THE DEVELOPMENT OF A THREE PHASE PLANT-WIDE MATHEMATICAL MODEL FOR SEWAGE TREATMENT

By

David S. Ikumi

This is a Full Dissertation Presented for the
Degree of
DOCTOR OF PHILOSOPHY
In the Water Research Group (WRG)
Department of Civil Engineering
UNIVERSITY OF CAPE TOWN
August 2011

Supervisor: Professor George A. Ekama

ABSTRACT

To aid in finding the most cost effective methods for the design and operation of wastewater treatment plants, for minimization of energy consumption and cost while maximizing nutrient recovery and improving effluent quality, the purpose of this project is to develop three phase (aqueous-gas-solid) steady state and dynamic mathematical models for the anaerobic and aerobic digestion of sludge; including waste activated sludge (WAS) produced by biological excess phosphorus removal (BEPR) plants, within a plant-wide setting. To accomplish this goal, the following four objectives were achieved:

1. Carry out an experimental investigation to generate the data required for both steady state and dynamic model development: The experimental set up was large to mimic three real wastewater treatment plant types at laboratory scale, viz nitrification-denitrification activated sludge treating raw wastewater, a nitrification-denitrification (ND) activated sludge (AS) system treating settled wastewater and a nitrification-denitrification biological excess phosphorus removal (NDBEPR) activated sludge system treating settled wastewater with separate anaerobic digestion (AD) of the WAS from each system, the primary sludge (PS) added to the settled wastewater to make up the raw wastewater and a PS - WAS blend.
2. Develop a steady state anaerobic digestion model including phosphorus: From the experimental data of the five anaerobic digesters, each operated at five different sludge ages, the hydrolysis kinetic rates of primary sludge, ND activated sludge system WAS and NDBEPR activated sludge system WAS were determined and included in the stoichiometric part of the anaerobic digestion model developed by Harding (2009) . Since mineral precipitation took place during the anaerobic digestion of NDBEPR WAS containing phosphorus accumulating organisms (PAOs), the steady state mixed weak

acid/base chemistry part of the AD model was extended to include three phases (aqueous-gas-solid).

3. Develop a dynamic anaerobic digestion model (ADM-3P) that includes phosphorus from NDBEPR WAS by extending the two phase (aqueous-gas) dynamic anaerobic digestion model for PS and ND activated sludge system WAS by Sötemann *et al.* (2005b), to include multiple organic types and three phase (aqueous-gas-solid) mixed weak acid/base chemistry for multiple mineral precipitation. Due to the significant increase in size and complexity to model the three wastewater treatment plants, as plant-wide configurations, in three phases, the models were coded in WEST®, which is a program capable of simulating many bioprocesses in various unit operations assembled into a wastewater treatment plant.
4. Develop a three phase activated sludge dynamic model (ASM2-3P) by extending the existing NDBEPR activated sludge model ASM2 (Henze *et al.*, 1995) and ensuring its compatibility with the three phase anaerobic digestion dynamic model. This three phase activated sludge model with BEPR was applied to plant-wide simulation of NDBEPR activated sludge with anoxic-aerobic digestion of concentrated phosphorus-rich waste activated sludge with mineral precipitation to produce dewatering liquor with low nitrogen and phosphorus.

The three phase steady state anaerobic digestion model (ADM-3P) developed in this investigation can be used on its own or linked with a steady state NDBEPR model, such as that developed by Wentzel *et al.* (1990), to construct a steady state plant-wide model, which is useful to make design decisions for the WWTP unit sizes and layout. Similarly, the ASM2-3P and ADM-3P models, which were linked form the plant-wide dynamic model, can be used independently for simulating anoxic-aerobic and anaerobic sludge stabilisation systems.

The steady state and dynamic models were developed simultaneously because the steady state models were required to determine kinetic rates and sludge

compositions for dynamic model input and calibration. This was possible because the steady state and dynamic activated sludge and anaerobic digestion models are based on the same basic principles, mass balanced stoichiometry, just in simplified form for the steady state model, without significant loss of accuracy. The steady state models allow sizing and optimization of individual wastewater treatment plant unit operations i.e. direct calculation of sludge age, reactor volumes and recycle flows for known wastewater characteristics or wastewater characteristics for existing wastewater treatment plants before performing dynamic simulations and so obviate much of the trial and error use of dynamic models. Once the wastewater treatment plant layout is established with steady state models, dynamic models can be applied to its operation to minimize energy consumption and cost while maximizing nutrient recovery and improving effluent quality.

David S. Ikumi, 2011
Dept. Of Civil Engineering,
University of Cape Town,
Rondebosch 7701,
South Africa

August 2011

DOCTORAL DEGREES BOARD
UNIVERSITY OF CAPE TOWN
Student Administration Building, University of Cape Town,
Private Bag X3, Rondebosch, 7701
Tel: **+27 21 650 2202** Fax: **+27 21 650 4913**
E-mail: janine.isaacs@uct.ac.za

Please complete Sections 1 and 2 and return to the Doctoral Degrees Board, University of Cape Town, when submitting your thesis for examination.

PhD Thesis title	THE DEVELOPMENT OF A THREE PHASE PLANT-WIDE MATHEMATICAL MODEL FOR SEWAGE TREATMENT

1. DECLARATIONS:

I DAVID SIDNEY IKUMI (full name) hereby:

(a) grant the University of Cape Town free licence to reproduce the above thesis in whole or in part, for the purpose of research;

(b) declare that:

(i) the above thesis is my own unaided work, both in concept and execution, and that apart from the normal guidance from my supervisor, I have received no assistance except as stated below:

_____
_____
_____
_____

(ii) neither the substance nor any part of the above thesis has been submitted in the past, or is being, or is to be submitted for a degree at this University or at any other university. except as stated below:

_____
_____
_____
_____

I am now presenting the thesis for examination for the degree of PhD.

Candidate's Signature		**Date**	

2. FUNDING AND FEES:

Candidates who submit have a choice in regards fee and funding options:

(a) to claim a fee rebate and discontinue funding through the PGFO (the student remains registered until graduation or the next academic year, see rule G5.2),

(b) to remain registered and engaged in the department while writing up a paper, with full student rights and full access to facilities, full liability for the fees for the year, and eligibility for continued (awarded) funding for that academic year.

Please indicate your preference:

To claim a fee rebate and discontinue funding and physical & library access*	
To continue fee liability, and funding eligibility and access to all facilities	

***Students asking for a fee rebate acknowledge:**

(a) the implications of the fee rebate on their access to facilities and eligibility for funding, and;

(b) that if they were to stay on in the department and receive payment though the payroll, such payment is taxable.

Candidate's Signature		**Date**	

PREFACE

This thesis is made on the topic of "the development of a three phase plant-wide mathematical model for sewage treatment" that is prepared by Mr. David S. Ikumi, under the supervision of Professor George A. Ekama. This thesis was solely prepared by the author, however, parts of the text are based on the research of others, and references for these sources have been provided to the best of the authors' efforts. This preface intends to clarify the contributions of the author, to avoid the reader from having any impressions that the full content of the mathematical models (for wastewater treatment plant (WWTP) unit processes of activated sludge (AS) and anaerobic digestion (AD)), presented in this thesis, were developed in this specific study.

It is first important to note that the experimental work described in Chapter 3 (i.e., mainly the operation and testing of the experimental set up, shown in Figure 3.1) of the thesis was done collaboratively with Harding (2009). However, the same data was used by Harding (2009) to answer different research questions. The main focus of the research by Harding was the determination of phosphorus release rates in AD of NDBEPR waste activated sludge (WAS) and the development of the stoichiometry section of the steady state model for the AD of phosphorus (P) rich sludge from the nitrification-denitrification biological excess P removal (NDBEPR) systems. Apart from Harding (2009), other major portions of work referred to in this thesis are from Sötemann (2005) for his developed two phase steady state and dynamic (UCTADM1) AD models (that do not include P) and Henze *et al.* (1995), for their developed ASM2 dynamic model.

The general project goal in this thesis is to develop three phase (aqueous-gas-solid) steady state and dynamic mathematical models for the anaerobic and aerobic digestion of WWTP sludge, including waste activated sludge produced by NDBEPR plants, in a plant-wide setting. This involved making extensions to models

developed in previous research, but for completeness, where it was deemed necessary, information from previous research is included and referenced in the text. The various sections of these developed models and the contributions by various authors have are presented below:

I. **The development of a steady state AD model that includes P**: The steady state AD model is an extension of the two phase (aqueous–gas) AD model developed by Sötemann (2005) and is described in Chapter 6 of this thesis. The steady state AD model comprises various sections:

   1. The kinetics of hydrolysis part that predicts the organics utilized in AD for a given sludge age. This part is reported in Sections 6.1 and 6.2 of Chapter 6 and is a part of the author's research, where methods similar to those used by Sötemann (2005) were also used.
   2. The stoichiometry and weak acid/base chemistry parts that predict the products formed in the AD, from the elements released with the degradation of organics predicted by part (1) above. This part was also developed by Sötemann (2005), using methods described by McCarty (1975), but without the inclusion of P. Harding (2009) extended this part to include P, as summarised in the whole of Section 6.3.1 of Chapter 6. The following Sections 6.3.2 to 6.4 comprise the work done by the author in the extension of this part. This includes the polyphosphate (PP) release with poly-3-hydoxyalkanoate (PHA) uptake in AD (with a review on methods proposed for the same process in NDBEPR AS systems, by other researchers such as Smolders *et al.*, (1995)) and the inclusion of a solid phase for the prediction of mineral precipitation, hence the extension of the two phase (aqueous-gas) AD model to three phase (aqueous-gas-solid). Methods carried out by previous researchers (such as Loewenthal *et al.*, 1994 and Musvoto *et al.*, 2000) are also included in the extension of the weak acid/base chemistry part. The author then calibrates the developed three phase steady state AD model in Section 6.5.

II. The development and calibration of a 3 phase dynamic AD model (ADM-3P):

This formed part of the main basis of the authors' work and is presented in Section 7.6 of Chapter 7. The ADM-3P model extends the two phase UCTADM1 (briefly described in Section 2.4.2.4 of Chapter 2) model developed by Sötemann *et al.* (2005b), by integrating it within a three phase mixed weak acid/base chemical and physical processes model of the inorganic carbon, ammonia, acetate, propionate and phosphate systems. The main extensions in the new model include:

1. Additional soluble and particulate biodegradable organic components to represent material which might be combined from different sources in the WWTP and fed to the anaerobic digester;
2. Digestion of waste activated sludge (WAS) from NDBEPR systems;
3. Additional processes for PP release and PHA hydrolysis.
4. Precipitation of $MgNH_4PO_4.6H_2O$ (struvite), $MgKPO_4.6H_2O$ (K-struvite) and $Ca_3(PO_4)_2$.
5. Modelling the "instantaneous" aqueous phase equilibrium reactions and ion paring with algebraic equations to reduce the stiffness of the system of differential equations.

In the development of this three phase AD model, the author worked closely with Chris Brouckaert from the University of Kwazulu Natal. Brouckaert *et al.* (2009) prepared an ionic speciation model, which could be integrated with the biological AD processes in the WEST® simulation platform to allow for ion paring and ionic speciation, which was an important requirement for the prediction of mineral precipitates in the AD model.

III. The development and calibration of the three phase activated sludge model number 2 (ASM2-3P)

The Activated Sludge Model No. 2 (ASM2) from IWA Task Group (Henze *et al.*, 1995) is a widely accepted activated sludge (AS) model that is broadly applied in NDBEPR system design and operation optimization. The ASM2-3P extends this ASM2 model by:

1. Including processes for the stripping of carbon dioxide (CO_2) and P precipitation (as would potentially occur in aerobic (AerD) or anoxic-aerobic (AnAerD) digestion).
2. Adding the same ionic speciation routine that is in the ADM-3P model described in (II) above.
3. Ensuring its compatibility with the ADM-3P model by extending the components to a general set, universal to both AS and AD processes of the ASM2-3P and ADM-3P models respectively and revising stoichiometric process coefficients in different units (from COD-based to mass-based)

The ASM2-3P model, developed and calibrated in Section 7.4 of Chapter 7, is also part of the main basis of the authors' work.

IV The development of a three phase plant-wide dynamic model:

This is also the main basis of the authors work and includes investigations into ancillary issues such as, whether the biodegradability of inert organic material remains consistent throughout all the linked upstream and downstream unit processes of the WWTP (this is important when coupling the primary settling tank (PST), AS, AerD and AD unit processes of the WWTP in a model). This aspect is discussed in Sections 5.1 and 5.2 of Chapter 5. The three phase plant-wide dynamic model is then prepared by linking the ASM2-3P and ADM-3P models (described in (II) and (III) above), which is done in Section 7.7 where the model is used to carry out scenario analysis for an NDBEPR AS system linked to an AD.

ACKNOWLEDGEMENTS

God Almighty – Thanks and praise to God for providing me this opportunity and giving me the strength to carry out this project. I could never have managed without the faith I have in you.

Professor George Ekama – Thank you for the opportunity to work with you in this high-ranking research group and for your guidance and assistance, which was of valuable contribution to the success of this project.

Chris Brouckaert – Thank you for your assistance, advice and input especially when working with the WEST® program.

Theodor Harding – Thank you for all the support and friendship, and for all the hard work you put in during our experimental investigation, without which this work would have not been completed.

Mark Wentzel – Thank you for all your suggestions and advice.

Taliep Lakay, Hector Mafungwa and Arnold Ramathla – Thankyou for all your support during the experimental investigation of this project.

My parents: Harry and Rehema Ikumi – Thank you for being supportive, encouraging and loving and for all the sacrifices you made to ensure that I get a good education.

My sisters: Michelle, Rhoda and Sonia Ikumi – Thank you for all your love and support and friendship.

All supportive friends – Thank you for your support and friendship and for all your positive input to my life.

The **Water Research Commission** (WRC), The **Water Research Group** (WRG) at the University of Cape Town, The **National Research Foundation** (NRF) for providing financial support.

The **Water Institute of South Africa** (WISA) and the **International Water Association** (IWA) for all opportunities awarded me to present this project at your conferences.

LIST OF SYMBOLS AND ABBREVIATIONS

A	Composition subscript for nitrogen in organics empirical formulation (i.e. $C_XH_YO_ZN_AP_B$)
Ac	Dissociated Acetic Acid (CH_3COO^-)
ACP	Amorphous calcium phosphate
AD	Anaerobic Digestion
ADM1	Anaerobic Digestion Model number 1
ADM-3P	Three phase Anaerobic Digestion Model
AerD	Aerobic Digestion
Alk	Alkalinity
Alk H_3PO_4	Phosphate Alkalinity (as $mgCaCO_3/l$)
ANO	Autotrophic Nitrifying Organism
AS	Activated Sludge
ASM1	Activated Sludge Model number 1
ASM2	Activated Sludge Model number 2
ASM2-3P	Three –Phase Activated Sludge Model number 2
A_T	Total acetate in acetate weak acid/base sub-system
atm.	Atmospheres
B	Composition subscript for phosphorus (P) in organics empirical formulation (i.e. $C_XH_YO_ZN_AP_B$)
BEPR	Biological Excess Phosphorus Removal
b_G	Specific endogenous mass loss rate of PAOs (0.04/d at 20°C)
b_H	Specific endogenous mass loss rate of OHOs (0.24/d at 20°C)
BPO	Biodegradable Particulate Organics
BSO	Biodegradable Soluble Organics
BNR	Biological Nutrient Removal

C	Carbon
Ca	Calcium
$CaCO_3$	Calcium Carbonate
CAS	Conventional Activated Sludge
CBIM	Continuity-Based Interfacing Model
CH_4	Methane
$C_XH_YO_ZN_AP_B$	Biomass empirical composition
CO_2	Carbon dioxide
COD	Chemical Oxygen Demand
CSTR	Continuously Stirred Tank Reactor
C_T	Total carbon in carbonate weak acid/base sub-system
d	Day
D_B	Electrons accepting capacity of biomass
˚C	Degrees Celcius
DO	Dissolved Oxygen (mgO)
DPAO	De-nitrifying Phosphate Accumulating Organism
D_s	Electron Donating Capacity of the Substrate
DSVI	Diluted Sludge Volume Index (ml/gTSS)
E	Fraction of the Biodegradable COD converted to Biomass
EBPR	Excess Biological Phosphorus Removal
ER	Endogenous Residue produced with biomass lysis
f	Value that relates the pH and equilibrium (pK_{p2}) in AD model
f_C or α^C	Total organic carbon (TOC) to mass (VSS or molar mass) ratio
f_{cv} or α^{COD}	Chemical oxygen demand (COD) to mass (VSS or molar mass) ratio

f_{EG}	Endogenous residue fraction of PAOs
f_{EH}	Endogenous residue fraction of OHOs
f_H **or** α^H	Hydrogen (H) to mass (VSS or molar mass) ratio
f_i	VSS to TSS ratio of the mixed liquor (mgN/mgCOD)
f_{iPAO}	ISS fraction of the PAOs (mgISS/mgPAOTSS)
f_{iOHO}	ISS fraction of the OHOs (mgISS/mgOHOTSS)
f_m, f_d **and** f_t	Activity Coefficient (mono-, di- and tri-valent) Ionic species
f_N **or** α^N	Nitrogen (N) to mass (VSS or molar mass) ratio
f_O **or** α^O	Oxygen (O) to mass (VSS or molar mass) ratio
f_P **or** α^P	Phosphorus (P) to mass (VSS or molar mass) ratio
FRBCOD	Fermentable Soluble Biodegradable Organic COD
FSA	Free and Saline Ammonia
$f_{S'up}$	Fraction of unbiodegradable particulate (with respect to total) COD in the influent wastewater
$f_{S'us}$	Fraction of unbiodegradable soluble (with respect to total) COD in the influent wastewater
$f_{up\text{-}WAS}$	UPO fraction of WAS in AS system
f_{XBGPP}	Fractional Polyphosphate P content of the PAOs (0.38mgP/mgPAOVSS)
f_{XBGP}	P fraction of the PAOs (mgP/mgPAOVSS)
f_{XBHPBM}	P fraction of OHOs (mgP/mgOHOVSS)
f_{XBGPBM}	Biological cell P fraction of the PAOs (mgP/mgPAOVSS)
F/M	Food to Microorganism ratio
g	Gram
H	Elemental Hydrogen
H^+	Hydrogen ion
H_2	Hydrogen molecule, denotes dissolved hydrogen concentration

HCO_3^-	Bi-carbonate
H_2CO_3* Alk.	Inorganic Carbon Alkalinity (as mg $CaCO_3$/*l*)
h	Hour
HRT	Hydraulic Retention Time
IC	Inorganic Carbon
ISS	Inorganic Settleable Solids
IWA	International Water Association
J_{BPO}	Molar fluxes for the total BPO (mol/d)
$J_{BPO\ (U)}$	Molar fluxes for the utilized BPO (mol/d)
K_a	Dissociation Constant for Weak Acid/Base
K_{c1}	Equilibrium Constant for H_2CO_3/HCO_3^- weak acid sub-system
K_{c2}	Equilibrium Constant for HCO_3^-/CO_3^{2-} weak acid sub-system
K_H	Henry's law constant
K_{LA}	Oxygen mass transfer coefficient (l/h)
K_s	Half Saturation Constant (mol/ l)
K_{spm}	Thermodynamic Solubility Product
K	Degrees Kelvin
l	Litre
Me	Counter-ion metals (include cations of Mg, K and Ca)
$MePO_3$	Polyphosphate
Mg	Magnesium
$MgNH_4PO_4.6H_2O$	Struvite
MLE	Modified Ludzack–Ettinger (activated sludge system)
MM_x	Molar Mass (g/mol) (where x refer to the relevant element)

MBR	Membrane Biological Reactor
mg	Milligram
min	Minute
ML	Mixed Liquor
MPWWTP	Mitchells Plain Wastewater Treatment Plant
MS_{ti}	Mass of total COD in the influent wastewater (mgCOD)
MX_a	Mass of active biomass (mgAVSS)
MX_v	Mass of volatile suspended solids (mgVSS)
Mg	Magnesium
MLSS	Mixed Liquor Suspended Solids (gSS/l)
MLVSS	Mixed Liquor Volatile Suspended Solids (gVSS/l)
N	Elemental Nitrogen
N_2	Di-nitrogen molecule
NaC*l*	Sodium Chloride
N_{ae}	Effluent ammonia concentration (mgN/ *l*)
ND	Nitrification-denitrification
NDBEPR	Nitrification-denitrification Biological Excess Phosphorus Removal
NH_4^+	Ammonium (mgN/ *l*)
NO_2^-	Nitrite (mgN/ *l*)
NO_3^-	Nitrate (mgN/ *l*)
N_{ousi}	Organic unbiodegradable soluble influent Nitrogen (mgN/ *l*)
N_T	Total nitrogen in ammonia weak acid/base sub-system
O	Elemental Oxygen
O_2	Oxygen molecule
OHO	Ordinary Heterotrophic Organism
OP	Ortho-phosphates

OUR	Oxygen Utilization Rate (mgO/ *l* /h)
Ortho P	Ortho-phosphates
P	Elemental Phosphorus
PAO	Phosphorus Accumulating Organism
p_{CO2}	Carbon dioxide (CO_2) partial pressure
pH	Activity of Hydrogen ions
p_{H2}	Hydrogen Partial Pressure (atm)
PHA	Poly-3-hydoxyalkanoates
PS	Primary Sludge
PST	Primary Settling Tank
P_T	Total phosphorus in phosphate weak acid/base sub-system
PP	Polyphosphate
pK_a	-Log10 of dissociation constant (K_a) in acetate weak acid sub-system
Q	Flow rate (*l*/d)
Q_e	Effluent flow rate (*l*/d)
Q_i	Influent flow rate (*l*/d)
Q_w	Sludge waste flow rate (*l*/d)
R_a	e^- acceptor reaction catabolism
RBCOD	Readily Biodegradable COD (mgCOD/ *l*)
R_c	synthesis reaction (anabolism) = f_e
R_d	e^- donor reaction (catabolism) for the organics = f_s
Rhn	Hydraulic Retention Time (d)
r_{HYD}	Rate of hydrolysis
Rs	Sludge age or sludge retention time (SRT, measured in days)
s	Second

SB	Sewage Batch
SBCOD	Slowly biodegradable COD (mgCOD/ *l*)
S_b	Biodegradable organics in reactor (mgCOD/ *l*)
S_{bi}	Influent biodegradable organics (mgCOD/ *l*)
S_{bp}	Biodegradable particulate organics (mgCOD/*l*)
S_{bpe}	Residual biodegradable particulate organics (mgCOD/*l*)
S_{bs}	Biodegradable soluble COD (mgCOD/ *l*)
SCFA	Short chain Fatty Acid
SRT	Solids (or sludge) Retention Time (d)
SS	Steady State
SST	Secondary Settling Tank
S_{te}	Total effluent COD concentration (mgCOD/ *l*)
S_{ti}	Total influent wastewater COD concentration (mgCOD/ *l*)
S_{up}	UPO in COD concentration (mgCOD/*l*)
S_{us}	Unbiodegradable COD in influent (mgCOD/ *l*)
T	Temperature (°C or K)
TDS	Total Dissolved Solids
TKN	Total Kjeldahl Nitrogen (mgN/ *l*)
TOC	Total Organic Carbon (mgC/ *l*)
TP	Total Phosphorus (mgP/ *l*)
TSS	Total Settleable Solids (mgTSS/ *l*)
UCT	University of Cape Town
UPO	Unbiodegradable Particulate Organics
USO	Unbiodegradable Soluble Organics
V	Volume
VFA	Volatile Fatty Acid

VSS	Volatile Suspended Solid (mgVSS/*l*)
WAS	Waste Activated Sludge
WRC	Water Research Commission
WRG	Water Research Group
WW	Wastewater
WWTP	Wastewater Treatment Plant
X	Composition subscript for carbon in organics' empirical formulation (i.e. $C_XH_YO_ZN_AP_B$)
$\mathbf{X_a}$	Active biomass concentration (mgAVSS/ *l*)
$\mathbf{X_{BG}}$	Active biomass of the PAOs (mgVSS/*l*)
$\mathbf{X_{BH}}$	Active biomass of the OHOs (mgVSS/*l*)
$\mathbf{X_{EG}}$	Endogenous residue of the PAOs (mgERVSS/*l*)
$\mathbf{X_{EH}}$	Endogenous residue of the OHOs (mgERVSS/*l*)
$\mathbf{X_i}$	Inert (unbiodegradable) organics concentration (mgUPOVSS/*l*)
$\mathbf{X_{Io}}$	Inorganic settleable solids concentration (mgISS/*l*)
$\mathbf{X_V}$	Volatile settleable solids concentration (mgVSS/ *l*)
Y	Composition subscript for hydrogen in organic empirical formulation (i.e. $C_XH_YO_ZN_AP_B$)
$\mathbf{Y_H}$	Ordinary heterotrophic cell yield coefficient
Z	Composition subscript for oxygen in organic empirical formulation (i.e. $C_XH_YO_ZN_AP_B$)
$\mathbf{Z_{AD}}$	Acidogenic biomass concentration
$\mathbf{\mu_{max}}$	Maximum Specific Growth Rate (/d)

LIST OF TABLES

Table S.1: Unbiodegradable Particulate Organic (UPO) Fractions and Hydrolysis Kinetic Determined by the Different Methods in the Experimental Investigation lvi

Table 2.1: Weak Acid Dissociation Constants (Truesdell and Jones, 1973; Loewenthal *et al.*, 1994) 69

Table 2.2: Solubility Products (pK_{sp}) for the Five Minerals likely to Precipitate in ADL 71

Table 2.3: Precipitation Process Reactions and Kinetics (Musvoto *et al.*, 2000 a) 72

Table 2.4: Rates of Aeration/Gas Stripping 79

Table 2.5: Advantages and Disadvantages of Aerobic or Anaerobic Treatment of PS and WAS....85

Table 3.1: Summary of Samples and Tests used in Research Experimental Period..111

Table 4.1a: Reference Guide and Timeline for 2007 Experimental Data....115

Table 4.1b: Reference Guide and Timeline for 2008 Experimental Data 116

Table 4.1c: Key for Tables 4.1a and 4.1 b 117

Table 4.2.5: Metallic Ion Concentrations (mg/*l*) in the NDBEPR AS System....127

Table 4.3.1: COD Removal with Increased AD Sludge Age 130

Table 4.3.2: FSA Release with Increased AD Sludge Age 134

Table 4.3.3: AD Gas Production and Composition Values 137

Table 4.3.4: AD Effluent VFA, H_2CO_3 Alkalinity and pH Values 141

Table 4.3.5: Ortho-phosphate Release with Increased AD Sludge Age 142

Table 4.3.6: NDBEPR WAS fed AD (AD 1) Metallic Ion Measurements 145

Table 4.4.1: Mass Balance over PST (%) 147

Table 4.4.2: MLE 1 AS System Mass Balances....148

Table 4.4.3: MLE 2 AS System Mass Balances....149

Table 4.4.4: NDBEPR AS System Mass Balances 150

Table 4.4.5: Percentage Mass Balances Over AD Systems 152

Table 5.2.1: Influent Unbiodegradable Particulate($f_{S'up}$) and Soluble ($f_{S'us}$) fractions for Operated AS systems.....161
Table 5.2.2: Comparison of Mitchell's Plain Sewage $f_{S'up}$ from Literature on ND Systems.....162
5.2.3b: Objectives, Scope and Distinctives of the 5 Investigations from Table 5.2.3a 164
Table 5.3.1: WAS Unbiodegradable Particulate Fraction ($f_{S'upWAS}$).....167
Table 5.4.1a: Methods used in Determination of Raw and Settled WW Characteristics 173
Table 5.4.1b: Methods used in Determination of PS Characteristics.....175
Table 5.4.2: Influent Chemical Oxygen Demand (COD) Characterisation.....179
Table 5.4.3: Influent Carbon (C) Characterisation.....183
Table 5.4.4a: Sludge Characteristics Obtained from Measurements in AS Systems and PS Anaerobic Digester Effluent.....186
Table 5.4.4.b: Influent Nitrogen (N) Characterisation 189
Table 5.4.4.c: Influent Phosphorus (P) Characterization 192
Table 5.4.6: NDBEPR AS System Influent Elemental Composition for Test Period 1 194
Table 5.5.1: Nutrient Removal Systems Waste Activated Sludge Characteristics.....201
Table 5.5.2: Methods used in Determination of WAS Characteristics 207
Table 5.5.3: Waste Activated Sludge Elemental Composition (Aerobic) for Test Period 1.....209
Table 5.3.4: Elemental composition for Biodegradable Organics (and Polyphosphate) of Influent Sludge to AD Calculated from the AS Systems. 213
Table 5.3.5: Elemental composition for Unbiodegradable Particulate Sludge Components, Calculated from the 60 day R_s AD Systems.....214
Table 5.6: Layout for Process Reactions on various Waste Components of the AS linked to AD Systems in a WWTP.....215
Table 6.2.1a: Primary Sludge Influent Experimental Data.....237

Table 6.2.1b: Primary Sludge Effluent Experimental Data 238
Table 6.2.1c: Summary of Results for First Order Kinetics in the AD of PS for $f_{PS'up}$ = 0.31.....242
Table 6.2.1d: From Sötemann *et al.* (2005) who used the Izzett *et al.* (1992) 7 to 20 d retention time (R_s) and O'Rourke (1968) 7.5 to 60 d R_s anaerobic digester measured influent* (S_{ti}) and effluent* (S_{te}) COD concentrations, influent unbiodegradable (S_{upi}) and biodegradable COD (S_{bpi}) concentrations for an unbiodegradable COD fraction ($f_{PS'up}$) of 0.36 (for Izzett data) and 0.338 (for O'Rourke data) to calculate the residual biodegradable COD concentration (S_{bp}), observed hydrolysis rate (r_{HYD}), specific hydrolysis rate [r_{HYD}/Z_{AD})] and the 1st order and 1st order specific hydrolysis rate constants (k_h and k_H). All mass units in gCOD.....244
Table 6.2.1e: Predicted S_{bpe} for the Determination of the Best Monod Kinetic Constants from the Three Linearization Methods 250
Table 6.2.1f: Monod Kinetics (Hydrolysis of PS).....252
Table 6.2.1g: Predicted S_{bpe} in gCOD/*l* for the Determination of the Best Saturation Kinetic Constants from the Three Linearization Methods.....254
Table 6.2.1h: Saturation Kinetics (Hydrolysis of PS) 255
Table 6.2.2a: WAS from MLE Fed Settled WW Influent Experimental Data 258
Table 6.2.2b: WAS from MLE Fed Settled WW Effluent Experimental Data.....259
Table 6.2.2c: Summary of Results for First Order Kinetics in the AD of MLE 1 WAS for $f_{SL'up}$ = 0.47 265
Table 6.2.2d: Predicted S_{bpe} in gCOD/*l* for the Determination of the Best Monod Kinetic Constants from the Three Linearization Methods.....269
Table 6.2.2e: Monod Kinetics (Hydrolysis of MLE 1 WAS).....270
Table 6.2.2f: Predicted S_{bpe} in gCOD/*l* for the Determination of the Best Saturation Kinetic Constants from the Three Linearization Methods.....273
Table 6.2.2g: Saturation Kinetics (Hydrolysis of MLE 1 WAS) 274
Table 6.2.3a: WAS from MLE Fed Raw WW Influent (MLE 2) Experimental Data ..275
Table 6.2.3b: WAS from MLE Fed Raw WW Effluent Experimental Data 276

Table 6.2.3c: Summary of Results for first order Kinetics in the AD of MLE 2 WAS280
Table 6.2.3d: Predicted S_{bpe} in gCOD/*l* for the Determination of the Best Monod Kinetic Constants from the Three Linearization Methods.....286
Table 6.2.3e: Monod Kinetics (Hydrolysis of MLE 2 WAS).....288
Table 6.2.3f: Saturation Kinetics (Hydrolysis of MLE 2 WAS).....290
Table 6.2.3g: Predicted S_{bpe} in gCOD/*l* for the Determination of the Best Saturation Kinetic Constants with the Three Linearization Methods and the Curve Expert program.....290
Table 6.2.4a: WAS from MBR NDBEPR UCT System Influent Experimental Data ..294
Table 6.2.4c: Summary of Results for First Order Kinetics in the AD of NDBEPR WAS for $f_{SL'up}$ = 0.54.....300
Table 6.2.4e: Monod Kinetics (Hydrolysis of NDBEPR WAS).....308
Table 6.2.5a: Primary Sludge-Waste Activated Sludge Blend Influent Experimental Data.....314
Table 6.2.5b: Primary Sludge-Waste Activated Sludge Blend Effluent Experimental Data.....315
Table 6.2.5c: Summary of Results for First Order Kinetics in the AD of PS-WAS for $f_{SL'up}$ = 0.37.....321
Table 6.2.5d: Predicted S_{bpe} in gCOD/l for the Determination of the Best Monod Kinetic Constants, for the AD of PS-WAS blend, from the Three Linearization Methods.....325
Table 6.2.5e: Monod Kinetics (Hydrolysis of PS-WAS).....326
Table 6.2.5f: Predicted S_{bpe} in gCOD/*l* for the Determination of the Best Saturation Kinetic Constants, for PS-WAS blend AD, from the Three Linearization Methods .328
Table 6.2.5g: Saturation Kinetics (Hydrolysis of PS-WAS).....329
Table 6.2.6a: Comparison of Experimentally Determined Monod and Saturation Kinetic Constants.....330
Table 6.2.6b: A Comparison of the Changes in Specific Hydrolysis Rates (r_{HYD}/Z_{AD}) of the Various Sludges with Increasing Biodegradable Organics Concentration (S_{bp}) .332

Table 6.5.1a: Parameters used to Calculate the AD predictions with the Steady State AD Model....360
Table 6.5.1c: Effluent Results and Mass Balance Calculations for NDBEPR WAS Steady State AD Model Versus Experimental Data....362
Table 7.2.1: The Universally Selected Model Components....382
Table 7.2.2: Ionic Species Selected for the Three Phase Modelling....384
Table 7.2.3: Example for Equilibrium and Mass Balance Equations for Ionic Speciation....386
Table 7.4.1: Mass Balance Results for NDBEPR AS Simulation....418
Table 7.4.2: Parameters used in Simulating the ASM2-3P Model....421
Table 7.4.3a: Summary of Measured and Simulated Results for NDBEPR AS System....426
Table 7.4.3a: Summary of Measured and Simulated Results for NDBEPR AS System....427
Table 7.4.4: Summary of Measured and Simulated Results for MLE 2 AS System....434
Table 7.4.5: Summary of Measured and Simulated Results for MLE 1 AS System....437
Table 7.5.1: Stoichiometric Processes of the ADM-3P Model....443
Table 7.5.2: Parameters used in Simulating the ADM-3P Model....450
Table 7.5.3a: Parameters (additional to those from Table 7.5.2) used for Simulating the AD of NDBEPR WAS....451
Table 7.5.3b: Measured and Simulated Results for Anaerobic Digestion of NDBEPR WAS....453
Table 7.5.3c: Comparison of Simulated to Measured Metals Data in Anaerobic Digestion of NDBEPR WAS....454
Table 7.5.5a: Parameters (additional to those from Table 7.5.2) for simulating the AD of MLE 1 WAS....460
Table 7.5.5b: Measured and Simulated Results for Anaerobic Digestion of MLE 1 WAS....462

Table 7.5.6a: Parameters (additional to those from Table 7.5.2) for simulating the AD of MLE 2 WAS 463
Table 7.5.6b: Measured and Simulated Results for Anaerobic Digestion of MLE 2 WAS 465
Table 7.5.7a: Parameters (additional to from Table 7.5.2) for simulating the AD of PS (data obtained from Izzett *et al.*, 1992) 469
Table 7.5.7b: Anaerobic Digestion of Primary Sludge (Using Experimental Results from Izzett *et al.* (1992) 471
Table 7.5.8a: Parameters (additional to those from Table 7.5.2) for simulating the AD of PS (data measured by author) 472
Table 7.5.9a: Adjustments made to parameters from Table 7.5.2 for simulating the AD of PS-MLE1 WAS blend (the same hydrolysis kinetics used for PS and WAS, i.e. the blend considered as a single sludge type, unique from PS or WAS, with only one k_M and K_S value used) 476
Table 7.5.9b: Measured and Simulated Results for Anaerobic Digestion of PS - MLE 1 WAS Blend 478
Table 7.5.10: Parameters Selected for Sensitivity Analysis 484
Table 7.6.2: Parameters used in Simulating Anoxic-Aerobic Digestion (AnAerD) with the Three phase ASM2 Model 521
Table 7.6.2a: Summary of Measured and Simulated Results for NDBEPR AS System, Parent to Anoxic- Aerobic Digester 527
Table 7.6.2b: Summary of Measured and Simulated Results for Anoxic - Aerobic Digester 528
Table 7.7.1a: Measured and Simulated Results for Plant-Wide AD of NDBEPR WAS 535
Table 8.1: Unbiodegradable Particulate Organic (UPO) fractions and hydrolysis kinetic determined by the different methods in the experimental investigation 551
Table A5.1: System Parameters in Steady State AD Model Spreadsheet 617
Table A5.2: Characterisation of Feed Sludge in AD Steady State Spreadsheet 618

Table A5.3: The AD Steady State Model Spreadsheet Calculated Stoichiometric Products for Infinite Solubility.....621
Table A5.4: Total Species Concentrations Before Precipitation in Steady State Model Spreadsheet (in mol/*l*) 622
Table A5.5: Post Precipitation AD Stoichiometric Products in AD Steady State Model Spreadsheet.....623
Table A5.6: Weak Acid Dissociation Constants used in Steady State Model.....624
Table A5.8: Influent Characteristics of Plant for Design Example.....625
Table A5.9a: plant-wide System Requirements for Selected Plant Configurations ..628
Table A5.9b: AS and AD System Effluent Quality for the Various Selected Plant Configurations.....629
Table A5.10: plant-wide System Requirements for Selected Plant Configurations ..632
Table A5.11: AS and AD System Effluent Quality for the Various Selected Plant Configurations.....634
Table A6.1a: Outline Formation of the Three phase Plant-Wide Model Gujer Matrix 637
Table A6.1b: ASM2-3P Section of the Stoichiometric Matrix for the Plant-Wide 3 Phase Model.....638
Table A6.1c: ASM2-3P Section of the Stoichiometric Matrix for the Plant-Wide 3 Phase Model.....640
Table A6.1d: ADM-3P Section of the Stoichiometric Matrix for the Plant-Wide 3 Phase Model.....642
Table A6.1e: ADM-3P Section of the Stoichiometric Matrix for the Plant-Wide 3 Phase Model.....644
6.1f: Process Rates for the ASM2-3P Section in the Stoichiometric Matrix for the Plant-Wide 3 Phase Model.....646
6.1g: Process Rates for the ADM-3P Section in the Stoichiometric Matrix for the Plant-Wide 3 Phase Model.....649

Table A7.1: Raw Measurements for the UCT Process Operated Nitrification-denitrification Biological Excess Phosphorus Removal System, fed settled wastewater and an extra 200mgCOD/*l* of acetate 665
Table A7.2: Raw Measurements for Modified Ludzack Ettinger System 2 (MLE 2) which carries out nitrification - denitrification process, operated using raw wastewater 671
Table A7.3: Raw Measurements for Modified Ludzack Ettinger System 1 (MLE 1) which carries out nitrification - denitrification process, operated using settled wastewater 677
Table A7.4: Influent for AD 2 (PS) Raw Measurements 683
Table A8.1: Raw Results for Anaerobic Digester 2 (AD 2), fed Primary Sludge (PS), when operated at sludge ages of 10, 18 and 25 days 687
Table A8.2: Raw Results for Anaerobic Digester 4 (AD 4), fed primary sludge blended with waste activated sludge (WAS) from MLE 1, when operated at sludge ages of 10, 18 and 25 days 692
Table A8.3: Raw Results for Anaerobic Digester 1 (AD 1), fed waste activated sludge (WAS) from the NDBEPR UCT Process System, when operated at sludge ages of 10, 18 and 25 days 697
Table A8.4: Raw Results for Anaerobic Digester 3 (AD 3), fed waste activated sludge (WAS) from MLE 1 system, when operated at sludge ages of 10, 18 and 25 days....702
Table A8.5: Raw Results for Anaerobic Digester 5 (AD 5), fed waste activated sludge (WAS) from MLE 2 System, when operated at sludge ages of 10, 18 and 25 days ...707

LIST OF FIGURES

Figure S.1: *Experimental set-up* xliv

Figure S.2: *The percentage biodegradable COD removed, calculated from measured results with increasing sludge age (R_s) for the different sludge type.* xlix

Figure S.3: *Process scheme for the ADM-3P model, as extended from the UCTADM1 model of Sötemann et al. (2005). Note that (1) ammonia is released in the NH_3 form and picks up a proton from H_2CO_3 to form NH_4^+, (2) Process 2 is for PP release with the uptake of acetate and (3) process 5 is for the PP hydrolysis with the death of the PAOs, (4) ER stands for the endogenous residue of biomass. Process 12 only shows for P precipitates, but other precipitates (i.e. newberyite, calcite and magnesite, which are less likely to form) are also included in the model.* lvii

Figure 1.1: *A mind map showing an overview of the project report, including the main contents of each chapter and the chapters that are associated with each other (green hidden lines).* 10

Figure 2.1: *Simplified WWTP layout* 12

Figure 2.2: *A simplified depiction of the anaerobic digestion process* 33

Figure 3.1: *Experimental set-up* 92

Figure 3.2: *MLE process used in research project.* 97

Figure 3.3: *NDBEPR system used in research project.* 98

Figure 3.4: *Anaerobic digester used in research project* 102

Figure 3.5: *Gas flow meter* 109

Figure 4.2.1: *The influent (S_{ti}) and filtered effluent (S_{te}) COD concentrations for the three AS systems at the test periods and respective sewage batch numbers.* 119

Figure 4.2.2: *The influent (N_{ti}) and filtered effluent (N_{te}) TKN concentrations for the three AS systems at the test periods and respective sewage batch numbers.* 121

Figure 4.2.3a: *The influent TKN and filtered effluent nitrate concentrations for the three AS systems over the AD test periods and respective sewage batch numbers.* 123

Figure 4.2.3b: *The mass of nitrates generated and de-nitrified in the three AS systems at the test periods and respective sewage batch numbers.* 124
Figure 4.2.4: *The variation of influent and filtered effluent total phosphate concentrations during the experimental research periods and respective sewage batch numbers.* 125
Figure 4.2.6: *The mixed liquor total and volatile suspended solids concentrations throughout the experimental period.*.....127
Figure 4.2.7: *Sewage batch average oxygen utilization rates (OUR) in the aerobic reactors of the NDBEPR, MLE 1 and MLE 2 systems.*.....129
Figure 4.3.1: *The change in the percentage COD removal with AD sludge age.* 132
Figure 4.3.2: *The percentage influent TKN released as FSA during anaerobic digestion.* ..134
Figure 4.3.3: *The fraction in influent unfiltered COD removed in the form of CH_4 during anaerobic digestion*.....136
Figure 4.3.4: *The variations of effluent VFA concentration with sludge age during anaerobic digestion*.....139
Figure 4.3.5: *The variations of effluent pH with sludge age during anaerobic digestion* 140
Figure 4.3.6: *The variations of effluent alkalinity concentration with sludge age during anaerobic digestion*.....140
Figure 4.3.7: *The percentage influent total phosphorus (TP) released as ortho-Phosphate (OP) during AD.* 143
Figure 5.4.1a: *The COD characteristics for raw and settled wastewater fed to MLE systems, all values are in mgCOD/l.*.....177
Figure 5.4.1b: *The COD characteristics for primary sludge (PS), all values are in mgCOD/l.* 178
Figure 5.4.1c: *The COD characteristics for settled wastewater fed to the MBR UCT system,all values are in mgCOD/l.*.....178
Figure 5.4.2a: *The TOC characteristics for raw and settled wastewater fed to MLE systems, all values are in mgC/l.* 181
Figure 5.4.2b: *The TOC characteristics for primary sludge, all values are in mgC/l.*.....181

Figure 5.4.2c: *The TOC characteristics for settled wastewater fed to the MBR UCT system, all values are in mgC/l.* 182
Figure 5.4.3a: *The nitrogen characteristics for raw and settled wastewater fed to MLE systems, all values in mgN/l.* 187
Figure 5.4.3b: *The nitrogen characteristics for primary sludge, all values in mgN/l.* 187
Figure 5.4.3c: *The nitrogen characteristics for settled wastewater fed to the MBR UCT system, all values in mgN/l.* 188
Figure 5.4.4a: *The phosphorus (P) characteristics for raw and settled wastewater fed to MLE systems, all values in mgP/l.* 190
Figure 5.4.4b: *The phosphorus (P) characteristics for primary sludge, all values in mgP/l.* 190
Figure 5.4.4a: *The phosphorus (P) characteristics for settled wastewater fed to the UCT MBR system, all values in mgP/l.* 191
Figure 6.1.0: *A typical Lineweaver-Burke plot.* 231
Figure 6.1.1: *Change in Monod curve for change in influent biodegradable COD concentration (S_{bpi}).* 232
Figure 6.2.1a: *The change in the coefficient of variation of the 1st order and 1st order specific hydrolysis equations kinetic constants with changing unbiodegradable particulate COD fraction of primary sludge ($f_{PS'up}$), without R_s = 40d data (see Table 6.2.1c).* 240
Figure 6.2.1b: *The regression correlation coefficient (R^2) for the Curve Expert program, Lineweaver-Burke (M1), double deciprocal (M2) and Eadie-Hofstee (M3) linearization methods of Monod hydrolysis kinetics versus unbiodegradable particulate COD fraction of the PS ($f_{PS'up}$).* 240
Figure 6.2.1c: *The regression correlation coefficient (R^2) for the Curve Expert program, Lineweaver-Burke (M1), double reciprocal (M2) and Eadie-Hofstee (M3) linearization methods of saturation hydrolysis kinetics versus unbiodegradable particulate COD fraction of the PS ($f_{PS'up}$).* 241

Figures 6.2.1d, e, f and g: *Volumetric hydrolysis rates (r_{HYD}) (d), specific volumetric hydrolysis rate (r_{HYD}/Z_{AD}) (e), first order kinetic constant (k_h) (f) and specific first order kinetic constant (k_H) (g) versus sludge age (R_s) for AD of PS*.....243

Figures 6.2.1h i, j and k: *Hydrolysis kinetics formulation curves plotted using experimental data and calculated from kinetic constants acquired from the three linearization methods for (h) Monod (see Table 6.2.1e column 9; k_m =4.30 and K_s = 1.523) and (i) saturation equations (see Table 6.2.1g column 9; k_M =1.796 and K_S = 7.962) and using the Curve Expert programme (j) for Monod (Table 6.2.1e) and (k) for saturation kinetics (Table 6.2.1h).* 246

Figures 6.2.1l, m and n: *The linearization of Monod kinetics for hydrolysis of PS at all five R_s (10, 18, 25, 40 and 60) using (l) Lineweaver–Burke (M1), (m) double reciprocal (M2) and (n) Eadie–Hofstee (M3) methods (R^2 values for all R_s data included – dark (black) lines. Numbers refer to column numbers in Table 6.2.1e, e.g. 5 refers to column 5 which lists the average k_m and K_s values obtained from line 5 in Figure 6.2.1l:M1 without the R_s =40d and 60d data, line 5 in Figure 6.2.1m:M2 (all data) and line 5 in Figure 6.2.1n: M3 without R_s = 40d data.*.....248

Figure 6.2.1o: *Comparison of tagret S_{bpe} values (calculated from measured values in Table 6.2.1b) with those predicted by different combinations of selected R_s data from the three linearization methods, for the determination of the best k_m and K_s values for modelling hydrolysis with the Monod kinetics. Numbers refer to column numbers in Table 6.2.1.e*....250

Figures 6.2.1p, q and r: *The linearization of saturation kinetics for hydrolysis of PS at all five R_s (10, 18, 25, 40 and 60) using (p) Lineweaver – Burke (M1), (q) double reciprocal (M2) and (r) Eadie–Hofstee (M3) methods. The R^2 values for all 5 R_s data included- dark (black) lines. Numbers refer to column numbers in Table 6.2.1g, e.g. 2 refers to column 2, which lists the average k_m and K_s values obtained from line 2 in Figure 6.2.1p:M1 all R_s data included, line 2 in Figure 6.2.1q:M2 with R_s =40d and 60d omitted and line 2 in Figure 6.2.1r:M3 with all R_s data included.*.....253

Figure 6.2.1s: *Comparison of tagret S_{bpe} values (calculated from measured values in Table 6.2.1b) with those predicted by different combinations of selected R_s data from the three*

*linearization methods, for the determination of the best k_M and K_S values for modelling hydrolysis with the saturation kinetics. Numbers refer to column number in Table 6.2.1g.*254

Figures 6.2.1t: *Comparison of S_{bp} removal for (i) Author data (Ikumi, 2011; $f_{PS'up}$ = 0.31) to data from (ii) Izzett et al. (1992) ($f_{PS'up}$ = 0.36), (iii) O'Rourke (1968) ($f_{PS'up}$ = 0.338), and (iv) Ristow et al. (2004a) ($f_{PS'up}$ = 0.3345).* 257

Figure 6.2.2a: *The change in the coefficient of variation of the 1st order and specific 1st order hydrolysis equations kinetic constants with changing unbiodegradable particulate COD fraction ($f_{SL'up}$) of MLE 1 WAS, without R_s = 25d (see Table 6.2.2c).* 261

Figure 6.2.2b: *The regression correlation coefficient (R^2) for the Curve Expert program, Lineweaver-Burke (M1), double reciprocal (M2) and Eadie-Hofstee (M3) linearization methods, of Monod hydrolysis kinetics versus unbiodegradable particulate COD fraction ($f_{SL'up}$) of the MLE 1 WAS.* 261

Figure 6.2.2c: *The regression correlation coefficient (R^2) for the Curve Expert program, Lineweaver-Burke (M1), double reciprocal (M2) and Eadie-Hofstee (M3) linearization methods of saturation hydrolysis kinetics versus unbiodegradable particulate COD fraction ($f_{SL'up}$) of the MLE 1 WAS.* 262

Figures 6.2.2d, e, f and g: *Volumetric hydrolysis rates (r_{HYD}, gCOD/ (l.d)) (d), specific volumetric hydrolysis rates (r_{HYD}/Z_{AD}, gCOD/(gCOD.d)) (e), first order kinetic constants (k_h) (f) and specific first order kinetic constants (k_H) (g), all versus sludge age (R_s) from 10, 18, 25, 40 and 60d, for MLE 1 WAS. Equation and correlation coefficient (R^2) given for results without R_s = 25d data.* 264

Figures 6.2.2h, i, j and k: *Hydrolysis kinetics formulation curves plotted using experimental data and calculated from kinetic constants acquired from the three linearization methods, for (h) Monod (see Table 6.2.2d column 7, or Table 6.2.2e; k_m =2.094 and K_s = 0.408) and (i) saturation (see Table 6.2.2f column 6, or Table 6.2.2g; k_M =1.603 and K_S = 5.387) equations and the Curve Expert programme (j) for Monod and (k) for saturation kinetics.* 266

Figures 6.2.2l, m and n: *The linearization of Monod kinetics for hydrolysis of MLE 1 WAS with all five R_s (10 to 60) data using: (l) Lineweaver–Burke (M1), (m) double reciprocal (M2)*

and (n) Eadie–Hofstee (M3). The R^2 values for all 5 R_s data included- dark (black) lines. Numbers refer to column numbers in Table 6.2.2d, e.g. 3 refers to column 3, which lists the average k_m and K_s values obtained from line 3 in Figure 6.2.2l:M1 with 25d R_s data excluded, line 3 in Figure 6.2.1m:M2 with 25d R_s data excluded and line 3 in Figure 6.2.1n:M3 with 25d R_s data excluded, i.e. M1, M2 and M3 (25d off all 3). 268

Figure 6.2.2o: *Comparison of tagret S_{bpe} values (calculated from measured values in Table 6.2.2b) with those predicted by different combinations of selected R_s data from the three linearization methods for the determination of the best k_m and K_s values for modelling MLE 1 WAS hydrolysis with the Monod kinetics. Numbers refer to column numbers in Table 6.2.2d.* 269

Figures 6.2.2p, q and r: *The linearization of saturation kinetics for hydrolysis of MLE 1 WAS at all five R_s (10 to 60) using (p) Lineweaver–Burke (M1), (q) double reciprocal (M2) and (r) Eadie–Hofstee (M3). Regression equations and R^2 values shown for all R_s data included – dark (black) lines. Numbers refer to column numbers in Table 6.2.2f, e.g. 3 refers to column 3, which lists the average k_m and K_s obtained from the line 3 in Figure 6.2.2p:M1 without R_s =25d, line 3 in Figure 6.2.2q: M2 without R_s = 25d and line 3 in Figure 6.2.2r: M3 without R_s = 25d, i.e. M1, M2 and M3 (25d off all 3)*.....272

Figure 6.2.2s: *Comparison of tagret S_{bpe} values (calculated from measured values in Table 6.2.2b) with those predicted by different combinations of selected R_s data from the three linearization methods, for the determination of the best k_M and K_S values for modelling hydrolysis with the saturation kinetics. Numbers refer to column numbers in Table 6.2.2f.* 273

Figure 6.2.3a: *The change in the coefficient of variation of the 1st order and 1st order specific hydrolysis equations kinetic constants with changing unbiodegradable particulate COD fraction ($f_{SL'up}$) of MLE 2 WAS. All data included – see Table 6.2.3c.* 278

Figure 6.2.3b: *The regression correlation coefficient (R^2) for the Curve Expert program, Lineweaver-Burke (M1), double reciprocal (M2) and Eadie-Hofstee (M3) linearization methods of Monod hydrolysis kinetics versus unbiodegradable particulate COD fraction ($f_{SL'up}$) of the MLE 2 WAS.*.....278

Figure 6.2.3c: *The regression correlation coefficient (R^2) for the Curve Expert program, Lineweaver-Burke (M1), double reciprocal (M2) and Eadie-Hofstee (M3) linearization methods of saturation hydrolysis kinetics versus unbiodegradable particulate COD fraction ($f_{SL'up}$) of the MLE 2 WAS.* 279

Figures 6.2.3d, e, f and g: *Volumetric hydrolysis rates (r_{HYD}) (d), specific volumetric hydrolysis rate (r_{HYD}/Z_{AD}) (e), first order kinetic constant (k_h) (f) and specific first order kinetic constant (k_H) (g) versus sludge age (R_s) of 10, 18, 25, 40 to 60 days for AD of MLE 2 WAS. Regression equation and R^2 given for all R_s data included (see Table 6.2.3c)* 281

Figures 6.2.3h, i, j and k: *Hydrolysis kinetics formulation curves plotted using experimental data and calculated from kinetic constants acquired from the three linearization methods for (h) Monod (see Table 6.2.3d column 6, k_m = 2.48 and K_s = 0.63) and (i) saturation equations (see Table 6.2.3f, k_M = 1.524 and K_S = 4.838) and using the Curve Expert programme (j) for Monod and (k) for saturation kinetics.*.....283

Figures 6.2.3j, k and l: *The linearization of Monod kinetics for hydrolysis of MLE 2 WAS with all five R_s (10 to 60) data using the three linearization methods: (j) Lineweaver–Burke (M1), (k) double reciprocal (M2) and (l) Eadie–Hofstee (M3). The R^2 values shown are for all 5 R_s data included- dark (black) lines. Numbers refer to column numbers in Table 6.2.3d, e.g. 4 refers to column 4, which lists the average k_m and K_s values obtained from line 4 in Figure 6.2.3j:M1 with all R_s data included (i.e. follows black line), line 4 in Figure 6.2.1k:M2 with R_s =10d omitted and line 4 in Figure 6.2.1l:M3 with all R_s data included.* 285

Figure 6.2.3o: *Comparison of target S_{bpe} concentrations (calculated from measured values in Table 6.2.3b)with those predicted by different combinations of selected R_s data from the three linearization methods for the determination of the best k_m and K_s values for modelling hydrolysis with the Monod kinetics. Numbers refer to the column numbers in Table 6.2.3d.* 286

Figures 6.2.3p, q and r: *The linearization of saturation kinetics for hydrolysis of MLE 2 WAS at all five R_s (10 to 60) with various methods: (p) Lineweaver–Burke (M1), (q) double reciprocal (M2) and (r) Eadie–Hofstee (M3). Regression equations and lines and R^2 values*

shown for all R_s data included – dark (black) lines. No R_s data were omitted to determine average k_M and K_S values from three linearization methods (Table 6.2.3f). 289

Figure 6.2.3s: *Comparison of measured S_{bpe} concentrations with those predicted by the average k_M and K_S values from the three linearization methods with all R_s data included and the Curve Expert program and experimentally measured to find the best k_M and K_S values for modelling hydrolysis with the saturation kinetics.*.....291

Figure 6.2.3t: *A comparison of the percentage COD removed for the AD of the sludge from the MLE 1 (blue graphs) and MLE 2 (red graphs) ND systems, measured and determined using obtained constants for the various kinetic formulations (1st order, specific 1st order, Monod and saturation).*.....292

Figure 6.2.4a: *The change in the coefficient of variation of the 1st order and 1st order specific hydrolysis equations kinetic constants with changing unbiodegradable particulate COD fraction ($f_{SL'up}$) of NDBEPR WAS, without R_s = 20d and 25d data (see Table 6.2.4c).*.....297

Figure 6.2.4b: *The regression correlation coefficient (R^2) for the Curve Expert program, Lineweaver-Burke (M1), double reciprocal (M2) and Eadie-Hofstee (M3) linearization methods of Monod hydrolysis kinetics versus unbiodegradable particulate COD fraction ($f_{SL'up}$) of the NDBEPR WAS.*.....298

Figure 6.2.4c: *The regression correlation coefficient (R^2), for the Curve Expert program Lineweaver-Burke (M1), double reciprocal (M2) and Eadie-Hofstee (M3) linearization methods of saturation hydrolysis kinetics versus unbiodegradable particulate COD fraction ($f_{SL'up}$) of the NDBEPR WAS.*.....298

Figures 6.2.4d, e, f and g: *Volumetric hydrolysis rates (r_{HYD}) (d), specific volumetric hydrolysis rate (r_{HYD}/Z_{AD}) (e), first order kinetic constant (k_h) (f) and Specific first order kinetic constant (k_H) (g) versus sludge age (R_s) ranging from 10, 12, 18, 20, 25, 40 to 60 days, for AD of NDBEPR WAS. Linear equation and R^2 given for regression without R_s 20 and 25d data (see Table 6.2.4c)*.....301

Figures 6.2.4h, i, j and k: *Hydrolysis kinetics formulation curves, plotted using experimental data and calculated from kinetic constants acquired from the three linearization methods for (h) Monod (see Table 6.2.4d column 8; k_m = 2.46 and K_s = 0.61) and (i)*

saturation (see Table 6.2.4f column 8; k_M = 1.951 and K_S = 9.109) equations and the Curve Expert programme (j) for Monod and (k) saturation kinetics. 303

Figures 6.2.4j, k and l: *The linearization of Monod kinetics for hydrolysis of NDBEPR WAS at all seven R_s (10 to 60) using three linearization methods: (j) Lineweaver–Burke (M1), (k) double reciprocal (M2) and (l) Eadie–Hofstee (M3). The R^2 values for all seven R_s data included - dark (black) lines. Numbers refer to column numbers in Table 6.2.4d, e.g. 5 refers to column 5, which lists the average k_m and K_s values obtained from line 5 in Figure 6.2.4j:M1 with R_s =20, 25, 40 and 60d omitted, line 5 in Figure 6.2.1k:M2 with R_s =20 and 25d omitted and line 5 in Figure 6.2.1l:M3 with R_s =20, 25 and 60d omitted.* 305

Figure 6.2.4o: *Comparison of tagret S_{bpe} values (calculated from measured values in Table 6.2.4b) with those predicted by different combinations of selected R_s data in the three linearization methods for the determination of the best k_m and K_s values for modelling hydrolysis with the Monod kinetics. Numbers refer to column numbers in Table 6.2.4d* 306

Figures 6.2.4p, q and r: *The linearization of saturation kinetics for hydrolysis of NDBEPR WAS at all seven R_s (10 to 60) using various methods in the order of: (p) Lineweaver–Burke (M1), (q) double reciprocal (M2) and (r) Eadie–Hofstee (M3). The R^2 values for all 5 R_s data included- dark (black) lines. Numbers refer to column numbers in Table 6.2.4f, e.g. 2 refers to column 2, which lists the average k_M and K_S values obtained from line 2 in Figure 6.2.4p: M1 with R_s =20 and 25d omitted, line 2 in Figure 6.2.1q: M2 with R_s =20 and 25d omitted and line 5 in Figure 6.2.1r: M3 with R_s =20 and 25d omitted, i.e. 20 and 25d R_s omitted for M1, M2 and M3* 309

Figure 6.2.4s: *Comparison of tagret S_{bpe} values (calculated from measured values in Table 6.2.4b) with those predicted by the average k_M and K_S values obtained from different combinations of selected R_s data in the three linearization methods to find the best k_M and K_S values for modelling hydrolysis with the saturation kinetics. Numbers refer to the column numbers in Table 6.2.4f.* 311

Figure 6.2.4t: *A comparison of the percentage COD removed for the AD of the sludge from the NDBEPR UCT system, measured and determined using obtained constants for the various kinetic formulations (1st order, specific 1st order, Monod and saturation).* 313

Figure 6.2.5a: *The change in the coefficient of variation of the 1st order and 1st order specific hydrolysis equations kinetic constants versus unbiodegradable particulate COD fraction ($f_{SL'up}$) of PS – MLE 1 WAS blend without R_s =25d data (see Table 6.2.5c).*.....317

Figure 6.2.5b: *The regression correlation coefficient (R^2) for the Curve Expert program, Lineweaver-Burke (M1), double reciprocal (M2) and Eadie-Hofstee (M3) linearization methods of the Monod hydrolysis kinetics versus unbiodegradable particulate COD fraction ($f_{SL'up}$) of the PS – MLE 1 WAS blend AD including all (10, 18, 25, 40 and 60 day R_s) data.* 317

Figure 6.2.5c: *The regression correlation coefficient (R^2) for the Curve Expert program, Lineweaver-Burke (M1), double reciprocal (M2) and Eadie-Hofstee (M3) linearization methods of the saturation hydrolysis kinetics versus unbiodegradable particulate COD fraction ($f_{SL'up}$) of the PS – MLE 1 WAS blend AD including all (10, 18, 25, 40 and 60 day R_s) data.*.....318

Figures 6.2.5d, e, f and g: *Volumetric hydrolysis rates (r_{HYD}) (d), specific volumetric hydrolysis rate (r_{HYD}/Z_{AD}) (e), first order kinetic constant (k_h) (f) and specific first order kinetic constant (k_H) (g) versus sludge age (R_s) ranging from 10, 18, 25, 40 and 60 days, for AD of PS-WAS blend. Linear Equation and correlation coefficient (R^2) is given for results without R_s = 40d data* 320

Figures 6.2.5h i, j and k: *Hydrolysis kinetics formulation curves, plotted using experimental data and calculated from kinetic constants acquired from the three linearization methods, for (h) Monod (see Table 6.2.5d column 7 and Table 6.2.5e; k_m =5.153 and K_s =1.710) and (i) saturation (see Table 6.2.5d column 7 and Table 6.2.5e; k_M = 1.915 and K_S =7.723) equations and using the Curve Expert programme (j) for Monod and (k) for saturation kinetics*.....322

Figures 6.2.5l, m and n: *The linearization of Monod kinetics for hydrolysis of PS – MLE 1 WAS with all five R_s data (10 to 60) for: (j) Lineweaver–Burke (M1), (k) double reciprocal (M2) and (l) Eadie–Hofstee (M3). The R^2 values are for all 5 R_s data included - dark (black) lines. Numbers refer to column numbers in Table 6.2.5d, e.g. 3 refers to column 3, which lists the average k_m and K_s values obtained from line 3 in Figure 6.2.5l: M1 with R_s = 40d omitted,*

line 3 in Figure 6.2.1m:M2 with all R_s data and line 3 in Figure 6.2.1n:M3 with R_s = 40d omitted 324

Figure 6.2.5o: *Comparison of tagret S_{bpe} values (calculated from measured values in Table 6.2.5b) with those predicted by different combinations of selected R_s data in the three linearization methods for the determination of the best k_m and K_s values for modelling hydrolysis with the Monod kinetics. Numbers refer to column numbers in Table 6.2.5d.* ...325

Figures 6.2.5p, q and r: *The linearization of saturation kinetics for hydrolysis of PS – MLE 1 WAS at all five R_s (10 to 60) using various methods in the order of: (p) Lineweaver–Burke (M1), (q) double reciprocal (M2) and (r) Eadie–Hofstee (M3). The R^2 values for all 5 R_s data included- dark (black) lines. Numbers refer to column numbers in Table 6.2.5f, e.g. 4 refers to column 4, which lists the average k_M and K_S values obtained from line 4 in Figure 6.2.5p: M1 with R_s = 40 and 60d omitted, line 4 in Figure 6.2.1q:M2 with all R_s data and line 4 in Figure 6.2.1r: M3 with R_s = 40d omitted.* 327

Figure 6.2.5s: *Comparison of tagret S_{bpe} values (calculated from measured values in Table 6.2.1b) with those predicted by the average k_M and K_S constants determined with different combinations of selected R_s data in the three linearization methods for the determination of the best k_M and K_S values for modelling hydrolysis of PS-WAS blend with the saturation kinetics. Numbers refer to the column numbers in Table 6.2.5f*.....329

Figure 6.2.6a: *Specific hydrolysis rate (r_{HYD}/Z_{AD}) versus biodegradable particulate organics (S_{bp}) for the five different sludge types.*.....332

Figure 6.2.6b: *The percentage biodegradable COD removed, calculated from measured results, with increasing sludge age (R_s) for the different sludge types.*.....333

Figures 6.2.6c - i to vi: *A comparison of the percentage COD removed for the AD of the different sludge types (i-MLE 1 WAS, ii- MLE 2 WAS, iii- NDBEPR WAS, iv- PS alone, v.- PS-WAS blended using the kinetic constants determined in Section 6.2.5, vi.- PS & WAS, where PS and MLE 1 WAS are given separate kinetic constants for hydrolysis of the blend) measured and determined using obtained constants for the various kinetic formulations (1^{st} order, specific 1^{st} order, Monod and saturation).*.....334

Figures 6.5.1a to d: *Comparison between the steady state model predicted results and experimentally measured data for the AD of NDBEPR WAS, in the order of: (a) COD removal, (b) FSA released, (c) OP released and (d) H_2CO_3* alkalinity.*.....363

Figures 6.5.1e to h: *Comparison between the steady state model predicted results and experimentally measured data for the AD of NDBEPR WAS, in the order of: (e) pH, (f) gas composition, (g) Struvite precipitated and (h) H_3PO_4 alkalinity.* 364

Figures 6.5.1i: *Comparison between the steady state model input Mg feed concentration value and experimentally measured influent and effluent Mg concentration for NDBEPR WAS AD.*.....365

Figure 7.4.1: *Configuration settings for the simulation of the Nitrification-Denitrification Biological Excess Phosphorus removal (NDBEPR) system with the ASM2-3P model.*.....415

Figure 7.4.2: *Configuration settings for the simulation of the Modified Ludzack Ettinger (MLE) AS system with the ASM2-3P model.*.....415

Figure 7.4.3: *Configuration settings for the simulation of the (a) aerobic digestion (AerD) and (b) anoxic-aerobic (AnAerD) digestion system with the ASM2-3P model.*.....416

Figures 7.4.4a to h: *A comparison between the results simulated by the ASM2-3P dynamic model and measured data per sewage batch test period for the NDBEPR AS system: (a) COD removal,(b) phosphorus removal, (c) biomass generated, (d) nitrates generated (aerobically) and removed (anoxically,) (e) oxygen utilization rates, (f) nitrogen removal, (g) total and volatile settleable solids concentrations and (h) Inorganic settleable solids concentration.*..425

Figures 7.4.5 a to f: *A comparison between the results simulated by the ASM2-3P dynamic model, the ASM1 model and measured data for 5 sewage batches (1-5) for the MLE 2 AS system: (a) COD removal, (b) phosphorus removal, (c) volatile settleable solids concentration, (d) nitrates generated (aerobically) and removed (anoxically), (e) oxygen utilization rate and (f) nitrogen removal.* 433

Figure 7.4.5g: *A comparison between the biomass generation results simulated by the ASM2-3P dynamic model, the ASM1 model and those detemined from the steady state model calculations for 5 sewage batches (1-5) for the MLE 2 AS system.*.....433

Figures 7.4.6a to d: *A comparison between the results simulated by the ASM2-3P dynamic model and measured data for 5 sewage batches (R_s) for the MLE 1 AS system in the order of: (a) COD removal, (b) phosphorus removal, (c) biomass generated and (d) nitrates generated (aerobically) and removed (anoxically).* 435

Figures 7.4.6a to h: *A comparison between the results simulated by the ASM2-3P dynamic model and measured data for 5 sewage batches (R_s) for the MLE 1 AS system in the order of: (e) oxygen utilization rates, (f) nitrogen removal, (g) total and volatile settleable solids concentration and (h) inorganic settleable solids concentration.* 436

Figure 7.5.1: *Process scheme for the ADM-3P model, as extended from the UCTADM1 model of Sötemann et al. (2005). Note that (1) ammonia is released in the NH_3 form and picks up a proton from H_2CO_3 to form NH_4^+, (2) Process 2 is for PP release with the uptake of acetate and (3) process 5 is for the PP hydrolysis with the death of the PAOs, (4) ER stands for the endogenous residue of biomass. Process 12 only shows for P precipitates, but other precipitates (i.e. newberyite, calcite and magnesite, which are less likely to form) are also included in the model.*.....445

Figures 7.5.2a to f: *Comparison between the results simulated by the three phase AD dynamic model and measured data versus sludge age (R_s) for the AD of NDBEPR WAS in the order of: (a) COD removal, (b) $H_2CO_3^*$ alkalinity, (c) total nitrogen released as free and saline ammonia (FSA), (d) digester pH, (e) phosphorus released as ortho-phosphate and (f) gas composition.*.....452

Figures 7.5.3a and b: *Comparison between experimentally measured and simulated results for a batch AD fed P rich WAS from Biological Excess P Removal (BEPR) Activated Sludge (AS) system blended with mixed liquor from the continous AD system treating BEPR waste AS in 50:50 ratio in the order of: (a) COD concentration and (b) settleable solids concentration.* 457

Figures 7.5.3c to e: *Comparison between experimentally measured and simulated results for a batch AD fed P rich WAS from Biological Excess P Removal (BEPR) Activated Sludge (AS) system blended with mixed liquor from the continous AD system treating BEPR waste*

AS in 50:50 ratio in the order of: (c) H_2CO_3 alkalinity, (d) pH and (e) ortho-phosphate released.* 458

Figures 7.5.4a to f: *Comparison between the results simulated by the three phase AD dynamic model, calculated by the three phase AD steady state model and measured data versus digester sludge age (R_s) for the AD of MLE 1 WAS in the order of: (a) COD removal, (b) digester H_2CO_3* alkalinity, (c) total nitrogen released as free and saline ammonia (FSA), (d) digester pH, (e) phosphorus released as ortho-phosphate and (f) gas composition.* 461

Figures 7.5.5a to f: *Comparison between the results simulated by the three phase AD dynamic model, calculated with the three phase AD steady state model and measured data versus digester sludge age (R_s) for the AD of MLE 2 WAS in the order of: (a) COD removal, (b) digester H_2CO_3* alkalinity, (c) total nitrogen released as free and saline ammonia (FSA), (d) digester pH, (e) phosphorus released as ortho-phosphate and (f) gas composition.* 464

Figures 7.5.6a to e: *Comparison between the results simulated by the ADM-3P and the validated UCTADM1 model of Sötemann et al. (2006) with measured data by Izzett et al. (1992) versus digester sludge age (R_s) for the AD of a primary and humus sludge mixture in the order of: (a) COD removal, (b) digester $H_2CO_3^*$ alkalinity, (c) total nitrogen released as free and saline ammonia (FSA), (d) digester pH and (e) gas composition.* 470

Figures 7.5.7a to e: *Comparison between the results simulated by UCTADM1 and ADM-3P and measured data versus digester sludge age (R_s) for the AD of PS in the order of: (a) COD removal, (b) digester H_2CO_3* alkalinity, (c) total nitrogen released as free and saline ammonia (FSA), (d) digester pH, (e) phosphorus released as ortho-phosphate and (f) gas composition.* 473

Figures 7.5.8 (i)a to f: *Comparison between the results simulated by the three phase AD dynamic model, calculated by the three phase AD steady state model and measured data versus AD sludge age (R_s) for the AD of PS-MLE 1 WAS in the order of: (a) COD removal, (b) digester H_2CO_3* alkalinity, (c) total nitrogen released as free and saline ammonia (FSA), (d) digester pH, (e) phosphorus released as ortho-phosphate and (f) gas composition.* 477

Figures 7.5.8 (ii)a to f: *Comparison between the results simulated by the three phase AD dynamic model, and the measured data versus AD sludge age (R_s) for the AD of PS-MLE 1*

WAS, using separate hydrolysis kinetics for PS and MLE 1 WAS: (a) COD removal, (b) digester H_2CO_3 alkalinity, (c) total nitrogen released as free and saline ammonia (FSA), (d) digester pH, (e) phosphorus released as ortho-phosphate and (f) gas composition.*.....481

Figures 7.5.9a to d: *Sensitivity analysis plot windows for struvite precipitation in AD of NDBEPR WAS showing (a) the reference simulation of struvite precipitated, and the relative sensitivity of struvite with change in parameter c_PP (Figure b), parameter A_o (Figure c) and parameter B_o (Figure d)*.....485

Figures 7.5.10 a to f: *Sensitivity analysis plot windows for carbon dioxide partial pressure (p_{CO2}) in AD of NDBEPR WAS showing (a) the reference simulation of p_{CO2}, and the relative sensitivity of p_{CO2} with change in parameter Mg_PlP (Figure b), parameter y_o (Figure c), parameter z_o (Figure d) parameter a_o (Figure e), parameter b_o (Figure f).* 487

Figures 7.5.11a to f: *Sensitivity analysis plot windows for carbon dioxide partial pressure (p_{CO2}) in AD of NDBEPR WAS showing (a) the reference simulation of p_{CO2}, and the relative sensitivity of p_{CO2} with change in parameter Mg_PlP (Figure b), parameter y_o (Figure c), parameter z_o (Figure d) parameter a_o (Figure e), parameter b_o (Figure f).* 490

Figures 7.5.12a to c: *Simulated AD failure exhibited by plot windows of (a) methane production, (b) digester pH and (c) digester total alkalinity.* 496

Figures 7.5.13a to c: *Simulated temporary AD failure exhibited by plot windows of (a) methane production, (b) digester pH and (c) digester total alkalinity.* 497

Figures 7.6.1a and b: *A comparison between the results simulated by the ASM2-3P dynamic model (with the precipitation process off) and those simulated by Mebrahtu (2007) with ASM2 (single phase) in Aquasim for the batch test 3 AerD system in the order of: (a) volatile settleable solids and (b) digester COD.*.....504

Figures 7.6.1c to f*: A comparison between the results simulated by the ASM2-3P dynamic model (with the precipitation process off) and those simulated by Mebrahtu (2007) with ASM2 (single phase) in Aquasim for the batch test 3 AerD system in the order of: (c) nitrogen releases, (d) phosphorus releases, (e) oxygen utilisation rates and (f) nitrates concentration.* 505

Figure 7.6.1g*: A comparison between the inorganic settleable solids concentration results simulated by the ASM2-3P dynamic model (with the precipitation process off) and those simulated by Mebrahtu (2007) with ASM2 (single phase) in Aquasim for the batch test 3 AerD.* 506

Figures 7.6.2a and b*: A comparison between the results simulated by the ASM2-3P dynamic model and measured data per sludge age (R_s) for the batch eight AerD system of Mebrahtu et al. (2007), in the order of: (a) volatile settleable solids concentrations and (b) COD concentration.* 507

Figures 7.6.2c to f*: A comparison between the results simulated by the ASM2-3P dynamic model and measured data per sludge age (R_s) for the batch eight AerD system of Mebrahtu et al. (2007) in the order of: (c) Nitrates concentration, (d) Nitrogen releases, (e) Phosphorus releases and (f) Inorganic settleable solids concentration.* 508

Figure 7.6.2g*: magnesium concentration results simulated by the ASM2-3P dynamic model per sludge age (R_s) for the batch eight AerD of Mebrahtu et al. (2007).* 509

Figures 7.6.3a and d: *A comparison between the results simulated by the ASM2-3P dynamic model and measured data for BT 1: (a) volatile settleable solids concentrations, (b) unfiltered COD concentration, (c) FSA released and (d) phosphorus releases,* 510

Figures 7.6.3e and f: *A comparison between the results simulated by the ASM2-3P dynamic model and measured data for BT 1: (e) inorganic settleable solids concentration and (f) simulated magnesium concentration.* 511

Figures 7.6.4a to d: *A comparison between the results simulated by the ASM2-3P dynamic model and measured data per sludge age (R_s) for the batch three AerD system in the order of: (a) Digester pH, (b) volatile solids concentrations, (c) COD concentration and (d) nitrates concentration.* 513

Figures 7.6.4e and f: *A comparison between the results simulated by the ASM2-3P dynamic model and measured data per sludge age (R_s) for the batch three AerD system in the order of: (e) TKN and FSA and (f) ortho-phosphate concentration.* 514

Figures 7.6.4g to i: *A comparison between the results simulated by the ASM2-3P dynamic model and measured data per sludge age (R_s) for the batch three AerD system in the order of:*

(g) magnesium (Mg) concentration, (h) inorganic settleable solids concentration and (i) simulated struvite concentration. 515

Figures 7.6.5a to c: *A comparison between the results simulated by the ASM2-3P dynamic model and measured data per sludge age (R_s) for the batch seven AerD system of Mebrahtu et al. (2007) in the order of: (a) volatile solids concentrations, (b) COD concentration and (c) nitrates concentration.* 517

Figures 7.6.5d to f: *A comparison between the results simulated by the ASM2-3P dynamic model and measured data per sludge age (R_s) for the batch seven AerD system of Mebrahtu et al. (2007) in the order of: (d) nitrogen releases, (e) phosphorus releases and (f) inorganic settleable solids concentration.* 518

Figures 7.6.5 g and h: *Results simulated by the ASM2-3P dynamic model per sludge age (R_s) for the batch seven AerD system of Mebrahtu et al. (2007) in the order of: (g) magnesium concentration and (h) struvite concentration.* 519

Figures 7.6.6 (i) a and b: *A comparison between the results simulated by the ASM2-3P dynamic model and measured data per sludge age (R_s) for the NDBEPR AS parent system to Vogts (2011) anoxic-aerobic digetster in the order of: (a) COD concentration and (b) Phosphorus removal.* 523

Figures 7.6.6 (i) c to f: *A comparison between the results simulated by the ASM2-3P dynamic model and measured data per test period for the NDBEPR AS parent system to Vogts (2011) anoxic-aerobic digetster in the order of: (c) Total and volatile solids concentrations, (d) nitrates generated and removed (e) Oxygen utilization rates and (f) Nitrogen removed.* 524

Figures 7.6.6 (ii) a to d: *A comparison between the results simulated by the ASM2-3P dynamic model and measured data per test period for the concentrated anoxic-aerobic digester of Vogts (2011) in the order of: (a) COD concentration, (b) Total and volatile solids concentrations (c) Nitrogen removal and (d) Phosphorus releases.* 525

Figures 7.6.6 (ii) e to h: *A comparison between the results simulated by the ASM2-3P dynamic model and measured data per test period for the concentrated anoxic-aerobic digester*

of Vogts (2011) in the order of: (e) pH, (f) H_2CO_3 alkalinity, (g) Oxygen utilization rates and (h) metals measured in solution.*.....526

Figure 7.7.1e and f: *Results from the application of the plant-wide ASM2-3P - ADM-3P model for simulating the NDBEPR system linked to AD, showing plot windows of (e) digester H_2CO_3* Alkalinity and (f) digester pH.* 533

Figures 7.7.2 a to d: *Results from the application of the plant-wide model in simulating the NDBEPR system linked to AD, showing scenario analysi plot windows of AD (a) Polyphosphate production in AS system, (b) struvite precipitated in AD, (c) AS efluent COD and (d) methane generated in AD.* 539

Figure A5.1: *Plant configuration 1* 626

Figure A5.2: *Plant configuration 2* 626

Figure A5.3: *Plant configuration 3* 627

SYNOPSIS

THE DEVELOPMENT OF A THREE PHASE PLANT-WIDE MATHEMATICAL MODEL FOR SEWAGE TREATMENT

Municipal wastewater usually contains a large quantity of nitrogen (N) and phosphorus (P), which if not removed is one of the main causes of eutrophication that negatively affects natural water bodies by excessive algae and plant growth. In general, phosphorus is removed in biological nutrient removal (BNR) wastewater treatment plants (WWTPs) through the use alternating anaerobic and aerobic conditions, which stimulate the growth of phosphorus accumulating organisms (PAOs) that mediate biological excess P removal (BEPR) in activated sludge systems. There is a need to find the most cost effective methods for the design and operation of WWTPs to minimize energy consumption and cost while maximizing nutrient recovery and effluent quality.

This required research into design procedures that were based on the behavioural patterns of microorganisms mediating the N and P removal processes of the WWTP. This research led to the development of a number of activated sludge kinetic theories and dynamic mathematical models, which were coded into computer simulation programmes. Also, simpler steady state models that use explicit algebraic equations, were deveoped to complement the dynamic models by allowing the WWTPs to be sized and/or wastewater characteristics to be determined before performing simulations, thereby obviating the inefficient trial and error use of dynamic models.

Previous steady state and dynamic simulation models concentrated mainly on the activated sludge (AS) unit operation because it is from this part of the WWTP that the effluent is produced. However, the mutual interaction between all the connected unit operations of the WWTP has recently triggered research interest in the development of mass balance based plant-wide WWTP models, which model all the unit operations of the WWTP together, linked with their connecting flows.

An integrated steady state model for the whole WWTP comprising nitrification-denitrification (ND) AS, anaerobic digestion (AD) of primary sludge (PS) and anoxic-aerobic digestion of waste activated sludge (WAS) was developed by Sötemann *et al.* (2006) and Ekama (2009) by coupling of the various existing WWTP individual unit operation steady state models. This model is being extended and modified as new information is added to it. Extending this plant-wide steady state model by adding P and inorganic settleable solid (ISS) with anoxic-aerobic and/or anaerobic digestion of the P-rich WAS is one of the objectives in this investigation.

The PAOs introduce several complex issues, which required investigation. For instance, the PAOs have a lower endogenous respiration rate compared with ordinary heterotrophic organisms (OHOs) and this affects the N and P nutrient releases in aerobic and anaerobic digestion (Sötemann *et al.*, 2006). Also, the release of P from polyphosphate (PP) could stimulate mineral precipitation in both aerobic or anaerobic digestion so three phase (aqueous-gas-solid) mixed weak acid/base chemistry needs to be considered.

PROJECT OBJECTIVES

The general project goal is to develop three phase (aqueous-gas-solid) steady state and dynamic mathematical models for the anaerobic and aerobic digestion of WWTP sludge, including waste activated sludge (WAS) produced by NDEPR plants, in a plant-wide setting. To accomplish this goal the following four objectives were established:

1. Carry out an experimental investigation to generate the data required for both steady state and dynamic model development: The experimental set up was large, to mimic three real WWTP types at laboratory scale, as shown in Figure S-1 below.
2. Develop a steady state AD model including P: From the experimental data of the ADs operated at five different sludge ages, the hydrolysis kinetics of PS, ND AS system waste activated sludge (WAS) and NDBEPR AS system WAS

are to be determined and included to the stoichiometric AD model that was developed by Harding (2009) . Since it was noted that mineral precipitation takes place in the AD of NDBEPR WAS containing PAOs, the steady state mixed weak acid/base chemistry part of the AD model needs extension to include three phases (aqueous-gas-solid).

3. Develop a plant-wide dynamic model that includes P from NDBEPR WAS: A dynamic AD model has previously been developed by Sötemann *et al.* (2005b) but this model was (i) two phase (aqueous-gas), (ii) applied for only a PS and ND system WAS and (iii) included only one biodegradable particulate organic (BPO) for PS or WAS digestion. Therefore the planned AD dynamic model is to include three phase (aqueous-gas-solid) mixed weak acid/base chemistry to include mineral precipitation and multiple organic types for anaerobic digestion to facilitate AD of primary sludge (PS) together with WAS within the plant-wide framework. Due to the significant increase in size and complexity to model the WWTP as a whole, the NDBEPR activated sludge system and the tertiary treatment processes of AD and aerobic digestion (AerD), both fed NDBEPR WAS required coding in WEST®, which is a program capable of simulating many bioprocesses in various unit operations assembled into a WWTP.
4. Develop a three phase AS dynamic model by extending an existing BEPR AS model, such as activated sludge model number 2 (ASM2; Henze *et al.*, 1995) and ensuring its compatibility with the AD dynamic model mentioned in objective 3 for the plant-wide model development. In addition, this three phase AS model with BEPR is to be extended to plant-wide simulation of BEPR AS with anoxic-aerobic digestion of P-rich WAS with mineral precipitation to produce concentrated dewatering liquor with low N and P.

The new knowledge contributed by this research is directly tied to the research objectives, which include:

1. The development of a three phase plant-wide model that includes phosphorous. This involves:
    - The development of the mixed weak acid/base chemistry part of the steady state AD model to include mineral (struvite) precipitation and digester pH prediction.
    - The development of a three phase dynamic model that includes phosphorus and mineral precipitation processes in aerobic (and/or anoxic-aerobic) and anaerobic digestion of concentrated WAS.
2. Investigating the biodegradability of organics within the WWTP, including:
    - The determination of organics biodegradability within the different unit operations of the WWTP, including primary settling tank (PST), AD and AS systems.
    - The comparison of the influent unbiodegradable particulate organic (UPO) fraction calculated from the ND AS system and NDBEPR AS system, treating the same settled wastewater and AD of the WAS from these systems.
3. Inclusion of the hydrolysis of multiple organic types in the plant-wide model, for the treatment of municipal sewage.

MATERIALS AND METHODS

The experimental layout to accomplish this research project replicates at laboratory scale three full scale wastewater treatment plant (WWTP) schemes, comprising (1) a Modified Ludzack – Ettinger (MLE) nitrogen (N) removal (ND) activated sludge (AS) system treating settled wastewater (WW) with the separate AD of PS, WAS and PS-WAS blends, (2) a MLE N removal AS system treating raw WW with AD of its WAS and (3) a University of Cape Town (UCT) N or P removal system treating settled WW with the AD of its WAS. All three AS systems were fed the same wastewater collected from the Mitchells Plain (MP) WWTP, in Cape Town. To ensure a consistent composition of the raw and settled watewater, measured masses

of macerated PS collected from the Athlone WWTP (in Cape Town) were added to the collected MP (settled) WW. Hence in this experimental programme, raw WW is MPs settled WW with added Athlone PS, and settled WW is MP settled WW only. In order to increase the biological excess P removal (BEPR) in the UCT system 200 mg/*l* of acetate was dosed to its settled wastewater feed.

EXPERIMENTAL SET UP

A diagrammatic representation of the experimental layout is shown in Figure S.1.

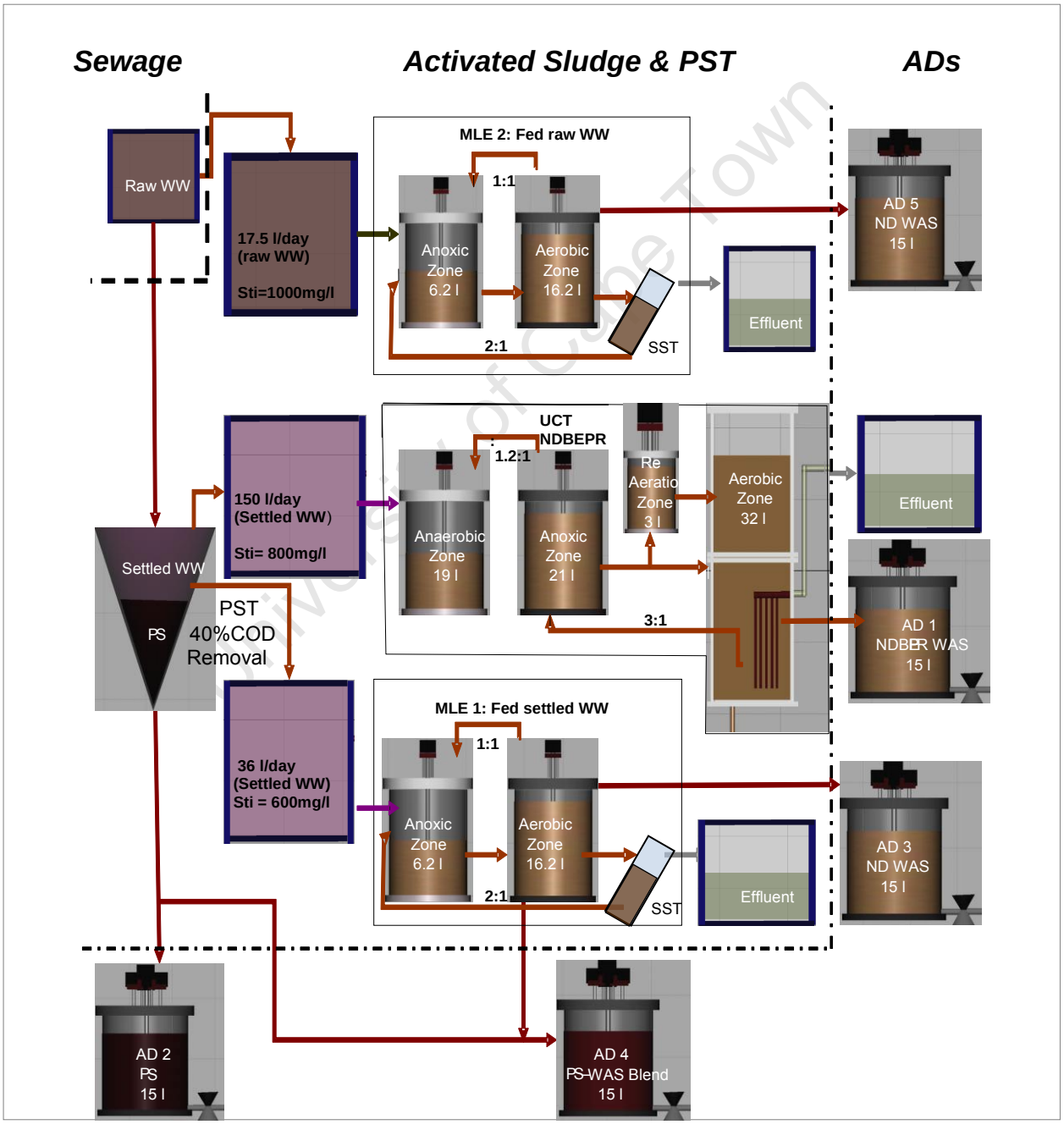

Figure S.1: *Experimental set-up*

Raw WW (18 *l*/d) was fed to one of the MLE systems (MLE 2) and settled WW to the UCT NDBEPR (150 *l*/d) and the other MLE system (MLE 1, fed at 36 *l*/d). The sludge age of all three AS systems was 10 days established by hydraulic control. The PS added to the collected WW to make the raw WW and the WAS from the three AS systems were fed to five completely mixed flow-through ADs: (1) UCT NDBEPR system WAS, (2) PS only, (3) settled WW MLE system (MLE 1) WAS, (4) MLE 1 WAS and PS blend and (5) raw WW MLE system (MLE 2) WAS.

Each digester was operated at five different sludge ages, i.e. 10, 18, 25, 40 and 60 days. The short sludge ages are useful to determine the hydrolysis rate of the different sludges and the very long 60-day sludge age is useful to determine the unbiodegradable fraction of the sludges, as recommeded by Sötemann *et al.* (2005). For the short and long sludge ages, once the time period of three sludge ages had elapsed, testing of the ADs commenced and continued for a period of about two weeks. The lab scale AS and AD systems, were operated over a two-year experimental period. The AS systems were also tested during this AD test period, because the source feed PS and WAS fed to the ADs was taken from them. During the periods when the systems were not intensively tested, random tests were performed on the AS and AD systems to check steady state conditions.

The results obtained in the experimental investigation were sufficiently reliable to provide data for (1) the development of a steady state model for the AD of PS, ND and NDBEPR WAS including P, (2) determination of the hydrolysis kinetic rates of the PS and WAS from the three AS systems and the PS-WAS blend and (3) experimental determination of whether or not the unbiodegradable particulate organics (UPO) from the influent wastewater and the unbiodegradable endogenous residue produced by the OHO and PAO biomass in the AS system, remain unbiodegradable under anaerobic digester conditions. If the similar unbiodegradable fractions are obtained from the AS and AD systems, this would

validate that unbiodegradable organics, as defined by the (aerobic) AS system remain unbiodegradable in the (anaerobic) AD system.

STEADY STATE KINETIC MODEL DEVELOPMENT

A steady state model for the anaerobic digestion (AD) of primary and secondary sludge from NDBEPR plants treating municipal wastewater was developed by modifying the existing steady state AD model for primary sludge of Sötemann *et al.* (2005). This involved adding:

1. Phosphorus (P), both organically bound P (OrgP) and polyphosphate (PP) in phosphorus accumulating organisms (PAOs), into the stoichiometry, taking due consideration of the pK ($-\log_{10}$ of the weak acid dissociation constant, K) value near 7 of the ortho-phosphate weak acid system.
2. The hydrolysis of WAS from ND and NDBEPR systems in the AD model.
3. Anaerobic digestion of primary sludge (PS) and WAS blends.
4. Mineral precipitation, in particular struvite, which involves three phase (liquid-gas-solid) mixed weak acid/base chemistry of the inorganic carbon (IC) and ortho-phosphate (OP) systems.

This will extend the steady state AD model to be able to deal with all the main types of municipal sludge thereby extending the plant-wide WWTP steady state model of Ekama (2009) to:

1. Predict the release of N and P in AD of PS and WAS from ND or NDBEPR activated sludge (AS) systems.
2. Optimizing plant operation procedures to minimize effluent N and P concentrations.
3. Tracking the various compounds and elements- mainly carbon (C), hydrogen (H), oxygen (O), N, P, magnesium (Mg), potassium (K) and calcium (Ca) - through the unit operations of the WWTP and identifying areas where mineral precipitation problems can occur.

In the steady state and dynamic AD models of Sötemann *et al.* (2005a,b) the hydrolysis of particulate biodegradable organics (BPO) was modified to include the three different organic materials (proteins, carbohydrates and lipids) of the International Water Association (IWA) anaerobic digestion model number 1 (ADM1, Batstone *et al.*, 2002) to a single hydrolysis process acting on a generic biodegradable particulate organic (BPO) representing sewage sludge, i.e. $C_XH_YO_ZN_A$. With complex organics like in WWTP sludges, the hydrolysis process is the rate-limiting step so that the AD processes that follow it, being much faster, can be dealt with stoichiometrically in steady state AD models to yield directly the digester end products, i.e. biomass, methane (CH_4), carbon dioxide (dissolved HCO_3^- and gaseous CO_2), ammonia (NH_4^+) and water. Thus, the extended steady state (SS) model also comprises three sequential parts:

1. A chemical oxygen demand (COD) based hydrolysis kinetic part from which the concentration of biodegradable COD utilized and methane and sludge production are determined for a given AD sludge age (R_s, which is also equal to hydraulic retention time for flow through ADs).
2. A COD, C, H, O, N, P and charge mass balance stoichiometry part from which gas production and composition (or partial pressure of CO_2), NH_4^+ released, biomass produced and alkalinity generated (HCO_3^-, $H_2PO_4^-$ and HPO_4^{2-}) are calculated from the biodegradable COD removal.
3. A three phase mixed inorganic carbon (IC) and ortho-phosphate (OP) weak acid/base chemistry part from which the digester pH and mineral precipitation is calculated.

AD KINETICS OF SLUDGE HYDROLYSIS

Like Sötemann *et al.* (2005), in this investigation four kinetic equations were proposed to model hydrolysis/acidogenesis in the breakdown of biodegradable particulate organics in AD. These are (1) First order with respect to the residual biodegradable particulate COD concentration (S_{bp}), (2) First order specific with

respect to S_{bp} and the acidogenic biomass concentration (Z_{AD}), (3) Monod kinetics and (4) Saturation kinetics. In order to use these kinetic formulations, the hydrolysis kinetic rate constants (k_h, k_H, k_m, K_s, k_M and K_S) in ADs fed the different sludges were determined. For this, the most useful data was that from the short sludge age ADs while long sludge age AD data was useful to determine the unbiodegradable particulate COD fraction ($f_{SL'up}$) of the different sludges.

The Monod and saturation kinetic constants, calibrated into the measured experimental AD data for the PS and WAS types are listed in Table S.1.

It was observed that the 1st order (k_h) and specific first order (k_H) hydrolysis rates of the different sludge types do not have a consistent relationship with AD sludge age and so are not the best to model the AD over a range of sludge ages. However, the Monod or saturation kinetics, obtained using selected sludge age data for improved correlation, can be used over the range of all sludge ages.

The different sludge types (PS, MLE 1 WAS, MLE 2 WAS, NDBEPR WAS and the PS-MLE 1 WAS blend) did not hydrolyse at the same rate. Although each sludge type has a unique hydrolysis rate Figure S.2 shows that the measured percentage biodegradable COD removed with sludge age for each of the sludges does not exhibit a very large difference between the PS and WAS. Therefore, anaerobic digestion of waste activated sludge (WAS) together with primary sludge (PS) does not have a significant impact on the hydrolysis rate of WAS compared with anaerobically digesting the WAS by itself.

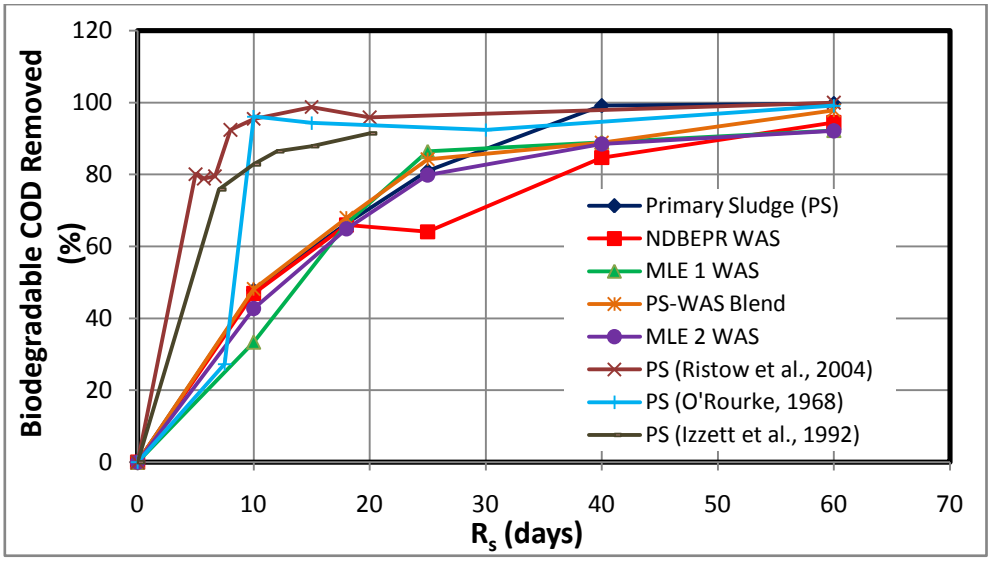

Figure S.2: *The percentage biodegradable COD removed, calculated from measured results with increasing sludge age (R_s) for the different sludge type.*

Table S.1: Unbiodegradable Particulate Organic (UPO) Fractions and Hydrolysis Kinetic Determined by the Different Methods in the Experimental Investigation									
Parameter		PS Author	WAS MLE 1	WAS MLE 2	WAS NDBEPR	PS -WAS PS + MLE 1	PS[1] Izzett	PS[2] O'Rourke	PS[3] Ristow
UPO value	Hydrolysis Kinetics Value	0.31	0.47	0.62	0.54	0.37	0.36	0.34	0.34
	60-day AD value	0.31	0.53	0.66	0.58	0.40			
	AS performance Value	0.30	0.47	0.62	0.53	0.36			
Hydrolysis kinetic rates	1st Order k_h								
	mk_h	0.013	0.003	0.003	0.033	0.015	0.0065	0.398	23205
	ck_h	-0.077	0.041	0.070	0.004	-0.165	0.432	1.030	-221130
	R^2	0.924	0.842	0.820	0.895	0.981	0.780	0.762	0.922
	Specific 1st order k_H								
	mk_H	0.372	0.096	0.092	0.216	0.430	0.007	0.2042	139.79
	ck_H	-0.303	0.970	1.147	0.131	-4.331	0.228	-1.5004	-1332.12
	R^2	0.852	0.974	0.980	0.872	0.956	0.780	0.874	0.922
	Monod								
	k_m	4.300	2.094	2.482	2.465	5.153	3.340	2.004	0.243
	k_s	1.523	0.408	0.626	0.607	1.710	6.760	0.355	640
	R^2	0.930	0.963	0.948	0.826	0.960	0.900	0.429	-
	Saturation								
	k_M	1.796	1.603	1.524	1.951	1.919	5.270	2.047	11.2
	k_S	7.962	5.387	4.838	9.109	7.723	7.980	0.263	13.0
	R^2	0.942	0.951	0.951	0.919	0.970	0.900	0.428	-

STOICHIOMETRIC MODEL FOR AD OF NDBEPR WAS

Sötemann *et al.* (2005a) developed a two phase (aqueous-gas) steady state model to describe the anaerobic digestion of organics, based on C, H, O, N and COD mass balanced stoichiometry developed with the method described by McCarty (1975). In the extension of this stoichiometric model, Harding (2009) added biomass P and polyphosphate (PP), with its associated Mg, K and Ca, into this mass balance stoichiometry. The complexities of including P into the mass balanced stoichiometry of the different WWTP unit operations were considered to hinge around (1) the different rates at which PP and

organically bound P are released in anoxic/aerobic and anaerobic digestion, (2) the effect of the 2nd dissociation constant of the OP weak acid/base system (pK_{p2}~7), and (3) the precipitation of metal phosphates resulting from the high metal (Mg^{2+}, K^{+}, Ca^{2+}) content which is also released with the OP in aerobic and anaerobic digestion (Harding *et al.*, 2011).

Harding (2009) noted that at AD sludge ages of five days or longer, only a part of the biodegradable organics of the NDBEPR WAS biomass was degraded but all of the PP in the PAOs was released. Also, the way in which PP is released affects the weak acid/base chemistry of the AD system.

In the anaerobic reactor of the NDBEPR system, PAOs take up short chain fatty acids and convert them to poly-3-hydoxyalkanoates (PHA), which are energy storage compounds that can be broken down aerobically by the PAOs to carry out their growth and respiration metabolism. In the dynamic AD model, PAOs fed to the AD, once entering the environment are deemed capable of carrying out the same P-release mechanisms as in the anaerobic reactor of the NDBEPR AS system. However, the PAOs cannot compete with the anaerobic bacteria because they require aerobic conditions to supply a terminal electron acceptor (oxygen) for their growth on the PHA and respiration. Therefore, the PAOs eventually die at a rate much faster than the hydrolysis of their biomass, releasing all remaining PP and PHA. Therefore, in the AD kinetic model, both the PP release with PHA formation, as mediated in the anaerobic reactor of the NDBEPR system, and PP and PHA release upon the death of PAOs is included. The hydrolysis of the dead PAO biomass is the slowest rate controlling process in the AD and governs the rate of release of organically bound P.

In the steady state model, PP, with its associated metals is assumed to be released instantaneously, which restricts the model to sludge ages larger than 5 days. The release of P (and N) from the hydrolysis of biomass biodegradable organics is modelled with the same hydrolysis/ acidogenesis kinetics in the steady state and dynamic kinetic models.

This release of PP and metals of Mg^{2+} (and K^{+} and Ca^{2+}) to high concentrations cause the precipitation of struvite. Therefore, steady state kinetic AD models for digestion of P rich

sludge containing PP requires three phase (solid-liquid-gas) weak acid/base stoichiometry to be included.

WEAK ACID/BASE CHEMISTRY AND THE INCLUSION OF A SOLID PHASE

The process of anaerobic digestion produces various aqueous chemical species at different molar concentrations within the AD liquor. These species belong to several weak acid/base sub-systems that are simultaneously present in solution. A methanogenic AD typically includes the carbonate, phosphate, ammonia, acetate and water weak acid/ base subsystems. Loewenthal *et al.* (1989) noted that each weak acid/base system requires characterisation through measurement of the P_T, N_T, C_T and A_T weak acid total species concentrations before they can be speciated (the total concentrations distributed between their ionic species). From the AD steady state model (described in Chapter 6 of this thesis), the digester products' concentrations and pH are completely defined by the influent organics composition and so the aqueous concentrations of the different weak acid/base species and pH (HCO_3^-, $H_2PO_4^-$, HPO_4^{2-}, NH_4^+, Ac^- and H^+) can be determined from the measured influent characteristics. These species concentrations can in turn be used in the determination of the digester pH.

Sötemann *et al.* (2005b) noted that the pH established within AD systems treating PS and ND WAS is primarily affected by the inorganic carbon system. Although other weak acid/base systems are present such as the ammonia (N_T), phosphate (P_T) and VFA sub-systems, these do not significantly affect pH, either because their concentration is low (as for the P and VFA system) or their pK values are far outside the normal pH range of ADs (as for the VFA [$pK_a = 4.7$] and ammonia [$pK_n = 9.1$] systems) (Loewenthal *et al.*, 1994).

Where the phosphate species are included in the AD stoichiometry, such as for the AD of NDBEPR WAS with high P concentrations, it is necessary to include the P_T system, since it significantly influences the AD pH via (1) its 2nd dissociation constant pK_{p2} at ~ 7.0, (2) the form in which it is released ($H_2PO_4^-$ from PP or H_3PO_4 from biomass P) and (3) precipitation of phosphate minerals, in particular struvite. These factors all affect the AD pH, causing it to decrease.

Calculation of Struvite Precipitation

The steady state model can also deal with mineral precipitation and because struvite is the main one from the Mg co-released from the PP, it is considered. The aqueous species concentrations and p_{CO2} predicted, by the steady state AD model are at infinite solubility of struvite. The struvite precipitation and AD pH can be calculated from these model outputs with the software STRUVITE (Morrison and Loewenthal, 2007) based on the algorithm of Loewenthal *et al.* (1994). The problem with struvite is that p_{CO2} is required as input to predict the pH and is kept constant. In reality with struvite precipitation in the AD, p_{CO2} increases (slightly, <10%) which causes a lower AD pH. A (not so simple) spreadsheet method was developed to solve for the AD pH and p_{CO2} with struvite precipitation. This requires simultaneous solution of the AD stoichiometry and 3 phase mixed weak acid/base chemistry of the IC and OP systems.

THREE PHASE PLANT-WIDE DYNAMIC MODEL DEVELOPMENT

A plant-wide three phase AD dynamic model was developed in the simulation program WEST®. The initial step in the preparation of this plant-wide aerobic and anaerobic digestion model was the selection of a general set of components, which are universal to all the unit operations of the plant. For this, 38 components were identified in mass concentrations (with the units of milligrams per litre) but further provisions were made to parameterise the component descriptions in terms of their COD and molar concentrations (molalities). Thereafter, ASM2 and the University of Cape Town anaerobic digestion model number 1 (UCTADM1) dynamic models were extended and linked to construct the integrated plant-wide model. These extensions include:

1. An algebraic equation based aqueous ionic speciation model (Brouckaert *et al.*, 2010) model, which includes pairing of ionic components.
2. The Activated Sludge Model 2 (ASM2, Henze *et al.*, 1995), modified to include the ionic speciation model (Brouckaert *et al.*, 2010) and the Inorganic Settleable Solids (ISS) model of Ekama and Wentzel (2004).

3. The three phase anaerobic digestion model (ADM-3P), including the hydrolysis of multiple biodegradable particulate organic (BPO) types to cater for PS, ND WAS, NDBEPR WAS and PS-WAS blends, the Ekama and Wentzel (2004) ISS model, the Brouckaert *et al.* (2010) ionic speciation model and multiple mineral precipitation. This ADM-3P model extends the UCTADM1 model developed by Sötemann *et al.* (2005b) by adding:
   - Additional soluble and particulate biodegradable organic components to represent organics which might be combined from different sources in the WWTP and fed to the anaerobic digester.
   - Hydrolysis kinetics of the polyphosphate for the AD of waste activated sludge (WAS) from BEPR systems.
   - Precipitation of $MgNH_4PO_4.6H_2O$ (struvite), $MgKPO_4.6H_2O$ (K-struvite) and $Ca_3(PO_4)_2$ (ACP).
   - Modelling separately as algebraic equations, the "instantaneous" aqueous phase equilibrium and ion-paring reactions to reduce the stiffness (i.e. when in simulations, the requisite step size in the integration of a differential equation used in preparing a model predictions is forced to an incorrectly small level in a region where the solution curve displays very low variation) of the system of differential equations for the slower biodegradable, gas exchange and mineral precipitation process.
   - Parameterised stoichiometry for the bioprocesses for the various organics compositions entered as X, Y, Z, A and B values in $C_XH_YON_AP_B$ and polyphosphate entered as $Mg_cK_dCa_ePO_3$. When linked to the ASM2-3P model, this parameter values are passed to the AD from the AS system.
   - Pre-processor and post-processor routines which transform measured influent parameters such as FSA, OP, H_2CO_3 Alk., VFA, pH and TDS to model components and the correct ionic strength for activity coefficient determination and model components back to predicted "measured" concentration for comparison with the actual measured concentrations.

4. An integrated plant-wide dynamic model that combines the ASM2-3P and ADM-3P models.

Ionic Speciation Routine and Inter-Phase Transfers

The ionic speciation routine, common in the ASM2-3P and ADM-3P models, provides a general algebraic approach to modelling the very rapid ionic dissociation and ion pairing equilibrium reactions separately from the slower biological and physical processes. Forty-four species were selected to represent the distribution of the mixed weak acid/base system species and ion pairs that can form from 14 ionic components (of the 38 universally selected model components). The 14 basic components represent the total concentrations of the various weak acid/base systems and are applied in the model material balance calculations.

The input pre-processor links to the ionic speciation routine as follows. Measured influent concentrations {OP (P_T), FSA (N_T), Mg^{2+}, K^+, Ca^{2+}, pH and the H_2CO_3* alkalinity and VFA (AT)} and TDS and temperature are entered into the ADM-3P. The pre-processor adds NaCl to achieve the correct ionic strength (TDS), calculates the ionic activity coefficients and disaggregates the total concentrations in the sub-species for each weak acid/base system at the given pH. The charge represented by this metal state forms the reference charge balance of the model against which all changes in charges are based. The post – processor does the reverse, giving the various species concentration to totals and H_2CO_3* alkalinity and pH at the effluent ionic strength (TDS).

The Three phase ASM2 (ASM2-3P) Model

The Activated Sludge Model No. 2 (ASM2) (Henze *et al.*, 1995) is widely accepted and widely applied in NDBEPR system design, operation and process optimisation and forms a platform for further model development (Vanrolleghem *et al.*, 2005). The ASM2, which was developed for NDBEPR AS systems, can also be applied to anoxic-aerobic digestion (AnAerD) because, at least theoretically, AnAerD is a continuation of the AS system endogenous respiration process of OHOs and PAOs. However, this may require

calibrating the kinetic rates of some of the bioprocesses and (if necessary) adjusting some of the kinetic and stoichiometric constants (Sötemann *et al.,* 2006).

The ASM2-3P model is calibrated against (1) the NDBEPR UCT activated sludge system of this investigation and (2) the modified Ludzack-Ettinger (MLE) AS systems of this investigation (all systems shown in Figure S.1) and ASM1 in the absence of BEPR (3) the batch aerobic digestion (AerD) tests on NDBEPR WAS conducted by Mebrahtu *et al.* (2007) and (4) the anoxic-aerobic digester (AnAerD) tested by Vogts *et al.* (2011), which was fed concentrated (2×) WAS from the same the NDBEPR UCT AS system as in this investigation.

The Three phase UCTADM (ADM-3P) Model

Figure S-3 shows a schematic overview of the three phase AD model chemical, physical and biological processes.

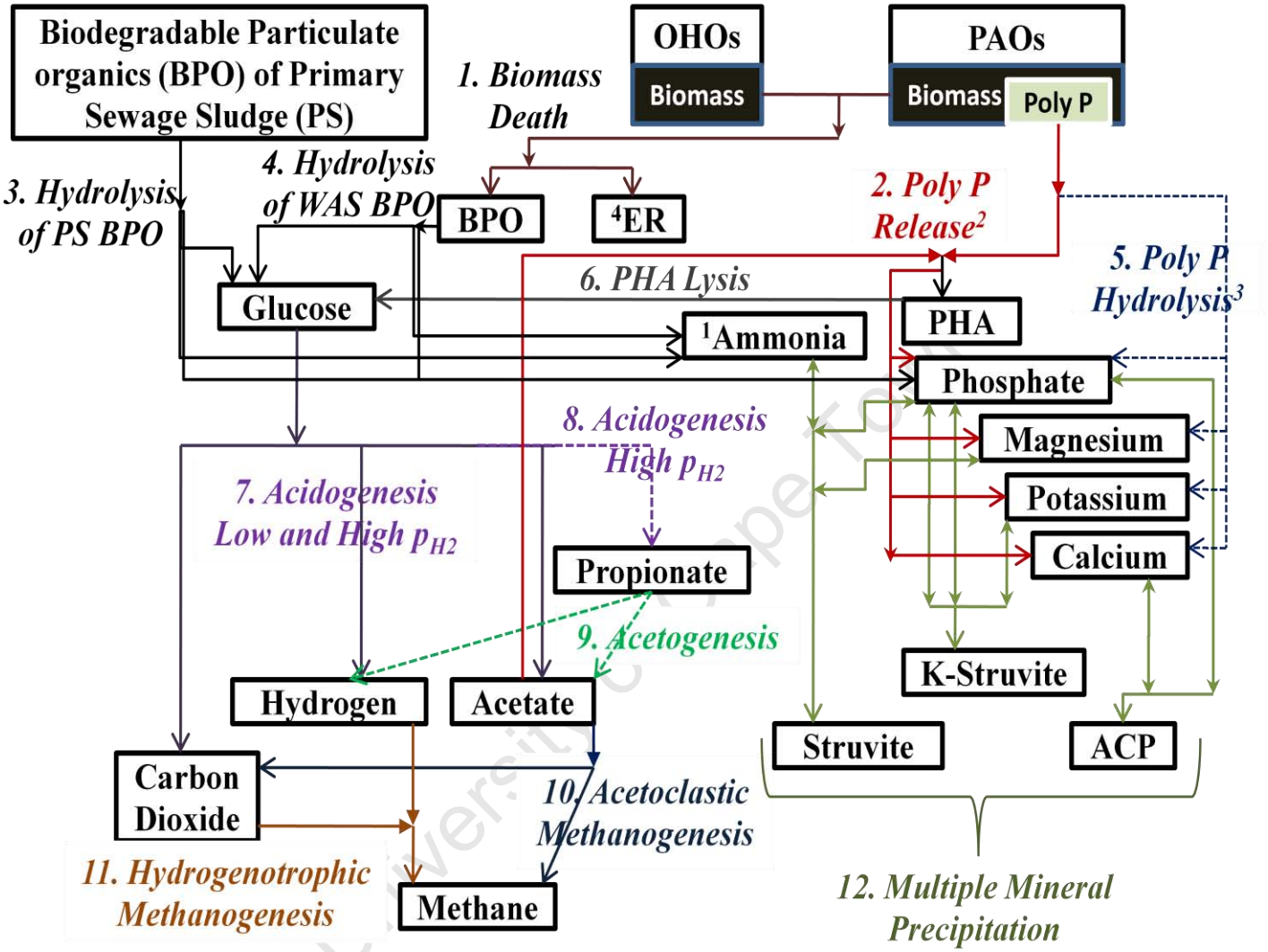

Figure S.3: *Process scheme for the ADM-3P model, as extended from the UCTADM1 model of Sötemann et al. (2005). Note that (1) ammonia is released in the NH_3 form and picks up a proton from H_2CO_3 to form NH_4^+, (2) Process 2 is for PP release with the uptake of acetate and (3) process 5 is for the PP hydrolysis with the death of the PAOs, (4) ER stands for the endogenous residue of biomass. Process 12 only shows for P precipitates, but other precipitates (i.e. newberyite, calcite and magnesite, which are less likely to form) are also included in the model.*

The ADM-3P model was calibrated against the ADs of this investigation, i.e. the AD of PS, MLE 1 WAS, MLE 2 WAS, PS-WAS (MLE 1) blend and NDBEPR WAS (the last with both continuous and batch AD tests to ensure that the P release is well matched). The ADM-3P was also validated with PS AD results of Izzett *et al.* (1992) and the predictions of the 2 phase UCTADM1 of Sötemann *et al.* (2005), which was calibrated against the Izzett *et al.* (1992) data.

The models were verified by checking that the material (COD, C, H, O N, P, Mg, K and Ca) mass balances are obtained. Calibration of the models generally involved matching the model results to measured variables on the different systems during selected steady state periods. Because the AS and AD systems were operated at steady state, the main calibration effort was determining the hydrolysis kinetic rates of the different sludges. This was accomplished with the COD based hydrolysis (first) part of the steady state model as detailed in Chapter 6. Because the hydrolysis /acidogenesis process is the slowest, all subsequent processes just need to be fast enough to produce a low component residual concentration. Therefore, the methanogenic bioprocesses (acetoclastic and hydrogenotrophic) were not actually calibrated – the yield coefficient endogenous respiration rate and Monod growth kinetic constants of these processes were taken directly from UCTADM1.

In calibration work, the unbiodegradable particulate COD fractions of the different sludge types were kept the same throughout all sludge ages. Its composition also was kept unchanged at elemental formulation (i.e. the X, Y, Z, A and B values of $C_XH_YO_ZN_AP_B$) that suited all the sludge ages best. The reason for this was because the AS systems were fed from the same wastewater and PS source throughout the investigation. It was deemed more important to observe that the model was predicting similar trends to experimentally measured results and to provide reason for any observed discrepancies, rather than to correct the discrepancies by changing the elemental formulation at each of the different experimental periods.

After separate calibration, the ASM2-3P and ADM-3P models were combined to build an integrated three phase plant-wide WWTP model in WEST with NDBEPR activated sludge, anaerobic digestion of primary sludge and anoxic-aerobic digestion or anaerobic digestion

of concentrated WAS. Therefore, since the ASM2-3P and ADM-3P models already had matching model components, the parameters and stoichiometric processes from the two models were easily combined into one Gujer matrix to form the integrated plant-wide model. However, in the WEST experimentation environment (where the model simulations are performed), it was ensured that only the AS reaction rates were activated in the simulation of AS system and only those of the AD were activated in simulation of the AD unit.

CONCLUSIONS

In this project, three phase (aqueous-gas-solid) plant-wide kinetic steady state and dynamic mathematical models are developed to simulate the anaerobic, aerobic and anoxic-aerobic digestion of sewage sludge including waste activated sludge (WAS) produced by Biological Excess phosphorus Removal (BEPR) plants. Determining whether or not the unbiodegradable organics of the influent wastewater and waste activated sludge (WAS) remained unbiodegradable also in the anaerobic digester was considered an important issue in the model development, when coupling the primary settling tank (PST), activated sludge (AS), aerobic digestion (AerD) and AD unit operations. Experimental observations carried out in this investigation led to the following conclusions regarding the fate of influent unbiodegradable particulate organics (UPO) and activated sludge generated (endogenous residue) unbiodegradable particulate organics in the wastewater treatment plant (WWTP):

1. The biodegradability of the influent wastewater organics remains closely consistent throughout the WWTP, i.e. the influent UPO component as established by the fully aerobic or ND AS systems remains unbiodegradable in the AD systems. The influent unbiodegradable soluble organics concentration is low enough (<50mgCOD/l) to be of little concern.
2. The material that is unbiodegradable in AS systems (i.e. endogenous residue and influent UPO) also is not further degraded in the AD system, even at very long sludge ages (60d). Hence, unbiodegradable material (influent UPO and AS

generated) is conserved throughout the plant, within experimental system operation error.

3. The remaining influent organic material that is biodegradable (particulate and soluble) gets transformed to active organisms (OHO) in the fully aerobic and ND AS systems, part of which undergoes endogenous respiration to form endogenous residue (which becomes part of the UPO in WAS). The OHO in WAS undergo further endogenous respiration in the anoxic-aerobic digestion (AnAerD) sludge treatment. In AD the BPO of the PS and WAS undergoes hydrolysis/acidogenesis to form acetate and hydrogen which is utilized by the AD biomass for growth, forming CH_4 and CO_2 gas as products. The concentration of BPO not hydrolysed depends on the kinetic rate of sludge hydrolysis. With complex organics like those found in WWTP sludge, the hydrolysis process is the rate-limiting step so that the AD processes that follow it, being much faster, invariably reach completion. The hydrolysis kinetic rate and unbiodegradable particulate fraction of the different sludges were determined from the measured AD influent and effluent COD concentrations of the sludge age range of 10-60 days. The WAS UPO (assuming 8% of OHO and PAO biomass was unbiodegradable) measured on the 60d AD and determined from the hydrolysis kinetics calibration matched reasonably close to the UPO determined for the WAS from measured activated sludge performance.
4. From 3 above, the higher UPO in the NDBEPR WAS (relative to that of the MLE system fed the same settled WW) is real and not an artifice of the NDBEPR AS model compared with the ND AS model. This has been a repeated observation in the UCT research (see Ekama and Wentzel, 1999). Determining where this extra UPO comes from was beyond the scope of this investigation. Because the NDBEPR system comprises a mixed culture of OHOs and PAOs, it becomes complex to account for this higher UPO. The endogenous residue fraction of OHOs (f_{EH} = 0.2, equivalent to 0.08 in death regeneration) used for modelling endogenous respiration and for determination of the unbiodegradable fraction of WAS has been validated in several investigations over the past decades (Marais and Ekama, 1976; van Haandel *et al.*, 1998; Ekama *et al.*, 2006; Randani *et al.*, 2011). Accounting for the

higher NDBEPR WAS UPO by changing the UPO of PAOs (f'_{EG}) distorts the f'_{EG} value beyond a reasonable range of that observed in enhanced PAO culture BEPR so this cannot be the reason for the difference.

5. The influent inorganic settleable (fixed) solids (ISS) is deemed not to take part in any reactions and is conserved through the plant as already investigated by Sötemann *et al.* (2006) and Ekama *et al.* (2006). Hence, it simply is enmeshed in the sludge mass and increases with sludge age. Moreover, as modelled by Ekama and Wentzel (2004), some influent inorganic dissolved solids (IDS) are taken up by the OHO and PAO and add to the mixed liquor (fixed) ISS concentration when VSS samples are dried. Therefore, the total reactor ISS comprises the ISS content of the OHO, PAO and ANO biomass (i.e. ISS_{BM} = 0.15 mgISS/mg biomass), the PAO stored PP (3.23 mgISS/mgP), all precipitates formed (struvite, amorphous calcium phosphate (ACP) and K-struvite ($MgKPO_4$)) and the influent ISS that is enmeshed with sludge. However, although the metals (Magnesium (Mg), potassium (K) and calcium (Ca)) and ortho-phosphate (OP) are taken up aerobically (from where the WAS is withdrawn), to make up polyphosphate (PP), and released anaerobically in the AS system, the mineral precipitation and dissolution of the influent ISS was found to be negligible in the AS systems. In contrast, significant phosphorus mineral precipitation does occur in the AD system fed concentrated WAS from the NDBEPR system (~10gTSS/*l*), increasing as the P removal of the parent NDBEPR system and concentration of the feed WAS increases.
6. Because polyphosphate (PP), a high-energy compound in the PAOs, is not a cell bound part of the biomass, it is released much faster than the organically bound biomass P during anaerobic digestion. This PP release from PAOs has no direct relation to the kinetics of hydrolysis/acidogenesis of the PAO (and OHO) biomass, and so the hydrolysis kinetics of the BEPR WAS are not significantly different from that of the WAS from fully aerobic or N removal AS systems. Aside from the PP, the composition of the OHO and PAO BPO material, which requires hydrolysis in the AD, was modelled to be the same because the experimental investigation did not allow these to be differentiated.

Some Observations from the Plant-Wide Model Development

The ASM2-3P and ADM-3P models were verified and validated individually before merging to construct the integrated plant-wide model. This model can be applied to simulate the whole WWTP plant comprising a NDBEPR AS system linked to an AD or an anoxic-aerobic digestion (AnAerD) for WAS stabilisation.

The following aspects were noted when modelling the anoxic-aerobic systems (AS, AerD and AnAerD) with the ASM2-3P model:

1. Since the MLE system with ND does not stimulate BEPR, its effluent P comprises mainly the OP that was not utilized by the biomass (mainly OHOs) for growth. This growth is limited by the flux of influent biodegradable COD available. With no PAO growth, no PP gets stored. Hence, the WAS produced from this type of system is not likely to cause struvite precipitation during sludge treatment, even with significant thickening before digestion.
2. The aeration that occurs in the aerobic zone of AS systems strips out most of the CO_2 generated by the bioprocesses. Consequently, this biologically generated CO_2 does not have a significant impact on the pH of the system – pH of the AS system reactors depends mostly on the loss and gain of alkalinity via protein hydrolysis (gain), nitrification (loss), denitrification (gain) and PP storage (loss). The degree of CO_2 super-saturation has little effect on pH.
3. In MLE systems with little or no nitrification taking place, high quantities of P and acetate in the unaerated ('anoxic') zone will result in the growth of PAOs rather than OHOs (and ANOs) only as expected in fully aerobic or nitrogen (N) removal systems. The concentration of acetate available for this PAO growth (and consequential excess P removal) depends on the rate of fermentation of biodegradable soluble organics (BSO) that occurs and the concentration of nitrate that gets recycled to the anaerobic reactor in these systems. This can also take place in 3 and 5-stage Bardenpho systems – during the winter months when denitrification is lower than in the summer, the nitrate concentration recycled to the anaerobic reactor can be sufficiently high to suppress BEPR, in which case the WAS

is not P-rich and AD of the WAS will not result in mineral precipitation even if thickened to 4 or 5% by flotation. In contrast, in summer the nitrate recycled to the anaerobic reactor is low resulting in BEPR in this system and mineral precipitation in AD and sludge dewatering systems. This happened at the Cape Flats WWTP in Cape Town, where the WAS was thickened to 3 to 4% by dissolved air flotation and anaerobically digested with PS. Seasonal BEPR in the 5-stage Bardenpho system caused mineral precipitation in the AD sludge dewatering centrifuges (van Rensburg *et al.*, 2003). The problem was solved by adding aeration to the AD sludge storage tank to raise the digester liquor pH by CO_2 stripping to stimulate mineral precipitation before discharge to the dewatering centrifuges. While not quantitatively validated the plant-wide ASM2-AD-3P does qualitatively predict this behaviour correctly.

4. In anoxic-aerobic digestion (AnAerD), the absence of VFA and an anaerobic period renders the PAOs to be unable to compete with the OHOs. Consequently, the PAOs do not grow and undergo endogenous respiration. The PAOs eventually die, releasing their stored PP that contains Magnesium, Calcium, potassium and OP. Struvite ($MgNH_4PO_4$) precipitation occurs when the concentration of Mg, ammonia and OP is high enough (i.e. the struvite is supersaturated) in the mixed liquor. If the ammonia is low (< 1mg/N/*l*), due to nitrification, the Mg and P would combine with K to form K-struvite ($MgKPO_4$). The precipitation of FSA-struvite and K-struvite is limited by the Mg concentration, which is usually the lowest of the Mg, K, FSA and P. Once the Mg is limited, no further OP reduction takes place. About one-third of the P released by PP precipitates with the co-released Mg. This was observed in both aerobic and anaerobic digestion**.**
5. From the application of the ASM2-AerD-3P model to the diluted (4gTSS/*l*) aerobic batch tests of Mebrahtu *et al.* (2007), in which mineral precipitation did not take place, it appears that the PAOs retain their PP until they 'die' at their very slow endogenous respiration rate (0.04/d). This means that after 20d aerobic digestion, a considerable proportion of PAOs, with a high PP content, are still "alive" (> 50%). If the WAS is concentrated (> 2% TSS) FSA-sruvite and K-struvite precipitation will

take place but will be limited by the co-released Mg. The P release behaviour in aerobic digestion is therefore distinctly different to that in anaerobic digestion, where all the PP is released in less than 5 days. The FSA and OP concentrations in dewatering liquor from aerobic digestion of P-rich WAS are therefore much lower than those from AD of P-rich WAS.

6. Application of the model to the anoxic –aerobic digestion of the concentrated P-rich WAS system of Vogts *et al.* (2010) validated that the effluent FSA, and nitrite was very low (< 1mgN/*l*) and that about 1/3rd of released P was precipitated as struvite with co-released Mg. While Vogts *et al.* (2010) also tested the effect of Ca and Mg dosing to the AnAerD on the aqueous OP concentration, this was not simulated but should be done in further work.

The following aspects were noted when modelling the AD systems using the steady state and dynamic (ADM-3P) three phase AD models:

1. In the AD of PS, biodegradable particulate organics (PS BPO) are directly available. For AD of WAS, the biomass (OHOs and/or PAOs) die and are converted to BPO rapidly – much faster than their aerobic endogenous respiration rate. The WAS BPO is hydrolyzed at a distinct rate (which was measured in this investigation). This hydrolysis rate of PS BPO and WAS BPO dictates the rate of all bound FSA and OP release in AD. The COD removal associated with FSA and OP release increases with increased AD sludge age. This increase is due to the increased time available for the hydrolysis of BPO material and hence release of the organically bound N and P, as FSA and OP, into the AD liquor.
2. Methane is produced via the COD removal; hence, methane production depends only on the electron donating capacity of the biodegradable organics degraded (minus the very small amount, 2-5% of COD in the AD biomass produced). The C not included in CH_4 (minus the very small amount of C in the biomass) becomes CO_2, either dissolved CO_2 (HCO_3^-) or gaseous CO_2. Being insoluble at close to atmospheric pressure, methane usually all escapes as gas as soon as it is formed by the biological reactions. The mole fraction of the CO_2 in the gas phase [CO_2/ (CO_2 +

CH_4)] sets the partial pressure of the gas phase (p_{CO2}), which together with the total alkalinity set the AD pH.

3. Organically bound N is released with the breakdown of biodegradable organics in the non-ionic NH_3 form, which are non-reference species for the ammonia weak acid/base system so the alkalinity increases by the concentration of NH_3 released. The NH_3, in the 6-8 pH range of ADs, picks up a H^+ ion from the bulk liquid which is supplied by the dissolved CO_2 (H_2CO_3*) forming HCO_3^-, according to $NH_3 + H_2O + CO_2 \rightarrow NH_4^+ + HCO_3^-$. Therefore, the total alkalinity (T.Alk) remains unchanged but is transferred from the FSA system to the inorganic carbon system. This is the main H_2CO_3*alkalinity generation process in an AD treating PS or WAS that is not P-rich. For P-rich systems with PP, H_2CO_3* alkalinity generation also depends on PP and cell bound P release.
4. Initially, polyphosphate (PP) release and PHA storage by PAOs takes place with the uptake of acetate, as would happen in the anaerobic part of the parent NDBEPR system. This results in increased alkalinity because the PP is released as $H_2PO_4^-$. Because the PAOs also require aerobic conditions to supply them with the terminal electron acceptor (oxygen) for their growth, they cannot grow in the AD. Therefore, the PAOs are modelled to "die" in AD at a rate faster than their endogenous respiration rate; releasing their PHA and rest of their stored PP, adding more $H_2PO_4^-$ and alkalinity. Depending on the charge/proton balance requirements, some of the $H_2PO_4^-$ species become HPO_4^{2-} species by reacting with HCO_3^- to form HPO_4^{2-}, H_2O and CO_2. In this exchange, again, the T.Alk remains constant but it causes an additional transfer of alkalinity from the HCO_3^- of the IC system to the HPO_4^{2-} of the OP system and increases the CO_2 that exits the digester as gas and so increases the p_{CO2} of the AD gas.
5. The organically bound P in the PAO (and OHO) biomass is released as H_3PO_4, at the much slower hydrolysis rate than the rapid PP release rate, which is complete in less than five days (Harding, 2009). Because H_3PO_4 is reference species for the OP weak acid/base system, the T.Alk does not change with this P release. In the AD pH

range 7 to 8, the H_3PO_4 reacts with HCO_3^- to become $H_2PO_4^-$ or HPO_4^{2-} species, the HCO_3^- becoming H_2O and CO_2. So while the total alkalinity does not change, the species that represent it do (there is a transfer of alkalinity from the HCO_3^- of the IC system to the $H_2PO_4^-$ and HPO_4^{2-} species of the OP system). The CO_2 that would have been retained in the aqueous phase as HCO_3^- now exits the AD as gas, which increases the p_{CO2} (the CH_4 gas production remains unchanged because it is fixed by the COD of the biodegraded organics).

6. The rapid release of PP and associated Mg^{2+} and the slow release of biomass N and P generate high concentrations of P, NH_4^+ and Mg^{2+} species in the AD liquor, which promotes struvite precipitation. This struvite precipitation decreases the T.Alk by 3×the struvite concentration precipitated and so results in re-speciation of the IC system, which increases p_{CO2} and decreases AD pH (Loewenthal *et al.*, 1994). If the T.Alk is low due to low N content of BPO and the P-rich WAS concentration high, precipitation of struvite results in decreased alkalinity and pH. However, the digester would not be at risk of failure, since for this precipitation to occur, the AD mixed liquor is required to be at above the required pH for stable AD operation, i.e. > 6.5, but preferably between 7 and 8, as reported by McCarty (1974).
7. Because the acetoclastic methanogens utilise only the associated form of VFA (HAc), all dissociated VFA fed to the AD, also cause an increase in alkalinity, i.e. $Ac^- + H_2O + CO_2 \rightarrow HAc + HCO_3^-$.
8. Therefore, alkalinity is generated only by the release of N, PP and utilization of dissociated VFA. These three alkalinity-generating processes (plus the influent alkalinity) establish the T.Alk in the AD. The T.Alk generated and p_{CO2} of the gas phase and hence, AD pH are therefore completely defined by the composition of the organics digested and the type of bioprocess, in this case methanogenesis, which itself does not generate alkalinity like sulphate reduction does (Poinapen and Ekama, 2010). However, it is also notable that physical processes that enhance CO_2 gas stripping, e.g. vigorous stirring of the AD tank could cause increased CO_2 expulsion (hence higher p_{CO2}), increased alkalinity and increased pH.

The material (COD, C, H, O, N, P, Mg, K and Ca) mass balance based three phase (solid – aqueous – gas) steady state AD and dynamic AD models have been developed in three steps, i.e. kinetics of hydrolysis, model stoichiometry and mixed weak acid/base chemistry. The ASM2-3P model was also developed to which the ADM-3P model can be connected to allow plant-wide simulation. Similarly, the 3 phase steady state AD model can be used on its own or linked to a steady state NDBEPR model, such as that developed by Wentzel *et al.* (1990), to construct a steady state plant-wide model, which is useful to make design decisions for the wastewater treatment plant layout (Ekama, 2009).

It was necessary to develop the steady state and dynamic models simultaneously because the steady state steady state models were required to determine kinetic rates and sludge compositions for dynamic model input and calibration. This was possible because the steady state models and dynamic AS and AD models are based on the same basic principles, mass balances stoichiometry, just in simplified form without significant loss of accuracy. Therefore, steady state models are a useful complement to dynamic models. They allow the WWTP to be sized and optimized (i.e. for direct calculation of sludge age, reactor volumes and recycle flows) or wastewater characteristics to be determined before performing simulations and so obviate much of the trial and error use of dynamic models, which require the plant unit operations to be sized and wastewater characteristics to be defined before simulations can be run. Once the WWTP layout is established with steady state models, dynamic models can be applied to its operation to minimize energy consumption and cost while maximizing nutrient recovery and effluent quality.

RECOMMENDATIONS

The steady state and dynamic three phase AD models have been developed and incorporated into plant-wide settings. However, when developing these models, there were a few aspects that would be considered useful in future research. These include:

1. Investigation into the reason behind the influent $f_{S'up}$ values, calculated from BEPR plants being higher than for ND systems treating the same wastewater. Two possible causes for this higher $f_{S'up}$ values have been reviewed in this thesis: (1) mistaken assumptions that may have been made when allocating to the PAOs the

same death regeneration unbiodegradable fraction (f_{EG} = 0.08) as for OHOs and/or the PAOs having sequestered more of the influent hydrolyzed biodegradable particulate organics than the assumed influent rapidly biodegradable organics (RBCOD) only and (2) the high influent $f_{S'up}$ in the MBR UCT system may be as a result of more unbiodegradable particulate organics (UPO) being enmeshed in the aerobic reactor (which has a higher sludge concentration and from which the waste sludge fed to the AD is taken) than the other reactors. To explore the validity of cause (1), the determination of f'_{EG} (the part of the NDBEPR WAS unbiodegradable fraction, which is generated by death regeneration in AD) could be done experimentally by digesting pure cultures of PAOs at a long AD sludge age (about 60 days or more). The exploration on the validity of cause (2) can be done by investigating the biodegradability of sludge from all reactors (aerobic, anoxic and anaerobic) of the NDBEPR system when fed to an AD operated at a long sludge age (about 60 days or more), hence confirming whether significantly higher mixed liquor concentrations in the aerobic reactor is a cause for more of the influent inert organics to get enmeshed, such that the ratio of sludge in the aerobic reactor to the whole system (f_{maer}) for the enmeshed influent unbiodegradable organics (X_i) is higher than that of the total measured volatile settleable solids (i.e. $f_{maer\text{-}Xi} > f_{maer\text{-}VSS}$).

2. It is important to stress that, when dealing with systems, under non-ideal conditions that are likely to have mineral precipitation, some parameters that do not ordinarily get tested would require rigorous testing. These include influent (and effluent) pH and alkalinity, ionic conductivity and for P precipitation, the OP should be tested before dissolution of precipitates and after dissolution (for distinguishing between the P that is bound in PP from that bound in the precipitate).
3. The steady state and dynamic plant-wide AD models have been used to predict the output of laboratory scale systems. However, when used to predict the output from full scale wastewater treatment plants, new challenges may arise, especially regarding the fluid dynamics of reactors (which we assumed in the models are completely mixed). It would be interesting to explore how well the models predict

full-scale systems and to see what type of modifications would be required to achieve this.

TABLE OF CONTENTS

ABSTRACT i

PREFACE vi

ACKNOWLEDGEMENTS x

LIST OF SYMBOLS AND ABBREVIATIONS xii

LIST OF TABLES xx

LIST OF FIGURES xxviii

SYNOPSIS xlvi

TABLE OF CONTENTS lxxvi

CHAPTER 1: INTRODUCTION 1

1.1 BACKGROUND TO PROBLEM 1

1.2 PROJECT OBJECTIVES 3

1.3 NEW KNOWLEDGE CONTRIBUTION 5

1.3.1 The Development of a Three Phase Plant-Wide Model that Includes Phosphorous 5

1.3.2 Biodegradability of Organics in the WWTP 7

1.3.3 Hydrolysis in the AD of Multiple Organic Types in Municipal Sewage Sludge 8

1.4 OVERVIEW OF REPORT 9

CHAPTER 2: LITERATURE REVIEW 11

2.1 INTRODUCTION 11

2.2 NATURE AND CHARACTERISTICS OF MUNICIPAL WASTEWATER 15

2.3 OVERVIEW OF WASTEWATER TREATMENT PLANT (WWTP) 15

2.3.1 Primary Treatment of Raw Wastewater 16

2.3.1.1 Primary Settling Tank 16

2.3.2 Secondary Treatment of Wastewater 17

2.3.2.1 Biological Processes 17

2.3.2.2 Activated Sludge Systems 18
2.3.2.3 Composition of the Activated Sludge (AS) 25
2.3.2.4 Separation of Effluent from RAS 29
2.3.3 Anaerobic Digestion 30
2.3.3.1 Anaerobic Digestion (AD) Processes 31
2.3.3.2 AD Systems 36
2.4 MATHEMATICAL MODELS FOR THE UNIT PROCESSES OF THE WWTP 40
2.4.1 Steady State Models 41
2.4.1.1 AS System Steady State Models 42
2.4.1.2 Anaerobic Digestion (AD) System Steady State Models 46
2.4.1.3 Plant-Wide Steady State Model 49
2.4.2 Dynamic Models 58
2.4.2.1 Stages in Development of the Dynamic Model. 59
2.4.2.2 Uses of Dynamic Modelling 59
2.4.2.3 AS System Dynamic Models 60
2.4.2.4 AD System Dynamic Models 65
2.4.3 Modelling Weak Acid/Base Processes 68
2.4.3.1 Mineral Precipitation 69
2.4.3.2 Gaseous Exchange 73
2.4.3.3 The C and N Removal AS System Model of Sötemann *et al. (2005a)* with Applications of the Musvoto *et al.* (1998; 2000a, b) Kinetic Model 76
2.4.4 The Formation of a Dynamic PWMM 80
2.4.4.1 Continuity Based Interfacing Method – CBIM (Volcke *et al.*, 2006) 81
2.4.4.2 The Supermodel Approach 85
2.4.4.4 Mass Balance Based Plant-Wide Modelling Approach 86
2.5 CLOSURE 88

CHAPTER 3: MATERIALS AND METHODS 91

3.1 INTRODUCTION 91
3.2 EXPERIMENTAL SET UP 92

3.2.1 Wastewater Collection and AS System Feed Preparation 93
3.2.2 Activated Sludge (AS) Systems 94
3.2.2.1 Feed Preparation for ND Activated Sludge Systems (MLE 1 and MLE 2) 94
3.2.2.2 Feed Preparation for the NDBEPR Activated Sludge System (UCT- MBR) 95
3.2.2.3 Description of ND Activated Sludge Systems (MLE 1 and MLE 2) 95
3.2.2.4 Description of NDBEPR Activated Sludge System (UCT- MBR) 97
3.2.2.5 Sampling 98
3.2.3 Anaerobic Digestion Systems 99
3.2.3.1 AD Feed Preparation 100
3.2.3.2 Description the of AD System used for Experimental Research 101
3.2.3.3 Sampling of AD Systems 103
3.3 EXPERIMENTAL TESTING METHODS 104
3.3.1 Chemical Oxygen Demand (COD) 104
3.3.2 Total Kjeldahl Nitrogen (TKN) and Free and Saline Ammonia (FSA) 105
3.3.3 Nitrate (NO_3^-) and Nitrite (NO_2^-) Test 105
3.3.4 Total Phosphates (TP) and Ortho-phosphates (OP) 106
3.3.5 Volatile Fatty Acids (VFAs), $H_2CO_3^*$ Alkalinity and pH 106
3.3.6 Mixed Liquor Settleable Solids (MLSS) 106
3.3.7 Oxygen Utilization Rate (OUR) 107
3.3.8 Gas Production and Composition 109
3.3.9 Total Organic Carbon (TOC) and Total Organic Nitrogen (TON) Analysis 109
3.3.10 Total and Dissolved Counter-ion Metal (Me) Analysis 110
3.3.10 Sampling from the Experimental Set-up 111
3.4 CLOSURE 112
CHAPTER 4: RESULTS AND DISCUSSIONS 114
4.1 INTRODUCTION 114
4.2 PERFORMANCE OF ACTIVATED SLUDGE (AS) SYSTEMS 118
4.2.1 COD Removal 119
4.2.2 TKN Removal 121

4.2.3 Nitrate Removal 122
4.2.4 Phosphorus Removal 125
4.2.5 Metallic Ions Removed in the Formation of Polyphosphate 126
4.2.5 Mixed Liquor Suspended Solids (MLSS) Concentration 127
4.2.7 Oxygen Utilization 128
4.3. PERFORMANCE OF THE ANAEROBIC DIGESTION (AD) SYSTEMS 130
4.3.1 COD Removal 130
4.3.2 Free and Saline Ammonia (FSA) Release during AD 132
4.3.3 Gas Production and Composition 134
4.3.4 Volatile Fatty Acids (VFA), H_2CO_3* Alkalinity and pH 137
4.3.5 Ortho-phosphate (OP) Release During AD 142
4.3.6 Metallic Ions and phosphorus Precipitation 143
4.4 EVALUATION OF EXPERIMENTAL DATA 146
4.4.1 Mass Balances over the PST 147
4.4.2 Mass Balances over the AS Systems 148
4.4.2.1 MLE Systems Operated on Raw (MLE 2) and Settled (MLE 1) Wastewater 148
4.4.3 Mass Balances over the AD Systems 151
4.5 CLOSURE 153

CHAPTER 5: CHARACTERISATION OF INFLUENT SEWAGE AND WASTE SLUDGE 157

5.1 INTRODUCTION 157
5.2 BIODEGRADABILITY OF INFLUENT WASTEWATER ORGANICS 157
5.2.1 The Determination of the $f_{S'up}$ Value for the Nitrification-denitrification (ND) Systems158
5.2.2 Primary Sludge Unbiodegradable Particulate Material 159
5.3 BIODEGRADABILITY OF ACTIVATED SLUDGE ORGANICS 165
5.4 CHARACTERISTICS OF INFLUENT WASTEWATER 172
5.4.1 Primary Sludge Characterisation and Elemental Composition 174
5.4.2 Influent COD Concentrations 176
5.4.3 Influent Carbon Characterisation 180

5.4.4 Influent N and P Characteristics 183
5.4.5 Elemental Compositions of Influent Wastewater Characteristic Components 193
5.5 CHARACTERISATION OF WASTE ACTIVATED SLUDGE 197
5.5.1 The Determination of Polyphosphate Concentrations in PAOs 202
5.5.2 Sludge Characterisation 205
5.6 CLOSURE 216
CHAPTER 6: STEADY STATE KINETIC MODEL DEVELOPMENT 220
6.1. INTRODUCTION 220
6.2 KINETIC SECTION OF STEADY STATE MODEL 222
6.2.1 The Determination of Kinetic Constants 225
6.2.2 Experimental Results 235
6.2.2.1. AD of Primary Sludge 236
6.2.2.2. MLE 1 Waste Activated Sludge (WAS) 258
6.2.2.3. MLE 2 Waste Activated Sludge 275
6.2.2.4 NDBEPR Waste Activated Sludge 293
6.2.2.5. AD of Primary Sludge – Waste Activated Sludge (PS-WAS) Blend 313
6.2.3 A Summary of the Constants Obtained for the Steady State AD Model Hydrolysis Kinetics 330
6.3. STOICHIOMETRIC MODEL FOR AD OF NDBEPR WAS 335
6.3.1 Extending the AD Model to Include P (Harding, 2009) 335
6.3.2 PAO Behaviour in the AD 340
6.4 WEAK ACID/BASE CHEMISTRY AND THE INCLUSION OF A SOLID PHASE 346
6.4.1 Determination of Digester pH for Infinite Solubility of Precipitates 346
6.4.2 Calculation of Precipitates Formed in AD 351
6.4.3 Determination of Digester pH after Precipitation 358
6.5 The Steady State AD Model Calibration 358
6.5.1 Comparison of SS Model Results to Experimental Measurements 358
6.5.2 Application of the Steady State AD Model in Design 370
6.6 CLOSURE 372

CHAPTER 7: THREE PHASE PLANT-WIDE DYNAMIC MODEL DEVELOPMENT 378

7.1 INTRODUCTION 378

7.2 UNIVERSALLY SELECTED MODEL COMPONENTS 380

7.3 IONIC SPECIATION ROUTINE AND INTERPHASE TRANSFERS 383

7.3.1 Ionic Speciation 383

7.3.2 Inter-Phase Transfers 387

7.4 THE THREE PHASE ASM2 (ASM2-3P) MODEL 392

7.4.1 Model Processes 393

7.4.2 Inclusion of Ekama and Wentzel (2004) ISS Model to ASM2 413

7.4.3 Programmed Configuration Settings 414

7.4.4 Model Verification 418

7.4.5 Model Calibration 419

7.5 THREE PHASE UCT AD (ADM-3P) MODEL 440

7.5.1 Implementation of the UCTADM Model 441

7.5.2 Calibration of UCTADM in WEST 446

7.5.3 Sensitivity Analysis of Model 482

7.5.4 Predicting Digester Failure 491

7.6 AEROBIC DIGESTER SIMULATION USING THE ASM2-3P MODEL 499

7.7 THE THREE PHASE PLANT-WIDE MODEL 530

7.7.1 Simulating NDBEPR linked to AD system 531

7.6.2 Scenario Analysis using the ASM2-3P-ADM-3P Plant-Wide Model 536

7.8 CLOSURE 540

CHAPTER 8: CONCLUSIONS 544

8.1 INTRODUCTION 544

8.2 UNBIODGRADABLE PARTICULATE MATERIAL IN THE WWTP 545

8.3 THE STEADY STATE KINETIC MODEL 549

8.3.1 Kinetics of Hydrolysis 549

8.3.2 Determination of Sludge Elemental composition 552

8.3.3 Stoichiometric Section of the Steady State Model 555

8.4 THE DEVELOPMENT OF A DYNAMIC PLANT-WIDE THREE PHASE MODEL 555
8.5 CLOSURE 564
8.6 RECOMMENDATIONS 565
REFERENCES 569
APPENDIX 588
APPENDIX 1: CALCULATIONS USED FOR DATA EVALUATION 589
1.1. The Determination of Solids and Hydraulic Retention Times for the AS Systems 589
1.2. Determination of Nitrogen Generated and De-nitrified in the AS System 591
1.3. The Determination of Oxygen Utilized for Nitrification and for Organics Utilization 593
APPENDIX 2: OHO AND PAO ORGANIC FORMULA DERIVATION 601
2.1. The Determination of OHO and PAO Biomass Generic Organic Formulae 601
2.2. The Determination of Polyphosphate Concentrations in PAOs 603
APPENDIX 3: EXPERIMENTAL SET UP 608
APPENDIX 4: ADDITIVES USED IN EXPERIMENT 611
APPENDIX 5: STEADY STATE AD SPREADSHEET DESIGN EXAMPLE 613
5.1 Description of Steady State AD Model Spreadsheet 615
5.2 Model Spreadsheet Example 616
APPENDIX 6: THE PLANT-WIDE THREE PHASE MODEL GUJER MATRIX 637
APPENDIX 7: RAW DATA FOR AS SYSTEMS 664
APPENDIX 8: RAW DATA FOR AD SYSTEMS 686

CHAPTER 1: INTRODUCTION

The project goal is to develop three phase (aqueous-gas-solid) steady state and dynamic mathematical models for the anaerobic and aerobic digestion of municipal sludge, including waste activated sludge (WAS) produced by Biological Excess phosphorus Removal (BEPR) plants, within a plant-wide setting. This research project is conducted in the Water Research Group (WRG) of the Civil Engineering Department and supervised by Professor G.A. Ekama. This thesis attempts to provide a comprehensive view on the aspects that entail this research, including the experimental findings and a detailed description of progress achieved in the development of the aforementioned steady state and dynamic models.

1.1 BACKGROUND TO PROBLEM

A large quantity of nitrogen (N) and phosphorus (P) is present in wastewater and if not removed, is one of the main causes of eutrophication, which negatively affects many natural water bodies with excessive algae and plant growth. In general, phosphorus is removed in biological nutrient removal (BNR) wastewater treatment plants (WWTPs) through the use of alternating anaerobic and aerobic conditions, which stimulate the growth of phosphorus accumulating organisms (PAOs) in a BEPR activated sludge system. Considerable resources are utilized in the construction and operation of these systems in order to meet the required effluent N and P criteria, prescribed for environmental safety. Therefore, there is a need to find the most cost-effective methods for their design and operation to minimize energy consumption and cost while maximizing nutrient recovery and effluent quality.

The design procedures for wastewater treatment systems that were used in the past (pre-1980) were mainly based on experience and empirical relationships. The inaccuracies and inadequacy brought about by using these methods, prompted research into improved design procedures that were based on the behavioural patterns of microorganisms mediating the N and P removal processes. As a result, over the past 20 years a number of

activated sludge kinetic theories and dynamic mathematical models have been developed. These models have been coded into computer simulation programmes by using the principle of material mass balances and are able to predict the system response when subjected to dynamic flows and material (chemical oxygen demand (COD), N and P) loads. However, these dynamic models are not compatible with design and operation procedures because they require, for design, the sludge age, reactor volumes and interconnecting recycle flows and for operation, the wastewater characteristics to be specified. Thus the dynamic models were usually exercised by iterative trial and error simulations. In contrast, steady state models are not only simpler but also allow direct calculation of sludge age, reactor volumes and recycle flows, for design, or wastewater characterisation, for operation, from explicit algebraic equations linking system parameters to reactor performance criteria. Therefore, steady state models are a useful complement to dynamic models allowing the WWTPs to be sized or wastewater characteristics to be determined before performing simulations and so obviate the trial and error use of dynamic models.

Previous steady state and dynamic simulation models concentrated mainly on the activated sludge (AS) unit operation because it is from this part of the WWTP that the effluent is produced. However, in WWTPs all the unit operations are connected, such as activated sludge, aerobic digester, primary settling and anaerobic digester, resulting in recycling mixed liquors from downstream to upstream unit operations. Therefore, the design and operation optimization of one unit operation may significantly affect the performance and economics of other up-stream or down-stream operations and therefore also of the WWTP as a whole. This mutual interaction has recently triggered research interest in developing mass balance based plant-wide WWTP models, which model all the unit operations of the WWTP together, linked with the connecting flows.

An integrated steady state model for the whole WWTP was formed from the coupling of the various existing WWTP individual unit operation steady state models. This model is being extended or modified as new information is added to it. Eventually, this plant-wide model shall deal with wastewater organics, N, P and inorganic settleable solid (ISS) compounds along links connecting the primary settling tank (PST), biological nutrient

removal activated sludge systems and aerobic and/or anaerobic digestion unit operations of the WWTP.

Progress to date in this research includes the completion of steady state models for primary settling, nitrification-denitrification (ND) activated sludge and aerobic digestion (AerD) or anaerobic digestion (AD) of primary and waste activated sludge treating raw or settled wastewater (WW) from Modified Ludzack-Ettinger (MLE) systems. Moreover, mass balance carbon (C), nitrogen (N), oxygen (O), hydrogen (H) and total oxygen demand (TOD) stoichiometry has also been developed to complement the steady state models so that the different products exiting the WWTP via the solid, liquid and gas streams can be calculated, such as N loads in recycle streams, methane (CH_4) production for energy recovery and green house gas (CO_2, CH_4) generation (Ekama, 2009). Sötemann *et al.* (2005) showed that the steady state and dynamic models yield closely similar outputs in this plant-wide model.

However, the anaerobic digestion (AD) of WAS from BEPR systems, containing phosphorus accumulating organisms (PAOs), has not yet been modelled. The PAOs introduce several complex issues, which require investigation. For instance, the PAOs have a lower endogenous respiration rate as compared to the ordinary heterotrophic organisms (OHOs). This would affect the N and P nutrient releases in aerobic and anaerobic digestion (Sötemann *et al.*, 2006).

1.2 PROJECT OBJECTIVES

With the focus of developing a steady state AD and dynamic three phase plant-wide simulation models, it was decided that the following four tasks needed to be accomplished:

1. An experimental investigation to generate the data required for both steady state and dynamic model development: The experimental set up was large, to mimic three real WWTP types at laboratory scale, and is described in Figure 3.1 in Chapter 3 of this thesis.
2. Steady state AD model development including P: From the experimental data of the ADs operated at five different sludge ages, the hydrolysis kinetics of primary

sludge (PS), ND AS system waste activated sludge (WAS) and NDBEPR AS system WAS are to be determined and included to the stoichiometric AD model that was developed by Harding (2009). Since it was noted that mineral precipitation takes place in the AD of NDBEPR WAS containing PAOs, the steady state mixed weak acid/base chemistry part of the AD model needs extension to include three phases (aqueous-gas-solid).

3. Plant-wide AD dynamic modelling including P from NDBEPR WAS: A dynamic AD model has previously been developed by Sötemann *et al.* (2005b) but this model was (i) two phase (aqueous-gas), (ii) applied for only a PS and ND system WAS and (iii) included only one biodegradable particulate organic (BPO) for PS or WAS digestion. Therefore the planned AD dynamic model is to include three phase (aqueous-gas-solid) mixed weak acid/base chemistry to include mineral precipitation and multiple organic types for anaerobic digestion to facilitate AD of primary sludge (PS) together with WAS within the plant-wide framework. Due to the significant increase in size and complexity to model the WWTP as a whole, the NDBEPR activated sludge system and AD fed NDBEPR WAS required coding in WEST®, which is a program capable of simulating many bioprocesses in various unit operations assembled into a WWTP.
4. Develop a three phase AS dynamic model by extending an existing BEPR AS model, such as activated sludge model number 2 (ASM2; Henze *et al.*, 1995) and ensuring its compatibility with the AD dynamic model mentioned in objective 3 for the plant-wide model development. In addition, this three phase AS model with BEPR is to be extended to plant-wide simulation of BEPR AS with anoxic-aerobic digestion of P-rich WAS with mineral precipitation to produce concentrated dewatering liquor with low N and P.

The main objectives of the research project are therefore to (i) include mineral precipitation into the steady state AD model and (ii) undertake the plant-wide dynamic modelling using the experimental systems and mass balance based steady state model as the basis for calibration and validation.

1.3 NEW KNOWLEDGE CONTRIBUTION

The new knowledge to be contributed by this research is directly tied to the research objectives, which include:

1. The development of a three phase plant-wide model that includes phosphorous. This involves:
    - The development of the mixed weak acid/base chemistry part of the steady state AD model to include mineral (struvite) precipitation and digester pH prediction.
    - The development of a three phase dynamic model that includes phosphorus and mineral precipitation processes in aerobic and anaerobic digestion of concentrated sludge.
2. Investigating the biodegradability of organics within the WWTP, including:
    - The determination of organics biodegradability within the various unit processes of the WWTP and throughout the WWTP primary settling tank (PST) – AD and AS system – AD connecting links.
    - The comparison of the influent unbiodegradable particulate fraction calculated from the ND MLE AS system and NDBEPR AS system, using the same wastewater.
3. Inclusion of the hydrolysis of multiple organic types in the plant-wide model, for the treatment of municipal sewage.

1.3.1 The Development of a Three Phase Plant-Wide Model that Includes Phosphorous

Because of the usefulness and benefits of steady state models, particularly because they require much less input information than dynamic models, both steady state and dynamic simulation plant-wide models are being developed progressively by adding unit operations as information becomes available. Moreover, the development of a mass balance based mathematical model for the entire wastewater treatment plant (WWTP) has, of late, been a major subject of research. Progress to date includes the completion of steady state and two phase kinetic simulation models for nitrification-

denitrification (ND) activated sludge and aerobic (AerD) or anaerobic digestion (AD) of primary and waste activated sludge from N removal systems (Sötemann *et al.*, 2005). Moreover, mass balance C, H, O, N and TOD stoichiometry has also been developed from which the different products exiting the WWTP via the solid, liquid and gas streams can be calculated, such as N loads in recycle streams, methane production for energy recovery and green house gas (CO_2, CH_4) generation (Ekama, 2009).

The primary objective of this investigation is to add phosphorus into this steady state plant-wide model so that the aerobic (AerD) and anaerobic digestion (AD) of WAS from BEPR systems, containing phosphorus accumulating organisms (PAOs), can be modelled. The PAOs introduce several complex issues which require experimental investigation. For instance, the PAOs contain polyphosphate (PP), which is a metal (magnesium (Mg^{2+}), potassium (K^{+}) and calcium (Ca^{2+})) phosphate ($MePO_3$) complex. This may be hydrolysed and released to the bulk liquid at a faster rate than aerobic or anaerobic digestion of the PAO biomass. This affects the N and P nutrient release rates in aerobic and anaerobic digestion (Sötemann *et al.*, 2006) and may also result in precipitation of minerals such as struvite ($MgNH_4PO_4$), calcium phosphate ($Ca_3(PO_4)_2$) and calcite ($CaCO_3$).

Currently, a steady state model including P (Harding, 2009) comprising hydrolysis, stoichiometry and weak acid/base chemistry parts has been completed. This model predicts very well the experimental data not affected by mineral precipitation, but predicts poorly the data affected by mineral precipitation. This is because the steady state mixed weak acid/base chemistry part of the AD model does not include the complexity of three phases (aqueous-gas-solid) and mineral precipitation. Mineral precipitation will be added to the AD and AerD models.

The recent proposals towards the development of whole WWTP simulation models have included only activated sludge model number 1 (ASM1, Henze *et al.*, 1987) and anaerobic digestion model number 1 (ADM1, Batstone *et al.*, 2002) and excluded phosphorus (P). Where P was included, mineral precipitation was ignored. Mineral precipitation significantly reduces the dissolved P recycled back to the influent in the AD dewatering liquor.

The proposed plant-wide kinetic simulation model will comprise a three phase activated sludge model for biological N and P removal, i.e. which includes magnesium (Mg), potassium (K), calcium (Ca), P, PAOs and BEPR, based on strict material (C, H, O, N, P, Mg, Ca and K) mass balances. This model will be modified to include the inorganic settleable solids (ISS) model of Ekama and Wentzel (2004) and combined with the University of Cape Town anaerobic digestion model 1 (UCTADM1) for kinetic simulation (Sötemann *et al.*, 2005b), which also will be extended to include P, PAOs, the AD of P-rich sludge, hydrolysis of multiple organics and the mineral precipitation processes, such as those from Musvoto *et al.* (2000). This dynamic plant-wide model will be validated using the results from the experimental systems and the mass balance based steady state model.

1.3.2 Biodegradability of Organics in the WWTP

Integral to achieving (1) above is determining whether or not unbiodegradable organics from the AS system remain unbiodegradable in the AD system. Biodegradability defines the extent to which organics that enter unit processes of the WWTP can be broken down. In the development of WWTP plant-wide models, the determination of whether or not the biodegradability of these organics remains consistent throughout all the linked upstream and downstream WWTP unit processes is very important when coupling the PST, AS, AerD and AD unit operations. The experimental plan described in Section 3.2 (of Chapter 3) will provide data to determine this.

There are two types of particulate unbiodegradable organics in the AS system (1) those from the influent wastewater (called UPO) and those produced by the biomass in the reactor called endogenous residue (ER). These two concentrations in the VSS of the AS system can be calculated from the experimental data measured on the AS system but their validity is strictly within the framework of the AS model used to calculate them. Therefore, from the experimental data measured on the two MLE systems, one fed raw WW and the other fed settled WW, the UPO in the raw and settled WW and unbiodegradable VSS in the reactor of each system can be calculated. From the

difference between the raw and settled UPO, the UPO in the PS can be calculated. From the experimental measurements on the ADs, the unbiodegradable fractions of the organics fed to them can be calculated, and again the unbiodegradable fraction is strictly valid within the framework of the AD model, because the AS model is for aerobic organisms and AD for anaerobic organisms. If the unbiodegradable fraction of the PS calculated from the AS systems is the same as that calculated from the AD system fed this sludge, then the unbiodegradable organics from the influent as defined by the aerobic AS system, remain unbiodegradable in the AD system. Similarly if the unbiodegradable fraction calculated from the experimental data of the AD system fed WAS is the same as that calculated from the experimental data measured on the AS system, then the endogenous residue (and influent UPO) from the AS system remain unbiodegradable in the AD. If the unbiodegradable fractions remain so between the AS and AD systems it follows also that the biodegradable fractions remain so. Now for the AS system only the live biomass has biodegradable organics. If the AD system fed WAS yields the same biodegradable fraction as the AS system, then this would be an important validation for the active fraction in the AS system being real and no longer only a consequence of the theoretical framework of the AS model.

Over the many years that BEPR research has been conducted at UCT, invariably a N removal MLE system and a P removal UCT system operated in parallel on the same wastewater yield different influent UPO fractions. Since influent UPO is a wastewater characteristic, one expects the same value for ND and NDBEPR AS systems. With WAS from MLE and UCT systems fed to separate ADs (as indicated in Section 3.2), it is possible to check if the difference in influent UPO is real or an artifice of the AS model including P removal.

1.3.3 Hydrolysis in the AD of Multiple Organic Types in Municipal Sewage Sludge

The anaerobic digestion of blended municipal primary sludge (PS) and waste activated sludge (WAS) seems to be an attractive method for environmental protection and energy savings. This is because it has potential benefits such as: dilution of potential toxic compounds, improved balance of nutrients, synergistic effects of microorganisms,

increased load of biodegradable organic matter, increased WAS digestion rate and higher biogas yield (Poggi-Varaldo and Oleszkiewicz, 1992). A disadvantage is significantly increased ammonia and phosphate concentrations in the AD dewatering liquor because the N and P content of WAS is 3 to 4 times higher than PS and the P content up to 15 times higher if the WAS is from a NDBEPR AS system. The organic material that makes up PS and WAS consists of carbon, hydrogen, oxygen, nitrogen and phosphorus, which can be represented by the generic composition formula $C_XH_YO_ZN_AP_B$, where the molar quantities in this generic organic material formula (i.e. X, Y, Z, A and B) for PS ($C_{3.5}H_7O_2N_{0.196}P_{0.01}$) are different from those of WAS ($C_5H_7O_2NP_{0.12}$). However, the PAOs are known to store polyphosphate, hence, their generic formula is as for ordinary WAS biomass but extended to include the PP, i.e. ($C_XH_YO_ZN_AP_B.(Mg_cK_dCa_ePO_3)_q$).

It is not clear whether anaerobic digestion of waste activated sludge (WAS) together with primary sludge (PS) has a beneficial effect on the hydrolysis rate of WAS compared with anaerobically digesting the WAS (with its high P content) by itself. The determination of hydrolysis rates of the PS, ND WAS and PS-WAS blends and NDBEPR WAS is part of the experimental set up, for the development of a plant-wide model that can accommodate the various municipal sludge types. The experimental set up will provide data to answer this question. If there is little advantage of co-digesting PS and WAS, it may be better to keep the PS and WAS separate and stabilize concentrated WAS in an anoxic- aerobic digester to (1) nitrify and denitrify the ammonia released and (2) allow universal precipitation to reduce the N and P concentrations in the dewatering liquor. For this reason the project includes the development of a three phase (aqueous-gas-solid) kinetic model for aerobic digestion of WAS from a NDBEPR system.

1.4 OVERVIEW OF REPORT

This thesis report comprises of various sections which have been divided over eight main chapters. The report is introduced through describing the background to the problem and clarifying the objectives to be met (Chapter 1) after which the literature related to the project is reviewed (Chapter 2). Following this is the

description of materials and methods used in carrying out the research (Chapter 3) then the presentation of the results and their evaluation (Chapter 4). Thereafter, the steady state model, with particular emphasis on the sludge characterisation (Chapter 5), kinetics of sludge hydrolysis, stoichiometry and weak acid/base chemistry (Chapter 6), is described through the use of experimental findings, theory, conceptual ideas and evaluated hypotheses. This is followed by a description of the dynamic three phase plant-wide model (Chapter 7), its preparation using the modelling platform WEST ® and its calibration using experimental results. Finally the report is concluded and a few recommendations are also made (Chapter 8). The Figure 1.1 below gives a detailed overview of the report.

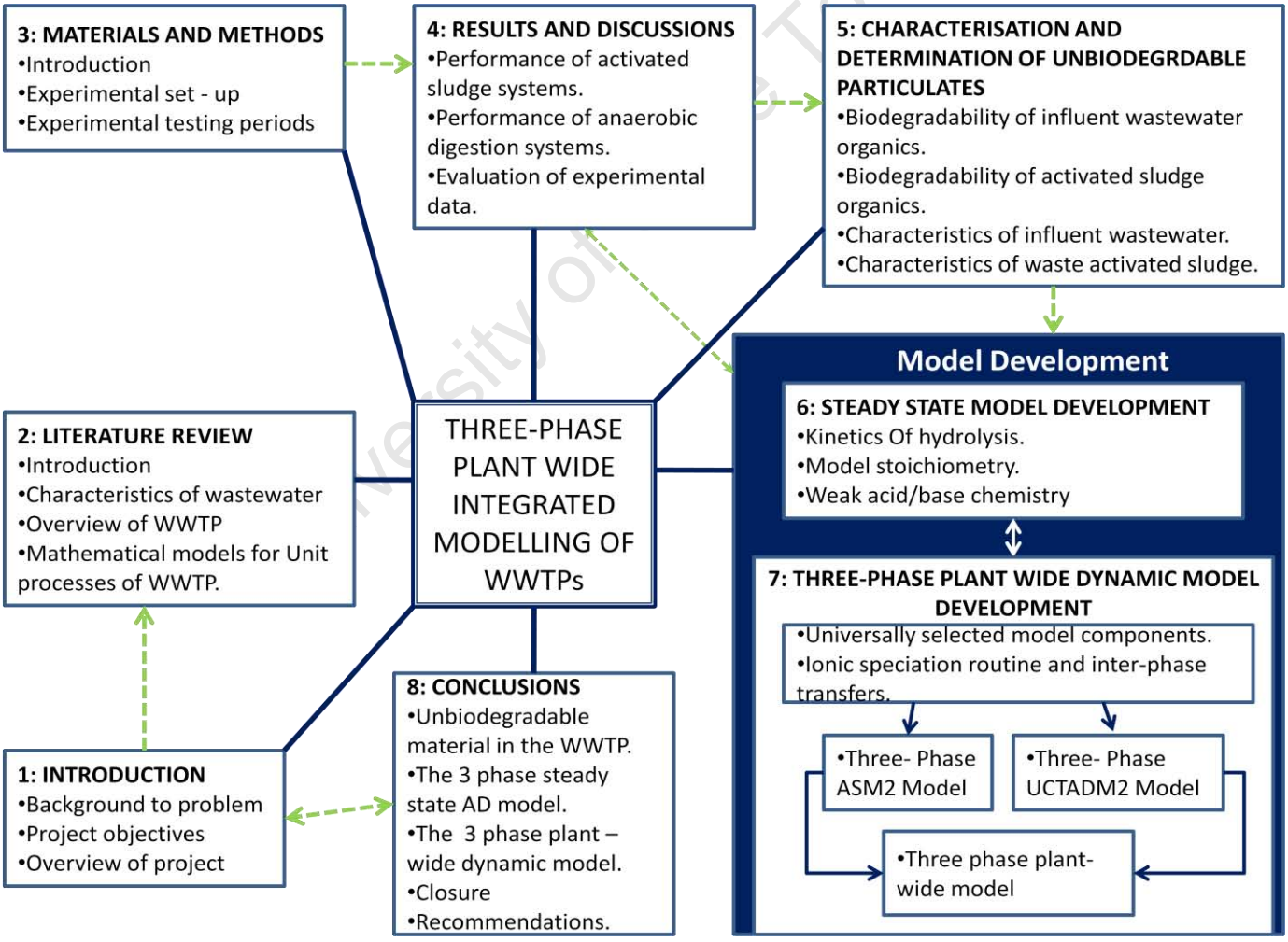

Figure 1.1: *A mind map showing an overview of the project report, including the main contents of each chapter and the chapters that are associated with each other (green hidden lines).*

CHAPTER 2: LITERATURE REVIEW

2.1 INTRODUCTION

Wastewater (WW) is known to have various detrimental effects on the environment such as groundwater and stream contamination and the transmission of human infectious waterborne diseases (e.g. cholera and typhoid). Moreover, once water pollution reaches water bodies, it stimulates harmful overgrowths of algae, which can endanger aquatic life through direct toxic effects or reduction in water clarity and oxygen. Wastewater comprises of various elements, the extent to which these individual elements are widely held depending on the source of pollution. Different microorganisms pre-dominate different water bodies, according to the nutrient availability and prevalent conditions necessary for the organism to carry out its metabolism. Various studies have been performed on these microorganisms and their metabolism in order to be able to optimize their growth and employment in the water treatment processes. A wastewater treatment plant (WWTP) is able to treat the water through providing conditions necessary for the physical separation of the various solid, liquid and gas phases in the wastewater and controlled, profitable utilization of the various elements in the wastewater. A general WWTP layout is shown in Figure 2.1 with aerobic (AerD) or anaerobic digestion (AD)of primary sludge (PS) and waste activated sludge (WAS).

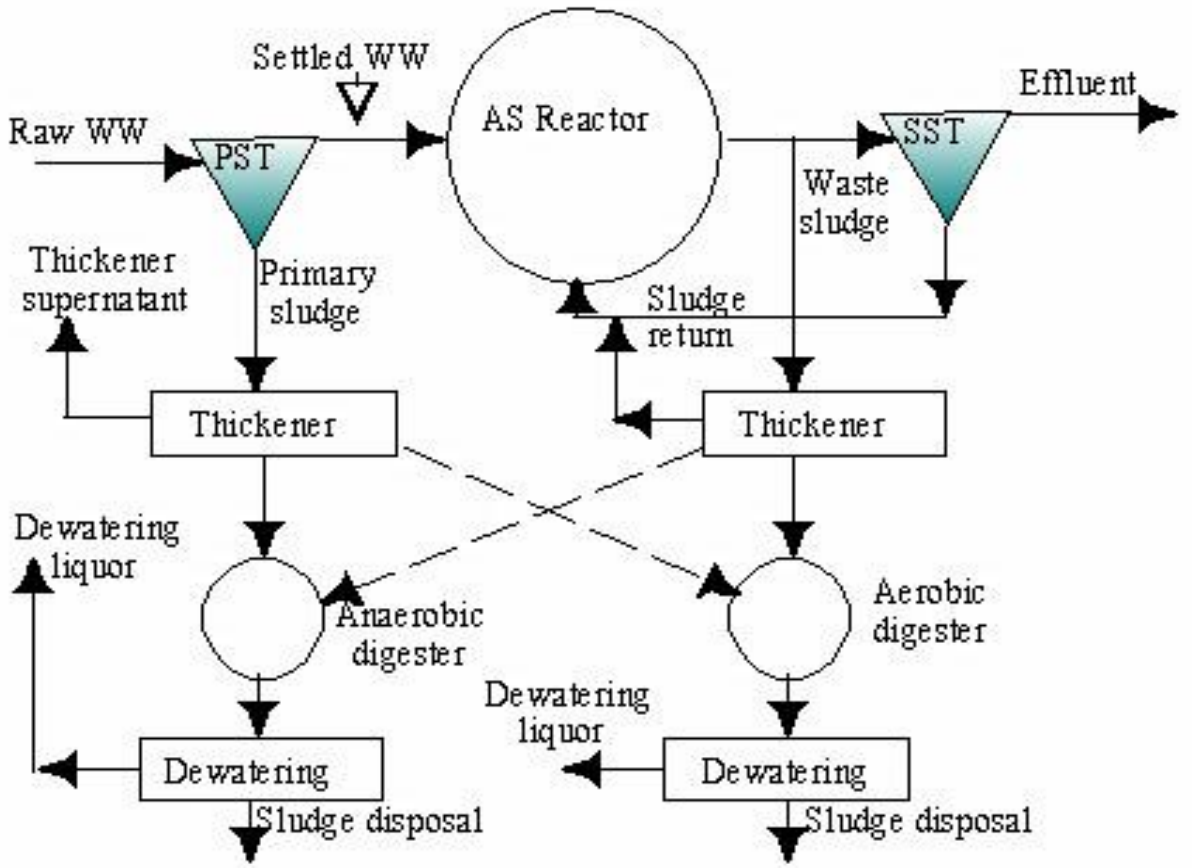

Figure 2.1: *Simplified WWTP layout*

Performing WWTP system optimization involves reviewing plant operations, facilities and field-testing to determine unit capacities and process bottlenecks. It is used as a means to bring about improvements or meet restraints within existing WWTP facilities through either operational changes or minor upgrades. There is increased pressure towards the optimization of WWTP facilities as effluent criteria and safety requirements become more stringent and available funds for investment, operation (especially energy costs) or upgrade become less available. Thus, the selection of the most appropriate plant design would require the measurement of numerous variables, which could consume a lot of time and become a difficult task, even for experienced designers. It is for this reason that predictive models for target quality variables have been widely considered.

Historically, wastewater treatment unit operation models such as activated sludge (AS) and AD have been developed in isolation. Unit operations have different functions and thus models for them are inherently different in their physical, chemical and biological

processes on which they are based. These differences have resulted in the development of models with different compound variables, e.g. Activated Sludge Model No 1 (ASM1, Henze *et al.*, 1987) and Anaerobic Digestion Model No 1 (ADM1, Batstone *et al.*, 2002). Therefore, incompatibilities exist when trying to couple unit operation models, i.e. the different unit operation models speak different languages. For example, state variables required in one model may be non-existent in other models - carbon is usually not included in AS models, but is required in AD models to predict the gas production and composition. Also, biodegradable compounds in one model may not be biodegradable in another (Ekama *et al.*, 2006; Vanrolleghem *et al.*, 2005).

Recent approaches to overcome these incompatibility problems to develop plant-wide WWTP simulation models include (i) the continuity based interfacing method (CBIM) of Vanrolleghem *et al.* (2005) and Volcke *et al.* (2006), (ii) the 'supermodel approach' of Jones &Takács (2004 cited in Grau *et al.*, 2007) and Seco *et al.* (2004 cited in Grau *et al.*, 2007), (iii) the transformation based approach of Grau *et al.* (2007) and (iv) the mass balances based plant-wide WWTP model approach of Ekama *et al.* (2006). All of these approaches have been aimed at overcoming the model interfacing difficulties caused by state variable incompatibilities. A general theme in these modelling approaches is the use of compounds, which mainly contain carbon (C), hydrogen (H), oxygen (O), nitrogen (N) and phosphorus (P), in their elemental composition forms, viz. $C_XH_YO_ZN_AP_B$. However, recent proposals towards the development of plant-wide WWTP simulation models have included only ASM1 and ADM1 and either excluded P or where P was included mineral precipitation was ignored in the AD part. Mineral precipitation significantly reduces the dissolved P recycled back to the influent in the AD dewatering liquor.

Because of the usefulness and benefits of steady state models, particularly since they require much less input information than dynamic models, both steady state and dynamic plant-wide models are being developed progressively by adding unit operations as information becomes available. The University of Cape Town (UCT) Water Research Group (WRG) has, of late, been involved in the development of a mass balance based mathematical model for the entire WWTP as a major subject of research. Progress to date includes the completion of steady state and two phase kinetic simulation models for

nitrification-denitrification (ND) activated sludge (AS) and aerobic (AerD) or anaerobic digestion (AD) of primary and waste activated sludge from N removal systems (Sötemann *et al.*, 2005). Moreover, mass balance carbon (C), nitrogen (N), oxygen (O), hydrogen (H) and total oxygen demand (TOD = COD + 4.57 TKN, see Section 5.4.5) stoichiometry has also been developed from which the different products exiting the WWTP via the solid, liquid and gas streams can be calculated, such as N loads in recycle streams, methane production for energy recovery and green house gas (CO_2, CH_4) generation (Ekama, 2009).

This thesis involves (1) a study on the biodegradability and kinetics of hydrolysis of primary and secondary municipal sewage sludge, a section that was done together with a parallel study on the stoichiometry of the AD of NDBEPR WAS (Harding, 2009) in order to extend the current plant-wide WWTP steady state model (Sötemann *et al.*, 2005) and (2) the use of this extended steady state model as a basis for the development of a dynamic model that could be used as a tool to simulate the plant against changing flows and material loads or to evaluate the efficiency of different operating strategies and upgrades. This proposed plant-wide dynamic model will comprise a three phase C, H, O, N, P mass balance based activated sludge model for biological N and P removal, i.e. which includes magnesium (Mg), potassium (K), calcium (Ca), P, P - accumulating organisms (PAOs) and biological excess P removal (BEPR). The PAOs introduce several complex issues, which require experimental investigation. For instance, the PAOs contain polyphosphate (PP), which is a metal (Mg, K and Ca) phosphate ($MePO_3$) complex. This may be hydrolysed and released to the bulk liquid at a faster rate in aerobic or anaerobic digestion than the PAO biomass. This affects the N and P nutrient release rates in aerobic and anaerobic digestion (Sötemann *et al.*, 2006) and also may result in precipitation of minerals such as struvite ($MgNH_4PO_4$), calcium phosphate ($Ca_3(PO_4)_2$) and calcite ($CaCO_3$).

This literature review includes a general outline of a WWTP, treating municipal wastewater and brief descriptions of the unit processes that make up this treatment plant, with particular reference to the unit processes that shall be used in this project. Moreover, the current progress in the modelling of WWTP systems (activated sludge aerobic digestion and anaerobic digestion units) treating municipal wastewater is discussed before closure.

2.2 NATURE AND CHARACTERISTICS OF MUNICIPAL WASTEWATER

Municipal wastewater is characterised according to quantities of organic and inorganic particulate or soluble material in the water.

Inorganic substances are those traditionally considered not to be of biological origin (e.g. sand, salt, iron, calcium salts and other mineral materials), which may also be dissolved in the form of chemical compounds or inorganic synthetic fertilizers.

Organic matter is that which has come from a recently living organism and is capable of decay, or the product of decay (e.g. decaying or living microorganisms, plants and animals). Organic material can be unbiodegradable (e.g. plastics and polyester) or biodegradable (e.g. food particles and cotton), i.e. can be broken down physically and/or chemically by the action of living things such as bacteria and other micro organisms into simple, stable products such as carbon-dioxide and water. Raw municipal wastewater usually contains higher concentrations of biodegradable matter (greater than 80%) and lower concentrations (about 10% to 20%) of unbiodegradable material. The biodegradable and unbiodegradable organics are usually broken down further into those that are soluble and those that are in particulate form (Davies, 2005).

2.3 OVERVIEW OF WASTEWATER TREATMENT PLANT (WWTP)

Each unit operation of a WWTP involves a physical or a chemical/biochemical process purposed towards removal or alteration of one contaminant or more in the wastewater.

Municipal wastewater is largely at solid and liquid phase, but could also exist at gas phase. The pollutant, if dissolved, requires transformation from the liquid phase to the gas or solid phase for its removal from the water. Furthermore, the solids can be physically separated from the liquid phase and concentrated within lower volumes. With the capability of separating the various state-phases (solid, liquid and gas) in wastewater, the WWTP treats the influent wastewater and has the solids removed from this influent, before (primary sludge) or/and after the biological transformation (secondary sludge) of

the dissolved pollutant. The solids are then treated through biological stabilization and thickening.

2.3.1 Primary Treatment of Raw Wastewater

Primary treatment involves removal of the material that can be easily collected from the raw wastewater and disposed of. The typical materials that are removed during primary treatment include fats, oils, and greases, sand, gravels and rocks (also referred to as grit), larger settleable solids including human waste and floating materials. Three major stages that occur in primary treatment of sewage include screening, de-gritting and finally primary settling of raw wastewater.

2.3.1.1 Primary Settling Tank

Primary settling tanks (PSTs) are employed to remove readily settleable particles from the wastewater. The settleable particles, settle at the bottom of the tank to form primary sludge and the settled influent wastewater proceeds for biological treatment. The purpose of the PST is to reduce the organic (COD) load, hence cut costs due to reactor size, aeration power and secondary sludge production. The amount of settleable material in raw wastewater determines the quantity of nutrient removal in the Primary Settling Tank (PST). This is because in municipal wastewater about 80% of this settleable material is removed; usually constituting about 40% COD and 45% total solids of the raw wastewater (Marais and Ekama, 1976). The Figure 2.2 below shows a typical depiction of a PST in a WWTP.

Figure 2.2: *Photo of a typical primary settling Tank*

2.3.2 Secondary Treatment of Wastewater

Secondary treatment is designed for the substantial removal of the biological content (mainly carbon, nitrogen and phosphorous) of the sewage such as are derived from human waste, food waste, soaps and detergent. The majority of municipal and industrial plants treat the settled sewage liquor using aerobic biological processes. This is because, to be effective, the active microorganisms require both oxygen and a substrate on which they have their being. The bacteria consume biodegradable soluble organic pollutants, such as organic short-chain carbon molecules, fats, etc. and also enmesh the less soluble fractions to form flocculi (Davies, 2005).

Secondary treatment systems are classified as fixed-film or suspended growth. Fixed-film treatment processes involve systems such as trickling filters where the biomass grows on media such as stones and the sewage passes over its surface. Settled sewage is usually used in these systems because the raw sewage would cause blockages of the rotating sewage distribution system on the top of the stone beds. In suspended growth systems, such as activated sludge, the biomass is well mixed with the sewage. However, fixed-film systems are more able to cope with drastic changes in the amount of biological material and can provide high removal rates for organic material and suspended solids than suspended growth systems (Beychok, 1971).

2.3.2.1 Biological Processes

The biological processes that occur in the secondary treatment wastewater refer to the growth and death behaviour of the mediating microorganisms. The growth behaviour of organism mass involves the utilization of a fraction of the biodegradable organic material (S_b) introduced into the bulk liquid, as the nutrient source for synthesis of new organism mass (anabolism) and the remaining fraction to provide energy for cell maintenance (catabolism). Oxygen would be required, as a terminal electron acceptor, to provide the energy needed for catabolism. However, nitrates or sulphates can also be used as alternative electron acceptors, in the absence of oxygen, for the oxidation of the substrates at a lower efficiency. The death behaviour of microorganisms involves loss of bacterial

mass through endogenous respiration. Endogenous respiration entails the utilization of a fraction of the live organism mass for catabolism while the remaining fraction (about ⅕) accumulates as unbiodegradable organic material known as endogenous residue (Marais and Ekama, 1976).

2.3.2.2 Activated Sludge Systems

Activated sludge (AS) systems are like miniature ecosystems, with biotic (competition, symbiosis and predation) and abiotic interrelationships occurring (Davies, 2005). In the AS systems the wastewater is retained in mixed tank(s) and the microorganisms, which make up the activated sludge, are suspended in the wastewater undergoing treatment. To ensure that this suspension of biomass occurs, it is necessary to create some form of turbulence through mixing and/or aeration. The combination of wastewater and biological mass is commonly known as mixed liquor. In all activated sludge plants, once the wastewater has received sufficient treatment, it is passed onto settling tanks or through membranes to separate the organisms from the clear effluent. The organisms are returned to the beginning of the mixed tank to continue treating the incoming water while the treated supernatant is discharged or taken through further final treatment. The fraction of the bacterial flocculi returned is called return activated sludge (RAS). Excess sludge is regularly removed from the treatment process to maintain a consistent sludge age (R_s) and to keep the ratio of biomass to food supplied (sewage or wastewater) in balance. This is called the waste activated sludge (WAS) and requires further treatment e.g. by digestion, either under anaerobic or aerobic conditions prior to disposal or utilization for agricultural purposes (Beychok, 1969). Therefore, R_s is a principle AS system design parameter that defines the average amount of time (in days) that activated sludge has been in the reactor(s) of the AS system. This is usually longer than the hydraulic retention time (R_{hn}) which defines the time that the soluble material has taken to go through the AS system reactor(s) (Marais and Ekama, 1976).

In poorly managed activated sludge systems, a range of mucilaginous filamentous bacteria can develop which produce a sludge that is difficult to settle and can result in

problems such as the sludge blanket decanting over the weirs in the settlement tank to severely contaminate the final effluent quality (Davies, 2005).

A photo showing a typical depiction of the activated sludge unit operation in a WWTP is given in Figure 2.3. The AS systems that shall be used in this research are Nitrification-Denitrification (ND) systems and Biological Excess phosphorus Removal (BEPR) systems. These systems and the processes are briefly described below.

Figure 2.3: *Photo of the activated sludge unit operation in a treatment plant, valves in the walls are usually provided to control flow from one zone (anaerobic, anoxic or aerobic) to another.*

Nitrification – Denitrification (ND) Systems

ND systems are used in WWTP within the secondary (biological) phase of wastewater treatment for removal of nitrogen from the wastewater. Nitrogen removal is desirable to reduce nutrient levels to the receiving water thereby inhibiting algae growth and reducing oxygen demand on the water.

Nitrification is the biological process whereby free and saline ammonia (FSA, in mgN/*l*) is converted to nitrate (NO_3^-) in a two-step process. It is mediated by two autotrophic bacteria groups, *Nitrosomonas*, which convert (oxidize) FSA to nitrite (NO_2^-) and *Nitrobacter*, which convert the nitrite to Nitrate. The *Nitrosomonas*, being slower, represent the rate limiting bacterial group. Thus, it is assumed that *Nitrobacter* rapidly convert all the

nitrite produced to nitrate. As the sludge age decreases, the FSA concentration in the reactor increases. Usually, a sludge age of greater than seven days is necessary to ensure that autotrophic organisms are not washed out of the system and for the nitrification process to be effective. Moreover, since nitrifiers are obligate aerobes, they require a sufficient supply of dissolved oxygen for their growth. The oxygen demand for nitrification is essentially 4.57 mgO/mgN times the mass concentration of nitrate produced per day (Marais and Ekama, 1976).

Therefore, with knowledge of the flux of nitrates generated (FNO_{3_gen}, in mgNO_3-N/d) the oxygen used in the nitrification process (FO_n, in mgO/d) can be calculated:

$$FO_n = 4.57 \cdot FNO_{3\_gen} \qquad (2.3.1)$$

To complete nitrogen removal from the wastewater, the nitrate produced in nitrification has to be converted to nitrogen gas (N_2), through a process known as denitrification. The reduction of nitrate to nitrogen gas requires anoxic conditions together with the provision of an electron donor, usually obtained from organic matter, sulphides, or in some cases an added donor like methanol. Once the nitrogen gas is produced, it is released to the atmosphere and thus removed from the water.

Apart from nitrogen removal, ND systems also operate to remove inflent biodegradable organics COD (S_{bi}, in mg COD/*l*). This is performed through the complete use of S_{bi} for growth of biomass (i.e. ordinary heterotrophic organisms - OHOs), which can physically be separated from the effluent. In steady state conditions, if the AS system sludge age is long enough for this complete use of S_{bi} the effluent can be said to entirely comprise of unbiodegradable soluble organics COD (S_{us}).

Two–thirds of the electrons in the S_{bi} are used in the formation of active biomass (anabolism) and the rest of the electrons in the influent biodegradable organics are passed to oxygen (catabolism). The two-thirds of electrons used for anabolism represent the yield for biomass growth (Y_H = 0.67). This yield, which is a COD fraction, can be employed in terms of a mass fraction when it is divided by the organism mass f_{cv} value (which is the electron donating capacity (COD) to molar mass ratio, COD/VSS ≈1.48). Hence as a mass

fraction, the Y_H has a value of 0.45. However, the other electrons passed to oxygen for catabolism represent the energy to produce new cell mass, which is then lost as heat (Marais and Ekama, 1976).

A fraction of the total organism mass formed can be progressively used to provide energy for cell maintenance, in a process known as endogenous respiration. The net loss due to endogenous respiration, per unit time, is proportional to the active mass in the bulk liquid. Thus, this endogenous respiration occurs at a certain rate according to the active biomass mediating the process, i.e. b_H of 0.24 (/d) for OHOs (Marais and Ekama, 1976).

The steady state equation used in modelling the concentration of organism active OHO mass (X_{BH}) was derived by Marais and Ekama (1976) as:

$$X_{BH} = \frac{Y_H (S_{bi} - S_b) \cdot R_s}{(1 + b_H \cdot R_s) \cdot R_{hn}} \quad (2.3.2)$$

Only a fraction of the organism active mass, which is used for endogenous respiration, is biodegradable. The other fraction of live biomass cannot be used further (f'_{epH} = 0.2) and remains as unbiodegradable organic material known as endogenous residue. Marais and Ekama (1976) derived the following steady state equation used in modelling the concentration of this endogenous residue (X_e, in mg/*l*):

$$X_e = f'_{epH} \cdot b_H \cdot X_{oh} \cdot R_s \quad (2.3.3)$$

Apart from the organism active mass and endogenous residue, the AS system reactor(s) mixed liquor also comprises of unbiodegradable particulate organic mass (X_i, in mg/*l*) from the influent that has been enmeshed with the sludge and accumulated in the reactors with sludge age. Marais and Ekama (1976) gave the formulation to calculate the steady state concentration of this X_i:

$$X_i = X_{ii} \cdot R_s = S_{ti} \cdot f_{S'up} \cdot \frac{R_s}{f_{cv}} \quad (2.3.4)$$

Where, X_{ii} is the influent X_i (mg/*l*) concentration, S_{ti} (mgCOD/*l*) is the total influent COD concentration and $f_{S'up}$ is the fraction of unbiodegradable particulate COD.

With the steady state activated sludge component (OHOs, X_e, X_i, S_{us}) masses known Marais and Ekama (1976) were able to determine the total mass of volatile solids in the AS reactor(s). This is represented by Equation 2.3.5 below:

$$MX_v = M_{sti} \cdot \left\{ (1 - f_{up} - f_{us}) . \left\lfloor \frac{(1 + f_{ep,H} . b_H . R_s) Y_H . R_s}{(1 + b_H . R_s)} \right\rfloor + \left\lfloor \frac{f_{up} . R_s}{f_{cv}} \right\rfloor \right\} \quad (2.3.5)$$

Moreover, the flux of oxygen demanded for the degradation of organics in the AS system reactors (FO_c), from catabolism and endogenous respiration at a steady state operation, could be determined by Marais and Ekama (1976) with the following Equation 2.3.6:

$$FO_c = \left(FS_{bi} \cdot (1 - f_{cv} \cdot Y_H)\right) + \left(FS_{bi} \cdot b_H \frac{(1 - f_{ep,H})}{1 + (b_H \cdot R_s)} \cdot Y_H \cdot R_s \cdot f_{cv} \right) \quad (2.3.6)$$

Where FS_{ti} (mgCOD/d) and FS_{bi} (mgCOD/d) are the fluxes of total influent COD and biodegradable influent COD respectively.

MLE Process

The Modified Ludzack-Ettinger (MLE) system is a nitrification-denitrification system, which is divided into anoxic and aerobic zones to ensure that the nitrates are utilized in the denitrification process. The first stage in the treatment process is anoxic, where influent wastewater and return sludge from the Secondary Settling Tank (SST) are mixed together with nitrate-rich mixed liquor from the aerobic tank. The influent wastewater serves as the carbon source for bacteria, return-activated sludge from the SST provides the active organisms and the sludge recycle from the aerobic tanks provides the nitrates, which serve as the electron acceptors in the process of denitrification. The second stage is the aerobic zone, where the nitrates are formed from free and saline ammonia (FSA) in the waste activated sludge and organics are transformed to active mass by heterotrophic organisms (Henze *et al.*, 2008).

Biological Excess Phosphorus Removal (BEPR) systems

Phosphorous is removed from wastewater by transforming it from the dissolved liquid phase to the solid phase. This can be done chemically, biologically or both. When done

chemically, aluminium sulphate or iron salts is added to the water to precipitate with the phosphate leaving the sulphate or chloride in solution. When done biologically phosphorus accumulating organisms (PAOs), able to take up large concentrations of phosphorous, are encouraged to grow in the Activated Sludge (AS) system.

The PAOs require rapidly biodegradable organics (S_{bsi}, in mgCOD/*l*) and high concentrations of phosphorus in the wastewater. Moreover, for phosphorus removal to occur, the AS system should be configured to include alternating aerobic and anaerobic conditions.

However, some BEPR systems are extended to NDBEPR systems via the inclusion of anoxic conditions, hence allowing nitrification and denitrification to also take place. Thus the anaerobic mass fraction (f_{Xa}) provided should also be adequate for the complete removal of phosphorus from the system (Wentzel *et al.*, 1990).

Wentzel *et al.* (1990) discovered that the mass of substrate required to be sequestered by the PAOs (MS_{eq}) in the NDBEPR systems could be calculated using the Equation 2.3.7:

$$MS_{eq} = \left(S'_{bsi} - (1+r)\cdot S_{bsn}\right)\cdot Q_i \qquad (2.3.7a)$$

Where:

- The ratio of anoxic to anaerobic reactor recycles flow to influent flow is denoted by the letter r.
- Q_i is the influent flow rate (*l*/d).
- S'_{bsi} (mgCOD/*l*) is the readily biodegradable COD (RBCOD) in the influent that is ready for utilization and conversion by PAOs, calculated using the Equation 2.3.7c below.
- S_{bsn} is the RBCOD concentration in the anaerobic reactor, calculated using the Equation 2.3.7b below.

$$S_{bsn} = \frac{\frac{S'_{bsi}}{(1+r)}}{\left(1 + k\cdot X_{B,Hn}\cdot\frac{R_N}{1+r}\right)} \qquad (2.3.7b)$$

Where:

- k is the first order rate constant for conversion of S_{bsn} by PAOs (with a measured value of $0.06 d^{-1}$).
- $X_{B,Hn}$ is the concentration of non-PAO organisms (mainly OHOs) in the anaerobic reactor, i.e. $X_{B,Hn} = f_{Xa} \cdot X_{BH}$, with X_{BH} determined using Equation 5.3.1d in Chapter 5.
- R_N is the sludge age of the anaerobic reactor (d).

$$S'_{bsi} = (S_{tsi} - S_{use}) - (r \cdot 8.6 \cdot NO_{3anaerobic}) \quad (2.3.7c)$$

Where:

- S_{tsi} is the total soluble organic COD in the influent (in mgCOD/*l*).
- S_{use} (which equals S_{usi}) is the concentration of total unbiodegradable soluble COD in the effluent (in mgCOD/*l*).
- The value of 8.6 represents observed COD removal per anaerobic reactor nitrate concentration.
- $NO_{3\ anaerobic}$ is the concentration of nitrates in the anaerobic reactor (mgNO_3-N/*l*).

NDBEPR systems thus provide an environment conducive for the growth of mixed cultures of organisms (OHOs and PAOs). In consideration of this, Wentzel *et al.* (1990) calculated the flux of oxygen used in catabolism and endogenous respiration (FO_c), at steady state operation, as:

$$FO_c = (FS_{bi} \cdot (1 - f_{cv} \cdot Y_H)) + \left((FS_{bi} - FS'_{bsi}) \cdot \left(b_H \cdot \frac{(1 - f_{ep,H})}{(1 + b_H \cdot R_s)} Y_H \cdot R_s \cdot f_{cv} \right) \right) + \left(FS'_{bsi} \cdot b_G \cdot \frac{(1 - fe_{p,G})}{(1 + b_G \cdot R_s)} Y_G \cdot R_s \cdot f_{cv} \right) \quad (2.3.8)$$

Where the yield for PAO biomass growth ($Y_G = 0.45$) is the same as that of OHOs but the rate of endogenous respiration ($b_G = 0.04$ /d) and fraction of endogenous residue to active biomass ($f_{ep,G} = 0.25$) are different.

Moreover, for NDBEPR systems with mixed cultures of OHOs and PAOs (Wentzel *et al.*, 1990), the total mass of volatile solids in the AS reactor(s) (MX_v, in mg) is represented by the Equation 2.3.9 below:

$$MX_v = FS_{ti}\left\{\left(\left(1 - f_{S'up} - f_{S'us} - \frac{S'_{bsi}}{S_{ti}}\right)\cdot\left(\frac{\left(1 + f_{ep,H}\cdot b_H \cdot R_s\right)\cdot Y_H \cdot R_s}{1 + b_H \cdot R_s}\right)\right) + \left(\frac{S_{'bsi}}{S_{ti}}\cdot\left(\frac{\left(1 + f_{ep,G}\cdot b_G \cdot R_s\right)\cdot Y_G \cdot R_s}{1 + b_G \cdot R_s}\right)\right) + \left(\frac{f_{S'up}\cdot R_s}{f_{cv}}\right)\right\} \quad (2.3.9)$$

Where $f_{'Sus}$ is the fraction of unbiodegradable soluble COD in the influent.

The NDBEPR Process

The Nitrification-Denitrification Biological Excess phosphorus Removal (NDBEPR) system is a system divided into anaerobic, anoxic and aerobic zones. In the anaerobic zone, the influent's SCFA content is taken up by the phosphorus accumulating organisms for energy and phosphorus is released in the process. The anoxic zone is included in order for denitrification to occur, thus protecting the biological excess phosphorus removal system from the detrimental effect of recycling nitrate to the anaerobic reactor. Hence the recycle from the aerobic to anoxic reactor needs regulation such that a minimum quantity of nitrate is recycled to the anaerobic reactor. In the aerobic zone phosphorus is taken up by PAOs and the ordinary heterotrophic organisms (OHOs), which also exist in this system, use wastewater organics for energy and growth (Wentzel *et al.*, 1990).

2.3.2.3 Composition of the Activated Sludge (AS)

The mixed liquor in the waste activated sludge system contains a wide variety of microorganisms. Usually, microorganisms that fulfil a particular function in the AS system are grouped together as a single entity, which is known as a "surrogate" organism. The "non-organism" components of the waste activated sludge systems are also all grouped together, e.g. as inert organics. Together, the surrogate organism and non-organism groups make up the WAS Mixed liquor Settleable Solids (MLSS) (Beeharry *et al.*, 2002).

In a NDBEPR system treating municipal wastewaters a mixed culture of organisms would develop. They can be categorized into five groups:

1. Phosphorous accumulating organism's (PAO's) active biomass, which mediate BEPR and removal of organics.
2. Ordinary heterotrophic organism's (OHO's) active biomass, mediating denitrification and removal of organics.
3. Autotrophic nitrifying organism's (ANO's) active biomass, mediating nitrification.
4. The endogenous residue produced from OHOs, PAOs and ANOs.
5. Influent inert material that remains conserved through the activated sludge process.

In an ND system all the above organisms are present except the PAOs, (i.e. 1 and 2 of the list) since the conditions are usually not conducive to their growth. Although all the above five groups are present in the NDBEPR system, investigations of Wentzel *et al.* (1989a, 1989b,1990) show that the PAO and OHO organism populations appear to act independently of each other in these mixed cultures and only tend to interact in the anaerobic zone. In this zone the rapidly biodegradable COD (RBCOD) component of the influent is converted to short chain fatty acids (SCFA) by the OHO's. The SCFA is, in turn, sequestered by the PAOs at a much faster rate than the RBCOD conversion. The influent COD is hence split into two fractions, one to be utilized by the PAO's and the other by the OHO's in order to determine the right sludge characteristics. The slowly biodegradable COD (SBCOD) of the influent usually requires a break down (hydrolysis) to RBCOD before it can be utilized by the microorganisms. This hydrolysis is a relatively slow process in the AS system. It is usually accepted that the RBCOD component of the influent wastewater is virtually all utilized by the PAO's (Wentzel *et al.*, 1990) and the influent SBCOD, which requires slow conversion to RBCOD, is taken up by the OHOs.

Phosphorus Accumulating Organisms (PAOs)

PAOs are organisms that develop the ability to store large quantities of phosphates, when they are subjected to alternating anaerobic and aerobic conditions by being recycled between the two flows and supplied with RBCOD (Rapidly Biodegradable Chemical Oxygen Demand) in the substrate feed. This happens because they are able to store phosphate internally, as chains of polyphosphate (PP) and other forms, at the expense of

carbon in the aerobic conditions and carbon at the expense of PP at the anaerobic zone of the AS system (Daigger *et al.*, 1999). The PP is a high-energy storage molecule that upon hydrolysis can supply ample energy for biochemical reactions within the cell. Thus the PAOs can use this metabolism to provide them with a selective advantage within the mixed microbial community of the activated sludge (AS) by consuming and storing readily biodegradable organics (RBCOD) as internal storage compounds (poly-3-hydoxyalkanoates [PHA]). Since RBCOD is stored in anaerobic conditions, without the presence of an external electron acceptor such as nitrate or oxygen, the energy and reduction equivalents have to be generated from the degradation of the internally stored PP and glycogen respectively. Therefore, with this degradation, the phosphate is released at the anaerobic stage of the AS system. Under subsequent aerobic conditions, the PAOs consume the stored PHA as a carbon and energy source for cell growth and maintenance using oxygen or nitrate as electron acceptor. The energy is also utilized in the uptake of ortho-phosphate (OP), used to manufacture PP. Thus a net phosphorus (P) removal can be achieved by wasting excess sludge of high P content since the aerobic phosphorus uptake is greater than the anaerobic P release (Liu *et al.*, 1996).

To favour the growth of the PAOs, acetate can be added as an additional carbon source. Moreover, phosphate loading is also essential for the development of the PAOs capacity for phosphorus accumulation. Calcium, magnesium and potassium are the principal metal components of PP granules and may be required in the influent for PP accumulation in the biological phosphorus removal process (luz *et al.,* 2004).

During investigations on BEPR systems by Hu *et al.* (2000) it was shown that under certain conditions PAOs are capable of utilizing nitrate as electron acceptor, resulting in the development of de-nitrifying phosphorus accumulating organisms (DPAOs). Conditions for this occurrence include the nitrate load to the anoxic reactor exceeding the OHO denitrification potential in the anoxic reactor and/or a high frequency of exposure of the activated sludge to anoxic rather than aerobic conditions. Nitrate is not as efficient as oxygen for phosphorus (P) uptake, thus DPAOs have a significantly low BEPR performance compared with the aerobic phosphorus uptake PAOs (APAOs) which use oxygen rather than nitrate as a terminal electron acceptor. Both populations (DPAOs and

APAOs) essentially compete for the same substrate (short chain fatty acids, such as acetate) and active APAOs will always out-compete DPAOs, via the organisms yield. Moreover, with limited nitrate available, OHOs tend to out-compete PAOs for nitrate.

In a study of BEPR system performance, Smolders *et al.* (1994a and 1994b) noted an increase in the ratio of phosphorus released to acetate taken up, with increasing pH. Liu *et al.* (1996) and Romansky *et al.* (1997) observed that this higher pH led to a greater phosphorus release, with the use of acetate wastewater, due to the increase in energy requirement for acetate transportation. The same result was reported by Pijuan *et al.* (2004) by observing phosphorus performance and propionate transformation using propionate as the sole carbon source. It was thus suggested that the pH in the BEPR system anaerobic phase should be maintained greater than 7.25 to enhance the rate of acetate uptake by PAOs (Liu *et al.*, 1996).

Ordinary Heterotrophic Organisms (OHOs) and Autotrophic Nitrifying Organisms (ANOs)

Heterotrophic organisms are a group of microorganisms which, when in the aerobic zone, degrade (oxidise) the organic compounds to energy, CO_2 and water. In this process more heterotrophic organisms are formed so that the energy is transformed to mass.

Autotrophic nitrifying organisms (ANOs) also require aerobic conditions for their growth and for the conversion of ammonia to nitrate (nitrification). To complete the nitrogen removal process, facultative heterotrophs biologically convert the nitrates to nitrogen gas (denitrification). This process occurs in the anoxic zone where the nitrate, instead of oxygen, is used as the terminal electron acceptor (Marais and Ekama, 1976). The creation of a mathematical model for the anaerobic digestion process requires the characterisation of the influent sludge through determination of the fractions of each organism group (i.e. active PAOs, endogenous PAOs, active OHOs, endogenous OHOs and inert material) that makes up the sludge mass. These characteristics are taken as the initial characteristics of the sludge in the anaerobic digester before the hydrolysis process.

Endogenous Residue from Microorganisms

Endogenous residue is the matter that remains within an organism after its death and oxidation for the generation of energy required for metabolic processes, a process known as endogenous respiration. This process takes place continually, at a certain rate (e.g. b_H = 0.24/d for OHOs) in an AS system, irrespectively of the availability of substrate in the influent. However, with the presence of influent biodegradable organics, growth takes place simultaneously with endogenous respiration. With about 24% of the OHO organism mass lost in a day, a fraction (20%) of this mass remains as unbiodegradable material that accumulates in the AS system as endogenous residue while the remaining fraction is used catabolically (Marais and Ekama, 1976).

The death regeneration model accounts for the net 24% active mass loss in a different manner to that of the endogenous respiration concept. In this model, 62 % of the active organisms are utilized in a day (0.08% of this active mass accumulates as unbiodegradable material, while the other 61.2% becomes slowly biodegradable COD (SBCOD). Therefore, with 62% used, there is 38% active mass remaining as unutilised. Of the 61.2% active biomass transformed to SBCOD, 38% is used to make new biomass (anabolism) and the rest used for and catabolism. Therefore the biomass that remains in the system in a day comprises the newly formed 38% active mass together with the originally unutilised 38% (100% - originally utilised 62%). This makes up a totalling of 76 % of biomass in a day, with 24% (100% - 76%) lost (Marais and Ekama, 1976).

2.3.2.4 Separation of Effluent from RAS

The final step in the secondary treatment stage is to settle out the biological floc or filter the material and produce the effluent water containing very low levels of organic material and suspended matter. In this case, either secondary settling tanks or membranes could be employed.

Secondary Settling Tanks and Membrane Technology

Secondary settling tanks (SSTs) are placed at the final stage of secondary treatment in a conventional AS process. The solid material is allowed to settle under gravity to the

bottom of SSTs while the clarified water overflows around the periphery to form the effluent. The settled sludge is returned to the head of the plant to continue treating the incoming sewage.

Membrane biological reactors (MBR) combine activated sludge treatment with a membrane liquid-solid separation process. The membrane component utilizes low-pressure micro-filtration or ultra-filtration membranes and eliminates the need for clarification and tertiary filtration. The membranes are typically immersed in the aeration tank. However, some applications utilize a separate membrane tank. Although the capital and operational costs are usually higher than that of conventional water treatment systems, there are some benefits that accompany the incorporation of MBR technology. Because it eliminates settling limitations, the MBR technology permits bioreactor operation with considerably higher mixed liquor suspended solids concentrations. Moreover, higher biomass concentration in the membrane bioreactor process allows for very efficient removal of biodegradable materials at higher organic loading rates and with the plant occupying reduced environmental footprint. MBR facilities can be considered a desirable option and have become increasingly popular and have gained wider acceptance throughout the industry (Lesjean *et al*., 2004; Ramphao *et al.,* 2004).

2.3.3 Anaerobic Digestion

Anaerobic digestion is a sludge treating, bacterial process that is carried out in the absence of oxygen. The main aims of anaerobic treatment are the purification of the wastewater so that it can be discharged into watercourses and the transformation of sludge to innocuous and easily dewatered substances (Pohland, 1992). Thus, there is a marked reduction in the amount of organic material, measured as COD. The sludge digested usually becomes stable and innocuous and can be used as a soil conditioner or co-disposed (when the sludge contains significant portions of undesirable constituents, such as metals, hence is unutilisable as soil conditioner, it is sometimes disposed in admixture with refuse on a sanitary ladfill site) (Pohland, 1992). Anaerobic digestion, unlike aerobic oxidation, provides relatively little energy to the microorganisms. Therefore, the rate of organism growth is slow and only a small portion of the waste is converted to new biomass with the

major portion converted to methane gas. This conversion to methane represents waste stabilization since methane is poorly soluble and escapes from the waste stream where it can be collected. Moreover, the methane production can be directly correlated with COD reduction (McCarty, 1974).

The methane constitutes about 65 to 75% of the gas produced in a digester. Other constituents are carbon dioxide (25 to 40%) and small volumes (1 to 5%) of nitrogen, hydrogen sulphide and hydrogen (Ross *et al.*, 1992).

An efficient anaerobic digestion system is one that offers the highest possible organic matter removal efficiency at the shortest possible hydraulic retention time, i.e. the volume of the system should be as small as possible (van Haandel and Lettinga, 1994).

The anaerobic digestion process is becoming a subject of interest because it is used in the conversion of organics to methane and carbon dioxide (CO_2), methane representing a renewable fuel for vehicle fuel, space heating, digester heating and/or electricity co-generation. Moreover, anaerobic digestion is linked to the other unit treatment systems and there are cases where products of this process require recycling to upstream unit processes of the WWTP.

However**,** as a disadvantage to the AD process, the methane gas has a global warming potential approximately 11 times greater than that of carbon dioxide. A 20% reduction in global warming may be achieved by utilization of organic wastes and residues for the production of bio-fuels and chemicals, both by preventing methane emission and by replacing fossil fuels (Ghosh, 1997).

2.3.3.1 Anaerobic Digestion (AD) Processes

Anaerobic digestion (AD) is a multiple process involving the action of four organism groups: Acidogens, acetogens, acetoclastic methanogens and hydrogenotrophic methanogens. Figure 2.2 provides a simplified depiction of the AD process.

The anaerobic digestion progresses through four metabolic stages:

1. Hydrolysis: Complex, polymeric organics (e.g. proteins, carbohydrates and lipids) are broken down, by extracellular enzymes, to simple products (usually

monomers or dimers) that are small enough to allow their transport across the cell membrane of acidogenic bacteria by this process.

2. Acidogenesis: Acidogenic bacteria ferment the products of hydrolysis (amino acids, sugars and fatty acids) to carbon dioxide (CO_2), Hydrogen (H_2) and short chain fatty acids (SCFA) such as acetic acid (HAc) and propionic acid (HPr). The biochemical pathways for which the substrate is fermented and the nature of the end product (i.e. type of SCFA produced) depends on the type of substrate and hydrogen partial pressure (Van Rensburg *et al.*, 2001**).**
3. Acetogenesis: Short chain fatty acids with more than two carbon atoms (such as propionic and butyric acids) cannot be fermented directly to methane (McInerney *et al.*, 1979). The acetogens convert these short chain fatty acids (e.g. HPr) which were produced in the acidogenesis process to acetic acid (HAc), carbon dioxide (CO_2) and hydrogen gas (H_2).
4. Methanogenesis: The acetoclastic methanogens convert HAc to CO_2 and methane (CH_4), in a process known as acetoclastic methanogenesis. Hydrogenotrophic methanogens, in turn, convert H_2 to CH_4 and water through hydrogen reduction with CO_2.

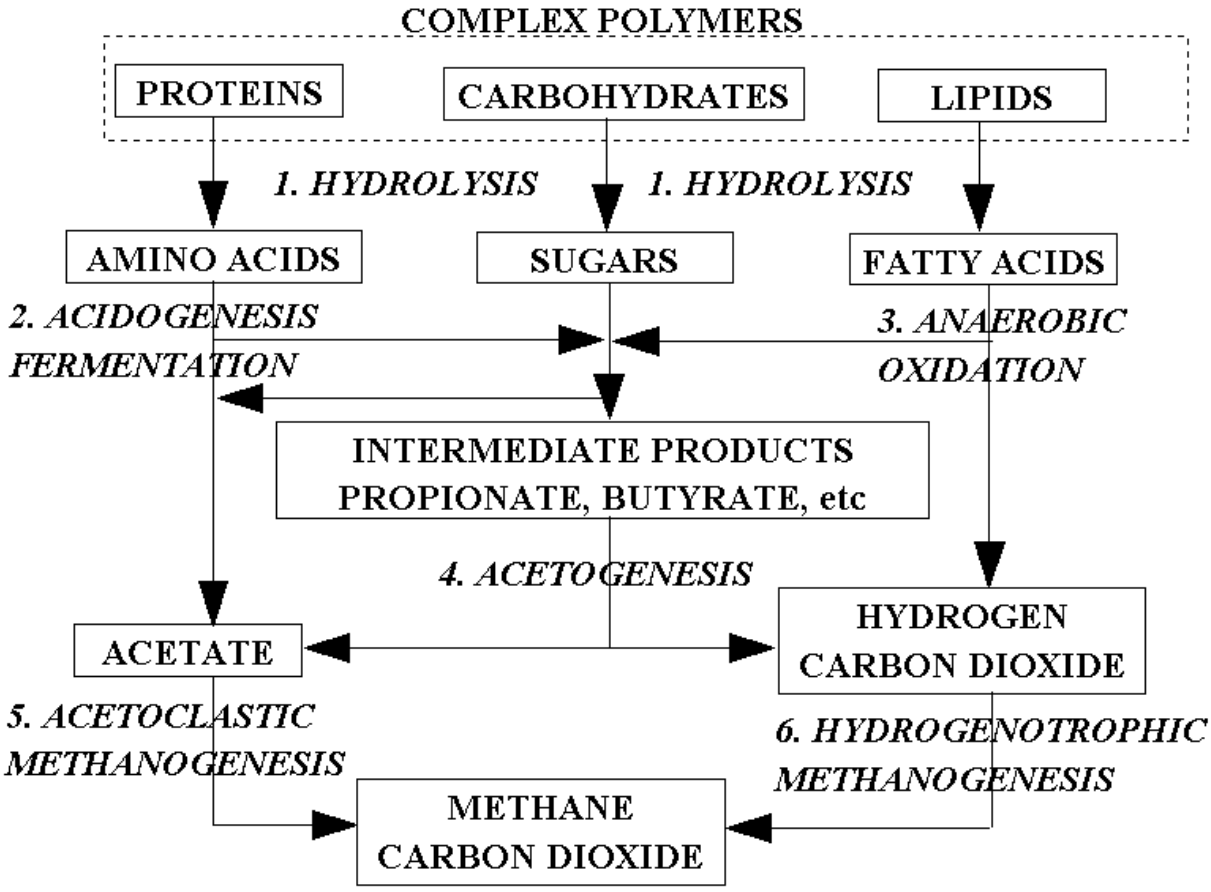

Figure 2.2: *A simplified depiction of the anaerobic digestion process*

The AD organism group known as methanogens are obligate anaerobes with strict requirements for low redox potentials and the absence of dissolved oxygen. They normally grow in close association with the other non-methanogenic bacteria to form a symbiotic community of microorganisms with a self-regulating fermentation, which automatically controls its own pH value, redox potential and oxygen tension (Sacks, 1997). Since the two methanogenic groups are sensitive to pH, the acetogens and acetoclastic methanogens must utilize the HPr and HAc respectively as soon as they are produced to maintain a near neutral pH for optimal operation of the anaerobic digester. An increase in SCFA concentrations would cause a drop in pH, which inhibits the hydrogen using methanogens, causing an increase in hydrogen partial pressure, a subsequent accumulation of propionic and butyric acids and the stalling of methane generation. Thus, in a well-balanced AD process, all products of a previous metabolic stage are converted into the next one without significant build up of intermediary products resulting in a near-

complete conversion of biodegradable organic material to end-products like methane, carbon dioxide, hydrogen sulphide and ammonia (Veeken *et al.*, 2000). For this to occur, a good monitoring system for acidity and pH in the digester is desirable, and an ability to add alkaline materials might be highly beneficial to maintaining the process (McCarty, 1974).

Many anaerobic bacteria can perform electron-transport phosphorylation (regeneration of adenosine tri-phosphate) under anaerobic conditions, by transferring electrons derived from a substrate via a short electron-transport chain to an external electron acceptor supplied in the nutrient medium or an internal electron acceptor derived from substrate degradation. Nitrate, sulphate, carbonate and fumarate ions, as well as sulphur and carbon dioxide can function as electron acceptors (Schlegel, 1992). The presence of alternative electron acceptors may inhibit methanogenesis since sulphate-reducing bacteria (SRB) and nitrate-reducing bacteria can out-compete methanogens for available substrates (Pohland, 1992).

Phosphorous Release and Precipitation Potential in AD of BEPR WAS

During digestion of BEPR WAS, P can be released into the bulk liquid, mostly as ortho-phosphate (OP) from the internally stored polyphosphate (PP) of the PAOs. The solid P is hydrolysed to organic P, which changes to OP. The quantity of P released in the anaerobic zone of the AS system depends on the amount of RBCOD used to form PHA and the pH of the mixed liquor in the anaerobic zone (see Section 2.3.3.2). The 'initial' P release during AD of BEPR WAS could be similar to the P release in the anaerobic zone of the AS system or can be due to the breakdown/hydrolysis of the organisms' cell wall and exposure of their cytoplasm, containing the OP. It is also likely that the organic P within the biomass is released at the same rate as the actual disintegration of the biomass. However, the total release of P during AD requires investigation in order to create a reasonable model. Another fundamental aspect within this study is the possibility of phosphorus precipitation during AD of BEPR sludge.

PAO polyphosphate (PP) is stabilized with cations such as magnesium (Mg), potassium (K) and calcium (Ca). These cations are released during the digestion process as a result of solids degradation. If the combined molar concentration of Mg^{2+}, NH_4^+ and PO_4^{3-} exceeds the solubility product, (K_{sp}, in mols/*l*) of struvite, then struvite precipitation occurs. Struvite is magnesium ammonium phosphate ($MgNH_4PO_4$), which forms a hard crystalline deposit. The Figure 2.5 below shows how struvite precipitation could lead to blockages in pipes and pumps of sludge treatment facilities, and thus the need for it to be controlled for its recovery and for successful AD to occur.

Figure 2.5: *The detrimental effects of struvite precipitation on WWTP sludge treatment facilities*

Due to the lack of oxygen in ADs, nitrification (described in Section 2.3.2.2) does not usually take place in these systems. Therefore, in AD systems treating PS or WAS, there is a high chance of the anaerobic digester liquor (ADL) to accumulate ammonia, which may have entered the AD as part of the influent or may have been formed from the release of organically bound nitrogen, with the degradation of biodegradable organic materials in the AD. In an AD system operated at a pH of below nine, NH_4^+ is usually available in the released FSA as the predominant species of the ammonium weak acid/base system. Also, since the AD of WAS from BEPR systems causes the release of PP, there is a high chance that the AD mixed liquor will also accumulate some Mg^{2+}, K^+, Ca^{2+} and OP, which are made available with the rapid breakdown of PP in the AD. Although in an AD operated at a pH of about seven, $H_2PO_4^-$ and HPO_4^{2-} are the predominant species in the phosphate weak acid/base system, there is also some PO_4^{3-} present in the released OP. This fraction of OP present as PO_4^{3-} increases with the increase in pH above 7.3 (Stumm and Morgan,

1970). Therefore, an AD treating WAS from BEPR systems is likely to accumulate significantly high concentrations of Mg^{2+}, NH_4^+ and PO_4^{3-}, enough to cause struvite ($MgNH_4PO_4$) precipitation to occur. Since increase in pH results in the increased PO_4^{3-} fraction of OP, the precipitation of struvite is also stimulated by the increase in pH. Increased pH in the AD system can be caused by the increase in H_2CO_3* alkalinity with CO_2 evolution (i.e. from its dissolved/aqueous phase (H_2CO_3) to CO_2 gas) and/or when highly alkaline additives, such as NaOH are introduced to the ADL. If not controlled, struvite precipitation could lead to blockages in pipes and pumps of sludge treatment facilities (van Rensburg *et al.*, 2003). Therefore, the extension of WWTP mathematical models, to include the prediction of struvite precipitation (with nutrient (N and P) and cation (e.g. Mg^{2+}) releases) would be useful to monitor AD systems treating P-rich sludge, hence aid in reducing damage to sludge treatment facilities, while assisting in the recovery of struvite.

2.3.3.2 AD Systems

There are various AD designs, each with their own benefits, constraints and treatment efficiencies. The design of an anaerobic digester and the engineering associated with it depend upon the type and volume of the waste it is required to process (Horton and Hawkes., 1979).

A number of design configurations have been used in anaerobic treatment. A conventional completely stirred tank reactor (CSTR) contains a mechanical agitation system consisting of a vertical shaft with a number of impellers and a number of baffles around the vessel perimeter. The impellers and baffle system provide an effective agitation system for the dispersion of the effluent (Sacks, 1997). The conventional process is generally used for treatment of municipal sludge and other concentrated wastes because of its simplicity in design and operation (McCarty, 1974). Figure 2.6 below shows the depiction of a typical AD system in a WWTP.

The AD systems are complex systems that unfortunately often suffer instability. The anaerobic digestion process is regarded as being unbalanced or upset when the process control indicators show deviations from normal (Ross *et al.*, 1992). This is usually

manifested as a decrease in methane production rate, decreases in pH, a rise in SCFA concentration, increased foaming or decreased volatile solids reduction.

Figure 2.6: *Photo of anaerobic digesters in the wastewater treatment plant.*

Sacks (1997) performed a study on the parameters that should be considered when assessing the extent of available capacity in an anaerobic digester. These include:

1. Composition of the feed sludge: Depending on the source of the wastewater, the sludge may contain organics, nutrients, trace elements and possibly some heavy metals (Ross *et al.*, 1992). In addition to the fundamental requirements for macro-nutrients such as carbon and nitrogen, the inability of many anaerobes to synthesize some essential vitamin or amino-acid often necessitates supplementation (Pohland, 1992; Lettinga, 1995). Moreover, four elements, iron, cobalt, nickel and sulphur have been found to be obligatory nutrient requirements for methanogens to convert acetate to methane (Speece, 1983). However, heavy metals, present in concentrations greater than those required for enzyme viability, can be potentially toxic and inhibitory, rather than stimulative (Pohland, 1992; van Haandel and Lettinga, 1994).
2. Organic loading rate: Digester problems can either be caused by feed overload or feed under-load. The best influent feed schedule is a continuous feed at a low rate as it promotes biomass stability and eliminates any abrupt flow rate or organic loading changes that could result in shock loading. Shock loading can result in fluctuations in gas production, pH, alkalinity, organism growth rate and volatile

acids concentration, with a concomitant reduction in degradation efficiency or even complete digester failure (Ross *et al.*, 1992). Thus, it is more favourable to feed small volumes frequently than to feed large volumes infrequently, especially during digester start-up.

3. Digester mixing efficiency: Digesters are usually mixed with paddles (mechanically turned impeller blades) or some other means, such as gas or sludge recirculation, to enhance their biological activity (Hill and Norstedt, 1980). This ensures that the concentrations of waste and microorganisms in the effluent are equal to the concentrations in the reactor itself, as a requirement where the theory development is limited to the concentration in the digester being fully uniform (Jeyaseelan, 1997). Furthermore, mixing in anaerobic digesters promotes an even distribution of contents throughout the digester that reduces the effects of toxic substances and enables efficient use of chemicals added for pH control, by promoting rapid dispersion and dilution (Kotze *et al.*, 1969; Pohland, 1992; Ross *et al.*, 1992; Lettinga, 1995). Mixing also reduces grit settlement, encourages contact between digester contents and eliminates scum, thereby preventing reduction in effective digester volume and thermal stratification, while promoting effective digestion (WEF, 1995). Although mixing improves the contact between microorganisms and the substrate, excessive mixing can disrupt the microorganisms, causing a reduction in their activity, hence slower mixing is usually preferred in AD systems (Monnet, 2003).
4. Sludge temperature: There are two temperature ranges generally used for anaerobic digestion: mesophilic (30 to 40^{o}C) and thermophilic (50 to 60^{o}C) (Zinder *et al.*, 1984). Most digesters are heated and operated in the mesophilic temperature range (optimum of approximately 35 to 37^{o}C). Anaerobic digesters are heated for two principal reasons: to increase the activity of the methane-producing bacteria thus reducing the digestion time; and to liquefy fats and greases to accelerate their decomposition (Ross *et al.*, 1992). The methane-producing bacteria are sensitive to temperature changes and their activity can be severely affected by sudden changes. The methanogens take a while to recover from the temperature shock, while the

acidogens remain unaffected and continue to produce volatile acids, causing a drop in pH. A rise in temperature results in a concurrent increase in metabolic activity to a certain point. Therefore, heating of a digester can result in a shorter hydraulic retention time and potentially increase the active or working volume. A decrease in temperature of the sludge can result in an organic overload as the drop in temperature would result in a decrease in the metabolic activity.

5. Hydraulic retention time: Longer sludge retention times are usually associated with increase in the digester solids concentration. Sludge thickening is important in promoting effective digestion, through preventing dilution or wash-out of the bacterial substrate, and maximizing the use of the available digester capacity and the amount of energy required to heat the sludge (Ross *et al.*, 1992; Sacks, 1997). For high rate digestion, retention times of 25 to 30 days may be used. For cold digestion, retention times in excess of 50 days are required (Ross *et al.*, 1992). Reduction in the effective retention time to a point where organisms cannot reproduce fast enough to avoid washout results in what is known as AD failure due to hydraulic overload. This can be caused by over-pumping a dilute feed sludge, sludge production exceeding digester capacity or reduction of effective digester volume by grit deposition, scum formation or poor mixing.
6. Sludge pH, SCFA and alkalinity concentrations: Most anaerobic conversion processes operate best at a near neutral pH and methanogenesis only proceeds at a high rate when the pH is maintained in the neutral range (Ross *et al.*, 1992). At pH values of lower than 6.8 or higher than 7.8, the rate of methanogenesis decreases (van Haandel and Lettinga, 1994). The eventual pH obtained in a specific anaerobic digester will be largely determined by the substrate supplied to the digester (Kotze *et al.*, 1969). Two factors closely associated with pH are the concentration of volatile fatty acids and the alkalinity of the system. The alkalinity of an anaerobic digester is a measure of the buffering capacity of the contents of the digester. Alkalinity is important to counteract sudden increases in the fatty acid content (Kotze *et al.*, 1969). If the pH, SCFA and alkalinity concentrations are not properly controlled, the biomass will not metabolize effectively and degradation rates will decrease.

The SCFA per alkalinity ratio (Ripley ratio) is important and, ideally, should be in the range of 0.1 to 0.35, but an increase in this value would suggest digester failure and the lower the Ripley ratio, the healthier the digester (Ross *et al.*, 1992).

7. Biomass activity and acclimation of the biomass: The degree of reduction of the substrate is dependent on the degree of acclimation of the biomass to the particular substrate (Sacks, 1997).

2.4 MATHEMATICAL MODELS FOR THE UNIT PROCESSES OF THE WWTP

Models of biological processes are used to aid design, as a tool for process optimization and as a method of reducing extensive and complex experimental data to simple, manageable formulae (McCarty and Mosey, 1991). A mathematical model incorporates a number of kinetic and stoichiometric expressions, which represent the biological interactions. These expressions are based on hypotheses, which are proposed for the biological processes occurring within the system (Billing and Dold, 1988a). To test these hypotheses, specific experiments are designed and data on the system response are collected. These experimental data can then be compared with the predictions obtained from the model. Models of biological processes tend to be empirical models based upon observed correlations between the performance of the plant and its main design and operating variables. Models based on empirical relationships are established by observation when the mechanisms and/or processes operating in the system are not known or are ignored. In contrast, a mechanistic model is based on some conceptualization of the biological/physical mechanisms operating in the system (Sam-Soon *et al.*, 1991). From the conceptual model, the process rates and their stoichiometric interactions with the compounds are formulated mathematically to develop the mechanistic model. Studies on wastewater treatment have resulted in the development of explicit equations, for the construction of mathematical models, by using fundamental kinetic relationships and application of material mass balances. Both steady state (used for constant material flow and load) and dynamic (used for changing material flows and

loads) models are developed and used for the design and operation optimization of WWTPs.

Sam-Soon *et al.* (1991) summarized the various uses of mathematical models in wastewater treatment as follows:

1. Gives mathematical expression to conceptual ideas and allows evaluation of hypotheses.
2. Provides information not apparent from laboratory-scale tests.
3. Provides guidance for the selection of feasible solutions for testing.
4. Assists in identifying the parameters that significantly influence the system response and thereby gives guidance for the establishment of design criteria.
5. Assists in identifying possible causes for system malfunction or failure, and in devising remedial measures.

Currently, mathematical models have also got other uses in wastewater treatment plants (WWTPs); including control diagnosis, monitoring of the systems, aid in system observance for early warning to avoid system malfunction, operation optimisation, decision support in design and operation of the plants and training of the staff that work in the WWTPs.

2.4.1 Steady State Models

Steady state models are based on the slowest process kinetic rate that governs the overall behaviour of the system and relates this process to system design and operating parameters. Therefore, steady state models allow the system design and operating parameters, such as reactor volume and recycle ratios, to be estimated reasonably simply and quickly from system performance criteria specified for the design, such as effluent quality. Once approximate design and operating parameters are known, these can serve as input to the more complex simulation models to investigate dynamic behaviour of the system and refine the design and operating parameters.

Some of the steady state models that have been developed in the past for AS and AD systems are briefly reviewed below.

2.4.1.1 AS System Steady State Models

Various AS system models, for organics, nitrogen and phosphorus removal have been developed in the past. A few such models are described below.

Steady State Models for Organics and Nitrogen Removal

The University of Cape Town (UCT) based research group (Marais and Ekama, 1976) developed an aerobic steady state model for organics removal and nitrification. This model, available in Corel Quattro® spreadsheets, caters for the design of aerobic activated sludge or aerobic digestion systems. It includes the following stoichiometric processes.

1. The ***anabolic process***, which involves adsorption, storage and utilization of biodegradable COD by heterotrophic organisms for growth. Part of this biodegradable COD (Y_H, the mass of organisms per unit COD mass of substrates synthesized) is used for the build up of cell mass and the rest ($1-Y_H$) to provide the energy for the growth process (see Section 2.3.2.2 above). The unbiodegradable organic COD remains untreated; hence, their particulates (S_{upi}) accumulate in the reactor with sludge age and the solubles (S_{usi}) flow through the activated sludge system to make up the final effluent. Some of the influent N and P, which is bound to the biodegradable organics or supplied by FSA and OP, are used as nutrients to build up heterotrophic cell mass.

   Since steady state conditions involve having a constant COD concentration in the bulk liquid (i.e. dS/dt, which denotes delta COD over delta time = 0), the adsorption rate increases until it equals the rate of utilization of the stored COD. With this the rate of COD consumption is governed by the organisms' metabolism, making it suitable for Marais and Ekama (1976) to use Monod kinetic formulations in modelling the rates of organism growth under steady state conditions. This formulation assumes that all other required items for growth (e.g. N and P) are in plentiful supply, except the substrate concentration. The specific growth rate formulation is as given in Equation 2.3.10 below.

$$\mu = \frac{\mu_m \cdot S_b}{K_s + S_b}$$

(2.4.1)

Where:

μ = Specific growth rate of organisms (g/g.d)

μ_m= Maximum specific growth rate

K_s = Substrate half maximum saturation coefficient

S_b = Concentration of biodegradable organic material (gCOD/*l*)

2. The ***catabolic process*** known as endogenous respiration, which involves the death and disintegration of a part of the biomass to provide energy for the cell maintenance of the remaining live biomass. In this process, the N and P that were organically bound by the biomass are also released into the reactor. Only the biodegradable portion (80%) of the dead biomass can be used to provide the energy (by endogenous respiration) and nutrients (from the released N and P). The remaining unbiodegradable fraction (20%) of the dead biomass is known as endogenous residue, which is allowed to accumulate in the reactor with sludge retention time. This endogenous residue combines with the influent unbiodegradable particulates to form the inert organics of the aerobic reactor (X_i). The equations used to model the active mass, endogenous residue and inert organics (see Equations 2.3.2 to 2.3.4 in Section 2.3.2.2 above) were conceptually derived, assuming that the WAS component masses remained constant (i.e. $dX_{BH}/dt = dX_e/dt = dX_i/dt = 0$), as required for steady state conditions and performing material mass balances over the AS system.
3. The ***nitrification process*** for the conversion of free and saline ammonia (FSA) to nitrates and nitrites. Nitrification is a two-step process, as described above in Section 2.3.2.2. However, Marais and Ekama (1976) noted that it was sufficient to model nitrification as a single step, whereby the slower organisms (*Nitrosomonas*) that convert the FSA to nitrite would set the overall rate, assuming that all these nitrites produced will all be rapidly oxidised by the faster organisms *(Nitrobacter)*. Although the growth of these autotrophic organisms was modelled in consistency

with that of the OHOs, the autotrophic organisms represent a relatively small organism population. Moreover, their endogenous respiration rate was deemed negligibly low.

4. The ***utilization of oxygen*** for the anabolic and catabolic respiration and nitrification. The mass of oxygen used in this process is proportional to the total biodegradable COD from the influent substrates used in anabolism and the dead biomass used in catabolism, as shown in Section 2.3.2.2.

The Incorporation of a Denitrification Model

In the steady state operation of ND systems, Stern and Marais (1974) observed denitrification in a plug-flow primary anoxic reactor taking place in two linear phases: first a short rapid phase, leading to a second slow phase. In a plug-flow secondary anoxic reactor only one slow linear denitrification phase was effective, at a slow rate (two-thirds the rate of the second phase in the primary anoxic reactor). It was then hypothesized by Ekama and Marais (1979) that the two linear phases in the primary anoxic reactor arose from the utilization of the two biodegradable COD fractions in the influent (RBCOD and SBCOD) with the first denitrification rate associated to the RBCOD and the second to SBCOD. The slow single denitrification phase, observed in the secondary anoxic reactor, was proposed to be associated with endogenous respiration. Thereafter, Ekama *et al.* (1979) developed a steady state denitrification design procedure for an in-series multi-reactor system, which was based on the above observations. van Haandel *et al.* (1981) incorporated the conceptual ideas of this denitrification design procedure into the aerobic synthesis death regeneration model of Dold *et al.* (1980) to produce a general ND AS kinetic model. After running simulations using this kinetic model, van Haandel *et al.* (1981) discovered that the ND kinetic behaviour could be modelled in terms of the RBCOD and SBCOD using the same formulations proposed by Dold *et al.* (1980) for RBCOD and SBCOD utilization under aerobic conditions to model their utilization under anoxic conditions. However, the rate of SBCOD hydrolysis under anoxic conditions required reduction, by about a third of that under aerobic conditions. With this van Haandel *et al.* was able to confirm the hypothesis by Ekama *et al.* (1979) that in the plug-

flow primary anoxic reactor the first phase linear denitrification rate arose mainly from utilization of secondary RBCOD and the second from utilization of adsorbed SBCOD only. Moreover, in the plug-flow secondary anoxic reactor the single denitrification phase arose from utilization of adsorbed SBCOD generated by organism death. This led to the development of a simplified steady state mathematical model for ND systems by Ekama *et al.* (1983) that could aid in estimating denitrification potential in design of ND systems (Wentzel *et al.*, 1992).

Biological Excess Phosphorus Removal Steady State Model

Wentzel *et al.* (1990) developed models (a kinetic model and its simplified steady state version) describing phosphorus release and P uptake design equations for biological excess phosphorus removal (BEPR) systems. With knowledge of the influent COD concentrations, for a specified sludge age and anaerobic mass fraction, the fraction of influent readily biodegradable COD converted to short-chain fatty acids (SCFA) by phosphorus accumulating organisms (PAOs) are calculated. Therefore, the influent substrate fractions available to the PAOs and non-PAOs (or ordinary heterotrophic organisms) are determined, for the calculation of the respective masses of organisms generated from the substrate. The concentration of phosphorus (P) removed from the influent is calculated from the mass of sludge wasted daily to maintain the solids retention time.

Following the behaviour of PAOs, as described earlier in the literature review, i.e. P release and uptake, the model assumes P release for anaerobic maintenance energy requirements is always small compared to P release for sequestration energy requirements, and thus can be neglected. Moreover, all the substrate taken up by the PAOs, in the anaerobic zone and stored as poly-3-hydoxyalkanoates (PHA) is utilized in the subsequent aerobic zone.

The models were firstly developed for the description of enhanced cultures of PAOs (Wentzel *et al.*, 1988) and later modified to include ordinary heterotrophic organisms (OHOs), i.e. to describe mixed cultures. This is necessary because a BEPR system treating municipal wastewaters promotes the development of a mixed culture of organisms. In

these mixed culture systems, the SCFA need to be converted from RBCOD form by the action of OHOs. Thereafter, the SCFA is sequestered by the PAOs. This SCFA is described in the model as S'_{bsi} , which is calculated using the above Equation 2.3.7.

Thus to maximise the phosphorus removal process the AS system must be designed to minimise, or completely eliminate, entry of nitrate or oxygen (as electron acceptors) to the anaerobic reactor. This is because the PAOs could participate in processes such as denitrification, resulting in inefficient P removal.

Because investigations by Wentzel *et al.* (1989a, 1989b) show that the PAOs and Non-PAOs (OHOs) act virtually independent of each other in the BEPR AS system, the two microorganism population groups are usually analysed separately in the model.

The phosphorus (P) content of the PAO endogenous mass ($f_{XEG,P}$) is usually measured at about 0.03mgP/mgVSS. However, the active mass of PAOs contains larger quantities of phosphorus (0.38mgP/mgVSS) due to the stored polyphosphate (Wentzel *et al.*, 1990). These values are used in the model and have proven to give good correlations between the theoretical predictions and experimental data.

2.4.1.2 Anaerobic Digestion (AD) System Steady State Models

Recognizing the potential usefulness of mathematical models, various researchers have developed such models to describe anaerobic digestion. Below is a description of some of the various AD models developed in the past.

Sötemann *et al.* (2005) Steady State AD model

Sötemann *et al.* (2005) developed an integrated (aqueous-gas) mixed weak acid/base chemical, physical and biological process kinetic model for the AD of sewage sludge. This steady state model comprises of three sequential parts:

1. Kinetic part from which the percentage COD removal and methane production are determined for a given retention time.
2. A stoichiometry part from which gas composition (or partial pressure of CO_2), NH_4 released and alkalinity generated are calculated from the percentage COD removal.

3. A carbonate system weak acid/base chemistry part from which the digester pH is calculated from the partial pressure of CO_2 and alkalinity generated.

The kinetic formulations and methods used by Sötemann *et al.* (2005) in the derivation of the kinetic part of the steady state model are similar to the ones used in this thesis and are reviewed in Chapter 6 (Section 6.2.1) which describes the extended steady state AD model. The stoichiometry and weak acid/base chemistry sections of the steady state model by Sötemann *et al.* (2005) are briefly described below.

Stoichiometry Section of Sötemann *et al.* (2005) Steady State AD Model

Sötemann *et al.* (2005b) used the generalized reaction stoichiometry for an overall AD system, developed by McCarty (1974), that caters for AD of complex organics from COD and N removal systems (but not including P). In this AD stoichiometry the organic substrate to the AD, having an empirical composition of $C_XH_yO_ZN_A$, is converted to methane, carbon dioxide and biomass that have an elemental composition of $C_5H_7O_2N$. This is shown by the Equation 2.4.2 below, comprising the anabolic and catabolic processes (McCarty, 1975).

$$C_X H_Y O_Z N_A + \left(2X + A - Z - \frac{9ED}{20} - \frac{(1-E)D}{4}\right) H_2O \rightarrow$$
$$\rightarrow \left(X - A - \frac{ED}{5} - \frac{ED}{8}\right) CO_2 + \frac{(1-E)D}{8} CH_4 + \frac{ED}{20} C_5H_7O_2N + \left(A - \frac{ED}{20}\right) NH_4^+ + \left(A - \frac{ED}{20}\right) HCO_3^- \quad (2.4.2)$$

Where:

$$D = 4X + Y - 2Z - 3A \text{ [e- equiv/mol]} \quad (2.4.3)$$

E = the ratio of biomass to hydrolyzed biodegradable organics, i.e.:

$$E = \frac{Z_{AD}}{S_{bpi} - S_{bp}} \quad (2.4.4)$$

Since PS can be fermented to produce fatty acids, the AD model assumes the measured influent VFA to be acetate with a molar mass of 60 and a COD of 64gCOD/mol. In the AD

stoichiometry, this acetate (both dissociated and undissociated) is used by methanogens and converted to methane gas as shown in the Equations 2.4.6 and 2.4.7 below:

$$CH_3COOH \rightarrow CH_4 + CO_2 \tag{2.4.6}$$

and

$$CH_3COO^- + H_2O \rightarrow CH_4 + HCO_3^- \tag{2.4.7}$$

Thus, the total of methane, carbon dioxide gas and bicarbonate predicted in the AD stoichiometry is the sum of that determined by Equations 2.4.2, 2.4.6 and 2.4.7.

Weak Acid/Base Chemistry Section of the Sötemann *et al.* (2005) Steady State AD Model

In the weak acid/base chemistry section of the Sötemann *et al.* (2005) steady state AD model, the partial pressure of CO_2 (p_{CO2}) is determined by calculating the ratio of gaseous CO_2 to total gas of CH_4 and CO_2. The proportion of dissolved CO_2 ($H_2CO_3^*$) that is converted to bicarbonate (HCO_3^-) is determined by the quantity of ammonia released during organic degradation, that at neutral pH, uses a proton from the ($H_2CO_3^*$) to form bicarbonate (HCO_3-) and saline ammonia NH_4^+. The rest of the bicarbonate is produced by the stoichiometric conversion of influent dissociated acetate species used during the AD process. With the acceptance that equilibrium exists between dissolved and gaseous inorganic carbon species, the relationship between bicarbonate, which is equivalent to the alkalinity generated, together with the p_{CO2} is used to determine the digester pH.

$$\rho_{CO_2} = \frac{\left[HCO_3^-\right] \cdot \left(1 + 10^{pKc1 - pH} + 10^{pH - pKc2}\right)}{10^{-pkHCO2}\left(1 + 10^{pH - pkc1} + 10^{2pH - pkc1 - pkc2}\right)} \tag{2.4.8}$$

where:

pK'_{HCO2} = -ve log 10 of Henry's law constant for CO_2.

and

pK'_{C1}, pK'_{C2}= -ve log 10 of the 1st and 2nd carbonate system apparent dissociation constants, corrected for ionic strength effects (Loewenthal *et al.* 1989).

2.4.1.3 Plant-Wide Steady State Model

The mutual interactions between the connected unit operations of WWTPs (e.g. primary settlers, activated sludge system, aerobic digester and anaerobic digesters) has led to studies in developing mass balance based plant-wide WWTP models, which model all the unit operations of the WWTP together, with their connecting flows. Some ancillary issues connected to this study have also been under investigation, such as the conservation of the influent unbiodegradable particulate material in aerobic and anaerobic systems and the tracking of inorganic settleable solids throughout the plant. The current progress on the development of an integrated materials mass balance based plant-wide steady state model spreadsheet and the above-mentioned ancillary issues are briefly discussed in this section of the literature review.

Material Balances Spreadsheet (Sötemann, 2005)

The steady state design and operation WWTP mass balances spreadsheet (developed in Corel Quattro® Pro8 software) includes comprehensive wastewater characterisation (mainly involving subdivision of COD, TKN and Total P to their biodegradable and unbiodegradable particulate and dissolved forms, together with FSA, ortho-phosphate (OP), nitrate and alkalinity) and WWTP unit processes (PST, ND and/or BEPR, together with thickening, AerD and/or AD of PS, ND system WAS or PS-WAS blends). This integrated plant-wide steady state model comprises 15 sheets:

1. Input worksheet: Here the input parameters, comprising mainly of particulate and soluble wastewater characteristic fractions that are determined from experimental results together with the kinetic and stoichiometric constants to be used in further calculations.
2. Loads worksheet: This worksheet uses the diurnal data variations in flow as well as in COD, TKN, FSA, TP, OP and settleable solids (SS) concentrations to provide estimates of the SS COD and nutrients (N and P) removed in primary settling and

present the load estimates for the raw and settled WW. Moreover, the PS characteristics (biodegradable and unbiodegradable COD, SS, OrgN and OrgP) are determined using mass balances around the PST.

3. Char worksheet: This sheet uses the values from the previous sheets 1 and 2 to calculate the raw and settled WWs COD, TKN, FSA, TP and OP unbiodegradable and biodegradable soluble and particulate characteristic components. These calculated characteristics are displayed graphically in corresponding block diagrams.
4. ASTmin worksheet: This is where design parameters for AS systems (i.e. volume of reactor, average and peak oxygen demand, effluent COD, TKN, FSA, nitrate, TP and OP concentrations and WAS flow and composition) for a chosen sludge age are calculated. The parameters are calculated for minimum expected temperatures.
5. ASTmax worksheet: This worksheet is used for the calculation of the same AS systems design parameters as for (4) above but for expected maximum temperatures.
6. AerDigSgl worksheet: Caters for the design of a single reactor for the aerobic digestion of PS (from the influent in worksheet 2), WAS (from the AS systems in worksheets 4, 5, 11 and 12) or blends of both. This includes the calculations for the thickening of the blended PS and WAS to a selected concentration, aerobic digestion to a selected residual biodegradable organic content, the quantities of N and P released during this digestion, the required digester volume, oxygen demand and effluent concentrations.
7. AerDTmin worksheet: The aerobic digestion of fully aerobic and nitrification/denitrification (ND) WAS sludge in single, double and triple compartment digesters with and without the blend of PS at expected minimum temperatures. The PS and WAS are thickened separately before blending, with the degree of thickening governed by (i) the selected capacity of PS and WAS thickening by gravity sedimentation and flotation respectively or (ii) selected maximum OUR in the digester. However, it should be noted that compartmentalizing, rather than providing a single completely mixed aerobic

digester is only beneficial (by lowering the sludge retention time, hence reducing digester volume) for WAS digestion. This is because unlike WAS, the thickened concentration of PS or PS-WAS blends as feed to the first compartment of the digester is limited by the high oxygen transfer requirements to values below the capacity for PS thickening. Therefore, it is the OUR in the digester that governs the reactor volume and the degree of sludge thickening required in the digestion of PS and PS-WAS blends.

8. AerDTmax worksheet: This spreadsheet replicates the previous one (AerDmin) but at expected maximum temperatures.
9. MBalAE worksheet: This sheet checks the COD, N and P mass balances around the WWTP for the fully aerobic system are at 100 (±0.5) % to confirm that the spreadsheet remains consistent.
10. MLEUCTConst Worksheet: The required input data for a MLE ND and a UCT NDBEPR AS system design is collected and the necessary temperature adjustments to kinetic constants are made.
11. MLESys Worksheet: Provides for the complete design of the MLE ND system at maximum and minimum design temperatures for both the raw and settled WW. This includes the calculation of anoxic and aerobic reactor volumes, recycles ratios, oxygen demand, effluent concentrations and WAS flow and composition.
12. UCTSys Worksheet: Provides for the complete design of the UCT NDBEPR system at maximum and minimum design temperatures for both the raw and settled WW, including the calculation of anaerobic, anoxic and aerobic reactor volumes, recycles ratios, oxygen demand, effluent concentrations and WAS flow and composition.
13. MLEBal Worksheet: Calculates the COD, N and P mass balances over the WWTP treating the raw and settled WW for the MLE system to check that they are within 100 (±0.5) %.
14. UCTBal Worksheet: Calculates the COD, N and P mass balances over the WWTP treating the raw and settled WW for the UCT system.
15. Tables and Summary Worksheet: Presents the tables and a summary of the results calculated in other previous worksheets.

Sötemann (2005) noted that the individual unit operations are interconnected through a network of flows, whereby outputs from a unit operation could become inputs to downstream or upstream (via recycles) unit operations. Therefore the steady state model for anaerobic digestion was integrated into the spreadsheet described above, linking it to the primary settler and AS system unit operations. This spreadsheet then collectively provides a mass balance based steady state model for the various configurations of the entire WWTP comprising the PST, AS system and anaerobic or aerobic digestion. This plant-wide steady state model could be applied in the designing of the overall WWTP scheme, tracking down materials of importance through this plant and quantifying the interdependencies of the various unit operations in the plant under steady state conditions. However, complex kinetic dynamic simulation models can be applied to the individual unit operations to refine their design and evaluate their performance under cyclic flow and load conditions.

The proposed three phase steady state AD model will be added to this spreadsheet, as an extension to the plant-wide materials mass balance based steady state model.

Biodegradability of Influent Wastewater Organics

Wentzel *et al.* (2006) investigated the continuity of wastewater organic chemical oxygen demand (COD) and nitrogen (N) compounds along the link connecting the primary settling tank (PST) and anaerobic digester (AD). The raw influent wastewater on reaching a WWTP will usually go through primary settling or direct to AS systems as the initial unit processes. The PST separates the raw wastewater (WW) into primary sludge (PS) and settled WW. The PS requires AD and the settled WW is usually treated using AS systems. To investigate biodegradability of the raw influent WW organics through the various unit processes of the WWTP requires considerations of whether the unbiodegradable particulate fraction obtained in fully aerobic or ND systems are the same as those obtained in anaerobic systems. The $f_{S'up}$ of aerobically treated influent PS can be calculated through obtaining the difference between the $f_{S'up}$ value acquired in settled WW from that of its original influent raw WW when treating the two (raw and settled) wastewaters

simultaneously, using fully aerobic or N removal AS systems. Thus the mass difference of this unbiodegradable particulate material in the raw ($MS_{upi\text{-}raw}$) and settled ($MS_{upi\text{-}settled}$) wastewater is that of the PS as if it was fed to the AS system. This primary sludge unbiodegradable particulate concentration ($S_{upi\text{-}PS}$) can thus be calculated using mass balances around the PST, expressed by the Equation 2.4.9 below:

$$S_{upi_{PS}} = \left(\frac{\left(M_{\text{sup}i_{raw}} - M_{\text{sup}i_{settled}} \right) \cdot Q_{e_{PST}}}{Q_{i_{PSAD}}} \right) \tag{2.4.9}$$

Where Qe_{PST} and Qi_{PSAD} are the flows of PS out of the PST and into the AD respectively.

To determine the biodegradability of this primary sludge under anaerobic conditions requires the anaerobic digester to be operated at long sludge retention times of about 60 days, which ensures that all the organics have been utilized. Thus the unbiodegradable particulate fraction obtained from the AS systems will have to match that from the AD systems before conclusions can be made on the conservation of this unbiodegradable mass in the WWTP.

This research aspect was semi-quantitatively performed in the past by Wentzel *et al.* (2006). This is because the PS $f_{S'up}$ ($f_{PS'up}$) value was calculated from the observed $f_{S'up}$ values in typical South African raw and settled municipal wastewaters, i.e. 0.15 and 0.04 respectively (WRC, 1984) to calculate an $f_{PS'up}$ value of 0.35.

This $f_{PS'up}$ value of 0.35 is also midway in the range of values reported in literature (Eckenfelder, 1980; O'Rouke, 1968) for the unbiodegradable fraction in PS when anaerobically digested on full scale at long sludge retention times.

To obtain this $f_{PS'up}$ value from AD of PS, Sötemann *et al.* (2005b) developed an anaerobic digestion model and calibrated the kinetic part of this model against the experimental data of Izzett *et al.* (1992) and O'Rouke (1968), with considerations to COD mass balance error. Hydrolysis kinetic rate constants calculated for the data by Izzett *et al.* (1992), who had experimented on AD of a PS and humus sludge mixture from a trickling filter plant, provided an $f_{PS'up}$ of 0.36. However, that calculated for the data by O'Rouke (1968), who

had anaerobically digested pure PS, gave an $f_{PS'up}$ of 0.33. The steady state AD model for pure PS by Ristow *et al.* (2004) gives an $f_{PS'up}$ value of 0.34.

Therefore, it was concluded that unbiodegradable particulate COD fraction of PS obtained from AD models closely matches that which was obtained using mass balances around the PST for typical South African raw and settled municipal wastewaters. This being so, there is a high possibility of the influent unbiodegradable particulate material following the principle of continuity, i.e. remaining the same in both aerobic and anaerobic treatment systems, enabling its characterisation to be performed using mass balances around the PST.

Wentzel *et al.* (2006) performed an elemental analysis of a data set from two WWTPs in Cape Town. The calculated CHON composition of the particulate biodegradable organics of the PS (i.e. $C_{3.65}H_7O_{1.97}N_{0.190}$) correlated closely with the CHON composition obtained from the VSS and COD removed and FSA generated using the Sötemann *et al.* (2005b) AD model (i.e. $C_{3.5}H_7O_2N_{0.196}$).

Quantitative confirmation of this research aspect using the same wastewater (including PS) in either the fully aerobic or ND AS systems as in the AD system, would be a valuable validation that AS unbiodegradable organics remains unbiodegradable in the AD.

Biodegradability of Activated Sludge Organics

The unbiodegradable organics in the influent to the digester comprise of the unchanged influent wastewater unbiodegradable material and the OHO endogenous residue generated in the AS reactors.

In tracking the unbiodegradable particulate material through the WWTP, it is necessary to investigate whether the unbiodegradable material (endogenous residue) formed through death and decay of the active mass in aerobic AS systems remains unbiodegradable in anaerobic systems. This is observed with anaerobic digestion of the WAS over long sludge retention times.

Sötemann *et al.* (2006) performed such an investigation, using a data set by Gossett and Belser (1982). Gossett and Belser (1982) fed synthetic wastewater to 2-day retention time AS systems. The sludge harvested from these systems was in turn fed to anaerobic

digesters with 15 days of sludge retention time. The synthetic wastewater has no particulates hence the only unbiodegradable particulates in the WAS fed to the anaerobic digester were in the form of endogenous residue of the active biomass.

Gossett and Belser (1982) had determined the unbiodegradable fraction of the WAS (f_{EH}), as 0.317, using a combination of the Christensen and McCarty (1975) and McKinney (1962) steady state AS models. In the steady state AD model of McCarty (1974) the methane gas production and AD biomass generation, negligible at long AD retention times, equals the biodegradable COD removal. Therefore, Gossett and Belser were also able to use this model to equate the theoretical cumulative methane production for the long retention time batch ADs to measured values. The f_{EH} they obtained using this model was similar to that in AS systems. However, a 15-day retention time in anaerobic digestion of WAS is not long enough for complete degradation of the sludge. Thus, the actual measured data was not used satisfactorily. Moreover, with the use of synthetic wastewater, it was not possible to know the biodegradability of real wastewater unbiodegradable organics.

To address the above shortcomings, Sötemann *et al.* (2006) applied the mass balances based steady state AS model of Marais and Ekama (1976) and AD model of Sötemann *et al.* (2005) to literature data involving investigations on AD of WAS. The data from van Haandel *et al.* (1998a; b), who had fed raw wastewater to a 2-day sludge age aerated lagoon, was used in this investigation. The sludge produced from this lagoon was fed to four aerobic digesters at sludge ages of 1.73, 2.14, 3 and 5.63 days. Thereafter, four, five, six, seven and eight litres per day (*l*/d) were taken from the feed to each aerobic digester and thickened to 0.4 *l*/d before being fed to five separate anaerobic digesters. This ensured that each anaerobic digester had a different unbiodegradable particulate fraction. The unbiodegradable fraction of the WAS feed to the ADs was calculated using the steady state AS model from Marais and Ekama (1976). This unbiodegradable particulate fraction closely matched that calculated using the AD model of Sötemann *et al.* (2005), as long as the unbiodegradable fraction of the OHOs is given the value from the death-regeneration model (f'_{EH} = 0.08). This was further confirmed by Sötemann *et al.* (2006) who fed raw wastewater to a 15-day R_s ND activated sludge system, with the sludge from this system in turn fed to a 60-day sludge age AD system. In this investigation, Sötemann *et al.* (2006)

included the CHON compositions of the anaerobic digester influent and effluent, using elemental analysis. He therefore concluded that (i) the influent wastewater unbiodegradable particulate organics determined from the response of the AS system and (ii) the unbiodegradable organics that are generated in the AS reactor, i.e. endogenous residue, using the well-established AS model values for the OHO endogenous respiration (b_H = 0.24/d) /death regeneration (b'_H=0.62/d) rates and unbiodegradable fraction (f_{EH}=0.20, f'_{EH}=0.08), should both be unbiodegradable under anaerobic digester conditions. From an investigation into the kinetics of aerobic and anaerobic digestion of WAS, Yasui *et al.* (2006) came to the same conclusions. Thus, we should be able to characterize the influent raw wastewater organic particulates to know the quantity that can be digested as primary sludge. Moreover, the biodegradable organics in WAS that can be anaerobically digested, may also be calculated from the active fraction of the WAS using the accepted stoichiometric and kinetic constants in steady state or dynamic simulation models. This would greatly simplify coupling the PST, AS and AD unit operations in plant-wide WWTP models. However, since the raw wastewater characteristics were mainly based on the steady state AS model from Marais and Ekama (1976) rather than data obtained using the same wastewater, we do not have absolute surety of the above conclusions.

ISS Conservation Model

Ekama and Wentzel (2004) developed an ISS model for AS systems. This was because ISS is a part of the TSS, which in turn is of major influence to downstream unit operations such as secondary settling tanks and aerobic or anaerobic digesters.

This model conceptualises the organism ISS content as the influent wastewater ISS that accumulates in the reactor with sludge age and the uptake of dissolved inorganic solids by active organisms, which when dried in the total suspended solids (TSS) test procedure, precipitate and manifest as ISS. Mineral precipitation and dissolution of the influent ISS is considered negligible. Furthermore, it is assumed that the particulate organic material in the influent contains negligible or no ISS content.

Ekama and Wentzel (2004) noted that the longer the sludge age, the less dissolved inorganic solids is taken up and the closer the effluent dissolved inorganic solids

approaches the influent value (particularly for ND systems). This is because the longer the sludge age, the longer the OHO and PAO endogenous processes have continued, resulting in increased return of dissolved inorganic solids back to the liquid phase. Thus, the contributions of fixed ISS flux by OHO and PAO biomass differs depending on their active fractions of the VSS.

The model by Ekama and Wentzel (2004) assigns ISS content to OHOs (known as f_{iOHO}) of 0.15 mgISS/mgOHO-VSS. Moreover, it was discovered that the difference between influent ISS and measured ISS at different stages of the WWTP would be much greater for WWTPs including biological excess phosphorus (P) removal (BEPR). This is because the PAOs take in polyphosphates, which are inorganic and increase the ISS content of the PAOs up to 6 times higher than that of OHOs, depending on the PAO phosphorus content (Ekama and Wentzel, 2004).

This resulted in the development of a linear relation between the P and ISS contents of PAOs, i.e. (fi_{PAO}, in mgP/mgISS):

$$f_{i\,PAO} = f_{i\,OHO} + 3.286 \cdot (f_{xBGP} - f_{p\,OHO}) \qquad (2.4.10)$$

Where 3.286 is the ISS content of intracellular PP as phosphorus (P) which precipitates in the drying step of the TSS-VSS test procedure and f_{pOHO} is the mgP/mgVSS, as normal to OHOs (which is usually about 0.03mgP/mgVSS). This value is calculated theoretically using measured Mg:K:Ca:P ratios of 0.275:0.295:0.05:1 from Wentzel *et al.* (1989b) and recognizing that P in PP exists as PO_3 (with a molar mass of 98.8 g/mol) to get a value of 3.19 mgISS/mgP. However, this value requires modification to take into account the reduced polyphosphate storage with anoxic P uptake to give a value close to 3.23 mgISS/mgP, which has been adopted in ASM2 and ASM2d models (Henze *et al.*, 2000). Moreover, when the generally observed biomass structural P content (f_{pOHO}) and intracellular polyphosphate content (f_{XBGP}) of 0.03 mgP/mgVSS and 0.38 mgP/mgPAO VSS are used respectively, an f_{iPAO} value of about 2.30 mgP/mgISS is calculated.

Sötemann *et al.* (2006) investigated the continuity of influent ISS along links connecting the PST, fully aerobic or N removal AS systems to anaerobic (AD) and aerobic digestion

(AerD) unit operations of the WWTP. They discovered that the ISS is conserved through the activated sludge and aerobic digestion unit operations. However, the influent ISS flux differed from the ISS flux at different stages of the WWTP unit operations. This is because, as already noted, the ISS flux depends on the active fraction of the VSS within these various stages. In the AerD unit process, the ISS concentration increases due to the inorganic dissolved (soluble) solids (IDS) being taken up with OHO growth. Also, this ISS decreases with OHO death (endogenous respiration) as would occur in a fully aerobic or N removal AS system. Therefore, the ISS model developed by Ekama and Wentzel (2004) can be readily incorporated into the AS mathematical models to track the ISS through AerD systems.

The literature from Moen *et al.* (2001) and Izzett *et al.* (1992) has shown that the conservation of the influent ISS through the primary sludge anaerobic digestion is within 10%, which is too wide a difference to be conclusive. The difference observed may be due to poor mixing, precipitation or dissolution of the inorganic material. Further work may be required with regard to conservation of ISS between the BEPR and AD link, whereby higher values in the digester effluent ISS would provide partial evidence of phosphorus precipitation during the sludge treatment.

2.4.2 Dynamic Models

The development of dynamic models is such that direct links between inputs and outputs are incorporated through ordinary and partial differential equations that seek to mimic reaction mechanisms for the various biological, physical and chemical processes acting on the individual influent components of the WWTP. Software packages for simulating this dynamic behaviour of wastewater treatment plants have recently become available (Meijer *et al.*, 2002). The development of the complex system component interactions in the presentation of these models is usually displayed in a matrix format. The Gujer Matrix is the widely used structure to construct chemical and biological WWTP models because it is concise and flexible. In the matrix, each row represents one process, where each column represents one component. The reaction rates of processes are displayed on the right side of the matrix, where the stoichiometric coefficients between processes and components are

distributed inside the matrix (see Tables A6.1a to c in Appendix 6 for a Gujer matrix example). Identification of the major processes and selection of the appropriate kinetic and stoichiometric expressions for each are the major conceptual tasks during development of the mathematical model.

2.4.2.1 Stages in Development of the Dynamic Model.

Mathematical modelling involves the provision of either steady state or dynamic simulation WWTP models. However, it is noted that steady state models of WWTP unit operations are a very useful complement to the complex simulation models and thus usually both would require development.

Siegrist *et al.* (2002) proposed a model development technique that generally involves the following steps:

1. Development of the model based on the necessary metabolic pathways
2. Verification of the model through inspecting material consistencies and analyses such as mass balances
3. Calibration of the model
4. Validation of the model using experimentally determined data.

2.4.2.2 Uses of Dynamic Modelling

The dynamic model can be used to predict effluent quality, system responses to dynamic conditions and the inhibitory effects of pH, temperature and metabolic products. This further enables:

- Conducting sensitivity analyses and assessments of the limits of the model through application of the model under 'what if' conditions that would be detrimental to the real system, if evaluated at full scale. Moreover, various operating strategies and future actions such as taking unit processes off-line, plant upsets and recovery time could be evaluated.
- Accurate sizing of unit processes and selection of the best design alternatives that achieve the effluent quality requirements. This also achieves confidence in design and minimises operational costs.

- Through the tools provided by dynamic models, assisting process designers to train operators by illustrating the effect of operating decisions on plant performance.

2.4.2.3 AS System Dynamic Models

The activated sludge models ASM1, ASM2, ASM2d and ASM3 (Henze *et al.*, 2000) were developed in an attempt to create widely acceptable common platform models, which would allow modellers to speak a common language when researching wastewater treatment modelling. These models have been commonly used as a basis for further model development (Vanrolleghem *et al.*, 2005).

The IWA Activated Sludge Models (ASM1-ASM2d)

Generally, most biological processes that are included in the original activated sludge model 1 (ASM1) are also included in ASM2 (Henze *et al.*, 1995), which is briefly described below. This is because the ASM2 is an extension of ASM1, with additional biological processes included, primarily in order to deal with BEPR. These additional processes also require that the biomass be defined to have a cell internal structure to cater for the PAO growth on cell internal stored organic materials poly-3-hydoxyalkanoates (denoted as PHA) as new components.

The processes for ASM2 can be outlined as:

1. Hydrolysis of organics, which are considered as surface reactions that occur with the hydrolytic enzyme producing organisms and slowly biodegradable substrate being in close contact and depend on electron acceptor conditions. These conditions being aerobic, anoxic and anaerobic, the aerobic hydrolysis being fastest. The hydrolysis of organics produces fermentable soluble organics together with nutrients to be used in biomass growth.
2. Aerobic and anoxic growth of heterotrophic organisms on fermentable substrates (S_f) modelled as separate processes with oxygen (aerobic conditions) and nitrates (anoxic conditions) respectively used as the electron acceptors. ASM2 also includes the use of nutrients (N and P) for this organism synthesis, where the N is obtained from ammonia (NH_4^+) or nitrate (NO_3^-, in the unlikely absence of ammonia) and P

from ortho-phosphates (OP).This quantity of N and P used for synthesis is parameterised as fractions of the active biomass COD, i.e. $f_{ZB,N}$ = 0.068 mgN/mgCOD_{OHO} and $f_{ZB,P}$ = 0.020 mgP/mgCOD_{OHO} respectively. For NO_3^- to be used as an N source for synthesis, it is reduced to NH_4^+ causing an increase in pH. Unlike ASM1, ASM2 excludes ammonification (conversion of the biodegradable soluble organically bound nitrogen to FSA) and instead links the release of this FSA to the utilization of the fermentable substrates (S_f) for growth.

3. Aerobic and anoxic growth of heterotrophic organisms on acetate (S_a), also modelled as two separate processes, with similar stoichiometry to the growth on S_f, but just that acetate is used as the substrate source. Ammonia and OP remain as the nutrient (N and P) sources.
4. Fermentation by heterotrophic organisms under anaerobic conditions.
5. Loss and decay of heterotrophic organisms, through the sum of endogenous respiration, lysis, predation and other such processes. This lysis results in the production of slowly biodegradable organics and endogenous residue together with the release of nutrients (N and P) as ammonia and OP. Anaerobic storage of PHA by PAOs, that requires their release of OP from PP and utilization of the energy produced from the hydrolysis of this PP.
6. Aerobic and anoxic storage of OP, in the form of cell internal PP using the energy obtained from the aerobic or anoxic respiration of PHA. To accommodate for the discontinued storage of PP due to significantly high phosphorus content in the PAO, as experimentally observed to occur, an inhibition term of PP storage is added. This inhibition term is reduced under anoxic conditions by the factor, ηNO3.
7. Aerobic and anoxic growth of PAOs using PHA, with the maximum growth rate of PAOs under anoxic conditions, reduced relative to its value under aerobic conditions by the reduction factor, ηNO3.
8. Lysis of PAOs and their storage products (i.e. PP and PHA), which are accounted for separately from the biomass PAO and thus have separate decay processes.

9. Aerobic growth of nitrifying organisms (ANOs), on ammonium (NH_4^+) to produce nitrate (NO_3^-) and reduce alkalinity. This two- stage process (see Section 2.3.2.2.1) is modelled as a single step occurring at a rate governed by the slow ammonia oxidation, with the conversion from nitrite to nitrate deemed as significantly faster. This oxidation provides the ANOs with their catabolic energy requirements, as defined by their parameterized yield coefficient i.e. Y_{ZA}=0.15 ($gCOD_{ANO}$ synthesized/gNH_4-N nitrified).
10. Lysis of nitrifying organisms, as a process with stoichiometry identical to that representing the lysis of other biomass (i.e. OHOs and PAOs).
11. Reverse processes of induced precipitation and re-dissolution of PO_4 to ferric – hydroxide, $Fe(OH)_3$ and ferric phosphate, FePO4, when iron is added to the AS system.

The ASM2d is an extension of ASM2. It includes two additional processes to account for de-nitrifying PAOs.

The aerobic digestion process can also be simulated using ASM2 or ASM2d. However, the relative rates of the various processes need to be calibrated and the switching function constants for processes competing for the same compounds examined and changed accordingly.

UCTOLD Model

The UCTOLD (Dold *et al.*, 1980 and 1991) is a dynamic model, programmed into Aquasim (Reichert, 1998), for activated sludge and aerobic digestion systems based on the steady state aerobic model of Marais *et al.* (1976).

The AS processes and their interactions with the compounds that are incorporated in the UCTOLD (Dold *et al.*, 1991) model are:

1. In UCTOLD, the influent SBCOD is first enmeshed in the sludge mass on entry into the reactor. It was hypothesized by Stern and Marais (1974) that the influent biodegradable COD consists of readily (RBCOD) and slowly biodegradable (SBCOD) fractions. The SBCOD comprises of large complex molecules that cannot move across organism cell walls, thus are initially enmeshed with the rest of the

sludge mass. The enmeshed SBCOD is adsorbed onto the organism cell wall in accordance with a saturation type kinetic rate. The enmeshment is instantaneous and thus is not modelled as an exclusive process but is linked to the adsorption, which is modelled according to saturation kinetics.

2. On the organism cell wall, the SBCOD is hydrolyzed (broken down) by enzymes to RBCOD molecules that can move across the organism cell wall. This hydrolysis process being relatively the slowest is known to be the rate-limiting step and is modelled according to Levenspiel's surface reaction kinetics (Dold *et al.*, 1980) in terms of the ratio of adsorbed SBCOD to active biomass. During the hydrolysis process, the N that is organically bound to the SBCOD is released as soluble organic N for its utilization together with the adsorbed SBCOD, in the aerobic and anoxic growth of organisms. Heterotrophic organisms then mediate the conversion of the remaining soluble organic N to ammonia (Dold *et al.*, 1980; van Haandel *et al.*, 1981).
3. Aerobic and anoxic growth of OHOs on biodegradable organics. The RBCOD together with other hydrolysis products (such as N released) are directly utilized by the active biomass for anabolic and catabolic processes. Part of the RBCOD is used for growth of active organisms and the rest for energy (with an associated oxygen demand) to be used in the growth process. Ammonia is usually taken as the N source for organism growth. However, the model also has a switching function, dependent on the ammonia concentration, to cater for the alternate utilization of nitrates when the ammonia is almost completely depleted. The utilization of ammonia and nitrates was therefore modelled as two processes, controlled by the switching function. Another switching function is also included to ensure the alteration in aerobic growth of biomass to anoxic growth when there is low oxygen supply. In this case, although the RBCOD remains the substrate, nitrate is used as the terminal electron acceptor. As was done for the aerobic growth, the anoxic growth using ammonia and nitrate as the N source are modelled as two separate processes, controlled by a switching function. Moreover, a switching function is included to halt these processes when the terminal electron acceptor (nitrates) is

depleted. Both aerobic and anoxic growth processes are modelled using Monod kinetics. The denitrification process as modelled by van Haandel *et al. (19*81) was also incorporated in the UCTOLD dynamic model (Dold *et al.*, 1991).

4. The aerobic and anoxic growth of heterotrophs on adsorbed SBCOD is also included as two separate processes. With the exception of the anoxic hydrolysis rate being slower, both processes are modelled identically. Thus, the anoxic hydrolysis rate is multiplied by a factor (n_NO_{Hyd}) to account for its slower rate as mentioned earlier (in Section 2.4.1.1). The growth on adsorbed SBCOD also includes the utilization of ammonia or nitrate as the N source as two separate processes, which are controlled by a switching function that depends on the ammonia concentration. Further switching functions are included to ensure the alternating from aerobic to anoxic growth (when oxygen supply is low) and to halt the anoxic growth (when nitrates are depleted).
5. Death of OHOs is based on the death-regeneration hypothesis, which is explained in Section 2.3.2.3 above. The death of heterotrophic organisms is modelled to occur at a specified rate (b_H), with its COD disintegrating in part to SBCOD and the rest to unbiodegradable endogenous residue. Some of the N from the biomass remains organically bound to the SBCOD and endogenous residue while the rest is released into the bulk liquid.
6. Nitrification: Autotrophic organisms convert ammonia to nitrate in a single-step process, for their consequential growth. Since this process occurs with an associated oxygen demand, a switching function is included to bring the process to a halt when the dissolved oxygen concentration is depleted.

When compared by Sötemann *et al.* (2006) the results in the simulation of AS and aerobic digestion systems by UCTOLD (Dold *et al.*, 1991) dynamic simulation model at constant flow and load conditions were found to have a close correlation to the much simpler steady state model.

Most of the processes were taken up into the International Water Association (IWA) ASM1 (Henze *et al.*, 1987) and thus both models are very similar, and can predict oxygen demand, sludge production, nitrification and denitrification for activated sludge systems,

i.e. COD and N removal from the wastewater. They both include the hydrolysis of particulate slowly biodegradable organics together with biological growth and death processes for two groups of organisms, i.e. ordinary heterotrophic (OHOs) and autotrophic nitrifying organisms (ANOs).

In ASM1, the SBCOD is instantaneously enmeshed in the sludge mass, where it is hydrolyzed (no adsorption process) in accordance with the same kinetics in UCTOLD. However, in contrast to UCTOLD, the hydrolysis products are RBCOD, which is returned to the bulk liquid where it adds to the RBCOD from the influent. Effectively, in ASM1 only RBCOD (no adsorbed SBCOD) is utilized by OHOs for growth with only ammonia (not nitrates) acting as the N source. This difference was carried over into the respective subsequent extensions of the models for biological nutrient removal (BNR) AS systems (i.e. from UCTOLD to UCTPHO, and from ASM1 to ASM2).

For the decay/death processes of the OHOs and ANOs, the death-regeneration concept is adopted in both UCTOLD and ASM1: For the OHOs, a fraction (62%, b_H = 0.62/d) of the OHOs die per day, and release all their organic content to the bulk liquid. Of this, a fraction (8%, f'_{EH}=0.08) is unbiodegradable particulate organics and adds to the endogenous residue, while the remainder (1-f'_{eH}=0.92) is biodegradable, adds to the SBCOD and is recycled through the processes of enmeshment, hydrolysis and utilization as the influent SBCOD. For the ANOs, the same concept applies, except that their decay/death rate is very low (b_A=0.05/d).

Since the UCTOLD and ASM1 models were developed, they have achieved wide application in system design, operation and process optimization of nitrification-denitrification (ND) AS systems.

ASM1 was later adapted to include other processes such as biological phosphorus removal and denitrification by phosphate accumulating organisms. This gave rise to activated sludge models ASM2, ASM2d and ASM3 (Henze *et al.*, 2002).

2.4.2.4 AD System Dynamic Models

Various AD system dynamic models have been developed in the past, this section of the reviews describes the ADM1 and UCTAD model, both of which have had great

conceptual contributions to the three phase AD model that is developed in this research report.

The IWA Anaerobic Digestion Model Number 1 (ADM1)

The Anaerobic Digestion Model No. 1 (ADM1), which is based on a variety of past anaerobic digestion models, was developed by the IWA task group as a common model that may be understood, used and, if necessary, extended or modified (Batstone *et al.*, 2002).

The ADM1 model structure is defined by the three general biological processes (acidogenesis, acetogenesis and methanogenesis), an extra-cellular degradation step and an extra-cellular hydrolysis step (refer to Fig. 1.2.).

Cellular kinetics is described by the uptake of substrates and organism growth (using Monod kinetics) together with biomass decay (independently expressed using first order kinetics).

Hydrolysis of influent organics is defined by disintegration of substrates to carbohydrates, proteins and lipids. These three substrates are then hydrolysed to produce monosaccharides, amino acids and long-chain fatty acids respectively. This hydrolysis is mediated by enzymes produced from the AD organisms that attach themselves to the substrate. To include multiple enzyme production, diffusion, adsorption reaction and enzyme deactivation, it was decided that first order kinetics is to be used because it reflects the cumulative effect of all microscopic processes occurring during hydrolysis (Eastman and Ferguson, 1981). The model continues to describe the subsequent degradation of the relatively simple and soluble hydrolysis products through fermentation (acidogenesis) or anaerobic oxidation to short-chain fatty acids (SCFAs) (acetate), alcohols, CO2, hydrogen and ammonia. A portion of the hydrolysis products are also converted to intermediate products (propionate, butyrate, etc.), which are then converted to acetate, hydrogen gas and CO2 through acetogenesis. Lastly, methanogenesis occurs by hydrogen reduction with CO2 (hydrogenotrophic methanogenesis) and from the acetate cleavage (acetoclastic methanogenesis) **(**Batstone *et al.*, 2002).

The UCTAD Model 1 (UCTADM1)

The University of Cape Town AD model number 1 (UCTADM1; Sötemann *et al.*, 2005b) is a two phase (aqueous-gas) chemical, physical and biological (CPB) anaerobic digestion (AD) model, which includes hydrolysis, biological growth and lysis processes of the four recognised AD organism groups. In addition, this model incorporates the system weak acid/base chemistry directly, in terms of the relevant species association and dissociation reactions, enabling the automatic redistribution of weak acid/base species, including the hydrogen ion (H^+) and the establishment of pH.

In UCTADM1 (Sötemann *et al.*, 2005b) the sludge to be fed to the AD is first characterized in terms of total COD, $f_{S'up}$ (fraction of unbiodegradable particulates), SCFA & CHON (carbon, hydrogen, oxygen and nitrogen) content, i.e. X, Y, Z and A in $C_XH_YO_ZN_A$ of the particulate organics. These sludge characteristics are obtained in the upstream unit processes and directly used as the input to the AD process. Mass balances over the PST are used where the sludge digested is PS and compatible AS models such as that developed by Henze *et al.* (2002) are used to characterize WAS where the AS system is the upstream unit process. This is convenient in linking the unit processes for the development of the plant-wide mass balance based model by Ekama *et al.* (2006). After the feed sludge has been characterized, hydrolysis, being the slowest process in anaerobic digestion, is considered to directly generate the idealised carbohydrate 'glucose'. In UCTADM1 (Sötemann *et al.*, 2005) the hydrolysis of the three separate organic materials (proteins, carbohydrates and lipids) of IWA ADM1 (Batstone *et al.*, 2002) is simplified to a single hydrolysis process acting on a generic organic material representing sewage sludge i.e. $C_XH_YO_ZN_A$.

This 'glucose' is directly fermented by the acidogens and converted to SCFAs. Therefore, in the model, 'glucose' does not accumulate but is an intermediate compound, which is acidified to SCFAs as soon as it is produced. Moreover, with the acceptance of a single hydrolysis process, separate anaerobic oxidation of fatty acids does not require inclusion. However, the influence of the hydrogen partial pressure (pH) on acidogenesis of glucose to acetate and propionate as proposed by Sam–Soon *et al.* (1991) was included, since it provided a better description of AD behaviour under failure conditions. In summary the

processes that follow hydrolysis/ acidogenesis being much faster, are dealt with stoichiometrically to yield digester end-products, i.e. biomass, CH_4, CO_2 and water.

2.4.3 Modelling Weak Acid/Base Processes

Initially the impact of the biological processes on pH was assessed graphically based on equilibrium chemistry principles of the carbonate weak acid/base system (e.g. Capri and Marais, 1975).

Loewenthal *et al.* (1989, 1991) then provided an approach that made it possible to include multiple mixed weak acid/base systems, both for estimating the digester pH and in the determination and interpretation of the commonly measured digester control parameters, short-chain (volatile) fatty acids (SCFA) and alkalinity.

Musvoto *et al.* (1997) discovered that it would be difficult to develop an integrated chemical/physical/biological kinetic model for the treatment of high nutrient (N and P) low organic (COD) wastes using the equilibrium chemistry approach. This is because of the practical difficulty that would arise in selection of a weak acid/base system reference species, such that resolving the on-going stoichiometric process calculations that simultaneously act on the various weak acid/base species would arrive at system equilibrium.

Musvoto *et al.* (1997) then used a kinetic approach when modelling mixed weak acid/base systems, to resolve the above complications, whereby the equilibria between weak acid/base systems are formulated according to kinetics of forward and reverse dissociation reactions. This kinetic approach enabled protons $[H^+]$ to be explicitly included together with all the individual weak acid/base systems in the model and hence the direct calculation of pH (where $pH=-\log[H^+]$, which is an important parameter required in the modelling. Thus, the kinetic model ensures that as the various stoichiometric processes continue to simultaneously adjust the relative weak acid/base species (including H^+), equilibrium is always achieved in the various weak acid/ base systems. The dissociation constants from various weak acid/base subsystems are shown in Table 2.1 below.

Table 2.1: Weak Acid Dissociation Constants (Truesdell and Jones, 1973; Loewenthal *et al.*, 1994)					
System	pK *	pK at 25°C	A	B	C
Water	pK_w	14.000			
	pK_{c1}	6.352	3404.7	14.8435	0.03279
Carbonate	pK_{c2}	10.329	2902.4	6.498	0.02379
Henry's constant	pK_{HCO2}	1.470	-1760	-9.619	-0.00753
	pK_{p1}	2.148	799.3	4.5535	0.01349
	pK_{p2}	7.198	1979.5	5.3541	0.01984
Phosphate	pK_{p3}	12.023			
Acetate	pK_a	4.756	1170.5	3.165	0.0134
Ammonium	pK_n	9.245	2835.8	0.6322	0.00123
* pK = (A/T) - B + CT, where T is in Kelvin					

Also using these forward and reverse reactions, for the dissociation of the weak acid/bases to formulate a kinetic model for the single aqueous phase behaviour of mixed weak acid/base systems, Musvoto *et al.* (2000a) included precipitation of $CaCO_3$, CO_2 gas exchange and ion-pairing effects. Musvoto *et al.* (2000b) extended the model to describe the three phase weak acid/base reactions that occur when AD liquor (ADL) is aerated, i.e. the forward and reverse dissociation processes of the weak acid/base species, the precipitation of various magnesium and calcium phosphates and carbonates, ion pairing and stripping of CO_2 and NH_3 gases.

The weak acid/base kinetic constants in Table 2.1 are used together with the weak acid base equilibrium equations, described in Section 6.4 of Chapter 6 in the development of the weak acid/base section of the AD model.

2.4.3.1 Mineral Precipitation

It has been discovered that in the AD and AerD systems (especially those treating BEPR sludge) Magnesium, potassium and calcium can be present at concentrations sufficient for the occurrence of precipitation. The solids most likely to precipitate are included in the model by Musvoto *et al.* (2000c). These solids are struvite ($MgNH_4PO_4$ and/or $mgKPO_4$ (K-

struvite)), newberyite ($MgHPO_4$), amorphous calcium phosphate ($Ca_3(PO_4)_2$), calcite ($CaCO_3$) and magnesite ($MgCO_3$).

Loewenthal *et al.* (1994) noted that the trigger mechanism for the precipitation of these solids is the reduction of the partial pressure of carbon dioxide (p_{CO2}). This is because it could cause expulsion of CO_2 from the aqueous phase leading to increase in pH, hence giving rise to a state of super saturation with respect to struvite. At saturation the total species product equals a pH dependent solubility product constant, termed the conditional solubility product (pK_{SP}). When the total species product is sufficiently high, to exceed the pK_{SP}, a state of super saturation exists with respect to struvite, and vice versa for under saturation.

A range of solubility products (pK_{SP}) for the five mineral salts identified above (struvite, newberyite, Amorphous calcium phosphate (ACP), calcite and magnesite) likely to precipitate on ADL aeration were found in the literature (Ferguson and McCarty, 1971; Musvoto *et al.*, 2000a) and are shown in Table 2.2 below. The stability constants for the ion pairs were then adjusted for ionic strength effects of non-ideal solutions with the Debye-Hückel theory (Musvoto *et al.*, 1998).

Table 2.2: Solubility Products (pK_{sp}) for the Five Minerals likely to Precipitate in ADL		
Precipitate	-Log Solubility Product (pK_{sp})	
	Musvoto *et al.* (2000a)	Other Literature Sources
ACP	25.46	24.0 – 32.7
Struvite	13.16	12.2 – 13.2
Newberyite	5.8	5.8
Magnesite	7	5 – 8.2
Calcite	6.45	6.3 – 8.5

To formulate the kinetics of this precipitation process, the kinetics of crystal growth of sparingly soluble salts, described by Nanchollas and Purdie (1964) is used. The salts grow from solutions of unequal cation and anion concentrations as shown in Equation 2.4.11:

$$-\frac{dm}{dt} = k \cdot s \cdot \left\{ \left(\left[M^{y+} \right]^x \cdot \left[A^{x-} \right]^y \right)^{\frac{1}{(x+y)}} - K_{sp}^{\frac{1}{(x+y)}} \right\} \tag{2.4.11}$$

where:
m = mass of salt precipitated (mo*l*/*l*)
k = rate constant (mo*l*/m^{2}s)
s = surface area of crystals (m^2/mol)
K_{sp} = solubility product of salt M_xA_y (molar form)

This equation was used by Kotsoukos *et al.* (1980) to describe the rate of precipitation of sparingly soluble salts, i.e. for a salt $M_{v+}A_{v-}$ the rate of precipitation can be expressed as:

$$-\frac{\left(dM_{V+}A_{V-}\right)}{dt} = k' \cdot s \cdot \left\{ \left(\left[M^{m+} \right]^{v+} \cdot \left[A^{a-} \right]^{v-} \right)^{\frac{1}{v}} - \left(\left[M^{m+} \right]_0^{v+} \cdot \left[A^{a-} \right]_0^{v-} \right)^{\frac{1}{v}} \right\}^n \tag{2.4.12}$$

Where:

- $[M^{m+}]$, $[A^{a-}]$, $[M^{m+}]_0$ and $[A^{a-}]_0$ are the concentrations in (mol/*l*) of crystal lattice ions in solution at time t and at equilibrium respectively.
- $K_{sp'} = ([M^{m+}]_0^{v+}[A^{a-}]_0^{v-})^{1/v}$ at equilibrium, $K_{SP'}$ is the apparent solubility product of the salt.
- k' = precipitation rate constant (mo*l*/m^{2}s).

- s is proportional to the total number of available growth sites on the added seed material.
- v^+ = number of cationic species.
- v^- = number of anionic species.
- $v = v^+ + v^-$.
- n is an experimentally determined parameter, which equals 2 for a number of divalent sparingly soluble salts.

In cases considered by Musvoto *et al.* (1998), no seed material of the precipitating crystal is added, therefore the term k's is replaced by the precipitation rate constant, k'.

The various forward and reverse reactions that describe precipitation or dissolution of struvite, newberyite, ACP, calcite and magnesite and the kinetics of these reactions as obtained from Musvoto *et al.* (2000 a, b and c) are given in Table 2.3 below:

Table 2.3: Precipitation Process Reactions and Kinetics (Musvoto *et al.*, 2000 a)

Precipitate	Reaction	Kinetic rate formulation	Kinetic constant (k'_r)*
ACP	$Ca_3(PO_4)_2.xH_2O \Leftrightarrow 3Ca^{2+} + 2PO_4^{3-} + x.H_2O$	$\frac{\partial[ACP]}{\partial t} = k'r_{ACP}\left\{\left[Ca^{2+}\right]^{\frac{3}{5}}\left[PO_4^{3-}\right]^{\frac{2}{5}} - K'sp_{ACP}^{\frac{1}{5}}\right\}^2$	350
NH_4-Struvite	$MgNH_4PO_4.6H_2O_{(s)} \Leftrightarrow Mg^{2+} + NH_4^+ + PO_4^{3-} + 6H_2O$	$\frac{\partial[Struv]}{\partial t} = k'r_{Struv}\left\{\left[Mg^{2+}\right]^{\frac{1}{3}}\left[NH_4^+\right]^{\frac{1}{3}}\left[PO_4^{3-}\right]^{\frac{1}{3}} - K'sp_{Struv}^{\frac{1}{3}}\right\}^2$	3000
K-Struvite	$MgKPO_4.6H_2O_{(s)} \Leftrightarrow Mg^{2+} + K^+ + PO_4^{3-} + 6H_2O$	$\frac{\partial[MgKP]}{\partial t} = k'r_{MgKP}\left\{\left[Mg^{2+}\right]^{\frac{1}{3}}\left[K^+\right]^{\frac{1}{3}}\left[PO_4^{3-}\right]^{\frac{1}{3}} - K'sp_{MgKP}^{\frac{1}{3}}\right\}^2$	
Newberyite	$MgHPO_4.3H_2O_{(s)} \Leftrightarrow Mg^{2+} + HPO_4^{2-} + 3H_2O$	$\frac{\partial[Newb]}{\partial t} = k'r_{Newb}\left\{\left[Mg^{2+}\right]^{\frac{1}{2}}\left[HPO_4^{2-}\right]^{\frac{1}{2}} - K'sp_{Newb}^{\frac{1}{2}}\right\}^2$	0.05
Magnesite	$MgCO_3 \Leftrightarrow Mg^{2+} + CO_3^{2-}$	$\frac{\partial[MgCO_3]}{\partial t} = k'r_{mgCO_3}\left\{\left[Mg^{2+}\right]^{\frac{1}{2}}\left[CO_3^{2-}\right]^{\frac{1}{2}} - K'sp^{\frac{1}{2}}\right\}^2$	50
Calcite	$CaCO_3 \Leftrightarrow Ca^{2+} + CO_3^{2-}$	$\frac{\partial[CaCO_3]}{\partial t} = k'r_{CaCO3}\left\{\left[Ca^{2+}\right]^{\frac{1}{2}}\left[CO_3^{2-}\right]^{\frac{1}{2}} - K'sp^{\frac{1}{2}}\right\}^2$	0.5

* The K'r constants given are as used by Musvoto *et al.* (2000a) in the simulations of aerobic batch tests on effluent from UASB reactor treating wine distillery waste.

As mentioned above the model for the three phase mixed weak acid/base system model by Musvoto *et al.* (2000a, b and c), Van Rensburg *et al.* (2003) and Loewenthal *et al.* (2004) could be used to simulate active gas exchange, which is briefly described below.

2.4.3.2 Gaseous Exchange

Gas exchange processes can occur passively (without gas bubbling) or actively (with gas bubbling, e.g. aeration). For both cases, the gas exchange formulations apply, except that of oxygen dissolution, which specifically requires aeration. However, the values of the gas exchange constants differ significantly for the two situations (Sötemann *et al.*, 2006).

Four gases (i.e. CO_2, CH_4, H_2 and NH_3) are considered in the application of integrating the AS and AD biological processes to the (aqueous-gas) mixed weak acid/base chemistry model of Musvoto *et al.* (2000a). Methane (CH_4) has very low solubility and is deemed unutilized in the biological or chemical processes, but directly produced through the AD methanogenic process. Therefore, this compound is included in the model in its gas phase. Hydrogen (H_2) is also quite insoluble but is utilized rapidly at an inter-organism species level in the hydrogenotrophic methanogenesis process, leaving only trace quantities of its residual concentration. Therefore, rather than its direct transfer to gas phase, H_2 has to be modelled as a dissolved compound (Musvoto *et al.*, 2000a).

Gases (CO_2 and NH_3) are expected to be stripped and the exchange of CO_2 and NH_3 between the liquid and gas phases has been outlined by Musvoto *et al.* (2000a, b).They noted that the atmospheric concentration of NH_3 is negligible (i.e. acts as an infinite sink), so that only NH_3 expulsion, due to bioprocesses, is included and its dissolution disregarded. However, carbon dioxide (CO_2) needs to be modelled with both expulsion and dissolution processes, because this gas is significantly soluble (Sötemann *et al.*, 2005a). This modelling could be done using the approach of Musvoto *et al.* (1997), described by two separate Equations 2.4.13 and 2.4.14 below;

$$H_2CO_3^* \xrightarrow{r_{fCO2}} CO_{2(g)} + H_2O \qquad (2.4.13)$$

$$CO_{2(g)} + H_2O \xrightarrow{r_{rCO2}} H_2CO_3^*$$

(2.4.14)

Where:

r_{fCO2} = k_{fCO2} $H_2CO_3^*$] = CO_2 Expulsion Rate [mol/*l*.d]

r_{rCO2} = k_{rCO2} [$CO_{2(g)}$] = CO_2 Dissolution Rate [mol/*l*.d].

The equilibrium between the dissolved (H_2CO_3) and gaseous CO_2 is maintained, i.e.

$$k' f_{CO2} = K' eq_{CO2} \cdot k' r_{CO2}$$

(2.4.15)

and the CO_2 dissolution and expulsion processes are correlated through the Henry's law constant for CO_2 (K_{HCO2}):

$$Keq_{CO2} = \frac{k' r_{CO2}}{k' f_{CO2}} = \frac{1}{K_{HCO2} \cdot R \cdot T_k} = CO_2 \text{ Equilibrium Constant (/d)}$$

(2.4.16)

Where:

K_{HCO2} (Henry's Law Constant) $= 10^{-pK_{HCO2}}$ [1/d], with pK_{HCO2} given in Table 2.3 above

R = Ideal Gas Law Constant = 0.08206 [J/mol. Kelvin]

T_k = Temperature [Kelvin]

To simulate gas exchange at dynamic situations, the rates at which the gas exchange processes take place were required. These rates were determined by Musvoto *et al.* (2000a) using experimental batch tests on the UASB reactors.

The equations used to model the rates of gas (CO_2 and NH_3) exchange are as outlined below:

1. For CO_2 gas exchange, Musvoto *et al.* (1997) noted that the process could occur

   i. When there is a difference in partial pressure of the CO_2 dissolved and gas phases causing CO_2 exchange to occur for the establishment of equilibrium;

$$\frac{\partial [CO_2 \text{ exp } ul]}{\partial t} = k_{fCO2} \{(\rho_{CO_2})(K_{HCO2})\}$$

(2.4.17)

   for CO_2 expulsion and

$$\frac{\partial[CO_2 dissol]}{\partial t} = k_{rCO2}\left[H_2CO_3^*\right]$$

(2.4.18)

for CO_2 dissolution.

ii. When aeration actively strips the dissolved CO_2 (H_2CO_3) from the liquid mass.

$$\frac{\partial[CO_2 Strip]}{\partial t} = K_{LaCO2}\left\{\left[H_2CO_3^*\right] - \rho_{CO_2} \cdot K_{HCO2}\right\}$$

(2.4.19)

Where K_{LaCO2} is the CO_2 overall liquid phase mass transfer rate coefficient, which is determined using Equation 2.4.22 below.

2. For NH_4, the atmosphere is assumed to act as an infinite sink, making the gas phase concentration at equilibrium negligible.

$$\frac{\partial[NH_3 Strip]}{\partial t} = k_{rNH3}[NH_3]$$

(2.4.20)

For various compounds stripped with the same aeration method, having similar geometric and hydrodynamic reactor conditions, Musvoto *et al.* (1997) noted that the rate constants for volatile solutes are proportional to each other. This made it possible to introduce the concept of measuring a single mass transfer coefficient value for a reference compound, which was then applied to calculate the mass transfer coefficient values for the other compounds (Munz and Roberts, 1989). Since aeration involves the transfer of oxygen, a compound that meets the required standards for volatility (shown below), Musvoto *et al.* (1997) selected oxygen as the reference compound. This was a suitable approach because only the mass transfer coefficient of oxygen required measurement. However, for this approach to be applicable to a compound, its solutes must also be sufficiently volatile, allowing the liquid phase resistance to be capable of controlling the inter-phase mass transfer rates. This volatility criterion is rated according to the compounds' dimensionless Henry's coefficient ($H_{ci} > 0.55$).

$$H_{ci} = \frac{1}{K_{Hi} \cdot R \cdot T_K}$$

(2.4.21)

Where:

K_{Hi} = Henry's law constant for the compound

R = Ideal Gas Law Constant = 0.08206 [J/mol. Kelvin]

T_k = Temperature [Kelvin]

Oxygen being the reference compound, the K_{La} for other gases is taken to be dependent on the magnitude of diffusivity of the other gases with respect to oxygen. Munz and Roberts (1989) provided a formulation that captured this relationship, in order to allow for the calculation of other gases' KLa values once that of oxygen (K_{LaO2}) is known:

$$K_{Lai} = K_{LaO2}\left[\frac{D_{Li}}{D_{LO2}}\right]^n \cdot \left[1 + \frac{1}{\frac{k_G}{k_L} \cdot H_{ci}}\right]^{-1}$$

(2.4.22)

Where:

K_{Lai} = overall liquid phase mass transfer rate coefficient for compound I [/d]

D_{Li} = Liquid phase molecular diffusion coefficient for compound i [cm^2/s]

k_G = Gas phase individual mass transfer coefficient [m/s]

k_L = Liquid phase individual mass transfer coefficient [m/s]

n = Diffusivity Coefficient = 0.5

2.4.3.3 The C and N Removal AS System Model of Sötemann *et al. (2005a)* with Applications of the Musvoto *et al.* (1998; 2000a, b) Kinetic Model

Van Rensburg *et al.* (2003) evaluated the kinetic model of Musvoto *et al.* (1998; 2000a, b) and investigated mineral precipitation problems at Cape Flats Wastewater Treatment Plant in order to provide possible solutions to mineral precipitation problems. His research included experimental investigations (batch aeration tests and pH-controlled experiments) on AD systems from the Cape Flats (CF) WWTP. The kinetic model of

Musvoto *et al.* (1998; 2000a, b) was then applied to the experimental results. The following were part of his findings:

- The dominant mineral that precipitated was struvite (97% of the mass of precipitant) followed by ACP (3%), and negligible newberyite, calcite and magnesite precipitate.
- The precipitation of struvite is stimulated by the increase in pH when CO_2 is lost from the AD systems, which can occur with aeration of the ADS.
- The rate of struvite precipitation is not limited by precipitation kinetics, but rather by the rate of increase in pH, which (with no buffer added) is limited by the rate of CO_2 stripping.
- The amount of struvite that precipitates is limited by the initial Mg concentration present, whereby if the initial concentration of Mg is increased, then more struvite precipitates.
- Theoretical modelling of the precipitation, using the default values of model constants that were suggested by Musvoto *et al.*, except for the struvite specific precipitation constant (increased from 300 to 1000/d), gave close correspondence with experimentally measured values.

In the formation of an integrated biological, chemical and physical processes kinetic model for anoxic/aerobic C and N removal in activated sludge systems Sötemann *et al.* (2005a) incorporated the gaseous exchange processes from the mixed weak acid/base model of Musvoto *et al.* (1997) into ASM1, in the computer simulation program Aquasim. This was specifically because the model by Musvoto *et al.* (1997) had a general approach and could be applied to include (or exclude) any weak acid/base system as well as the stripping of virtually any gas.

When integrating the biological processes of C and N removal of ASM1 into the chemical-physical model of Musvoto *et al.* (1997, 2000a, b, c), Sötemann *et al.* (2005a) needed to define interactions between:

1. The chemical and biological processes:
    a) The influence of the biological processes on the production and/or utilization of H^+ ions and CO_2 together with carbonate, ammonia and phosphate weak

acid /base system species. This required reformulating the kinetic rates of the relevant biological processes to utilize specific species of the weak acid/base systems, by adding new stoichiometric coefficients and modifying existing ones.

b) The effect of pH on the relevant biological process rates. To incorporate its effect pH was included in the kinetic rate formulation of the processes to which it was a direct influence.

2. The chemical and physical processes:
    a) Production and loss of N_2 species with gas exchange processes.
    b) Provision of dissolved oxygen via aeration and its utilization in biological processes.

Sötemann *et al.* (2005a) noted that since ammonia did not meet the volatility criterion (Hc = 0.011, hence < 0.55 at 20°C), it was required that the K_{LaNH3} be determined independently of the K_{La} rate of oxygen (the selected reference compound).

Unlike the mixed weak acid/base model of Musvoto *et al.* (2000a), the concentration of non-dissolved gases is not constant because Sötemann *et al.* (2005a) considered dynamic variation of gases under production and consumption. This was done by substituting the gas species (e.g. CO_2) concentration for the relevant gas partial pressure and Henry's law constant (e.g. p_{CO2} and K_{HCO2}). Thus with the dissolved and gaseous phases of the relevant compounds considered as separate model components, removal of the gas from the reactor was modelled to occur hydraulically, i.e. with the effluent flow.

For simulations, Sötemann *et al.* (2005a) set the k_G/k_L ratio to 40 as recommended by Munz and Roberts (1989) for the high turbulent mixing conditions created by power inputs (P/V) greater than 70 W/m^3, which was characteristic of aerated activated sludge reactors. During simulations they discovered that the increases in K_{LaO2} rate caused increased aerobic reactor dissolved oxygen (DO) and decreased CO_2 (H_2CO_3*) concentrations, but did not affect the pH. However, the anoxic reactor pH increased as the K_{LaO2} rate decreased due to increasing denitrification and greater alkalinity generation resulting from recycling less DO to the anoxic reactor (at a mixed liquor recycle ratio of 1:1). Sötemann *et al.* (2005a) then decided to set the K_{LaO2} rate at 600/d to ensure that the

simulated aerobic reactor effluents had low (about 20%) dissolved CO_2 concentrations, as measured from two full-scale activated sludge plants with fine bubble aeration. They set the mass transfer coefficient for ammonia (K_{LaNH3}) at a very low value of 3.2/d to ensure an extremely low loss of ammonia by aeration stripping. Table 2.4 shows the rates of gas stripping reported by Musvoto *et al.* (2000) and Sötemann *et al.* (2006).

Table 2.4: Rates of Aeration/Gas Stripping

		K_{La}/d	
		Musvoto *et al.* (2000)*	Sötemann *et al.* (2006)
Oxygen	O_2	670	600
Carbon Dioxide	CO_2	610	Based on O_2 (see Equation 2.4.22)
Ammonia	NH_3	1.92	3.2

* The K_{LA} constants given are as used by Musvoto *et al.* (2000a) in the simulations of aerobic batch tests on effluent from UASB reactor treating wine distillery waste.

To incorporate the biological processes of the activated sludge model, Sötemann *et al.* (2005a) added gas exchange processes for N_2, formulated in the same way as for CO_2, together with the process of O_2 dissolution by aeration. To include these processes, it was required for Sötemann *et al.* (2005a) to add the gaseous oxygen and nitrogen as model components, their dissolved phases already being compounds of the biological processes section of the model.

Sötemann *et al.* (2005a) also noted that to incorporate the biological processes of anaerobic digestion (in the formation of a plant-wide model) only methane (CH_4) would be the added gaseous compound. Since CH_4 has a velry low solubility, it was assumed that the CH_4 gas is formed directly by the biological processes. Although dissolved hydrogen is also produced and utilized in anaerobic digestion Sötemann *et al.* (2005a) noted that hydrogen gas production is negligible compared with CO_2 and CH_4 and hence included hydrogen only as a dissolved species.

The two phase (aqueous-gas) integrated chemical-physical-biological (CPB) processes activated sludge system model of Sötemann *et al.* (2005a) for C and N removal can be summarized to comprise of:

1. The biological activated sludge processes includes the biological C and N removal processes from ASM1 and additional processes of aerobic and anoxic OHO growth on ammonium and nitrate with their associated new compounds NH_4^+, H_2CO_3*, H^+, HPO_4^{2-}.
2. The physical gas exchange processes, including the exchange of ammonia, carbon dioxide and nitrogen gases together with aeration dissolution of oxygen with associated compounds of dissolved ammonia, dissolved and gaseous carbon dioxide, oxygen and nitrogen. A gaseous ammonia compound was not included, because the gas stream is deemed negligible.

However, the integrated chemical, physical and biological model of Sötemann *et al.* (2005a) did not include chemical ion pairing and physical mineral precipitation processes. This is because the model only considered the two (aqueous-gas) phases (no solid phase) for activated sludge systems treating municipal wastewater.

2.4.4 The Formation of a Dynamic PWMM

Until recently, research was focussed on modelling activated sludge systems, since the effluent water is produced from these systems and high costs of aeration were involved and of prime importance. However, recently there has been interest in other unit processes of the WWTP. This recent interest triggered the research into modelling the WWTP as a whole.

In these 'plant –wide' models the WWTP is itself considered a unit, where primary/secondary clarification units, activated sludge reactors, anaerobic digesters, thickeners, dewatering systems, etc. are linked together and thus operated and controlled, not only on a local level as individual processes but by supervisory systems as well, taking into account all the interactions between the processes.

Whole wastewater treatment plant mass balances models can have a number of potential advantages. These may include

1. The tracking of compounds through the WWTP in order to identify the characteristics of streams between different links in order to assess the impact on downstream unit operations.

2. Assessment of the impact of recycled flows such as sludge thickening and dewatering liquors from downstream on upstream unit operations.
3. Avoidance of sub-optimisation, which could lead to reduced effluent quality or higher operational costs.
4. The possibility of identifying the potential of overloading unit operations, optimisation of unit operations, prediction of mineral precipitation problems and the identification of parameters that do not conform to mass balance and continuity principles (Wentzel *et al.*, 2006).

Attempts towards the coupling of different unit process models for the purpose of creating a whole WWTP simulation model has not been straight forward. This is due to the incompatibilities promoted by various process differences between the individual units of the plant and different state variable meanings that resulted from isolated development of the individual unit process models.

Thus the recent proposals towards the development of whole WWTP simulation models have included the continuity based interfacing method (CBIM) of Vanrolleghem *et al.* (2005) and Volcke *et al.* (2006), the 'supermodel approach' of Jones and Takács (2004) and Seco *et al.* (2004), the transformation based approach of Grau *et al.* (2007) and the mass balances based whole WWTP model approach of Ekama *et al.* (2006). All of these approaches have been aimed at circumventing the model interfacing difficulties caused by state variable incompatibilities. A general theme in the model approaches is the use of compounds in their elemental composition forms, viz. C, H, O, N, P and charge content, as part of a method to transform incompatible unit process state variables into compatible forms. The different model approaches are further discussed below.

2.4.4.1 Continuity Based Interfacing Method – CBIM (Volcke *et al.*, 2006)

The CBIM approach is based on the idea of creating interfacing models between the origin (e.g. AS system) and destination (e.g. AD system) unit process models from which, and to which, the WWTP streams flow respectively. The interfacing models are used to transform the origin model state variable compositions and units to become compatible with those required in the destination model. In this approach, the unit process sub-models are left

unchanged and mass conservation is adhered to in variables e.g. C, H, O, N, P, COD and charge (Volcke *et al.*, 2006).

The CBIM approach comprises of four generally applied steps:

i. Formulation of component elemental mass fractions:

Components of all sub models are described according to charge (ch) and constant mass fraction elements C, H, O, N, and P. In this step, it is assumed that the mass of each model component (k) consists of a constant elemental mass fraction (α), i.e.:

$$\alpha_k^C + \alpha_k^H + \alpha_k^O + \alpha_k^N + \alpha_k^P = 1 \tag{2.4.23}$$

The general formula for 1 gram of a model component, after charge has also been incorporated, is then given as:

$$\left[C\left(\frac{\alpha_k^C}{12}\right) H\left(\alpha_k^H\right) O\left(\frac{\alpha_k^O}{16}\right) N\left(\frac{\alpha_k^N}{14}\right) P\left(\frac{\alpha_k^P}{31}\right) \right]^{\alpha Ch} \tag{2.4.24}$$

ii. Establishment of composition matrices for each unit process model:

The interface method uses a Gujer matrix description of the origin and destination unit process to develop a set of algebraic equations that can be used to transform variables in the interface between these models.

iii. Definition of transformation matrices:

The interface, with inputs consisting of output state-variable fluxes from the origin sub-model and outputs consisting of input state-variable fluxes to the destination model, is created.

iv. Development of component transformation equations:

Transformation equations are defined by stoichiometric considerations. Therefore, they specify the amount of an origin model component that is transformed to an amount of a destination model component (Vanrolleghem *et al.*, 2005).

Once transformation equations have been designed, the unknowns (stoichiometric coefficients and transformation rates) may be calculated through a set of linear equations.

These unknowns can then be used to calculate the destination model influx components with the transformation equations. Because it is not likely that all users will specify the same transformation equations for the destination model influx components, the model solutions for a specific problem may vary significantly from one user to another. Therefore, it was proposed that such specifications be performed based on process knowledge and insight.

Volcke *et al.* (2006) illustrated the CBIM approach by means of four different interfacing case studies, viz. the creation of interfaces between the ASM1 and SHARON models, SHARON and Anammox models as well as Anammox and ASM1 models.

In developing the Benchmark Simulation model number 2 (BSM2), which links the ASM1 model of Henze *et al.* (2000) and the ADM1 model of Batstone *et al.* (2002), Jeppsson *et al.* (2006) adopted an Ad hoc research interface maintaining continuity to CBIM approach, which leaves the existing ASM1 and ADM1 unit process models unchanged. The rationale was that since ASM1 and ADM1 models are good representations of reality, why change them? In linking ASM1 and ADM1, they made a number of educated guesses (which may require some experimental validation), the most important of which are:

The unbiodegradable organics as defined in the AS system, i.e. the influent unbiodegradable particulate organics and the activated sludge endogenous residue, remain unbiodegradable in the AD.

This assumption, if validated, has some major implications, i.e.:

1. The unbiodegradable fraction of the primary sludge organics can be calculated by mass balance (e.g. COD, N and P) from the raw and settled wastewater characteristics.
2. Only the biodegradable part of the live biomass in the waste activated sludge is anaerobically digestible. If (1) above is experimentally validated, it suggests a way to validate the theoretically predicted live biomass concentration from ASM1, which has not been possible very confidently to date with microbiological techniques, such as FISH, DGGE, PCR etc. If the unbiodegradable fraction of the WAS from the AS system is closely the same as that measured in long sludge age AD fed this WAS, then it validates that

the live biomass concentration predicted by ASM1 is very similar to the measured value.

One purpose of plant-wide models is to evaluate the impact of recycling liquor from downstream unit operation, particularly the liquor from sludge digesters back to the influent (see Figure 2.1), on the effluent quality from the AS system. However, aerobic and anaerobic digestion of PS and/or WAS have significantly different N and P concentration in the dewatering liquor, energy foot-prints and economic considerations (see Table 1) making sludge treatment unit operation selection complex. In order to deal with the high nutrient (N and P) content of anaerobic digester liquor (ADL), SHARON and ANAMMOX systems for N removal and struvite crystallization systems for P removal have been developed (Volcke *et al.*, 2006). An important process affecting the N and P content of the digester liquors from AD (of WAS) is mineral precipitation both in the AD and its effluent. In order to assess the significance of this, the aerobic and anaerobic digester models will be developed in three phases (aqueous-gas-solid) to include prediction of mineral precipitation. Previous plant-wide models are two phase (aqueous-gas) and are therefore unable to predict the impact of mineral precipitation on ADL N and P concentration. Table 2.5 below compares aerobic and anaerobic digestion sludge treatment processes.

Table 2.5: Advantages and Disadvantages of Aerobic or Anaerobic Treatment of PS and WAS

	Anaerobic				Anoxic - Aerobic			
	Advantage		Disadvantage		Advantage		Disadvantage	
	1	High energy (CH4) production	1	Complex operation	1	Simple operation	1	Energy intensive
	2	Low N and P content digestion liquor (DL)			2	Low N and P content DL	2	Low VSS removal
	3	High hydrolysis rate						
PS	4	High biodegradability						
	1	Some CH_4 produced	1	Low biodegradability	1	Simple operation	1	Energy intensive
	2	Limited P precipitation	2	Slow hydrolysis rate	2	Low N and P content DL	2	Lower VSS removal
			3	Complex operation	3	High N removal and P precipitation		
			4	High N and P content DL				
WAS			5	Mineral precipitation problems				

2.4.4.2 The Supermodel Approach

In the super-model approach (Jones and Takács, 2004), all components and transformations from the sub-model of each unit process are combined to form the plant-wide model, with state-variable transforming interfaces between unit-process models deemed unnecessary. This increases the size of all unit process models and thus increases computation time.

2.4.4.3 The Transformation–Based Approach

The transformation-based approach (Grau *et al.*, 2007) uses the most suitable process transformations, selected from a created and universally accepted list of transformations, for specific WWTP simulations.

The proposed transformation-based methodology consists of three main steps, viz.

1. The creation of a general list of transformations (LT) with the resultant construction of a specific plant transformation model (see Grau *et al.*, 2007).

2. The construction of a plant transformation model (PTM) - A specific plant transformation model (PTM), comprising selected transformation processes and a plant components vector (PCV) may be constructed for each unique whole WWTP simulation problem. Thus, the relevant transformation processes are selected from the list created in (1) and a PCV, which is a set of model components that includes their elemental compositions, is constructed (Grau *et al.*, 2007).
3. Direct Interfacing of Unit Process Models (UPMs) to construct the plant-wide model (PWM). To complete this step it is required that the selected components and transformation processes are displayed in a Gujer Matrix format.

Grau *et al.* (2007) noted that the following actions are substantial to reduce the model complexity of this step:

a. The use of mass transport considerations only in processes where biochemical activity is not assumed to exist (e.g. clarifiers),
b. elimination of transformations where irrelevant e.g. anaerobic processes during activated sludge treatment and
c. the lumping of variables where required e.g. TSS requirements in clarifiers.

The transformation-based approach incorporates a selection of process transformations that may be used to model all unit process elements in a specific WWTP. Unit process transformations need to be compatible among different unit processes and thus a requirement of this approach is the re-writing of current unit process models (Grau *et al.*, 2007). This is a major requirement as many current unit process models are generally accepted and well known and may become highly time-consuming with little or no gain in unit process optimisation.

2.4.4.4 Mass Balance Based Plant-Wide Modelling Approach

For the development of a plant-wide mass balance based model, investigations were carried out to track the wastewater organic, inorganic and N compounds over the unit process links of the primary settling tank (PST), N removal AS systems, the AD and the

aerobic digester (AerD) unit processes (Ekama *et al.*, 2006; Sötemann *et al.*, 2006 and Wentzel *et al.*, 2006). From these semi-quantitative investigations, it was noted that the PS can be characterised using mass balances over the PST, and that the organics of sewage and waste activated sludge that are unbiodegradable in fully aerobic or N removal systems remain unbiodegradable in anaerobic systems (see Section 2.4.1.3).

This mass balance based plant-wide modelling approach uses developed calculation methods for the characterisation of organic components, in terms of total COD, $f_{S'up}$ (fraction of unbiodegradable particulates), SCFA and CHON (carbon, hydrogen, oxygen and nitrogen) content, i.e. X, Y, Z and A in the $C_XH_YO_ZN_A$ elemental composition of organics. This characterisation methods together with the developed stoichiometric equations for the various unit processes (AS, AD and AerD) allow the tracking of materials over the WWTP (where sludge characteristics from upstream AS unit processes are used as input to downstream AD or AerD processes) and the calculation of material (COD, C, H, O and N) mass balances over the plant.

Together with developing an integrated steady state mass balances model for the whole WWTP system (useful for sizing of WWTP unit operations and interconnecting flows), it was required that a similar integrated dynamic plant-wide model be developed. As the steady state mass balances model, this dynamic model was to consider the same links of PST, AS, AD and AerD unit processes and also be based on the same mass balances principles of Ekama *et al.* (2006), Sötemann *et al.* (2006) and Wentzel *et al.* (2006).

An integrated chemical (C), physical (P) and biological (B) processes kinetic model for the N removal activated sludge system was developed by Sötemann *et al.* (2005a), by integrating the biological processes of the International Water Association (IWA) Activated Sludge Model No 1 (ASM1, Henze *et al.*, 1987) into a two phase (aqueous-gas) subset of the three phase mixed weak acid/base C-P model of Musvoto *et al.* (1997, 2000a,b,c), and included additionally gas exchange of N_2 (see Section 2.4.3.3). Following this, an integrated two phase (aqueous-gas) chemical (C), physical (P) and biological (B) processes AD model for sewage sludges, was developed by Sötemann *et al.* (2005b) by integrating the biological processes for AD with the same two phase subset of the three phase CP model of Musvoto *et al.* (1997, 2000a,b,c) (see Section 2.4.2.4). Therefore, the two

models (i.e. the N removal activated sludge model of Sötemann *et al.* (2005a) and AD model of Sötemann *et al.* (2005b)) have been programmed into a two phase mixed weak acid/base framework to form a two phase integrated mixed weak acid/base chemical, physical and biological process models for simulating the WWTP systems (Sötemann et al 2005; Ekama *et al.*, 2007).

However, the mass balance based modelling approach of Ekama *et al.* (2006), Sötemann *et al.* (2006) and Wentzel *et al.* (2006) requires stronger validation towards the continuity of unbiodegradable organics in the WWTP. This is because the investigation by Wentzel *et al.* (2006) was done semi-quantitatively, whereby the unbiodegradble fraction of PS (0.35) was calculated from the observed unbiodegradable particulate fraction values in typical South African raw and settled municipal wastewaters, i.e. 0.15 and 0.04 respectively (WRC, 1984). A more quantitative investigation into this research aspect, by using the same wastewater in AS systems as in the AD system, would be useful in the confirmation of the Wentzel *et al.* (2006) findings. Also, the integrated chemical, physical and biological model of Sötemann *et al.* (2005a) does not include chemical ion pairing and physical mineral precipitation processes. The three phase plant-wide mass balance based model (which extends the one developed by Ekama *et al.* (2006), Sötemann *et al.* (2006) and Wentzel *et al.* (2006)) developed in this thesis intends to address these issues (see Sections 1.2 and 1.3) in the extended mass balance based .

2.5 CLOSURE

Wastewater Treatment Plants (WWTP) are considered useful in the treatment of water for the production of environmentally safe effluents and the recovery of various useful elements in the wastewater. This literature review includes an outline on the characterisation of municipal wastewater and a general overview of WWTP systems, used in treating municipal wastewater, together with brief descriptions of primary secondary and tertiary unit processes that form a WWTP. This is done with particular reference to the unit processes directly related to the investigations performed in this research project (including PST, N removal (such as MLE system) and NDBEPR AS systems, SSTs and AD systems). The municipal WWTP secondary treatment systems are distinguished, between

those that are defined as fixed-film and those of suspended growth. Thereafter, the AS systems, which shall be used in this research project are reviewed, including Nitrification-Denitrification (ND) systems (with MLE process description given as example) and Biological Excess Phosphorus Removal (BEPR) systems. The various zones (anaerobic, anoxic and aerobic) of these AS systems are described and the composition of the activated sludge, including the microorganisms that constitute it and the biological treatment processes that the microorganisms carry out in the various AS system zones. This is followed by a brief discussion on the settling tanks and membrane technology used in separating the waste sludge in these AS systems from the treated effluent. A comprehensive review on AD systems used in treating the primary sludge that is collected from the PST and/or the sludge wasted from AS systems is then presented.

Predictive WWTP models are required to assist in making the most appropriate decisions on design and operation optimisation of the WWTP facilities. Some of the various mathematical models developed in the past for this purpose have been described in this chapter. In the past, the WWTP individual unit operation models (such as AS and AD systems) were developed in isolation. The currently developed unit process (activated sludge aerobic digestion and anaerobic digestion units) mathematical models for WWTP, treating municipal wastewater, are presented. It is noted that attempts to model the whole WWTP by coupling the unit process models were complicated due to the state variable incompatibilities between these unit process models. However, there have been various recent proposals on how to overcome these model-interfacing difficulties. These proposals were reviewed in this chapter together with the investigations over ancillary issues regarding the development of plant-wide models (such as the biodegradability of influent wastewater organics and exploring the possibility of the unbiodegradable material being continuous throughout the WWTP). It is noted that this thesis involves the extension of a plant-wide model using the approach of Ekama *et al.* (2006), Sötemann *et al.* (2006) and Wentzel *et al.* (2006). The models to be extended in this regard are the nitrogen (N) removal activated sludge and anaerobic digestion (AD) models of Sötemann (2005), which are two compatible parts of a single larger model for simulating the entire wastewater treatment plant (WWTP) on materials mass balance and continuity principles of Ekama *et*

al. (2006). It is intended to modify this mathematical model through including the AD of phosphorus (P) rich waste activated sludge, from biological excess P removal (BEPR) systems. A step towards this modification is the advancement of the sludge elemental characterisation with the addition of phosphorus (P) as a component of the generic material, which would be useful in the characterisation of WAS from BEPR systems. Furthermore, the PAOs, which exist in these systems, have a different endogenous respiration rate (b_H) which influences the rates at which the nutrients (N and P), which are bound in the cell mass, are released during AerD or AD. The release rates need to be investigated to include BEPR systems into the plant-wide mathematical model PWMM (Sötemann *et al.*, 2006). Also, the unbiodegradable portion of the substrate needs to be accounted for to avoid error of describing reduced rates in these mathematical models. A review of literature would suggest that the unbiodegradable particulates in aerobic systems remain unbiodegradable when moved to anaerobic systems. However, since the raw wastewater characteristics were mainly based on the steady state AS model from Marais and Ekama (1976) rather than data obtained using the same wastewater, there is no absolute surety of the above conclusions.

CHAPTER 3: MATERIALS AND METHODS

3.1 INTRODUCTION

The core objective of this chapter is to explain the experimental set-up and analytical procedures used in performing the experimental work. This chapter is largely similar to the equivalent by Harding (2009), because the experimental work for both projects was done collaboratively. However, the same data is used for different research questions. Harding (2009) focused on the anaerobic digestion (AD) of nitrification-denitrification biological excess phosphorus removal (NDBEPR) waste activated sludge (WAS) and the development of a steady state stoichiometric AD model, including phosphorus (P), while this report focuses on (1) biodegradability and kinetics of hydrolysis of various organic types, including primary sludge (PS) and WAS, (2) the inclusion of a solid phase to the steady state AD model and (3) the development of a three phase (aqueous-gas-solid) dynamic mathematical model for anaerobic and aerobic digestion, within a plant-wide setting.

The experimental layout replicates, at laboratory scale three full scale wastewater treatment plant (WWTP) schemes, comprising (1) a Modified Ludzack – Ettinger (MLE) nitrogen (N) removal activated sludge (AS) system treating settled wastewater (WW) with the separate AD of PS, WAS and PS-WAS blends, (2) a MLE N removal AS system treating raw WW with AD of its WAS and (3) a University of Cape Town (UCT) N or P removal system treating settled WW with the AD of its WAS. All three AS systems were fed the same wastewater collected from the Mitchells Plain wastewater treatment plant (WWTP), in Cape Town. To ensure a consistent composition of the raw and settled wastewater, measured masses of macerated PS collected from the Athlone WWTP, in Cape Town was added to the collected Mitchells Plain (settled) WW. Hence, in this experimental programme, raw WW is Mitchells Plains' settled WW with added Athlone PS, and settled WW is Mitchells Plain (MP) settled WW only. In order to increase the biological excess P removal (BEPR) in the UCT system 200 mg/*l* of acetate was dosed to the settled wastewater feed.

3.2 EXPERIMENTAL SET UP

A diagrammatic representation of the experimental layout is shown in Figure 3.1.

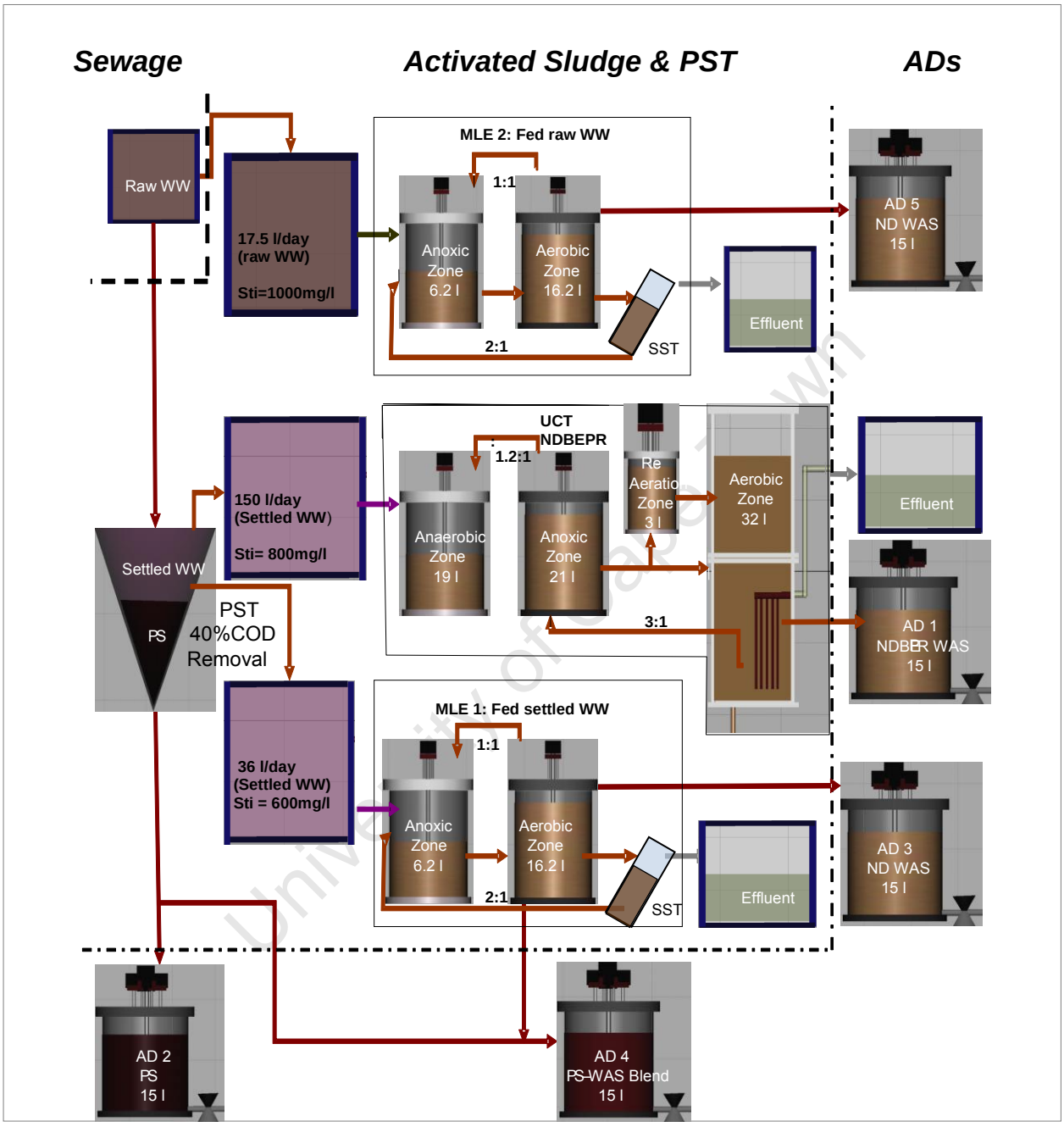

Figure 3.1: ***Experimental set-up***

Raw WW was fed to one of the MLE systems (MLE 2) and settled WW to the UCT NDBEPR and the other MLE system (MLE 1). The PS added to the collected WW to make the raw WW and the WAS from the three AS systems were fed to five completely mixed flow-through

ADs: (1) UCT NDBEPR system WAS, (2) PS only, (3) settled WW MLE system WAS, (4) settled WW MLE system WAS and PS blend and (5) raw WW MLE system WAS.

3.2.1 Wastewater Collection and AS System Feed Preparation

Wastewater obtained was pumped from the main collection sump at the Mitchell's Plain wastewater treatment plant (MP WWTP) in Cape Town (South Africa). This WWTP treats mainly domestic sewage with a small (less than 10%) industrial component. The raw WW was collected in 2m^3 batches and transported with a small tanker truck to the laboratory. While being mixed with high-pressure compressed air, the collected WW was transferred by gravity through an in-line macerator into five 400-litre stainless steel storage tanks. These storage tanks are located in a laboratory cold room and are maintained at 4˚C. A batch of sewage normally lasted about 12 to 14 days, after which it was discarded and a new sewage batch collected. The storage of sewage for longer than three weeks usually caused the sewage to become septic (accumulate hydrogen sulphide) and significant sewage characteristic changes. Upon arrival, Chemical Oxygen Demand (COD) analysis was performed on the collected sewage. Typically, undiluted sewage from the MP WWTP ranges between 1000 and 1200 mg COD/*l*, but may tend to vary because of rainfall, causing dilution, especially during the winter rainy season. Daily, after thoroughly mixing the sewage, the required volume of wastewater was withdrawn from the refrigerated tanks and diluted, with tap water, to a target COD of 600 mg/*l* while it was stored in the cold room. This was done to ensure that the COD load to the AS systems remained consistent throughout the experimental period. The 600 mg COD/*l* feed represented the settled WW and was fed to the UCT NDBEPR system and one MLE system (MLE 1). A measured mass (volume × concentration) of PS was dosed into one of the stainless steel tanks to make the raw WW. The PS was obtained from the underflow of the primary settling tank (PST) at the Athlone WWTP. Although it would be natural for the PS to be taken from the same plant that the wastewater was collected, i.e. MP WWTP, this was not the case because, from past experience in the UCT laboratory, the PS from the MP WWTP was known to cause problems in experimental AD systems. This PS taken from Athlone WWTP was generated from the settling of domestic raw sewage at the treatment plant. It

was collected in about 50 litre batches and stored in the 4˚C cold room. Primary sludge (PS) usually undergoes considerable anaerobic fermentation, even at low temperatures of 4˚C. This causes an increase in short chain fatty acid (SCFA) concentration of the stored PS. To limit the prospect of characteristic alterations, PS storage was limited to a maximum of three months. The PS was thoroughly macerated before use to reduce its particle size, thus preventing blockages in the experimental systems.

The PS from the Athone WWTP had a COD concentration of around 80000mgCOD/*l*, but this also varied with different batches. The PS was diluted to 60000mgCOD/*l*, which was the consistent target PS COD concentration, maintained to make the mass balance calculations over the virtual PST easier.

3.2.2 Activated Sludge (AS) Systems

Although all three AS systems were fed the same basic settled wastewater, the COD of two of the three systems feed was adjusted to conform to the objectives for this research. All three AS systems were operated at constant temperature of 20˚C (± 1˚C) and at a sludge age (R_s) of 10 days, by harvesting the required volume of sludge from the aerobic reactor (taking due account of the mixed liquor abstract for samples from the different reactors).

3.2.2.1 Feed Preparation for ND Activated Sludge Systems (MLE 1 and MLE 2)

The MLE 2 and MLE 1 were fed raw and settled wastewater respectively. The settled wastewater was set at a COD of 600mg/*l* and fed (36 *l*/d) to MLE 1 at a constant 24h rate. The daily 36*l* influent to this system was stored in a 50-litres feed tank mounted inside a chest refrigerator to maintain the temperature of the influent below 8°C. The influent was gently stirred to keep the wastewater particulates in suspension.

The raw wastewater feed for MLE 2 was produced by adding a measured mass of PS to the settled WW, with the basic 600mgCOD/*l* concentration, to increase the COD to 1000mgCOD/*l* raw WW. Due to the higher influent COD, the MLE 2 was fed at half the daily volume of MLE 1, i.e. 18*l*/d. The daily influent was stored in a 30-litre feed tank,

housed in the chest refrigerator and gently stirred to prevent settling of the PS settleable solids.

To ensure that each AS system was fed its required mass of COD per day, at the end of a 24h period, any sewage (both liquid and solid components) left in the feed tank (usually less than 0.5*l*) was collected and added batch-wise into the first reactor of the AS system.

3.2.2.2 Feed Preparation for the NDBEPR Activated Sludge System (UCT- MBR)

The UCT NDBEPR system was fed the same basic 600mgCOD/*l* settled WW with 200mgCOD/*l* acetate added to promote BEPR by the system. This was achieved by adding 40g of sodium acetate (CH_3COONa) to the daily required feed volume of 150*l*/d. Also, to avoid P limitation di-Potassium hydrogen ortho-phosphate (K_2HPO_4) was added to the feed to provide potassium and to increase the phosphorus concentration to 40mgP/*l* (see Appendix 4 for calculations on the required quantities of these additives).

The daily influent volume was stored in a 200*l* tank housed in a chest refrigerator at 4°C. Because the influent flow is very high (150*l*/d), the feed pipe to the reactor was coiled in a 20*l* , heated water bucket to raise its temperature, consequently keeping the temperature in the anaerobic reactor above 19°C. Also, as for the MLE systems, any feed and particulates left in the feed tank after a 24-hour period was added batch-wise into the anaerobic reactor. To prevent wall growth in the feed drums and feed pipes of the three AS systems, they were brushed daily and cleared with hot water and chlorine every second week.

3.2.2.3 Description of ND Activated Sludge Systems (MLE 1 and MLE 2)

Both MLE systems comprised of two reactors and a secondary settling tank (Figure 3.2). The first reactor was a 6.2-litre anoxic tank followed by a 16.2-litre aerobic tank both made from clear cylindrical Perspex. The influent wastewater enters the anoxic reactor and thereafter flows through to the aerobic reactor. In both the anoxic and aerobic reactors, motorized stirrers create agitation to keep the mixed liquor suspended solids (MLSS) completely mixed. The outflow from the aerobic reactor enters the secondary settling tank (SST), which separates the biological sludge from the treated water. The SST was made

from a 600mm long, 100mm diameter clear Perspex cylindrical tube filled with a wiper blade to keep its inner walls clear of sludge. The wiper blade made three revolutions in 15 seconds of every 10 minutes. The SST was set up at an angle of about 60 degrees to enable the sludge entering the SST at its base to be rapidly removed by the recycle flow diagonally opposite to the entry point. The effluent (clear, treated water) overflows the top of the cylinder. The two reactors and SST were connected with 12mm, soft, clear, plastic tubing. The outflow was withdrawn from the base of the reactor via an inverse U-tube, mounted on the side of the reactor, with which the liquid volume of the reactor could be set. A 2:1 mixed liquor recycle returned mixed liquor from the aerobic to anoxic tanks and a 1:1 underflow sludge recycle returned sludge from the secondary settling tank to the anoxic reactor.

Compressed air was supplied via a fine bubble diffuser at the bottom of the aerobic reactor to provide aeration. As the air bubbles rose to the surface, oxygen from the air bubbles dissolved into the mixed liquor. A Hi-Tech Microsystems oxygen utilization rate (OUR) meter was used to control the dissolved oxygen (DO) concentration between 2.0mgO/*l* and 5.0mgO/*l*, low and high set points respectively, via a solenoid valve on the air line. When the DO reached the high set point, aeration stopped and the OUR meter recorded the OUR by measuring the slope of the decreasing DO versus the time line. When the DO reached the low DO set point, aeration commenced again. The OUR readings accumulated in the OUR meter over 24h were downloaded daily to a data collection computer.

Each MLE system was operated with one multi-channel peristaltic pump set to deliver the daily influent feed volume over 23.5 to 24h. The recycle flows were delivered by the same pump, one channel for the sludge return (s =2:1) and two for the mixed liquor recycle (a = 1:1). These flows were checked regularly with a measuring cylinder and stopwatch to check that they correctly paced the influent flow.

The two MLE systems were operated at a 10-day sludge age by wasting 2.2 *l* of mixed liquor from the aerobic reactor daily, which included any mixed liquor taken for samples.

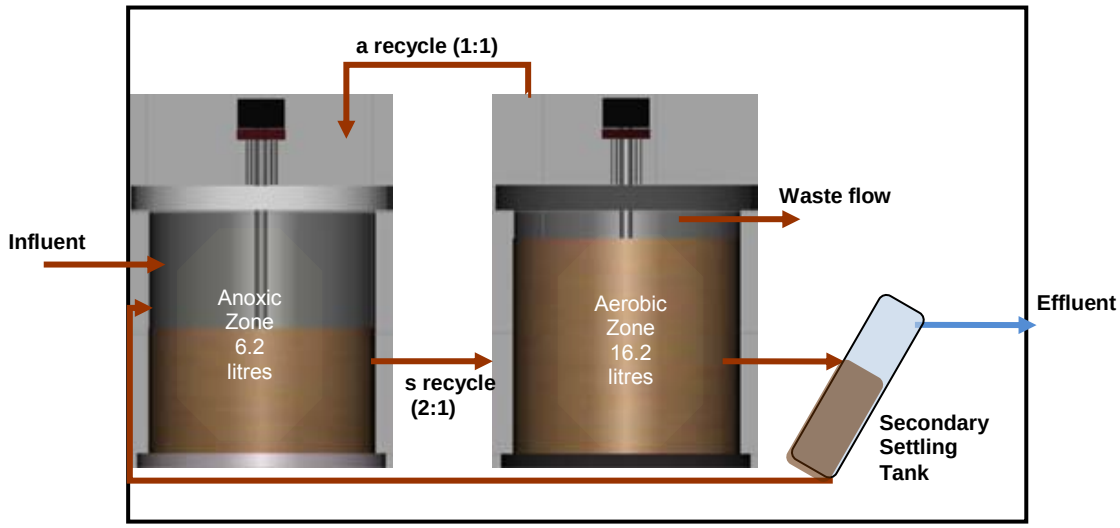

Figure 3.2: ***MLE process used in research project.***

3.2.2.4 Description of NDBEPR Activated Sludge System (UCT- MBR)

The nitrification-denitrification biological excess phosphorus removal (NDBEPR) AS system was set up at the UCT configuration with sequential anaerobic, anoxic and aerobic reactors (Figure 3.3). The anaerobic reactor was 19*l*, the anoxic 21*l* and aerobic zone 35*l* in volume. The aerobic zone comprised two reactors – a 32*l* membrane reactor and a 3*l* side stream aeration tank, used for OUR measurements. The membrane tank was fitted with Kubota™ A4 size membranes through which the final effluent was produced. The membrane panels were fitted vertically in the bottom section of the main aerobic tank. Continuous coarse-bubble aeration was supplied at the base of the reactor. The air bubbles were forced to rise between the membrane panels to provide scurr and minimize fouling. The 3 *l* side-stream aeration reactor was fitted with a DO controller/ OUR meter to measure the OUR. The flow rate from the anoxic reactor to the side-stream reactor was set to give the same actual retention time as in the MBR reactor.

The UCT system was operated with one peristaltic pump set to deliver the influent feed volume of 150*l* in 23.5 to 24 h. The mixed liquor recycles were set at 3:1 (3 channels) for the as-recycle from the aerobic to the anoxic and 1.2:1 for the r-recycle from the anoxic to the anaerobic reactors. These recycle flows were regularly checked with a measuring cyclinder and stop watch and recorded as a ratio with respect to the influent flow. For the fixed volume reactors the anaerobic, anoxic and aerobic mass fractions are set by the recycle

ratios. The relationships between the mass and volume fractions in terms of the recycle ratios are given by Ramphao *et al.* (2005). The long term averages of the measured reactor MLSS concentrations could therefore be used to check the measured recycle ratios. The anaerobic, anoxic and side-stream re-aeration tanks were fitted with stirrers for mixing while the main aerobic MBR reactor was mixed by continuous coarse-bubble aeration.

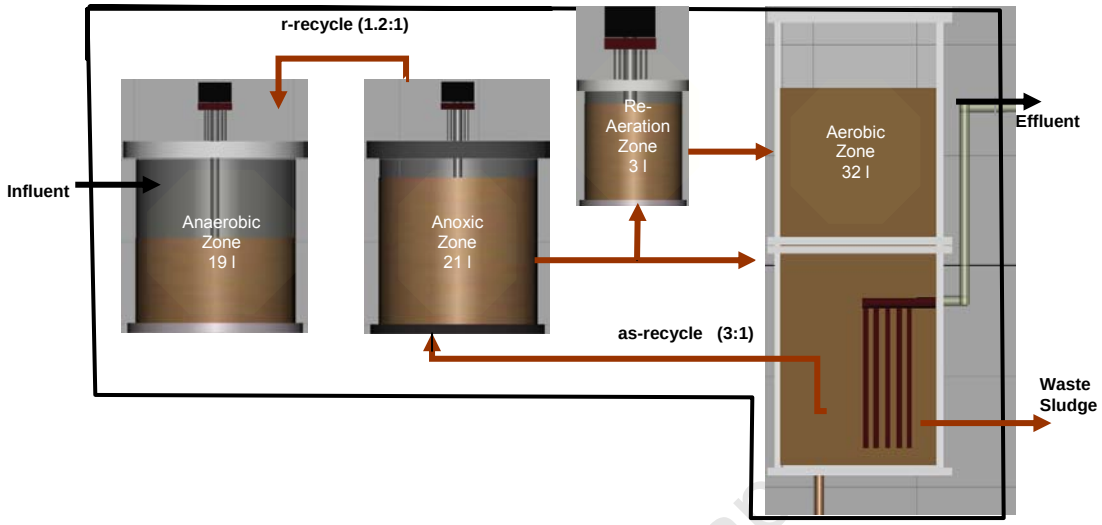

Figure 3.3: *NDBEPR system used in research project.*

The UCT NDBEPR sludge age is maintained by wasting a total equivalent volume of 5.74*l* of sludge daily from the aerobic membrane reactor, which includes the mixed liquor taken from the anaerobic and anoxic reactors for testing, taking due account of the differences in reactor MLSS concentrations.

3.2.2.5 Sampling

Filtered and unfiltered samples were taken from the two MLE systems. These samples were collected from the influent, anoxic reactor, aerobic reactor and effluent. In the case of the UCT-MBR system, 50ml samples were drawn from the anaerobic, anoxic and aerobic reactors and two drops of polyelectrolyte flocculent (1g/*l*) added to make subsequent filtration easier, due to the high concentration of non-settleable solids in the MBR system. These samples were immediately placed in 50ml centrifuge tubes and centrifuged at 3500rpm for 10 minutes. The centrifuge supernatants are filtered through 0.45 micrometer membrane filters and stored in the cold room for later analysis. This filtrate was analysed

for COD, TKN, FSA, NO_3, NO_2, TP and OP as will be discussed, in more detail, in the subsequent section on analytical procedures (Chapter 4). The MBR NDBEPR system effluent was not filtered because the pore sizes of the membranes (0.1 μm), through which this effluent is produced, are smaller than those of the 0.45 micrometer membrane filter paper. In fact the effluent COD from the UCT MBR system was consistently lower than the 0.45 μm membrane filtered COD in the aerobic reactor. The solid residue, which remained in the centrifuge tube was used for the TSS, VSS and ISS tests. The pH was measured in-situ in the aerobic reactors of the AS systems.

Furthermore, 500ml and 100ml samples were drawn from aerobic reactors of the MLE and NDBEPR systems respectively and used to measure the DSVI (dilute sludge volume index). However, this test was only performed occasionaly, to check the settleability of the WAS, since the DSVI parameter was mainly required for the operation of the experimental systems and not for the modelling exercise of the project.

3.2.3 Anaerobic Digestion Systems

The PS and WAS from the three AS systems were fed daily to the five completely mixed ADs, three of the ADs receiving WAS from each AS system (MLE 1 for AD 3, MLE 2 for AD 5 and UCT MBR for AD 1), one receiving the PS used to make the raw WW (AD 2) and one recieving a 1.5:1 blend (by COD mass) of PS and MLE 1 (fed settled WW) WAS. In this way the experimental set-up replicates the connection of a 'virtual' PST to an AD system (AD 2 is fed the PS) and AS systems (i.e. MLE 1 and UCT MBR systems are fed 'virtualy' settled WW). The five ADs were operated at mesophilic temperatures of about 35°C. All five ADs were not fed continuously over a day but batch-wise, once daily for the ADs fed WAS and two or three times per day in the case of PS and the PS-WAS blend. Initially, when the AD 2 (fed PS) and AD 4 (fed PS-WAS) were fed once per day, their reactor volatile fatty acids (VFAs) concentration increased rapidly resulting in a drop in pH over time and eventual AD failure. The spreading of the daily feed mass over two to three feed portions per day prevented system failure. The digesters used had a 20*l* capacity but AD 2, AD 3 and AD 4 contained 12*l*, AD 1 had 16*l* and AD 5 had 15*l* liquid volume. Each digester was fed a consistent target COD concentration (with the

expectation of attaining steady state) daily, with the daily feed volume determined by the sludge age (R_s or sludge retention time, which in this case also equals the hydraulic retention time, R_{hn}, established on the AD in conformity with: influent flow(Q)=volume (V)/R_s).

Each digester was operated at five different sludge ages, i.e. 10, 18, 25, 40 and 60 days. The short sludge ages are useful to determine the hydrolysis rate of the different sludges and the very long 60-day sludge age is useful to determine the unbiodegradable fraction of the sludges, as recommended by Sötemann *et al.* (2005). For the short and long sludge ages, once the time period of three steady states had elapsed, testing of the ADs commenced and continued for a period of about two weeks.

3.2.3.1 AD Feed Preparation

Anaerobic digesters 1, 3 and 5 were fed WAS from the UCT-MBR system, MLE 1 and MLE 2, respectively. The WAS from the UCT-MBR system (~ 9gTSS/*l* with 10gCOD/*l*) was fed directly to AD 1 without any thickening. Consequently, there was a change in the COD mass load for every change in the sludge age i.e. 1.5, 0.83, 0.6, 0.38 and 0.25 *l*/d for 10, 18, 25, 40 and 60 days sludge age, because a large volume of WAS was available from the UCT MBR system to feed a high flow at the short sludge ages. In contrast, because the two MLE systems did not produce a large mass of WAS daily, the WAS from these systems was thickened to a higher concentration, with change in the sludge age, to maintain a constant daily mass load (~ 1.7gTSS/d with 2.1gCOD/d for MLE 1 WAS fed to AD 3 and ~ 2.2gTSS/d with 2.7gCOD/d for MLE 2 WAS fed to AD 5) throughout the duration of this study. Before the WAS was fed to the three ADs, it was heated to above 35˚C to avoid causing a temperature shock to the temperature-sensitive methanogenic biomass.

Anaerobic digesters 2 and 4 were fed PS and a 1.5:1 ratio (by COD mass) of PS-WAS mixture respectively. The daily TSS load of PS fed to AD 2 and used in the mixture of AD 4 was equal to the PS TSS mass dosed in the 'settled' WW to make the raw WW fed to MLE 1 (i.e. 18 *l*/d × 400mgCOD/*l* = 7.2gCOD/d). The daily WAS from the MLE 2 treating the settled WW was split into two halves. One half was fed to AD 3 as mentioned above, the other half was blended with the 7.2 gCOD/d PS and fed to AD 4. It was possible to

split the WAS from MLE 2 while maintaining the approximate relative proportions of PS and WAS because MLE 2 treated double the settled WW flow (36 *l*/d) compared with MLE 1 treating raw WW (18 *l*/d).

As mentioned above, the feed to AD 2 and AD 4 receiving PS was spread over the day on 2 to 3 batches. A fixed mass of COD/d was fed to ADs 2 and 4, with the volume of feed per day fixed by the sludge age of the ADs. The PS and the PS-WAS blend were diluted or thickened as required to contain the fixed COD mass load into the required feed volume. In the initial start-up stage or after changes of sludge age, half of this sludge was fed in the mornings and the other half in the evenings to avoid shock loading, which would result in digester failure. This shock loading occurred because, unlike the WAS fed directly from the AS systems, the VFA concentration of the PS was quite high. These high concentrations of VFAs batch-fed to the ADs caused the digester pH to drop suddenly, negatively affecting the methanogenic biomass, which is highly sensitive to pH variations. The high VFA concentration in the PS was the result of anaerobic fermentation during its storage period in the cold room. In instances where the AD showed signs of failure, the loading rate on the digester was reduced to half the sludge mass per day and hydrogen carbonate added to the influent feed.

3.2.3.2 Description the of AD System used for Experimental Research

The anaerobic digesters (ADs) were continuously stirred tank reactors (CSTR) as depicted in Figure 3.4. The reactor tank was manufactured from Perspex and cylindrical stainless steel rods for structural support and to ensure a gas-tight seal. A stirrer driven by a single-phase motor was mounted on the top lid of the unit. The stirring shaft passed through the lid via a sealed bearing to ensure the reactor was gas-tight under low positive gas pressures (< 50 mm water). A valve was fitted at the base of the reactor to allow for feeding of influent sludge and removal of waste sludge in sampling and/or maintaining the AD sludge age.

A gas outlet part was provided in the top lid. The gas-outlet pipe was connected to a wall-mounted gas counter. The anaerobic digesters were operated at a temperature of approximately 35 ˚C, optimal for mesophilic organisms. This temperature was controlled

by means of heating coils wrapped around the outside of the digester walls and connected to a temperature controller with a temperature probe in the reactor mixed liquor. The ADs were all completely sealed, except for the provision of the gas outlet pipe and the access port, which was closed with a rubber bung. The access port was opened only once daily to measure the pH. The sludge inlet/ outlet pipe at the base of the AD, controlled by a valve, was only opened during the feeding process when waste sludge was drawn and new feed sludge added.

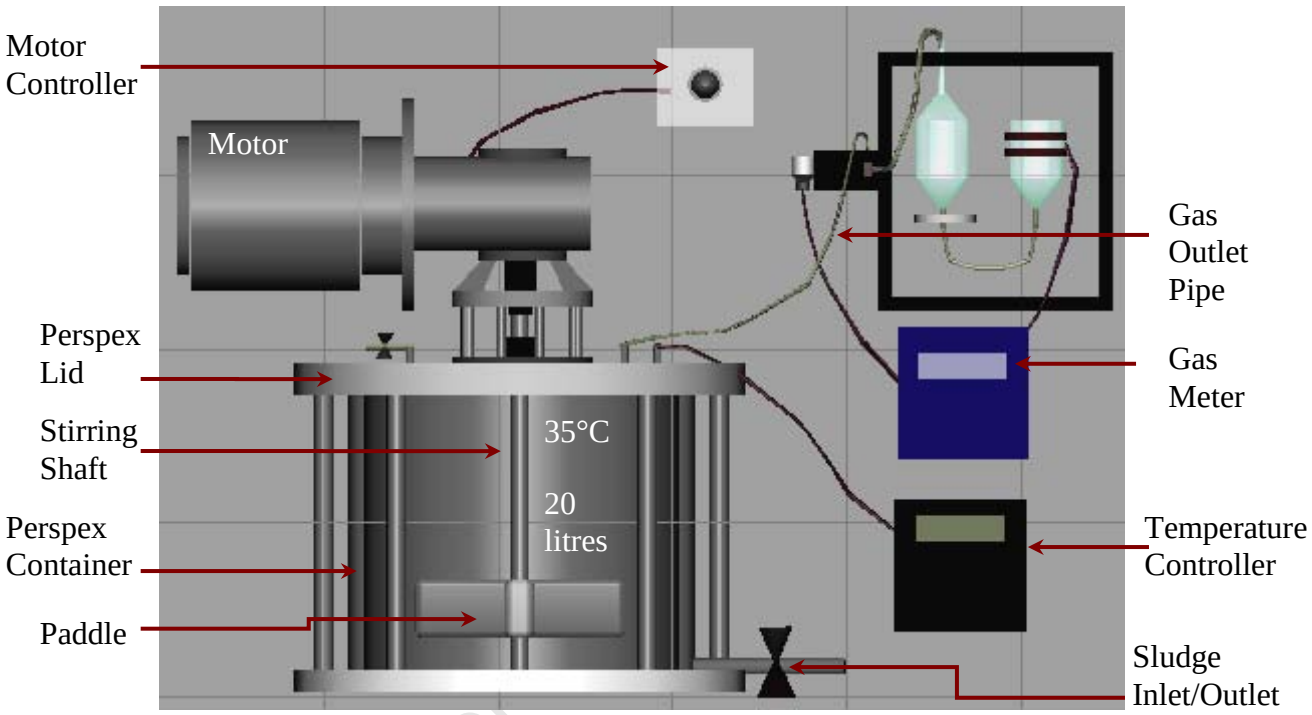

Figure 3.4: *Anaerobic digester used in research project*

The total volume of each reactor tanks was 20 litres. However, the operating volume of AD 1 was set at 16 litres, AD 5 at 15 litres and those of ADs 2, 3 and 4 were each set at 12 litres. Each digester was operated at three short sludge ages (i.e. 10, 18 and 25 days) and two long sludge ages of 40 and 60 days. Because it was difficult to grow and maintain a stable methanogenic population at short sludge ages, the digester operation commenced with the longer sludge ages. Then for the shorter sludge ages, the methanogenic biomass was already established allowing the AD systems to continue operating stably.

The access point was opened once daily for the ADs receiving WAS but two or three times daily for the ADs receiving PS. First, the in-situ pH was measured and then the required

volume of waste sludge withdrawn via the stop-cock at the AD base. Then the liquid volume wasted was restored back to the operating volume by adding the required volume of feed sludge, thereby maintaining this prescribed sludge age.

When a period of three sludge ages had elapsed, experimental tests and measurements were performed on the anaerobic digesters.

3.2.3.3 Sampling of AD Systems

Samples for analysis were collected from the AD influent and effluent taken from the digester. However, for the ADs fed WAS only, sampling was not required because the WAS fed to these ADs had been tested and characterized already as part of the measurements conducted on the AS systems. Therefore, influent samples were only collected for the ADs fed PS (AD 2) and PS-WAS mixture feed (AD 4).

In order to check the stability of the ADs on a routine basis, a five-point titration was conducted on a filtered effluent sample at least every second day. The in-situ pH and five-point titration method (Moosbrugger *et al.*, 1992) gives the H_2CO_3 alkalinity and VFA concentration. For optimal operation, the in-situ pH should be above 6.5 but preferably within the range of 7 and 8 (McCarty, 1974) and the H_2CO_3 alkalinity to VFA ratio should be maintained at more than 3:1 (Ripley *et al.*, 1986). During the intensive measuring periods, once the ADs reached steady state at a particular sludge age, the influent (for ADs 2 and 4) and effluent (for all ADs), unfiltered and membrane filtered VFA, COD, TKN and FSA, TP and OP tests were performed to determine the extent of digestion and the COD, N and P mass balances over these digesters. For the AD 1, fed NDBEPR WAS the unfiltered and membrane filtered metallic ions, i.e. magnesium (Mg), potassium (K) and calcium (Ca) were also tested.

The daily gas flow was measured by means of the gas counter and gas samples were collected in 5-litre impermeable Tedlar gasbags connected to the AD gas outlet pipes. The gas was analysed to determine the CO_2 and CH_4 content as a requirement to establish a COD and carbon balance over the digesters.

3.3 EXPERIMENTAL TESTING METHODS

The analytical measurements performed on the sample collected from influent wastewaters, PST, AS systems and ADs include the following:

1. Chemical oxygen demand (COD) tests
2. Total Kjeldahl nitrogen (TKN) test and free and saline ammonia (FSA) test
3. Nitrate (NO_3) and nitrite (NO_2) analysis
4. Total phosphate (TP) and ortho-phosphate concentration test
5. Volatile fatty acids (VFA) , H_2CO_3 alkalinity and pH measurements
6. Mixed liquor total and volatile settleable solids (MLSS, MLVSS)
7. Oxygen utilization rate (OUR)
8. Gas composition analysis and flow rate measurement
9. Organic carbon analysis

All the above analyses were performed in the laboratory at the WRG of the Department of Civil Engineering, UCT, except for the gas composition and organic carbon analysis.

These measurements were sufficient to allow for the characterisation of wastewater and sludge components and perform COD, nitrogen (N) and phosphorus (P) mass balances over all unit process systems of the research project's experimental layout (shown in Figure 3.1). Furthermore, this data set was used in the calibration and validation of the mathematical models developed from this work. The tests performed on the AD system effluents included all above-mentioned tests for AS systems with the exception of OUR and nitrate analysis. These tests are briefly described below.

3.3.1 Chemical Oxygen Demand (COD)

The COD was measured using the dichromate and sulphuric acid open flux method, followed by a titration with ferrous ammonium sulphate (FAS) (Standard Methods, 1985). The COD test involves the reflux of a 10ml sample in strongly acidic solution (5ml sulphuric acid) with a known excess (~ 5ml at 0.25N (i.e. N= normality)) of potassium dichromate ($K_2Cr_2O_7$). In principle, the organic matter is oxidised by the boiling dichromate. After boiling, the quantity of potassium di-chromate reduced is determined

by titration, which gives the electron donating capacity of the oxidised organic matter in terms of oxygen equivalent (Sawyer *et al.*, 1994).

3.3.2 Total Kjeldahl Nitrogen (TKN) and Free and Saline Ammonia (FSA)

The TKN and FSA concentration was measured using a micro-distillation method (Standard Methods, 1985, Semi-micro Kjeldahl method, 420B). The TKN is the combination of organic nitrogen (Org-N) and FSA. In the TKN test, the sample is digested with a sulphuric acid solution containing potassium sulphate (K_2SO_4) while using mercuric sulphate as a catalyst. The digestion converts all organic nitrogen compounds such as proteins and peptides to ammonia. The sample is then steam distilled using a micro-distillation apparatus with sodium hydroxide and sodium thio-sulphate. On being stripped from sample as a gas, the ammonia generated from the organically bound N and any ammonia originally present in the sample is condensed and dissolved in a boric acid solution turning it from purple to green. A sample is then titrated with standard sulphuric acid solution of normality 0.001 until it regains its purple colour and the volume of acid titrated is deemed proportional to the TKN concentration. For the FSA concentration only, the sample is not digested but only steam distilled. The difference between the TKN and FSA is the organically bound N (Org-N).

3.3.3 Nitrate (NO_3^-) and Nitrite (NO_2^-) Test

The Technicon Auto-Analyser Automated Method was applied for the measurement of nitrate and nitrite concentration in solution. This test procedure is described in the operational procedures for the Technicon Auto-Analyser Methodology (Industrial Methods 33, 68 and 35.67W). The method is based on nitrate reduction to nitrite and then measuring the nitrite concentration. The chemical reagents for nitrate reduction are hydrazine sulphate, sodium hydroxide and copper sulphate. The colour reagent with nitrite makes a pink colour, the intensity of which is proportional to the nitrite concentration and which is measured using a colorimeter. The nitrate concentration is the difference between the nitrite concentration with nitrate reduction (nitrate + nitrite) and

the nitrite only (with no reduction). For more details on this method, refer to the source indicated above.

3.3.4 Total Phosphates (TP) and Ortho-phosphates (OP)

The TP and OP were measured using the persulphate digestion method (Standard Methods, 1985, Method 424CIII) and the molybdate-vanadate colorimetric method (Standard Methods, 1985, Vanado-molybdo-phosphoric acid colometric method). In principle, ortho-phosphates react with molybdate, in the presence of vanadate, to form a yellow phospho-vando-molybdate solution. The intensity of the yellow colour is proportional to the concentration of ortho-phosphate present and is measured by absorbance using a spectrophotometer. A Unicam 8625 UV/VIS spectrophotometer, set at a wavelength of 470μm, was used for this colour intensity measurement and is valid up to a concentration of 300mgP/*l*. Measurement of total phosphates requires conversion of organic and polyphosphates to ortho-phosphate through boiling the sample with sulphuric acid and potassium persulphate.

3.3.5 Volatile Fatty Acids (VFAs), $H_2CO_3^*$ Alkalinity and pH

The pH, volatile fatty acid (VFA in mgAc/*l*) and $H_2CO_3^*$ alkalinity (measured as mg$CaCO_3$/*l*) were measured using the 5-point titration method (Moosbrugger *et al.*, 1992). In this test, a sample of digester supernatant is titrated to five predetermined pH points with dilute hydrochloric acid. The acid added to the 4 predetermined pH points and the in-situ pH are keyed into a computer program (Titra 5) which calculates the required $H_2CO_3^*$ alkalinity (as mg$CaCO_3$/*l*) and VFA (as mgHAc/*l*) concentrations. A Metrohm Dosimat (715) and Metrohm pH meter (744) combo was used in the 5-point titration method.

3.3.6 Mixed Liquor Settleable Solids (MLSS)

The MLSS concentration (measured in mg/*l*) was measured using the Total Settleable Solids (TSS) and Inorganic Settleable Solids (ISS) tests (Standard Methods, 1985). The TSS is obtained by first centrifuging a known volume (usually 2 × 50ml) of mixed liquor,

decanting all the (usually) clear supernatant, transferring the collected solids to a clean and dry crucible of known mass and drying the solids at 105˚C for 24 hours. The ISS, performed subsequently, is obtained by incinerating the sample in a furnace at about 600˚C for over 20 minutes. The difference between the TSS and ISS gives us the Volatile (organic) Settleable Solids (VSS).

3.3.7 Oxygen Utilization Rate (OUR)

This is an electronic online measurement that is collected during the operation of the AS systems. The Hi-Tech Microsystems automated oxygen utilization rate (OUR) meter (Sections 3.2.2.3 and 3.2.2.4 of this chapter), which was used to control the dissolved oxygen (DO) concentration between low (2.0mgO/*l*) and high (5.0mgO/*l*) set points was connected to a DO probe, which was placed in the aerobic reactor of each activated sludge system. When the aerobic reactor mixed liquor DO concentration reached the low set point (2mgO/*l*), aeration commenced and continued until the DO concentration reached the high set point (5mgO/*l*), and the aeration went off automatically. The OUR meter then monitored the decrease in DO with time until the low DO set point was reached again, and aeration recommenced for a repeat in the cycle. During each aeration-off period of the cycle, the OUR (mgO/*l*/h) at that time was automatically calculated by the slope of the linear regression of the change in DO concentration versus time curve. This OUR was stored by the OUR meter, together with the time, correlation coefficient and temperature. These OUR results for each day's feed cycle were downloaded from the OUR meter to a computer, where the data was imported into a spreadsheet program for it to be plotted and the average OUR (mgO/*l*/h) for the day calculated.

It was noted that the 3 *l* side-stream aeration reactor of the NDBEPR system, in which the OUR probe was placed to measure the OUR, had a lower concentration (effectively that of the anoxic reactor) than that of the fully aerated membrane reactor (which was higher due to the membrane concentration effect). Therefore, the OUR (mgO/*l*/hour) for the fully aerated tank (OUR_{aer}) was obtained by dividing the measured OUR (mgO/*l*/hour, $OUR_{re\text{-}aer}$), by the mixed liquor settleable solids mass fraction of the re-aeration tank ($MLSS_{re\text{-}aer}$) to that of the fully aerated tank ($MLSS_{aer}$) as shown in Equation 3.1 below.

$$OUR_{aer} = OUR_{re\_aer}.\frac{MLSS_{aer}}{MLSS_{re\_aer}}$$

(3.1)

Procedure to Obtain the Flux of Oxygen Consumed:

The measured oxygen utilization rate (OUR_M) includes both the oxygen used in nitrification and that used in formation of active mass and its endogenous respiration.

The total flux of oxygen used (FO_M, mgO/d) equals the measured OUR (mgO/*l*/hour) multiplied by the total aerobic volume and the hours per day (24 hours) i.e.:

$$FO_M = OUR_M \cdot V \cdot 24$$

(3.2)

The oxygen in the aerobic zone of the activated sludge systems is used for nitrification and for conversion of organics. The change in nitrates (ΔNO_3, mgN-NO_3/*l*) concentration, relative to influent flow rate (Q_i), i.e. due to the nitrification and denitrification, is calculated and then multiplied by Q_i to give the change in flux of nitrates denitrified in the systems (ΔFNO_{3_denit}, see Equations A1.2a, b and c in Appendix 1).

The total change in flux of nitrates generated (FNO_{3_gen}, mgN-NO_3/d) in the AS system is then determined by the sum of the flux of nitrates de-nitrified (ΔFNO_{3_denit}, mgN-NO_3/d) and nitrates not de-nitrified (i.e. which are found in the effluent, NO_{3_eff} (mgN-NO_3/*l*)) as shown in Equation 3.3 below:

$$FNO_{3\_gen} = \left(NO_{3\_eff} \cdot Q_i\right) + \Delta FNO_{3\_denit}$$

(3.3)

With knowledge of the flux of nitrates generated aerobically (FNO_{3_gen}, mgN-NO_3/d), the flux of oxygen used in the nitrification process (FO_n, mgO/d) can be determined by:

$$FO_n = 4.57 \cdot FNO_{3\_gen}$$

(3.4)

Where 4.57 is the mgO/mgFSA nitrified (i.e. 64/14).

Thereafter, the flux of oxygen used in the conversion of organics (FO_c, mgO/d) can be calculated by subtracting the FO_n (mgO/d) from the FO_M (mgO/d), using the following Equation 3.5:

$$FO_c = FO_M - FO_n \,.$$

(3.5)

3.3.8 Gas Production and Composition

The biogas volume produced is measured using gas meters connected to the AD system's gas outlet pipe, shown in Figure 3.4. Once the biogas production was known for a given AD steady state period, 5-litre impermeable Tedlar gasbags were connected to the gas outlet pipes for the collection of gas samples. Thereafter, these samples were sent to a laboratory at the University of Stellenbosch (Department of Food Sciences) for analysis, using a gas chromatograph to give the percentage composition of methane, carbon dioxide and nitrogen of the total gas sample.

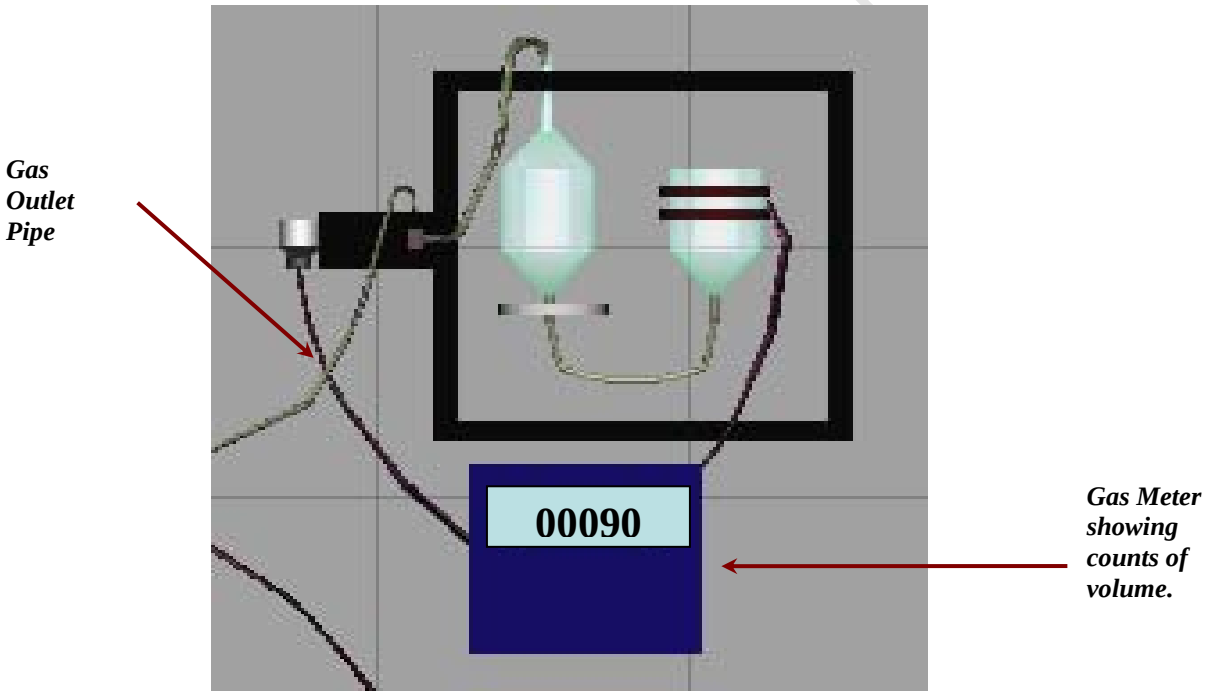

Figure 3.5: *Gas flow meter*

3.3.9 Total Organic Carbon (TOC) and Total Organic Nitrogen (TON) Analysis

The total organic carbon and total organic nitrogen analysis was done by an external laboratory. The CSIR marine analytical service laboratory was used for this purpose. This analysis was performed on 104°C dried WAS samples from the UCT-MBR system and waste sludge from AD 1 for a sludge age exceeding 60 days.

3.3.10 Total and Dissolved Counter-ion Metal (Me) Analysis

The analytical measurement of the counter-ions metals contained within the polymer structure of polyphosphate, magnesium (Mg^{2+}), potassium (K^{+}) and calcium (Ca^{2+}), consists of two parts, (1) the preparation of the samples in the WRG laboratory and (2) the sample analysis in the external Chemical Engineering laboratory, at UCT, equipped to perform the analysis.

The preparation of the NDBEPR WAS sample in the WRG laboratory entails the digestion of the sludge using a strong acid (H_2SO_4). This digestion procedure is the same as that used in the case of the TKN analysis but the digestion mixture is slightly altered by replacing the K_2SO_4 component (used in the TKN digestion mix) with Na_2SO_4, since potassium is one of the counter-ion metals being analysed in this study. As mentioned, the sample is analyzed at an external facility (the Chemical Engineering laboratory of UCT) using the Atomic Absorption Spectrophotometer (AAS) method to determine the Mg, Ca and K elements in the sample. These results are then used to determine the counter-ion metal Mg: K: Ca ratio of the sludge, which in turn can be linked to the polyphosphate P content of the sludge.

3.3.10 Sampling from the Experimental Set-up

Table 3.1, below presents a guide indicating all measurements performed on samples taken from the experimental setup:

Table 3.1: Summary of Samples and Tests used in Research Experimental Period.

		TEST	COD	TKN	FSA	NO_3	NO_2	OP	T-P	TSS	VSS	OUR	DSVI	pH
Activated Sludge Systems	Membrane NDBEPR System	**Influent**	Unf & Filt	Unf & Filt	Filt	Occ	Occ	Filt	Unf	Unf	Unf	-	-	-
		Anaerobic	-	-	-	Filt	Filt	Filt	Filt	Unf	Unf	-	-	-
		Anoxic	-	-	-	Filt	Filt	Filt	Filt	Unf	Unf	-	-	-
		Aerobic	Unf	Unf		Filt	Filt	Filt	Unf	Unf	Unf	dir	Occ	dir
		Final Effluent 1*	Unf	Unf	Unf	Unf	Unf	Unf	Unf	-	-	-	-	-
	MLE System	**Influent**	Unf & Filt	Unf & Filt	Filt	Occ	Occ	Filt	Unf	Unf	Unf	-	-	-
		Anoxic	-	-	-	Filt	Filt	Filt	Filt	Unf	Unf	-	-	-
		Aerobic	Unf	Unf	-	Filt	Filt	Filt	Unf	Unf	Unf	dir	Occ	dir
		Final Effluent	Unf & Filt	Unf & Filt	Filt	Unf	Unf	Unf	Unf	-	-	-	-	-
Anaerobic Digesters		TEST	**COD**	**TKN**	**FSA**	**VFA**	**Gas**	**Ortho-P**	**TP**	**TSS**	**VSS**	**H_2CO_3* Alk.**	**%CO2**	**pH**
		Influent	Unf & Filt	Unf & Filt	Unf	Unf		Filt	Unf	Unf	Unf			dir
		Final Effluent	Unf & Filt	Unf & Filt	Unf	Unf	dir	Filt	Unf	Unf	Unf	dir	dir	dir

Abbreviations	Meaning
COD	Chemical oxygen demand, Open flux method
TKN	Total Kjeldahl Nitrogen, micro-Kjeldahl method
FSA	Free and saline ammonia, titrimetric method
NO_3	Nitrates, Hydrazine reduction (Technicon Auto-Analyzer)
NO_2	Nitrites, Hydrazine reduction (Technicon Auto-Analyzer)
OP	Ortho-phosphate, molybdate vanadate colour development
TP	Total phosphorous, sulphuric acid/ persulphate digestion at 100°C followed by molybdate-vanadate colour development for ortho-phosphate
TSS	Total suspended solids, sample dried at 103-105 °C
VSS	Volatile suspended solids, sample ignited at 600°C
DSVI	Dilute Sludge Volume Index, (Ekama and Marais, 1984b)
OUR	Oxygen Utilization Rate, automated
pH	Hydrogen power, pH meter (Hanna Instruments model)
VFA	Volatile Fatty Acid content (as mgHAc/*l*), 5-point titration.
H_2CO_3* Alk.	Hydrogen bicarbonate alkalinity (as mg$CaCO_3$/*l*), 5-point titration.
Filt	Filtered through Schleicher & Schull ME 25/21 0.45 micrometer membrane filters
Unf	Unfiltered samples.
dir	Direct measurement taken.
Occ	Occasional.
1*	Membrane pore size < 0.45 μm membranes.

3.4 CLOSURE

This chapter has presented the experimental set-up, operation and testing of three laboratory-scale wastewater treatment plant schemes, comprising of the various activated sludge (AS) and anaerobic digestion (AD) systems, used in this study.

The experimental set up is described as three laboratory scale wastewater treatment plant (WWTP) schemes that comprise (1) a Modified Ludzack – Ettinger (MLE) nitrogen (N) removal activated sludge (AS) system (which is given the name MLE 1) treating settled wastewater (WW) with the separate AD of PS, WAS and PS-WAS blends, (2) a MLE N removal AS system (MLE 2) treating raw WW with AD of its WAS and (3) a University of Cape Town (UCT) N or P removal system (UCT NDBEPR) treating settled WW with the AD of its WAS. To make up the raw WW, PS was added to the same basic settled WW that was fed to the MLE1 and NDBEPR systems. Hence it is this PS and the WAS from the 3 AS systems that were fed to 5 completely mixed flow-through ADs (i.e. AD1 (fed UCT NDBEPR system WAS), AD 2 (fed PS only), AD3 (fed MLE 1 WAS), AD 4 (fed MLE 1 WAS and PS blend) and AD 5 (fed MLE 2 WAS)).

The collection of municipal sewage to be fed to the experimental systems (settled wastewater from Mitchells Plain WWTP and PS from Athlone WWTP) is explained together with how the feed was prepared for the various AS and AD systems. These AS and AD systems are then described together with how they were fed, operated, sampled and tested during the experimental period of this research project. The experimental period was for 16 months from July 2007 to October 2008. The AS systems were each operated at 10 day R_s and the 5 ADs each operated at 5 sludge ages (i.e. 10, 18, 25, 40 and 60 days). For the AD systems, it was noted that the short sludge ages were useful to determine the hydrolysis rate of the different sludge types and the very long 60-day sludge age was useful to determine the unbiodegradable fraction of the sludges, this was as recommended by Sötemann *et*

al. (2005). Table 1 reports the measurements performed on samples taken from the experimental set-up.

The test procedures used to obtain data from the various influent, effluent and reactor locations of AS and AD systems are presented and the analytical measurements performed on samples taken from the experimental set up are summarised in Table 3.1.

The results obtained from the steady state operation of the systems in the experimental set up are reported in Chapter 4.

CHAPTER 4: RESULTS AND DISCUSSIONS

4.1 INTRODUCTION

The laboratory-scale Activated Sludge (AS) and Anaerobic Digestion (AD) systems, described in Chapter 3, were operated over a two-year experimental period (Figure 4.1a and 4.1b). The AD systems were tested for 10 to 20 consecutive days each during their steady state periods at a particular sludge age. Each digester was operated at four short sludge ages (i.e. 10, 18, 25 and 40 days) and a long sludge age of 60 days. Once a period of three sludge ages had elapsed, and the AD systems were at steady state, experimental tests and measurements were performed on the ADs. Although the experimental research period commenced in June 2007, the experimental data for the ADs in the initial 10-day and 25-day AD sludge age periods were erratic and thus were not used for this research report. However, the data acquired in 2008, after the operational details of the various systems and the testing methods were mastered, achieved good mass balances and so were useful to meet the research objectives. This chapter reports the results accumulated during this research period. Tables 4.1a and 4.1b (with a key for these tables given in Table 4.1c) show a timeline of the operating and testing periods of each sewage batch of 2007 and 2008 fed to the AS systems, aligned with the sludge ages of the ADs. The day-to-day data of the steady state 2008 results are shown in Appendices 7 and 8 as indicated in the timeline Table 4.1b. Also shown in Table 4.1b is the testing periods, during the AD steady state periods. The AS systems were also tested during this AD test period, because the source feed primary sludge (PS) and waste activated sludge (WAS) fed to the ADs was taken from them. During the periods when the systems were not intensively tested, random tests were performed on the AS and AD systems to check steady state conditions. However, the data from these random tests have not been included in the steady state period results.

Table 4.1a: Reference Guide and Timeline for 2007 Experimental Data

Year			2007 (NB: data acquired for this year not included as part of report)																	
Sewage Batch			3		4		5		6			7		8		9				
			Start	End	Start	End	Start	End	Start		End	Start	End	Start	End	Start				End
Plant Unit System	Feed to System	Date / Rs	17-Jul	25-Jul	26-Jul	8-Aug	8-Sep	22-Sep	23-Sep	1-Oct	14-Oct	15-Oct	13-Nov	14-Nov	29-Nov	30-Nov	20-Dec	31-Dec		
NDBEPR AS	Settled WW (+acetate)	10 day																		
MLE 1 AS	Settled WW	10 day																		
MLE 2 AS	Raw WW	10 day																		
AD 1	NDBEPR AS WAS	10 day																		
		25 day																		
AD 2	Primary sludge	10 day																		
		25 day																		
AD 3	MLE 1 WAS	10 day																		
		25 day																		
AD 4	PS and MLE 1 WAS (blended at 1.5:1)	10 day																		
		25 day																		
AD 5	MLE 2 WAS	10 day																		
		25 day																		

Table 4.1b: Reference Guide and Timeline for 2008 Experimental Data

Plant Unit System	Feed to system	Date Rs	2008 (NB: data acquired for this year is included in the report and can be referred to in given appendix numbers)	Appendix Ref. Table no.
Year			2008 (NB: data acquired for this year is included in the report and can be referred to in given appendix numbers)	
Sewage Batch			10 to 13 / 14 / 16 / 17 / 19 / 20 / 21	
			Start / End	
			1-Feb / 15-Mar / 31-Mar / 8-Apr / 15-May / 2-Jun / 12-Jun / 13-Jun / 25-Jun / 4-Jul / 30-Jul / 18-Aug / 28-Aug / 29-Aug / 5-Oct / 26-Oct / 2-Nov	
NDBEPR AS	Settled WW (+acetate)	10 day		A7.1
MLE 1 AS	Settled WW	10 day		A7.3
MLE 2 AS	Raw WW	10 day		7.2
AD 1	NDBEPR AS WAS	10 day		8.3
		18 day		
		25 day		
		40 day		
AD 2	Primary sludge	10 day		8.1
		18 day		
		25 day		
		40 day		
AD 3	MLE 1 WAS	10 day		8.4
		18 day		
		25 day		
		40 day		
AD 4	PS and MLE 1 WAS (blended at 1.5:1)	10 day		8.2
		18 day		
		25 day		
		40 day		
AD 5	MLE 2 WAS	10 day		8.5
		18 day		
		25 day		
		40 day		
AD 6	NDBEPR AS WAS	12 day		8.3
		60 day		
		20 day		
AD 7	PS	60 day		8.1
AD 8	MLE 1 WAS	60 day		8.4
AD 9	PS -MLE 1 WAS blend	60 day		8.2
AD 10	MLE 2 WAS	60 day		8.5

Table 4.1c: Key for Tables 4.1a and 4.1 b		
System	**Activity**	**Colour type**
NDBEPR AS (fed settled WW)	Testing	
	Operation	
MLE 1 AS (fed settled WW)	Testing	
	Operation	
MLE 2 AS (fed raw WW)	Testing	
	Operation	
AD 1 and AD 6 (fed NDBEPR WAS)	Testing	
	Operation	
AD 2 and AD 7 (fed PS)	Testing	
	Operation	
AD 3 and AD 8 (fed MLE 1 WAS)	Testing	
	Operation	
AD 4 and AD 9 (fed PS-MLE 1 WAS blend)	Testing	
	Operation	
AD 5 and AD 10 (fed MLE 2 WAS)	Testing	
	Operation	

4.2 PERFORMANCE OF ACTIVATED SLUDGE (AS) SYSTEMS

The Activated Sludge (AS) system performance is assessed in terms of the nitrogen (N) and phosphorus (P) removal, sludge produced and oxygen consumed. The operation of the three AS systems that were used in this research project was described in detail in Chapter 3. The University of Cape Town (UCT) Nitrification-denitrification Biological Excess Phosphorus Removal (NDBEPR) system was fed 150*l*/d of settled wastewater, one Modified Ludzack Ettinger (MLE) system was fed 36*l*/d settled wastewater (MLE 1) and the other MLE system fed 18*l*/d raw wastewater (MLE 2). The sludge age of all three AS systems was 10 days established by hydraulic control.

The MLE systems incorporate Chemical Oxygen Demand (COD) removal and biological N removal through the processes of nitrification and denitrification and the use of wastewater organics (COD) as substrate. The NDBEPR system also incorporates biological excess P removal (BEPR) to COD and N removal. For biological N and P removal to take place, oxygen is used as a terminal electron acceptor in processes of nitrification, the growth of ordinary heterotrophic organism (OHO) and P accumulating organism (PAO) active mass and their endogenous residue. The active biomass grows by the utilization of organics and nutrients available in the wastewater, causing an increase in the volatile settleable solids (VSS, activated sludge) concentration in the systems. To keep this VSS concentration as constant as possible, the daily COD flux feed is kept constant and a fixed volume of the sludge mixed liquor VSS is wasted daily. Thus, with constant flow and load operation, the reactor solids VSS concentration achieves steady state and remains approximately constant with time. This way, the characteristics of the AS systems' waste sludge, as feed to the ADs are kept as constant as possible. Thus AS system stability required consistency of sludge age, influent COD, total Kjeldahl nitrogen (TKN) and total phosphorus (TP) fluxes and COD, N and P removal. This was

observed in the difference between the influent and effluent COD, TKN and TP concentrations. Consistency of oxygen utilization and sludge production (reactor VSS concentrations) are also very good indicators of steady state system operation. All these aspects, as observed from the AS system test results, are discussed below.

4.2.1 COD Removal

The AS systems' unfiltered influent COD, membrane filtered effluent COD concentration and their difference (COD removal) is evaluated below. Figure 4.2.1 shows the daily concentrations of the unfiltered influent and membrane filtered effluent COD concentrations from the AS systems during the various AD test periods (1 to 5) of the experimental investigation. In Figure 4.2.1, the AD test periods have been aligned with the batch numbers of the sewage fed to the AS systems.

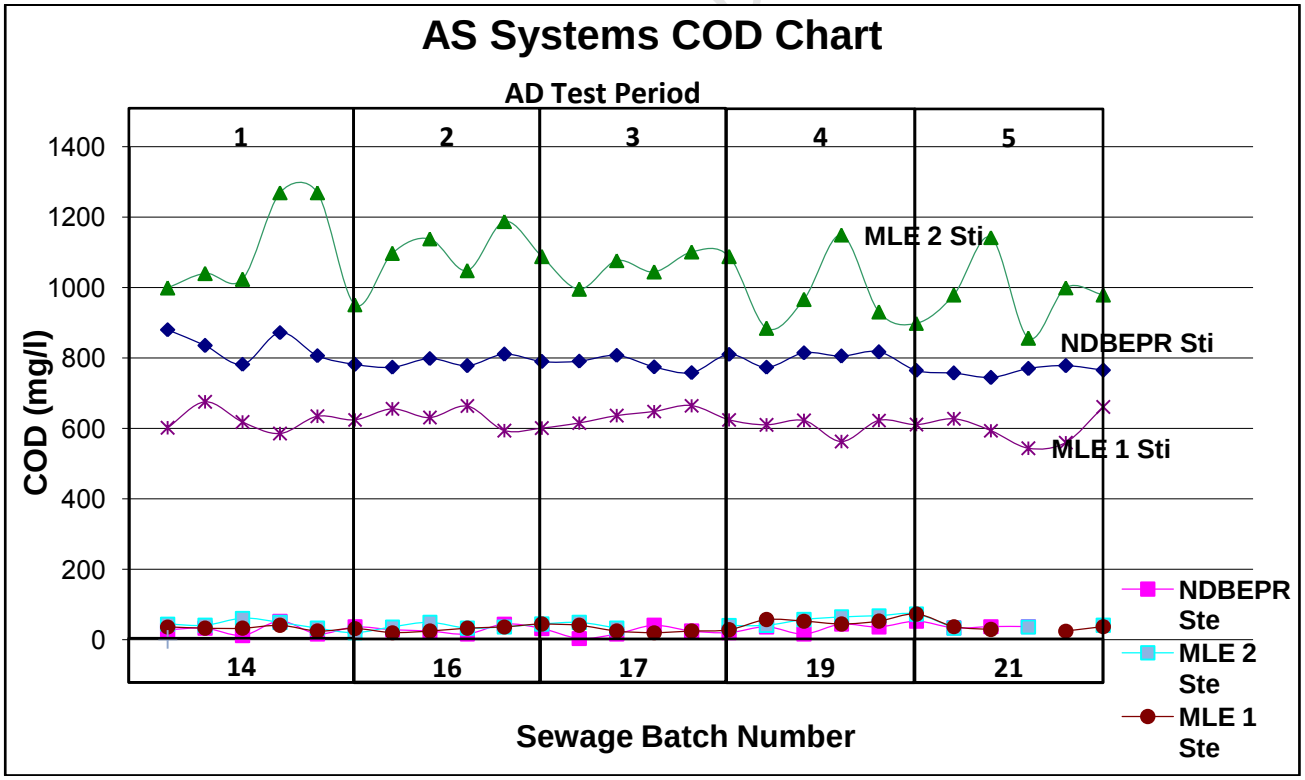

Figure 4.2.1: *The influent (S_{ti}) and filtered effluent (S_{te}) COD concentrations for the three AS systems at the test periods and respective sewage batch numbers.*

The COD of the settled wastewater fed to MLE 1 averaged at 619 (±29.5) mgCOD/*l* (the target was 600mgCOD/*l*) (refer to Figure 4.2.1). This was done through sourcing the wastewater from the same location and applying the necessary dilutions (see Section 3.2 of Chapter 3). To obtain the raw wastewater fed to MLE 2, at the target influent COD concentration of 1000mgCOD/*l*, primary sludge was added to the settled sewage. The raw wastewater average COD is 1046.6 (±95.4) mgCOD/*l*. For the NDBEPR system, an extra 38.5g/day of sodium acetate that was added to 150*l*/day of settled wastewater, which added 200mgCOD/*l*. The average influent COD of this augmented settled WW was 786.8 (±29.0) mgCOD/*l* (target 600 + 200 = 800mgCOD/*l*).

Despite the variation in the feed concentrations, the 0.45µm membrane filtered effluent COD concentrations for the 2 MLE and Kubota membrane filtered effluent COD concentrations from the UCT system were similar, i.e. 29.0 ±11.4, 44.8 ±11.8 and 36.3 ±11.3 for the UCT, MLE 2 and MLE 1 systems respectively. Since all three systems were fed wastewater from the same source, the unbiodegradable soluble COD concentration (S_{use}) was expected to be similar because the PS and acetate added did not significantly affect the effluent filtered COD. The only expected difference is that the NDBEPR effluent COD concentration should be the lowest because it exits through the membranes, which are known to remove more organics than the 0.45µm membrane filters (Du Toit *et al.*, 2007) used for the filtered effluent COD of the MLE 1 and MLE 2 systems.

The very low filtered effluent COD concentration from the three AS systems confirms that the operational sludge age (10 days) is sufficient for the acclimatized active mass at steady state to remove all the biodegradable organics. Therefore, the filtered effluent COD concentration (S_{use}) can be taken as equal to the influent's unbiodegradable soluble COD concentration (S_{usi}). The NDBEPR, MLE 1 and MLE 2 AS systems remove 96%, 94% and 96% of the influent COD respectively.

For the settled wastewater feed to MLE 1, the S_{usi} fraction of the S_{ti} $\left(f_{S'us} = {}^{S_{use}}\!/_{S_{ti}} \right)$ is ${}^{36}\!/_{619} = 0.058$. For the raw WW feed to MLE 2 the $f_{S'us}$ fraction is lower $\left({}^{45}\!/_{1047} = 0.043\right)$

from the low volume, high COD concentration PS added to the settled WW. The $f_{S'us}$ for the settled WW (without acetate) feed to the UCT system is $^{29}/_{619} = 0.047$, which is lower than the 0.058 as expected from the smaller pore size of the Kubota membranes compared with the 0.45µm membranes.

4.2.2 TKN Removal

The TKN removal performance of the AS system is evaluated from the difference between the influent and filtered effluent TKN concentrations. Figure 4.2.2 shows the daily concentrations for the unfiltered influent and membrane filtered effluent TKN concentrations from the AS systems during the various AD test periods (1 to 5) of the experimental investigation.

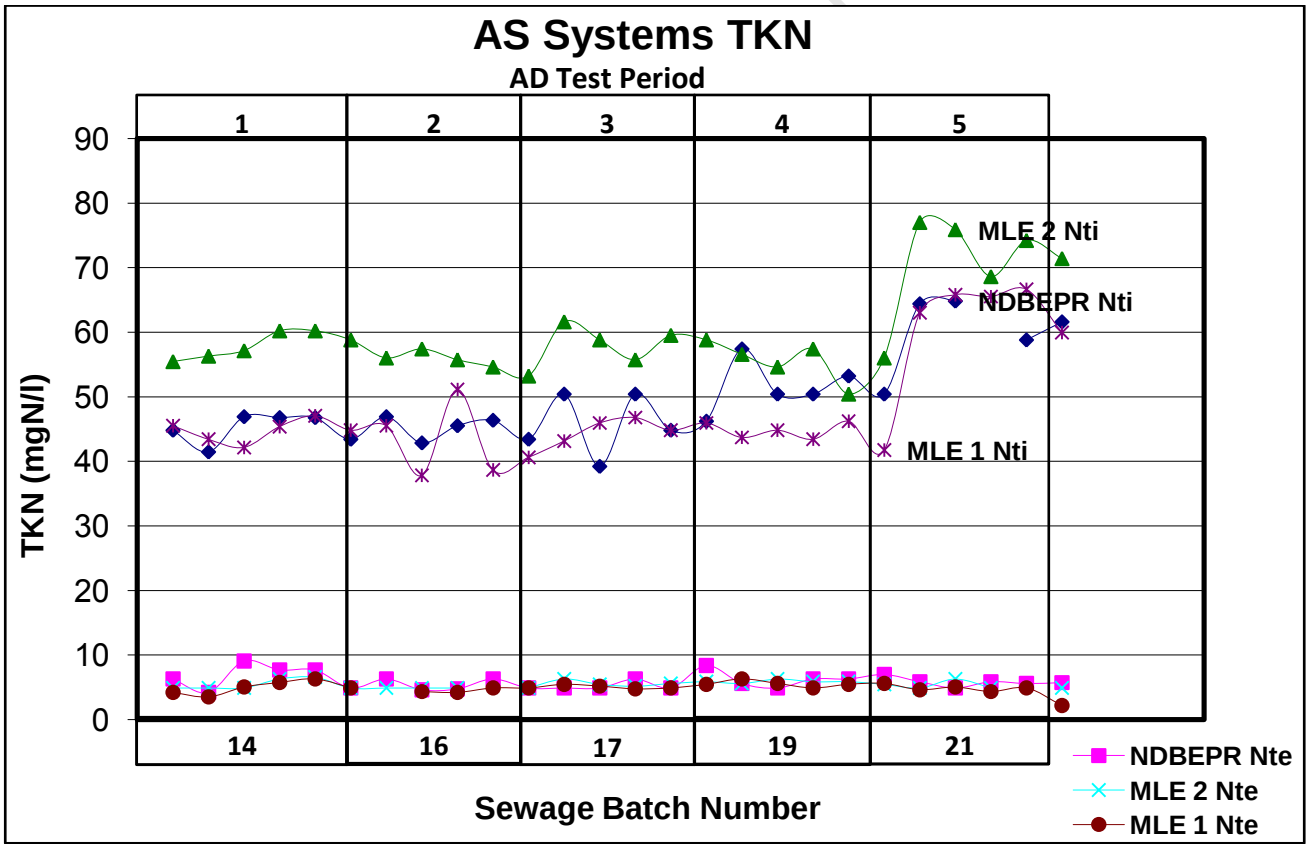

Figure 4.2.2: *The influent (N_{ti}) and filtered effluent (N_{te}) TKN concentrations for the three AS systems at the test periods and respective sewage batch numbers.*

The influent TKN comprised a significant proportion of FSA (Free and Saline Ammonia), and relatively little organic N was present. Thus the influent FSA values

for NDBEPR, MLE 1 and MLE 2 AS systems (36.1 ±7.8, 34.5 ±6.5 and 34.7 ±4.9mgN/*l* respectively) were about 25% lower than the influent TKN values (49.5 ±9.2, 48.0 ±7.6 and 60.0 ±6.3mgN/*l* respectively). The influent TKN concentration for the raw wastewater fed to MLE 2 is expected to be higher than the other two systems due to the organic N addition from the PS. For the NDBEPR, MLE 1 and MLE 2 systems, about 88%, 90% and 90% of the influent TKN was removed indicating nearly complete nitrification throughout the test period and resulting in low filtered effluent TKN values of 5.8 ±1.1, 4.9 ±0.8 and 5.4 ±0.5 mgN/*l* respectively – the effluent FSA concentrations from all three systems were below 1 mgN/*l*.

4.2.3 Nitrate Removal

For the ND (MLE) and NDBEPR systems to achieve N removal, aerobic conversion of influent TKN to nitrate (nitrification) and the anoxic conversion of nitrates to nitrogen gas (denitrification) which escapes to the atmosphere, are required. Figure 4.2.3a shows the relationship between the unfiltered influent TKN (N_{ti}) and effluent nitrate (N_{ne}) concentrations (N_{ne} having the same concentration as that in the aerobic reactor). Because near complete nitrification took place in the AS systems, increased effluent nitrate concentrations were produced with higher influent TKN concentrations because the anoxic reactor volumes and mixed liquor recycles from the aerobic to anoxic reactor were not changed during the investigation. Figure 4.2.3b shows a comparison between the mass of nitrate generated and nitrate de-nitrified, calculated for each AD test period (1 to 5). The average concentration (with respect to influent flow) of nitrate de-nitrified in the NDBEPR, MLE 1 and MLE 2 AS systems (16.1, 15.2 and 11.2mgN/*l* respectively) are about 72.8, 44.5 and 52.3% of those generated (22.1, 34.2 and 21.5 mgN/*l* respectively). The membrane (MBR) UCT NDBEPR system de-nitrified significantly better than the two MLE systems and was not affected by the increased influent TKN concentration during sewage batch 21. This is due to the much higher reactor VSS concentration (about 2.5 times higher) in the MBR UCT system with the result that the dissolved oxygen (DO) in the recycles

not affecting denitrification as much as in the MLE systems. In addition, the MLE 2 system fed the raw wastewater de-nitrified better than MLE 1 fed the settled wastewater. This is due to the additional organics (400mgCOD/*l*), but little additional TKN (12.0mgN/*l*) from the PS, which decreases the influent TKN/COD concentration ratio from $\left(48/619 = 0.078\right)$ mgN/mgCOD to $\left(60/1047 = 0.057\right)$ mgN/mgCOD.

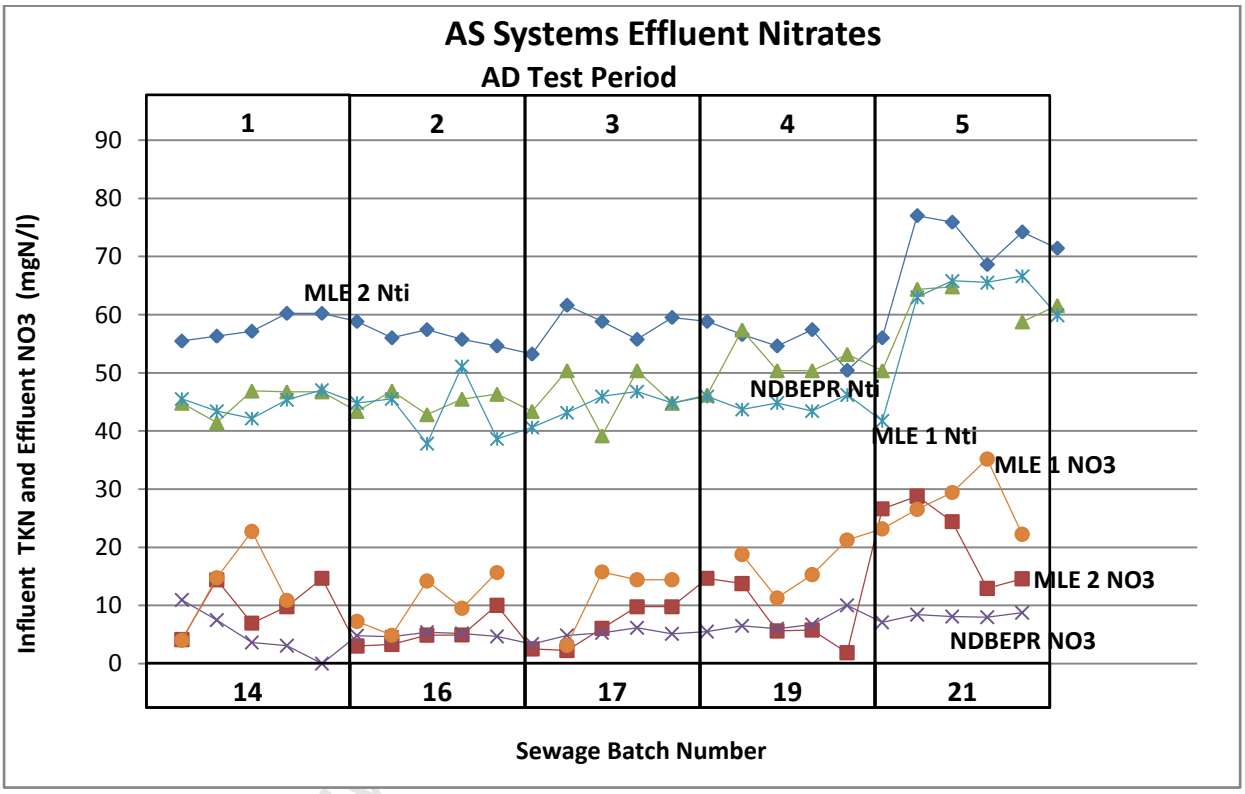

Figure 4.2.3a: *The influent TKN and filtered effluent nitrate concentrations for the three AS systems over the AD test periods and respective sewage batch numbers.*

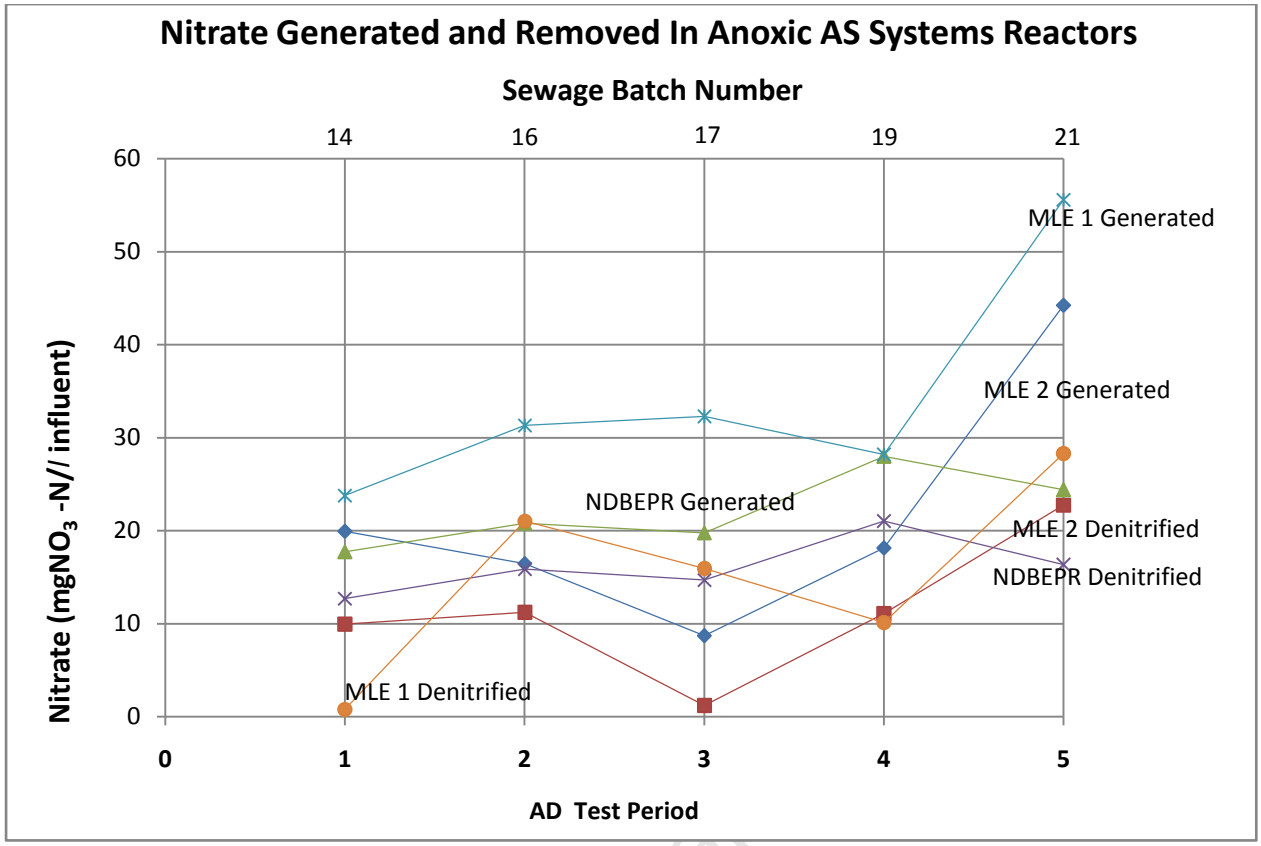

Figure 4.2.3b: *The mass of nitrates generated and de-nitrified in the three AS systems at the test periods and respective sewage batch numbers.*

Negligible concentrations of nitrate (NO_3) were measured in the anaerobic reactor of the UCT NDBEPR system (average of 0.17mgNO_3-N/*l* over the complete experimental investigation). The BEPR process was therefore unrestrained by nitrate (the potential for this BEPR restraint explained in Section 2.3.2.3 of Chapter 2). Although the two MLE systems did not de-nitrify as well as the NDBEPR system, this was not of any significance because the major objective was to ensure that (1) no BEPR occurred in the MLE systems, in order to compare the biodegradability of their WAS organics in the ADs with that of the NDBEPR system and that (2) the BEPR in the UCT system was not affected by any nitrate recycle to the anaerobic reactor. Both these objectives were met at all times in the investigation. The composition of the WAS from the three systems was of primary importance in this investigation, not the effluent concentrations.

4.2.4 Phosphorus Removal

The system P removal performance is evaluated from the removals achieved by the system, which is the difference between the influent and filtered effluent total phosphorus (TP) concentrations. Figure 4.2.4 shows the unfiltered influent and membrane filtered effluent total phosphate concentrations over the various AD test periods (1 to 5) of the experimental investigation, aligned with the respective sewage batch numbers.

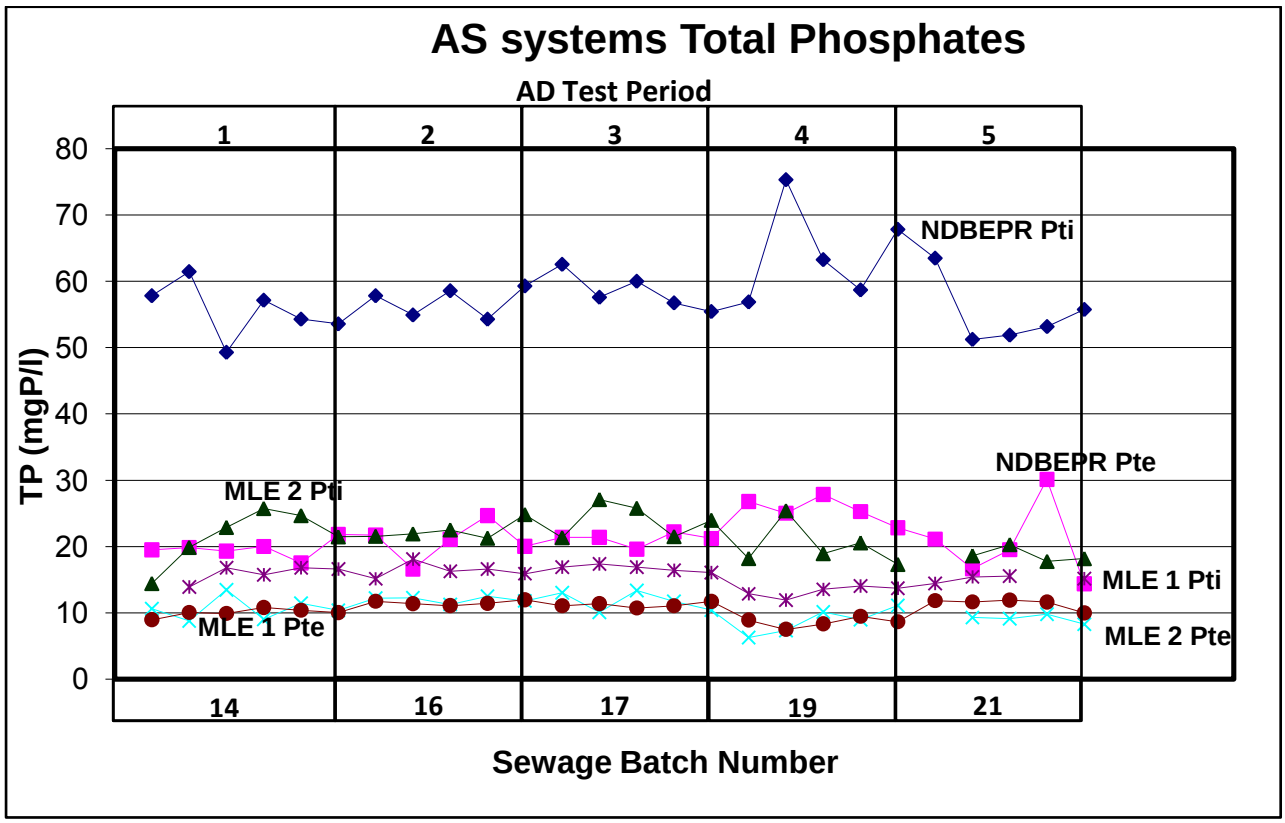

Figure 4.2.4: *The variation of influent and filtered effluent total phosphate concentrations during the experimental research periods and respective sewage batch numbers.*

The influent TP for the NDBEPR, MLE 1 and MLE 2 systems comprised mainly of ortho-phosphate (OP), i.e. 44.3 ±7.1, 13.5 ±1.4 and 14.9 ±1.4 mgP/*l* respectively and so the influent organic P concentrations were low. The respective average unfiltered TP concentrations were 57.4 ±4.7, 16.0 ±1.4 and 21.9 ±2.8 mgP/*l*. The NDBEPR system influent TP concentration was much higher because 40mgOP -P/*l* was added to its influent feed to avoid P limitation so that the PAOs could acquire maximum

polyphosphate (PP) content. The higher influent TP concentration for the raw wastewater fed to MLE 2 (the extra 5.9 mgP/*l*) is from the organic P added with the 400 mgCOD/*l* PS.

The average effluent filtered TP concentrations from the NDBEPR, MLE 1 and MLE 2 AS systems were 21.1 ±3.2, 10.4 ±1.1and 10.5 ±1.6 respectively. The low P removals in the MLE 1 and MLE 2 systems confirm that no BEPR took place in these systems and the phosphorus was utilized for sludge production (assimilation) only. In contrast, the very high removal of TP obtained in the NDBEPR system (36.3 mgP/*l*) indicated that there was substantial growth of phosphorus accumulating organism (PAO) biomass, on the influent rapidly biodegradable COD (RBCOD) and added 200 mgCOD/*l* acetate.

4.2.5 Metallic Ions Removed in the Formation of Polyphosphate

Calcium, magnesium and potassium metallic ions are required components in the formation of PP which is accumulated in the PAOs. To avoid limitation of these metals they were supplemented into the system as part of the NDBEPR influent feed. To quantify their utilization from system mass balances, samples from the influent, effluent and mixed liquor were tested for these metals. The results are shown in Table 4.2.5. An average of 202.8, 348.4 and 33.4 mg/*l* of magnesium (Mg), potassium (K) and calcium (Ca) respectively became a part of the WAS from the NDBEPR system. These values were used to determine the PAO PP elemental composition (as reported in Chapter 5). Although the metal concentration in the sludge is high, the difference between the influent and effluent metal concentration is quite low due to the high influent flow-rate, relative to the waste flow rate. The Mg, K and Ca concentrations removed from the wastewater were 18.9, 11.3 and 1.1 mg/*l* respectively.

Table 4.2.5: Metallic Ion Concentrations (mg/*l*) in the NDBEPR AS System							
Experimental Testing Period		1	2	3	4	5	
Sewage Batch Number		14	16	17	19	21	Average
	Influent	90.5	94.2	98.7	101.1	101.0	97.0
	Unfiltered mixed liquor	290.9	289.5	279.3	313.1	235.7	285.3
	Aerobic (filtered)	59.6	74.1	93.2	81.8	89.2	79.2
	Stored in Biomass	231.3	215.5	186.1	231.3	146.5	206.2
Magnesium (Mg)	Effluent	61.3	72.9	91.9	80.6	84.2	78.1
	Influent	110.0	117.3	105.8	84.5	99.7	102.5
	Unfiltered mixed liquor	494.0	442.3	401.8	447.9	400.0	440.3
	Aerobic (filtered)	80.6	98.7	98.1	75.4	95.0	88.2
	Stored in Biomass	413.4	343.7	303.7	372.5	305.0	352.1
Potassium (K)	Effluent	97.5	107.0	95.4	72.1	89.9	91.2
	Influent	22.9	22.3	21.3	21.5	15.7	21.1
	Unfiltered mixed liquor	54.0	58.5	56.4	52.9	50.7	54.4
	Aerobic (filtered)	22.8	27.2	21.1	21.8	12.3	21.3
	Stored in Biomass	31.2	31.3	35.3	31.1	38.3	33.1
Calcium (Ca)	Effluent	22.1	23.0	19.9	21.3	11.7	20.0

4.2.5 Mixed Liquor Suspended Solids (MLSS) Concentration

Figure 4.2.6 shows the mixed liquor total and volatile suspended solids concentrations throughout the various AD test periods (1 to 5) of the experimental investigation aligned with the respective sewage batch numbers.

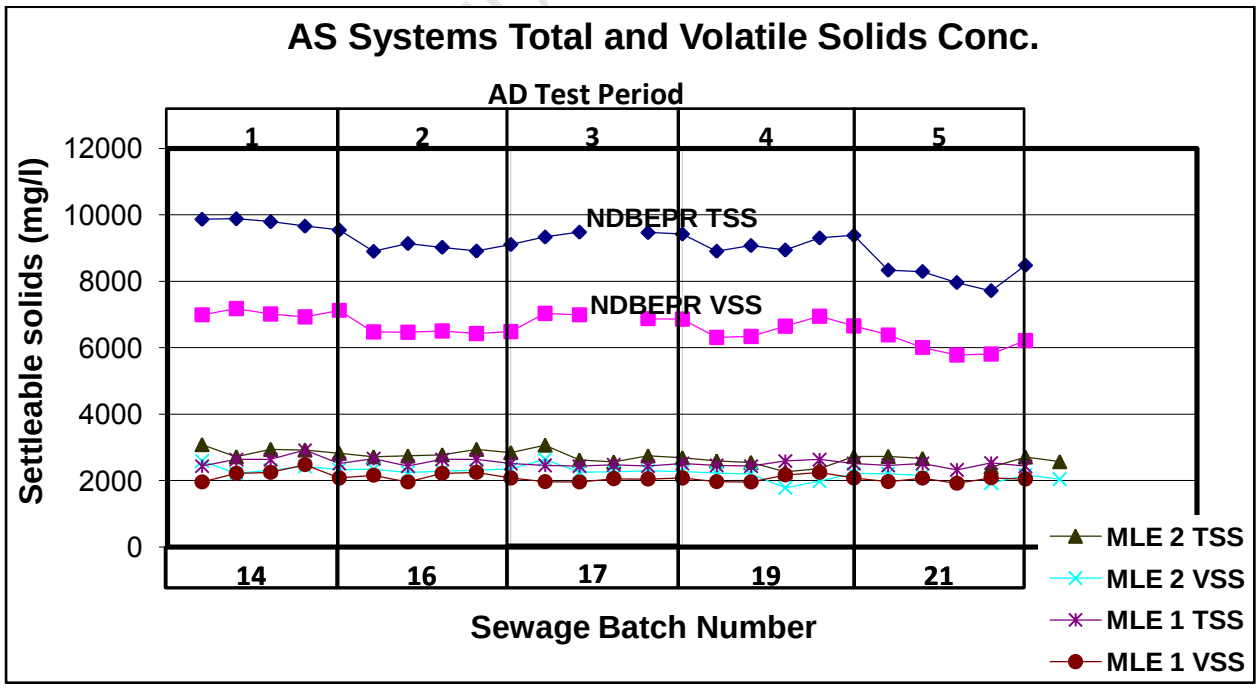

Figure 4.2.6: *The mixed liquor total and volatile suspended solids concentrations throughout the experimental period.*

With the constant influent flow and COD concentrations (as shown in Figure 4.2.1) together with the maintenance of a constant sludge age at 10 days (i.e. steady state conditions), the systems' total settleable solids (TSS) and volatile settleable solids (VSS) concentrations did not vary much. Average TSS concentrations of 9392 ±517, 2533 ±106 and 2714 ±178 and average VSS of 6814 ±358, 2095 ±118 and 2243 ±162 mgVSS/*l* in the aerobic reactors of the NDBEPR, MLE 1 and MLE 2 systems were measured respectively. The VSS/TSS ratios for the aerobic reactor mixed liquor solids were therefore 0.726, 0.826 and 0.827 for the NDBEPR, MLE 1 and MLE 2 systems respectively. The concentrations of inorganic settleable solids (ISS = TSS-VSS) in the aerobic reactors of the MLE systems remained low (438 ±34mgISS/*l* for MLE 1 and 471 ±72mgISS/*l* for MLE 2) while that in the aerobic reactor of the NDBEPR system was about five times higher (at 2578 ±225 mgISS/*l*) partly due to the high TSS concentration in the MBR UCT system and partly due to the high PP content of the PAOs. From Ekama and Wentzel (2004), the MLE system reactor ISS concentration is a combination of influent (fixed) ISS and a small ISS contribution from the OHOs (0.15mgISS/mgOHOVSS) so the VSS/TSS ratios are high (0.827, low ISS). With BEPR the reactor ISS concentration increases significantly due to the very high ISS content of the PAOs from the stored PP, i.e. 3.826mgISS/ mgPP as P. Therefore, if the PAOs contain their maximum PP (f_{XBGP} = 0.35mgP/mgPAOVSS), their ISS contribution is 0.15 + 0.35 × 3.286 = 1.3mgISS/mgPAOVSS. This makes the VSS/TSS ratio significantly lower (0.727, high TSS) than in the two MLE systems.

4.2.7 Oxygen Utilization

Figure 4.2.7 shows the sewage batch average oxygen utilization rate (OUR) measured by the OUR meters during the various AD test periods (1 to 5) of the experimental investigation, aligned with the respective sewage batch numbers.

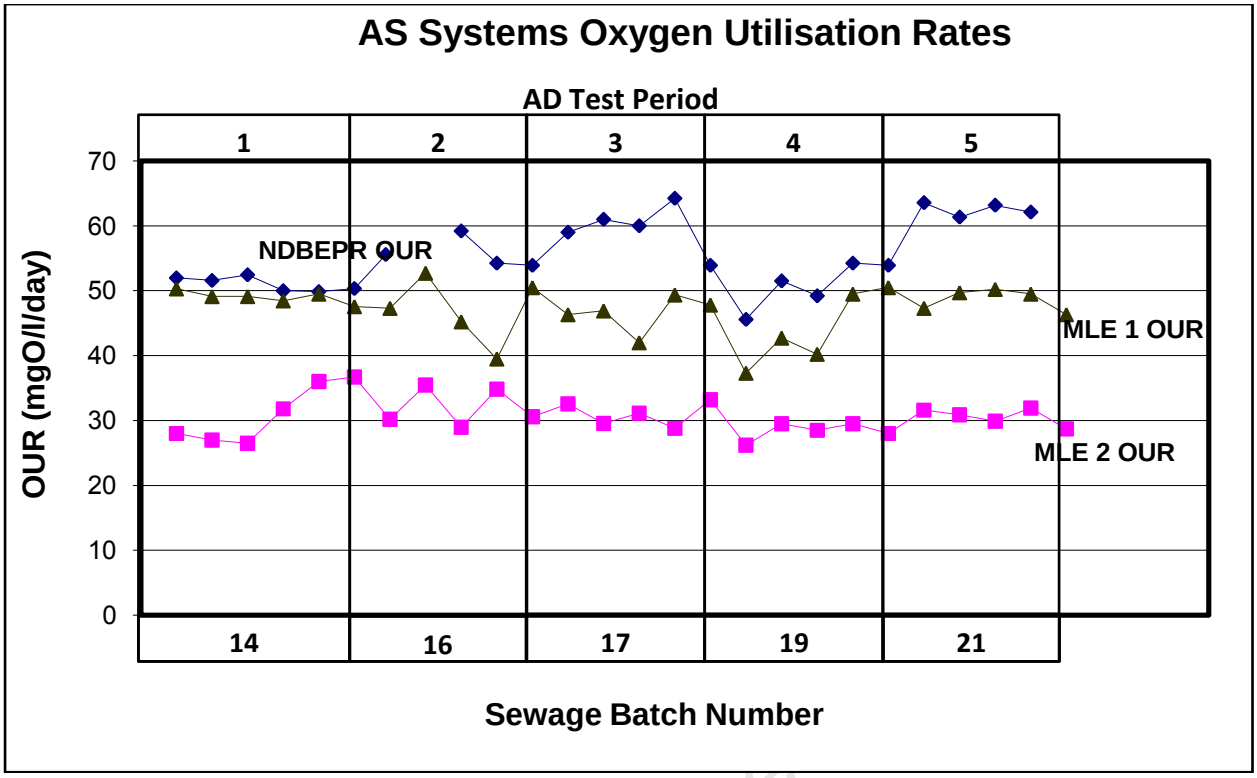

Figure 4.2.7: *Sewage batch average oxygen utilization rates (OUR) in the aerobic reactors of the NDBEPR, MLE 1 and MLE 2 systems.*

Oxygen is used in the processes of nitrification and aerobic substrate utilization for growth and endogenous respiration. The magnitude of the aerobic OUR depends on the flux (g/d) of COD and TKN (or FSA) in the wastewater feed, the system volume (i.e. the system hydraulic retention time, HRT) and the aerobic mass fraction (proportion of system sludge mass in the aerobic reactor). The OUR for MLE 1 (47.0 ±3.4 mgO/*l*/h) is higher than that of MLE 2 (30.6 ±2.5mgO/*l*.h) because although MLE 2 was fed higher concentrations of COD and TKN from the raw wastewater, MLE 1 (fed settled WW) was fed at double the influent flow of wastewater (36*l*/d) and so had half the HRT (0.62d). The HRT of the NDBEPR system also was low (0.5d) due to the high influent flow of 150 *l*/d through the 75*l* system volume. Hence, it also had a higher OUR (55.5 ±4.7mgO/*l*/d).

4.3. PERFORMANCE OF THE ANAEROBIC DIGESTION (AD) SYSTEMS

In this section the results from the steady state periods of the seven different sludge ages (10, 12, 18, 20, 25, 40 and 60) of the Anaerobic Digesters (AD) fed NDBEPR WAS and five different sludge ages (10, 18, 25, 40 and 60) of the other ADs (fed PS, MLE 1 WAS, MLE 2 WAS and PS-MLE 2 WAS blend) are presented. These results include COD removal, FSA release, ortho-phosphate (OP) release, pH, volatile fatty acids (VFA), $H_2CO_3^*$ alkalinity, gas production and gas composition.

4.3.1 COD Removal

Figure 4.3.1 shows the change in the percentage COD removal with AD sludge age (equal to the retention time). The corresponding results are presented in Table 4.3.1.

Table 4.3.1: COD Removal with Increased AD Sludge Age

Sludge Age (R_s)	Test Period	Percentage of Influent COD Removed				
		NDBEPR WAS (AD1)	PS (AD2)	MLE 1 WAS (AD3)	PS-WAS (AD4)	MLE 2 WAS (AD5)
10	5 (SB 21)	19.6	31.3	14.3	25.1	14.4
12	5 (SB 21)	20.7	-	-	-	-
18	1 (SB 14)	28.1	42.9	31.3	43.4	22.6
20	5 (SB 21)	23.8	-	-	-	-
25	2 (SB 16)	27.5	52.2	41.6	50.3	28.0
40	4 (SB 19)	37.0	64.3	44.7	54.8	31.9
60	3 (SB 17)	41.6	63.8	46.9	57.3	33.6

SB: Sewage Batch Number

In all AD systems, there is an increase in the percentage COD removal with increase in sludge age, since the AD biomass has more time to degrade the feed sludge. The increase in percentage COD removal with sludge age is more rapid for the digesters

fed Primary Sludge (PS) than for the ADs fed WAS. This is due to the faster hydrolysis rate of the PS biodegradable organics than the WAS biodegradable organics, a commonly reported observation in the literature. The PS and WAS are also different in composition. The elemental composition of the biodegradable particulate organics were calculated to be ($C_{1.0}H_{2.19}O_{0.65}N_{0.06}P_{0.01}$ for PS and $C_{1.0}H_{1.46}O_{0.35}N_{0.23}P_{0.03}$, $C_{1.0}H_{1.35}O_{0.37}N_{0.21}P_{0.03}$ and $C_{1.0}H_{1.45}O_{0.36}N_{0.23}P_{0.03}$ for MLE 1, MLE 2 and NDBEPR WAS respectively, see later in Chapter 5). Thus, it is expected that the AD of WAS from the three AS systems (NDBEPR, MLE 1 and MLE 2) would have similar trends in % COD removal with increase in sludge age but all lower than the PS and PS-WAS sludge blend. However, differences between the WAS sludges arise due to differences in their unbiodegradable particulate fractions, which in turn are different to the UPO fraction of the PS and PS-WAS blend - one of the objectives of the project is to determine the UPO fractions of the different sludges. Figure 4.3.1 gives rise to some questions with regards to the percentage COD removal for the AD of NDBEPR WAS at 20 and 25 –day sludge ages because they do not follow the trend of the other sludge ages of the AD treating this WAS and the ADs treating the other WAS sludges. Although no reasonable explanation could be given for this different behaviour in COD removal, it will be taken into account when using the 20d and 25d NDBEPR results to determine the hydrolysis rate of the NDBEPR WAS.

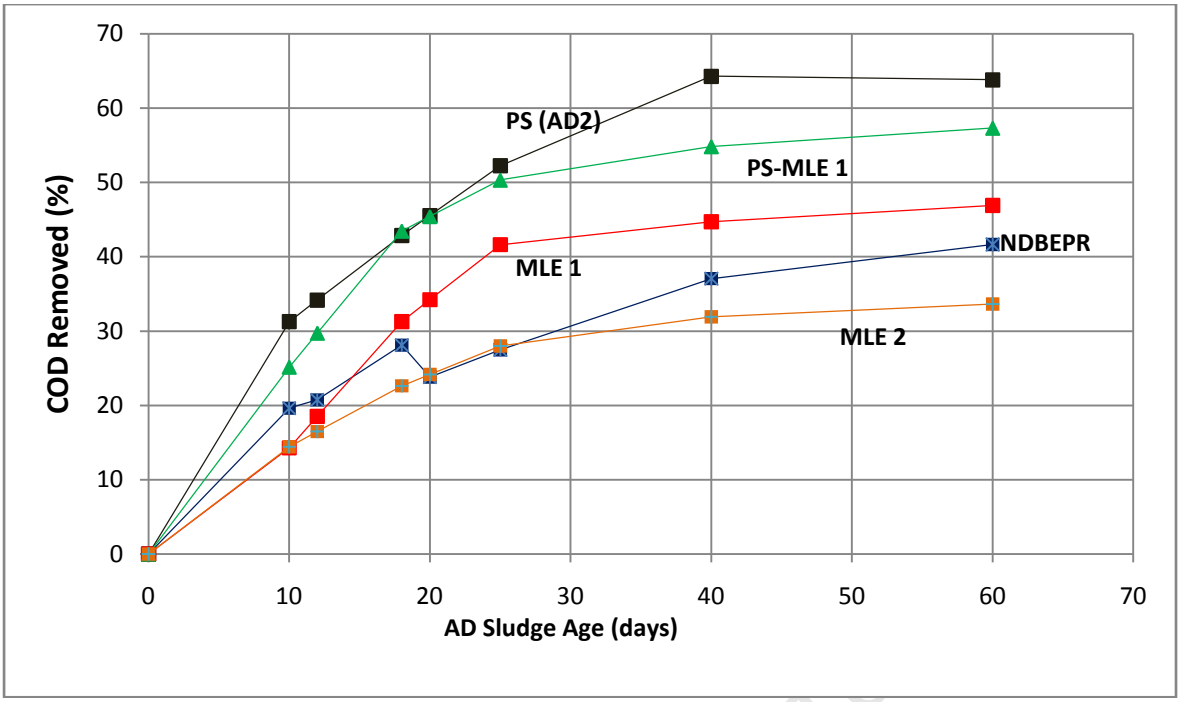

Figure 4.3.1: *The change in the percentage COD removal with AD sludge age.*

4.3.2 Free and Saline Ammonia (FSA) Release during AD

Figure 4.3.2 shows the % influent TKN fed to the ADs released as FSA to the bulk liquid. In general this is similar to the % COD reduction at various sludge ages of the AD systems, i.e. the FSA release tends to increase with sludge age like % COD removal. This is because the organically bound nitrogen in the biodegradable particulate organics (BPO) is released to the AD liquor as the organics are degraded. The release of organically bound N, which is in the non-ionic NH_3 form, are non-reference species for the ammonia weak acid/base system. The NH_3 pick up a H^+ from the bulk liquid which is supplied by the dissolved CO_2 ($H_2CO_3^*$) of the inorganic carbon (IC) system forming HCO_3^- i.e.:

$$NH_3 + H_2CO_3 \rightarrow NH_4^+ + HCO_3^- . \qquad (4.3.1)$$

This production of [HCO_3^-] is the crucial generation of alkalinity in the AD treating ND system WAS. The CO_2 released in the breakdown of the BPO (since the biodegradable soluble organics in WAS are negligible) that cannot be 'held' in solution as HCO_3^-, escapes as CO_2 gas. The methane production depends only on the

electron donating capacity (COD) of the biodegradable organics, and being insoluble, all escape as gas. The mole fraction of the CO_2 in the gas phase [CO_2/ (CO_2 + CH_4)] sets the partial pressure of carbon dioxide (p_{CO2}) which together with the total alkalinity (equal to $H_2CO_3^*$ alkalinity ≈ [HCO_3^-] when the inorganic carbon system dominates the mixed weak acid/base systems), set the AD pH. With PAOs in the WAS, it is a little more complex. The phosphate from the PP is released as $H_2PO_4^-$ which are not reference species for the ortho-phosphate (OP) weak acid/base system, and so adds alkalinity. Because the phosphate weak acid/base sub-system (for $H_2PO_4^-$/HPO_4^{2-} speciation, shown by the Equation 6.4.1e of Section 6.4.1) has a pK_{p2} value at 7.13, some of the $H_2PO_4^-$ consumes $H_2CO_3^*$ Alk. i.e.

$$H_2PO_4^- + HCO_3^- \rightarrow HPO_4^{2-} + H_2O + CO_2 \quad (4.3.2)$$

So while the total alkalinity does not change, the partial pressure of CO_2 (p_{CO2}) in the gas changes.

The pH of the digester is therefore established by both the OP and inorganic carbon (IC) systems, the H_2PO_4 and HPO_4^{2-} concentration of the former and the p_{CO2} and HCO_3^- of the latter.

Because the OP release affects the mixed weak acid/base chemistry of the AD liquor and is affected by mineral precipitation, the OP release is discussed later (in Section 4.3.5) after presenting the gas production and composition, the $H_2CO_3^*$ alkalinity, VFA concentrations and pH of the ADs.

Table 4.3.2: FSA Release with Increased AD Sludge Age						
Sludge Age (R_s)	**Test Period**	**Percentage of Influent TKN Released as FSA**				
		NDBEPR WAS (AD1)	PS (AD2)	MLE 1 WAS (AD3)	PS-WAS (AD4)	MLE 2 WAS (AD5)
10	5 (SB 21)	15.8	0.0	19.0	4.1	18.5
12	5 (SB 21)	20.3	-	-	-	-
18	1 (SB 14)	22.8	19.6	33.2	15.7	21.8
20	5 (SB 21)	28.0	-	-	-	-
25	2 (SB 16)	29.0	37.8	39.8	29.1	34.0
40	4 (SB 19)	35.7	40.7	46.7	42.2	36.3
60	3 (SB 17)	41.5	42.4	53.4	37.7	38.7
SB: Sewage Batch Number						

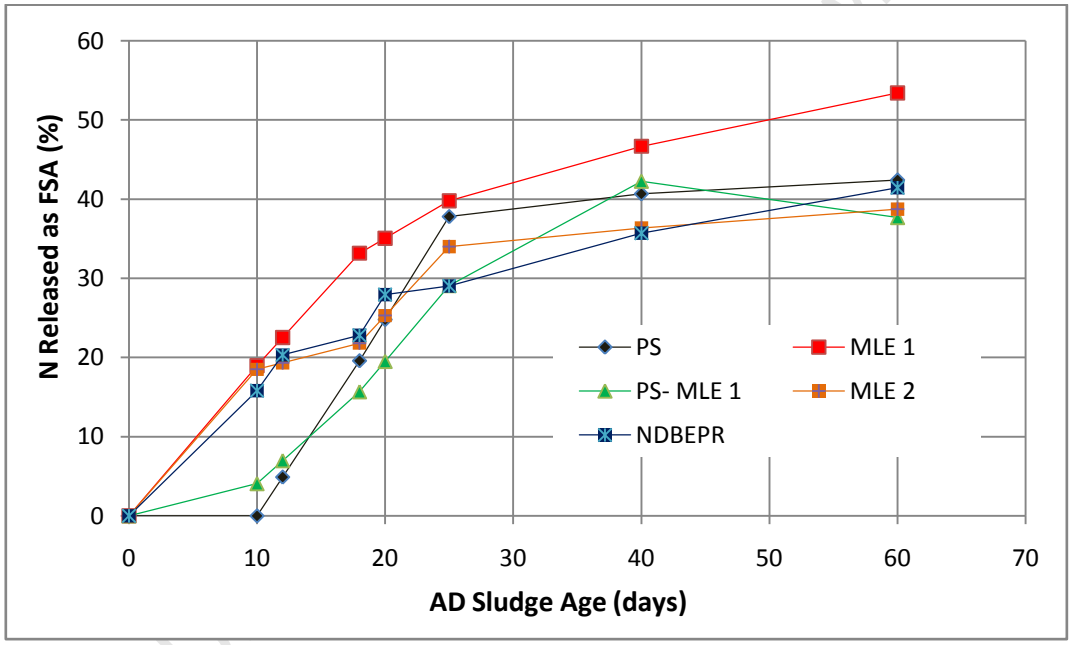

Figure 4.3.2: *The percentage influent TKN released as FSA during anaerobic digestion.*

4.3.3 Gas Production and Composition

At all of the sludge ages, including the lowest (10 day), all the AD systems produced methane, indicating that the systems remained stable and methanogenic. This was probably because the ADs were started at the long sludge ages, at which it is easier to build up and sustain a stable methanogenic population. Then, when the sludge age was decreased to test the short sludge ages, the methanogens were already acclimatized in the system to keep it operating at the short sludge age.

For AD 3 (fed MLE 1 WAS) and AD 4 (fed PS-MLE 1 WAS blend) the feed COD flux (gCOD/d) was kept constant by increasing the feed concentration for a decrease in feed volume/d (the ADs were batch-fed once daily) with an increase in sludge age. However, for the AD 1 (fed NDBEPR WAS), the feed concentration was kept constant and the feed COD flux (and volume/d) decreased with increase in sludge age. In Table 4.3.3 below, the volume of biogas produced per day per litre influent feed volume/d is compared with the sludge age and concentration of COD fed daily to each AD. The biogas produced in the 60-day sludge age was not measured. Because the COD balances on the ADs at the short sludge ages were acceptable, the gas production was calculated from 100% COD balance for the 60d sludge age ADs.

The AD gas composition usually changes negligibly with sludge age (SRT) - it is in fact independent of SRT at constant feed COD concentration. This was observed by Izzett *et al.* (1992) and is confirmed by the stoichiometry that is developed in this project. The gas composition is fixed by the electron donating capacity (EDC or COD/mol) of the organics and the N and PP (not organic P) content, which generate alkalinity, as explained above, of the digested organics.

Ideally, the gas produced by methanogenic digesters comprises only methane (CH_4) and CO_2. However, the way the digesters were fed and sludge wasted from them allowed air into the headspace of the ADs. Although this does not influence the gas volume produced per day, it does affect the gas composition because other gases, including water vapour and nitrogen, exited the system. The CH_4 and CO_2 fraction of the total gas was measured and the observed increase in CH_4 COD with sludge age for the various sludge types is as shown in Figure 4.3.3 below, followed by Table 4.3.3 that reports the fractions of CO_2 and CH_4.

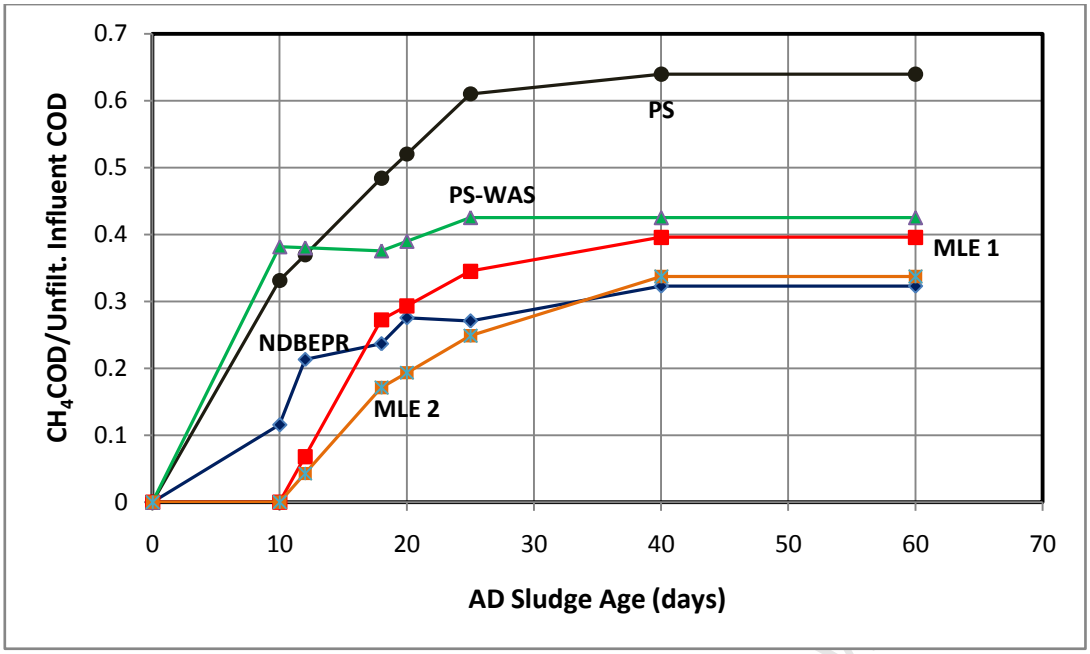

Figure 4.3.3: *The fraction in influent unfiltered COD removed in the form of CH_4 during anaerobic digestion.*

Table 4.3.3: AD Gas Production and Composition Values							
Sludge age (R_s)		**10**	**12**	**18**	**20**	**25**	**40**
AS Sewage Batch		21	21	14	21	16	19
Test Period		5	5	1	5	2	4
AD 2 (AD of PS)	Influent COD, S_{ti} (mgCOD/*l*)	5684		8053		8910	18707
	Gas production (litres/d)	2.60		1.68		1.30	1.03
	Gas composition: CO_2 fraction of total gas	0.40		0.40		0.40	0.40
	Gas composition : CH_4 fraction of total gas	0.23		0.23		0.23	0.23
	COD of CH_4 (mgCOD/*l* feed)	1883		3899		5435	11962
AD 4 (AD of PS-WAS	Influent COD (mgCOD/*l*)	8308		13407		12592	28067
	Gas production (litres)	3.77		1.87		1.11	0.89
	Gas composition: CO_2 fraction of total gas	0.46		0.46		0.46	0.46
	Gas composition : CH_4 fraction of total gas	0.27		0.27		0.27	0.27
	COD of CH_4 (mgCOD/*l* feed)	3170		5035		5354	11931
AD 3 (AD of MLE 1 WAS)	Influent COD (mgCOD/*l*)	2673		3648		5151	8053
	Gas production (litres)	0.00		0.36		0.33	0.23
	Gas composition: CO_2 fraction of total gas	0.47		0.47		0.47	0.31
	Gas composition : CH_4 fraction of total gas	0.31		0.31		0.31	0.31
	COD of CH_4 (mgCOD/*l* feed)	0		995		1777	3188
AD 5 (AD of MLE 2 WAS)	Influent COD (mgCOD/*l*)	3027		6717		8210	17693
	Gas production (litres)	0.00		0.63		0.58	0.42
	Gas composition: CO_2 fraction of total gas	0.49		0.49		0.49	0.32
	Gas composition : CH_4 fraction of total gas	0.32		0.32		0.32	0.32
	COD of CH_4 (mgCOD/*l* feed)	0		1151		2042	5966
AD 1 (AD of NDBEPR WAS)	Influent COD (mgCOD/*l*)	9355	9355	10062	9355	9589	10127
	Gas production (litres)	2.51	3.22	1.71	1.50	0.97	0.47
	Gas composition: CO_2 fraction of total gas	0.42	0.42	0.42	0.42	0.42	0.42
	Gas composition : CH_4 fraction of total gas	0.23	0.23	0.23	0.23	0.23	0.23
	COD of CH_4 (mgCOD/*l* feed)	1082	1995	2383	2579	2598	3271

4.3.4 Volatile Fatty Acids (VFA), H_2CO_3* Alkalinity and pH

The VFA and $H_2CO_3^*$ alkalinity was measured with the five-point titration method of Moosbrugger *et al.* (1992) and results are shown in Table 4.3.4. The effluent VFA concentration was low (generally less than 50 mgHAc/*l* or 54 mgCOD/*l*, apart from the PS-WAS AD at 60- day R_s with an average of 69mgCOD/*l*) in all ADs at all sludge ages 10 to 60d (see Figure 4.3.4). This demonstrates that all ADs had stable

methanogenic conditions. In addition, such low VFA concentrations make a negligible contribution to the total alkalinity in the ADs. Using the terminology of Loewenthal *et al.* (1989), the total alkalinity is therefore the sum of the $H_2CO_3^*$ alk and alk H_3PO_4 ($\approx [H_2PO_4^-] + 2[HPO_4^{2-}]$), where alk as suffix means the water alkalinity ($[OH^-] - [H^+]$) is included and alk as prefix means the water alkalinity is excluded. The total alkalinity generated is a function of the N and PP content of the BPO concentration digested – the higher the N and PP content and concentration (COD or VSS) of organics digested, the higher the total alkalinity. If the organics contain a high organic P content, the P released as H_3PO_4 reference species does not increase the total alk, but some of the alk $H_2CO_3^*$ is replaced by alk H_3PO_4. This decreases the $H_2CO_3^*$ alk and increases the p_{CO2}, but the total alkalinity stays unchanged as shown earlier (see Section 4.3.2). The increase in total alkalinity with sludge age increases the pH with sludge age. The $H_2CO_3^*$ alk increases with sludge age due to the increase in concentration of organics digested. The $H_2CO_3^*$ alkalinity is higher for the PS - WAS blend (AD 4) than the PS (AD 2) because the WAS has a higher N content than the PS. The $H_2CO_3^*$ alk for the different WAS is quite low because of their higher organic P content, so that some of the $H_2CO_3^*$ alk has been replaced by alk H_3PO_4. With the NDBEPR sludge, the PP released increases the total alk but the increase is less than the alk H_3PO_4 it contributes, so that the net effect on the $H_2CO_3^*$ alk is to decrease it. This is evident in Table 4.3.4 which shows the $H_2CO_3^*$ alk of the WAS ADs to be low. If the total alkalinity comprises mostly $H_2CO_3^*$ alk (i.e. alkaline H_3PO_4 is low as for the AD 4 fed PS), then the digester pH is established by the $H_2CO_3^*$ alk and the partial pressure of CO_2 (p_{CO2}). If alk H_3PO_4 is a significant proportion of the total alk, then the digester pH is established by both the inorganic carbon system ($H_2CO_3^*$ alk and p_{CO2}) and the phosphate system (Harding, 2009). If significant mineral precipitation takes place, e.g. struvite, then the phosphate concentration, total alkalinity and digester pH decrease but the p_{CO2} remains unchanged. This can be seen in AD 5 treating the NDBEPR WAS - its pH is low (≤ 7.1) at all the sludge ages. The pH measured for all anaerobic digesters showed no trends with changing

retention time. This can be explained in terms of the mixed weak acid/base chemistry described above. Usually, a low pH and high effluent VFA would be an indication of impending digester failure, due to accumulation of SCFA and subsequent loss of methanogenic biomass, but for AD 1 (fed the NDBEPR WAS), this is not the case. The low VFA concentration indicated that methanogenesis was functional and the AD system stable at all times. The following graphs, in Figures 4.3.4, 4.3.5 and 4.3.6, show variation to sludge age of the effluent VFA, pH and alkalinity respectively for the various operated AD systems, as illustrations to the above discussions.

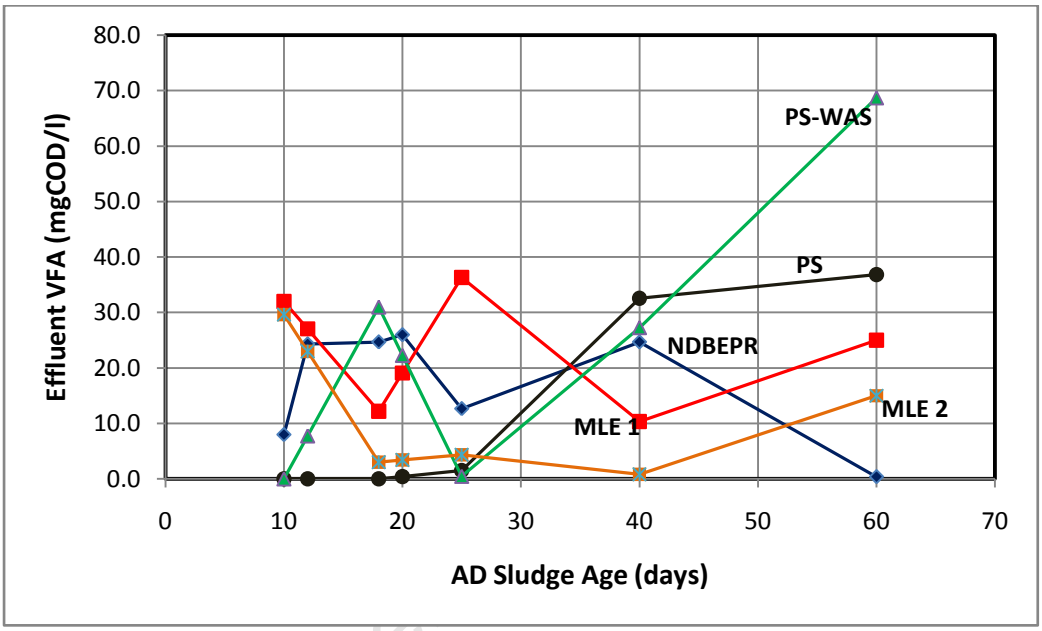

Figure 4.3.4: *The variations of effluent VFA concentration with sludge age during anaerobic digestion*

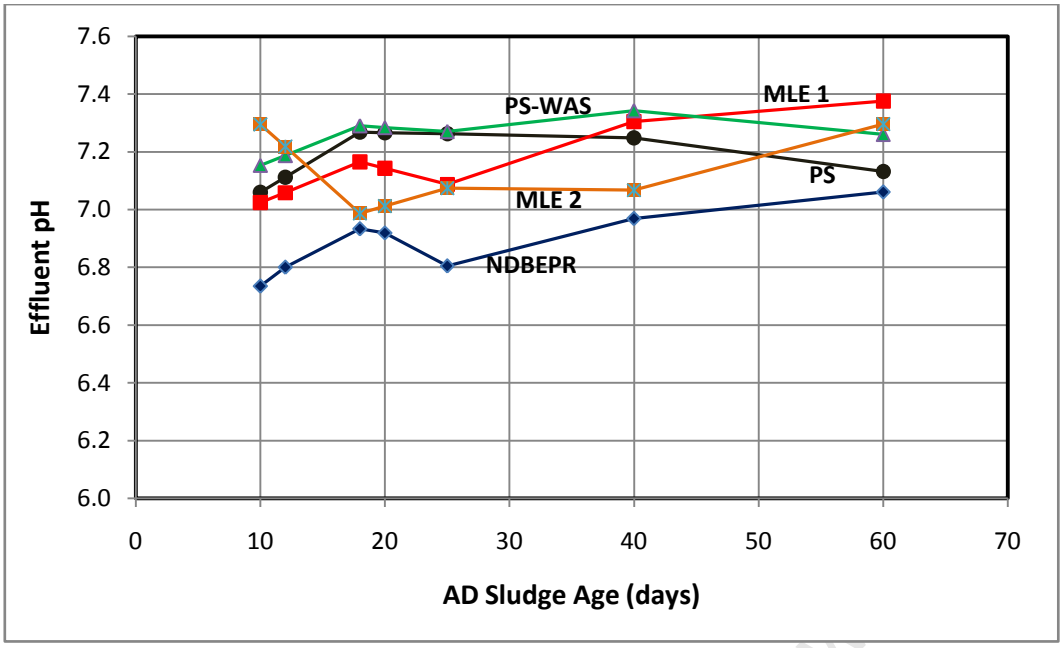

Figure 4.3.5: *The variations of effluent pH with sludge age during anaerobic digestion*

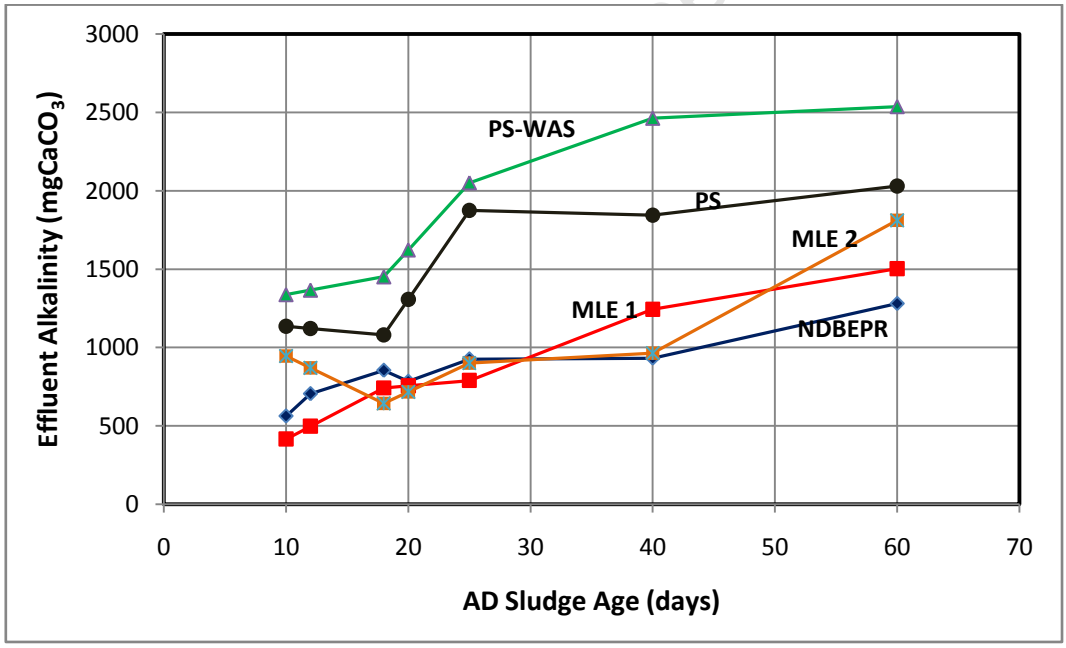

Figure 4.3.6: *The variations of effluent alkalinity concentration with sludge age during anaerobic digestion*

Table 4.3.4: AD Effluent VFA, H_2CO_3 Alkalinity and pH Values								
AD Sludge Age (R_s)		**10**	**12**	**18**	**20**	**25**	**40**	**60**
AS Sewage Batch		21	21	14	21	16	19	17
Test Period		5	5	1	5	2	4	3
AD 1 (Fed NDBEPR WAS)	Effluent VFA, S_{ase} (mgCOD/*l*)	8.0	24.3	24.7	26.0	12.7	24.7	0.4
	Effluent $H_2CO_3^*$ Alk	562.5	705.0	854.6	784.0	926.7	932.3	1281.0
	Measured in situ digester pH	6.7	6.8	6.9	6.9	6.8	7.0	7.1
AD 2 (Fed PS)	Effluent VFA, S_{ase} (mgCOD/*l*)	0.0	-	0.0	-	1.5	32.5	36.8
	Effluent $H_2CO_3^*$ Alk	1135.5	-	1079.8	-	1875.4	1844.5	2031.1
	Measured in situ digester pH	7.1	-	7.3	-	7.3	7.2	7.1
AD 3 (Fed MLE 1 WAS)	Effluent VFA, Sase (mgCOD/*l*)	32.0	-	12.2	-	36.3	10.3	25.0
	Effluent $H_2CO_3^*$ Alk	415.3	-	742.2	-	789.3	1243.7	1504.0
	Measured in situ digester pH	7.0	-	7.2	-	7.1	7.3	7.4
AD 4 (Fed PS - MLE 1 WAS)	Effluent VFA, Sase (mgCOD/*l*)	0.0	-	31.0	-	0.5	27.3	68.7
	Effluent $H_2CO_3^*$ Alk	1338.3	-	1451.9	-	2052.3	2463.7	2537.9
	Measured in situ digester pH	7.2	-	7.3	-	7.3	7.3	7.3
AD 5 (Fed MLE 2 WAS)	Effluent VFA, Sase (mgCOD/*l*)	29.6	-	3.0	-	4.4	0.8	15.0
	Effluent $H_2CO_3^*$ Alk	946.2	-	643.5	-	901.5	964.2	1812.6
	Measured digester pH	7.3	-	7.0	-	7.1	7.1	7.3
	Where * means mg/*l* as CaCO3							

4.3.5 Ortho-phosphate (OP) Release During AD

Table 4.3.5: Ortho-phosphate Release with Increased AD Sludge Age

Sludge Age (R_s)	Test Period	Percentage of Influent TP Released as Ortho-P				
		NDBEPR WAS (AD1)	PS (AD2)	MLE 1 WAS (AD3)	PS-WAS (AD4)	MLE 2 WAS (AD5)
10	5 (SB 21)	54.6	0.0	8.7	0.0	8.3
12	5 (SB 21)	58.5	-	-	-	-
18	1 (SB 14)	48.0	4.1	36.8	9.3	19.5
20	5 (SB 21)	62.6	-	-	-	-
25	2 (SB 16)	44.1	17.2	44.6	17.0	30.9
40	4 (SB 19)	54.1	13.4	52.8	27.2	36.2
60	3 (SB 17)	43.8	15.8	53.5	26.2	40.1
SB: Sewage Batch Number						

The above Table 4.3.5 and Figure 4.3.7 show the percentage influent total phosphorus (TP) released as ortho-phosphate (OP). It is evident that the phosphorus release follows the same increasing trend as substrate degradation, i.e. increases with sludge age, for all AD systems except the one fed NDBEPR sludge. It would appear that the decrease in P release from 40 to 60d sludge age for the PS and PS - MLE 1 sludge blend AD is spurious. Moreover, the OP releases for the PS are generally low in comparison to the percentage N release (shown in Figure 4.3.2). This may be because of the TP in the PS being generally low, thus most of it being used in the formation of AD biomass. The similarity of trends between the P release and COD removal for these four AD systems is due to the release of the organically bound P (compare Figures 4.3.1 and 4.3.7). However, with steady state anaerobic digestion of the NDBEPR sludge, phosphorus release appears to remain within the ranges of 45% to 62%, while the COD removal tends to increase with increased sludge age (Figure 4.3.1). This is because the PAOs wasted from the aerobic zone of the BEPR system contain a high concentration of PP. This PP is released much more quickly than the organically bound P in the PAO and OHO biomass. The PAOs being essentially aerobic organisms, cannot survive in the AD system very long and are likely to utilize their PP to survive as long as possible. It is therefore expected that the entire

PAO PP is released within a few days (Harding, 2009). Thus at steady state AD operation, the release of all the PP will occur at very short sludge ages (< 10d), while the biomass P, which is relatively a much lower concentration, is released separately at a slower rate i.e. the same rate as that of the biomass degradation in the AD system.

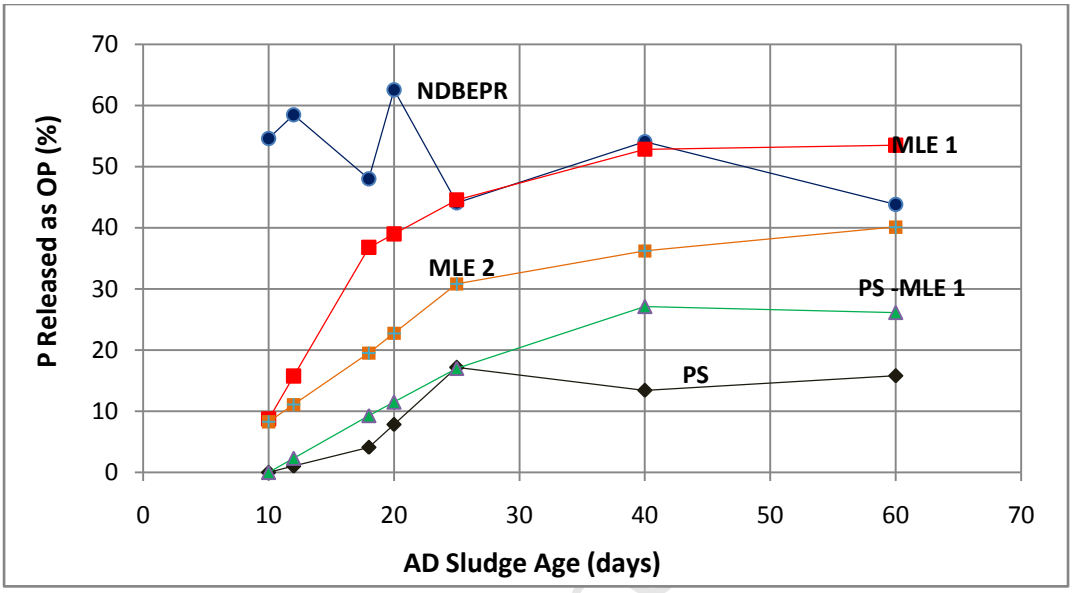

Figure 4.3.7: *The percentage influent total phosphorus (TP) released as ortho-Phosphate (OP) during AD.*

However, for AD 1 (fed NDBEPR WAS), not all the released P is observed in the bulk liquid as OP. This is because once the P exeeds 48% of the influent P (about 400mgP/*l* in this investigation) struvite precipitation took place with the Mg and P release from PP, preventing further significant increases of soluble P (and Mg) concentration in the AD liquor. Because the PP is released rapidly within a few days, precipitation also took place at the lowest AD sludge age of 10 days. This aspect of struvite precipitation, as observed in this experiment, is discussed in more detail in Harding (2009) and accounts for the low AD 1 liquor pH.

4.3.6 Metallic Ions and phosphorus Precipitation

The PP contains metal ions magnesium (Mg), potassium (K) and calcium (Ca) to charge balance it. These ions are taken up together with the phosphate in the PAO P uptake process in the NDBEPR system and thus form part of the feed to the AD. The

Mg, K and Ca metal ions are taken up in proportion to the OP taken up. From the enhanced PAO cultures of Comeau *et al.* (1985) and Wentzel *et al.* (1989), the metal to P proportions in PP formation are approximately:

$$0.22Mg^{2+} + 0.27K^{+} + 0.12Ca^{2+} + H_2PO_4^{-} \rightarrow \left(0.22Mg^{2+} + 0.27K^{+} + 0.12Ca^{2+}\right)PO_3 + H_2O \quad (4.3.3)$$

This stoichiometry of P uptake makes the P to ISS ratio of the PP equal to 3.126mgISS/mgP, which is very close to the 3.286 mgISS/mgP measured by Ekama and Wentzel (2004). The metal ions were measured in the AD influent and effluent filtered and unfiltered samples in order to check whether or not they were used in the formation of struvite or other precipitates. Table 4.3.6 below lists the results as measured within the steady state experimental periods for AD 1 fed the NDBEPR WAS. The influent and filtered effluent concentrations are shown in Fig. 4.3.6. The metal ions were not measured for AD 1 to AD 4 fed the PS and WAS from the MLE systems because the changes on these metal ion concentrations are negligible in these AS and AD systems.

Table 4.3.6: NDBEPR WAS fed AD (AD 1) Metallic Ion Measurements							
AD Sludge Age (R_s)	**10**	**12**	**18**	**20**	**25**	**40**	**60**
AS Sewage Batch	21	21	14	21	16	19	17
Test Period	5	5	1	5	2	4	3
Unfiltered Influent magnesium (mg/*l*)	235.7	235.7	290.9	235.7	289.5	313.1	279.3
Filtered Influent magnesium (mg/*l*)	89.2	89.2	59.6	89.2	74.1	81.8	93.2
Unfiltered Influent potassium (mg/*l*)	400.0	400.0	494.0	400.0	442.3	447.9	401.8
Filtered Influent potassium (mg/*l*)	95.0	95.0	80.6	95.0	98.7	75.4	98.1
Unfiltered Influent calcium (mg/*l*)	50.7	50.7	54.0	50.7	58.5	52.9	56.4
Filtered Influent calcium (mg/*l*)	12.3	12.3	22.8	12.3	27.2	21.8	21.1
Unfiltered Effluent magnesium (mg/*l*)	225.1	252.1	296.7	273.2	299.0	251.8	274.3
Filtered Effluent magnesium (mg/*l*)	24.1	23.8	24.1	22.6	25.0	25.6	24.8
Unfiltered Effluent potassium (mg/*l*)	307.6	391.9	394.8	373.3	400.3	376.6	404.8
Filtered Effluent potassium (mg/*l*)	273.3	355.8	362.5	362.5	372.4	369.0	382.3
Unfiltered Effluent calcium (mg/*l*)	42.8	43.4	43.2	42.8	39.8	26.1	48.6
Filtered Effluent calcium (mg/*l*)	41.6	37.4	28.8	34.1	26.8	20.0	45.7
% Recovery Magnesium	95.5	107.0	102.0	115.9	103.3	80.4	98.2
% Recovery potassium	76.9	98.0	79.9	93.3	90.5	84.1	100.7
% Recovery Calcium	84.5	85.6	79.9	84.5	68.0	49.4	86.3

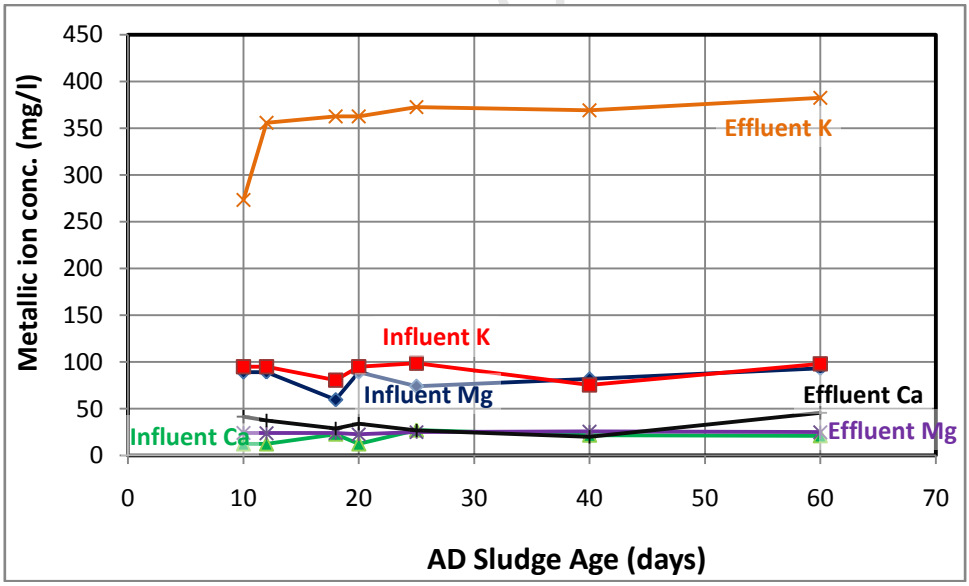

Figure 4.3.8: *The AD influent and filtered effluent metallic ion concentrations.*

Figure 4.3.8, shows that the filtered effluent Mg and Ca concentrations remain very low and constant with sludge age. The dissolved effluent magnesium concentration is much lower than its influent (both unfiltered and filtered) values while that of potassium is much higher. The very high filtered K concentration (close to the influent unfiltered value) validates that the PP in the PAOs has been fully

hydrolysed (reverse of Equation 4.3.3) and released. Therefore, a filtered effluent Mg concentration that is close to the unfiltered influent Mg concentration was expected but was not observed. This confirms that precipitation took place in AD 1. The concentration of struvite precipitated is the difference between the unfiltered influent and filtered effluent Mg concentrations, i.e. 200 – 270 mgMg/*l*. The difference between the unfiltered influent and filtered effluent Ca concentrations indicate that a small concentration of $(Ca)_3(PO_4)_2$ (~10–30 mgCa/*l*) also precipitated.

4.4 EVALUATION OF EXPERIMENTAL DATA

The results that were obtained during the experimental investigation required continuous review and evaluation to check their reliability and validity before further calculations were undertaken. This evaluation mainly involved performing material mass balance calculations over the AS and AD systems.

Materials mass balances calculations are a good way of checking the reliability and accuracy of experimental results. They are based on the principle that at steady state the flux of the material exiting the system must be equal to the flux entering the system. Therefore, mass balance checks on COD, N, P, Mg, K and Ca were determined immediately on completing a steady state test period. These test periods were defined by the seven sludge age periods of (AD 1) and the five sludge age periods (AD 2 - 5) at which the AD systems were operated at steady state. The AS systems sludge age remained constant at 10 days throughout the experimental period. Material mass balances were calculated over the PST (difference between raw and settled wastewater from which PS characteristics can be calculated) and the AS and AD systems. Materials mass balances within the range of 90% - 110% are indicative of accurate and reliable experimental measurements. In some cases, the mass balances within the range of 80% to 120% are also acceptable if the reasons for it can be determined. If the mass balances are outside this range, one or more of the measured parameters may be incorrect and then the results require careful interpretation. The mass balances reported below are the values obtained after

careful evaluation of the data and removal of visually outlying and inconsistent data, which would otherwise alter the level of accuracy in the results.

4.4.1 Mass Balances over the PST

The materials mass balance over the PST is simply based on the reasonable assumption that the materials in the raw wastewater entering the primary settling tank should equal the materials leaving the PST, in settled wastewater and primary sludge. Since primary settling is a physical process, with (usually) no biological reactions involved, it was straightforward to account for COD, N and P and all other parameters that were measured or calculated in the raw and settled wastewater. The COD mass balance calculation over the PST is given by Equation 4.4.2:

$$CODmassbal. = \left[\frac{\left(Sti_{PS} \cdot \left(Qi_{raw} - Qi_{settled}\right)\right) + \left(Sti_{settled} \cdot Qi_{settled}\right)}{Sti_{raw} \cdot Qi_{raw}} \right] \cdot 100 \quad (4.4.1)$$

This procedure can also be applied to all the other material properties like TKN and TP.

The average COD, N and P mass balances over the PST obtained in this investigation are listed in Table 4.4.2. In these mass balance calculations the dissolved material were also included in order to ensure that the settled wastewater does not have higher concentrations than the raw wastewater for all the measured parameters.

Table 4.4.1: Mass Balance over PST (%)

Test Period	1	2	3	4	5
COD	94.4	96.9	102.9	98.6	96.3
COD (filtered)	101.7	100.8	105.7	99.3	113.9
TKN	100.6	92.1	97.3	99.9	108.8
TKN (filtered)	99.8	100.3	99.6	102.6	103.4
FSA	100.3	101.7	99.7	103.6	105.2
TP	116.6	91.2	90.5	106.6	108.8
TP (filtered)	98.2	99.2	88.6	87.3	97.1
OP	97.1	99.6	84.2	85.8	99.1

Good material mass balances were generally obtained in all the five test periods, with the COD, N and P balances ranging between 94.4% to 102.9%, 92.1% to 108.8%

and 90.5% to 116.6% respectively. This indicates that all the influent data to the AS systems was accurately measured and acceptable for subsequent analysis.

4.4.2 Mass Balances over the AS Systems

The mass balance calculations over the AS systems are more complicated because of the various biological reactions taking place within these systems. Thus, the mass balance procedure is specific to each material, i.e. COD, N, P Mg, K and Ca.

4.4.2.1 MLE Systems Operated on Raw (MLE 2) and Settled (MLE 1) Wastewater

The mass balance procedures that account for the COD, N and P exiting the MLE systems are described in Appendix 1. In principle, the COD, N and P removed from the system, calculated by the difference between the measured influent and effluent, at steady state, should equal the COD, N and P taken up by the system, measured in waste sludge, oxygen utilized and nitrogen de-nitrified.

MLE 1 AS System

Table 4.4.2: MLE 1 AS System Mass Balances

Test Period	Nitrogen In	Nitrogen Out	N Balance	COD In	COD Out	COD Balance	P wasted	P removed	P Balance
	(mgN/d)	(mgN/d)	Per-cent	(mg/d)	(mg/d)	Per-cent	(mgP/d)	(mgP/d)	Per-cent
1	1538	1556	**101.1**	22640	22292	**98.5**	175	176	**100.5**
2	1609	1865	**115.9**	22452	23737	**105.7**	230	214	**92.9**
3	1631	1715	**105.2**	22977	21938	**95.5**	201	199	**98.7**
4	1583	1800	**113.7**	21818	22328	**102.3**	188	167	**89.1**
5	2310	2584	**111.9**	21509	20553	**95.6**	155	134	**86.7**

COD, N and P mass balances obtained over the MLE 1 AS system, within the experimental testing period, are listed in Table 4.4.2. The COD mass balance values are within a good range from 95.5 % to 105.7%, thus lending credibility to the experimental data.

The N balance values for this AS system are between 101.1% and 115.9%. As noted earlier, the N balance is very sensitive to the measured recycle ratios and nitrate

concentrations. A difference of 1 mgN/*l* nitrate concentration in the aerobic reactor or effluent and a small error in the measured recycle flow can make 5% difference to the % mass balance. Error of 1 mgN/*l* can occur because with the Auto Analyser, the samples are diluted 10 to 20 times which multiplies the error. However, errors in the N balance arising from the estimate of the nitrate de-nitrified in the anoxic reactor of the AS systems do not affect the N fed to the ADs via the waste sludge and so will not affect the N mass balances over the ADs.

The P balance range of between 86.7% and 100.5 is acceptable because the P concentration between the influent and effluent is relatively small 15.5mgP/*l* and 10.5mgP/*l*, with very little P removed from the system. A good P balance indicates that the P content of the WAS is accurately measured.

MLE 2 AS System

Table 4.4.3: MLE 2 AS System Mass Balances

Test Period	Nitrogen In (mgN/d)	Nitrogen Out (mgN/d)	N Balance Per-cent	COD In (mg/d)	COD Out (mg/d)	COD Balance Per-cent	P wasted (mgP/d)	P removed (mgP/d)	P Balance Per-cent
1	997	1017	**102.0**	20021	19732	**98.6**	201	187	**93.2**
2	1044	880	**84.3**	19665	19861	**101.0**	235	196	**83.4**
3	1060	997	**94.1**	19107	19179	**100.4**	208	220	**105.5**
4	990	891	**90.0**	17391	18113	**104.2**	193	204	**105.3**
5	1322	1284	**97.2**	17846	16753	**93.9**	159	172	**108.4**

Table 4.4.3 shows the materials mass balances obtained over the MLE 2 AS system over the five AD steady state test periods. The COD, N and P balances ranged between 93.9% to 104.2%, 84.3% to 102.9% and 93.2% to 108.4% respectively. Considering the reasons given above for the low N and P mass balances for the MLE 1 AS system, the mass balances for the MLE 2 AS system are also generally acceptable. As mentioned before, the primary purpose of the COD, N and P mass balances over the AS systems is to check the reliability of the COD/VSS, TKN/VSS and TP/VSS ratios of the particulate organics in the WAS fed to the ADs. In the experimental period 5, MLE 1 and MLE 2 had N balances of 113.7% and 90.0%. The

large (23.7%) difference in N balance could be due to the influent (PS and settled WW) TKN measurements, not capturing the actual difference between raw and settled wastewater influent TKN values. This will be considered when the data is used for calibrating the steady state AD model.

NDBEPR AS System

Table 4.4.4: NDBEPR AS System Mass Balances

Test Period	Nitrogen In	Nitrogen Out	N Balance	COD In	COD Out	COD Balance	P wasted	P removed	P Balance
	(mgN/d)	(mgN/d)	Percentage	(mg/d)	(mg/d)	Percentage	(mgP/d)	(mgP/d)	Percentage
1	6749	6850	**101.5**	118572	114104	**96.2**	5213	5426	**104.1**
2	6752	7746	**114.7**	124003	109662	**88.4**	5255	5392	**102.6**
3	6930	8332	**120.2**	119173	115505	**96.9**	4777	5112	**107.0**
4	7854	7389	**94.1**	112706	106503	**94.5**	5635	5025	**89.2**
5	9361	7607	**81.3**	114474	118887	**103.9**	4939	5215	**105.6**

Table 4.4.4 shows the materials mass balances obtained over the NDBEPR AS system over the five steady state test periods. Good mass balances were obtained in all test periods, apart from one period where the COD balance was somewhat lower, i.e. 88.4%. Historically, in the Water Research Group (WRG) at UCT, COD mass balances over NDBEPR AS systems have been lower (80 - 90%) than over N removal AS systems, (90 – 100%). Therefore, in this investigation to achieve COD balances for the NDBEPR system between 90 to 100% is very good compared with many NDBEPR systems operated in the past (Ekama and Wentzel 1999). For the NDBEPR system of this investigation it was particularly important to achieve good mass balances so that accurate COD/VSS (f_{cv}), OrgN/VSS (f_n) and the OrgP/VSS (f_P) ratios of the particulate WAS organics could be established because these ratios are used to calculate the elemental composition (X, Y, Z, A and B in $C_XH_YO_ZN_AP_B$) of the organics fed to the ADs. The low COD balances for test period 2 may be due to error in OUR values, since the OUR calculation requires the ratio of the VSS concentration in the re-aeration and aerobic reactors which is subject to variability in the MLSS/VSS test. However, the TKN and TP values are within reasonable range.

4.4.3 Mass Balances over the AD Systems

In AD systems, the anaerobic biomass has a very low yield so only a very small portion of the feed COD is converted to new organism mass. Most of the biodegradable organics (> 95%) are converted to methane gas, which is insoluble and so escapes as gas. Therefore, for the COD mass balances over methanogenic systems to be accurate, the difference between the influent and effluent COD should equal the COD 'lost' as methane gas. The N, P, Mg, K and Ca, which are bound or stored in the biodegradable organics, are released as the digestion progresses. Therefore, for 100% N, P, Mg, K and Ca mass balances the total unfiltered TKN, TP, Mg, K and Ca in the influent sludge to the AD should equal the effluent total unfiltered TKN, TP, Mg, K and Ca respectively, the only difference being a change in the dissolved fractions of these elements. The mass balances obtained in the various AD systems are presented in Table 4.4.5 below.

Table 4.4.5: Percentage Mass Balances Over AD Systems								
AD Sludge Age (R_s)		**10**	**12**	**18**	**20**	**25**	**40**	**60**
AS Sewage Batch		21	21	14	21	16	19	17
Test Period		5	5	1	5	2	4	3
AD 1 (Fed NDBEPR WAS)	COD balance (%)	99.7	100.6	98.9	103.8	99.6	97.1	92.5
	Nitrogen balance (%)	108.3	107.8	98.4	106.4	100.0	104.5	87.9
	Phosphorous balance (%)	105.3	104.6	100.0	104.0	86.5	105.8	92.6
	Magnesium balance (%)	95.5	107.0	102.0	115.9	103.3	80.4	98.2
	Potassium balance (%)	76.9	98.0	79.9	93.3	90.5	84.1	100.7
	Calcium balance (%)	84.5	85.6	79.9	84.5	68.0	49.4	86.3
AD 2 (Fed PS)	COD balance (%)	101.8		104.6		107.6	98.5	98.9
	Nitrogen balance (%)	93.0		102.6		81.6	99.7	101.9
	Phosphorous balance (%)	97.3		100.8		106.5	102.9	88.7
AD 3 (Fed MLE 1 WAS)	COD balance (%)	91.3		92.2		95.9	94.9	92.7
	Nitrogen balance (%)	100.7		91.5		103.5	85.0	86.2
	Phosphorous balance (%)	95.5		102.1		100.2	104.7	93.5
AD 4 (Fed PS - MLE 1 WAS)	COD balance (%)	108.3		102.5		88.8	91.2	85.6
	Nitrogen balance (%)	96.8		85.8		80.9	81.3	88.8
	Phosphorous balance (%)	107.0		101.6		97.0	86.4	85.3
AD 5 (Fed MLE 2 WAS)	COD balance (%)	103.7		97.6		101.4	108.0	106.2
	Nitrogen balance (%)	95.5		100.0		108.7	89.3	85.5
	Phosphorous balance (%)	108.4		118.4		109.2	101.3	92.2

Of the 75 COD, TKN and TP mass balances in Table 4.4, 39 are between 95 - 105%, 24 between 90 – 95% and 105 – 110%, 13 between 85 – 90% and 110 – 115% and four between 80 – 85% and 115 – 120%. Therefore, above 80% of the COD, TKN and TP mass balances are between 90 and 110%, which is deemed sufficiently accurate to meet the objectives of the research. The Mg mass balances are very good with four of the five test periods between 95 – 116%, with that of test period 4 being low at 80% Mg recovery. The K balances, ranging between 76 to 101%, are lower than the Mg mass balances. For some unidentified reason the Ca balances are very low ranging between 49% and 86%. This is not a serious concern because the calcium data are not

required – as noted above, calcium phosphate precipitation was very small (10 to 30 mgCa/*l*). The Mg and K results are sufficiently accurate for the purposes of this project, i.e. the K to validate that the entire PAO PP was hydrolysed and the Mg to quantify struvite precipitation that took place in the AD treating NDBEPR WAS. Taken overall, the mass balances over the five AD systems, obtained over the seven test periods as shown in Table 4.4.5 above, are generally within satisfactory ranges, indicating that the data, with the exceptions noted above, are acceptable for use in this investigation.

4.5 CLOSURE

In this chapter, the results that were obtained from data collected during the experimental research period of the project are reported. A timeline for this experimental research period showing when the operated AS and AD systems of the experimental set up were tested is presented (see Tables 4.1a and 4.1, with a key for these tables given in Table 4.1c). The day-to-day data collected from the tests performed on the experimental set-up are provided in Appendices 7 and 8 as indicated in the timeline Table 4.1b.

An assessment of how the Activated Sludge (AS) systems performed, in terms of the COD removal, nitrogen (N) and phosphorus (P) removal, sludge production and oxygen consumed, is presented. It was confirmed from the very low filtered effluent COD concentration of the three AS systems, that their 10-day operational sludge age at steady state was adequate for the acclimatized active mass to satisfactorily remove all the biodegradable organics. Also, the high removals of TKN (above 88%) and low filtered effluent TKN values, in the AS systems, indicated that nearly complete nitrification occurred in these systems during the test period. However, it was important to note that the BEPR process of the NDBEPR system was not restrained by the nitrate (nitrate is significantly less efficient than oxygen for phosphorus uptake by PAOs, see Section 2.3.2.3). The two MLE systems did not denitrify as well as the NDBEPR system, but this was not considered to have major implications, with

regards to the achievement of their major project objective, which was to ensure that no BEPR occurred in these MLE systems, such that the biodegradability of their WAS (containing no PAOs) can be compared with that of the NDBEPR system (containing both OHOs and PAOs). The low P removals in these MLE 1 and MLE 2 systems confirm that this objective was met and the phosphorus fed to the MLE systems was utilized for OHO biomass growth only. Also, the very high P removal observed in the NDBEPR system indicated PP was formed and accumulated by PAO biomass that grew this system. A further confirmation of this occurrence was shown by the high difference in concentration of the influent and effluent metalic ions (Mg, K and Ca), which was brought about by their usage in the formation of PP, as was also notable from their high concentrations in the sludge from the aerobic reactor (where PP storage by PAOs normally occurs in NDBEPR systems). In the AS systems, which were all operated at the 10-day R_s, it was observed that TSS and VSS concentrations were fairly stable throughout the experimental period, indicating the maintenance of steady state conditions.

The AD systems results from the steady state periods of the various sludge ages at which they were operated are presented. An assessment of the AD systems results was performed in terms of the obtained COD removals, FSA releases, ortho-phosphate (OP) releases, pH, VFA content, H_2CO_3* alkalinity, gas production and gas composition. There was a notable trend of the percentage COD removal increasing with increase in sludge age, which was expected in these systems since the increased sludge age meant increased time made available for the AD biomass to degrade the feed sludge. The FSA release followed a similar increasing trend due to the release of organically bound N with the degradation of organics. It was expected for the OP release to also follow a similar trend, but this only occurred with the ADs that were not fed P-rich sludge (i.e. ADs 2, 3, 4 and 5). In the AD 1, which was fed NDBEPR WAS, containing PAOs and their stored PP, the P release was observed to remain within the ranges of 45% to 62%, even at the low 10 day R_s, regardless of the increasing trend of COD removal with R_s. From these observations, it was apparent

that the PP (which contain significantly higher P content than that of organically bound P) is released much faster than the P that is organically bound in the OHO and PAO biomass (which, from the observing the P release of the other AD systems followed a similar trend to COD removal with sludge age). The observation of rapid PP release and hydrolysis in AD is validated further by the very high filtered effluent K concentration (close to the influent unfiltered value) at low sludge ages (by 10d R_s). However, with this observation, a filtered effluent Mg concentration that is close to the unfiltered influent Mg concentration was also expected (since they both form part of the released PP) but was not observed. This confirmed that precipitation took place in AD 1 (which was fed NDBEPR WAS).

The low VFA concentration and reasonably stable pH (which was maintained above 6.5, as recommended by McCarty 1974 for stable AD operation) indicated that methanogenesis was functional and the AD systems were stable at all times.

The results that were obtained during the experimental investigation required continuous review and evaluation to check their reliability and validity before further calculations were undertaken. This evaluation mainly involved performing material mass balance calculations over the 'virtual' PST (see Section 3.1), AS and AD systems.

Good material mass balances over the PST AS and AD systems were generally obtained in all the five test periods. However, for some unidentified reason the Ca balances in the AD were very low ranging between 49% and 86%. This was not a serious concern because the calcium data are not required – as noted above, since calium content in PP was usually low and deemed to have very low (of any) precipitation in this system. The Mg and K results are sufficiently accurate for the purposes of this project, i.e. the K to validate that the entire PAO PP was hydrolysed and the Mg to quantify that struvite precipitation took place in the AD treating NDBEPR WAS.

The results obtained in the experimental investigation have been shown to be sufficiently reliable to meet the research objectives, which is to provide data for (1)

the development of a steady state model for the AD of PS, ND and NDBEPR WAS in extending the plant-wide model to include P, (2) determination of the hydrolysis kinetic rates of the PS and WAS from the three AS systems and the PS-WAS blend and (3) experimental determination of whether or not the unbiodegradable particulate organics (UPO) from the influent wastewater and the unbiodegradable endogenous residue produced by the OHO and PAO biomass in the AS system, remain unbiodegradable in the anaerobic digester. This investigation into biodegradability of organics will require using the data from the AS systems to characterize the WAS into biodegradable and unbiodegradable organics (as reported on in the following Chapter 5) and using the results from the five AD systems to determine the unbiodegradable fraction of the particulate organics (UPO) and the hydrolysis kinetic rate of the biodegradable particulate organics (BPO) in the AD (which is described in Chapter Six). If the same unbiodegradable fraction is obtained from the AS and AD systems, this would validate that unbiodegradable organics, as defined by the (aerobic) AS system remain unbiodegradable in the (anaerobic) AD system.

CHAPTER 5: CHARACTERISATION OF INFLUENT SEWAGE AND WASTE SLUDGE

5.1 INTRODUCTION

This chapter focuses on determining the characteristics of the influent raw and settled wastewaters and the waste activated sludge (WAS) products generated from feeding them into the AS systems. In the project's experimental investigation these WAS products and the primary sludge (PS), which was added to the settled wastewater (WW) to make up the raw WW, were fed to the five anaerobic digesters (ADs). From the performance of the ADs, the characteristics of the PS and WAS could be determined and compared with those obtained from the activated sludge (AS) systems. Also considered is the biodegradability, under anaerobic conditions, of raw wastewater organic material that settles out as primary sludge and whether this biodegradability correlates with the biodegradability that is determined from the AS systems through mass balances over the primary settling tank (PST). Therefore, this chapter considers whether the unbiodegradable material from the influent wastewater and the endogenous residue generated in the AS reactors remain unbiodegradable, throughout the wastewater treatment plant (WWTP). The determination of the biodegradability of the PS and WAS in AD is required for the calibration of the AD hydrolysis kinetic model from which the hydrolysis kinetic rates of the PS and the WAS are obtained, which is also an important objective of this investigation.

5.2 BIODEGRADABILITY OF INFLUENT WASTEWATER ORGANICS

In this section of the chapter, the unbiodegradable particulate fraction ($f_{S'up}$) of the influent raw and settled wastewaters is determined. From these the unbiodegradable particulate fraction of primary sludge ($f_{PS'up}$) is calculated from mass balances over the primary settling tank (PST). This calculated value of $f_{PS'up}$ from the AS system is

then compared with the fraction of unbiodegradable material obtained through the anaerobic digestion of the same primary sludge at a long sludge age (R_s) of 60 days.

5.2.1 The Determination of the $f_{S'up}$ Value for the Nitrification-denitrification (ND) Systems

The mass of volatile settleable solids (VSS) in the reactor (MX_v), flux of oxygen consumed (FO_c) and flux of total COD (FS_{ti}) are experimentally measurable parameters. Moreover, the unbiodegradable soluble influent COD concentration and fraction ($f_{S'us}$ = S_{usi}/S_{ti}) can be measured as the filtered effluent soluble COD concentration (S_{usi} = S_{tse}) of the AS process, provided the reactor sludge age is above three days (Marais and Ekama, 1976). The unbiodegradable particulate COD fraction ($f_{S'up}$) is determined by finding the $f_{S'up}$ value at which the calculated mass of VSS (MX_v, gVSS), or flux of oxygen utilized (gO/d), corrected for nitrification and denitrification (FO_c, see Section 3.3.7 of Chapter 3) in the AS system match those measured. If the system COD balance is 100%, the same $f_{S'up}$ value will be obtained from the measured VSS mass and flux of oxygen utilized. Therefore, the influent unbiodegradable particulate fraction ($f_{S'up}$) can be determined by making it the subject of Equations 2.3.5 and 2.3.9 (in Chapter 2), which are used to calculate MX_v from the measured influent COD flux (FS_{ti}) and sludge age (R_s), i.e.:

$$f_{S'up} = \frac{\frac{MX_v}{FS_{ti}} - \left[(1 - f_{S'us}) \cdot \left(\frac{Y_H \cdot R_s}{1 + (b_H \cdot R_s)} \cdot (1 + f_{EH} \cdot b_H \cdot R_s) \right) \right]}{\left[\frac{R_S}{f_{cv}} - \left(\frac{Y_H \cdot R_s}{1 + (b_H \cdot R_s)} \cdot (1 + f_{EH} \cdot b_H \cdot R_s) \right) \right]} \quad (5.2.1)$$

for the MLE systems, which includes ordinary heterotrophic organisms (OHOs) only and

$$f_{S'up} = \frac{\frac{MX_v}{FS_{ti}} - \left(\left(1 - f_{S'us} - \frac{S'_{bsi}}{S_{ti}}\right).\left(\frac{Y_H \cdot R_s}{1+(b_H \cdot R_s)} \cdot (1 + f_{EH} \cdot b_H \cdot R_s)\right)\right) - \left(\frac{S'_{bsi}}{S_{ti}}\right).\left(\frac{Y_G \cdot R_s}{1+(b_G \cdot R_s)} \cdot (1 + f_{EG} \cdot b_G \cdot R_s)\right)}{\left(\frac{R_s}{f_{cv}} - \left(\frac{Y_H \cdot R_s}{1+(b_H \cdot R_s)} \cdot (1 + f_{EH} \cdot b_H \cdot R_s)\right)\right)} \quad (5.2.2)$$

for the NDBEPR system. This includes both OHOs and phosphorus accumulating organisms (PAOs).

In terms of the flux of oxygen employed for COD utilization (FO_c), the rearranged Equations 2.3.6 and 2.3.8 (in Chapter 2) are:

$$f_{S'up_{FOC}} = 1 - \left\{ \frac{FO_C}{FS_{ti}.\left\{\left(1-(f_{cv}.Y_H)\right) + \left(f_{cv}.(1-f_{EH}).b_H.\frac{Y_H.R_s}{(1+b_H.R_s)}\right)\right\}} \right\} - \frac{S_{use}}{S_{ti}} \quad (5.2.3)$$

for the MLE systems (includes OHOs only) and

$$f_{S'up_{FOC}} = 1 - \left\{ \frac{\left\lfloor \left(\frac{FO_C}{Qi}\right) + (S'_{bsi} \cdot f_{cv}) \cdot \left(\left((1-f_{EH}) \cdot b_H \cdot \frac{Y_H \cdot R_s}{(1+b_H.R_s)}\right) - \left((1-f_{EH}) \cdot b_G \cdot \frac{Y_G \cdot R_s}{(1+b_G.R_s)}\right)\right) \right\rfloor}{FS_{ti}.\left\{\left(1-(f_{cv}.Y_H)\right) + \left(f_{cv} \cdot (1-f_{EH}).b_H.\frac{Y_H \cdot R_s}{(1+b_H.R_s)}\right)\right\}} \right\} - \frac{S_{use}}{S_{ti}} \quad (5.2.4)$$

for the NDBEPR system (includes both OHOs and PAOs), where S'_{bsi} is the readily biodegradable COD obtained by the PAOs for their growth.

5.2.2 Primary Sludge Unbiodegradable Particulate Material

Primary sludge (PS) is the settleable part of the raw influent wastewater captured by the primary settling tank (PST). It is usually concentrated by gravity thickening after the PST before feeding into the AD. The mass of a material component in the

primary sludge is obtained by performing materials mass balance over the PST, i.e. by subtracting the flux of the material measured in the settled wastewater from that in the raw wastewater. This mass balance assumes that there is no biological activity in the PST and gravity thickener and no accumulation in the PS.

With $f_{S'up}$ known for the raw and settled wastewaters, the unbiodegradable particulate COD concentrations in each can be calculated. The difference between these two concentrations must then be the unbiodegradable particulate COD concentration in the 400mgCOD/*l* PS (see Section 3.2.2.1) added to the settled WW to make the raw WW. Hence the unbiodegradable particulate COD fraction of the primary sludge ($f_{PS'up}$) is:

$$f_{PS'up} = \frac{f_{S'up_{raw}} \cdot S_{ti_{raw}} - f_{S'up_{set}} \cdot S_{ti_{set}}}{S_{ti_{PS}}} \qquad (5.2.5)$$

Where: $f_{S'up\_raw}$ and $f_{S'up\_set}$ represent the raw and settled influent $f_{S'up}$ respectively.

In the Equation 5.2.5, the underflow in the 'virtual' PST is zero, which is correct for this project because the PS was added to the settled WW to make up raw WW. However, this equation is not correct for a real PST with an underflow.

The AD, at long sludge ages (60 days and above), should be able to completely remove all the biodegradable organics of the PS providing a remnant of only AD biomass (which is very small), unbiodegradable particulate and soluble organics in the effluent. Therefore, it is possible to determine the unbiodegradable particulate organic fraction of the PS in the AD and compare this with that obtained from the AS systems.

Table 5.2.1 below lists the unbiodegradable particulate fraction ($f_{S'up}$) values for the raw and settled wastewater from the MLE systems (Equation 5.2.1) and the resulting $f_{PS'up}$ values for PS obtained from Equation 5.2.5, together with the $f_{S'up}$ values of the NDBEPR system (Equation 5.2.2), as obtained in this research programme. In these calculations, the $f_{S'up}$ was determined with both MX_v and FO_c equations. However,

more confidence was placed in the $f_{S'up}$ values determined using MX_v (Equations 5.2.1 and 5.2.2) because MX_v is less sensitive to day-to-day variability in influent COD flux (FS_{ti}).

Table 5.2.1: Influent Unbiodegradable Particulate($f_{S'up}$) and Soluble ($f_{S'us}$) fractions for Operated AS systems

	PS	Raw WW		Settled WW to MLE 1		Settled WW to NDBEPR		
Test Period	$f_{S'up}$[1]	$f_{S'up}$[1]	$f_{S'us}$	$f_{S'up}$[1]	$f_{S'us}$	$f_{S'up}$[2]	$f_{S'us}$[2]	S_{bsi}/S_{ti}[2]
1	0.28	0.15	0.04	0.04	0.05	0.18	0.04	0.37
2	0.28	0.16	0.04	0.06	0.05	0.19	0.04	0.33
3	0.34	0.15	0.04	0.02	0.04	0.16	0.02	0.30
4	0.33	0.17	0.06	0.07	0.09	0.19	0.05	0.38
5	0.25	0.13	0.04	0.05	0.05	0.17	0.05	0.32
Average	0.30	0.15	0.04	0.05	0.06	0.18	0.04	0.34
[1]Based on Equation 5.2.1 for MX_v								
[2]S_{ti} includes 200mgCOD/*l* acetate dosed to settled WW								

From Table 5.2.1 the average $f_{S'up}$ obtained for the raw and settled wastewater were 0.15 and 0.05.

The $f_{S'up}$ of municipal wastewater organics (COD) usually ranges between 0.12 to 0.15 for raw WW and 0.03 to 0.05 for settled WW (WRC, 1984). Table 5.2.2 below shows a very good comparison of the $f_{S'up}$ values obtained in the past using Mitchells Plain raw WW fed fully aerobic ND systems.

Table 5.2.2: Comparison of Mitchell's Plain Sewage $f_{S'up}$ from Literature on ND Systems			
Literature Source	Highest $f_{S'up}$ [1]	Lowest $f_{S'up}$ [1]	Average $f_{S'up}$
Ikumi *et al.* (2011)	0.07	0.02	0.05
Ubisi *et al. (1997)*	0.167	0.059	0.1165
Warbuton *et al.* (1991) - 1	0.182	0.001	0.0912
Warbuton *et al.* (1991) - 2	0.224	0.095	0.162
[1]Of the sewage batch in the investigation.			

As reported by Ekama and Wentzel (1999), most investigations in the UCT laboratory used Mitchells Plain raw WW for the experimental operation of ND and NDBEPR AS systems. The variation in the above $f_{S'up}$ values (Table 5.2.2) could mainly be due to the differences in time and location at which the feed was sourced from the plant.

The values obtained from the MLE systems, presented in Table 5.2.2 above, are within reasonable range of these values; therefore, they can confidently be used in calculating further characteristics of influent organics. However, the unbiodegradable particulate fraction of settled influent wastewater calculated in the NDBEPR system is higher (0.18) than that of MLE 1, fed the same settled wastewater. This shows that, compared with the MLE 1 system, the NDBEPR system "displays" a higher flux of influent unbiodegradable particulates than the MLE system fed the same wastewater. Ramphao *et al.* (2004) also reported having an increased value for the $f_{S'up}$ determined from the membrane bioreactor UCT system ($f_{S'up}$ = 0.224) as compared with a conventional UCT system ($f_{S'up}$ = 0.067) treating the same wastewater.

Table 5.2.3a: Comparison of $f_{S'up}$ Values Calculated from NDBEPR Systems (Ekama and Wentzel 1999)				
	Unbiodegradable particulate fraction ($f_{S'up}$)			
Literature Source	**Mean**	**Std. Deviation**	**Max**	**Min**
Clayton *et al.* (1989)	0.15	-	-	-
Musvoto *et al.* (1992)	0.287	0.056	0.371	0.163
	0.317	0.074	0.456	0.23
Pilson *et al.* (1995)	0.111	0.017	0.026	0.01
	0.153	0.014	0.026	0.02
Sneyders *et al.* (1997)	0.062	0.023	0.107	0.023
	0.04	0.055	0.132	-0.042
Mellin *et al.* (1997)	0.14	0.06	0.25	0.03
	0.18	0.05	0.24	0.09
	0.12	0.03	0.17	0.08
[1] The 582 days of HUCT30 was divided into 3 parts, i.e. I: day 1 - 237; II: 238 - 468; III 469 - 582.				

5.2.3b: Objectives, Scope and Distinctives of the 5 Investigations from Table 5.2.3a					
Literature Source	Clayton *et al.* (1989)	Musvoto *et al.* (1992)	Pilson *et al.* (1995)	Sneyders *et al.* (1997)	Mellin *et al.* (1997)
Objectives	Delineate NDBEPR kinetics and determine whether or not PAOs contribute to denitrification	Establish the role of nitrate/nitrite concentration entering aerobic zone in AA (low F/M) filament bulking	Determine temperature sensitivity of denitrification kinetics and BEPR at 12 and 20°C	Examine effect of unstabilized landfill leachate addition on BEPR and ND	Determine temperature sensitivity of denitrification kinetics and BEPR at 20°C and 30°C
Scope of Investigat-ion	29 plug flow anoxic reactor NO_3, NO_2, PO_4 soluble COD profiles on 1st anoxic reactor - 12MUCT, 17UCT. 19 denitrification batch tests - 8 on anaerobic reactor sludge, 6 on aerobic sludge and 5 on anoxic. Several different batch tests with PHB measurement to determine activity of PAOs	10 anoxic batch tests on MMUCT 1 blended 1st anoxic and aerobic reactor sludge - 7 with nitrate and 3 with nitrite dose. 8 anoxic batch tests on MMUCT2 blended 1st anoxic and aerobic reactor sludge - 4 with nitrate and 4 with nitrite addition	34 anoxic batch tests at each temperature - 27 with nitrate dose, 3 with nitrate and nitrite dose, 1 with initial nitrate and after 100min a nitrite dose, 1 with initial nitrite dose and after 100min a nitrate dose and 2 on sludges from one temperature and tested at the other temperature with nitrate dose	On each system: 3 anaerobic, 6 anoxic and 5 aerobic batch tests. 17.7% of influent COD to MSUCTEX was leachate - 147 out of 830mgCOD/*l*. Added 5, 10, 15 mgP/*l* extra P to influent of both systems on days 80, 104, 446, to ensure > 5mgP/*l* in effluent	Batch tests: On UCT systems at 30°C and 20°C; 13 and 4 aerobic nitrification and P uptake, 21 and 10 denitrification and P uptake, 33 and 8 anaerobic P release , 12 and 3, 11 and 3 and 10 and 2 with sewage, acetate and excess acetate respectively
Investigat-ion distinctives	CMUCT day 1 - 198; CUCT day 199 - 311; PF 1st anoxic day 1-311; CSTR 1st anoxic day 312 - 570	MMUCT1: Dosed nitrate to 2nd anoxic from day 129 - 239. MMUCT2: Dosed nitrite to 2nd anoxic from day 291 - 340	PMUCT12 at 12°C; PMUCT20 at 20°C	Dosed leachate to MSUCTEX from day 37 - 495	Operated 30°C UCT from day 1 to 582; MSUCTCL was 20°C UCT system day 280 - 582

The unbiodegradable fraction of influent PS as calculated from the MLE systems, i.e. using mass balances over the PST as shown in Equation 5.2.5, gave an average value of 0.30. This result will be compared with the value obtained from the AD of PS over long (60 days) sludge age (see Section 6.2.2 - 1 of Chapter 6) and it will also be investigated whether or not the unbiodegradability of the influent UPO is consistent throughout the WWTP, i.e. the material that is unbiodegradable in the fully aerobic or ND AS systems remains unbiodegradable in the AD systems. This aspect will also be checked for the NDBEPR WAS to determine whether or not the higher $f_{S'up}$ observed in this system is real – i.e. remains unbiodegradable in the AD – or whether or not this is a consequence error in the NDBEPR model, in that it produces less sludge (MX_i) theoretically than experimentally, which is compensated for by a higher $f_{S'up}$ (see Section 6.2.2 - 4).

5.3 BIODEGRADABILITY OF ACTIVATED SLUDGE ORGANICS

The determination of the $f_{S'up}$ values from Equations 5.2.1 and 5.2.2 also fractionate the measured VSS into OHO biomass (which is denoted as X_{BH}, in mgOHOVSS/*l*), OHO endogenous residue (X_{EH}, in mgERVSS/*l*) and unbiodegradable particulate organics from the influent (X_i, in mgUPOVSS/*l*) for the MLE systems and additionally PAO biomass (X_{BG}, in mgPAOVSS/*l*) and PAO endogenous residue (X_{EG}, in mgERVSS/*l*) for the NDBEPR system. To determine the unbiodegradable fraction of the WAS from the AS model, it is assumed that the only biodegradable organics in the WAS is the biodegradable part of the OHO and PAO biomass. During AD of WAS a fraction of this OHO and PAO biomass (the unbiodegradable f'_{EH} and f'_{EG} respectively) does not get degraded and remains as the endogenous residue that would have formed in the AS system. So the unbiodegradable part of the OHO and PAO biomass adds to the WAS unbiodegradable organics after complete digestion of the WAS. For this reason, the total unbiodegradable fraction of the VSS can be calculated as the biomass OHO and PAO unbiodegradable fraction (f'_{EH} and f'_{EG}), the OHO and PAO endogenous residue (f_{EH} and f_{EG}) and the enmeshed unbiodegradable

particulate organics (X_i/VSS) from the influent. However, here an interesting question arises - what is the unbiodegradable fraction of the OHOs (f'_{EH}) and PAOs (f'_{EG}) insofar as the AD is concerned? In the AS system for the OHOs, f_{EH} = 0.20 for the endogenous respiration model but f'_{EH} = 0.08 for the death regeneration model (Dold *et al.*, 1980) of organism loss. This f'_{EH} of 0.08 was accepted to be used for the AD of OHOs, as previously validated by Ekama *et al.* (2006) using the AD of WAS from a single MLE AS system. The PAOs 'loss' is only modelled with the endogenous respiration approach primarily because it is simpler and avoids the complex questions of what happens to the storage compounds (poly-3-hydoxyalkanoates, PHA and polyphosphate, PP) and how these compounds would be regenerated without an anaerobic phosphorus (P) release and volatile fatty acid (VFA) uptake phase? The f_{EG} of the PAOs in terms of the endogenous approach is 0.25 in steady state (Wentzel *et al.*, 1990) and dynamic models (ASM2, Henze *et al.*, 1995; UCTPHO, Wentzel *et al.*, 1992). For the purposes of determining the unbiodegradable fraction of the PAOs (f'_{EG}), 0.08 was also accepted, but accuracy of this value will be checked in this investigation by comparing the unbiodegradable fraction of the WAS obtained from the AS system and AD system.

In summary, the concentration of unbiodegradable COD in WAS ($S_{up\ WAS}$) can be calculated as:

$$S_{up_{WAS}} = \left(X_I + X_{EH} + X_{EG} + \left(f'_{EH} \cdot X_{BH} + f'_{EG} \cdot X_{BG}\right)\right) \cdot f_{cv} \qquad (5.3.1a)$$

This is extended as:

$$S_{up_{WAS}} = \frac{F_{sti} \cdot f_{S'upi} \cdot R_s}{V_{AS}} + \left(\left(X_{BH} \cdot f_{EH}.b_H.R_s\right) + \left(X_{BG} \cdot f_{EG}.b_G.R_s\right) + \left(f'_{EH} \cdot X_{BH} + f'_{EG} \cdot X_{BG}\right)\right) \cdot f_{cv} \qquad (5.3.1b)$$

Where X_{BH} and X_{BG} are the concentrations of OHO and PAO biomass respectively. With the influent readily biodegradable COD (S_{bsi}) known from measurement (and acetate addition) and unbiodegradable soluble influent COD ($f_{S'us}$) and $f_{S'up}$

determined as shown in Section 5.2.1 above, X_{BH} and X_{BG} can be calculated using Equations 5.3.1c and d below:

$$X_{BG} = \frac{\left(\frac{Y_G \cdot Q_i \cdot S'_{bPAO} \cdot R_s}{1 + (R_s \cdot b_G)} \right)}{V_{AS}} \quad (5.3.1c)$$

$$X_{BH} = \frac{\left\{ \frac{Y_H \cdot Q_i \cdot \left[\left(S_{ti} \cdot \left(1 - f_{S'us} - f_{S'up} \right) \right) - S_{bPAO} \right] \cdot R_s}{1 + (R_s \cdot b_H)} \right\}}{V_{AS}} \quad (5.3.1d)$$

Where

- S_{bPAO} is the influent biodegradable COD obtained by the PAOs and
- V_{AS} is the equivalent volume of the AS systems at the aerobic reactor VSS concentration at which the WAS is harvested from the systems.

The unbiodegradable fraction of the WAS from MLE 2, MLE 1 and NDBEPR AS systems, as calculated from the above Equation 5.3.1a, with the $f'_{EG} = f'_{EH}$ value of 0.08, are listed in Table 5.3.1 below. It must be remembered that these WAS unbiodegradable fractions are associated with, and a consequence of, the wastewater unbiodegradable particulate COD fraction determination, with the ND and NDBEPR models based on the measured experimental data in the three activated sludge systems.

Table 5.3.1: WAS Unbiodegradable Particulate Fraction ($f_{S'upWAS}$)

Test Period	MLE 2 to AD 5	MLE 1 to AD 3	NDBEPR to AD 1
1	0.61	0.46	0.52
2	0.63	0.50	0.55
3	0.62	0.42	0.53
4	0.64	0.51	0.53
5	0.60	0.47	0.53
Average	0.62	0.47	0.53

From Table 5.3.1 above, the average unbiodegradable fraction of WAS from MLE 1, MLE 2 and the NDBEPR systems are 0.47, 0.62 and 0.53 respectively. These values are quite close to the unbiodegradable (effluent) COD fractions obtained from the 60d sludge age ADs fed these WAS (0.53, 0.66 and 0.58 for MLE 1, MLE 2 and NDBEPR WAS respectively). Therefore, it can be concluded with reasonable certainty that the unbiodegradable material is conserved through the WWTP because the organics that are unbiodegradable in the WAS are not degraded further in the AD system. Interestingly, this also applies to the NDBEPR WAS, even though the influent unbiodegradable particulate organics fraction ($f_{S'up}$) was found to be significantly higher than that of MLE 1 fed the same wastewater.

If UPO is really a WW characteristic then AS systems fed the same WW are expected to yield the same influent $f_{S'up}$ value. This is true for fully aerobic and ND systems as a group and NDBEPR systems as a group, but not for ND and NDBEPR systems – the $f_{S'up}$ for NDBEPR systems have always been found to be considerably higher than for ND systems (Ekama and Wentzel, 1999). Therefore, the question that has been asked for many years is whether this difference is real (which is not expected if $f_{S'up}$ is really a wastewater characteristic) or if there is a factor that is unaccounted for in the NDBEPR model. The surprising outcome from the AD fed the NDBEPR WAS is that it reflects a similar unbiodegradable fraction as estimated by the NDBEPR model. This indicates that the much higher unbiodegradable particulates found for the NDBEPR system than for the MLE 1 system (see Table 5.2.1), fed the same WW, are registering in the AD system also as unbiodegradable. Furthermore, this suggests that the higher UPO in the NDBEPR WAS is real and not an artifice of the NDBEPR AS model with respect to the ND AS model.

There may be two possible causes for this phenomenon: (1) mistaken assumptions could have been made when allocating to the PAOs the same death regeneration unbiodegradable fraction (f_{EG} = 0.08) as for OHOs and/or the PAOs may have sequestered more of the influent biodegradable organics than the assumed RBCOD only and (2) the high influent $f_{S'up}$ in the MBR UCT system may be a result of more

unbiodegradable particulate organics (UPO) being enmeshed in the aerobic reactor (which has a higher sludge concentration and from which the waste sludge fed to the AD is taken) than the other reactors.

To explore the validity of cause (1) above, the determination of f'_{EG} could be done experimentally by digesting pure cultures of PAOs at a long AD sludge age. The f'_{EG} is a part of the NDBEPR WAS unbiodegradable fraction, as shown in the Equation 5.3.1a above, which is generated by death regeneration in AD. If the lower influent unbiodegradable particulate fraction that was measured in the MLE system fed the same wastewater ($f_{S'up}$ = 0.05) is accurate, then the resultant, 'true' X_i (see Equation 5.5.3 and 5.3.1a) is expected to be lower. This is only true with the assumption that the quantities of UPO enmeshed in individual reactors are proportional to their relative VSS concentrations. Moreover, with the validated f'_{EH} value and all known kinetic and stoichiometric constants applied in determination of X_{EG} and X_{EH} (both in mgERVSS/*l*, as measured by Wentzel *et al.*, 1990) deemed accurate, only the f'_{EG} could be increased to ensure that the unbiodegradable fraction of WAS as calculated in Equation 5.3.1a remains as measured in the AD, despite the lower 'true' estimate of the X_i value. Making f'_{EG} the subject of Equation 5.3.1a gives us:

$$f'_{EG} = \frac{S_{up_{WAS}} - \left\{ \frac{MS_{upi} \cdot R_s}{V_{AS}} + \left(\left(X_{BH} \cdot f_{EH} . b_H . R_s \right) + \left(X_{BG} \cdot f_{EG} . b_G . R_s \right) + \left(f'_{EH} \cdot X_{BH} \right) \right) \cdot f_{cv} \right\}}{f_{cv} \cdot X_{BG}} \tag{6.24}$$

Further, making S'_{bsi} (the concentration of influent COD allocated to growth of PAOs in the NDBEPR system) the subject of Equation 2.3.9 (in Chapter 2) which is used to calculate MX_v from the measured influent COD flux (FS_{ti}) and sludge age (R_s) gives:

$$S'_{bsi} = \left(\frac{\frac{MX_v}{MS_{ti}} - \left\{ \left\lfloor \left(1 - f_{up} - f_{us}\right) . \left(\frac{(1 + f_{EH} . b_H . R_s) \cdot Y_H . R_s}{(1 + b_H . R_{s)}} \right) \right\rfloor + \left[\frac{f_{up} . R_s}{f_{cv}} \right] \right\}}{\left(\frac{(1 + f_{EG} . b_G . Rs) \cdot Y_G . R_s}{(1 + b_G . R_s)} \right) - \left(\frac{(1 + f_{EH} . b_H . R_s) \cdot Y_H . R_s}{(1 + b_H . R_{s)}} \right)} \right) \cdot S_{ti} \tag{6.25}$$

When applying Equations 5.3.2 and 5.3.3 simultaneously, it is noted that to obtain an increased f'_{EG} value would require also having an increased S'_{bsi} value (and a corresponding reduction in the remaining fraction of the influent biodegradable COD, allocated for OHO growth). Using the average MLE system $f_{S'up}$ of 0.05 together with the kinetic and stoichiometric constants for NDBEPR systems (from Wentzel *et al.*, 1990, see Section 2.3.2.2 of Chapter 2) in the simultaneous application of the Equations 5.3.2 and 5.3.3, gives an f'_{EG} value of 0.45 and S'_{bsi} of 654.9mgCOD/*l* (i.e. with OHOs allocated the remainder BPO of 135.2mgCOD/*l* for their growth). However, the PAOs are known to utilise only readily biodegradable COD (RBCOD), which was measured in the influent to have ranged between 237.8 and 292.4mgCOD/*l* (i.e. less than the 654.9mgCOD/*l*). Moreover, equating the average measured RBCOD value of 264.8 mgCOD/*l* to the S'_{bsi} value, used for the growth of PAOs, would require an f'_{EG} of 0.92 to establish the measured $S_{up\text{-}WAS}$. This f'_{EG} value is unreasonably higher than the endogenous respiration f_{EG} value of 0.25.

The other possible explanation for the higher influent $f_{S'up}$ value is that the ratio of enmeshed influent unbiodegradable particulate sludge in the aerobic reactor to that of the whole AS system (i.e. $X_{i\text{-}aerobic}/X_{i\text{-}system} = f_{maer\text{-}Xi}$), is not proportionate to the relative ratio of reactor VSS concentrations (i.e.$VSS_{aerobic}/VSS_{system} = f_{maer\text{-}VSS}$); hence it is higher than accounted for. The amount of sludge wasted daily is certainly containing a higher than anticipated fraction of unbiodegradable organics (as confirmed by the AD of the MBR UCT system WAS at a long, 60d sludge age). This infers that the active biomass, which is the only biodegradable organic portion of sludge in the WAS (see Section 4.2.1 of Chapter 4), is well predicted if the MBR influent $f_{S'up}$ is kept at the high values calculated in the NDBEPR system (shown in Table 5.2.1). Since the endogenous residue is mainly from this active biomass, and it is accepted that all kinetic and stoichiometric values from Wentzel *et al.* (1990) are accurate, the source of excess unbiodegradable WAS could be from the influent inert organics. This could be true if, although the reactors are completely mixed, the significantly higher mixed liquor concentrations in the aerobic reactor cause more of the influent inert organics

to get enmeshed, such that the ratio of sludge in the aerobic reactor to the whole system (f_{maer}) for the enmeshed influent unbiodegradable organics is higher than that of the total measured volatile solids (i.e. $f_{maer\text{-}Xi} > f_{maer\text{-}VSS}$). This would cause more of the reactor sludge enmeshed influent unbiodegradable organics ($X_{i\text{-}aer}$) to be wasted daily, in order to maintain the system sludge age. The aerobic reactor X_i concentration can be given by the Equation 5.3.4 below:

$$X_{i-aer} = f_{maer-Xi} \cdot \frac{\left(Q_i \cdot f_{upi} \cdot \frac{S_{ti}}{f_{cv}} \cdot R_s \right)}{V} \tag{6.26}$$

Making the aerobic mass fraction of enmeshed unbiodegradable influent organics ($f_{maer\text{-}Xi}$) the subject of the above Equation 5.3.4 results in:

$$f_{maer-Xi} = \frac{V \cdot X_{i-aer} \cdot f_{cv}}{Q_i \cdot f_{upi} \cdot S_{ti} \cdot R_s} \tag{6.27}$$

To obtain the right $f_{maer\text{-}Xi}$ value requires application of the above Equation 5.3.5, using the lower $f_{S'up}$ (0.05) value that was obtained from the MLE system that was operated without membranes, together with the $X_{i\text{-}aer}$ value that would result from applying the higher NDBEPR influent $f_{S'up}$ (0.18) value to Equation 5.5.3. This results in an $f_{maer\text{-}Xi}$ of 4.64, which is significantly higher (about four times) than the measured ratio of sludge VSS in the aerobic reactor to the whole MBR UCT system ($f_{maer\text{-}VSS} \approx 1.3$). However, the acceptance of this high $f_{maer\text{-}Xi}$ value allows for this MBR system and the conventional MLE system, fed the same sewage (MLE 1), to use the same average influent $f_{S'up}$ value of 0.05. A further exploration on the validity of this cause can be done by investigating the biodegradability of sludge from the other reactors (anoxic and anaerobic) when fed to an AD operated at a long sludge age (about 60 days or more), hence confirming whether their X_i component of VSS is indeed lower than that of the aerobic reactor.

With the experimental investigation, it has been established that the biodegradable particulate organics in the activated sludge system remain unbiodegradable in the AD. However, with the above review, it is also apparent that the aspect regarding high influent $f_{S'up}$ values, calculated from BEPR plants requires further investigations, which extend beyond the scope of this research report.

5.4 CHARACTERISTICS OF INFLUENT WASTEWATER

The settleable and non-settleable/dissolved organics (and inorganics) of the raw wastewater can be treated together in the activated sludge system or separated by primary settling tank into primary sludge (settleable organics and inorganics) and settled wastewater (with non-settleable organics and inorganics). The primary sludge requires stabilization (digestion) and the settled wastewater is treated in activated sludge systems. The organics of raw wastewater, primary sludge and settled wastewater sub-divide into biodegradable or unbiodegradable, each of which has soluble and particulate components, i.e. biodegradable soluble organics (BSO), unbiodegradable soluble organics (USO), biodegradable particulate organics (BPO) and unbiodegradable particulate organics (UPO). The soluble organics are usually sub-divided further into those that are fermentable (FBSO) and volatile fatty acids (VFAs). Also, the N and P compositions of these organics and the inorganic ammonia and ortho-phosphates are included in this characterization (see block structures in Figures 5.4.1 to 5.4.4).

Table 5.4.1a: Methods used in Determination of Raw and Settled WW Characteristics			
No.	Name	Denotation	Determination Method
1	Total	S_{ti}	Unfiltered COD test on WW (Open flux method)
2	VFA	S_{bsai}	[1]5 point titration = 64/60 mgHAc/*l*
3	FBSO	S_{bsfi}	S_{bsai} and S_{usi} deducted from filtered*WW COD test result (S_{tsi})
4	USO	S_{usi}	COD test on filtered* AS system effluent
5	UPO	S_{upi}	Using Equation 5.2.1 to 5.2.4
6	BPO	S_{bpi}	$S_{tpi} - S_{upi} = S_{ti} - S_{tsi} - S_{upi}$.
7	Total	C_{ti}	$C_{bsai} + C_{bsfi} + C_{usi} + C_{bpi} + C_{upi}$
8	VFA	C_{bsai}	[1]5 point titration = 24/60 mgHAc/*l*
9	FBSO	C_{bsfi}	Using f_{cv} = 1.42 and f_c = 0.487, from Brink and Ekama (2008),
10	USO	C_{usi}	Using f_{cv} = 1.42 and f_c = 0.47, from Brink and Ekama (2008),
11	UPO	C_{upi}	Using f_{cv} =1.48 and f_c = 0.515, from Poinapen and Ekama (2010)
12	BPO	C_{bpi}	Using results from AD of PS by difference between influent PO and effluent UPO f_{cv} and f_c ratios and COD concentrations (see Section 5.4.3)
13	Total	N_{ti}	TKN test on WW (micro-Kjeldahl method)
14	FSA	N_{ai}	FSA test (titrimetric method) on filtered* WW
15	Org N	N_{oi}	N_{ai} deducted from N_{ti}
16	USO	N_{ousi}	AS system effluent filtered* (TKN - FSA) test result
17	FBSO	N_{obsi}	(N_{ousi} + N_{ai}) deducted from filtered* WW TKN test result (N_{tsi})
18	UPO	N_{oupi}	$f_n \times S_{upi} / f_{cv}$, where f_n and f_{cv} are the ratios measured on the effluent solids of the WAS (which is obtained from the AS system treating the wastewater) AD operated at the long 60 day R_s.
19	BPO	N_{obpi}	$N_{tpi} - N_{oupi} = N_{ti} - N_{tsi} - N_{oupi}$
20	Total	P_{ti}	Unfiltered TP test on WW (Sulphuric acid/Persulphate digestion at 100°C followed by OP test)
21	OP	P_{ai}	OP test (Molybdate vanate colour development) on filtered* WW
22	Org P	P_{oi}	OP deducted from P_{ti}
23	USO	P_{ousi}	(P_{ousi} + P_{ai}) deducted from filtered* WW TKN test result (P_{tsi})
24	FBSO	P_{obsi}	AS system effluent filtered* (TP - OP) test result
25	UPO	P_{oupi}	$f_p * S_{upi} / f_{cv}$, where f_p and f_{cv} are the ratios measured on the effluent solids of the WAS (which is obtained from the AS system treating the wastewater) AD operated at the long 60 day R_s
26	BPO	P_{obpi}	$P_{bi} - P_{oupi} = P_{ti} - P_{tsi} - P_{oupi}$
filtered* -means sample filtered through Schleicher & Schull ME 25/21 0.45 micrometer membrane filters			
[1] - Means the VFA test was carried out mainly in the PS added to make up raw wastewater and the settled wastewater assumed to have a VFA of zero, with occasional tests on the settled sewage to check that VFA mass balances over the 'virtual' PST are satisfied.			

5.4.1 Primary Sludge Characterisation and Elemental Composition

The PS is the settleable part of the raw wastewater that is separated from settled wastewater in the PST. As in the determination of the unbiodegradable fraction of PS ($f_{PS'up}$), the mass of COD, carbon (C), nitrogen (N) and phosphorus (P) contents of the various PS organic concentrations are obtained by performing materials mass balances over the PST from known raw and settled WW BPO fluxes (g/d) and concentrations (mg/*l*). Thus the flux of COD, C, N and P in the settled WW is subtracted from that in raw WW giving the flux of COD, C, N and P in the PS, which is then divided by the PST underflow to obtain the total COD, C, N and P concentrations in the PS. For example, to obtain the concentration of N in the FBSO component of PS as influent to the AD ($N_{obsi\text{-}PS}$), the calculation below can be used:

$$N_{obsi-PS} = \frac{\left(FN_{obsi-raw} - FN_{obsi-settled}\right)}{Q_{PS}} = \frac{\left(Q_{i-raw} \cdot N_{obsi-raw} - Q_{i-settled} \cdot N_{obsi-settled}\right)}{Q_{i-raw} - Q_{i-settled}} \quad (5.4.1)$$

The PS total COD, C, N and P concentrations also fractionate into USO, BSO, BPO, UPO, FBSO, VFA, FSA and OP (where applicable) concentrations like the raw and settled COD, C, N and P. Theoretically, the soluble BSO, USO, VFA, FSA, OP are the same in the raw, settled and PS flows (since theoretically biological activity is assumed not to take place in the PST and gravity thickener). However, in this investigation with real wastewater and PS, this is not the case because PS, which contained some dissolved concentrations of its own, was added to the wastewater with different dissolved concentrations to make up the raw wastewater. This can be seen in the characterization block diagrams which show the different measured dissolved concentrations in the raw, settled wastewaters and PS. The particulates (UPO and BPO) concentrations (of COD, C, N and P) are about two orders of magnitude higher in the PS than in the raw or settled wastewaters due to the concentrating effect of the PST from which the PS was collected.

Table 5.4.1b: Methods used in Determination of PS Characteristics			
No.	Name	Denotation	Determination Method
1	Total	S_{ti}	Unfiltered COD test on WW (Open flux method)
2	VFA	S_{bsai}	5 point titration = 64/60 mgHAc/*l*
3	FBSO	S_{bsfi}	($S_{bsai} + S_{usi}$) deducted from filtered* WW COD test result (S_{tsi})
4	USO	S_{usi}	COD test on filtered* AS system effluent
5	UPO	S_{upi}	Using the concept of material (UPO) mass balances over the 'virtual' PST, illustrated in Equation 5.4.1
6	BPO	S_{bpi}	$S_{tpi} - S_{upi} = S_{ti} - S_{tsi} - S_{upi}$.
7	Total	C_{ti}	$C_{bsai} + C_{bsfi} + C_{usi} + C_{bpi} + C_{upi}$
8	VFA	C_{bsai}	5 point titration = 24/60 mgHAc/*l*
9	FBSO	C_{bsfi}	Using f_{cv} = 1.42 and f_c = 0.487, from Brink and Ekama (2008),
10	USO	C_{usi}	Using f_{cv} = 1.42 and f_c = 0.47, from Brink and Ekama (2008),
11	UPO	C_{upi}	Using f_{cv} =1.48 and f_c = 0.515, from Poinapen and Ekama (2010)
12	BPO	C_{bpi}	Using results from AD of PS by difference between influent PO and effluent UPO f_{cv} and f_c ratios and COD concentrations (see Section 5.4.3).
13	Total	N_{ti}	TKN test on WW (micro-Kjeldahl method)
14	FSA	N_{ai}	FSA test (titrimetric method) on filtered* WW
15	Org N	N_{oi}	N_{ai} deducted from N_{ti}
16	USO	N_{ousi}	AS system effluent filtered* (TKN - FSA) test result
17	FBSO	N_{obsi}	($N_{ousi} + N_{ai}$) deducted from filtered* WW TKN test result (N_{tsi})
18	UPO	N_{oupi}	$f_n \times S_{upi} / f_{cv}$, where f_n and f_{cv} are the ratios measured on the effluent solids of the PS AD operated at the long 60 day R_s.
19	BPO	N_{obpi}	$N_{tpi} - N_{oupi} = N_{ti} - N_{tsi} - N_{oupi}$.
20	Total	P_{ti}	Unfiltered TP test on WW (Sulphuric acid/Persulphate digestion at 100°C followed by OP test)
21	OP	P_{ai}	OP test (Molybdate vanate colour development) on filtered* WW
22	Org P	P_{oi}	OP deducted from P_{ti}
23	USO	P_{ousi}	($P_{ousi} + P_{ai}$) deducted from filtered* WW TKN test result (P_{tsi})
24	FBSO	P_{obsi}	AS system effluent filtered* (TP - OP) test result
25	UPO	P_{oupi}	$f_p \times S_{upi} / f_{cv}$, where f_p and f_{cv} are the ratios measured on the effluent solids of the PS AD operated at the long 60 day R_s.
26	BPO	P_{obpi}	$P_{bi} - P_{oupi} = P_{ti} - P_{tsi} - P_{oupi}$
filtered* - means sample filtered through Schleicher & Schull ME 25/21 0.45 micrometer membrane filters			

5.4.2 Influent COD Concentrations

The COD concentrations obtained for the characterisation of the influent COD components were determined using results from the COD tests on the membrane filtered (S_{tsi}) and unfiltered (S_{ti}) influent and the membrane-filtered effluent (S_{tse} = S_{usi}). To determine the COD of UPO required calculating the influent $f_{S'up}$ with the above Equation 5.2.1 or 5.2.2 (which necessitates also measuring the system MX_v) and multiplying the result with the measured S_{ti} value (i.e. $S_{upi} = f_{S'up} \times S_{ti}$). The VFA COD was determined using the 5-point titration method (Moosbrugger *et al.*, 1992) and converting the resultant unit mgHAc/*l* to mgCOD/*l* by multiplying by 64/60 mgCOD/mgHAc. Other influent COD components were then determined algebraically, i.e. for FBSO: $S_{bsfi} = S_{tsi} - S_{ai} - S_{usi}$ and for BPO: $S_{bp} = S_{ti} - S_{tsi} - S_{upi}$.

For the NDBEPR system further influent COD characteristics, which show the COD to be taken up by OHOs and the COD to be sequestered by PAOs, are required. Wentzel *et al.* (1990) discovered that the S_{bsi} required to be sequestered by the PAOs (S_{bPAO}) in the NDBEPR systems could be calculated iteratively using the Equations 2.3.7a and b (in Chapter 2). It is known that, with large quantities of P in the influent, as was the case in this experimental set-up, the PAOs in a NDBEPR system usually take up almost all of the rapidly biodegradable (mainly soluble) influent COD (S_{bsi}). Therefore, it was assumed that all the S_{bsi} was used for the growth and metabolism of PAOs. However, the influent COD sequestered by the PAOS was adjusted by including Equation 2.3.7b, to cater for cases where denitrification may occur in the anaerobic (rather than anoxic) zone of the NDBEPR system (i.e. the presence of de-nitrifying PAOs). This resulted in the Equation 5.4.2 below:

$$S_{bPAO} = (S_{tsi} - S_{use}) - (r * 8.6 * NO_{3anaerobic}) \qquad (5.4.2)$$

Where S_{tsi} is the total soluble organic material in the influent, r is the ratio of anoxic to anaerobic reactor recycles flow to influent flow and 8.6 is the value that represents observed COD removal per anaerobic reactor nitrate concentration (denoted by $NO_{3anaerobic}$).

The COD characteristic component concentrations of the influent PS, and the raw and settled wastewaters (from the MBR UCT and MLE systems) are as shown in Table 5.4.2 and a summary of the average resultant values are given in the block structures of Figures 5.4.1 a to c. It is notable from Table 5.4.2 that there are some differences in the PS characteristics. The PS was liable to changes because the batches collected, from the Athlone treatment plant, for the different experimental test periods were taken at different times and there was chances of variability in the components of the sewage particulates (as can be noted with the variability of PS charactersictics for different batches in Table 5.4.2) that were fed to this plant according to the extent of contributions from various waste sources. However, unlike PS, WAS largely comprises of the same microorganisms, depending on the AS system from which it is taken, hence has less chances of variability in its component charateristics.

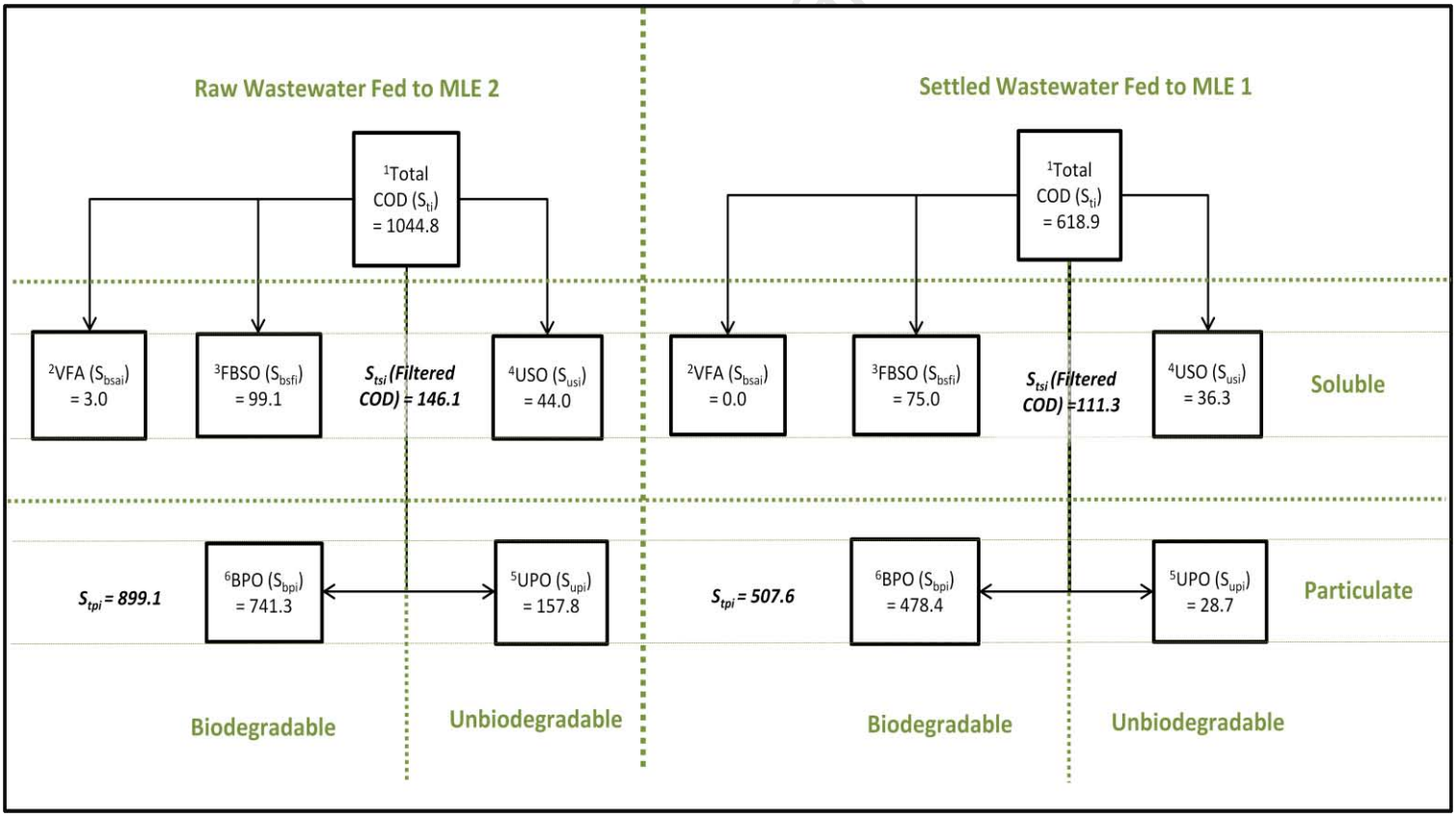

Figure 5.4.1a: *The COD characteristics for raw and settled wastewater fed to MLE systems, all values are in mgCOD/l.*

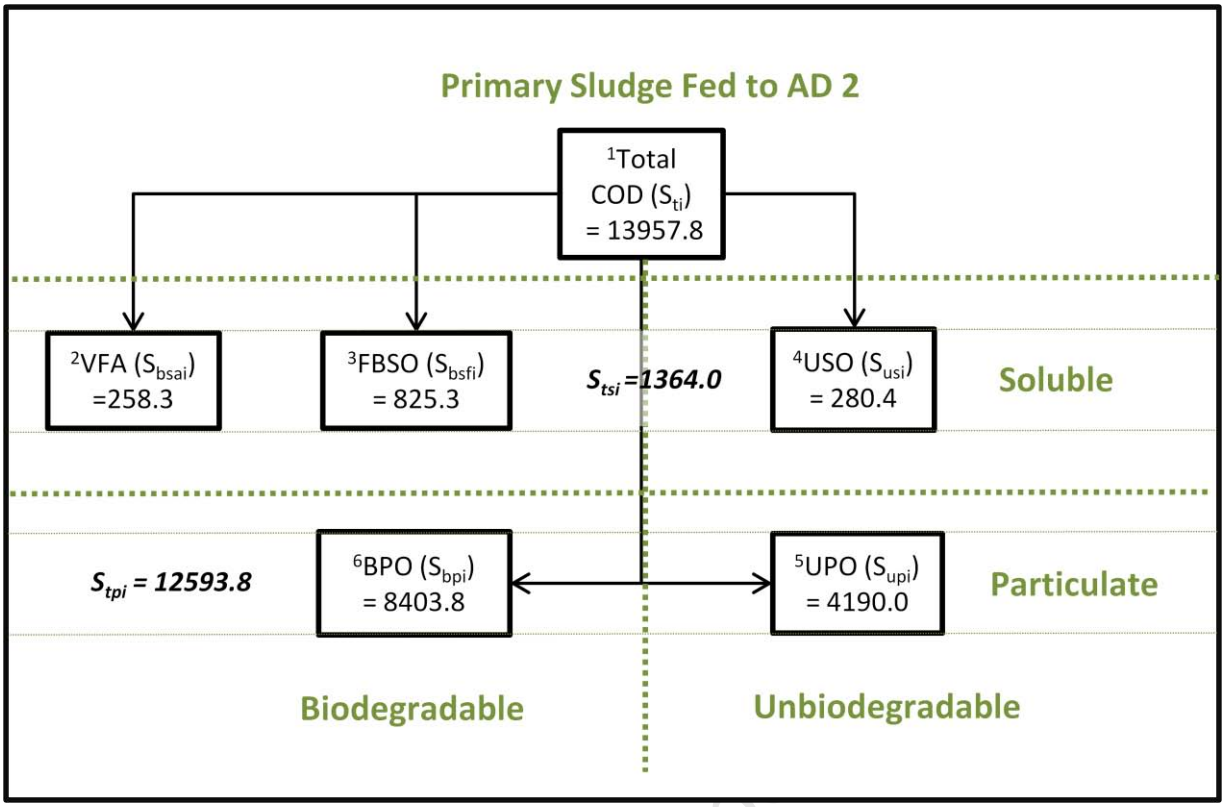

Figure 5.4.1b: *The COD characteristics for primary sludge (PS), all values are in mgCOD/l.*

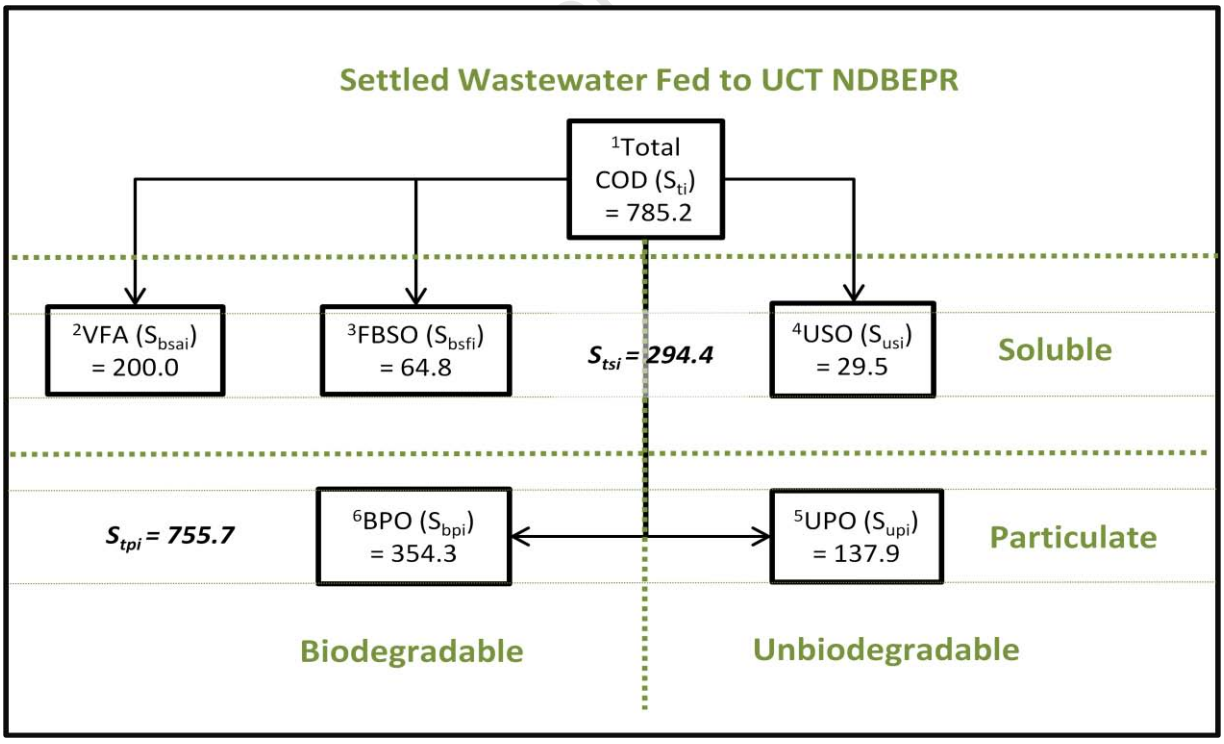

Figure 5.4.1c: *The COD characteristics for settled wastewater fed to the MBR UCT system,all values are in mgCOD/l.*

Table 5.4.2: Influent Chemical Oxygen Demand (COD) Characterisation												
	[a]Test period	$^{1}S_{ti}$	$^{m}S_{tsi}$	$^{d}S_{tpi}$	$^{2}S_{ai}$	$^{3}S_{bPAO}$	$^{2+3}S_{bsi}$	$^{4}S_{usi}$	$^{5}S_{upi}$	$^{4+5}S_{ui}$	$^{6}S_{bpi}$	$^{3+6}S_{bi}$
Primary Sludge (PS)	1	8053	816	7899	185	477	662	154	2240	2394	4997	5659
	2	28435	2626	27903	441	1654	2095	531	7971	8502	17837	19932
	3	18707	1673	18179	311	834	1145	528	6368	6896	10666	11811
	4	8910	1242	8789	199	922	1121	122	2947	3069	4721	5841
	5	5684	462	5617	156	239	395	67	1424	1491	3798	4193
	Average	13958	1364	13677	258	825	1084	280	4190	4470	8404	9487
	Fraction	1.00	0.10	0.98	0.02	0.06	0.08	0.02	0.30	0.32	0.60	0.68
Raw WW to MLE 2	1	1112	164	1072	1	123	123	40	163	203	786	909
	2	1092	159	1051	2	115	117	42	173	214	761	878
	3	1061	145	1021	5	99	104	41	159	200	757	862
	4	966	173	905	6	107	112	61	161	222	632	744
	5	991	89	955	1	51	51	37	133	169	771	822
	Average	1045	146	1001	3	99	102	44	158	202	741	843
	Fraction	1.00	0.14	0.96	0.00	0.09	0.10	0.04	0.15	0.19	0.71	0.81
Settled WW to MLE 1	1	629	125	597	0	93	93	32	24	56	480	573
	2	624	120	590	0	86	86	33	39	72	465	551
	3	638	113	611	0	86	86	28	11	39	514	599
	4	606	125	550	0	69	69	56	40	96	441	510
	5	597	73	565	0	41	41	32	29	61	496	536
	Average	619	111	583	0	75	75	36	29	65	479	554
	Fraction	1.00	0.18	0.94	0.00	0.12	0.12	0.06	0.05	0.10	0.77	0.90
Settled WW to NDBEPR	1	790	322	761	200	92	292	29	139	168	330	622
	2	827	301	797	200	71	271	30	156	186	373	641
	3	794	252	780	200	38	238	15	126	141	418	654
	4	751	320	714	200	82	282	37	139	177	294	575
	5	763	277	727	200	41	241	36	129	165	357	598
	Average	785	294	756	200	65	265	30	138	167	354	618
	Fraction	1.00	0.37	0.96	0.25	0.08	0.34	0.04	0.18	0.21	0.45	0.79

[a] - See Tables 4.1 a and b for the time-line with the dates and sewage batch that correspond to the indicated test period, also included are appendix reference numbers for day to day results

[m] – Indicates total soluble COD, which is measured from filtered influent sample

[d] – Indicates the total particulate COD, which is obtained by $S_{ti} - S_{tsi}$

[1] to [6] – Reference to the corresponding characteristics in the block diagrams of Figures 5.4.1a, b and c

5.4.3 Influent Carbon Characterisation

The influent total organic carbon (TOC) characteristic component concentrations were either obtained using values from literature or by indirect calculations from other tests. This is because the direct carbon (C) analysis tests were not performed during the experimental investigation. For instance, the C concentration of influent VFA was simply determined by using the 5-point titration method (Moosbrugger *et al.*, 1992) and converting the resultant unit mgHAc/*l* to mgTOC/*l* through multiplication by 24/60 mgC/mgHAc. The other dissolved organics (FBSO and USO) C concentrations were obtained from Brink and Ekama (2008) who performed wastewater characteristic tests and obtained f_c (carbon ratio per unit mol) values of 0.47 for FBSO and 0.487 for USO, using an assumed f_{cv} value of 1.42 for both components. In the case of BPO carbon characteristics, the carbon production (from CO_2, CH_4 and alkalinity change) with the AD of PS BPO was measured, and its ratio to the unit COD removed calculated. This determined TOC/COD ratio could then be multiplied to the known influent sewage BPO COD to calculate influent BPO TOC. Similarly, the unbiodegradable particulate organic C concentrations were obtained from the TOC/COD ratio values obtained from Wentzel *et al.* (2006) investigations on the particulate organic characteristics of PS. Wentzel *et al.* (2006) determined the CHONP characteristics of PS using the experimental data of Izzett *et al.* (1992), Moen *et al.* (2001) and Ristow *et al.* (2005) and applied these characteristics into the AD model of Sötemann *et al.* (2006) to predict COD removal and FSA releases. Thereafter, these model predictions were matched to measured results from the elemental analysis of PS from two full-scale WW treatment plants. In this investigation, Wentzel *et al.* (2006) obtained a UPO f_{cv} value of 1.48 and f_c value of 0.515. Therefore, for this investigation, this f_c (TOC/COD) ratio was multiplied by the known influent COD UPO values to obtain the UPO TOC concentrations. The influent carbon concentrations for components of the primary sludge (fed to AD 2 of the experimental set-up shown in Chapter 3), raw (fed to MLE 2) and settled

wastewater (fed to the MLE 1 and UCT NDBEPR systems) are as presented in Table 5.4.3 below with the averages summarised in the block structures Figure 5.4.2 a to c.

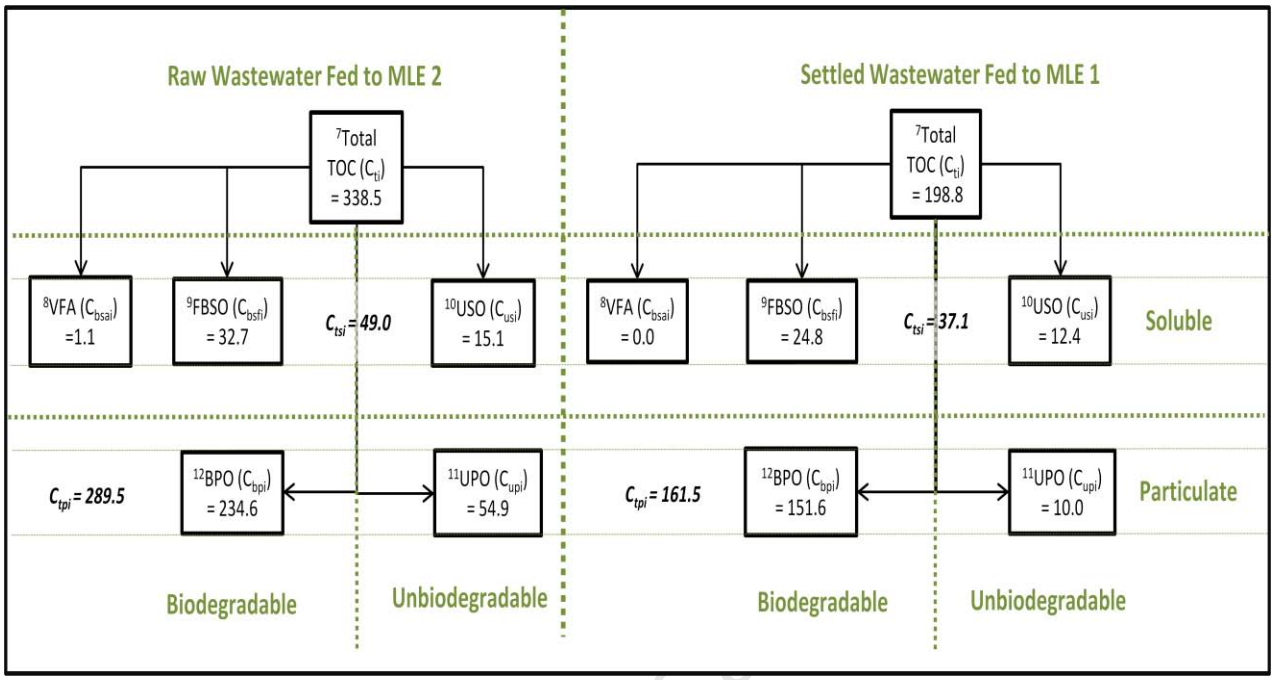

Figure 5.4.2a: *The TOC characteristics for raw and settled wastewater fed to MLE systems, all values are in mgC/l.*

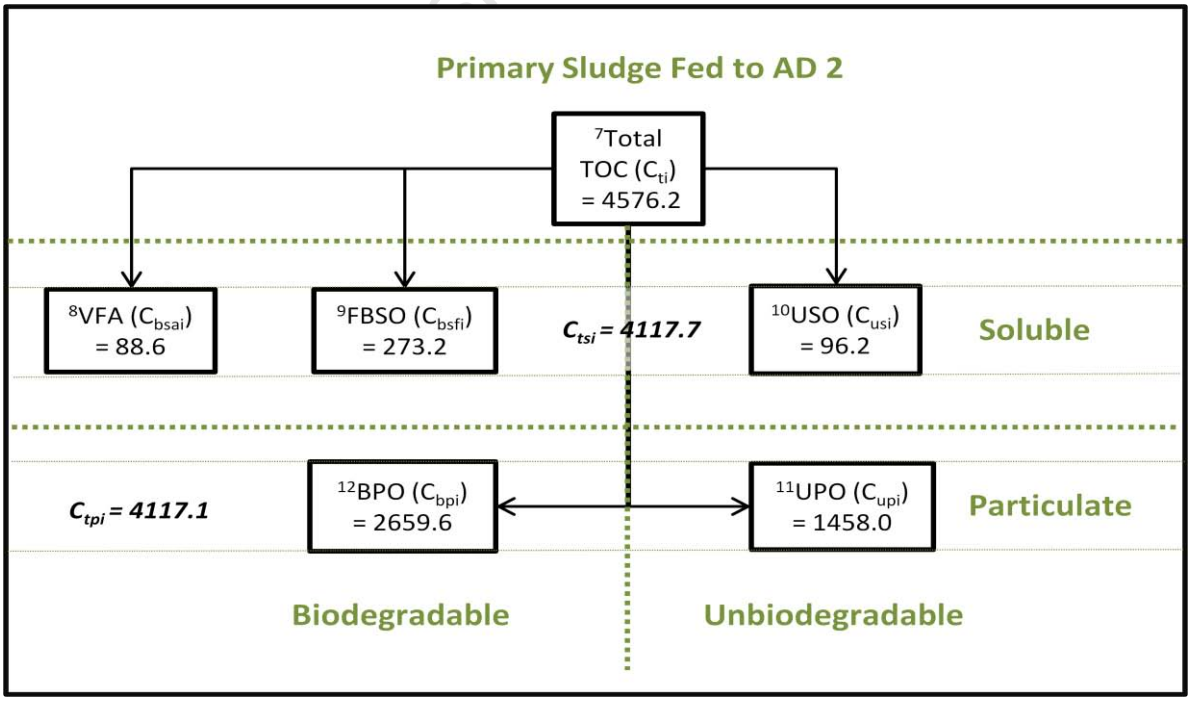

Figure 5.4.2b: *The TOC characteristics for primary sludge, all values are in mgC/l.*

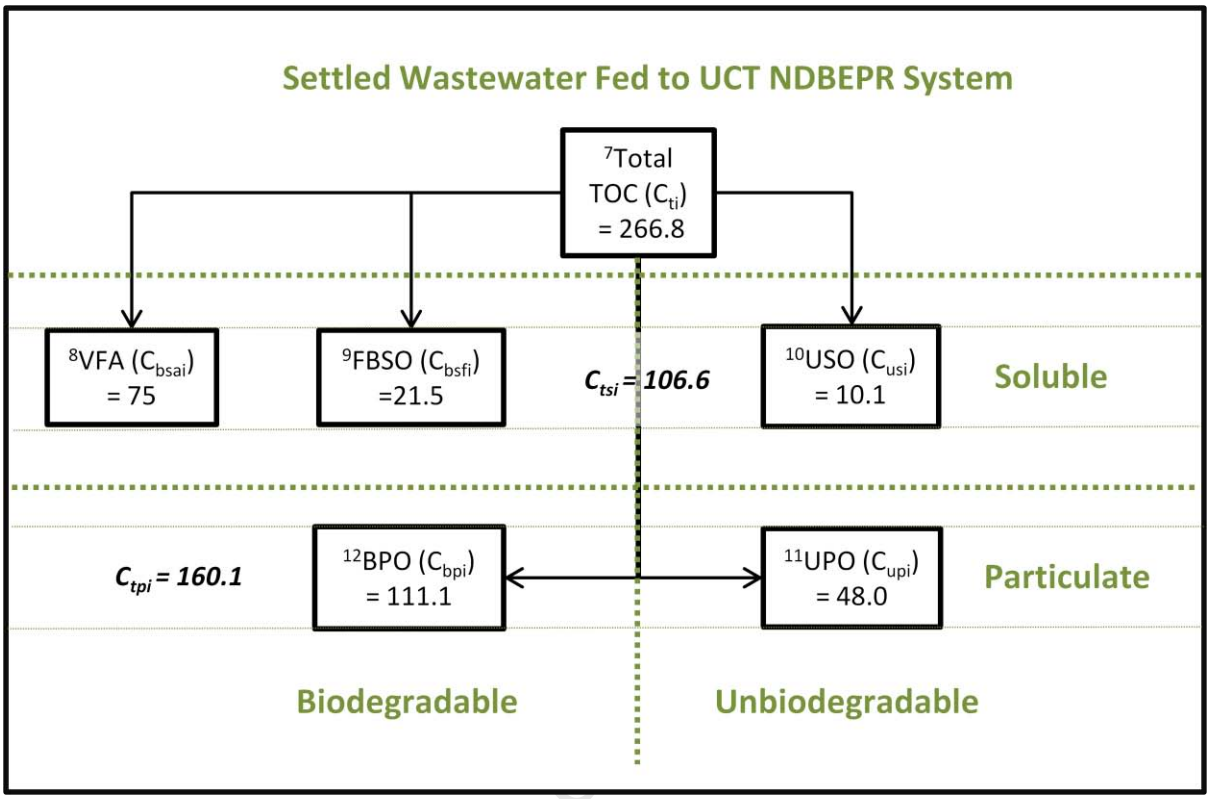

Figure 5.4.2c: *The TOC characteristics for settled wastewater fed to the MBR UCT system, all values are in mgC/l.*

Table 5.4.3: Influent Carbon (C) Characterisation												
	[a]Test period	$^{7}C_{ti}$	$^{m}C_{tsi}$	$^{d}C_{tpi}$	$^{8}C_{ai}$	$^{9}C_{bPAO}$	$^{8+9}C_{bsi}$	$^{10}C_{usi}$	$^{11}C_{upi}$	$^{10+11}C_{ui}$	$^{12}C_{bpi}$	$^{9+12}C_{bi}$
Primary Sludge (PS)	1	2635	274	2361	64	158	221	53	779	832	1581	1803
	2	9299	881	8418	151	548	699	182	2774	2956	5645	6343
	3	6156	564	5592	107	276	383	181	2216	2397	3376	3759
	4	2934	415	2519	68	305	373	42	1026	1067	1494	1867
	5	1853	156	1697	53	79	133	23	495	518	1202	1335
	Average	4576	458	4118	89	273	362	96	1458	1554	2660	3021
	Fraction	1.00	0.10	0.90	0.02	0.06	0.08	0.02	0.32	0.34	0.58	0.66
Raw WW to MLE 2	1	360	55	305	0	40	41	14	57	70	249	290
	2	354	53	301	1	38	39	14	60	74	241	280
	3	344	49	295	2	33	35	14	55	69	240	274
	4	314	58	256	2	35	37	21	56	77	200	237
	5	320	30	290	0	17	17	13	46	59	244	261
	Average	338	49	289	1	33	34	15	55	70	235	268
	Fraction	1.00	0.14	0.86	0.00	0.10	0.10	0.04	0.16	0.21	0.69	0.79
Settled WW to MLE 1	1	202	42	160	0	31	31	11	8	19	152	183
	2	201	40	161	0	29	29	11	14	25	147	176
	3	204	38	167	0	28	28	9	4	13	163	191
	4	196	42	153	0	23	23	19	14	33	139	162
	5	191	25	167	0	14	14	11	10	21	157	170
	Average	199	37	162	0	25	25	12	10	22	152	176
	Fraction	1.00	0.19	0.81	0.00	0.12	0.12	0.06	0.05	0.11	0.76	0.89
Settled WW to NDBEPR	1	268	116	153	75	31	106	10	48	58	104	210
	2	281	109	172	75	24	99	10	54	65	118	217
	3	269	93	176	75	13	88	5	44	49	132	220
	4	256	115	141	75	27	102	13	48	61	93	195
	5	259	101	158	75	13	88	12	45	57	113	202
	Average	267	107	160	75	21	96	10	48	58	112	209
	Fraction	1.00	0.40	0.60	0.28	0.08	0.36	0.04	0.18	0.22	0.42	0.78

[a] - See Tables 4.1 a and b for the time line with the dates and sewage batch that correspond to the indicated test period, also included are appendix reference numbers for day to day results

[m] – Indicates total soluble TOC, which equals the sum of C_{bsi} and C_{usi}

[d] – Indicates the total particulate TOC, which is obtained by $C_{ti} - C_{tsi}$

[7] to [12] – Reference to the corresponding Influent characteristics in the block diagrams of Figures 5.4.2a, b and c

5.4.4 Influent N and P Characteristics

The N and P characteristics of the influent PS, raw and settled wastewaters (from MLE and NDBEPR systems) are as shown in Table 5.4.4b and 5.4.4c respectively.

These characteristic component concentrations were obtained as described in Table 5.4.1 using measured N (N_{ti}, N_{ai}, N_{tse} and N_{ae}) and P (P_{ti}, P_{ai}, P_{tse} and P_{ae}) values. The calculated S_{upi} concentrations (as described in Section 5.4.2) were also used in determining the N_{oupi} and P_{oupi} concentrations as shown below:

$$N_{oupi} = S_{upi} \cdot \frac{f_{n-up}}{f_{cv-up}} \qquad (5.4.3a)$$

and $$P_{oupi} = S_{upi} \cdot \frac{f_{p-up}}{f_{cv-up}} \qquad (5.4.3b)$$

Where $f_{cv\text{-}up}$, $f_{n\text{-}up}$ and $f_{p\text{-}up}$ are the fractions of influent unbiodegradable particulate organic material nitrogen to VSS, COD to VSS and phosphorus to VSS that can be measured, for PS, in the unbiodegradable particulate material which remains after the AD of PS at a long sludge age (about 60 days). The $f_{cv\text{-}up}$, $f_{n\text{-}up}$ and $f_{p\text{-}up}$ values of influent X_i going into the AS systems (noting that this influent X_i eventually gets enmeshed and accumulates in the AS reactors, to form a large portion of the WAS unbiodegradable component) are given the same values as for the WAS endogenous residue (X_e). This is because in the WAS, the influent X_i and X_e collectively form the unbiodegradable particulate organics, which have $f_{cv\text{-}up}$, $f_{n\text{-}up}$ and $f_{p\text{-}up}$ values that can be obtained from the measured VSS, COD, TKN and TP concentrations on the effluent of the WAS AD, when operated at 60d sludge age.

Organically bound phosphorus is usually low in both the biomass and unbiodegradable particulate material, measured by Wentzel *et al.* (1990) to be at a value of about 0.03 mgP/mgVSS. In this investigation, the P/VSS ratio of the unbiodegradable particulate influent material, which was measured in the AD effluent particulate organics after the complete degradation of PS at a long AD sludge age of 60 days, was 0.048mgP/mgVSS. In this 60-day AD sludge age, the

measured N/VSS ratio of PS UPO was similar (0.061) to that measured by Poinapen *et al.* (2008) who measured this unbiodegradable particulate organics in PS, f_n as 0.06. Table 5.4.4a shows the mass ratios f_{cv}, f_n, f_p of the WAS, obtained from the measured VSS, COD, TKN and TP concentrations of the AS systems' aerobic reactor (from where the sludge is wasted) mixed liquor and the $f_{cv\text{-}up}$, $f_{n\text{-}up}$ and $f_{p\text{-}up}$, obtained from the effluent of WAS AD and PS AD when operated at 60d sludge age. For all systems, the f_{cv}, f_n and f_p of the corresponding influent biodegradable particulates ($f_{cv\text{-}bp}$, $f_{n\text{-}bp}$ and $f_{p\text{-}bp}$) could be determined by subtracting the $f_{cv\text{-}up}$, $f_{n\text{-}up}$ and $f_{p\text{-}up}$ values from the measured influent sewage total particulate f_{cv}, f_n and f_p values. Moreover, the f_{cv}, f_n and f_p of the corresponding WAS biodegradable particulate organics (which for a steady state AS system almost solely comprises of active biomass, i.e. X_{BG} or/and X_{BH}, influent sewage biodegradable organics having all been used up) could be determined by subtracting the $f_{cv\text{-}up}$, $f_{n\text{-}up}$ and $f_{p\text{-}up}$ values from the measured WAS total particulate f_{cv}, f_n and f_p values. This is essential when modelling the systems on a plant-wide basis because the nitrogen and phosphorus that is organically bound in the biodegradable WAS (X_{BG} and X_{BH}), is released during tertiary treatment processes such as AD. This N and P release usually has significant influence on important variables such as pH, alkalinity and struvite precipitation potentials. The influent N and P characteristic components concentrations for raw and settled WW and PS are as presented in Table 5.4.4b and c below with the averages summarised in the block structures Figure 5.4.3a to c.

Table 5.4.4a: Sludge Characteristics Obtained from Measurements in AS Systems and PS Anaerobic Digester Effluent

Test Period	Measured Sludge Characteristics	Units	[1]MLE 1	[1]MLE 2	[2]NDBEPR	[3]PS influent	[4]PS AD effluent
Period 5 (Sewage batch 21, 10-day AD sludge age)	f_{cv} (COD/VSS)[a]	mgCOD/mgVSS	1.48	1.44	1.44	1.47	1.58
	f_c (TOC/VSS)[b]	mgC/mgVSS	0.52	0.52	0.52	0.51	0.51
	f_n (OrgN/VSS)[a]	mgN/mgVSS	0.1	0.09	0.08	0.07	0.08
	f_p (OrgP/VSS)[a]	mgP/mgVSS	0.03	0.03	0.03	0.02	0.03
Period 1 (Sewage batch 14, 18-day AD sludge age)	f_{cv} (COD/VSS)[a]	mgCOD/mgVSS	1.43	1.46	1.45	1.79	1.64
	f_c (TOC/VSS)[b]	mgC/mgVSS	0.52	0.52	0.52	0.62	0.53
	f_n (OrgN/VSS)[a]	mgN/mgVSS	0.12	0.11	0.09	0.06	0.07
	f_p (OrgP/VSS)[a]	mgP/mgVSS	0.03	0.03	0.03	0.04	0.06
Period 4 (Sewage batch 19, 25-day AD sludge age)	f_{cv} (COD/VSS)[a]	mgCOD/mgVSS	1.45	1.45	1.45	1.61	1.53
	f_c (TOC/VSS)[b]	mgC/mgVSS	0.52	0.52	0.52	0.56	0.51
	f_n (OrgN/VSS)[a]	mgN/mgVSS	0.1	0.11	0.09	0.05	0.05
	f_p (OrgP/VSS)[a]	mgP/mgVSS	0.04	0.04	0.04	0.03	0.07
Period 3 (Sewage batch 17, 40-day AD sludge age)	f_{cv} (COD/VSS)[a]	mgCOD/mgVSS	1.48	1.45	1.45	1.59	1.41
	f_c (TOC/VSS)[b]	mgC/mgVSS	0.52	0.52	0.52	0.55	0.49
	f_n (OrgN/VSS)[a]	mgN/mgVSS	0.12	0.11	0.08	0.04	0.06
	f_p (OrgP/VSS)[a]	mgP/mgVSS	0.04	0.04	0.04	0.01	0.03
Period 2 (Sewage batch 16, 60-day AD sludge age)	f_{cv} (COD/VSS)[a]	mgCOD/mgVSS	1.47	1.46	1.45	1.74	1.51
	f_c (TOC/VSS)[b]	mgC/mgVSS	0.52	0.52	0.52	0.61	0.52
	f_n (OrgN/VSS)[a]	mgN/mgVSS	0.11	0.12	0.09	0.04	0.06
	f_p (OrgP/VSS)[a]	mgP/mgVSS	0.04	0.04	0.04	0.01	0.05
[5] Effluent for WAS AD 60-day R_s	f_{cv} (COD/VSS)[a]	mgCOD/mgVSS	1.48	1.52	1.45		
	f_c (TOC/VSS)[b]	mgC/mgVSS	0.52	0.52	0.52		
	f_n (OrgN/VSS)[a]	mgN/mgVSS	0.07	0.09	0.04		
	f_p (OrgP/VSS)[a]	mgP/mgVSS	0.03	0.03	0.02		

[1] - Mixed OHO, OHO endogenous residue and influent UPO organics.

[2] - As for 1 but also PAO and PAO endogenous residue.

[3] – Mixed settleable influent BPO and UPO.

[4] - Settleable UPO only (plus a relatively small quantity of AD biomass) for the longer (40 to 60d) AD R_s, but also including some unhydrolyzed influent BPO for the shorter (10-25d) AD R_s.

[5] – Mixed settleable UPO and endogenous residue (plus a relatively small quantity of AD biomass).

[a] – Obtained from direct measurements of reactor mixed liquor COD (i.e. from unfiltered COD-filtered COD = COD of solids) and VSS (i.e. TSS - ISS).

[b] - The f_c value for OHO, PAO and UPO is given the value (0.515) obtained by Wentzel *et al. (2006)*. The f_c value for S_{bpi}, in PS, is obtained by multiplying the PS AD BPO (mgVSS) to the ratio of TOC removed (from CO_2, CH_4 and H_2CO_3* alkalinity change) to COD removed in the operation of the PS AD at 60 day R_s.

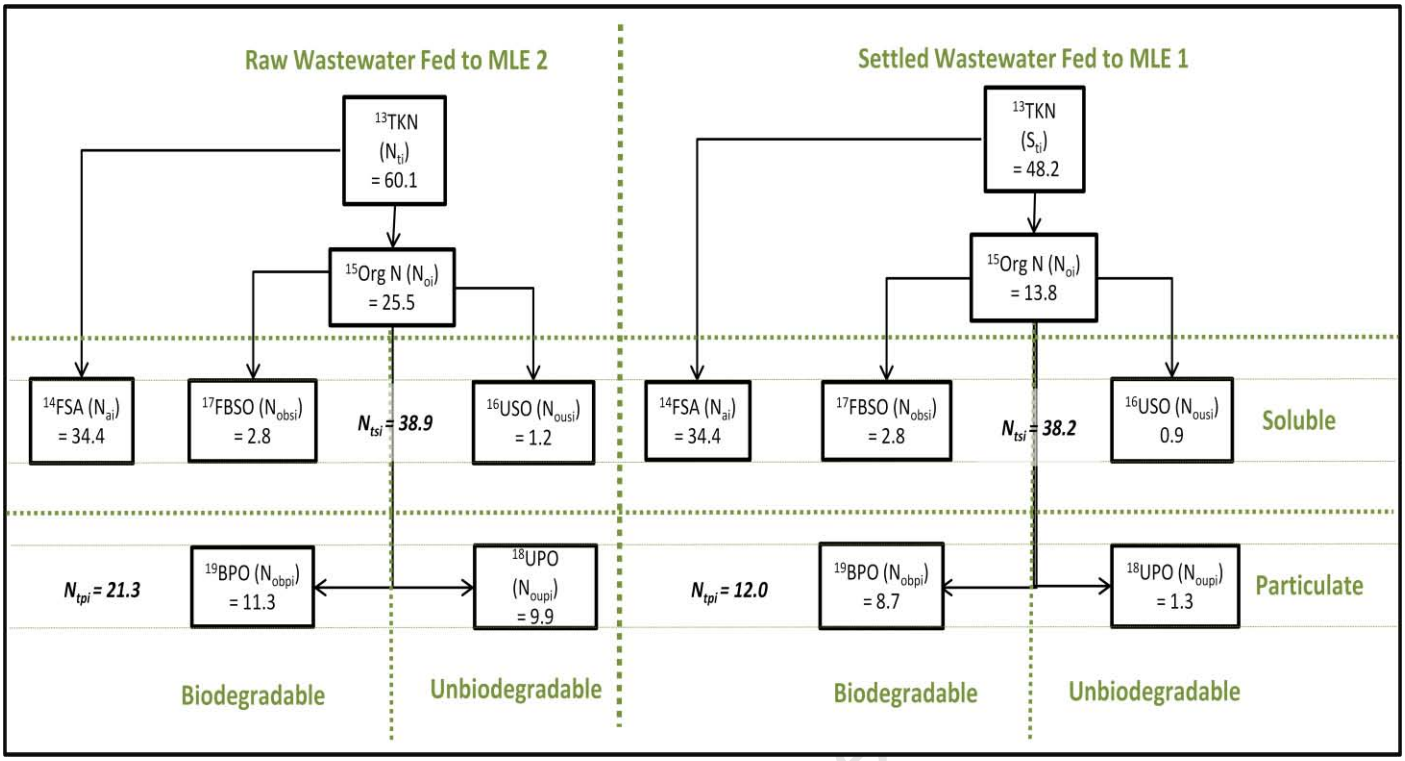

Figure 5.4.3a: *The nitrogen characteristics for raw and settled wastewater fed to MLE systems, all values in mgN/l.*

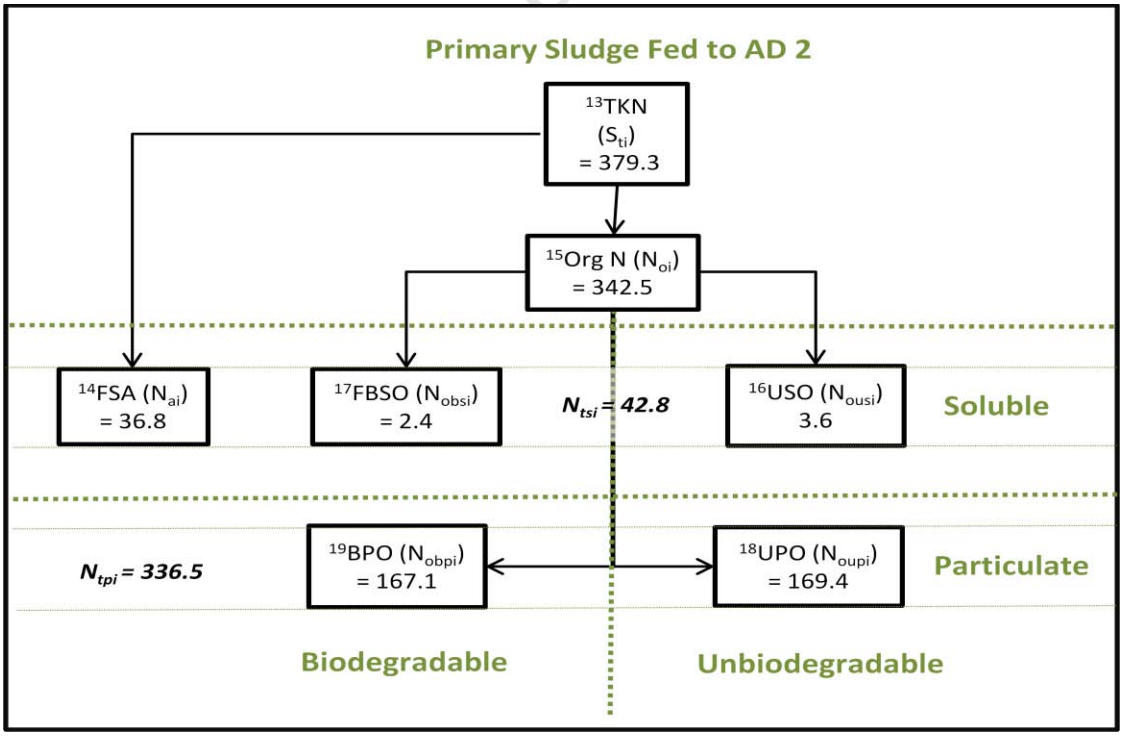

Figure 5.4.3b: *The nitrogen characteristics for primary sludge, all values in mgN/l.*

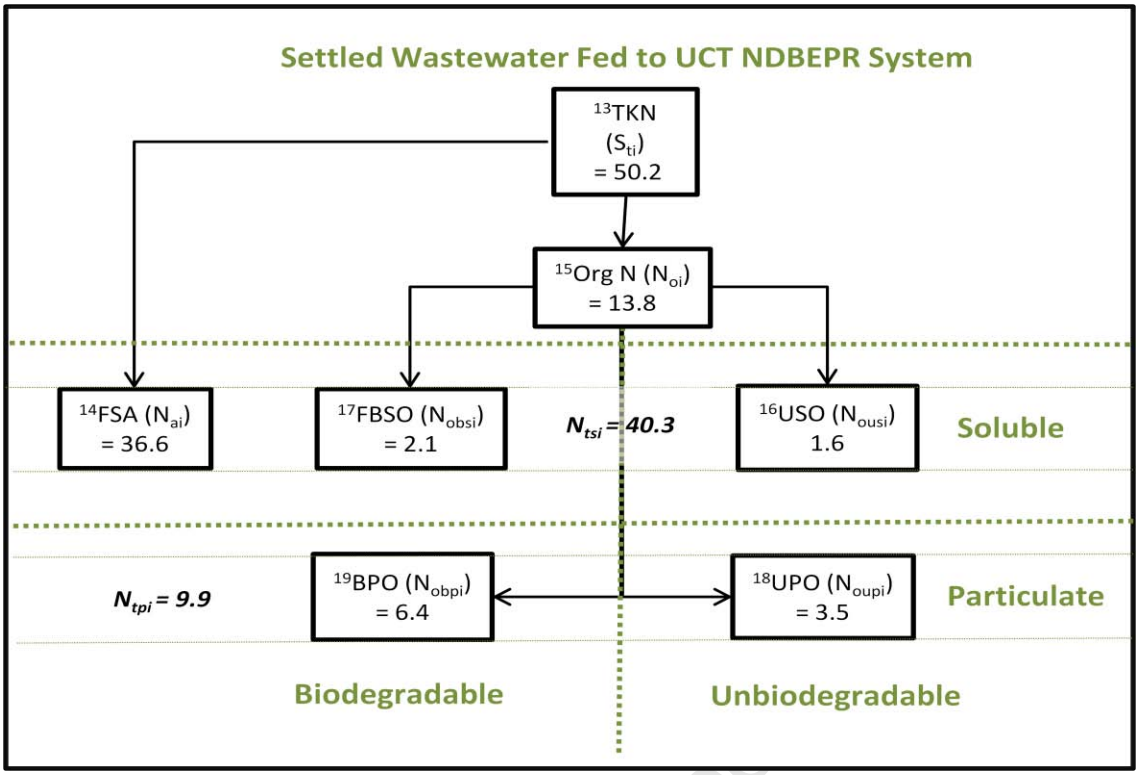

Figure 5.4.3c: *The nitrogen characteristics for settled wastewater fed to the MBR UCT system, all values in mgN/l.*

Table 5.4.4.b: Influent Nitrogen (N) Characterisation												
	[a]Test period	$^{13}N_{ti}$	$^{m}N_{tsi}$	$^{d}N_{tpi}$	$^{14}N_{ai}$	$^{15}N_{oi}$	$^{16}N_{ousi}$	$^{17}N_{obsi}$	$^{18}N_{oupi}$	$^{19}N_{obpi}$	$^{16+18}N_{oui}$	$^{17+19}N_{obi}$
Primary Sludge (PS)	1	254.8	33.3	221.6	27.5	227.3	4.9	0.9	90.6	131.0	95.5	131.9
	2	588.0	51.6	536.4	49.0	539.0	2.6	0.0	322.3	214.0	325.0	214.0
	3	506.8	57.8	449.1	52.5	454.3	1.1	4.1	257.5	191.5	258.7	195.6
	4	290.5	34.1	256.4	24.5	266.0	3.5	6.1	119.2	137.2	122.7	143.3
	5	256.2	37.1	219.1	30.5	225.8	5.8	0.8	57.6	161.6	63.4	162.4
	Average	379.3	42.8	336.5	36.8	342.5	3.6	2.4	169.4	167.1	173.0	169.4
	Fraction	1.00	0.11	0.89	0.10	0.90	0.01	0.01	0.45	0.44	0.46	0.45
Raw WW to MLE 2	1	55.4	40.3	15.1	36.7	18.7	0.6	3.0	10.2	4.8	10.9	7.8
	2	58.0	38.9	19.1	35.6	22.4	0.9	2.4	10.8	8.3	11.8	10.7
	3	58.9	43.4	15.5	39.8	19.1	1.4	2.2	10.1	5.4	11.4	7.6
	4	55.0	40.4	14.6	35.8	19.2	1.9	2.7	10.2	4.4	12.1	7.0
	5	73.4	31.3	42.1	25.4	48.0	0.9	4.9	8.4	33.7	9.3	38.7
	Average	60.1	38.9	21.3	34.7	25.5	1.2	3.0	9.9	11.3	11.1	14.4
	Fraction	1.00	0.65	0.35	0.58	0.42	0.02	0.05	0.17	0.19	0.18	0.24
Settled WW to MLE 1	1	42.7	39.0	3.7	35.8	6.9	0.4	2.8	1.1	2.6	1.5	5.4
	2	44.7	38.5	6.2	35.7	9.0	0.5	2.3	1.8	4.4	2.3	6.7
	3	45.3	42.2	3.1	38.8	6.6	1.3	2.1	0.5	2.6	1.9	4.7
	4	44.0	40.7	3.3	36.6	7.4	1.8	2.3	1.9	1.5	3.6	3.7
	5	64.2	30.4	33.7	25.2	39.0	0.5	4.7	1.3	32.4	1.8	37.1
	Average	48.2	38.2	10.0	34.4	13.8	0.9	2.8	1.3	8.7	2.2	11.5
	Fraction	1.00	0.79	0.21	0.71	0.29	0.02	0.06	0.03	0.18	0.05	0.24
Settled WW to NDBEPR	1	45.0	38.1	6.9	34.3	10.7	0.4	3.3	3.5	3.4	3.9	6.8
	2	45.0	32.4	12.6	29.1	15.9	1.6	1.8	4.2	8.3	5.8	10.1
	3	46.2	35.3	10.9	35.3	10.9	0.9	-0.9	3.2	7.8	4.1	6.9
	4	52.4	40.9	11.5	33.3	19.0	1.4	6.2	3.5	8.0	4.9	14.2
	5	62.4	54.9	7.5	51.1	11.3	3.8	0.0	3.2	4.3	7.0	4.3
	Average	50.2	40.3	9.9	36.6	13.6	1.6	2.1	3.5	6.4	5.1	8.4
	Fraction	1.00	0.80	0.20	0.73	0.27	0.03	0.04	0.07	0.13	0.10	0.17

[a] - See Tables 4.1a and b for the time-line with the dates and sewage batch that correspond to the indicated test period, also included are appendix reference numbers for day to day results

[m] – Indicates total soluble N, which is measured from filtered influent sample

[d] – Indicates the total particulate N, which is obtained by $N_{ti} - N_{tsi}$

[13] to [19] – Reference to the corresponding characteristics in the block diagrams of Figures 5.4.3a, b and c

Similarly to N, the influent P concentrations for components of raw and settled WW and PS are also presented in Table 5.4.4.2 below with the averages summarised in the block structures in Figure 5.4.4a to c.

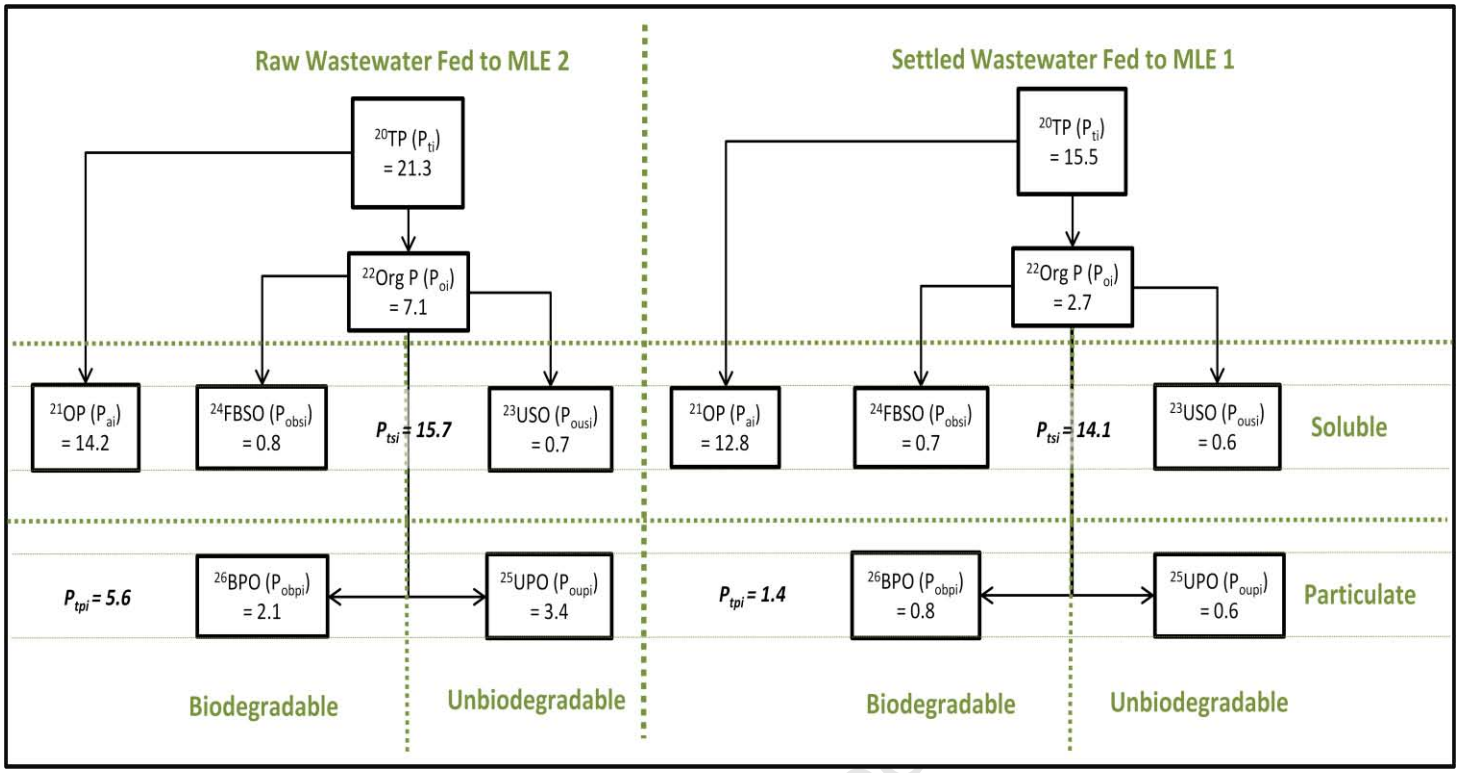

Figure 5.4.4a: *The phosphorus (P) characteristics for raw and settled wastewater fed to MLE systems, all values in mgP/l.*

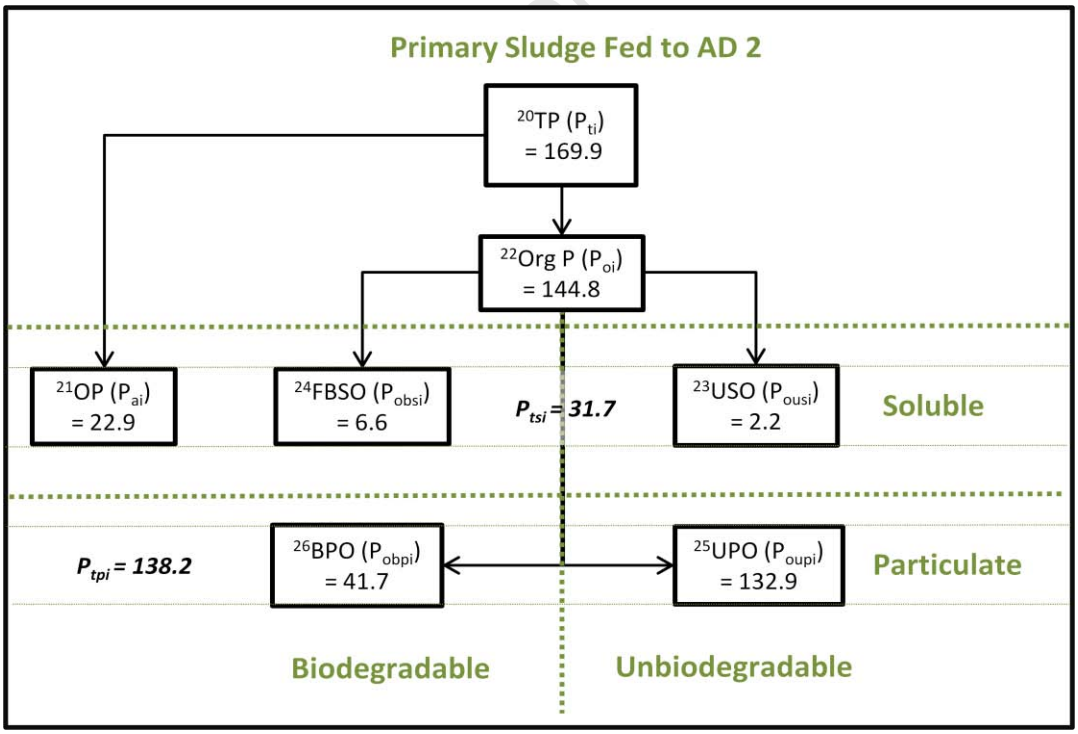

Figure 5.4.4b: *The phosphorus (P) characteristics for primary sludge, all values in mgP/l.*

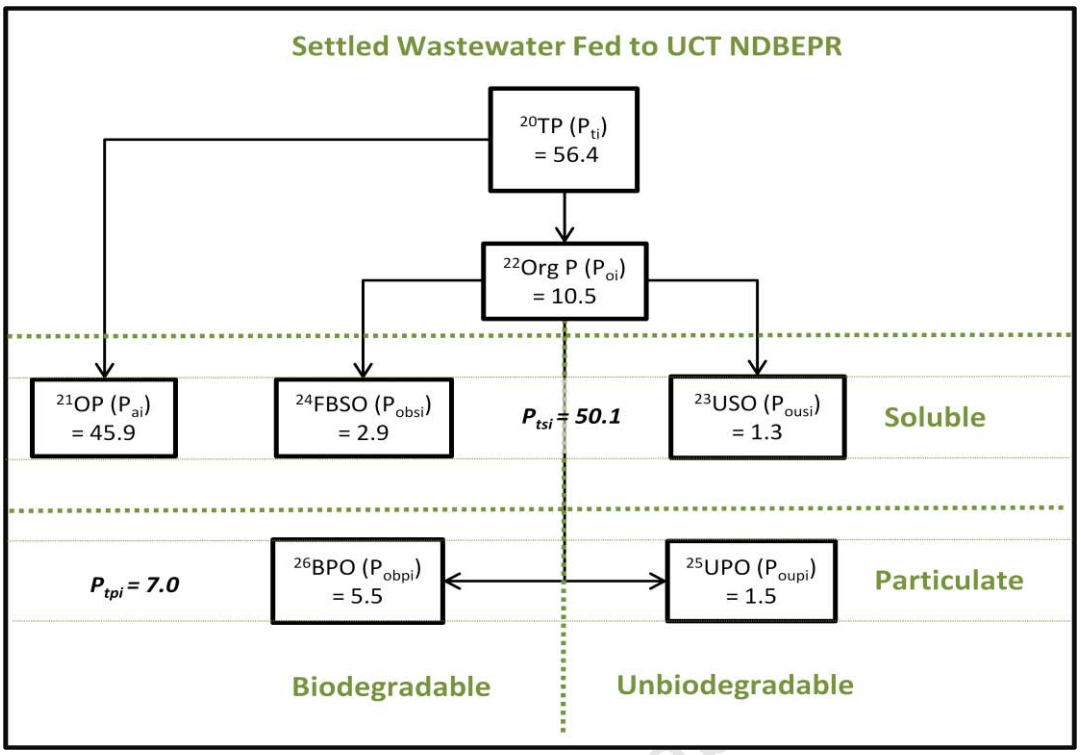

Figure 5.4.4a: *The phosphorus (P) characteristics for settled wastewater fed to the UCT MBR system, all values in mgP/l.*

Table 5.4.4.c: Influent Phosphorus (P) Characterization												
	[a]Test period	$^{20}P_{ti}$	$^{m}P_{tsi}$	$^{d}N_{tpi}$	$^{21}P_{ai}$	$^{22}P_{oi}$	$^{23}P_{ousi}$	$^{24}P_{obsi}$	$^{25}P_{oupi}$	$^{26}P_{obpi}$	$^{23+25}P_{oui}$	$^{24+26}P_{obi}$
Primary Sludge (PS)	1	171.3	34.5	136.8	23.6	147.7	1.2	9.7	71.1	89.3	72.2	99.1
	2	221.5	32.9	188.6	25.9	195.6	7.0	0.0	252.9	0.0	259.8	0.0
	3	190.5	40.4	150.0	23.0	167.4	0.4	17.0	202.0	0.0	202.4	17.0
	4	192.6	30.7	161.9	22.8	169.9	1.7	6.2	93.5	91.2	95.2	97.4
	5	73.9	20.0	53.8	19.5	54.4	0.6	0.0	45.2	28.1	45.7	28.1
	Average	169.9	31.7	138.2	22.9	147.0	2.2	6.6	132.9	41.7	135.1	48.3
	Fraction	1.00	0.19	0.81	0.14	0.86	0.01	0.04	0.78	0.25	0.79	0.28
Raw WW to MLE 2	1	22.4	17.0	5.4	15.4	7.0	0.7	0.9	3.7	1.6	4.4	2.6
	2	21.5	15.5	6.0	14.6	6.8	0.6	0.2	4.8	1.2	5.4	1.5
	3	23.9	16.1	7.8	13.8	10.1	1.0	1.4	4.0	3.8	5.0	5.2
	4	20.1	14.8	5.2	13.7	6.3	0.8	0.4	4.2	1.0	5.0	1.4
	5	18.7	15.3	3.3	13.6	5.1	0.4	1.4	2.8	0.5	3.2	1.9
	Average	21.3	15.7	5.6	14.2	7.1	0.7	0.8	3.9	1.6	4.6	2.5
	Fraction	1.00	0.74	0.26	0.67	0.33	0.03	0.04	0.18	0.08	0.22	0.12
Settled WW to MLE 1	1	16.4	15.5	0.9	14.3	2.1	0.6	0.6	0.5	0.3	1.2	0.9
	2	16.0	15.0	0.9	14.4	1.6	0.4	0.2	1.1	0.0	1.6	0.2
	3	16.7	13.6	3.1	11.3	5.4	0.9	1.3	0.3	2.8	1.2	4.2
	4	13.2	12.1	1.1	11.2	2.0	0.7	0.2	1.0	0.1	1.7	0.3
	5	15.1	14.4	0.8	12.9	2.2	0.3	1.1	0.6	0.2	0.9	1.3
	Average	15.5	14.1	1.4	12.8	2.7	0.6	0.7	0.7	0.7	1.3	1.4
	Fraction	1.00	0.91	0.09	0.83	0.17	0.04	0.04	0.05	0.04	0.09	0.09
Settled WW to NDBEP R	1	57.0	53.7	3.3	50.1	6.8	0.4	3.1	3.1	0.2	3.5	3.4
	2	55.6	38.0	17.6	35.1	20.5	0.9	2.0	4.6	12.9	5.5	14.9
	3	55.3	51.6	3.8	42.4	13.0	3.1	6.1	3.5	0.3	6.5	6.4
	4	59.0	54.0	5.1	50.3	8.7	0.6	3.1	3.5	1.6	4.1	4.6
	5	55.1	53.3	1.8	51.6	3.6	1.8	0.0	2.6	2.6	4.4	2.6
	Average	56.4	50.1	6.3	45.9	10.5	1.3	2.9	3.5	3.5	4.8	6.4
	Fraction	1.00	0.89	0.11	0.81	0.19	0.02	0.05	0.06	0.06	0.09	0.11

[a] – See Tables 4.1a and b for the time-line with the dates and sewage batch that correspond to the indicated test period, also included are appendix reference numbers for day to day results

[m] – Indicates total soluble P, which is measured from filtered influent sample

[d] – Indicates the total particulate P, which is obtained by $P_{ti} - P_{tsi}$

[20] to [26] – Reference to the corresponding characteristics in the block diagrams of Figures 5.4.4a, b and c

5.4.5 Elemental Compositions of Influent Wastewater Characteristic Components

Each of the influent characteristic components, quantified in the above section 5.4.4, are transformed into their carbon (C), hydrogen (H), oxygen (O), nitrogen (N) and phosphorus (P) elemental compositions in the form $C_XH_YO_ZN_AP_B$, with the various molar units X, Y, Z, A and B calculated from the determined concentrations (shown in Tables 5.4.2 to 5.4.4c above). The calculation of the elemental composition of the different influent and WAS organics is required for the CHONP, COD and charge mass balance AD model. The elemental compositions of the influent organic components not transformed to other organic types by the various biological or chemical processes (e.g. UPO, USO and residual BPO), remain unchanged throughout the plant (provided the unbiodegradable organics from the AS system do not become biodegradable in the AD). The elemental composition of the influent components that are transformed to other AS organic types (like OHO and PAO biomass) are strictly not required to be known but the elemental composition of the organics that are produced is required to be known for the subsequent AD. The elemental compositions of the AS organic types are calculated from COD/VSS (f_{cv}), TOC/VSS (f_c), N/VSS (f_n) and P/VSS (f_p) ratios of the aerobic reactor VSS because the sludge, which is wasted from the AS system to maintain the system R_s, is fed as influent to the AD and is transformed in AD to AD biomass, methane and other non-COD containing products. The Table 5.4.5 below lists the elemental compositions of the influent characteristic components, obtained for the Test period 1 (using sewage batch 14) of the experimental research period, with the molar quantities (i.e. X, Y, Z, A and B of $C_XH_YO_ZN_AP_B$) highlighted. The method for calculating these elemental compositions is outlined below.

Table 5.4.6: NDBEPR AS System Influent Elemental Composition for Test Period 1								
	UPCOD		USCOD		AMMONIA		Ortho-Phosphate	
	mg/*l* (conc.)	mg/d (flux)	mg/*l* (conc.)	mg/d (flux)	mg/*l* (conc.)	mg/d (flux)	mg/*l* (flux	mg/d (flux)
COD	139.1	20861.1	29.4	4408.3	0.0	0.0	0.0	0.0
TOD	155.0	23246.1	31.3	4696.2	156.9	23531.8	0.0	0.0
Carbon (C)	49.5	7426.5	10.1	1511.9	0.0	0.0	0.0	0.0
Hydrogen (H)	5.9	879.4	1.4	208.8	9.8	1471.2	1.6	242.6
Oxygen (O)	35.8	5370.3	8.4	1261.7	0.0	0.0	103.5	15525.1
Nitrogen (N)	3.5	521.9	0.4	63.0	34.3	5149.2	0.0	0.0
Phosphorous (P)	1.5	222.2	0.4	59.2	0.0	0.0	50.1	7520.0
Metal (Me)	0.0	0.0	0.0	0.0	0.0	0.0	0.0	0.0
MM	96.1	4.9	20.7	4.2	44.1	0.0	148.8	0.0
COD/MM (f_{cv})	1.5	7.0	1.4	7.0	0.0	4.0	0.0	1.0
TOC/MM (f_c)	0.5	2.7	0.5	2.6	0.0	0.0	0.0	4.0
TKN/MM (f_n)	0.0	0.3	0.0	0.2	0.8	1.0	0.0	0.0
TP/MM (f_p)	0.0	0.1	0.0	0.1	0.0	0.0	0.3	1.0
Me/MM	0.00		0.0	0.0	0.0	0.0	0.0	0.0
	SBCOD		FRBCOD		HAC		Total	
	mg/*l* (conc.)	mg/d (flux)	mg/*l* (conc.)	mg/d (flux)	mg/*l* (conc.)	mg/d (flux)	mg/*l* (conc.)	mg/d (flux)
COD	329.7	49447.4	92.4	13854.7	200.0	30000.0	790.5	118571.5
TOD	345.4	51803.3	107.6	16138.8	200.0	30000.0	996.1	149416.3
Carbon (C)	104.3	15647.9	30.6	4585.7	75.0	11250.0	269.5	40422.0
Hydrogen (H)	16.0	2392.6	4.5	675.4	12.5	1875.0	51.6	7745.0
Oxygen (O)	72.6	10893.7	23.5	3526.3	100.0	15000.0	343.9	51577.1
Nitrogen (N)	3.4	515.5	3.3	499.8	0.0	0.0	45.0	6749.4
Phosphorous (P)	1.8	275.9	3.1	469.6	0.0	0.0	57.0	8546.8
Metal (Me)	0.0	0.0	0.0	0.0	0.0	0.0		**Key**
MM	198.2	3.8	65.1	4.0	187.5	3.5		X
COD/MM (f_{cv})	1.7	7.0	1.4	7.0	1.1	7.0		Y
TOC/MM (f_c)	0.5	2.0	0.5	2.3	0.4	3.5		Z
TKN/MM (f_n)	0.0	0.1	0.1	0.4	0.0	0.0		A
TP/MM (f_p)	0.0	0.0	0.1	0.2	0.0	0.0		B
M/MM	0.0		0.0		0.0			q

In determining the component elemental formulations, as in the example above, the known COD, carbon, nitrogen and phosphorus concentrations and the mass

concentration (mg/*l* influent) for each characteristic component is calculated by dividing the obtained COD values by their corresponding f_{cv} values.

The total oxygen demand (TOD) for each characteristic component is the total electron donating capacity (EDC) of the organics, which includes the EDC of the N part of the organics when oxidized to nitrate. In nitrification, two oxygen molecules (with a molecular mass of 64gO) are required to accept the eight electrons donated by one mole of ammonia (with an atomic mass of 14gN) when oxidized to nitrate. Therefore, the TOD is calculated using the expression below:

$$TOD = COD + \left(\frac{64}{14}\right).TKN \qquad (5.4.4)$$

Each organic type in the influent (VFA, FBSO, USO, UPO and BPO) comprises carbon, hydrogen, oxygen, nitrogen and phosphorus, which give it a representative generic empirical formula of $C_XH_YO_ZN_AP_B$. If the Y value is equated to 7, the other molar quantities of this generic organic (i.e. X, Z, A and B) can be calculated with respect to this value[1] for each specified influent sewage organic type, using the following Equations 5.4.5 to 5.4.8 (see Appendix 2 for the detailed derivation) in terms of the organic types f_{cv}, f_c, f_n and f_p mass ratios[1].

$$X = \frac{C}{MM}.\frac{(Y+16Z)}{12.\left[1-\left(\frac{C}{MM}\right)-\left(\frac{N}{MM}\right)-\left(\frac{P}{MM}\right)\right]} \qquad (5.4.5)$$

$$Z = \frac{Y}{2}.\frac{\left[1-\left(\frac{COD}{8.MM}\right)-\left(\frac{8.C}{12.MM}\right)-\left(\frac{17.N}{14.MM}\right)-\left(\frac{26.P}{31.MM}\right)\right]}{\left[1+\left(\frac{COD}{MM}\right)-\left(\frac{44.C}{12.MM}\right)+\left(\frac{10.N}{14.MM}\right)-\left(\frac{71.P}{31.MM}\right)\right]} \qquad (5.4.6)$$

$$A = \frac{N}{MM} \cdot \frac{(Y + 16Z)}{14.\left[1 - \left(\frac{C}{MM}\right) - \left(\frac{N}{MM}\right) - \left(\frac{P}{MM}\right)\right]}$$

(5.4.7)

$$B = \frac{P}{MM} \cdot \frac{(Y + 16Z)}{31.\left[1 - \left(\frac{C}{MM}\right) - \left(\frac{N}{MM}\right) - \left(\frac{P}{MM}\right)\right]}$$

(5.4.8)

Using the characterization methods shown in Table 5.4.1b to get the f_{cv} (or COD/MM), f_n (N/MM), f_p (P/MM) and f_c (C/MM) ratios, together with the above Equations 5.4.5 to 5.4.8 the elemental formulations of the influent organics could be calculated. On average, the influent PS had calculated generic unbiodegradable and biodegradable particulate organic elemental formulations of $C_{1.0}H_{1.32}O_{0.44}N_{0.1}P_{0.04}$ and $C_{1.0}H_{2.19}O_{0.65}N_{0.06}P_{0.01}$ respectively.

After obtaining the X, Y, Z, A and B values of the organic generic formula, the hydrogen (H) and oxygen (O) could be calculated by multiplying their molar fractions by the concentration of VSS, which was the total mass of particulate organics per unit volume (Equations 5.4.9 and 5.4.10).

$$H = \frac{MM \cdot Y}{(Y + 12X + 16Z + 14A + 31B)}$$

(5.4.9)

$$O = \frac{MM \cdot 16 \cdot Z}{(Y + 12X + 16Z + 14A + 31B)}$$

(5.4.10)

---

[1] - *$C_XH_YO_ZN_AP_B$ can also be expressed as $C_{fc/12}H_{fH/1}O_{fO/16}N_{fn/14}P_{fp/31}$ and if the composition needs to be expressed in terms of C = 1 rather than Y = 7 then it can be simply found from $C_1H_{Y/X}O_{Z/X}N_{A/X}P_{B/X}$.*

5.5 CHARACTERISATION OF WASTE ACTIVATED SLUDGE

As already described in Section 2.3.2.2 of Chapter 2, an AS system treating municipal wastewaters has a mixed culture of organism groups that fulfil a particular function in the AS system, which occur together with the unbiodegradable organics to make up the WAS mixed liquor volatile settleable solids (MLVSS). The mixed liquor suspended solids (MLSS) comprises inorganic settleable solids (ISS) and the volatile settleable solids (VSS). In WAS characterisation, the VSS components of this mixed liquor are categorized into six groups:

1. Phosphorous accumulating organism (PAO) active biomass, denoted as X_{BG}, which mediate BEPR and removal of some influent organics. The determination of PAO biomass concentrations in the MLSS is as shown in Equation 5.3.1c.
2. The endogenous residue of the PAOs, which can be calculated using Equation 5.5.1 below.

$$X_{EG} = f_{EG} \cdot b_G \cdot X_{BG} \cdot R_s \qquad (5.5.1)$$

3. Ordinary heterotrophic organism (OHO) biomass, mediating denitrification and removal of the remaining organics. The OHO biomass concentration is determined as shown in Equation 5.3.1d.
4. The endogenous residue of the OHOs, which is calculated using Equation 5.5.2 below.

$$X_{EH} = f_{EH} \cdot b_G \cdot X_{BH} \cdot R_s \qquad (5.5.2)$$

5. Autotrophic nitrifying organisms (ANOs) active biomass, mediating nitrificationand their endogenous residue (ANO ER): These are relatively small in concentration (<2% of VSS) and hence, since disaggregating the

measured organics (VSS) into the five major components was already complicated enough, they are not included as separate components of the WAS during the characterisation process. However, they are they are lumped together with the much higher OHO and PAO organism concentrations and are also included in the WWTP models.

6. Inert material from the influent, which remains and accumulates in the AS reactor(s) in proportion with sludge age. The concentration of this inert material (X_i) in the AS reactor MLSS is calculated as shown in Equation 5.5.3 below.

$$X_I = \frac{\left(\frac{\left(FS_{ti} \cdot R_s \cdot f_{S'up}\right)}{f_{cv}}\right)}{V_{AS}} \quad (5.5.3)$$

All of the above organism groups (OHO, PAO and ANO) exist in NDBEPR AS systems. However, the PAOs (i.e. X_{BG} (mgPAOVSS/*l*) and X_{EG} (in mgERVSS/*l*)) are usually excluded from fully aerobic ND systems, since the conditions are not favourable to their growth and metabolism. Further descriptions of the above-mentioned WAS organism groups (OHOs, PAOs and their endogenous residues) and their various interactions can be found in Section 2.3.2.2 (in Chapter 2).

Since the sludge wasted from the AS system is fed to the AD system, the AS systems were operated at a sludge age of ten days to allow for the wastage of a sufficient quantity of active biomass (X_{BH} and X_{BG}). This was necessary because the active biomass is the only biodegradable particulate organics to be utilized by the anaerobic bacteria in the AD. The remaining particulate fraction of the waste sludge is deemed to be 'unbiodegradable' (X_{EH} (mgERVSS/*l*), X_{EG} (mgERVSS/*l*) and X_i (mgUPOVSS/*l*)). Since the sludge is wasted from the aerobic reactor, which is the final treatment stage of the AS system, the dissolved concentrations in the waste sludge are taken to have the same concentrations as those measured

in the treated effluent of this system. Moreover, with the operation of all three AS systems at a sludge age of ten days, the dissolved fraction of the WAS (AS system effluent) can be accepted to comprise only unbiodegradable soluble COD (S_{use}) and very low free and saline ammonia (FSA), because complete nitrification took place at all times. However, complete denitrification, and complete P removal did not take place but this was accepted because it was a project requirement to obtain a greater quantity of active mass for AD than to produce a very good effluent quality in terms of nitrate and phosphate.

Apart from the above-mentioned six organic components of WAS VSS, the MLSS includes inorganic suspended solids (ISS). This reactor ISS arises from influent ISS accumulation and biomass intracellular dissolved solids that precipitate as ISS in the drying step of TSS procedure. The total ISS concentration at various stages of the WWTP can be measured directly. Further descriptions on how the ISS is made up in the AS system has been explained in Chapter 2. It has been noted that the PAOs in NDBEPR systems take up phosphate to make polyphosphate (PP) chains that are inorganic and increase the ISS content of the PAOs up to nine times higher than that of OHOs.

This aspect was investigated by Ekama and Wentzel (2004) who developed a linear relation between the P and ISS contents of PAOs:

$$f_{iPAO} = f_{iOHO} + 3.286 \cdot (f_{XBGP} - f_{pOHO}) \quad (5.5.4)$$

Where

- The 3.286 is the ISS content of PP (as mgISS/mgP),
- f_{XBGP} is the P content of PAOs (as mgP/mgPAOVSS)
- f_{pOHO} is the mgP/mgVSS, for OHO's (i.e. ≈ 0.03mgP/mgOHOVSS)

Table 5.4.6 lists the WAS obtained during the experimental research period by reconciling the calculated VSS with that which was calculated with Equations 5.2.1 to 5.2.4.

Table 5.5.1: Nutrient Removal Systems Waste Activated Sludge Characteristics

	Exp. Period [a]	X_{BG} (mgPAO/*l*)	X_{EG} (mgER/*l*)	PP (mgP/*l*)	X_{BH} (mgOHO/*l*)	X_{EH} (mgER/*l*)	X_i (mgVSS/*l*)	X_V (mgVSS/*l*)	X_{IO} (mgISS/*l*)	X_T (mgTSS/*l*)	f_{vaer} Ratio (VSS_{aer}/VSS_{AS})
MLE 2 AS System	1	0	0	0	970	470	894	2334	519	2853	1.0
	2	0	0	0	938	456	949	2342	513	2855	1.0
	3	0	0	0	919	445	871	2235	385	2619	1.0
	4	0	0	0	797	392	897	2087	459	2545	1.0
	5	0	0	0	879	429	733	2040	549	2589	1.0
MLE 1 AS System	1	0	0	0	1226	601	270	2097	452	2549	1.0
	2	0	0	0	1178	574	429	2181	447	2628	1.0
	3	0	0	0	1284	632	127	2043	443	2486	1.0
	4	0	0	0	1090	531	442	2063	462	2525	1.0
	5	0	0	0	1143	552	312	2007	417	2424	1.0
UCT NDBEPR AS System	1	1873	186	545	871	416	1914	5261	1658	6919	1.3
	2	1695	166	429	945	444	2295	5545	1935	7480	1.3
	3	1562	163	431	1121	562	1822	5229	2301	7530	1.3
	4	1809	181	462	778	374	1930	5073	2424	7498	1.3
	5	1543	154	547	943	451	1783	4873	1641	6514	1.3

a - See Tables 4.1 a and b for the time-line with the dates and sewage batch that correspond to the indicated test period, also included are appendix reference numbers for day to day results.
The X_{IO} (ISS) concentrations were obtained with Equations 5.5.3 and 5.5.4.

In an AS system that is at steady state and operated at a sludge age of more than 3 days, the influent unbiodegradable soluble material that is retained in the system with HRT is usually the main soluble component of the WAS mixed liquor. The FRBCOD may also contribute a relatively small (usually negligible) fraction of this total soluble mixed liquor COD. Therefore, COD in the effluent is usually taken to be unbiodegradable, but the FRBCOD (S_{bsfml}) can be calculated using the Equation 5.5.5 below:

$$S_{bsfml} = \frac{1}{\left(\frac{(Y_H \cdot R_s)}{(1 + R_s \cdot b_H)} \cdot k_v \right)} \qquad (5.5.5)$$

Where k_v is the rate of substrate (S_{bsf}) utilization, which was measured by Marais and Ekama (1976) to be about 108 *l*/mgOHOVSS/d.

5.5.1 The Determination of Polyphosphate Concentrations in PAOs

Unlike ND or fully aerobic AS systems, where the P content is a small part of the biomass (≈0.03 mgP/mgOHOVSS), NDBEPR AS systems contain PAOs, which store significant quantities of phosphorus. Apart from the organic P that is a part of all the AS organism biomass (both OHOs and PAOs), the PAOs are able to store P internally as chains of PP, a high-energy storage molecule. Thus P is removed from the AS system when sludge is wasted from the aerobic zone of the NDBEPR system, when the P uptake process is complete. This is because it is in the aerobic zone that PAOs take up the phosphorus and store it as PP. This PP content has to be included as a characteristic of the WAS, that is fed as influent to the AD, as it has a profound influence on the AD stoichiometry and weak acid/base chemistry, when released into the AD liquor. The total P removed by the AS system is the P bound in the 5 VSS components of the WAS and at steady state is equal to the difference between the influent and effluent P as shown in Equation 5.5.6 below:

$$P\ removed = P_{ti} - P_{te} = \frac{1}{R_s \cdot Q_i} \cdot \left(f_{XBGPP} \cdot MX_{BG} + f_p \cdot MX_V \right) \tag{5.5.6}$$

Where:

- f_{xBGPP} is the PP content of the PAOs (mgP/mgPAOVSS).
- f_p is the Org P content of the 5 VSS components.

With experiments performed on the ND systems (containing OHOs only) it was possible to measure the Org P fraction of the P VSS mass (X_{BH} + X_{EH} +X_I) excluding the PP containing PAOs and their endogenous residue by calculating the organic particulate P content of the VSS:

$$f_p = \frac{(TP - OP)_{aer}}{VSS_{aer}} \tag{5.5.7}$$

Where:

- f_P is the organic P content of OHOs (X_{BH}), their endogenous residue (X_{EH}) and the UPO VSS from the influent (X_I) and
- $(TP - OP)_{aer}$ the total P (unfiltered) and OP (filtered) concentrations in the aerobic reactor of the MLE systems.

The f_P value is usually about 0.03 mgP/ mgVSS.

Equation 5.5.6 can also be written as:

$$P_{removed} = \left(\frac{1}{(R_s \cdot Q_i)}\right) \cdot \left(\left(MX_{BG} \cdot f_{XBGP}\right) + \left(f_{pOHO} \cdot \left(MX_{BG} + MX_{EG} + MX_{EH} + MX_I\right)\right)\right) \quad (5.5.8)$$

Where:

f_{XBGP} is the total P content of PAOs $= f_{XBGPP} + f_{pPAO}$, (5.5.9)

f_{pOHO} is the P content of other VSS components. The Org P content of the PAOs (f_{pPAO}) is equal to that of the OHOs (f_{pOHO}).

$$Then: f_{XBGP} = \frac{\left(P_{removed} \cdot R_s \cdot Q_i\right) - \left(f_{pOHO} \cdot \left(MX_i + MX_{BH} + MX_{EH} + MX_{EG}\right)\right)}{MX_{BG}} \quad (5.5.10)$$

The PP has an elemental composition of $_q(MePO_3)$, where Me is the sum of metallic atoms of magnesium (Mg), potassium (K) and calcium (Ca) and q is the factor that links the PAO concentration to PP concentration, hence giving the PAO elemental composition of $C_XH_YO_ZN_AP_{B\cdot q}(MePO_3)$. Therefore, the difference in influent and effluent measured Mg, K and Ca concentration is equal to the quantity taken up in the formation of the PP mass.

To know the molar mass of PP, the molar ratio of each metallic component of PP (e.g. Mg) to P is first calculated as shown in Equation 5.5.11 below:

$$\frac{Mg_{mol}}{P_{mol}} = \frac{\left(\frac{Mg_{polyP}}{24.305}\right)}{\left(\frac{P_{polyP}}{30.974}\right)},$$

(5.5.11)

where the 24.305 and 30.974 in the above Equation 5.5.11, are the relative atomic masses of Mg and P respectively.

However, PP is a stable molecule so the total Me^{+} should have a charge of +1 to balance the charge of PO_3 of -1. Therefore, the sum of the molar fractions of each metal component should be 1 (i.e. $2\cdot\frac{Mg}{P}+\frac{K}{P}+2\cdot\frac{Ca}{P}=1$) and if it is not 1, it can be corrected by dividing it by the total metallic charge per mol of P in PP,

i.e. $$Corrected\ \frac{Mg_{mol}}{P_{mol}} = \frac{\left(\frac{Mg_{mol}}{P_{mol}}\right)}{\left[\frac{\left(\frac{2\,Mg}{24.305}+\frac{K}{39.098}+\frac{2Ca}{40.078}\right)}{\left(\frac{P_{polyP}}{30.974}\right)}\right]}.$$

(5.5.12)

After the above calculations the sum of metallic atoms and oxygen atoms per mol of P in PP are known. Therefore, we can calculate the resultant mass concentration of PP by dividing the concentration of P in PP, which was determined using Equation 5.5.12 above, by the molar fraction of this P to PP i.e.:

$$Mass\_Conc._{PolyP} = \frac{P_{polyP}}{\left[\frac{30.974}{30.974+\left(24.305\cdot\frac{Mg_{mol}}{P_{mol}}\right)+\left(39.098\cdot\frac{K_{mol}}{P_{mol}}\right)+\left(40.078\cdot\frac{Ca_{mol}}{P_{mol}}\right)+(3\cdot 16)}\right]}$$

(5.5.13)

Where 39.098, 40.078 and 16 are the atomic masses of K, Ca and oxygen (O) respectively and 3 atoms of O are linked to one atom of P in PP.

The corrected Me^{+} concentration in PP is then calculated by multiplying the corrected molar fraction of total Me in PP by the molar mass, determined using Equation 5.5.13 above i.e.:

$$Me_{polyP} = MolarMass_{PolyP} \cdot \frac{\left[\left(24.305 \cdot \frac{Mg_{mol}}{P_{mol}}\right) + \left(39.098 \cdot \frac{K_{mol}}{P_{mol}}\right) + \left(40.078 \cdot \frac{Ca_{mol}}{P_{mol}}\right)\right]}{\left[30.974 + \left(24.305 \cdot \frac{Mg_{mol}}{P_{mol}}\right) + \left(39.098 \cdot \frac{K_{mol}}{P_{mol}}\right) + \left(40.078 \cdot \frac{Ca_{mol}}{P_{mol}}\right) + (3 \cdot 16)\right]} \quad (5.5.14)$$

Similarly, the oxygen in PP is obtained by multiplying its molar fraction in PP by the molar mass of PP. i.e.:

$$O_{polyP} = MolarMass_{PolyP} \cdot \frac{[3 \cdot 16]}{\left[30.974 + \left(24.305 \cdot \frac{Mg_{mol}}{P_{mol}}\right) + \left(39.098 \cdot \frac{K_{mol}}{P_{mol}}\right) + \left(40.078 \cdot \frac{Ca_{mol}}{P_{mol}}\right) + (3 \cdot 16)\right]} \quad (5.5.15)$$

Because PP is not a part of the cell biomass, it is released a lot faster than the organic P during anaerobic digestion. The release of PP in AD is described in more detail in Section 6.3 of Chapter 6 .

5.5.2 Sludge Characterisation

The sludge to be fed to the AD is characterized and defined according to the representative generic organic material formula, given as $C_XH_YO_ZN_AP_B$, as input to the AD predictive mass balance based mathematical model. In this case, the carbon, hydrogen, oxygen, nitrogen and phosphorus content, i.e. X, Y, Z, A and B in $C_XH_YO_ZN_AP_B$ of the particulate organics is calculated using Equations 5.4.5 to 5.4.8, but with the molar mass equivalently substituted with the volatile settleable solids concentration. For instance, X is calculated by:

$$X = \frac{C}{VSS} \cdot \frac{(Y + 16Z)}{12.\left[1 - \left(\frac{C}{VSS}\right) - \left(\frac{N}{VSS}\right) - \left(\frac{P}{VSS}\right)\right]}$$

(5.5.16)

Since the atoms of P in each $C_XH_YO_ZN_AP_B$ molecule are known (i.e. the quantity of B), q as the factor linking the biomass PAO to PP in $C_XH_YO_ZN_AP_{B \cdot q}(Mg_cK_dCa_ePO_3)$, can be determined by multiplying this value of B to the ratio of f_{XGBP} to f_{pOHO}, i.e.:

$$q = B \cdot \frac{f_{XBGP}}{f_{P_{OHO}}}$$

(5.5.17)

The methods used in determining the sludge characteristics are shown in Table 5.5.2 and an example of the way in which these characteristics were presented (for the test period 1, i.e. the same period as the influent characteristics of Table 5.4.6) are as shown below (Table 5.5.3):

Table 5.5.2: Methods used in Determination of WAS Characteristics			
No.	**Name**	**Denotation**	**Determination Method**
1	Total	S_{tml}	Unfiltered COD test on WAS (Open flux method)
2	VFA	S_{bsaml}	5-point titration = 64/60 mgHAc/*l* on filtered* AS system effluent
3	FBSO	S_{bsfml}	Using Equation 5.5.5
4	USO	S_{usml}	COD test on filtered* AS system effluent (i.e. S_{usml} =S_{use})
5	UPO	$S_{up\text{-}WAS}$	[1]Using Equation.5.3.1b
6	BPO	S_{bpml}	[1]Using Equations 5.3.1c and d
7	Total	C_{tml}	By the addition of all C characteristic components
8	VFA	C_{bsaml}	5-point titration = 24/60 mgHAc/*l* on filtered sample (or AS system effluent)
9	FBSO	C_{bsfml}	Using f_{cv} = 1.42 and f_c = 0.487, from Brink and Ekama (2008)
10	USO	C_{usml}	Using f_{cv} = 1.42 and f_c = 0.47, from Brink and Ekama (2008)
11	UPO	C_{upml}	Using f_{cv} =1.48 and f_c = 0.515, from Poinapen and Ekama (2010)
12	BPO	C_{bpml}	Using f_{cv} from measured values in of COD and VSS in mixed liquor and f_c = 0.515, from Wentzel *et al.* (2006)
13	Total	N_{tml}	TKN test on WAS (micro-Kjeldahl method)
14	FSA	N_{aml}	FSA test (titrimetric method) on filtered* AS system effluent
15	Org N	N_{oml}	N_{aml} deducted from N_{tml}
16	USO	N_{ousml}	AS system effluent filtered* (TKN - FSA) test result
17	FBSO	N_{obsml}	Multiplying the N_{obsi}/S_{bsfi} ratio (with values found using methods in Table 5.4.1a) to S_{bsfml}
18	UPO	N_{oupml}	$f_n \times S_{up\ WAS} / f_{cv}$, where f_n and f_{cv} are the ratios measured on the effluent of the WAS AD operated at the long 60 day R_s
19	BPO	N_{obpml}	$N_{tpml} – N_{oupml} = N_{tml} - N_{tsml} - N_{oupml}$, where $N_{tsml} = N_{ousml}+N_{obsml}+N_{aml}$
20	Total	P_{tml}	Unfiltered TP test on WAS (Sulphuric acid/Persulphate digestion at 100°C followed by OP test)
21	OP	P_{aml}	OP test (Molybdate vanate colour development) on filtered*effluent
22	Org P	P_{oml}	OP deducted from P_{tml}

Table 5.5.2: Methods used in Determination of WAS Characteristics			
No.	**Name**	**Denotation**	**Determination Method**
23	USO	P_{ousml}	AS system effluent filtered* (TP - OP) test result
24	FBSO	P_{obsml}	Multiplying the P_{obsi}/S_{bsfi} ratio (with values found using methods in Table 5.4.1a) to S_{bsfml}
25	UPO	P_{oupi}	$f_p \times S_{up\ WAS} / f_{cv}$, where f_p and f_{cv} are the ratios measured on the effluent of the WAS AD operated at the long 60 day R_s
26	BPO	P_{obpi}	$P_{bi} - P_{oupi} = P_{ti} - P_{tsi} - P_{oupi}$, where $P_{tsml} = P_{ousml}+P_{obsml}+P_{aml}$
27	TSS	X_t	Measured from AS mixed liquor samples - the total suspended solids dried at 103-105 °C
28	VSS	X_v	Measured from AS mixed liquor samples -the volatile suspended solids ignited at 600°C
29	ISS	X_i	Calculated from ISS = TSS-VSS.
filtered* - means sample filtered through Schleicher & Schull ME 25/21 0.45 micrometer membrane filters			
1 - Influent BPO assumed to equal zero for SS AS system operation of 10 day R_s (Ekama and Marais, 1976). The BPO is mainly from active organisms present in mixed liquor (i.e. OHOs and PAOs, see Sections 5.3 and 5.5).			

Table 5.5.3: Waste Activated Sludge Elemental Composition (Aerobic) for Test Period 1								
Unbiodegradable Organics	UPCOD		USCOD			FRBCOD		
	mg/*l* (conc.)	mg/d (flux)	mg/*l* (conc.)	mg/d (flux)			mg/*l* (conc.)	mg/d (flux)
COD	3642.1	20760.0	29.4	167.5		COD	0.0	0.0
TOD	4058.5	23133.4	31.3	178.5		TOD	0.0	0.1
Carbon (C)	1267.4	7223.9	10.1	57.5		Carbon (C)	0.0	0.0
Hydrogen (H)	42.6	243.0	1.4	7.9		Hydrogen (H)	0.0	0.0
Oxygen (O)	260.3	1483.7	8.4	47.9		Oxygen (O)	0.0	0.0
Nitrogen (N)	91.1	519.4	0.4	2.4		Nitrogen (N)	0.0	0.0
Phosphorous (P)	38.8	221.1	0.4	2.3		Phosphorous (P)	0.0	0.0
Metal (Me)	0.0	0.0	0.0	0.0		Metal (Me)	0.0	0.0
MM	2517.6	4.5	20.7	4.2		MM	0.0	4.0
COD/MM (f_{cv})	1.5	7.0	1.4	7.0		COD/MM (f_{cv})	1.4	7.0
TOC/MM (f_c)	0.5	2.5	0.5	2.6		TOC/MM (f_c)	0.5	2.3
TKN/MM (f_n)	0.0	0.3	0.0	0.2		TKN/MM (f_n)	0.1	0.4
TP/MM (f_p)	0.0	0.1	0.0	0.1		TP/MM (f_p)	0.1	0.2
Me/MM	0.o	0.0	0.0	0.0		Me/MM	0.0	0.0

Phosphorous Accumulating Organisms (PAO's)								
	Active PAO		Endogenous PAO		Polyphosphate			
PAO's	mg/*l* (conc.)	mg/d (flux)	mg/*l* (conc.)	mg/d (flux)	mg/*l* (conc.)	mg/d (flux)		
COD	3578.9	20399.8	354.9	2022.6	0.0	0.0		
TOD	5055.6	28817.1	395.4	2253.9	0.0	0.0		
Carbon (C)	1269.1	7233.9	123.5	703.8	0.0	0.0		
Hydrogen (H)	158.8	905.4	16.1	91.9	0.0	0.0		
Oxygen (O)	629.8	3589.6	93.0	530.3	1115.5	6358.2		
Nitrogen (N)	323.1	1841.9	8.9	50.6	0.0	0.0		
Phosphorous (P)	83.4	475.6	3.8	21.5	720.4	4106.3		
Metal (Me)	0.0	0.0	0.0	0.0	495.0	2821.3		**KEY**
MM	2464.3	4.7	245.3	4.5	2330.8	0.0		X
COD/MM (f_{cv})	1.5	7.0	1.5	7.0	0.0	0.0		Y
TOC/MM (f_c)	0.5	1.7	0.5	2.5	0.0	3.1		Z
TKN/MM (f_n)	0.1	1.0	0.0	0.3	0.0	0.0		A
TP/MM (f_p)	0.0	0.1	0.0	0.1	0.3	1.0		B
Me/MM	0.0	0.0	0.0	0.0	0.2	1.0		q

Ordinary Heterotrophic Organisms (OHOs)						Total		
	Active OHO		Endogenous OHO					
OHO"s	mg/*l* (conc.)	mg/d (flux)	mg/*l* (conc.)	mg/d (flux)			mg/*l* (conc.)	mg/d (flux)
COD	1664.8	9489.5	792.3	4516.3		COD	10062.4	57355.8
TOD	2351.8	13405.1	882.9	5032.6		TOD	12775.6	72820.7
Carbon (C)	590.4	3365.0	275.7	1571.5		Carbon (C)	3536.1	20155.6
Hydrogen (H)	73.9	421.2	36.0	205.2		Hydrogen (H)	328.9	1874.5
Oxygen (O)	293.0	1669.8	207.7	1184.1		Oxygen (O)	2607.7	14863.7
Nitrogen (N)	150.3	856.8	19.8	113.0		Nitrogen (N)	598.6	3384.0
Phosphorous (P)	38.8	221.3	8.4	48.1		Phosphorous (P)	913.7	5096.2
Metal (Me)	0.0	0.0	0.0	0.0		Metal (Me)	495.0	2821.3
MM	1146.3	4.7	547.7	4.5				X
COD/MM (f_{cv})	1.5	7.0	1.5	7.0				Y
TOC/MM (f_c)	0.5	1.7	0.5	2.5				Z
TKN/MM (f_n)	0.1	1.0	0.0	0.3				A
TP/MM (f_P)	0.0	0.1	0.0	0.1				B
Me/MM	0.0	0.0	0.0	0.0				q

Using the characterization methods shown in Table 5.4.5.2 to get the f_{cv} (or COD/MM), f_n (N/MM), f_P (P/MM) and f_c (C/MM) ratios, together with the above Equations 5.4.5 to 5.4.8 and 5.5.16, the elemental formulations of the influent organics are calculated and placed to give values as shown in the Table 5.5.3. However, in this thesis it was decided that the generic organic material elemental formulations, i.e. $C_XH_YO_ZN_AP_B$ is presented with the carbon component (represented by X) given a value of 1. Therefore, after determining the elemental formulations using the above methods, the X, Y, Z, A, B and q values are all divided by the X value to present the final elemental formulation., where the new X value is now equal to 1 (i.e. from X /X).

In summary, the input required for the model (steady state AD, which is presented in the following Chapter 6 and dynamic plant-wide AD, which is presented in Chapter 7) is (1) the mol/*l* BPO utilized in the AD, (2) the f_{cv}, f_c, f_n and f_P mass ratios, from which X, Y, Z, A and B are calculated, (3) the PAO PP content, f_{xBGPP} (from which q is calculated) and (4) the PP Mg, K and Ca content

(c, d, e). Noting that the VSS in the UCT system comprises 5 components, viz. OHO (X_{BH}) and PAO (X_{BG}) biomass, OHO ER (X_{EH}) and PAO ER (X_{EG}) and the unbiodegradable particulate organics (UPO) from the influent (X_I), the stoichiometric model inputs were obtained by:

1. Checking the UCT and AD system COD, N, P, Mg, K and Ca mass balances (see Section 4.4 of Chapter 4).
2. Calculating from the measured data on the AS systems the influent UPO (X_{Ii}) and active biomass (OHO and PAO) VSS concentrations (i.e. X_{BH} and X_{BG} respectively), and PAO PP content (f_{xBGPP}) from the Wentzel *et al.* (1990) BEPR model (for the calculations associated with the NDBEPR system that contains mixed cultures of OHOs and PAOs) and the Marais and Ekama (1976) model for the N removal systems (i.e. MLE 1 and MLE 2, which only contain OHO biomass). This at the same time fractionates the VSS into its five components.
3. Grouping the five VSS components into biodegradable (BPO) and unbiodegradable (UPO) particulate organics.
4. Comparing the AS system UPO VSS fraction, UPO/ (BPO+UPO) with that measured on the effluent from the AD when operated at 60d sludge age.
5. Determining the BPO utilized in the AD at different sludge ages via the BPO hydrolysis kinetics of the steady state AD model, which also yields the BPO hydrolysis kinetics rates and the average UPO fraction of the VSS across all AD sludge ages (this is done in detail in Section 6.2 of Chapter 6).
6. Calculating the mass ratios f_{cv}, f_c, f_n, f_p of the UPO VSS from the measured VSS, COD, TOC, TKN and TP concentrations on the

effluent of AD of the various sludge types operated at 60d sludge age (as shown in this Section 5.5.).

7. Calculating the mass ratios f_{cv}, f_c, f_n and f_p of the BPO VSS from the difference between the measured compositions of the AD feed particulate organics (PO) and the UPO (BPO=PO-UPO).
8. Calculating the X, Y, Z, A and B of the OHO and PAO BPO from the f_{cv}, f_c, f_n and f_p mass ratios.

From the averages of the calculated X, Y, Z, A, B, c, d and e values of $C_XH_YO_ZN_AP_{B\cdot q}(Mg_cK_dCa_ePO_3)$, the generic organic formula, determined for OHOs and PAOs in the NDBEPR system is $C_{1.0}H_{1.45}O_{0.36}N_{0.23}P_{0.03}$ and $C_{1.0}H_{1.45}O_{0.36}N_{0.23}P_{0.03}(Mg_{0.31}K_{0.31}Ca_{0.04}PO_3)_{0.19}$ respectively. That obtained for the MLE 1 and MLE 2 are $C_{1.0}$ $H_{1.46}O_{0.35}N_{0.23}P_{0.03}$ and $C_{1.0}H_{1.35}O_{0.37}N_{0.21}P_{0.03}$ respectively. The Tables 5.3.4 and 5.3.5 show the elemental formulations for the BPO and UPO of the PS and various WAS from the three AS systems, as influent to the AD.

The detailed derivation calculations for the above components of the generic WAS formula are given in Appendix 2.

Table 5.3.4: Elemental composition for Biodegradable Organics (and Polyphosphate) of Influent Sludge to AD Calculated from the AS Systems.								
Test Period			5	1	4	3	2	
Batch Number			21	14	19	17	16	
AD Sludge Age			10	18	25	40	60	**Average**
PS	BPO	X	1.00	1.00	1.00	1.00	1.00	1.00
		Y	2.55	1.71	2.30	2.31	1.93	2.19
		Z	0.76	0.45	0.74	0.72	0.55	0.65
		A	0.12	0.08	0.08	0.05	0.04	0.06
		B	0.02	0.03	0.03	0.01	0.00	0.01
	FBSO	X	1.00	1.00	1.00	1.00	1.00	1.00
		Y	1.99	1.79	1.93	1.80	1.98	1.90
		Z	0.71	0.68	0.69	0.68	0.72	0.70
		A	0.01	0.00	0.02	0.01	0.00	0.01
		B	0.00	0.02	0.01	0.02	0.00	0.01
BIOMASS	OHOs from MLE 2	X	1.00	1.00	1.00	1.00	1.00	1.00
		Y	1.29	1.45	1.30	1.34	1.39	1.35
		Z	0.47	0.37	0.37	0.35	0.31	0.37
		A	0.13	0.22	0.22	0.24	0.27	0.21
		B	0.02	0.03	0.04	0.03	0.04	0.03
	OHOs from MLE 1	X	1.00	1.00	1.00	1.00	1.00	1.00
		Y	1.60	1.40	1.39	1.52	1.40	1.46
		Z	0.39	0.35	0.36	0.33	0.33	0.35
		A	0.20	0.25	0.22	0.24	0.24	0.23
		B	0.02	0.03	0.03	0.03	0.04	0.03
	OHOs and PAOs from NDBEPR system	X	1.00	1.00	1.00	1.00	1.00	1.00
		Y	1.47	1.50	1.48	1.40	1.42	1.45
		Z	0.38	0.37	0.35	0.37	0.31	0.36
		A	0.22	0.22	0.23	0.21	0.26	0.23
		B	0.02	0.03	0.03	0.03	0.04	0.03
POLYPHOSPHATE (from NDBEPR system only)		q	0.27	0.27	0.22	0.19	0.21	0.23
		c	0.28	0.28	0.31	0.32	0.32	0.30
		d	0.35	0.35	0.33	0.30	0.32	0.33
		e	0.04	0.04	0.03	0.03	0.03	0.03

Table 5.3.5: Elemental composition for Unbiodegradable Particulate Sludge Components, Calculated from the 60 day R_s AD Systems				
Sludge Type	PS	MLE 1 WAS	MLE 2 WAS	NDBEPR WAS
Unbiodegradable Particulate Components	UPO	*UPO and ER	UPO and ER	UPO and ER
X	1.00	1.00	1.00	1.00
Y	1.32	1.51	1.48	1.42
Z	0.44	0.43	0.47	0.54
A	0.10	0.15	0.11	0.06
B	0.04	0.02	0.02	0.01
* Where UPO is the unbiodegradable particulate organics found in the sewage that is fed as a component part of primary sludge (PS) to the AD directly or gets enmeshed and accumulates in activated sludge reactors when fed as a component of influent wastewater to the AS systems (see Table 5.6).				

With the wastewater characterized, its constituent characteristics can be entered into the steady state or dynamic simulation models to be tracked through the plant processes for the prediction of plant behaviour and/or effluent quality. The Table 5.6 below shows a layout for the process reactions of the waste constituents of the AS systems linked to the AD.

Table 5.6: Layout for Process Reactions on various Waste Components of the AS linked to AD Systems in a WWTP

Influent				Activated Sludge System			Anaerobic Digestion System				
WASTEWATER CONSTITUENTS				REACTION		SLUDGE CONSTITUENTS	REACTION IN AD				AD WASTE SLUDGE & PRODUCTS
ORGANIC	Soluble	Dissolved Unbiodegradable	USO	Escapes With Effluent		USO	Escapes With Effluent				USO
		Dissolved Biodegradable	VFA / FBSO	Transforms to Active Organisms		Biomass in Reactor, All Settleable None Suspended	Death, forming BPO, which Transforms to AD Biomass	Total Settleable Solids (TSS)	Volatile Settleable Solids (VSS)		CH_4 / CO_2 / BPO / AD Biomass
	Particulate	Biodegradable Suspended / Biodegradable Settleable	BPO	Transforms to Active Organisms							
		Unbiodegradable Suspended / Unbiodegradable Settleable	UPO	Enmeshed with Sludge Mass		UPO	Enmeshed with Sludge Mass				UPO
INORGANIC	Particulate	Suspended / Settleable	ISS	Enmeshed with Sludge Mass					Inorganic Settleable Solids (ISS)		
		Precipitable	IDS[a]	Transforms to Settleable Solids			Enmeshed with Sludge Mass			R / I D S / P	
		Biologically Utilizable	IDS[a]	Transferred to Solids		ISS					ISS
		Non-precipitable	IDS[a]	Escapes With Effluent		IDS[a]	Escapes With Effluent				IDS[a]
	Soluble	Biologically Utilizable	IDS[a]	Transferred to gas	Gas						

Gas; VSS; TSS

a– IDS are inorganic dissolved solids; **R** refers to redissolution of ISS (inorganic settleable solids) to IDS and **P** refers to the precipitation of IDS back to ISS.

5.6 CLOSURE

This chapter focuses on the characterisation of the waste inputs to various unit processes of the WWTP, including the influents sewage that is treated in the AS systems and the municipal sludge of PS and/or WAS, which is to be treated in AD (or AnAerD) systems, with consideration towards these sewage or waste sludge component characteristics being used as input to the WWTP mass balance based unit process models developed in this project. The extent to which these wastes can be treated in the various unit processes of the WWTP, in terms of the biodegradability of their organics is also investigated. This included considerations on whether the unbiodegradable material from the influent wastewater and the endogenous residue generated in the AS reactors remain unbiodegradable throughout the WWTP and an assessment on whether the PS unbiodegradable organic fraction, determined in the AS systems through mass balances over the PST, correlates well with that determined from the AD system operated at a long R_s of 60 days. Foreknowledge of these aspects would greatly simplify the coupling the PST, AS and AD unit operations in plant-wide WWTP models.

In the characterisation procedure of influent sewage (PS, raw WW and settled WW) organics, their total COD was divided into the quantity that is biodegradable or unbiodegradable, and these subdivided further into soluble and particulate components, i.e. biodegradable soluble organics (BSO), unbiodegradable soluble organics (USO), biodegradable particulate organics (BPO) and unbiodegradable particulate organics (UPO). The BSO usually undergo further characterisation into those that are fermentable (FBSO) and volatile fatty acids (VFAs). Thereafter, the N and P characteristics are determined according to those that are in the inorganic soluble form (i.e. FSA and OP) and those that are bound in the various particulate and soluble organic components.

Hence the total COD, C, N and P concentrations, for the PS, raw WW and settled WW, and their fractionation into USO, BSO, BPO, UPO, FBSO, VFA, FSA and OP (where applicable) concentrations were presented in tables and block diagrams (See Tables 5.4.2 to 5.4.4 and Figures 5.4.1 to 5.4.4). Once quantified, each of the influent characteristic organic components (i.e. VFA, FBSO, USO, UPO and BPO), are transformed into their carbon (C), hydrogen (H), oxygen (O), nitrogen (N) and phosphorus (P) elemental compositions to give the elemental formula of $C_XH_YO_ZN_AP_B$, with the various molar units X, Y, Z, A and B calculated from the determined concentrations (i.e. using Equations 5.4.5 to 5.4.8).

The waste activated sludge (WAS) produced from AS systems is characterized according to five organic components of WAS VSS (i.e. OHO (X_{BH}) and PAO (X_{BG}) biomass, OHO ER (X_{EH}) and PAO ER (X_{EG}) and the UPO from the influent (X_i)) together with the inclusion of inorganic settleable solids (ISS), which adds to form the MLSS. The f_{cv}, f_c, f_n and f_p mass ratios of the five organic components are then determined from experimentally measured values and used in the calculation of X, Y, Z, A and B values for the definition of these organics according to their representative elemental formula, given as $C_XH_YO_ZN_AP_B$. The quantity of PP stored in the PAOs (f_{xBGPP}) is then calculated (see Equations 5.5.6 to 5.5.10) since they form a significant part of ISS and contain Mg, K and Ca, which when released in the subsequent AD process can be used in the formation of mineral precipitates. This PP is given an empirical composition of $q(Mg_cK_dCa_ePO_3)$, whereby q is the average molar quantity of PP stored in every PAO molecule that is determined from f_{xBGPP}. This gives the PAO an empirical composition of $C_XH_YO_ZN_AP_{B\cdot q}(Mg_cK_dCa_ePO_3)$.

In the characterization of the influent sewage and waste sludge, a number of interesting aspects were discovered:

- The unbiodegradable fraction of influent PS as calculated from the MLE systems, i.e. using mass balances over the PST, gave an average value of

0.31. This result is close to the value obtained from the AD of PS over long (60 days) sludge age (0.35). Therefore, the biodegradability of the influent is conserved throughout the WWTP, i.e. the material that is unbiodegradable in the fully aerobic or ND AS systems remains unbiodegradable in the AD systems.

- The unbiodegradable fractions of WAS from MLE 1, MLE 2 and the NDBEPR systems are 0.47, 0.62 and 0.56 respectively, which is close to the ones obtained over the AD of these WAS over a long sludge age of 60 days (0.52, 0.65, and 0.58 for AD 3, AD5 and AD 1 respectively). This indicates that the material that is unbiodegradable in the WAS is not further degraded in the AD system of the plant and thus remains conserved throughout the WWTP. However, although this aspect is also observed in the NDBEPR WAS, the influent $f_{S'up}$, which eventually gets enmeshed in the WAS, was calculated to give a significantly higher than expected value. This could mean that, for the NDBEPR AS system, if the influent $f_{S'up}$ is overpredicted, to give the right WAS $f_{S'up}$, the fraction of unbiodegradable material contained in the growing biomass (endogenous residue) of WAS or its rate of production in the AS system is underpredicted. Two possible causes for this phenomenon were presented: (1) mistaken assumptions that could have been made when allocating to the PAOs the same death regeneration unbiodegradable fraction (f_{EG} = 0.08) as for OHOs and/or the PAOs may have sequestered more of the influent biodegradable organics than the assumed RBCOD only and (2) the high influent $f_{S'up}$ in the MBR UCT system may be as a result of more unbiodegradable particulate organics (UPO) being enmeshed in the aerobic reactor (which has a higher sludge concentration and from which the waste sludge fed to the AD is taken) than the other

reactors. However, it was noted that this aspect may require further investigation, which extend beyond the scope of this research report.

- On average, the influent PS had calculated generic unbiodegradable and biodegradable organic formulas of $C_{4.9}H_7O_{2.33}N_{0.5}P_{0.13}$ and $C_{3.2}H_7O_{1.84}N_{0.4}P_{0.04}$ respectively. Moreover, the generic organic formula, determined for OHOs and PAOs in the NDBEPR system is $C_{1.0}H_{1.45}O_{0.36}N_{0.23}P_{0.03}$ and $C_{1.0}H_{1.45}O_{0.36}N_{0.23}P_{0.03}(Mg_{0.31}K_{0.31}Ca_{0.04}PO_3)_{0.19}$ respectively. Those obtained for the MLE 1 and MLE 2 are $C_{1.0}$ $H_{1.46}O_{0.35}N_{0.23}P_{0.03}$ and $C_{1.0}H_{1.35}O_{0.37}N_{0.21}P_{0.03}$ respectively.

CHAPTER 6: STEADY STATE KINETIC MODEL DEVELOPMENT

6.1. INTRODUCTION

The investigation into aspects associated with the design and operation of wastewater treatment plants (WWTPs) is driven by the need for improved use of resources in the provision of wastewater treatment facilities.

Steady state models allow for the sizing of system design parameters, such as reactor volumes and recycle flows within reasonable ranges, to provide sufficient capacity for the plant in the treatment of incoming wastewater. These estimated design parameters can then be used as input to dynamic simulation models to investigate the dynamic behaviour of the wastewater treatment system, when subjected to changing flows and material loads likely to occur during plant operation.

A steady state model for the anaerobic digestion (AD) of primary and secondary sludge from biological nutrient removal (BNR) plants treating municipal wastewater is presented. This steady state model is developed by modifying the existing steady state anaerobic digestion (AD) model for primary sludge of Sötemann *et al.* (2005). This involves adding:

1. Phosphorus (P), both organically bound (OrgP) and polyphosphate (PP) in phosphorus accumulating organisms (PAOs), into the stoichiometry.
2. The hydrolysis of WAS from nitrification-denitrification (ND) and nitrification-denitrification biological excess phosphorus removal (NDBEPR) systems to the AD model.
3. Anaerobic digestion of primary sludge (PS) and secondary sludge (or waste activated sludge, WAS) blends.

4. Mineral precipitation, in particular struvite, which involves three phase (liquid-gas-solid) mixed weak acid/base chemistry of the inorganic carbon (IC) and ortho-phosphate (OP) systems.

This will extend the steady state AD model to the greater capacity required to deal with the main types of municipal sludges thereby extending the plant-wide WWTP steady state model of Ekama (2009) to:

1. Predict the release of N and P in AD of PS and WAS from ND or NDBEPR activated sludge (AS) systems.
2. Optimizing plant operation procedures to minimize effluent N and P concentrations.
3. Tracking the various compounds and elements (C, H, O, N, P, Mg, Ca and K) through the unit operations of the WWTP and identifying areas where mineral precipitation problems can occur.

In the steady state AD model of Sötemann *et al.* (2005) the hydrolysis of the three different organic materials (proteins, carbohydrates and lipids) of the International Water Association (IWA) ADM1 model (Batstone *et al.*, 2002) was modified to a single hydrolysis process acting on a generic particulate biodegradable organic material representing sewage sludge i.e. $C_XH_YO_ZN_A$. With complex organics, like in WWTP sludges, the hydrolysis process is the rate-limiting step so that the AD processes that follow it, being much faster, are dealt with stoichiometrically to yield the digester end products, i.e. biomass, CH_4, CO_2 (dissolved HCO_3^- and gaseous CO_2) and water. Thus, the extended steady state (SS) model will also comprise three sequential parts:

1. A COD based kinetic part from which the concentration of biodegradable COD utilization and methane and sludge production are determined for a given AD sludge age (which is also equal to hydraulic retention time for flow through ADs).

2. A COD, C, H, O, N, P and charge mass balance stoichiometry part from which gas production and composition (or partial pressure of CO_2), NH_4^+ released, biomass produced and alkalinity generated (HCO_3^-, $H_2PO_4^-$ and HPO_4^{2-}) are calculated from the biodegradable COD removed.
3. A three phase mixed inorganic carbon (IC) and ortho-phosphate (OP) weak acid/base chemistry part from which the digester pH and mineral precipitation is calculated.

This chapter presents the extended steady state AD model with a focus on the first hydrolysis kinetic part and the extension of the weak acid/base part of the stoichiometric model developed by Harding (2009).

6.2 KINETIC SECTION OF STEADY STATE MODEL

A number of kinetic expressions can represent the biological process of enzymatic action, hydrolysis, and acidogenesis in the breakdown of biodegradable particulate organics under anaerobic conditions.

Biological process kinetics is based on two fundamental relationships: (1) The acidogen organism growth rate and associated substrate utilization rate and (2) the acidogen organism decay rate as proposed by Lawrence and McCarty (1970). Four kinetic equations have been proposed to model the hydrolysis /acidogenesis process in AD:

1. First order with respect to the residual biodegradable particulate COD concentration (S_{bp}), which has been widely used (e.g. Henze and Harremoës, 1983; Bryers, 1985; Eastman and Ferguson, 1981; Gujer and Zehnder, 1983; Henze and Harremoës, 1983; Bryers, 1985; Pavlostathis and Giraldo-Gomez, 1991). First order kinetics has a simple formulation where the rate of hydrolysis is directly proportional to the concentration of available substrate:

$$r_{HYD} = k_h \cdot S_{bp} \qquad \text{[gCOD/ (}l\text{.d)]} \tag{6.01}$$

Where r_{HYD} is the volumetric rate of sludge hydrolysis in the anaerobic digester and k_h is the first order kinetic rate constant (1/d).

2. First order specific with respect to S_{bp} and the acidogenic biomass concentration (Z_{AD}), which was used in modelling conversion of readily biodegradable organics to short chain fatty acids in the anaerobic reactor of BEPR systems (Wentzel *et al.*, 1988). The first order specific rate equation models the rate of hydrolysis as being proportional to the residual biodegradable particulate COD concentration (S_{bp}) and the acidogen biomass (Z_{AD}) concentration:

$$r_{HYD} = k_H \cdot S_{bp} \cdot Z_{AD} \qquad \text{[gCOD/ (}l\text{.d)]} \tag{6.02}$$

Where k_H is the specific first order kinetic rate constant [l/ (mgZ_{AD}.d)]. This form of equation is conceptually superior to the first order rate equation since the r_{HYD} is dependent on Z_{AD} (gCOD/*l*), the organism group (acidogens) which mediates the hydrolysis process.

3. Monod kinetics: The empirical equation presented by Monod can estimate the growth rate of a given species of organisms growing on a single growth limiting substrate (S_{bp}) by relating the rate of uptake of that substrate to its concentration in the growth medium (Mitchell, 1972). All other substrates and nutrients are assumed present in excess, such that the products of the reaction do not accumulate sufficiently enough to inhibit the fermentation (McCarty and Mosey, 1991). Thus, the Monod equation describes the relationship between the specific hydrolysis rate (r_{HYD}/Z_{AD}) and the concentration of the growth limiting substrate (S_{bp}). This formed the basis for most modern bacterial growth models (e.g. Activated Sludge Models, ASM1 and ASM2 and

Anaerobic Digestion Model, ADM1) and includes k_m, the upper limit of the specific hydrolysis rate and K_s, the substrate concentration at which this specific hydrolysis rate is half of k_m (Bailey and Ollis, 1986). Thus the Monod equation is given as:

$$r_{HYD} = \frac{k_m \cdot S_{bp}}{K_s + S_{bp}} \cdot Z_{AD} \qquad \text{[gCOD/ (}l\text{.d)]} \tag{6.03}$$

The Monod model is widely used in bioprocess kinetics because of its mathematical simplicity, stability and its automatic transition between zero and first order at high and low limiting substrate concentrations respectively.

4. Saturation kinetics: This kinetic formulation is used to model the utilization of slowly biodegradable particulate organics (BPO) in activated sludge models (Dold *et al.*, 1980; Henze *et al.*, 1987) and hydrolysis of sewage sludge (McCarty, 1974). Like Monod kinetics, saturation kinetics includes acidogenic biomass concentration (Z_{AD}) and incorporates a maximum rate of hydrolysis under conditions of high substrate/biomass concentration ratio (S_{bp}/Z_{AD}). Saturation kinetics is based on the quantity of BPO attached to the organic biomass active sites, whereby the rate of hydrolysis reaches a maximum at saturation of the active sites of the acidogens. Unlike the Monod expression, in saturation kinetics the hydrolysis rate is independent of the bulk liquid residual biodegradable COD concentration (S_{bp}), but rather dependent on its concentration with respect to the acidogenic biomass concentration (Z_{AD}). Thus the saturation kinetic equation used to predict the rate of hydrolysis is:

$$r_{HYD} = \left(\frac{k_M \cdot \left(\frac{S_{bp}}{Z_{AD}} \right)}{K_S + \left(\frac{S_{bp}}{Z_{AD}} \right)} \right) \cdot Z_{AD} \qquad [\text{gCOD/ } (l.\text{d})]$$

(6.04)

Where K_S is the substrate and acidogenic biomass concentration ratio, at which the specific hydrolysis rate is half its upper limit (k_M) at saturation.

In order to use the above process formulations, the kinetic constants (k_h, k_H, k_m, K_s, k_M and K_S) need to be determined for particular sludge types.

6.2.1 The Determination of Kinetic Constants

The same methods as in Sötemann *et al.* (2005a) are used here to determine the constants in the hydrolysis rate equations. These methods are based on mass balance principles over the anaerobic digester, whereby the total influent COD flux (FS_{ti}) is linked to the total effluent COD flux (FS_{te}) via the volumetric hydrolysis rate (r_{HYD}). For completely mixed flow through anaerobic digester conditions, at steady state, the influent and effluent COD concentrations are given by:

$$S_{ti} = S_{bpi} + S_{bsfi} + S_{bsai} + S_{usi} + S_{upi}$$

(6.10)

and

$$S_{te} = S_{bpe} + S_{bsfe} + S_{bsae} + S_{use} + S_{upe} + Z_{AD}$$

(6.11)

Where the S_{bsf}, S_{bsa} are the COD's of fermentable readily biodegradable organics (FRBCOD) and acetate (VFA) respectively, and S_{us} and S_{up} are unbiodegradable soluble and particulate COD concentration respectively in the influent ($_i$) and effluent ($_e$).

In these equations, the acidogenic biomass (Z_{AD}) concentration represents the biomass formation of all the AD microorganism groups, i.e. not only the

acidogens, to have better predictions of the methane gas and sludge production. Therefore, Sötemann *et al.* (2005a) increased the yield coefficient (Y_{AD}) from 0.089 to 0.113 (units in mgCOD organism/mgCOD substrate) to account for the growth of Acetoclastic Methanogen (Z_{AM}) and Hydrogenotrophic Methanogen (Z_{HM}) biomass in the AD system. Although the Z_{AM} and Z_{HM} have very low yield coefficients (Y_{AM} = 0.04, Y_{HM} = 0.01), they still contribute to the overall biomass production. Since acidogenesis produces 67% acetic acid for Z_{AM} growth (and 33% hydrogen), 67% of the Y_{AM} value was added to Y_{AD}. The hydrogenotrophic methanogens (Z_{HM}), being a very small part of AD biomass were neglected in the adjustment of the Y_{AD}. Although this increase in Y_{AD} improves the sludge and gas production prediction of the steady state model, the hydrolysis kinetic rates based on it in the steady state model are slightly lower than used for the dynamic AD model on which all three AD biomass graphs are modelled separately.

In this development, the influent fermentable biodegradable soluble organics (FBSO = S_{bsfi}) is included with the influent biodegradable particulate organics (BPO = S_{bpi} + S_{bsfi}) because it also requires hydrolysis and so produces acidogens. The influent VFA (assumed all acetate) is kept separate because it does not undergo hydrolysis and so does not produce acidogens.

At steady state, the change in BPO in the system arises from BPO entering and exiting the flow through AD and utilization via hydrolysis, so a mass balance on BPO yields:

$$V \cdot \partial S_{bp} = Q_i \cdot \partial t \cdot S_{bpi} - Q_e \cdot \partial t \cdot S_{bpe} - r_{HYD} \cdot V \cdot \partial t + \left(b_{AD} \cdot Z_{AD}\right) \cdot V \cdot \partial t \tag{6.12}$$

Dividing the above Equation 6.12 by V.δt, and setting $\delta S_{bp}/\delta t$ to zero for steady state, then rearranging it gives:

$$r_{HYD} = \left(\frac{\left(S_{bpi} - S_{bpe}\right)}{R_s} \right) + \left(b_{AD} \cdot Z_{AD}\right) \qquad [\text{gCOD}/ (l.\text{d})] \tag{6.13}$$

Where b_{AD} (/d) is the acidogen endogenous respiration rate constant and the FBSO is included with the BPO.

Applying the mass balance to the acidogenic biomass (Z_{AD}) concentration in the flow through AD yields:

$$V \cdot \delta Z_{AD} = 0 - (Q_e \cdot Z_{AD} \cdot \delta t) + (Y_{AD} \cdot r_{HYD} \cdot V \cdot \delta t) - (b_{AD} \cdot Z_{AD} \cdot V \cdot \delta t) \tag{6.14}$$

Dividing the above Equation 6.14 by V.δt and noting that $\frac{Q_e}{V} = \frac{1}{R_s}$ yields:

$$\frac{\delta Z_{AD}}{\delta t} = \left(- \frac{Z_{AD}}{Rs} \right) + Y_{AD} . r_{HYD} - b_{AD} . Z_{AD} . \tag{6.15}$$

Setting $\delta Z_{AD}/\delta t$ to zero for steady state, then rearranging it gives:

$$r_{HYD} = \frac{Z_{AD}}{Y_{AD}} \cdot \left(\frac{1}{R_s} + b_{AD} \right). \tag{6.16}$$

However, Equation 6.13 as also gives r_{HYD} as:

$$r_{HYD} = \left(\frac{(S_{bpi} - S_{bpe})}{R_s} \right) + (b_{AD} \cdot Z_{AD}), \tag{6.17}$$

Therefore, equating the above Equations 6.16 and 6.17 yields for Z_{AD}:

$$Z_{AD} = (S_{bpi} - S_{bpe}) \cdot \left(\frac{Y_{AD}}{1 + b_{AD} \cdot R_s \cdot (1 - Y_{AD})} \right) = E \cdot (S_{bpi} - S_{bpe}) \tag{6.18}$$

In the above Equation 6.18, it is accepted that the acidogen endogenous residue fraction (f_{AD}) is zero. Therefore, no endogenous residue (Z_{EAD}) accumulates in the AD. In Equation 6.18, the sludge mass produced (Z_{AD}/R_s) per flux BPO utilized $Q_i \cdot (S_{bpi} - S_{bpe})$ is represented as E, and substituting Equation 6.18 for Z_{AD} yields:

$$E = \frac{Z_{AD}}{R_s \cdot Q_i \cdot (S_{bpi} - S_{bpe})} = \left(\frac{Y_{AD}}{1 + b_{AD} \cdot R_s \cdot (1 - Y_{AD})} \right) \tag{6.19}$$

The validity of Equation 6.19 is established by recognising that for the flow-through AD, $V = R_s \cdot Q_i$, from which Equation 6.18 can be obtained.

Equation 6.19 establishes the link between the influent and effluent unfiltered COD concentration (S_{ti} and S_{te}) as follows:

1. Accepting the S_{usi} (USO) as negligible (<100 mgCOD/*l* in 50000 mgCOD/*l*).
2. Assuming S_{bsae} (effluent VFA) is zero.
3. Eliminating S_{bsai} (influent VFA) from Equation 6.10 because it is dealt with separately.
4. Setting S_{upi} (influent UPO COD) = $f_{SL'up}$ S_{ti}, where $f_{SL'up}$ is the unbiodegradable COD fraction of the sludge and $S_{upe} = S_{upi}$.
5. Substituting Equation 6.18 for Z_{AD} in Equation 6.11 yields:

$$S_{te} = S_{bpe} + f_{SL'up} \cdot S_{ti} + E \cdot \left(\left(1 - f_{SL'up}\right) \cdot S_{ti} - S_{bpe} \right), \text{ from which}$$

$$S_{bpe} = \frac{\left[S_{te} - S_{ti} \cdot f_{SL'up} - S_{ti} \cdot \left(1 - f_{SL'up}\right) . E \right]}{E} \qquad (6.20)$$

Where

- $f_{SL'up}$ = Unbiodegradable fraction of the feed sludge with respect to total COD (minus unbiodegradable soluble which is extremely low with respect to total COD ~0.1%)
- S_{ti} = Total influent COD concentration to AD (gCOD/*l*) excluding the influent VFA (if significant)
- S_{te} = Particulate effluent COD concentration (gCOD/*l* and equal to Equation 6.11)

Therefore, with an estimate of $f_{SL'up}$, E known from the acidogenic constants and AD sludge age (Equation 6.19) and measured influent and effluent particulate COD concentrations (S_{ti} and S_{te}), S_{bpe} can be calculated. If the USO is significant, then this should be subtracted from both influent and effluent COD

concentration to give the total particulate COD in influent and effluent. With S_{bpe} known, Z_{AD} can be calculated from Equation 6.18 and r_{HYD} from Equation 6.16 and 6.13. With S_{bpe}, Z_{AD} and r_{HYD} known, the variables in the four hydrolysis kinetic equations (6.01 to 6.04) are known and thus hydrolysis rate constants can be calculated. For the first order Equation 6.01, the first order kinetic rate constant k_h is given by:

$$k_h = \frac{r_{HYD}}{S_{bpe}} \qquad (6.21a)$$

For the specific first order Equation 6.02, the rate constant k_H is given by:

$$K_H = \frac{r_{HYD}}{S_{bpe} \cdot Z_{AD}} \quad (l/\text{gCOD.d}) \qquad (6.21b)$$

Being kinetic constants, one expects the k_h and k_H to be constant with sludge age, but they are not, so for each selected unbiodegradable particulate COD fraction ($f_{SL'up}$) the coefficient of variation is determined for the range of sludge ages tested, where the coefficient of variation = $k_{std.dev}/k_{average}$, where $k_{average}$ is the average k and $k_{std.dev}$ is its standard deviation over the sludge age range. The $f_{SL'up}$ that gives the lowest coefficient of variation is deemed the best estimate of the $f_{SL'up}$ value of the sludge for the first order and specific first order hydrolysis models.

It was found that the determined constants of k_h and k_H (for first order and specific first order kinetics respectively) usually increased approximately linearly with increase in retention time (R_s), so the slope (m) and intercept (c) of this linear relationship were determined by linear regression, i.e. the k rates can be replaced in the first order hydrolysis equations by:

$k_h = m_{kh} \cdot R_s + c_{kh}$ and $k_H = m_{kH} \cdot R_s + c_{kH}$. (6.21c, 6.21d)

For the Monod and saturation rate equations, the S_{bpe}, Z_{AD} and r_{HYD} are calculated in the same way for each sludge age. Then the constants (k_m, K_s, k_M and K_S) in the rate equations (6.03 and 6.04) are obtained with a curve-fitting programme like Curve Expert or through linearization of the rate equations and linear regression over the sludge age range. This linearization and regression were performed using the three different linearization methods i.e. Lineweaver-Burke (or Inversion), double reciprocal and Eadie-Hofstee (Lehninger, 1977) and the correlation coefficient (R^2) is calculated for each method. A general Lineweaver-Burke inversion plot used in determination of the Monod kinetic constants is depicted in Figure 6.1.0 below. The procedure is repeated for different selected influent COD unbiodegradable fractions ($f_{SL'up}$). The $f_{SL'up}$ fraction that yields the highest regression correlation coefficient (R^2) is accepted to be the best estimate of the $f_{SL'up}$ value for the influent organics. Whereas Curve Expert does not linearize the equations and so gives equal weight to each S_{bpe} (for Monod) or S_{bpe}/Z_{AD} (for saturation) values over the range obtained for the different R_s, the different linearization methods emphasize the data in different R_s ranges of the r_{HYD} versus S_{bp} or S_{bp}/Z_{AD} domain and therefore yield different k_m, K_s and k_M and K_S values. The averages of the kinetic constants obtained by the three linearization methods for the highest average correlation coefficient were accepted as the best hydrolysis rate kinetic constants for the organics. The unbiodegradable particulate COD fraction so determined was then compared with the measured effluent particulate COD from the 60d sludge age AD system. Between the values obtained from curve fitting software and those from the linearization methods, the kinetic rate constants (k_m and K_s for Monod and k_M and K_S for saturation hydrolysis kinetics) that provided the closest predictions were selected for application in the AD model.

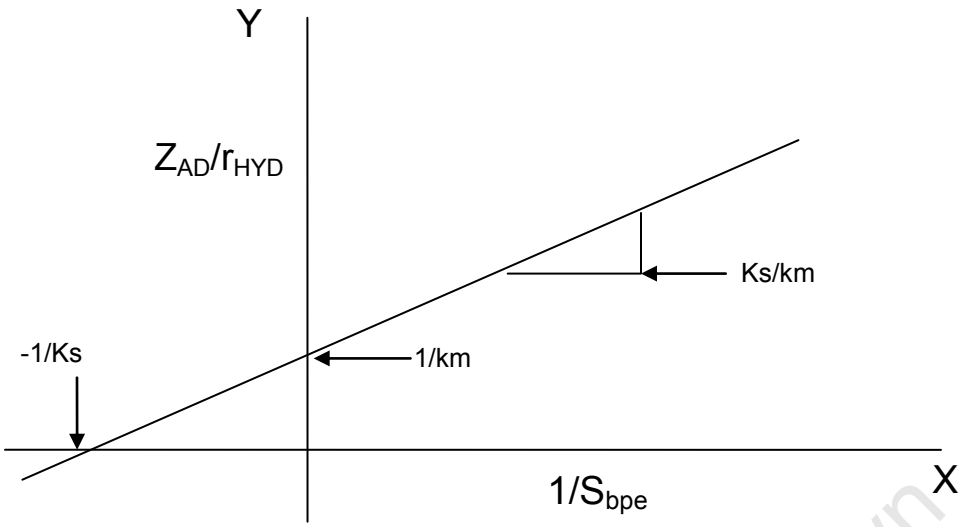

Figure 6.1.0: *A typical Lineweaver-Burke plot.*

Variations of K_s with S_{bpi}

For the Monod kinetics, which is based on the bulk liquid S_{bpe} concentration, if the kinetic model is applied to increased (or decreased) biodegradable influent COD concentration (S_{bpi}), the K_s value (K_s 1) will change since the S_{bpe} will have increased (or decreased) accordingly to maintain the correct fraction of biodegradable particulate organics removed (S_{bpi} - S_{bpe}) in the kinetic rate equations. For example, if the influent biodegradable COD concentration (S_{bpi}) is doubled, the S_{bpe} will also double (Equation 6.20) to maintain the same fraction of COD removed, thus causing the K_s 1 to double (K_s 2) as shown below:

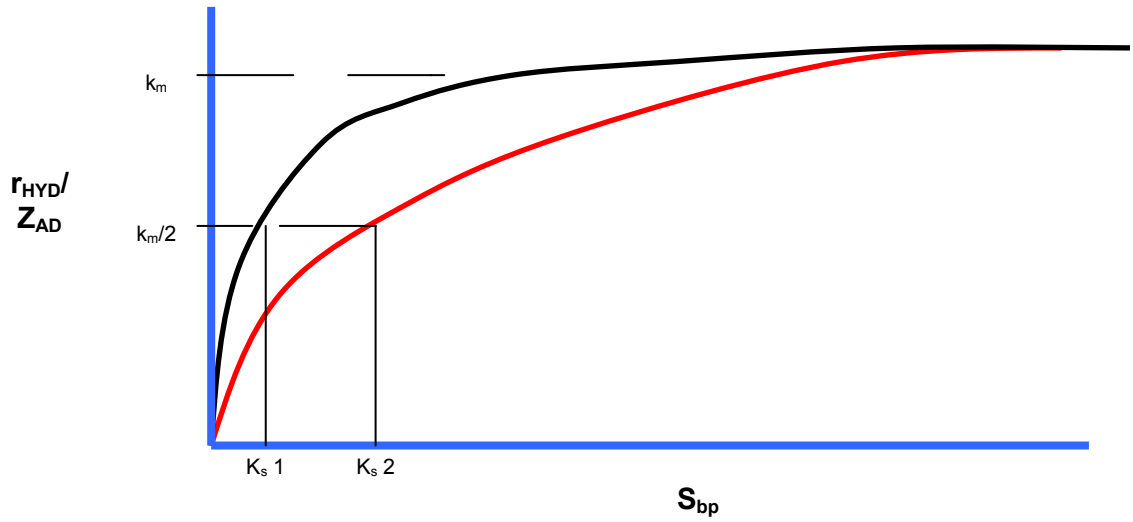

Figure 6.1.1: *Change in Monod curve for change in influent biodegradable COD concentration (S_{bpi}).*

However, the k_m value must not change because it influences the fraction of COD removal at a specific sludge age rather than variations in S_{bpi}. Therefore, a reference K_s (K_{s_ref}) value, relative to a reference S_{bpi} (S_{bpi_ref}), was established from which the actual K_s values were determined relative to the actual S_{bpi} concentrations, i.e.

$$K_{s\_actual} = \left(\frac{K_{s\_ref}}{S_{bpi\_ref}} \right) \cdot S_{bpi\_actual} \quad . \tag{6.22.a}$$

Where S_{bpi_actual} is the biodegradable particulate organic influent concentration that is specific to a particular AD experiment, calculated from:

$$S_{bpi\_actual} = S_{ti} - S_{upi} - S_{usi} - S_{bsi} \tag{6.22b}$$

Where,

- S_{ti} is the measured total unfiltered influent COD concentration.
- S_{upi} is the influent unbiodegradable particulate COD, which is determined from $f_{SL'up}$ S_{ti}, where $f_{SL'up}$ is approximated from the COD of the residual particulate organics from the 60d sludge age AD or

estimated in the hydrolysis kinetic rate determination procedure described above.

- S_{usi} is the influent unbiodegradable soluble COD concentration, assumed to equal the residual soluble filtered organics COD from the 60d sludge age AD.
- S_{bsi} is the total soluble influent biodegradable organics COD, calculated by subtracting the S_{usi} from the filtered influent COD (S_{tsi}). The S_{bsi} in primary sludge usually comprises mostly volatile fatty acids (S_{bsai}) and a low concentration of fermentable rapidly biodegradable COD (S_{bsfi}). The S_{bsi} concentration of WAS is negligible, almost zero mgCOD/*l* for both S_{bsfi} (fermentable) and S_{bsai} (VFA). Because the soluble COD concentration (S_{usi} and S_{bsi}) are very low relative to the total COD (S_{ti}), it is reasonable to define the unbiodegradable particulate COD fraction ($f_{SL'up}$) with respect to the total COD (S_{ti}).

To simplify this process, the experimental COD concentrations used for calculating the Monod hydrolysis rate constants were all divided by S_{bpi} to set the S_{bpi_ref} to 1gramCOD/*l*, while maintaining the correct percentage of COD removal at each sludge age. Thus the K_{s_actual} is:

$$K_{s\_actual} = K_{s\_ref} \cdot S_{bpi\_actual} \tag{6.22c}$$

In contrast to Monod kinetics, the kinetic constants for saturation kinetics (i.e. k_M and K_S) do not change with increased (or decreased) S_{bpi} concentration because these constants consider the rate of hydrolysis relative to the biomass concentration (Z_{AD}) i.e. (S_{bp}/Z_{AD}), not the bulk liquid concentration (S_{bp}).

Once the kinetic constants have been determined, the calibrated hydrolysis rate equation can be applied to calculate the residual biodegradable organics in the effluent (S_{bpe}). For the first order kinetics, the expression used in determining the

residual S_{bpe} concentration, obtained using from Equations 6.01 (the first order equation), 6.17 (that defines r_{HYD}) and 6.21c (that defines k_H), is shown in Equation 6.22d below:

$$S_{bpe} = \frac{\left(\frac{S_{bpi}}{R_s} + \left(S_{bpi} \cdot b_{AD} \cdot \frac{Y_{AD}}{1 + b_{AD} \cdot R_s \cdot (1 - Y_{AD})}\right)\right)}{(m_{kh} \cdot R_s + c_{kh}) + \left(\frac{1}{R_s}\right) + \left(b_{AD} \cdot \frac{Y_{AD}}{1 + b_{AD} \cdot R_s \cdot (1 - Y_{AD})}\right)}$$

(6.22d)

The above equation can be applied to the model ADs because it depends on known hydrolysis rate kinetic rate constants, sludge age and the influent biodegradable particulate COD can be determined by subtracting the unbiodegradable fraction ($f_{SL'up}$) of the influent from its total COD (S_{ti}), i.e. $S_{bpi} = S_{ti} \cdot (1 - f_{SL'up})$.

For the specific first order hydrolysis kinetics the residual undegraded biodegradable COD (S_{bpe}) is calculated from Equations 6.16 and 6.21d that define r_{HYD} and k_H respectively, to give:

$$S_{bpe} = \left(\frac{1}{Y_{AD} \cdot (m_{k_H} \cdot R_s + C_{k_H})}\right) \cdot \left(\frac{1}{R_s} + b_{AD}\right)$$

(6.22e)

For the Monod kinetics, once the kinetic constants have been determined (i.e. k_m and K_{s_ref}) Equation 6.16 for r_{HYD} can be equated to the Monod hydrolysis rate (Equation 6.03) to find the S_{bpe}, as shown below in Equations 6.22f and 6.22g.

$$\frac{Z_{AD}}{Y_{AD}} \cdot \left(\frac{1}{R_s} + b_{AD}\right) = \left(\frac{k_m \cdot S_{bp}}{K_s + S_{bp}}\right) \cdot Z_{AD}$$

(6.22f)

When S_{bpe} is made the subject of the Equation 6.22f, Equation 6.22g is obtained:

$$S_{bpe} = \frac{K_{s\_ref} \cdot S_{bpi} \cdot \left(\frac{1}{R_s} + b_{AD}\right)}{\left(Y_{AD} \cdot k_m\right) - \left(\frac{1}{R_s} + b_{AD}\right)}.$$

(6.22g)

To find the S_{bpe} in terms of the saturation kinetics with k_M and K_S known, Equation 6.17 for r_{HYD} and Equation 6.18 that defined Z_{AD} are applied to the saturation kinetic equation (6.04) to give:

$$\left(\frac{S_{bpi} - S_{bpe}}{R_s}\right) + \left(b_{AD} \cdot \left(S_{bpi} - S_{bpe}\right) \cdot E\right) = \left(\frac{k_M \cdot \frac{S_{bpe}}{\left(S_{bpi} - S_{bpe}\right) \cdot E}}{K_s \cdot \frac{S_{bpe}}{\left(S_{bpi} - S_{bpe}\right) \cdot E}}\right) \cdot \left(S_{bpi} - S_{bpe}\right) \cdot E,$$

(6.23.a)

where E is obtained from Equation 6.18. Solving Equation 6.23a for S_{bpe} yields:

$$S_{bpe} = \frac{S_{bpi} \cdot K_s \cdot E}{\left(\frac{k_M \cdot E \cdot R_s}{1 + b_{AD} \cdot E \cdot R_s}\right) - 1 + \left(K_s \cdot E\right)}.$$

(6.23b)

6.2.2 Experimental Results

The procedure described in Section 6.2.1 above allows determination of the unbiodegradable particulate COD fraction ($f_{SL'up}$) and hydrolysis kinetic rate constants in the four different hydrolysis rate expressions from experimentally measured AD results – mainly influent and effluent particulate COD concentrations and AD sludge age. This procedure is applied below to determine the hydrolysis kinetic rate constants in ADs fed PS, WAS from nitrification-denitrification (ND) activated sludge (AS) systems fed raw and settled wastewater (WW), WAS from a ND biological excess P removal (BEPR) system fed settled WW to which acetate was added, WAS and a PS-WAS blend from

MLE system fed settled WW. For the kinetic rates, the most useful data is that from the short sludge age ADs while long sludge age AD data is useful to determine the unbiodegradable particulate COD fraction ($f_{SL'up}$).

6.2.2.1. AD of Primary Sludge

Tables 6.2.1a and 6.2.1b show the average influent and effluent experimental results respectively that were measured in the AD of primary sludge (PS) at the different sludge ages. The hydrolysis kinetic rates were determined from these experimental data by following the calculation procedure presented above.

Table 6.2.1a: Primary Sludge Influent Experimental Data										
Retention Time (d)	10		18		25		40		60	
Influent flow (*l*/d)	1.2		0.67		0.50		0.30		0.09	
Digester Volume (*l*)	12		12		12		12		12	
Units	Conc. (g/*l*)	Flux (g/d)	Conc. (g/*l*)	Flux (g/d)	Conc. (g/*l*)	Flux (g/d)	Conc. (g/*l*)	Flux (g/d)	Conc. (g/*l*)	Flux (g/d)
Influent COD[3], S_{ti} (gCOD/*l*)	5.68	1.64	8.05	1.70	8.91	1.82	18.71	1.67	28.43	1.67
Influent COD[1], S_{upi} (gCOD/*l*)	1.76	0.51	2.50	0.53	2.76	0.56	5.80	0.52	8.81	0.52
Influent COD, S_{usi}[2] (gCOD/*l*)	0.07	0.02	0.09	0.02	0.10	0.02	0.21	0.02	0.33	0.02
Influent filtered COD, S_{tsi} (gCOD/*l*)	0.46	0.13	0.82	0.17	1.24	0.25	1.67	0.15	2.63	0.15
Influent COD, S_{bpi}[6] (gCOD/*l*)	3.46	1.00	4.74	1.00	4.91	1.00	11.23	1.00	16.99	1.00
Influent COD, S_{bsfi}[5] (gCOD/*l*)	0.24	0.07	0.54	0.11	0.94	0.19	1.15	0.10	1.86	0.11
Influent VFA, S_{bsai}[4] (gCOD/*l*)	0.16	0.05	0.19	0.04	0.20	0.04	0.31	0.03	0.44	0.03
Influent TKN[3] (gN/*l*)	0.26	0.07	0.25	0.05	0.29	0.06	0.51	0.05	0.59	0.03
Influent filtered TKN (gN/*l*)	0.04	0.01	0.03	0.01	0.03	0.01	0.06	0.01	0.05	0.00
Influent FSA (gN/*l*)	0.03	0.01	0.03	0.01	0.02	0.00	0.05	0.00	0.05	0.00
Influent Alk g/*l* as $CaCO_3$	0.40	0.12	0.32	0.07	0.35	0.07	0.39	0.03	0.32	0.02
Influent pH	5.88		6.16		5.93		6.07		5.54	
Influent TP[3] (gP/*l*)	0.09	0.03	0.19	0.04	0.22	0.04	0.21	0.02	0.25	0.01
Influent filtered TP (gP/*l*)	0.02	0.01	0.03	0.01	0.03	0.01	0.04	0.00	0.03	0.00
Influent OP (gP/*l*)	0.02	0.01	0.02	0.00	0.02	0.00	0.02	0.00	0.03	0.00
Influent TSS (gTSS/*l*)	4.94	1.43	5.56	1.17	6.95	1.42	14.75	1.31	19.73	1.16
Influent VSS (gVSS/*l*)	3.84	1.11	4.49	0.95	5.49	1.12	11.78	1.05	16.34	0.96
Influent ISS (gISS/*l*)	1.10	0.32	1.06	0.22	1.46	0.30	2.97	0.26	3.39	0.20

[1] S_{upi} is the unbiodegradable particulate COD calculated for $f_{PS'up}$ = 0.31, obtained for best coefficients of variation and correlation coefficients

[2] S_{usi} is the unbiodegradable soluble COD measured from the filtered effluent from 60d sludge age AD

[3] Unfiltered samples

[4] S_{bsai} is the COD in short chain fatty acids that is measured in the influent using the 5-point titration method

[5] S_{bsfi} is the fermentable biodegradable soluble influent COD calculated from the measured filtered influent COD (S_{tsi}) – S_{usi} – S_{bsai}

[6] S_{bpi} is the biodegradable particulate influent COD which is calculated by the total influent COD (S_{ti}) – S_{tsi} – S_{upi}

Table 6.2.1b: Primary Sludge Effluent Experimental Data										
Retention Time (d)	10		18		25		40		60	
Effluent flow (*l*/d)	1.2		0.67		0.50		0.30		0.09	
Units	Conc. (g/*l*)	Flux (g/d)	Conc. (g/*l*)	Flux (g/d)	Conc. (g/*l*)	Flux (g/d)	Conc. (g/*l*)	Flux (g/d)	Conc. (g/*l*)	Flux (g/d)
Effluent COD[1], S_{te} (gCOD/*l*)	3.91	1.13	4.60	0.97	4.26	0.87	6.68	0.59	10.29	0.61
Effluent COD, S_{upe} [5] (gCOD/*l*)	1.76	0.51	2.50	0.53	2.76	0.56	5.80	0.52	8.81	0.52
Effluent COD, S_{use}[2] (gCOD/*l*)	0.07	0.02	0.09	0.02	0.10	0.02	0.21	0.02	0.33	0.02
Effluent filtered COD, S_{tse} (gCOD/*l*)	0.12	0.03	0.18	0.04	0.25	0.05	0.37	0.03	0.33	0.02
Effluent COD, S_{bpe}[6] (gCOD/*l*)	2.03	0.56	1.93	0.38	1.24	0.24	0.51	0.05	1.15	0.06
Effluent COD, S_{bsfe}[4] (gCOD/*l*)	0.05	0.02	0.08	0.02	0.15	0.03	0.16	0.01	0.00	0.00
Effluent VFA, S_{bsae}[3] (gCOD/*l*)	0.00	0.00	0.00	0.00	0.00	0.00	0.03	0.00	0.04	0.00
Effluent TKN[1] (gN/*l*)	0.24	0.07	0.26	0.06	0.24	0.05	0.51	0.04	0.60	0.04
Effluent filtered TKN (gN/*l*)	0.06	0.02	0.08	0.02	0.11	0.02	0.26	0.02	0.27	0.02
Effluent FSA (gN/*l*)	0.03	0.01	0.06	0.01	0.10	0.02	0.25	0.02	0.27	0.02
Effluent TP[1] (mgP/*l*)	0.09	0.03	0.20	0.04	0.23	0.05	0.22	0.02	0.22	0.01
Effluent filtered TP (gP/*l*)	0.01	0.00	0.03	0.01	0.06	0.01	0.08	0.01	0.09	0.01
Effluent OP (gP/*l*)	0.01	0.00	0.03	0.01	0.06	0.01	0.08	0.01	0.07	0.00
Effluent TSS	3.48	1.01	4.20	0.89	3.95	0.80	6.71	0.60	8.93	0.53
Effluent VSS	2.40	0.69	2.70	0.57	2.62	0.53	4.48	0.40	5.85	0.34
Effluent ISS	1.08	0.31	1.45	0.31	1.33	0.27	2.23	0.20	3.07	0.18
Effluent Alk mg/*l* as $CaCO_3$	1.14	0.33	1.08	0.23	1.88	0.38	1.84	0.16	2.03	0.12
Measured digester pH	7.06		7.27		7.26		7.25		7.13	
COD removed (gCOD/*l*)	0.43	0.51	1.09	0.73	1.90	0.95	3.57	1.07	12.56	1.07
Gas production (litres/d)	2.60		1.68		1.30		1.03		-	
Gas prod. (l gas/*l* influent)	2.17		2.50		2.60		3.44			
Gas composition : CH_4 fraction	0.39		0.39		0.39		0.39			
Gas composition: CO_2 fraction	0.24		0.24		0.24		0.24			
Flow of CH_4 (litres/d)	0.84		0.98		1.02		1.34			
Flow of CO_2 (litres/d)	0.51		0.59		0.61		0.81			
COD of CH_4 (gCOD/*l* feed)	1.85		3.82		5.33		11.74		17.84	
pCO_2 (atm)	0.38		0.38		0.38		0.38		0.37	
CT dissolved (mmol/*l*)	9.77		9.77		9.77		9.77			
H_2CO_3 diss. (mg/*l*)	976.59		976.59		976.59		976.59			
Moles of CO_2/*l* feed	0.02		0.02		0.03		0.03			
Moles of CH_4	0.03		0.04		0.04		0.06			
COD balance (%)	101.22		104.64		107.60		98.45		98.92	
Nitrogen balance (%)	93.03		102.56		81.63		99.72		101.93	
Phosphorous balance (%)	97.34		100.81		106.56		102.93		88.66	
f_{cv} (gCOD/gVSS)	1.63		1.70		1.62		1.49		1.76	
$f_{SL'up}$ (PS)	0.31		0.31		0.31		0.31		0.31	

[1] Unfiltered sample

[2] S_{use} is the unbiodegradable soluble COD measured in filtered effluent from the 60d sludge age AD

[3] S_{bsae} is the COD in short chain fatty acids that is measured in the effluent using the 5-point titration method

[4] S_{bsfe} is the fermentable biodegradable soluble COD calculated from the filtered effluent COD (S_{tse}) – S_{use} – S_{bsae}

[5] S_{upe} is the unbiodegradable particulate effluent COD which equals the S_{upi} value from Table 6.2.1a

[6] S_{bpe} is the biodegradable particulate effluent COD which equals the total effluent COD (S_{te}) – S_{tse} – S_{upe}

Selection of PS Unbiodegradable Particulate COD Fraction $f_{PS'up}$

The coefficients of variation for first order and first order specific hydrolysis kinetic equations versus increasing $f_{PS'up}$ fractions are shown in Figure 6.2.1a and correlation coefficients (R^2) for Monod and saturation hydrolysis kinetic equations versus the same range of $f_{SL'up}$ fractions in Figures 6.2.1b and 6.2.1c respectively. The same range of $f_{PS'up}$ is selected in order to obtain the best $f_{PS'up}$ estimate for good coefficients of variation and correlation coefficients for all four hydrolysis kinetic equations to best predict the effluent COD in the AD of PS. The correlation coefficients for the Monod and saturation kinetics are shown for the three linearization methods of Lineweaver-Burke (M1 and M1*), Double Reciprocal (M2) and Eadie-Hofstee (M3 and M3*). The M1, M2 and M3 (without asterisks) were obtained using the data for all five PS AD sludge ages, i.e. 10, 18, 25, 40 and 60 days. The M1* is the result when the 40 and 60 day R_s data are omitted both from linearising the Monod and saturation kinetics using the Lineweaver-Burke method and M3* is for the plot obtained when the 25, 40 and 60 day R_s data are omitted from linearising the Monod and saturation kinetics using the Eadie-Hofstee method. The omission of these data sets to form M1* and M3* was done in order to improve the R^2 value. Certainly with only two data sets for M3*, a perfect fit is achieved (R^2 =1). The curve fitting results are evaluated in greater detail below after selecting the best $f_{PS'up}$ value.

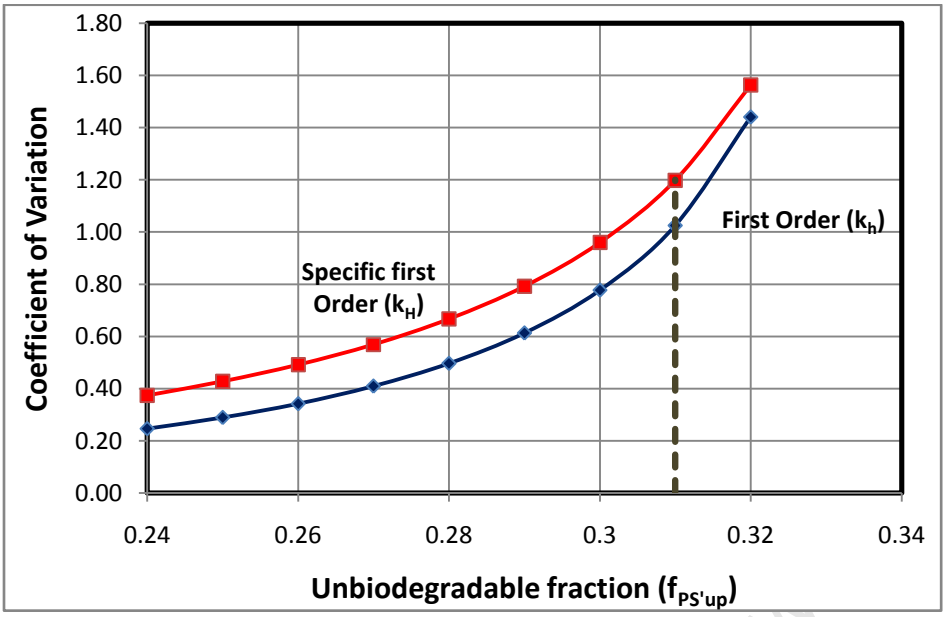

Figure 6.2.1a: *The change in the coefficient of variation of the 1st order and 1st order specific hydrolysis equations kinetic constants with changing unbiodegradable particulate COD fraction of primary sludge ($f_{PS'up}$), without R_s = 40d data (see Table 6.2.1c).*

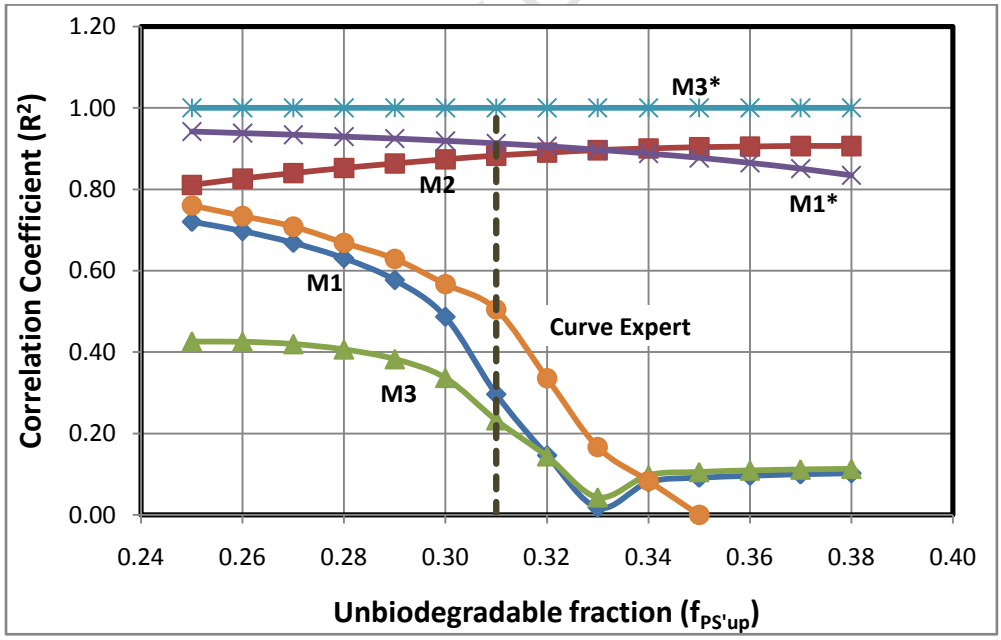

Figure 6.2.1b: *The regression correlation coefficient (R^2) for the Curve Expert program, Lineweaver-Burke (M1), double deciprocal (M2) and Eadie-Hofstee (M3) linearization methods of Monod hydrolysis kinetics versus unbiodegradable particulate COD fraction of the PS ($f_{PS'up}$).*

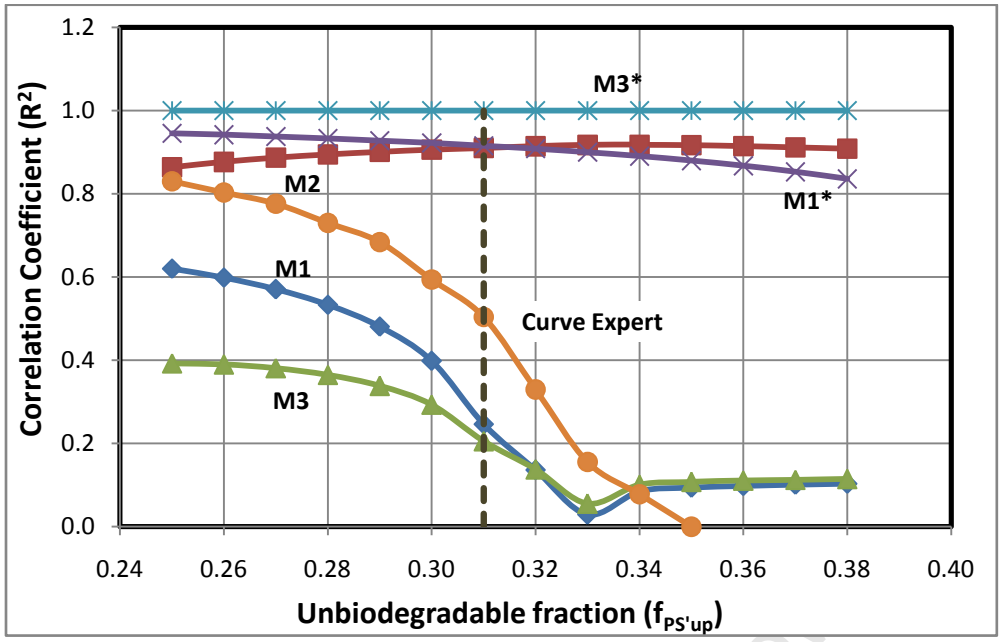

Figure 6.2.1c: *The regression correlation coefficient (R^2) for the Curve Expert program, Lineweaver-Burke (M1), double reciprocal (M2) and Eadie-Hofstee (M3) linearization methods of saturation hydrolysis kinetics versus unbiodegradable particulate COD fraction of the PS ($f_{PS'up}$).*

In Figure 6.2.1a, the coefficient of variation (C_{var}) is increasing slowly with increase in unbiodegradable particulate fraction, from 0.24 to 0.32 after which it increases sharply. Figures 6.2.1b and 6.2.1c show that the Monod and saturation kinetics exhibit maximum R^2 values, for all three linearization methods, at the $f_{PS'up}$ value of around 0.31. This value is also equal to that determined from the AD of the PS at a very long sludge (60 days). Therefore, the best compromise $f_{PS'up}$ value between the four hydrolysis kinetic formulations and the 60d sludge age AD is 0.31. Therefore, this value (0.31) was selected as the $f_{PS'up}$ value to be used in the determination of the relevant kinetic constants.

First Order Kinetics

The experimentally obtained values (Tables 6.2.1a and 6.2.1b) and above-mentioned calculations were used to determine the volumetric hydrolysis rates (r_{HYD}), the residual biodegradable COD concentrations (S_{bpe}) and the first order kinetic rate constants (k_h and k_H), which are shown in Table 6.2.1c below. Thereafter, the variations of these values with sludge age are plotted as shown in Figures 6.2.1d to 6.2.1g.

Table 6.2.1c: Summary of Results for First Order Kinetics in the AD of PS for $f_{PS'up}$ = 0.31

R_s (d)	r_{HYD} (g/*l*/d)	Z_{AD} (g/*l*)	S_{bpe} (g/*l*)	k_h (/d)	Spec r_{HYD} (gS_{bp}/gZ_{AD}/d	k_H (*l*/gZ_{AD}/d)
10	0.050	0.044	0.522	0.095	1.128	2.160
18	0.039	0.052	0.336	0.116	0.756	2.250
25	0.035	0.057	0.190	0.183	0.610	3.212
40	0.027	0.049	0.008	3.211	0.543	64.980
60	0.018	0.038	0.026	0.673	0.466	17.644
		Mean		0.86	-	18.05
		Standard deviation		1.34	-	27.04
		Coefficient of variation		1.56	-	1.50

$k_h = c_{kh} + m_{kh} \times R_s$; c_{kh} = -0.077; m_{kh} = 0.0132; R^2 = 0.924 (excluding R_s = 40d)
$k_H = c_{kH} + m_{kH} \times R_s$; c_{kH} = -0.303; m_{kH} = 0.372; R^2 = 0.852 (excluding R_s = 40d)

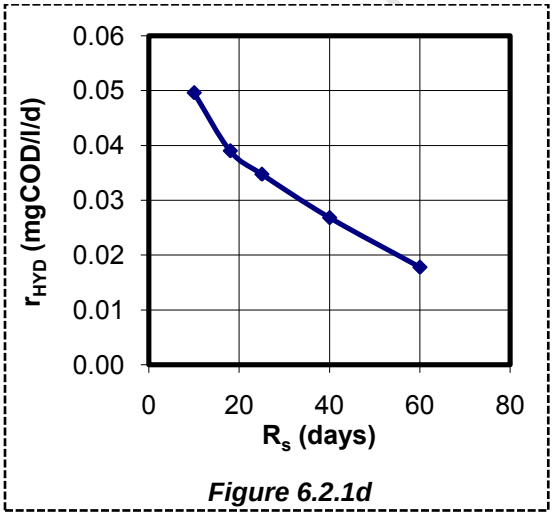

Figure 6.2.1d

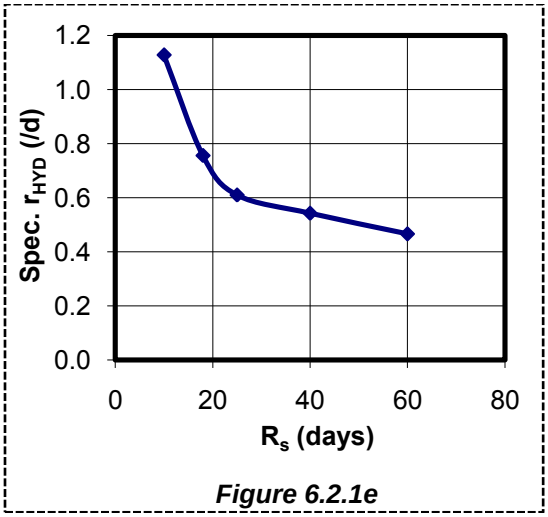

Figure 6.2.1e

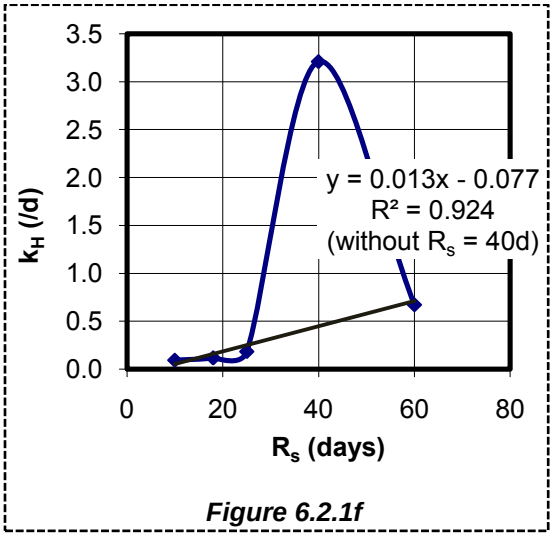

Figure 6.2.1f

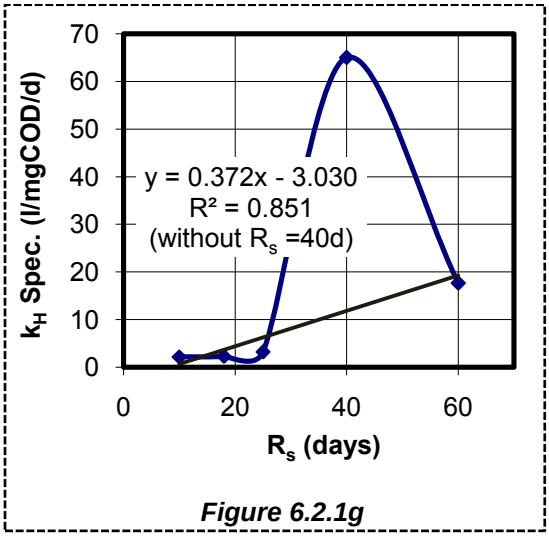

Figure 6.2.1g

Figures 6.2.1d, e, f and g: *Volumetric hydrolysis rates (r_{HYD}) (d), specific volumetric hydrolysis rate (r_{HYD}/Z_{AD}) (e), first order kinetic constant (k_h) (f) and specific first order kinetic constant (k_H) (g) versus sludge age (R_s) for AD of PS.*

As notable from Figures 6.2.1f and 6.2.1g, for first order and specific first order, the R_s 40d data do not fit the trends exhibited by the rest of the data. Therefore, this data is omitted when establishing the linear relationship (from Equation 6.21c and d) of k_h and k_H with sludge age. This gives us $k_h = 0.0132 \cdot R_s - 0.077$ (R^2 = 0.924) for first order hydrolysis kinetics and $k_H = 0.372 \cdot R_s - 0.30304$ (R^2 = 0.8516) for specific first order hydrolysis kinetics (Table 6.2.1c). Sötemann *et al.* (2005a) also calculated k_h and k_H values, using data from Izzett *et al.* (1992) and O'Rourke (1968). Izzett *et al.* (1992) operated the AD of a PS and humus sludge mixture from a trickling filter plant at sludge ages of 7 to 20 days (results shown in Table 6.2.1d). The calculated relationship of the resulting k_h and k_H values with sludge age (all data) gives $k_h = 0.0065 \cdot R_s + 0.432$ (R^2 = 0.78) and $k_H = 0.00737 \cdot R_s + 0.228$ (R^2 = 0.78) which are different from those calculated in this project. This could be because the data from Izzett *et al.* (1992) is for a range of sludge ages shorter (7 – 20d R_s) than the range used in this project (10 – 60d R_s) but probably more so because the PS characteristics vary depending on the

sewage source and type. O'Rourke (1968) operated the AD of 'pure' PS at sludge ages of 7.5 to 60 days (results shown in Table 6.2.1d) and obtained $k_h = 0.398 \cdot R_s + 1.03$ (R^2 = 0.762) (all data) and $k_H = 0.2042 \cdot R_s - 1.5004$ (R^2 = 0.874) (all data), which are also different from those calculated in this project.

Table 6.2.1d: From Sötemann *et al.* (2005) who used the Izzett *et al.* (1992) 7 to 20 d retention time (R_s) and O'Rourke (1968) 7.5 to 60 d R_s anaerobic digester measured influent* (S_{ti}) and effluent* (S_{te}) COD concentrations, influent unbiodegradable (S_{upi}) and biodegradable COD (S_{bpi}) concentrations for an unbiodegradable COD fraction ($f_{PS'up}$) of 0.36 (for Izzett data) and 0.338 (for O'Rourke data) to calculate the residual biodegradable COD concentration (S_{bp}), observed hydrolysis rate (r_{HYD}), specific hydrolysis rate [r_{HYD}/Z_{AD})] and the 1st order and 1st order specific hydrolysis rate constants (k_h and k_H). All mass units in gCOD.

Data Reference	R_s	*S_{ti}	*S_{te}	S_{upi}	S_{bpi}	S_{bpe}	r_{HYD}	r_{HYD}/Z_{AD}	k_h	k_H
	d	g/*l*	g/*l*	g/*l*	g/*l*	g/*l*	g/(l.d)	(gS_{bpe}/gZ_{AD}/d)	/d	l/(gZAD.d)
From Izzett *et al.* (1992) Data	7	43.286	23.637	15.584	25.832	6.240	2.871	1.586	0.460	0.261
	10	40.721	20.521	14.660	24.100	4.142	2.064	1.207	0.498	0.301
	12	39.222	18.678	14.120	22.230	3.018	1.663	1.059	0.551	0.365
	15	42.367	19.969	15.252	25.291	3.065	1.548	0.912	0.505	0.311
	20	42.595	19.005	15.334	25.012	2.151	1.204	0.764	0.560	0.374
								Mean	0.515	0.322
From O'Rourke (1968) Data	7.5	28.400	12.400	9.599	17.781	1.188	2.273	1.543	1.914	1.299
	10	28.400	11.700	9.599	17.781	0.586	1.778	1.248	3.034	2.129
	15	28.400	11.800	9.599	17.781	0.907	1.175	0.953	1.296	1.050
	30	28.400	11.800	9.599	17.781	1.247	0.588	0.658	0.471	0.527
	60	28.400	10.300	9.599	17.781	0.04	0.321	0.510	7.876	12.503
								Mean**	2.081	1.493
								Mean***	2.474	1.714

* Measured total unfiltered COD fractionated into different organic types (USO, BPO, FBSO, VFA and UPO), in the same way as this investigation – see Section 6.2.1
** Mean of 7.5, 10 and 15d R_s values
*** Mean of 7.5 and 10d R_s values only

Monod and Saturation Kinetics

The Figures 6.2.1.h to 6.2.1.k below show the specific hydrolysis rates (r_{HYD}/Z_{AD}) versus the residual BPO (S_{bpe}) of PS for the Monod equation and versus the residual BPO per acidogenic biomass (S_{bpe} / Z_{AD}) for the saturation kinetics equation. The plots were obtained from the data in Table 6.2.1c, which are directly calculated from experimental results and are compared with the plots calculated using the determined Monod and saturation kinetic constants from the 3 linearisation methods (Figures 6.2.1h and i) and the Curve Expert program (Figures 6.2.1j and k). The kinetic constants used are determined as shown in Table 6.2.1e (for Monod kinetics) and 6.2.1g (for saturation kinetics) and the selected constants listed in Table 6.2.1f (for Monod kinetics) and 6.2.1h (for saturation kinetics). It can be seen from these plots that the measured data do not conform to the form of the Monod and saturation equations and is the reason for the low correlation coefficient (R^2) values (Figure 6.2.1b and c). It is evident that the measured data at the long sludge ages of 25d to 60d deviate from the plots of Monod and saturation kinetics, which are plotted using the kinetic constants determined in Tables 6.2.1f and h below. This shows that the methods used in selecting the best kinetic constants from the measured data were more appropriate for the shorter sludge ages. The main focus of this hydrolysis kinetics evaluation is determining the unbiodegradable fraction $f_{PS'up}$ of the sludge and the hydrolysis kinetic rate to be able to calculate as accurately as possible the biodegradable COD utilized, $\Delta S_{bp} = \left[\left(1 - f_{PS'up}\right) \cdot S_{ti} - S_{bpe}\right]$ for input to the stoichiometric model. Therefore, finding a precise $f_{PS'up}$ is more important than accurate kinetic constants determination because even inaccurate kinetic constants do not change S_{bpe} much (< 0.1 gCOD/*l*) particularly at long sludge age. However, a 0.31 or 0.32 value of $f_{PS'up}$ has a much bigger effect on ΔS_{bp}. The methods used in selecting the kinetic constants (k_m = 4.300 and K_s = 1.523, for

Monod and k_M = 1.796 and K_S = 7.962 for saturation kinetics) are discussed further below (see Tables 6.2.1 e, f, g and h).

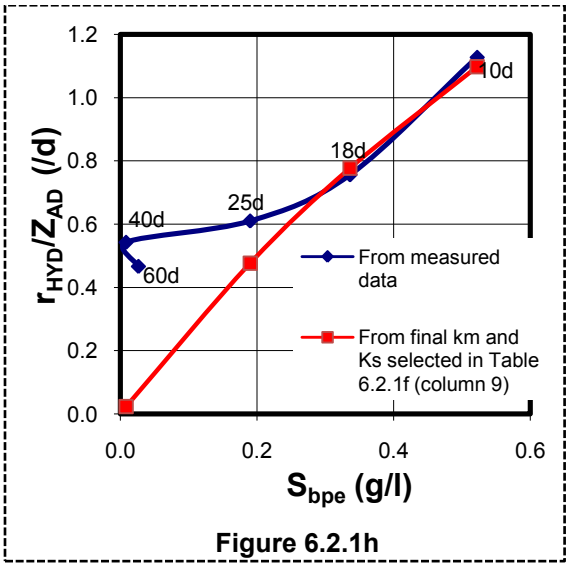

Figure 6.2.1h

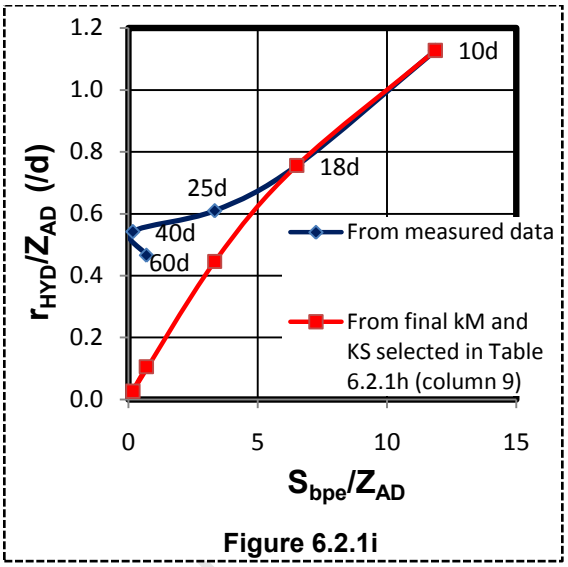

Figure 6.2.1i

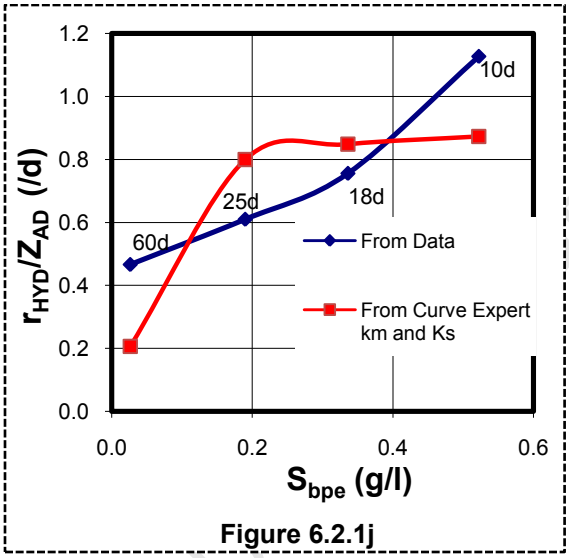

Figure 6.2.1j

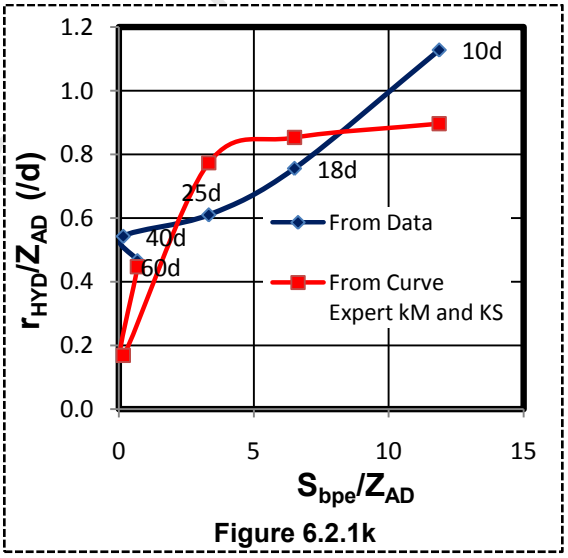

Figure 6.2.1k

Figures 6.2.1h i, j and k: *Hydrolysis kinetics formulation curves plotted using experimental data and calculated from kinetic constants acquired from the three linearization methods for (h) Monod (see Table 6.2.1e column 9; k_m =4.30 and K_s = 1.523) and (i) saturation equations (see Table 6.2.1g column 9; k_M =1.796 and K_S = 7.962) and using the Curve Expert programme (j) for Monod (Table 6.2.1e) and (k) for saturation kinetics (Table 6.2.1h).*

The r_{HYD}, S_{bpe} and Z_{AD} values determined from the experimental results (shown in Table 6.2.1c) were used in the linearization of the Monod and saturation kinetic equations to determine their kinetic constants (i.e. k_m and K_s for Monod and k_M and K_S for saturation kinetics). The plots (Figures 6.2.1l to 6.2.1n, for Monod and 6.2.1p to 6.2.1r for saturation kinetics) below show the measured and best fit results ($f_{PS'up}$ = 0.31) for the three different linearisation methods, i.e. Lineweaver-Burke (M1), double reciprocal (M2) and Eadie-Hofstee (M3) used in this linear regression. The resultant R^2 values together with the slope and y-coefficient for calculating the kinetic constants are presented in following Tables 6.2.1d (for Monod kinetics) and 6.2.1g (for saturation kinetics).

Monod Kinetics

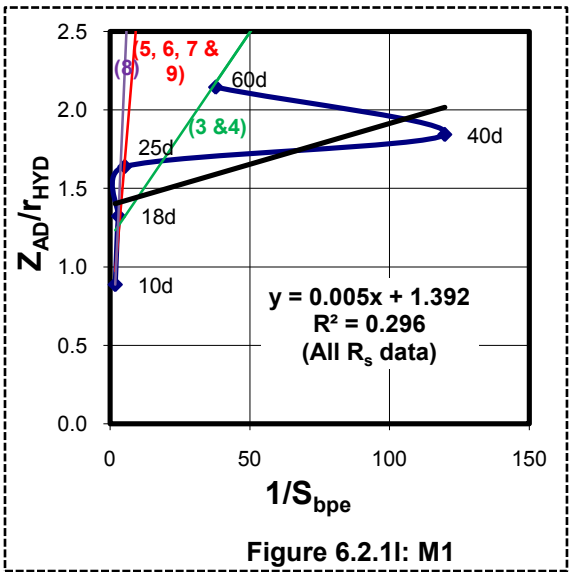

Figure 6.2.1l: M1

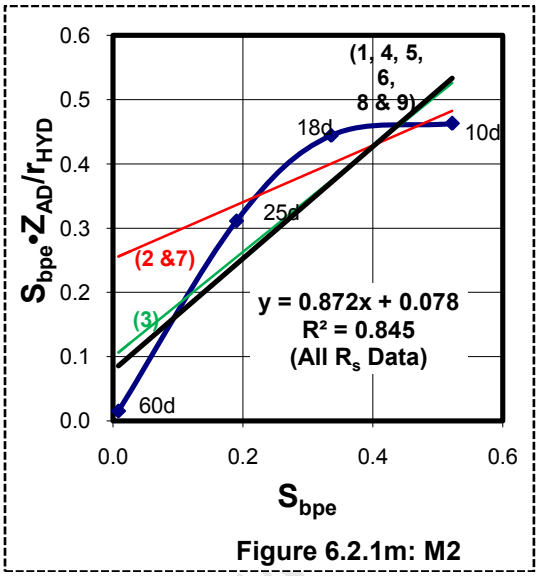

Figure 6.2.1m: M2

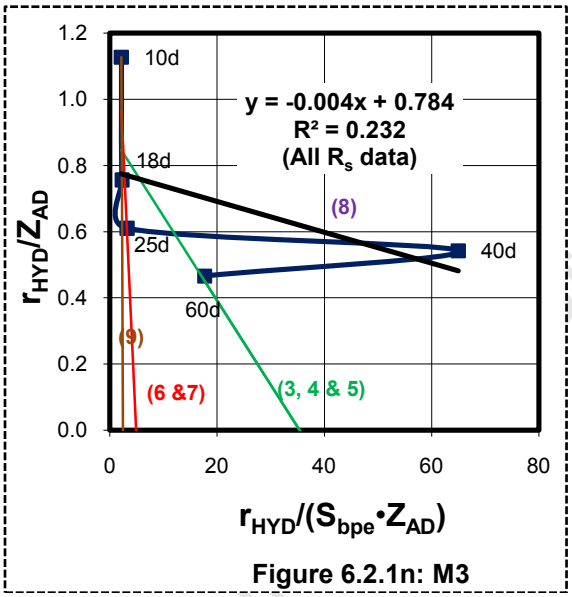

Figure 6.2.1n: M3

Key for Figures 6.2.1 l, m and n	
Column No. in Table 6.2.1e	**Data used or omitted (R_s off) in determining the k_m and K_s values using the 3 linearization methods (M1, M2 and M3)**
1	Only M2 used
2	Only M2 (40 and 60 off)
3	M1, M2 & M3 (40d off all 3)
4	M1 (40d off), M2, M3 (40d off)
5	M1 (40 & 60d off), M2, M3 (40d off)
6	M1 (40 & 60d off), M2, M3 (40 & 60d off)
7	M1, M2 and M3 (40 and 60 off all 3)
8	M1 (25, 40 & 60d off), M2, M3 (40 & 60d off)
9	M1 (40 & 60d off), M2, M3 (25, 40 & 60d off)

Figures 6.2.1l, m and n: *The linearization of Monod kinetics for hydrolysis of PS at all five R_s (10, 18, 25, 40 and 60) using (l) Lineweaver–Burke (M1), (m) double reciprocal (M2) and (n) Eadie–Hofstee (M3) methods (R^2 values for all R_s data included – dark (black) lines. Numbers refer to column numbers in Table 6.2.1e, e.g. 5 refers to column 5 which lists the average k_m and K_s values obtained from line 5 in Figure 6.2.1l:M1 without the R_s =40d and 60d data, line 5 in Figure 6.2.1m:M2 (all data) and line 5 in Figure 6.2.1n: M3 without R_s = 40d data.*

To select the best Monod and saturation kinetic constants that result from the three linearization methods, the formulations for these methods are plotted, together with experimental data, the linear regression equations and correlation coefficients that result from the plots (Figures 6.2.1*l* to m for Monod). These linear regression equations provide the slope and intercept values as functions of the Monod and saturation kinetic constants. If poor (low) correlation coefficient (R^2) values are obtained from the linear regression, it shows that some of the data do not conform well to the Monod and saturation kinetics formulation, hence requiring omission as outlying data to improve the R^2 values e.g. the 40d R_s data in Figures 6.2.1 *l* to n. However, it must be noted that the different linearization methods emphasize different parts of the Monod or saturation kinetics curve, so it is useful to average the resultant kinetic constants from the 3 methods to get results that are better for predicting the hydrolysis rates over the whole range of long and short sludge ages. Therefore, apart from evaluating whether the R^2 values are good ($R^2 \geq 0.8$), it was necessary also to check how well the predicted S_{bpe} values matched those calculated from experimentally measured results. This was done by omitting one or more R_s data, which appear to set the wrong gradient trend to the slope of the linear regression line. This data evaluation for the selection of the best kinetic constants for the hydrolysis of PS is shown in Table 6.2.1e and Figure 6.2.1o, for Monod kinetics and Table 6.2.1g and Figure 6.2.1s for saturation kinetics.

Table 6.2.1e: Predicted S_{bpe} for the Determination of the Best Monod Kinetic Constants from the Three Linearization Methods											
	Data used or omitted (for R_s off) in determining the average k_m and K_s values from the 3 linearization methods (M1, M2 and M3)										
	1	2	3	4	5	6	7	8	9		
R_s	Only M2 (All R_s)	Only M2 (40 and 60 off)	M1, M2 & M3 (40d off all 3)	M1 (40d off), M2, M3 (40d off)	M1 (40 & 60d off), M2, M3 (40d off)	M1 (40 & 60d off), M2, M3 (40 & 60d off)	M1, M2 and M3 (40 and 60 off all 3)	M1 (25, 40 & 60d off), M2, M3 (40 & 60d off)	M1 (40 & 60d off), M2, M3 (25, 40 & 60d off)	Curve Expert	Target S_{bpe}
10	-0.51	0.70	-0.27	-0.15	125.10	1.18	0.80	0.61	0.62	-0.11	0.52
18	0.24	0.35	0.36	0.35	0.33	0.33	0.35	0.38	0.38	0.37	0.34
25	0.12	0.26	0.15	0.12	0.21	0.23	0.26	0.30	0.30	0.10	0.19
40	0.07	0.20	0.08	0.06	0.13	0.16	0.19	0.24	0.24	0.05	0.01
60	0.06	0.17	0.06	0.04	0.11	0.13	0.16	0.21	0.21	0.04	0.03
									Selected		
k_m	1.09	2.27	0.99	0.95	1.25	1.52	1.92	4.68	**4.30**	0.92	
K_s	0.06	0.57	0.06	0.04	0.15	0.26	0.43	1.69	**1.52**	0.03	
R^2	0.88	0.79	0.68	0.69	0.75	0.80	0.76	0.79	0.93	0.34	

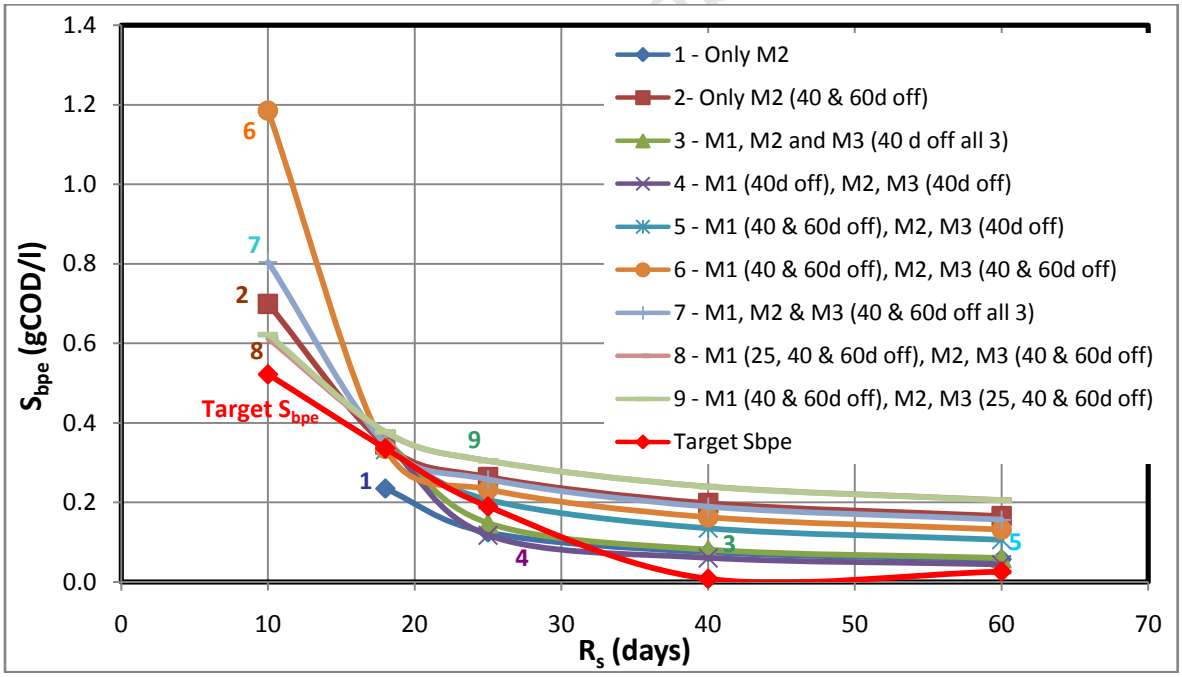

Figure 6.2.1o: *Comparison of tagret S_{bpe} values (calculated from measured values in Table 6.2.1b) with those predicted by different combinations of selected R_s data from the three linearization methods, for the determination of the best k_m and K_s values for modelling hydrolysis with the Monod kinetics. Numbers refer to column numbers in Table 6.2.1.e.*

The reason for the poor R^2 observed with Lineweaver-Burke (M1: R^2 = 0.297, see Figure 6.2.1*l*) and Eadie-Hofstee (M3: R^2 = 0.232, see Figure 6.2.1m) is because the R_s 40d data are far out of line of the other data sets. In order to get the better k_m and K_s values and higher R^2, it is required that this data set is excluded. The improved fit should result in k_m and K_s values that yield predictions of S_{bpe} closer to experimentally measured data. For M1 and M3, taking the slope given by the 10d to 25d R_s data, by removing the 40 and 60d R_s data, results in the best predictions for the short R_s (10 to 18d) (see Figures 6.2.1l and 6.2.1n and Table 6.2.1e). However, for M1 and M3, although the slope emphasized the 25 to 60d R_s data results and so producing unreasonable predictions of S_{bpe} for the 10-day R_s, including this data yields better predictions for the longer 40 and 60 day R_s. Therefore, selecting the best k_m and K_s values was a matter of knowing how far to trade-off between the data that worked best for the shorter (10 to 25d) and longer (25 to 60d) R_s, in order to obtain reasonable S_{bpe} predictions. In fact, the accuracy of prediction of the S_{bpe} at long R_s has very little impact on the accuracy of the biodegradable COD utilized for the stoichiometric part of the model - finding the best $f_{PS'up}$ has a greater impact on the accuracy of the biodegradable COD concentration utilized. After evaluating the results from the different slopes, using Table 6.2.1e and Figure 6.2.1o, it was decided that all the data (10 to 60d R_s) should be applied with M2, since it gave a good R^2 with the complete data set, including all R_s. However, M2 by itself resulted in unreasonable predictions of S_{bp} for the 10d R_s (-ve value; column1 of Table 6.2.1e) and under-predictions of S_{bp} for the 18d R_s. Therefore, the k_m and K_s from the linearization with M1, using only the 10 to 25d R_s data, and M3, using only the 10 to 18d R_s data, were averaged with the M2 (all data) for the determination of the k_m and K_s values to yield better 10 and 18d R_s predictions of the S_{bp} value (although not improving the 40 and 60d over-prediction of S_{bp}). The final k_m and K_s values, resulting from

this data selection (column 9 in Table 6.2.1e and line 9 in Figure 6.2.1o), are presented in Table 6.2.1f below.

To further verify that the best $f_{PS'up}$ was selected, similar evaluations as shown in Table 6.2.1 e and 6.2.1g were performed for $f_{PS'up}$ = 0.30 and 0.32. These attempts did not show any significant improvement on S_{bpe} predictions than with $f_{PS'up}$ = 0.31, thus this value remained the best estimate for $f_{PS'up}$.

Table 6.2.1f: Monod Kinetics (Hydrolysis of PS)						
Linearization	Lineweaver-Burke (M1)	Double reciprocal (M2)	Eadie-Hofstee (M3)	**Average**	**Curve Expert**	**Notes**
Slope	0.005	0.917	-4.133			AD sludge ages of 10, 18, 25, 40 and 60 days are used in all methods.
Y-Intercept	1.392	0.060	10.054			
k_m	0.718	1.090	10.054		**0.922**	
K_s	0.004	0.065	4.133		**0.029**	
R^2	0.297	0.883	0.232		0.336	
Slope	0.211	0.917	-4.133			40 and 60 day R_s is omitted in M1; 25, 40 and 60 day R_s is omitted in M3 to improve R^2
Y-Intercept	0.569	0.060	10.054			
k_m	1.757	1.090	10.054	**4.300**		
K_s	0.370	0.065	4.133	**1.523**		
R^2	0.913	0.883	1.000	0.932		

Saturation Kinetics

Following the same procedure as described above for the Monod kinetics, the k_M and K_S values for saturation kinetics were obtained, after using Table 6.2.1g and Figure 6.2.1s to evaluate the best data used in the linearization methods. These resultant saturation kinetics k_M and K_S values are presented in Table 6.2.1g below.

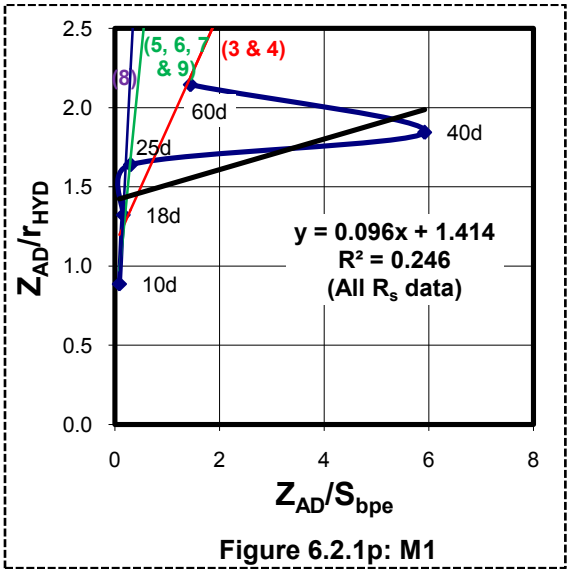

Figure 6.2.1p: M1

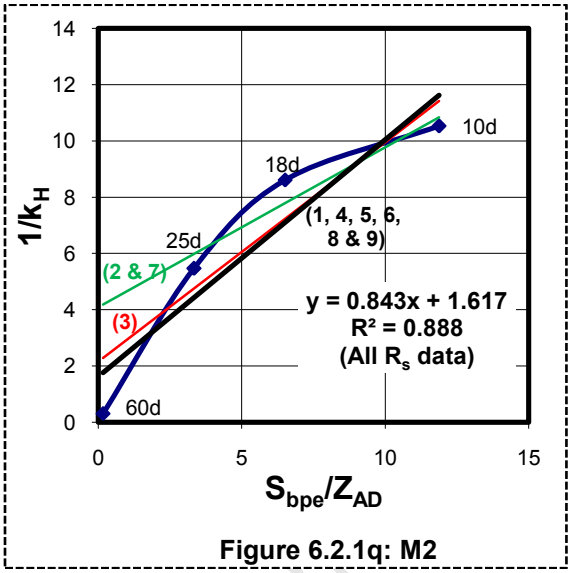

Figure 6.2.1q: M2

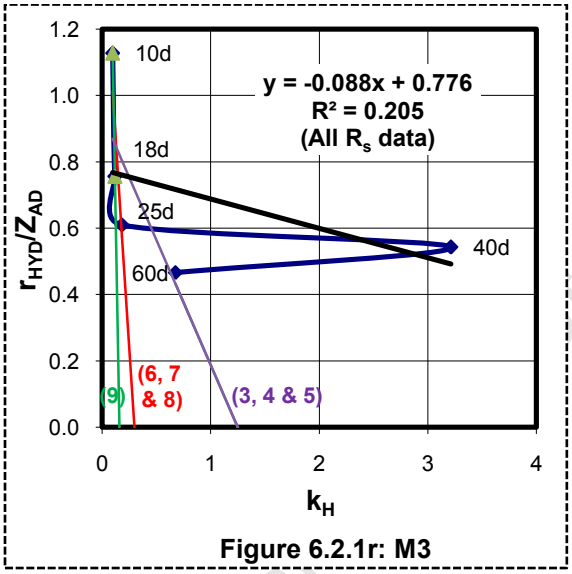

Figure 6.2.1r: M3

Key for Figures 6.2.1 p, q and r	
Column No. in Table 6.2.1g	**Data used or omitted (for R_s off) in determining the k_M and K_S values using the 3 linearization methods (M1, M2 and M3)**
1	Only M2 used
2	Only M2 (40 and 60 off)
3	M1, M2 & M3 (40d off all 3)
4	M1 (40d off), M2, M3 (40d off)
5	M1 (40 & 60d off), M2, M3 (40d off)
6	M1 (40 & 60d off), M2, M3 (40 & 60d off)
7	M1, M2 and M3 (40 and 60 off all 3)
8	M1 (25, 40 & 60d off), M2, M3 (40 & 60d off)
9	M1 (40 & 60d off), M2, M3 (25, 40 & 60d off)

Figures 6.2.1p, q and r: *The linearization of saturation kinetics for hydrolysis of PS at all five R_s (10, 18, 25, 40 and 60) using (p) Lineweaver – Burke (M1), (q) double reciprocal (M2) and (r) Eadie–Hofstee (M3) methods. The R^2 values for all 5 R_s data included- dark (black) lines. Numbers refer to column numbers in Table 6.2.1g, e.g. 2 refers to column 2, which lists the average k_m and K_s values obtained from line 2 in Figure 6.2.1p:M1 all R_s data included, line 2 in Figure 6.2.1q:M2 with R_s =40d and 60d omitted and line 2 in Figure 6.2.1r:M3 with all R_s data included.*

Table 6.2.1g: Predicted S_{bpe} in gCOD/*l* for the Determination of the Best Saturation Kinetic Constants from the Three Linearization Methods											
	Data used or omitted (for R_s off) in determining the average k_M and K_S values from the 3 linearization methods (M1, M2 and M3)										
	1	2	3	4	5	6	7	8	9		
R_s	Only M2	Only M2 (40 and 60 off)	M1, M2 & M3 (40d off all 3)	M1 (40d off), M2, M3 (40d off)	M1 (40 & 60d off), M2, M3 (40d off)	M1 (40 & 60d off), M2, M3 (40 & 60d off)	M1, M2 and M3 (40 and 60 off all 3)	M1 (25, 40 & 60d off), M2, M3 (40 & 60d off)	M1 (40 & 60d off), M2, M3 (25, 40 & 60d off)	**Curve Expert**	**Target S_{bpe}**
10	2.77	0.59	-2.05	-0.64	1.42	0.78	0.65	0.60	0.60	-0.39	0.52
18	0.24	0.32	0.31	0.30	0.30	0.30	0.32	0.33	0.33	0.31	0.34
25	0.13	0.23	0.16	0.13	0.18	0.20	0.22	0.24	0.24	0.12	0.19
40	0.07	0.14	0.08	0.06	0.10	0.12	0.13	0.15	0.15	0.05	0.01
60	0.04	0.09	0.05	0.04	0.06	0.07	0.09	0.10	0.10	0.03	0.03
									Selected		
k_m	1.146	1.760	1.035	0.989	1.176	1.358	1.563	1.811	**1.796**	0.956	
K_s	1.537	7.202	1.386	0.979	2.341	3.755	5.643	8.049	**7.962**	0.788	
R^2	0.910	0.920	0.736	0.739	0.784	0.854	0.858	0.882	0.942	0.330	

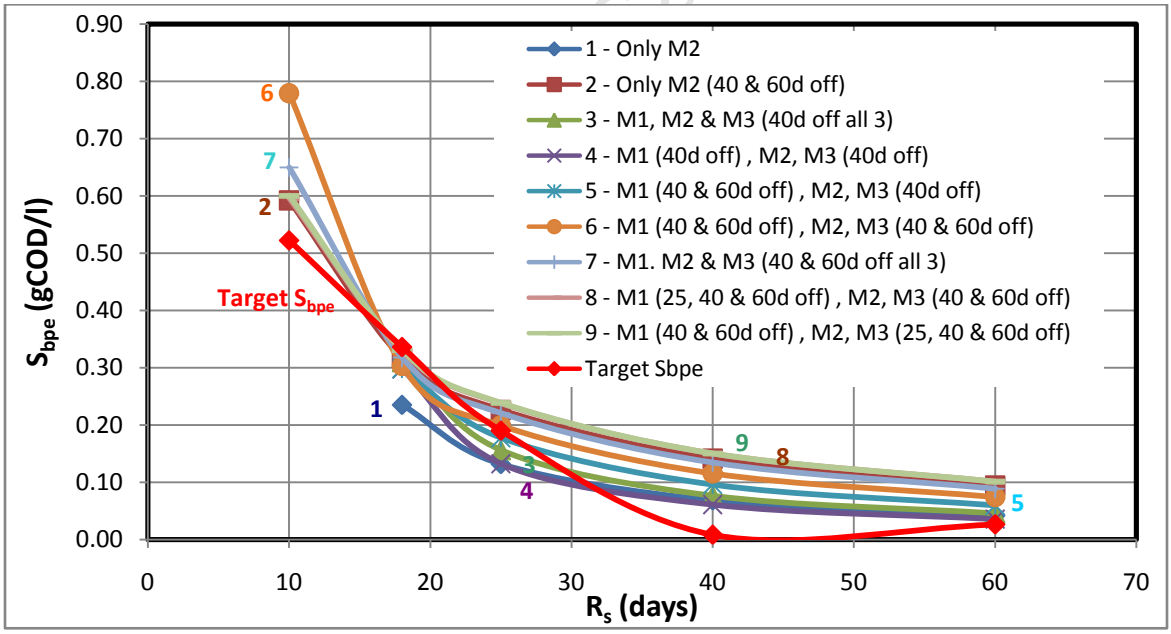

Figure 6.2.1s: *Comparison of tagret S_{bpe} values (calculated from measured values in Table 6.2.1b) with those predicted by different combinations of selected R_s data from the three linearization methods, for the determination of the best k_M and K_S values for modelling hydrolysis with the saturation kinetics. Numbers refer to column number in Table 6.2.1g.*

Table 6.2.1h: Saturation Kinetics (Hydrolysis of PS)						
Linearization	Lineweaver-Burke (M1)	double reciprocal (M2)	Eadie-Hofstee (M3)	**Average**	**Curve Expert**	**Notes**
Slope	0.097	0.872	-0.089			AD sludge ages of 10, 18, 25, 40 and 60 days are used in all methods.
Y-Intercept	1.415	1.341	0.776			
k_M	0.707	1.146	0.776		**0.956**	
K_S	0.068	1.537	0.089		**0.788**	
R^2	0.247	0.910	0.205		0.330	
Slope*	3.285	0.872	-17.617			40 and 60 day R_s is omitted in M1; 25, 40 and 60 day R_s is omitted in M3 to improve R^2.
Y-Intercept*	0.694	1.341	2.801			
k_M*	1.440	1.146	2.801	**1.796**		
K_S*	4.732	1.537	17.617	**7.962**		
R^2*	0.916	0.910	1.000	0.942		

In summary, from Tables 6.2.1f and 6.2.1h, the double reciprocal method (M2) gives the best correlation with all the experimental data (R^2 = 0.883 for Monod kinetics and R^2 = 0.910 for saturation kinetics). In contrast, linearization by the other two methods (M1 and M3) shows poor correlation because the PS data do not conform to the form of the Monod and saturation equations (Figures 6.2.1h and i). Removal of the 40 and 60-day R_s data for M1 and the 25, 40 and 60-day R_s data for M3 gave better correlation values, but resulting K values are valid only for short (10 – 20) sludge age ADs.

Selected PS Hydrolysis Monod and Saturation Kinetic Constants

The average kinetic constants obtained from the three linearization methods with the removal of the above-mentioned outliers gives a k_m of 4.3 gCOD /(gCOD.d) and K_s of 1.523 (gCOD/*l*) for Monod kinetics and a k_M of 1.796 gCOD /(gCOD.d) and K_S of 7.962 (gCOD/*l*) for saturation kinetics. These kinetic constants are different from those of Sötemann *et al.* (2005a) obtained for the Izzett *et al.* (1992) Primary and humus sludge mixture and the O'Rourke (1968) 'pure'PS. The determined kinetic constants were k_m of 3.34 gCOD /(gCOD.d) and K_s of 6.76 (gCOD/*l*) for Monod kinetics and a k_M of 5.27 gCOD /(gCOD.d) and K_S of 7.98

(gCOD/*l*) for saturation kinetics, for the Izzett *et al.* (1992) sludge and k_m of 2.004 gCOD /(gCOD.d), K_s of 0.355 (gCOD/*l*), k_M of 2.047 gCOD /(gCOD.d) and K_S of 0.263 (gCOD/*l*), for the O'Rourke (1968) PS. The Figure 6.2.1t below shows a comparison of the biodegradable COD removals predicted with the selected hydrolysis kinetic constants for the PS of this investigation with those obtained with the same procedures by Sötemann *et al.* (2005) for the Izzett *et al.* (1992) PS and the O'Rourke (1968) PS and for Ristow *et al.* (2004) PS.

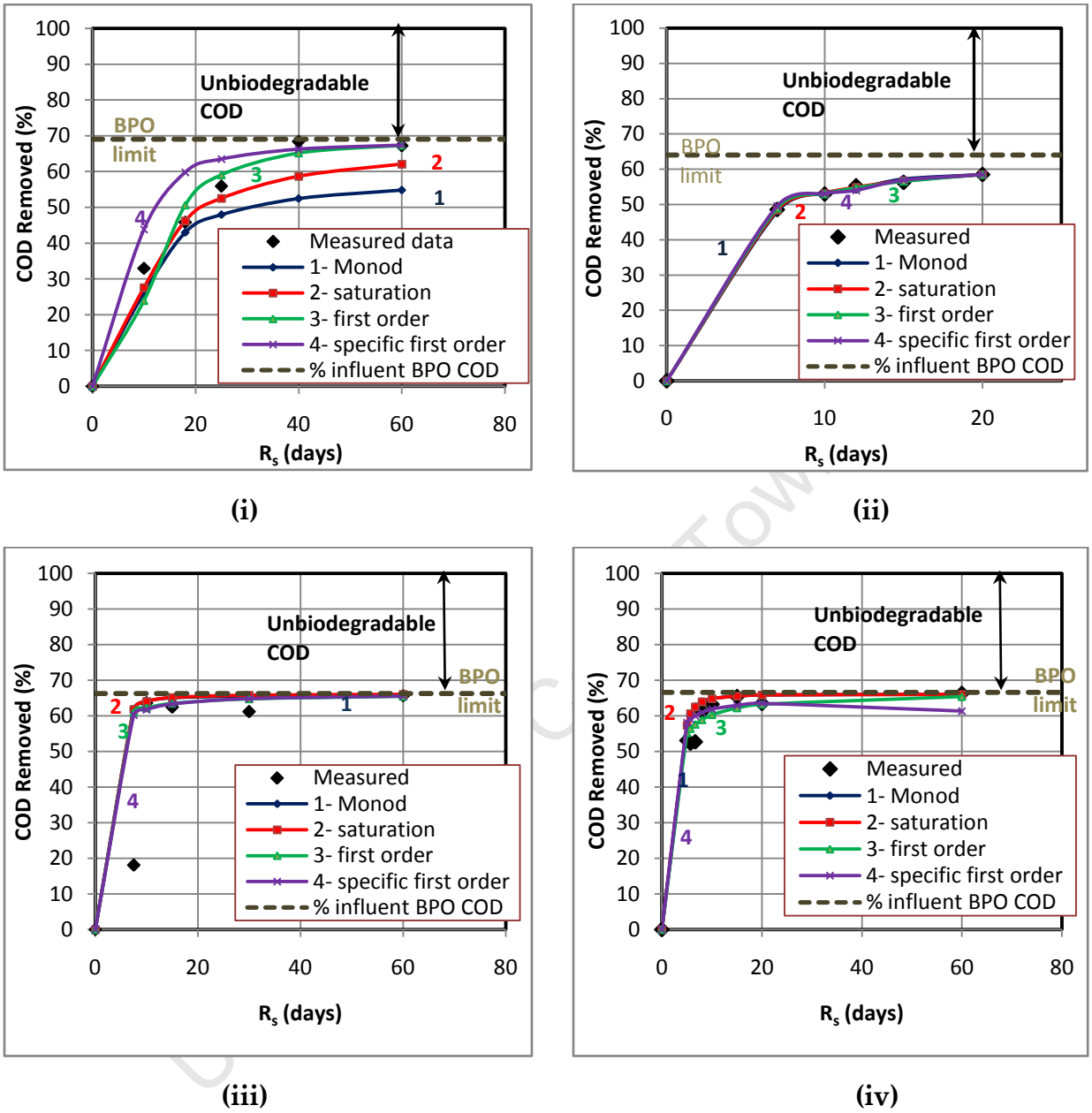

Figures 6.2.1t: *Comparison of S_{bp} removal for (i) Author data (Ikumi, 2011; $f_{PS'up}$ = 0.31) to data from (ii) Izzett et al. (1992) ($f_{PS'up}$ = 0.36), (iii) O'Rourke (1968) ($f_{PS'up}$ = 0.338), and (iv) Ristow et al. (2004a) ($f_{PS'up}$ = 0.3345).*

6.2.2.2. MLE 1 Waste Activated Sludge (WAS)

The same procedure applied for the determination of the hydrolysis kinetic constants of the PS was also applied to determine the hydrolysis kinetic constants of the WAS. Tables 6.2.2a and 6.2.2b show the average influent and effluent experimental results obtained in the AD of WAS from the Modified Ludzack Ettinger (MLE) system fed the settled wastewater (MLE 1).

Table 6.2.2a: WAS from MLE Fed Settled WW Influent Experimental Data

Retention Time (d)	10		18		25		40		60	
Digester Volume (*l*)	12		12		12		12		12	
Influent flow (*l*/d)	1.2		0.67		0.48		0.3		0.08	
Units	Conc. (g/*l*)	Flux (g/d)	Conc. (g/*l*)	Flux (g/d)	Conc. (g/*l*)	Flux (g/d)	Conc. (g/*l*)	Flux (g/d)	Conc. (g/*l*)	Flux (g/d)
Influent COD[3], S_{ti} (gCOD/*l*)	2.67	1.93	3.65	1.92	5.15	1.93	8.05	1.9	11.71	1.9
Influent COD[1], S_{upi} (gCOD/*l*)	1.26	0.91	1.71	0.9	2.42	0.91	3.78	0.89	5.5	0.89
Influent COD, S_{usi}[2] (gCOD/*l*)	0.03	0.02	0.03	0.02	0.06	0.02	0.03	0.01	0.03	0.01
Influent COD, S_{bpi}[6] (gCOD/*l*)	1.38	1	1.9	1	2.67	1	4.24	1	6.17	1
Influent COD, S_{bsfi}[5] (gCOD/*l*)	0	0	0	0	0	0	0	0	0	0
Influent VFA, S_{bsai}[4] (gCOD/*l*)	0.16	0.12	0.06	0.03	0	0	0.06	0.02	0.02	0
Influent TKN[3] (gN/*l*)	0.18	0.13	0.3	0.16	0.36	0.14	0.63	0.15	0.86	0.14
Influent filtered TKN (gN/*l*)	0	0	0	0	0.01	0	0.01	0	0	0
Influent FSA (gN/*l*)	0	0	0	0	0	0	0	0	0	0
Influent Alk g/*l* as $CaCO_3$	0.44	0.31	0.69	0.37	0.51	0.19	0.46	0.11	0.52	0.08
Influent pH	7.7		7.84		7.64		7.63		7.8	
Influent TP[3] (gP/*l*)	0.06	0.05	0.09	0.05	0.14	0.05	0.23	0.05	0.35	0.06
Influent filtered TP (gP/*l*)	0.01	0.01	0.01	0.01	0.01	0	0.01	0	0.01	0
Influent OP (gP/*l*)	0.01	0.01	0.01	0.01	0.01	0	0.01	0	0.01	0
Influent TSS (gTSS/*l*)	2.15	1.55	3.05	1.6	4.22	1.58	6.58	1.55	9.49	1.54
Influent VSS (gVSS/*l*)	1.78	1.29	2.52	1.32	3.48	1.3	5.4	1.27	7.91	1.28
Influent ISS (gISS/*l*)	0.37	0.26	0.53	0.28	0.74	0.28	1.18	0.28	1.59	0.26

[1] S_{upi} is the unbiodegradable particulate COD calculated using best-determined $f_{SL'up}$ = 0.47, obtained for good coefficients of variation and correlation coefficients as shown in the section below

[2] S_{usi} is the unbiodegradable soluble COD measured from the filtered effluent of parent MLE 1 AS system

[3] Unfiltered samples

[4] S_{bsai} is the COD in short chain fatty acids that is measured in the influent using the 5-point titration method

[5] S_{bsfi} is the fermentable biodegradable soluble influent COD, assumed to be zero (completely utilized) from MLE 1

[6] S_{bpi} is the biodegradable particulate influent COD, calculated by the total influent COD (S_{ti}) – S_{usi} – S_{bsai} – S_{upi}

Table 6.2.2b: WAS from MLE Fed Settled WW Effluent Experimental Data										
Retention Time (d)	10		18		25		40		60	
Effluent flow (*l*/d)	1.20		0.67		0.48		0.30		0.08	
Units	Conc. (g/*l*)	Flux (g/d)	Conc. (g/*l*)	Flux (g/d)	Conc. (g/*l*)	Flux (g/d)	Conc. (g/*l*)	Flux (g/d)	Conc. (g/*l*)	Flux (g/d)
Effluent COD[1], S_{te} (gCOD/*l*)	2.29	1.66	2.51	1.32	3.01	1.12	4.45	1.05	6.22	1.01
Effluent COD, S_{upe} [5] (gCOD/*l*)	1.26	0.91	1.71	0.90	2.42	0.91	3.78	0.89	5.50	0.89
Effluent COD, S_{use}[2] (gCOD/*l*)	0.03	0.02	0.03	0.02	0.06	0.02	0.03	0.01	0.03	0.01
Effluent filtered COD, S_{tse} (gCOD/*l*)	0.07	0.05	0.07	0.04	0.09	0.03	0.03	0.01	0.03	0.01
Effluent COD, S_{bpe}[6] (gCOD/*l*)	0.96	0.69	0.72	0.38	0.50	0.19	0.64	0.15	0.68	0.11
Effluent COD, S_{bsfe}[4] (gCOD/*l*)	0.04	0.03	0.04	0.02	0.03	0.01	0.00	0.00	0.00	0.00
Effluent VFA, S_{bsae}[3] (gCOD/*l*)	0.03	0.02	0.01	0.01	0.04	0.01	0.01	0.00	0.03	0.00
Effluent TKN[1] (gN/*l*)	0.18	0.13	0.27	0.14	0.38	0.14	0.54	0.13	0.74	0.12
Effluent filtered TKN (gN/*l*)	0.04	0.03	0.11	0.06	0.17	0.06	0.34	0.08	0.48	0.08
Effluent FSA (gN/*l*)	0.04	0.03	0.10	0.05	0.15	0.06	0.30	0.07	0.47	0.08
Effluent TP[1] (mgP/*l*)	0.06	0.04	0.09	0.05	0.14	0.05	0.24	0.06	0.33	0.05
Effluent filtered TP (gP/*l*)	0.02	0.02	0.05	0.02	0.07	0.03	0.14	0.03	0.21	0.03
Effluent OP (gP/*l*)	0.02	0.01	0.05	0.02	0.07	0.03	0.13	0.03	0.20	0.03
Effluent TSS	1.92	1.39	1.98	1.04	2.43	0.91	4.02	0.95	5.39	0.87
Effluent VSS	1.54	1.11	1.49	0.78	1.84	0.69	2.82	0.66	3.95	0.64
Effluent ISS	0.38	0.28	0.49	0.26	0.59	0.22	1.21	0.28	1.44	0.23
Effluent Alk mg/*l* as $CaCO_3$	0.42	0.30	0.74	0.39	0.79	0.30	1.24	0.29	1.50	0.24
Measured digester pH	7.02		7.17		7.09		7.31		7.38	
COD removed (gCOD/*l*)		0.28		0.60		0.80		0.85		0.89
Gas production (litres/d)	0.24		0.43		0.50		0.33			
Gas prod. (l gas/*l* influent)	0.20		0.65		1.05		1.08		No data	
Gas composition : CH_4 fraction	0.34		0.34		0.34		0.34		0.34	
Gas composition: CO_2 fraction	0.17		0.17		0.17		0.17		0.17	
Volume of CH_4 (litres)	0.07		0.22		0.35		0.36			
Volume of CO_2 (litres)	0.03		0.11		0.18		0.18			
COD of CH_4 (gCOD/*l* feed)	0.15		0.86		1.93		3.19		4.63	
p_{CO2} (atm.)	0.34		0.34		0.34		0.34			
C_T dissolved (mmol/*l*)	8.72		8.72		8.72		8.72			
H_2CO_3 diss. (mg/*l*)	871.54		871.54		871.54		871.54			
Moles of CO_2/*l* feed	0.00		0.00		0.01		0.01			
Moles of CH_4/*l* feed	0.00		0.01		0.01		0.01			
COD balance (%)	91.31		92.21		95.86		94.87		92.66	
Nitrogen balance (%)	100.74		91.50		103.54		84.96		86.20	
Phosphorous balance (%)	95.52		102.12		100.22		104.66		93.46	
f_{cv} (gCOD/gVSS)	1.49		1.68		1.64		1.58		1.57	
$f_{SL'up}$ (MLE 1 WAS)	0.47		0.47		0.47		0.47		0.47	

[1] Unfiltered sample

[2] S_{use} is the unbiodegradable soluble COD that equals the S_{usi} value from Table 6.2.2a.

[3] S_{bsae} is the COD in short chain fatty acids that is measured in the effluent using the 5-point titration method.

[4] S_{bsfe} is the fermentable biodegradable soluble COD calculated from the measured filtered effluent COD (S_{tse}) – S_{use} – S_{bsae}.

[5] S_{upe} is the unbiodegradable particulate effluent COD which equals the S_{upi} value from Table 6.2.2a.

[6] S_{bpe} is the biodegradable particulate effluent COD which equals the total effluent COD (S_{te}) – S_{tse} – S_{upe}.

The Selection of the Best $f_{SL'up}$ Value

The influence of $f_{SL'up}$ on the hydrolysis rate kinetic constants of the AD of MLE 1 WAS is shown below by plotting the coefficients of variation for first order and first order specific hydrolysis kinetic equations versus increasing $f_{SL'up}$ fractions (shown in Figure 6.2.2a) and correlation coefficients (R^2) for Monod and saturation hydrolysis kinetic equations versus the same range of $f_{SL'up}$ fractions (in Figures 6.2.2b and 6.2.2c respectively). This is done in order to obtain the most suitable $f_{SL'up}$ fraction that gives the best correlation coefficients when applying the four hydrolysis kinetic equations to predict, as accurately as possible, the effluent COD from the AD fed the MLE 1 WAS. The correlation coefficients for the Monod and saturation kinetics are shown for the Curve Expert program and the three linearization methods of Lineweaver-Burke (M1), double reciprocal (M2) and Eadie-Hofstee (M3) and (M3*). The M1, M2 and M3 (without asterisks) were obtained using the data for all five MLE 1 WAS AD sludge ages, i.e. 10, 18, 25, 40 and 60 days R_s. The M3* is the result with the omission of 25, 40 and 60-day sludge age AD data when linearising the Monod kinetics and saturation kinetics with the Eadie-Hofstee method. The M3* was included to improve the R^2 value for the M3 method but of course with only two sludge ages (data parts), the correlation is perfect (R^2 =1). Overall the coefficients of variation are lower and the correlation coefficients are higher over the entire range of $f_{SL'up}$ for all four hydrolysis kinetic equations for the MLE 1 WAS than the PS indicating that these equations fit the MLE1 WAS data better. But as for the PS, it is more important to find the best $f_{SL'up}$ than very accurate kinetic constants because the $f_{SL'up}$ has a greater effect on the $\Delta S_{bp} = (1 - f_{SL'up}) \cdot S_{ti} - S_{bpe}$ than the kinetic constants especially at long sludge ages.

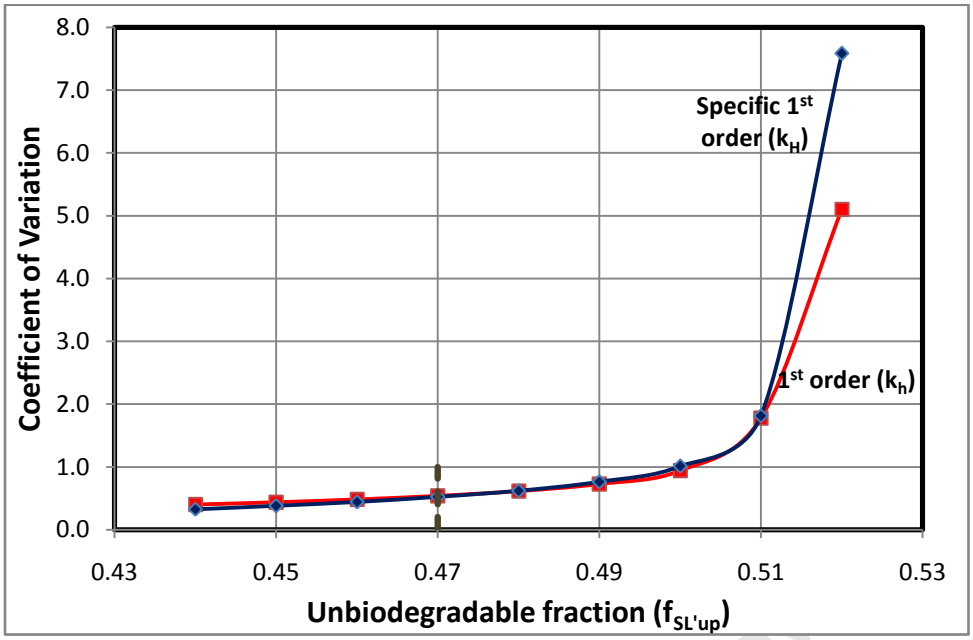

Figure 6.2.2a: *The change in the coefficient of variation of the 1st order and specific 1st order hydrolysis equations kinetic constants with changing unbiodegradable particulate COD fraction ($f_{SL'up}$) of MLE 1 WAS, without R_s = 25d (see Table 6.2.2c).*

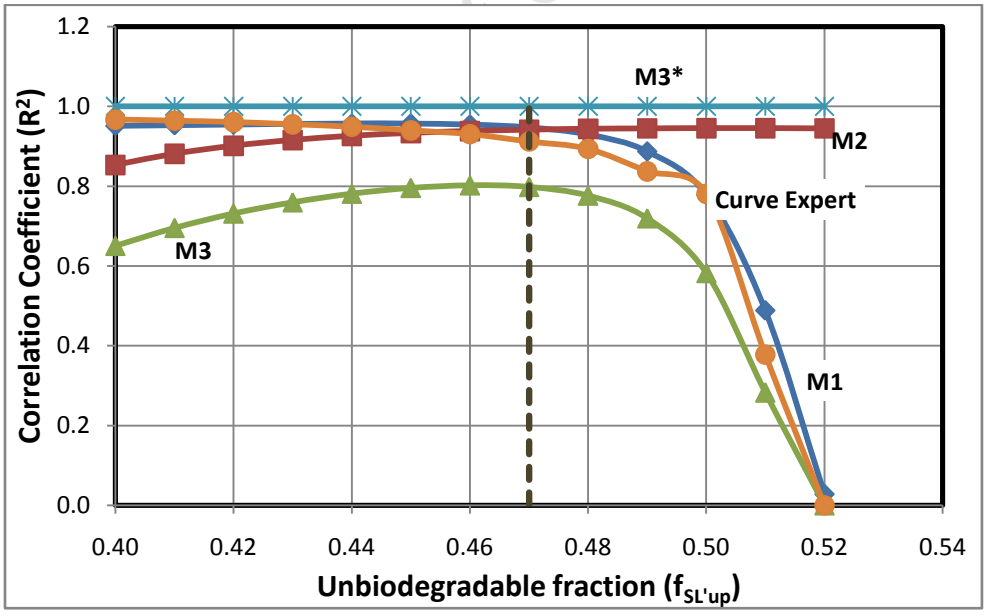

Figure 6.2.2b: *The regression correlation coefficient (R^2) for the Curve Expert program, Lineweaver-Burke (M1), double reciprocal (M2) and Eadie-Hofstee (M3) linearization methods, of Monod hydrolysis kinetics versus unbiodegradable particulate COD fraction ($f_{SL'up}$) of the MLE 1 WAS.*

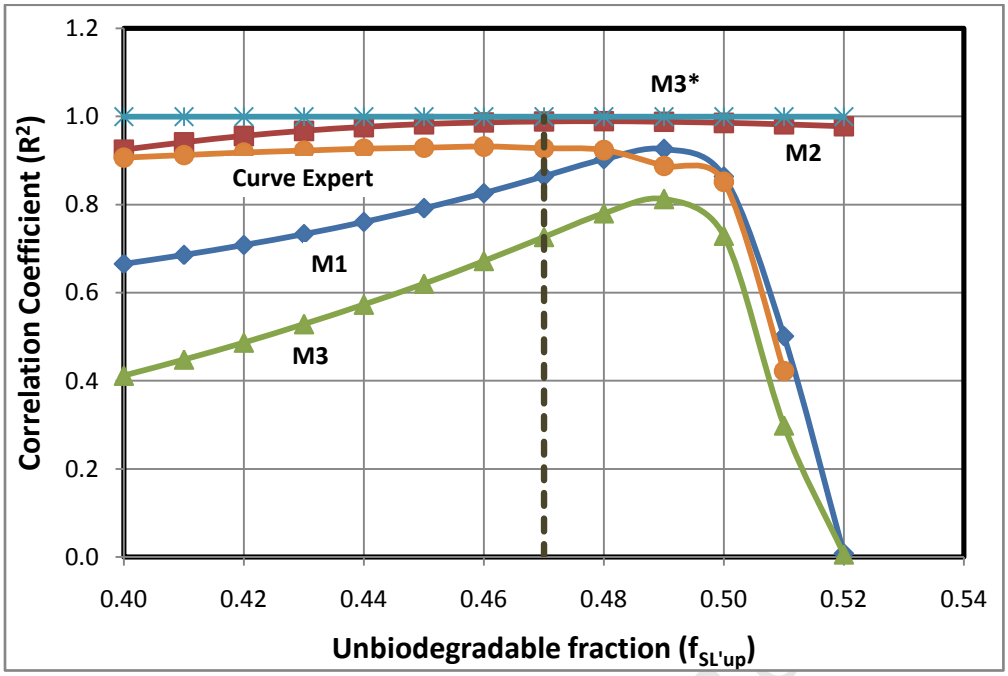

Figure 6.2.2c: *The regression correlation coefficient (R^2) for the Curve Expert program, Lineweaver-Burke (M1), double reciprocal (M2) and Eadie-Hofstee (M3) linearization methods of saturation hydrolysis kinetics versus unbiodegradable particulate COD fraction ($f_{SL'up}$) of the MLE 1 WAS.*

As for the case in the AD of PS, Figure 6.2.2a shows that the coefficient of variation (C_{var}) increases with increase in the unbiodegradable particulate fraction from 0.45 to 0.5, after which it increases sharply. Figures 6.2.2b and 6.2.2c show that Monod and saturation kinetics exhibit maximum R^2 values at $f_{SL'up}$ value of around 0.46 and 0.49 respectively. Therefore, the best compromise $f_{SL'up}$ value for all four kinetic equations is 0.47. This value is quite close to that measured when the AD was operated at the long sludge of 60 days (0.53) and equal to that calculated with the AS model for the AS system VSS (MLE 1) from the influent wastewater $f_{S'up}$ fraction and organism endogenous residue (ER) (0.47, see Section 5.3 of Chapter 5). Therefore, $f_{SL'up}$ = 0.47 was selected for determination of the hydrolysis kinetic constants.

First Order Kinetics

The experimentally measured influent (S_{ti}) and effluent (S_{te}) concentrations for the steady state AD of WAS from the MLE 1 (Tables 6.2.2a and 6.2.2b) were used in the above-mentioned kinetic calculations (Section 6.2.1) to determine the volumetric hydrolysis rates (r_{HYD}, gCOD/(*l*.d)), the specific hydrolysis rate (r_{HYD}/Z_{AD}, gCOD hydrolysed/(gCOD biomass.d)), the residual biodegradable COD concentrations (S_{bp}) and the first order and first order specific kinetic rate constants (k_h and k_H). These rates are listed in Table 6.2.2c below and their variations with sludge age are plotted in Figures 6.2.2d to 6.2.2g. The graphs of k_h and k_H show that the 25d R_s AD data do not conform to the pattern of the other AD sludge ages, so the linear relationship (from Equation 6.21c and d) of k_h and k_H with sludge age was determined without the 25d data set. This gives $k_h = 0.0033 \cdot R_s + 0.0413$ (R^2 = 0.8415) for 1st order hydrolysis kinetics and $k_H = 0.0963 \cdot R_s + 0.97$ (R^2 = 0.9742) for specific first order hydrolysis kinetics.

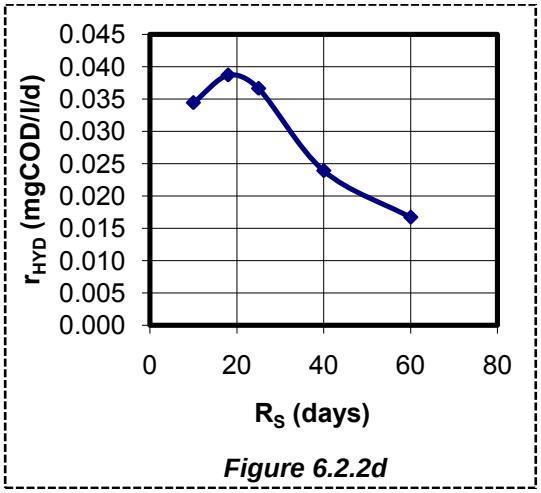

Figure 6.2.2d

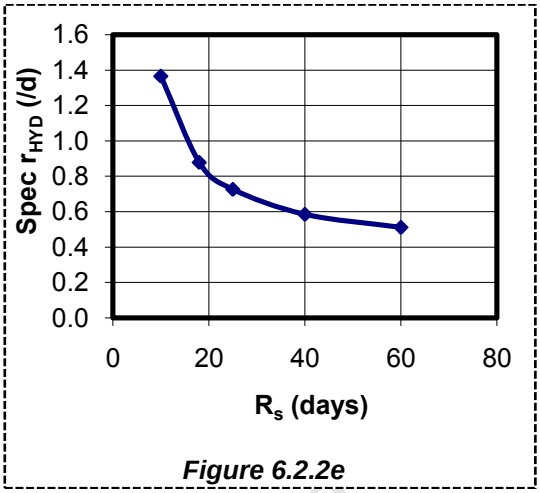

Figure 6.2.2e

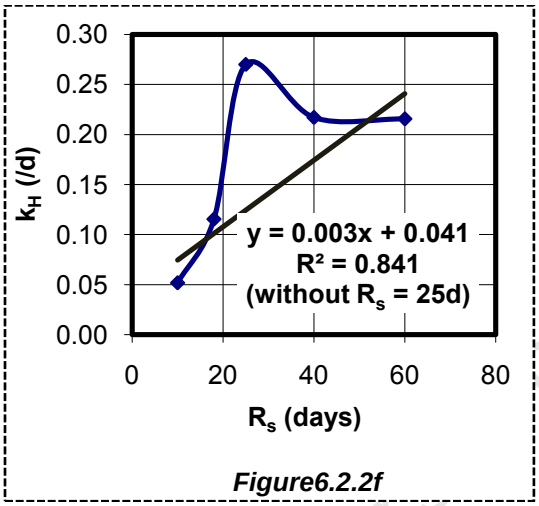

Figure6.2.2f

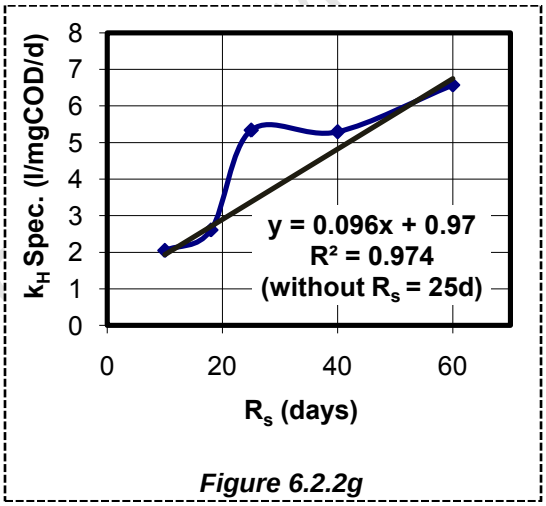

Figure 6.2.2g

Figures 6.2.2d, e, f and g: *Volumetric hydrolysis rates (r_{HYD}, gCOD/ (l.d)) (d), specific volumetric hydrolysis rates (r_{HYD}/Z_{AD}, gCOD/(gCOD.d)) (e), first order kinetic constants (k_h) (f) and specific first order kinetic constants (k_H) (g), all versus sludge age (R_s) from 10, 18, 25, 40 and 60d, for MLE 1 WAS. Equation and correlation coefficient (R^2) given for results without R_s = 25d data.*

Table 6.2.2c: Summary of Results for First Order Kinetics in the AD of MLE 1 WAS for $f_{SL'up}$ = 0.47						
R_s (d)	**r_{HYD} (g/*l*/d)**	**Z_{AD} (g/*l*)**	**S_{bpe} (g/*l*)**	**k_h (/d)**	**Spec. r_{HYD} ($gS_{bp}/gZ_{AD}/d$**	**k_H ($l/gZ_{AD}/d$)**
10	0.034	0.025	0.666	0.052	1.365	2.050
18	0.039	0.044	0.336	0.115	0.878	2.614
25	0.037	0.051	0.136	0.270	0.725	5.340
40	0.024	0.041	0.110	0.217	0.584	5.296
60	0.017	0.033	0.078	0.215	0.510	6.578
		Mean		0.174	-	4.376
		Standard deviation		0.088	-	1.945
		Coefficient of variation		0.567	-	0.445
$k_h = c_{kh} + m_{kh} \times R_s$; c_{kh} = 0.0413; m_{kh} = 0.0033; R^2 = 0.8415(without R_s = 25d data) $k_H = c_{kH} + m_{kH} \times R_s$; c_{kH} = 0.97; m_{kH} = 0.0963; R^2 = 0.9742 (without R_s = 25d data)						

Monod and Saturation Kinetics

The Figures 6.2.2h and 6.2.2i below show the specific hydrolysis rates (r_{HYD}/Z_{AD}) of the BPO of the MLE 1 WAS versus the residual BPO (S_{bpe}) for the Monod equation and versus the residual BPO per acidogenic biomass (S_{bpe} / Z_{AD}) for the saturation kinetics equation. The specific hydrolysis rate (r_{HYD}/Z_{AD}) obtained from the data in Table 6.2.2c, which are directly calculated from experimental results, are compared with those calculated from the determined Monod and saturation kinetic constants from the 3 linearisation methods, including all five R_s data, in Figures 6.2.2h and i and the Curve Expert program in Figures 6.2.2j and k.

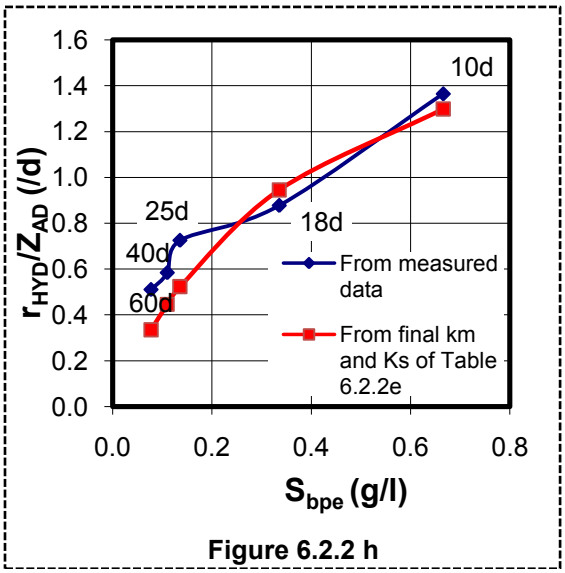

Figure 6.2.2 h

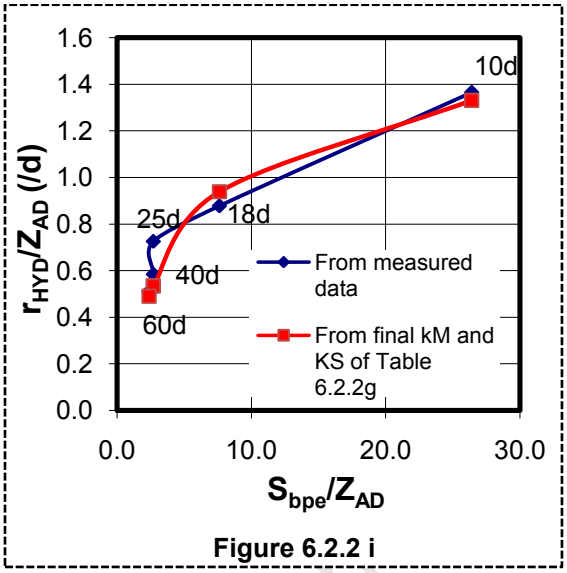

Figure 6.2.2 i

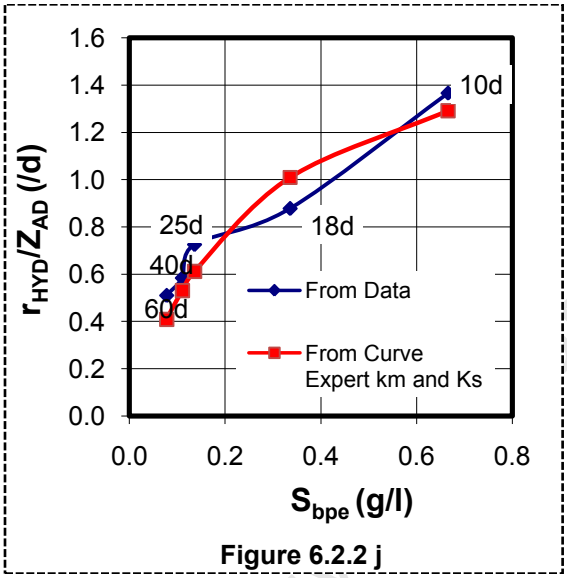

Figure 6.2.2 j

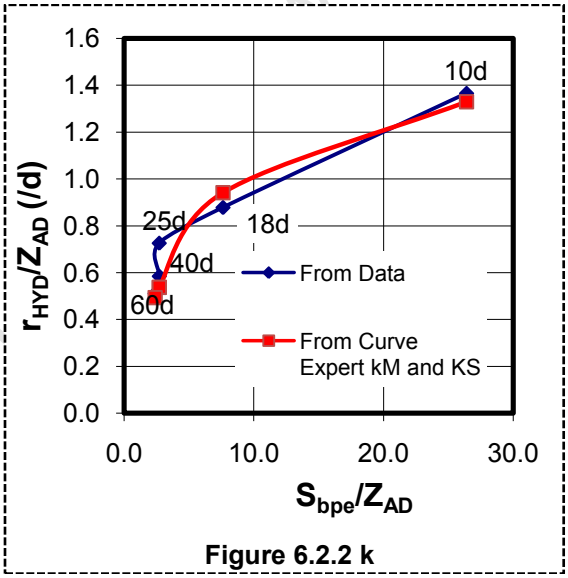

Figure 6.2.2 k

Figures 6.2.2h, i, j and k: *Hydrolysis kinetics formulation curves plotted using experimental data and calculated from kinetic constants acquired from the three linearization methods, for (h) Monod (see Table 6.2.2d column 7, or Table 6.2.2e; k_m =2.094 and K_s = 0.408) and (i) saturation (see Table 6.2.2f column 6, or Table 6.2.2g; k_M =1.603 and K_S = 5.387) equations and the Curve Expert programme (j) for Monod and (k) for saturation kinetics.*

The determined values of r_{HYD}, S_{bp}, Z_{AD} (shown in Table 6.2.2c) for the AD of MLE 1 WAS were used in the three linearization methods of the Monod and saturation kinetic equations to obtain the kinetic constants (i.e k_m and K_s for

Monod kinetics and k_M and K_S for saturation kinetics). The results for Monod kinetics and saturation kinetics are shown in (i) Figures 6.2.2l and 6.22p for Lineweaver-Burke, (ii) Figures 6.2.2m and 6.22q for double Reciprocal, (iii) Figures 6.2.2n and 6.22r for Eadie-Hofstee. The resultant R^2 values together with the graphical slope and y-coefficient used for calculating the kinetic constants are presented in Tables 6.2.2e (Monod kinetics) and 6.2.2g (saturation kinetics).

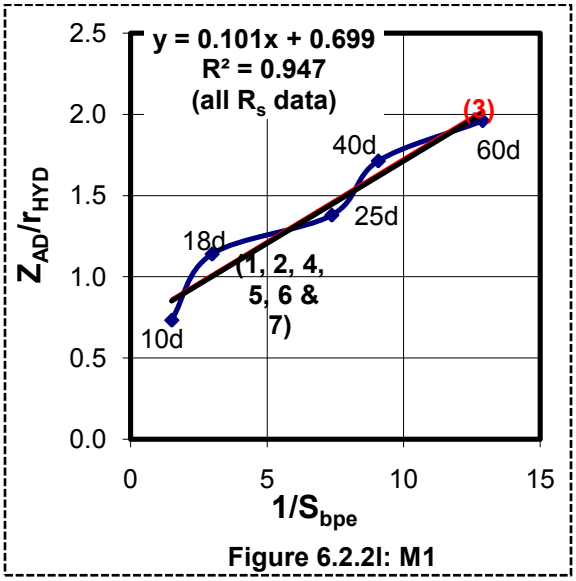

Figure 6.2.2l: M1

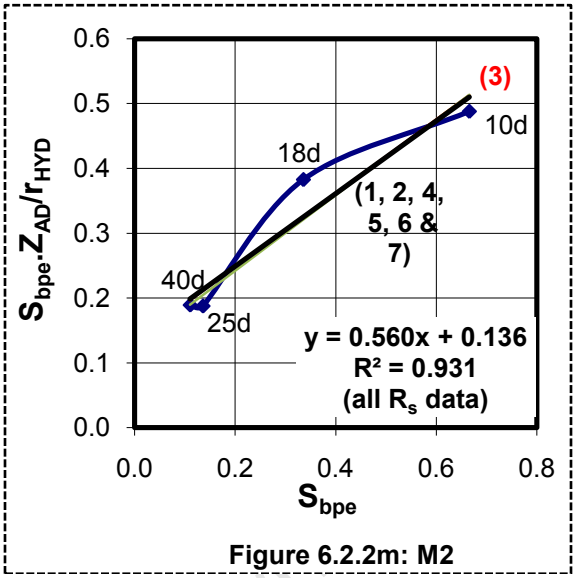

Figure 6.2.2m: M2

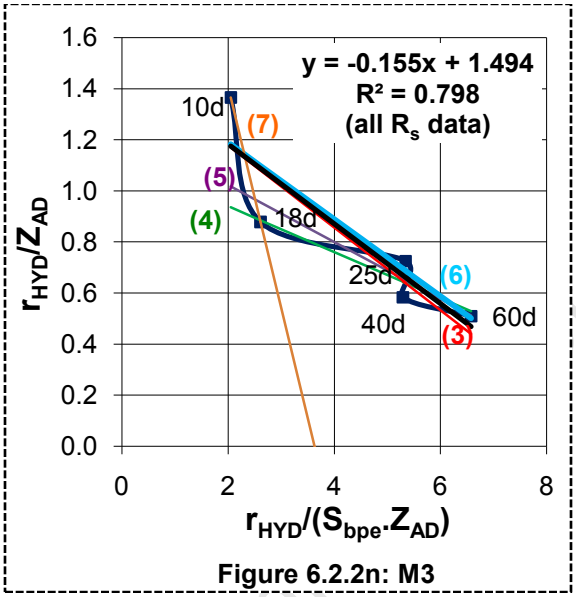

Figure 6.2.2n: M3

Key for Figures 6.2.2 l, m and n	
Column No. in Table 6.2.2d	Data used or omitted (R_s off) in determining the k_m and K_s values using the 3 linearization methods (M1, M2 and M3)
1	All Inclusive
2	without M3
3	M1, M2, M3 (25d off all 3)
4	M1, M2, M3 (10d off)
5	M1, M2, M3 (10 & 18d off)
6	M1, M2, M3 (40 & 60d off)
7	M1, M2, M3 (25, 40 & 60d off)

Figures 6.2.2l, m and n: *The linearization of Monod kinetics for hydrolysis of MLE 1 WAS with all five R_s (10 to 60) data using: (l) Lineweaver–Burke (M1), (m) double reciprocal (M2) and (n) Eadie–Hofstee (M3). The R^2 values for all 5 R_s data included-dark (black) lines. Numbers refer to column numbers in Table 6.2.2d, e.g. 3 refers to column 3, which lists the average k_m and K_s values obtained from line 3 in Figure 6.2.2l:M1 with 25d R_s data excluded, line 3 in Figure 6.2.1m:M2 with 25d R_s data excluded and line 3 in Figure 6.2.1n:M3 with 25d R_s data excluded, i.e. M1, M2 and M3 (25d off all 3).*

Table 6.2.2d: Predicted S_{bpe} in gCOD/*l* for the Determination of the Best Monod Kinetic Constants from the Three Linearization Methods									
	Data used or omitted (for R_s off) in determining the average k_m and K_s values from the 3 linearization methods								
	1	2	3	4	5	6	7		
R_s	All Inclusive	without M3	M1, M2, M3 (25d off all 3)	M1, M2, M3 (10d off)	M1, M2, M3 (10 & 18d off)	M1, M2, M3 (40 & 60d off)	M1, M2, M3 (25, 40 & 60d off)	Curve Expert	Target S_{bpe}
10	0.72	0.69	0.73	1.07	0.91	0.69	0.60	2.09	0.67
18	0.21	0.21	0.22	0.23	0.22	0.22	0.28	0.24	0.34
25	0.15	0.15	0.15	0.15	0.15	0.15	0.21	0.15	0.14
40	0.10	0.11	0.11	0.10	0.10	0.11	0.16	0.10	0.11
60	0.08	0.09	0.09	0.08	0.08	0.09	0.13	0.08	0.08
							Selected		
k_m	1.55	1.57	1.55	1.42	1.46	1.58	**2.09**	1.33	
K_s	0.17	0.18	0.18	0.15	0.16	0.19	**0.41**	0.13	
R^2	0.90	0.94	0.90	0.92	0.81	0.89	0.96	0.59	

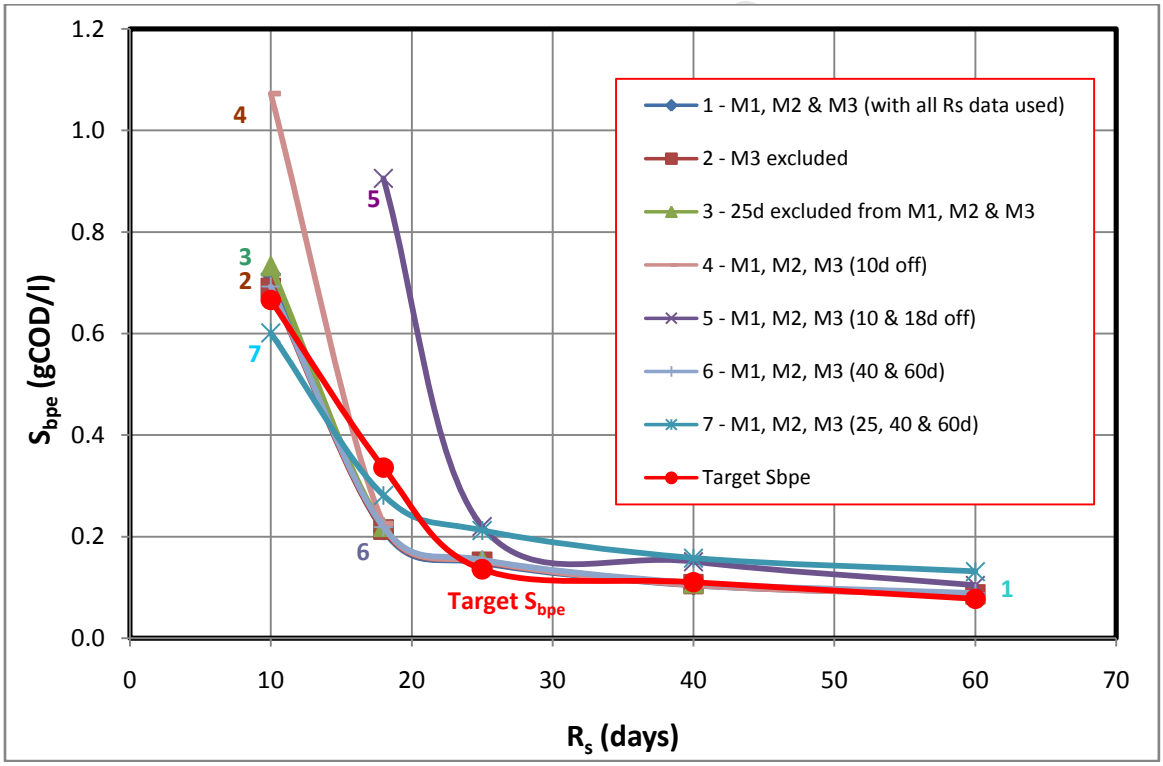

Figure 6.2.2o: *Comparison of tagret S_{bpe} values (calculated from measured values in Table 6.2.2b) with those predicted by different combinations of selected R_s data from the three linearization methods for the determination of the best k_m and K_s values for modelling MLE 1 WAS hydrolysis with the Monod kinetics. Numbers refer to column numbers in Table 6.2.2d.*

Table 6.2.2e: Monod Kinetics (Hydrolysis of MLE 1 WAS)						
Linearization	**Lineweaver-Burke (M1)**	**Double Reciprocal (M2)**	**Eadie-Hofstee (M3)**	**Average**	**Curve Expert**	**Notes**
Slope	0.101	0.582	-0.156			AD sludge ages of 10, 18, 25, 40 and 60 days are used in all methods.
Y-Intercept	0.700	0.125	1.495			
k_m	1.429	1.717	1.495		**1.804**	
K_s	0.145	0.215	0.156		**0.265**	
R^2	0.947	0.942	0.798		0.912	
Slope	0.101	0.582	-0.864			All R_s data included for M1 and M2. 25, 40 and 60 day R_s omitted in M3 to improve R^2.
Y-Intercept	0.700	0.125	3.136			
k_m	1.429	1.717	3.136	**2.094**		
K_s	0.145	0.215	0.864	**0.408**		
R^2	0.947	0.942	1.000	0.963		

The same methods applied in selecting the best Monod kinetic constants from the three linearization methods for hydrolysis of PS (in Section 6.2.1) were used here for the MLE 1 WAS. This involved evaluating how well the S_{bpe} concentrations predicted by the resultant kinetic constants matched those calculated from experimentally measured concentrations and that the resultant linear regression from each method had good correlation coefficients ($R^2 \geq 0.8$).

After evaluating the results (using Table 6.2.2e and Figure 6.2.2o) from the linear regressions for the three methods (M1, M2 and M3), it was decided that all the data (10 to 60d R_s) should be applied with M1 and M2, since they both gave good R^2 values with the complete data set (including all R_s). However, since M3 was seen as the only linearisation method that gave less than satisfactory results it was removed altogether and the average of the kinetic constants from the other two linearisation methods (M1 and M2) were accepted. This resulted in improved overall S_{bp} predictions (column 2 in Table 6.2.2d and Figure 6.2.2o), but under-prediction for the 18d R_s data (Figure 6.22o). In attempts to improve this 18d R_s data prediction it was discovered that two slopes, formed by the 10 to 18 day data (steeper) and by the 25 to 60d R_s was the cause of the lower R^2 value.

The application of the data from the 10 to 18d R_s data resulted in an R^2 of 1 (since it is only two data points used in the linear regression) but improved the 18d R_s S_{bp} prediction, although slightly compromising the other R_s S_{bp} predictions (column 7 in Table 6.2.2d and Figure 6.2.2o). Therefore, linearization with M3 using the 10 and 18d R_s data was used together with M1 and M2 (both using all the R_s data) to determine the k_m and K_s values. The final k_m and K_s values, resulting from this data selection, are presented in Table 6.2.2e, i.e. k_m = 2.094 $gS_{bp}/ (gZ_{AD}.d)$ and K_s = 0.408 gCOD/*l*.

Saturation Kinetics

Again, following the same procedure as for the Monod kinetics, the k_m and K_s values for saturation kinetics were obtained.

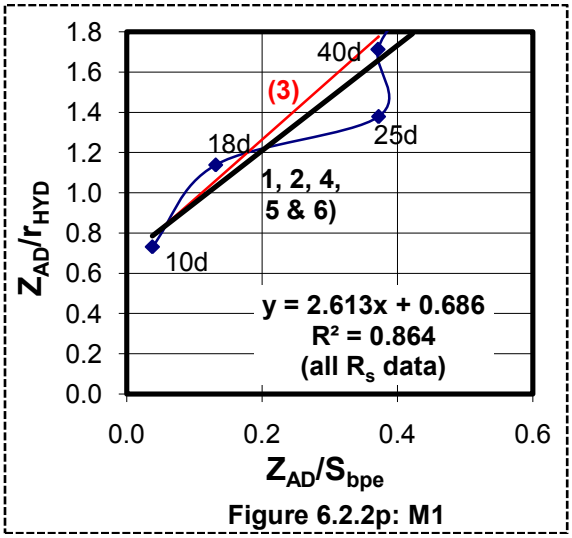

Figure 6.2.2p: M1

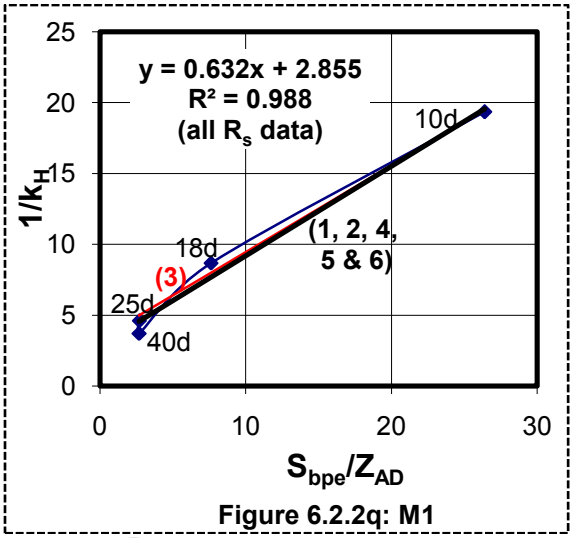

Figure 6.2.2q: M1

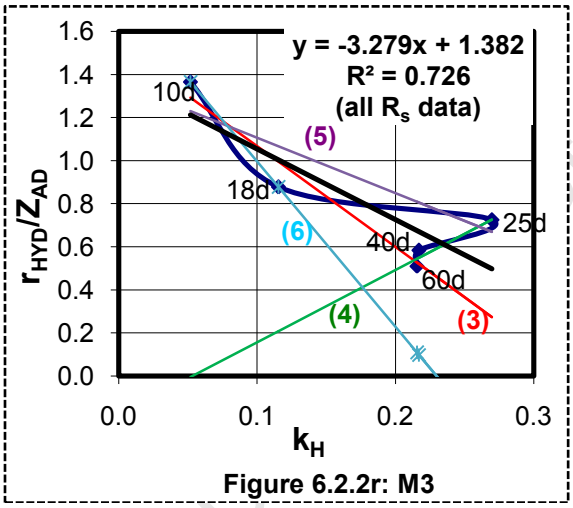

Figure 6.2.2r: M3

Key for Figures 6.2.2p, q and r	
Column No. in Table 6.2.2f	Data used or omitted (R_s off) in determining the k_M and K_S values using the 3 linearization methods (M1, M2 and M3)
1	All Inclusive
2	Without M3
3	M1, M2, M3 (25d off all 3)
4	M1, M2, M3 (10 & 18d off)
5	M1, M2, M3 (40 & 60d off)
6	M1, M2, M3 (25, 40 & 60d off)

Figures 6.2.2p, q and r: *The linearization of saturation kinetics for hydrolysis of MLE 1 WAS at all five R_s (10 to 60) using (p) Lineweaver–Burke (M1), (q) double reciprocal (M2) and (r) Eadie–Hofstee (M3). Regression equations and R^2 values shown for all R_s data included – dark (black) lines. Numbers refer to column numbers in Table 6.2.2f, e.g. 3 refers to column 3, which lists the average k_m and K_s obtained from the line 3 in Figure 6.2.2p:M1 without R_s =25d, line 3 in Figure 6.2.2q: M2 without R_s = 25d and line 3 in Figure 6.2.2r: M3 without R_s = 25d, i.e. M1, M2 and M3 (25d off all 3)*

Table 6.2.2f: Predicted S_{bpe} in gCOD/*l* for the Determination of the Best Saturation Kinetic Constants from the Three Linearization Methods								
	Data used or omitted (for R_s off) in determining the average k_M and K_S values from the 3 linearization methods							
	1	2	3	4	5	6		
R_s	All Inclusive	Without M3	M1, M2, M3 (25d off all 3)	M1, M2, M3 (10 & 18d off)	M1, M2, M3 (40 & 60d off)	M1, M2, M3 (25, 40 & 60d off)	Curve Expert	Target S_{bpe}
10	0.64	0.61	0.62	-1.57	0.63	0.61	0.61	0.67
18	0.27	0.27	0.28	0.49	0.26	0.30	0.29	0.34
25	0.18	0.18	0.19	0.23	0.17	0.20	0.20	0.14
40	0.11	0.11	0.11	0.11	0.10	0.12	0.12	0.11
60	0.07	0.07	0.07	0.07	0.07	0.08	0.08	0.08
						Selected		
k_M	1.477	1.524	1.527	0.957	1.471	**1.603**	1.596	
K_S	3.926	4.249	4.389	1.716	3.690	**5.387**	5.306	
R^2	0.860	0.927	0.934	0.918	0.866	0.951	0.928	

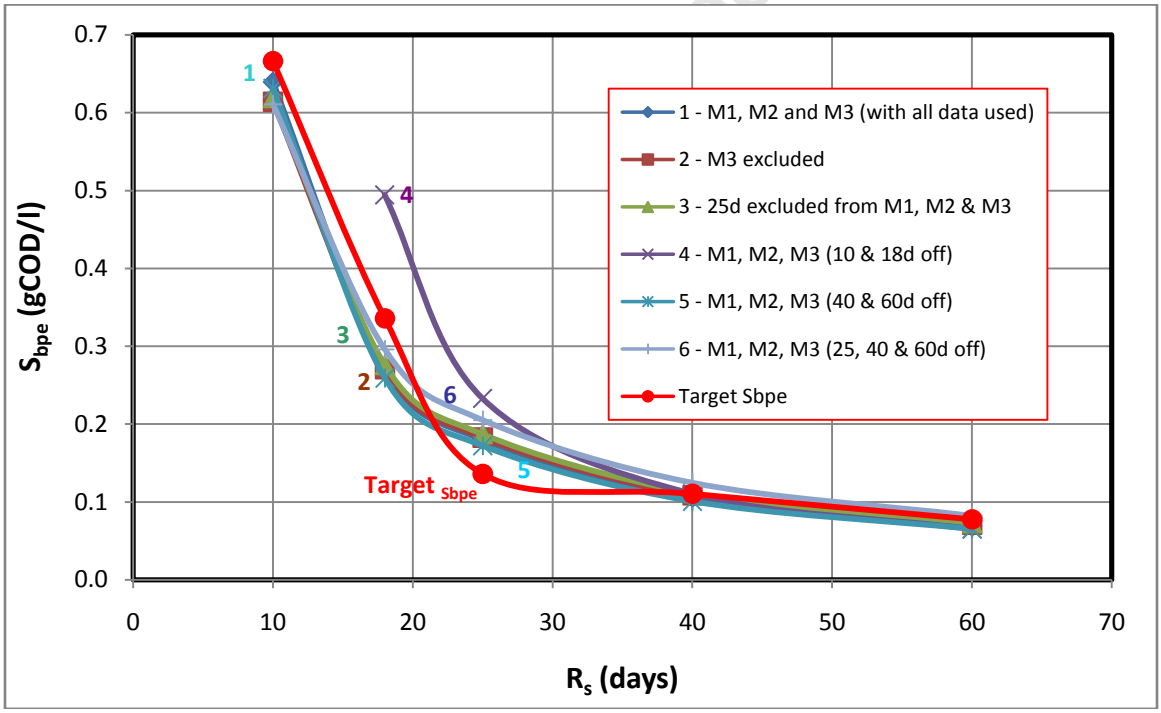

Figure 6.2.2s: *Comparison of tagret S_{bpe} values (calculated from measured values in Table 6.2.2b) with those predicted by different combinations of selected R_s data from the three linearization methods, for the determination of the best k_M and K_S values for modelling hydrolysis with the saturation kinetics. Numbers refer to column numbers in Table 6.2.2f.*

Table 6.2.2g: Saturation Kinetics (Hydrolysis of MLE 1 WAS)						
Linearization	**Lineweaver-Burke (M1)**	**double reciprocal (M2)**	**Eadie-Hofstee (M3)**	**Average**	**Curve Expert**	**Notes**
Slope	2.613	0.628	-3.280			AD sludge ages of 10, 18, 25, 40 and 60 days are used in all methods.
Y-Intercept	0.687	2.947	1.383			
k_M	1.456	1.592	1.383		**1.596**	
K_S	3.806	4.692	3.280		**5.306**	
R^2	0.865	0.989	0.727		0.928	
Slope	2.613	0.628	-7.665			25, 40 and 60 day R_s is omitted in M3 to improve R^2.
Y-Intercept	0.687	2.947	1.762			
k_M	1.456	1.592	1.762	**1.603**		
K_S	3.806	4.692	7.665	**5.387**		
R^2	0.865	0.989	1.000	0.951		

Apart from the results with the Eadie–Hofstee method (M3), generally good correlation coefficients (R^2 > 86%) were obtained in the linearization of Monod and saturation kinetics for the MLE 1 WAS, with the best given by the double reciprocal method (M2) (R^2 Monod = 0.94 and R^2 saturation = 0.99). The improvement of the correlation values for linearization with M3 required the removal of the 25, 40 and 60 day R_s data, which apparently were outliers in the application of this method. Since the resultant R^2 values without the R_s 25 to 60d data appear satisfactory (which shows that the M3 method emphasizes the long sludge age data), the average Monod kinetic constants (k_m and K_s of 2.094 gCOD /(gCOD.d) and 0.408 gCOD/*l* respectively) or the saturation kinetic constants (i.e. k_M and K_S of 1.603 gCOD /(gCOD.d) and 5.387 gCOD/*l* respectively) can be used in calculating the r_{HYD} for the AD of MLE 1 WAS and hence ΔS_{bp} for the stoichiometry part of the AD model. As before with the PS, the entire procedure was checked for $f_{SL'up}$ = 0.46 and 0.48. While different kinetic constants were obtained, better C_{var} and R^2 coefficients and S_{bpe} concentrations were not obtained, validating that 0.47 was the best estimate for $f_{SL'up}$. No activated sludge hydrolysis rate data were found in the literature with which to compare the data here.

6.2.2.3. MLE 2 Waste Activated Sludge

Apart from the unbiodegradable fraction, the hydrolysis rate of the MLE 2 WAS from the raw WW system should be similar to that of the MLE 1 WAS from the settled WW system. For the determination of hydrolysis kinetic constants of the MLE 2 WAS, the same procedures applied to the determination of the hydrolysis kinetic constants of the PS and MLE 1 WAS are used. Tables 6.2.3a and 6.2.3b show the average influent and effluent experimental results obtained in the AD of WAS from the MLE system fed the raw wastewater (MLE 2).

Table 6.2.3a: WAS from MLE Fed Raw WW Influent (MLE 2) Experimental Data

Retention Time (d)	10		18		25		40		60	
Digester Volume (*l*)	15		15		15		15		5	
Influent flow (*l*/d)	1.50		0.83		0.60		0.30		0.09	
Units	Conc. (g/*l*)	Flux (g/d)	Conc. (g/*l*)	Flux (g/d)	Conc. (g/*l*)	Flux (g/d)	Conc. (g/*l*)	Flux (g/d)	Conc. (g/*l*)	Flux (g/d)
Influent COD[3], S_{ti} (gCOD/*l*)	3.03	2.72	6.72	2.67	8.21	2.68	17.69	2.65	24.75	2.64
Influent COD[1], S_{upi} (gCOD/*l*)	1.88	1.69	4.16	1.66	5.09	1.66	10.97	1.64	15.34	1.64
Influent COD, S_{usi}[2] (gCOD/*l*)	0.04	0.03	0.04	0.02	0.06	0.02	0.04	0.01	0.04	0.00
Influent COD, S_{bpi}[6] (gCOD/*l*)	1.11	1.00	2.51	1.00	3.06	1.00	6.68	1.00	9.36	1.00
Influent COD, S_{bsfi}[5] (gCOD/*l*)	0.00	0.00	0.00	0.00	0.00	0.00	0.00	0.00	0.00	0.00
Influent VFA, S_{bsai}[4] (gCOD/*l*)	0.00	0.00	0.00	0.00	0.00	0.00	0.00	0.00	0.00	0.00
Influent TKN[3] (gN/*l*)	0.18	0.17	0.50	0.20	0.60	0.20	1.38	0.21	2.01	0.22
Influent filtered TKN (gN/*l*)	0.01	0.00	0.00	0.00	0.01	0.00	0.01	0.00	0.01	0.00
Influent FSA (gN/*l*)	0.00	0.00	0.00	0.00	0.00	0.00	0.00	0.00	0.00	0.00
Influent Alk g/*l* as $CaCO_3$	-		-		-		280.00	41.90	-	
Influent pH	7.50		-		-		-		-	
Influent TP[3] (gP/*l*)	0.07	0.06	0.16	0.07	0.22	0.07	0.45	0.07	0.69	0.07
Influent filtered TP (gP/*l*)	0.01	0.01	0.01	0.00	0.01	0.00	0.01	0.00	0.01	0.00
Influent OP (gP/*l*)	0.01	0.01	0.01	0.00	0.01	0.00	0.01	0.00	0.01	0.00
Influent TSS (gTSS/*l*)	2.59	2.33	5.52	2.20	6.74	2.20	14.11	2.11	20.26	2.16
Influent VSS (gVSS/*l*)	2.07	1.86	4.55	1.81	5.54	1.81	12.07	1.81	16.74	1.79
Influent ISS (gISS/*l*)	0.52	0.47	0.98	0.39	1.20	0.39	2.03	0.30	3.52	0.38

[1] S_{upi} is the unbiodegradable particulate COD calculated using best-determined $f_{SL'up}$ = 0.62, obtained for good coefficients of variation and correlation coefficients as shown in the section below.

[2] S_{usi} is the unbiodegradable soluble COD measured from the filtered effluent of parent MLE 2 AS system.

[3] Unfiltered samples.

[4] S_{bsai} is the COD in short chain fatty acids that is measured in the influent using the 5-point titration method.

[5] S_{bsfi} is the fermentable biodegradable soluble influent COD, assumed zero (completely utilized) from MLE 2.

[6] S_{bpi} is the biodegradable particulate influent COD, calculated by the total influent COD (S_{ti}) – S_{usi} – S_{bsai} – S_{upi}.

Table 6.2.3b: WAS from MLE Fed Raw WW Effluent Experimental Data										
Retention Time (d)	10		18		25		40		60	
Effluent flow (*l*/d)	1.50		0.83		0.60		0.30		0.09	
Units	Conc. (g/*l*)	Flux (g/d)	Conc. (g/*l*)	Flux (g/d)	Conc. (g/*l*)	Flux (g/d)	Conc. (g/*l*)	Flux (g/d)	Conc. (g/*l*)	Flux (g/d)
Effluent COD[1], S_{te} (gCOD/*l*)	2.59	2.33	5.20	2.07	5.91	1.93	12.05	1.80	16.43	1.75
Effluent COD, S_{upe} [5] (gCOD/*l*)	1.88	1.69	4.16	1.66	5.09	1.66	10.97	1.64	15.34	1.64
Effluent COD, S_{use}[2] (gCOD/*l*)	0.04	0.03	0.04	0.02	0.06	0.02	0.04	0.01	0.04	0.00
Effluent filtered COD, S_{tse} (gCOD/*l*)	0.04	0.03	0.04	0.02	0.06	0.02	0.04	0.01	0.04	0.00
Effluent COD, S_{bpe}[6] (gCOD/*l*)	0.68	0.61	0.99	0.40	0.76	0.25	1.04	0.16	1.04	0.11
Effluent COD, S_{bsfe}[4] (gCOD/*l*)	0.00	0.00	0.00	0.00	0.00	0.00	0.00	0.00	0.00	0.00
Effluent VFA, S_{bsae}[3] (gCOD/*l*)	0.03	0.03	0.00	0.00	0.00	0.00	0.00	0.00	0.02	0.00
Effluent TKN[1] (gN/*l*)	0.18	0.16	0.50	0.20	0.65	0.21	1.24	0.18	1.72	0.18
Effluent filtered TKN (gN/*l*)	0.04	0.04	0.12	0.05	0.20	0.06	0.51	0.08	0.77	0.08
Effluent FSA (gN/*l*)	0.04	0.03	0.11	0.05	0.21	0.07	0.51	0.08	0.78	0.08
Effluent TP[1] (mgP/*l*)	0.08	0.07	0.19	0.08	0.24	0.08	0.46	0.07	0.63	0.07
Effluent filtered TP (gP/*l*)	0.01	0.01	0.05	0.02	0.09	0.03	0.20	0.03	0.32	0.03
Effluent OP (gP/*l*)	0.01	0.01	0.04	0.02	0.08	0.03	0.18	0.03	0.29	0.03
Effluent TSS	2.24	2.01	4.24	1.69	4.96	1.62	9.76	1.46	13.07	1.40
Effluent VSS	1.70	1.53	3.37	1.34	3.88	1.27	7.85	1.17	10.09	1.08
Effluent ISS	0.54	0.49	0.87	0.35	1.08	0.35	1.91	0.29	2.98	0.32
Effluent Alk mg/*l* as $CaCO_3$	0.95	0.85	0.64	0.26	0.90	0.29	0.96	0.14	1.81	0.19
Measured digester pH	7.30		6.99		7.07		7.07		7.30	
COD removed (gCOD/*l*)		0.39		0.60		0.75		0.84		0.89
Gas production (litres/d)	0.82		0.63		0.58		0.42			
Gas prod. (l gas/*l* influent)	0.55		0.75		0.96		1.40		-	
Gas composition : CH_4 fraction	0.58		0.58		0.58		0.58			
Gas composition: CO_2 fraction	0.22		0.22		0.22		0.22			
Volume of CH_4 (litres)	0.31		0.43		0.55		0.81			
Volume of CO_2 (litres)	0.12		0.16		0.21		0.30			
COD of CH_4 (gCOD/*l* feed)	0.55		1.36		2.41		7.05		9.87	
p_{CO2} (atm.)	0.27		0.27		0.27		0.27			
CT dissolved (mmol/*l*)	7.07		7.07		7.07		7.07			
H_2CO_3 diss. (mg/*l*)	706.76		706.76		706.76		706.76			
Moles of CO_2/*l* feed	0.00		0.01		0.01		0.01			
Moles of CH_4/*l* feed	0.01		0.02		0.02		0.03			
COD balance (%)	103.77		97.64		101.42		107.98		106.24	
Nitrogen balance (%)	95.51		100.03		108.71		89.33		85.47	
Phosphorous balance (%)	108.39		118.37		109.19		101.31		92.21	
f_{cv} (gCOD/gVSS)	1.52		1.54		1.52		1.54		1.63	
$f_{SL'up}$ (MLE 2 WAS)	0.62	0.62	0.62	0.62	0.62	0.62	0.62	0.62	0.62	0.62

[1] Unfiltered sample

[2] S_{use} is the unbiodegradable soluble COD that equals the S_{usi} value from Table 6.2.3a

[3] S_{bsae} is the COD in short chain fatty acids that is measured in the effluent using the 5-point titration method

[4] S_{bsfe} is the fermentable biodegradable soluble COD calculated from the measured filtered effluent COD (S_{tse}) – S_{use} – S_{bsae}

[5] S_{upe} is the unbiodegradable particulate effluent COD which equals the S_{upi} value from Table 6.2.3a

[6] S_{bpe} is the biodegradable particulate effluent COD which equals the total effluent COD (S_{te}) – S_{tse} – S_{upe}

The Selection of a Suitable $f_{SL'up}$ Value

The influence of $f_{SL'up}$ on the hydrolysis rate kinetic constants of the AD of MLE 2 WAS is shown below in plots of coefficients of variation for first order and first order specific hydrolysis kinetic equations versus increasing $f_{SL'up}$ fractions (shown in Figure 6.2.3a) and correlation coefficients (R^2) for Monod and saturation hydrolysis kinetic equations versus the same range of $f_{SL'up}$ fractions (0.56 to 0.64, shown in Figures 6.2.3b and 6.2.3c respectively). This is done in order to obtain the most suitable $f_{SL'up}$ estimate that gives the best correlation coefficients when applying the various hydrolysis kinetic equations for accurate prediction of the ΔS_{bp} in the AD of MLE 2 WAS. The correlation coefficients for the Monod and saturation kinetics are determined for the Curve Expert program results and the three linearization methods of Lineweaver-Burke (M1), double reciprocal (M2) and Eadie-Hofstee (M3) and (M3*). The M1, M2 and M3 (without asterisks) were obtained using the data for the AD of MLE 2 WAS at 10, 18, 25, 40 and 60 days R_s. However, (M3*) is for the plot obtained when the 25, 40 and 60 day R_s data are omitted when linearising the Monod kinetics with the Eadie-Hofstee (M3) method which emphasizes the long sludge age data, which are not very sensitive for determining the hydrolysis kinetic rates. These data sets omitted to form (M3*) appeared as outliers, which if included (as the case with M3) significantly decreases the R^2 value and yield kinetic constants that deviate significantly from those of the other two linearisation methods. The curve fitting results are evaulated in more detail below after selecting the best $f_{SL'up}$.

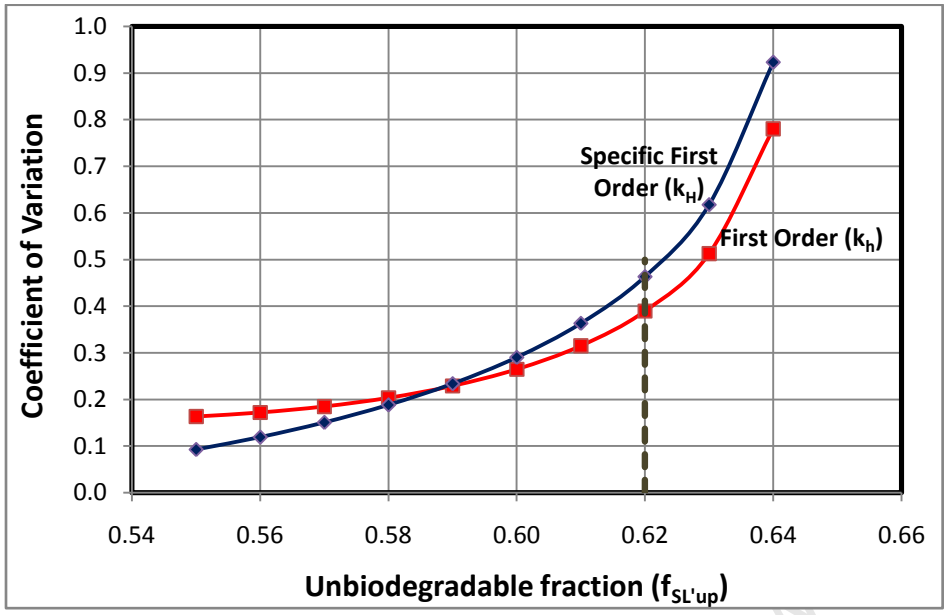

Figure 6.2.3a: *The change in the coefficient of variation of the 1st order and 1st order specific hydrolysis equations kinetic constants with changing unbiodegradable particulate COD fraction ($f_{SL'up}$) of MLE 2 WAS. All data included – see Table 6.2.3c.*

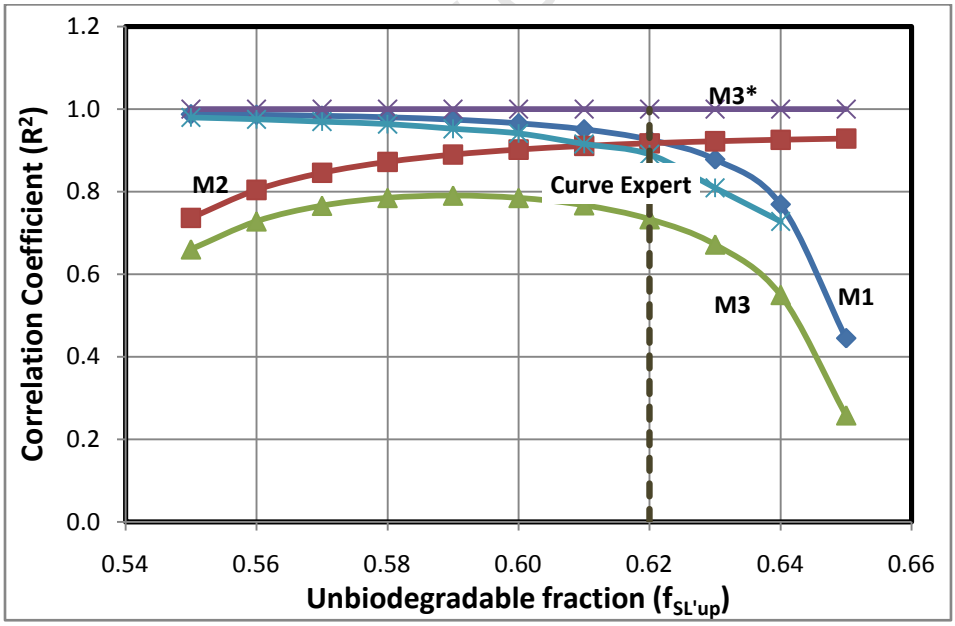

Figure 6.2.3b: *The regression correlation coefficient (R^2) for the Curve Expert program, Lineweaver-Burke (M1), double reciprocal (M2) and Eadie-Hofstee (M3) linearization methods of Monod hydrolysis kinetics versus unbiodegradable particulate COD fraction ($f_{SL'up}$) of the MLE 2 WAS.*

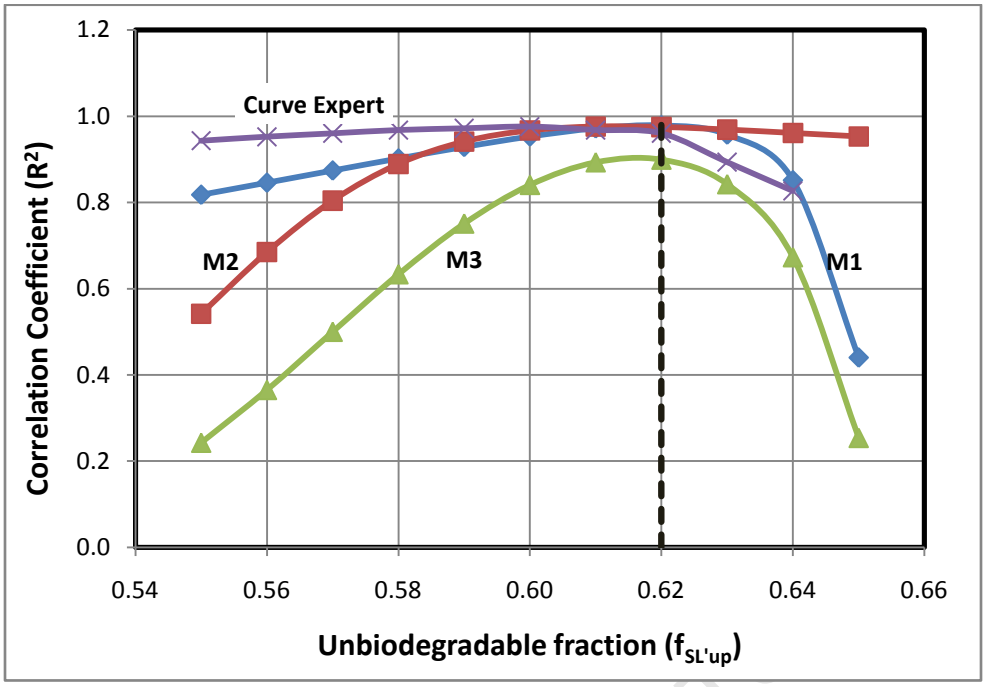

Figure 6.2.3c: *The regression correlation coefficient (R^2) for the Curve Expert program, Lineweaver-Burke (M1), double reciprocal (M2) and Eadie-Hofstee (M3) linearization methods of saturation hydrolysis kinetics versus unbiodegradable particulate COD fraction ($f_{SL'up}$) of the MLE 2 WAS.*

As was the case with the other sludge types discussed above (PS and MLE 1 WAS), Figure 6.2.3a, shows a gradual increase in the coefficient of variation (C_{var}) with increasing unbiodegradable particulate fraction from 0.56 to 0.62, after which C_{var} increases sharply. Figures 6.2.3b and 6.2.3c show that Monod and saturation kinetics exhibit maximum R^2 values for all three linearization methods at the $f_{SL'up}$ value of around 0.62. This value is close to that determined from the AD of the MLE 2 WAS at 60d sludge age (0.66) and equal to that calculated with the AS model for the AS system VSS (MLE 2) from the influent wastewater $f_{S'up}$ fraction and organism endogenous residue (ER) (see Section 5.3 of Chapter 5). Therefore, $f_{SL'up}$ = 0.62 was selected as best for the determination of the hydrolysis kinetic constants.

First Order Kinetics

The experimentally measured influent and effluent concentrations for the steady state anaerobic digestion of WAS from the MLE 2 (Tables 6.2.3a and 6.2.3b) were used in the above-mentioned kinetic calculations (Section 6.2.1) to determine the volumetric hydrolysis rates (r_{HYD}), the residual biodegradable COD concentrations (S_{bp}) and the first order kinetic rate constants (k_h and k_H). These rates are listed in Table 6.2.3c below and their variations with sludge age are shown plotted in Figures 6.2.3d to 6.2.3g.

Figures 6.2.3f and 6.2.3g show that, for first order and specific first order kinetics, all the data have a reasonable linear relationship with R_s. This is notable from the good correlation coefficients $R^2 = 0.82$ for first order and $R^2 = 0.98$ for specific first order kinetics. This linear relationship of k_h and k_H with sludge age is given from linear regression $k_h = 0.0028 \cdot R_s + 0.0703$ ($R^2 = 0.82$) for first order hydrolysis kinetics and $k_H = 0.0917 \cdot R_s + 1.1472$ ($R^2 = 0.98$) for specific first order hydrolysis kinetics (Table 6.2.3c).

Table 6.2.3c: Summary of Results for first order Kinetics in the AD of MLE 2 WAS

R_s (d)	r_{HYD} (g/*l*/d)	Z_{AD} (g/*l*)	S_{bpe} (g/*l*)	k_h (/d)	Spec r_{HYD} (gS_{bp}/gZ_{AD}/d)	k_H (/d)
10	0.044	0.035	0.572	0.077	1.248	2.180
18	0.038	0.045	0.342	0.112	0.854	2.498
25	0.034	0.047	0.202	0.168	0.717	3.555
40	0.024	0.041	0.115	0.207	0.584	5.086
60	0.017	0.033	0.078	0.213	0.510	6.510
		Mean		0.155	-	3.966
		Standard deviation		0.059	-	1.819
		Coefficient of variation		0.384	-	0.206

$k_h = c_{kh} + m_{kh} \times R_s$; $c_{kh} = 0.070$; $m_{kh} = 0.0028$; $R^2 = 0.82$ (all R_s; Figure 6.2.3f)
$k_H = c_{kH} + m_{kH} \times R_s$; $c_{kH} = 1.147$; $m_{kH} = 0.092$; $R^2 = 0.98$ (all R_s; Figure 6.2.3g)

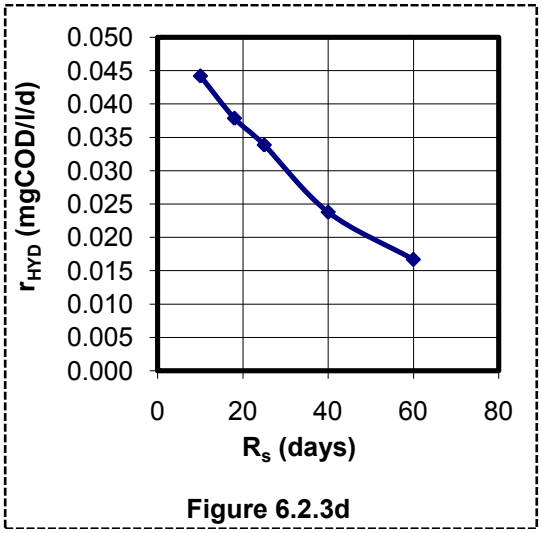

Figure 6.2.3d

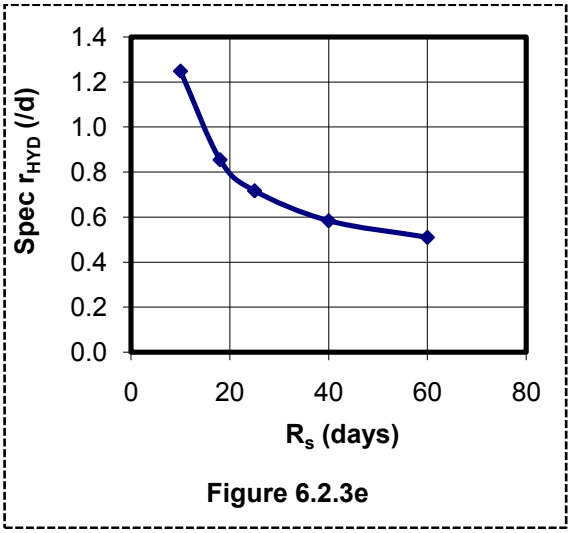

Figure 6.2.3e

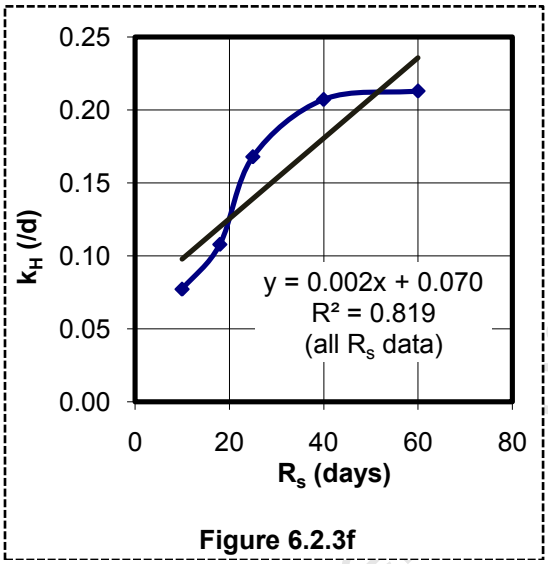

Figure 6.2.3f

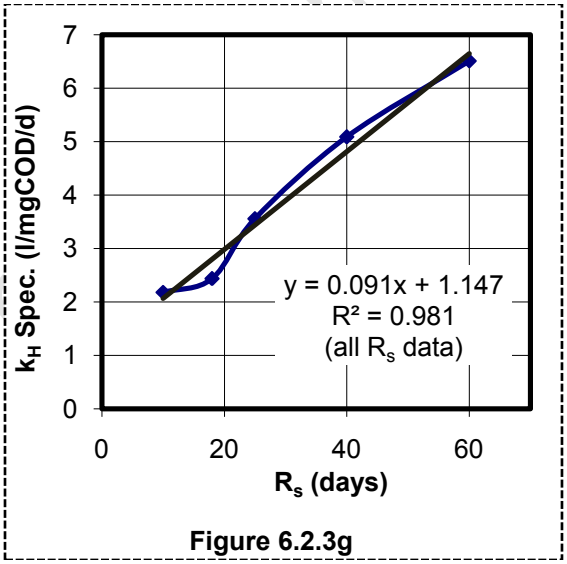

Figure 6.2.3g

Figures 6.2.3d, e, f and g: *Volumetric hydrolysis rates (r_{HYD}) (d), specific volumetric hydrolysis rate (r_{HYD}/Z_{AD}) (e), first order kinetic constant (k_h) (f) and specific first order kinetic constant (k_H) (g) versus sludge age (R_s) of 10, 18, 25, 40 to 60 days for AD of MLE 2 WAS. Regression equation and R^2 given for all R_s data included (see Table 6.2.3c)*

Monod and Saturation Kinetics

Figures 6.2.3h to 6.2.3k below show the specific hydrolysis rates (r_{HYD}/Z_{AD}) versus the residual BPO of MLE-2 WAS as the essential substrate (S_{bp}) for the Monod equation, and versus this residual BPO per acidogenic biomass (S_{bp}/Z_{AD}) for the saturation kinetics equation. The specific hydrolysis rate (r_{HYD}/Z_{AD}) obtained from the data from Table 6.2.3c, which is directly calculated from experimental results,

and compared with those calculated from the Monod and saturation kinetic constants determined with the 3 linearisation methods and the Curve Expert program in Table 6.2.3d (for Monod kinetics) and Table 6.2.3f (for saturation kinetics) and are shown plotted in Figures 6.2.3h and i and the Curve Expert program (Figures 6.2.3j and k).

It can be seen that the measured data at the longer sludge ages of 25d to 60d does not conform well to the Monod kinetic curve generated using the k_m and K_s values with the 3 linearization methods, but shows values close to that expected for the saturation kinetics. This shows that the methods used in selecting the best kinetic constants with the 3 linearization methods for this MLE 2 WAS AD data were more appropriate to the saturation kinetic formulation. However, the kinetic constants obtained with the Curve Expert program generated Monod and saturation kinetic plots that are more in conformity with the measured data for the long (25 to 60d) sludge ages. The methods used in selecting the kinetic constants (k_m = 2.482 and K_s = 0.626, for Monod and k_M = 1.524 and K_S = 4.838 for saturation kinetics) are discussed further below.

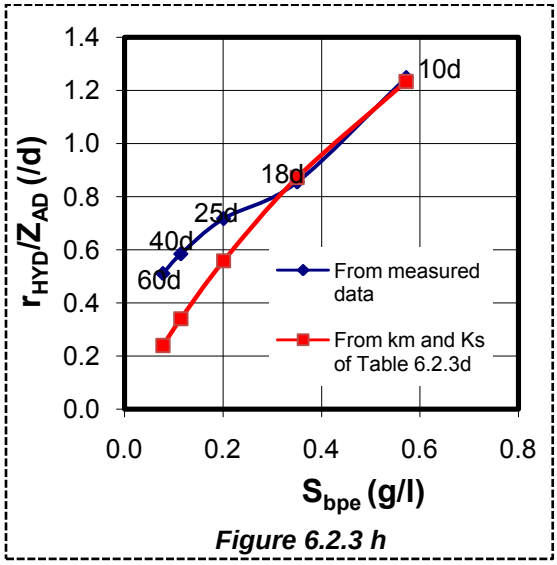

Figure 6.2.3 h

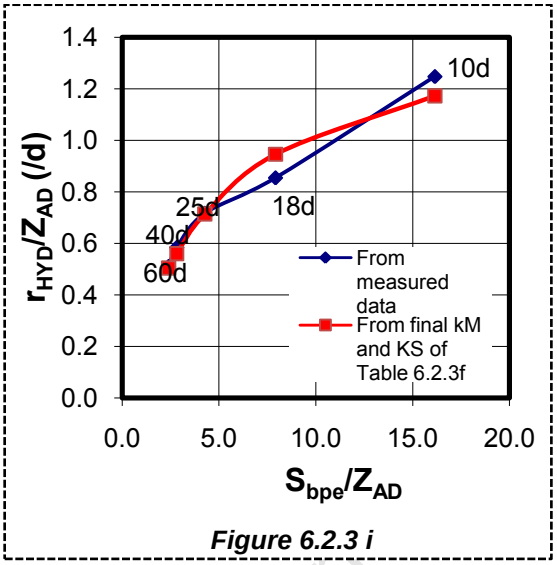

Figure 6.2.3 i

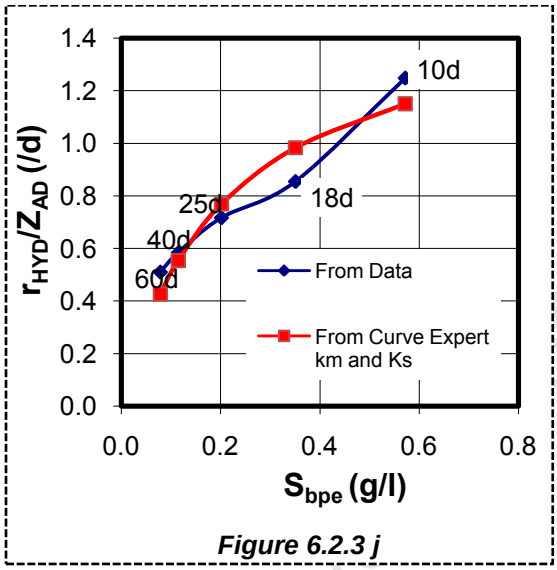

Figure 6.2.3 j

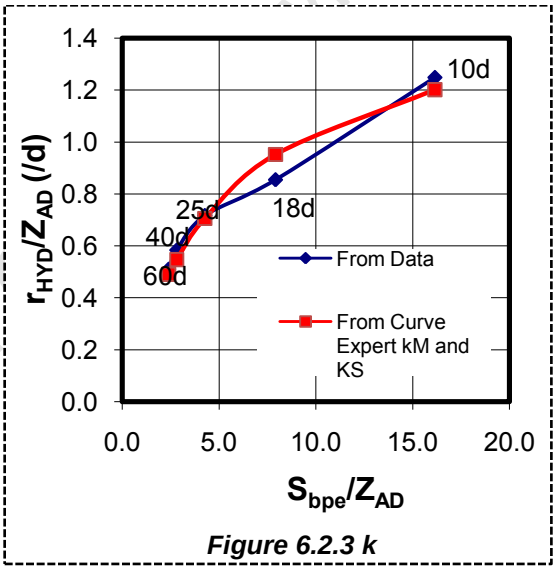

Figure 6.2.3 k

Figures 6.2.3h, i, j and k: *Hydrolysis kinetics formulation curves plotted using experimental data and calculated from kinetic constants acquired from the three linearization methods for (h) Monod (see Table 6.2.3d column 6, k_m = 2.48 and K_s = 0.63) and (i) saturation equations (see Table 6.2.3f, k_M = 1.524 and K_S = 4.838) and using the Curve Expert programme (j) for Monod and (k) for saturation kinetics.*

The r_{HYD}, S_{bp} and Z_{AD} values determined from experimental results (Table 6.2.3c) for the AD of MLE 2 WAS were used in the linearization of the Monod and saturation kinetic equations to determine their kinetic constants (i.e. k_m and K_s for Monod and k_M and K_S for saturation kinetics). The plots (Figures 6.2.3j to 6.2.3l

for Monod kinetics and Figures 6.2.3m to 6.2.3o for saturation kinetics) below show the measured and best fit results ($f_{SL'up}$ = 0.62) for the three different linearisation and regression methods, i.e. (i) Lineweaver-Burke (M1, Figure 6.2.3*l*), (ii) double Reciprocal (M2, Figure 6.2.3m) and (iii) Eadie-Hofstee (M3, Figure 6.2.3n). The resultant R^2 values together with the graphical slope and y-coefficient obtained in calculating the kinetic constants are presented in Tables 6.2.3d (Monod kinetics) and 6.2.3f (saturation kinetics).

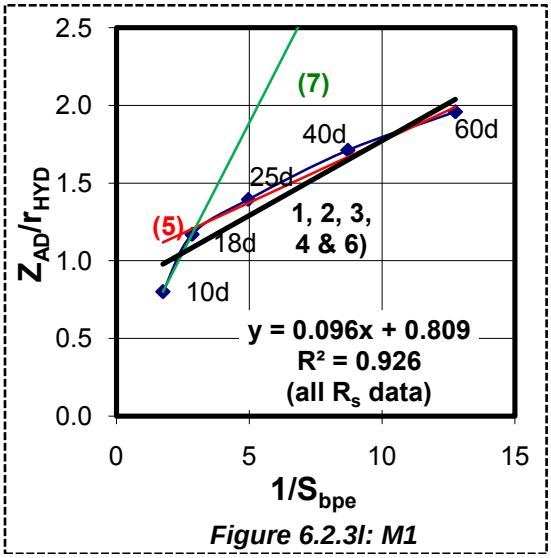

Figure 6.2.3l: M1

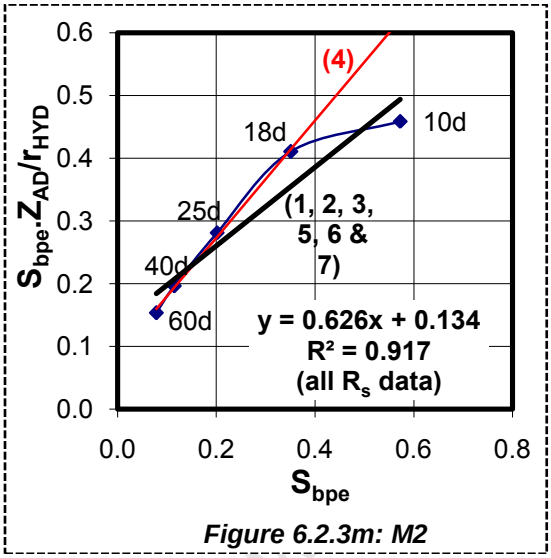

Figure 6.2.3m: M2

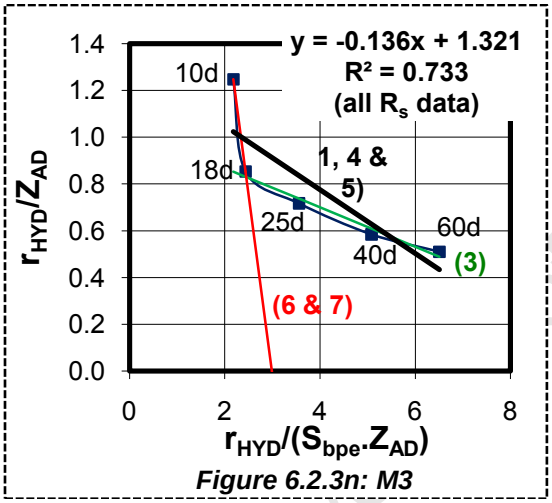

Figure 6.2.3n: M3

Key for Figures 6.2.3 l, m and n	
Column No. in Table 6.2.3d	**Data used or omitted (R_s off) in determining the k_m and K_s values using the 3 linearization methods (M1, M2 and M3)**
1	All inclusive
2	M3 Out
3	M1, M2, M3 (10d off)
4	M1, M2 (10d off), M3
5	M1 (10d off), M2, M3
6	M1, M2, M3 (25, 40, 60 off)
7	M1(25, 40, 60 off), M2, M3 (25, 40, 60 off)

Figures 6.2.3j, k and l: *The linearization of Monod kinetics for hydrolysis of MLE 2 WAS with all five R_s (10 to 60) data using the three linearization methods: (j) Lineweaver–Burke (M1), (k) double reciprocal (M2) and (l) Eadie–Hofstee (M3). The R^2 values shown are for all 5 R_s data included- dark (black) lines. Numbers refer to column numbers in Table 6.2.3d, e.g. 4 refers to column 4, which lists the average k_m and K_s values obtained from line 4 in Figure 6.2.3j:M1 with all R_s data included (i.e. follows black line), line 4 in Figure 6.2.1k:M2 with R_s =10d omitted and line 4 in Figure 6.2.1l:M3 with all R_s data included.*

Table 6.2.3d: Predicted S_{bpe} in gCOD/*l* for the Determination of the Best Monod Kinetic Constants from the Three Linearization Methods									
	Data used or omitted (for R_s off) in determining the k_m and K_s values with the 3 linearization methods								
	1	2	3	4	5	6	7		
R_s	All Inclusive	M3 Excluded	M1, M2, M3 (10d off)	M1, M2 (10d off), M3	M1 (10d off), M2, M3	M1, M2, M3 (25, 40, 60 off)	M1(25, 40, 60 off), M2, M3 (25, 40, 60 off)	Curve Expert	Target S_{bpe}
10	1.44	1.25	4.25	-3.75	-0.52	0.63	0.58	0.81	0.57
18	0.25	0.25	0.27	0.28	0.39	0.33	0.34	0.25	0.35
25	0.17	0.17	0.17	0.17	0.19	0.25	0.27	0.18	0.20
40	0.11	0.12	0.12	0.11	0.11	0.19	0.21	0.12	0.11
60	0.09	0.09	0.09	0.08	0.08	0.16	0.18	0.10	0.08
						Selected			
k_m	1.38	1.42	1.29	1.21	1.04	**2.48**	3.61	1.58	
K_s	0.16	0.17	0.14	0.12	0.09	**0.63**	1.10	0.21	
R^2	0.86	0.92	0.94	0.96	0.99	0.95	0.97	0.89	

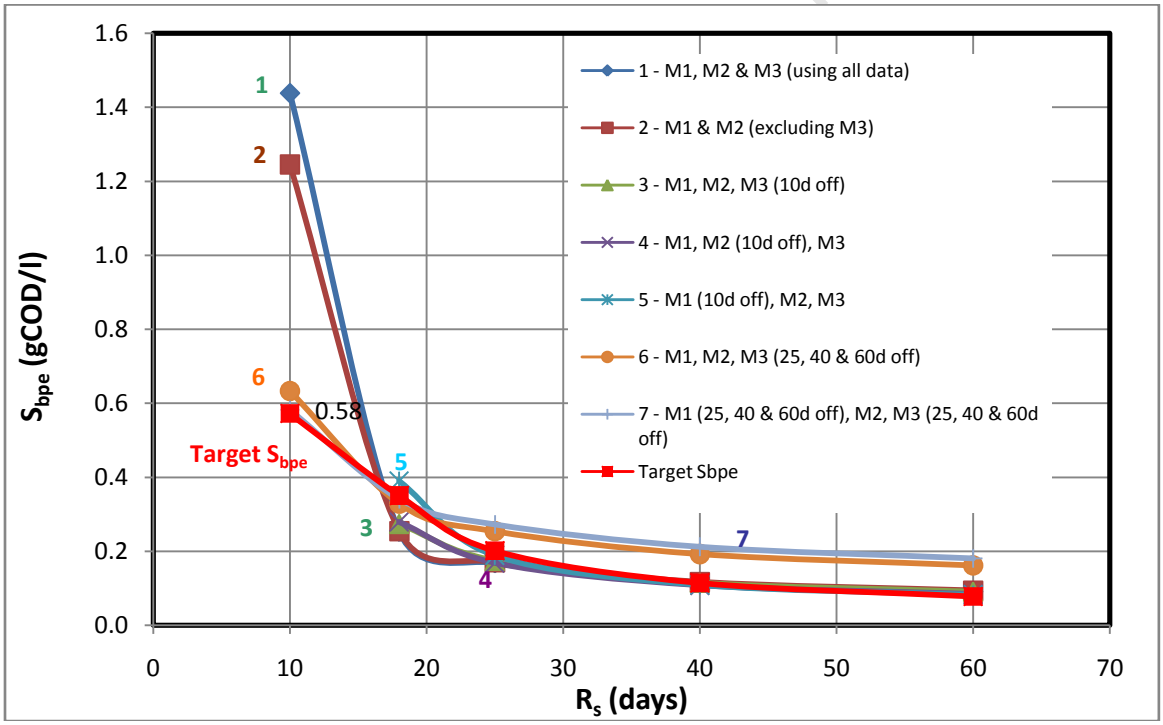

Figure 6.2.3o: *Comparison of target S_{bpe} concentrations (calculated from measured values in Table 6.2.3b)with those predicted by different combinations of selected R_s data from the three linearization methods for the determination of the best k_m and K_s values for modelling hydrolysis with the Monod kinetics. Numbers refer to the column numbers in Table 6.2.3d.*

The procedure used to select the best Monod kinetic constants from the three linearization methods are the same as applied for the PS and MLE1 WAS. The Table 6.2.3d lists the correlation coefficients (R^2) between predicted and measured S_{bpe} obtained from the average k_m and K_s from different combinations of selected R_s data for the three linearization methods and Figure 6.2.3o shows how well the predicted S_{bpe} by the resultant kinetic constants matched the experimentally measured results. Good R^2 values ($R^2 > 0.8$) were obtained from the linear regression methods M1 and M2. Hence, it was first checked whether the omission of the M3 k_m and K_s values would result in the best k_m and K_s. However, omission of M3 values resulted in poor predictions of S_{bpe} for the 10 and 18d R_s. Therefore, it was decided that k_m and K_s obtained from M3 with some R_s data be included to generate better predictions at these shorter sludge ages. Deciding which data to include for M3 was done by trial and error, whereby for the various data omitted the resultant S_{bpe} values were assessed. This resulted in selecting the 10 and 18-day R_s data for M3. Although this gives the obvious R^2 value of 1 for M3 (since there are only 2 points used in the linear regression), it generated better predictions for the shorter R_s (10 to 18d) without over compromising the predictions from the other longer R_s. The final k_m and K_s values resulting from this data selection are presented in Table 6.2.3e below as k_m = 2.48 gCOD/ (gCOD.d) and K_s = 0.63 gCOD/*l*.

Table 6.2.3e: Monod Kinetics (Hydrolysis of MLE 2 WAS)						
Linearization	**Lineweaver-Burke (M1)**	**Double Reciprocal (M2)**	**Eadie-Hofstee (M3)**	**Average**	**Curve Expert**	**Notes**
Slope	0.096	0.627	-0.136			AD sludge ages of 10, 18, 25, 40 and 60 days are used in all methods.
Y-Intercept	0.810	0.135	1.321			
k_m	1.235	1.595	1.321		**1.575**	
K_s	0.119	0.215	0.136		**0.212**	
R^2	0.926	0.917	0.734		0.891	
Slope*	0.096	0.627	-1.545			All data for M1 and M2 but 25, 40 and 60 day R_s are omitted in M3 to improved R^2.
Y-Intercept*	0.810	0.135	4.615			
k_m*	1.235	1.595	4.615	**2.482**		
K_s*	0.119	0.215	1.545	**0.626**		
R^2*	0.926	0.917	1.000	0.948		

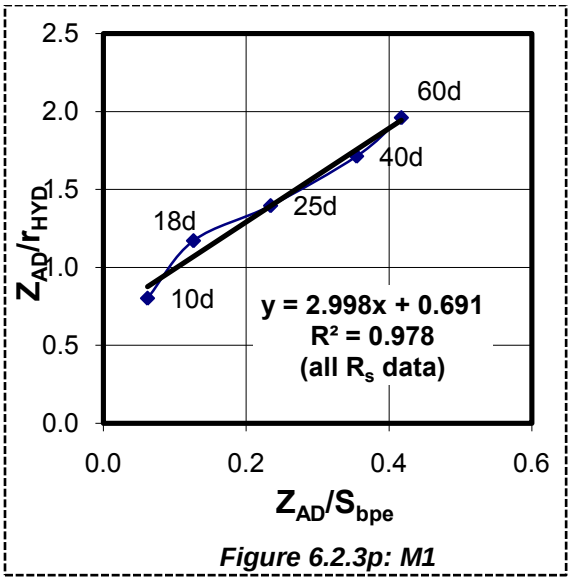

Figure 6.2.3p: M1

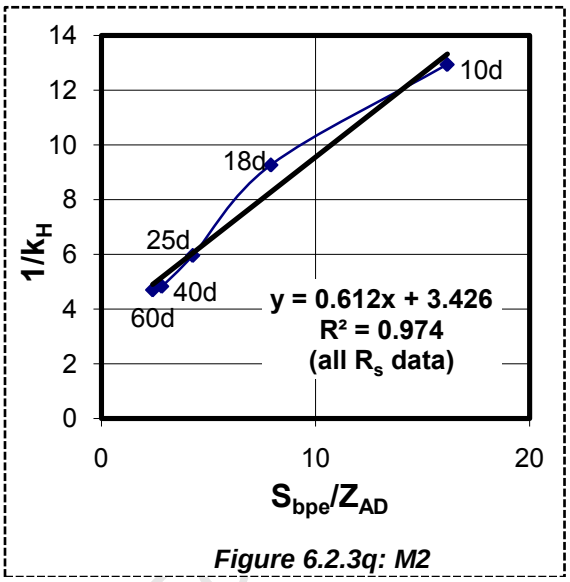

Figure 6.2.3q: M2

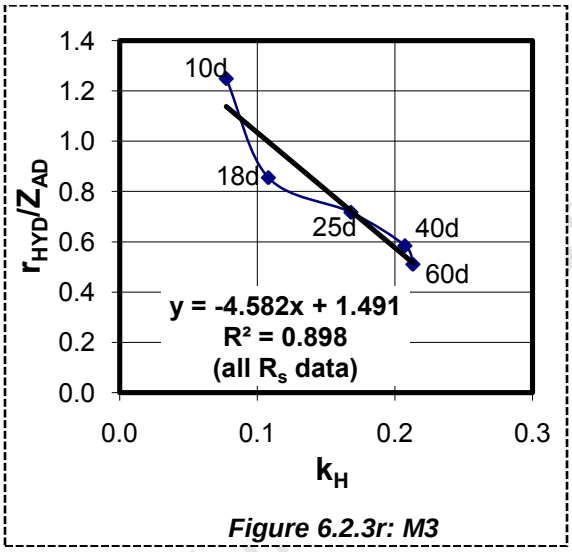

Figure 6.2.3r: M3

Figures 6.2.3p, q and r: *The linearization of saturation kinetics for hydrolysis of MLE 2 WAS at all five R_s (10 to 60) with various methods: (p) Lineweaver–Burke (M1), (q) double reciprocal (M2) and (r) Eadie–Hofstee (M3). Regression equations and lines and R^2 values shown for all R_s data included – dark (black) lines. No R_s data were omitted to determine average k_M and K_S values from three linearization methods (Table 6.2.3f).*

Unlike Monod kinetics, all the R^2 values for the three linearization methods and Curve Expert were very good ($R^2 > 0.9$) for saturation kinetics; Hence, the resultant

kinetic constants for saturation kinetics were accepted without the omitting any R_s data for the three linearization methods and Curve Expert program (see Figure 6.2.3s and Table 6.2.3g).

Table 6.2.3f: Saturation Kinetics (Hydrolysis of MLE 2 WAS)						
Linearization	**Lineweaver-Burke (M1)**	**Double Reciprocal (M2)**	**Eadie-Hofstee (M3)**	**Average**	**Curve Expert**	**Notes**
Slope	2.998	0.613	-4.583			AD sludge ages of 10, 18, 25, 40 and 60 days are used in all methods.
Y-Intercept	0.691	3.426	1.492			
k_M	1.447	1.633	1.492	**1.524**	**1.606**	
K_S	4.338	5.594	4.583	**4.838**	**5.442**	
R^2	0.978	0.975	0.899	0.951	0.960	

Table 6.2.3g: Predicted S_{bpe} in gCOD/*l* for the Determination of the Best Saturation Kinetic Constants with the Three Linearization Methods and the Curve Expert program			
R_s	**All three methods (All data included)**	**Curve Expert**	**S_{bpe} Measured**
10	0.64	0.57	0.61
18	0.30	0.35	0.30
25	0.20	0.20	0.21
40	0.12	0.11	0.13
60	0.08	0.08	0.08
	Selected		
k_M	**1.52**	1.61	
K_S	**4.84**	5.44	

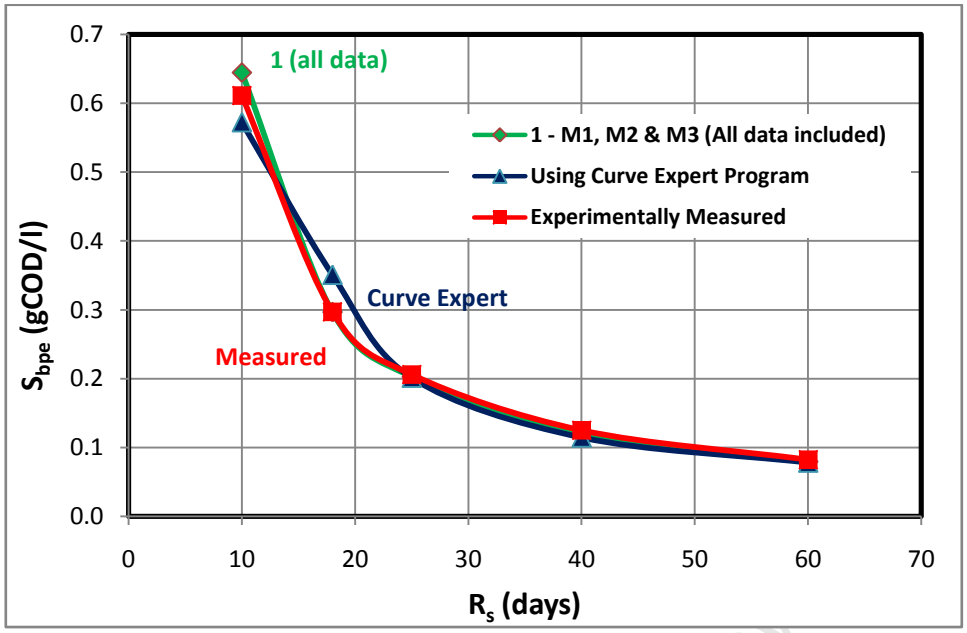

Figure 6.2.3s: *Comparison of measured S_{bpe} concentrations with those predicted by the average k_M and K_S values from the three linearization methods with all R_s data included and the Curve Expert program and experimentally measured to find the best k_M and K_S values for modelling hydrolysis with the saturation kinetics.*

Reliable application of the Monod kinetics required removal of the 25, 40 and 60-day R_s in the M3 linearization method. The removal of these data from M3 yielded better correlation coefficients and S_{bpe} prediction. The resulting average k_m and K_s values are 2.482 (gCOD/gCOD.d) and 0.626 (gCOD/*l*) respectively (for Monod kinetics, Table 6.2.3e). In contrast for saturation kinetics, no R_s data needed to be omitted for any of the three linearization methods and the average k_M and K_S values obtained are of 1.524 (gCOD/gCOD.d) and 4.838 (gCOD/*l*) respectively. A comparison of the predicted and measured linearized plots for the three linearization methods are shown in Figures 6.2.3p to r respectively and can be seen to correlate well ($R^2 > 0.9$) for all three methods. Comparing the S_{bpe} predicted by the average saturation kinetic constants from the three linearization methods and those from the Curve Expert program with the S_{bpe} calculated from the

experimental data (Figure 6.2.3s), it can be seen that the Curve Expert program predicts S_{bpe} almost just as well as the average k_M and K_S obtained from the three linearization methods. Therefore, the kinetic constants determined with the Curve Expert program would also be suitable to model the hydrolysis kinetics of this sludge (MLE 2 WAS). These kinetic constants are also reported in Tables 6.2.3f where k_M and K_S values are 1.606 (gCOD/gCOD.d) and 5.442 (gCOD/*l*) respectively.

A comparison of the percentage (of total influent) COD removed versus sludge age for the MLE1 (fed settled WW) and MLE 2 (fed raw WW) sludges is shown in Figure 6.2.3t. It shows the significantly different unbiodegradable fractions ($f_{SL'up}$) and the predicted % COD removed by the four calibrated kinetic hydrolysis rates, as well as the experimental results. The similar curvature of these lines indicates the similar hydrolysis rates of the WAS from the MLE 1 and MLE 2 systems.

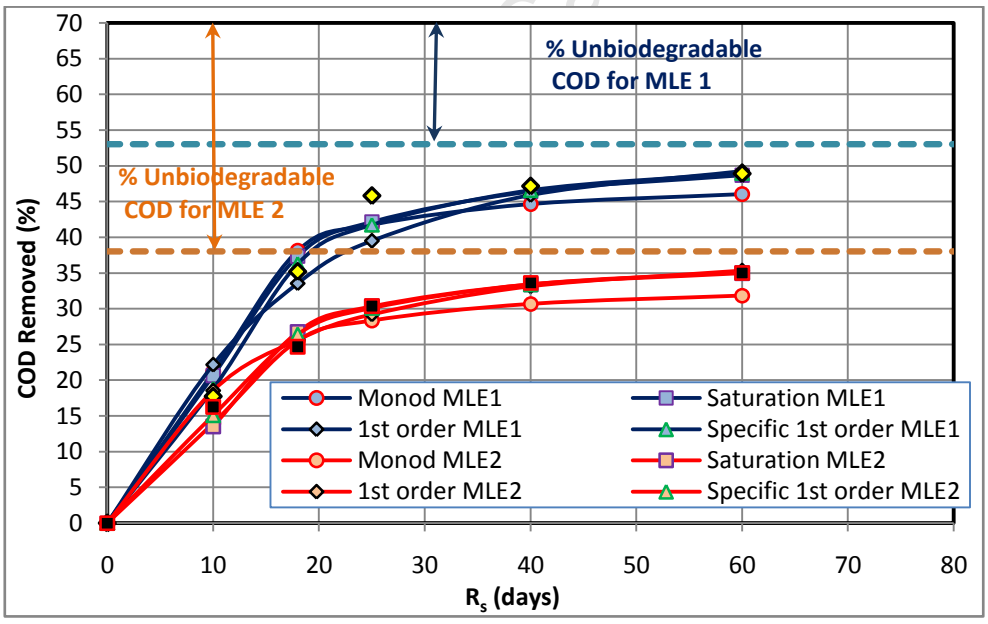

Figure 6.2.3t: *A comparison of the percentage COD removed for the AD of the sludge from the MLE 1 (blue graphs) and MLE 2 (red graphs) ND systems, measured and determined using obtained constants for the various kinetic formulations (1st order, specific 1st order, Monod and saturation).*

6.2.2.4 NDBEPR Waste Activated Sludge

The same procedure applied to the determination of the hydrolysis kinetic constants of the other sludge types (PS and MLE WAS) was also applied to determine the hydrolysis kinetic constants of the NDBEPR WAS. Tables 6.2.4a and 6.2.4b show the average influent and effluent experimental results obtained for all seven sludge ages of the AD fed WAS from the Nitrification-Denitrification Biological Excess Phosphorus Removal (NDBEPR) system fed settled wastewater. Since the sludge fed from the NDBEPR system to the AD (AD 1) was not thickened, the concentration of influent sludge was constant at about 9gTSS/*l* but the flux fed was varied with change in R_s. Therefore, the NDBEPR influent BPO (S_{bpi}) remained in the range of 4 to 5g/*l* but the Monod K_s obtained were divided by the S_{bpi} value to calculate $K_{s\text{-}ref}$. The kinetic values obtained using the experimental data (Table 6.2.4a and 6.4.2b), together with the calculation procedures described above (in Section 6.2.1), are presented in this section.

Table 6.2.4a: WAS from MBR NDBEPR UCT System Influent Experimental Data							
Retention Time (d)	10	12	18	20	25	40	60
Digester Volume (*l*)	16	5	16	5	16	16	5
Influent flow (*l*/d)	1.60	1.33	0.89	0.80	0.64	0.40	0.09
Units	Conc. (g/*l*)	Flux (g/d)	Conc. (g/*l*)	Flux (g/d)	Conc. (g/*l*)	Flux (g/d)	Conc. (g/*l*)
Influent COD[3], S_{ti} (gCOD/*l*)	9.36	9.36	10.06	9.36	9.59	10.13	10.42
Influent COD[1], S_{upi} (gCOD/*l*)	5.05	5.05	5.43	5.05	5.18	5.47	5.63
Influent COD, S_{usi}[2] (gCOD/*l*)	0.04	0.04	0.03	0.04	0.04	0.01	0.03
Influent COD, S_{bpi}[6] (gCOD/*l*)	4.27	4.27	4.60	4.27	4.37	4.64	4.76
Influent COD, S_{bsfi}[5] (gCOD/*l*)	0.00	0.00	0.00	0.00	0.00	0.00	0.00
Influent VFA, S_{bsai}[4] (gCOD/*l*)	0.00	0.00	0.00	0.00	0.00	0.00	0.00
Influent TKN[3] (gN/*l*)	0.55	0.55	0.60	0.55	0.60	0.58	0.67
Influent filtered TKN (gN/*l*)	0.01	0.01	0.01	0.01	0.01	0.01	0.01
Influent FSA (gN/*l*)	0.00	0.00	0.00	0.00	0.00	0.00	0.01
Influent Alk g/*l* as $CaCO_3$	-	-	-	-	230.00	-	-
Influent pH	7.89	7.89	-	7.89	7.60	-	-
Influent TP[3] (gP/*l*)	0.87	0.87	0.91	0.87	0.99	0.84	0.92
Influent filtered TP (gP/*l*)	0.02	0.02	0.02	0.02	0.04	0.02	0.02
Influent OP (gP/*l*)	0.02	0.02	0.02	0.02	0.02	0.02	0.02
Influent TSS (gTSS/*l*)	8.60	8.60	9.18	8.60	9.88	9.49	9.87
Influent VSS (gVSS/*l*)	6.48	6.48	6.92	6.48	6.58	6.99	7.17
Influent ISS (gISS/*l*)	2.11	2.11	2.25	2.11	3.30	2.50	2.70
Influent magnesium (gMg/*l*)	0.24	0.24	0.29	0.24	0.29	0.31	0.28
Filtered Influent magnesium (gMg/*l*)	0.09	0.09	0.06	0.09	0.07	0.08	0.09
Influent potassium (gK/*l*)	0.40	0.40	0.49	0.40	0.44	0.45	0.40
Filtered Influent potassium (gK/*l*)	0.09	0.09	0.08	0.09	0.10	0.08	0.10
Influent calcium (gCa/*l*)	0.05	0.05	0.05	0.05	0.06	0.05	0.06
Filtered Influent calcium (gCa/*l*)	0.01	0.01	0.02	0.01	0.03	0.02	0.02

[1] S_{upi} is the unbiodegradable particulate COD calculated using best-determined $f_{SL'up}$ = 0.54, obtained for good coefficients of variation and correlation coefficients as shown in the section below

[2] S_{usi} is the unbiodegradable soluble COD measured from the filtered effluent of parent NDBEPR AS system

[3] Unfiltered samples

[4] S_{bsai} is the COD in short chain fatty acids that is measured in the influent using the 5-point titration method

[5] S_{bsfi} is the fermentable biodegradable soluble influent COD, assumed to zero (completely utilized) from parent NDBEPR AS system

[6] S_{bpi} is the biodegradable particulate influent COD, calculated by the total influent COD (S_{ti}) – S_{usi} – S_{bsai} – S_{upi}

Table 6.2.4b: WAS from MBR NDBEPR UCT System Effluent Experimental Data							
Retention Time (d)	10	12	18	20	25	40	60
Effluent flow (*l*/d)	1.6	1.33	0.89	0.8	0.64	0.4	0.09
Units	Conc. (g/*l*)	Flux (g/d)	Conc. (g/*l*)	Flux (g/d)	Conc. (g/*l*)	Flux (g/d)	Conc. (g/*l*)
Effluent COD[1], S_{te} (gCOD/*l*)	7.52	7.42	7.23	7.13	6.95	6.38	6.08
Effluent COD, S_{upe} [5] (gCOD/*l*)	5.05	5.05	5.43	5.05	5.18	5.47	5.63
Effluent COD, S_{use}[2] (gCOD/*l*)	0.04	0.04	0.03	0.04	0.04	0.01	0.03
Effluent filtered COD, S_{tse} (gCOD/*l*)	0.04	0.04	0.03	0.04	0.04	0.01	0.03
Effluent COD, S_{bpe}[6] (gCOD/*l*)	2.43	2.33	1.77	2.04	1.74	0.89	0.42
Effluent COD, S_{bsfe}[4] (gCOD/*l*)	0	0	0	0	0	0	0
Effluent VFA, S_{bsae}[3] (gCOD/*l*)	0.01	0.02	0.02	0.03	0.01	0.02	0
Effluent TKN[1] (gN/*l*)	0.6	0.59	0.59	0.59	0.6	0.6	0.59
Effluent filtered TKN (gN/*l*)	0.09	0.12	0.15	0.17	0.18	0.22	0.29
Effluent FSA (gN/*l*)	0.09	0.11	0.14	0.16	0.18	0.21	0.28
Effluent TP[1] (mgP/*l*)	0.91	0.91	0.91	0.9	0.86	0.89	0.85
Effluent filtered TP (gP/*l*)	0.51	0.53	0.46	0.56	0.47	0.48	0.47
Effluent OP (gP/*l*)	0.49	0.53	0.46	0.56	0.46	0.47	0.42
Effluent TSS	7.21	7.3	7.4	7.25	7.2	6.73	6.57
Effluent VSS	5.04	4.97	4.93	4.89	4.76	4.32	4.18
Effluent ISS	2.17	2.33	2.46	2.36	2.44	2.41	2.27
Effluent Alk. mg/*l* as $CaCO_3$	0.25	0.27	0.32	0.38	0.64	0.75	0.93
Effluent Alk. mg/*l* as $CaCO_3$ (No P)	0.56	0.71	0.85	0.78	0.93	0.93	1.28
Measured digester pH	6.74	6.8	6.93	0.01	6.81	6.97	7.06
Effluent magnesium (g/*l*)	0.23	0.25	0.3	0.27	0.3	0.25	0.27
Filtered Effluent magnesium (g/*l*)	0.02	0.02	0.02	0.02	0.03	0.03	0.02
Effluent potassium (g/*l*)	0.35	0.39	0.39	0.37	0.4	0.38	0.4
Filtered Effluent potassium (g/*l*)	0.33	0.36	0.36	0.36	0.37	0.37	0.38
Effluent calcium (g/*l*)	0.04	0.04	0.04	0.04	0.04	0.03	0.05
Filtered Effluent calcium (g/*l*)	0.04	0.04	0.03	0.03	0.03	0.02	0.05

Table 6.2.4b: WAS from MBR NDBEPR UCT System Effluent Experimental Data							
Retention Time (d)	10	12	18	20	25	40	60
COD removed (gCOD/*l*)	1.84	1.94	2.83	2.23	2.64	3.75	4.34
Gas production (litres)	4.19	3.22	1.94	1.5	0.97	0.5	0.28
Gas prod. (l gas/*l* influent)	2.62	2.41	2.19	1.87	1.51	1.25	
Gas composition : CH_4 fraction	0.42	0.42	0.42	0.42	0.42	0.42	
Gas composition: CO_2 fraction	0.23	0.23	0.23	0.23	0.23	0.23	
Vol. CH_4 (litres)	1.1	1.01	0.92	0.79	0.63	0.53	
Vol. CO_2 (litres)	0.6	0.56	0.5	0.43	0.35	0.29	
COD of CH_4 (gCOD/*l* feed)	1.8	2	2.71	2.58	2.6	3.46	3.56
p_{CO2} (atm)	0.35	0.35	0.35	0.35	0.35	0.35	
CT dissolved (mmo*l*/*l*)	0.04	0.04	0.04	0.04	0.04	0.04	
H_2CO_3 diss. (mg/*l*)	4.41	4.41	4.41	4.41	4.41	4.41	
Moles of CO_2/*l* feed	0.02	0.02	0.02	0.02	0.01	0.01	
Moles of CH_4/*l* feed	0.05	0.04	0.04	0.03	0.03	0.02	
COD balance (%)	99.66	100.59	98.87	103.75	99.61	97.1	92.5
Nitrogen balance (%)	108.34	107.83	98.41	106.39	100	104.47	87.91
Phosphorous balance (%)	105.33	104.55	100.02	103.98	86.51	105.75	92.55
Magnesium balance (%)	95.54	106.96	102	115.92	103.26	80.42	98.2
Potassium balance (%)	87.14	97.98	79.91	93.32	90.5	84.07	100.74
Calcium balance (%)	84.54	85.56	79.92	84.54	68	49.44	86.27
f_{cv} (gCOD/gVSS)	1.48	1.48	1.46	1.45	1.45	1.47	1.45
$f_{SL'up}$ (NDBEPR WAS)	0.54	0.54	0.54	0.54	0.54	0.54	0.54
[1] Unfiltered sample							
[2] S_{use} is the unbiodegradable soluble COD that equals the S_{usi} value from Table 6.2.4a							
[3] S_{bsae} is the COD in short chain fatty acids that is measured in the effluent using the 5-point titration method							
[4] S_{bsfe} is the fermentable biodegradable soluble COD calculated from the measured filtered effluent COD (S_{tse}) – S_{use} – S_{bsae}							
[5] S_{upe} is the unbiodegradable particulate effluent COD which equals the S_{upi} value from Table 6.2.4a							
[6] S_{bpe} is the biodegradable particulate effluent COD which equals the total effluent COD (S_{te}) – S_{tse} – S_{upe}							

The Selection of a Suitable $f_{SL'up}$ Value

The influence of $f_{SL'up}$ on the results from hydrolysis rate equations of NDBEPR WAS are shown below by plotting the coefficients of variation for first order and first order specific hydrolysis kinetic equations versus increasing $f_{SL'up}$ fractions

(shown in Figure 6.2.4a) and correlation coefficients (R^2) for Monod and saturation hydrolysis kinetic equations versus the same range of $f_{SL'up}$ fractions (in Figures 6.2.4b and 6.2.4c respectively). This is done in order to obtain the most suitable $f_{SL'up}$ fraction that gives the best correlation coefficients when applying the various hydrolysis kinetic equations to as accurately as possible predict the effluent COD from the AD of NDBEPR WAS. The correlation coefficients of the Monod and saturation kinetics are shown for the Curve Expert program and the three linearization methods of Lineweaver-Burke (M1) and (M1*), double reciprocal (M2) and Eadie-Hofstee (M3) and (M3*). The M1, M2 and M3 (without asterisks) were obtained with the 10, 12, 18, 25, 40 and 60-day R_s data i.e., with the 20-day data set omitted. The M1* for Lineweaver-Burke has the 20, 25, 40 and 60 day R_s data omitted and M3* has 20 and 25-day R_s data omitted for both the Monod and the saturation kinetics. The omission of these R_s data sets from M1 and M3 was done in order to improve the corresponding R^2 values for M1 and M3 linearization methods.

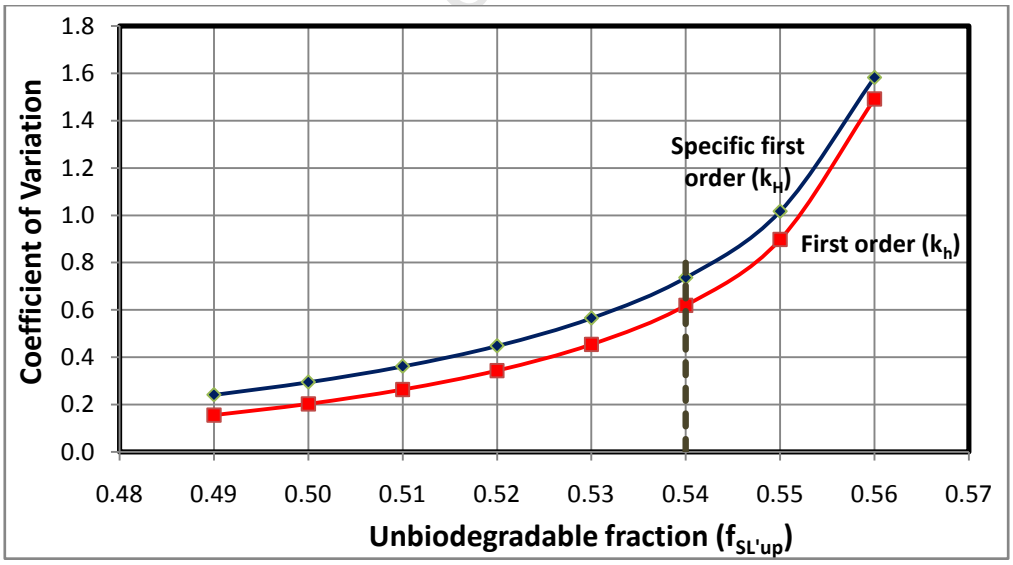

Figure 6.2.4a: *The change in the coefficient of variation of the 1st order and 1st order specific hydrolysis equations kinetic constants with changing unbiodegradable particulate COD fraction ($f_{SL'up}$) of NDBEPR WAS, without R_s = 20d and 25d data (see Table 6.2.4c).*

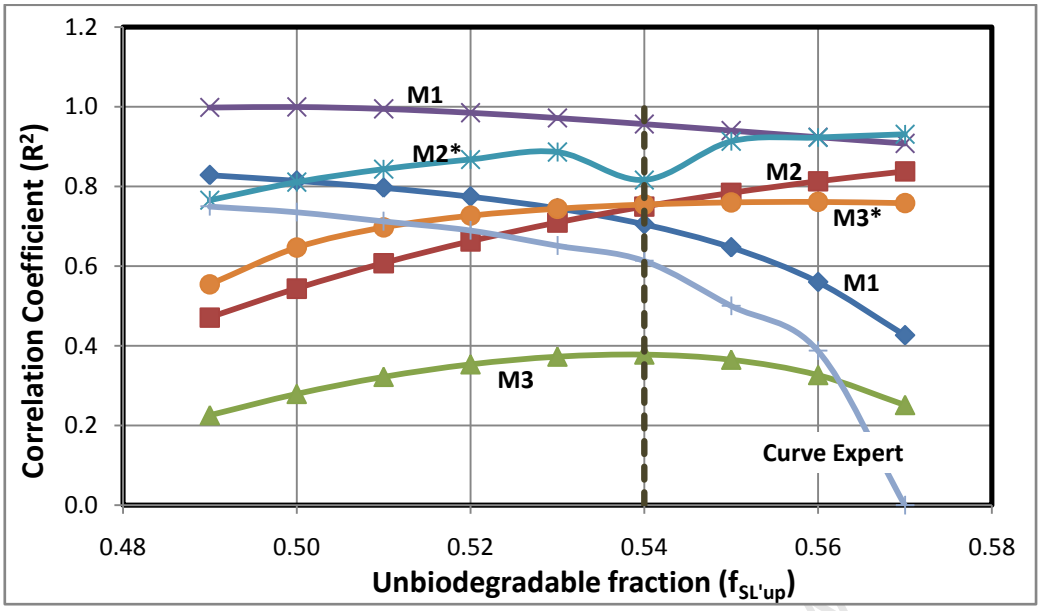

Figure 6.2.4b: *The regression correlation coefficient (R^2) for the Curve Expert program, Lineweaver-Burke (M1), double reciprocal (M2) and Eadie-Hofstee (M3) linearization methods of Monod hydrolysis kinetics versus unbiodegradable particulate COD fraction ($f_{SL'up}$) of the NDBEPR WAS.*

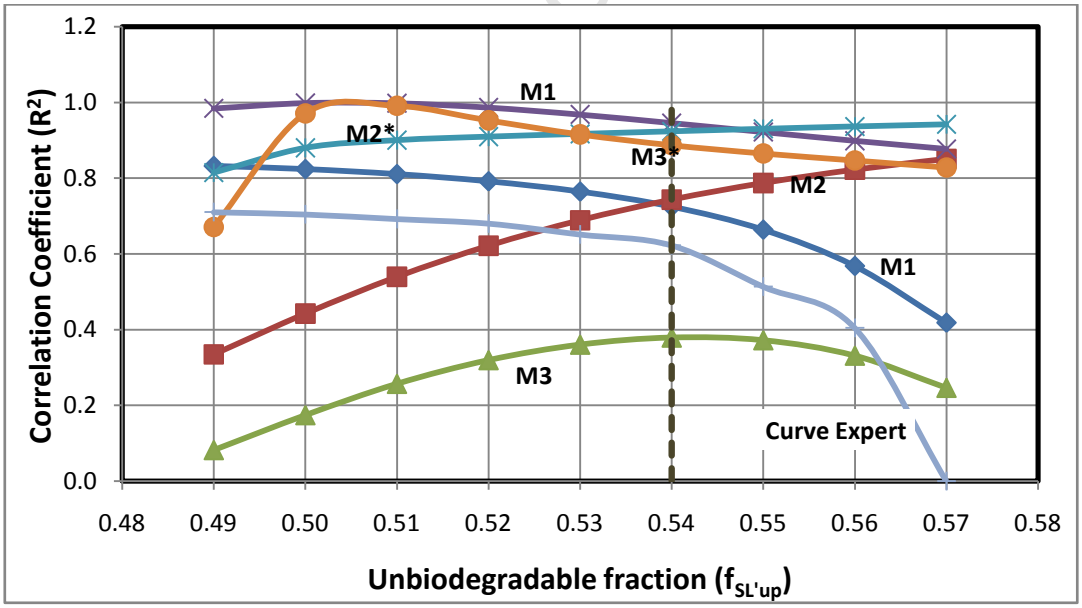

Figure 6.2.4c: *The regression correlation coefficient (R^2), for the Curve Expert program Lineweaver-Burke (M1), double reciprocal (M2) and Eadie-Hofstee (M3) linearization methods of saturation hydrolysis kinetics versus **u**nbiodegradable particulate COD fraction ($f_{SL'up}$) of the NDBEPR WAS.*

As was the case with the other sludges considered earlier (PS, MLE 1 WAS and MLE 2 WAS), Figure 6.2.4a, shows a gradual increase in the coefficient of variation (C_{var}) with increasing unbiodegradable particulate fraction from 0.49 to 0.55, after which it increases sharply. Figures 6.2.4b and 6.2.4c show that Monod and saturation kinetics exhibit maximum R^2 values for all three linearization methods at an $f_{SL'up}$ value of around 0.54. This value is close to that measured from the AD at the very long sludge age of 60 days (0.58) and also to that calculated with the NDBEPR AS model for NDBEPR AS system for the influent wastewater $f_{S'up}$ fraction and OHO and PAO endogenous residue (X_{EH} and X_{EG}, both in mgERVSS/*l*) (0.53, see Section 5.3 of Chapter 5). This means that the best compromise $f_{SL'up}$ value between the four hydrolysis kinetic formulations and the 60d sludge age AD is 0.54. Therefore, $f_{SL'up}$= 0.54 was selected for the determination of the hydrolysis kinetic constants.

Comparison of Biodegradability Determined from AD to that of AS System

As was noted in Chapter 5 (Section 5.3), the surprising outcome from the AD fed the NDBEPR WAS is that it reflects a similar WAS unbiodegradable fraction as estimated by the NDBEPR model, which requires a significantly higher settled WW $f_{S'up}$ (0.18) than for the MLE 1 ($f_{S'up}$ = 0.05) fed the same settled WW. This means that the much higher unbiodegradable particulate organics (UPO) found for the NDBEPR system ($f_{S'up}$ = 0.18) than for the MLE 1 system ($f_{S'up}$ = 0.05) fed the same WW, is measured also in the AD system. This indicates that the higher UPO in the NDBEPR WAS is real and not an artifice of the NDBEPR AS model compared with the ND AS model. Determining where this extra UPO comes from is beyond the scope of this research, but has been a repeated observation in the UCT research (see Ekama and Wentzel, 1999). To account for it by changing, e.g. the UPO of PAOs (f_{EG}) requires a value way outside the reasonable range. This

applies also to the f_{EH} of the OHOs. Moreover, the OHO f_{EH} (and f'_{EH}) have been validated in several investigations over the past decades (Marais and Ekama, 1976 and van Haandel *et al.*, 1998). Therefore, the additional UPO are unlikely to originate from this source. This aspect requires further investigation.

First Order Kinetics

The experimentally measured influent and effluent concentrations from the steady state AD of the NDBEPR WAS (Table 6.2.4a and 6.2.4b) were used in the above-mentioned kinetic calculations (Section 6.2.1) to determine the volumetric hydrolysis rates (r_{HYD}), the residual biodegradable COD concentrations (S_{bp}) and the first order kinetic rate constants (k_h and k_H). These rates are listed in Table 6.2.4c below and their variations with sludge age are shown plotted in Figures 6.2.4d to 6.2.4g. The graphs of k_h and k_H show that the 20d and 25d R_s AD data do not conform to the pattern of the other AD sludge ages, so this data is omitted when establishing the linear relationship (from Equation 6.21c and d) of k_h and k_H with sludge age. This yields $k_h = 0.0041 \cdot R_s + 0.0332$ (R^2 = 0.895) for first order hydrolysis kinetics and $k_H = 0.1309 \cdot R_s + 0.2163$ (R^2 = 0.872) for specific first order hydrolysis kinetics.

Table 6.2.4c: Summary of Results for First Order Kinetics in the AD of NDBEPR WAS for $f_{SL'up}$ = 0.54

R_s (d)	r_{HYD} (g/*l*/d)	Z_{AD} (g/*l*)	S_{bpe} per unit S_{bpi} (g/*l*)	k_h (/d)	Spec r_{HYD} (gS_{bp}/gZ_{AD}/d)	k_H spec (*l*/gZ_{AD}/d)
10	0.048	0.039	0.531	0.091	1.248	2.350
12	0.04	0.039	0.51	0.084	1.100	2.172
18	0.039	0.045	0.340	0.113	0.854	2.512
20	0.029	0.037	0.441	0.067	0.805	1.825
25	0.027	0.038	0.360	0.076	0.717	1.994
40	0.023	0.038	0.153	0.148	0.599	3.911
60	0.017	0.034	0.056	0.308	0.510	9.186
		Mean		0.127	-	3.421
		Standard deviation (all R_s data)		0.084	-	2.633
		Coefficient of variation (all R_s data)		0.661	-	0.770

$k_h = c_{kh} + m_{kh} \times R_s$; c_{kh} = 0.0332; m_{kh} = 0.0041; R^2 = 0.895 (excluding R_s = 20d and 25d)
$k_H = c_{kH} + m_{kH} \times R_s$; c_{kH} = 0.2163; m_{kH} = 0.1309; R^2 = 0.872 (excluding R_s = 20d and 25d)

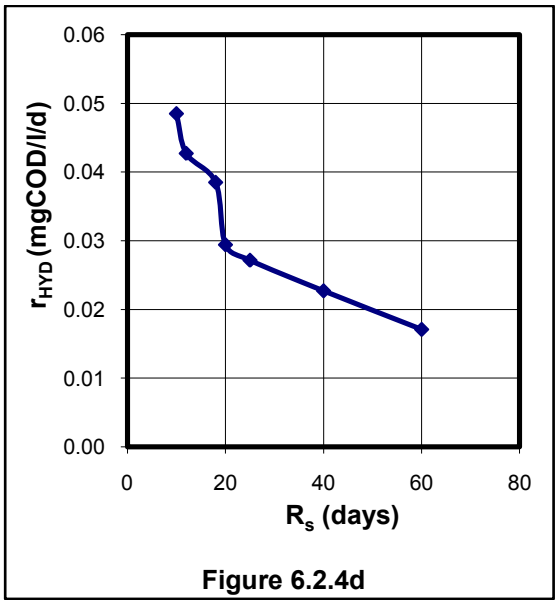

Figure 6.2.4d

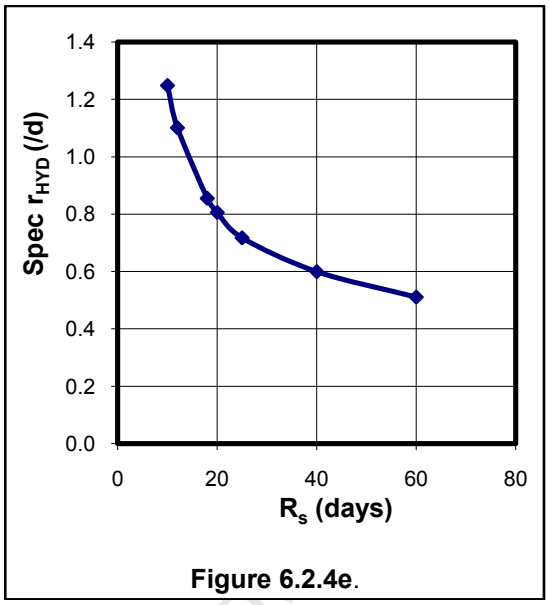

Figure 6.2.4e.

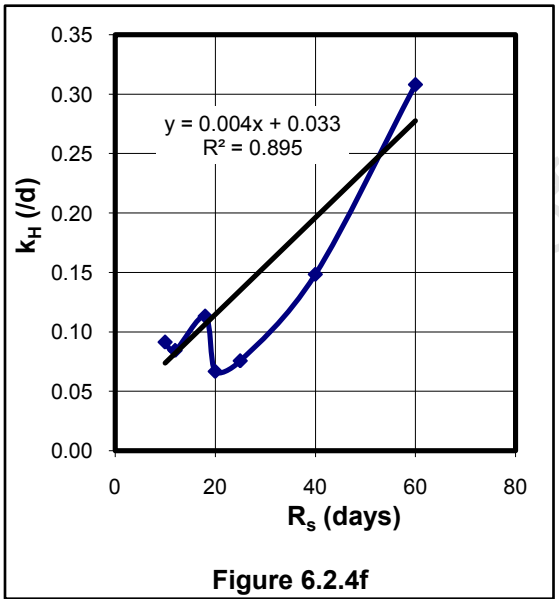

Figure 6.2.4f

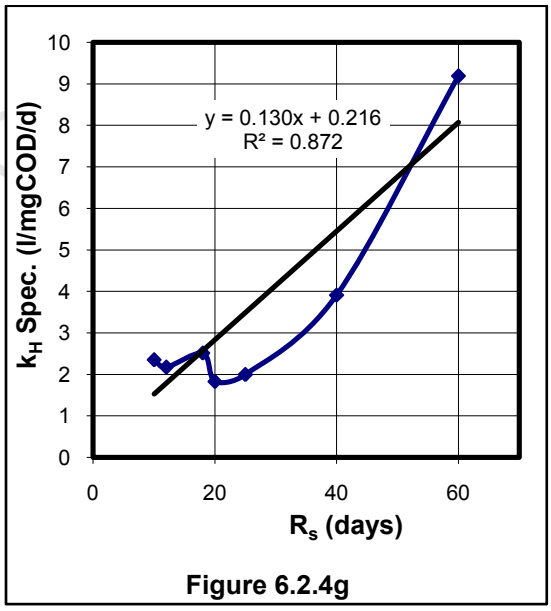

Figure 6.2.4g

Figures 6.2.4d, e, f and g: *Volumetric hydrolysis rates (r_{HYD}) (d), specific volumetric hydrolysis rate (r_{HYD}/Z_{AD}) (e), first order kinetic constant (k_h) (f) and Specific first order kinetic constant (k_H) (g) versus sludge age (R_s) ranging from 10, 12, 18, 20, 25, 40 to 60 days, for AD of NDBEPR WAS. Linear equation and R^2 given for regression without R_s 20 and 25d data (see Table 6.2.4c)*

Monod and Saturation Kinetics

The Figures 6.2.4h to 6.2.4k below show the specific hydrolysis rates (r_{HYD}/Z_{AD}) versus the residual BPO (S_{bp}) for the Monod equation and versus the residual BPO per unit acidogenic biomass (S_{bp} / Z_{AD}) for the saturation kinetics equation. The specific hydrolysis rate (r_{HYD}/Z_{AD}) obtained using the data from Table 6.2.4c, which are directly calculated from experimental results, are compared with those calculated from the Monod and saturation kinetic constants determined with the 3 linearisation methods (Figures 6.2.4h and i) and the Curve Expert program (Figures 6.2.4j and k) (see Table 6.2.4d). It can be seen from these plots that the measured data do not conform to the form of the Monod and saturation equations and is the reason for the low correlation coefficient values (Figure 6.2.4b and c). As expected from Table 6.2.4c, the measured data for 20 and 25 day R_s do not conform to the trends of the rest of the data so these should be omitted to improve the correlation coefficient R^2. The methods used in selecting the kinetic constants (k_m = 2.465 and K_s = 0.607 for Monod and k_M = 1.951 and K_S = 9.109 for saturation kinetics) are discussed further below (See Tables 6.2.4 d, e, f and g).

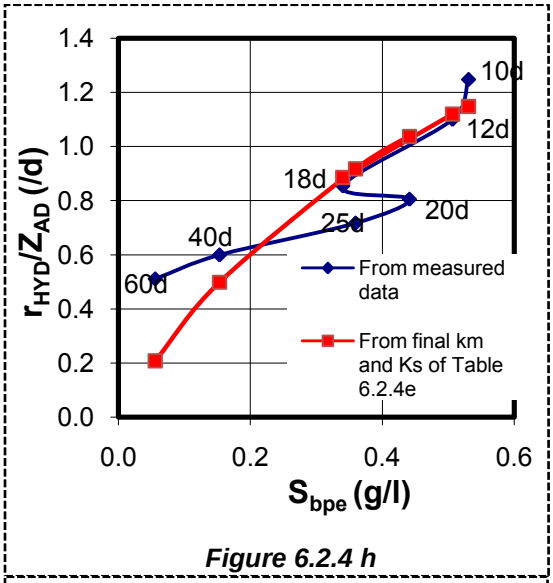

Figure 6.2.4 h

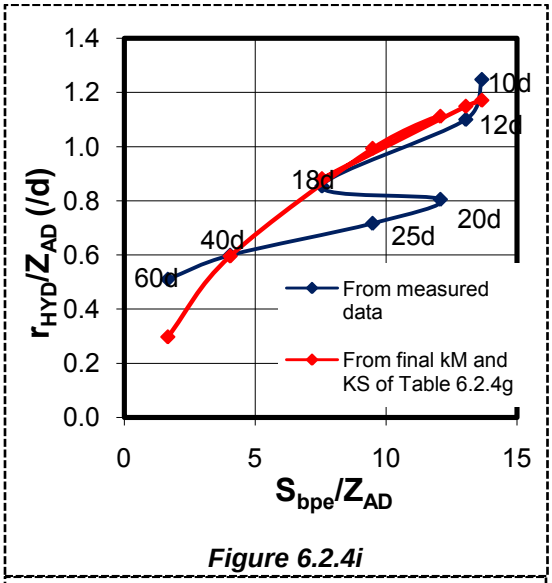

Figure 6.2.4i

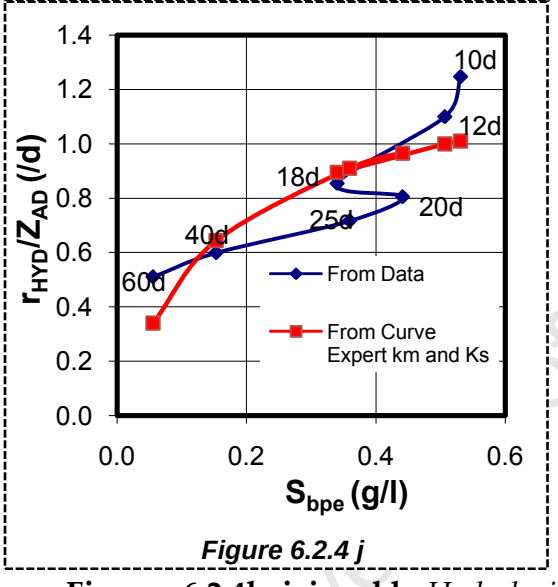

Figure 6.2.4 j

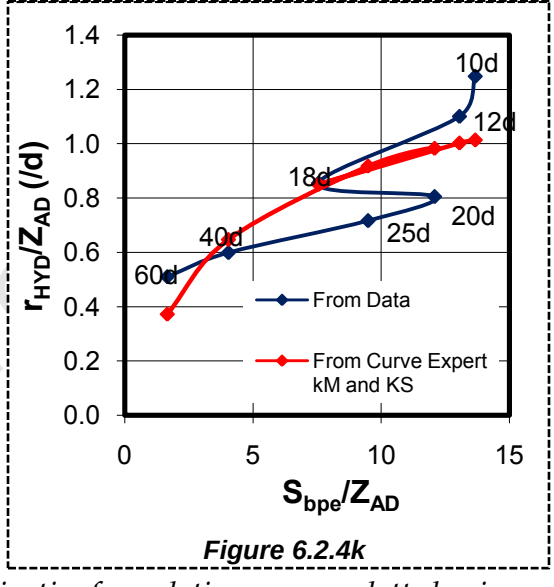

Figure 6.2.4k

Figures 6.2.4h, i, j and k: *Hydrolysis kinetics formulation curves, plotted using experimental data and calculated from kinetic constants acquired from the three linearization methods for (h) Monod (see Table 6.2.4d column 8; k_m = 2.46 and K_s = 0.61) and (i) saturation (see Table 6.2.4f column 8; k_M = 1.951 and K_S = 9.109) equations and the Curve Expert programme (j) for Monod and (k) saturation kinetics.*

The r_{HYD}, S_{bp} and Z_{AD} values determined from the experimental results (Table 6.2.4c) were used in the linearization of the Monod and saturation kinetic equations to determine their kinetic constants (i.e. k_m and K_s for Monod and k_M and K_S for saturation kinetics). The results for linearisation of Monod kinetics and

saturation kinetics with the three different linearization methods are shown below, i.e. (i) Lineweaver-Burke (M1, Figure 6.4.2j and 6.4.2n), (ii) double reciprocal (M2, Figure 6.4.2k and 6.4.2o) and (iii) Eadie-Hofstee (M3, Figure 6.4.2l and 6.4.2p). The resultant R^2 values together with the graphical slope and y-coefficient used for calculating the kinetic constants are presented in Tables 6.2.4d (Monod kinetics) and 6.2.4e (saturation kinetics).

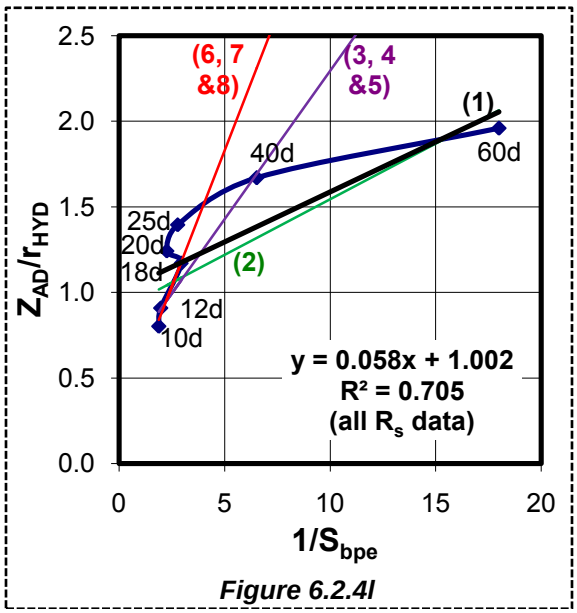

Figure 6.2.4l

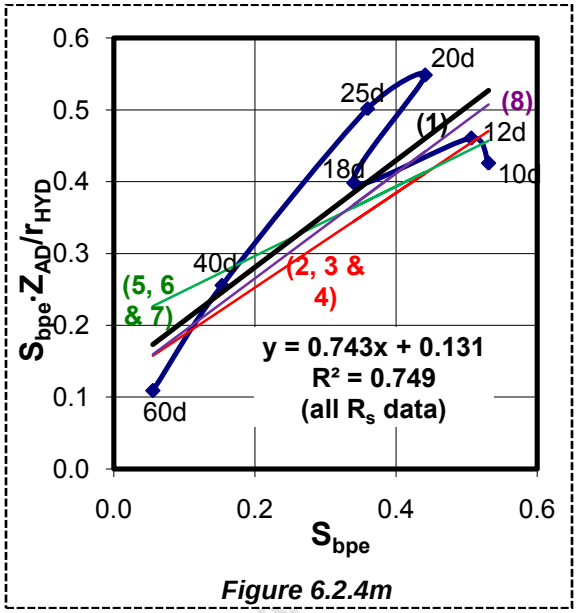

Figure 6.2.4m

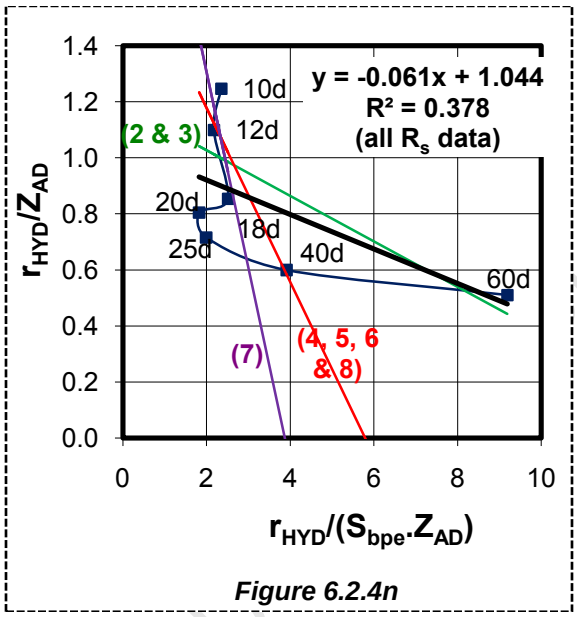

Figure 6.2.4n

Key for Figures 6.2.4j, k and l	
Attempt No.	**Data used or omitted (for R_s off) in determining the k_m and K_s values using the 3 linearization methods (M1, M2 and M3)**
1	Excluding M3
2	M1, M2 & M3 (20 & 25d off all)
3	M1, M2 & M3 (20, 25 & 60d off all)
4	M1(20, 25 & 60d off), M2 (20 & 25d off), M3 (20, 25 & 60d off)
5	M1(20, 25, 40 & 60d off), M2 (20 & 25d off), M3 (20, 25 & 60d off)
6	M1(20, 25, 40 & 60d off), M2 (20 & 25d off), M3 excluded

Figures 6.2.4j, k and l: *The linearization of Monod kinetics for hydrolysis of NDBEPR WAS at all seven R_s (10 to 60) using three linearization methods: (j) Lineweaver–Burke (M1), (k) double reciprocal (M2) and (l) Eadie–Hofstee (M3). The R^2 values for all seven R_s data included - dark (black) lines. Numbers refer to column numbers in Table 6.2.4d, e.g. 5 refers to column 5, which lists the average k_m and K_s values obtained from line 5 in Figure 6.2.4j:M1 with R_s =20, 25, 40 and 60d omitted, line 5 in Figure 6.2.1k:M2 with R_s =20 and 25d omitted and line 5 in Figure 6.2.1l:M3 with R_s =20, 25 and 60d omitted.*

Table 6.2.4d: Predicted Sbpe in gCOD/*l* for the Determination of the Best Monod Kinetic Constants from the Three Linearization Methods										
	Data used or omitted (for R_s off) in determining the average k_m and K_s values from the 3 linearization methods (M1, M2 and M3)									
	1	2	3	4	5	6	7	8		
R_s	Exclu-ding M3	M1, M2 & M3 (20 & 25d off all)	M1 (20, 25 & 60d off), M2 (20, & 25d off) & M3 (20, & 25d off)	M1 (20, 25 & 60d off), M2 (20, & 25d off) & M3 (20, 25 & 60d off)	M1, M2 & M3 (20, 25 & 60d off all)	M1(20, 25, 40 & 60d off), M2 (20, 25 & 60d off) & M3 (20, 25 & 60d off)	M1(20, 25, 40 & 60d off), M2 (20, 25 & 60d off) & M3 (20, 25, 40 & 60d off)	M1 (20, 25, 40 & 60d off); M2 (20d off); M3 (20, 25 & 60d off)	**Curve Expert**	**Target S_{bpe}**
10	-1.91	4.97	0.95	0.74	0.67	0.60	0.59	0.62	3.00	0.53
12	1.83	0.71	0.53	0.49	0.48	0.48	0.48	0.49	0.82	0.51
18	0.32	0.23	0.25	0.27	0.29	0.32	0.33	0.32	0.30	0.34
20	0.26	0.19	0.22	0.24	0.26	0.29	0.30	0.29	0.25	0.44
25	0.19	0.14	0.18	0.20	0.21	0.25	0.26	0.25	0.19	0.36
40	0.12	0.10	0.12	0.14	0.15	0.19	0.20	0.19	0.13	0.15
60	0.09	0.08	0.10	0.11	0.13	0.16	0.17	0.16	0.10	0.06
								Selected		
k_m	1.17	1.28	1.50	1.70	1.88	2.67	2.97	**2.46**	1.31	
K_s	0.12	0.11	0.19	0.27	0.34	0.68	0.81	**0.61**	0.16	
R^2	0.73	0.76	0.82	0.87	0.87	0.87	0.74	**0.83**	0.61	

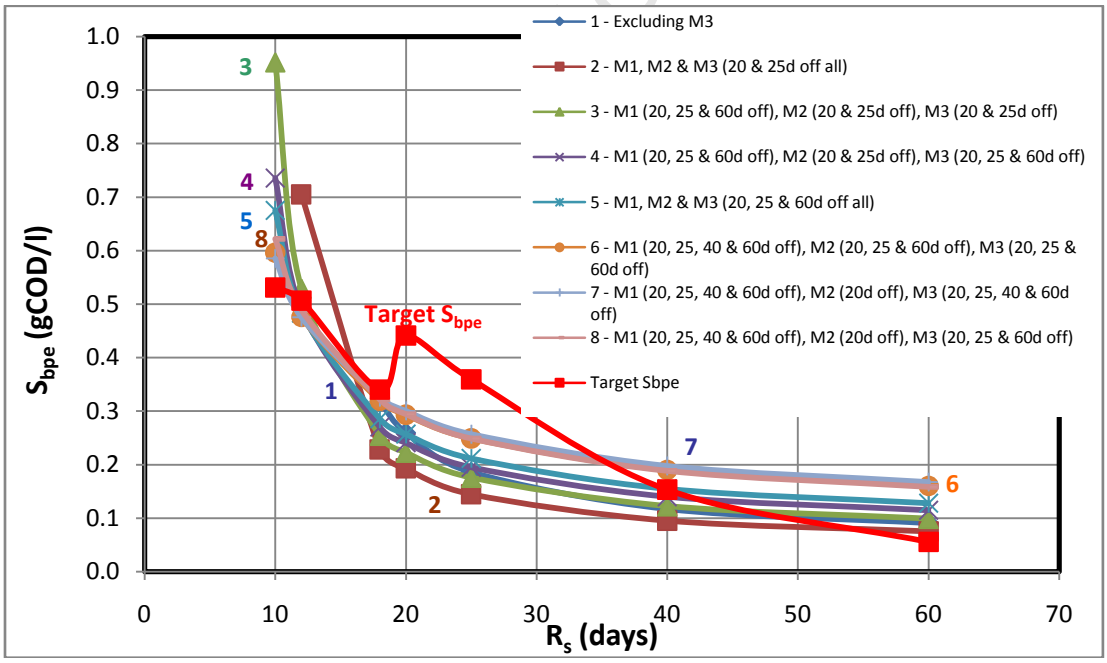

Figure 6.2.4o: *Comparison of tagret S_{bpe} values (calculated from measured values in Table 6.2.4b) with those predicted by different combinations of selected R_s data in the three linearization methods for the determination of the best k_m and K_s values for modelling hydrolysis with the Monod kinetics. Numbers refer to column numbers in Table 6.2.4d*

The procedure used to select the best Monod kinetic constants for the NDBEPR WAS, from the three linearization methods, are the same as applied for the other sludge types (PS and MLE WAS). Table 6.2.4d and Figure 6.2.4o show whether or not the R^2 values are satisfactory ($R^2 \geq 0.8$) and how well the S_{bpe} concentrations predicted by the resultant kinetic constants matched those calculated from the experimentally measured results. The 20 and 25d R_s were observed to be outliers, since their measured S_{bpe} do not conform to the trend of the rest of the S_{bpe} data, which show the expected decreasing trend in S_{bpe} with R_s. Therefore, these data (20 and 25d R_s) were excluded from all three linearization methods. However, the resultant S_{bpe} predictions were still not satisfactory. The 60-day R_s data was then removed from the linearization with M1 and M3 (column 3 of Table 6.2.4d). Although this resulted in improved predictions of S_{bpe} from 10 to 40d R_s, the 10-day R_s S_{bpe} still appeared to be significantly over-predicted by the resultant k_m and K_s values. It was noted that omission of the 40d R_s data (for M1 and M3) resulted in better predictions for the shorter R_s (10 to 25d) but over-predictions for the longer R_s (40 and 60d). Thus, the 40d R_s was also omitted, but only for M1 to provide some positive influence on the S_{bpe} predictions of the lower (10 to 25d) R_s, while not over-compromising the longer R_s S_{bpe} predictions, which are very low anyway. It was also observed that inclusion of the initially removed 25d R_s for M2 also improved this shorter R_s data with no negative impact on the longer R_s data. The final k_m and K_s values, resulting from this data selection, are presented in Table 6.2.4e below.

Table 6.2.4e: Monod Kinetics (Hydrolysis of NDBEPR WAS)						
Linearization	**Lineweaver-Burke (M1)**	**Double reciprocal (M2)**	**Eadie-Hofstee (M3)**	**Average**	**Curve Expert**	**Notes**
Slope	0.058	0.744	-0.062			AD sludge ages of 10, 12, 18, 20, 25, 40 and 60 days are used in all methods.
Y-Intercept	1.003	0.132	1.044			
k_m	0.997	1.345	1.044		**1.314**	
K_s	0.058	0.177	0.062		**0.159**	
R^2	0.705	0.750	0.378		0.613	
Slope*	0.317	0.686	-0.311			20, 25, 40 and 60 day R_s is omitted in M1; 20d R_s omitted in M2 and 20, 25 and 60 day R_s omitted from M3 to improve R^2.
Y-Intercept*	0.242	0.136	1.802			
k_m*	4.135	1.457	1.802	**2.465**		
K_s*	1.311	0.198	0.311	**0.607**		
R^2*	0.957	0.767	0.755	0.826		

Saturation Kinetics

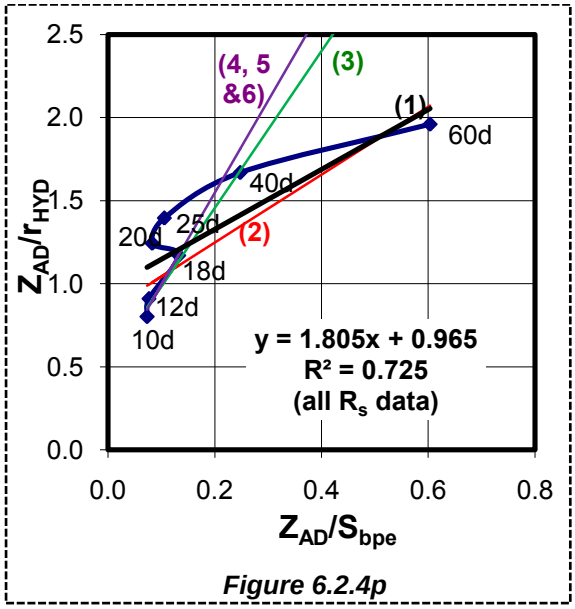

Figure 6.2.4p

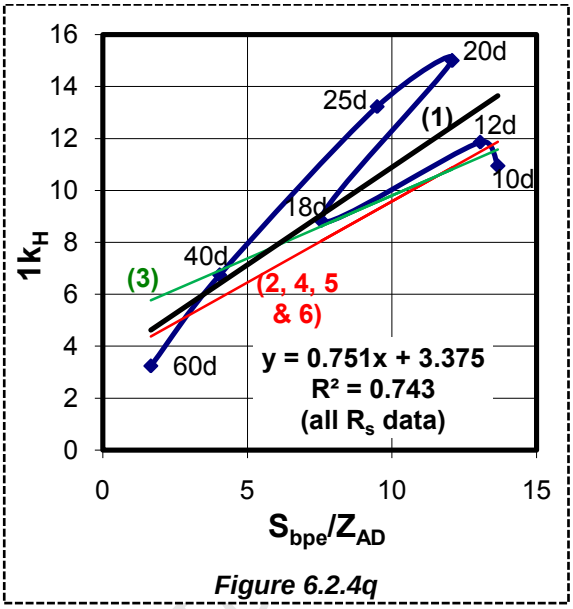

Figure 6.2.4q

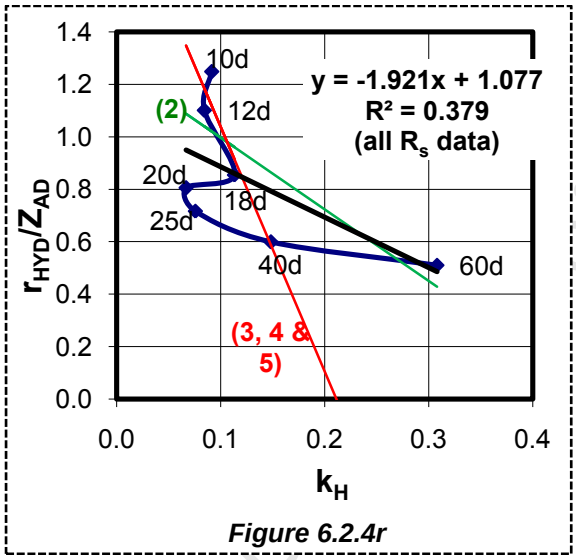

Figure 6.2.4r

Key for Figures 6.2.4p, q and r	
Column No. in Table 6.2.4f	**Data used or omitted (for R_s off) in determining the k_M and K_S values using the 3 linearization methods (M1, M2 and M3)**
1	Excluding M3
2	M1, M2 & M3 (20 & 25d off all)
3	M1, M2 & M3 (20, 25 & 60d off all)
4	M1(20, 25 & 60d off), M2 (20 & 25d off), M3 (20, 25 & 60d off)
5	M1(20, 25, 40 & 60d off), M2 (20 & 25d off), M3 (20, 25 & 60d off)
6	M1(20, 25, 40 & 60d off), M2 (20 & 25d off), M3 excluded

Figures 6.2.4p, q and r: *The linearization of saturation kinetics for hydrolysis of NDBEPR WAS at all seven R_s (10 to 60) using various methods in the order of: (p) Lineweaver–Burke (M1), (q) double reciprocal (M2) and (r) Eadie–Hofstee (M3). The R^2 values for all 5 R_s data included- dark (black) lines. Numbers refer to column numbers in Table 6.2.4f, e.g. 2 refers to column 2, which lists the average k_M and K_S values obtained from line 2 in Figure 6.2.4p: M1 with R_s =20 and 25d omitted, line 2 in Figure 6.2.1q: M2 with R_s =20 and 25d omitted and line 5 in Figure 6.2.1r: M3 with R_s =20 and 25d omitted, i.e. 20 and 25d R_s omitted for M1, M2 and M3*

The determination of the best kinetic constants for saturation kinetics was all done the same way as those for Monod kinetics by evaluating which R_s data in each of the 3 linearization methods gave the best R^2 values and S_{bpe} predictions. The results of this evaluation are given in Table 6.2.4f and shown in Figure 6.2.4s below.

Table 6.2.4f: Predicted S_{bpe} in gCOD/*l* for the Determination of the Best Saturation Kinetic Constants from the Three Linearization Methods

	Data used or omitted (for R_s off) in determining the average k_M and K_S values with the 3 linearization methods							
	1	**2**	**3**	**4**	**5**	**6**		
R_s	Excluding M3	M1, M2 & M3 (20 & 25d off all)	M1, M2 & M3 (20, 25 & 60d off all)	M1(20, 25 & 60d off), M2 (20 & 25d off), M3 (20, 25 & 60d off)	M1(20, 25, 40 & 60d off), M2 (20 & 25d off), M3 (20, 25 & 60d off)	M1(20, 25, 40 & 60d off), M2 (20 & 25d off), M3 excluded	**Curve Expert**	**Target S_{bpe}**
10	1.24	0.77	0.57	0.58	0.57	0.57	0.84	0.53
12	0.77	0.54	0.48	0.48	0.48	0.48	0.62	0.51
18	0.36	0.29	0.33	0.32	0.33	0.33	0.34	0.34
20	0.31	0.25	0.30	0.29	0.30	0.29	0.30	0.44
25	0.22	0.19	0.24	0.23	0.24	0.24	0.23	0.36
40	0.12	0.11	0.15	0.15	0.15	0.15	0.13	0.15
60	0.08	0.07	0.10	0.10	0.10	0.10	0.09	0.06
					Selected			
k_M	1.183	1.355	1.996	1.842	**1.951**	1.942	1.330	
K_S	3.181	3.507	9.601	7.965	**9.109**	9.002	4.264	
R^2	0.73	0.80	0.94	0.93	0.92	0.93	0.62	

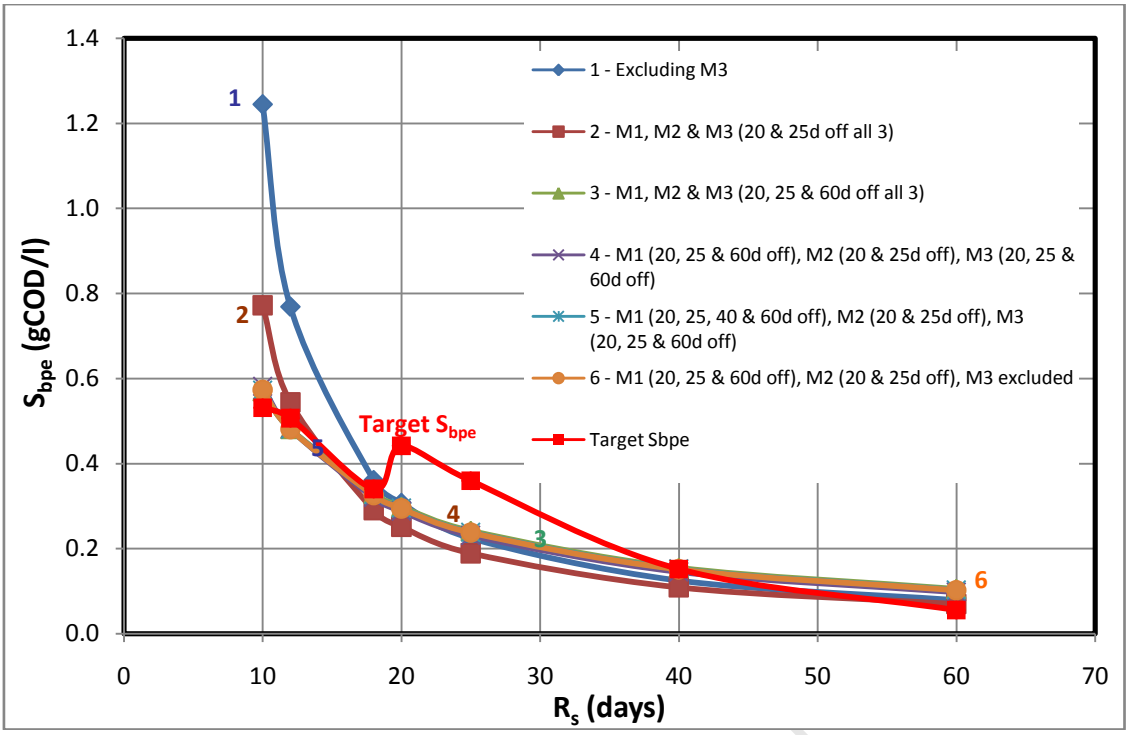

Figure 6.2.4s: *Comparison of tagret S_{bpe} values (calculated from measured values in Table 6.2.4b) with those predicted by the average k_M and K_S values obtained from different combinations of selected R_s data in the three linearization methods to find the best k_M and K_S values for modelling hydrolysis with the saturation kinetics. Numbers refer to the column numbers in Table 6.2.4f.*

Table 6.2.4g: Saturation Kinetics (Hydrolysis of NDBEPR WAS)

Linearization	Lineweaver-Burke (M1)	double reciprocal (M2)	Eadie-Hofstee (M3)	Average	Curve Expert	Notes
Slope	1.806	0.752	-1.922			AD sludge ages of 10, 12, 18, 20, 25, 40 and 60 days are used in all methods.
Y-Intercept	0.966	3.375	1.077			
k_M	1.036	1.331	1.077		**1.330**	
K_S	1.870	4.492	1.922		**4.264**	
R^2	0.725	0.743	0.379		0.623	
Slope*	5.547	0.624	-9.322			20, 25, 40 and 60 day R_s omitted in M1; 20 and 25 day R_s omitted in M2; 20, 25 and 60d R_s omitted in M3 to improve R^2.
Y-Intercept*	0.438	3.338	1.969			
k_M*	2.282	1.602	1.969	**1.951**		
K_S*	12.655	5.348	9.322	**9.109**		
R^2*	0.946	0.924	0.887	0.919		

The Lineweaver-Burke and double reciprocal method (M1 and M2) gives the best correlation with all the experimental data (R^2 = 0.705 and 0.750 for Monod kinetics

and R^2 = 0.725 and 0.743 for saturation kinetics for M1 and M2 respectively). The Eadie-Hofstee method (M3) gives unsatisfactory correlation values (R^2 < 0.4). Therefore, the 20d R_s data was removed from all three linearization methods because it had a higher S_{bpe} than the 18-day R_s data. However, the Eadie-Hofstee method (M3) still showed poor correlation because it emphasizes the long R_s data so the 25 and 60-day R_s data were also removed from this linearization. Removal of these two data from the M3 linearization method gave better correlation values for S_{bpe}. Moreover, it was also beneficial to remove the 25, 40 and 60-day R_s data from M1 because, although the linear correlation value was satisfactory, the result was not suitable for providing accurate effluent COD (S_{bpe}) predictions (Table 6.2.4f).

The averages of kinetic constants obtained from the above three linear regression plots, with the removal of the above-mentioned R_s data, yielded good correlation coefficients and S_{bpe} predictions for both Monod and saturation kinetics. Therefore, the resulting average kinetic constants k_m of 2.465gCOD/ (gCOD.d) and K_s value of 0.607 gCOD/ *l* for Monod kinetics (Table 6.2.4e) and k_M of 1.951 gCOD/ (gCOD.d) and K_S of 9.109 gCOD/ *l* for saturation kinetics were accepted (Table 6.2.4g).

Graphs showing the percentage (of total influent) COD removed (by the four calibrated kinetic hydrolysis rates, as well as the experimental results) versus sludge age for the NDBEPR WAS is shown in Figure 6.2.4t. The unbiodegradable COD fraction of the sludge is also shown. The NDBEPR WAS was found to have a different unbiodegradable fraction ($f_{SL'up}$ = 0.54) from the ND systems (see Figure 6.2.3t, MLE 1 ($f_{SL'up}$ = 0.47) which is fed the same settled WW and MLE 2 ($f_{SL'up}$ = 0.62) fed raw WW).

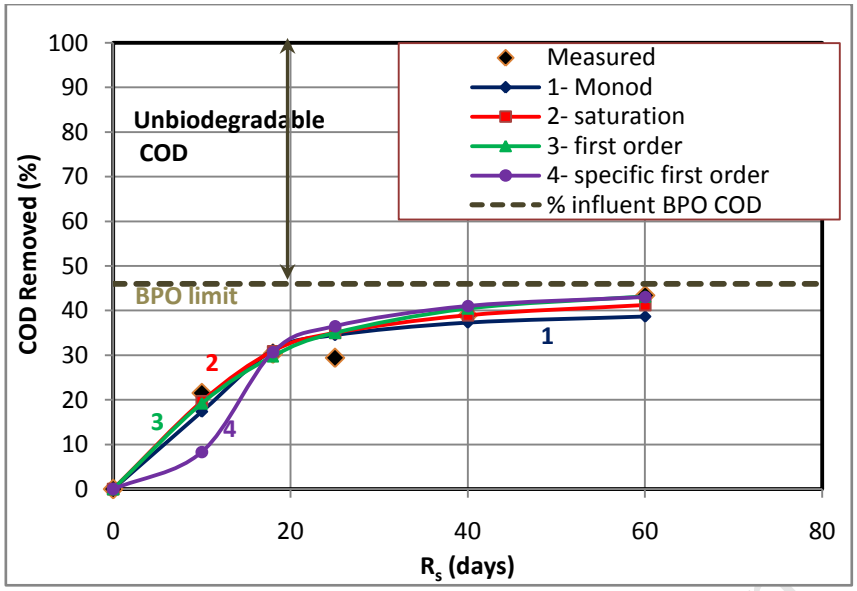

Figure 6.2.4t: *A comparison of the percentage COD removed for the AD of the sludge from the NDBEPR UCT system, measured and determined using obtained constants for the various kinetic formulations (1st order, specific 1st order, Monod and saturation).*

6.2.2.5. AD of Primary Sludge – Waste Activated Sludge (PS-WAS) Blend

Again the same procedure was applied to determine the hydrolysis kinetic constants of the PS-WAS blend. Tables 6.2.5a and 6.2.5b list the average respective influent and effluent experimental results that were obtained from the AD fed PS –WAS, blended at a ratio of 1.5:1 (by COD mass). The hydrolysis kinetic constants obtained from this experimental data over the various sludge ages and the calculation procedures applied (in Section 6.2.1) are presented below.

Table 6.2.5a: Primary Sludge-Waste Activated Sludge Blend Influent Experimental Data										
Retention Time (d)	10		18		25		40		60	
Digester Volume (*l*)	16		12		12		12		5	
Influent flow (*l*/d)	1.60		0.67		0.48		0.30		0.09	
Units	Conc. (g/*l*)	Flux (g/d)	Conc. (g/*l*)	Flux (g/d)	Conc. (g/*l*)	Flux (g/d)	Conc. (g/*l*)	Flux (g/d)	Conc. (g/*l*)	Flux (g/d)
Influent COD[3], S_{ti} (gCOD/*l*)	8.44	1.75	11.65	1.80	13.77	1.87	26.70	1.78	41.46	1.78
Influent COD[1], S_{upi} (gCOD/*l*)	3.12	0.65	4.31	0.67	5.09	0.69	9.88	0.66	15.34	0.66
Influent COD, S_{usi}[2] (gCOD/*l*)	0.04	0.01	0.06	0.01	0.07	0.01	0.13	0.01	0.20	0.01
Influent filtered COD, S_{tsi} (gCOD/*l*)	0.46	0.10	0.82	0.13	1.24	0.17	1.67	0.11	2.63	0.11
Influent COD, S_{bpi}[6] (gCOD/*l*)	4.82	1.00	6.46	1.00	7.36	1.00	15.02	1.00	23.30	1.00
Influent COD, S_{bsfi}[5] (gCOD/*l*)	0.21	0.04	0.46	0.07	0.90	0.12	0.83	0.06	1.62	0.07
Influent VFA, S_{bsai}[4] (gCOD/*l*)	0.15	0.03	0.17	0.03	0.20	0.03	0.31	0.02	0.44	0.02
Influent TKN[3] (gN/*l*)	0.44	0.09	0.54	0.08	0.63	0.09	1.13	0.08	1.46	0.06
Influent filtered TKN (gN/*l*)	0.04	0.01	0.03	0.01	0.03	0.00	0.06	0.00	0.05	0.00
Influent FSA (gN/*l*)	0.03	0.01	0.03	0.00	0.02	0.00	0.05	0.00	0.05	0.00
Influent Alk g/*l* as $CaCO_3$	0.40	0.08	0.38	0.06	0.35	0.05	0.77	0.05	1.04	0.04
Influent pH	6.20		6.43		5.93		6.07		5.83	
Influent TP[3] (gP/*l*)	0.15	0.03	0.28	0.04	0.34	0.05	0.43	0.03	0.60	0.03
Influent filtered TP (gP/*l*)	0.02	0.00	0.03	0.01	0.03	0.00	0.04	0.00	0.03	0.00
Influent OP (gP/*l*)	0.02	0.00	0.02	0.00	0.02	0.00	0.02	0.00	0.03	0.00
Influent TSS (gTSS/*l*)	7.05	1.46	9.70	1.50	9.70	1.32	19.24	1.28	28.58	1.23
Influent VSS (gVSS/*l*)	5.60	1.16	7.82	1.21	7.82	1.06	15.45	1.03	23.69	1.02
Influent ISS (gISS/*l*)	1.45	0.30	1.88	0.29	1.88	0.26	3.79	0.25	4.90	0.21

[1] S_{upi} is the unbiodegradable particulate COD calculated using best-determined $f_{SL'up}$ = 0.37, obtained for good coefficients of variation and correlation coefficients as shown in the section below.

[2] S_{usi} is the unbiodegradable soluble COD measured from the filtered effluent from 60d sludge age AD.

[3] Unfiltered samples.

[4] S_{bsai} is the COD in short chain fatty acids that is measured in the influent using the 5-point titration method.

[5] S_{bsfi} is the fermentable biodegradable soluble influent COD calculated from the measured filtered influent COD (S_{tsi}) – S_{usi} – S_{bsai}.

[6] S_{bpi} is the biodegradable particulate influent COD which is calculated by the total influent COD (S_{ti}) – S_{tsi} – S_{upi}.

Table 6.2.5b: Primary Sludge-Waste Activated Sludge Blend Effluent Experimental Data										
Retention Time (d)	10		18		25		40		60	
Effluent flow (*l*/d)	1.60		0.67		0.48		0.30		0.09	
Units	Conc. (g/*l*)	Flux (g/d)	Conc. (g/*l*)	Flux (g/d)	Conc. (g/*l*)	Flux (g/d)	Conc. (g/*l*)	Flux (g/d)	Conc. (g/*l*)	Flux (g/d)
Effluent COD[1], S_{te} (gCOD/*l*)	5.97	1.24	6.91	1.07	6.87	0.93	12.42	0.83	16.94	0.73
Effluent COD, S_{upe} [5] (gCOD/*l*)	3.12	0.65	4.31	0.67	5.09	0.69	9.88	0.66	15.34	0.66
Effluent COD, S_{use}[2] (gCOD/*l*)	0.04	0.01	0.06	0.01	0.07	0.01	0.13	0.01	0.20	0.01
Effluent filtered COD, S_{tse} (gCOD/*l*)	0.18	0.04	0.20	0.03	0.21	0.03	0.15	0.01	0.20	0.01
Effluent COD, S_{bpe}[6] (gCOD/*l*)	2.67	0.56	2.40	0.37	1.57	0.21	2.39	0.15	1.40	0.06
Effluent COD, S_{bsfe}[4] (gCOD/*l*)	0.14	0.03	0.14	0.02	0.14	0.02	0.02	0.00	0.00	0.00
Effluent VFA, S_{bsae}[3] (gCOD/*l*)	0.00	0.00	0.03	0.00	0.00	0.00	0.03	0.00	0.07	0.00
Effluent TKN[1] (gN/*l*)	0.42	0.09	0.47	0.07	0.51	0.07	0.92	0.06	1.30	0.06
Effluent filtered TKN (gN/*l*)	0.04	0.01	0.09	0.01	0.21	0.03	0.41	0.03	0.55	0.02
Effluent FSA (gN/*l*)	0.04	0.01	0.09	0.01	0.16	0.02	0.39	0.03	0.53	0.02
Effluent TP[1] (mgP/*l*)	0.16	0.03	0.28	0.04	0.33	0.04	0.37	0.02	0.51	0.02
Effluent filtered TP (gP/*l*)	0.02	0.00	0.04	0.01	0.06	0.01	0.12	0.01	0.18	0.01
Effluent OP (gP/*l*)	0.02	0.00	0.04	0.01	0.05	0.01	0.11	0.01	0.16	0.01
Effluent TSS	5.72	1.19	7.82	1.21	7.73	1.05	10.78	0.72	14.86	0.64
Effluent VSS	4.03	0.84	6.11	0.95	5.70	0.77	7.39	0.49	10.60	0.45
Effluent ISS	1.69	0.35	1.71	0.26	2.03	0.28	3.38	0.23	4.26	0.18
Effluent Alk mg/*l* as $CaCO_3$	1.34	0.28	1.45	0.22	2.05	0.28	2.46	0.16	2.54	0.11
Measured digester pH	7.15		7.29		7.27		7.34		7.26	
COD removed (gCOD/*l*)	2.47	0.51	4.74	0.73	6.89	0.94	14.28	0.95	24.52	1.05
Gas production (litres/d)	3.77		1.87		1.11		0.89		-	
Gas prod. (l gas/*l* influent)	3.15		2.79		2.21		2.96			
Gas composition : CH_4 fraction	0.46		0.46		0.46		0.46			
Gas composition: CO_2 fraction	0.27		0.27		0.27		0.27			
Volume of CH_4 (litres)	1.45		1.28		1.02		1.36			
Volume of CO_2 (litres)	0.85		0.75		0.60		0.80			
COD of CH_4 (gCOD/*l* feed)	3.17		5.03		5.35		11.93		18.53	
p_{CO2} (atm.)	0.37		0.37		0.37		0.37			
CT dissolved (mmol/*l*)	9.58		9.58		9.58		9.58			
H_2CO_3 diss. (mg/*l*)	958.41		958.41		958.41		958.41			
Moles of CO_2/*l* feed	0.03		0.03		0.02		0.03			
Moles of CH_4/*l* feed	0.06		0.05		0.04		0.06			
COD balance (%)	108.28		102.54		88.83		91.19		85.55	
Nitrogen balance (%)	96.84		85.81		80.94		81.31		88.81	
Phosphorous balance (%)	107.01		101.62		96.96		86.35		85.25	
f_{cv} (gCOD/gVSS)	1.48		1.13		1.21		1.68		1.60	
$f_{SL'up}$ (MLE 1 WAS)	0.37		0.37		0.37		0.37		0.37	

[1] Unfiltered sample

[2] S_{use} is the unbiodegradable soluble COD measured in filtered effluent from the 60d sludge age AD.

[3] S_{bsae} is the COD in short chain fatty acids that is measured in the effluent using the 5-point titration method.

[4] S_{bsfe} is the fermentable biodegradable soluble COD calculated from the measured filtered effluent COD (S_{tse}) – S_{use} – S_{bsae}.

[5] S_{upe} is the unbiodegradable particulate effluent COD which equals the S_{upi} value from Table 6.2.5a.

[6] S_{bpe} is the biodegradable particulate effluent COD which equals the total effluent COD (S_{te}) – S_{tse} – S_{upe}.

The Selection of a Suitable $f_{SL'up}$ Value

The influence of $f_{SL'up}$ on the results from hydrolysis rate equations of PS-MLE 1 WAS blend are shown below by plotting the coefficients of variation for first order and first order specific hydrolysis kinetic equations versus increasing $f_{SL'up}$ fractions (shown in Figure 6.2.5a) and correlation coefficients (R^2) for Monod and saturation hydrolysis kinetic equations versus the same range of $f_{SL'up}$ fractions (in Figures 6.2.5b and 6.2.5c respectively). This is done in order to find the most suitable $f_{SL'up}$ fraction that gives the best correlation coefficients when applying the various hydrolysis kinetic equations to as accurately as possible predict the effluent COD from the AD of PS-MLE 1 WAS blend. The correlation coefficients of the Monod and saturation kinetic equations are shown for the Curve Expert program and the three linearization methods of Lineweaver-Burke (M1) and (M1*), double reciprocal (M2) and Eadie-Hofstee (M3) and (M3*). The M1, M2 and M3 (without asterisks) were obtained with all 5 R_s data (10, 18, 25, 40 and 60 days). M1* and M3* are for the Lineweaver-Burke and the Eadie-Hofstee both with the 40 and 60 day R_s data omitted in linearising both the Monod and saturation kinetics. The omission of these R_s data sets from M1 and M3 was done in order to improve the R^2 values for these linearisation methods. The curve fitting results are evaluated in greater detail below after first selecting the best $f_{SL'up}$ value.

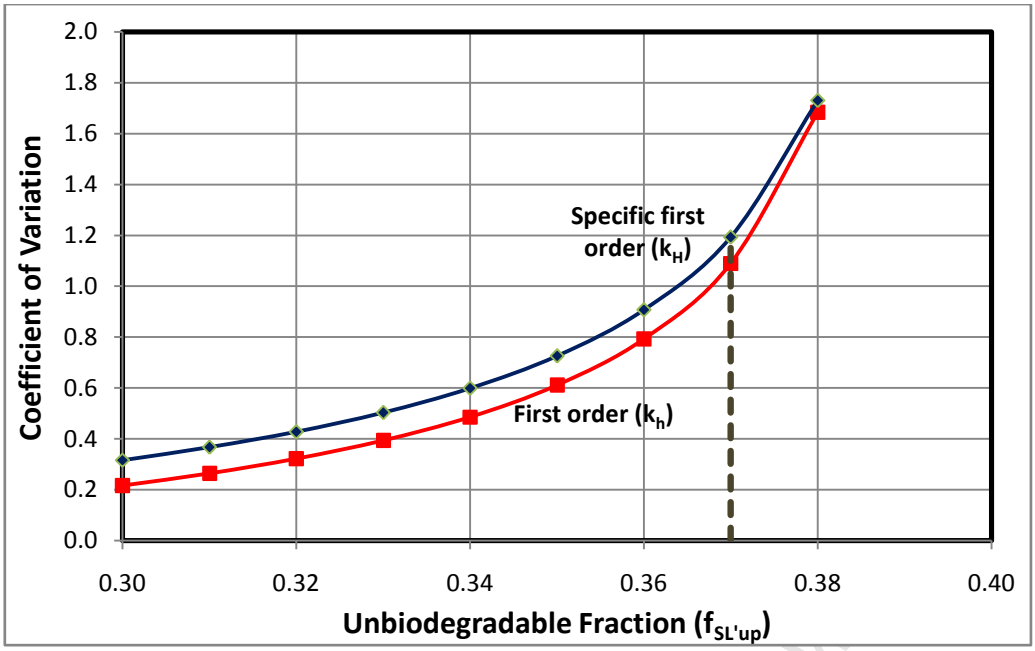

Figure 6.2.5a: *The change in the coefficient of variation of the 1st order and 1st order specific hydrolysis equations kinetic constants versus unbiodegradable particulate COD fraction ($f_{SL'up}$) of PS – MLE 1 WAS blend without R_s =25d data (see Table 6.2.5c).*

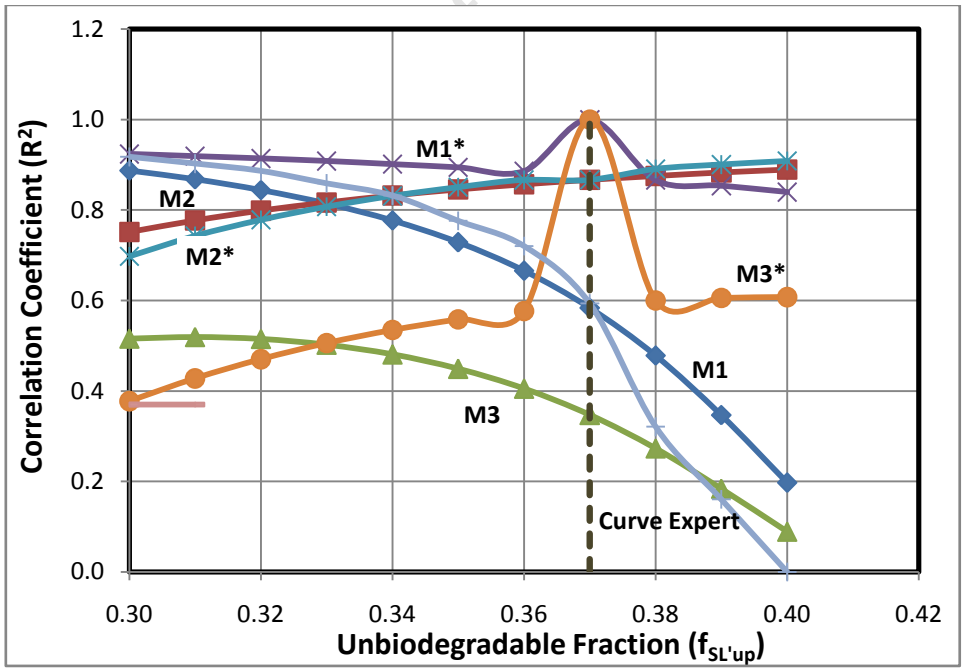

Figure 6.2.5b: *The regression correlation coefficient (R^2) for the Curve Expert program, Lineweaver-Burke (M1), double reciprocal (M2) and Eadie-Hofstee (M3) linearization methods of the Monod hydrolysis kinetics versus unbiodegradable particulate COD fraction ($f_{SL'up}$) of the PS – MLE 1 WAS blend AD including all (10, 18, 25, 40 and 60 day R_s) data.*

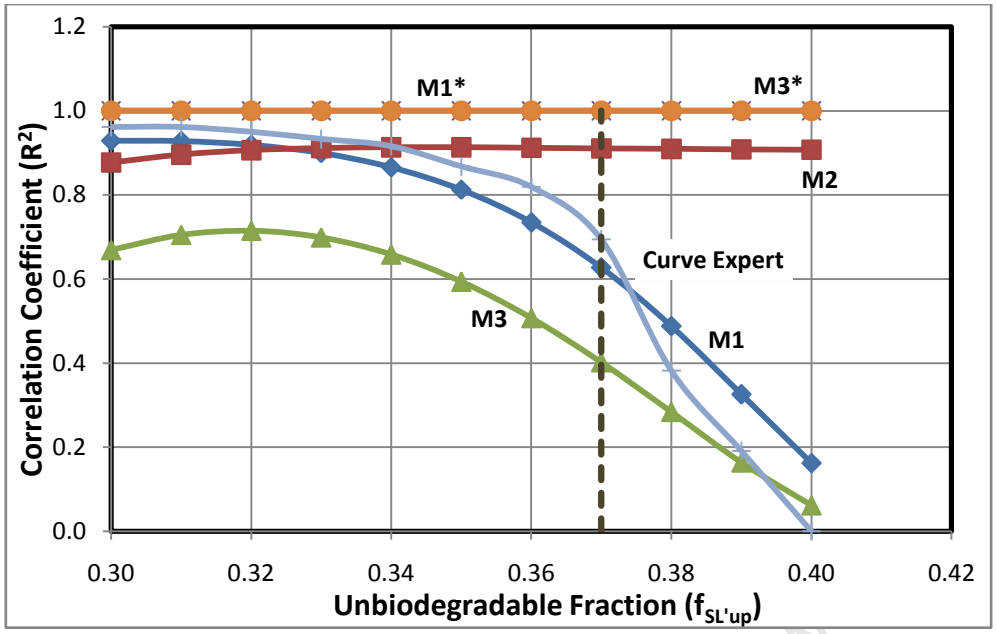

Figure 6.2.5c: *The regression correlation coefficient (R^2) for the Curve Expert program, Lineweaver-Burke (M1), double reciprocal (M2) and Eadie-Hofstee (M3) linearization methods of the saturation hydrolysis kinetics versus unbiodegradable particulate COD fraction ($f_{SL'up}$) of the PS – MLE 1 WAS blend AD including all (10, 18, 25, 40 and 60 day R_s) data.*

As the case with all the other sludges, Figure 6.2.5a shows a gradual increase in the coefficient of variation (C_{var}) with increasing unbiodegradable particulate fraction (from 0.31 to 0.37). Figures 6.2.5b and 6.2.5c show that Monod and saturation kinetics exhibit maximum R^2 values at an $f_{SL'up}$ value of around 0.37. This value is also close to the value that was determined from the AD of the PS-WAS blend at the very long sludge age of 60 days (0.40) and to that obtained from the earlier $f_{SL'up}$ of the PS and MLE 1 WAS individually (0.36). Therefore, this value (0.37) was selected as the best compromise $f_{SL'up}$ value of the PS-WAS blend to be applied for the determination of the relevant kinetic constants.

First Order Kinetics

The experimentally measured influent and effluent COD concentrations for the AD of the PS-WAS blend at steady state (Table 6.2.5a and 6.2.5b) and above-mentioned calculations procedure (in Section 6.2.1) were applied to determine the volumetric hydrolysis rates (r_{HYD}), the residual biodegradable COD concentrations (S_{bp}) and the first order and specific first order kinetic rate constants (k_h and k_H). These rates are listed in Table 6.2.5c below and their variations with sludge age are plotted in Figures 6.2.5d to 6.2.5g. The k_h and k_H graphs show that the 40d R_s data do not conform to the trend of the other sludge ages**.** Therefore, this data is omitted in establishing the linear relationship (from Equation 6.21c and d) of k_h and k_H with sludge age. This yields $k_h = 0.0154 \cdot R_s - 0.165$ (R^2 = 0.981) for first order hydrolysis kinetics and $k_H = 0.4296 \cdot R_s - 4.3307$ (R^2 = 0.956) for specific first order hydrolysis kinetics.

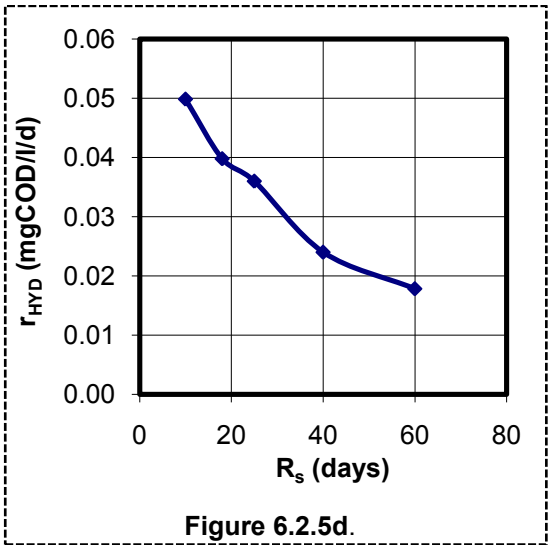

Figure 6.2.5d.

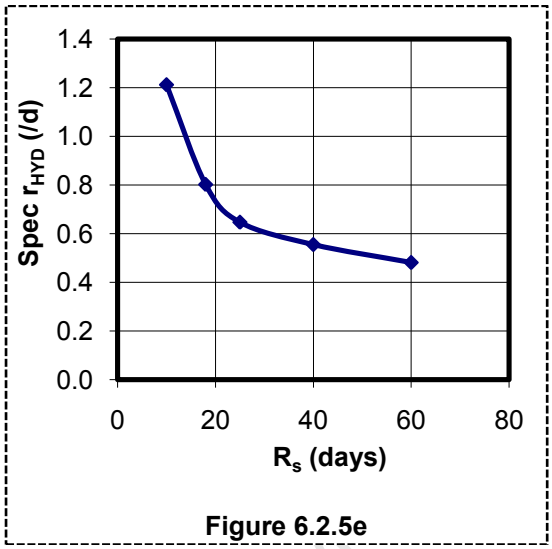

Figure 6.2.5e

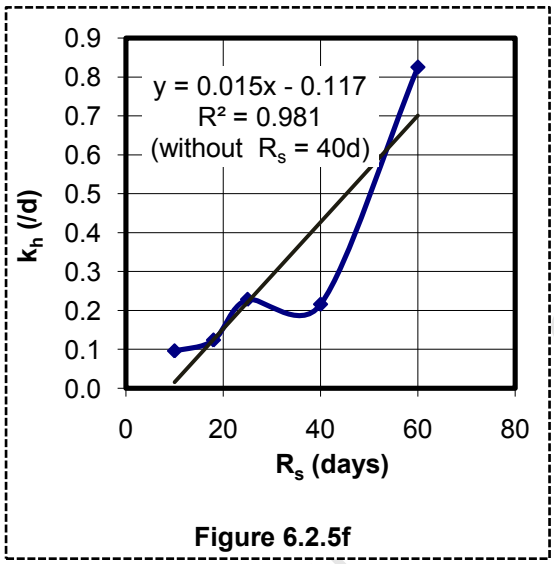

Figure 6.2.5f

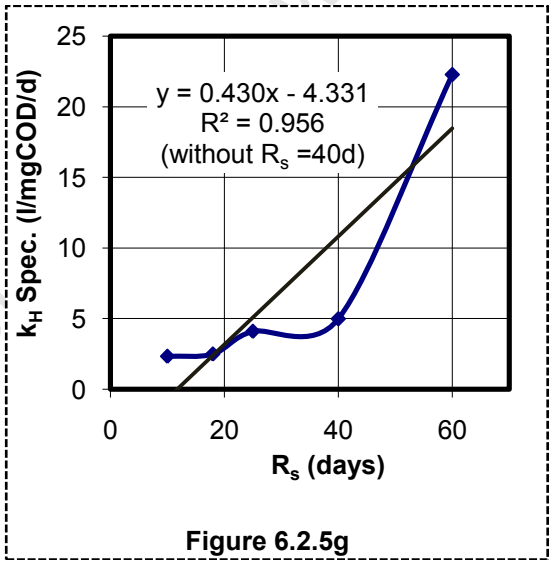

Figure 6.2.5g

Figures 6.2.5d, e, f and g: *Volumetric hydrolysis rates (r_{HYD}) (d), specific volumetric hydrolysis rate (r_{HYD}/Z_{AD}) (e), first order kinetic constant (k_h) (f) and specific first order kinetic constant (k_H) (g) versus sludge age (R_s) ranging from 10, 18, 25, 40 and 60 days, for AD of PS-WAS blend. Linear Equation and correlation coefficient (R^2) is given for results without R_s = 40d data*

Table 6.2.5c: Summary of Results for First Order Kinetics in the AD of PS-WAS for $f_{SL'up}$ = 0.37						
R_s (d)	r_{HYD} (g/*l*/d)	Z_{AD} (g/*l*)	S_{bpe} (g/*l*)	k_h (/d)	Spec r_{HYD} (gS_{bp}/gZ_{AD}/d	k_H (*l*/gZ_{AD}/d)
10	0.050	0.041	0.519	0.096	1.212	2.336
18	0.040	0.050	0.321	0.124	0.802	2.500
25	0.036	0.056	0.158	0.228	0.647	4.107
40	0.024	0.043	0.111	0.216	0.555	4.995
60	0.018	0.037	0.022	0.825	0.482	22.283
Where * means that the values are for all R_s data		Mean		0.298*	-	7.244*
		Standard deviation		0.300*	-	8.480*
		Coefficient of variation		1.008*	-	1.171*
$k_h = c_{kh} + m_{kh} \times R_s$; c_{kh} = -0.1165; m_{kh} = 0.0154; R^2 = 0.981 (excluding R_s = 40d) $k_H = c_{kH} + m_{kH} \times R_s$; c_{kH} = -4.3307; m_{kH} =0.4296; R^2 = 0.956 (excluding R_s = 40d)						

Monod and Saturation Kinetics of PS-WAS

The Figures 6.2.5h to 6.2.5k below show the specific hydrolysis rates (r_{HYD}/Z_{AD}) versus the residual BPO (S_{bp}) for the Monod equation and versus the residual BPO per acidogenic biomass (S_{bp} / Z_{AD}) for the saturation kinetics equation. The specific hydrolysis rate obtained using the values in Table 6.2.5c, which are directly calculated from experimental results, are compared with those calculated from the Monod and saturation kientic constants determined with the 3 linearisation methods (Figures 6.2.5h and i) and the Curve Expert program (Figures 6.2.5j and k). It can be seen from these plots that the measured data do not conform to the form of the Monod and saturation equations, which is the reason for the low correlation coefficient values (Figure 6.2.5b and c). It can be seen that the measured data conform better to saturation kinetics (Figure 6.2.5k) than the Monod kinetics (Figure 6.2.5j), especially at the longer sludge ages of 25d to 60d. Thus for this sludge the method applied in selecting the best kinetic constants from the measured data were more appropriate to the saturation kinetic formulation than the Monod. Because of this it would be more favorable to use the saturation kinetics in modelling the hydrolysis of this sludge, in order to ensure that resonable predictions are made for the longer sludge ages (25 to 60 days). The methods used in selecting the kinetic

constants k_m = 5.153 and K_s = 1.710 for Monod and k_M = 1.919 and K_S = 7.723 for saturation kinetics are discussed further below (see Tables 6.2.5 d, e, f and g).

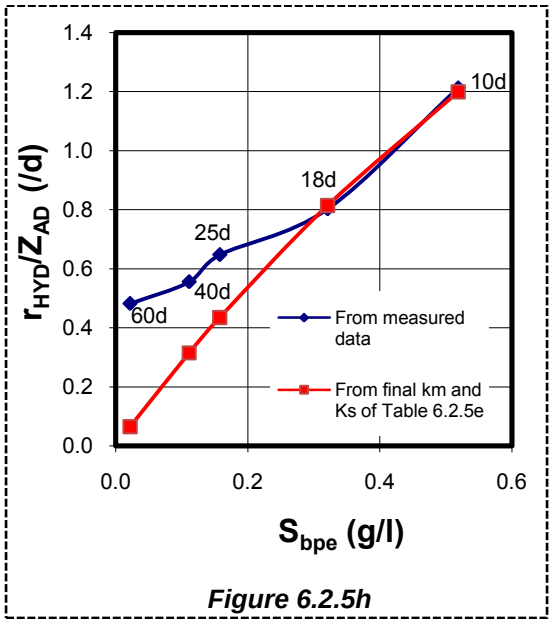

Figure 6.2.5h

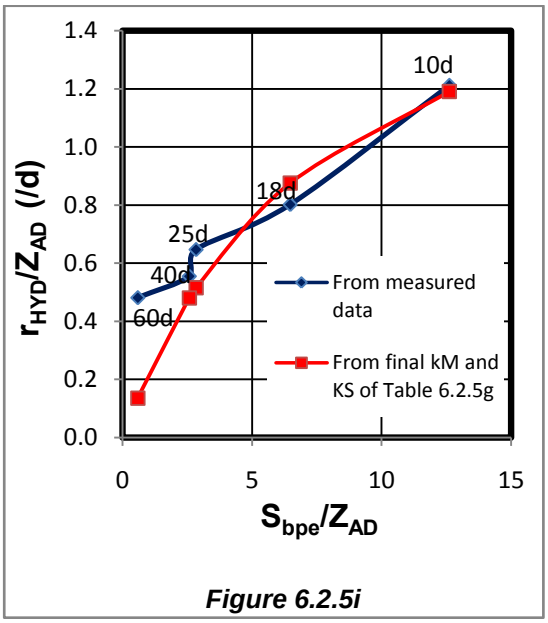

Figure 6.2.5i

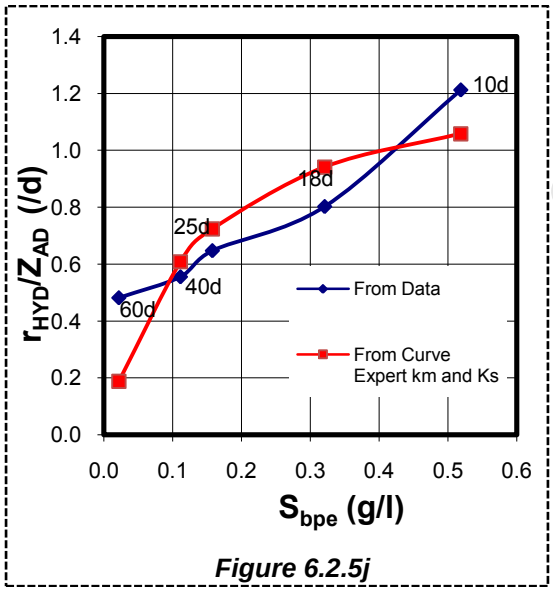

Figure 6.2.5j

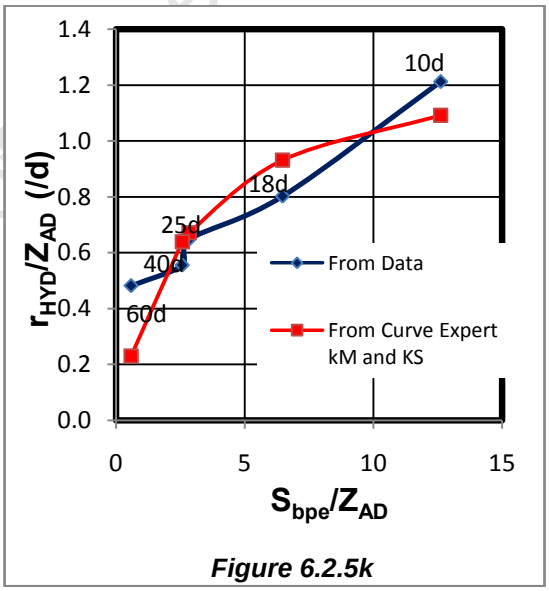

Figure 6.2.5k

Figures 6.2.5h i, j and k: *Hydrolysis kinetics formulation curves, plotted using experimental data and calculated from kinetic constants acquired from the three linearization methods, for (h) Monod (see Table 6.2.5d column 7 and Table 6.2.5e; k_m =5.153 and K_s =1.710) and (i) saturation (see Table 6.2.5d column 7 and Table 6.2.5e; k_M = 1.915 and K_S =7.723) equations and using the Curve Expert programme (j) for Monod and (k) for saturation kinetics*

The r_{HYD}, S_{bp} and Z_{AD} values determined from experimental results (Table 6.2.5c) for the AD of the PS-WAS blend were used in the three linearization methods of the Monod and saturation kinetic equations to determine the average kinetic constant values of the 3 (i.e. k_m and K_s for Monod and k_M and K_S for saturation kinetics). The results experimentally measured and regression best fit results for the Monod and saturation kinetic equation with $f_{SL'up}$ = 0.37 are shown for (i) Lineweaver-Burke in Figures 6.25j and 6.25n, (ii) double reciprocal in Figures 6.25k and 6.25o and (iii) Eadie-Hofstee in Figure 6.25l and 6.25p. The R^2 values together with the slope and y-coefficient used to calculate the kinetic constants in the different linearizations are presented in Tables 6.2.5d (Monod kinetics) and 6.2.5e (saturation kinetics).

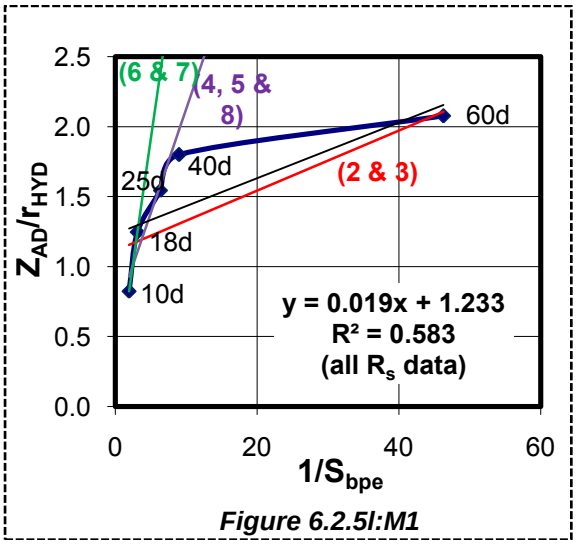

Figure 6.2.5l:M1

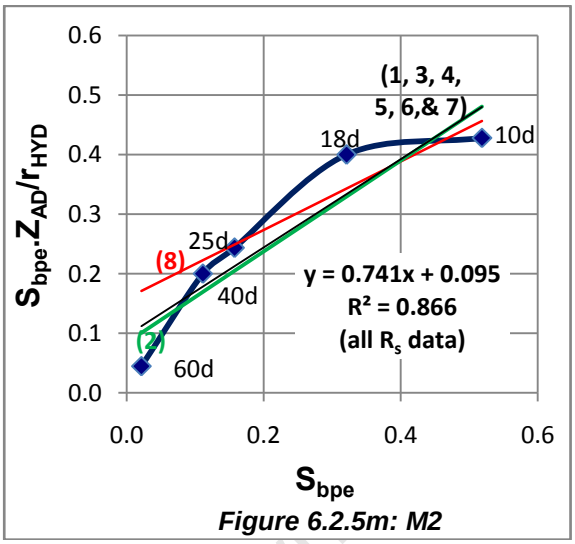

Figure 6.2.5m: M2

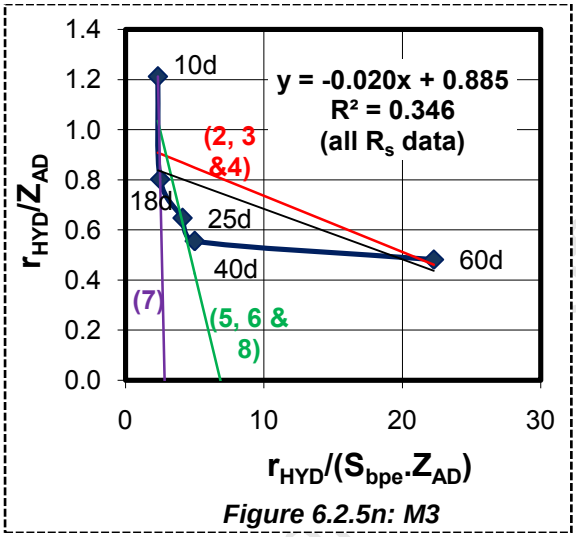

Figure 6.2.5n: M3

Key for Figures 6.2.5 l, m and n	
Column No. in Table 6.2.5d	**Data used or omitted (for R_s off) in determining the k_m and K_s values using the 3 linearization methods (M1, M2 and M3)**
1	Only M2
2	M1, M2 & M3 (40d off all)
3	M1 (40d off), M2, M3 (40d off)
4	M1 (40 & 60d off), M2, M3 (40d off)
5	M1 (40 & 60d off), M2, M3 (40 & 60d off)
6	M1 (25, 40 & 60d off), M2, M3 (40 & 60d off)
7	M1 (25, 40 & 60d off), M2, M3 (25, 40 & 60d off)
8	M1 (40 & 60d off), M2 (60d off), M3 (40 & 60d off)

Figures 6.2.5l, m and n: *The linearization of Monod kinetics for hydrolysis of PS – MLE 1 WAS with all five R_s data (10 to 60) for: (j) Lineweaver–Burke (M1), (k) double reciprocal (M2) and (l) Eadie–Hofstee (M3). The R^2 values are for all 5 R_s data included - dark (black) lines. Numbers refer to column numbers in Table 6.2.5d, e.g. 3 refers to column 3, which lists the average k_m and K_s values obtained from line 3 in Figure 6.2.5l: M1 with R_s = 40d omitted, line 3 in Figure 6.2.1m:M2 with all R_s data and line 3 in Figure 6.2.1n:M3 with R_s = 40d omitted*

Table 6.2.5d: Predicted S_{bpe} in gCOD/l for the Determination of the Best Monod Kinetic Constants, for the AD of PS-WAS blend, from the Three Linearization Methods										
	Data used or omitted (for R_s off) in determining the average k_m and K_s values from the 3 linearization methods									
	1	2	3	4	5	6	7	8		
R_s	Only M2	M1, M2 & M3 (40d off all)	M1 (40d off), M2, M3 (40d off)	M1 (40 & 60d off), M2, M3 (40d off)	M1 (40 & 60d off), M2, M3 (40 & 60d off)	M1 (25, 40 & 60d off), M2, M3 (40 & 60d off)	M1 (25, 40 & 60d off), M2, M3 (25, 40 & 60d off)	M1 (40 & 60d off), M2 (60d off), M3 (40 & 60d off)	Curve Expert	Target S_{bpe}
10	1.60	-0.49	-0.59	2.27	0.95	0.57	0.55	0.79	2.09	0.52
18	0.22	0.23	0.24	0.26	0.27	0.34	0.34	0.28	0.24	0.32
25	0.15	0.12	0.13	0.17	0.19	0.27	0.28	0.20	0.15	0.16
40	0.10	0.07	0.08	0.11	0.13	0.21	0.22	0.14	0.10	0.11
60	0.08	0.06	0.06	0.09	0.11	0.18	0.19	0.12	0.08	0.02
							Selected			
k_m	1.39	1.24	1.10	1.33	1.53	3.69	**5.15**	1.67	1.33	
K_s	0.15	0.12	0.07	0.14	0.22	1.12	**1.71**	0.27	0.13	
R^2	0.86	0.72	0.71	0.75	0.78	0.82	**0.96**	0.78	0.59	

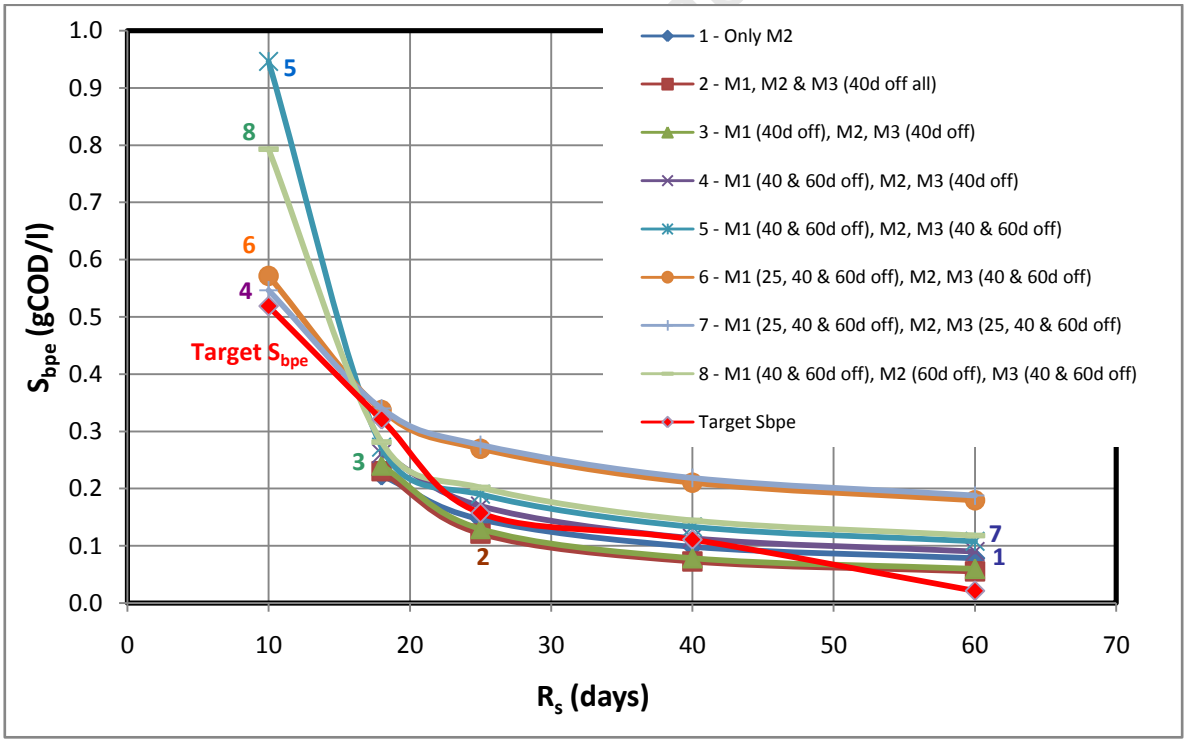

Figure 6.2.5o: *Comparison of tagret S_{bpe} values (calculated from measured values in Table 6.2.5b) with those predicted by different combinations of selected R_s data in the three linearization methods for the determination of the best k_m and K_s values for modelling hydrolysis with the Monod kinetics. Numbers refer to column numbers in Table 6.2.5d.*

The procedure to select the best Monod kinetic constants for the PS-WAS blend, from the three linearization methods is the same as that applied above for the other sludge types. Table 6.2.5d and Figure 6.2.5o show whether or not the R^2 values are satisfactory ($R^2 \geq 0.8$) and how well the S_{bpe} concentrations are predicted by the determined kinetic constants compared with the experimentally measured results. Firstly, the effect of removing the 40d R_s from all 3 linearization methods was checked. This did not bring about significant improvements in the R^2 values and S_{bpe} predictions. Therefore the 60d R_s was also removed when linearizing with M2, since this data appeared (from Figures 2.3.5l and n) to be forcing a change in gradient of the lines for M1 and M3. This resulted in improved S_{bpe} predictions and R^2 values, but the 10d R_s S_{bpe} was still highly over-predicted. The removal of the 25d R_s from M1 and M2 significantly improved this 10d S_{bp} prediction, but at the same time resulted in higher S_{bpe} predictions for longer R_s of 25, 40 and 60d. The final k_m and K_s values resulting from this data selection are listed in Table 6.2.5e below.

Table 6.2.5e: Monod Kinetics (Hydrolysis of PS-WAS)

Linearization	Lineweaver-Burke (M1)	Double reciprocal (M2)	Eadie-Hofstee (M3)	Average	Curve Expert	Notes
Slope	0.020	0.742	-0.020			AD sludge ages of 10, 18, 25, 40 and 60 days are used in all methods.
Y-Intercept	1.233	0.096	0.885			
k_m	0.811	1.349	0.885		**1.326**	
K_s	0.016	0.129	0.020		**0.131**	
R^2	0.584	0.867	0.347		0.593	
Slope*	0.355	0.742	-2.501			25, 40 and 60 day R_s are omitted in M1 and in M3 to improve R^2.
Y-Intercept*	0.142	0.096	7.055			
k_m*	7.055	1.349	7.055	**5.153**		
K_s*	2.501	0.129	2.501	**1.710**		
R^2*	1.000	0.880	1.000	0.960		

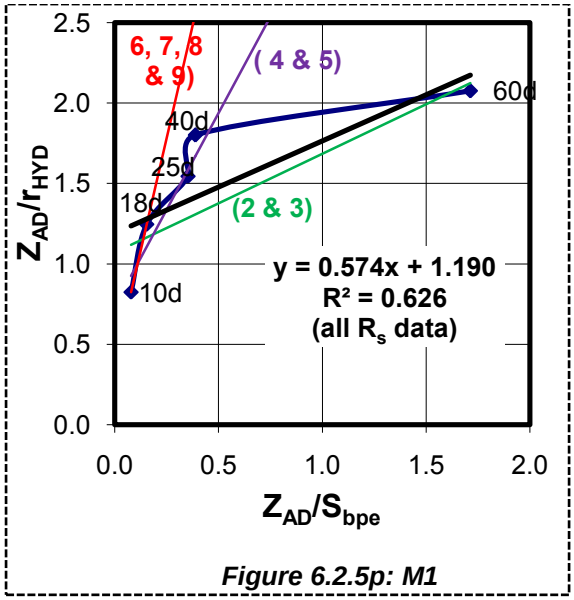

Figure 6.2.5p: M1

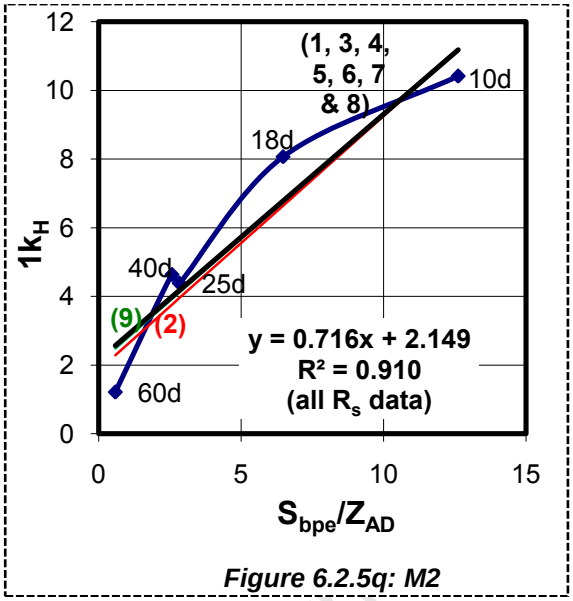

Figure 6.2.5q: M2

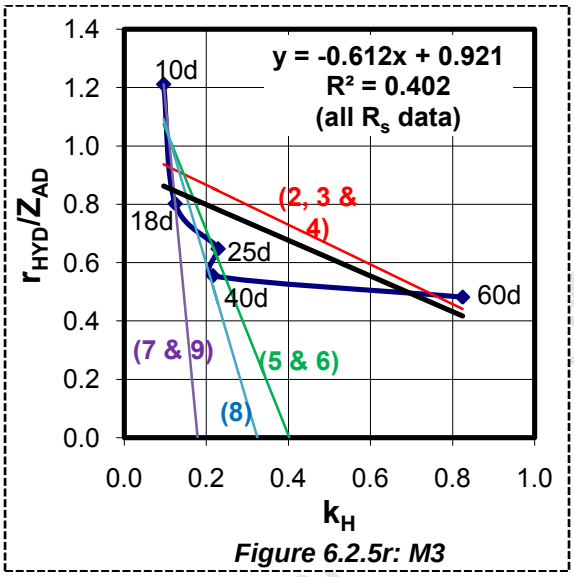

Figure 6.2.5r: M3

Key for Figures 6.2.5p, q and r	
Column No. in Table 6.2.5f	**Data used or omitted (for R_s off) in determining the k_M and K_S values using the 3 linearization methods (M1, M2 and M3)**
1	Only M2
2	M1, M2 & M3 (40d off all)
3	M1 (40d off), M2, M3 (40d off)
4	M1 (40 & 60d off), M2, M3 (40d off)
5	M1 (40 & 60d off), M2, M3 (40 & 60d off)
6	M1 (25, 40 & 60d off), M2, M3 (40 & 60d off)
7	M1 (25, 40 & 60d off), M2, M3 (25, 40 & 60d off)
8	M1 (25, 40 & 60d off), M2, M3 (18, 25 & 60d off)
9	M1 (25, 40 & 60d off), M2 (25d off), M3 (18, 25 & 60d off)

Figures 6.2.5p, q and r: *The linearization of saturation kinetics for hydrolysis of PS – MLE 1 WAS at all five R_s (10 to 60) using various methods in the order of: (p) Lineweaver–Burke (M1), (q) double reciprocal (M2) and (r) Eadie–Hofstee (M3). The R^2 values for all 5 R_s data included- dark (black) lines. Numbers refer to column numbers in Table 6.2.5f, e.g. 4 refers to column 4, which lists the average k_M and K_S values obtained from line 4 in Figure 6.2.5p: M1 with R_s = 40 and 60d omitted, line 4 in Figure 6.2.1q:M2 with all R_s data and line 4 in Figure 6.2.1r: M3 with R_s = 40d omitted.*

The determination of the best kinetic constants for saturation kinetics was done the same way as that for Monod kinetics above. The contribution of each R_s with data used in each of the 3 linearization methods was checked to see which combination gave the best R^2 values and S_{bpe} predictions. The results of this evaluation process are given in Table 6.2.5f and shown in Figure 6.2.5s below.

Table 6.2.5f: Predicted S_{bpe} in gCOD/*l* for the Determination of the Best Saturation Kinetic Constants, for PS-WAS blend AD, from the Three Linearization Methods

	Data used or omitted (for R_s off) in determining the average k_M and K_S values from the 3 linearization methods										
	1	**2**	**3**	**4**	**5**	**6**	**7**	**8**	**9**		
R_s	Only M2	M1, M2 & M3 (40d off all)	M1 (40d off), M2, M3 (40d off)	M1 (40 & 60d off), M2, M3 (40d off)	M1 (40 & 60d off), M2, M3 (40 & 60d off)	M1 (25, 40 & 60d off), M2, M3 (40 & 60d off)	M1 (25, 40 & 60d off), M2, M3 (25, 40 & 60d off)	M1 (25, 40 & 60d off), M2, M3 (18, 25 & 60d off)	M1 (25, 40 & 60d off), M2 (25d off), M3 (18, 25 & 60d off)	**Curve Expert**	**Target S_{bpe}**
10	0.66	2.67	1.91	0.86	0.69	0.57	0.54	0.54	0.55	0.77	0.52
18	0.25	0.25	0.26	0.26	0.27	0.31	0.32	0.30	0.30	0.25	0.32
25	0.17	0.14	0.15	0.17	0.18	0.22	0.24	0.21	0.22	0.16	0.16
40	0.10	0.07	0.08	0.09	0.10	0.14	0.16	0.13	0.14	0.09	0.11
60	0.06	0.04	0.05	0.06	0.07	0.09	0.11	0.09	0.09	0.06	0.02
								Selected			
k_M	1.431	1.143	1.159	1.292	1.419	1.854	2.271	**1.919**	1.974	1.334	
K_S	3.370	1.623	1.801	2.690	3.609	7.625	11.558	**7.723**	8.420	2.798	
R^2	0.91	0.79	0.79	0.80	0.83	0.87	0.97	**0.97**	0.97	0.69	

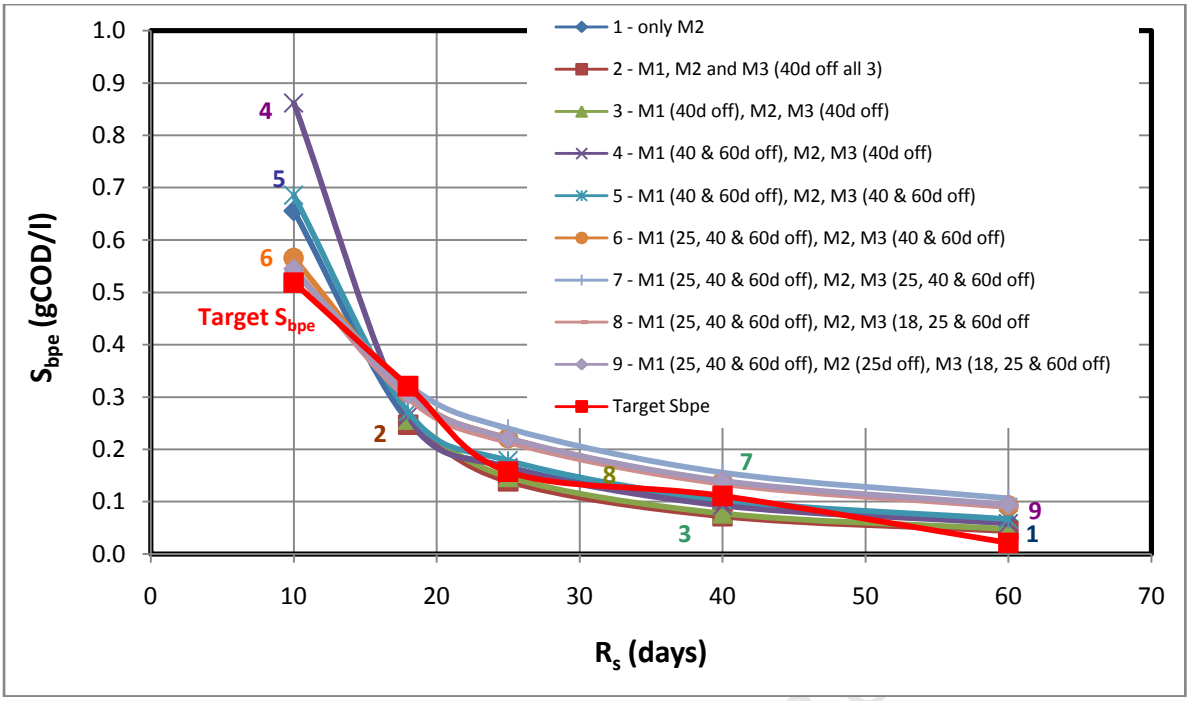

Figure 6.2.5s: *Comparison of tagret S_{bpe} values (calculated from measured values in Table 6.2.1b) with those predicted by the average k_M and K_S constants determined with different combinations of selected R_s data in the three linearization methods for the determination of the best k_M and K_S values for modelling hydrolysis of PS-WAS blend with the saturation kinetics. Numbers refer to the column numbers in Table 6.2.5f*

Table 6.2.5g: Saturation Kinetics (Hydrolysis of PS-WAS)						
Linearization	**Lineweaver-Burke (M1)**	**Double reciprocal (M2)**	**Eadie-Hofstee (M3)**	**Average**	**Curve Expert**	**Notes**
Slope	0.574	0.716	-0.612			AD sludge ages of 10, 18, 25, 40 and 60 days are used in all methods.
Y-Intercept	1.190	2.149	0.922			
k_M	0.840	1.396	0.922		**1.334**	
K_S	0.483	3.001	0.612		**2.798**	
R^2	0.627	0.911	0.402		0.694	
Slope*	5.600	0.716	-5.481			25, 40 and 60 day R_s are omitted in M1 and 18, 25 and 60 day R_s are omitted in M3 to improve R^2.
Y-Intercept*	0.381	2.149	1.738			
k_M*	2.622	1.396	1.738	**1.919**		
K_S*	14.687	3.001	5.481	**7.723**		
R^2*	1.000	0.911	1.000	0.970		

As in the case with the AD of PS by itself, the double reciprocal method (M2) gives the best correlation with all the R_s data included (R^2 = 0.867 for Monod kinetics and R^2 = 0.911 for saturation kinetics, see column 1 of Tables 6.2.5d and f). Linearization

by the other two methods (M1 and M3) shows poor correlation because the 40 and 60-day R_s data deviate from the trend of the other data. Removing these two R_s data did not improve the correlation (columns 4 and 5 in Tables 6.2.5e and f) for both methods. So the 25-day data was also omitted from the M1 and M3 linearization methods, which gave good correlation values for S_{bpe} (columns 6 to 9 in Table 6.2.5e and f).

The average kinetic constants obtained from the three linearization methods with the removal of the 25, 40 and 60d R_s data yielded a k_m of 5.153gCOD/(gCOD.d) and K_s value of 1.710 for Monod kinetics (Table 6.2.5e) and a k_M of 1.919gCOD/(gCOD.d) and K_S of 7.723gCOD/*l* for saturation kinetics (Table 6.2.5g). These kinetic constants predict the effluent S_{bpe} well and hence also the hydrolysis rate of the AD of PS-WAS blend.

6.2.3 A Summary of the Constants Obtained for the Steady State AD Model Hydrolysis Kinetics

The Monod and saturation kinetic constants, calibrated from the measured experimental AD data for the various primary and secondary municipal sludge types are listed in Table 6.2.6a.

Table 6.2.6a: Comparison of Experimentally Determined Monod and Saturation Kinetic Constants

	Monod kinetics		saturation kinetics	
AD Feed Source	**k_m**	**K_s**	**k_M**	**K_S**
PS	4.3	1.523	1.796	7.962
PS-MLE1	5.153	1.71	1.919	7.723
MLE 1	2.094	0.408	1.603	5.387
MLE 2	2.482	0.626	1.524	4.838
NDBEPR	2.465	0.607	1.951	9.109
PS (1)	3.34	6.76	5.27	7.98
PS (2)	2.004	0.355	2.047	0.263
PS (3)	0.243	640	11.2	13

Where:
PS (1) is from Sötemann *et al.* (2005a), determined using data from Izzett *et al.* (1992).
PS (2) is from Sötemann *et al.* (2005a), determined using data from O'Rourke (1968).
PS (3) is from Ristow *et al.* (2004).

As observed in the previous Section 6.2.2 from the plots of r_{HYD}, spec r_{HYD}, k_h and k_H for the various sludge types, the first order kinetics do not have a consistent relationship with sludge age, hence are not ideal to model the AD of sludge under various R_s. However, the Monod or saturation kinetics, obtained using selected data for improved correlation values, can be used over the range of all sludge ages.

Table 6.2.6b and the following Figure 6.2.6a below show that the various sludge types have dissimilarities in the trends of specific hydrolysis rates, with increasing residual biodegradable particulate organics (S_{bpe}). These dissimilarities resulted in each sludge type having unique hydrolysis rate kinetic constants. However, the following Figure 6.2.6b shows that the measured percentage of biodegradable COD removed with sludge age for each of the AD systems does not exhibit a significant difference between the PS and WAS degradation rates. It is thus evident that the anaerobic digestion of waste activated sludge (WAS) together with primary sludge (PS) does not have a significant impact on the hydrolysis rate of WAS compared with anaerobically digesting the WAS by itself. The following Figure 6.26c shows how well the different kinetic constants from the various sludge types compare with each other and which ones best fit the measured data for COD removal versus sludge age. This Figure 6.2.6c shows how the various sludge types have different unbiodegradable particulate COD fractions but exhibit similarities in the curvature of the lines, in the graphs for the various sludge types, which also confirms how the different sludge types have similar rates of biodegradable COD removal.

Table 6.2.6b: A Comparison of the Changes in Specific Hydrolysis Rates (r_{HYD}/Z_{AD}) of the Various Sludges with Increasing Biodegradable Organics Concentration (S_{bp})										
	AD 1 (NDBEPR WAS)		AD 2 (PS)		AD 3 (MLE 1 WAS)		AD 4 (PS-WAS blend)		AD 5 (MLE 2 WAS)	
R_s	S_{bpe}	r_{HYD}/Z_{AD}	S_{bpe}	r_{HYD}/Z_{AD}	S_{bpe}	r_{HYD}/Z_{AD}	S_{bpe}	r_{HYD}/Z_{AD}	S_{bpe}	r_{HYD}/Z_{AD}
10	0.531	1.248	0.522	1.128	0.666	1.365	0.519	1.212	0.572	1.248
18	0.340	0.854	0.336	0.756	0.336	0.878	0.321	0.802	0.351	0.854
25	0.360	0.717	0.190	0.610	0.136	0.725	0.158	0.647	0.202	0.717
40	0.153	0.599	0.008	0.543	0.110	0.584	0.111	0.555	0.115	0.584
60	0.056	0.510	0.003	0.466	0.078	0.510	0.022	0.482	0.078	0.510

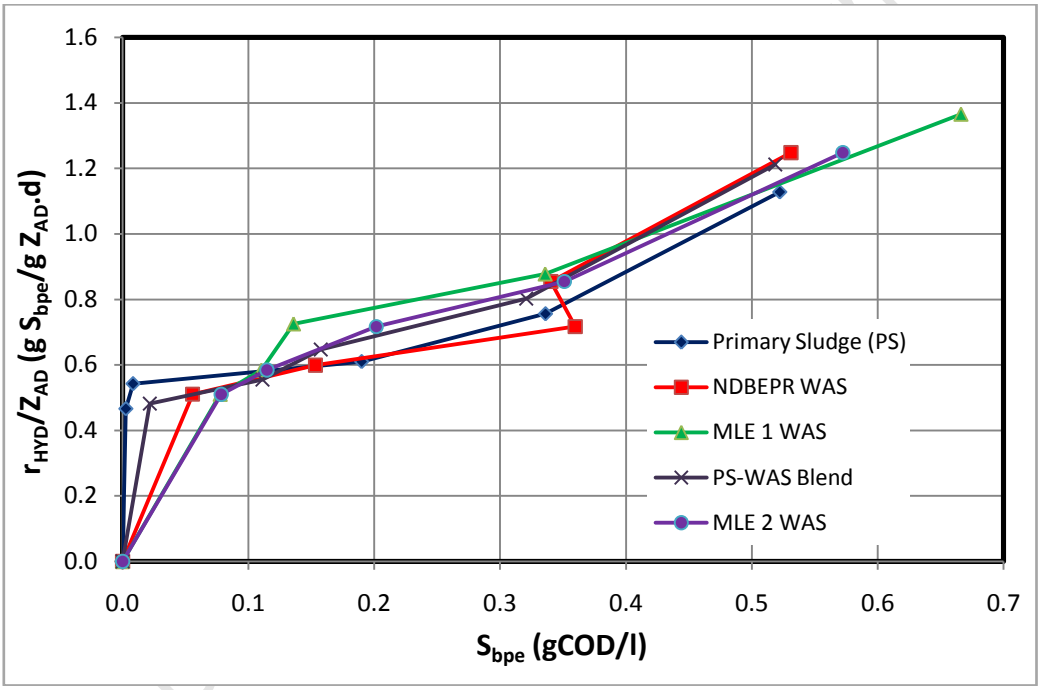

Figure 6.2.6a: *Specific hydrolysis rate (r_{HYD}/Z_{AD}) versus biodegradable particulate organics (S_{bp}) for the five different sludge types.*

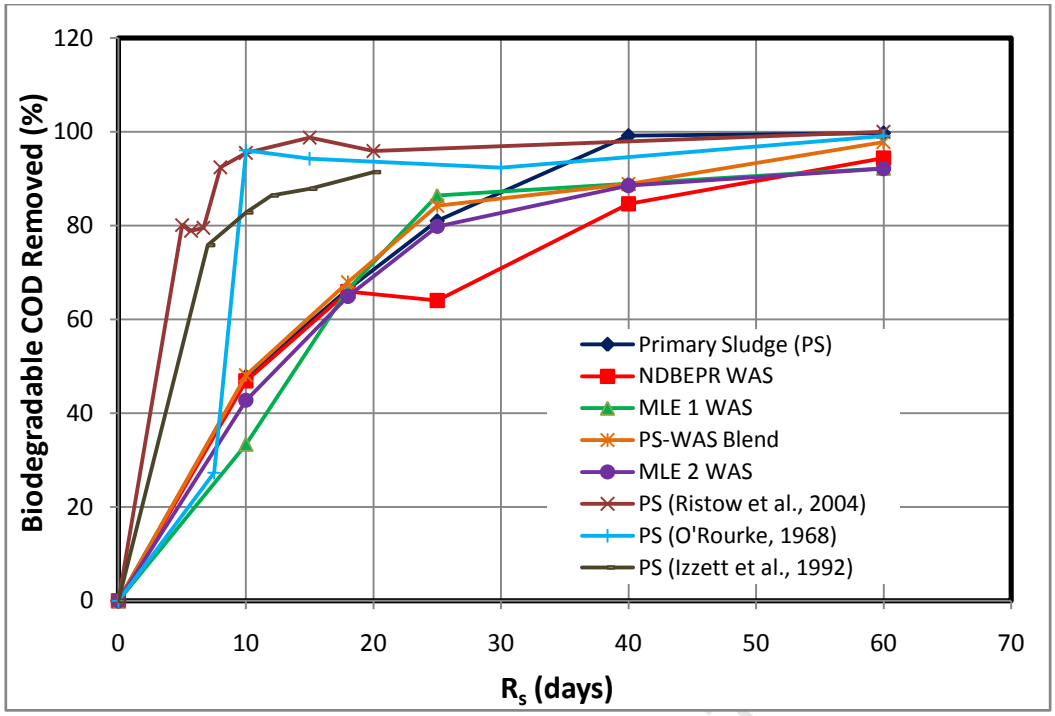

Figure 6.2.6b: *The percentage biodegradable COD removed, calculated from measured results, with increasing sludge age (R_s) for the different sludge types.*

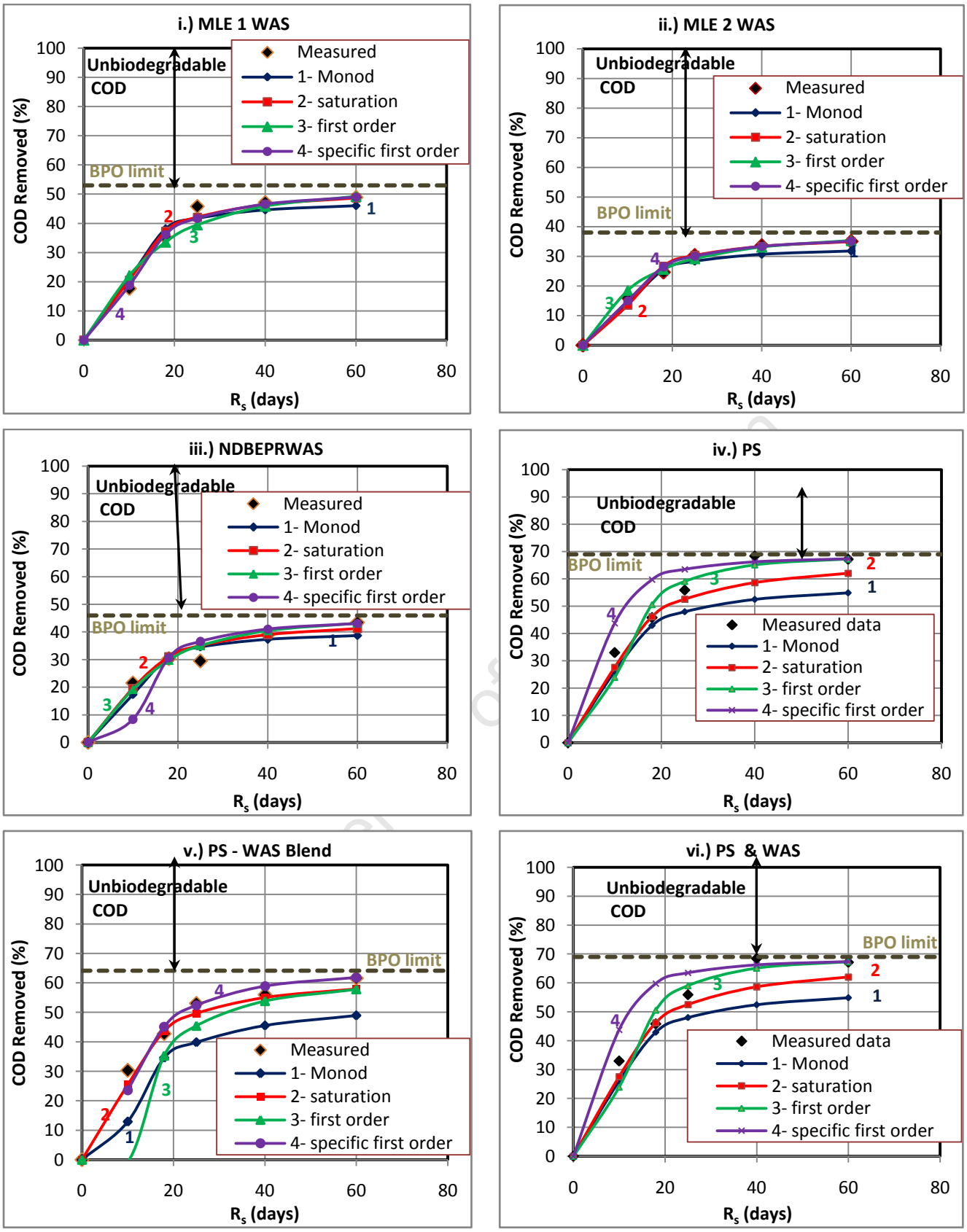

Figures 6.2.6c - i to vi: *A comparison of the percentage COD removed for the AD of the different sludge types (i-MLE 1 WAS, ii- MLE 2 WAS, iii- NDBEPR WAS, iv- PS alone, v.- PS-WAS blended using the kinetic constants determined in Section 6.2.5, vi.- PS & WAS, where PS and MLE 1 WAS are given separate kinetic constants for hydrolysis of the blend) measured and determined using obtained constants for the various kinetic formulations (1st order, specific 1st order, Monod and saturation).*

6.3. STOICHIOMETRIC MODEL FOR AD OF NDBEPR WAS

6.3.1 Extending the AD Model to Include P (Harding, 2009)

Sötemann *et al.* (2005a) developed a two phase (aqueous-gas) steady state model to describe the anaerobic digestion of organics, that includes the C, H, O, N and COD mass balanced stoichiometry developed with the method described by McCarty (1975). In the extension of this CHON, COD and charge mass balanced stoichiometric model, Harding (2009) added biomass P and polyphosphate (PP) in NDBEPR WAS and so includes P and metals Mg, Ca and K mass balance stoichiometry. The complexities of including P in the mass balanced stoichiometry of the different WWTP unit operations were considered to hinge around (1) the different rates at which PP and organically bound P are released in anoxic/aerobic and anaerobic digestion, (2) the effect of the 2nd dissociation constant of the OP weak acid/base system (pK_{p2}~7), and (3) the precipitation of metal phosphates because PP has a high metal (Mg^{2+}, K^{+}, Ca^{2+}) content which is released with the OP in aerobic and anaerobic digestion (Harding *et al.*, 2011). The development of this AD model stoichiometry is briefly described below.

Harding (2009) determined the mass balanced redox half reactions of substrate electron (and H^{+}) donation by splitting phosphate products from organically bound and polyphosphate ($MePO_3$) between HPO_4^{2-} and $H_2PO_4^{-}$ to include the effect of the 2nd pK_{p2} at 7.0 of the ortho-phosphate system. These reactions are given in Equations 6.31a and 6.31b below i.e.

$$R_d\left[\begin{array}{l} C_X H_Y O_Z N_A P_B.q[MePO_3] + (2X - Z + A + 2B)H_2O \rightarrow (X - A + 2B + q)CO_2 + \\ + ANH_4^+ + (B + q)HPO_4^{2-} + (A - 2B - q)HCO_3^- + qMe^+ + \gamma_S(H^+ + e^-) \end{array}\right] \quad (6.31a)$$

and,

$$R_d\left[\begin{array}{l} C_X H_Y O_Z N_A P_B.q[MePO_3]+(2X-Z+A+3B)H_2O \rightarrow (X-A+B)CO_2 \\ +ANH_4^+ +(B+q)H_2PO_4^- +(A-B)HCO_3^- +qMe^+ +\gamma_S\left(H^+ +e^-\right) \end{array}\right]$$

(6.31b)

Where γ_s = electron donating capacity of the organics (e^- eq/mol) and given by Equation 6.36a. The mass balance reaction stoichiometry of the anabolic process (R_a) half reaction with the uptake of $H_2PO_4^-$ (Equation 6.31c) or HPO_4^{-2} (Equation 6.31d) for biomass production of composition $C_kH_lO_mN_nP_p$ is given by:

$$R_a=\left[\begin{array}{l} (k-n+p)\frac{\gamma_S}{\gamma_B}CO_2+(n-p)\frac{\gamma_S}{\gamma_B}HCO_3^- +n\frac{\gamma_S}{\gamma_B}NH_4^+ +p\frac{\gamma_S}{\gamma_B}H_2PO_4^- \\ +\gamma_S\left[H^+ +e^-\right]\rightarrow \frac{\gamma_S}{\gamma_B}C_kH_lO_mN_nP_p+(2k-m+n+3p)\frac{\gamma_S}{\gamma_B}H_2O \end{array}\right] \quad . \quad .$$

(6.31c)

and

$$R_a=\left[\begin{array}{l} (k-n+2p)\frac{\gamma_S}{\gamma_B}CO_2+(n-2p)\frac{\gamma_S}{\gamma_B}HCO_3^- +n\frac{\gamma_S}{\gamma_B}NH_4^+ +p\frac{\gamma_S}{\gamma_B}HPO_4^{2-} \\ +\gamma_S\left[H^+ +e^-\right]\rightarrow \frac{\gamma_S}{\gamma_B}C_kH_lO_mN_nP_p+(2k-m+n+2p)\frac{\gamma_S}{\gamma_B}H_2O \end{array}\right]$$

(6.31d)

Where γ_B = electron donating capacity of the biomass organics and is described in Equation 6.36b. The stoichiometry describing the e^- acceptor half reaction for the catabolic pathway (R_c) with CO_2 as electron acceptor is as given by Equation 6.31e below,

$$R_c=\left[\frac{\gamma_S}{8}CO_2+\gamma_S\left[H^+ +e^-\right]\rightarrow\frac{\gamma_S}{8}CH_4+\frac{2\gamma_S}{8}H_2O\right]$$

(6.31e)

To balance the COD (e^-) donated by the organic substrate (R_d) and conserved as biomass (anabolism) and passed to the e^- acceptor (catabolism) (R_a and R_c), Harding (2009) equated the e^- donated by the organics to the electrons captured into new cell mass (anabolism) and

transferred to the e^- acceptor CO_2. Thus if a fraction E of the e^- are new cell mass and (1-E) passed to e^- acceptor CO_2 then: $R = R_d - (1-E)R_a - ER_c$

(6.31f)

Substituting Equations 6.31a to e into Equation 6.31f yields the generalised stoichiometric model for the phosphate products $H_2PO_4^-$ (presented by Equation 6.32a below) and HPO_4^{-2-} (presented by Equation 6.32b below).

$$C_X H_Y O_Z N_A P_B .q[MePO_3] + \left(2X - Z + A + 2B - E\frac{\gamma_S}{\gamma_B}(2k - m + n + 2p) - \frac{2\gamma_S}{8}(1-E)\right)H_2O \rightarrow$$
$$\left(X - A + 2B + q - E\frac{\gamma_S}{\gamma_B}(k - n + 2p) - \frac{(1-E)\gamma_S}{8}\right)CO_2 + \left(\frac{\gamma_S}{8}(1-E)\right)CH_4 + \left(E\frac{\gamma_S}{\gamma_B}\right)C_k H_l O_m N_n P_p$$
$$+\left(A - nE\frac{\gamma_S}{\gamma_B}\right)NH_4^+ + \left(B + q - pE\frac{\gamma_S}{\gamma_B}\right)HPO_4^{2-} + \left(A - 2B - q - E\frac{\gamma_S}{\gamma_B}(n - 2p)\right)HCO_3^- + qMe^+$$

(6.32a)

and,

$$C_X H_Y O_Z N_A P_B .q[MePO_3] + \left(2X - Z + A + 3B + q - E\frac{\gamma_S}{\gamma_B}(2k - m + n + 3p) - \frac{2\gamma_S}{8}(1-E)\right)H_2O \rightarrow$$
$$\left(X - A + B - E\frac{\gamma_S}{\gamma_B}(k - n + p) - \frac{(1-E)\gamma_S}{8}\right)CO_2 + \left(\frac{\gamma_S}{8}(1-E)\right)CH_4 + \left(E\frac{\gamma_S}{\gamma_B}\right)C_k H_l O_m N_n P_p$$
$$+\left(A - nE\frac{\gamma_S}{\gamma_B}\right)NH_4^+ + \left(B + q - pE\frac{\gamma_S}{\gamma_B}\right)H_2PO_4^- + \left(A - B - E\frac{\gamma_S}{\gamma_B}(n - p)\right)HCO_3^- + qMe^+$$

(6.32b)

In the above Equations 6.32a and b, the phosphate products $H_2PO_4^-$ and HPO_4^{-2} are equal to the ortho-phosphate (OP) released from the biomass and polyphosphate (PP) and establish the digester pH together with the inorganic carbon (IC) system via the aqueous phase equilibrium chemistry that exists within the AD reactor environment.

Noting that the OP species in the AD almost entirely comprises of $H_2PO_4^-$ and HPO_4^{2-} in the pH range of 5 to 9, Harding (2009) added the two phosphate products to equal the OP concentration (P_T) i.e.

$$f\left[H_2PO_4^-\right]+(1-f)HPO_4^{2-}=P_t,$$

(6.33)

which is dependent on the molar concentration of protons [H^+] and therefore digester pH i.e.:

$$K'_{P2}=\frac{\left(H^+\right)\left[HPO_4^{-2}\right]}{\left[H_2PO_4^-\right]}$$

$$\left[H_2PO_4^-\right]=fP_T=\frac{P_T\cdot\left[H^+\right]}{\left[H^+\right]+K'p_2}$$
$$\left[H^+\right]\cdot(f-1)=-f\cdot K'p_2$$
$$\left[H^+\right]=\frac{-f\cdot K'p_2}{(f-1)}$$

(6.34a, b, c, d)

In the AD stoichiometry of Harding *et al.*(2009) it is noted that at a sludge age of five days or longer, only a part of the biodegradable organics of the NDBEPR WAS biomass are degraded but all of the PP inside the phosphorus accumulating organisms (PAOs) is released. Since in the empirical composition of the PAO (i.e. CHONP[$MePO_3$], in Equation 6.32) there is a fixed ratio (q) between the PAO biomass and PP, it is better to separate the biomass P from the PP in the general reaction stoichiometry, which yields for any biodegradable organics.

$$C_XH_YO_ZN_AP_B+\left(2X-Z+A+(2+f)B-E\frac{\gamma_S}{\gamma_B}(2k-m+n+(2+f)p)-\frac{2\gamma_S}{8}(1-E)\right)H_2O\leftrightarrow$$
$$\left(X-A+(2-f)B-E\frac{\gamma_S}{\gamma_B}(k-n+(2-f)p)-\frac{(1-E)\gamma_S}{8}\right)CO_2+\left(\frac{\gamma_S}{8}(1-E)\right)CH_4+$$
$$\left(E\frac{\gamma_S}{\gamma_B}\right)C_kH_lO_mN_nP_p+\left(A-nE\frac{\gamma_S}{\gamma_B}\right)NH_4^++f\left(B-pE\frac{\gamma_S}{\gamma_B}\right)H_2PO_4^-$$
$$+(1-f)\left(B-pE\frac{\gamma_S}{\gamma_B}\right)HPO_4^{2-}+\left(A-(2-f)B-E\frac{\gamma_S}{\gamma_B}(n-(2-f)p)\right)HCO_3^-$$

(6.35a)

and for polyphosphate:

$$q\left[Mg_cK_dCa_ePO_3\right]+fqH_2O+(1-f)qHCO_3^-\leftrightarrow(1-f)qCO_2+fqH_2PO_4^-$$
$$+(1-f)qHPO_4^{2-}+qcMg^{2+}+qdK^++qeCa^{2+}$$

(6.35b)

Where:

- ɣS and ɣB refer to the electron donating capacity of the substrate and the biomass respectively and can be determined using the Equations 6.36a and 6.36b below:

$$\gamma_S = 4X + Y - 2Z - 3A + 5B \quad \text{(e-/ mol)} \tag{6.36a}$$

and

$$\gamma_B = 4k + l - 2m - 3n + 5p \quad \text{(e-/ mol)} \tag{6.36b}$$

- E is the fraction of biodegradable COD for the flow through AD of this investigation and (where there is no endogenous residue of AD biomass (f_{AD} = 0)) COD utilized (S_{bpi} - S_{bpe}) that is converted to biomass (Z_{AD})

$$E = \frac{Z_{AD}}{S_{bpi} - S_{bpe}} = \frac{Y_{AD}\left(1 + b_{AD} R_S\right)}{\left[1 + b_{AD} R_s \left(1 - Y_{AD}\right)\right]} \tag{6.37}$$

Where:

- Y_{AD} is the yield coefficient (gCOD biomass/gCOD organics hydrolysed).
- b_{AD} is the acidogen endogenous respiration rate (/d).
- R_s is the digester sludge age.
- The f value is the fraction of $H_2PO_4^-$ in the total phosphate species (comprising mainly of $H_2PO_4^-$ and HPO_4^{2-}, which are in equilibrium with each other according to pH and is described further in the Section 6.4 below).

With the mol/*l* organics hydrolysed and PP released known the only unknown in Equation 6.35 is the f factor and hence also the AD pH.

The above stoichiometry can also be applied to any biodegradable organics including primary sludge (PS). However, PS contains a significant concentration of SCFA in the influent, which requires separate consideration, as was done by Sötemann *et al.* (2005). They

assumed the influent SCFA is all acetate and its reaction stoichiometry (shown in Equations 6.38a and 6.38b) derived, assuming zero biomass growth because it does not require acidogenesis. In this reaction stoichiometry, the undissociated and dissociated acetate species are utilized by methanogenic AD biomass with no AD sludge produced in the process.

$$CH_3COOH \rightarrow CH_4 + CO_2$$

(6.38a)

and

$$CH_3COO^- + H_2O \rightarrow CH_4 + HCO_3^-$$

(6.38b)

As stated by Loewenthal *et al.* (1989) the undissociated and dissociated acetate species are maintained in equilibrium with each other according to the pH of the AD liquor, whereby higher pH causes a higher fraction of dissociated acetate species.

The final stoichiometry of the AD model for the various municipal sludge types, including WAS from NDBEPR systems, comprises a combination of Equations 6.35a and b and 6.38a and b, with the influent total alkalinity and pH to define the initial carbonate and OP concentrations that influence the final alkalinity and AD pH. In order to utilize this steady state AD model for the digestion of P rich sludge containing PP, three phase (solid-liquid-gas) weak acid/base stoichiometry requires inclusion. This is because the hydrolysis of PP during AD causes release of Mg^{2+} (and K^+ and Ca^{2+}) and P which when in high concentrations cause the precipitation of struvite.

6.3.2 PAO Behaviour in the AD

In the anaerobic reactor of the NDBEPR system, PAOs take up short chain fatty acids and convert them to poly-3-hydoxyalkanoates (PHA), which are energy storage compounds that can be broken down aerobically by the PAOs to carry out their growth and respiration metabolism. The PAOs fed to the AD, once entering the environment are deemed capable of carrying out the same P-release mechanisms as in the anaerobic reactor of the NDBEPR AS

system. However, the PAOs would not compete with the anaerobic bacteria because they require alternating anaerobic and aerobic conditions to supply them with the terminal electron acceptor (oxygen) for their growth and respiration. Therefore, the PAOs eventually die at a rate much faster than the hydrolysis of their biomass, releasing all remaining PP and PHA. Therefore, in the AD, both the PP release with PHA formation, as mediated in the anaerobic reactor of the NDBEPR system, and P release upon the death of PAOs (as reported by Harding, 2009), is required in modelling. The hydrolysis of the dead PAO biomass is the slowest rate controlling process in the AD.

Smolders *et al.* (1995) presented the anaerobic uptake of acetate and storage of PHA using the following Equation 6.39.1a. First, the acetate is taken up and converted to Acetyl-CoA, which requires 0.5mol ATP, then subsequently converted to PHA with the use of 0.25 mol $NADH_2$ per mol of acetic acid used, viz.

$$CH_2O + \frac{1}{4}NADH_2 + \left(\frac{1}{2} + \alpha 1\right)ATP \rightarrow CH_{1.5}O + H_2O \tag{6.39.1a}$$

Mino *et al.* (1994) confirms these two stages by reporting the two equations below:

$$CH_3COOH + CoA - SH + ATP \rightarrow Acetyl - CoA + H_2O \tag{6.39.1b}$$

and

$$Acetyl - CoA + \frac{1}{2}NADH_2 \rightarrow \frac{1}{2}C_4H_6O_2 \tag{6.39.1c}$$

Each mol of ATP used for the uptake and storage of acetate is produced by the degradation of one P-mol PP and phosphate (one mol) is released in the process, as shown by Smolders *et al.* (1995), using the Equation 6.39.2a below.

$$HPO_3 + H_2O \rightarrow ATP + H_3PO_4 \tag{6.39.2a}$$

Cole and Hughes (1964) reports that two separate enzymes are used in this process. One used for the formation of ATP from the degradation of PP in the presence of adenosine di-phosphate (ADP), and the other used for hydrolysis of adenosine tri-phosphate (ATP) to release ortho-phosphate (OP) and regenerate ADP. These processes are summarized by the Equations 6.39.2b to 6.39.2d below.

$$(Polyphosphate)_n + ADP \rightarrow ATP + (Polyphosphate)_{n-1} \quad (6.39.2b)$$

$$ATP + H_2O \rightarrow ADP + H_3PO_4 \quad (6.39.2c)$$

ATP is formed as an intermediate and can be utilized for other energy consuming processes and to drive some enzyme controlled reactions. Ultimately, the reaction is:

$$(Polyphosphate)_n + ADP \rightarrow Ortho-phosphate + ADP \quad (6.39.2d)$$

Smolders *et al.* (1995) took the HPO_3 of the above Equation 6.39.2a as a representation of the PP ($Mg_{0.31}K_{0.32}Ca_{0.03}PO_3$), since the proton provided equivalent electro-neutrality (as the metals Mg, K and Ca) to the phosphorus group. The only $NADH_2$ available to PAOs in the AD is present in the PAO cytoplasm in the AD feed WAS. This is because in the NDBEPR parent system the $NADH_2$ (formed as $NADH\text{-}H^+$, when NAD^+ molecules take up two electrons and two H^+ atoms) is produced in the aerobic reactor, with PP uptake and PHA degradation but this aerobic synthesis of $NADH_2$ cannot take place in the AD. However, Smolders *et al.* (1995) reports that some $NADH_2$ can be produced anaerobically from the conversion of some of the acetate in the tri-carboxylic acid (TCA) cycle, using the Equation 6.39.3 below.

$$CH_2O + ATP + H_2O \rightarrow 2NADH_2^+ + CO_2 \quad (6.39.3)$$

With the supply of $NADH_2$, which is produced in the aerobic reactor of the parent NDBEPR system with PP uptake and hence included with the influent to the AD, the outcome results in less CO_2 evolution and increased alkalinity. The use of undissociated acetate in Equation 6.39.1a may result in CO_2 production instead of HCO_3^-, but the digester is operated at a pH of about seven, hence mostly dissociated acetate is used in PHA uptake. As shown in the above Equation 6.39.1a, the PP release provides ATP for PHA uptake. According to results from Smolders *et al.* (1995), at a pH of 7 about 0.5 moles of P in PP are used to provide 0.5mols ATP to form 1 mol of C in PHA (specifically poly-hydroxy-butyrate, PHB), in the TCA cycle. Hence, for 4 C-moles of PHA, 2 moles ATP are provided by the PP released (which is 2mol P-PP). This gives the following reaction for anaerobic PP release:

$$2Mg_cK_dCa_ePO_3 + 2CH_3COOH + NADH_2^+ \rightarrow C_4H_6O_2 + NAD^+ + 2H_2PO_4^- + 2cMg^{2+} + 2dK^+ + 2eCa^{2+} \quad (6.39.4)$$

The PHA that is produced from this reaction (Equation 6.39.4 above) is broken down in the anaerobic digester, with the growth of AD biomass, to form carbon dioxide and methane as shown below:

$$4C_4H_6O_2 + 6H_2O \rightarrow 9CH_4 + 7CO_2 \quad (6.39.5)$$

In addition, the dissociated acetate available in the AD system is converted to bi-carbonate and methane as shown below (Equation 6.39.6)

$$CH_3COO^- + H_2O \rightarrow CH_4 + HCO_3^- \quad (6.39.6)$$

Thus, the PAOs do not compete with the AD biomass for the acetate, but after an initial rapid uptake of acetate and release of PP, leave the acetate to be degraded by AD biomass and give up the PHA with their hydrolysis. Therefore, the Equation 6.39.4 can be converted to Equation 6.39.7 below:

$$2CH_3COOH + 2Mg_cK_dCa_ePO_3 + \frac{6}{4}H_2O + NADH_2^+ \rightarrow \frac{7}{4}CO_2 + 2H_2PO_4^-$$
$$+ 2cMg^{2+} + 2dK^+ + 2eCa^{2+} + \frac{9}{4}CH_4 + NAD^+$$

(6.39.7)

However, as described above, $NADH_2^+$ is formed by the uptake of $2e^-$ and $2H^+$, as shown by the Equation 6.39.8 below:

$$NAD^+ + 2H^+ + 2e^- \rightarrow NADH_2^+$$

(6.39.8)

Hence, the above Equation 6.39.7 can be given as:

$$2CH_3COOH + 2Mg_cK_dCa_ePO_3 + \frac{6}{4}H_2O + NAD^+ + 2H^+ + 2e- \rightarrow \frac{7}{4}CO_2 + 4H^+ + 2PO_4^{3-}$$
$$+ 2cMg^{2+} + 2dK^+ + 2eCa^{2+} + \frac{9}{4}CH_4 + NAD^+$$

(6.40.1)

then simplified to:

$$CH_3COOH + Mg_cK_dCa_ePO_3 + \frac{3}{4}H_2O + e- \rightarrow \frac{7}{8}CO_2 + HPO_4^{2-}$$
$$+ cMg^{2+} + dK^+ + eCa^{2+} + \frac{9}{8}CH_4$$

(6.40.2)

Also, as reported by Harding (2009) , the total phosphates are fractionated, according to pH, by the f value to HPO_4^{2-} and $H_2PO_4^-$, i.e.:

$$PO_4^{3-} + (1+f)H_2CO_3 \rightarrow (1+f)HCO_3^- + fH_2PO_4^- + (1-f)HPO_4^{2-}$$

(6.40.3)

Therefore, the PP release Equation 6.48 can be included in the steady state AD model as Equation 6.40.4 below:

$$CH_3COOH + Mg_cK_dCa_ePO_3 + \left(\frac{3}{4} + f\right)H_2O + e- \rightarrow fH_2PO_4^- +$$
$$(1-f)HPO_4^{2-} + fHCO_3^- + cMg^{2+} + dK^+ + eCa^{2+} + \frac{9}{8}CH_4 + \left(\frac{7}{8} - f\right)CO_2$$

(6.40.4)

In the case where this $NADH_2$ is produced within the AD, the result is a combination of the above three Equations 6.39.1a, 6.39.2a and 6.39.3 together with the Equation 6.40.3 for fractionation of P species to give the following Equation 6.40.5.

$$(8f-1)H_2CO_3 + 8Mg_cK_dCa_ePO_3 + 9CH_3COO^- + 4H_2O \rightarrow 4C_4H_6O_2 + (1+8f)HCO_3^-$$
$$+ 8fH_2PO_4^- + (8-8f)HPO_4^{2-} + 8cMg^{2+} + 8dK^+ + 8eCa^{2+}$$

(6.40.5)

The outcome of this Equation 6.40.5 with the anaerobic breakdown of PHA (to CO_2 and CH_4 as shown in Equation 6.39.5) and acetate (to HCO_3^- and CH_4, see Equation 6.39.6) is equivalent to the PP release occurring with the death of PAOs, as was reported by Harding (2009), and can be simplified to:

$$Mg_cK_dCa_ePO_3 + fH_2O + (1-f)HCO_3^- \rightarrow (1-f)CO_2$$
$$+ fH_2PO_4^- + (1-f)HPO_4^{2-} + cMg^{2+} + dK^+ + eCa^{2+}$$

(6.40.6)

It was decided that both Equations (6.40.4 and 6.40.6) be entered into the model, since there was a possibility of both processes occurring in the AD. This is because in the anaerobic and anoxic zones of the parent NDBEPR system, the PP release ranged between 65 and 75% of its uptake. It could be safe to assume that similar amounts are released in the AD using the $NADH_2$ that is present in the biomass feed (i.e. a fraction of ϕ via Equation 6.40.4) and the rest (1-ϕ) is released with the death of the PAOs (via Equation 6.40.6). The ϕ value can be calibrated using the AD partial pressure and alkalinity results. Thus, the generalized stoichiometric model for PP release (Equation 6.35b) is extended (to accommodate Equations 6.40.4 and 6.40.6) as:

$$\phi \cdot CH_3COOH + [Mg_cK_dCa_ePO_3] + \left(\phi \cdot \left(\frac{3}{4} + f\right) + (1-\phi)\cdot f\right) \cdot H_2O + \phi \cdot e^- \rightarrow fH_2PO_4^- +$$

$$(1-f)HPO_4^{2-} + (\phi \cdot f - (1-\phi)\cdot(1-f)) \cdot HCO_3^- + cMg^{2+} + dK^+ + eCa^{2+} + \phi \cdot \frac{9}{8} CH_4$$

$$+ \left(\phi \cdot \left(\frac{7}{8} - f\right) + (1-\phi)\cdot(1-f)\right) CO_2$$

(6.40.7)

6.4 WEAK ACID/BASE CHEMISTRY AND THE INCLUSION OF A SOLID PHASE

6.4.1 Determination of Digester pH for Infinite Solubility of Precipitates

The process of anaerobic digestion results in the production of various chemical species at different molar concentrations within the AD liquor. Some of these chemical species belong to one of the weak acid/base sub-systems that are simultaneously present in solution. A methanogenic AD typically includes the carbonate, phosphate, ammonia, acetate and water weak acid/ base subsystems. Loewenthal *et al.* (1994) has described the influence of the digester pH on the molar concentrations of the chemical species within each of these subsystems using a set of equilibrium and mass balance equations as shown below:

A. <u>Aqueous phase equilibrium Equations</u>

(i) Carbonate sub-system (C_T) :

$$K'_{C1} = \frac{\left(H^+\right)\left[HCO_3^-\right]}{\left[H_2CO_3^*\right]}$$

(6.41a)

$$K'_{C2} = \frac{\left(H^+\right)\left[CO_3^{-2}\right]}{\left[HCO_3^-\right]}$$

(6.41b)

(ii) Ammonia sub-system:

$$K'_N = \frac{\left(H^+\right)\left[NH_3\right]}{\left[NH_4^+\right]} \tag{6.41c}$$

(iii) Phosphate sub-system:

$$K'_{P1} = \frac{\left(H^+\right)\left[H_2PO_4^-\right]}{\left[H_3PO_4\right]} \tag{6.41d}$$

$$K'_{P2} = \frac{\left(H^+\right)\left[HPO_4^{-2}\right]}{\left[H_2PO_4^-\right]} \tag{6.41e}$$

$$K'_{P3} = \frac{\left(H^+\right)\left[PO_4^{-3}\right]}{\left[HPO_4^{-2}\right]} \tag{6.41f}$$

(iv) Acetate sub-system (assumed to represent the SCFA):

$$K'_{A1} = \frac{\left(H^+\right)\left[Ac^-\right]}{\left[HAc\right]} \tag{6.41g}$$

(v) Water sub-system:

$$K'_W = \left(H^+\right)\left[OH^-\right] \tag{6.41h}$$

Where (H^+) is the hydrogen ion activity, [X] the molar concentration of species X and $K_{X'}$ is the thermodynamic equilibrium constant for species X (see Table 2.1 for the pK values, where pKx= -log[Kx]), adjusted for Debye Hückel effects to account for the activity of ions in low salinity water (Stumm and Morgan 1996).

B. <u>Mass Balance Equations</u>

$$C_t = \left[H_2CO_3^*\right] + \left[HCO_3^-\right] + \left[CO_3^{-2}\right] \tag{6.42a}$$

$$P_t = \left[H_3PO_4\right] + \left[H_2PO_4^-\right] + \left[HPO_4^{-2}\right] + \left[PO_4^{-3}\right] \tag{6.42b}$$

$$N_t = \left[NH_4^+\right] + \left[NH_3\right] \tag{6.42c}$$

$$A_t = \left[HAc\right] + \left[Ac^-\right] \tag{6.42d}$$

It was noted by Loewenthal *et al.* (1989) that a weak acid/base system requires characterisation of the various sub-systems through measurement of the P_T, N_T, C_T and A_T weak acid total species concentrations before they can be speciated. The AD kinetic and stoichiometric model that has been described in Sections 6.2 and 6.3 above is able to use the measured influent characteristics to predict the aqueous concentrations of the weak acid/base species as final AD products (HCO_3^-, $H_2PO_4^-$, HPO_4^{2-}, NH_4^+, and Ac^-). These species concentrations can in turn be used in the determination of the digester pH.

Sötemann *et al.* (2005b) noted that the pH established within AD systems treating PS and ND WAS is primarily affected by the inorganic carbon system. Although other weak acid/base systems are present such as the ammonia (N_T), phosphate (P_T) and SCFA sub-systems, these do not significantly affect pH, either because their concentration is low (as for the P system) or their pK values are far outside the normal pH range of ADs (as for the VFA [pK_a = 4.7] and ammonia [pK_n = 9.1] systems) (Loewenthal *et al.,* 1994). The AD stoichiometric model can predict the bi-carbonate concentration generated from the N and VFA content of the PS and ND WAS (Sötemann *et al*, 2005b). However, the H_2CO_3* species of the inorganic carbon system exists at equilibrium in both a gaseous CO_2 and aqueous (H_2CO_3*) phase. Moreover, the gas-liquid transfer equilibrium within the AD is dependent on the partial pressure of the gas phase (Moosbrugger *et al.*, 1992). This CO_2 partial pressure (p_{CO2}) can be calculated (as shown in Equation 6.43) using the molar concentrations of gaseous CO_2 and CH_4, which are the chief biogas components predicted by the AD stoichiometric model. The CH_4 is insoluble and hence does not significantly affect the system mass balances or participate in the aqueous phase reactions.

$$p_{CO2} = \frac{[CO_2]_g}{([CO_2]_g + [CH_4]_g)}$$

(6.43)

Since, in steady state, the dissolved CO_2 species concentration ($[H_2CO_3^*]$) in the aqueous phase is in equilibrium with the pCO_2 in the AD headspace, it can be determined using the Henry's law expression (Loewenthal *et al.,* 1994):

$$[H_2CO_3^*] = K_{HCO2} \times p_{CO_2}$$

(6.44)

Where:

K'_{HCO2} = Henry's law constant, which is 1.59 at 37°C (calculated using the pK_{HCO2}, which is -log $[K_{HCO2}]$, value shown in Table 2.1).

$[H_2CO_3^*]$ = the dissolved CO_2 concentration in mo*l/l.*

The $[H_2CO_3^*]$ that is calculated using the p_{CO2} can then be applied together with the stoichiometrically predicted $[HCO_3^-]$ concentration and the known K'_H, K'_{c1} and K'_{c2} values (shown in Table 2.1 of Chapter 2) in the calculation of $[H^+]$, hence pH, using the above carbonate aqueous phase Equations 6.41 a and b.

Where the phosphate species are included in the AD stoichiometry, such as for the AD of NDBEPR WAS with high P concentrations, it is necessary to include the P_T system, since it significantly influences the AD pH via its 2nd dissociation constant pK_{p2} at ~ 7.0. As can be seen in the general stoichiometric model (Equation 6.41d to f) the *f* value, which fractionates the phosphate species ($H_2PO_4^-$ and HPO_4^{2-}) as AD products, is required for the calculation of the AD pH (see Equation 6.34 of Section 6.3). Accepting that $P_T = [H_2PO_4^-] + [HPO_4^{2-}]$ i.e. $[H_3PO_4]$ and $[PO_4^{3-}]$ are effectively zero in the 5 to 9 pH range, the *f* value can be related to pH and the dissociation constant, relating $H_2PO_4^-$ and HPO_4^{2-} (pK'_{p2}):

$$[H_2PO_4^-] = f.P_t = f\left\lfloor B + q - pE\frac{\gamma_S}{\gamma_B}\right\rfloor$$

(6.46a)

and:

$$\left[H_2PO_4^-\right] = \frac{P_t}{1+10^{pH-pKp2}}$$

(6.46b)

So:

$$f = \frac{1}{1+10^{pH-pKp2}}$$

(6.46c)

It should be noted that this iterative pH calculation method could also be used when predicting the AD pH for digesters where precipitation has taken place but then the stoichiometry needs to be modified to include the mineral as an AD product (Harding *et al.*, 2011). This is because precipitation would cause a change in some of the AD products from aqueous to solid phase, hence influencing the final digester pH and p_{CO2}. The calculation of the digester pH after precipitation is discussed in Section 6.4.4 below.

In order to have a convenient basis to deal with problems involving determination of change of state due to chemical changes, Loewenthal *et al.* (1991) used the proton donating/accepting capacity parameters relative to a reference species for a specified weak acid subsystem or/and solution. These capacity parameters are termed alkalinities (to exhibit proton acceptance) and acidities (to exhibit proton donation). The Equations 6.47a to 6.47e below describe the total alkalinity, where proton balance is based on the weak acid reference species in the most protonated form. Accepting the nomenclature of Loewenthal *et al.* (1989), where alk as a suffix includes the water species and Alk as a prefix excludes the water species:

1. inorganic carbon:

$$H_2CO_3 * Alk = \left[HCO_3^-\right] + 2\left[CO_3^{2-}\right] + \left[OH^-\right] - \left[H^+\right],$$

(6.47a)

2. phosphate:

$$Alk.H_3PO_4 = \left[H_2PO_4^-\right] + 2\left[HPO_4^{2-}\right] + 3\left[PO_4^{3-}\right],$$

(6.47b)

3. ammonia:

$$Alk.NH_4^+ = \left[NH_3\right] \text{ and}$$

(6.47c)

4. acetate:

$$Alk.HAc = \left[Ac^-\right].$$

(6.47d)

So for a mixture of inorganic carbon, phosphate, ammonia and acetate weak acid/base subsystems.

$$\begin{aligned} Total\ \ Alk &= H_2CO_3 * Alk + Alk.H_3PO_4 + Alk.NH_4^+ + Alk.HAc \\ &= \left[HCO_3^-\right] + 2\left[CO_3^{2-}\right] + \left[H_2PO_4^-\right] + 2\left[HPO_4^{2-}\right] + 3\left[PO_4^{3-}\right] + \left[NH_3\right] + \left[Ac^-\right] + \left[OH^-\right] - \left[H^+\right] \\ &\approx \left[HCO_3^-\right] + 2\left[CO_3^{2-}\right] + \left[H_2PO_4^-\right] + 2\left[HPO_4^{2-}\right], \text{ in the pH range } 6-8. \end{aligned}$$

(6.47e)

6.4.2 Calculation of Precipitates Formed in AD

The AD hydrolysis of BEPR WAS usually results in the release of magnesium (Mg), potassium (K), calcium (Ca) and phosphates (mainly from polyphosphate) together with ammonia and inorganic carbon species as dissolved AD products. At favourable conditions, when these dissolved products are at high concentrations, mineral precipitates are likely to form within the AD liquor. The minerals that are likely to precipitate are (1) calcium phosphate ($Ca_3(PO_4)_2$), (2) calcium carbonate ($CaCO_3$) and (3) struvite ($MgNH_4PO_4$) (Musvoto *et al.*, 2000).

To determine the quantity of precipitant that can be formed during AD requires comparing the calculated ionic product of the soluble AD products with the thermodynamic solubility

product (K_{spm}) of the potential precipitant. The methods used in determining the precipitation potentials of struvite, calcium phosphate and calcium carbonate are presented below.

1. Struvite

Struvite precipitation occurs when the ionic product of the molar activity of Mg^{2+}, NH_4^+ and PO_4^{3-} in solution exceed the thermodynamic solubility product of struvite ($K_{spm\_struv} = 12.6$) in the aqueous phase (Loewenthal *et al.*, 1994).

$$\left[Mg^{2+}\right]\cdot\left[NH_4^+\right]\cdot\left[PO_4^{3-}\right] = \frac{K_{spm}}{f_d f_m f_t} = K'_{spm} \tag{6.48}$$

Where f_m, f_d and f_t are the activity coefficients of mono- , di- and tri-valent ionic species. Loewenthal *et al.* (1989) provides a method of determining the activity coefficients for the ionic species through modification of the Debye-Hückel theory, which describes the activity of ions in low salinity water (Harding, 2009; Butler, 1964). The above Equation 6.48 indicates that struvite will either precipitate or dissolve into solution until equilibrium exists between the aqueous Mg, NH_4^+ and PO_4^{3-} concentrations in the aqueous phases and the ionic product K_{sp}. With the precipitation of R mo*l*/*l* $MgNH_4PO_4$, the R mol/*l* Mg, NH_4^+ and PO_4^{3-} are species used and hence are removed from the aqueous phase of the initial stoichiometrically predicted species concentrations, i.e.:

in the case of magnesium,

$$\left[Mg^{2+}\right]_{final} \approx \left[Mg^{2+}\right]_{initial} - R \tag{6.49}$$

Since N_T is mainly NH_4^+, R mo*l*/*l* of NH_4^+ is used to form the struvite:

$$\left[NH_4\right]_{final} \approx \left[NH_4\right]_{initial} - R \tag{6.50}$$

For the supply of P_T in this precipitation, although the least protonated species of the phosphate system species is likely to be used up first, the result is a net decrease in P_T by R mol/*l* and a a decrease in Total Alk. by 3R mol/*l*. This is because of $[PO_4^{3-}]$ being in the struvite, i.e. it is $3H^+$ away from the H_3PO_4 reference species. This P_T and T.Alk change will determine the final molar concentrations of all the weak acid/base species, including the $H_2PO_4^-$ / HPO_4^{2-} species concentrations (Loewenthal *et al.*, 1994). The molar product of the new ionic species can then be compared with the solubility product of struvite to determine the molar concentration (R) of struvite formed. This is represented by the following Equation 6.51 below, which shows that struvite precipitation will take place as long as the molar product of Mg_T, N_T and PO_{4T} are above the solubility product.

$$([Mg_T]-[R])\cdot([N_T]-[R])\cdot([P_T]-[R])=Ksp_{Struvite} \tag{6.51}$$

Once the molar concentration of struvite is calculated, the final PT, NT and MgT aqueous concentrations can be calculated by deducting the R moles/*l* from their initial stoichiometrically predicted molar concentrations. Thereafter, the aqueous phase equilibrium equations can be applied to speciate (i.e. determine the relevant, HPO_4 and H_2PO_4, species concentrations) the AD liquor. Whereby, since R moles/*l* of P_T are used in the formation of struvite.

$$[H_2PO_4]_{final}=[H_2PO_4]_{initial}-(f\cdot R) \tag{6.52}$$

and

$$[HPO_4^-]_{final}=[HPO_4^-]_{initial}-((1-f)\cdot R) \tag{6.53}$$

The precipitation process influences the final digester pH and p_{CO2} since the formation of struvite involves the release of H^+ ions by the phosphate species. These H^+ ions are taken up by bicarbonate (HCO_3^-) to form dissolved CO_2 (H_2CO_3). Some of this H_2CO_3, to maintain aqueous-gas phase equilibrium according to Henry's law, is converted to its gas (CO_2) and released to the head space, which increases the p_{CO2}. This means that the precipitation of

struvite also brings a change in the gaseous CO_2 concentration and hence carbon dioxide partial pressure (p_{CO2}).

The continued release of H^+ ions results in an increased H_2CO_3/HCO_3^- ratio that corresponds with a decreased pH in the digester. However, the struvite has been experimentally observed to precipitate only at pH ranges of 6.9 and above (but this depends on the P_T concentration), i.e. at pH ranges that allow for stable operation of the digester, possibly averting the AD system from failure caused by low pH. The precipitation of struvite in the digester can be formulated with the following Equation (6.54a).

$$RMg^{2+} + RNH_4^+ + 6RH_2O + ((1-f)\cdot R)HPO_4^- + ((1+f)\cdot R)HCO_3^- + (f\cdot R)H_2PO_4 \\ \rightarrow RMgNH_4PO_4\cdot 6H_2O + ((1+f)\cdot R)H_2CO_3 \quad (6.54a)$$

This above Equation 6.54 can be included to the post precipitation stoichiometry that is used to predict the final AD effluent in the steady state AD model. Since the f value that fractionates the phosphate species changes with precipitation, the AD pH also changes with precipitation (Harding *et al.*, 2011). Thus, if it is accepted that the mineral precipitated is struvite, then the affect of this on the AD behaviour can be evaluated by including struvite as an AD product in the above Equation 6.35b, viz.

$$Mg_cK_dCa_ePO_3 + RNH_4^+ + (f + R\cdot(5-f))H_2O + ((1-f)+R\cdot(1+f))HCO_3^- \rightarrow \\ ((1-f)+R\cdot(1+f))CO_2 + f\cdot(1-R)H_2PO_4^- + (1-f)\cdot(1-R)HPO_4^{2-} \\ + (c-R)Mg^{2+} + dK^+ + eCa^{2+} + RMgNH_4PO_4.6H_2O \quad (6.54b)$$

The above Equation 6.54b extends Equation 6.35b (the PP hydrolysis part of stoichiometry), rather than 6.35a (the biomass products utilization part of the stoichiometry) because the struvite precipitation is limited by the availability of Mg from the PP. Then knowing the concentrations (mol/*l*) of PP hydrolyzed and PAO and OHO biomass utilized, it will be noted that the (gaseous) CO_2 terms are different with and without struvite precipitation but the CH_4 term remains the same (i.e. since it is not included in the Equations for PP release and/or

struvite precipitation). Therefore, the p_{CO2} changes when struvite precipitation takes place in the AD.

2. Calcite

For precipitation of Q moles/*l* of $CaCO_3$, the Ca and CO_3 species molar concentrations that are predicted as stoichiometric products, before precipitation (when assuming infinite solubility of AD final products, shown in Section 6.3 above), are transformed from aqueous to solid phase, i.e.:

$$[C_T]_{final} \approx [C_T]_{initial} - Q \tag{6.55}$$

and

$$[Ca_T]_{final} \approx [Ca_T]_{initial} - Q \tag{6.56}$$

As the case of struvite precipitation there is also a T.Alk loss with $CaCO_3$ precipitation of 2 ×[CaCO3] precipitated because the $[CO_3^{2-}]$ species are $2H^+$ from the $H_2CO_3^*$ reference species. The C_T and T.Alk define the final molar concentrations of HCO_3^- and H_2CO_3 species concentrations after precipitation of calcite are ultimately established by weak acid /base equilibrium conditions. Therefore, the total carbonate (C_T) species that is in the AD liquor is first determined from the AD stoichiometric products. The product of this C_T and stoichiometrically (before precipitation) predicted Ca_T is continuously adjusted against the solubility product of calcite ($Ksp_{calcite}$) to determine the molar concentration (Q) of calcite ultimately formed. This is as shown by Equation 6.57 below:

$$([Ca_T]-[Q])\cdot([C_T]-[Q]) = Ksp_{calcite} \tag{6.57}$$

With the precipitation of calcite, the inorganic carbon system species concentrations change, which affects the $[H_2CO_3^*]$ concentration and hence the p_{CO2} of the headspace. This is mainly due to the release of H^+ ions when bicarbonate loses its carbonate mass to calcite and/or the

uptake of H^+ ions by bicarbonate in the formation of H_2CO_3, to re-adjust the molar ratios of the carbonate system species according to pH.

The precipitation of calcite is thus represented by Equation 6.58a, which can also be added to the general post-precipitation stoichiometry for the prediction of the final AD effluent to give Equation 6.58b.

$$QCa^{2+} + 2QHCO_3^- \rightarrow QCaCO_3 + QH_2O + QCO_2 \tag{6.58a}$$

$$Mg_cK_dCa_ePO_3 + (f - Q)H_2O + (1 - f + 2Q)HCO_3^- \rightarrow (1 - f + Q)CO_2 + fH_2PO_4^- + (1 - f)HPO_4^{2-} + cMg^{2+} + dK^+ + (e - Q)Ca^{2+} + QCaCO_3 \tag{6.58b}$$

The reduction in bicarbonate to form struvite would result in lower alkalinity (by 2Q mol/*l*) and reduced AD pH. Moreover, as the case in the formation of struvite, the production of H_2CO_3 in calcite precipitation would result in the production of more CO_2 gas, which in turn would also increase the p_{CO2}.

3. Precipitation of Amorphous Calcium Phosphate (ACP or $Ca_3(PO_4)_2$)

With the precipitation of V mol/*l* $Ca_3(PO_4)_2$, 3Vmol/*l* of Ca^{2+} and 2V mol/*l* PO_4^{3-} aqueous species are lost to the solid phase, resulting in the following changes in total calcium and phosphorus (Ca_T and P_T respectively) species concentrations:

$$[P_T]_{final} \approx [P_T]_{initial} - 2V \tag{6.59}$$

and

$$[Ca_T]_{final} \approx [Ca_T]_{initial} - 3V \tag{6.60}$$

To obtain the molar concentration of the ACP precipitate (V), the molar product of stoichiometrically predicted P_T and Ca_T is adjusted and compared with the solubility product of ACP (Ksp_{ACP}) as shown in the Equation 6.61 below:

$$([Ca_T]-[3V])\cdot([P_T]-[2V])=Ksp_{ACP} \tag{6.61}$$

Once V has been calculated and 2V and 3V moles/*l* have respectively been deducted from the initially predicted (before precipitation) P_T and Ca_T species, the weak acid/base equilibrium equations for the phosphate subsystem (Equations 6.41d to f) can be used to determine the final HPO_4^{2-} and $H_2PO_4^-$ species concentrations. In this case, since 2V moles/*l* of P_T are used in the formation of ACP:

$$[H_2PO_4]_{final}=[H_2PO_4]_{initial}-(f\cdot 2V) \tag{6.62}$$

and

$$[HPO_4^-]_{final}=[HPO_4^-]_{initial}-((1-f)\cdot 2V) \tag{6.63}$$

Therefore, the precipitation of ACP can be represented by the following Equation 6.64a, which is also to be added to the general post-precipitation stoichiometry for the prediction of the final AD effluent, i.e. by extending Equation 6.35b to Equation 6.64b.

$$3VCa^{2+}+(2V\cdot(f+1))HCO_3^-+(2V\cdot(1-f))HPO_4^-+(2V\cdot f)H_2PO_4\rightarrow VCa_3(PO_4)_2 + (2V\cdot(f+1))H_2CO_3 \tag{6.64a}$$

$$Mg_cK_dCa_ePO_3+(f-2V\cdot(f+1))H_2O+(1-f+2V\cdot(f+1))HCO_3^-\rightarrow(1-f+2V\cdot(f+1))CO_2 + f\cdot(1-2V)H_2PO_4^-+(1-f)\cdot(1-2V)HPO_4^{2-}+cMg^{2+}+dK^++(e-3V)Ca^{2+}+VCa_3(PO_4)_2 \tag{6.64b}$$

Similar to the precipitation of struvite, the release of H^+ ions by the phosphate species to reduce bicarbonate concentration and increase dissolved CO_2 brings about further changes in the system pH, alkalinity and carbon dioxide partial pressure (p_{CO2}).

6.4.3 Determination of Digester pH after Precipitation

Solving for the system pH after precipitation is complex because it includes both the inorganic C and P systems, whose species concentrations are intricately related to each other within the AD post-precipitation stoichiometry and weak acid/base chemistry. The final general stoichiometric equation is given by the sum of Equation 6.35a (for biomass utilization) and an extension of Equation 6.40.7 for PP release, to include the changes described above of the various species after precipitation, to the Equation 6.65 below:

$$\begin{aligned}&\phi\cdot CH_3COOH + Mg_cK_dCa_ePO_3 + RNH_4^+ + \left(\phi\cdot\left(\frac{3}{4}+f\right)+(1-\phi)\cdot f+(5-f)\cdot R-Q-2V\cdot(f+1)\right)\cdot H_2O\\&+\phi\cdot e^-\rightarrow f\cdot(1-R-2V)H_2PO_4^- + (1-f)\cdot(1-R-2V)HPO_4^{2-}\\&+\left(\phi\cdot f-(1-\phi)\cdot(1-f)-(1+f)\cdot R-2Q-2V\cdot(f+1)\right)\cdot HCO_3^- + (c-R)Mg^{2+}+dK^+ + (e-Q-3V)Ca^{2+}\\&+\phi\cdot\frac{9}{8}CH_4+\left(\phi\cdot\left(\frac{7}{8}-f\right)+(1-\phi)\cdot(1-f)+(1+f)\cdot R+Q+2V\cdot(f+1)\right)CO_2\\&+RMgNH_4PO_4.6H_2O+QCaCO_3+VCa_3(PO_4)_2\end{aligned}$$

(6.65)

Since the final carbonate and species concentrations have changed in the general stoichiometry, the new (post-precipitation expressions for CO_2, and HCO_3^- in the above stoichiometric equation need to replace the previous (pre-precipitation) stoichiometric expressions in the calculation of pH as shown in Section 6.4.1.

6.5 The Steady State AD Model Calibration

In this section, the steady state AD model is calibrated against experimental data from the NDBEPR WAS AD and verified by checking that during these calibrations the material (COD, C, H, O, N, P, Mg, K and Ca) mass balances are always maintained. Thereafter the model application to plant design is discussed.

6.5.1 Comparison of SS Model Results to Experimental Measurements

The steady state AD model that has been developed in this chapter is calibrated by checking how well it fits the experimentally measured AD data. In this section the steady state model

predicted results of the AD fed NDBEPR WAS is compared with measured results. However, to avoid this report being too long, all the AD systems (AD1 to AD5, described in the experimental set-up shown in Chapter 3) are included in the steady state AD model predictions, together with the dynamic model results in Chapter 7. The NDBEPR WAS was selected as a validation example in this section because it tests all aspects of the extended steady state model, including polyphosphate release and multiple mineral precipitation. An example of the steady state model, as programmed into a spreadsheet and its use in predicting AD system results and in plant design is shown in Appendix 5.

In carrying out these SS model predictions it is known that the elemental composition (X, Y, Z, A, B in $C_XH_YO_ZN_AP_B$ $qMg_cK_dCa_ePO_3$) of the active organisms dictate the quantities of AD products predicted. All elemental compositions are determined, as shown in Section 5.5.2 of Chapter 5, for each AD sludge age, using the steady state AS models such as that of Wenzel *et al.* (1990). The average of the elemental compositions obtained for all AD sludge ages is then used as input to the SS model. These selected elemental compositions, shown in Table 6.5.1, are kept the same for all R_s when predicting the AD results with the SS model. The steady state model predicted results are compared with the experimental data in Figure 6.5.1 and the corresponding Tables 6.5.1b and c below.

Table 6.5.1a: Parameters used to Calculate the AD predictions with the Steady State AD Model

	Component		UPO	PAOs	OHOs	ER	FBSO	USO
Sludge Feed components Elemental composition	Biomass	C	1.00	1.00	1.00	1.00	1.00	1.00
		H	1.421	1.454	1.454	1.421	2.004	1.648
		O	0.542	0.357	0.357	0.542	0.660	0.511
		N	0.060	0.227	0.227	0.060	0.058	0.135
		P	0.012	0.031	0.031	0.012	0.005	0.030
	Poly-phosphate	q		1.10				
		c		0.31				
		d		0.32				
		e		0.03				
Kinetic Constants	k_M	1.951	Where • k_M (given in gCOD/gCOD.d) and K_S (in gCOD/*l*) are the respective kinetic constants of saturation kinetics, obtained as shown in Section 6.1 and 6.2.2.4. • Y_{AD} is the AD organism yield coefficient (mol/mol) and b_{AD} (/d) is its endogenous respiration rate (see Section 6.2.1).					
	K_S	9.109						
	Y_{AD}	0.113						
	b_{AD}	0.041						
Reactor Volume	V	16 litres	The reactor volume is maintained at 16 litres, apart from the 60-day R_s where the volume is reduced to 5 litres.					
Weak Acid Dissociation Constants	pK'_{C1}	6.31	The weak acid dissociation constants, Henry's law constant and minerals solubility products were obtained from literature sources (e.g. Truesdell and Jones, 1973; Loewenthal *et al.*, 1994) and adjusted for Debye Hückel effects to account for the activity of ions in low salinity water (Butler *et al.*, 1964).					
	pK'_{C2}	10.25						
	pK'_{P2}	7.18						
	pK'_n	8.95						
	pK'_a	38.64						
Henry's Law constant	pK_H	1.61						
Solubility Products for Mineral precipitation	Struvite (R)	2.51E-13						
	ACP (V)	3.47E-26						
	Calcite (Q)	3.80E-09						
AD Temperature (in °C)		34.85						

Table 6.5.1b: Influent Results for NDBEPR WAS Steady State AD Model Vs Experimental Data										
Retention Time (d)	10		18		25		40		60	
Influent flow (l/d)	1.60		0.67		0.50		0.30		0.09	
	Exp	Model	Exp	Model	Exp	Model	Exp	Model	Exp	Model
S_{ti} (mgCOD/*l*)	9355.4	9415.4	10061.8	10043.4	9589.4	9561.7	10126.7	10128.9	10417.9	10417.9
S_{upi} (mgCOD/*l*)	5051.9	5453.2	5433.4	5782.9	5178.3	5500.5	5468.4	5842.1	5625.7	6006.7
S_{usi} (mgCOD/*l*)	36.3	36.3	29.4	29.4	37.4	37.4	14.7	14.7	29.9	29.9
S_{bpi} (mgCOD/*l*)	4267.2	3925.8	4599.0	4231.1	4373.8	4023.9	4643.6	4272.1	4762.3	4381.3
S_{bsfi} (mgCOD/*l*)	0.0	0.0	0.0	0.0	0.0	0.0	0.0	0.0	0.0	0.0
S_{asi} (mgCOD/*l*)	0.0	0.0	0.0	0.0	0.0	0.0	0.0	0.0	0.0	0.0
Influent TKN (mgN/*l*)	550.5	533.6	598.6	575.2	596.4	546.8	576.2	580.1	670.1	586.4
Filtered TKN (mgN/*l*)	5.6	3.8	5.4	6.5	6.0	6.0	5.9	5.9	6.7	6.7
FSA (mgN/*l*)	1.9	1.9	5.0	5.0	4.6	4.6	5.0	5.0	5.1	5.1
H_2CO_3 Alk mg/*l* as $CaCO_3$	-	150.0	-	150.0	230.0	150.0	-	150.0	-	150.0
Influent pH	7.9	8.0	-	8.0	7.6	8.0	-	8.0	-	8.0
TP (mgP/*l*)	866.6	866.6	914.5	914.5	988.5	855.2	838.0	838.0	921.9	853.2
Filtered TP (mgP/*l*)	19.0	19.7	22.8	20.4	38.6	25.3	19.9	19.5	21.1	19.8
OP (mgP/*l*)	18.8	18.8	19.6	19.6	24.8	24.8	16.4	16.4	18.9	18.9
TSS (mg/*l*)	8595.9	8595.9	9175.6	9175.6	9882.0	9882.0	9494.5	9494.5	9870.8	9882.1
VSS (mg/*l*)	6482.4	6482.4	6921.2	6921.2	6582.8	6582.8	6990.5	6990.5	7168.4	7179.7
ISS (mg/*l*)	2113.5	2113.5	2254.4	2254.4	3299.2	3299.2	2504.0	2504.0	2702.4	2702.4
Magnesium (Mg, in mg/*l*)	235.7	235.7	290.9	290.9	289.5	299.0	313.1	251.8	279.3	279.3
Filtered Mg (mg/*l*)	89.2	74.5	59.6	121.4	74.1	142.7	81.8	100.9	93.2	126.0
Potassium (K, in mg/*l*)	400.0	400.0	494.0	494.0	442.3	442.3	447.9	447.9	401.8	401.8
Filtered K (mg/*l*)	95.0	128.2	80.6	208.2	98.7	178.8	75.4	193.5	98.1	143.4
Calcium (Ca, in mg/*l*)	50.7	50.7	54.0	54.0	58.5	58.5	52.9	52.9	56.4	56.4
Filtered Ca (mg/*l*)	12.3	22.6	22.8	24.5	27.2	31.3	21.8	26.6	21.1	29.7

Table 6.5.1c: Effluent Results and Mass Balance Calculations for NDBEPR WAS Steady State AD Model Versus Experimental Data										
Retention Time (d)	10		18		25		40		60	
	Exp	Model	Exp	Model	Exp	Model	Exp	Model	Exp	Model
S_{te} (mgCOD/*l*)	7519.8	7923.9	7234.6	7419.8	6953.9	6701.3	6375.5	6688.5	5625.7	6006.7
S_{upe} (mgCOD/*l*)	5051.9	5453.2	5433.4	5782.9	5178.3	5500.5	5468.4	5842.1	29.9	29.9
S_{use} (mgCOD/*l*)	36.3	36.3	29.4	29.4	37.4	37.4	14.7	14.7	29.9	29.9
S_{tse} (mgCOD/*l*)	36.3	36.3	29.4	29.4	37.4	37.4	14.7	14.7	424.4	648.6
S_{bpe} (mgCOD/*l*)	2431.6	2434.4	1771.8	1607.6	1738.3	1163.5	892.4	831.7	0.0	0.0
S_{bsfe} (mgCOD/*l*)	0.0	0.0	0.0	0.0	0.0	0.0	0.0	0.0	0.4	0.0
S_{ase} (mgCOD/*l*)	8.0	0.0	24.7	0.0	12.7	0.0	24.7	0.0	589.1	586.4
TKN (gN/*l*)	596.4	533.6	589.1	575.2	596.4	546.8	602.0	580.1	294.0	225.3
Filtered TKN (mgN/*l*)	92.3	86.3	147.0	155.2	184.6	157.2	219.1	224.4	282.9	223.8
FSA (mgN/*l*)	88.9	84.3	141.5	153.6	177.8	155.8	210.7	223.5	853.2	853.2
TP (mgP/*l*)	912.8	866.6	914.6	914.5	855.2	855.2	886.2	838.0	470.5	439.2
Filtered TP (mgP/*l*)	509.4	555.8	459.9	529.1	466.9	444.7	477.1	458.4	422.8	438.4
OP (mgP/*l*)	492.1	554.8	458.7	528.3	460.4	444.2	469.6	455.4	6566.1	7865.4
TSS (mg/*l*)	7209.9	6855.3	7395.0	7292.9	7199.4	8335.3	6727.0	7420.0	4182.1	4600.3
VSS (mg/*l*)	5042.6	5453.6	4933.0	5110.8	4759.7	4608.6	4319.8	4615.3	2273.1	3265.1
ISS (mg/*l*)	2167.3	1401.8	2462.0	2182.1	2439.8	3726.7	2407.3	2804.7	927.4	846.9
H_2CO_3 Alk mg/*l* as $CaCO_3$	247.3	557.4	317.3	690.9	639.0	611.8	749.5	809.4	5625.7	6006.7
pH	6.7	6.6	6.9	6.6	6.8	6.5	7.0	6.6	7.1	6.6
Magnesium (Mg, in mg/*l*)	225.2	235.7	296.7	290.9	299.0	299.0	251.8	251.8	274.3	279.3
Filtered Mg (mg/*l*)	24.1	91.4	24.1	72.2	25.1	48.4	25.6	21.0	24.8	19.4
Potassium (K, in mg/*l*)	348.5	400.0	394.8	494.0	400.3	442.3	376.6	447.9	404.8	401.8
Filtered K (mg/*l*)	325.7	400.0	362.5	494.0	372.4	442.3	369.0	447.9	382.3	401.8
Calcium (Ca, in mg/*l*)	42.8	50.7	43.2	54.0	39.8	58.5	26.1	52.9	48.6	56.4
Filtered Ca (mg/*l*)	41.6	50.6	28.8	54.0	26.8	58.5	20.0	52.9	45.7	56.4
Gas production (litres)	4.2	1.3	1.9	1.4	1.0	1.2	0.5	0.9	0.3	0.2
p_{CO2} (atm)	0.4	0.2	0.4	0.3	0.4	0.3	0.4	0.3	0.4	0.3
COD balance (%)	99.7	100.0	98.9	100.0	99.6	100.0	97.1	100.0	92.5	100.0
Nitrogen balance (%)	108.3	100.0	98.4	100.0	100.0	100.0	104.5	100.0	87.9	100.0
Phosphorous balance (%)	105.3	100.0	100.0	100.0	86.5	100.0	105.8	100.0	92.6	100.0
Mg balance (%)	95.5	100.0	102.0	100.0	103.3	100.0	80.4	100.0	98.2	100.0
K balance (%)	87.1	100.0	79.9	100.0	90.5	100.0	84.1	100.0	100.7	100.0
Ca balance (%)	84.5	100.0	79.9	100.0	68.0	100.0	49.4	100.0	86.3	100.0

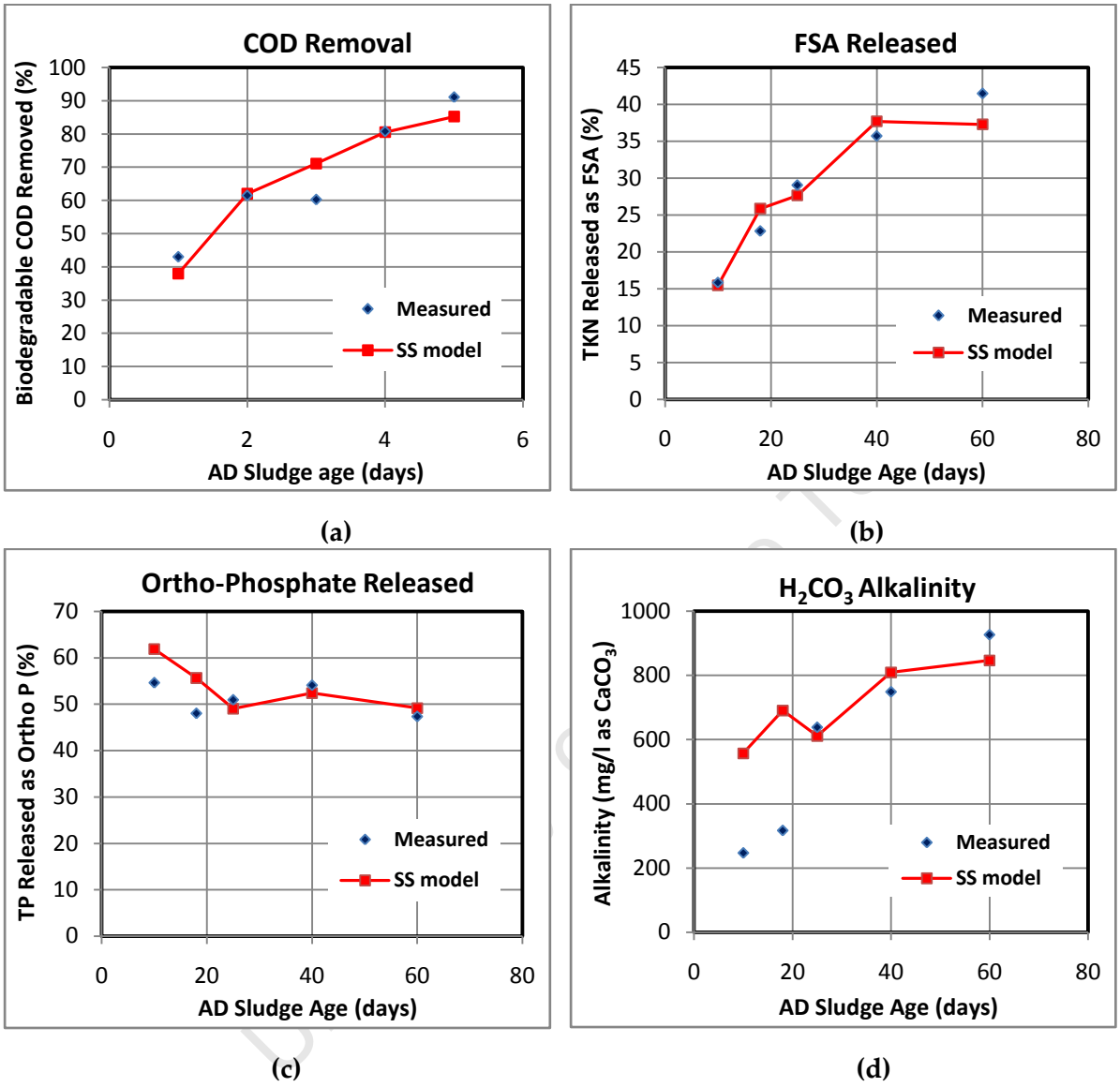

Figures 6.5.1a to d: *Comparison between the steady state model predicted results and experimentally measured data for the AD of NDBEPR WAS, in the order of: (a) COD removal, (b) FSA released, (c) OP released and (d) H_2CO_3* alkalinity.*

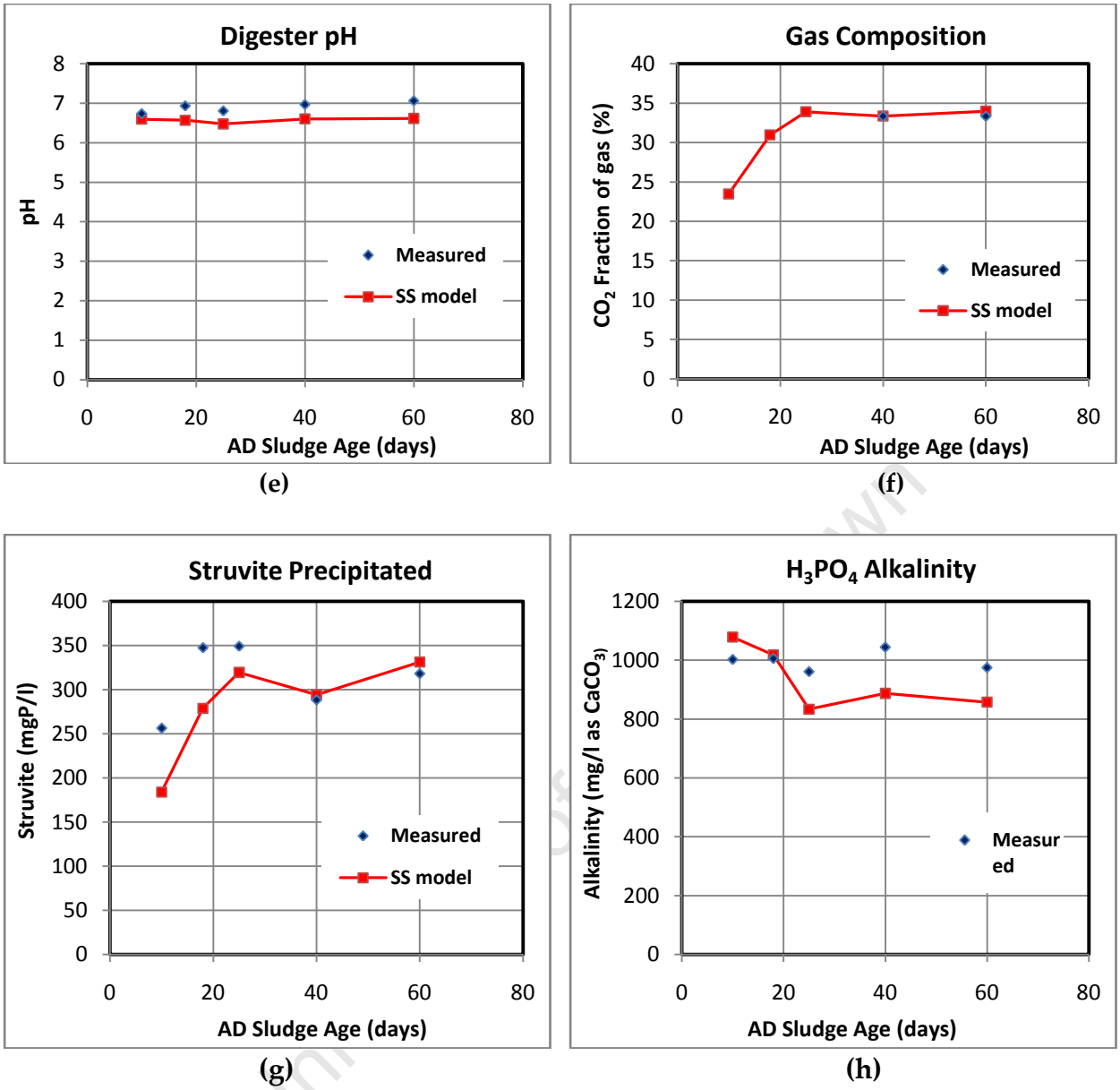

Figures 6.5.1e to h: *Comparison between the steady state model predicted results and experimentally measured data for the AD of NDBEPR WAS, in the order of: (e) pH, (f) gas composition, (g) Struvite precipitated and (h) H_3PO_4 alkalinity.*

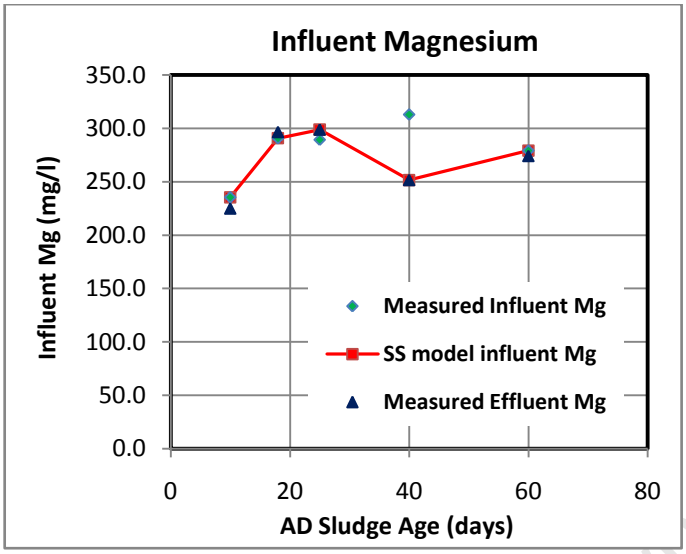

Figures 6.5.1i: *Comparison between the steady state model input Mg feed concentration value and experimentally measured influent and effluent Mg concentration for NDBEPR WAS AD.*

As noticeable in the Figure 6.5.1, the model predicted COD removal, FSA releases and OP releases have a reasonably good correlation to the experimentally measured results. This confirms that the determined hydrolysis kinetic constants calibrated in Section 6.2.2.4 (see Tables 6.2.4f and g) work well to predict the degradation of biodegradable organics (apart from the 25-day R_s data of Figure 6.5.1a, which does not conform to the trend of the other COD removal results). For the AD of sludge that is not P-rich (without PP content or P precipitation), the good predictions of COD removal and proper characterisation of the N and P content of biodegradable organics, simplifies the model predictions of the anaerobic digestion liquor (ADL) FSA and OP concentrations. This is because the production of OP and FSA in the ADL would depend on the quantity of N and P bound in biodegradable organics of the feed sludge and the extent of degradation of these biodegradable organics in the AD. However, in this AD system, the P released at all R_s largely depends on the quantity of PP available in the feed sludge, since PP was observed to have been released and hydrolysed (to form OP) much faster than organically bound P (which also had significantly less quantity of P than PP). Section 6.3.2 provides more detail on the release of this P and how it is captured in the AD model. In the AD of WAS (and also PS) organically bound N is usually released in

the non-ionic NH_3 form (which is a non-reference species for the ammonia weak acid/base system). On its release, the NH_3 picks up a H^+ ion, supplied by the dissolved CO_2 ($H_2CO_3^*$) in the bulk liquid, to form HCO_3^- i.e.:

$$NH_3 + H_2CO_3 \rightarrow NH_4^+ + HCO_3^- .$$

(6.5.6)

The production of this HCO_3^- is usually the main generation of alkalinity in an AD treating PS or WAS that is not P rich, hence during model calibration there can be a trade-off between the predicted alkalinity generated and FSA released in these systems. However, this is not the case in this digester treating BEPR WAS since, significant quantities of $H_2PO_4^-$ and HPO_4^{2-} are also produced to contribute, together with HCO_3^-, to the total alkalinity (see Equations 6.4.7a to e). Moreover, the quantity of this HCO_3^-, $H_2PO_4^-$ and HPO_4^{2-} in the AD aqueous phase depends on how the PP is released during AD (see Equations 6.40.4 to 6.40.7). Despite this, the occurrence of struvite precipitation takes up some of the ADL OP and FSA, also decreasing the total alkalinity and so resulting in re-speciation of the inorganic carbon system, which causes a change in the carbon dioxide partial pressure (p_{CO2}) and a lower AD pH (Loewenthal *et al.*, 1994) (see Section 6.4.2).

$$Mg + NH_4^+ + PO_4^{3-} \rightarrow MgNH_4PO_4$$

(6.5.7)

Therefore, the rapid release of significant quantities of OP from PP and the utilisation of some of this OP in the precipitation of struvite explains why the OP release results seem to be within the region of 50% rather than increasing with R_s as COD removal and FSA release. If the same feed component concentrations were entered to this steady state AD model, the struvite precipitation would increase with increase in sludge age. This is because increased sludge age results in more ammonia (NH_4^+) to be formed, with greater degradation of biodegradable organics, increasing the ionic product of the molar activity of Mg^{2+}, NH_4^+ and PO_4^{3-} in solution, hence promoting more struvite precipitation. However, since FSA and OP are normally available in this AD system, it is usually the availability of Mg^{2+} that limits the

struvite precipitation potential. Therefore, the variation in influent Mg^{2+} is what influenced the irregular trend (rather than an expected steady increasing trend) of struvite precipitation with R_s. Figure 6.5.1i shows how the Mg^{2+} input concentration trend is similar to that of struvite precipitation. It can be noted that in the 40-day R_s, the measured influent Mg^{2+} is significantly higher than that of the effluent (about 80 % Mg^{2+} balance was obtained over the AD system). In this case, the measured effluent Mg^{2+} was considered to give a better representation of the model input Mg^{2+} value, since it worked better with the measured results of struvite precipitation and OP release.

It is notable in Figure 6.5.1 that although the COD removal, pH and FSA releases are reasonable matched, the H_2CO_3* alkalinity (mainly from HCO_3^- production) is not well matched for the 10 and 18 day Rs. In the AD model the increase in struvite precipitation causes reduction of HCO_3^-, also it is notable that if the model prediction of struvite precipitation was increased, it would result in better matches (lower predicted values) for the OP releases and H_2CO_3* alkalinity in the 10 and 18 day R_s. However, this would also result in significantly lower pH and FSA values. Also, in Figure 6.5.1, the H_3PO_4 alkalinity are under predicted for the 25, 40 and 60d R_s. This makes the measured H_3PO_4 alkalinity values seem spurious, because it is expected that reasonable predictions of OP and pH (which are used in the model to calculate H_3PO_4 alkalinity) should also result in good predictions of H_3PO_4 alkalinity. Therefore there has to be a trade off between having further increases in the struvite precipitation to cause further reductions in H_2CO_3* alkalinity, H_3PO_4 alkalinity, OP, FSA and pH.

Considering the systems' complexity of interrelated variables and allowing for the possibilities of error in experimental data (both from the AS systems used in characterising the AD influent and the AD systems, which did not get 100% mass balances, see Chapter 5) the overall results show that the steady state AD model gives satisfactory predictions of AD performance when fed NDBEPR WAS.

Harding *et al.* (2011) report the following observations in the model stoichiometry, for 1 mol/*l* WAS BPO digested:

(1) The COD of the CH_4 is defined by the COD of the biodegradable organics (minus the very small amount, 2-5% of COD in the AD biomass produced). CH_4 and biomass are the only two AD products that have COD.

(2) The C content of the organics defines the C in the CO_2 and CH_4 (minus the very small amount of C in the biomass).

(3) The C not included in CH_4 becomes CO_2, either dissolved CO_2 (HCO_3^-) or gaseous CO_2.

(4) The N content of the biodegradable organics (minus the very small amount in AD biomass) produces NH_4^+. The N released in the breakdown of organics is released as NH_3. This is not the reference species for the FSA (N_T) weak acid/base system so the alkalinity increases by the concentration of NH_3 released (= a mol/*l*). However, in the 6-8 pH range of ADs, the NH_3 reacts with CO_2 (and H_2O) to form HCO_3^- so the total alkalinity (T.Alk) remains unchanged but transfers from the N system to the HCO_3^- of the IC system.

(5) When organic P is released from the breakdown of organics, it is released as H_3PO_4. This is the reference species for the OP system so the T.Alk does not change. However, in the 6-8 pH range of ADs the H_3PO_4 will react with HCO_3^- to form CO_2, so the total alkalinity remains the same but there is a transfer of alkalinity from the HCO_3^- of the IC system to the $H_2PO_4^-$ and HPO_4^{2-} species of the OP system. So the release of organic P decreases the H_2CO_3*Alk, which increases the CO_2 that exits the AD as gas, increasing the p_{CO2} of the gas but the aqueous T.Alk remains unchanged.

6) When polyphosphate is hydrolysed, it is released as $H_2PO_4^-$ i.e. $(Mg_cK_dCa_e)PO_3 + H_2O \rightarrow cMg^{2+}+dK^{+}+eCa^{2+}+H_2PO_4^-$. The $H_2PO_4^-$ is not the reference species for the OP system and so increases the T.Alk by q mmol/ℓ per mmol PP released. Some of the $H_2PO_4^-$ reacts with HCO_3^- to form HPO_4^{2-}, H_2O and CO_2. In this exchange, again the T.Alk remains constant (a+q) but it causes an additional transfer of alkalinity from the HCO_3^-

of the IC system to the HPO_4^{2-} of the OP system. This further increases the CO_2 that exits the digester as gas and so increases the p_{CO2} of the AD gas.

(7) So from 5 and 6, with the release of OrgP and PP, the CO_2 from the organics that remains dissolved as HCO_3^- decreases while the CO_2 exiting as gas increases. Because the methane gas is fixed by the COD of the organics, the increased CO_2 gas increases the partial pressure of CO_2 (p_{CO2}).

(8) If dissociated VFA were fed to the AD (h mol/*l*), then alkalinity would be generated by this also (h mol/*l*), i.e. $Ac^- + H_2O + CO_2 \rightarrow HAc + HCO_3^-$. This is because the acetoclastic methanogens utilise only the associated form of VFA (HAc).

(9) From 4, 6 and 8, alkalinity is generated only by the release of N and PP by the organics and utilization of dissociated VFA, i.e. ΔT. Alk = a+q+h mol/*l*. These 3 alkalinity generating processes (plus the influent Alk) establish the T.Alk in the AD.

(10) The other processes, like the release of OP from the breakdown of organic P (5) and the release of PP, which remains as $H_2PO_4^{-2}$ (6), do not change the T.Alk, only the species that represent it.

(11) The T.Alk generated (= a+q+h mol/*l*) and hence the AD pH is completely defined by the composition of the organics digested and the type of bioprocess, in this case methanogenesis, which itself does not generate alkalinity like sulphate reduction does (Poinapen and Ekama, 2010).

(12) With struvite precipitation, the T.Alk (in mol/*l*) decreases by 3x the struvite precipitated because the PO_4^{3-} is $3H^+$ away from the H_3PO_4 reference species and NH_4^+ is reference species. If all the Mg precipitates as struvite, the T.Alk decreases by 3qc mol/*l*. This decrease in T.Alk results in a re-speciation of the species that represent T.Alk and if the T.Alk is already low (due to the organics N content a being low and pH < 7) then the HCO_3^- decreases. This results in less CO_2 retention in the aqueous phase and p_{CO2} increases. So with struvite precipitation the p_{CO2} increases and the AD pH decreases. With complete Mg precipitation as struvite, the final T.Alk (mol/*l*)=

influent T.Alk +(a+q+h)–3cq (mol/*l*). So struvite precipitation with the co-released Mg from PP virtually nullifies the increase in T.Alk from the $H_2PO_4^-$ release {(q-3cq) = q(1-3c) = q(1-3x0.27) = 0.19q mol/*l*}.

6.5.2 Application of the Steady State AD Model in Design

The most important factor in a successful (most economical and attractive in terms of operability, maintainability and safety) design of an integrated WWTP facility is ensuring that the facility is able to meet the required effluent quality criteria to ensure environmental sustainability. Moreover, it is also important to consider the upstream and downstream effects that each unit process of the plant design has on the performance of the overall WWTP scheme. The steady state plant-wide AD model can be useful in the design of such a WWTP scheme because it is able to predict, given known influent characteristics, the removals of biodegradable COD, carbon (C), hydrogen (H), oxygen (O), nitrogen (N) and phosphorus (P) and to track the unbiodegradable organic and inorganic material, which cannot be removed but add to the total settleable solids (TSS), hence affect the system volumes, retention times and sludge production.

Presented in Appendix 5 is an example of the steady state (assuming constant load and flow conditions) AD model spreadsheet and its use in the design of a wastewater treatment plant (WWTP) for COD, C, H, O, N and P removal. In this example the activated sludge (AS) system volume requirements, oxygen demand and sludge production are calculated, using known influent sewage characteristics and the specified system sludge age. With increased sludge age, it is known that the active fraction of the WAS decreases but the mass of total sludge in the reactor and oxygen consumption increases. Moreover, an AS system treating raw sewage is known to require more oxygen and larger reactor sizes than one treating settled sewage. Other aspects also considered in the plant design include evaluating the impact on design requirements and effluent quality at recycling liquors from the downstream AD unit processes to the upstream AS system.

The WWTP framework for this demonstration are the WWTP layouts of the experimental systems of this investigation i.e. (1) the treatment of raw sewage with an NDBEPR system (described in Section 2.3.2.2 of Chapter 2) with anaerobic digestion (AD) of its waste activated sludge (WAS); (2) the treatment of settled sewage with the NDBEPR system and the AD of its primary sludge and WAS separately and (3) the treatment of settled wastewater with the same NDBEPR system but with the AD of its primary sludge and WAS blended together. The results obtained from the most favourable design of each of these examples shall thereafter be discussed.

The examples are intentionally focused on AD design, because a major objective of this thesis was to develop and incorporate the three phase AD into the plant-wide steady state model. However, it should be noted that anoxic-aerobic digestion (AerD) is also suitable as a tertiary treatment process for WAS, because it is able to deal with the high N and P sludge concentrations through nitrification-denitrification and promoting P precipitation (Mebrahtu *et al.*, 2010). High N and Phosphorus (P) also occurs in AD of P-rich sludge, hence with careful monitoring of the AD and controlled precipitation the AD process can be beneficial in treating secondary sludge. The excess N released from the AD process is commonly treatable later using the SHARON –ANAMMOX process (Volcke *et al.*, 2006). Table 2.5 in Section 2.4.4.1 of Chapter 2 shows more about the comparison between AD and AerD treatment processes.

In these simplified design examples, the main design parameters include the sludge age (R_s) and the reasonably selected AS and AD sludge concentrations. Thus for the specified AS sludge age, the AS system volume requirements, oxygen demand, sludge production, sludge active fraction and effluent prediction are determined using the steady state (SS) formulations of an NDBEPR system (developed by Wentzel *et al.*, 1990; see Section 2.3.2.2). Also, for a specified AD sludge age, the AD volume requirements and the quantities of COD, C, H, O, N and P removed are predicted using the SS model (developed in this chapter, see Sections 6.1 to 6.4). This shows how the SS AD model can be used to aid in predicting system

requirements for production of completely stabilised sludge and effluent that complies with advancing environmental standards.

6.6 CLOSURE

The material (COD, C, H, O, N, P, Mg, K and Ca) mass balance based three phase (solid – aqueous –gas) steady state model for the anaerobic digestion (AD) of primary and secondary sludge from biological nutrient removal (BNR) plants treating municipal wastewater has been developed by modifying the existing steady state AD model for primary sludge of Sötemann *et al.* (2005). This model has been described according to its developed sections, i.e.:

1. COD based kinetics of hydrolysis part from which the concentration of biodegradable COD utilized and methane and sludge production are determined for a given AD sludge age.
2. A COD, C, H, O, N, P and charge mass balance stoichiometry part from which gas production and composition (or partial pressure of CO_2), NH_4^+ released, biomass produced and alkalinity generated (HCO_3^-, $H_2PO_4^-$ and HPO_4^{2-}) are calculated from the biodegradable COD removal.
3. A three phase mixed inorganic carbon (IC) and ortho-phosphate (OP) weak acid/base chemistry part from which the digester pH and mineral precipitation is calculated.

The sludge hydrolysis section of the AD model was a modification of the one developed by Sötemann *et al.* (2005), with the addition of the hydrolysing biodegradable organics of primary sludge (PS) and secondary sludge (or waste activated sludge, WAS) blends, and also the hydrolysis of WAS from nitrification-denitrification (ND) and nitrification-denitrification biological excess phosphorus removal (NDBEPR) systems. As was done by Sötemann *et al.* (2005), four kinetic equations (first order, specific first order, Monod and saturation kinetics) are proposed and evaluated, in modelling the hydrolysis /acidogenesis process in AD.

The process used to determine the constants in the hydrolysis rate equations require the initial determination of S_{bpe}, r_{HYD}, and Z_{AD} parameters (which are calculated using b_{AD} and adjusted Y_{AD} and measured COD values, see Equations 6.20, 6.13 and 6.18 respectively) are first determined for the different R_s at which the ADs were operated (i.e. 10, 18, 25, 40 and 60 days). These values are then applied in the calculation of kinetic constants for the four kinetic equations that are used to model the sludge hydrolysis in AD (i.e. Equations 6.01 to 6.04).

It was found that the determined constants of k_h and k_H (for first order and specific first order kinetics respectively) usually increased approximately linearly with increase in retention time (R_s), so the slope (m) and intercept (c) of this linear relationship were determined by linear regression.

The Monod and Saturation kinetic constants (k_m, K_s, k_M and K_s) were obtained for a selected range of influent COD unbiodegradable fraction ($f_{SL'up}$) values, using a curve-fitting programme like Curve Expert or through linearization of the rate equations and linear regression over the sludge age range. The linearization and regression was performed using three different linearization methods i.e. Lineweaver-Burke (or Inversion), double reciprocal and Eadie-Hofstee (Lehninger, 1977). The correlation coefficient (R^2) was calculated for each of the four methods (i.e. the three linearization methods and the non-linear method, using the Curve Expert program), with each $f_{SL'up}$ fraction of influent organics, such that the $f_{SL'up}$ that yielded the highest R^2 value is accepted to be the best estimate of the $f_{SL'up}$ value. When necessary, various R_s data would be omitted in certain linearization methods to improve the R^2 values. The averages of the kinetic constants obtained by the three linearization methods for the reasonably high average R^2 values were then evaluated by checking how well these kinetic constants predicted the S_{bpe} concentrations as compared with the experimentally measured results. The kinetic constants that best predicted S_{bpe} concentrations were accepted as the best hydrolysis rate kinetic constants for the organics.

It was observed in Section 6.2.2, from the plots of r_{HYD}, spec r_{HYD}, k_h and k_H for the various sludge types, that the first order kinetics do not have a consistent relationship with sludge

age, hence are not ideal to model the AD of sludge under various R_s. However, the Monod or saturation kinetics, obtained using selected data for improved correlation values, can be used over the range of all sludge ages.

The Monod and saturation kinetic constants, calibrated from the measured experimental AD data for the various primary and secondary municipal sludge types are listed in Table 6.2.6a. It is noted that each sludge type has unique hydrolysis rate kinetic constants, as a result of their dissimilar trends in specific hydrolysis rates, with increasing residual biodegradable particulate organics (S_{bpe}), as shown in Figure 6.2.6a. However, the following Figure 6.2.6b shows that the measured percentage of biodegradable COD removed with sludge age for each of the AD systems does not exhibit a significant difference between the PS and WAS degradation rates, hence the AD of PS-WAS blended did not have a significant impact on the hydrolysis rate of WAS compared with the AD of the WAS by itself. A further confirmation on how the different sludge types have similar rates of biodegradable COD removal, is shown by similarities in linear curvatures of the graphs in Figure 6.2.6c, which presents a comparison of the predicted COD removals for the various sludge types, using the determined kinetic constants. This Figure 6.2.6c also shows how the various sludge types have different unbiodegradable particulate fractions.

The next section of this chapter the AD model stoichiometry and Weak acid/base chemistry part is presented. Previously, Sötemann *et al.* (2005a) had developed a C, H, O, N and COD mass balance based stoichiometry, in a two phase steady state model, using the method described by McCarty (1975). This stoichiometric model was extended by Harding (2009) with the addition of biomass P and PP in NDBEPR WAS, hence to a COD and C, H, O, N, P, Mg, K and Ca steady state mass balance based stoichiometric model.

Harding (2009) performed this extension to the model by splitting the OP released from biomass P and PP between HPO_4^{2-} and H_2PO^{4-} (which almost entirely make-up OP in the pH range of 5 to 9, i.e. within the pH bounds of steady state AD operation that normally is between 6.5 and 8) and including the function of these P products in the establishment of

digester pH, together with the inorganic carbon (IC) system via the aqueous phase equilibrium chemistry that exists in the AD. In the model of Harding (2009), all the PP is released (even at the low operating AD R_s) and the quantity of organic P released is directly related to the quantity of P bound in the portion of organics degraded. The amount of HPO_4^{2-} and H_2PO^{4-} predicted from this released OP is dependent on the molar concentration of protons [H^+] and therefore digester pH (see Equations 6.33 and 6.34a, b and c). The final stoichiometric Equation for AD of NDBEPR WAS developed by Harding (2009) is given by Equation 6.35a (for biomass degradation) and 6.35b (for PP release and hydrolysis).

To extend application of the stoichiometric model by Harding (2009) for its application also to biodegradable organics of PS, which are likely to have significant concentrations of SCFA (deemed in the model to all be acetate) in the influent, the reaction stoichiometry of Sötemann *et al.* (2005) for the utilisation of undissociated and dissociated acetate species by methanogenic AD biomass (however, without AD sludge production) was added separately.

Because the hydrolysis of PP during AD causes release of Mg^{2+} (and K^+ and Ca^{2+}) and P, which when in high concentrations cause the precipitation of struvite and consequently changes in the weak acid/base chemistry for the prediction of the AD p_{CO2}, H_2CO_3* alk alkalinity and pH, three phase (solid-liquid-gas) weak acid/base stoichiometry required inclusion to the AD model. Also, although all the PP eventually gets released in AD at a very short sludge age (less than 10 days), the distinct behaviour of PAOs in the AD was studied further and the stoichiometry also extended to include the initial release of PP with the anaerobic uptake of acetate and storage of PHA, as would happen in the NDBEPR system. The fraction of PP released in the anaerobic reactor of the NDBEPR system in the experimental set up of this project was about 65 to 75%; it was deemed possible that similar quantities would be initially released in the AD in this way (i.e. with uptake of acetate), but this quantity was parameterised and would require calibration using the AD partial pressure and alkalinity results. Because the PAOs require alternating anaerobic and aerobic conditions for their growth, they do not compete with the AD biomass for acetate, but eventually die at

a rate much faster than the hydrolysis of their biomass, releasing all remaining PP (the release of this remaining PP with death of PAOs was already available in the stoichiometric model of Harding (2009)) and PHA (which in the modified stoichiometric model is broken down by AD organisms to carbon dioxide and methane (see Equation 6.39.5)). Thus, the Equation 6.35b, which was the generalized stoichiometric model for PP release developed by Harding (2009) is extended to Equation 6.40.7.

The minerals that are likely to precipitate in the NDBEPR AD are (1) calcium phosphate ($Ca_3(PO_4)_2$), (2) calcium carbonate ($CaCO_3$) and (3) struvite ($MgNH_4PO_4$) (Musvoto *et al.*, 2000).

To determine the quantity of precipitant that can be formed during AD requires comparing the calculated ionic product of the soluble AD products with the thermodynamic solubility product (K_{spm}) of the potential precipitant. This Chapter presents the methods used in determining the precipitation potentials of struvite, calcium phosphate and calcium carbonate in the steady state model. The final general AD post-precipitation stoichiometric equation is given by the sum of Equation 6.35a (for biomass utilization) and an extension of Equation 6.40.7 for PP release to the Equation 6.65, which includes the changes (from aqueous to solid phase) in the various precipitated species. This final stoichiometric equation also considers the complexity of the weak acid/base chemistry, which includes both the inorganic C and P systems, whose species concentrations are intricately related to each other within the AD post-precipitation stoichiometry. Therefore, expressions are also included to accommodate the changes in CO_2, and HCO_3^- and for the prediction of pH after precipitation in the AD model.

After its preparation, the steady state AD model was calibrated against experimental data from the NDBEPR WAS AD and verified by checking that during these calibrations the material (COD, C, H, O, N, P, Mg, K and Ca) mass balances are always maintained.

It is noted that this model can be used individually and is also compatible to be linked with the steady state activated sludge UCT models (such as that developed by Wentzel *et al.* (1990)

for NDBER AS systems) in the construction of a plant-wide-AD steady state model. The model can be a useful aid in making design choices for the AD and/or for the entire wastewater treatment plant (i.e. in predicting the effluent quality for given influent flows and material loads and sizing of unit processes).

CHAPTER 7: THREE PHASE PLANT-WIDE DYNAMIC MODEL DEVELOPMENT

7.1 INTRODUCTION

Dynamic wastewater treatment plant models are tools that incorporate direct links between the plant inputs (wastewater) and outputs (treated effluents) using ordinary and partial differential equations, which seek to mimic reaction mechanisms. They can be implemented using recently developed computational platforms (or instrumentation-programming software packages) which provide efficient methods of dealing with numerical analysis (Copp, 2002).

Due to technological advancements and the continuous demands for optimisation of energy and resource use, dynamic models can be valuable tools that complement steady state models, for wastewater treatment plant operators and designers. The uses of dynamic models include:

1. Forecasting the performance of the wastewater treatment plant: This includes predicting effluent quality and assessing the effects of recycling products from one unit operation on another and on the system as a whole. Moreover, the impact of plant upsets and recovery time can be predicted.
2. Explaining the behavioural performances that occur within a wastewater treatment plant, hence train operators through illustrating the effects that various operating decisions have on plant performance.
3. Evaluation of the system responses to dynamic conditions: This may include assessing the plants' response to various process control strategies, changes in material flows and loads and/or adjustments that would cater for operational necessities (such as taking one unit operation off-line for maintenance). This not only ensures that

important decisions are made based on the extent of performance variations but also enables the periodic refinement of overall treatment strategies.

4. To establish better design and operational procedures through the evaluation of various optimization scenarios that can result in significant cost savings while still meeting effluent quality requirements.

The creation of a dynamic model involves ensuring that reactions that are representative of the fundamental system processes are identified and coded, such that the model is mathematically tractable and capable of providing realistic predictions. The coding of these reactions requires appropriate selection and quantification of the kinetics (rate-concentration dependence) and the stoichiometry (relationship of one component to another in a process reaction) of each major system process. The Gujer matrix provides a concise and flexible structure, into which the kinetics and stoichiometry of the system processes can be coded. This matrix comprises rows and columns, whereby each row represents a system process and each column represents a component that may partake in single or multiple system processes. The reaction rates of processes are displayed on the right side of the Gujer matrix on the same row as the stoichiometric coefficients in the matrix. Negative stoichiometric coefficients represent utilization and positive stoichiometric coefficients represent production of the relevant component. Continuity may be checked by moving across the matrix, provided consistent units have been used because then the sum of the stoichiometric coefficients must be zero i.e. all masses (CHONP, COD and charge) must be balanced within each process (horizontal row) which can be checked by adding the particular mass component of each stoichiometric coefficient/formula in the row. The Gujer matrix allows rapid and easy recognition of the fate of each component which aids in the calculation of material mass balances for each component, within a given system boundary (e.g. a completely mixed reactor).

This chapter presents the dynamic models of the unit operations that are linked to construct a plant-wide model through their description, verification and calibration.

The dynamic models that are extended and/or linked to achieve this are:

1. The ionic speciation model (Brouckaert *et al.*, 2010). This model includes pairing of ionic components and inter-phase transfers of component species.
2. The ASM2-3P model: This is the Activated Sludge Model 2 (ASM2, Henze *et al.*, 1995), modified to include the ionic speciation model (Brouckaert *et al.*, 2010) and the Inorganic Settleable Solids (ISS) model of Ekama and Wentzel (2004).
3. The ADM-3P Model: This is the University of Cape Town Anaerobic Digestion Model 1 (UCTADM1), modified to include the hydrolysis of multiple organic sludge types (PS, ND WAS, NDBEPR WAS and PS-WAS blends), the Ekama and Wentzel (2004) ISS model and the Brouckaert *et al.* (2010) speciation model which facilitates ionic speciation and multiple mineral precipitation.
4. An integrated plant-wide dynamic model, which combines the above-mentioned models 2 and 3.

7.2 UNIVERSALLY SELECTED MODEL COMPONENTS

A step towards the construction of the plant-wide aerobic and anaerobic digestion model was to select a general set of components, which will be universal to all the unit processes of the plant. These components were entered in mass concentrations (with the units of milligrams per litre) but further provisions were made to parameterise the component descriptions in terms of their COD and molar concentrations (molalities). These parameterised values were useful in formulating some of the models' stoichiometric coefficients and variables. For example, it was necessary to express some of the components in molar concentrations, e.g. [H_2CO_3], to model the carbon dioxide (CO_2) partial pressure with the weak acid/base chemistry section of the model.

Setting up the COD, C, H, O, N and P mass balances, over the unit operations and the whole WWTP to be modelled, required knowledge of each component's composition formulation. All components included in the model have distinct chemical composition formulations enabling direct calculation of the molar and material (COD, C, H, O, N and P) masses. The inorganic and some organic (VFA) components have known composition, but other organic components (i.e. the seven organism groups and the sewage FBSO, USO, BPO, UPO, see Table 7.2.1) were given parameterized (variable) compositions in the general form ($C_XH_YO_ZN_AP_B$), so their compositions can be entered as model inputs. Therefore, the elemental molar ratios (i.e. the X, Y, Z, A and B values) of their composition formulations were coded as model parameters to cater for the variability in sewage characteristics. All organism groups (aerobic and anaerobic) were given the same elemental formulation of $C_{X\_o}H_{Y\_o}O_{Z\_o}N_{A\_o}P_{B\_o}$, where each organism component (or species) is taken to represent a "surrogate" of its kind performing a particular function of interest, as has generally been accepted in WWTP modelling (Henze *et al.*, 1995). As already mentioned in Chapter 5 of this report, the organism biomass elemental formulation was experimentally measured, in the NDBEPR system to be, on average, $C_{1.0}H_{1.45}O_{0.36}N_{0.23}P_{0.03}$ (equivalent to $C_{4.8}H_7O_{1.73}N_{1.11}P_{0.14}$), which is different from that of wastewater organics and PS ($C_{3.5}H_7O_2N_{0.196}P_{0.01}$, Sötemann *et al.*, 2005b). Phosphorus accumulating organisms (PAOs, denoted in the model as PAO) are known to store polyphosphate (PP, denoted as PP), hence their generic formula is as for ordinary heterotrophic biomass (OHO) but extended to include the PP, i.e. ($C_{1.0}H_{1.45}O_{0.36}N_{0.23}P_{0.03}$·q($Mg_{0.c}K_dCa_ePO_3$)), where q is the PP content of PAOs in mol/mol and c, d and e the Mg, K and Ca content of PP). Table 7.21 presents the set of universally selected model components. The subscripts in the elemental formulae for the generic organics are adjustable parameters in the model.

Table 7.2.1: The Universally Selected Model Components			
	Component Name	**Empirical formula**	**Notation**
Total Dissolved Ionic Concentrations	Water	H_2O	H_2O
	Hydrogen ion	H^+	H
	Sodium	Na^+	Na
	Potassium	K^+	K
	Calcium	Ca^{2+}	Ca
	Magnesium	Mg^{2+}	Mg
	Ammonium	NH_4^+	NH_4
	Chloride	Cl^-	Cl
	Acetate	CH_3COO^-	Ac
	Propionate	$CH_3CH_2COO^-$	Pr
	Carbonate	CO_3^{2-}	CO_3
	Sulphate	SO_4^{2-}	SO_4
	Phosphate	PO_4^{3-}	PO_4
	Nitrate	NO_3^-	NO_3
Soluble Organics	Dissolved hydrogen	H_2	H_2
	Dissolved oxygen	O_2	O_2
	Unbiodegradable Soluble Organics	$CH_{Yu}O_{Zu}N_{Au}P_{Bu}$	USO
	Fermentable Biodegradable Soluble Organics	$CH_{Yf}O_{Zf}N_{Af}P_{Bf}$	FBSO
	Glucose	$C_6H_{12}O_6$	GLU
Particulates	Unbiodegradable particulate organics	$CH_{Yup}O_{Zup}N_{Aup}P_{Bup}$	UPO
	Biodegradable particulate organics	$CH_{Ybp}O_{zbp}N_{Abp}P_{Bbp}$	BPO
	Primary sludge biodegradable particulate organics	$CH_{Ybps}O_{Zbps}N_{Abps}P_{Bbps}$	BPO_{PS}
	Polyphosphate	$K_{kp}Mg_{mp}Ca_{cp}PO_3$	PP
	Poly-hydroxy-alkanoate	$C_4H_6O_2$	PHA
	Struvite	$MgNH_4PO_4.6H_2O$	Struv
	Calcium Phosphate	$Ca_3(PO_4)_2$	ACP
	K-struvite	$MgKPO_4.6H_2O$	MgKP
Microorganism Biomass	Ordinary heterotrophic organisms	$CH_{Yo}O_{Zo}N_{Ao}P_{Bo}$	OHO
	Phosphate accumulating organisms	$CH_{Yo}O_{Zo}N_{Ao}P_{Bo}$	PAO
	Autotrophic nitrifying organisms	$CH_{Yo}O_{Zo}N_{Ao}P_{Bo}$	ANO
	Acidogens	$CH_{Yo}O_{Zo}N_{Ao}P_{Bo}$	Z_{AD}
	Acetogens	$CH_{Yo}O_{Zo}N_{Ao}P_{Bo}$	Z_{AC}
	Acetoclastic Methanogens	$CH_{Yo}O_{Zo}N_{Ao}P_{Bo}$	Z_{AM}
	Hydrogenotrophic methanogens	$CH_{Yo}O_{Zo}N_{Ao}P_{Bo}$	Z_{HM}
	Endogenous residue	$CH_{ye}O_{ze}N_{ae}P_{be}$	ER
	Inorganic settleable solids		ISS
Gases	Carbon dioxide	CO_2	CO_2
	Methane	CH_4	CH_4

7.3 IONIC SPECIATION ROUTINE AND INTERPHASE TRANSFERS

The ionic speciation routine, contained in the three phase AD model (Brouckaert *et al.*, 2010a) provides a general algebraic approach to modelling the very rapid ionic dissociation and ion pairing equilibrium reactions separately from the slower biological and physical processes and can be applied to any combination of mixed weak acid/base systems. Because the weak acid/base chemistry processes for precipitation and gas exchange are slow, they are included with the slow bioprocesses, which are modelled with kinetic equations. The algebraic-based ionic equilibrium model can be readily integrated with models incorporating kinetics for biologically mediated unit processes that occur in the WWTP, provided the interaction between these and weak acid/base species is known.

The ionic speciation and physical inter-phase transfer processes included in the model are briefly described below.

7.3.1 Ionic Speciation

As already described in Section 6.4.1 of Chapter 6, the concentrations of ionic species belonging to various weak acid/base sub-systems that are simultaneously present in solution, and govern pH, are governed by sets of aqueous phase equilibrium dissociation and mass balance equations (such as those described by Equations 6.41 and 6.42).

Since total concentrations are the appropriate quantities to use in material balance calculations, Brouckaert *et al.* (2010) included the total species components (shown in Table 7.2.1) to represent the total concentrations of the various weak acid/base systems concerned, e.g. CO_3 represents CO_3^{2-} plus HCO_3^- plus H_2CO_3 plus various other aqueous ion pair (not precipitates) carbonate complexes present in the solution, such as $MgCO_3$ and $CaHCO_3^+$. The ion pairs that can be formed are listed in Table 7.2.2.

Table 7.2.2: Ionic Species Selected for the Three Phase Modelling					
1	H^+	Hydrogen ion	**23**	$NH_4SO_4^-$	Ammonium sulphate
2	Na^+	Sodium	**24**	$MgPO_4^-$	Magnesium phosphate
3	K^+	Potassium	**25**	$CaCH_3COO^+$	Calcium acetate
4	Ca^{2+}	Calcium	**26**	$CaCH_3CH_2COO^+$	Calcium propionate
5	Mg^{2+}	Magnesium	**27**	$CaHCO_3^+$	Calcium bi-carbonate
6	NH_4^+	Ammonium	**28**	$NaSO_4^-$	Sodium sulphate
7	Cl^-	Chloride	**29**	$MgHPO_4$	Magnesium hydrogen phosphate
8	CH_3COO^-	Acetate	**30**	CH_3COONa	Sodium Acetate
9	$CH_3CH_2COO^-$	Propionate	**31**	H_2CO_3	Di-hydrogen carbonate
10	CO_3^{2-}	Carbonate	**32**	$MgSO_4$	Magnesium sulphate
11	SO_4^{2-}	Sulphate	**33**	HPO_4^{2-}	Hydrogen phosphate
12	PO_4^{3-}	Phosphate	**34**	NH_3	Ammonia
13	NO_3^-	Nitrate	**35**	$MgCO_3$	Magnesium carbonate
14	OH^-	Hydroxide ion	**36**	$ACPO_4^-$	Calcium Phosphate
15	CH_3COOH	Acetic acid	**37**	$MgHCO_3^+$	Magnesium hydrogen carbonate
16	CH_3CH_2COOH	Propionic acid	**38**	$CaHPO_4^-$	Calcium hydrogen phosphate
17	HCO_3^-	Bi-carbonate	**39**	$NaCO_3^-$	Sodium carbonate
18	$CaSO_4$	Calcium sulphate	**40**	$MgH_2PO_4^+$	Magnesium di-hydrogen phosphate
19	$H_2PO_4^-$	Di-hydrogen phosphate	**41**	$NaHCO_3$	Sodium hydrogen carbonate
20	$MgCH_3COO^+$	Magnesium acetate	**42**	$NaHPO_4^-$	Sodium hydrogen phosphate
21	$MgCH_3CH_2COO^+$	Magnesium propionate	**43**	$CaOH^+$	Calcium hydroxide
22	$CaCO_3$	Calcium carbonate	**44**	$MgOH^+$	Magnesium hydroxide

The forty-four ionic species were selected to represent the distribution of the mixed weak acid/base system species and ion pairs that can form from the 14 ionic components shown in Table 7.2.1. The 14 ionic components are total solution concentrations as sums of their representative species used for the determination of material balances in the model. The ionic speciation reactions in the aqueous phase are solved algebraically and so are considered to reach equilibrium instantaneously at each time step because they are much faster than the biological and phase transfer reactions occurring in the anaerobic digester. Thus, the model instantly redistributes weak acid/base species including the hydrogen ion (H^+) for the direct

calculation of pH but keeps the fast and slow processes separate to avoid solver instability and reduce model runtimes.

Ionic speciation involves the determination of each of the species concentrations within weak acid/base subsystems existing in a solution, through the disaggregation of total ionic concentrations. Noting that a number of the models' reaction processes depend on the concentration of the speciated rather than the total solution concentrations, the algebraic speciation model is solved at each time step interval of the dynamic simulation. This makes the rates of the ionic speciation reactions in the aqueous phase, which are many orders of magnitude faster than the bioprocess, gas stripping and precipitation process reactions occurring in a biological reactor, effectively instantaneous. Therefore, the weak acid/ base subsystems that are present in solution are deemed to remain in a state of chemical equilibrium, whereby the speciated equilibrium composition of the solution is completely determined by the total concentrations, temperature and pressure. In summary, the model calculations involve using differential mass balances to determine component total concentrations directly produced or utilized in the kinetic/stoichiometric processes, and applying these to equilibrium speciation calculations for the determination of the detailed ionic concentrations of the weak acid/base systems, including the water system from which pH is calculated.

The more detailed principles of ionic speciation calculations are set out in Stumm and Morgan (1996). The concentrations of the 44 ionic species are related to the total concentrations of the 14 components by a set of 14 stoichiometric balances, together with a set of 30 equilibrium relationships. The equilibrium relationships are formulated in terms of species activities, which are related to their concentrations by activity coefficients. Activity coefficients were modelled using the Davies equation (Stumm and Morgan, 1996), which is an empirical extension of the Debye-Hückel theory that is used in the adjustment of stability constants for ionic strength effects and temperature of non-ideal solutions.

$$-\log f\pm = 0.5 \cdot a_1 \cdot a_2 \cdot \left(\frac{\sqrt{I}}{1+1.5\sqrt{I}} - 0.301 \right)$$

(7.0.0)

Where:

- $f\pm$ is the mean molal activity coefficient of the electrolyte that dissociates into ions
- a_1 and a_2 are the charges of the ions into which the electrolyte dissociates
- I is the ionic strength

The second term, 0.301 reduces to zero as ionic strength decreases to zero, but becomes progressively significant as the concentration of the solution increases.

The Table 7.2.3 gives an example of a set of equilibrium and mass balance equations used in the ionic speciation subroutine.

Table 7.2.3: Example for Equilibrium and Mass Balance Equations for Ionic Speciation

Weak Acid Sub-System	*Aqueous Phase Equilibrium Equations	Mass Balance Equation
Ammonia	$[NH_3] = \frac{K_{NH_4} \cdot [NH_4^+]}{(H^+)}$ $[NH_4SO_4^-] = \frac{[SO_4^{2-}][NH_4^+]}{K_{NH_4SO_4}}$	$N_T = [NH_4^+] + [NH_3] + [NH_4SO_4^-]$

*Where (H^+) is the hydrogen ion activity, [X] the molar concentrations of species X and $K_{X'}$ is the thermodynamic equilibrium constant for species X, adjusted for Debye Hückel effects to account for the activity of ions in low salinity water (Stumm and Morgan, 1996).

In developing the speciation model, Brouckaert *et al.* (2010) used for its validation the MINTEQA2 modelling software (Allison *et al.*, 2009) available from the United States Environmental Protection Agency. MINTEQA2 was useful because it has an extensive and critical user-base and is expected to provide reliable results within its range of applicability. The MINTEQA2 simulations of a range of ionic compositions, which could be encountered in

an anaerobic digestion unit process, were used to choose which species to include in the model and also validate algebraic ionic speciation model outputs.

The ionic speciation model forms an important part of the extended three phase AS and AD models (ASM-3P and ADM-3P). To include this ionic speciation model in ASM-3P and ADM-3P, required coding the ionic speciation routine (containing the aqueous phase equilibrium and mass balance reactions, example shown in Table 7.2.3) in a separate C++ file, which is then linked to the WEST® (the platform that was used for developing the ASM-3P and ADM-3P models) model-base. This separate coding was done to alleviate the numerical handling of these 'instantaneous' equilibrium reactions.

7.3.2 Inter-Phase Transfers

The AD model considers three phases (liquid, gas and solid) and so can simulate active gas exchange through liquid to gaseous phase evolution and multiple mineral precipitation from liquid to solid or dissolution from solid into liquid phase.

Liquid – Gaseous Phase Transfers

Six gases are considered in the model (i.e. CO_2, CH_4, H_2, NH_3, N_2 and O_2). Ammonia (NH_3) is known to have a (virtually) zero atmospheric concentration, i.e. it has an infinite sink (Sötemann *et al.*, 2005b) and its dissolution is effectively zero. Therefore, unlike the other five gases, NH_3 is not included as a model component but is calculated in the equilibrium speciation routine mentioned above in Section 7.3.1 and also described in Section 6.4.1.

Methane (CH_4) is insoluble in water (at atmospheric pressure) and is not utilized in the biological or chemical processes. It is a model component (because it does not affect pH) and is modelled to be directly produced in its gaseous phase by the AD methanogenic processes (acetoclastic and hydrogenotrophic methanogenesis). Carbon dioxide (CO_2) is significantly soluble and is evolved relatively slowly, hence needs to be modelled with the CO_2 evolution process such as that presented by Musvoto *et al.* (1997) and Sötemann *et al.* (2005) i.e.:

$$H_2CO_3^* \xrightarrow{k_{fCO2}} CO_{2(g)} + H_2O$$

(7.01a)

$$CO_{2(g)} + H_2O \xrightarrow{k_{rCO2}} H_2CO_3^*$$

(7.01b)

Where:

k_{fCO2} = CO_2 expulsion rate [mol/l.d]

k_{rCO2} = CO_2 dissolution rate [mol/l.d]

The CO_2 expulsion and dissolution were coded in the model, as a single evolution process, i.e.:

$$2H^+ + CO_3^{2-} \leftrightarrow CO_2 + H_2O$$

(7.01c)

For simulating the AD (i.e. with this CO_2 evolution process as part of the three phase AD model (ADM-3P), described in Section 7.5 below), an equilibrium constant of log K_{CO2} = 1.466 is used together with the enthalpy of reaction (Delta H) of 19700 J/mol as sourced from the MINTEQA2 database, which in turn references the NIST46.4 thermodynamic database. However, in simulating the aerobic systems (using the ASM2-3P model, described in Section 7.4 below) it is considered that, due to continuous aeration, the CO_2 aqueous and gas phase do not reach equilibrium (Sötemann *et al.*, 2005). This aeration results in CO_2 stripping, which is modelled using active CO_2 gas exchange rates by aeration.

Hydrogen (H_2) is sparingly soluble but is utilized very rapidly at an inter-organism species level by the hydrogenotrophic methanogenesis process, leaving only trace quantities of residual concentration. Therefore, rather than its direct transfer to gas phase, H_2 was modelled to remain a dissolved compound and establish a hydrogen partial pressure which influences the acidogenesis process (Sötemann *et al.*, 2005). Oxygen is also added as a dissolved compound since it is modelled to be utilized by the active organisms in its

dissolved state within aerobic (aerated) biological reactors. It is set to zero in the AD, which does not affect the COD balance of the AD or WWTP as a whole.

Liquid-Solid Phase Transfers:

In the anaerobic (AD) and aerobic digestion (AerD) unit operations, (especially those treating sludge from biological excess phosphorus removal (BEPR) systems); Magnesium, potassium and calcium can be present at sufficiently high concentrations for the occurrence of precipitation. The solids most likely to precipitate were identified by Musvoto *et al.* (2000c) as struvite ($MgNH_4PO_4$), newberyite ($MgHPO_4$), amorphous calcium phosphate ($Ca(PO_4)_2$), calcite ($CaCO_3$) and magnesite ($MgCO_3$). The ionic speciation described above plays a significant role in the dynamics of multiple mineral precipitation. This is because, as free ions (usually the least protonated) get incorporated into the precipitating minerals, other ions of the same type, bound in ion pairs, get released into the aqueous solution in the process of maintaining equilibrium in the aqueous phase. This continues to happen and influences pH for as long as the ionic product of the relevant species concentrations exceeds species concentrations of the weak acid/base subsystem.

Musvoto *et al.* (2000) modelled mineral precipitation or dissolution, with equations from Kotsoukos *et al.* (1980), in terms of five reversible reactions (one for each mineral), which are driven backwards or forwards depending on whether the solubility products of the respective minerals are exceeded by the ionic product. Although they found that newberyite, calcite and magnesite hardly precipitated at all, these three minerals were included in this plant-wide model, as well as potassium struvite for situations where NH_4^+ is low like in aerobic digestion. These mineral precipitation/dissolution reactions are given below:

1. **Struvite dissociation:**

$$6H_2O + Mg^{2+} + NH_4^{+} + PO_4^{3-} \leftrightarrow MgNH_4PO_4 \cdot 6H_2O \quad (7.02a)$$

Modelled to occur at the rate of:

$$\frac{\partial[Struv]}{\partial t} = k' r_{Struv} \left\{ \left[Mg^{2+}\right]^{\frac{1}{3}} \left[NH_4{}^{+}\right]^{\frac{1}{3}} \left[PO_4{}^{3-}\right]^{\frac{1}{3}} - K' sp_{Struv}{}^{\frac{1}{3}} \right\}^2$$

(7.02b)

2. Calcium phosphate (ACP) dissociation:

$$Ca_3(PO_4)_2 \leftrightarrow 3Ca^{2+} + 2PO_4{}^{3-}$$

(7.03a)

Modelled to occur at the rate of:

$$\frac{\partial[ACP]}{\partial t} = k' r_{ACP} \left\{ \left[Ca^{2+}\right]^{\frac{3}{5}} \left[PO_4{}^{3-}\right]^{\frac{2}{5}} - K' sp_{ACP}{}^{\frac{1}{5}} \right\}^2$$

(7.03b)

3. Magnesium potassium phosphate (MgKP) dissociation:

$$MgKPO_4 \cdot 6H_2O \leftrightarrow 6H_2O + Mg^{2+} + K^{+} + PO_4{}^{3-}$$

(7.04a)

Modelled to occur at the rate of:

$$\frac{\partial[MgKP]}{\partial t} = K' r_{MgKP} \left\{ \left[Mg^{2+}\right]^{\frac{1}{3}} \left[K^{+}\right]^{\frac{1}{3}} \left[PO_4{}^{3-}\right]^{\frac{1}{3}} - K' sp_{MgKP}{}^{\frac{1}{3}} \right\}^2$$

(7.04b)

4. Calcite ($CaCO_3$) dissociation:

$$CaCO_3 \leftrightarrow Ca^{2+} + CO_3{}^{2-}$$

(7.05a)

Modelled to occur at the rate of:

$$\frac{\partial[CaCO_3]}{\partial t} = K' r_{CaCO3} \left\{ \left[Ca^{2+}\right]^{\frac{1}{2}} \left[CO_3{}^{2-}\right]^{\frac{1}{2}} - K' sp_{CaCO_3}{}^{\frac{1}{2}} \right\}^2$$

(7.05b)

5. **Magnesite ($MgCO_3$) dissociation:**

$$MgCO_3 \leftrightarrow Mg^{2+} + CO_3^{2-}$$

(7.06a)

Modelled to occur at the rate of:

$$\frac{\partial[MgCO_3]}{\partial t} = K' r_{MgCO_3} \left\{ \left[Mg^{2+}\right]^{\frac{1}{2}} \left[CO_3^{2-}\right]^{\frac{1}{2}} - K' sp_{MgCO_3}^{\frac{1}{2}} \right\}^2$$

(7.06b)

6. **Newberyite ($MgHPO_4$) dissociation:**

$$MgHPO_4.3H_2O_{(s)} \leftrightarrow Mg^{2+} + HPO_4^{2-} + 3H_2O$$

(7.06a)

Modelled to occur at the rate of:

$$\frac{\partial[Newb]}{\partial t} = K' r_{Newb} \left\{ \left[Mg^{2+}\right]^{\frac{1}{2}} \left[HPO_4^{2-}\right]^{\frac{1}{2}} - K' sp_{Newb}^{\frac{1}{2}} \right\}^2$$

(7.06b)

The range of solubility products (pK_{SP}) used in the model for the six minerals identified above (struvite, newberyite, amorphous calcium phosphate (ACP), calcite, magnesite and potassium struvite) as likely to precipitate were found in the literature (Ferguson and McCarty, 1971; Musvoto *et al.*, 2000a).

Charge Loss and Gain

The aqueous ionic species input to the model is determined from the measured influent conductivity, temperature, pH, ortho-phosphate (OP), free and saline ammonia (FSA), NO_3^-, SO_4^{2-}, H_2CO_3 alkalinity and volatile fatty acids (VFA), where the last two were measured with the 5-point titration of Moosbrugger *et al.* (1992). These measurements allow complete speciation of the OP, FSA, VFA, inorganic carbon (IC) and water weak acid/base systems

including ion-pairing, which is executed in a pre-processor spreadsheet. All the ions of the 5 weak acid/base systems (and NO_3^-, SO_4^{2-}) do not produce sufficient ionic strength to obtain the measured conductivity, so NaCl is hypothetically added to the model influent characterisation pre-processor, to match the conductivity to the measured value. The addition of sodium chloride adds the necessary ionic strength for correct adjustment of dissociation and stability constants and solubility products and establishes the initial charge concentration associated with the measured conductivity.

The species and ions so determined comprise the total charge input to the model. With this influent charge established, the model then accounts for any charge gains or losses due to the bioprocess, physical and chemical reactions, such as mineral precipitation or ion pairing from which the output charge and pH is predicted. Together with the final weak acid/base species concentrations, this output charge is then transformed back to proton balance alkalinity parameters (for which the conductivity may be quite different due to *inter alia* mineral precipitation) with a post-processor spreadsheet to enable comparison between the predicted and measured parameters (since measured results are based on the proton balance approach) and the determination of pH. So the influent and effluent are characterised (speciated) by means of conductivity and proton balance (alkalinity) parameters (to facilitate measurement) while the model is based on charge accounting (to facilitate simulation), with transformation calculations to link them.

7.4 THE THREE PHASE ASM2 (ASM2-3P) MODEL

The Activated Sludge Model No. 2 (ASM2) from IWA Task Group (Henze *et al.*, 1995) is a widely accepted model that is broadly applied in NDBEPR system design, operation and process optimisation for activated sludge systems and is commonly used as a platform for further model development (Vanrolleghem *et al.*, 2005). The ASM2 includes the biological growth and death processes for OHO, PAO and ANO biomass (denoted in the models as OHO, PAO and ANO respectively and predicts oxygen demand and sludge production

together with storage and lysis of polyphosphate (PP) and poly-3-hydoxyalkanoates (PHA) for PAOs for strictly aerobic P uptake BEPR. The ASM2, which was developed for simulating AS systems, can also be used to simulate the aerobic digestion (AerD) because, at least theoretically, AerD is a continuation of the biomass aerobic endogenous process and the endogenous respiration rate of PAOs (b_G) was measured in long-term aerobic digestion batch tests. However, this may require calibrating the relative rates of the various processes and (if necessary) adjusting the appropriate kinetic and stoichiometric constants (Sötemann *et al.*, 2006). For instance, the release of polyphosphate by PAOs without acetate uptake may be different to the endogenous respiration rate. Mebrahtu *et al.* (2008) and Vogts *et al.* (2010) conducted aerobic digestion tests on concentrated NDBEPR WAS, in which mineral precipitation also took place, to measure this. These results will be simulated with the ASM2-3P model.

The AS model extension to ASM2-3P was based on ASM2, and not ASM2d (which is a common choice among modellers for the inclusion of P), because at this initial stage of including P into the three phase models, model selection was based on experimental system performance rather than model user performance. The experimental UCT system only demonstrated aerobic P uptake BEPR, so there was no need to use ASM2d. In addition, ASM2 stands a much stronger experimental validation base.

The ASM2 model was modified to include the inorganic settleable solids (ISS) model of Ekama and Wentzel (2004) and also the three phase ionic speciation model (described in Section 7.3) developed for the AD system. The integration of these models together with the set of universally selected components required converting the model process stoichiometry from COD-based to mass-based. The kinetic and stoichiometric coefficients for the ASM2 rates were also evaluated and transformed to be compatible with the revised components and stoichiometric process coefficients in different units. In some cases the kinetic equations, together with their included parameters, were changed to make them consistent with the components of the ASM2-3P model.

7.4.1 Model Processes

The ASM2-3P model processes, together with the modified molar stoichiometric equations, are presented below. However, it should be noted that since the model was converted to have a mass–based stoichiometry, the molar stoichiometric coefficients for each component participating in the model process reactions shown in the stoichiometric equations below, were multiplied by their relevant component molecular mass before their inclusion to the Gujer matrix based on mass (which can be found in Appendix 6). There are five influent organic components in the model, each with its own composition (X, Y, Z, A and B in $C_XH_YO_ZN_AP_B$), viz., UPO, USO, FBSO, BPO and VFA. While the VFA, FBSO, USO and UPO each have a different composition, these compositions are the same in the raw WW, PS and settled WW, but the BPO has a different composition in raw WW, PS and settled WW subject to the COD, C, H, O, N and P mass balances over the PST. Hence below BPO_{PS} is the BPO in the PS that settles out from the raw WW in the PST. The non-settleable BPO in the raw WW is the settled WW BPO_{SW}. The raw WW (BPO_{RW}) is the combined BPO_{PS} and BPO_{SW}.

1. Hydrolysis:

Hydrolysis processes are considered surface reactions, which occur when the slowly biodegradable substrates are enmeshed with the organisms, which provide hydrolytic enzymes (Dold *et al.*, 1980; Henze *et al.*, 1995). The COD of slowly biodegradable particulates (primary sludge, denoted as BPO_{PS}) is enmeshed in the sludge mass, where it is broken down to fermentable biodegradable soluble COD (FBSO). To add this process into the stoichiometry of the ASM2-3P model, it is assumed (as shown in Equation 7.10a) that the COD of the reactant (BPO_{PS}) is equal to the COD of the product (FBSO). The FBSO is released into the bulk liquid to add to the influent FBSO, which may have a different composition (different X, Y, Z, A, B in $C_XH_YO_ZN_AP_B$) than the BPO_{PS}. Any release or uptake of nutrients (N and P), carbonates or protons are speciated to add to or subtract from the ions of the bulk liquid.

$$BPO_{PS}(mgCOD/l) = FBSO(mgCOD/l)$$

(7.10a)

Thereafter, the unit particulate and soluble COD's are divided by their COD to molar mass ratios (denoted as gam_{ps} for BPO_{PS} and gam_f for FBSO) and converted to unit moles as shown in Equation 7.10 below.

$$BPO_{PS}[mol/l] = \frac{gam_{PS}}{gam_f} FBSO[mol/l]$$

(7.10b)

With this established, the stoichiometric coefficients for the other component products of the hydrolysis process can be determined using material mass balances:

- The CO_3^{2-} is obtained through the carbon mass balance over each stoichiometric reaction.
- The NH_4^+ and PO_4^{3-} are obtained using N and P mass balances respectively.
- The water (H_2O) used to maintain the oxygen mass balance.
- Finally, the hydrogen (H^+) ions produced to maintain the hydrogen mass balance over each stoichiometric reaction. The reference species selected for the weak acid/base systems involved in the bioprocesses are CO_3^{2-} for inorganic C, PO_4^{3-} for the Ortho-P, NH_4^+ for the ammonia, and H^+ and H_2O for water.

This process is given in the following molar stoichiometric reaction:

$$C_{X_{PS}} H_{Y_{PS}} O_{Z_{PS}} N_{A_{PS}} P_{B_{PS}} + \left\{ \left(\frac{gam_{ps}}{gam_f} \right) \cdot \left(Z_f - 3X_f - 4B_f \right) - \left(Z_{ps} - 3X_{ps} - 4B_{ps} \right) \right\} H_2O$$
$$\rightarrow \left(\frac{gam_{ps}}{gam_f} \right) C_{X_f} H_{Y_f} O_{Z_f} N_{A_f} P_{B_f} + \left\{ A_{ps} - \left(\frac{gam_{ps}}{gam_f} \right) \cdot A_f \right\} NH_4^+ + \left\{ B_{ps} - \left(\frac{gam_{ps}}{gam_f} \right) \cdot B_f \right\} PO_4^{3-}$$
$$+ \left\{ X_{ps} - \left(\frac{gam_{ps}}{gam_f} \right) \cdot X_f \right\} CO_3^{2-} + \left\{ 8B_{ps} - 2Z_{ps} + 6X_{ps} + Y_{ps} - 4A_{ps} - \left(8B_f - 2Z_f + 6X_f + Y_f - 4A_f \right) \cdot \left(\frac{gam_{ps}}{gam_f} \right) \right\} H^+$$

(7.10c)

However, as mentioned above, the stoichiometric coefficients of this reaction in mol/*l* require multiplication by their component molar masses to convert them to concentrations before they are used to construct the actual Gujer matrix (see Appendix 6).

Hydrolysis reactions occur at different rates, according to the different electron acceptor conditions, i.e. aerobic (oxygen available), anoxic (oxygen unavailable but nitrates available) and anaerobic (both oxygen and nitrates unavailable). The reaction rates in the model are presented below:

i. Aerobic:

$$k_h \left(\frac{O_2}{K_O + O_2} \right) \cdot \frac{\left(\frac{BPO_{PS}}{OHO} \right)}{\left(K_X \cdot \frac{MM_{BPO\_PS} \cdot gam_o}{MM_{OHO} \cdot gam_{b\,ps}} + \frac{BPO_{PS}}{OHO} \right)} \cdot OHO \qquad (7.10d)$$

Where:

- k_h is the hydrolysis rate constant (gCOD/gCOD·d)
- K_x is the saturation coefficient for particulate COD (gCOD/gCOD)
- K_o is the saturation coefficient for oxygen (gO/m^3)
- MM_{BPO_PS} is the molar mass of BPO_{PS} (g/mol)
- MM_{OHO} is the molar mass of OHO (g/mol).

ii. Anoxic:

$$k_h \cdot n_{NO_{HYD}} \cdot \left(\frac{K_O}{K_O + O_2} \right) \cdot \left(\frac{NO_3}{\frac{62}{14} \cdot K_{NO} + NO_3} \right) \cdot \frac{\left(\frac{BPO_{PS}}{OHO} \right)}{\left(K_X \cdot \frac{MM_{BPO\_PS} \cdot gam_o}{MM_{OHO} \cdot gam_{b\,ps}} + \frac{BPO_{PS}}{OHO} \right)} \cdot OHO \qquad (7.10e)$$

Where:

- n_{NO_Hyd} is the anoxic hydrolysis reduction factor relative to aerobic concentrations
- K_{NO} is the saturation coefficient for nitrate ($mgNO_3/l$)

- The K_{NO} is multiplied by 62/14 (i.e. divided by the molar mass ratio of N in NO_3) to convert it from mgN/*l* to mg NO_3/*l*.

iii. Anaerobic:

$$k_h \cdot n_{fe} \cdot \left(\frac{K_O}{K_O + O_2} \right) \cdot \left(\frac{\frac{62}{14} \cdot K_{NO}}{\frac{62}{14} \cdot K_{NO} + NO_3} \right) \cdot \frac{\left(\frac{BPO_{PS}}{OHO} \right)}{\left(K_X \cdot \frac{MM_{BPO\_PS} \cdot gam_o}{MM_{OHO} \cdot gam_{b\,ps}} + \frac{BPO_{PS}}{OHO} \right)} \cdot OHO \quad (7.10f)$$

Where:

- n_{fe} is the anaerobic hydrolysis reduction factor relative to aerobic conditions.

2. Aerobic growth of OHO:

During the aerobic growth of OHOs, the appropriate substrate (fermentable rapidly biodegradable organics, FBSO, or acetate, Ac) is taken up, together with ammonia (NH_4^+) and phosphates (PO_4^{3-}), which are used as nutrients in an environment where oxygen (the electron acceptor) is supplied. The biomass formed is given prescribed biomass C, H, O, N and P characteristics (xo, yo, zo, ao, bo in $C_{X_o}H_{Y_o}O_{Z_o}N_{A_o}P_{B_o}$), which are included as model stoichiometric parameters. The aerobic growth of OHO is modelled in ASM2 as two parallel processes, shown below, according to the substrate FBSO or VFA used:

In ASM2 (Henze *et al.*, 1995), the bio-energetics of AS organism growth are quantified in terms of the electron donating capacity parameter (COD) with each unit substrate COD distributed to the biomass (Y_H, for anabolism) and the rest (1-Y_H) to oxygen for respiration to form CO_2 (the catabolic process):

$$Y_H \cdot Substrate(mgCOD/l) = Biomass(mgCOD/l) \quad (7.11a)$$

$$(1-Y_H)\cdot Substrate(mgCOD/l) = Oxygen(\ mgO_2/l)$$

(7.11b)

Therefore,

$$\left(\frac{1-Y_H}{Y_H}\right)Oxygen(mgO_2/l) + \left(\frac{1}{Y_H}\right)Substrate(mgCOD/l) \rightarrow Biomass(mgCOD/l)\,.$$

(7.11c)

The unit substrate COD is converted to unit substrate molar concentrations by multiplying the Y_H and (1-Y_H) by the substrate (FBSO) COD to molar mass ratio (gam_f). In ASM2 (Henze *et al.*, 1995), oxygen (since it has a COD directly equal to its molar mass) is already included as a mass component. However, to convert the COD of biomass formed to moles, requires further division of the Y_H by the biomass COD to molar mass ratio (gam_o).This gives us

$$Substrate[mol/l] = \frac{gam_o}{Y_H \cdot gam_f} Biomass[mol/l]$$

(7.11d)

and

$$Oxygen\ (mgO_2/l) = \left(\frac{(1-Y_H)\cdot gam_o}{Y_H}\right)\cdot Biomass[mol/l]\ .$$

(7.11e)

Hence, stoichiometrically

$$\left(\frac{(1-Y_H)\cdot gam_o}{Y_H}\right)Oxygen\ (mgO_2/l) + \left(\frac{gam_o}{Y_H \cdot gam_f}\right)Substrate[mol/l] \rightarrow Biomass[mol/l]\ .$$

(7.11f)

- The CO_3^{2-} is then obtained through the carbon mass balance over each stoichiometric reaction.
- The NH_4^+ and PO_4^{3-} are obtained using N and P mass balances respectively.

- Thereafter, the H_2O used is obtained using the oxygen mass balance and the H^+ ions produced obtained is using the hydrogen mass balance over each stoichiometric reaction.

  i. The aerobic growth of OHO on FBSO, as shown in Equations 7.11g and h below:

$$\left(\frac{gam_o}{gam_f \cdot Y_H}\right)C_{X_f}H_{X_f}O_{Z_f}N_{A_f}P_{B_f} + \left\{(1-Y_H)\cdot\frac{gam_o}{Y_H}\cdot\frac{1}{32}\right\}O_2 +$$
$$\left\{A_0 - \left(A_f \cdot \frac{gam_o}{gam_f \cdot Y_H}\right)\right\}NH_4^{+} + \left\{B_0 - \left(B_f \cdot \frac{gam_o}{gam_f \cdot Y_H}\right)\right\}PO_4^{3-} + \left\{X_o - \left(\frac{gam_o}{gam_f \cdot Y_H}\right)X_f\right\}CO_3^{2-} +$$
$$\left\{\left(\frac{(2Z_f - 8B_f - 6X_f - Y_f + 4A_f)\cdot gam_o}{gam_f \cdot Y_H}\right) + \left(\frac{(1-Y_H)\cdot gam_o}{8\cdot Y_H}\right) - (2Z_o - 8B_o - 6X_o - Y_o + 4A_o)\right\}H^+$$
$$\rightarrow C_{Z_o}H_{Y_o}O_{Z_o}N_{A_o}P_{B_o} + \left\{\left(\frac{(Z_f - 4B_f - 3X_f)\cdot gam_o}{gam_f \cdot Y_H}\right) + 4B_o - Z_o + 3X_o + \left(\frac{(1-Y_H)\cdot gam_o}{16\cdot Y_H}\right)\right\}H_2O \quad (7.11g)$$

This process is modelled to occur at the rate of:

$$\mu_H \cdot \left\{\begin{array}{l}\left(\frac{O_2}{K_O + O_2}\right)\cdot\left(\frac{FBSO}{\frac{MM_{FBSO}}{gam_f}\cdot K_f + FBSO}\right)\cdot\left(\frac{FBSO}{Ac + FBSO}\right)\cdot\left(\frac{CO_3^{-}}{60\cdot K_{Alk} + CO_3^{-}}\right)\cdot \\ \left(\frac{NH_4}{\frac{18}{14}\cdot K_{NH} + NH_4}\right)\cdot\left(\frac{PO_4}{\frac{95}{31}\cdot K_P + PO_4}\right)\end{array}\right\}\cdot OHO \quad (7.11h)$$

Where:

- μ_H is the maximum growth rate of OHOs on substrate (/d);
- K_f is the saturation coefficient for growth on FBSO (mgCOD/*l*);
- K_{Alk} is the saturation coefficient for alkalinity (mol/*l*);
- K_{NH} is the saturation coefficient for ammonia (mgN/*l*);
- K_P is the saturation coefficient for phosphorus (mgP/*l*);

- MM denotes the molar mass of a component (e.g. MM_{FSBSO} denotes the molar mass of FBSO).

ii. The aerobic growth of OHOs on acetate (Ac), as shown in Equations 7.11i and j below:

$$\left(\frac{gam_o}{64\cdot Y_H}\right)CH_3COO^- + \left\{(1-Y_H)\cdot\frac{gam_o}{Y_H}\cdot\frac{1}{32}\right\}O_2 + (A_0)NH_4^+ + (B_0)PO_4^{3-} + \left\{X_o - \left(\frac{gam_o}{32\cdot Y_H}\right)\right\}CO_3^{2-}$$
$$+\left\{\left(\frac{gam_o\cdot 2\cdot(1-Y_H)}{16\cdot Y_H}\right) - \left(\frac{11\cdot gam_o}{64\cdot Y_H}\right) - (2Z_o - 8B_o - 6 - Y_o + 4A_o)\right\}H^+$$
$$\rightarrow C_{X_o}H_{Y_o}O_{Z_o}N_{A_o}P_{B_o} + \left\{4B_o - Z_o + 3X_o + \left(\frac{gam_o\cdot(2\cdot(1-Y_H)-2)}{32\cdot Y_H}\right)\right\}H_2O \quad (7.11i)$$

This process is modelled to occur at the rate of:

$$\mu_H\left\{\begin{array}{l}\left(\frac{O_2}{K_O+O_2}\right)\cdot\left(\frac{Ac}{\frac{59}{64}\cdot K_A+Ac}\right)\cdot\left(\frac{Ac}{Ac+FBSO}\right)\cdot\left(\frac{CO_3^-}{60\cdot K_{Alk}+CO_3^-}\right)\cdot \\ \left(\frac{NH_4}{\frac{18}{14}\cdot K_{NH}+NH_4}\right)\cdot\left(\frac{PO_4}{\frac{95}{31}\cdot K_P+PO_4}\right)\end{array}\right\}\cdot Xoho \quad (7.11j)$$

Where:

- K_A = saturation coefficient for acetate (mgCOD/*l*).

3. Anoxic Growth of OHO:

The anoxic growth of OHOs is similar to the aerobic growth; however nitrates (NO_3^-, denoted as NO_3) are used as the electron acceptor, instead of oxygen (O_2 denoted as O_2). In this, it is assumed that the NO_3 is reduced to N_2 gas (S_N2), which escapes into the atmosphere (the process of denitrification). The anoxic growth of OHOs is also modelled in ASM2, according to the substrate used (FBSO or VFA), as two parallel processes:

i. The anoxic growth of OHOs on FBSO, as shown in Equations 7.12a and b below:

$$\left(\frac{gam_o}{gam_f \cdot Y_H}\right)C_{X_f}H_{Y_f}O_{Z_f}N_{A_f}P_{B_f} + \left\{(1-Y_H)\cdot\frac{gam_o}{Y_H}\cdot\frac{1}{(2.86\cdot 14)}\right\}NO_3 +$$
$$\left\{A_0 - \left(A_f \cdot \frac{gam_o}{gam_f \cdot Y_H}\right)\right\}NH_4^{+} + \left\{B_0 - \left(B_f \cdot \frac{gam_o}{gam_f \cdot Y_H}\right)\right\}PO_4^{3-} + \left\{X_o - \left(\frac{gam_o}{gam_f \cdot Y_H}\right)X_f\right\}CO_3^{2-} +$$
$$\left\{\left(\frac{(2Z_f - 8B_f - 6X_f - Y_f + 4A_f)\cdot gam_o}{gam_f \cdot Y_H}\right) + \left(\frac{6\cdot(1-Y_H)\cdot gam_o}{2.86\cdot 14\cdot Y_H}\right) - (2Z_o - 8B_o - 6X_o - Y_o + 4A_o)\right\}H^+$$
$$\rightarrow C_{X_o}H_{Y_o}O_{Z_o}N_{A_o}P_{B_o} + \left\{\left(\frac{(Z_f - 4B_f - 3X_f)\cdot gam_o}{gam_f \cdot Y_H}\right) + 4B_o - Z_o + 3X_o + \left(\frac{3\cdot(1-Y_H)\cdot gam_o}{2.86\cdot 14\cdot Y_H}\right)\right\}H_2O +$$
$$\left\{(1-Y_H)\cdot\frac{gam_o}{2.86\cdot Y_H}\right\}N_2$$

(7.12a)

This process is modelled to occur at the rate of:

$$\mu_H \cdot n_{NO_{HET}} \cdot \left\{\begin{array}{l}\left(\frac{K_O}{K_O + O_2}\right)\cdot\left(\frac{S_{bsf}}{\frac{MM_{FBSO}}{gam_f}\cdot K_f + S_{bsf}}\right)\cdot\left(\frac{FBSO}{Ac + FBSO}\right)\cdot\left(\frac{CO_3^{-}}{60\cdot K_{Alk} + CO_3^{-}}\right)\cdot \\ \left(\frac{NH_4}{\frac{18}{14}\cdot K_{NH} + NH_4}\right)\cdot\left(\frac{PO_4}{\frac{95}{31}\cdot K_P + PO_4}\right)\cdot\left(\frac{NO_3}{\frac{62}{14}\cdot K_{NO} + NO_3}\right)\end{array}\right\}\cdot OHO$$

(7.12b)

Where the reduction factor for denitrification (n_{NO_Het}) accounts for the incapability of all heterotrophic organisms (OHOs) to grow on nitrate and for the reduced rate at which denitrification occurs.

ii. The anoxic growth of OHOs on Ac as shown in Equations 7.12c and d below:

$$\left(\frac{gam_o}{64\cdot Y_H}\right)CH_3COO^- + \left\{(1-Y_H)\cdot\frac{gam_o}{Y_H}\cdot\frac{1}{(2.86\cdot 14)}\right\}NO_3 + (A_0)NH_4^+ + (B_0)PO_4^{3-}$$
$$+\left\{X_o - \left(\frac{gam_o}{32\cdot Y_H}\right)\right\}CO_3^{2-} + \left\{\left(\frac{6\cdot gam_o\cdot(1-Y_H)}{2.86\cdot 14\cdot Y_H}\right) - \left(\frac{11\cdot gam_o}{64\cdot Y_H}\right) - (2Z_o - 8B_o - 6X_o - Y_o + 4A_o)\right\}H^+$$
$$\rightarrow C_{X_o}H_{Y_o}O_{Z_o}N_{A_o}P_{B_o} + \left\{4B_o - Z_o + 3X_o - \left(\frac{2\cdot gam_o}{32\cdot Y_H}\right) + \left(\frac{3\cdot gam_o\cdot(1-Y_H)}{2.86\cdot 14\cdot Y_H}\right)\right\}H_2O$$
$$+\left\{(1-Y_H)\cdot\frac{gam_o}{2.86\cdot Y_H}\right\}N_2$$

(7.12c)

This process is modelled to occur at the rate of:

$$\mu_H\cdot n_{NO_{HET}}\cdot\left\{\left(\frac{K_O}{K_O+O_2}\right)\cdot\left(\frac{Ac}{\frac{59}{64}\cdot K_A + Ac}\right)\cdot\left(\frac{Ac}{A_c+FBSO}\right)\cdot\left(\frac{CO_3^-}{60\cdot K_{Alk}+CO_3^-}\right)\cdot\left(\frac{NH_4}{\frac{18}{14}\cdot K_{NH}+NH_4}\right)\cdot\left(\frac{PO_4}{\frac{95}{31}\cdot K_P+PO_4}\right)\cdot\left(\frac{NO_3}{gam_o\cdot\frac{62}{14}\cdot K_{NO}+NO_3}\right)\right\}\cdot OHO$$

(7.12d)

4. Fermentation:

Fermentation by heterotrophic organisms is modelled to occur under anaerobic conditions and involves the transformation, by OHOs, of fermentable rapidly biodegradable substrates (FBSO) to acetate (Ac) accompanied with the release of excess nutrients (in the form of NH_4^+ and PO_4^{3-}).

The unit COD of the FBSO used is equated to that of acetate produced to establish the molar fraction of acetate produced to FBSO utilized. Thereafter, the CO_3^{2-}, NH_4^+, PO_4^{3-}, H_2O and H^+ produced are determined using C, N, P, O and H mass balances respectively over the stoichiometric reaction. The molar stoichiometric process is as shown by the Equations 7.14a and b below:

$$C_{X_f}H_{Y_f}O_{Z_f}N_{A_f}P_{B_f} \rightarrow \left(\frac{gam_f}{64 \cdot Y_H}\right)CH_3COO^- + (A_f)NH_4^+ + (B_f)PO_4^{3-} + \left\{X_f - \left(\frac{2 \cdot gam_f}{64}\right)\right\}CO_3^{2-}$$
$$+ \left\{Z_f - 4B_f - 3X_f + \left(\frac{4 \cdot gam_f}{64}\right)\right\}H_2O + \left\{8B_f - 2Z_f + 6X_f + Y_f - 4A_f - \left(\frac{11 \cdot gam_f}{64}\right)\right\}H^+$$

(7.14a)

This process is modelled to occur at the rate of:

$$q_{fe} \cdot \left\{\left(\frac{K_O}{K_O + O_2}\right) \cdot \left(\frac{FBSO}{K_{fe} \cdot \frac{MM_{FBSO}}{gam_f} + FBSO}\right) \cdot \left(\frac{CO_3^-}{60 \cdot K_{Alk} + CO_3^-}\right) \cdot \left(\frac{NO_3}{\frac{62}{14} \cdot K_{NO} + NO_3}\right)\right\} \cdot OHO$$

(7.14b)

Where:

- q_{fe} is the maximum rate of fermentation (/d)
- K_{fe} is the saturation coefficient for fermentation on FBSO (mgCOD/*l*).

5. Lysis:

In ASM2, the 'lysis' process is considered to be the sum of endogenous respiration, lysis, predation and other decay processes. In this lysis process, the death-regeneration concept is adopted for OHOs whereby a fraction (b'_H) of the organism mass dies per day and releases all its organic content together with excess nutrients (ammonia and phosphates) to the mixed liquor. A fraction of the organic content (f'_{EH} = 0.08) is unbiodegradable particulate organics and adds to the endogenous residue (ER), while the remainder (1- f_{EH}) is slowly biodegradable substrate (BPO) which goes through the same processes (enmeshment and hydrolysis) as the influent BPO_{PS}. The lysis of PAOs and ANOs is modelled in ASM2 as endogenous respiration, not death-regeneration like the OHOs. With endogenous respiration a fraction, b_G (for PAOs) and b_A (for ANOs), is lost per day. The e^- (COD) associated with the biodegradable organics of the 'lost' biomass are passed to oxygen (PAOs and ANOs are inactive under anoxic conditions, in ASM2) and the e^- associated with the unbiodegradable part of the 'lost'

biomass (f_{EG} =0.25 for PAOs, f_{EA}=0 for ANOs) accumulates as endogenous residue (ER, denoted as X_{EG} (in mgER/*l*) for PAOs and X_{EA} (in mgER/*l*) =0 for ANOs). The loss/lysis of OHOs, PAOs and ANOs is modelled in ASM2 as three separate processes, since each surrogate organism type has its own death rate. The stoichiometry that was entered to represent lysis is as shown in Equation 7.15a below, followed by the kinetics exhibited by each organism type (Equations 7.15b to 7.15d).

$$
\begin{aligned}
&C_{X_o}H_{Y_o}O_{Z_o}N_{A_o}P_{B_o} \rightarrow \left(f_{ep}\cdot\frac{gam_o}{gam_e}\right)C_{X_e}H_{Y_e}O_{Z_e}N_{A_e}P_{B_e}+\left(\left(1-f_{ep}\right)\cdot\frac{gam_o}{gam_{ps}}\right)C_{X_{ps}}H_{Y_{ps}}O_{Z_{ps}}N_{A_{ps}}P_{B_{ps}}\\
&+\left\{A_0-\left(f_{ep}\cdot\frac{gam_o}{gam_e}\right)\cdot A_e-\left(\left(1-f_{ep}\right)\cdot\frac{gam_o}{gam_{ps}}\right)\cdot A_{ps}\right\}NH_4^{+}\\
&+\left\{B_0-\left(f_{ep}\cdot\frac{gam_o}{gam_e}\right)\cdot B_e-\left(\left(1-f_{ep}\right)\cdot\frac{gam_o}{gam_{ps}}\right)\cdot B_{ps}\right\}PO_4^{3-}\\
&+\left\{X_o-\left(f_{ep}\cdot\frac{gam_o}{gam_e}\right)\cdot X_e-\left(\left(1-f_{ep}\right)\cdot\frac{gam_o}{gam_{ps}}\right)\cdot X_{ps}\right\}CO_3^{2-}\\
&+\left\{Z_0-\left(f_{ep}\cdot\frac{gam_o}{gam_e}\right)\cdot\left(Z_e-3X_e-4B_e\right)-\left(\left(1-f_{ep}\right)\cdot\frac{gam_o}{gam_{ps}}\right)\cdot\left(Z_{ps}-3X_{ps}-4B_{ps}\right)-3X_o-4B_o\right\}H_2O+\\
&\left\{\begin{array}{l}8B_o-2Z_o+6+Y_o-4A_o-\left(8B_e-2Z_e+6X_e+Y_e-4A_e\right)\cdot\left(\dfrac{f_{ep}\cdot gam_o}{gam_e}\right)\\-\left(8B_{ps}-2Z_{ps}+6X_{ps}+Y_{ps}-4A_{ps}\right)\cdot\left(\dfrac{\left(1-f_{ep}\right)\cdot gam_o}{gam_{ps}}\right)\end{array}\right\}H^+
\end{aligned}
\qquad (7.15a)
$$

With b_H, b_{PAO} and b_A as the rate constants for lysis and decay of OHOs, PAOs and ANOs biomass, the rates at which this process occurs for the various AS system organisms are:

- **OHOs:**

$$b'_H\cdot OHO \qquad (7.15b)$$

Where b'_H = 0.62/d at 20°C and f'_{EH} = 0.08 for death-regeneration.

- **PAOs:**

$$b_{PAO} \cdot PAO \tag{7.15c}$$

Where b_G = 0.04/d at 20°C and f_{EG} = 0.25 for endogenous respiration.

- **ANOs:**

$$b_A \cdot ANO \tag{7.15d}$$

Where b_A = 0.04/d at 20°C and f_{EA} = 0.0 for endogenous respiration.

6. Storage of PHA (anaerobic):

The PAO use the energy obtained from the anaerobic utilization of polyphosphate (PP), and phosphate release, to store acetate (Ac) in the form of cell internal energy storage material known as poly-hydroxy-alkanoate (PHA, $C_4H_6O_2$). The stoichiometry that was entered to represent storage of PHA, occurring with the utilization of PP and P release is as shown in Equation 7.16d below. The yield value (Y_{PO4}) is the amount of PP utilized per unit COD of PHA stored (i.e. mgP/mgCOD, as shown in the Equation 7.16 below).

$$Y_{PO4} = \frac{PP(mgP/l)}{PHA(mgCOD/l)} \tag{7.16a}$$

Because a unit mole of PP has 31 mgP and a unit mole of PHA has 144 mgCOD,

$$31 \cdot PP[mol/l] = 144 \cdot YPO_4 \cdot PHA[mol/l] \tag{7.16b}$$

and hence,

$$PP[mol/l] = \left(\frac{144}{31}\right) \cdot YPO_4 \cdot PHA[mol/l] \tag{7.16c}$$

With this established, the molar stoichiometric process of the storage of PHA is as represented by Equation 7.16d below.

$$\left(\frac{144\cdot Y_{PO4}}{31}\right)Mg_cK_dCa_ePO_3+\frac{144}{64}CH_3COO^-+2\cdot\left\{\left(\frac{144\cdot Y_{PO4}}{31}\right)-\frac{144}{64}\right\}H^+\rightarrow\left(\frac{144}{2\cdot 64}\right)C_4H_6O_2$$
$$+\left(\frac{144\cdot Y_{PO4}}{31}\right)PO_4^{3-}+\left(\frac{144\cdot Y_{PO4}\cdot c}{31}\right)Mg^{2+}+\left(\frac{144\cdot Y_{PO4}\cdot d}{31}\right)K^++\left(\frac{144\cdot Y_{PO4}\cdot e}{31}\right)Ca^{2+} \quad (7.16d)$$
$$+\left\{\left(\frac{144\cdot Y_{PO4}}{31}\right)-\frac{144}{64}\right\}H_2O$$

The process rate is given by:

$$qPHA\cdot\left(\frac{A_c}{\frac{59}{64}\cdot K_A+A_C}\right)\cdot\left(\frac{CO_3^-}{60\cdot K_{Alk}+CO_3^-}\right)\cdot\frac{PP}{K\_PP\cdot\frac{101.2}{31}\cdot\frac{gam_o}{MM_{Xpao}}+\frac{PP}{PHA}} \quad (7.16e)$$

Where,

- qPHA represents the rate constant for the storage of PHA (/d)
- K_PP is the saturation coefficient for PP.

Because the process is also known to take place in anoxic conditions, the model does not contain inhibition terms for the lack of oxygen (O_2) and the presence of nitrate (NO_3).

7. Storage of PP (aerobic):

As aforementioned, the PAOs store phosphate (PO_4^{3-}) in the form of cell internal polyphosphate (PP). This requires energy, which is gained from the aerobic respiration of PHA. The oxygen (O_2) has a negative COD per unit mol (-32 mgCOD/molO_2) and the PHA is positive (144 mgCOD/molPHA). The Y_{PHA} is the yield value corresponding to the catabolic PHA requirement for PP storage (0.2 mgCOD PHA/mgP PP). Equation 7.1.a gives the molar stoichiometric equation representing storage of PP:

$$\left(\frac{Y_{PHA}}{32}\right)O_2+\left(\frac{Y_{PHA}}{144}\right)C_4H_6O_2+PO_4^{3-}+cMg^{2+}+dK^++eCa^{2+}$$
$$\rightarrow Mg_cK_dCa_ePO_3+\left\{4\cdot\frac{Y_{PHA}}{144}\right\}CO_3^{2-}+\left\{1-\left(10\cdot\frac{Y_{PHA}}{144}\right)+\left(\frac{Y_{PHA}}{16}\right)\right\}H_2O$$
$$\left\{\left(26\cdot\frac{Y_{PHA}}{144}\right)-2-\left(\frac{Y_{PHA}}{8}\right)\right\}H^+$$

(7.17a)

The process rate is given by:

$$Q\_PP \cdot \left(\frac{O_2}{K_O + O_2}\right) \cdot \frac{PO4\_t}{PO4\_t + K\_PS \cdot \frac{95}{31}} \cdot \left(\frac{\left(\frac{PHA}{Xpao}\right)}{K\_PHA \cdot \frac{86}{144} \cdot \frac{gam_o}{MM_{Xpao}} + \frac{PHA}{Xpao}}\right) \cdot \left(\frac{CO_3^-}{60 \cdot K_{Alk} + CO_3^-}\right)$$

$$\frac{\left(K\_MAX - \frac{PP}{PHA}\right)}{\left(\left(K\_IPP \cdot \frac{101.2}{31} \cdot \frac{gam_o}{MM_{Xpao}}\right) + (K\_MAX) - \left(\frac{PP}{Xpao}\right)\right)} \cdot Xpao$$

(7.17b)

The storage of PP (molar mass 101.2) is observed to stop when the phosphorus content of the PAOs becomes too high. This has led to an inhibition term of PP storage (K_IPP) that becomes active as the ratio of PP/ PAO approaches the maximum allowable value, K_MAX.

8. Aerobic growth of PAO:

The PAO are assumed to grow under aerobic conditions (where oxygen is supplied and used as the electron acceptor) on PHA, while utilising ammonia (NH_4^+) and phosphate (PO_4^{3-}) as nutrients. The biomass formed is given the same prescribed (parameterised) biomass C, H, O, N and P characteristics as for the OHO and ANO. The PAO can also grow in anoxic conditions (with the utilization of nitrates), but this process is not included in the ASM2 model. The PAO growth molar stoichiometry is similar to that of OHO biomass, but with the substrate yield value for anabolism given as Y_{PAO}:

$$\left\{(1 - Y_{PAO}) \cdot \frac{gam_o}{Y_{PAO}} \cdot \frac{1}{32}\right\} O_2 + (A_0) NH_4^+ + (b_0) PO_4^{3-} + \left(\frac{gam_o}{144 \cdot Y_{PAO}}\right) C_4H_6O_2 +$$

$$\left\{X_o - \left(\frac{4 \cdot gam_o}{144 \cdot Y_{PAO}}\right)\right\} CO_3^{2-} + \left\{\left(\frac{(1 - Y_{PAO}) \cdot gam_o}{8 \cdot Y_{PAO}}\right) - \left(\frac{26 \cdot gam_o}{144 \cdot Y_{PAO}}\right) - (2Z_o - 8B_o - 6X_o - Y_o + 4A_o)\right\} H^+ \quad (7.18a)$$

$$\rightarrow C_{X_o} H_{Y_o} O_{Z_o} N_{A_o} P_{B_o} + \left\{\left(\frac{(1 - Y_{PAO}) \cdot gam_o}{16 \cdot Y_{PAO}}\right) - \left(\frac{10 \cdot gam_o}{144 \cdot Y_{PAO}}\right) + 4B_o - Z_o + 3X_o\right\} H_2O$$

This process is modelled to occur at the rate of:

$$\mu_{PAO} \cdot \left\{ \left(\frac{O_2}{K_O + O_2} \right) \cdot \left(\frac{CO_3^-}{60 \cdot K_{Alk} + CO_3^-} \right) \cdot \left(\frac{\left(\frac{PHA}{PAO} \right)}{K\_PHA + \frac{PHA}{PAO}} \right) \cdot \left(\frac{NH_4}{\frac{18}{14} \cdot K_{NH} + NH_4} \right) \cdot \left(\frac{PO_4}{\frac{95}{31} \cdot K_P + PO_4} \right) \right\} \cdot PAO$$

(7.18b)

Where:

- μ_{PAO} = Maximum growth rate for PAO biomass (/d).

9. Lysis of PAO storage products:

The storage products, PP and PHA are accounted for separately from the biomass PAO and hence have separate decay processes. The decay of PHA is assumed to produce acetate and that of PP produces phosphate (denoted in the model as PO_4), both processes occurring at different rates as shown below:

i. Lysis of PHA:

$$\left(\frac{1}{144} \right) C_4H_6O_2 \rightarrow \frac{1}{64} CH_3COO^- + \left\{ \frac{4}{144} - \frac{2}{64} \right\} CO_3^{2-} + \left\{ \frac{4}{64} - \frac{10}{144} \right\} H_2O + \left\{ \frac{26}{144} - \frac{11}{64} \right\} H^+$$

(7.19a)

The PHA is modelled to decay at the rate of:

$$b_{PHA} \cdot PHA \cdot \left(\frac{CO_3^-}{60 \cdot K_{Alk} + CO_3^-} \right)$$

(7.19b)

Where, b_{PHA} is the rate constant for lysis of PHA.

ii. Lysis of PP:

Although the lysis of polyphosphate (which is denoted in the model as PP) has already been included as a joint process, with the storage of PHA, it is re-entered into the model to ensure that the model captures the discrepancies between the rates of this process and that of the PHA storage:

$$Mg_cK_dCa_ePO_3 + H_2O \rightarrow PO_4^{3-} + cMg^{2+} + dK^{+} + eCa + 2H^{+} \quad (7.20a)$$

The PP is modelled to decay at the rate of:

$$b_{PP} \cdot PP \cdot \left(\frac{CO_3^{-}}{60 \cdot K_{Alk} + CO_3^{-}} \right) \quad (7.20b)$$

The PP is modelled to decay at a slower rate, b_{PP}, than the PAO biomass that stores it, to ensure that a consistent ratio of PAO to PP is maintained during the endogenous respiration that occurs in aerobic digestion but the validity of this will be checked with experimental observation.

10. Aerobic Growth of ANOs:

The autotrophic nitrifying organisms (ANOs) are assumed to grow aerobically with the process of nitrification, where ammonium (NH_4^+, which is taken as the substrate and nutrient) is oxidised to nitrate (NO_3^-, denoted as NO_3).

Although nitrification takes two steps, i.e. the conversion of ammonia to nitrite (NO_2) and nitrite to nitrate (NO_3^-), ASM2 (Henze *et al.*, 1995) models it as a single process (direct conversion of ammonia to NO_3^-). However, since the ASM2-3P model includes strict material, e^- and charge accounting, if appreciable NO_2^- concentrations are observed experimentally, the NO_2^- may require addition as an ionic component to ensure that e^- and charge are conserved.

The nitrification process is as shown in the Equation 7.21a below:

$$NH_4^+ + 2O_2 \rightarrow NO_3^- + H_2O + 2H^+$$

(7.21a)

As shown by the Equation 7.21a above, the nitrification process without biomass production uses two moles of oxygen per unit mol of nitrate produced. Thus, the oxygen requirement for each mgN of nitrate produced in this process is 4.57 (mgCOD/mgNO_3-N), but this will be slightly lower (< 1%; Ekama, 2009) when ANO biomass yield is taken into account. The catabolic energy requirement for the nitrification process corresponds to the ANO yield coefficient (Y_A, which is 0.15 mg COD ANO/mgN NH_4).

$$Y_A \cdot NH_4(mgN/l) = Biomass(mgCOD/l)$$

(7.21b)

Since there are 14 mgN in each unit mol of ammonia and gam_o is the COD per unit mol of biomass, the above equation can be re-written as:

$$NH_4[mol/l] = \left(\frac{gam\_o}{14 \cdot Y_A}\right) \cdot Biomass[mol/l]$$

(7.21c)

This is the stoichiometric coefficient for ammonia, per unit ANO biomass formed in the molar nitrification reaction.

The growth process of ANOs combines the nitrification process shown above with the utilization of carbonate, ammonia and phosphate, for the C, H, O, N and P ANO biomass requirements (i.e. their cell synthesis). The stoichiometric coefficients of these components are obtained through performing C, N and P mass balances and the H_2O used and H^+ generated is obtained using O and H mass balances.

The stoichiometry and kinetics that was used to represent this process are as shown in Equations 7.21d and 7.21e respectively:

$$\left(\frac{4.57-Y_A}{32\cdot Y_A}\cdot gam_o\right)O_2+\left(\frac{gam_o}{14\cdot Y_A}+A_0\right)NH_4{}^{+}+(B_0)PO_4{}^{3-}+(X_o)CO_3{}^{2-}+$$
$$\left\{\left(\frac{4.57-Y_A}{8\cdot Y_A}\cdot gam_o\right)-\left(10\cdot\frac{gam_o}{14\cdot Y_A}\right)-(2Z_o-8B_o-6X_o-Y_o+4A_o)\right\}H^{+}$$
$$\rightarrow C_{X_o}H_{Y_o}O_{Z_o}N_{A_o}P_{B_o}+\left(\frac{gam_o}{14\cdot Y_A}\right)NO_3{}^{-}$$
$$\left\{\left(\frac{4.57-Y_A}{16\cdot Y_A}\cdot gam_o\right)-3\cdot\frac{gam_o}{14\cdot Y_A}+4B_o-Z_o+3X_o\right\}H_2O$$

(7.21d)

This process is modelled to occur at a rate of:

$$\mu_{AUT\,7.2}\cdot\frac{O_2}{(O_2+K\_O\_AUT)}\cdot\frac{NH_4}{\left(NH_4+\left(K\_NH\_AUT\cdot\frac{18}{14}\right)\right)}\cdot\left(\frac{PO_4}{\frac{95}{31}\cdot K_P+PO_4}\right)\cdot$$
$$\frac{CO_3}{CO_3+60\cdot KALK\_AUT}\cdot\left\{2.35^{(pH-7.2)}\cdot K_I\cdot\frac{K_{\max}-pH}{K_{\max}+K_{II}-pH}\right\}\cdot X\_AUT$$

(7.21e)

The final term in {}, was added to the ASM2-3P to model the effect of pH on nitrification, following past studies (Sötemann, 2006; WRC, 1984). According to these studies, it is noted that the maximum specific growth rate of nitrifiers is very sensitive to pH, whereby nitrification rates are optimum at pH range of 7.2 to 8.5, outside which a sharp decline in μ_{AUT} is observed (Downing *et al.*, 1964; Loveless and Painter, 1968). Thus, the variation of μ_{AUT} with pH < 7.2 is modelled by WRC (1984) as $\mu_{AUT\,7.2}\cdot 2.35^{(pH-7.2)}$, where 2.35 is the sensitivity coefficient (WRC, 1984; Sötemann, 2006).

For pH > 8.5, nitrification rates have also been observed to decline and to effectively stop at a pH of 9.5 (Wild *et al.*, 1971; Antoniou *et al.*, 1990 (as Cited in Sötemann, 2005)). Therefore, Sötemann *et al.* (2005) included an additional term to model this decline with increased pH: $K_I\cdot\frac{K_{\max}-pH}{K_{\max}+K_{II}-pH}$, where K_I is 1.13, K_{max} (coefficient for maximum pH) is 9.5 and K_{II} is approximately 0.3 to best fit the literature μ_{AUT} rates.

11. Aeration

Aeration was included as a simple process whereby oxygen is the only component involved, i.e. with a stoichiometric coefficient of 1. This process is modelled at the rate of:

$$KLa \cdot (S_{O\_sat} - O_2) \tag{7.22}$$

Where KLa is the rate of oxygen transfer and S_{O_sat} is the concentration at which the oxygen is saturated.

12. Carbon Dioxide (CO_2) Evolution

The dissolved CO_2 is dealt with as part of the aqueous phase, as $H_2CO_3^*$ (a carbonate species) and as a separate gaseous phase. Equilibrium between the aqueous and gas CO_2 phases is not reached during aeration in the aerobic reactor due to its continuous generation by the bioprocess (Sötemann *et al.*, 2005). Therefore, active CO_2 gas exchange rates by aeration have been included to model CO_2 stripping from the aeration reactor, to aid in simulating the process. The molar equation that was used to represent this process in the model is given as:

$$CO_3^{2-} + 2H^+ \rightarrow CO_2(gas) \tag{7.23a}$$

With the rate of this CO_2 evolution modelled to be similar to that of Musvoto *et al.* (see Section 2.4.3.2), i.e.:

$$KLa_{CO2} \cdot ([H_2CO_3] - p_{CO2} \cdot K_{HCO2}) \tag{7.23b}$$

Where KLa_{CO2} is the CO_2 overall liquid phase mass transfer (due to aeration) rate coefficient, p_{CO2} is the partial pressure of CO_2 and K_{HCO2} is the Henry's Law constant (also described in Section 6.4.1) for CO_2 evolution.

13. Mineral precipitation

The liquid-solid transfer processes described in Section 7.3.2 were added as part of the ASM2-3P model, mainly to cater for potential phosphorus precipitation in the aerobic or anoxic-aerobic digestion of NDBEPR WAS, using the given equations 7.02 to 7.04 above.

7.4.2 Inclusion of Ekama and Wentzel (2004) ISS Model to ASM2

The principle of Gujer (1993) for calculating total settleable solids (TSS) from stoichiometric TSS/COD ratios of the individual mixed liquor organic compounds is employed in ASM2. Hence the TSS concentration is computed via stoichiometric TSS/COD ratios for the active biomass ($iTSS_{BM}$ = 0.9mgTSS/mgCOD), for slowly biodegradable particulate substrate and unbiodegradable organic matter (iTSSXs = 0.75mgTSS/mgCOD and $iTSS_{Xi}$ = 0.75 mgTSS/mgCOD respectively). Further, for the polyphosphate (PP) content of the PAOs, a ratio of 3.23 mgISS/mgP is employed to add to the solids concentration (Henze *et al.*, 2000). The difference between TSS and volatile settleable solids (VSS) is then the inorganic settleable solids (ISS). However, with the addition of ISS and PP as components in the model, new provisions can be made for tracking the effect of this on the ionic mix and conductivity. The influent ISS (silt) and clay is deemed not to take part in any reactions; hence, it simply gets enmeshed in the sludge mass and increases with sludge age. Moreover, as modelled by Ekama and Wentzel (2004), influent inorganic dissolved ions are taken up by the organism biomass as intracellular ions. These ions precipitate as ISS in the drying step of the TSS/VSS test and so in effect add to the mixed liquor ISS concentration. An ISS content of OHO and PAO (without PP) of 0.15 mgISS/mg biomass VSS was measured by Ekama and Wentzel (2004). Because the uptake of these ions by the biomass has a small effect on the conductivity, this process is not included in the model. However, the effect of the uptake and release of the metals and OP that make up PP in the PAOs on the ionic mix is included in the model. Compared with the ion exchange between the biomass and

aqueous phase, the effect of the PP is much greater, up to nine times higher, at high PAO PP content. So (1) the effect of the ion exchange between the biomass and the aqueous phase ionic matrix and conductivity was not included but (2) its affect on the reactor TSS was included by adding 0.15 (f_{iOHO} and f_{iPAO}) times the OHO and PAO biomass concentrations to the ISS arising from the influent wastewater. In contrast, the effect of the metal ion and OP exchange between the biomass and aqueous ionic matrix and conductivity and the reactor ISS concentration by the release and uptake of PP were both included in the model. So the total reactor ISS concentration comprises the ISS content of the OHO and PAO and ANO biomass (i.e. ISS_{BM} = 0.15 mgISS/mg biomassVSS), the stored PP in the PAOs, all precipitates (struvite, ACP, and $MgKPO_4$) formed and the influent ISS that is enmeshed with the sludge. This was simple to include because all components are already mass-based (given in units of mg/*l*). Moreover, the TSS is also included in the model base as a variable, which is calculated as the sum of all the aforementioned particulate components. Other lumped parameter variables that provide useful interpretation of the simulated results were also included by coding in the necessary component additions and transformation calculations. These include pH, total alkalinity (in mg$CaCO_3$/*l*), TKN and FSA (in mg N/*l*), TP, OP (in mgP/*l*), total COD (in mgCOD/*l*), VSS (in mg/*l*), and total metal concentrations (i.e. Mg, Ca, K all in mg/*l*).

7.4.3 Programmed Configuration Settings

To calibrate the ASM2-3P model, the three experimentally operated system configurations (ND and NDBEPR systems, shown in Figure 3.1 of Chapter 3) and aerobic digestion continuous reactor and batch tests conducted on the NDBEPR system WAS by Mebrahtu *et al.* (2007) were coded into the configuration editor of the WEST® programme. These configurations are shown in Figures 7.4.1 to 7.4.3 below:

1. The NDBEPR Activated Sludge System

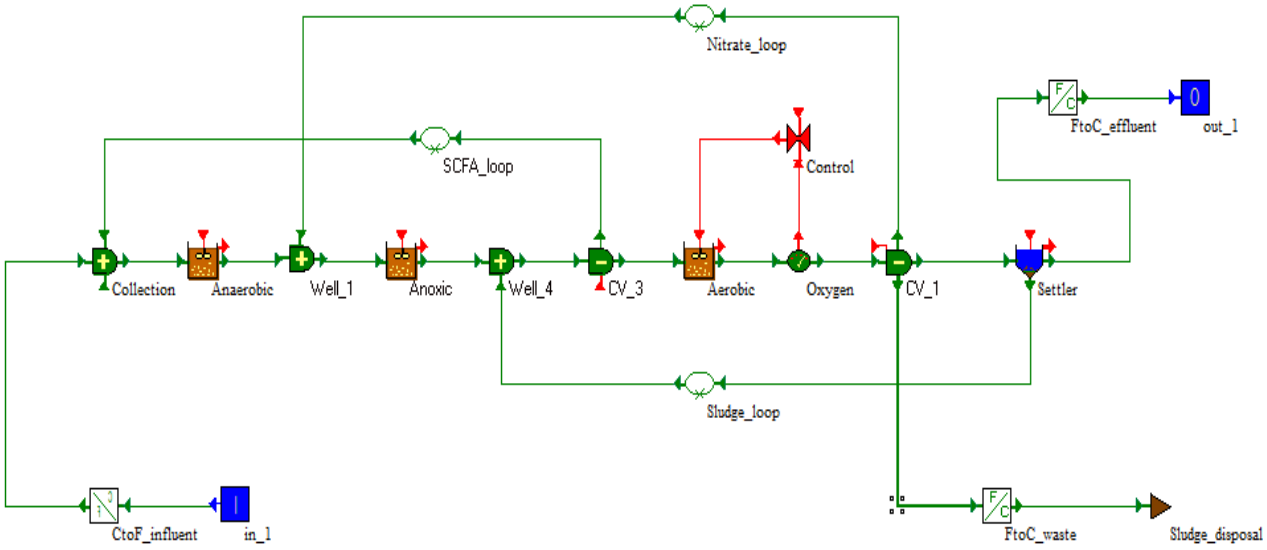

Figure 7.4.1: *Configuration settings for the simulation of the Nitrification-Denitrification Biological Excess Phosphorus removal (NDBEPR) system with the ASM2-3P model.*

2. The MLE Activated Sludge System

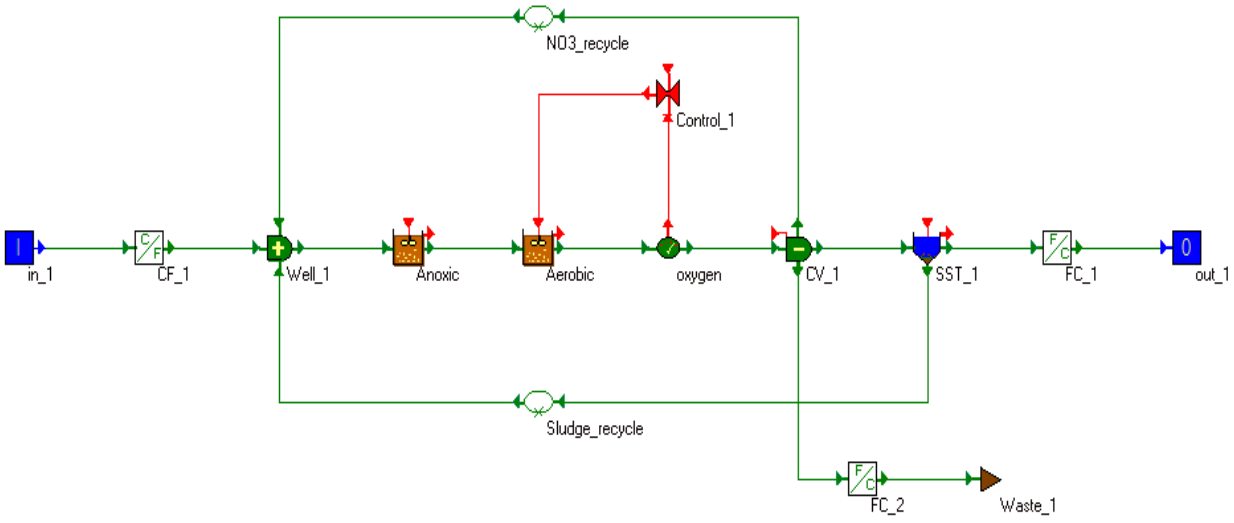

Figure 7.4.2: *Configuration settings for the simulation of the Modified Ludzack Ettinger (MLE) AS system with the ASM2-3P model.*

3. The Aerobic Digester:

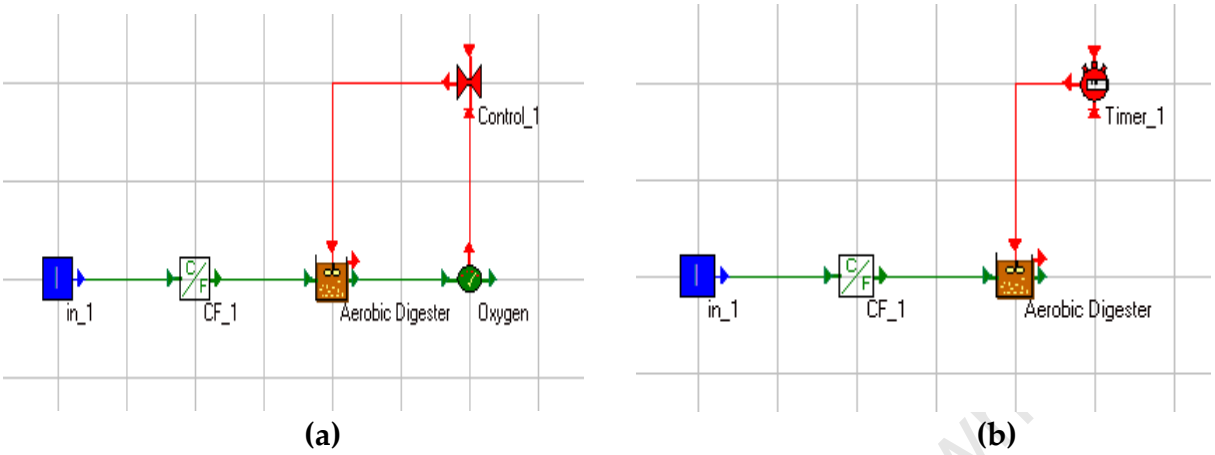

Figure 7.4.3: *Configuration settings for the simulation of the (a) aerobic digestion (AerD) and (b) anoxic-aerobic (AnAerD) digestion system with the ASM2-3P model.*

In the WEST simulation program, each icon represents a distinct in-built model that carries out a particular function of the WWTP. In the above model configurations, these icons are arranged to replicate the WWTP being modelled. The icons in the above configurations (Figures 7.4.1, 7.4.2 and 7.4.3), each of which represents a component of the WWTP model, are briefly described below:

- Input icons, which once included in the configuration indicate that a set of influent values (of prescribed units i.e. mg/*l*) shall be entered for the simulation of the unit process or plant. This incoming data, expressed in concentrations, is converted to fluxes (by multiplication by flow) by the CF icons. The FC icons do the opposite (convert fluxes into concentrations and flow) and are usually followed by an outlet icon.
- The activated sludge unit sets the boundaries for the processes that have been defined to occur in activated sludge unit operation. The fixed volume

activated sludge unit that is used in the above configurations signifies that the flows going in and out of this unit are equal.

- The secondary settling tank is modelled by what is defined in WEST® as a 'secondary point settler'. This settler is modelled to be a phase separator with no real volume, hence its retention time is not considered, and is modelled to implement only physical separation, with no biological processes included. The secondary point settler calculates its effluent particulate concentration as a fraction of its influent concentration and its underflow concentration is resolved by mass balances over the settler.
- The modelling of the recycle flows shown in the above configurations is facilitated by 'differential loop breakers'(loop breakers use iteration to solve algebraic loops, such as those caused by recycle flows, which result when the input to a sub model is directly dependent on its own output). Selecting the right recycle rates is important because as stated by Meijer *et al.* (2001), errors in flows often prove to be more sensitive to the simulation model than the model parameters themselves (i.e. hydrolysis can have a larger impact on variable change than bioprocess kinetic rates).
- Aeration control has been included in the above configurations, which the model identifies in the configuration editor as 'PI_saturation'. This icon controls the dissolved oxygen by keeping the dissolved oxygen between upper and lower limits on a proportional-integral control action (the control action is what effects a step change input and specifies the function of integration to produce the model predictions during simulation). This means that when the dissolved oxygen is within specified limits, the control action is performed with according to the proportional-integral control but limitedto a prescribed minimum or maximum value. An oxygen sensor, which is in effect a 'DO' probe, is attached to this controller to measure the dissolved oxygen

concentration in the aerobic reactors. In anoxic-aerobic digestion (using a single tank digester), a timer is used to control the supply of oxygen (during aerobic phase) and to stop the oxygen input for anoxic phases (Figure 7.4.3b).

7.4.4 Model Verification

In order to verify the model, materials mass balances must be obtained for COD, carbon (C), hydrogen (H), oxygen (O), nitrogen (N) and phosphorus (P). All model components have known material (COD, C, H, O, N and P) characteristics; hence, the total output of each material characteristic was calculated as a variable percentage and matched against its total input. Since chemical balances were achieved and used in the determination of the molar stoichiometric processes shown above (Section 7.4.1) it is expected that when simulated the results of this calculation would be 100%. However, it is also noted that some of the processes are very slow and would require very long simulations to reach steady state to achieve values close to 100% mass balance. The NDBEPR AS system was simulated for 250 days and the results presented in Table 7.4.1 below:

Table 7.4.1: Mass Balance Results for NDBEPR AS Simulation

	Input	Output	Balance
COD balance	121350.4	121323.3	100.0
Carbon (C) balance	50651.8	50589.6	99.9
Hydrogen (H) balance	8916.3	8843.3	99.2
Oxygen (O) balance	86102.5	152943.7	100.3
Nitrogen (N) balance	10760.2	10734.7	99.8
Phosphorus (P) balance	7945.5	7934.5	99.9

Because these results are very close to 100%, the model was accepted to be internally consistent and can be confidently calibrated against experimental data.

The mass balances were not exactly 100.00% due to minor integration rounding errors.

7.4.5 Model Calibration

The model calibration generally involved matching the model results to variables measured from experimental systems in this case NDBEPR, MLE and aerobic digestion (AerD) systems, each for selected steady state periods. This was done in order to establish the performance of the model and adjust the model parameters, including kinetic and stoichiometric constants.

With the Gujer matrix coded in the model editor (as shown in Appendix 6) and the WWTP configuration settings coded in the model configuration (as shown on Figures 7.4.1 to 7.4.3), trial and error simulations can be executed in the experimental environment of the (WEST®) program. However, before these simulations can be carried out, the system parameters (including sludge age, reactor volumes and interconnecting recycle flows) must be defined to represent the systems against which the model is calibrated. Moreover, for all simulations, the initial reactor concentrations for each model component need to be specified together with the influent feed component concentrations for each day of the model specified experimental period.

Initial values for suitable kinetic (such as hydrolysis, growth and lysis rates) and stoichiometric (such as composition characteristics of sewage and sludge components) constants as obtained from literature are entered, and then adjusted in successive trial and error simulations to fit the predicted results as best as possible to the observed experimental behaviour. These adjustments require knowledge of the model structure, stoichiometric processes and experimental behaviour because the model is fairly intricate and contains many parameters that can be changed. In this respect, the influent sewage and sludge characterisation are the most important part of the calibration exercise and were fine-tuned around the measured values before kinetic constants were changed. Of the many sewage and sludge types within the model, those considered in the calibration of the ASM2-3P model are OHO, PAO (together with the stored PP), ANO, endogenous residue (ER), UPO, BPO_{PS}, BPO_{SW}, USO and FBSO.

The C, H, O, N and P composition values (i.e. X, Y, Z, A and B) selected for the biomass (OHO and PAO and ANO), endogenous residue and influent WW UPO was not changed for all systems and sludge ages because the AS systems were all fed the same wastewater and the wastewater source and handling was consistent. This composition was obtained from the COD/VSS (f_{cv}), C/VSS (f_c), N/VSS (f_n) and P/VSS (f_p) ratios measured in this and previous investigations, i.e. f_{cv} = 1.48gCOD/gVSS, f_c = 0.53gC/gVSS, f_n = 0.1gN/gVSS and f_p = 0.025gP/gVSS (Ekama, 2009). However, the BPO_{PS} and FBSO were considered components that would require some characteristic adjustment, since they are more specific to each sewage batch and directly influence the extent of N and P release, which in turn affects the system stoichiometry (i.e. nitrates generated, biomass growth, alkalinity change, etc). The variable parameters that were chosen for calibration in the ASM2-3P model are shown in Table 7.4.2 below. Note that for OHOs the death-regeneration (b'_H = 0.62 and f'_{EH} of 0.08) instead of the endogenous respiration model constants (b_H of 0.24 and f_{EH} = 0.2) are used because OHO mass loss is modelled in ASM2 (and ASM1) with death-regeneration.

Table 7.4.2: Parameters used in Simulating the ASM2-3P Model			
Parameter	**Value**	**Units**	**Description**
A_bp	0.227	dUnit/dUnit	N/C: biodegradable particulate organics (BPO_{SW})
A_bps	0.033	dUnit/dUnit	N/C: PS biodegradable particulate organics (BPO_{PS})
A_e	0.062	dUnit/dUnit	N/C: endogenous residue organics (ER)
A_f	0.058	dUnit/dUnit	N/C: fermentable biodegradable soluble organics (FBSO)
A_o	0.227	dUnit/dUnit	N/C : organisms
A_up	0.062	dUnit/dUnit	N/C: unbiodegradable particulate organics (UPO)
A_us	0.135	dUnit/dUnit	N/C: unbiodegradable soluble organics (USO)
b_{AUT}	0.150	1/d	Decay rate
B_bp	0.031	dUnit/dUnit	P/C: biodegradable particulate organics (BPO_{SW})
B_bps	0.013	dUnit/dUnit	P/C: PS biodegradable particulate organics (BPO_{PS})
B_e	0.012	dUnit/dUnit	P/C: endogenous residue organics (ER)
B_f	0.005	dUnit/dUnit	P/C: fermentable biodegradable soluble organics (FBSO)
b_H	0.620	1/d	Rate constant for lysis and decay
B_o	0.031	dUnit/dUnit	P/C : organisms
b_G	0.040	1/d	Rate constant for lysis of PAO
b_PHA	0.040	1/d	Rate constant for lysis of PHA
b_PP	0.017	1/d	Rate constant for lysis of PP
B_up	0.012	dUnit/dUnit	P/C: unbiodegradable particulate organics (UPO)
B_us	0.030	dUnit/dUnit	P/C: unbiodegradable soluble organics (USO)
e_PP	0.030	dUnit/dUnit	Ca/P: Polyphosphate
F_BOD_COD	0.650	gBOD/gCOD	Conversion factor BOD/COD
f_X_IH	0.08	gCOD/gCOD	Fraction of inert COD generated in X_oHO lysis
f_X_IP	0.08	gCOD/gCOD	Fraction of inert COD generated in PAO lysis
ISS_BM	0.15	g/gCOD	ISS to biomass for OHO and PAO
$k'r_{ACP}$	0.001	/d	Dissolution of calcium phosphate
$k'r_{MgKP}$	0.001	/d	Dissolution of K-struvite
$k'r_{Struv}$	0.001	/d	Dissolution of struvite
K_A	4	-	Saturation coeff for Ac (acetate)
K_ALK	0.1	-	Saturation coeff for alkalinity (HCO3-)
K_ALK_AUT	0.5	-	Saturation coeff of autotrophs for alkalinity
k_CO2	0.1	-	Rate constant for CO2 exchange
K_F	4	-	Saturation/inhibtion coeff for growth on FBSO
K_fe	20	-	Saturation coeff for fermentation on FBSO
k_h	3	gCOD/(gCOD*d)	Hydrolysis rate constant
K_IPP	0.02	-	Inhibition coeff for PP storage
K_MAX	0.78	-	Maximum ratio of PP/PAO
K_NH	0.05	-	saturation coeff for ammonium (nutrient)

Table 7.4.2: Parameters used in Simulating the ASM2-3P Model			
Parameter	**Value**	**Units**	**Description**
K_NH_AUT	1	-	saturation coeff of autotrophs for ammonium
K_NO	0.5	-	saturation/inhibition coeff fir nitrate
K_O	0.2	-	saturation/inhibition coeff for oxygen
K_O_AUT	0.5	-	saturation/inhibition coeff of autotrophs for oxygen
K_P	0.01	-	saturation coeff for phosphorus (nutrient)
k_pa	0.38	1/d	Decay rate constant for PAO
K_PHA	0.01	-	saturation coeff for PHA
d_PP	0.32	Unit/Unit	K/P ratio in Polyphosphate
K_PP	0.01	-	saturation coeff for poly-phosphate
K_PS	0.2	-	saturation coeff for phosphorus in PP storage
K_X	0.1	-	saturation coeff for particulate COD
c_PP	0.32	Unit/Unit	Mg/P:Polyphosphate
mu_AUT	1	1/d	Maximum growth rate
mu_H	6	1/d	Maximum growth rate on substrate
mu_hm	1.2	1/d	Max specific growth rate for hydrogenotrophic methanogens
mu_PAO	1	1/d	Maximum growth rate
n_fe	0.1	-	Anaerobic hydrolysis reduction factor
n_NO_Het	0.3	-	Reduction factor for denitrification
n_NO_Hyd	0.6	-	Anoxic hydrolysis reduction factor
P_{CO2_AS}	0.3	-	Partial pressure of CO2 in the AS liquor
q_fe	3	1/d	Maximum rate for fermentation
q_PHA	3	1/d	Rate constant for storage of PHA (base: PP)
q_PP	4.5	1/d	Rate constant for storage of PP
S_O_Sat	8.9	g/m3	Oxygen saturation concentration
TempCoeff	0.0667	-	Rate temperature coefficient
Temperature	20	°C	System Temperature
Y_{AUT}	0.240	gCOD/gN	Yield For Autotrophic Biomass
Y_bp	1.454	dUnit/dUnit	H/C: biodegradable particulate organics (BPO_{SW})
Y_bps	2.469	dUnit/dUnit	H/C: PS biodegradable particulate organics (BPO_{PS})
Y_e	1.567	dUnit/dUnit	H/C: endogenous residue organics (ER)
Y_f	2.004	dUnit/dUnit	H/C: fermentable biodegradable soluble organics (FBSO)
Y_H	0.670	gCOD/gCOD	Yield For Heterotrophic Biomass
Y_o	1.454	dUnit/dUnit	H/C : organisms
Y_G	0.670	-	Yield coeff (biomass/PHA)
Y_PHA	0.200	-	PHA requirement for PP storage
Y_PO	0.400	-	PP requirement (S_PO4 release) per PHA stored
Y_up	1.567	dUnit/dUnit	H/C: unbiodegradable particulate organics (UPO)
Y_us	1.648	dUnit/dUnit	H/C: unbiodegradable soluble organics (USO)

Table 7.4.2: Parameters used in Simulating the ASM2-3P Model			
Parameter	**Value**	**Units**	**Description**
Z_bp	0.357	dUnit/dUnit	O/C: biodegradable particulate organics (BPO_{SW})
Z_bps	0.848	dUnit/dUnit	O/C: PS biodegradable particulate organics (BPO_{PS})
Z_e	0.565	dUnit/dUnit	O/C: endogenous residue organics (ER)
Z_f	0.660	dUnit/dUnit	O/C: fermentable biodegradable soluble organics (FBSO)
Z_o	0.357	dUnit/dUnit	O/C : organisms
Z_up	0.565	dUnit/dUnit	O/C: unbiodegradable particulate organics (UPO)
Z_us	0.511	dUnit/dUnit	O/C: unbiodegradable soluble organics (USO)

This section of the chapter captures the calibration of the ASM2-3P model by presenting the simulation model results in comparison with the measured results of COD removal, N removal, P removal, solids (TSS, VSS and ISS) concentrations, nitrate generation, denitrification, oxygen utilization and biomass generation. The experimental unit operation systems against which this model is calibrated include the NDBEPR, MLE 1 and MLE 2 AS systems (of the experimental set up shown in Section 3.2 of this report) and the aerobic digestion (AerD) system operated and tested by Mebrahtu *et al.* (2007), which is described further below. Since the AS systems (NDBEPR, MLE 1 and MLE 2) were operated at steady state (at a 10-day R_s throughout the two-year experimental research period), the input characteristic components to the model (shown in Tables 7.43a, 7.44 and 7.45) were kept the same, i.e. the input data was constant in the simulation of each experimental period. Moreover, the simulation run time used for these AS systems was about 100 days (which is greater than 3 times the 10-day sludge age at which the AS systems were operated, for the simulation period to be more than enough, to model the AS systems at when steady state). Therefore, although the ASM2-3P model is dynamic (in the sense that it is based on differential equations) the validation was limited to steady state constant flow and load conditions.

1. NDBEPR AS SYSTEM

The Figure 7.4.4 below shows a comparison between the results simulated by the ASM2-3P dynamic model and measured NDBEPR AS system data. The corresponding results are presented in Table 7.4.3 below.

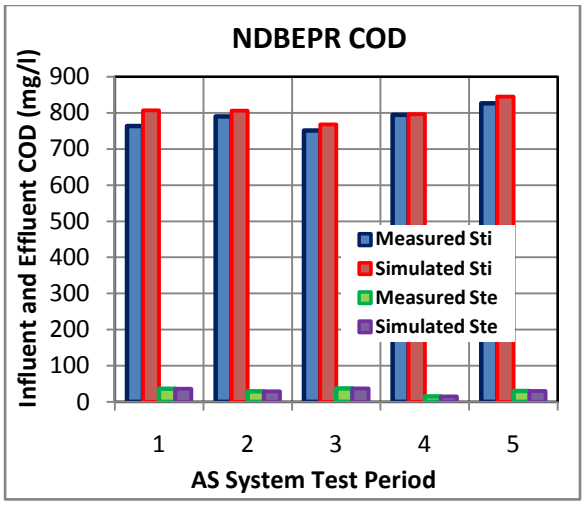

(a)

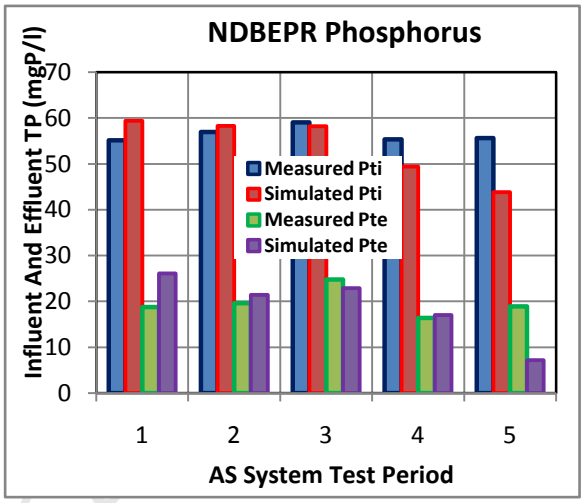

(b)

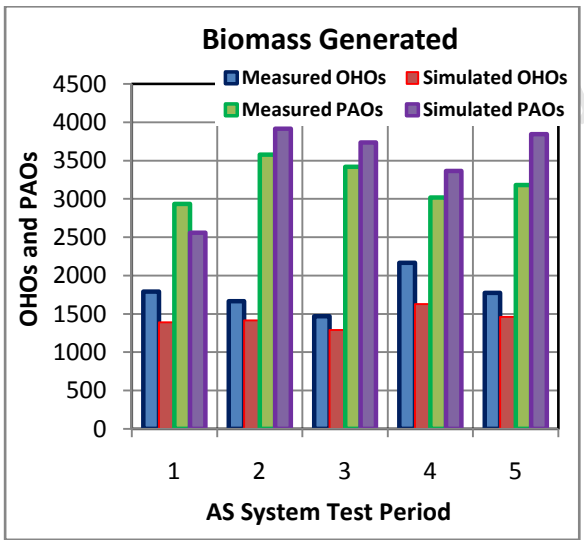

(c)

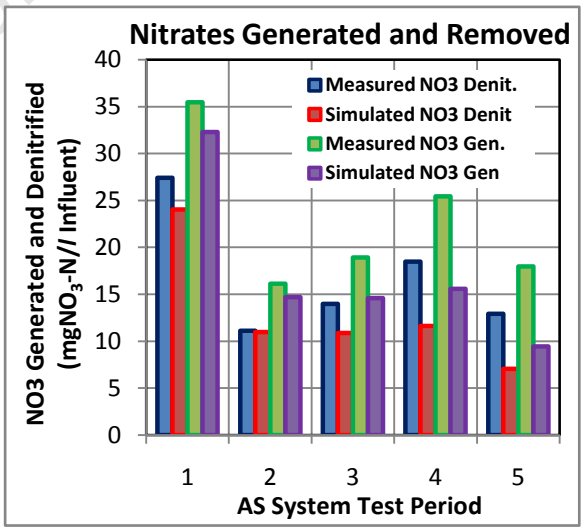

(d)

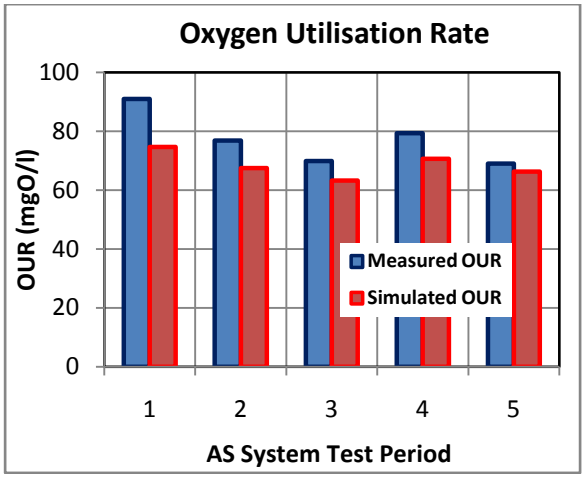

(e)

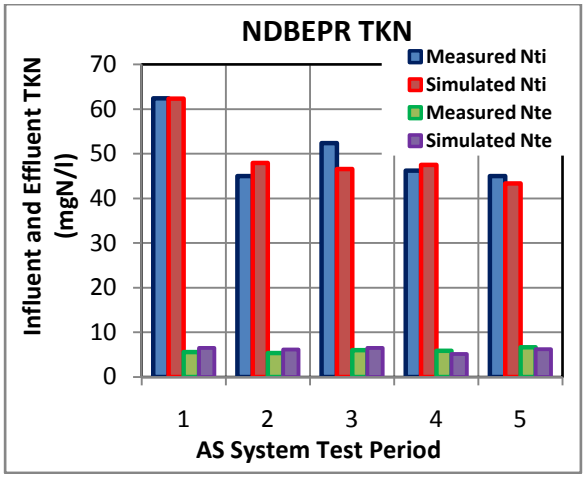

(f)

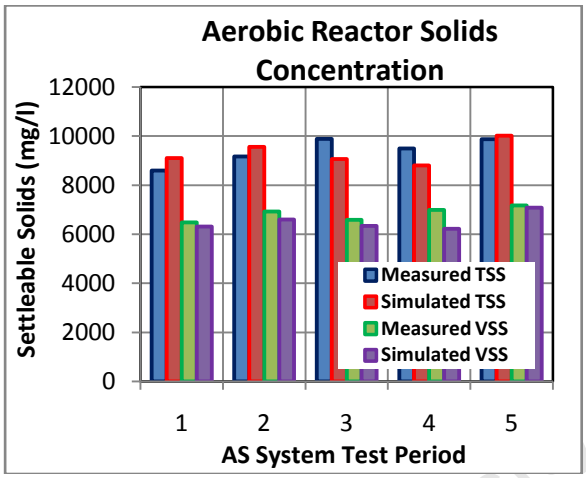

(g)

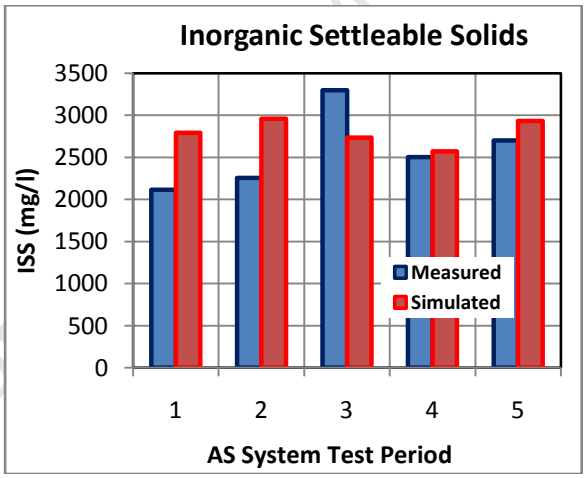

(h)

Figures 7.4.4a to h: *A comparison between the results simulated by the ASM2-3P dynamic model and measured data per sewage batch test period for the NDBEPR AS system: (a) COD removal,(b) phosphorus removal, (c) biomass generated, (d) nitrates generated (aerobically) and removed (anoxically,) (e) oxygen utilization rates, (f) nitrogen removal, (g) total and volatile settleable solids concentrations and (h) Inorganic settleable solids concentration.*

Table 7.4.3a: Summary of Measured and Simulated Results for NDBEPR AS System											
Experimental Testing Period		1		2		3		4		5	
Sewage Batch Number		14		16		17		19		21	
Parameter		Measd	Sim	Measd	Sim	Measd	Sim	Measd	Sim	Measd	Sim
Influent	COD (mgCOD/*l*)	763.2	807.1	790.5	805.9	751.4	768.1	794.5	796.7	826.7	845.4
	TKN (mgN/*l*)	62.4	62.3	45	48	52.4	46.6	46.2	47.5	45	43.4
	FSA (mgN/*l*)	51.1	51.1	34.3	34.3	33.3	33.3	35.3	35.3	29.1	29.1
	TP (mgP/*l*)	55.1	59.4	57	58.3	59	58.2	55.3	49.4	55.6	43.9
	OP (mgP/*l*)	51.6	51.6	50.1	50.1	50.3	50.3	42.4	42.4	35.1	35.1
Anaerobic Tank	TSS (mg/*l*)	3548.4	4645.2	3602.8	4856.3	3943.5	4599.9	4765.2	4514.1	3906.2	5111.5
	VSS (mg/*l*)	2633.6	3270.8	2924.4	3420.8	2876	3288	2742.4	3209.2	3158.5	3667.2
	Nitrates (mgN/*l*)	0	0	0	0	0.1	0	0.2	0	0.3	0
	OP (mgP/*l*)	97.4	104.7	101	106.5	142	104.2	84.4	91.7	105.4	89.5
Anoxic Tank	TSS (mg/*l*)	6091.6	7299.4	6524.4	7657.5	7115.6	7262.7	7095.5	7063.8	7193.7	8033.4
	VSS (mg/*l*)	4544.4	5090.6	4868	5320.5	4780	5110.3	4845	5012.5	5230.3	5707.6
	Nitrates (mgN/*l*)	0	0.2	1	0.1	0.2	0.1	0.6	0.1	0.6	0
	OP (mgP/*l*)	50.1	61.9	57.3	61.7	52.5	61	68.1	53.4	62.3	46.7

Table 7.4.3a: Summary of Measured and Simulated Results for NDBEPR AS System											
Experimental Testing Period		1		2		3		4		5	
Sewage Batch Number		14		16		17		19		21	
	Parameter	Measd	Sim	Measd	Sim	Measd	Sim	Measd	Sim	Measd	Sim
Aerobic Tank	COD (mgCOD/*l*)	9355.4	9426.3	10061.8	9862.4	9589.4	9460.1	10126.7	9366.5	10417.9	10613.1
	Filtered COD (mgCOD/*l*)	36.3	36.2	29.4	29.4	37.4	37.4	14.6	14.6	29.9	29.9
	TKN (mgN/*l*)	550.5	583.9	598.6	613.7	596.4	583.3	576.2	576.6	670.1	630
	FSA (mgN/*l*)	1.8	1.6	5	1.5	4.6	1.6	5	1.4	5.1	1.4
	TP (mgP/*l*)	866.6	776.2	914.5	849.4	988.5	812.5	838	744.5	921.9	830.8
	OP (mgP/*l*)	18.8	26.1	19.6	21.4	24.8	22.9	16.4	17.1	18.9	7.2
	TSS (mg/*l*)	8595.9	9101.6	9175.6	9556.8	9882	9066.8	9494.5	8799.9	9870.8	10013.5
	VSS (mg/*l*)	6482.4	6307.4	6921.2	6596.1	6582.8	6332.8	6990.5	6226.5	7168.4	7081.4
	Nitrates (mgN/*l*)	8.1	8.3	5	3.7	4.9	3.7	7	4	5.1	2.4
	VFA (mgCOD/*l*)	0	0	0	0	0	0	0	0	0	0
	Alkalinity (mg/*l* as $CaCO_3$)	-	195.2	-	226.1	230	211.3	-	234.3	-	188.9
	Measured pH	7.9	7.7	-	7.8	7.9	7.9	-	7.8	-	7.7
	OHO Biomass (mgCOD/*l*)	1792.7	1563.1	1664.8	1415.3	1469.8	1290.8	2167.3	1628.6	1774.8	1460.1
	PAO Biomass (mgCOD/*l*)	2933	3492.7	3578.9	3917.1	3417.5	3737.6	3020.1	3364.9	3181.2	3845.4
	Polyphosphate (mgP/*l*)	701.7	634.3	720.4	711.3	769.3	678.7	600	610.6	657.8	697.8
	Endogenous Residue (mgCOD/*l*)	1163.1	1048.7	1147.2	961.9	1043.4	880.2	1401.8	1069.3	830.6	982.1
	Unbiodegradable Particulate COD (mgCOD/*l*)	3430.7	3001.5	3642.1	3227.6	3622.2	3233.2	3523.1	2926.1	4291.9	3935.8
	OUR (mgO/l/d)	90.9	74.7	76.9	67.5	69.9	63.3	79.3	70.6	69	66.3
	Mg (mg/*l*)	260.8	235.3	290.9	241.1	289.5	237.8	313.1	230.1	279.3	246.4
	K (mg/*l*)	369.5	322.4	494	359.6	442.3	355.5	447.9	298.4	401.8	350.7
	Ca (mg/*l*)	46.5	36	54	45.7	58.5	44.1	52.9	41	56.4	43.7
	Filtered Mg (mg/*l*)	84.2	92.5	61.3	81.6	72.9	85.4	80.6	92.5	91.9	89.7
	Filtered K (mg/*l*)	89.9	87.9	97.5	96.7	107	104.3	21.3	73	95.4	92.9
	Filtered Ca (mg/*l*)	11.7	14.3	22.1	21.3	23	20.8	72.1	20	19.9	19.8

Table 7.4.3b: Mass Balances for the Measured and Simulated Results of Table 7.4.3a										
Experimental Testing Period	1		2		3		4		5	
Sewage Batch Number	14		16		17		19		21	
Parameter	Measd	Sim	Measd	Sim	Measd	Sim	Measd	Sim	Measd	Sim
COD balance (%)	103.9	99.5	96.2	101.2	94.5	101	96.9	100.8	88.4	100.8
N balance (%)	81.3	99.4	101.5	99.5	94.1	100.4	120.2	97.7	114.7	96.4
P balance (%)	105.6	100	104.1	98.6	89.2	99	107	98.1	102.6	98
Mg balance (%)	89	100.4	77.4	100.3	86.2	100.3	88.5	100.1	100.3	100.3
K balance (%)	90.5	100.4	89.1	100.3	91.5	100.4	85.8	99.8	90.5	100.3
Ca balance (%)	74.6	100.3	96.5	100.4	103.7	100.4	99.4	100.3	93.5	100.4

COD and Nutrient Removal

As can be seen in the Figures 7.4.4a, f and b, the dynamic model simulated results exhibit trends in COD, TKN and TP removal that are close to the experimental results. The 10d sludge age at which the experimental NDBEPR was operated was sufficiently long for complete utilization of the influent biodegradable organics together with the nutrients (N and P) that are not bound in influent unbiodegradable components (USO and UPO). The model replicates the experimentally observed behaviour well. The effluent comprises mainly of the USO component with very little or no ammonia and low ortho-phosphate concentrations. Also, the model exhibits P removal via anaerobic P release and aerobic storage of PP by PAOs. The simulated PP concentrations (689.8 mgP/*l*) can be seen to fall within very close range of those measured (666.6 mgP/*l*). This is important for plant-wide modelling because the PP is the main source of ortho-phosphate (OP) and metals (Mg, Ca and K) in the subsequent WAS treatment systems (AD or AerD) and hence determines the extent to which precipitation and other weak acid/base processes take place.

Sludge Produced

The influent biodegradable COD and nutrients (N and P) are used for biomass growth and hence the generation of sludge. The Figure 7.4.4c above, shows a good correlation between the predicted PAO and OHO concentrations by the dynamic model and those calculated from measured results with the steady state model (see Equations 5.3.1c and 5.3.1d of Section 5.3). The endogenous residue generated from the biomass lysis, which adds to the reactor unbiodegradable particulate mass, is also similar to that calculated from experimentally measured results. Because the $f_{S'up}$ (UPO) fraction was determined by calibration onto the measured VSS, the UPO (X_I) VSS concentration in the reactor also matches well. This is also reflected by the measured and predicted VSS concentrations as presented in Figure 7.4.4g. Moreover, predicted reactor ISS can be seen to correlate reasonably well with the measured

results (as shown in Figure 7.4.4h), which validates the ISS model of Ekama and Wentzel (2004) included in the extension of the ASM2-3P model. Considering that the ISS is very sensitive to the system P removal, this confirms the good correlation between predicted and measured P removal.

Nitrate Generated and Denitrified

The influent ammonia and that produced by the N released from the biodegradable organics (FBSO and BPO) less that taken up for OHO and PAO growth is used by ANOs for nitrification. Therefore, it was important to ensure that the right organic elemental C, H, O, N, and P compositions were entered as parameters into the dynamic model, since a higher nitrogen content of BPO_{PS} and/or FBSO results in higher FSA release and hence increased nitrate generation. Also, a high N content in the biomass results in more N uptake for biomass growth leaving less for nitrification. The anoxic/aerobic BPO hydrolysis reduction factor for denitrification (n_NO_Het), which is usually calibrated to the experimental system to correctly predict the extent of denitrification, also required adjustment to ensure that the predicted effluent nitrate matched the measured values. Reducing n_NO_Het reduces the rate of anoxic OHO hydrolysis/utilization of BPO, which decreases the FBSO product available for denitrification. The n_NO_Het value of 0.3 was selected since it accurately predicted the denitrification in the UCT system (i.e. effluent NO_3-N).

Accurate prediction of denitrification and effluent nitrate concentration is not important for determining the WAS composition fed to the AD or AerD. For this it is much more important that the CHONP and COD of the WAS (via the X, Y, Z, A, B in $C_XH_YO_ZN_AP_B$) are determined as accurately as possible to match the measured results. For this the OUR is important because it is related to the OHO and PAO growth and endogenous respiration that has taken place in the NDBEPR system.

Oxygen Utilized

The predicted average oxygen utilization rate (OUR) is 68.5 (mgO/*l*.h) and that from the measured results is 77.2 (mgO/*l*.h). The OUR was experimentally measured in a side stream aeration reactor (Chapter 3) and depended on the ratio of VSS concentration of the main aerobic reactor and re-aeration reactor. The OUR therefore had the potential to be subject to some error, and this accounts for the 8.7mgO/*l* difference between the measured and simulated results (Figure 7.4.4e). With consideration to this error, it is notable that the model is capable of predicting reasonably accurate responses in OHO and PAO biomass aerobic growth, endogenous respiration and nitrification for which the oxygen is utilized.

VFA, Alkalinity and pH

The VFA, alkalinity and pH of the main aerobic reactor were not tested often, but when measured were found to be around zero mgCOD/*l*; 230mg/*l* as $CaCO_3$ and 7.9 respectively. The simulated values of VFA (about zero mgCOD/*l*) match the measured values and the alkalinity (ranged from 189 to 235 mg/*l* as $CaCO_3$) and pH (ranged from 7.7 to 7.9) are within reasonable range to the measured values. It was also noted that these parameters (VFA, alkalinity and pH) should also require rigorous testing from the parent systems (which in this case is the NDBEPR) to aid in tracking the H^+ and carbonate components through the plant. As found by Sötemann *et al.* (2005), the aeration that occurs in the aerobic reactor of AS systems strips out most of the CO_2 generated by the bioprocesses and consequently does not have a significant impact on the alkalinity and the pH of the system.

2. Calibration of the ASM2-3P model to the MLE AS System Results

Comparisons between the results simulated by the ASM2-3P dynamic model and measured data from MLE 2 (Figure 7.4.5) and MLE 1 (Figure 7.4.6) are shown below. The corresponding results are presented in the succeeding Tables 7.4.4 and 7.4.5 respectively. The ASM2 can be used for the simulation of MLE systems but it must be established that BEPR

does not take place (PAO = 0). Therefore, the results from the simulation of MLE 2, using the ASM2-3P model are compared with results obtained when simulating this system with (single phase) ASM1 to verify that the same results are obtained, in particular the VSS concentration, in Fig 7.4.5 and 7.4.6 and Tables 7.4.3 and 7.4.4 respectively. The parameters used in ASM1 for these simulations are given in Table 7.4.4a. The AS systems (including MLE 2) were operated at a sludge age that was long enough (10 days) for all the biodegradable organics to be utilized, therefore the default stoichiometric constants in Table 7.44a could be used without expecting the kinetic rates of biodegradable organics degradadation to affect the ASM1 system results.

Table 7.4.4a: Parameters used in Simulating The ASM1 Model

Parameter	Value	Units	Description
b_A	0.15	1/d	Decay Coefficient For Autotrophic Biomass
b_H	0.62	1/d	Decay Coefficient For Heterotrophic Biomass
f_P	0.08	Ratio	Fraction Of Biomass Converted To Inert Matter
i_X_B	0.059	gN/gCOD	Mass Of Nitrogen Per Mass Of COD In Biomass
i_X_P	0.059	gN/gCOD	Mass Of Nitrogen Per Mass Of COD In Products Formed
k_a	0.06	m^3/(gCOD*d)	Maximum Specific Ammonification Rate
k_h	3	gCOD/(gCOD*d)	Maximum Specific Hydrolysis Rate
K_NH	1	gNH_3-N/m^3	Ammonia Half-Saturation Coefficient For Autotrophic Biomass
K_NO	0.5	gNO_3-N/m^3	Nitrate Half-Saturation Coefficient For Denitrifying Heterotrophic Biomass
K_OA	0.5	gO_2/m^3	Oxygen Half-Saturation Coefficient For Autotrophic Biomass
K_OH	0.2	gO_2/m^3	Oxygen Half-Saturation Coefficient For Heterotrophic Biomass
K_S	20	gCOD/m^3	Half-Saturation Coefficient For Heterotrophic Biomass
K_X	0.1	gCOD/gCOD	Half Saturation Coefficient For Hydrolysis Of Slowly Biodegradable Substrate
mu_A	1	1/d	Maximum Specific Growth Rate For Autotrophic Biomass
mu_H	6	1/d	Maximum Specific Growth Rate For Heterotrophic Biomass
n_g	0.8	-	Correction Factor For Anoxic Growth Of Heteritrophs
n_h	0.6	-	Correction Factor For Anoxic Hydrolysis
S_O_Sat	8.9	g/m^3	Oxygen saturation concentration
Vol	16.2	Litres	Volume of the tank
Y_A	0.24	gCOD/gN	Yield For Autotrophic Biomass
Y_H	0.65	gCOD/gCOD	Yield For Heterotrophic Biomass

The MLE 2 system (fed raw WW):

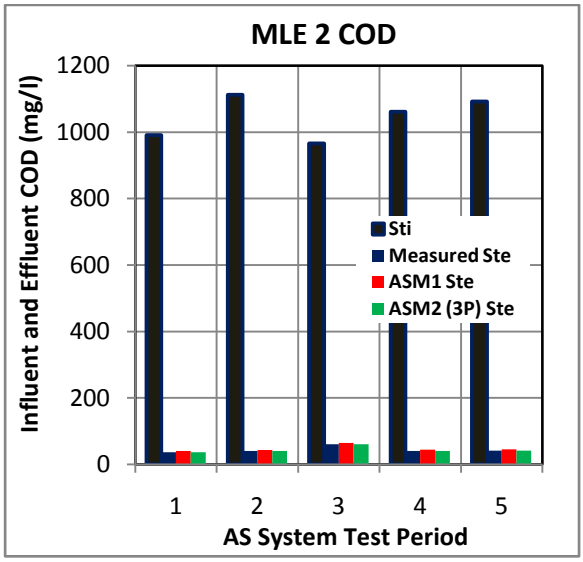

(a)

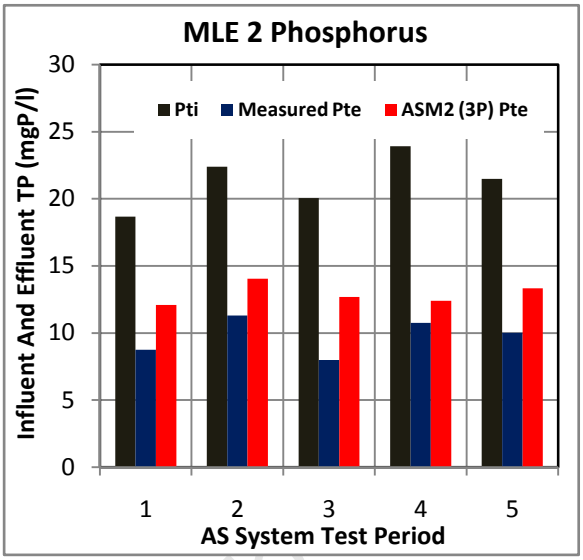

(b)

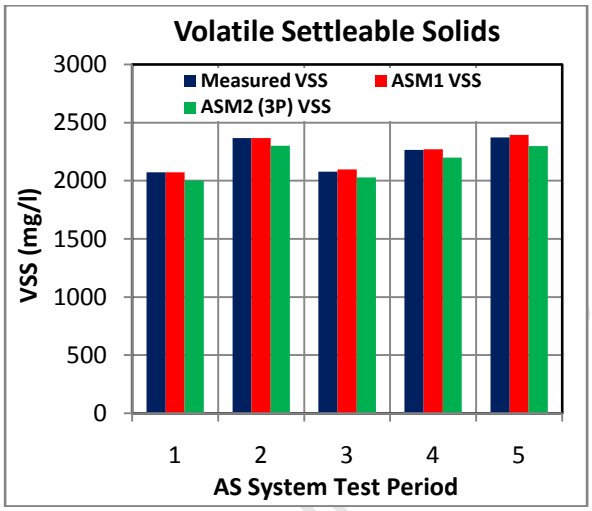

(c)

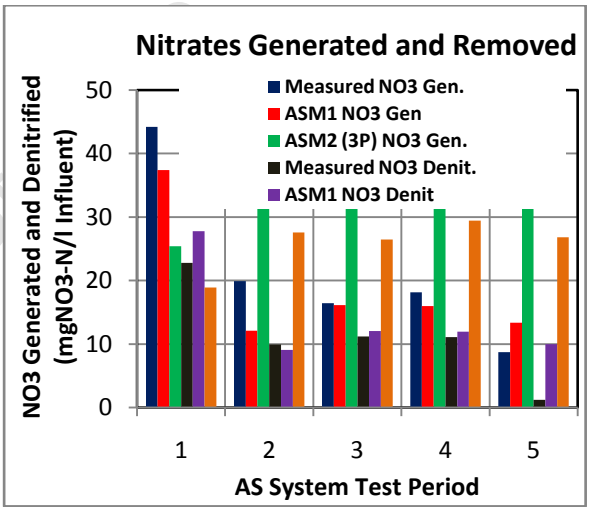

(d)

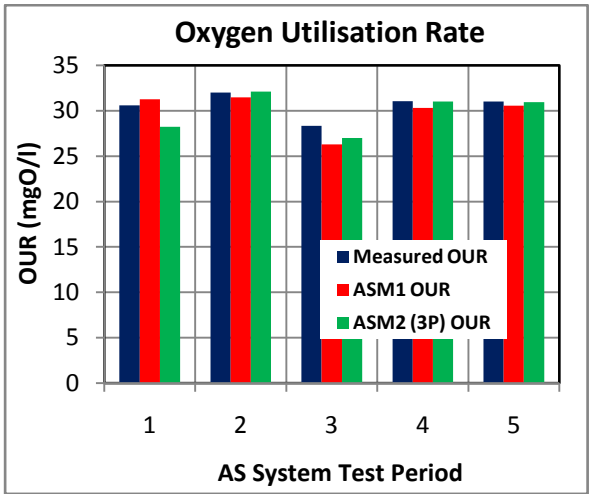

(e)

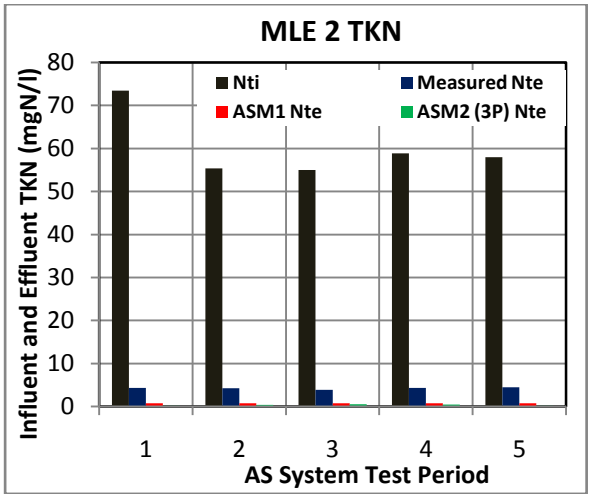

(f)

Figures 7.4.5 a to f: *A comparison between the results simulated by the ASM2-3P dynamic model, the ASM1 model and measured data for 5 sewage batches (1-5) for the MLE 2 AS system: (a) COD removal, (b) phosphorus removal, (c) volatile settleable solids concentration, (d) nitrates generated (aerobically) and removed (anoxically), (e) oxygen utilization rate and (f) nitrogen removal.*

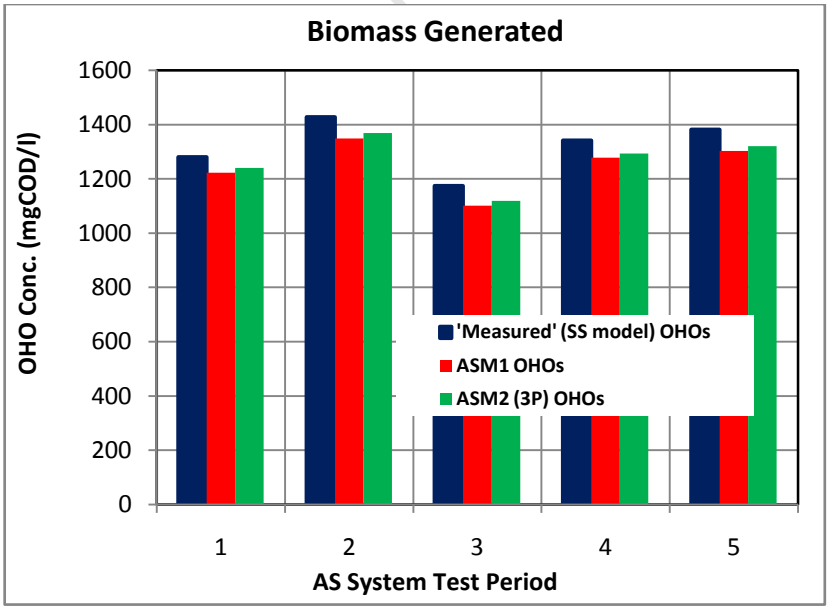

Figure 7.4.5g: *A comparison between the biomass generation results simulated by the ASM2-3P dynamic model, the ASM1 model and those detemined from the steady state model calculations for 5 sewage batches (1-5) for the MLE 2 AS system.*

Table 7.4.4: Summary of Measured and Simulated Results for MLE 2 AS System											
	Experimental Testing Period	1		2		3		4		5	
	Sewage Batch Number	14		16		17		19		21	
Parameter		Measd.	Sim	Measd.	Sim	Measd.	Sim	Measd.	Sim	Measd.	Sim
Influent	COD (mgCOD/*l*)	991.4	991.4	1112.3	1112.3	966.1	966.1	1061.5	1061.5	1092.5	1092.5
	Filtered COD (mgCOD/*l*)	88.1	88.1	163.3	163.3	173.3	173.3	145.0	145.0	158.5	158.5
	TKN (mgN/*l*)	73.4	73.4	55.4	55.4	55.0	55.0	58.9	58.9	58.0	58.0
	FSA (mgN/*l*)	25.4	25.4	36.7	36.7	35.8	35.8	39.8	39.8	35.6	35.6
	TP (mgP/*l*)	18.7	18.7	22.4	22.4	20.1	20.1	23.9	23.9	21.5	21.5
	OP (mgP/*l*)	13.6	13.6	15.4	15.4	13.7	13.7	13.8	13.8	14.6	14.6
	TSS (mg/*l*)	732.1	732.1	761.5	761.5	1012.5	1012.5	676.9	676.9	763.4	763.4
	VSS (mg/*l*)	590.8	590.8	643.9	643.9	650.9	650.9	557.7	557.7	653.4	653.4
Anoxic Tank	TSS (mg/*l*)	2581.6	3235.6	2788.0	3378.6	2592.0	5033.7	2552.0	3294.5	2814.3	3324.0
	VSS (mg/*l*)	2025.2	1941.2	2287.6	2238.9	2172.0	1980.8	2228.4	2144.8	2311.3	2240.9
	Nitrates (mgN/*l*)	10.4	0.1	5.0	0.2	1.1	0.5	2.5	0.4	5.3	0.2
Aerobic Tank	COD (mgCOD/*l*)	3027.4	3052.8	3498.2	3501.1	3078.9	3105.9	3317.5	3348.5	3506.1	3500.2
	Filtered COD (mgCOD/*l*)	36.7	36.7	40.0	40.0	61.0	60.9	40.6	40.6	41.6	41.6
	TKN (mgN/*l*)	184.1	221.5	264.0	252.8	252.8	221.1	204.3	241.4	264.0	251.3
	FSA (mgN/*l*)	4.3	0.2	4.3	0.4	3.9	0.5	4.3	0.4	4.5	0.2
	TP (mgP/*l*)	72.2	85.6	91.2	98.0	87.8	86.4	94.6	92.6	106.7	96.9
	OP (mgP/*l*)	8.7	12.1	11.3	14.1	8.0	12.7	10.8	12.4	10.0	13.3
	TSS (mg/*l*)	2592.5	3160.8	2877.6	3305.2	2527.6	4983.0	2644.8	3232.9	2870.7	3250.8
	VSS (mg/*l*)	2072.0	2001.7	2367.6	2300.0	2077.6	2027.1	2264.0	2199.7	2371.3	2299.3
	Nitrates (mgN/*l*)	21.5	6.5	10.0	9.4	5.2	9.4	7.1	10.4	7.5	9.2
	VFA (mgCOD/*l*)	0.0	0.1	0.0	0.2	0.0	0.2	0.0	0.2	0.0	0.1
	Measured pH	7.5	7.5	-	3.3	-	2.9	-	2.7	-	7.4
	OHO Biomass (mgCOD/*l*)	1280.0	1240.8	1428.4	1369.2	1174.0	1118.7	1341.8	1293.9	1381.6	1320.2
	Endogenous Residue (mgCOD/*l*)	624.9	615.4	692.1	683.3	577.8	556.7	649.4	645.1	671.5	659.0
	Unbiodegradable Particulate COD (mgCOD/*l*)	1103.6	1045.2	1345.1	1284.1	1365.8	1269.3	1311.8	1252.6	1428.5	1358.5
	Polyphosphate (mgP/*l*)	0.0	0.0	0.0	0.0	0.0	0.0	0.0	0.0	0.0	0.0
	OUR (mgO/l/h)	30.6	28.2	32.0	32.1	28.3	27.0	31.0	31.0	31.0	30.9
Mass Balances	COD balance (%)	93.9	100.2	98.6	100.2	104.2	99.9	100.4	100.1	101.0	100.1
	N balance (%)	97.2	99.4	102.0	99.4	90.0	99.4	94.1	99.4	84.3	99.4
	P balance (%)	108.4	99.5	93.2	97.1	105.3	97.2	105.5	97.3	83.4	97.2
Where measd. and sim. stand for measured and simulated results respectively.											

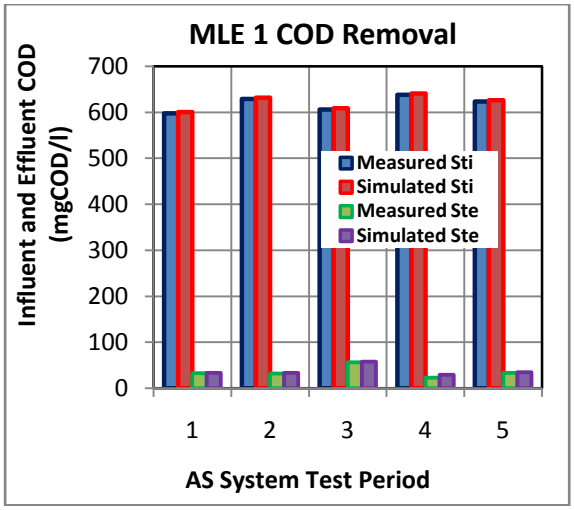

(a)

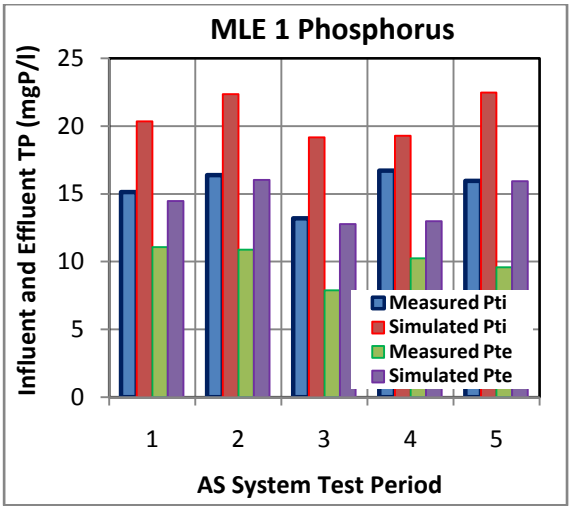

(b)

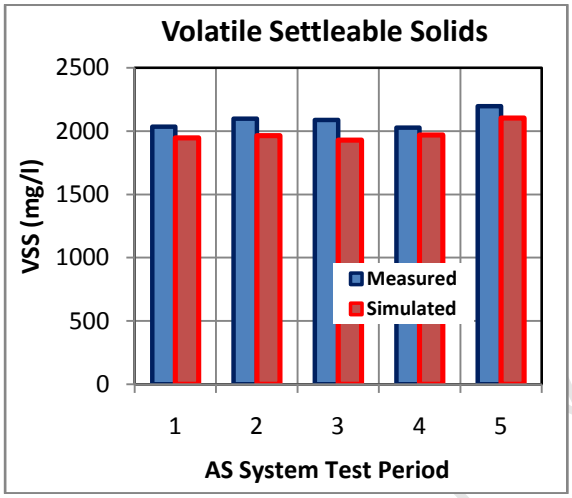

(c)

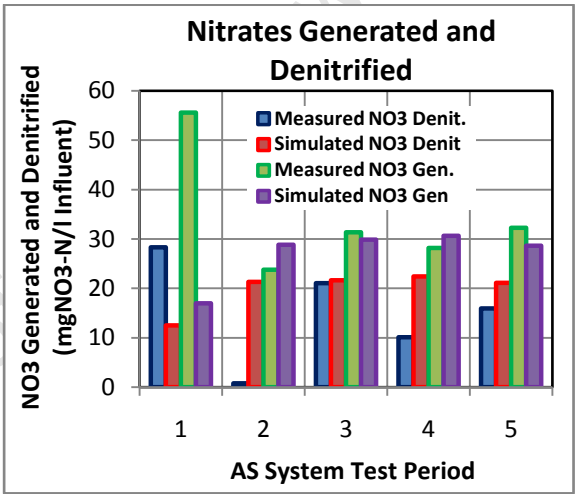

(d)

Figures 7.4.6a to d: *A comparison between the results simulated by the ASM2-3P dynamic model and measured data for 5 sewage batches (R_s) for the MLE 1 AS system in the order of: (a) COD removal, (b) phosphorus removal, (c) biomass generated and (d) nitrates generated (aerobically) and removed (anoxically).*

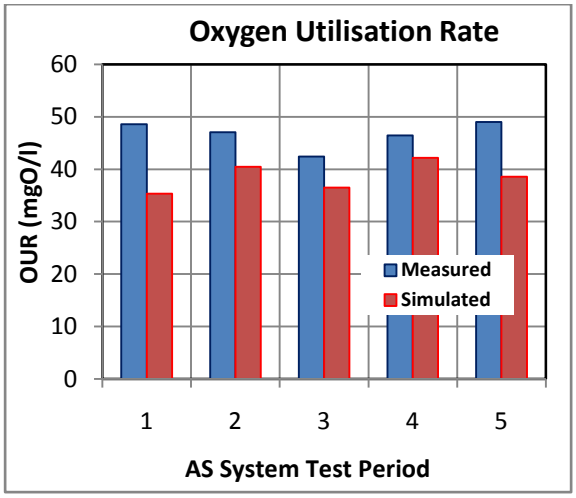

(e)

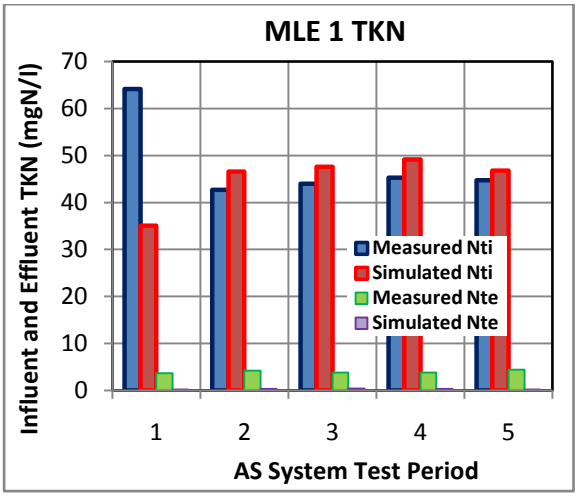

(f)

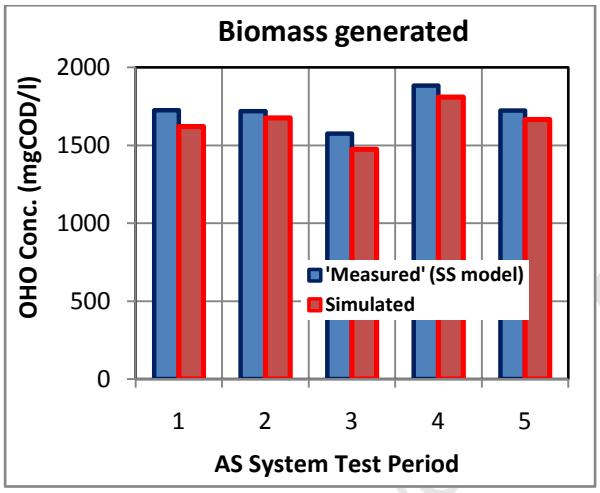

(g)

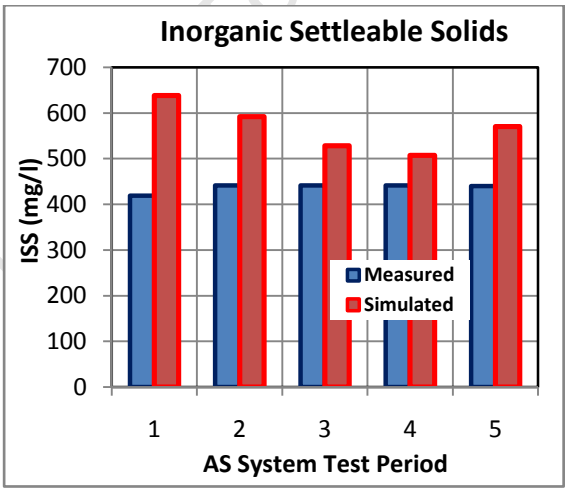

(h)

Figures 7.4.6a to h: *A comparison between the results simulated by the ASM2-3P dynamic model and measured data for 5 sewage batches (R_s) for the MLE 1 AS system in the order of: (e) oxygen utilization rates, (f) nitrogen removal, (g) total and volatile settleable solids concentration and (h) inorganic settleable solids concentration.*

Table 7.4.5: Summary of Measured and Simulated Results for MLE 1 AS System											
	Experimental Testing Period	1		2		3		4		5	
	Sewage Batch Number	14		16		17		19		21	
Parameter		Measd.	Sim	Measd.	Sim	Measd.	Sim	Measd.	Sim	Measd.	Sim
Influent	COD (mgCOD/*l*)	597.5	600.4	628.9	631.8	606.0	609.0	638.3	641.2	623.7	626.6
	Filtered COD (mgCOD/*l*)	73.2	73.2	124.9	124.9	125.3	125.3	113.2	113.2	119.8	119.8
	TKN (mgN/*l*)	64.2	35.1	42.7	46.6	44.0	47.6	45.3	49.2	44.7	46.8
	FSA (mgN/*l*)	25.2	25.2	35.8	35.8	36.6	36.6	38.8	38.8	35.7	35.7
	TP (mgP/*l*)	15.1	20.3	16.4	22.3	13.2	19.2	16.7	19.3	16.0	22.5
	OP (mgP/*l*)	12.9	12.9	14.3	14.3	11.2	11.2	11.3	11.3	14.4	14.4
	TSS (mg/*l*)	199.5	430.8	231.4	412.5	380.8	517.9	167.0	423.5	230.3	410.0
	VSS (mg/*l*)	166.0	397.3	201.2	382.3	226.3	363.4	142.8	399.3	201.3	381.0
Anoxic Tank	TSS (mg/*l*)	2343.6	2644.6	2572.0	2613.8	2512.0	4435.2	2532.0	2532.8	2605.3	2729.5
	VSS (mg/*l*)	1928.0	1907.7	2125.6	1930.0	2025.6	1901.6	2085.6	1931.9	2157.3	2070.7
	Nitrates (mgN/*l*)	13.4	0.2	17.0	0.4	2.5	0.7	11.0	0.5	8.3	0.4
Aerobic Tank	COD (mgCOD/*l*)	3054.3	3053.6	3040.0	3084.8	3090.3	3041.0	3019.9	3091.9	3251.4	3287.1
	Filtered COD (mgCOD/*l*)	32.4	33.7	31.8	33.3	56.1	57.7	27.7	29.2	33.4	34.5
	TKN (mgN/*l*)	200.2	212.8	247.2	216.6	219.7	205.0	239.4	223.3	243.4	225.4
	FSA (mgN/*l*)	3.7	0.2	4.2	0.3	3.8	0.4	3.8	0.4	4.4	0.2
	TP (mgP/*l*)	70.4	87.1	79.3	89.5	85.2	83.8	91.5	87.6	104.6	93.4
	OP (mgP/*l*)	11.1	14.5	10.9	16.0	7.9	12.8	10.2	13.0	9.6	15.9
	TSS (mg/*l*)	2454.5	2584.7	2540.0	2556.1	2530.4	4385.5	2468.0	2475.3	2636.3	2673.4
	VSS (mg/*l*)	2035.5	1946.5	2098.4	1963.7	2088.8	1929.2	2026.4	1968.1	2196.0	2103.0
	Nitrates (mgN/*l*)	27.3	4.4	23.0	7.6	10.3	8.2	18.1	8.2	16.3	7.5
	VFA (mgCOD/*l*)	0.0	0.1	61.1	0.1	0.0	0.1	65.0	0.1	23.0	0.1
	Measured pH	7.7	7.4	7.8	3.3	7.6	2.8	7.6	2.7	7.8	7.3
	OHO Biomass (mgCOD/*l*)	1725.1	1620.5	1718.0	1675.8	1575.6	1474.1	1883.1	1810.0	1723.1	1665.2
	Endogenous Residue (mgCOD/*l*)	828.1	790.8	890.3	824.3	796.4	741.6	927.9	889.7	855.0	820.0
	Unbiodegradable Particulate COD (mgCOD/*l*)	468.7	432.5	399.9	367.9	662.1	605.6	186.1	172.1	639.9	589.0
	Polyphosphate (mgP/*l*)	0.0	0.0	0.0	0.0	0.0	0.0	0.0	0.0	0.0	0.0
	OUR (mgO/*l*/h)	48.6	35.3	47.0	40.5	42.4	36.5	46.5	42.2	49.0	38.6
Mass Balances	COD balance (%)	95.2	99.0	98.5	99.2	102.3	99.0	95.5	99.3	105.7	98.9
	N balance (%)	110.7	97.5	101.1	100.3	113.7	99.3	105.2	99.5	115.9	99.9
	P balance (%)	86.7	100.3	100.5	98.9	89.1	98.7	98.7	97.7	92.9	99.0
Where measd. and sim. stand for measured and simulated results respectively.											

COD and Nutrient Removal

With the change in system configuration from NDBEPR to MLE, the ASM2-3P dynamic model simulated the experimental data COD, TKN and TP removal (as shown in Figure 7.4.5 and 7.4.6) very well. It can be noticed that the P removal, both in the measured and simulated results are low (4-6 mgP/*l* for MLE 1 and 9-12 mgP/*l* for MLE 2) despite the low influent P concentration (15-22 mgP/*l* for MLE 1 and 18-25 mgP/*l* for MLE 2). This is expected as typical of an MLE system since BEPR does not take place in it, which has been captured well by the model. The effluent P comprises mainly OP that was not taken up by OHO growth, which is limited to the amount of influent biodegradable COD available.

Sludge Produced

As observable in Figures 7.4.5 (for MLE 1), and 7.4.6 (for MLE 2), the OHO (OHO) concentration calculated with the steady state model equations (which are given in Chapter 5) is slightly higher than that simulated. This is because when calculating the biomass measured results, it was accepted that there are zero PAOs (PAO). However, the ASM2 simulation model predicts a very low concentration of PAO, which would account for the slightly lower OHO concentration. Since the specific concentrations of the various organism types (OHOs and PAOs) were not directly measured, it is not certain whether there are trace concentrations of PAO present in the MLE system. The close match of reactor settleable solids (VSS and ISS which is strongly influenced by PP storage) and close correspondence between measured and predicted effluent OP indicated that the ASM2-3P model satisfactorily simulates the MLE 1 and MLE 2 systems and can be confidently connected to an AD for MLE WAS digestion. For the ASM1, the VSS values were calculated by dividing the COD results predicted by the model by the COD/VSS ratio (which was not a parameter in ASM1) measured from the WAS in the MLE 2 systems aerobic reactor. With negligible PAO growth, low quantities of PP stored (see Table 7.4.5) validate that the sludge produced from

the MLE systems will not cause any struvite precipitation during aerobic or anaerobic digestion.

Nitrates Generated and Denitrified

It can be noticed, in Figure 7.4.5d, that the measured values for nitrates generated and de-nitrified vary considerably between sewage batches. The simulated values are not varying as much and are different to the measured values. The main reason for this difference is that the experimental data do not have a 100% N balance like the model, and the denitrification is not accurately predicted. This is because the anoxic/aerobic BPO hydrolysis rate factor (n_NO_Hyd) in ASM1 (for N removal only) is 0.33 whereas in ASM2 (for N and P removal) it is much higher at 0.6 to account for the faster OHO denitrification rate on BPO in NDBEPR systems (Clayton *et al.*, 1991; Wentzel *et al.*, 1992). This n_NO_Hyd was not decreased to 0.3 in the ASM2-3P to simulate the MLE systems. However, the extent of denitrification in the MLE system does not affect the WAS aerobic and anaerobic digestion systems. Therefore, it is expected that the predicted effluent nitrate is much lower for those sewage batches where the anoxic reactor was overloaded with nitrate i.e. for high influent TKN loading to high nitrate generated. For those sewage batches where the denitrification is nitrate limited, the faster denitrification kinetic rate would not make much difference in effluent nitrate concentration.

Oxygen Utilized

The average oxygen utilization rate for the MLE 2 simulated values is 29.9 (mgO/*l*.h) and that from the measured results is 30.6 (mgO/*l*.h). These close results show that the ASM2-3P model replicates the experimental behaviour of endogenous respiration, nitrification and biomass growth very well. This demonstrates that the important parameters required for simulating the WAS aerobic and anaerobic digestion accurately are predicted well by the ASM2-3P model.

7.5 THREE PHASE UCT AD (ADM-3P) MODEL

The two phase (aqueous-gas) UCTADM1 (Sötemann *et al.*, 2005b) was developed in stages. First, the biological processes mediating the growth and death of AD biomass were defined and these were then integrated into the mixed weak acid/base chemistry model of Musvoto *et al.* (1997, 2000a, b, c), with all processes included in the Gujer matrix of the dynamic model. Thus in order to model the AD, the AD bioprocesses need integration with the mixed weak acid/base chemistry processes at least in two phases (aqueous-gas). For methanogenic AD of low P organics (like PS and ND WAS), two phase inorganic carbon, acetate and ammonium mixed weak acid/base chemistry is acceptable since mineral precipitation, if any, is very minor (Sötemann *et al.*, 2005b). However, to model the AD of P-rich sludge (e.g. from NDBEPR AS systems) the phosphate weak acid/base system requires inclusion together with three phase mixed weak acid/base chemistry, since the hydrolysis of polyphosphate in PAOs and organic P in concentrated WAS results in precipitation of minerals such as struvite which also leads to changes in alkalinity (van Rensburg *et al.*, 2003; Harding, 2009). Therefore, to predict AD pH and dewatering liquor aqueous metal, P and N concentrations in a plant-wide modelling context, the AD bioprocesses need to be integrated within a three phase mixed weak acid/base chemical and physical processes system. The ADM-3P model extends the UCTADM1 model developed by Sötemann *et al.* (2005b), by integrating it within a three phase mixed weak acid/base chemical and physical processes model of the inorganic carbon, ammonia, acetate and phosphate systems.

This extension was done by coding the AD reaction processes in the model editor of the modelling platform WEST and including an ionic speciation model subroutine (i.e. the same ionic speciation and interphase transfers described in Sections 7.3.1 and 7.3.2), coded separately (to alleviate the numerical handling of these 'instantaneous' reactions) via a C++ program file linked to the WEST model-base. Thus, the slow AD biological gas-exchange and mineral precipitation processes are modelled as differential equations and generate total species concentrations, these total species concentrations are speciated into their respective

subspecies concentrations by the algebraic equations speciation subroutine. The ionic speciation routine includes ion pairing and maintains aqueous phase equilibrium at each time step of the simulation. Hence, the weak acid/base species are re-distributed, facilitating the establishment of the free, unassociated H^+ ion concentration and hence the determination of digester pH at each time step. Therefore, the AD model is useful in simulating the interactions between the biological processes and weak acid/base chemistry for the dynamic operation of anaerobic digesters (Brouckaert *et al.*, 2010).

7.5.1 Implementation of the UCTADM Model

The IWA AD model (ADM1, Batstone *et al.*, 2002) has a structure defined by the three general biological processes (acidogenesis, acetogenesis and methanogenesis) together with an extracellular degradation step and an extracellular hydrolysis step. These multiple processes involve the action of four organism groups: acidogens, acetogens, acetoclastic methanogens and hydrogenotrophic methanogens. In ADM1, the degradation of influent organics is defined by disintegration of substrates to carbohydrates, proteins and lipids, which are further hydrolysed to produce monosaccharides, amino acids and long chain fatty acids respectively. The UCTADM1 model (Sötemann *et al.*, 2005) is similar in that it includes the reactions mediated by the same four organism groups as for IWA ADM1, but with a single hydrolysis process acting on a generic organic material representing sewage sludge i.e. $C_XH_YO_ZN_A$. This hydrolysis process directly generates an idealised carbohydrate 'glucose' while maintaining COD, C, N, H and O mass balances also producing NH_3 and taking up H_2CO_3. The processes that follow hydrolysis, being much faster, are dealt with stoichiometrically to yield digester end products i.e. biomass, CH_4, CO_2 and water.

This ADM-3P model extends the UCTADM1 model developed by Sötemann *et al.* (2005b), by integrating it within a three phase mixed weak acid/base chemical and physical processes model of the inorganic carbon, ammonia, acetate, propionate and phosphate systems. The main extensions in the new model include:

1. additional soluble and particulate biodegradable organic components to represent material which might be combined from different sources in the WWTP and fed to the anaerobic digester;
2. digestion of waste activated sludge (WAS) from BEPR systems;
3. precipitation of $MgNH_4PO_4.6H_2O$ (struvite), $MgKPO_4.6H_2O$ (K-struvite) and $Ca_3(PO_4)_2$ (ACP);
4. modelling the "instantaneous" aqueous phase equilibrium reactions and ion paring with algebraic equations to reduce the stiffness (i.e. when in simulations, the requisite step size in the integration of a differential equation used in preparing a model predictions is forced to an incorrectly small level in a region where the solution curve displays very low variation) of the system of differential equations.

Model Components and Processes

The components used in the ADM-3P model are the same as those of the ASM2-3P model, to ensure compatibility between the two models, when linked to simulate the whole AS-AD plant. These components are described in the above Section 7.2.

The processes that have been coded into the ADM-3P model are summarised in the Table 7.5.1 below. These biological reactions essentially follow the treatment of Sötemann *et al.* (2005b), with additions and modifications to account for the P content of organisms and to account for the AD of additional OHO and PAO components. This includes the release of polyphosphate from PAOs and the formation of endogenous residue, the small fraction of unbiodegradable particulate organics, with the death of biomass. The process equations and rates, as coded into the Gujer matrix of this model are reported in Appendix 6.

Table 7.5.1: Stoichiometric Processes of the ADM-3P Model	
1	Hydrolysis of fermentable soluble organics (FBSO)
2	Hydrolysis of biodegradable particulate organics (BPO) produced by dead biomass
3	Hydrolysis of (BPO) from primary sludge (PS)
4	Lysis of ordinary heterotrophic organisms (OHOs)
5	Lysis of phosphorus accumulating organisms (PAOs)
6	Release of polyphosphate (PP) with uptake of poly-hydroxy-alkanoate (PHA)
7	Release of PP in PAOs
8	Release of PHA in PAOs
9	Low hydrogen partial pressure (p_{H2}) Acidogenesis
10	High p_{H2} Acidogenesis
11	Lysis of acidogens
12	Acetogenesis
13	Lysis of acetogens
14	Acetoclastic methanogenesis
15	Lysis of acetoclastic methanogens
16	Hydrogenotrophic methanogenesis
17	Lysis of hydrogenotrophic methanogens

Reactions 1 to 3 and 9 to 17 are essentially the same as in UCTADM1, except that they have additional terms to account for the P content of organics, biomass and polyphosphate (PP). Reactions 4 and 5 are added merely because the OHOs and PAOs are additional components of the new model; the lysis (death) reactions have the same stoichiometry for all the organism groups, but their rates may be different. The AD organism lysis reactions are slightly modified from the UCTADM1 model, in that they account for the P content of these organisms and the production of a small fraction of unbiodegradable endogenous residue, both of which were taken to be negligible in the earlier model. The AD biomass endogenous residue is assumed to have the same elemental composition as that of the AD biomass itself, which is assumed the same for all four AD biomass species.

The only completely new reactions are 6 to 8, which model the release of PP with the uptake of acetate by PAOs while they are still alive (6), the release of P from PP on the death of PAOs (7) and the release of poly-hydroxy-alkanoate (PHA) on the death of PAOs (8). The processes are represented by the following stoichiometry:

Reaction 6, which is the same as that of Equation 7.16d (in Section 7.4.1) of the ASM2-3P model, which caters for the anaerobic PP release with the uptake of PHA, occurring when live PAOs initially enter the AD environment:

$$\left(\frac{144\cdot YPO_4}{31}\right)Mg_cK_dCa_ePO_3+\frac{144}{64}CH_3COO^-+2\cdot\left\{\left(\frac{144\cdot YPO_4}{31}\right)-\frac{144}{64}\right\}H^+\rightarrow\left(\frac{144}{2\cdot 64}\right)C_4H_6O_2$$
$$+\left(\frac{144\cdot YPO_4}{31}\right)PO_4^{3-}+\left(\frac{144\cdot YPO_4\cdot c}{31}\right)Mg^{2+}+\left(\frac{144\cdot YPO_4\cdot d}{31}\right)K^++\left(\frac{144\cdot YPO_4\cdot e}{31}\right)Ca^{2+}$$
$$+\left\{\left(\frac{144\cdot YPO_4}{31}\right)-\frac{144}{64}\right\}H_2O \qquad (7.24)$$

Reaction 7, which represents the hydrolysis of PP after the death of PAOs, without PHA uptake:

$$K_{0.32}Mg_{0.31}Ca_{0.03}PO_3+H_2O\rightarrow 0.32K^++0.31Mg^{2+}+0.03Ca^{2+}+PO_4^{3-}+2H^+ \qquad (7.25)$$

Reaction 8, which represents the hydrolysis of PHA to glucose that can be used by the AD biomass:

$$4C_4H_6O_2+4H^++2CO_3^{2-}+4H_2O\rightarrow 3C_6H_{12}O_6\ (glu\cos e) \qquad (7.26)$$

Note that the reversible mineral precipitation or dissolution (see Equations 7.02 to 7.06) and the CO_2 gas expulsion and dissolution (see Equation 7.01) reactions, described in Section 7.3.2 are also included as model reactions. This is especially to be able to cater for the precipitation of struvite and other minerals, which has been observed to occur in AD treating P-rich WAS from BEPR systems.

Figure 7.5.1 below, presents an overview of the three phase AD model process scheme.

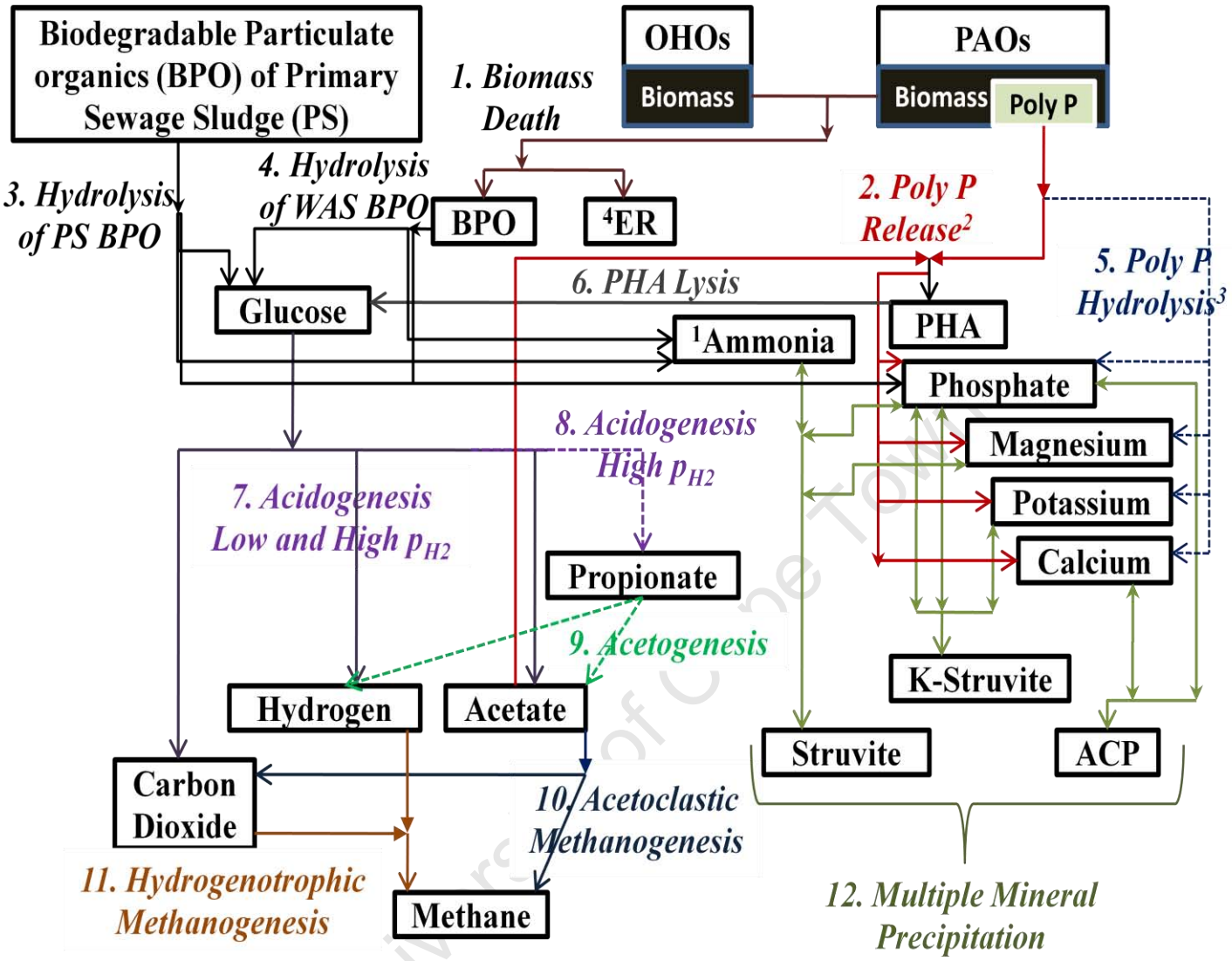

Figure 7.5.1: *Process scheme for the ADM-3P model, as extended from the UCTADM1 model of Sötemann et al. (2005). Note that (1) ammonia is released in the NH_3 form and picks up a proton from H_2CO_3 to form NH_4^+, (2) Process 2 is for PP release with the uptake of acetate and (3) process 5 is for the PP hydrolysis with the death of the PAOs, (4) ER stands for the endogenous residue of biomass. Process 12 only shows for P precipitates, but other precipitates (i.e. newberyite, calcite and magnesite, which are less likely to form) are also included in the model.*

7.5.2 Calibration of UCTADM in WEST

For all simulations, the initial reactor concentration for each model component needs to be entered together with the influent feed component concentrations for each day of the model specified experimental period. Most of these values were obtained or calculated from directly measured results.

Initial values for suitable kinetic (such as hydrolysis, growth and lysis rates) and stoichiometric (such as empirical characteristics of sewage and sludge components) constants as obtained from experimental measurements or given from literature are entered, and then adjusted during the trial and error AD simulations to fit the best-replicated experimental behaviour. The sewage and sludge characterisation was an important part of the simulation exercise. The UCTAD model considers all of the multiple sludge component types from municipal wastewater treatment, i.e. OHO, PAO (together with the stored PP) and ANO which are biomass from the AS systems used as feed to the AD systems; ER and UPO which are deemed to remain unchanged but add to the solids mass in the reactor; BPO_{PS} which could also provide organic substrate to AD feed and the AD biomass that partake in the growth and death processes (Z_{AD}, Z_{AC}, Z_{AM} and Z_{HM}).

This section of the chapter presents the calibration of the three phase AD model by a comparison of the results simulated using the AD model to measured results of COD removal, nutrient (N and P) releases, solids (TSS, VSS and ISS) concentrations, alkalinity generation, digester pH and gas composition. The dynamic AD model results were compared with data generated from the laboratory scale plant-wide experimental set-up (shown in Section 3.2 of Chapter 3) evaluated by Harding (2009) and Ikumi (2011). This set up comprised three activated sludge (AS) systems, one of which was a membrane (MBR) University of Cape Town (UCT) nitrification-denitrification (ND) biological excess P removal (BEPR) system treating real wastewater (WW) with added acetate to increase the BEPR. The WAS from this system was fed to a mesophilic (37°C) AD (AD1) which was operated at 5 different sludge ages, i.e. 10, 18, 25, 40 and 60 days. At each sludge age, once a period of three

sludge ages had elapsed, experimental tests were performed on the ADs. For the measured results the COD, N, P, Mg, K and Ca mass balances over the UCT and AD systems were between 85% and 105%, which is reasonable for these systems. Determination of the (i) first order, (ii) specific first order, (iii) Monod and (iv) saturation hydrolysis kinetic rates of the WAS followed the procedure of Sötemann *et al.* (2005a,b). The dynamic AD model includes saturation hydrolysis kinetics so the determined saturation kinetic constants were entered into the AD model. Because the hydrolysis is the slowest rate, the remaining AD bioprocesses are essentially stoichiometric. So for these processes, determination of the elemental composition of the organics and PP was more important than establishing the kinetic rates.

Aside from the sludge age (volume and influent flow), the input required for the dynamic AD model is (1) the X, Y, Z, A and B values of the composition of the biodegradable part of the OHO and PAO biomass and/or the BPO of influent PS (BPO_{PS}), (2) the PAO PP content (f_{XBGPP}) from which q is calculated, (3) the PP Mg, K and Ca content (c, d, e). Noting that the UCT system WAS comprises 5 components, i.e. OHO (denoted as X_{BH}, in mgOHO/*l*) and PAO (X_{BG}, in mgPAO/*l*) biomass, OHO (X_{EH}, in mgER/*l*) and PAO (X_{EG}, in mgER/*l*) endogenous residue, and the unbiodegradable particulate organics (UPO) from the influent wastewater (X_I, in mgUPO/*l*), the AD model input was obtained by (1) checking the Activated sludge (AS) system (i.e. either the BEPR UCT , MLE 1 or MLE 2 system, depending on where the feed sludge is coming from) COD, N, P, Mg, K and Ca mass balances, (2) calculating from the measured data on the AS system the influent UPO (X_{Ii}) and PAO VSS (X_{BG}) concentrations, and the PAO PP content (f_{XBGPP} from which q in mol/mol is obtained) with the Wentzel *et al.* (1990) NDBEPR model, which at the same time fractionates the measured VSS into its 5 components, (3) grouping the 5 VSS components into biodegradable particulate (BPO) and unbiodegradable particulate (UPO) organics, (4) comparing the AS system UPO VSS fraction, UPO/(BPO+UPO) with that measured on the effluent from the AD1 when operated at 60d sludge age, (5) determining the BPO hydrolysis kinetics rates (first order, specific first order, Monod and saturation) and VSS

unbiodegradable fraction ($f_{SL'up}$) of the WAS and/or of the PS ($f_{PS'up}$) with the data from all 5 AD sludge ages with the steady state AD model of Sötemann *et al.* (2005a), (6) calculating the mass ratios f_{cv}, f_c, f_n and f_p of the BPO VSS from the difference between the measured mass ratios of the AD WAS or PS feed (PO=UPO+BPO) and the UPO (BPO=PO-UPO), (7) calculating the X, Y, Z, A and B values of the BPO from the f_{cv}, f_c, f_n and f_p mass ratios (with the method shown in Section 5.5.2 of Chapter 5), (8) determining the PP metals content (c, d, e) from the metal mass balance over the AS system (for when dealing with WAS from the BEPR UCT system). The release of P from PP is modelled at a faster rate than the release of P from the hydrolysis of PAO and OHO biomass.

The parameters that were chosen in the three phase AD model are as shown in the Table 7.5.2 below. The parameters shown in this Table 7.5.2 do not include the empirical formulations of the organic compounds (the X, Y, Z, A and B values in the $C_XH_YO_ZN_AP_B$ empirical formulation of each organic component), hydrolysis kinetics (k_M and K_S) and AD reactor volume (V). This is because these parameters were specific to the AD of the individual sludge types (i.e. the X, Y, Z, A and B values, k_M, K_S and V are different for each of the AD experimental systems against which the model is calibrated). The biomass, ER, UPO and USO components remained the same when simulating the AD of a particular sludge feed at all the different sludge ages. However, the BPO_{PS} and FBSO required adjustment in their empirical characteristic values, for each simulation (i.e. at the different AD sludge ages) especially when they made significant contributions to the AD feed.

Since the AD systems were tested when at steady state (i.e. after three steady states periods had elapsed, see Section 3.2.3 of Chapter 3) the results predicted by the model during the simulation of the AD systems at steady state were the ones to be checked against experimental results. This means that the input characteristic components to the model were kept under constant flows and loads, when simulating each AD system at each sludge age, and the results predicted after the simulation of these systems for a period of beyond three steady states (i.e. simulation time was always greater than 3 times the operating AD sludge

age) were taken as the 'model predicted' results. Therefore, although the ADM-3P model is dynamic (in the sense that it is based on differential equations), its validation was limited to steady state constant flow and load conditions. Moreover, because the hydrolysis process in the AD is slowest, this process required a calibration as best as possible. The bioprocesses following hydrolysis are effectively stoichiometric and goverened by the hydrolysis kinetic rate. The calibration of the hydrolysis rate (and the determination of the unbiodegradable fraction of the sludge) was the focus in Section 6.2 of Chapter 6. These constants, for the kinetics of hydrolysis, obtained from the Section 6.2, were applied in the ADM-3P model and the stoichiometric and kinetic constants for other subsequent processes were obtained from literature (without any calibration done for them).

Table 7.5.2: Parameters used in Simulating the ADM-3P Model			
Parameter	**Value**	**Units**	**Description**
e_PP	0.053	-	Molar fraction of calcium in PP
F_E	0.08	-	Fraction of dead biomass to ER
ISS_BM	0.15	g/gCOD	ISS to biomass for OHO and PAO
$k'r_{ACP}$	350	-	Dissolution of calcium phosphate
$k'r_{MgKP}$	1	-	Dissolution of K-struvite
$k'r_{Struv}$	8000	-	Dissolution of struvite
ki_am	1.15E-6	mol.kg-1	H+ inhibition for acetoclastic methanogens
ki_H2	1.25	g/m3	Inhibition coefficient for H2 in acidogenesis
ki_hm	0.00053	mol.kg-1	H+ inhibition for hydrogenotrophic methanogens
KLa_{CO2}	50	1/d	CO_2 transfer coefficient
$K_{S,AC}$	6.59	g/m3	Half Sat coeff for acetogens
$K_{S,AD}$	140	g/m3	Half Sat coeff for acidogens
$K_{S,AM}$	0.78	g/m3	Half Sat coeff for acetoclastic methanogens
$K_{S,HM}$	0.3145	g/m3	Half Sat coeff for hydrogenotrophic methanogens
b_{AC}	0.015	1/d	Decay rate constant for Z_{AC}
b_{AD}	0.041	1/d	Decay rate constant for Z_{AD}
b_{AM}	0.037	1/d	Decay rate constant for Z_{AM}
k_fs	10	1/d	Hydrolysis rate constant for FBSO
b_{HM}	0.01	1/d	Decay rate constant for Z_{HM}
$b_{H\text{-}AD}$	0.38	1/d	Decay rate constant for OHO in ADs
b_{G_AD}	0.38	1/d	Decay rate constant for PAO in ADs
k_pha	0.2	1/d	Hydrolysis rate constant for PHA
d_PP	0.312	-	Molar fraction of potassium in PolyP
k_pp	0.2	1/d	Hydrolysis rate constant for PP
c_PP	0.297	-	Molar fraction of magnesium in PolyP
$\mu_{max,AC}$	1.15	1/d	Max specific growth rate for acetogens
$\mu_{max,AD}$	0.8	1/d	Max specific growth rate for acidogens
$\mu_{max,AM}$	4.39	1/d	Max specific growth rate for acetoclastic methanogens
$\mu_{max,HM}$	1.2	1/d	Max specific growth rate for hydrogenotrophic methanogens
Temperature	37	°C	System Temperature
Y_{ZAC}	0.0278	-	Acidogenesis yield (COD/COD)
Y_{ZAD}	0.1074		Lo H2 Acetogenesis yield (COD/COD)
Y_{ZAH}	0.1074		Hi H2 Acetogenesis yield (COD/COD)
Y_{ZAM}	0.0157		Acetoclastic Methanogenesis yield (COD/COD)

1. Anaerobic Digestion of NDBEPR WAS

Figure 7.5.2 below shows a comparison between the results simulated by the three phase AD dynamic model (ADM-3P) and data measured with AD sludge age for the AD of the NDBEPR WAS. The corresponding results are presented in Tables 7.5.3b and 7.5.3c below. Table 7.5.3a shows the additional parameters (added to those in Table 7.5.2) for the feed sludge characteristics, reactor volume and hydrolysis kinetics that were used in these simulations.

Table 7.5.3a: Parameters (additional to those from Table 7.5.2) used for Simulating the AD of NDBEPR WAS

Parameters	Name	Modifications					
		UPO (ϕ=up)[1]	BPO$_{PS}$ (ϕ=bps)[1]	Organisms (ϕ=o)[1]	ER (ϕ=e)[1]	FBSO (ϕ=f)[1]	USO (ϕ=us)[1]
	Y_ ϕ : H/C	1.567	2.450	1.484	1.567	2.004	1.648
	Z_ ϕ : O/C	0.565	0.839	0.362	0.565	0.660	0.511
	A_ ϕ : N/C	0.062	0.033	0.227	0.062	0.058	0.135
	B_ ϕ : P/C	0.012	0.013	0.027	0.012	0.005	0.030
Organics Empirical Formulations		[1]Whereby the empirical formula for each organic is $CH_{Y\_\phi}O_{Z\_\phi}N_{A\_\phi}P_{B\_\phi}$, and each components' parameterised CHONP molar fraction denotations are extended by its ϕ replacements (e.g. the empirical formulation for UPO is $CH_{Y\_up}O_{Z\_up}N_{A\_up}P_{B\_up}$)					
Hydrolysis Kinetics	k_M	1.917	Where k_M and K_S are the constants of saturation kinetics , obtained as shown in Section 6.1 and 6.2 of Chapter 6				
	K_S	9.149					
Reactor Volumes	V	The reactor volume is maintained at 16 litres, apart from the 60-day R_s where the volume is reduced to 5 litres.					

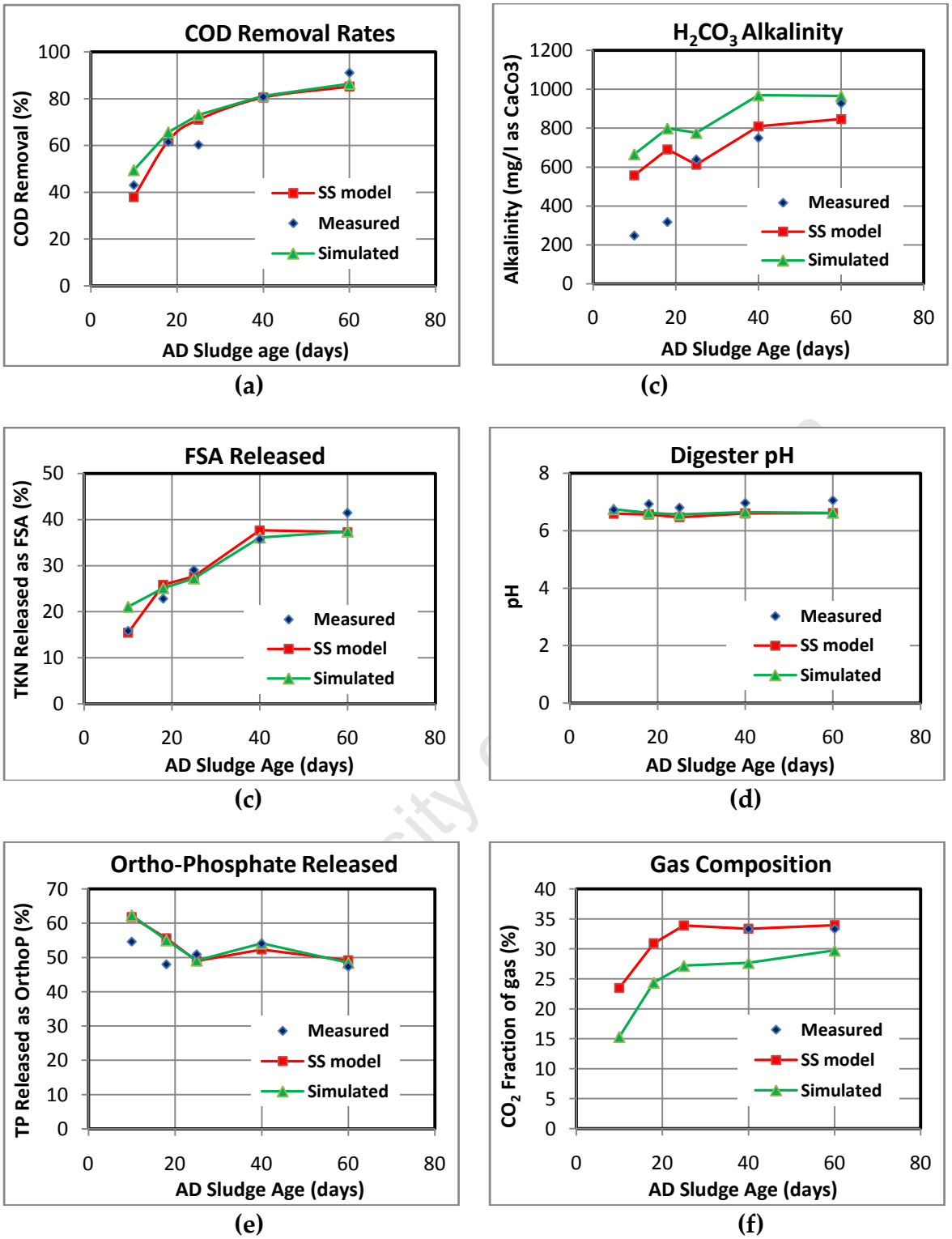

Figures 7.5.2a to f: *Comparison between the results simulated by the three phase AD dynamic model and measured data versus sludge age (R_s) for the AD of NDBEPR WAS in the order of: (a) COD removal, (b) $H_2CO_3^*$ alkalinity, (c) total nitrogen released as free and saline ammonia (FSA), (d) digester pH, (e) phosphorus released as ortho-phosphate and (f) gas composition.*

Table 7.5.3b: Measured and Simulated Results for Anaerobic Digestion of NDBEPR WAS										
Retention Time (d)	10		18		25		40		60	
Influent flow (*l*/d)	1.6		0.89		0.65		0.4		0.09	
	Measd.	Sim	Measd.	Sim	Measd.	Sim	Measd.	Sim	Measd.	Sim
Influent COD (mgCOD/*l*)	9355.4	9355.4	10061.8	10061.8	9589.4	9589.4	10126.7	10126.7	10417.9	10417.9
Influent unbiodegradable particulate COD, Supi (mgCOD/d)	5051.9	5051.9	5433.4	5433.4	5178.3	5178.3	5468.4	5468.4	5625.7	5625.7
Influent biodegradable particulate COD, Sbpi (mgCOD/*l*)	4267.2	4267.2	4599.0	4599.0	4373.8	4373.8	4643.6	4643.6	4762.3	4762.3
Influent VFA, S_{asi} (mgCOD/*l*)	0.0	0.0	0.0	0.0	0.0	0.0	0.0	0.0	0.0	0.0
Influent TKN (mgN/*l*)	550.5	533.5	598.6	577.2	596.4	549.6	560.0	581.5	670.1	597.8
Influent FSA (mgN/*l*)	1.8	1.8	5.0	5.0	4.6	4.6	5.0	5.0	5.1	5.1
Influent Alkalinity (mg/*l* as $CaCO_3$)	-	350.0	-	350.0	230.0	350.0	-	350.0	-	350.0
Influent pH	7.9	8.0	-	8.0	7.6	8.0	-	8.0	-	8.0
Influent TP (mgP/*l*)	866.6	850.3	914.5	922.3	988.5	851.1	866.0	864.7	921.9	860.2
Influent OP (mgP/*l*)	18.8	18.6	19.6	20.4	24.8	25.0	16.4	18.2	18.9	18.8
Influent TSS (mg/*l*)	8595.9	8561.5	9175.6	9269.9	9882.0	9908.4	9494.5	9251.0	9870.8	9890.0
Influent VSS (mg/*l*)	6482.4	6448.0	6921.2	6941.6	6582.8	6609.2	6990.5	6996.6	7168.4	7187.6
Influent ISS (mg/*l*)	2113.5	2113.5	2254.4	2328.4	3299.2	3299.2	2504.0	2254.4	2702.4	2702.4
Effluent COD, Ste (mgCOD/*l*)	7519.8	7911.0	7234.6	7635.7	6953.9	6921.4	6375.5	6888.6	6080.0	6829.9
Effluent VFA, Sase (mgCOD/*l*)	8.0	208.1	24.7	132.1	12.7	98.9	24.7	84.7	0.4	68.5
Effluent FSA (gN/*l*)	88.9	114.3	141.5	150.0	177.8	154.3	210.7	215.0	282.9	228.7
Effluent OP (mgP/*l*)	492.1	550.2	458.7	528.1	460.4	443.5	469.6	486.5	422.8	436.0
Effluent Alkalinity (mg/*l* as $CaCO_3$)	562.5	1212.8	854.6	1213.8	926.7	1095.3	932.3	1322.6	1281.0	1266.0
Measured digester pH	6.7	6.8	6.9	6.6	6.8	6.6	7.0	6.7	7.1	6.6
COD removed (%)	43.0	49.5	61.5	65.7	60.3	73.1	80.8	81.2	91.1	86.5
Volume of CH_4 (litres)	412.4	2.6	906.8	2.4	974.5	1.8	1246.2	1.4	0.0	1.0
Volume of CO_2 (litres)	225.8	0.5	496.6	0.8	533.7	0.7	682.5	0.5	0.0	0.4
FSA released (%)	15.8	21.1	22.8	25.1	29.0	27.2	36.7	36.1	41.5	37.4
OP released (%)	54.6	62.5	48.0	55.0	44.1	49.2	52.3	54.2	43.8	48.5
Gas composition (%CO2)	0.4	0.2	0.4	7.0	0.4	0.2	0.4	7.5	0.4	0.3
COD balance (%)	92.0	101.8	95.6	101.9	99.6	101.8	95.3	101.8	90.7	101.7
N balance (%)	108.3	100.2	98.4	100.3	100.0	100.3	96.5	100.3	87.9	100.3
P balance (%)	105.3	99.1	100.0	100.3	86.5	100.3	93.5	101.4	90.2	100.4

Table 7.5.3c: Comparison of Simulated to Measured Metals Data in Anaerobic Digestion of NDBEPR WAS										
Retention Time (d)	10		18		25		40		60	
Influent flow (*l*/d)	1.6		0.89		0.65		0.4		0.085	
	Meas.	Sim	Meas.	Sim	Meas.	Sim	Meas.	Sim	Meas.	Sim
Influent magnesium (g/*l*)	235.7	227.8	290.9	291.3	289.5	299.4	313.1	252.2	279.3	279.7
Filt. Influent magnesium (g/*l*)	89.2	70.5	59.6	118.1	74.1	142.2	81.8	90.3	93.2	122.3
Influent potassium (g/*l*)	400.0	386.9	494.0	495.0	442.3	443.2	447.9	448.8	401.8	402.7
Filt. Influent potassium (g/*l*)	95.0	121.6	80.6	202.7	98.7	178.1	75.4	175.7	98.1	137.2
Influent calcium (g/*l*)	50.7	48.9	54.0	53.7	58.5	58.2	52.9	52.6	56.4	56.1
Filt. Influent calcium (g/*l*)	12.3	21.9	22.8	23.9	27.2	31.2	21.8	24.7	21.1	29.0
Effluent magnesium (g/*l*)	225.1	228.0	252.1	179.2	296.7	291.6	273.2	179.2	299.0	299.6
Filt. Effluent magnesium (g/*l*)	24.1	90.7	23.8	74.1	24.1	63.7	22.6	60.9	25.0	50.7
Effluent potassium (g/*l*)	307.6	383.6	391.9	302.0	394.8	491.9	373.3	301.3	400.3	440.4
Filt. Effluent potassium (g/*l*)	273.3	381.0	355.8	211.8	362.5	490.3	362.5	239.7	372.4	439.4
Effluent calcium (g/*l*)	42.8	48.9	43.4	51.7	43.2	53.7	42.8	51.8	39.8	57.5
Filt. Effluent calcium (g/*l*)	41.6	55.9	37.4	36.8	28.8	61.6	34.1	41.6	26.8	65.5
Magnesium balance (%)	95.5	100.1	102.0	100.1	103.3	100.1	102.3	100.1	98.2	100.1
Potassium balance (%)	76.9	99.2	79.9	99.4	90.5	99.4	84.1	99.4	100.7	99.3
Calcium balance (%)	84.5	99.8	79.9	100.0	68.0	98.8	49.4	100.4	86.3	99.3
Where measd. and sim. stand for measured and simulated results respectively.										

Apart from gas composition and H_2CO_3* alkalinity, the results predicted by the ADM-3P simulation model (Figure 7.5.2) correspond reasonably well to those measured. The steady state model shows reasonably close matches to the measured results, and (apart from the gas composition and H_2CO_3* alkalinity) to the ADM-3P dynamic model. The poor correlation for the ADM-3P predicted gas composition and H_2CO_3* alkalinity is different from the SS model because CO_2 gas-liquid transfer equilibrium is determined using Henry's law equation (with $pK_{HCO2} = 1.59$, see Equation 6.44), while the ADM-3P uses a lower equilibrium constant (log K = 1.466, see Equation 7.01).

The FSA releases show a similar trend to COD removal, indicating its steady release as the sludge is degraded. The breakdown of sludge biodegradable organics, results in the release

of organically bound N, which is in the non-ionic NH_3 form and are non-reference species for the ammonia weak acid/base system. On release, the NH_3 picks up a H^+ ion from the bulk liquid which is supplied by the dissolved CO_2 ($H_2CO_3^*$) forming HCO_3^- i.e.:

$$NH_3 + H_2CO_3 \rightarrow NH_4^+ + HCO_3^- .$$

(7.3a)

Since the production of this HCO_3^- is the main generation of alkalinity in an AD treating PS or WAS that is not P rich, it is reasonable, during calibration, to have a trade-off between the predicted alkalinity generated and FSA released in these systems. However, in this digester treating waste activated sludge from biological excess phosphorus removal (BEPR) systems that contains high concentrations of polyphosphate ($Mg_cK_dCa_ePO_3$), the total alkalinity generation also depends on how this PP is released.

Initially, once entering the environment of the anaerobic digester, the PAOs are modelled to carry out the same PP release mechanisms as in the anaerobic reactor of the parent BEPR AS system. This initial polyphosphate release occurs with the uptake of acetate and results in increased alkalinity by the addition of $H_2PO_4^-$, viz.

$$2Mg_cK_dCa_ePO_3 + 2CH_3COOH + NADH_2^+ \rightarrow C_4H_6O_2 + NAD^+ + 2H_2PO_4^- + 2cMg^{2+} + 2dK^+ + 2eCa^{2+}$$

(7.3b)

However, because the PAOs also require an aerobic condition to supply them with the terminal electron acceptor (oxygen) for their growth, they cannot grow in the anaerobic digester. Therefore, the PAOs are also modelled to eventually die; releasing the rest of their stored PP and poly-hydroxy butyrate (PHB) as they are hydrolysed by the AD biomass. Depending on the charge/proton balance requirements, some of the $H_2PO_4^-$ species may become HPO_4^{2-} species while keeping the total alkalinity constant but increasing the partial pressure of the AD gas (p_{CO2}), viz.

$$H_2PO_4^- + HCO_3^- \rightarrow HPO_4^{2-} + H_2O + CO_2$$

(7.3c)

The organic P in the PAO (and OHO) biomass is released as H_3PO_4. Because this is the reference species for the OP weak acid/base system, the total alkalinity does not change. However, in the AD pH range 7 to 8, the H_3PO_4 species lose 1 or 2 H^+ to become $H_2PO_4^-$ or HPO_4^{2-} species. The H^+ reacts with HCO_3^- to become H_2O and CO_2. So while the total alkalinity does not change, the species that represent it do, and the CO_2 that would have been retained in the aqueous phase as HCO_3^- now exits the AD as gas, which increases the pCO_2 (the CH_4 gas production remains unchanged because it is fixed by the COD of the biodegraded organics).

Therefore, overestimating the PP and biomass P content of the PAO (and OHO) biomass could lead to underprediction of bicarbonate (HCO_3^-) alkalinity and pH. Moreover, the rapid release of PP and associated Mg^{2+} (yielding high concentrations of P species in the AD liquor already at short sludge ages (< 10d)) and the increased release of ammonia with sludge age promote struvite precipitation. This struvite precipitation requires phosphate system species, which decreases the total alkalinity and so results in re-speciation of the inorganic carbon system, which causes changes in p_{CO2} and AD pH (Loewenthal *et al.*, 1994).

$$Mg + NH_4^+ + PO_4^{3-} \rightarrow MgNH_4PO_4 \qquad (7.3d)$$

However, as already mentioned total alkalinity (T.Alk) is significantly reduced, with struvite precipitation. As can be seen in Figure 7.11e, struvite precipitation is responsible for the OP exhibiting a steady decrease rather than an increasing trend with sludge age, similar to FSA release.

With all the above-mentioned interrelated variables it is important to know which of the measurements is most reliable and how far to trade-off between simulated results, in order to get reasonable predictions. The best elemental formulation was maintained for all sludge ages because it was deemed more important to observe that the model is predicting similar trends to experimentally measured results and then to provide reasons for observed

discrepancies, rather than to correct the discrepancies by changing the elemental formulation at each sludge age.

Batch-AD of NDBEPR WAS to Observe P Release

To observe the rate of phosphorus release in AD, Harding (2009) conducted experimental AD batch tests on the NDBEPR WAS. These batch tests were performed using a 5 litre continuously stirred mesophilic (35 °C) AD reactor. This reactor was seeded with a 50:50 ratio mixture of NDBEPR WAS to effluent waste sludge from the continuous AD system described above, for the 18-day R_s operation. One batch test was conducted on undiluted NDBEPR WAS (~ 10gTSS/*l*), the other was diluted five times. Figure 7.5.3 below shows a comparison between the results measured in the undiluted batch test and results simulated with the three phase AD model, with and without struvite precipitation.

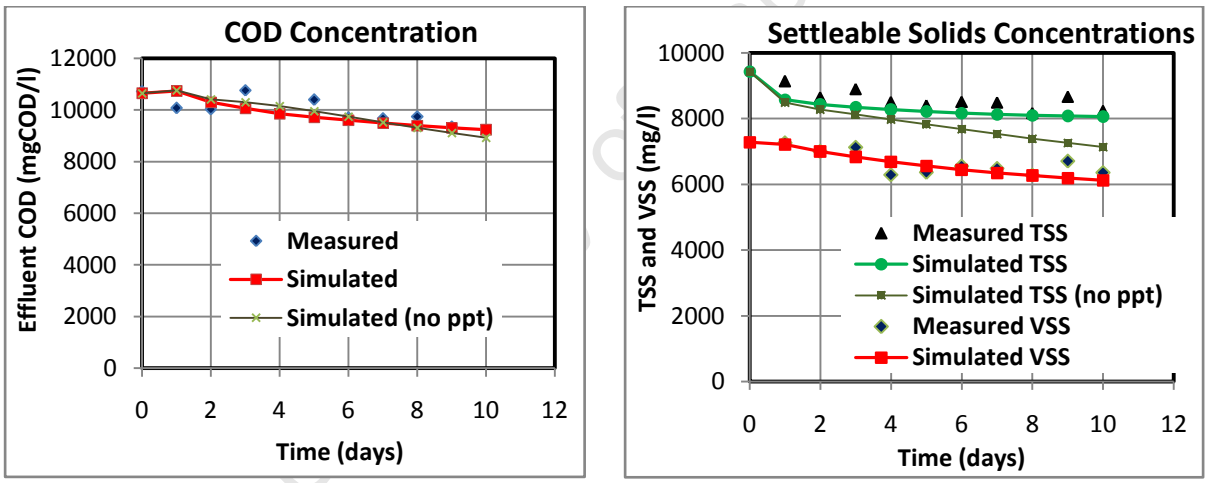

(a) (b)

Figures 7.5.3a and b: *Comparison between experimentally measured and simulated results for a batch AD fed P rich WAS from Biological Excess P Removal (BEPR) Activated Sludge (AS) system blended with mixed liquor from the continous AD system treating BEPR waste AS in 50:50 ratio in the order of: (a) COD concentration and (b) settleable solids concentration.*

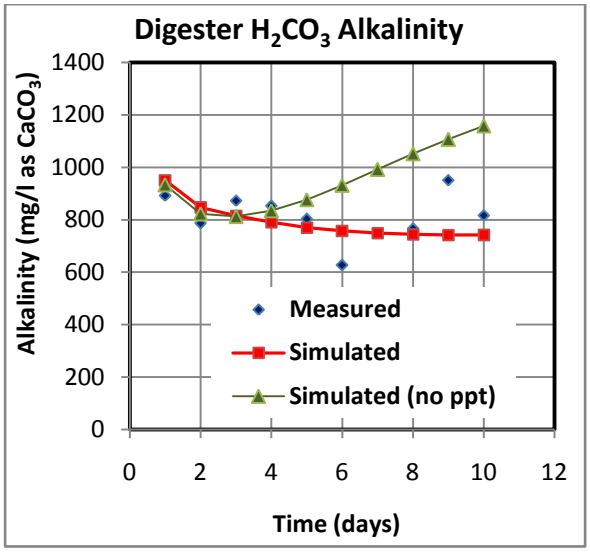

(c)

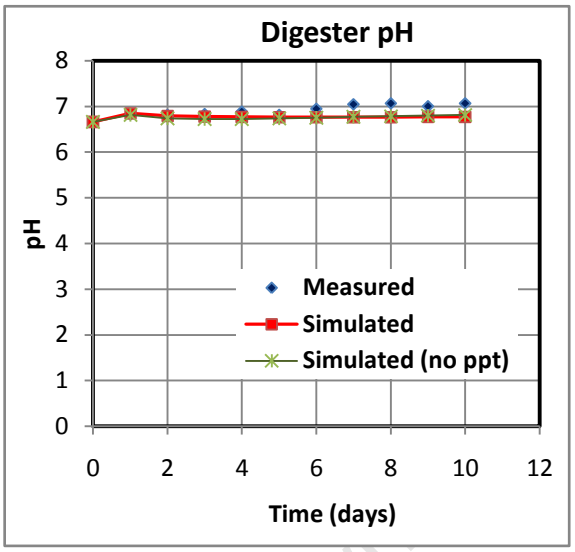

(d)

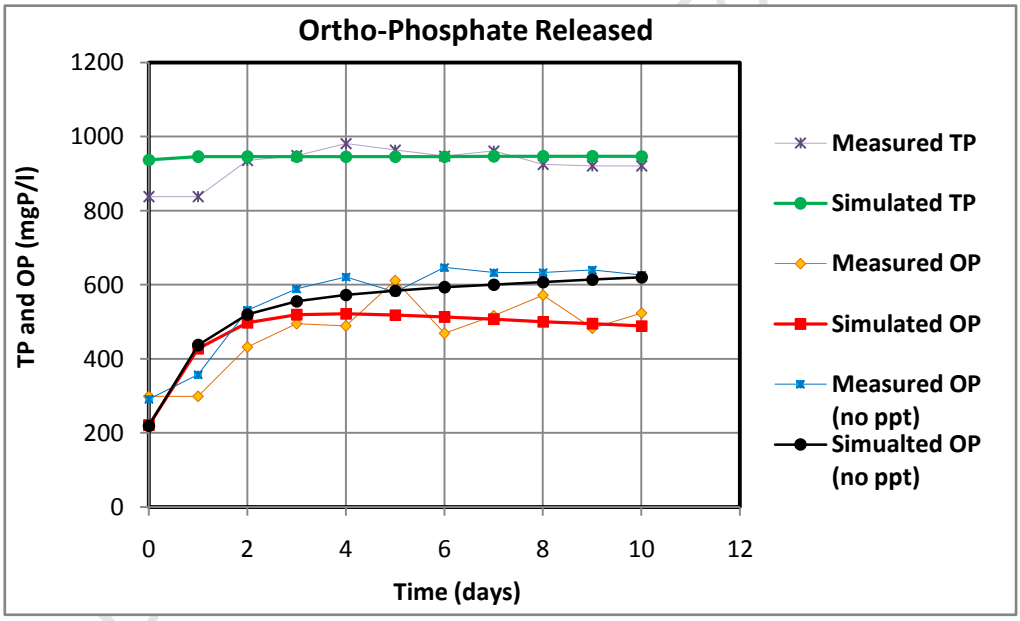

(e)

Figures 7.5.3c to e: *Comparison between experimentally measured and simulated results for a batch AD fed P rich WAS from Biological Excess P Removal (BEPR) Activated Sludge (AS) system blended with mixed liquor from the continous AD system treating BEPR waste AS in 50:50 ratio in the order of: (c) H_2CO_3* alkalinity, (d) pH and (e) ortho-phosphate released.*

Figures 7.5.3a to e show that a closer match between experimental and simulated results is made, when including struvite precipitation than without precipitation. Most of the P is

released (as ortho-phosphate, OP) within 4 days, after which the P release, if any was very slow or gradual. This conforms to the observation by Jardin *et al.* (1994), confirming that stored polyphosphate in PAOs (which forms a large portion of the TP content) is released within seven days. The OP simulated for infinite solubility of struvite matches well with that measured in the diluted batch test (multiplied by the dilution factor), while the OP simulated with inclusion of struvite precipitation matches the OP measured in the undiluted batch test. This validates the capability of the model to predict mineral precipitation during AD. The other graphs (Figure 7.5.3c) which show reduced H_2CO_3 alkalinity and increased TSS (Figure 7.5.3b, since struvite contributes to inorganic solids concentration in the AD) provide further support of the reduced simulated OP being due to struvite precipitation.

2. Anaerobic Digestion of ND WAS from MLE Systems

Figures 7.5.4 and 7.5.5 below show a comparison between the results simulated by the three phase AD dynamic model and data measured with different AD sludge ages for the AD of the MLE 1 and MLE 2 WAS respectively. The corresponding results are presented in Tables 7.5.5b and 7.5.5b below.

The parameters for simulating the AD of MLE 1 and MLE 2 are the same as shown in Table 7.5.2 above with, as the AD of NDBEPR WAS, additional parameters for the feed sludge characteristics, reactor volume and hydrolysis kinetics. These added parameters are listed in Tables 7.5.5a (for MLE 1) and 7.5.5a (for MLE 2) below.

Table 7.5.5a: Parameters (additional to those from Table 7.5.2) for simulating the AD of MLE 1 WAS							
Parameters	Name	Modifications					
		UPO (ϕ=up) [1]	BPO_{PS} (ϕ=bps)[1]	Organisms (ϕ=o)[1]	ER (ϕ=e)[1]	FBSO (ϕ=f)[1]	USO (ϕ=us)[1]
	Y_ ϕ : H/C	1.482	2.450	1.463	1.482	2.010	1.646
	Z_ ϕ : O/C	0.472	0.839	0.355	0.472	0.592	0.593
	A_ ϕ : N/C	0.113	0.033	0.229	0.113	0.119	0.062
	B_ ϕ : P/C	0.022	0.013	0.031	0.022	0.012	0.020
Organics Empirical Formulations		[1]Whereby the empirical formula is for all each of the organic is $CH_{Y\_\phi}O_{Z\_\phi}N_{A\_\phi}P_{B\_\phi}$, and each components' parameterised CHONP molar fraction denotations are extended by its ϕ replacements (e.g. the empirical formulation for UPO is $CH_{Y\_up}O_{Z\_up}N_{A\_up}P_{B\_up}$)					
Hydrolysis Kinetics	k_M	1.603	Where k_M and K_S are the constants of saturation kinetics, obtained as shown in Section 6.1 and 6.2 of Chapter 6				
	K_S	5.387					
Reactor Volumes	V	The reactor volume is maintained at 12 litres, apart from the 60-day R_s where the volume is reduced to 5 litres.					

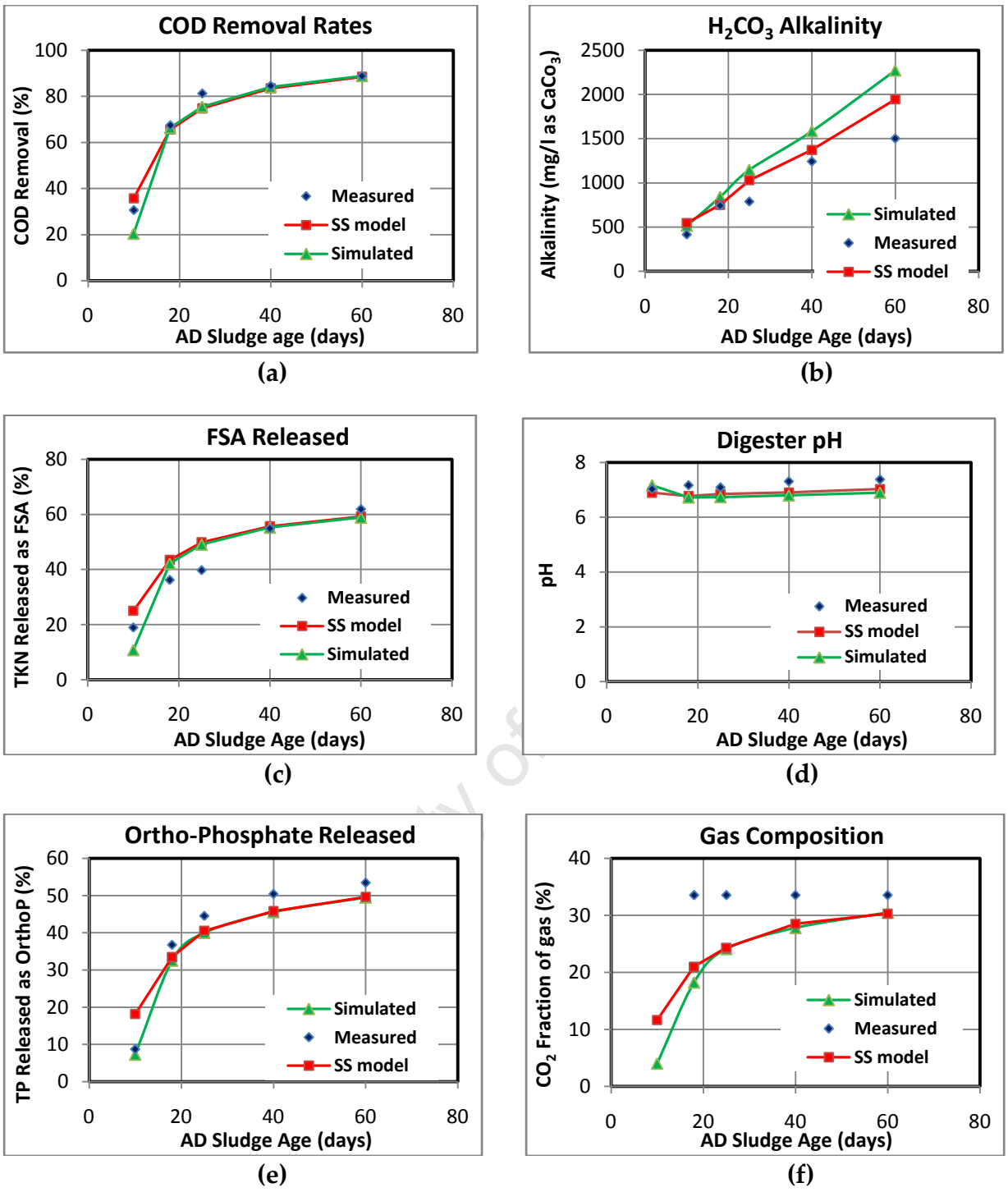

Figures 7.5.4a to f: *Comparison between the results simulated by the three phase AD dynamic model, calculated by the three phase AD steady state model and measured data versus digester sludge age (R_s) for the AD of MLE 1 WAS in the order of: (a) COD removal, (b) digester H_2CO_3* alkalinity, (c) total nitrogen released as free and saline ammonia (FSA), (d) digester pH, (e) phosphorus released as ortho-phosphate and (f) gas composition.*

Table 7.5.5b: Measured and Simulated Results for Anaerobic Digestion of MLE 1 WAS										
Retention Time (d)	10		18		25		40		60	
Influent flow (*l*/d)	1.2		0.67		0.48		0.3		0.085	
	Measd.	Sim	Measd.	Sim	Measd.	Sim	Measd.	Sim	Measd.	Sim
Influent COD (mgCOD/*l*)	2672.5	2512.6	3648.0	3648.0	5150.5	5150.5	8053.1	8053.1	11705.1	11695.9
Influent unbiodegradable particulate COD, Supi (mgCOD/d)	1256.1	1256.1	1714.6	1714.6	2420.7	2420.7	3785.0	3785.0	5501.4	5501.4
Influent biodegradable particulate COD, Sbpi (mgCOD/*l*)	1224.1	1224.1	1840.5	1840.5	2673.6	2673.6	4175.5	4175.5	6147.3	6147.3
Influent VFA, Sasi (mgCOD/*l*)	159.9	0.0	61.1	61.1	0.0	0.0	65.0	64.9	23.0	13.8
Influent TKN (mgN/*l*)	175.7	178.4	295.8	258.6	362.4	370.3	629.8	574.9	863.3	841.8
Influent FSA (mgN/*l*)	3.7	3.7	4.2	4.2	3.8	3.8	3.8	3.8	4.4	4.4
Influent Alkalinity (mg/*l* as $CaCO_3$)	550.0	550.0	694.7	694.7	506.5	506.5	460.0	460.0	523.0	523.0
Influent pH	7.7	7.7	7.8	7.8	7.6	7.6	7.6	7.6	7.8	7.8
Influent TP (mgP/*l*)	63.0	71.3	92.9	97.7	136.3	132.8	225.5	204.3	350.6	293.7
Influent OP (mgP/*l*)	11.1	11.1	10.9	10.9	7.9	7.9	10.2	10.2	9.6	9.6
Influent TSS (mg/*l*)	2147.7	2062.3	3048.0	2961.8	4217.3	4221.3	6581.3	6623.7	9490.8	9555.1
Influent VSS (mg/*l*)	1781.1	1695.7	2518.1	2431.8	3481.3	3485.3	5403.7	5446.1	7905.6	7969.9
Influent ISS (mg/*l*)	366.6	366.6	529.9	529.9	736.0	736.0	1177.6	1177.6	1585.2	1585.2
Effluent COD, Ste (mgCOD/*l*)	2291.0	2472.9	2507.8	2621.7	3007.0	3453.0	4454.0	4932.8	6215.6	6867.1
Effluent VFA, Sase (mgCOD/*l*)	32.0	84.2	12.2	83.5	36.3	80.1	10.3	80.7	25.0	90.8
Effluent FSA (gN/*l*)	37.0	22.9	102.3	113.3	148.0	185.6	297.9	321.6	465.7	500.3
Effluent OP (mgP/*l*)	16.6	16.2	45.1	42.6	68.6	61.0	129.4	103.3	197.2	154.9
Effluent Alkalinity (mg/*l* as $CaCO_3$)	415.3	516.9	742.2	842.9	789.3	1148.9	1243.7	1585.7	1504.0	2272.7
Measured digester pH	7.0	7.2	7.2	6.7	7.1	6.7	7.3	6.8	7.4	6.9
COD removed (%)	21.6	20.4	60.6	66.3	81.3	75.5	84.6	84.1	88.9	88.8
Volume of CH_4 (litres)	-	39.4	326.1	899.9	735.4	1078.0	1213.6	1240.6	-	1294.3
Volume of CO_2 (litres)	-	1.6	164.7	200.8	371.4	342.5	612.9	478.0	-	568.0
FSA released (%)	19.0	10.8	33.2	42.2	39.8	49.1	46.7	55.3	53.4	58.9
OP released (%)	8.7	7.3	36.8	32.5	44.6	40.0	52.8	45.5	53.5	49.5
Gas composition (%CO2)	39.0	4.0	33.6	18.2	33.6	24.1	33.6	27.8	39.0	30.5
COD balance (%)	91.3	99.9	92.2	100.3	95.9	100.5	94.9	100.7	92.7	101.2
N balance (%)	100.7	100.0	91.5	100.1	103.5	100.1	85.0	100.2	86.2	100.3
P balance (%)	95.5	100.0	102.1	100.1	100.2	100.1	104.7	100.2	93.5	100.3
Where measd. and sim stand for measured and simulated results respectively.										

Table 7.5.6a: Parameters (additional to those from Table 7.5.2) for simulating the AD of MLE 2 WAS							
Parameters	Name	Modifications					
		UPO (ϕ=up)[1]	BPO$_{PS}$ (ϕ=bps)[1]	Organisms (ϕ=o)[1]	ER (ϕ=e)[1]	FBSO (ϕ=f)[1]	USO (ϕ=us)[1]
	Y_ ϕ : H/C	1.449	2.158	1.352	1.449	1.986	1.669
	Z_ ϕ : O/C	0.420	0.583	0.374	0.420	0.612	0.595
	A_ ϕ : N/C	0.154	0.120	0.214	0.154	0.097	0.064
	B_ ϕ : P/C	0.024	0.022	0.031	0.024	0.012	0.018
Organics Empirical Formulations		[1]Whereby the empirical formula is for all each of the organic is $CH_{Y\_\phi}O_{Z\_\phi}N_{A\_\phi}P_{B\_\phi}$, and each components' parameterised CHONP molar fraction denotations are extended by its ϕ replacements (e.g. the empirical formulation for UPO is $CH_{Y\_up}O_{Z\_up}N_{A\_up}P_{B\_up}$).					
Hydrolysis Kinetics	k_M	1.52	Where k_M and K_S are the constants of saturation kinetics, obtained as shown in Section 6.1 and 6.2 of Chapter 6.				
	K_S	4.84					
Reactor Volumes	V	The reactor volume is maintained at 15 litres, apart from the 60-day R_s where the volume is reduced to 5 litres.					

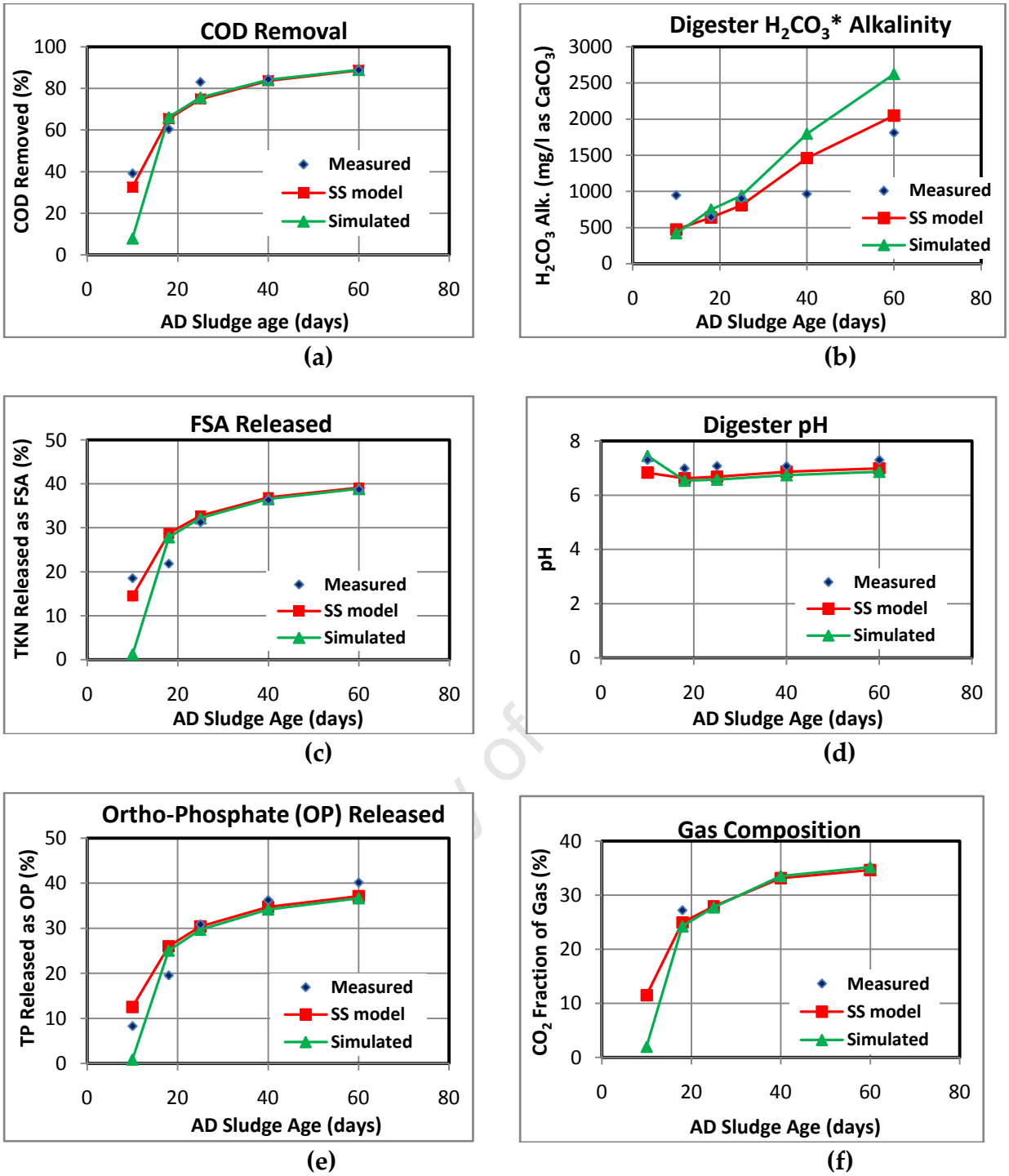

Figures 7.5.5a to f: *Comparison between the results simulated by the three phase AD dynamic model, calculated with the three phase AD steady state model and measured data versus digester sludge age (R_s) for the AD of MLE 2 WAS in the order of: (a) COD removal, (b) digester H_2CO_3* alkalinity, (c) total nitrogen released as free and saline ammonia (FSA), (d) digester pH, (e) phosphorus released as ortho-phosphate and (f) gas composition.*

Table 7.5.6b: Measured and Simulated Results for Anaerobic Digestion of MLE 2 WAS										
Retention Time (d)	10		18		24		40		60	
Influent flow (*l*/d)	1.2		0.67		0.5		0.3		0.085	
	Measd.	Sim	Measd.	Sim	Measd.	Sim	Measd.	Sim	Measd.	Sim
Influent COD (mgCOD/*l*)	3027.4	2807.7	6743.6	6743.6	8210.3	8210.4	17693.2	17693.2	24749.2	24749.2
Influent unbiodegradable particulate COD, Supi (mgCOD/d)	1877.0	1657.3	4181.0	4181.0	5090.4	5090.4	10969.8	10969.8	15344.5	15344.5
Influent biodegradable particulate COD, Sbpi (mgCOD/*l*)	1113.7	1113.7	2522.6	2522.6	3059.0	3059.0	6682.8	6682.8	9363.1	9363.1
Influent VFA, Sasi (mgCOD/*l*)	0.0	0.0	0.0	0.0	0.0	0.0	0.0	0.0	0.0	0.0
Influent TKN (mgN/*l*)	184.1	202.6	504.4	499.1	601.8	605.6	1383.6	1306.8	2014.5	1827.4
Influent FSA (mgN/*l*)	4.3	4.3	4.3	4.3	3.9	3.9	4.3	4.3	4.5	4.5
Influent H_2CO_3 Alkalinity (mg/*l* as $CaCO_3$)	0.0	0.0	0.0	0.0	0.0	0.0	280.0	280.0	0.0	0.0
Influent pH	7.5	7.5	-	-	-	-	-	-	-	-
Influent TP (mgP/*l*)	72.2	75.1	164.6	176.5	222.9	209.0	453.6	445.2	688.6	617.8
Influent OP (mgP/*l*)	8.7	8.7	11.3	11.3	8.0	8.0	10.8	10.8	10.0	10.0
Influent TSS (mg/*l*)	2592.5	2430.1	5547.2	5597.4	6740.3	6809.2	14105.6	14182.9	20263.5	20533.7
Influent VSS (mg/*l*)	2072.0	1909.6	4564.0	4614.3	5540.3	5609.2	12074.7	12152.0	16738.8	17009.0
Influent ISS (mg/*l*)	520.5	520.5	983.1	983.1	1200.0	1200.0	2030.9	2030.9	3524.7	3524.7
Effluent COD, Ste (mgCOD/*l*)	2590.6	2807.7	5197.4	5374.8	5912.7	6239.9	12050.1	12769.6	16426.5	17397.7
Effluent VFA, Sase (mgCOD/*l*)	29.6	0.1	3.0	70.7	4.4	68.1	0.8	92.9	15.0	105.7
Effluent FSA (gN/*l*)	38.4	6.8	113.8	143.3	208.4	198.8	507.0	482.0	784.8	714.8
Effluent OP (mgP/*l*)	14.7	9.4	43.3	55.5	76.8	70.1	175.2	162.9	286.5	236.6
Effluent H_2CO_3 Alkalinity (mg/*l* as $CaCO_3$)	946.2	420.1	643.5	750.6	901.5	943.1	964.2	1798.8	1812.6	2624.6
Measured digester pH	7.3	7.4	7.0	6.5	7.1	6.6	7.1	6.7	7.3	6.9
COD removed (%)	39.2	8.0	61.3	66.2	75.1	75.7	84.4	84.2	88.9	89.0
Volume of CH_4 (litres)	209.9	0.0	522.5	1200.6	919.8	1250.1	2149.9	1981.1	0.0	1990.2
Volume of CO_2 (litres)	78.5	0.0	195.3	384.1	343.9	480.0	803.7	998.8	0.0	1079.8
FSA released (%)	18.5	1.2	21.7	27.9	34.0	32.2	36.3	36.6	38.7	38.9
OP released (%)	8.3	0.9	19.5	25.1	30.9	29.7	36.2	34.2	40.1	36.7
Gas composition (%CO2)	40.0	2.0	27.2	24.2	27.2	27.7	27.2	33.5	41.0	35.2
COD balance (%)	103.8	100.0	97.4	100.3	101.4	100.4	108.0	100.8	106.2	100.6
N balance (%)	95.5	100.2	99.6	100.1	108.7	100.1	89.3	100.3	85.5	100.4
P balance (%)	108.4	100.7	117.9	100.1	109.2	100.1	101.3	100.3	92.2	100.4
Where measd. and sim stand for measured and simulated results respectively.										

As can be seen in the Figures 7.5.4 and 7.5.5, the dynamic model simulated results reasonably match the experimentally measured values, but the alkalinity measurements for the last three sludge ages are poorly correlated. Both simulated and measured results show trends of increased COD removal together with FSA and OP release, which is expected with increased AD sludge age. This increase is attributed to the increased retention time available for the degradation of WAS BPO and hence release of organically bound N and P into the AD liquor. The higher measured FSA releases could be due to the feed to the AD in the last three sludge ages having an increased organic N content. The H_2CO_3* alkalinity is also expected to increase as sludge age increases due to the increase in ammonia contributing to the formation of HCO_3^- (via $NH_3 + H_2O + CO_2 \rightarrow NH_4 + HCO_3^-$). In this case, it is hard to find a reasonable trade-off between the predicted $H_2CO_3^*$ alkalinity generated (which is mainly $[HCO_3^-]$) and FSA released, since some of the measured results show a high FSA release and low alkalinity. It was concluded that this inconsistency is due to either unreliable influent alkalinity or biodegradable sludge concentrations, since these parameters were tested only during the steady state period.

The simulated and measured methane production mirrors the COD removal trend, which is expected because the methane production is directly proportional to the COD removal. The methane production depends only on the electron donating capacity of the biodegradable organics, and being insoluble at atmospheric pressure, all exits as gas. The mole fraction of the CO_2 in the gas phase $[CO_2/ (CO_2 + CH_4)]$ sets the partial pressure of the gas phase (p_{CO2}) which together with the $H_2CO_3^*$ alkalinity ($\approx [HCO_3^-]$) set the AD pH. Thus, the dynamic AD model requires adjustment of CO_2 gas stripping kinetic constants to provide a good prediction of alkalinity (which decreases with increased CO_2 expulsion rate) and pH (which increases with increased CO_2 expulsion rate). For $R_s < 25d$, the OP concentration is too low to significantly affect digester pH. Because dissolved metals concentrations are very low and

OP concentration low, with AD of ND WAS, no mineral precipitation took place in these ADs.

3. Anaerobic Digestion of PS only

a. Comparison of ADM-3P predictions to Izzett *et al.* (1992) data and UCTADM1:

Figure 7.5.6 compares the simulated results from the AD of PS with the results from the mass balance based dynamic two phase (aqueous-gas) AD model, UCTADM1 (Sötemann *et al.*, 2005b). The corresponding results are presented in Table 7.5.7b. This UCTADM1 model was validated using results from Izzett *et al.* (1992) who conducted a series of experiments investigating the mesophilic anaerobic digestion of primary sewage sludge at AD sludge ages of 20, 15, 12, 10 and 7 days. The same influent data from Izzett *et al.* (1992) was used as input to the UCTADM1 and ADM-3P models and the simulation results of both are compared with the effluent concentrations measured by Izzett *et al.* (1992). Parameters for sludge characteristics, AD volume and hydrolysis kinetics, which match the AD conditions to those reported by Sötemann *et al.* (2005b), were added to those in Table 7.5.2. The PS elemental composition of $C_{3.5}H_7O_2N_{0.196}P_{0.01}$ was applied by Sötemann *et al.* (2006) in simulating the AD data with UCTADM1 at the various AD sludge ages. The additional parameters are listed below in Table 7.5.7a. The comparison of the UCTADM1 model to that of ADM-3P, for the AD of PS, with no occurrence of precipitation was mainly done for verification through testing the different model implementations, since the ADM-3P is a model prepared in WEST®, and UCTADM1 (which ADM-3P extends) is prepared in Aquasim.

Table 7.5.7a: Parameters (additional to from Table 7.5.2) for simulating the AD of PS (data obtained from Izzett *et al.*, 1992)							
Parameters	Name	Modifications					
		UPO (ϕ=up)[1]	BPO_{PS} (ϕ=bps)[1]	Organisms (ϕ=o)[1]	ER (ϕ=e)[1]	FBSO (ϕ=f)[1]	USO (ϕ=us)[1]
	Y_ ϕ : H/C	1.465	2.000	1.400	1.400	2.000	1.966
	Z_ ϕ : O/C	0.484	0.571	0.400	0.400	0.571	0.689
	A_ ϕ : N/C	0.100	0.056	0.200	0.200	0.056	0.027
	B_ ϕ : P/C	0.023	0.003	0.030	0.030	0.003	0.005
Organics Empirical Formulations		[1]Whereby the empirical formula is for all each of the organic is $CH_{Y\_\phi}O_{Z\_\phi}N_{A\_\phi}P_{B\_\phi}$, and each components' parameterised CHONP molar fraction denotations are extended by its ϕ replacements (e.g. the empirical formulation for UPO is $CH_{Y\_up}O_{Z\_up}N_{A\_up}P_{B\_up}$).					
Hydrolysis Kinetics	k_{M_PS}	6.797	Where k_{M_PS} and K_{S_PS} are the respective k_M and K_s constants of saturation kinetics for PS hydrolysis, obtained as reported by Sötemann *et al.* (2005b).				
	K_{S_PS}	10.829					
Reactor Volumes	V	The reactor volume is maintained at 14 litres.					

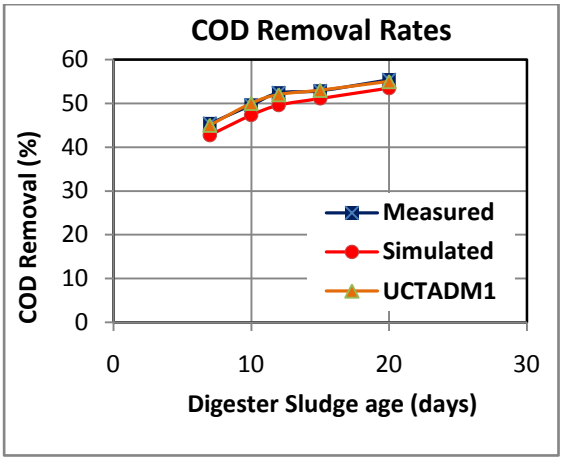

(a)

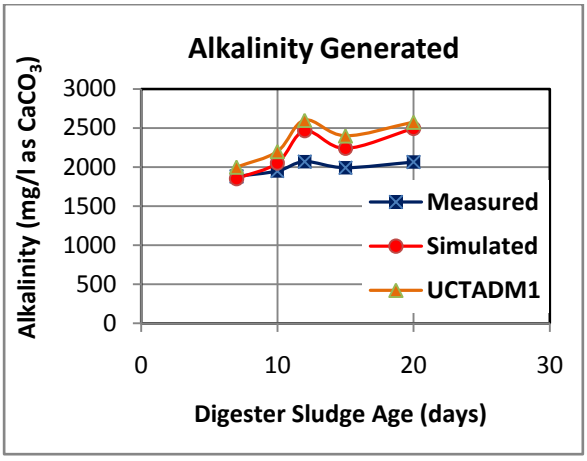

(b)

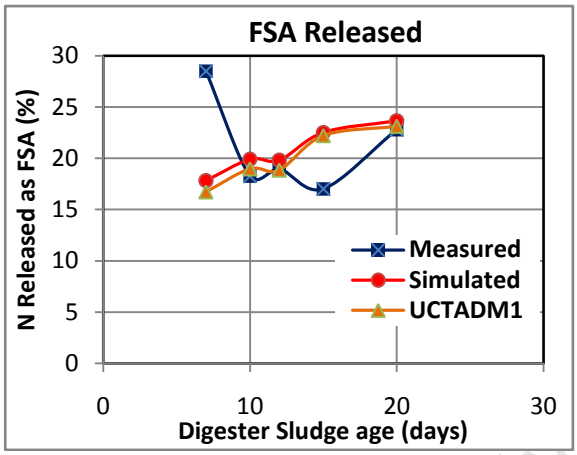

(c)

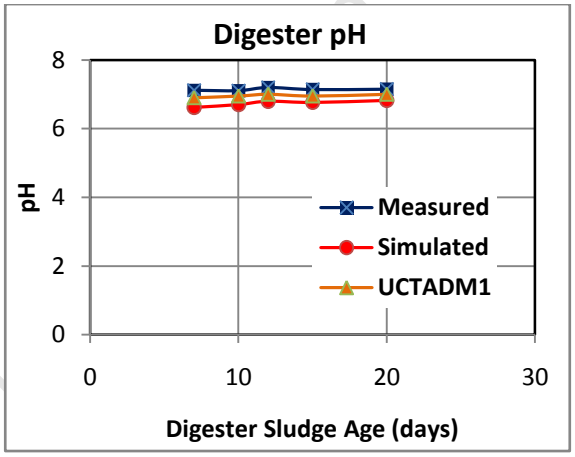

(d)

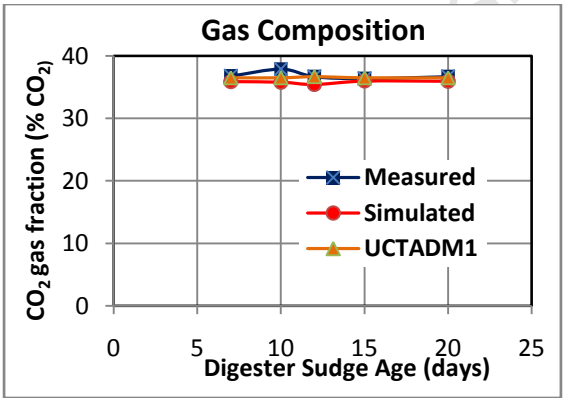

(e)

Figures 7.5.6a to e: *Comparison between the results simulated by the ADM-3P and the validated UCTADM1 model of Sötemann et al. (2006) with measured data by Izzett et al. (1992) versus digester sludge age (R_s) for the AD of a primary and humus sludge mixture in the order of: (a) COD removal, (b) digester $H_2CO_3^*$ alkalinity, (c) total nitrogen released as free and saline ammonia (FSA), (d) digester pH and (e) gas composition.*

Table 7.5.7b: Anaerobic Digestion of Primary Sludge (Using Experimental Results from Izzett *et al.* (1992)										
Retention Time (d)	20		15		12		10		7	
Influent flow (*l*/d)	0.70		0.93		1.17		1.40		2.00	
	Measd	Sim	Measd	Sim	Measd	Sim	Measd	Sim	Measd	Sim
Influent Total COD (mgCOD/*l*)	42595.0	42596.9	42367.0	42467.9	39222.0	39322.8	40721.0	40821.9	43286.0	43386.9
Influent Unbiodegradable Particulate COD (mgCOD/*l*)	15334.2	15334.2	15252.1	15252.1	14119.9	14119.9	14659.6	14659.6	15583.0	15583.0
Influent Biodegradable Particulate COD (mgCOD/*l*)	25011.8	25011.8	25290.9	25290.9	22230.1	22230.1	24100.4	24100.4	25832.0	25832.0
Influent VFA (mgCOD/*l*)	2249.0	2248.9	1824.0	1823.9	2872.0	2871.8	1961.0	1960.9	1871.0	1870.9
Influent TKN (mgN/*l*)	1171.0	1388.0	1075.0	1368.5	1028.0	1272.7	1100.0	1301.6	1105.0	1368.2
Influent Free and Saline Ammonia, FSA (mgN/*l*)	244.0	244.0	221.0	221.0	235.0	235.0	203.0	203.0	196.0	196.0
Influent Alkalinity (mg/*l* as $CaCO_3$)	56.0	56.0	82.0	82.0	90.0	90.0	81.0	81.0	80.0	80.0
Influent pH	5.3	5.3	5.4	5.4	5.2	5.2	5.3	5.3	5.3	5.3
Influent VSS (mg/*l*)	25690.0	26352.9	25863.0	26475.6	24727.0	23754.4	25768.0	25314.3	25971.0	27045.2
Effluent Total COD (mgCOD/*l*)	19005.0	19805.4	19969.0	20759.7	18678.0	19818.3	20521.0	21503.9	23637.0	24833.5
Effluent VFA (mgCOD/*l*)	23.0	497.2	28.0	585.4	28.0	659.7	28.0	741.4	50.0	980.8
Effluent, FSA (mgN/*l*)	511.0	572.5	404.0	529.3	430.0	487.3	404.0	462.3	511.0	440.1
Effluent Alkalinity (mg/*l* as $CaCO_3$)	2066.0	2495.5	1994.0	2239.7	2072.0	2464.9	1951.0	2052.6	1882.0	1851.9
Measured Digester pH	7.2	6.8	7.1	6.8	7.2	6.8	7.1	6.7	7.1	6.6
COD Removed (%)	55.4	53.5	52.9	51.1	52.4	49.6	49.6	47.3	45.4	42.8
FSA Released (%)	22.8	23.7	17.0	22.5	19.0	19.8	18.3	19.9	28.5	17.8
Gas Composition (%CO2)	36.7	36.0	36.4	36.0	36.7	35.4	37.9	35.8	36.8	35.9
COD Balance (%)	107.3		106.9		109.1		1086.0		108.4	
N Balance (%)	98.8		90.8		96.5		94.5		94.2	
Where Measd and Sim stand for measured and simulated results respectively.										

As can be seen the COD removal, ammonia release, alkalinity generation and gas composition for the ADM-3P model are very similar to those of UCTADM1. This provides

a good verification and validation of the ADM-3P model, without precipitation. The differences between ADM-3P and the experimental results are the same as for UCTADM1 and are given by Sötemann *et al.* (2005).

b. Comparison of ADM-3P predictions to data measured in the project's experimental investigation: The data obtained by anaerobically digesting the PS that was added to make up the raw wastewater feed in this project's experimental set up (see Figure 3.1 in Chapter 3) was also compared with simulations by the ADM-3P. As in the aforementioned calibrations of the AD model with the other sludge types, the model parameters in these simulations were the same as those shown in Table 7.5.2, with added parameters for the sludge characteristics, AD volume and hydrolysis kinetics , which are given in Table 7.5.8a.

Table 7.5.8a: Parameters (additional to those from Table 7.5.2) for simulating the AD of PS (data measured by author)

Parameters	Name	Modifications					
		UPO (ϕ=up)[1]	BPO_{PS} (ϕ=bps)[1]	Organisms (ϕ=o)[1]	ER (ϕ=e)[1]	FBSO (ϕ=f)[1]	USO (ϕ=us)[1]
	Y_ ϕ : H/C	1.320	2.190	1.485	1.320	1.899	1.753
	Z_ ϕ : O/C	0.443	0.653	0.424	0.443	0.698	0.586
	A_ ϕ : N/C	0.100	0.064	0.166	0.100	0.009	0.086
	B_ ϕ : P/C	0.035	0.010	0.023	0.035	0.011	0.010
Organics Empirical Formulations		[1]Whereby the empirical formula is for all each of the organic is $CH_{Y\_\phi}O_{Z\_\phi}N_{A\_\phi}P_{B\_\phi}$, and each components' parameterised CHONP molar fraction denotations are extended by its ϕ replacements (e.g. the empirical formulation for FBSO is $CH_{Y\_f}O_{Z\_f}N_{A\_f}P_{B\_f}$).					
Hydrolysis Kinetics	k_{M_PS}	1.796	Where k_{M_PS} and K_{S_PS} are the respective k_M and K_s constants of saturation kinetics in hydrolysis of PS BPO, obtained as shown in Section 6.1 and 6.2 of Chapter 6.				
	K_{S_PS}	7.962					
Reactor Volumes	V	The reactor volume is maintained at 12 litres, apart from the 60-day R_s where the volume is reduced to 5 litres..					

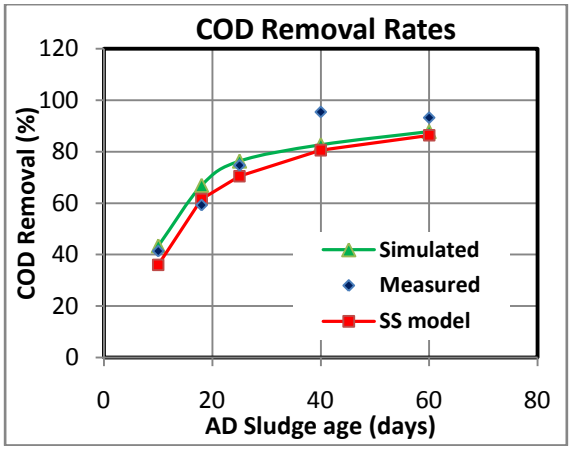

(a)

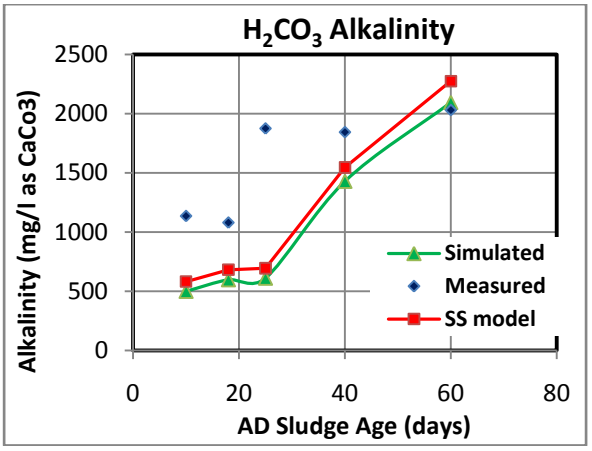

(b)

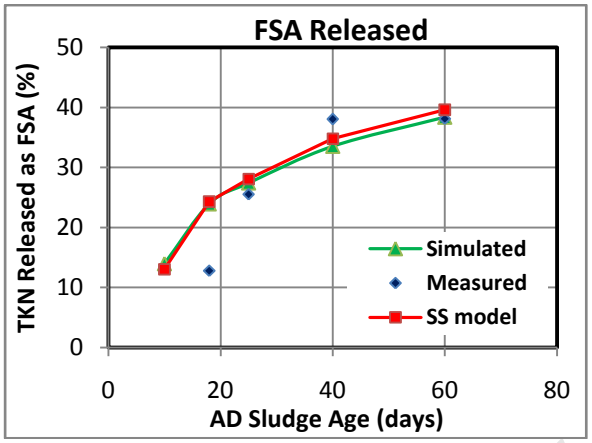

(c)

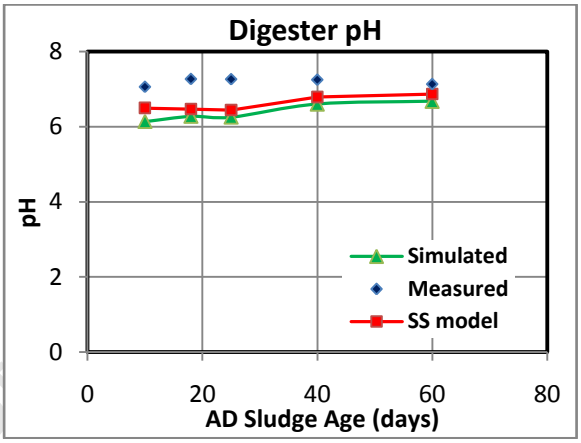

(d)

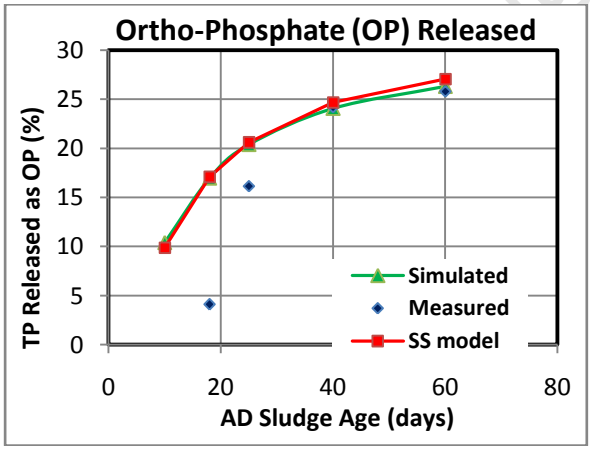

(e)

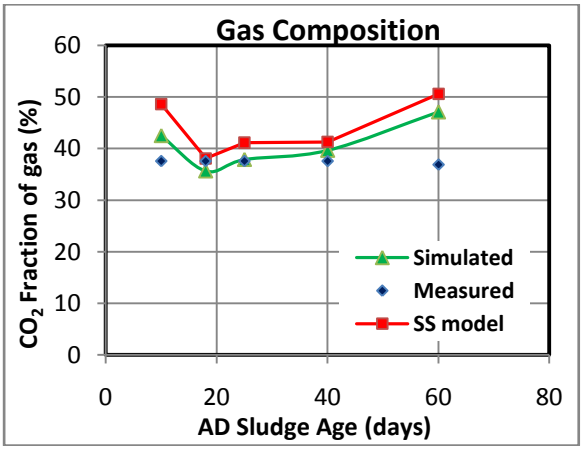

(f)

Figures 7.5.7a to e: *Comparison between the results simulated by UCTADM1 and ADM-3P and measured data versus digester sludge age (R_s) for the AD of PS in the order of: (a) COD removal, (b) digester H_2CO_3* alkalinity, (c) total nitrogen released as free and saline ammonia (FSA), (d) digester pH, (e) phosphorus released as ortho-phosphate and (f) gas composition.*

In the above Figure 7.5.7, the COD removal and nutrient (N and P) releases (apart from the N and P released in the 18d R_s) trends show reasonably close matches between the model and experimental results. However, there are some discrepancies in the effluent pH and H_2CO_3* alk. results. With the N release (which significantly affects H_2CO_3* alk. generation in this system) being reasonably well matched, a possible reason for this mismatch is inaccuracies (pH and H_2CO_3* alk. values being too low) in the measured influent H_2CO_3* alkalinity, which is used as input to the AD model to effect the effluent pH and H_2CO_3* alk. values. This is because the influent pH and H_2CO_3* alk. were not measured as frequently as in the effluent and thus, there is less distribution of error in the average values used.

Table 7.5.8b: Anaerobic Digestion of PS										
Retention Time (d)	10		18		24		40		60	
Influent flow (l/d)	1.2		0.67		0.5		0.3		0.085	
	Measd.	Sim	Measd.	Sim	Measd.	Sim	Measd.	Sim	Measd.	Sim
Influent COD (mgCOD/*l*)	5684.2	5684.4	8053.2	8053.5	8910.3	8910.5	18706.8	18707.0	28434.7	28436.4
Influent unbiodegradable particulate COD, Supi (mgCOD/d)	1762.1	1762.1	2496.5	2496.5	2762.2	2762.2	5799.1	5799.1	8814.7	8814.7
Influent biodegradable particulate COD, Sbpi (mgCOD/*l*)	3459.9	3460.1	4740.3	4740.5	4905.8	4906.0	11234.9	11235.1	16993.5	16993.7
Influent VFA, Sasi (mgCOD/*l*)	155.7	155.7	185.2	185.2	198.6	198.6	311.3	311.3	440.6	442.1
Influent TKN (mgN/*l*)	256.2	187.0	254.8	246.1	290.5	259.5	506.8	565.3	588.0	826.8
Influent FSA (mgN/*l*)	30.5	30.4	27.5	27.5	24.5	24.5	52.5	52.5	49.0	49.0
Influent Alkalinity (mg/*l* as CaCO3)	398.0	398.0	316.3	316.3	347.2	347.2	392.3	392.3	316.1	316.1
Influent pH	5.9	5.9	6.2	6.2	5.9	5.9	6.1	6.1	5.5	5.5
Influent TP (mgP/*l*)	93.3	105.5	194.9	145.7	215.4	158.3	213.5	307.5	247.4	458.7
Influent OP (mgP/*l*)	19.5	19.5	23.6	23.6	22.8	22.8	23.0	23.0	25.9	25.9
Influent TSS (mg/*l*)	4941.0	4632.7	5556.0	5957.8	6949.6	6638.9	14749.6	14485.3	19725.6	20841.6
Influent VSS (mg/*l*)	3840.0	3531.7	4491.6	4893.4	5493.6	5182.9	11783.6	11519.3	16336.4	17452.4
Influent ISS (mg/*l*)	1101.0	1101.0	1064.4	1064.4	1456.0	1456.0	2966.0	2966.0	3389.2	3389.2
Effluent COD, Ste (mgCOD/*l*)	3906.4	4011.6	4602.1	4442.4	4255.4	4353.1	6682.2	8334.5	10291.0	11711.1
Effluent VFA, Sase (mgCOD/*l*)	0.0	84.3	0.0	90.2	1.5	81.6	32.5	128.3	36.8	151.1
Effluent FSA (gN/*l*)	25.5	56.6	60.1	86.4	98.7	95.7	245.4	242.1	273.4	366.3
Effluent OP (mgP/*l*)	11.6	30.4	31.6	48.3	59.8	55.0	76.2	97.0	65.0	146.5
Effluent Alkalinity (mg/*l* as CaCO3)	1135.5	500.6	1079.8	598.2	1875.4	611.5	1844.5	1429.5	2031.1	2095.3
Measured digester pH	7.1	6.1	7.3	6.3	7.3	6.3	7.2	6.6	7.1	6.7
COD removed (%)	43.8	43.4	61.9	66.9	76.2	76.4	94.6	82.7	93.9	87.8
Volume of CH4 (litres)	-	2618.4	1457.0	3146.7	2031.1	2858.8	4470.4	4066.5	-	4375.8
Volume of CO2 (litres)	-	1937.2	877.9	1743.5	1223.9	1743.8	2693.7	2673.2	-	3900.2
FSA released (%)	-1.9	14.0	12.8	24.0	25.5	27.4	38.1	33.5	38.2	38.4
OP released (%)	-8.4	10.4	4.1	17.0	17.2	20.4	24.9	24.1	15.8	26.3
Gas composition (%CO2)	36.9	42.5	37.6	35.7	37.6	37.9	37.6	39.7	37.6	47.1
COD balance (%)	101.2	100.0	104.6	99.9	107.6	100.2	98.5	100.2	98.9	100.3
N balance (%)	93.0	100.0	102.6	100.1	81.6	100.1	99.7	99.8	101.9	100.0
P balance (%)	97.3	100.0	100.8	100.5	106.6	100.8	102.9	100.5	88.7	100.4
Where Measd. and Sim stand for measured and simulated results respectfully.										

4. Anaerobic Digestion of PS - MLE 1 WAS Blend

a. Simulation of PS-MLE 1 WAS blend AD with the blend considered to be a unique sludge type (i.e. the same hydrolysis kinetics used for both PS and MLE 1 WAS): To model the AD of this PS-MLE 1 WAS blend required characterising the influent sludge by using the AD model kinetics to determine the unbiodegradable fraction of sludge (as shown in Section 6.2 of Chapter 6) and the AS steady state model equations (shown in Chapter 5) to fractionate the components of this biodegradable and unbiodegradable COD concentrations. This facilitated the determination of influent organics component concentrations and their parameterised empirical elemental formulations. The empirical formulations of the sludge, together with the hydrolysis kinetics and reactor volume (as additions to the general set of AD model parameters in the above Table 7.5.2) are reported below, in Table 7.5.9a.

Table 7.5.9a: Adjustments made to parameters from Table 7.5.2 for simulating the AD of PS-MLE1 WAS blend (the same hydrolysis kinetics used for PS and WAS, i.e. the blend considered as a single sludge type, unique from PS or WAS, with only one k_M and K_S value used)

Parameters	Name	Modifications					
		UPO (ϕ=up)[1]	BPO_{PS} (ϕ=bps)[1]	Organisms (ϕ=o)[1]	ER (ϕ=e)[1]	FBSO (ϕ=f)[1]	USO (ϕ=us)[1]
	$Y_{\_\phi}$: H/C	1.303	1.913	1.468	1.303	1.907	1.690
	$Z_{\_\phi}$: O/C	0.317	0.576	0.356	0.317	0.691	0.623
	$A_{\_\phi}$: N/C	0.207	0.006	0.229	0.207	0.016	0.044
	$B_{\_\phi}$: P/C	0.054	0.000	0.031	0.054	0.011	0.012
Organics Empirical Formulations		[1]Whereby the empirical formula is for all each of the organic is $CH_{Y\_\phi}O_{Z\_\phi}N_{A\_\phi}P_{B\_\phi}$, and each components' parameterised CHONP molar fraction denotations are extended by its ϕ replacements (e.g. the empirical formulation for FBSO is $CH_{Y\_f}O_{Z\_f}N_{A\_f}P_{B\_f}$).					
Hydrolysis Kinetics	k_M	1.919	Where k_M and K_S are the respective k_M and K_S constants of saturation kinetics, obtained as shown in Section 6.1 and 6.2 of Chapter 6.				
	K_S	7.723					
Reactor Volumes	V	The reactor volume is maintained at 12 litres, apart from the 60-day R_s where the volume is reduced to 5 litres.					

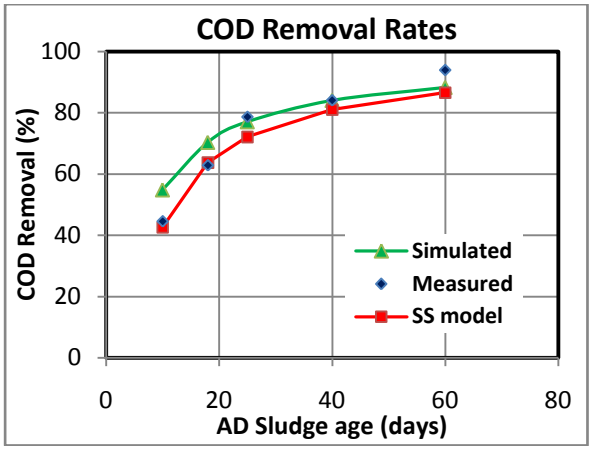

(a)

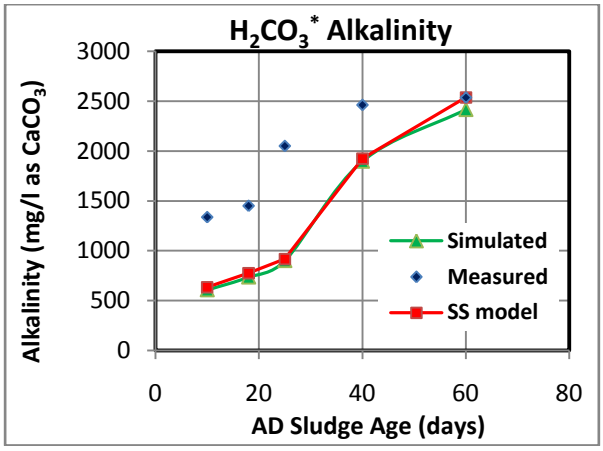

(b)

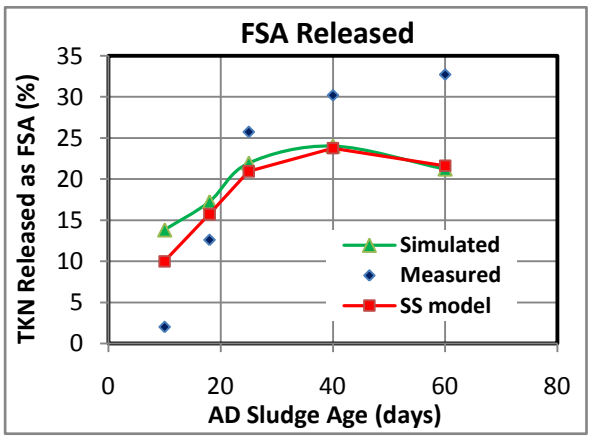

(c)

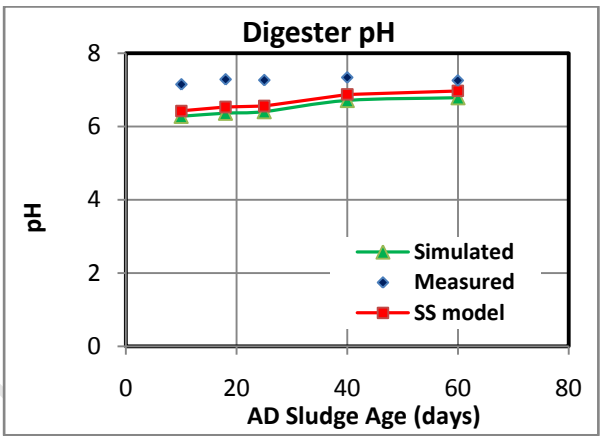

(d)

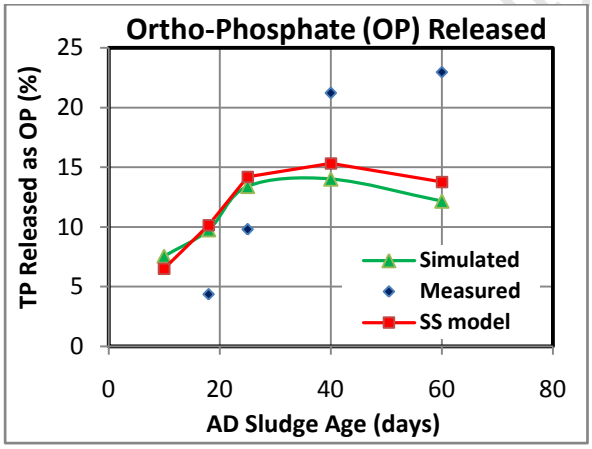

(e)

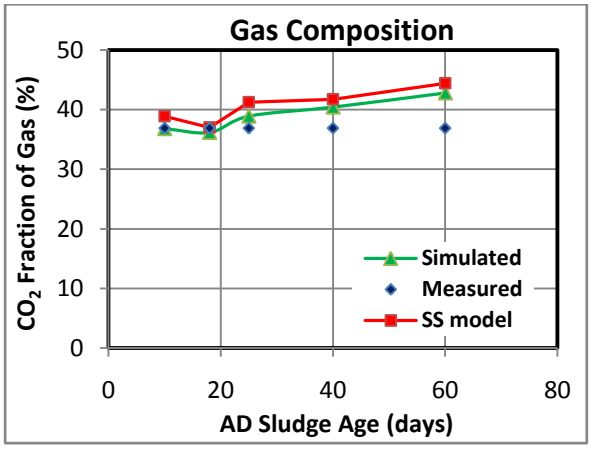

(f)

Figures 7.5.8 (i)a to f: *Comparison between the results simulated by the three phase AD dynamic model, calculated by the three phase AD steady state model and measured data versus AD sludge age (R_s) for the AD of PS-MLE 1 WAS in the order of: (a) COD removal, (b) digester H_2CO_3* alkalinity, (c) total nitrogen released as free and saline ammonia (FSA), (d) digester pH, (e) phosphorus released as ortho-phosphate and (f) gas composition.*

Table 7.5.9b: Measured and Simulated Results for Anaerobic Digestion of PS - MLE 1 WAS Blend										
Retention Time (d)	10		18		25		40		60	
Influent flow (l/d)	1.2		0.67		0.5		0.3		0.085	
	Measd.	Sim	Measd.	Sim	Measd.	Sim	Measd.	Sim	Measd.	Sim
Influent COD (mgCOD/*l*)	8443.4	8339.5	11645.1	11461.5	13765.0	13621.4	26699.1	26167.5	41463.1	40870.6
Influent unbiodegradable particulate COD, Supi (mgCOD/d)	3081.8	3081.8	4250.5	4250.5	5024.2	5024.2	9745.2	9745.2	15134.0	15134.0
Influent biodegradable particulate COD, Sbpi (mgCOD/*l*)	4859.2	4860.2	6523.0	6524.0	7433.2	7433.2	15154.5	15155.5	23505.9	23506.0
Influent VFA, Sasi (mgCOD/*l*)	146.0	211.4	173.6	458.2	198.6	900.1	311.3	828.9	440.6	1620.8
Influent TKN (mgN/*l*)	435.1	146.0	544.5	173.6	633.0	198.6	1131.5	311.3	1463.8	413.0
Influent FSA (mgN/*l*)	30.5	34.9	27.5	36.5	24.5	41.5	52.5	69.3	49.0	81.0
Influent Alkalinity (mg/*l* as $CaCO_3$)	398.0	30.4	378.0	27.5	347.2	24.5	769.3	52.5	1043.5	49.0
Influent pH	6.2	6.2	6.4	6.4	5.9	5.9	6.1	6.1	5.8	5.8
Influent TP (mgP/*l*)	147.2	147.2	275.8	275.8	338.0	338.0	427.8	427.8	595.3	595.3
Influent OP (mgP/*l*)	19.5	22.1	23.6	29.0	22.8	33.0	23.0	33.2	25.9	45.2
Influent TSS (mg/*l*)	7053.2	19.5	9704.0	23.6	9704.0	22.8	19242.1	23.0	28584.8	25.9
Influent VSS (mg/*l*)	5598.3	6594.0	7820.4	8856.5	7820.4	9982.1	15449.3	19939.8	23688.3	29812.3
Influent ISS (mg/*l*)	1454.8	5139.2	1883.6	6972.9	1883.6	8098.5	3792.8	16147.0	4896.5	24915.8
Effluent COD, Ste (mgCOD/*l*)	5972.7	1454.8	6906.1	1883.6	6872.4	1883.6	12415.8	3792.8	16942.4	4896.5
Effluent VFA, Sase (mgCOD/*l*)	0.0	32.5	31.0	22.1	0.5	19.5	27.3	14.8	68.7	13.7
Effluent FSA (gN/*l*)	39.1	0.0	86.5	0.0	156.5	0.0	394.3	0.0	528.1	0.0
Effluent OP (mgP/*l*)	19.4	0.0	35.6	0.0	54.9	0.0	113.7	0.0	162.5	0.0
Effluent Alkalinity (mg/*l* as $CaCO_3$)	1338.3	1483.5	1451.9	1925.5	2052.3	1931.0	2463.7	3873.4	2537.9	5002.0
Measured digester pH	7.2	608.3	7.3	736.6	7.3	901.5	7.3	1898.1	7.3	2417.0
COD removed (%)	44.2	6.3	62.3	6.4	77.9	6.4	83.4	6.7	93.1	6.8
Volume of CH_4 (litres)	1207.5	54.8	1070.8	70.3	849.9	77.0	1136.2	84.0	0.0	88.3
Volume of CO_2 (litres)	706.1	4342.2	626.2	4342.0	497.0	4086.1	664.4	5284.2	0.0	5868.0
FSA released (%)	2.0	0.4	10.8	0.4	20.9	0.4	30.2	0.4	32.7	0.4
OP released (%)	0.0	13.8	4.4	17.3	9.5	21.9	21.2	24.0	23.0	21.2
Gas composition (%CO2)	36.9	7.6	36.9	9.8	36.9	13.4	36.9	14.0	0.0	12.2
COD balance (%)	108.3	100.5	102.5	100.7	88.8	100.7	91.2	101.3	85.5	101.6
N balance (%)	96.8	99.5	85.8	99.2	80.9	98.7	81.3	99.6	88.8	99.4
P balance (%)	107.0	99.9	101.6	99.9	97.0	99.8	86.3	100.1	85.2	100.1
Where measd. and sim stand for measured and simulated results.										

The Figures 7.5.8 (i)a to f show the comparisons between simulated and experimentally measured results for the AD of PS-MLE 1 WAS blend, over various sludge ages. The corresponding data for this simulation is reported in Table 7.5.9b. It is noticeable in the above Figures 7.5.8 (i)a to f that the general trend in biodegradable COD removal, as predicted by the hydrolysis saturation kinetics in the model is at a reasonable match to the trends from the measured data. However, the trends in nutrient (N and P) releases are poorly matched and the H_2CO_3* alkalinity and pH are underpredicted. It would be possible to predict well the nutrient releases, if N and P content of the BPO_{PS} and FBSO, which are capable of changing with the sewage batch, were adjusted for each sludge age simulation. With the BPO N content increased for the 25 and 40d R_s, higher N releases pH and alkalinity generation will be predicted, which is in agreement with the measured results. However, for the lower sludge ages (10, and 18d), a decrease in the BPO N content, to match the measured N releases, is not in agreement to the prediction of the effluent H_2CO_3* alkalinity (i.e. would result in a worse, much lower, match to the measured value). Thus, as in the case of PS digested by itself (see Figures 7.5.7b and d), the underpredicted effluent pH and H_2CO_3* alkalinity for these sludge ages are possibly due to inaccurate influent pH and H_2CO_3 values that are used as input to the AD model. Another possible cause for the underpredicted pH values is that some CO_2 could have been actively stripped during the effluent sampling and testing process, resulting in higher measured pH, since these pH measurements were not carried out in-situ.

b. Simulation of PS-MLE1 WAS blend AD with the PS and MLE 1 sludges considered as separate entities of a blend: To model the AD of the PS-WAS in this way required determining the MLE 1 WAS and PS hydrolysis kinetics and influent characteristics (see Tables 7.5.5a and 7.5.8a respectively) separately and applying them in the same model simulation of the PS-MLE 1 WAS blend. Table 7.5.9c shows the empirical formulations of these sludge components, the hydrolysis kinetics used for each of the MLE1 and PS sludge

types and the reactor volume (all as additions to the general set of AD model parameters in the above Table 7.5.2). The results predicted from this simulation are also compared to the measured values (Figure 7.5.9).

Table 7.5.9c: Adjustments made to parameters from Table 7.5.2 for simulating the AD of PS-WAS blend (where the PS and WAS are modelled to hydrolyze individually using separate kinetics for PS and WAS)

Parameters	Name	Modifications					
		UPO (ϕ=up)	BPO$_{PS}$ (ϕ=bps)	Organisms (ϕ=o)	ER (ϕ=e)	FBSO (ϕ=f)	USO (ϕ=us)
	Y_ ϕ : H/C	1.358	2.190	1.463	1.482	1.907	1.690
	Z_ ϕ :O/C	0.450	0.653	0.355	0.472	0.691	0.623
	A_ ϕ : N/C	0.103	0.064	0.229	0.113	0.016	0.044
	B_ ϕ : P/C	0.032	0.010	0.031	0.022	0.011	0.012
Organics Empirical Formulations		Where the empirical formula is for all each of the organic is $CH_{Y\_\phi}O_{Z\_\phi}N_{A\_\phi}P_{B\_\phi}$, and each components' parameterised CHONP molar fraction denotations are extended by its ϕ replacements (e.g. the empirical formulation for UPO is $CH_{Y\_up}O_{Z\_up}N_{A\_up}P_{B\_up}$)					
Hydrolysis Kinetics PS	k_{M_PS}	1.80	Where k_{M_PS} and K_{S_PS} (for PS) and k_M and K_S (for WAS) are the respective k_M and K_s constants of saturation kinetics of PS and WAS, obtained as shown in Section 6.1 and 6.2 of Chapter 6.				
	K_{S_PS}	7.96					
Hydrolysis Kinetics WAS	k_M	1.52					
	K_S	4.84					
Reactor Volumes	V	The reactor volume is maintained at 12 litres, apart from the 60-day R_s where the volume is reduced to 5 litres.					

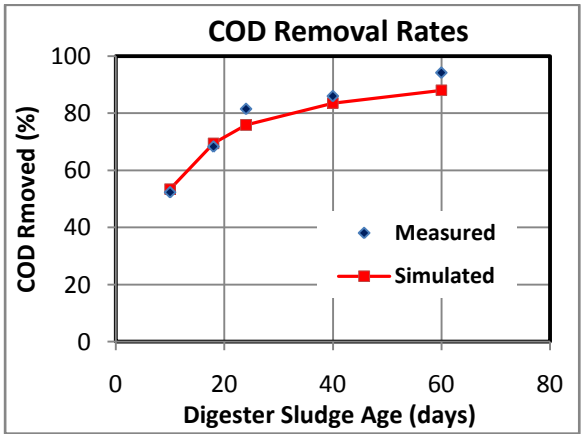

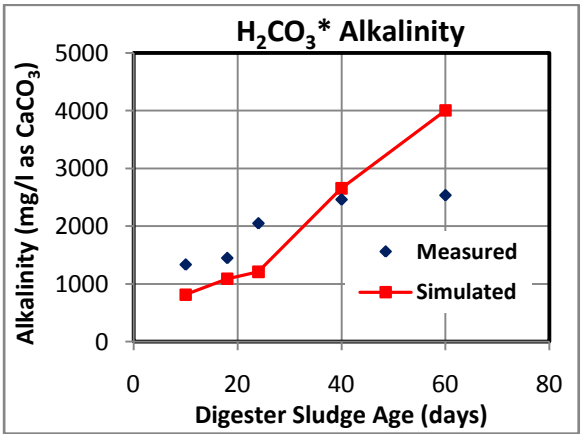

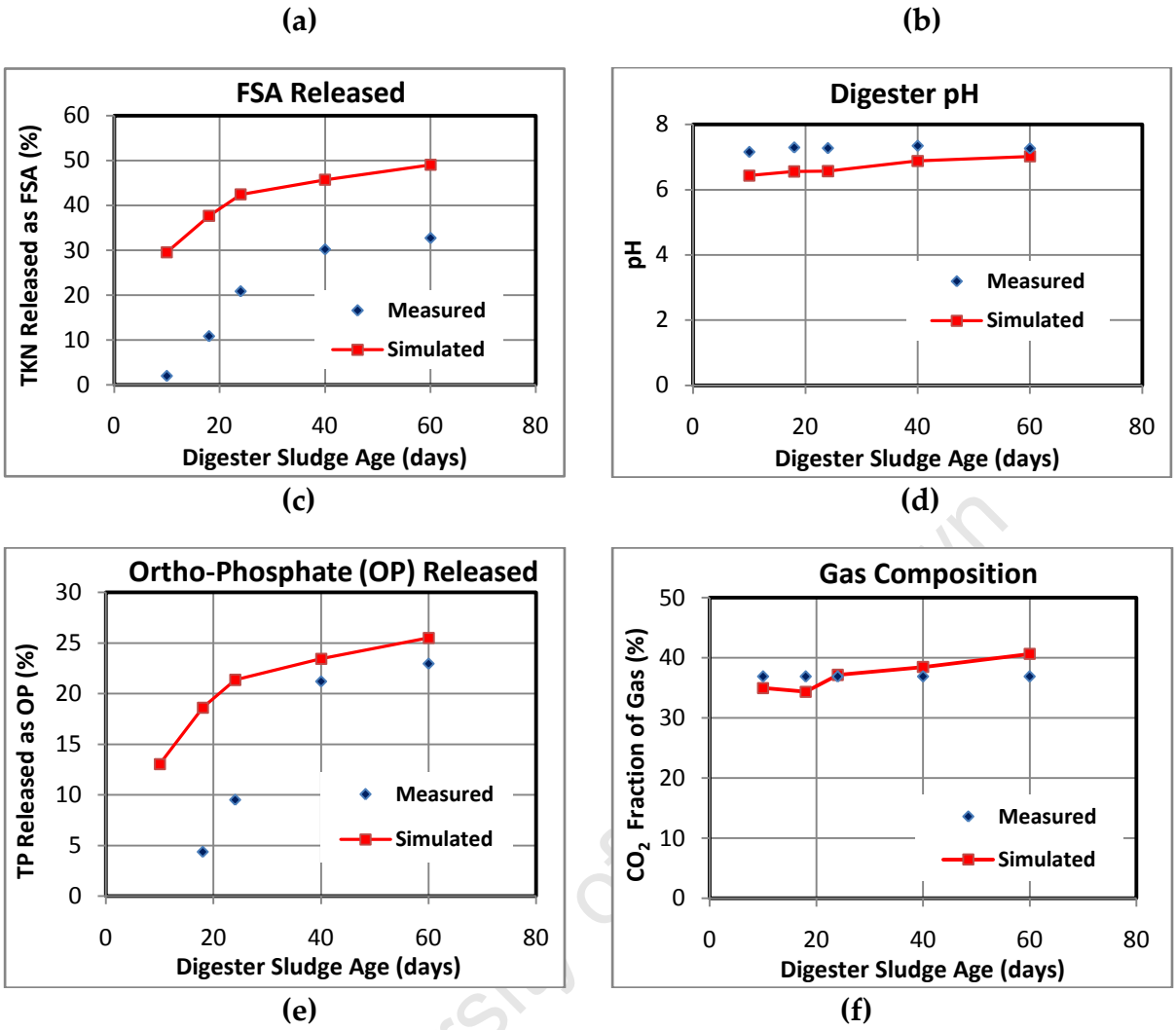

Figures 7.5.8 (ii)a to f: *Comparison between the results simulated by the three phase AD dynamic model, and the measured data versus AD sludge age (R_s) for the AD of PS-MLE 1 WAS, using separate hydrolysis kinetics for PS and MLE 1 WAS: (a) COD removal, (b) digester H_2CO_3* alkalinity, (c) total nitrogen released as free and saline ammonia (FSA), (d) digester pH, (e) phosphorus released as ortho-phosphate and (f) gas composition.*

As for the simulations carried out with PS and WAS given the same hydrolysis kinetic constants (see Tables 7.5.9a and b and Figures 7.5.8 (i)a to f) the COD removal trends for this simulation closely match the measured values (Figure 7.5.8 (ii)a). The predicted H_2CO_3* alkalinity has an improved (i.e. Figure 7.5.8 (i)b in comparison to 7.5.8 (ii)b) match to the experimentally measured values. These improved H_2CO_3* alkalinity values are a result of this simulation having increased BPO N, which when released with sludge hydrolysis are released as NH_3, leading to the generation of alkalinity (see Equation 7.3a). However, the

increased BPO N content is also the cause of the overpredicted FSA releases in Figure 7.5.8 (ii)c.

7.5.3 Sensitivity Analysis of Model

Sensitivity analysis is a crucial stage in model development which allows for the identification of model parameters that have a major impact (can cause significant alteration when slightly changed) on the outcome of essential model variables. Takács (2008) outlined the uses of sensitivity analysis as follows:

1. Help in selection of model parameters that can be estimated with the most accuracy, given a set of measurements.
2. Help in developing a sampling program to gather data for the particular process objective to target the most sensitive model elements.
3. Identify the parameters that have negligible effect on model variables – or conversely, identify those variables that are not sensitive to any model parameters. Those parameters can usually be left at default values and the variables do not warrant inclusion in a detailed sample program.

The sensitivity analysis is performed in the WEST software experimental environment (Vanhooren *et al.*, 2003). During the analysis a reference simulation is run, after which alteration is performed sequentially on each selected parameter by an appropriate perturbation factor and another simulation is run to check the impact of this alteration on the variable(s). The absolute sensitivity (SF_p) is then calculated for each simulation time point using the formulation below:

$$SF_p = \frac{V_p - V_r}{P_p - P_r} \tag{7.4a}$$

Where:

- The parameter and variable value during the reference simulation are P_r and V_r respectively.

- The parameter and variable value, with the simulation after the parameter perturbation, are P_P and V_P respectively.

With this done the relative sensitivity (R_SF_P) is calculated by multiplying the absolute sensitivity (SF_P) to the parameter over variable ratio, i.e.:

$$RSF_p = SF_p \times \frac{P_p}{V_p} \tag{7.4b}$$

A control simulation is also done to evaluate the accuracy of the sensitivity analysis. This level of accuracy is determined by how close the sensitivity for this control simulation is to that of the perturbation simulation.

This section reports an investigation on the sensitivity of the model predicted digester pH and carbon dioxide partial pressure (with the assessment of methane production), which are good indicators of methanogenic AD operational health, and struvite production (which does not impair the digestion process but could cause blockages, hence associated maintenance problems) in relation to selected stoichiometric parameters of the main feed components' empirical formula (i.e. X, Z, A and B of $C_XH_YO_ZN_AP_B$). The sensitivity analysis is performed on the model using the same experimentally operated conditions of the AD that was fed NDBEPR WAS and operated at a sludge age of 18 days and using the calibrated model parameter values as the initial conditions. This sensitivity analysis is performed under steady state conditions. To prepare these conditions, the AD was simulated for over 150 days (above three sludge ages), and then the final results from this simulation used as initial AD concentrations for the reference simulation. The reference simulation was carried out for a 100-day period. With the feed sludge being NDBEPR WAS, it was decided that in this investigation, the parameters defining the active organisms empirical formulation (i.e. X_o = 1, Y_o, Z_o, A_o and B_o) shall be selected for the analysis together with the parameter that defined the magnesium content of polyphosphate (c_PP). These parameters were selected because they can be easily estimated (using laboratory tests carried out over a short period)

and are deemed to have a significant role in the model stoichiometric processes that lead to the prediction of pH, p_{CO_2} and struvite precipitation.

Table 7.5.10: Parameters Selected for Sensitivity Analysis		
Parameter	**Description**	**Initial Value[2]**
A_o	Molar ratio of N/C[1]	0.25
B_o	Molar ratio of H/C[1]	0.045
Y_o	Molar ratio of P/C[1]	1.437
Z_o	Molar ratio of P/C[1]	0.367
c_PP	Molar fraction of Mg in PP	0.307
[1]The molar ratio is specifically for the WAS (and AD) organisms' generic empirical formula.		
[2]The default perturbation factor of 10^{-6} is used for all parameters during the sensitivity analysis.		

Sensitivity Analysis Results

The results from the sensitivity analysis of struvite, p_{CO_2} and pH with changes in the above-mentioned parameters (Table 7. 5.10) are briefly described below.

1. Struvite

The Figure 7.5.9 below shows various plot windows containing reference simulation and the relative sensitivity (perturbation and control) values of the struvite with change in parameters (Y_o, Z_o, A_o, B_o and c_PP) for each simulated time point.

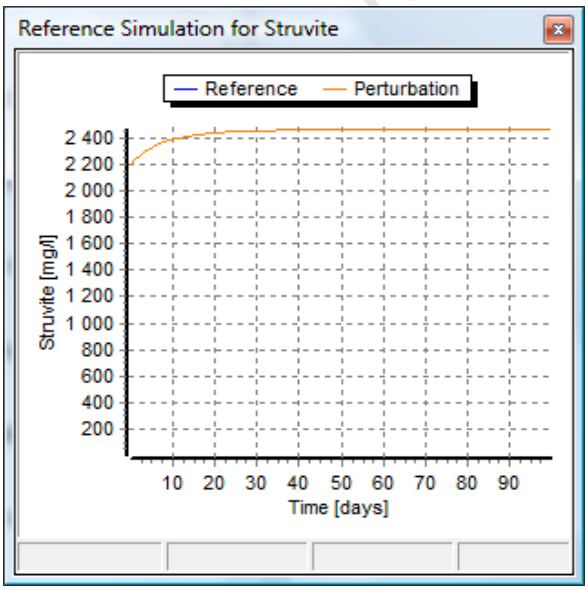

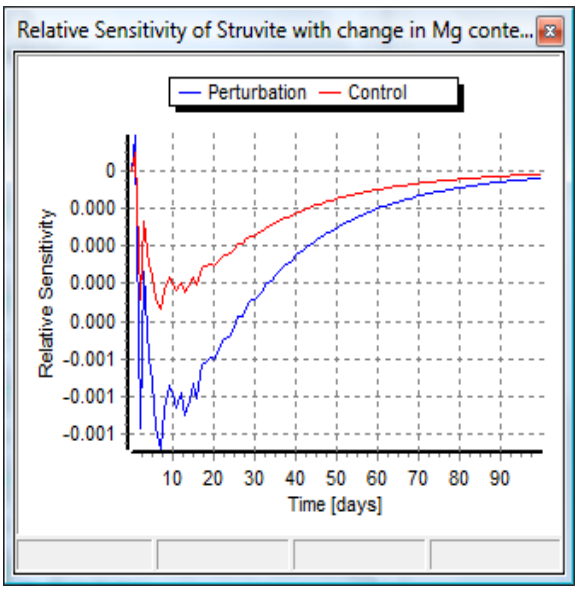

(a)

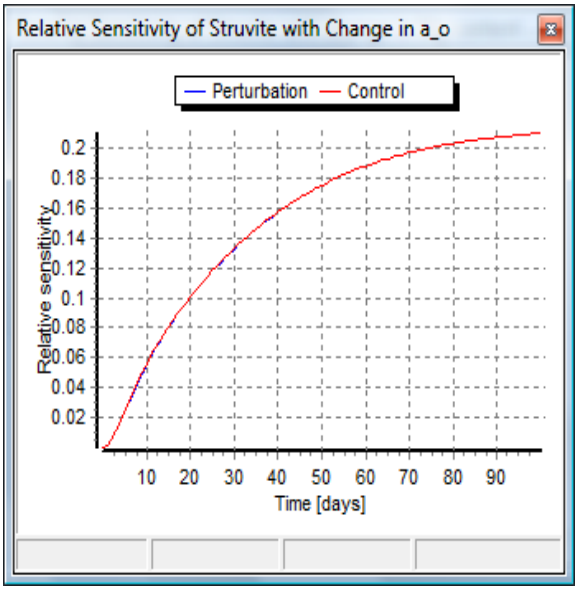

(b)

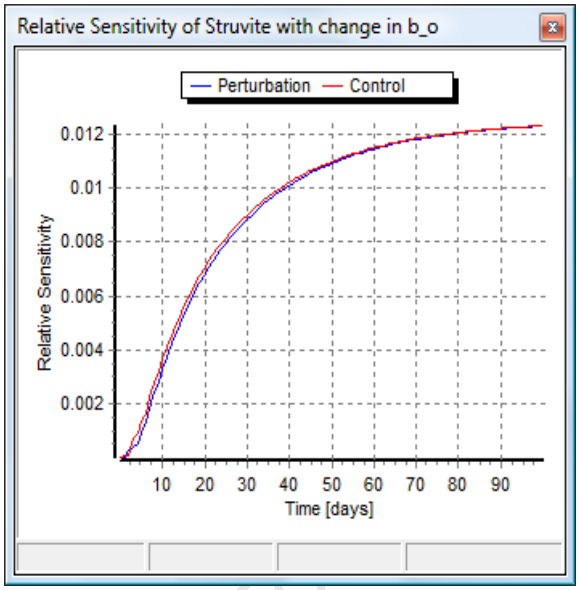

(c) (d)

Figures 7.5.9a to d: *Sensitivity analysis plot windows for struvite precipitation in AD of NDBEPR WAS showing (a) the reference simulation of struvite precipitated, and the relative sensitivity of struvite with change in parameter c_PP (Figure b), parameter A_o (Figure c) and parameter B_o (Figure d)*

As can be seen in the above Figure 7.5.9, the relative sensitivity of struvite is highest to changes in A_o (20%), followed by B_o (1%), with a much lower (about 10 times less) sensitivity effect and the least being the c_PP with almost no sensitivity effect (0.1%). Therefore, if the A_o parameter is increased in the model it is likely to result in a uniform increase in struvite precipitation. This is true because the A_o parameter affects the quantity of ammonia (NH_3) released with hydrolysis of sludge and hence the $H_2CO_3^*$ Alk (via $NH_3 + H_2O + CO_2 \rightarrow HCO_3^- + NH_4^+$). The higher alkalinity increases the pH, which increases the $[PO_4^{3-}]$ concentration and hence increases struvite precipitation. The B_o parameter represents the lower quantity (organically bound in the biodegradable particulates of WAS) of phosphorus which is released with sludge hydrolysis. Although the molar fraction of B_o in the organism generic formula is significantly lower than that of A_o, a higher value results in greater P release and higher $[PO_4^{3-}]$. However, sensitivity analysis is situation specific, and

with less influent magnesium present and more polyphosphate present, it is expected that the c_PP, depending on how fast the PP is released, would have higher effect on the sensitivity of struvite precipitation.

2. Carbon Dioxide Partial Pressure

The Figure 7.5.10 shows various plot windows containing reference simulation and the relative sensitivity (perturbation and control) values of the p_{CO2} with change in parameters (Y_o, Z_o, A_o, B_o and c_PP) for each simulated time point.

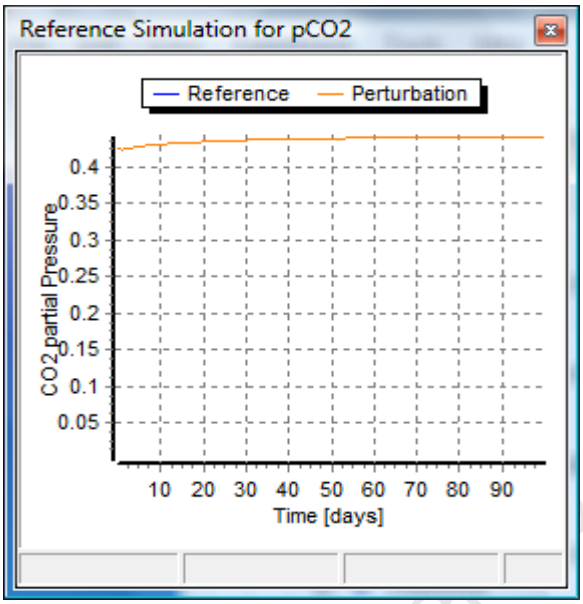

(a)

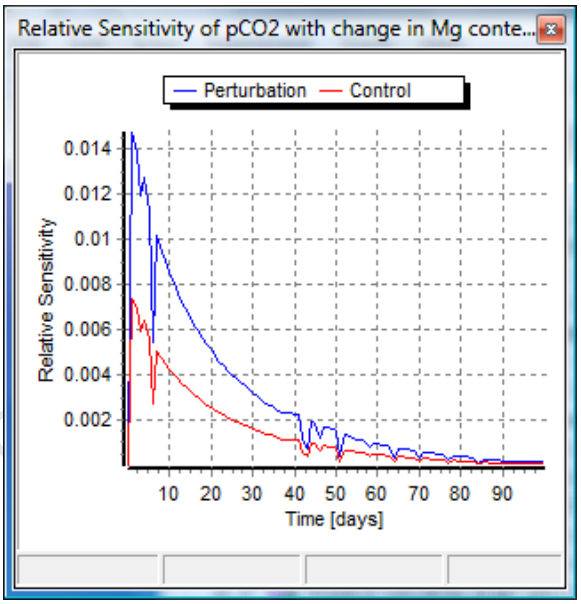

(b)

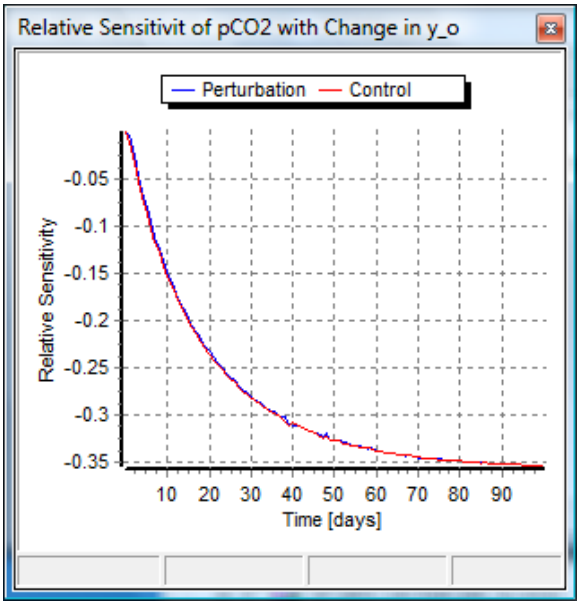

(c)

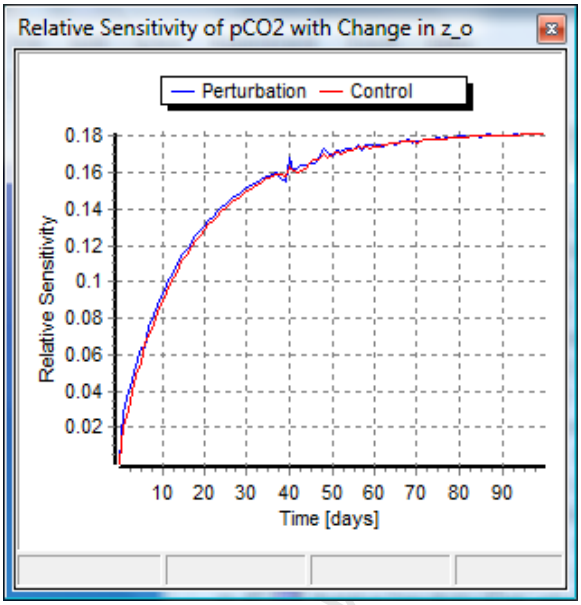

(d)

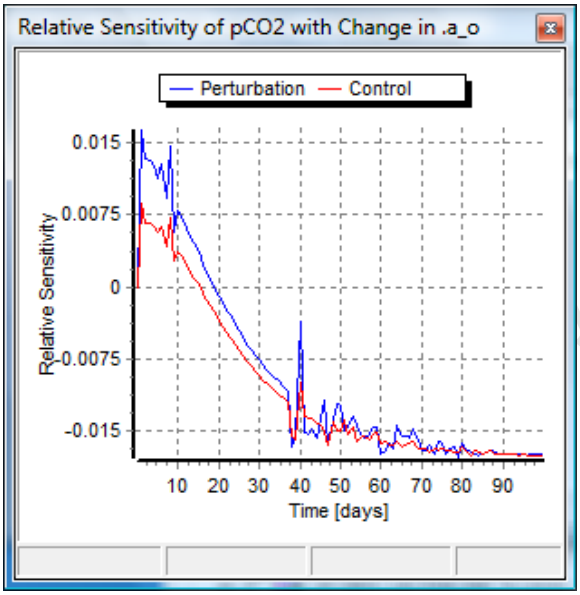

(e)

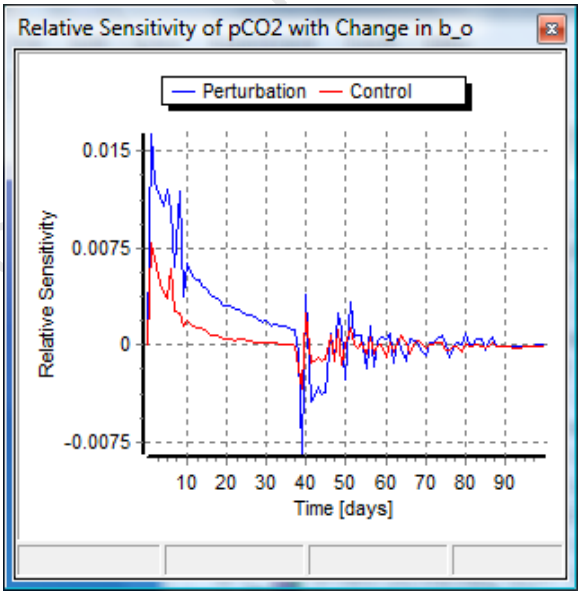

(f)

Figures 7.5.10 a to f: *Sensitivity analysis plot windows for carbon dioxide partial pressure (p_{CO2}) in AD of NDBEPR WAS showing (a) the reference simulation of p_{CO2}, and the relative sensitivity of p_{CO2} with change in parameter Mg_PlP (Figure b), parameter y_o (Figure c), parameter z_o (Figure d) parameter a_o (Figure e), parameter b_o (Figure f).*

The Figure 7.5.10 shows the relative sensitivity of Z_o exhibits positive values, which increase with time, and increasing p_{CO2}, while the other parameters are decreasing. This shows that if the parameter Z_o were increased, it would result in increased p_{CO2}. This is because an increase in Z_o decreases the COD of the biodegradable organics, which decrease the CH_4 production. Less CH_4 means less carbon (C) in methane, so more of the C in the organics goes to CO_2. Because Z_o does not change the T.Alk, the CO_2 exits as gas. In this analysis, the p_{CO2} is observed to be most sensitive to changes in Y_o, with the highest relative sensitivity values, and least sensitive to c_PP. An increase in Y_o increases the COD of the organics, via COD = 8(4X_o + Y_o – 2Z_o – 3A_o + 5B_o), which increases CH_4 production and hence decreases CO_2 gas production, which in turn decreases p_{CO2}. The sensitivity exhibited by c_PP (together with A_o and B_o) is due to their influence on struvite precipitation, which causes more CO_2 release during AD. However, although increasing the parameter A_o to promote ammonia release would cause struvite precipitation, it also causes more CO_2 to be retained in the aqueous phase as bi-carbonate (HCO_3^-). This is why the graphs (Figure 7.5.10) show that for this specific situation, despite promoting precipitation, the increase in ammonia cause a reduction in p_{CO2}. This decreasing trend is also observed with the parameters B_o and c_PP but their relative sensitivity values are very low, tending towards zero.

3. Digester pH

The Figure 7.5.11 shows the various plot windows, containing the reference simulation and the relative sensitivity (perturbation and control) values of the pH with change in parameters (Y_o, Z_o, A_o, B_o and c_PP) for each simulated time point.

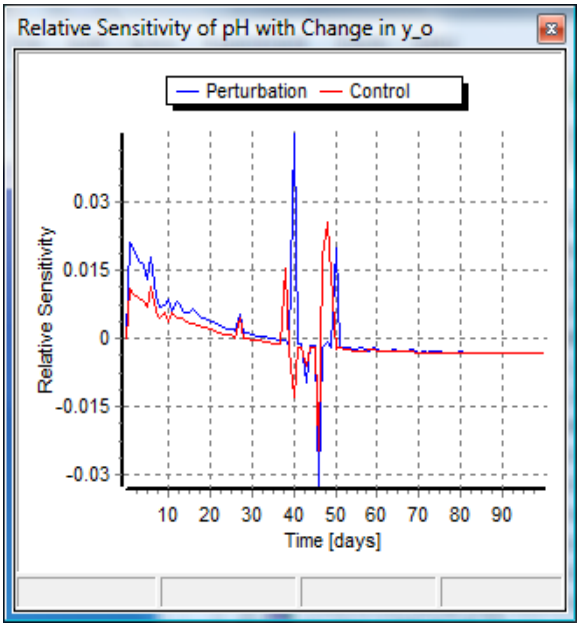
Relative Sensitivity of pH with Change in y_o
Perturbation
Control
Relative Sensitivity
0.03
0.015
0
-0.015
-0.03
10 20 30 40 50 60 70 80 90
Time [days]

(a)

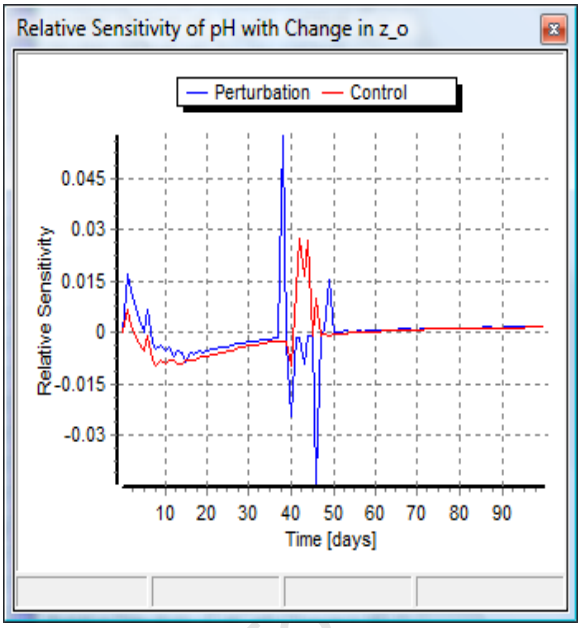
Relative Sensitivity of pH with Change in z_o
Perturbation
Control
Relative Sensitivity
0.045
0.03
0.015
0
-0.015
-0.03
10 20 30 40 50 60 70 80 90
Time [days]

(b)

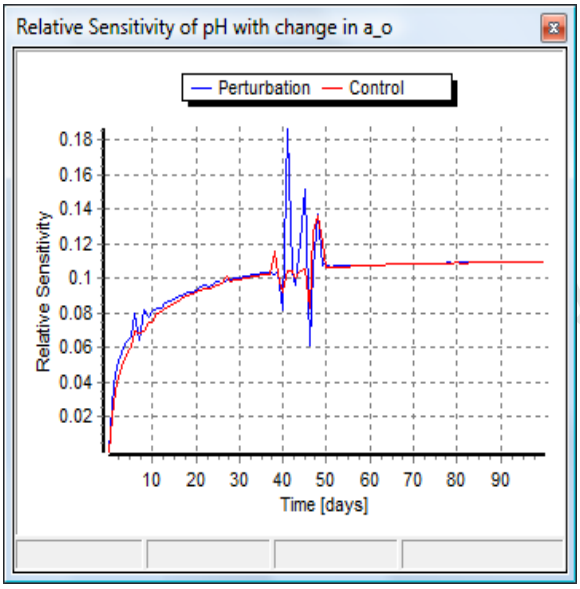
Relative Sensitivity of pH with change in a_o
Perturbation
Control
Relative Sensitivity
0.18
0.16
0.14
0.12
0.1
0.08
0.06
0.04
0.02
10 20 30 40 50 60 70 80 90
Time [days]

(c)

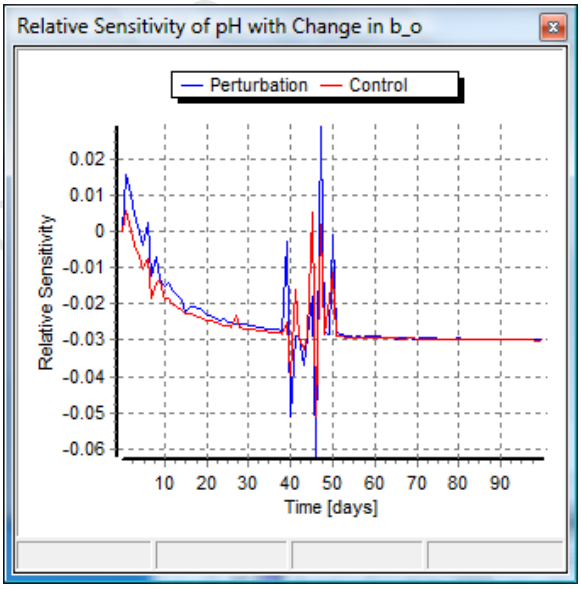
Relative Sensitivity of pH with Change in b_o
Perturbation
Control
Relative Sensitivity
0.02
0.01
0
-0.01
-0.02
-0.03
-0.04
-0.05
-0.06
10 20 30 40 50 60 70 80 90
Time [days]

(d)

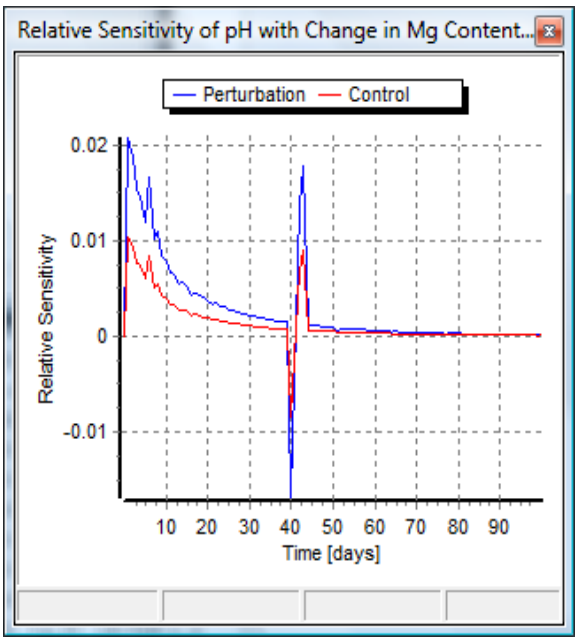

(e)

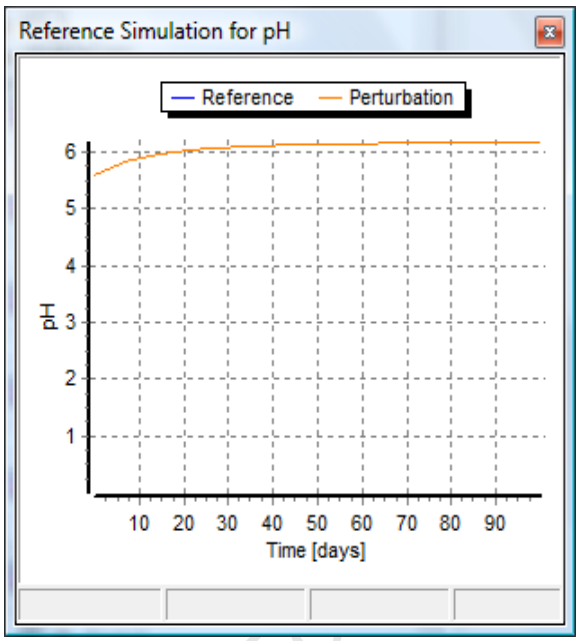

(f)

Figures 7.5.11a to f: *Sensitivity analysis plot windows for carbon dioxide partial pressure (p_{CO_2}) in AD of NDBEPR WAS showing (a) the reference simulation of p_{CO_2}, and the relative sensitivity of p_{CO_2} with change in parameter Mg_PlP (Figure b), parameter y_o (Figure c), parameter z_o (Figure d) parameter a_o (Figure e), parameter b_o (Figure f).*

The pH of the digester is subject to the T.Alk (comprising $H_2CO_3^*$ Alk ≈ $[HCO_3^-]$ and Alk H_3PO_4 ≈ $[H_2PO_4^-]$ + 2$[HPO_4^{2-}]$), the OP concentration (≈ $[H_2PO_4^-]$ + $[HPO_4^{2-}]$) and the p_{CO_2}. The higher the p_{CO_2} the lower the pH, but the higher the T.Alk the higher the pH. In this contrary effect of T.Alk and p_{CO_2} on pH, the p_{CO_2} is relatively insensitive to parameter changes compared with the T.Alk. Therefore, the digester pH is more sensitive to the parameters that affect T.Alk, such as A_o (via NH_3 release). While PP release increases, T.Alk struvite precipitation with the associated Mg virtually nullifies this increase.

The above Figure 7.5.11 shows that the pH has a highest sensitivity to changes in the parameter A_o, (with the relative sensitivity values levelling off at 0.1). This is as expected because it is known that the increase in ammonia released due to higher A_o values would cause a higher T.Alk (via $[HCO_3^-]$), as shown in Equation 7.3a) resulting in pH increase. The

pH has a lower sensitivity to the parameters Y_o and Z_o because these affect the p_{CO2}. The pH is marginally sensitive to B_o and least sensitive to c_PP (which has relative sensitivity values that are observed to be approaching zero). Although B_o increases T.Alk, struvite precipitation reduces this to only 20% of the increase without struvite precipitation, which is reflected in the low sensitivity of these parameters on pH.

7.5.4 Predicting Digester Failure

The three phase AD kinetic (ADM-3P) model is an extension of that (UCTADM1) developed by Sötemann *et al* (2005) and also includes the various acetogenic and methanogenic organism inhibition functions together with the accommodation of failure due to low pH. As indicated by Sötemann *et al.* (2005) the AD system failure is usually due to disturbances in the methanogenic processes. The acidogens continue to produce acetic acid and H_2 but under high partial pressure of H_2 also produce propionate. The methanogenic process disturbances usually occur due to shock loading the digester, sudden temperature drop or the presence of toxic substances in the feed. They usually lead to increased concentrations of acetic acid, hydrogen partial pressure and propionic acid due to slowing down of the growth rate of the acetoclastic methanogens and, hydrogenotrophic methanogens. The increase in HAc and HPr causes the pH to decrease resulting in further reduction in acetoclastic and hydrogenotrophic methanogen activity. The digester pH should not drop below a value of 6.6 to maintain methanogenesis processes uninhibited by low pH (Moosbrugger *et al.*, 1993). The methanogenic organisms inhibition terms that are present in the model, included in the growth rate equations, as reported by Sötemann *et al.* (2005), are listed below:

1. **Growth and Inhibition of Acidogens:** As was mentioned in the review of AD processes (Section 2.3.3.2 of Chapter 2) acidogenesis occurs with the fermentation of hydrolysis products to form carbon dioxide (CO_2), hydrogen (H_2) and short chain fatty acids (SCFA) such as acetic acid (HAc, produced under low H_2 partial pressure) and propionic acid (HPr, produced under high H_2 partial pressure). This process is

modelled according to the growth rate of the mediating acidogens (r_{ZAD}) using the Monod equation (Gujer and Zehnder, 1983; Pavlostathis and Giraldo Gomez, 1991; Sötemann *et al.*, 2005).

$$r_{Z\,AD} = \frac{\mu_{\max,AD} \cdot [S_{bsf}]}{K_{S,AD} + [S_{bsf}]} \cdot \left\{ 1 - \frac{[H_2]}{k_{H2} + [H_2]} \right\} \cdot [Z_{AD}] \qquad (7.5a)$$

Where:

$[H_2]$ = Molar concentration of hydrogen.

$[S_{bsf}]$ = Molar concentration of rapidly biodegradable organic substrate.

$\mu_{max,AD}$ = Acidogenic biomass maximum specific growth rate constant.

$K_{S,AD}$ = Half saturation coefficient for acidogens (molar concentration).

K_{H2} = Inhibition constant for hydrogen in acetogenesis.

$[Z_{AD}]$ = Molar concentration of acidogenic biomass.

The section in brackets {} within the growth rate Equation 7.5a is a non-competitive inhibition function that accounts for the reduced rates of acidogenic growth at high p_{H2}. Moreover, this above equation is for the growth rate of acidogens to produce acetic acid.

The growth rate of acidogens with the production of propionic acid is modelled using the same Monod equation as for Equation 7.5a but with a change in the bracketed term to accommodate a non-competitive inhibition when the hydrogen partial pressure (p_{H2}) is high, since these conditions favour the production of propionic acid.

$$r_{Z\,AD} = \frac{\mu_{\max,AD} \cdot [S_{bsf}]}{K_{S,AD} + [S_{bsf}]} \cdot \left\{ \frac{[H_2]}{k_{H2} + [H_2]} \right\} \cdot [Z_{AD}] \qquad (7.5b)$$

Thus K_{H2}, in both acidogenesis Equations 7.5a and 7.5b, is a switching constant because it controls the switching of the above process under conditions of high p_{H2}

(while simultaneously reducing the acetate production rate with Equation 7.5a) and off under conditions of low p_{H2}.

2. **Growth and Inhibition of Acetogens:** Acetogens grow with the conversion of short chain fatty acids with more than 2 carbon atoms (such as propionic and butyric acids) to HAc, CO_2 and H_2 (McInerney *et al.*, 1979). The growth of acetogenic organisms slows with increase in the hydrogen partial pressure p_{H2}. This in turn causes a reduction in the rate at which the propionic acid is converted to acetic acid and hydrogen.

$$r_{Z\,AC} = \frac{\mu_{\max,AC} \cdot [H\,\mathrm{Pr}]}{K_{S,AC} + [H\,\mathrm{Pr}]} \cdot \left(1 - \frac{[H_2]}{k_{H2} + [H_2]}\right) \cdot [Z_{AC}] \qquad (7.5c)$$

Where:

$r_{Z,AC}$ = Growth rate of acetogenic biomass.

[HPr] = Molar concentration of undissociated propionic acid.

$\mu_{max,AC}$ = Acetogenic biomass maximum specific growth rate constant.

$K_{S,AC}$ = Half saturation coefficient for acetogenic biomass.

$[Z_{AC}]$ = Molar concentration of acetogenic biomass.

3. **Growth Inhibition of Acetoclastic Methanogens:** The acetoclastic methanogens grow with the conversion of HAc to CO_2 and methane (CH_4). The growth of acetoclastic methanogens is inhibited by digester operational pH being low, i.e. below 6.6 (Gujer and Zehnder, 1983; Zehnder and Wuhrmann, 1977).

$$r_{Z\,AM} = \frac{\mu_{\max,AM} \cdot [HAc]}{\left(K_{S,AM} + [HAc]\right) \cdot \left(1 + \frac{[H^+]}{K_{I,AM}}\right)} \cdot [Z_{AM}] \qquad (7.5d)$$

Where:

$r_{Z,AM}$ = Growth rate of acetoclastic methanogens.

$[H^+]$ = Molar concentration of the hydrogen ions.

$[H_{AC}]$ = Molar concentration of the undissociated acetic acid.

$\mu_{max,AM}$ = Acetoclastic methanogens' maximum specific growth rate constant.

$K_{S,AM}$ = Half saturation coefficient for acetoclastic methanogens.

$[Z_{AM}]$ = Molar concentration of acetoclastic methanogens.

$K_{I,AM}$ = The molar concentration of hydrogen ions at which the growth of acetoclastic methanogens is reduced to half the normal rate (Batstone *et al.*, 2002).

4. **Growth Inhibition of Hydrogenotrophic Methanogens**: Hydrogenotrophic methanogens grow by converting H_2 to CH_4 and water through hydrogen reduction with CO_2. As is the case with acetoclastic methanogens, hydrogenotrophic methanogens are also inhibited by low pH values.

$$r_{Z\,HM} = \frac{\mu_{\max,HM} \cdot [H_2]}{(K_{S,HM} + [H_2]) \cdot \left(1 + \frac{[H^+]}{K_{I,HM}}\right)} \cdot [Z_{HM}] \qquad (7.5e)$$

Where:

$r_{Z,HM}$ = Growth rate of hydrogenotrophic methanogens.

$\mu_{max,HM}$ = Hydrogenotrophic methanogens' maximum specific growth rate constant.

$K_{S,HM}$ = Half saturation coefficient for hydrogenotrophic methanogens.

$[Z_{HM}]$ = Molar concentration of hydrogenotrophic methanogens.

$K_{I,HM}$ = The molar concentration of hydrogen ions at which the growth of hydrogenotrophic methanogens is reduced to half the normal rate (Batstone *et al.*, 2002).

The above-mentioned inhibition functions were applied in the ADM-3P model to predict the response of the AD system when methanogenic inhibition is induced.

The MLE 2 AD system at its 40 day R_s operation (using same model parameters and 40-day input values reported in Tables 7.5.5a and 7.5.5b respectivley) was run to a steady state. Thereafter, to induce AD failure the H^+ component in the influent was significantly increased for 10 days (day 30 to 40) of a 120 day simulation period. This was done so in order to ensure that the H^+ ions (the inhibitor) would increase to beyond the $k_{I,AM}$ and $k_{I,HM}$ (of Equations 7.5d and 7.5e respectively) in the AD causing methanogenic inhibition. The Figure 7.5.12 below shows that this caused the system to collapse without recovery for the remaining simulation time of 80 days (2 sludge ages).

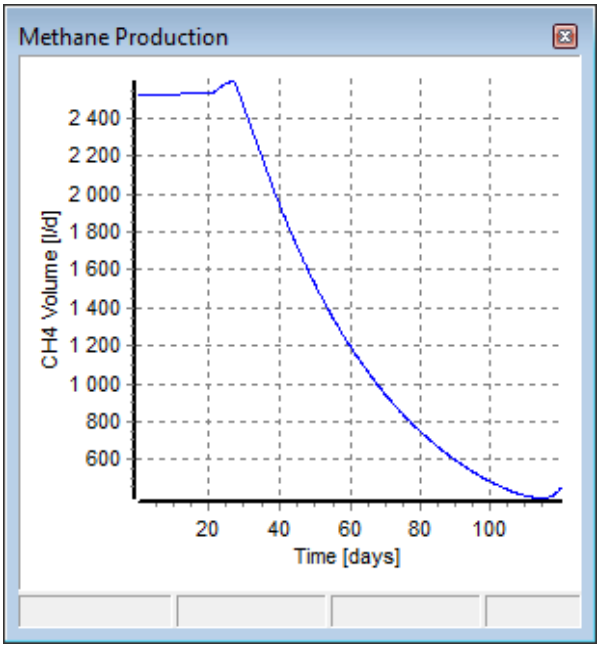

(a)

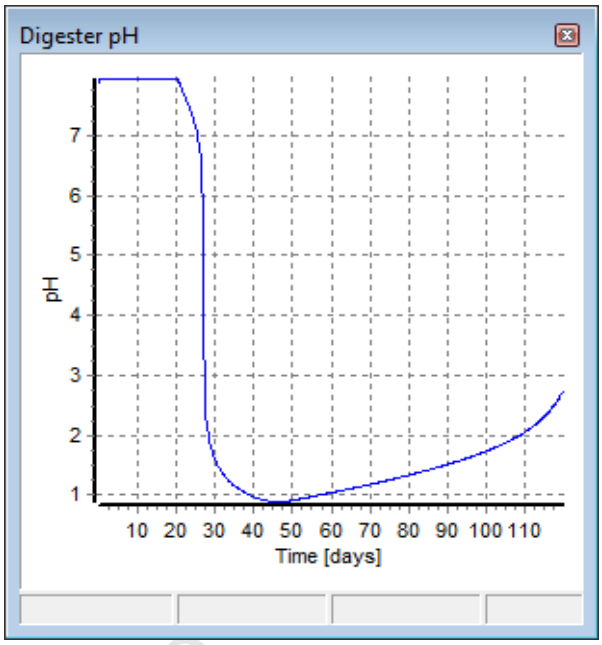

(b)

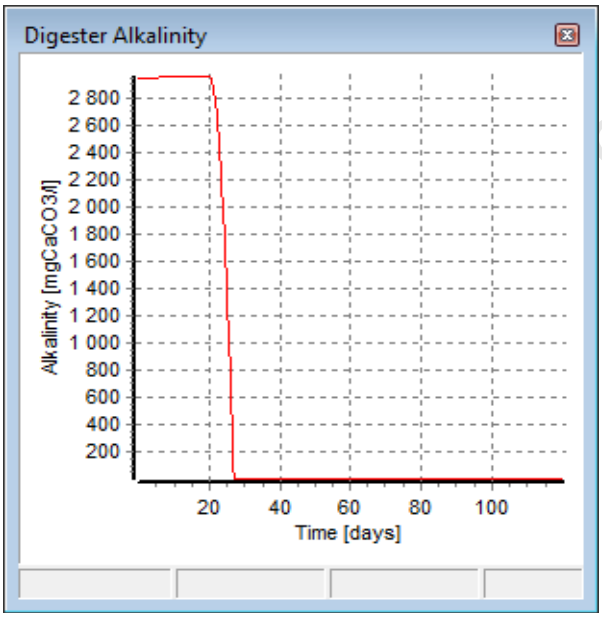

(c)

Figures 7.5.12a to c: *Simulated AD failure exhibited by plot windows of (a) methane production, (b) digester pH and (c) digester total alkalinity.*

The same 40-day R_s MLE 2 AD simulation was repeated but with the increase in H^+ only done for a period of one day. The Figure 7.5.13 below show that this only caused a temporary

AD failure with the methane production exhibiting a steady decrease for 40 days and then rapidly rising back to its original volume. This same trend, which is also observed with the digester pH, shows that the model is also capable of predicting a temporary reduction in the methanogenic growth rate. However, in reality these trends of AD failure prediction would also depend on the specific cause of failure and its magnitude in order to forecast the degree at which the AD system would fail and the extent of intervention required to ensure recovery.

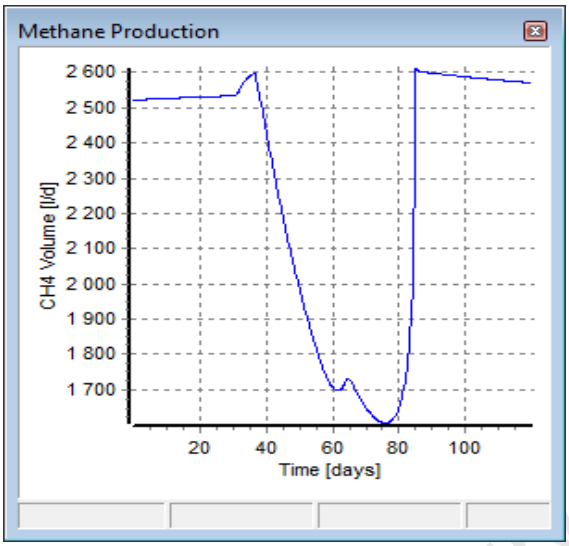

(a)

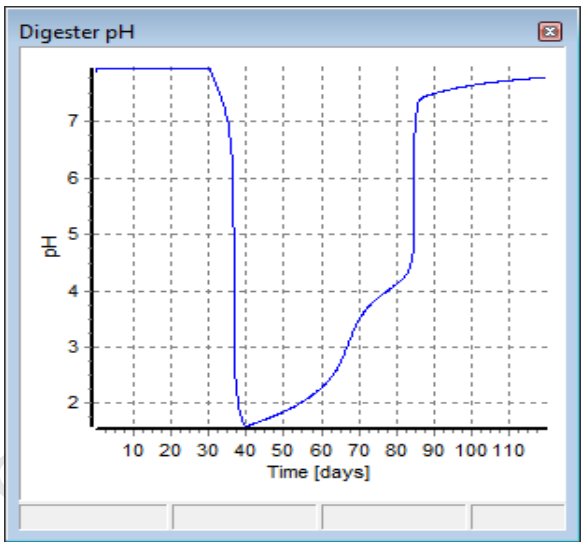

(b)

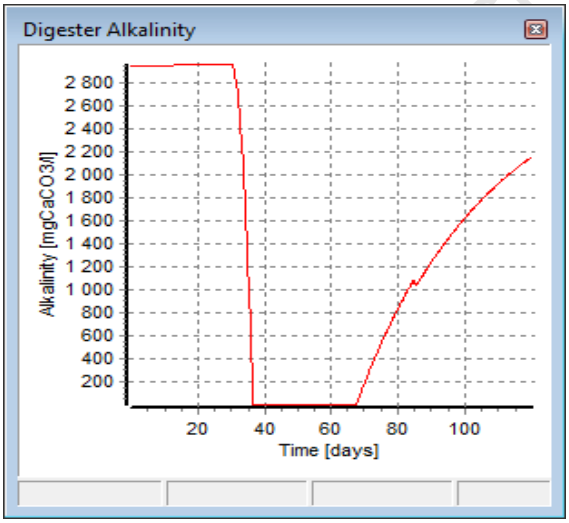

(c)

Figures 7.5.13a to c: *Simulated temporary AD failure exhibited by plot windows of (a) methane production, (b) digester pH and (c) digester total alkalinity.*

Closure

Important criteria in the design of this 3 phase dynamic AD model were (1) rapid and stable mathematical solutions, (2) alignment with routine and common measurement parameters used in practice and (3) ready integration into plant-wide models by aligning model components with those used in other wastewater treatment plant unit operation models such as activated sludge models, in particular ASM2, which includes biological excess P removal. These criteria were met by (1) separating the differential mass balance equations for the slow biological and chemical precipitation processes and the algebraic equations for the rapid aqueous equilibrium and ion-paring reactions by making use of an external equilibrium speciation model, (2) characterizing the AD influent organics with a generic elemental composition formula $C_XH_YO_ZN_AP_B$, and the polyphosphate by $Mg_cK_dCa_ePO_3$ where the X,Y,Z,A and B values are determined from the measured mass ratios fcv, fc, fn and fp for each organic type and the Mg, K and Ca content of polyphosphate from measured metals composition of the solids entering the AD. The influent aqueous phase concentration characterization is based on the widely used proton balance (alkalinity) approach, which is transformed by a model pre-processor to a charge balance system to facilitate AD simulation. The predicted effluent aqueous concentrations are transformed back to the proton balance basis by a post-processor to facilitate comparison with experimentally measured concentrations.

The ADM1, developed by an IWA task group (Batstone *et al.*, 2002), combines and fine-tunes work done in past years of research and modelling of AD systems. To expand its prediction capabilities, over the past few years extensions and modifications have been added to ADM1, including aspects such as toxic effects of cyanide in acidogenic inhibition (Zaher, 2004) or anaerobic degradation of other compounds (Wolfberger and Holubar, 2006; Batstone and Keller, 2003; Fezzani and Ben Cheikh, 2009). The conceptual three phase AD model developed here could also be useful in further extensions to the ADM1, mainly by including (1) multiple mineral precipitation, whereby weak acid/base reactions together with the final

state of equilibrium in situations where simultaneous and/or sequential precipitation of multiple minerals competing for the same species (or not) can be predicted; (2) correction of ion activity, together with some ion pairing behaviour for accurate prediction of pH kinetics. Later (see Section 7.7), the external equilibrium speciation model has been integrated with ASM2 to build a 3 phase BEPR AS model and linked with the 3 phase AD model to build a 3 phase plant-wide model with NDBEPR activated sludge, anaerobic digestion of primary sludge and anoxic-aerobic digestion or anaerobic digestion of concentrated WAS.

7.6 AEROBIC DIGESTER SIMULATION USING THE ASM2-3P MODEL

The ASM2-3P model described in Section 7.4 above was also used to simulate aerobic digestion, by calibrating the model against data obtained from Mebrahtu *et al.* (2007) who ran laboratory scale batch aerobic digesters started with NDBEPR WAS and Vogts (2011) who operated a lab scale continuous aerobic digester fed NDBEPR WAS.

Aerobic Digester: Calibration with Mebrahtu *et al.* (2007) Data

Mebrahtu *et al.* (2007) carried out eight aerobic batch digestion tests on WAS from the laboratory scale MBR UCT NDBEPR, at a controlled pH of 7.2 and in the temperature regulated (20°C) Water Research Laboratory of the University of Cape Town (UCT). The MBR UCT NDBEPR system that provided the WAS was operated at steady state by Du Toit *et al.* (2010) at a sludge age of 20 days and a high aerobic reactor TSS concentration of about 20gTSS/*l*. This UCT MBR system was identical to that operated in this investigation to supply WAS for the ADs except that its sludge age was 20d rather than 10d as in this investigation. Six of the eight batch tests were performed in a 5 *l* aerobic digester, while the last two batch tests were carried out in parallel using two separate 3 *l* aerobic digesters, one with concentrated WAS (~20gTSS/*l*) and the other with WAS diluted 5 times (~ 4gTSS/*l*).

The influent COD concentration fed to the parent NDBEPR system was 800 mgCOD/*l* real wastewater, to which 200 mgCOD/*l* of acetate was added to increase PAO growth. To maintain the 20-day sludge age, 2.85 *l*/day of mixed liquor WAS was harvested from the aerobic reactor.

Mebrahtu *et al.* (2007) simulated in Aquasim (Reichert, 1998) both the NDBEPR parent system and the eight batch digestion tests using Activated Sludge Model No. 2 (ASM2, Henze *et al.*, 1995) that had been modified to include the ISS model of Ekama and Wentzel (2004). To calibrate this ASM2 model against the parent NDBEPR system data, Mebrahtu *et al.* (2007) set as input the measured influent VFA, FRBO and total COD concentrations and influent unbiodegradable soluble organics (USO) to total influent COD concentration ratio ($f_{S'us} = S_{use}/S_{ti}$) and selected the unbiodegradable particulate COD fraction ($f_{S'up}$) such that the predicted VSS concentrations in the system matched those measured – an average value of $f_{S'up}$ of 0.183 was obtained. This procedure simultaneously splits influent RBCOD between the OHOs and to PAOs. Then the PP content of the PAOs (f_{XBGPP}) was adjusted so that the predicted P removal matches that measured. This calibration method assumes that the variable P removal observed experimentally was due to variable P content of PAOs, due to variable P uptake rates. The model was also calibrated with a second method, which assumes that the variable P removal was due to a variable PAO biomass concentrations in the VSS. In this method, with a fixed P uptake rate, which fixes the PAO PP content at 0.35 mgP/mgPAOVSS, the FBSO hydrolysis rate was adjusted such that the predicted P removal matched that measured. They also affected the VSS mass in the system, so the $f_{S'up}$ value was adjusted so that the predicted VSS mass matched that measured. Finally, Mebrahtu *et al.* (2007) iteratively selected the influent ISS concentration such that the ISS mass predicted in the system matched that measured. The ASM2-3P model was calibrated the same way.

To simulate the AerD system with the ASM2-3P model, the predicted results from the calibrated model were set as initial conditions for the simulation of the aerobic batch tests, just as Mebrahtu *et al.* (2007) had done when simulating batch tests with Aquasim. To ensure

that the input simulated values matched the measured initial (day-zero) values of the aerobic batch reactors, these initial values were re-calculated by multiplying them by the ratio of day-one predicted to measured values. The day-one predicted to measured VSS ratio was applied to the particulate organics, the TP ratio was applied to the PP, and the ISS (from the influent sewage) was calculated by subtracting this PP ISS from the calculated day zero ISS.

Before comparing the ASM2-3P model predicted results to those measured experimentally, the results obtained by Mebrahtu (2007) from the simulation of Batch Test 3 (BT 3) with ASM2 (single phase) in Aquasim are compared with results from the simulation of BT 3 using the ASM2-3P model, with its precipitation process turned off, to verify that the results obtained are reasonably similar (Fig 7.6.1). The parameters used in this simulation are shown below, in Table 7.6.1.

Table 7.6.1: Parameters used in Simulating the ASM2-3P Model			
Parameter	**Value**	**Units**	**Description**
A_bp	dUnit/dUnit	N/C: biodegradable particulate	0.2
A_bps	dUnit/dUnit	N/C: PS biodegradable particulate	0.05
A_e	dUnit/dUnit	N/C: endogenous residue	0.15
A_f	dUnit/dUnit	N/C: fermentable soluble	0.06
A_o	dUnit/dUnit	N/C : organisms	0.2
A_up	dUnit/dUnit	N/C: unbiodegradable particulate	0.15
A_us	dUnit/dUnit	N/C: unbiodegradable soluble	0.061887
b_{AUT}	1/d	Decay rate	0.15
B_bp	dUnit/dUnit	P/C: biodegradable particulate	0.015
B_bps	dUnit/dUnit	P/C: PS biodegradable particulate	0.002857
B_e	dUnit/dUnit	P/C: endogenous residue	0.026042
B_f	dUnit/dUnit	P/C: fermentable soluble	0.007502
b_H	1/d	Rate constant for lysis and decay of OHOs	0.62
B_o	dUnit/dUnit	P/C : organisms	0.015
b_G	1/d	Rate constant for lysis of PAO	0.2
b_PHA	1/d	Rate constant for lysis of PHA	0.02
b_PP	1/d	Rate constant for lysis of PP	0.025
B_up	dUnit/dUnit	P/C: unbiodegradable particulate	0.026042
B_us	dUnit/dUnit	P/C: unbiodegradable soluble	0.008221
e_PP			0.05
f_e	-	Fraction of dead biomass to ER	0.08
$k'r_{ACP}$	-	Dissolution of calcium phosphate	1.64346E-5
$k'r_{MgKP}$	-	Dissolution of K-struvite	0.001
$k'r_{Struv}$	-	Dissolution of struvite	0.001
K_A	-	Saturation coeff for Ac (acetate)	4
K_ALK	-	Saturation coeff for alkalinity (HCO_3^-)	5
K_ALK_AUT	-	Saturation coeff of autotrophs for alkalinity	0.5
k_CO2	-	Rate constant for CO_2 exchange	0.1
K_F	-	Saturation/inhibtion coeff for growth on FBSO	4
K_fe	-	Saturation coeff for fermentation on FBSO	20
k_fs	1/d	Hydrolysis rate constant for FBSO	10
k_h	gCOD/(gCOD*d)	Hydrolysis rate constant	8
K_IPP	-	Inhibition coeff for PP storage	0.02
K_MAX	-	Maximum ratio of PP/PAO	1.05

Table 7.6.1: Parameters used in Simulating the ASM2-3P Model			
Parameter	**Value**	**Units**	**Description**
K_NH	-	Saturation coeff for ammonium (nutrient)	0.05
K_NH_AUT	-	Saturation coeff of autotrophs for ammonium	1
K_NO	-	Saturation/inhibition coeff fir nitrate	0.5
K_O	-	Saturation/inhibition coeff for oxygen	0.5
K_O_AUT	-	Saturation/inhibition coeff of autotrophs for oxygen	0.5
K_P	-	Saturation coeff for phosphorus (nutrient)	0.01
K_PHA	-	Saturation coeff for PHA	0.01
K_pha	1/d	Hydrolysis rate constant for PHA	0.2
d_PP	Unit/Unit	K/P:Polyphosphate	0.32
K_PP	-	Saturation coeff for poly-phosphate	0.01
K_PS	-	Saturation coeff for phosphorus in PP storage	0.2
K_X	-	Saturation coeff for particulate COD	0.1
mu_AUT	1/d	Maximum growth rate for XAUT	0.45
c_PP	1/d	Maximum growth rate on substrate	0.29
mu_H	1/d	Maximum growth rate on substrate	6
mu_hm	1/d	Max specific growth rate for hydrogenotrophic methanogens	1.2
mu_PAO	1/d	Maximum growth rate	1.2
n_fe	-	Anaerobic hydrolysis reduction factor	0.1
n_NO_Het	-	Reduction factor for denitrification	0.1
n_NO_Hyd	-	Anoxic hydrolysis reduction factor	0.6
P_{CO2_AS}	-	Partial pressure of CO2 in the AS liquor	0.3
PCO2_headspace	-	Headspace CO2 partial pressure (Pa)	50500
q_fe	1/d	Maximum rate for fermentation	20
q_PHA	1/d	Rate constant for storage of PHA (base: PP)	3
q_PP	1/d	Rate constant for storage of PP	5
R_gas	-		0.082057
S_O_Sat	g/m3	Oxygen saturation concentration	9.5
TempCoeff	-	Rate temperature coefficient	0.0667
Temperature	°C	System Temperature	20
Tref	°C	Reference temperature for kinetics	20
Vol	L	Volume of the tank	5
Y_{AUT}	gCOD/gN	Yield For Autotrophic Biomass	0.24

Table 7.6.1: Parameters used in Simulating The ASM2-3P Model			
Parameter	**Value**	**Units**	**Description**
Y_bp	dUnit/dUnit	H/C: biodegradable particulate	1.458333
Y_bps	dUnit/dUnit	H/C: PS biodegradable particulate	1.990487
Y_e	dUnit/dUnit	H/C: endogenous residue	1.458333
Y_f	dUnit/dUnit	H/C : fermentable soluble	1.567209
Y_o	dUnit/dUnit	H/C : organisms	1.458333
Y_G	-	Yield coeff (biomass/PHA)	0.67
Y_PHA	-	PHA requirement for PP storage	0.5
Y_PO	-	PP requirement (S_PO4 release) per PHA stored	0.5
Y_up	dUnit/dUnit	H/C: unbiodegradable particulate	1.458333
Y_us	dUnit/dUnit	H/C: unbiodegradable soluble	1.546307
Z_bp	dUnit/dUnit	O/C: biodegradable particulate	0.416667
Z_bps	dUnit/dUnit	O/C: PS biodegradable particulate	0.561719
Z_e	dUnit/dUnit	O/C: endogenous residue	0.416667
Z_f	dUnit/dUnit	O/C : fermentable soluble	0.587228
Z_o	dUnit/dUnit	O/C : organisms	0.416667
Z_up	dUnit/dUnit	O/C: unbiodegradable particulate	0.416667
Z_us	dUnit/dUnit	O/C: unbiodegradable soluble	0.543126

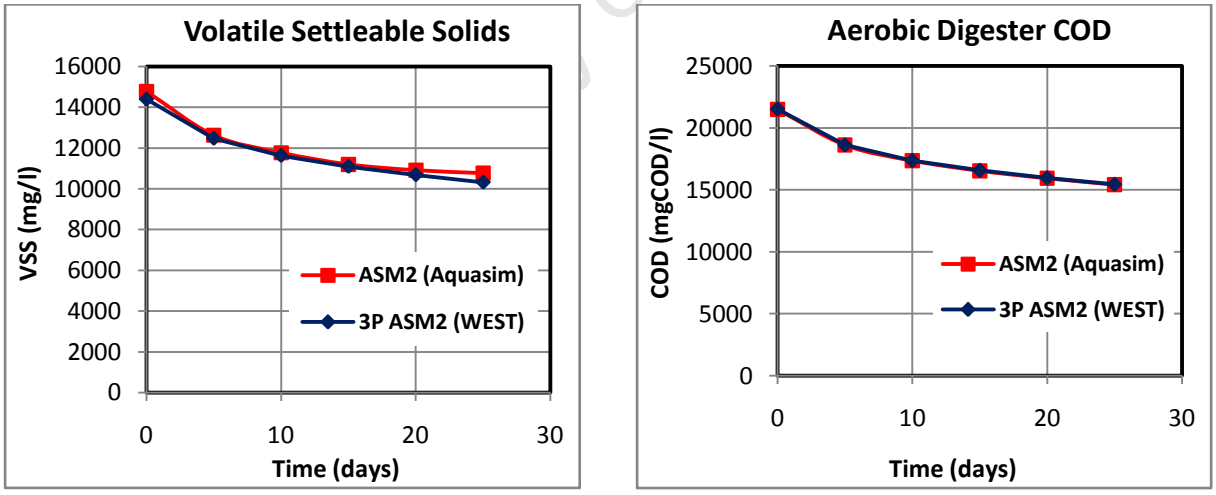

(a) (b)

Figures 7.6.1a and b: *A comparison between the results simulated by the ASM2-3P dynamic model (with the precipitation process off) and those simulated by Mebrahtu (2007) with ASM2 (single phase) in Aquasim for the batch test 3 AerD system in the order of: (a) volatile settleable solids and (b) digester COD.*

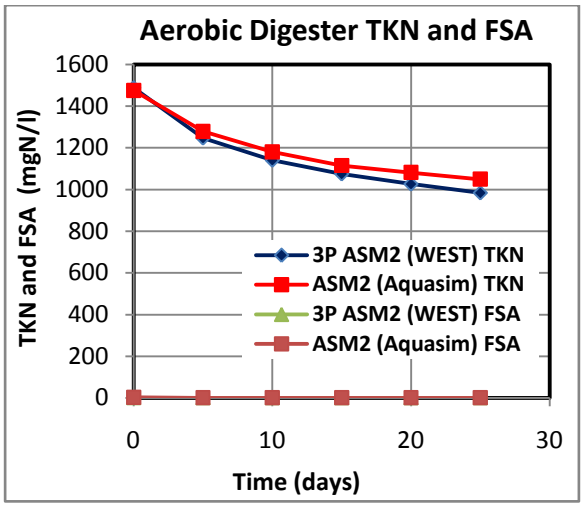

(c)

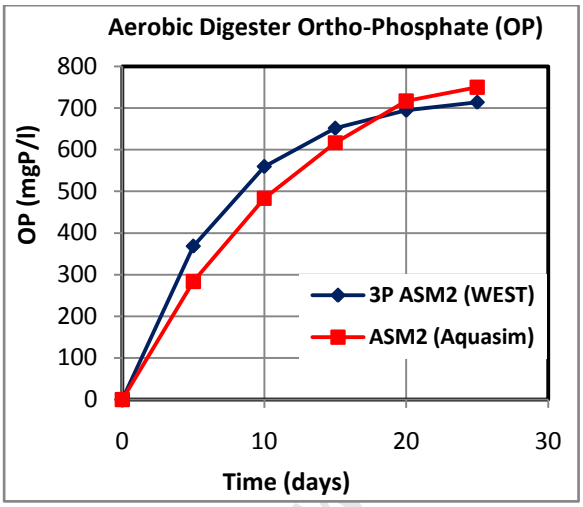

(d)

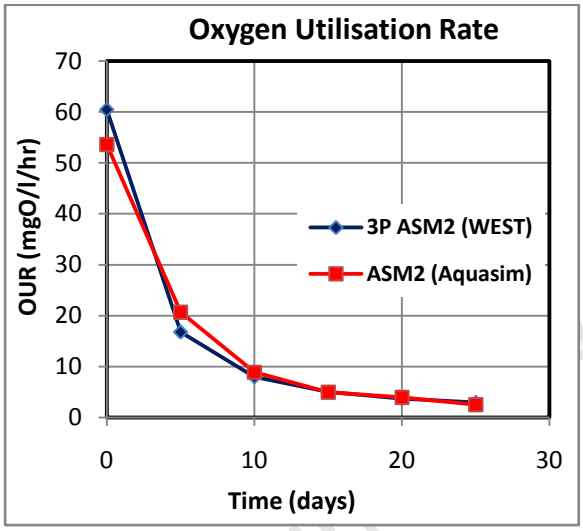

(e)

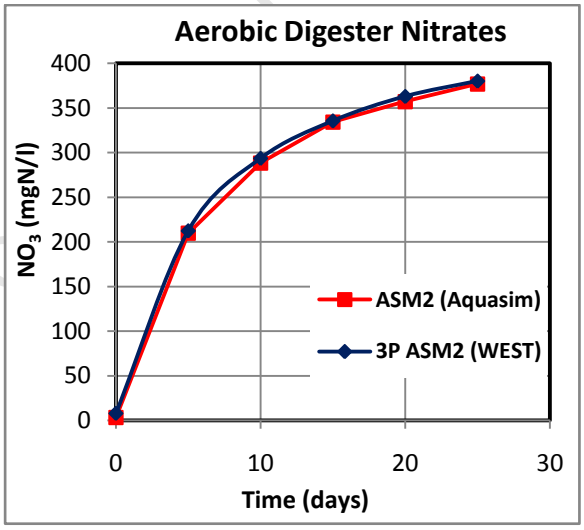

(f)

Figures 7.6.1c to f: *A comparison between the results simulated by the ASM2-3P dynamic model (with the precipitation process off) and those simulated by Mebrahtu (2007) with ASM2 (single phase) in Aquasim for the batch test 3 AerD system in the order of: (c) nitrogen releases, (d) phosphorus releases, (e) oxygen utilisation rates and (f) nitrates concentration.*

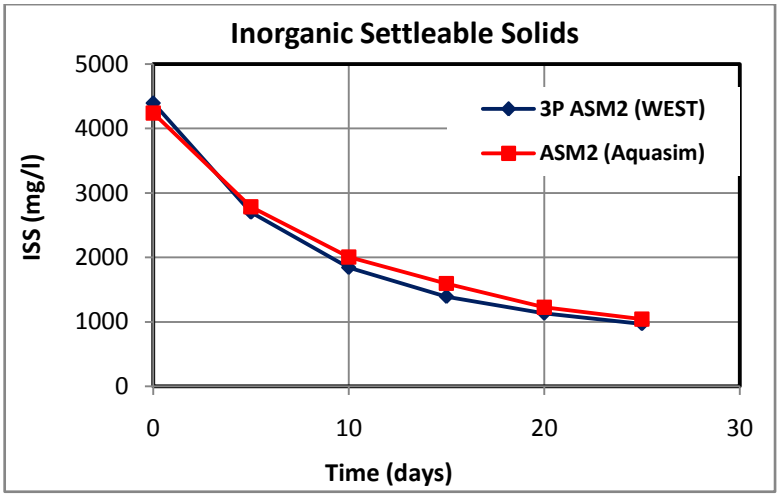

Figure 7.6.1g: *A comparison between the inorganic settleable solids concentration results simulated by the ASM2-3P dynamic model (with the precipitation process off) and those simulated by Mebrahtu (2007) with ASM2 (single phase) in Aquasim for the batch test 3 AerD.*

As notable the organics degradation (from the COD and VSS graphs 7.6.1a and b), nitrification (from TKN reduction and nitrate generation graphs 7.6.1c and f), oxygen utilization (Figure 7.6.1e) and phosphate release (Figures 7.6.1 d and g, since PP makes up a significant portion of ISS) predicted by the ASM2-3P model (in WEST®) are reasonably similar to those predicted by Mebrahtu (2007) using ASM2 in Aquasim. This provides a good verification of the ASM2-3P model in the simulation of batch AerD, without precipitation.

Given below is a comparison between the concentrations simulated with the ASM2-3P model and those measured by Mebrahtu *et al.* (2007) for AerD Batch Tests 1, 3, 7 and 8. Struvite precipitation took place in the concentrated Batch Tests 1, 3 and 7 and not in the diluted BT8.

Batch Test Eight of Mebrahtu *et al.* (2007) Aerobic Digestion (AerD) Data

The comparisons between the results simulated by the ASM2-3P dynamic model and measured data from the batch 8 (with the same influent as batch 7, but diluted 5 times) aerobic digester are shown in Figure 7.6.2 below.

To match the predicted P release in the diluted BT8, in which no precipitation took place, to the observed P release the polyphosphate lysis rate (b_{PP}) is reduced from the value of 0.04/d to a value of 0.025/d. Therefore, it is notable from these low PP release values, that in aerobic digestion the PAOs that are alive still withhold their stored PP and release it at a similarly slow rate as associated with PAO endogenous respiration. This release behaviour is completely different to that in AD, where all the PP was released in about 5-7 days.

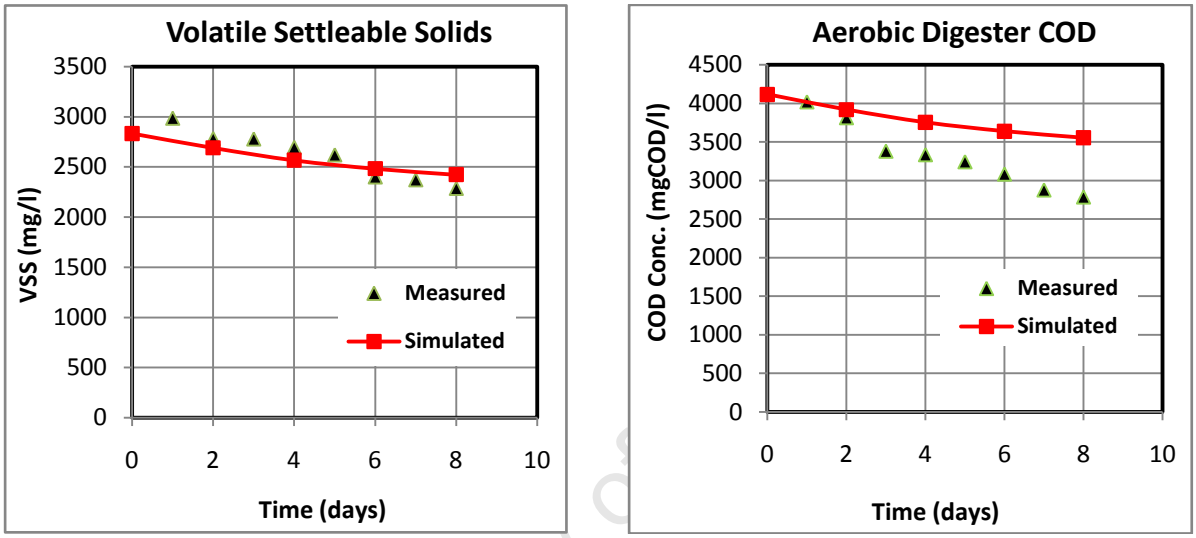

Figures 7.6.2a and b: *A comparison between the results simulated by the ASM2-3P dynamic model and measured data per sludge age (R_s) for the batch eight AerD system of Mebrahtu et al. (2007), in the order of: (a) volatile settleable solids concentrations and (b) COD concentration.*

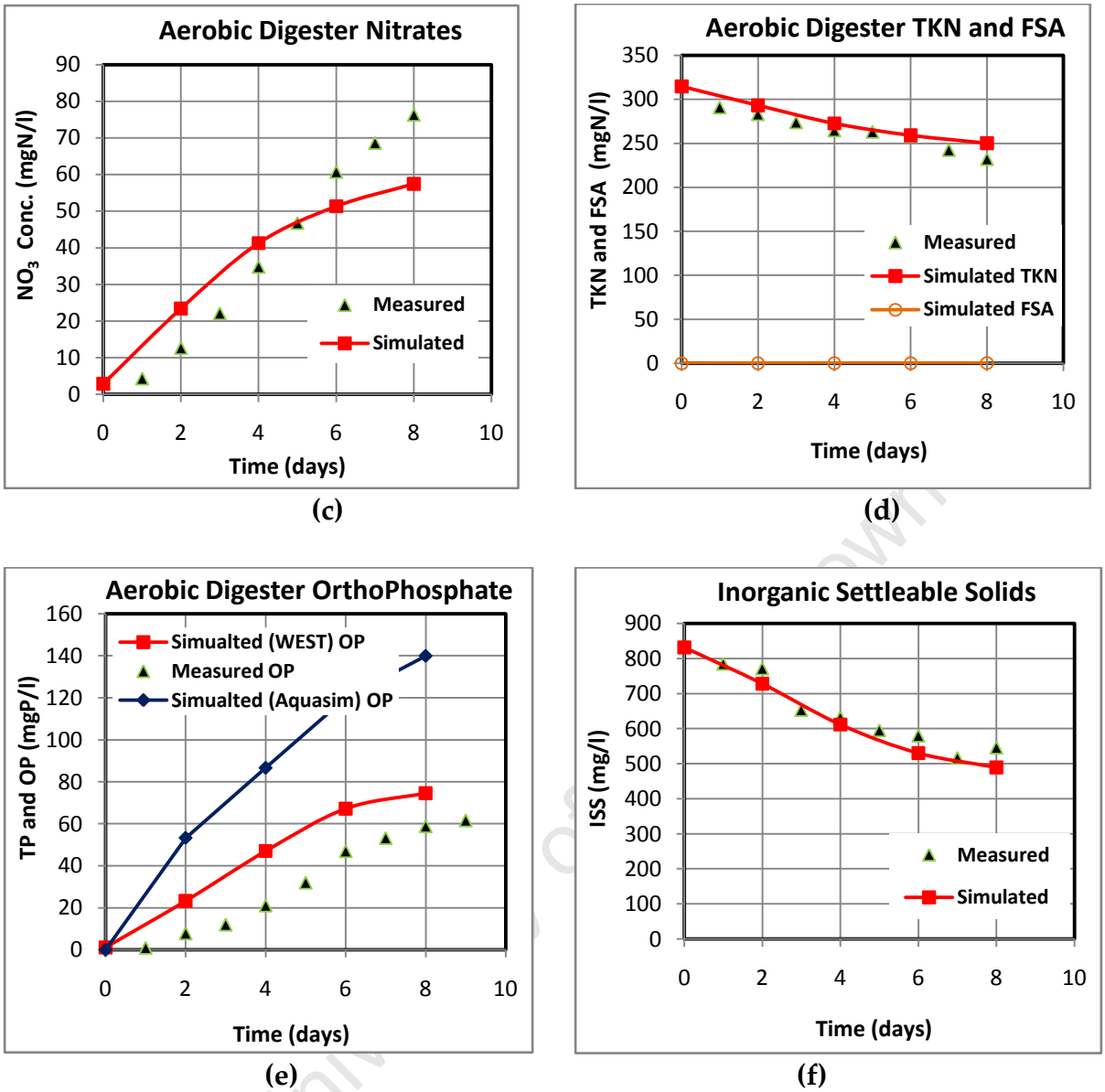

Figures 7.6.2c to f: *A comparison between the results simulated by the ASM2-3P dynamic model and measured data per sludge age (R_s) for the batch eight AerD system of Mebrahtu et al. (2007) in the order of: (c) Nitrates concentration, (d) Nitrogen releases, (e) Phosphorus releases and (f) Inorganic settleable solids concentration.*

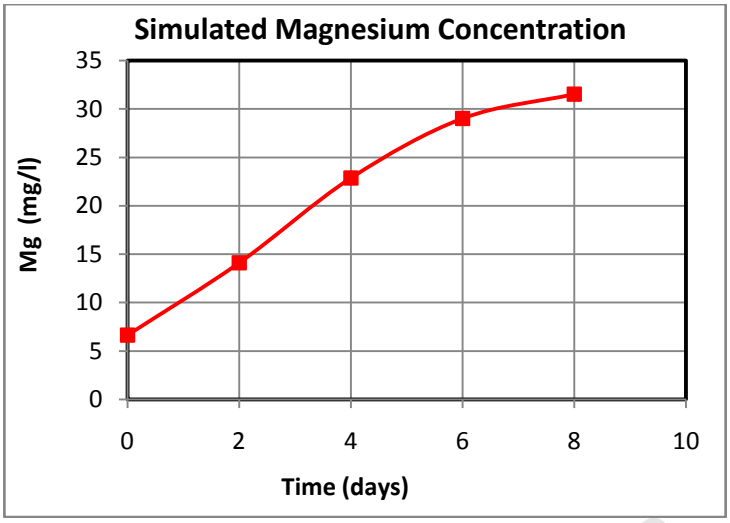

Figure 7.6.2g: *magnesium concentration results simulated by the ASM2-3P dynamic model per sludge age (R_s) for the batch eight AerD of Mebrahtu et al. (2007).*

Organics degradation is reflected by COD and VSS removal. However, although the measured COD results are observed to be lower than the simulated COD, the measured VSS concentrations are reasonably matched to those simulated. However, since the measured VSS removal is similar to that simulated, similar quantities of ammonia are made available by the organic N reduction (noted by the close match in declining trends of TKN of Figure 7.6.2d) resulting in the similar quantities of nitrates being generated.

It was noted that the measured TP values seemed to be spurious because the corresponding ISS concentration should be much higher (due to PP). Moreover, the values did not reflect the dilution of batch 7 sludge to a fifth of the concentration. Therefore, the ISS was used to determine the concentration of influent PP that is usable as input for the ASM2-3P model simulations. This explains why the effluent OP simulated by the ASM2-3P has lower concentrations, than those obtained from simulations by Mebrahtu *et al.* (2007), using ASM2 (without the coded precipitation process). Using the influent ISS to determine the influent PP (which contributes the major portion of ISS) resulted in the ASM2-3P having a better match of effluent OP and similar effluent ISS concentrations to those experimentally measured.

Batch Test One of Mebrahtu *et al.* (2007) AerD Data

The comparisons between the results simulated by the ASM2-3P dynamic model and measured data in the BT 1 are shown in Figure 7.6.3 below.

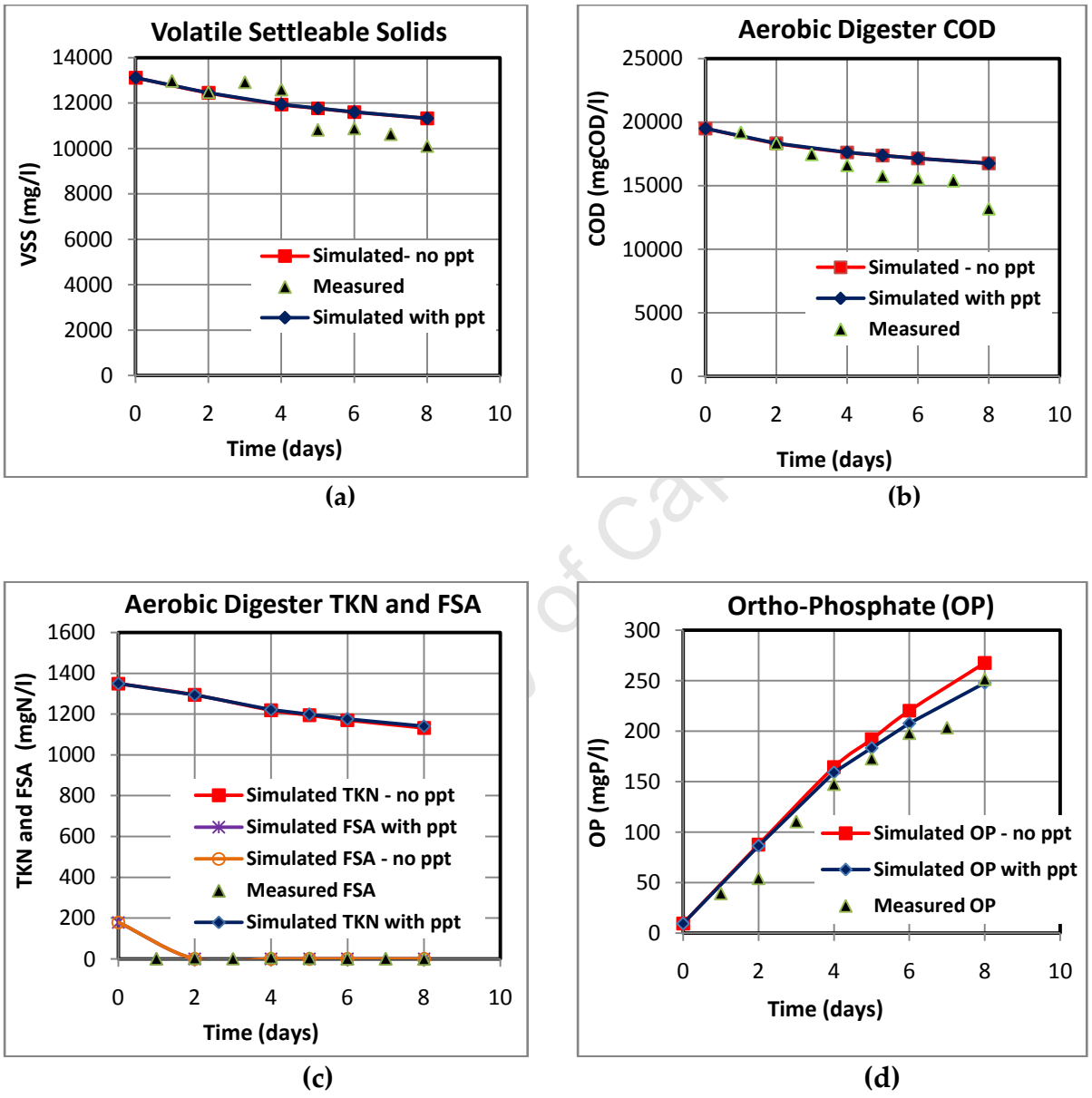

Figures 7.6.3a and d: *A comparison between the results simulated by the ASM2-3P dynamic model and measured data for BT 1: (a) volatile settleable solids concentrations, (b) unfiltered COD concentration, (c) FSA released and (d) phosphorus releases,*

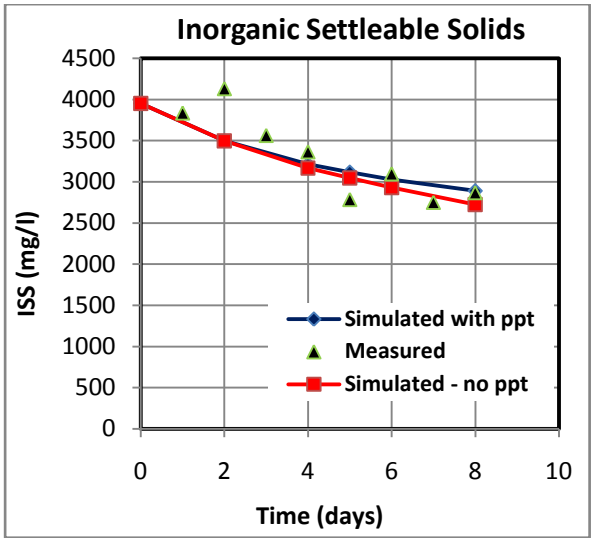

(e)

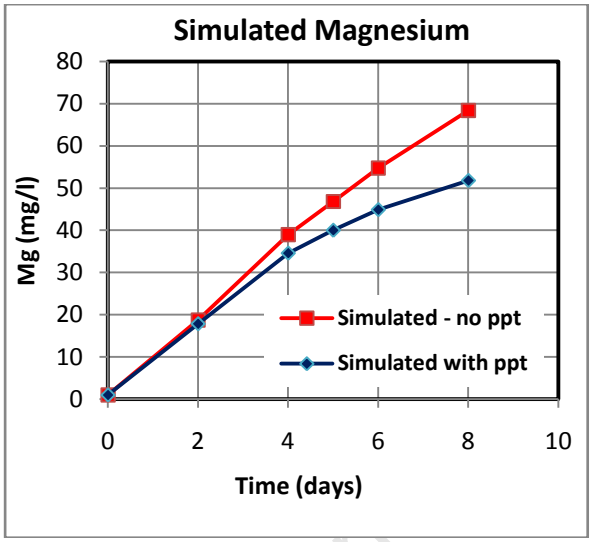

(f)

Figures 7.6.3e and f: *A comparison between the results simulated by the ASM2-3P dynamic model and measured data for BT 1: (e) inorganic settleable solids concentration and (f) simulated magnesium concentration.*

Comparing the measured and simulated results, it is notable that the reactor VSS, ISS, COD, FSA and OP concentrations, give reasonably identical results.

The simulated and measured OP and Mg concentrations for this batch of sludge (BT 1), when simulated using the ASM2-3P model are slightly lower and the ISS concentration higher when the precipitation rate is activated than when it is turned off (Figures 7.6.3 d, e and f). Its seems, from the measured OP concentration tending more towards the lower concentrations, to have closer match to those simulated with the activated precipitation process that small concentrations of struvite precipitated. However, to substantiate the evidence of this precipitation requires further experimental measurements. These include TKN, nitrates and TP (including PP and its characteristics) concentrations to indicate the quantities of N and P released to provide precipitation potential and metals, especially Mg and K, to show their decline due to this precipitation). In this case, the values simulated from the parent (NDBEPR) system were used as input to the AerD simulations, and the measured ISS was the

only variable that could be used to aid in re-adjusting the influent PP concentration. Nevertheless, this may still not have been sufficient because the ratio of PP to ISS may not be consistent with the values simulated in the parent system. Hypothetically, it is expected that the precipitation of struvite would take place in the AerD of concentrated NDBEPR WAS, if high concentrations of N, P, Mg and K are released in the AerD during the endogenous respiration process.

Batch Three of Mebrahtu *et al.* (2007) AerD Data

The comparisons between the results simulated by the ASM2-3P dynamic model and measured data from the batch 3 aerobic digester are shown in Figure 7.8 below. The pH usually keeps decreasing during the AerD process, thus as was done experimentally by Mebrahtu (2007), $NaHCO_3$ was added when simulating the batch AerD, in an attempt to maintain the pH above 7.2. As can be seen in Figure 7.6.4a, the simulated effluent pH is within reasonable range of that measured.

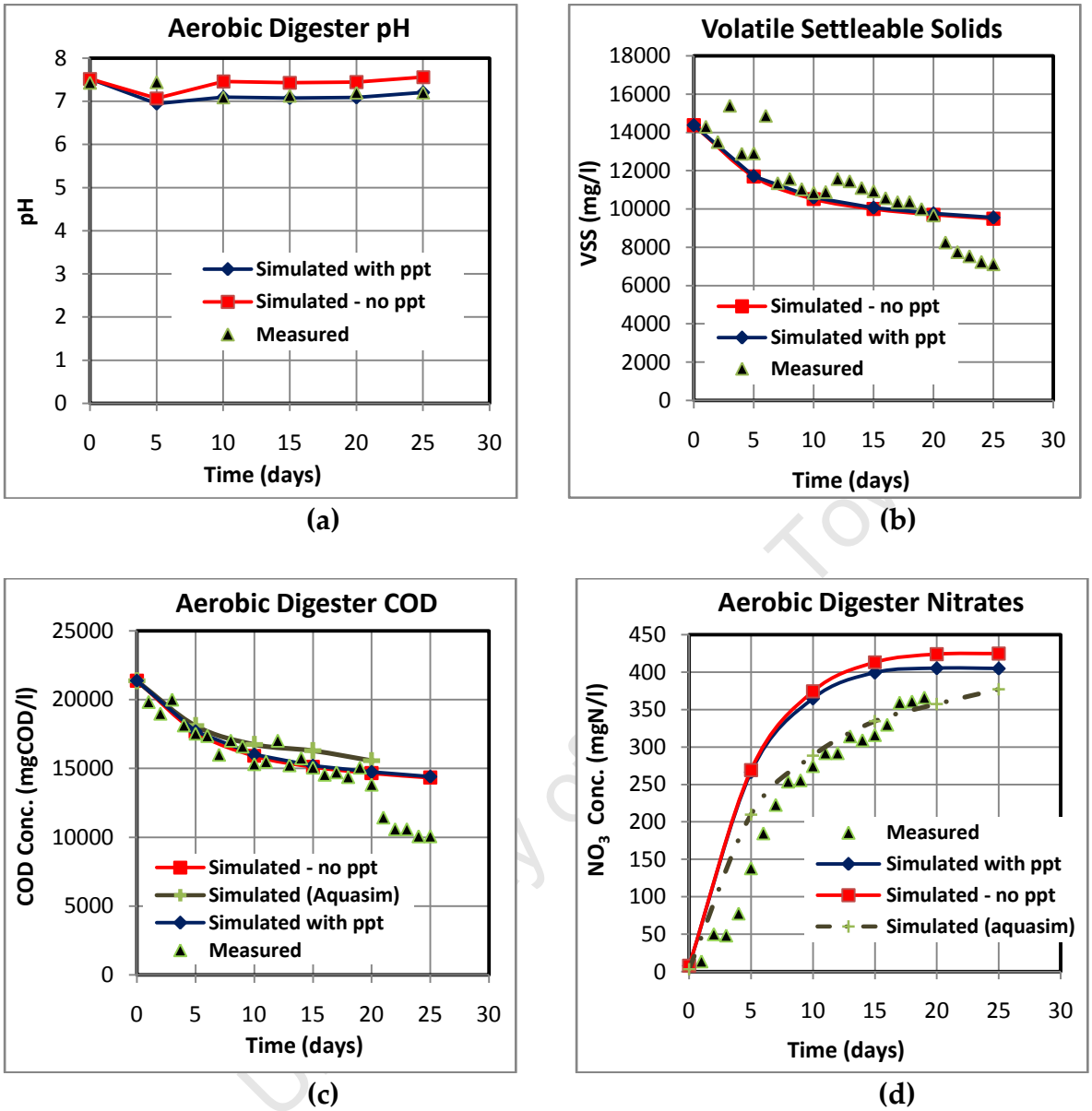

Figures 7.6.4a to d: *A comparison between the results simulated by the ASM2-3P dynamic model and measured data per sludge age (R_s) for the batch three AerD system in the order of: (a) Digester pH, (b) volatile solids concentrations, (c) COD concentration and (d) nitrates concentration.*

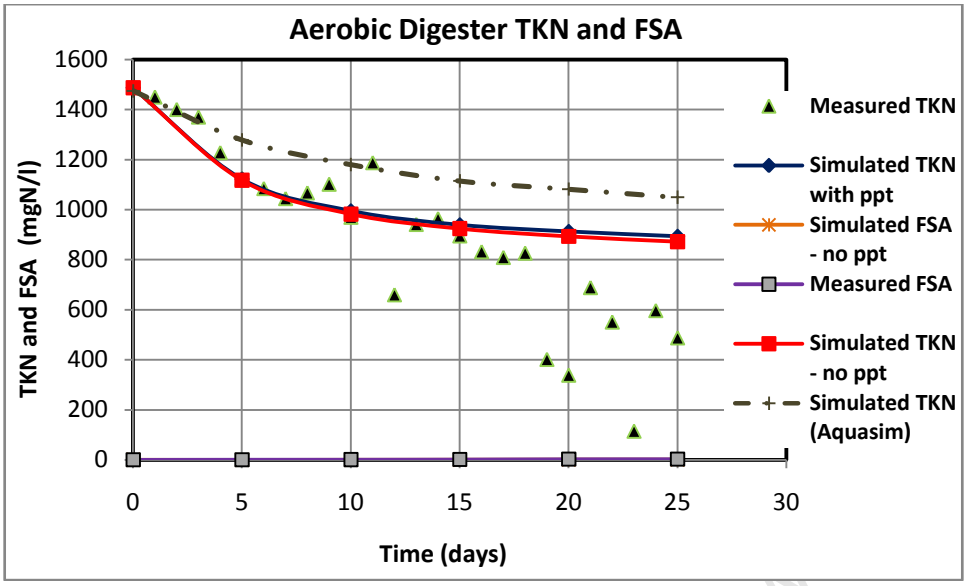

(e)

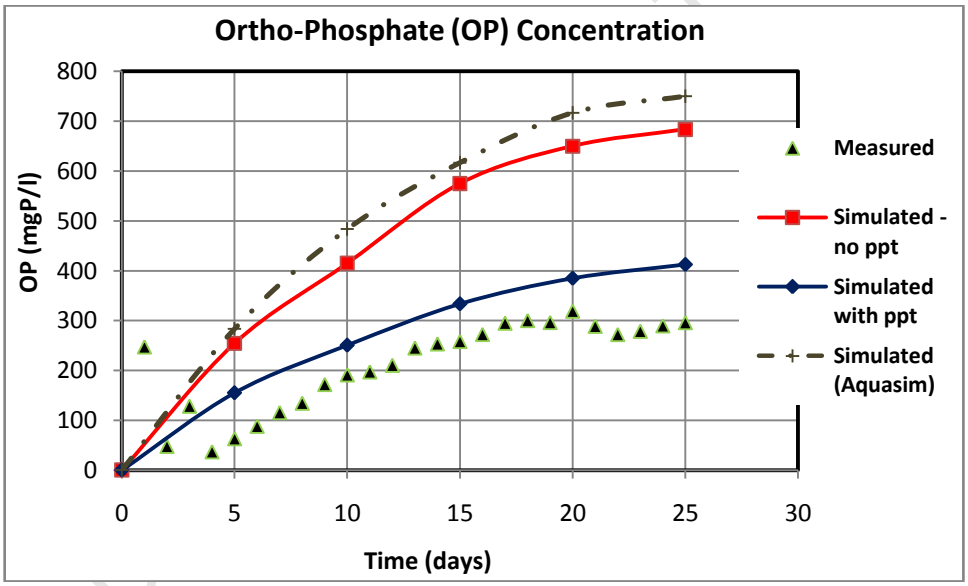

(f)

Figures 7.6.4e and f: *A comparison between the results simulated by the ASM2-3P dynamic model and measured data per sludge age (R_s) for the batch three AerD system in the order of: (e) TKN and FSA and (f) ortho-phosphate concentration.*

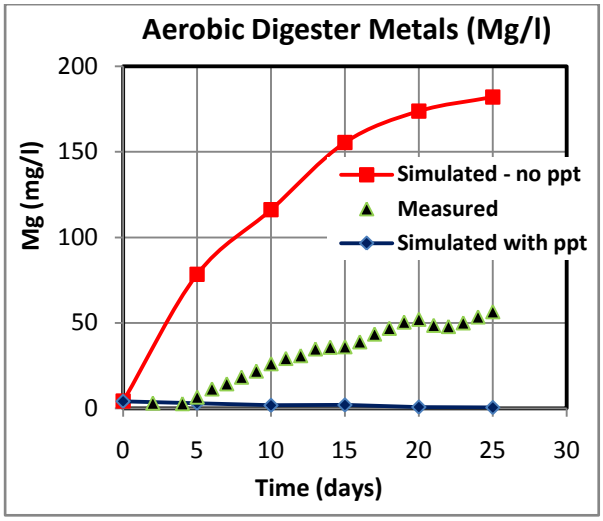

(g)

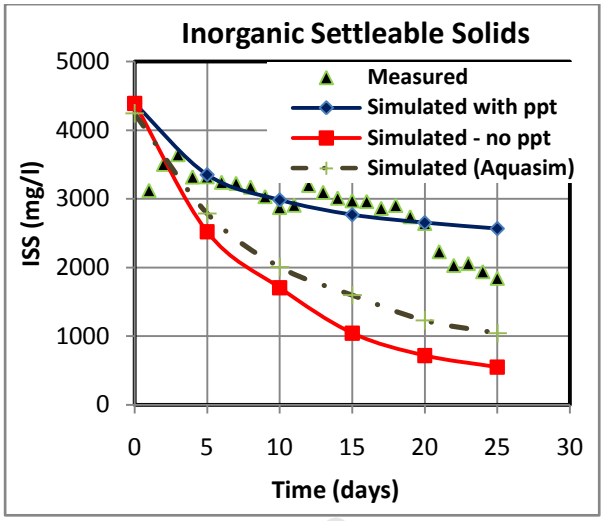

(h)

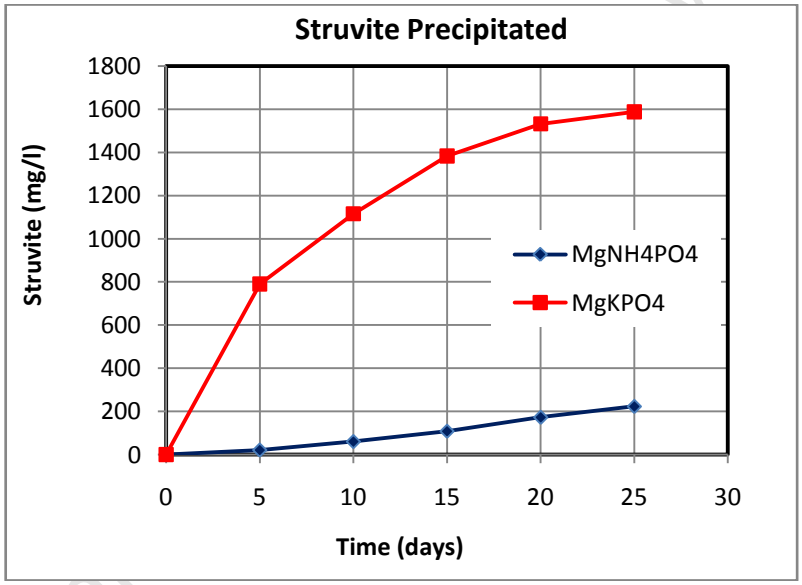

(i)

Figures 7.6.4g to i: *A comparison between the results simulated by the ASM2-3P dynamic model and measured data per sludge age (R_s) for the batch three AerD system in the order of: (g) magnesium (Mg) concentration, (h) inorganic settleable solids concentration and (i) simulated struvite concentration.*

The measured and simulated AerD effluent results for COD and VSS concentrations are reasonably close, showing that the model predicts organic degradation, due to endogenous respiration, reasonably well. In addition, the measured effluent TKN and nitrates

concentration matches the simulated values, both with and without the struvite precipitation. When struvite ($MgNH_4PO_4$) precipitation occurs in AerD, it is expected that the TKN will increase since some of the released nitrogen gets transformed into solid phase ($MgNH_4PO_4$, which is part of TKN) instead of nitrates (which is not measured in TKN). It is notable that the nitrate concentrations simulated with and without precipitation are close to each other. This shows that most of the organic N released with endogenous respiration was used for nitrification rather than struvite ($MgNH_4PO_4$) precipitation. However, the effluent OP concentration, which is lower than that simulated, is closer to the one predicted with struvite precipitation, while the one simulated without struvite precipitation is much higher. Also, the measured effluent ISS concentration has values close to that predicted by the model with the precipitation process activated, while that simulated without precipitation is significantly lower. This all points towards the possibility of precipitation taking place in this AD, but in the form of K-struvite ($MgKPO_4$) rather than $MgNH_4PO_4$. To further substantiate that this K-struvite mineral precipitated requires further measurements (of influent PP characteristics, especially the ratios of Mg and K to PP, together with the influent and effluent Mg and K concentrations) to show the decline in the K and to know how much Mg and K are used for struvite precipitation. This is because the Mg and K are usually made available in this AerD, with their release (together with P and Ca) from hydrolysed PP.

Batch Seven of Mebrahtu *et al.* (2007) AerD Data

The comparisons between the results simulated by the ASM2-3P dynamic model and measured data from the batch 7 aerobic digester are shown in Figure 7.9 below.

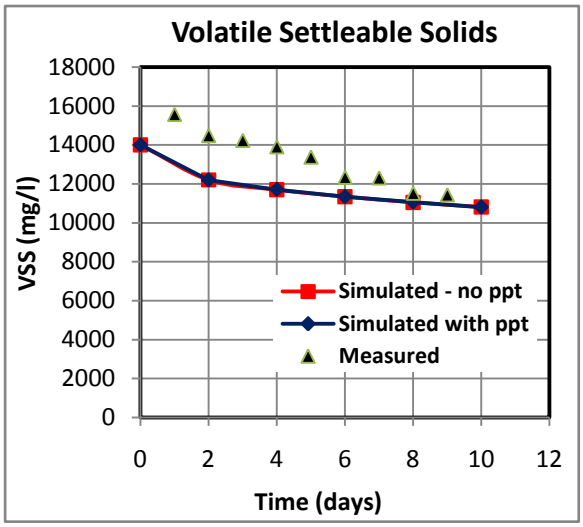

(a)

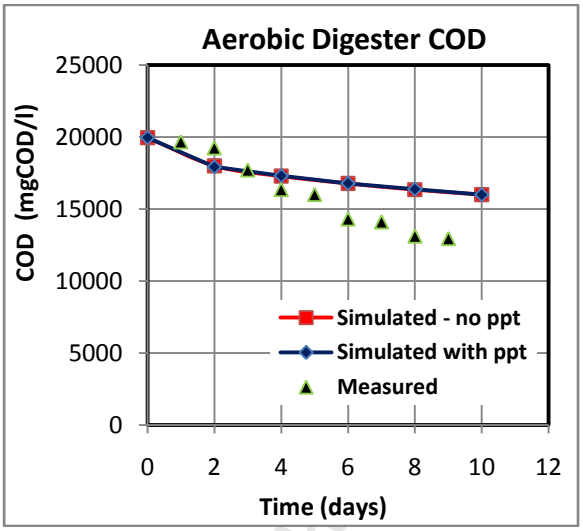

(b)

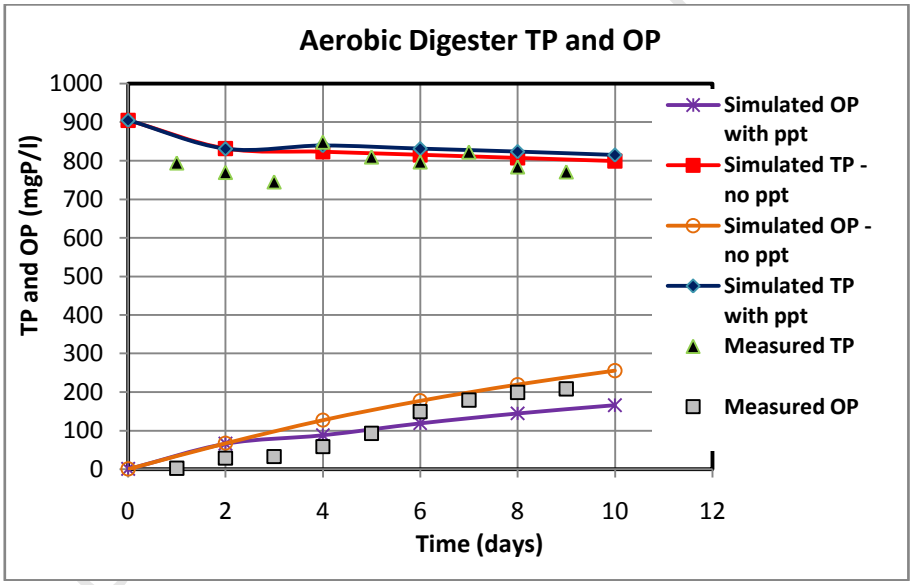

(c)

Figures 7.6.5a to c: *A comparison between the results simulated by the ASM2-3P dynamic model and measured data per sludge age (R_s) for the batch seven AerD system of Mebrahtu et al. (2007) in the order of: (a) volatile solids concentrations, (b) COD concentration and (c) nitrates concentration.*

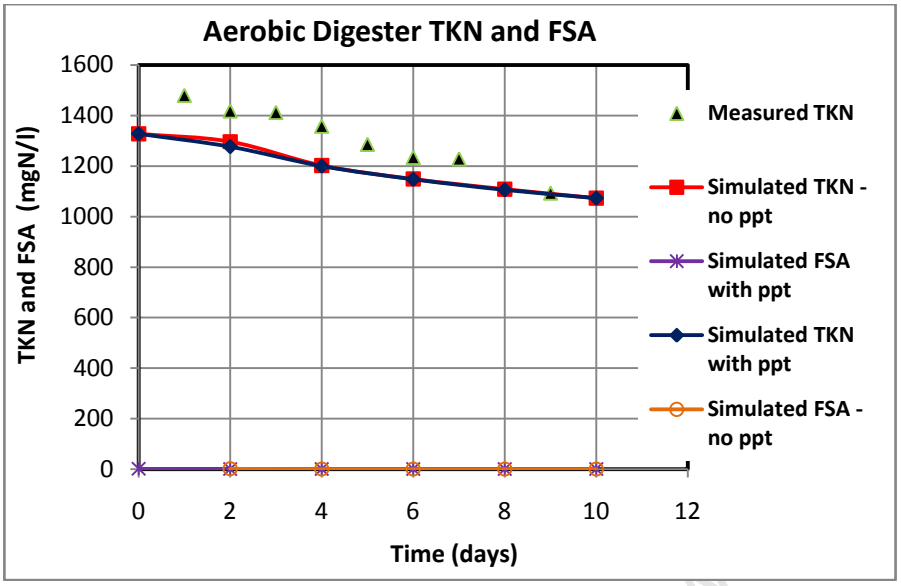

(d)

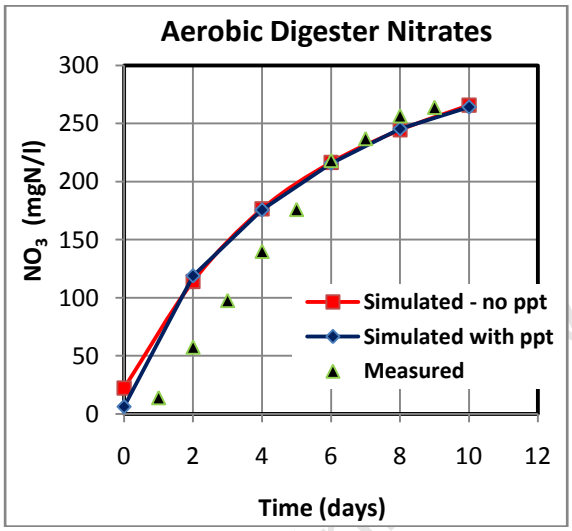

(e)

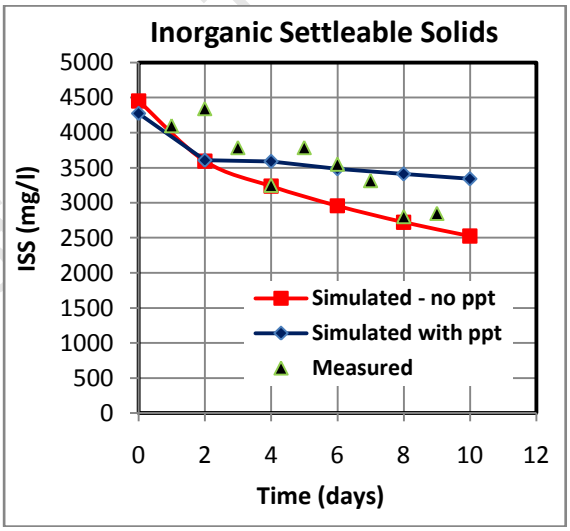

(f)

Figures 7.6.5d to f: *A comparison between the results simulated by the ASM2-3P dynamic model and measured data per sludge age (R_s) for the batch seven AerD system of Mebrahtu et al. (2007) in the order of: (d) nitrogen releases, (e) phosphorus releases and (f) inorganic settleable solids concentration.*

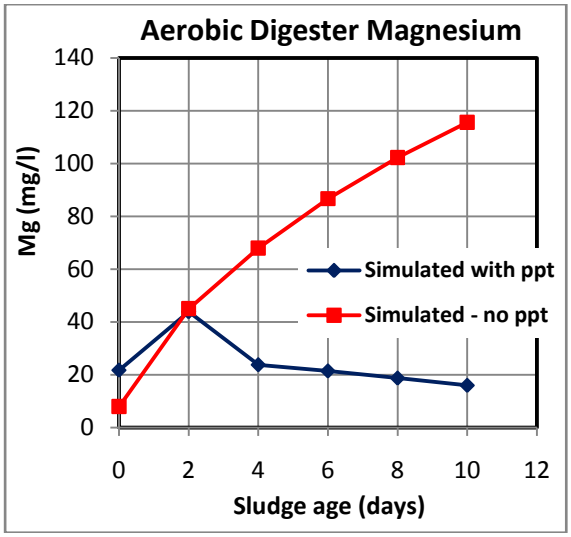

(g)

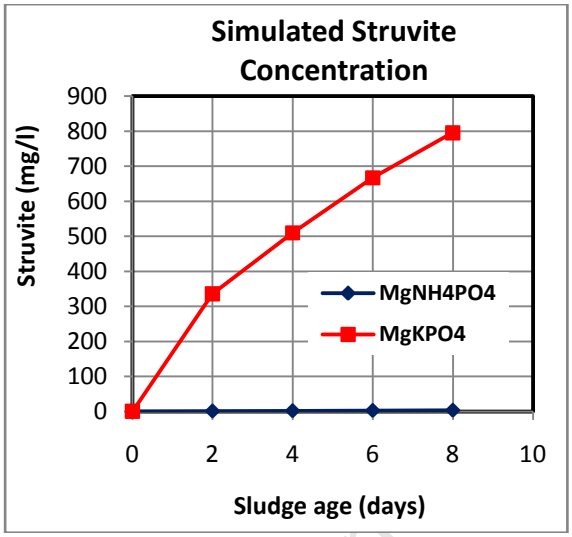

(h)

Figures 7.6.5 g and h: *Results simulated by the ASM2-3P dynamic model per sludge age (R_s) for the batch seven AerD system of Mebrahtu et al. (2007) in the order of: (g) magnesium concentration and (h) struvite concentration.*

As is noticeable in Figure 7.6.5 the simulated and measured results are fairly similar. The similarities between the measured and simulated TP (about 900mgP/*l*) and ISS, together with the small difference between the results (mainly OP, ISS and Mg) simulated with and without precipitation indicates that the phosphorus precipitation was low.

Aerobic Digester: Comparison of Model Simulations to Vogts (2011) Data

To observe the effect of intermittent aeration and P precipitation on N and P removal in anoxic-aerobic digestion of P rich WAS, Vogts (2011) set up two anoxic-aerobic digesters, one fed concentrated NDBEPR WAS (20g/ℓ), the other fed dilute NDBEPR WAS (3g/*l*). Both were fed WAS from the same NDBEPR UCT AS system, from which the feed for the ADs of this investigation was taken. The two systems were operated with the same intermittent aeration cycle (3h aeration on, 3h aeration off).

The two digesters were operated at a 20d sludge age over four experimental time periods spanning about two years. In the first period, both digesters were operated at steady state for about 6 months, without pH control. In period two, which also lasted about 6 months, the pH was controlled by the addition of sodium bicarbonate. In period three, the pH was controlled by dosing magnesium hydroxide ($Mg(OH)_2$) to observe the increase in precipitation of phosphate. However, the $Mg(OH)_2$ dose to the anoxic- aerobic digester fed dilute WAS (at 3g/*l*) was soon stopped since no precipitation was observed in it, so only NaOH was added to maintain its pH. In period four, the dilute anoxic- aerobic digester was turned fully aerobic (no longer on the intermittent aeration cycle) and for the concentrated (fed 20g/*l* of WAS) digester, the $Mg(OH)_2$ dose was changed to $Ca(OH)_2$. Through all pH-controlled periods, Vogts (2011) maintained the pH of both digesters to between 7.3 and 7.5. For ease of operation the continuous digesters were fed batch-wise once daily.

The ASM2-3P model was applied to simulate the UCT NDBEPR system linked to the continuous anoxic-aerobic digester and the model results were compared with the average experimental results (shown in the Figures 7.6.6i and ii and corresponding Tables 7.6.3). While the experimental systems were batch-fed, the simulated systems were continuously fed.

The Table 7.6.2 shows the list of parameters, and their values, that were used for the simulation of the anoxic- aerobic digester. The parent NDBEPR AS system had the same parameters, apart from the precipitation constants ($k'r_{ACP}$, $k'r_{MgKP}$ and $k'r_{Struv}$) that were reduced to 0.001 to avoid precipitation in the AS system and the anaerobic fermentation rate (q_fe), for the production of acetate, increased from 3 to 20 to simulate PAO growth.

Table 7.6.2: Parameters used in Simulating Anoxic-Aerobic Digestion (AnAerD) with the Three phase ASM2 Model			
Parameter	**Value**	**Units**	**Description**
A_bp	0.13	dUnit/dUnit	N/C: biodegradable particulate
A_bps	0.039	dUnit/dUnit	N/C: PS biodegradable particulate
A_e	0.135	dUnit/dUnit	N/C: endogenous residue
A_f	0.057026	dUnit/dUnit	N/C: fermentable soluble
A_o	0.135	dUnit/dUnit	N/C : organisms
A_up	0.166667	dUnit/dUnit	N/C: unbiodegradable particulate
A_us	0.061887	dUnit/dUnit	N/C: unbiodegradable soluble
b_{AUT}	0.15	1/d	Decay rate
B_bp	0.026042	dUnit/dUnit	P/C: biodegradable particulate
B_bps	0.02	dUnit/dUnit	P/C: PS biodegradable particulate
B_e	0.026042	dUnit/dUnit	P/C: endogenous residue
B_f	0.007502	dUnit/dUnit	P/C: fermentable soluble
b_H	0.62	1/d	Rate constant for lysis and decay
B_o	0.026042	dUnit/dUnit	P/C : organisms
b_G	0.04	1/d	Rate constant for lysis of PAO
b_PHA	0.04	1/d	Rate constant for lysis of PHA
b_PP	0.025	1/d	Rate constant for lysis of PP
B_up	0.026042	dUnit/dUnit	P/C: unbiodegradable particulate
B_us	0.008221	dUnit/dUnit	P/C: unbiodegradable soluble
e_PP	0.09	dUnit/dUnit	Ca/P: Polyphosphate
F_BOD_COD	0.65	gBOD/gCOD	Conversion factor BOD/COD
f_X_IH	0.08	gCOD/gCOD	Fraction of inert COD generated in X_oHO lysis
f_X_IP	0.25	gCOD/gCOD	Fraction of inert COD generated in PAO lysis
ISS_BM	0.15	g/gCOD	ISS to biomass for OHO and PAO
$k'r_{ACP}$	0.001	/d	Precipitation of calcium phosphate
$k'r_{MgKP}$	0.001	/d	Precipitation of K-struvite
$k'r_{Struv}$	0.001	/d	Precipitation of struvite
K_A	4	-	saturation coeff for Ac (acetate)
K_ALK	0.1	-	saturation coeff for alkalinity (HCO3-)
K_ALK_AUT	0.5	-	saturation coeff of autotrophs for alkalinity
k_CO2	0.1	-	Rate constant for CO2 exchange
K_F	4	-	saturation/inhibtion coeff for growth on FBSO
K_fe	1	-	saturation coeff for fermentation on FBSO
k_h	3	gCOD/(gCOD*d)	Hydrolysis rate constant
K_IPP	0.02	-	Inhibition coeff for PP storage
K_MAX	1.05	-	Maximum ratio of PP/PAO
K_NH	0.05	-	saturation coeff for ammonium (nutrient)

Table 7.6.2: Parameters used in Simulating AnAerD with the Three phase ASM2 Model			
Parameter	**Value**	**Units**	**Description**
K_NH_AUT	1	-	saturation coeff of autotrophs for ammonium
K_NO	0.5	-	saturation/inhibition coeff fir nitrate
K_O	0.2	-	saturation/inhibition coeff for oxygen
K_O_AUT	0.5	-	saturation/inhibition coeff of autotrophs for oxygen
K_P	0.01	-	saturation coeff for phosphorus (nutrient)
K_pa	0.38	1/d	Decay rate constant for PAO
K_PHA	0.01	-	saturation coeff for PHA
d_PP	0.09	Unit/Unit	K/P:Polyphosphate
K_PP	0.01	-	saturation coeff for poly-phosphate
K_{PS}	0.2	-	saturation coeff for phosphorus in PP storage
K_X	0.1	-	saturation coeff for particulate COD
c_PP	0.37	Unit/Unit	Mg/P:Polyphosphate
mu_AUT	0.8	1/d	Maximum growth rate
mu_H	6	1/d	Maximum growth rate on substrate
mu_PAO	1	1/d	Maximum growth rate
n_fe	0.1	-	Anaerobic hydrolysis reduction factor
n_NO_Het	0.6	-	Reduction factor for denitrification
n_NO_Hyd	0.6	-	Anoxic hydrolysis reduction factor
P_{CO2_AS}	0.3	-	Partial pressure of CO_2 in the AS liquor
q_fe	20	1/d	Maximum rate for fermentation
q_PHA	3	1/d	Rate constant for storage of PHA (base: PP)
q_PP	1.5	1/d	Rate constant for storage of PP
S_O_Sat	8.9	g/m3	Oxygen saturation concentration
TempCoeff	0.0667	-	Rate temperature coefficient
Temperature	20	°C	System Temperature
Y_{AUT}	0.24	gCOD/gN	Yield For Autotrophic Biomass
Y_bp	1.458333	dUnit/dUnit	H/C: biodegradable particulate
Y_bps	1.990487	dUnit/dUnit	H/C: PS biodegradable particulate
Y_e	1.458333	dUnit/dUnit	H/C: endogenous residue
Y_f	1.567209	dUnit/dUnit	H/C : fermentable soluble
Y_H	0.67	gCOD/gCOD	Yield For Heterotrophic Biomass
Y_o	1.458333	dUnit/dUnit	H/C : organisms
Y_G	0.67	-	Yield coeff (biomass/PHA)
Y_PHA	0.2	-	PHA requirement for PP storage
Y_PO	0.4	-	PP requirement (S_PO4 release) per PHA stored
Y_up	1.458333	dUnit/dUnit	H/C: unbiodegradable particulate
Y_us	1.546307	dUnit/dUnit	H/C: unbiodegradable soluble

Table 7.6.2: Parameters used in Simulating AnAerD with the Three phase ASM2 Model			
Parameter	**Value**	**Units**	**Description**
Z_bp	0.416667	dUnit/dUnit	O/C: biodegradable particulate
Z_bps	0.561719	dUnit/dUnit	O/C: PS biodegradable particulate
Z_e	0.416667	dUnit/dUnit	O/C: endogenous residue
Z_f	0.587288	dUnit/dUnit	O/C : fermentable soluble
Z_o	0.4166667	dUnit/dUnit	O/C : organisms
Z_up	0.416667	dUnit/dUnit	O/C: unbiodegradable particulate
Z_us	0.543126	dUnit/dUnit	O/C: unbiodegradable soluble

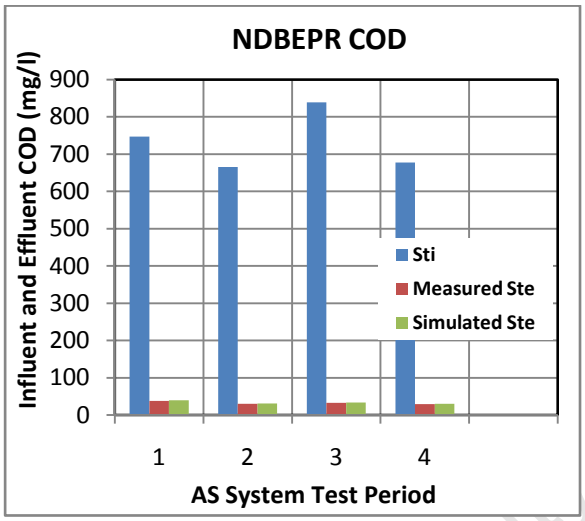

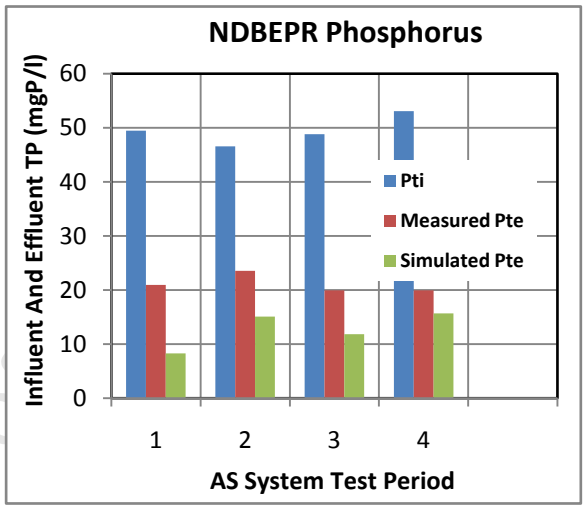

(a) **(b)**

Figures 7.6.6 (i) a and b: *A comparison between the results simulated by the ASM2-3P dynamic model and measured data per sludge age (R_s) for the NDBEPR AS parent system to Vogts (2011) anoxic-aerobic digetster in the order of: (a) COD concentration and (b) Phosphorus removal.*

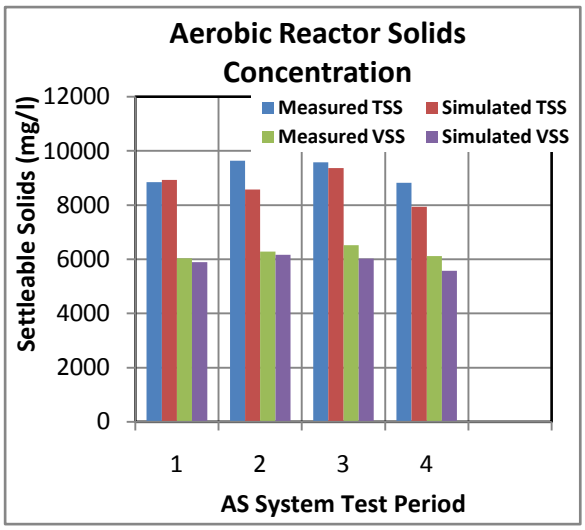

(c)

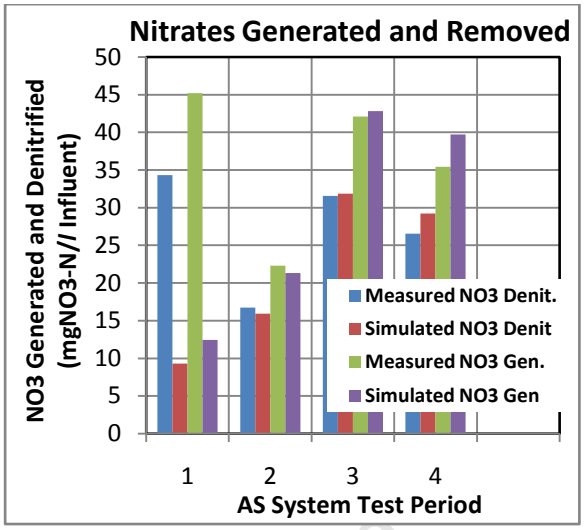

(d)

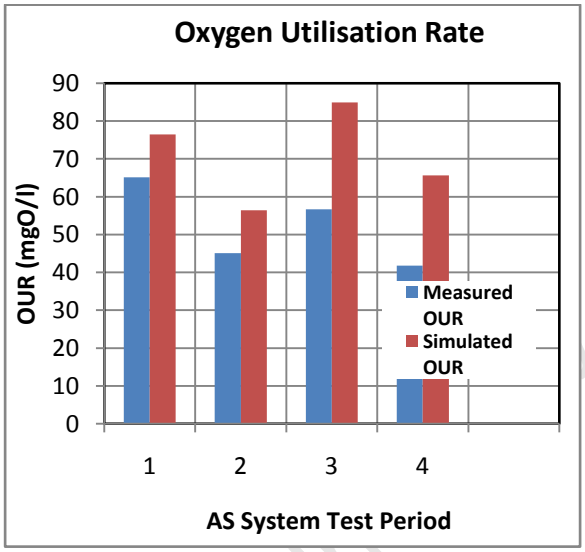

(e)

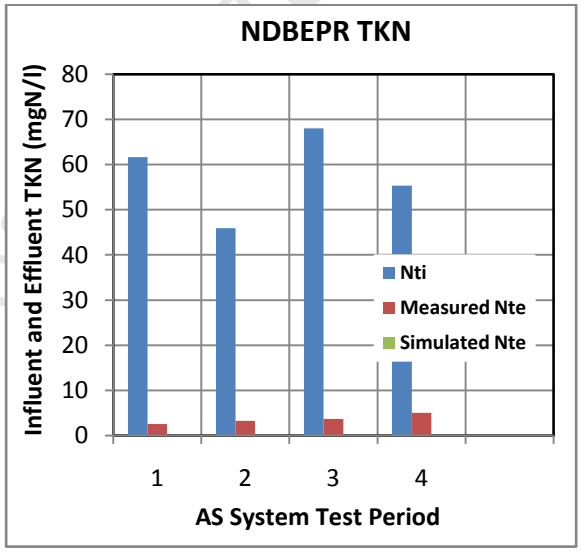

(f)

Figures 7.6.6 (i) c to f: *A comparison between the results simulated by the ASM2-3P dynamic model and measured data per test period for the NDBEPR AS parent system to Vogts (2011) anoxic-aerobic digetster in the order of: (c) Total and volatile solids concentrations, (d) nitrates generated and removed (e) Oxygen utilization rates and (f) Nitrogen removed.*

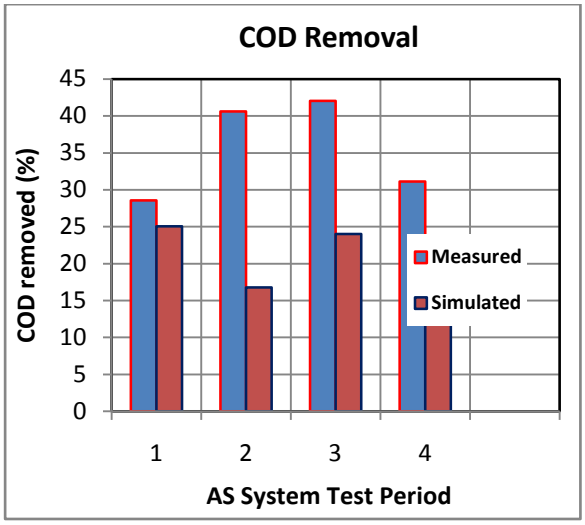

(a)

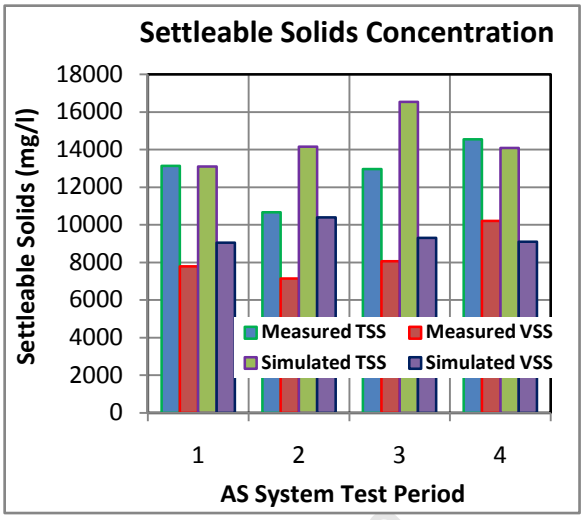

(b)

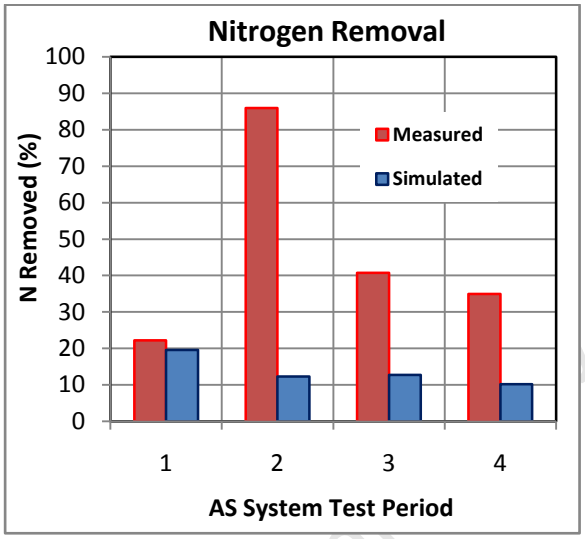

(c)

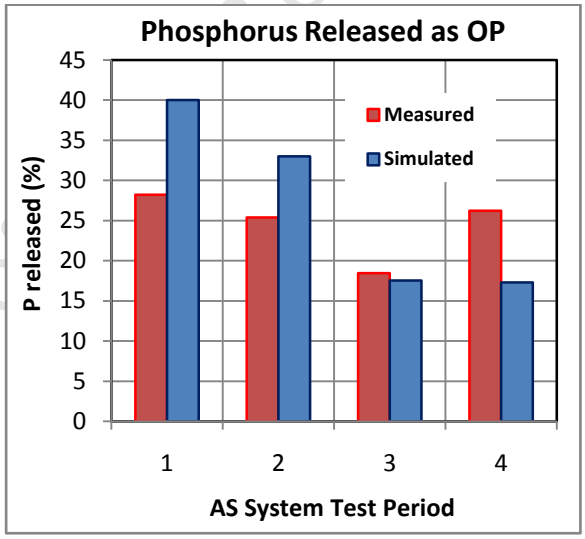

(d)

Figures 7.6.6 (ii) a to d: *A comparison between the results simulated by the ASM2-3P dynamic model and measured data per test period for the concentrated anoxic-aerobic digester of Vogts (2011) in the order of: (a) COD concentration, (b) Total and volatile solids concentrations (c) Nitrogen removal and (d) Phosphorus releases.*

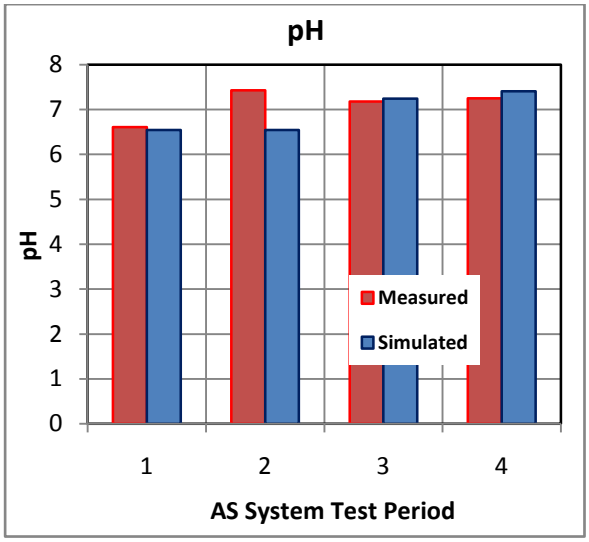

(e)

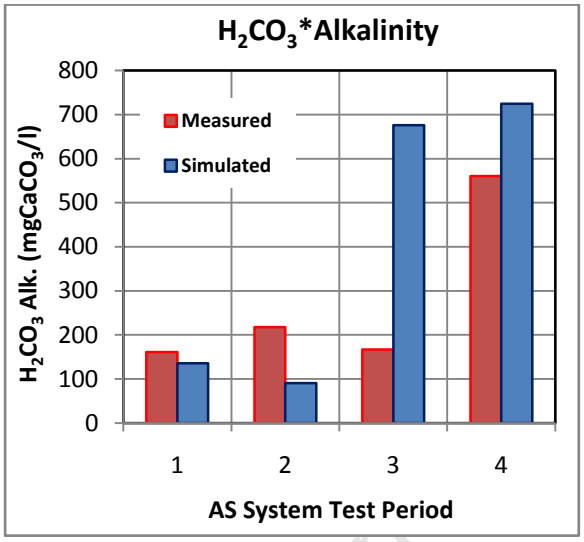

(f)

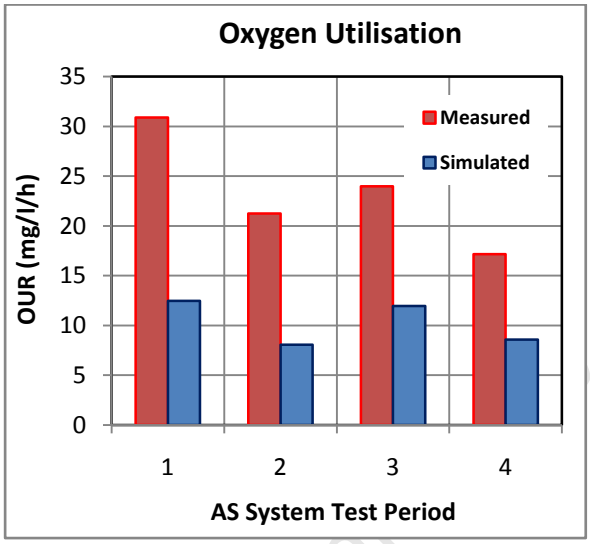

(g)

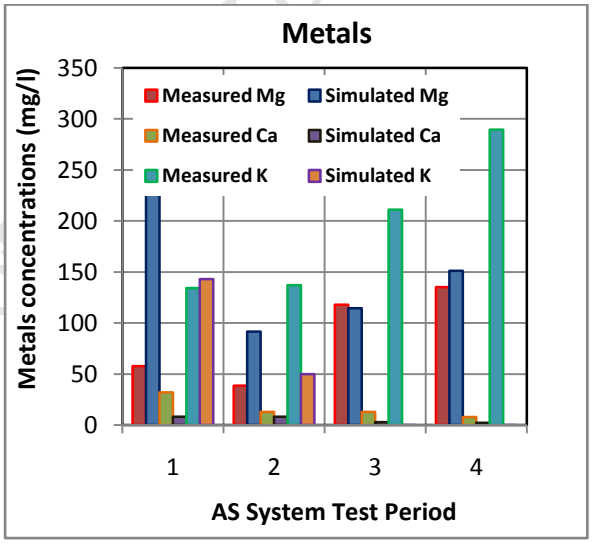

(h)

Figures 7.6.6 (ii) e to h: *A comparison between the results simulated by the ASM2-3P dynamic model and measured data per test period for the concentrated anoxic-aerobic digester of Vogts (2011) in the order of: (e) pH, (f) H_2CO_3* alkalinity, (g) Oxygen utilization rates and (h) metals measured in solution.*

Table 7.6.2a: Summary of Measured and Simulated Results for NDBEPR AS System, Parent to Anoxic- Aerobic Digester									
Experimental Testing Period		1		2		3		3	
Sewage Batch Number		3		11		13		15	
Parameter		Measd.	Sim	Measd.	Sim	Measd.	Sim	Measd.	Sim
Influent	COD (mgCOD/*l*)	746.99	746.99	665.82	665.82	839.42	839.42	677.86	677.86
	TKN (mgN/*l*)	61.64	61.64	45.89	45.89	68.04	68.04	55.32	55.32
	FSA (mgN/*l*)	23.35	23.35	30.14	30.14	50.84	50.84	42.37	42.37
	TP (mgP/*l*)	49.45	49.45	46.59	46.59	48.83	48.83	53.10	53.10
	OP (mgP/*l*)	47.29	47.29	45.56	45.56	46.61	46.61	46.61	46.61
Anaerobic Tank	TSS (mg/*l*)	3294.80	4305.38	3404.50	4199.55	4005.82	4555.95	5525.56	3861.20
	VSS (mg/*l*)	2557.80	3034.22	2694.00	3211.18	3003.64	3114.95	3835.78	2907.84
	Nitrates (mgN/*l*)	0.08	0.00	0.00	0.00	0.00	0.00	0.00	0.00
	OP (mgP/*l*)	110.60	108.79	77.34	101.02	69.61	110.19	69.61	104.27
Anoxic Tank	TSS (mg/*l*)	6545.80	7060.55	5893.00	6818.72	7091.09	7441.57	7288.44	6304.92
	VSS (mg/*l*)	4795.60	4747.36	4126.50	4985.69	5137.09	4862.49	5085.56	4517.52
	Nitrates (mgN/*l*)	0.62	0.00	0.00	0.06	0.00	0.26	0.00	0.55
	OP (mgP/*l*)	80.05	54.44	55.36	51.73	60.45	53.77	60.45	53.72
Aerobic Tank	COD (mgCOD/*l*)	7903.59	9193.70	8301.33	9353.21	8121.19	9273.67	8702.32	8500.76
	Filtered COD (mgCOD/*l*)	37.98	39.50	30.03	31.24	32.53	33.84	28.81	29.96
	TKN (mgN/*l*)	426.49	509.53	535.15	556.36	598.15	519.95	577.11	494.19
	FSA (mgN/*l*)	2.17	0.11	2.86	0.66	3.03	0.63	4.19	0.65
	TP (mgP/*l*)	629.54	1021.81	727.80	876.50	930.89	943.96	822.51	836.35
	OP (mgP/*l*)	20.93	8.27	23.52	15.07	19.93	11.81	19.93	15.67
	TSS (mg/*l*)	8841.20	8934.32	9641.00	8571.10	9576.00	9369.11	8818.00	7937.26
	VSS (mg/*l*)	6034.20	5894.77	6284.50	6163.19	6515.80	6018.04	6117.33	5580.68
	Nitrates (mgN/*l*)	10.89	3.11	5.58	5.39	10.53	10.97	8.85	10.48
	VFA (mgCOD/*l*)	0.00	0.01	0.00	0.00	0.00	0.00	0.00	0.01
	Alkalinity (mg/*l* as $CaCO_3$)	175.17	216.76	200.00	134.61	230.00	263.32	-	258.17
	pH	7.43	7.76	7.47	7.60	7.92	7.78	-	7.92
	OHO Biomass (mgCOD/*l*)	1455.94	2036.29	960.73	1215.38	1748.65	2047.98	892.96	1356.57
	PAO Biomass (mgCOD/*l*)	2894.88	3640.28	2871.86	3013.31	3157.54	3367.67	3730.67	2945.84
	Polyphosphate (mgP/*l*)	460.06	758.27	455.00	607.90	605.17	679.25	634.50	589.11
	Endogenous Residue (mgCOD/*l*)	956.77	1385.13	669.40	908.92	1169.70	1383.84	864.53	976.91
	Unbiodegradable Particulate COD (mgCOD/*l*)	2596.00	1797.74	3799.33	4023.59	2045.31	2175.09	3214.16	3009.53
	Mg (mg/*l*)	263.50	324.45	270.42	269.76	356.25	294.35	278.93	274.42
	K (mg/*l*)	126.11	103.54	148.89	93.43	121.25	101.10	111.72	89.67
	Ca (mg/*l*)	166.13	189.84	200.78	182.25	241.48	198.04	184.11	154.40
	Filtered Mg (mg/*l*)	9.80	91.29	10.12	82.83	11.95	85.49	11.73	93.27
	Filtered K (mg/*l*)	73.33	95.92	92.43	106.95	91.12	113.90	85.93	81.43
	Filtered Ca (mg/*l*)	14.24	11.76	15.99	19.78	17.86	18.84	23.00	18.30

Table 7.6.2aii: Mass balance Results for NDBEPR AS System, Parent to Anoxic- Aerobic Digester								
COD balance (%)	68.94	101.34	81.85	98.84	66.74	98.81	76.43	96.78
Nitrogen balance (%)	114.43	99.97	87.4	98.04	88.57	98.45	98.31	97.85
Phosphorous balance (%)	99.07	97.89	64.81	98.41	72.75	99.1	87.76	101.22
Mg balance (%)	58.73	99.96	75.1	100.15	93.76	100.04	107.64	99.88
K balance (%)	98.33	100.6	119.96	100.71	131.76	100.68	109.39	100.5
Ca balance (%)	80.18	97.97	40.95	99.38	51.44	99.09	99.94	98.65

Table 7.6.2b: Summary of Measured and Simulated Results for Anoxic - Aerobic Digester									
Experimental Testing Period		1		2		3		3	
Sewage Batch Number		3		11		13		15	
Anoxic-Aerobic Tank	COD (mgCOD/*l*)	11264.16	13754.02	9838.10	15541.68	9394.28	14064.22	11969.84	13680.27
	Filtered COD (mgCOD/*l*)	37.98	39.47	30.03	31.11	32.53	33.70	28.81	29.85
	TKN (mgN/*l*)	661.20	819.68	692.13	975.96	706.44	907.59	747.36	888.11
	FSA (mgN/*l*)	5.30	0.15	2.57	0.08	3.63	0.03	5.83	0.02
	TP (mgP/*l*)	1329.58	2013.31	1330.35	1710.51	1591.64	1852.94	1597.80	1635.95
	OP (mgP/*l*)	264.54	814.12	258.26	579.79	275.73	336.49	413.01	298.97
	TSS (mg/*l*)	13133.00	13108.55	10671.50	14161.71	12969.48	16536.96	14544.25	14086.17
	VSS (mg/*l*)	7789.84	9056.79	7142.00	10386.93	8063.73	9304.79	10200.50	9108.30
	Nitrates (mgN/*l*)	0.03	2.04	0.00	1.35	0.00	1.35	0.03	0.97
	VFA (mgCOD/*l*)	0.00	0.00	0.00	0.00	0.00	0.00	0.00	0.00
	Alkalinity (mg/*l* as $CaCO_3$)	161.20	135.81	217.57	90.87	166.70	676.20	560.40	724.40
	pH	6.61	6.55	7.43	6.54	7.18	7.25	7.25	7.41
	OHO Biomass (mgCOD/*l*)	624.11	940.76	406.55	603.48	766.24	904.11	337.96	634.03
	PAO Biomass (mgCOD/*l*)	3998.57	4521.38	3915.93	3699.65	4458.24	4223.11	4549.62	3655.33
	Polyphosphate (mgP/*l*)	635.47	689.11	620.42	554.17	854.46	780.59	773.79	704.18
	Endogenous Residue (mgCOD/*l*)	3383.63	4597.77	2381.46	3133.03	4177.59	4473.01	2594.48	3290.19
	Unbiodegradable Particulate COD (mgCOD/*l*)	5192.00	3584.86	7598.66	8013.72	4090.62	4333.61	6428.33	5995.73
	Mg (mg/*l*)	168.75	559.60	354.00	382.56	737.50	618.18	961.25	563.18
	K (mg/*l*)	302.81	283.07	204.25	257.87	371.25	283.86	336.04	228.49
	Ca (mg/*l*)	284.78	126.44	236.89	105.72	200.37	125.72	81.11	111.85
	Filtered Mg (mg/*l*)	57.55	253.56	38.55	91.60	117.80	114.36	135.28	151.04
	Filtered K (mg/*l*)	134.23	143.03	137.05	49.82	211.13	0.04	289.58	0.02
	Filtered Ca (mg/*l*)	31.93	8.17	12.78	8.17	12.95	2.75	7.78	2.27
	OUR (mgO/l/d)	30.89	12.47	21.23	8.06	23.98	11.97	17.17	8.59

Table 7.6.2aii: Mass balance Results for Anoxic- Aerobic Digester								
COD balance (%)	126.62	97.22	93.95	96.55	97.5	94.69	94.99	95.17
Nitrogen balance (%)	- [a]	101.68	- [a]	101.98	- [a]	101.76	- [a]	101.97
Phosphorous balance (%)	107.73	98.52	92.98	97.58	86.41	98.15	98.32	97.8
Mg balance (%)	32.63	100.36	66.7	99.88	105.27	101.68	176.01	101.88
K balance (%)	116.95	99.75	66.07	100.12	94.74	100.59	119.05	100.49
Ca balance (%)	119.67	97.95	84.07	97.9	89.2	98.91	40.47	98.39
a - The Nitrogen balance could not be obtained from measurements fron the reactor since the nitrogen evolved during the denitrification phase was not measured. However, N balance was assumed to be 100% to calculate the nitrogen denitrified in the anoxic phase.								

Although the simulated results for the parent NDBEPR system matched the measured results reasonably well, those of the continuous anoxic-aerobic digester simulation are not well matched to the measured data. This is mainly due to the variations in the measured COD removal and its under-prediction by the model. A possible reason for the deviation in COD removal is varied concentrations of the feed WAS from the NDBEPR system, which required thickening before being fed to the anoxic-aerobic digester. Because ammonia is released with the hydrolysis of biomass, the under-prediction of COD removal also resulted in lower predictions of released ammonia, hence a limitation in the quantity of nitrogen to be removed by the nitrification - denitrification process or used for struvite precipitation. With less COD removal, lower oxygen is used for endogenous respiration and nitrification, hence the model prediction for oxygen utilization rate in the anoxic- aerobic digester is less than that measured. The difficulties in calibrating the model for P removal in aerobic digestion arise with the uncertainty of how much particulate P is retained in PP and how much in precipitates formed. Thus it was noted that for such systems, in tertiary treatment of BEPR WAS, the analysis of P should include testing samples that are both measured directly (for correct characterization of particulate P) and diluted before measurement (to dissolve the P precipitates in the sample, for distinguishing between PP and precipitated P). For cases where very little or no nitrification is occurring, high quantities of P and acetate in the unaerated ('anoxic') zone could result in the growth PAOs in the digester, rather than the

OHO pre-domination, as would occur in the BEPR system and hence poor prediction of biomass (and PP) quantities. This meant that simulating this type of system with mixed cultures of OHO and PAO biomass, requires careful monitoring of the fermentation rate (q_fe) to control the quantity of acetate produced, hence direct PAO growth (and the consequential PP storage). The pH prediction is very close to that measured because the model is safeguarded against decline in pH that would occur due to nitrification (which occurs at a reduced rate when the pH is less than 7.2, see Section 7.4.1) and / or precipitation (which is modelled not to occur at low pH of <6.7). Also, due to low metals balances, not much confidence could be achieved on the quantity of metals to have precipitated.

Closure

The above calibration exercise has demonstrated that the ASM2-3P model can be used individually to simulate various AS and/or fully aerobic systems. In Section 7.7, this model is combined with a compatible three phase AD model (UCTAD) to develop a single larger model, for the simulation of the entire wastewater treatment plant (WWTP), based on strict material (COD, C, H, O, N, P, Mg, K and Ca) mass balance principles.

7.7 THE THREE PHASE PLANT-WIDE MODEL

Once calibrated, the ASM2-3P-ISS and ADM-3P models were combined to build a three phase plant-wide WWTP model in WEST. Therefore, since the ASM2-3P-ISS and ADM-3P models already had matching model components, the parameters and stoichiometric processes from the two models were easily combined into one Gujer matrix to form the super model. However, in the WEST experimentation environment (where the model simulations are performed), it was ensured that only the AS reaction rates were activated in the simulation of AS system components and only those of the AD were activated in simulation of the AD unit.

In this section, the plant-wide model will be applied to simulate the NDBEPR AS system linked to the AD system as was done in part of the experimental set-up of this project (shown in Figure 3.1 of Chapter 3). This configuration allows for the comparison of the results simulated by the plant-wide super model to those experimentally measured and those obtained from the models when operated individually. Thereafter, the model shall be used in a scenario analysis to investigate the effects on P removal when changing the sludge ages in the NDBEPR AS system and a linked AD system. The plant-wide model could also be applied to simulate the NDBEPR AS system with anoxic – aerobic digestion of concentrated WAS with lime dosing or source separated urine addition, but these aspects will be investigated by Vogts (2011) and Motlomelo (2011) who operated the experimental anoxic aerobic - digesters for this research.

7.7.1 Simulating NDBEPR linked to AD system

To simulate the plant-wide scenario, the same model parameters and input values of the 10 day R_s operation of the NDBEPR AS system in the experimental period number three (as shown in Tables 7.4.3) are used to define the AS system parameters and plant input values. The parameters that defined the linked AD system are as those for the 40 day R_s AD of NDBEPR WAS (shown in Table 7.5.3a). The ASM2-3P and ADM-3P were simulated under constant flow and load conditions. Because the NDBEPR TSS concentration was around 10g TSS/*l*, due to the membrane aerobic reactor solid – liquid separation, the WAS was not thickened before AD. The composition of the different influent and WAS organics is given in Table 7.7.1a. The Figure 7.7.1 shows some output graphs of this simulation for a runtime period of 250 days and the corresponding results are reported in Tables 7.7.1a and 7.7.1b below. The result after 250 days is the steady state system response behaviour.

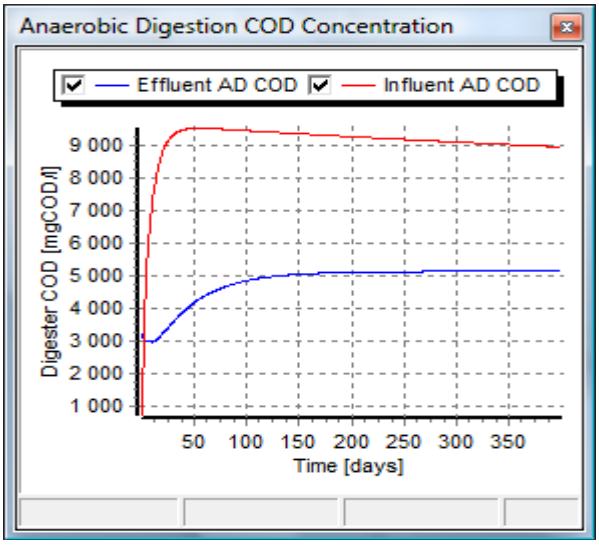

(a)

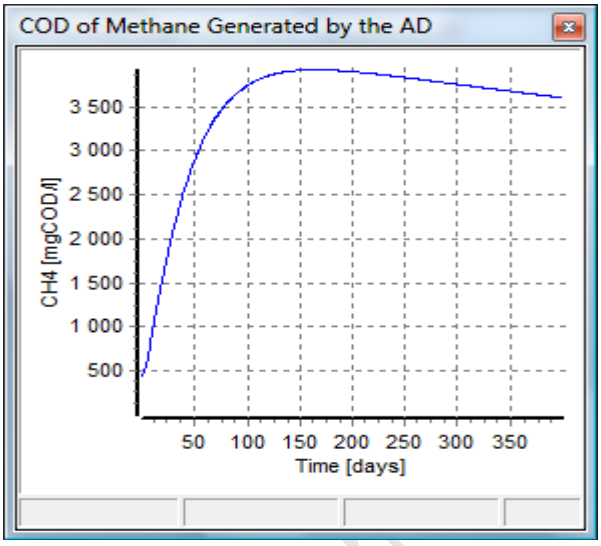

(b)

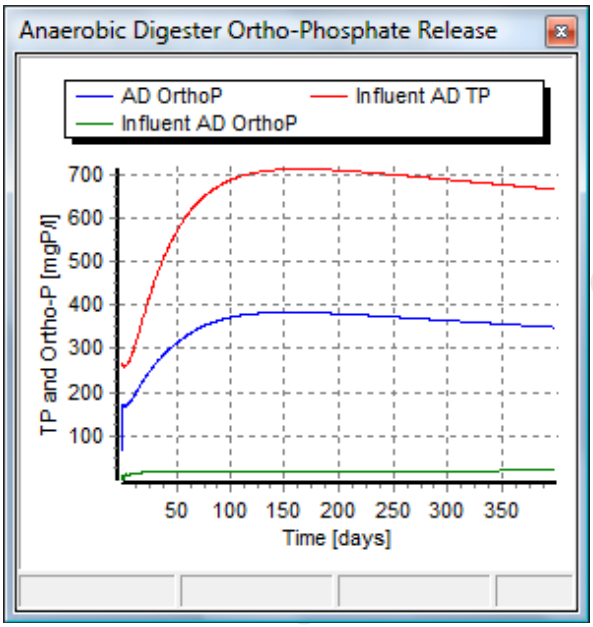

(c)

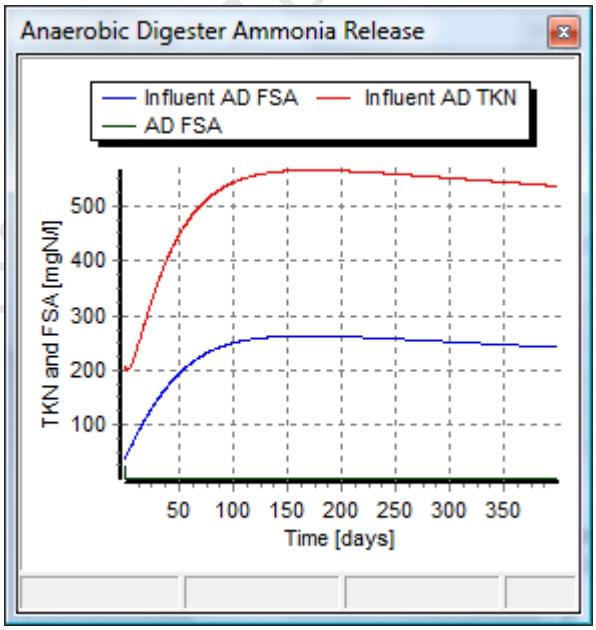

(d)

Figures 7.7.1a to d: *Results from the application of the plant-wide ASM2-3P - ADM-3P model for simulating the NDBEPR system linked to AD, showing plot windows of AD (a) unfiltered influent and effluent COD, (b) COD of methane generated, (c) effluent TP and OP and (d) effluent TKN and FSA*

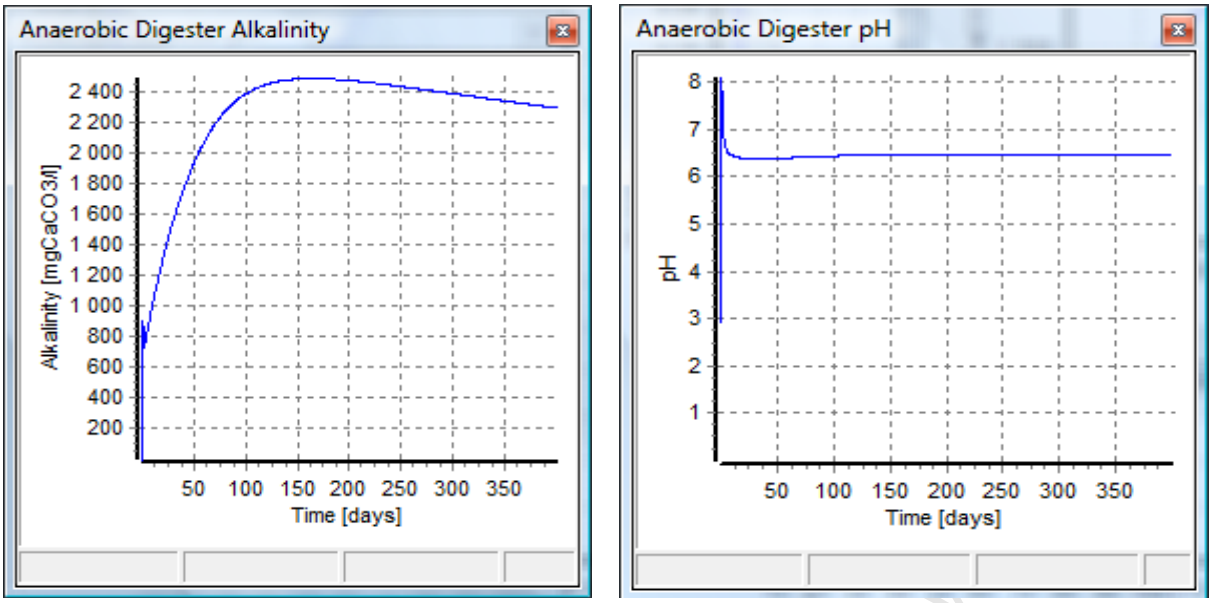

(e) **(f)**

Figure 7.7.1e and f: *Results from the application of the plant-wide ASM2-3P - ADM-3P model for simulating the NDBEPR system linked to AD, showing plot windows of (e) digester H_2CO_3* Alkalinity and (f) digester pH.*

The simulated AS system results are similar to the ones predicted by the ASM2-3P model when used in isolation (results shown in Table 7.4.3a and b, for experimental period 3) because the model input values are applied to the same AS system. However, the results for the AD system are slightly different from those predicted when the three phase AD model is used independently because the characteristics and composition of the WAS are the same as those measured and used as input to the independent AD model. This has led to some differences in some of the output results between the AD model used independently and the plant-wide model. For instance, the total alkalinity and pH predicted by the plant-wide model, although closer to the experimentally measured results, is higher than that predicted by the AD model when applied in isolation. Moreover, these simulations, run from day zero, show the periods when the system acclimatization till when the results appear more stable. This steady state period is expected to have reached after more than three steady states of the

AD system sludge age system. However, there seems to be some slight decreases in the variables of Figure 7.71 a and b. This may be due to the water produced in the AS aerobic reactor, which provides the feed to the AD directly in this simulation. The water production in the aerobic reactor of the AS system is expected but the model did not cater for the loss (as would naturally occur) of this water with evaporation processes.

Tables 7.16b and 7.16c below show the comparisons between the influent AD (simulated as WAS wasted from the aerobic reactor) and effluent AD.

Table 7.7.1a: Measured and Simulated Results for Plant-Wide AD of NDBEPR WAS			
Retention Time (d)	40		
Influent flow (*l*/d)	0.4		
	Measured	AD Model	Plant-Wide Model
Influent COD (mgCOD/*l*)	10126.7	10126.7	8941.8
Influent unbiodegradable particulate COD, Supi (mgCOD/d)	5468.4	5468.4	4095.3
Influent biodegradable particulate COD, Sbpi (mgCOD/*l*)	4643.6	4643.6	4823.3
Influent VFA, Sasi (mgCOD/*l*)	0	0	0.0
Influent TKN (mgN/*l*)	560	581.5	540.2
Influent FSA (mgN/*l*)	5	5	0.5
Influent Alkalinity (mg/*l* as $CaCO_3$)	-	350	519.3
Influent pH	-	8	7.4
Influent TP (mgP/*l*)	866	864.7	658.8
Influent OP (mgP/*l*)	16.4	18.2	20.9
Influent TSS (mg/*l*)	9494.5	9251	8357.8
Influent VSS (mg/*l*)	6990.5	6996.6	6026.4
Influent ISS (mg/*l*)	2504	2254.4	2331.4
Effluent COD, Ste (mgCOD/*l*)	6375.5	6888.6	5139.5
Effluent VFA, Sase (mgCOD/*l*)	24.7	84.7	28.6
Effluent FSA (gN/*l*)	210.7	215	241.3
Effluent OP (mgP/*l*)	469.6	486.5	349.0
Effluent Alkalinity (mg/*l* as $CaCO_3$)	932.3	1322.6	2295.0
Measured digester pH	7	6.7	6.4
COD removed (%)	80.8	81.2	78.3
Volume of CH_4 (litres)	1246.2	1.4	1418.9
Volume of CO_2 (litres)	682.5	0.5	583.8
FSA released (%)	36.7	36.1	44.6
OP released (%)	52.3	54.2	49.8
Gas composition (%CO2)	0.4	7.5	0.3
COD balance (%)	95.3	101.8	
N balance (%)	96.5	100.3	
P balance (%)	93.5	101.4	

Table7.7.1b: Metals Data for Plant-Wide AD of NDBEPR WAS			
Retention Time (d)	40		
Influent flow (*l*/d)	0.4		
	Measured	AD model	plant-wide model
Influent magnesium (g/*l*)	313.1	252.2	206.9
Filt. Influent magnesium (g/*l*)	81.8	90.3	96.3
Influent potassium (g/*l*)	447.9	448.8	268.5
Filt. Influent potassium (g/*l*)	75.4	175.7	76.4
Influent calcium (g/*l*)	52.9	52.6	39.3
Filt. Influent calcium (g/*l*)	21.8	24.7	20.6
Effluent magnesium (g/*l*)	273.2	179.2	206.6
Filt. Effluent magnesium (g/*l*)	22.6	60.9	13.8
Effluent potassium (g/*l*)	373.3	301.3	257.3
Filt. Effluent potassium (g/*l*)	362.5	239.7	256.9
Effluent calcium (g/*l*)	42.8	51.8	49.0
Filt. Effluent calcium (g/*l*)	34.1	41.6	49.0
Magnesium balance (%)	102.3	100.1	
Potassium balance (%)	84.1	99.4	
Calcium balance (%)	49.4	100.4	

7.6.2 Scenario Analysis using the ASM2-3P-ADM-3P Plant-Wide Model

This section presents a scenario analysis when simulating the NDBEPR AS system directly linked to an AD system, using the plant-wide model. The objective of this scenario analysis was to observe the extent to which the AS system R_s (that is controlled by its waste flow, which is also its link to the AD) influences the removal of phosphorus in the plant. This required the inspection of which option promoted the most polyphosphate generation in the AS system and struvite precipitation in the AD system, while promoting reasonable energy efficiency, with low oxygen utilization and more methane generation (AD COD removal). Fortunately, for the AD, the methane production is linked to the COD removal hence effluent quality. However, with the AS system COD and nutrient removal occurs at the expense of oxygen utilisation. The proposed scenario analysis was run at five different AS system Rs as shown in the Table 7.7.2 below. Assuming that the AS system is directly linked to the AD

(which was given a fixed volume of 120 litres), the variation in waste flow volume from the AS system also allowed variations in the AD system R_s for this analysis.

Table 7.7.2: Scenario Analysis for P Removal in Plant-Wide Model

	AS system (fed 150l/d wastewater *)									AD System (120-litres)		
Run no.	Waste flow (l/d)	Anae-robic (19-litres) TSS (mg/*l*)	Anoxic (21 - litres) TSS (mg/*l*)	Aerobic (35-litres) TSS (mg/*l*)	R_s (d)	O_2 used (mgO/l/h)	PP formed (mgP/*l*)	Reactor TP conc. (mgP/*l*)	P removed (mgP/d)	R_s (d)	CH_4 vol. (l/d)	Struvite ppt. (mg/*l*)
1	3	6447.09	10191.2	13158	20.19	56.3698	722.149	1015.4	3046.211	40	746.849	2469.39
2	6	4139.22	6485.18	8072.1	10.27	53.7872	444.847	641.179	3847.073	20	349.652	1647.61
3	9	3117.81	4834.32	6004.21	6.864	50.5892	335.178	488.46	4396.138	13.3	185.217	1064.53
4	12	2542.33	3971.91	4952.32	5.133	46.65	293.062	420.617	5047.41	10	106.365	738.458
5	15	2153.3	3322.74	4131.93	4.119	45.0961	239.262	348.676	5230.137	8	64.9764	485.428

* To simulate the plant-wide scenario, the same model parameters and input values of the 10 day R_s operation of the NDBEPR AS system in the experimental period number three (as shown in Tables 7.4.3) areused to define the AS system parameters and plant input values

As expected the polyphosphate and settleable solids concentration in the AS system are highest at the longest AS sludge age (run no. 1). However, the flux of P removed (3046.2mgP/day) from the AS system is lowest with this option, and highest when the AS system R_s is lowest (5230.1mgP/*l*). This is because endogenous respiration loss of PAOs is least at the shortest AS R_s, hence the fraction of PAO biomass which contains the polyphosphate in the sludge concentration is highest. Moreover, despite the sludge wasted to maintain this low R_s having a lower solids concentration, its higher flow rate contributed significantly to more mass of P wasted (P removed/d). The reduced endogenous respiration also promotes less oxygen utilization in this system. The highest struvite concentration in the AD was predicted at the highest AD sludge age (40 d). This is because the longer the AD sludge age, the more the sludge is hydrolysed, hence the more the ammonia and P is released, which promotes increased struvite precipitation (as long as there is still sufficient Mg and P available, and the system T.Alk and pH are high enough). The 20-day AD

simulation exhibited the highest flux of P removed by struvite precipitation in the system (higher than the 40d one, due to higher effluent flow). Despite this, the 40d R_s AD would still be preferable, because of the significantly higher COD removal, exhibited by the high methane volume generated. A low AD sludge age is not desirable in this plant configuration because high concentrations of biodegradable WAS feed are required to generate a sufficiently high H_2CO_3* alkalinity concentration, since some of this alkalinity is lost with the high PP release and struvite precipitation. The best option requires a compromise between the AS and AD system sludge ages to achieve optimum P removal, and good overall effluent quality, with the best efficiency in energy use. Thickening of the WAS with dissolved air flotation (to avoid anaerobic P release) will facilitate finding such an optimum.

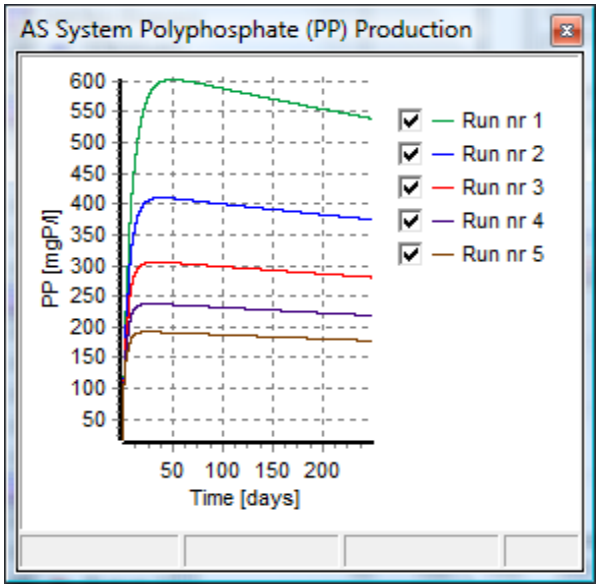

(a)

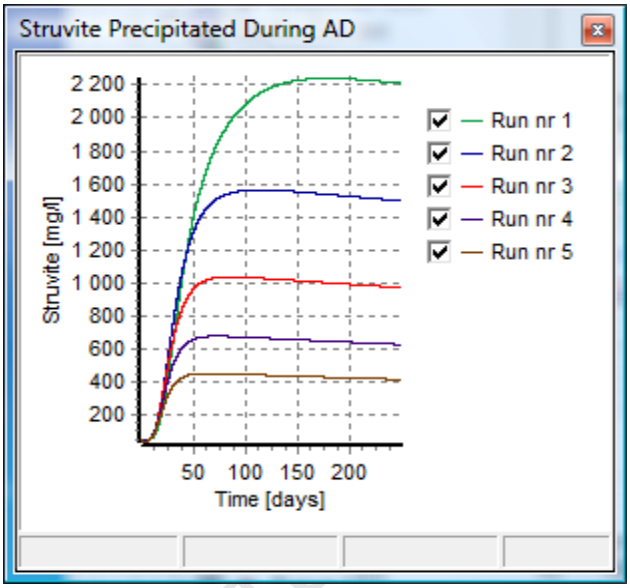

(b)

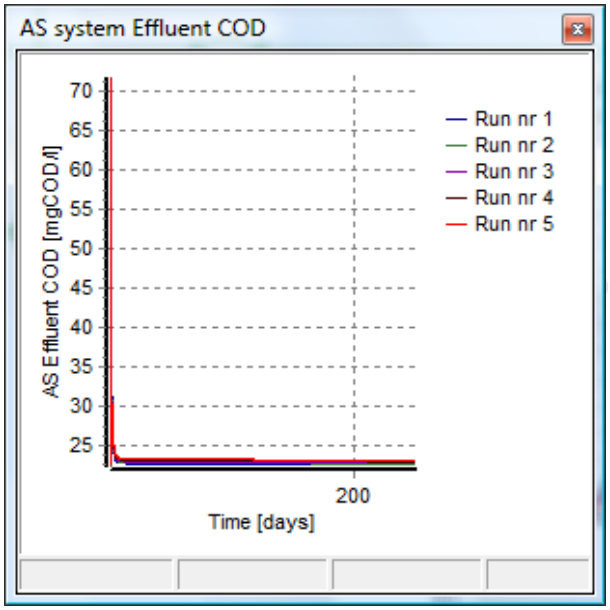

(c)

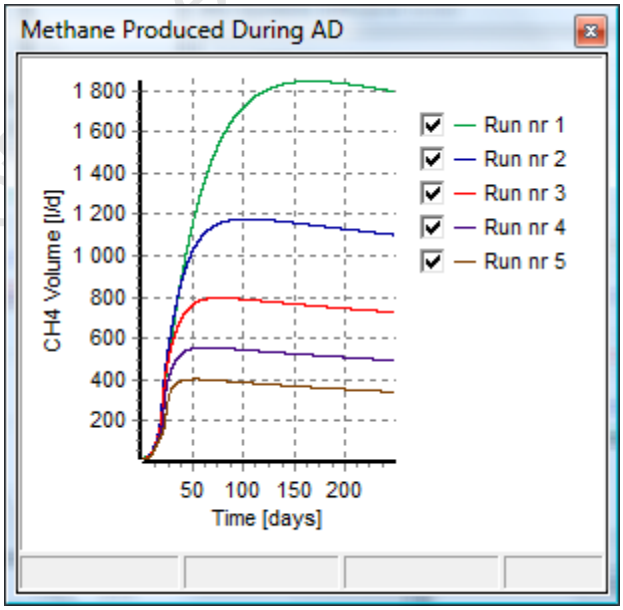

(d)

Figures 7.7.2 a to d: *Results from the application of the plant-wide model in simulating the NDBEPR system linked to AD, showing scenario analysi plot windows of AD (a) Polyphosphate production in AS system, (b) struvite precipitated in AD, (c) AS efluent COD and (d) methane generated in AD.*

7.8 CLOSURE

In this chapter the development of a three phase model including P that can be used in simulation of AS, AerD and AD systems linked in a plant-wide configuration was presented. This model was developed in the simulation program WEST®. In summary, the following steps were taken to develop this model:

- The selection of a general set of components that will be common to all biological and chemical processes occurring in all the modeled unit processes of the WWTP (i.e. AS, AnAerD and AD). All components were to be entered into the model in mass concentrations (all component units in mg/l) and additional provisions were made to parameterize the components of their elemental formulation (i.e. for organic materials this is the X, Y, Z, A and B values in $C_XH_YO_ZN_AP_B$). These provisions allowed for the direct calculation of the components COD, molar concentrations and compositions. Hence, it was possible to calculate certain output variables such as COD, N and P characteristics, and total molalities of components.
- The incorporation of an ionic speciation routine, which is a model coded in C++, containing algebraic equations for the instantaneous ionic dissociation and ion pairing equilibrium reactions, and was linked to form part of the ASM2-3P and ADM-3P models in WEST®. This ionic speciation routine was prepared by (Brouckaert *et al.*, 2010a) and provides a general algebraic approach to modelling the very rapid ionic dissociation and ion pairing equilibrium reactions separately from the slower biological and physical processes, hence can be applied to any combination of mixed weak acid/base systems. Because the weak acid/base chemistry processes for precipitation and gas exchange are slow, they are included with the slow bioprocesses, which are modelled with kinetic equations. This algebraic-based ionic equilibrium was ready to be integrated with the AD and AS developed in this project once knowledge was obtained for the interaction between biologically mediated unit processes and weak acid/base species. The Ionic speciation involved the determination of each of the species

concentrations within weak acid/base subsystems existing in a solution, through the disaggregation of total ionic concentrations. The solutions for this ionic speciation were to be solved at each time interval of the kinetic simulation, since some of the model reaction processes depended on concentration of the speciated rather than total solution component concentrations.

- Modification of the Activated Sludge Model No. 2 (ASM2) from IWA Task Group (Henze *et al.*, 1995) by including the inorganic settleable solids (ISS) model of Ekama and Wentzel (2004), together with an algorithmic mixed weak acid/base chemistry model of Brouckaert *et al.* (2010). This ASM2 model also required further extensions to be compatible with the ADM3P model, for the construction of a plant-wide model. This involved the inclusion of the above-mentioned universally selected components and the conversion of the model process stoichiometry of ASM2 from COD-based to mass-based. Consequently, the kinetic and stoichiometric constants for the COD-based ASM2 model were assessed and transformed to ensure their compatibility with the revised model components and stoichiometric process coefficients. Also added to the ASM2 model, is the process of CO_2 stripping from the aerated reactor together with processes that cater for mineral ($MgNH_4PO_4$, $MgKPO_4$ and $Ca_3(PO_4)_2$) precipitation and dissolution processes (see Equations 7.02 to 7.04) that could take place during the aerobic or anoxic-aerobic digestion of NDBEPR WAS. For the aerobic CO_2 striping process, the CO_2 is continuously generated with aeration, hence no equilibrium is achieved between the aqueous ($H_2CO_3^*$) and gas phase CO_2 (Sötemann *et al.*, 2005).
- Once developed, this ASM2-3P model was calibrated against the AS (NDBEPR UCT and MLE) systems, that were operated in the experimental investigation of this project (see Section 3.1. and 3.2 of Chapter 3) as parent systems to the ADs that digested their WAS, a batch aerobic digester (which was operated and tested by Mebrahtu *et al.* (2007)) and a NDBEPR UCT AS system linked to an AnAerD system (operated and

tested by Vogts (2011)). The MLE system results of ASM-3P were also compared with simulation results obtained from ASM1 to ensure that the similar results are obtained. This calibration exercise generally involved matching the model results to variables measured from the appropriate systems.

- Developing the ADM-3P model by modifying the UCTADM1 (Sötemann *et al.*, 2005) model through addition of compounds, rate parameters constants and stoichiometry for the AD of P-rich BEPR WAS and PS-WAS blends, together with the inclusion of the algorithmic mixed weak acid/base chemistry model (Brouckaert *et al.*, 2010). The main extensions in the new ADM-3P model include:
  1. Additional soluble and particulate biodegradable organic components to represent material that might be combined from different sources in the WWTP and feed to the anaerobic digester.
  2. New process reactions for (i) the release of PP with the uptake of acetate by PAOs while they are still alive (see Equation 7.24), (ii) release of P from PP on the death of PAOs (see Equation 7.25), (iii) the release of poly-hydroxy-alkanoate (PHA) on the death of PAOs (see Equation 7.26) and (iv) mineral precipitation processes (see next point, below).
  3. The AD model considers three phases (liquid, gas and solid) and so can simulate active gas exchange through liquid to gaseous phase evolution and multiple mineral precipitation from liquid to solid or dissolution from solid into liquid phase. The solids most likely to precipitate in AD, for inclusion in this model were the ones identified by Musvoto *et al.* (2000c) as struvite ($MgNH_4PO_4$ and/or $MgKPO_4.6H_2O$ (K-struvite)), newberyite ($MgHPO_4$), amorphous calcium phosphate ($Ca(PO_4)_2$), calcite ($CaCO_3$) and magnesite ($MgCO_3$) (see Equations 7.02 to 7.06 for the precipitation process reaction equations).
  4. Parameterised stoichiometry for the bioprocesses so the various organics compositions are entered as X, Y, Z, A and B values.

5. Pre-processor and post-processor routines which transform measured influent parameters such as FSA, OP, H_2CO_3 Alk., VFA, pH and TDS to model components and correct equilibrium, Henry's law and solubility products for ionic strength and can form model components back to predicted 'measured' concentrations for comparison with the actual measured concentrations.

- This AD model also required calibration by matching simulation predictions to experimental results of the AD systems operated in this investigation, at selected steady state periods. The ADM-3P model was calibrated against the ADs fed MLE 1 WAS, MLE 2 WAS and NDBEPR WAS (including batch AD - to ensure that the P release was well matched), primary sludge (PS) and PS-WAS blends of the experimental set up. The ADM-3P predictions were also compared with the predictions of the 2-phase UCTADM1 model of Sötemann *et al.* (2005) and the PS AD results of Izzett *et al.* (1992), whose results were used to validate the UCTADM1 model.
- Combining the ASM2-3P and ADM-3P models into the three phase plant-wide model. Developing this three phase plant-wide model including P for activated sludge and anoxic – aerobic or anaerobic digestion of P rich WAS accomplishes the objectives of this project. Thus after the separate validation of the ASM2-3P and ADM-3P models, the two were combined to construct a plant-wide model, which was applied to simulate the whole plant (NDBEPR AS system linked to AD or anoxic-aerobic digestion (AnAerD)).

CHAPTER 8: CONCLUSIONS

8.1 INTRODUCTION

The primary aim of this study was to develop three phase (aqueous-gas-solid) plant-wide kinetic steady state and dynamic mathematical models to simulate the anaerobic and aerobic digestion of sewage sludge including waste activated sludge (WAS) produced by Biological Excess phosphorus Removal (BEPR) plants.

In order to accomplish this research goal, the following objectives, as described in chapter 1, were identified:

1. Carry out an experimental investigation to generate the data required for both steady state and dynamic model calibration and validation.
2. Develop a steady state anaerobic digestion (AD) model that includes phosphorus (P) together with three phase (aqueous-gas-solid) mixed weak acid/ base chemistry for the prediction of mineral precipitation.
3. Develop a plant-wide dynamic model, in WEST® for simulating BEPR AS systems with three phase (aqueous-gas-solid) mixed weak acid/base chemistry and multiple organic types to simulate AD of primary sludge (PS) and P-rich WAS either separately or blended.
4. Extend the three phase AS model with BEPR to plant-wide simulation of BEPR AS with anoxic-aerobic digestion of concentrated P-rich WAS with mineral precipitation to produce a concentrated dewatering liquor with low N and P.

The operation and testing of the large experimental set-up allowed accomplishment of objective 1 and to confirm or investigate various aspects related to and useful for the development of the steady state and dynamic models to achieve objectives 2 and 3. Results from investigations by Mebrahtu *et al.* (2007) and Vogts *et al.* (2011) were used to achieve objective 4. This chapter focuses on the conclusions drawn from this experimental

investigation together with the important and interesting aspects observed in the development of the steady state and dynamic plant-wide models.

8.2 UNBIODGRADABLE PARTICULATE MATERIAL IN THE WWTP

Biodegradability defines the extent to which organics that enter unit operations of the wastewater treatment plant (WWTP) can be broken down. In the development of WWTP plant-wide models, the determination of whether or not the biodegradability of these organics remains consistent throughout all the linked upstream and downstream WWTP unit operations is very important when coupling the primary settling tank (PST), activated sludge (AS), aerobic digestion (AerD) and AD unit operations.

From the unbiodegradable particulate (UPO) COD fraction ($f_{S'up}$) of the raw and settled wastewater (WW) determined from two nitrification-denitrification (ND) Modified Ludzack Ettinger (MLE) systems (i.e. MLE 1 fed settled WW and MLE 2 fed raw WW), the unbiodegradable COD fraction of the primary sludge ($f_{PS'up}$) added to the settled WW to make the raw WW was calculated and compared with the biodegradability of the same PS when anaerobically digested. The unbiodegradable fraction of influent PS ($f_{PS'up}$) as calculated from the measured performance of two MLE systems with mass balances over the PST (Equation 5.2.5, in Chapter 5) was 0.30, which matched well with the value obtained from the AD of the PS at long (60 days) sludge age (0.31). This proves that the particulate organics in the influent wastewater as defined by the 'aerobic' AS system are also unbiodegradable in the AD. This simplifies plant–wide modelling because the influent components that are unbiodegradable remain unbiodegradable through AS and AD unit operations of the WWTP.

Although the MLE 1 and the (ND) BEPR systems were fed the same settled wastewater, the unbiodegradable particulate fraction ($f_{PS'up}$) of this settled influent wastewater calculated for the NDBEPR system is much higher (0.18) than that calculated for the MLE system (0.05).

The average unbiodegradable fraction of waste activated sludge (WAS) from MLE 1 (fed raw WW), MLE 2 (fed settled WW) and the NDBEPR systems, which include the influent UPO, the AS endogenous residue (f_{EH} = 0.2 and f_{EG} =0.25) and 8% of the OHO and PAO biomass, are 0.47, 0.62 and 0.56 respectively. These values are equal or close to unbiodegradable fractions measured in the ADs fed these WAS at the long sludge age of 60 days (0.47, 0.62, and 0.54 respectively). Therefore, the material that is unbiodegradable in the WAS is not significantly further degraded in the AD system. Interestingly, this applies to the NDBEPR WAS also, even though the influent unbiodegradable particulate organics fraction ($f_{S'up}$) was found to be significantly higher (0.18) than that of MLE 1 system ($f_{S'up}$ = 0.05) fed the same settled wastewater. This means that the much higher unbiodegradable particulate organics (UPO) fraction found for the NDBEPR system ($f_{S'up}$ = 0.18) than for the MLE 1 system ($f_{S'up}$ = 0.05) fed the same WW, is measured also in the AD system. Therefore, this high UPO fraction is real and not an artifice in the model.

The above experimental observations have thus led to the following conclusions regarding the fate of influent and AS generated (endogenous residue) unbiodegradable particulate organics in the wastewater treatment plant (WWTP):

1. The biodegradability of the influent wastewater organics remains closely consistent throughout the WWTP, i.e. the influent UPO component as established by the fully aerobic or ND AS systems remains unbiodegradable in the AD system.
2. The material that is unbiodegradable in AS systems (i.e. endogenous residue and influent UPO) also is not further degraded in the AD system, even at very long sludge ages (60d). Hence, unbiodegradable material (influent UPO and AS generated) is conserved throughout the plant, within experimental system operation error.
3. The remaining influent organic material that is biodegradable (particulate and soluble) gets transformed to active organisms (OHO) in the fully aerobic and ND AS systems, which undergoes endogenous respiration to form endogenous residue

(which becomes part of the UPO in WAS). The OHO in WAS undergo further endogenous respiration in the anoxic-aerobic digestion (AnAerD) sludge treatment. In AD, the BPO of the PS and WAS undergoes hydrolysis/acidogenesis to form acetate and hydrogen which are utilized by the AD biomass for growth. The AD end products include AD biomass, CH_4, CO_2 (dissolved HCO_3^- and gaseous CO_2), NH_4^+ and water. The extent of sludge BPO hydrolysis depends on the rate of hydrolysis of the sludge type and the length of time that the sludge spends in the AD (i.e. sludge age, R_s). The hydrolysis rates in terms of 1st order (k_h), specific 1st order (k_H), Monod (k_m, K_s) and saturation (k_M, K_S) kinetics of the PS BPO and WAS BPO were measured in this investigation. PS BPO hydrolyses faster than the WAS BPO, but the difference was not as large as expected.

4. From 3 above, the higher UPO in the NDBEPR WAS (relative to that of the MLE system fed the same settled WW) is real and not an artifice of the NDBEPR AS model compared with the ND AS model. This has been a repeated observation in the UCT research (see Ekama and Wentzel, 1999). Determining where this extra UPO may come from was beyond the scope of this investigation. Because the NDBEPR system comprises a mixed culture of ordinary heterotrophic (OHOs) and phosphorus accumulating (PAOs) organisms, there are several possibilities that may account for this higher UPO. However, the endogenous residue fraction of OHOs (f_{EH} = 0.2 in steady state models and f'_{EH} = 0.08 in dynamic models) used for modelling endogenous respiration and for determining the unbiodegradable fraction of WAS has been validated in several investigations over the past decades (Marais and Ekama, 1976; van Haandel *et al.*, 1998; Ekama *et al.*, 2006; Randani *et al.*, 2011). Accounting for the higher NDBEPR WAS UPO by changing the UPO of PAOs (f'_{EG}) distorts the f'_{EG} value far beyond a reasonable range of that observed in enhanced PAO culture BEPR systems (f_{EG} = 0.25) so this cannot be the reason for the difference.

5. The influent inorganic settleable (fixed) solids (ISS) is deemed not to take part in any reactions and is conserved through the plant as already investigated by Sötemann *et al.* (2006) and Ekama *et al.* (2006). Hence, it simply is enmeshed in the sludge mass and increases with sludge age. Moreover, as modelled by Ekama and Wentzel (2004), some influent inorganic dissolved solids (IDS) are taken up by the OHO and PAO and add to the mixed liquor (fixed) ISS concentration when VSS samples are dried. Therefore, the total reactor ISS comprises the ISS content of the OHO, PAO and ANO biomass (i.e. ISS_{BM} = 0.15 mgISS/mg biomass), the PAO stored PP (3.23 mgISS/mgP), all precipitates formed (struvite, amorphous calcium phosphate (ACP), and K-struvite ($MgKPO_4$)) and the influent ISS that is enmeshed with sludge. However, although the metals (Magnesium (Mg), potassium (K) and calcium (Ca)) and ortho-phosphate (OP) are taken up aerobically (from where the WAS is withdrawn) to make up polyphosphate (PP), and released anaerobically in the AS system, the mineral precipitation and dissolution of the influent ISS was found to be negligible in the AS systems. In contrast, significant phosphorus mineral precipitation does occur in the AD and AnAerD systems fed concentrated WAS from the NDBEPR system (~10gTSS/*l*), increasing as the P removal of the parent NDBEPR system and concentration of the feed WAS increases.
6. Because polyphosphate (PP), a high-energy compound in the PAOs, is not a cell bound part of the biomass, it is released much faster than the organically bound biomass P during anaerobic digestion. This PP release from PAOs has no direct relation to the kinetics of hydrolysis/acidogenesis of the PAO (and OHO) biomass, and so the hydrolysis kinetics of the BEPR WAS are not significantly different from that of the WAS from fully aerobic or N removal AS systems. Aside from the PP content of PAOs, the composition of the OHO and PAO BPO material, both of which requires hydrolysis in the AD, was modelled to be the same because the experimental investigation did not allow these to be differentiated.

8.3 THE STEADY STATE KINETIC MODEL

This section presents the conclusions drawn in the development of the three phase steady state AD model, including the COD based kinetics of hydrolysis, the CHONP and COD mass balanced stoichiometry and 3 phase mixed weak acid/base chemistry with the inclusion of P and PP for the digestion of P rich sludge.

8.3.1 Kinetics of Hydrolysis

The procedure described in Section 6.2.1 was applied to determine the unbiodegradable particulate COD fraction ($f_{SL'up}$) and hydrolysis kinetic rate constants in four different hydrolysis rate expressions (first order, specific first order, Monod and saturation kinetics) from the experimentally measured AD performance results – mainly influent and effluent particulate COD concentrations at 10, 18, 25, 40 and 60 days AD sludge age. This procedure was applied to the five AD systems treating WAS from the NDBEPR system (AD 1), PS (AD 2), WAS from MLE 1 (AD 3), a blend of PS and MLE 1 WAS (AD 4) and WAS from MLE 2 (AD 5). It was noted that for the kinetic rates, the most useful data is that from the short sludge age ADs while long sludge age AD data was useful to determine the unbiodegradable particulate COD fraction ($f_{SL'up}$).

1. It was found that the determined hydrolysis rate constants of the first order (k_h) and specific first order (k_H) kinetics increased approximately linearly with increase in retention time (R_s), so the slope (m) and intercept (c) of this linear k_h and k_H versus R_s relationship were determined by linear regression, i.e. the k rates can be replaced in the first order and specific first order hydrolysis equations by:

$$k_h = m_{kh} \cdot R_s + c_{kh} \text{ and } k_H = mk_{KH} \cdot R_s + c_{kH} .$$

(8.1a, 8. 1b)

The observed hydrolysis rates of the PS and WAS are listed in Table 8.1.

2. For the Monod and saturation rate equations, the residual unhydrolysed BPO COD concentration (S_{bpe}), acidogen biomass concentration (Z_{AD}, gCOD/*l*) and volumetric hydrolysis rate (r_{HYD}, gCOD/*l*.d) are calculated in the same way as for first order and specific first order kinetics for each sludge age. In fact, the S_{bpe}, Z_{AD} and r_{HYD} are independent of the hydrolysis kinetic equation. The constants (k_m, K_s, k_M and K_S) in the Monod and saturation rate equations (6.03 and 6.04) were obtained by four methods, a curve-fitting program (Curve Expert) and three different linearization methods of the rate equations with subsequent linear regression over the sludge age range. The three linearization and regression methods were Lineweaver-Burke (or Inversion), double reciprocal and Eadie-Hofstee (Lehninger, 1977) and the correlation coefficient (R^2) was calculated for each method for each of the Monod and saturation kinetic equations. For the Monod equation, for which the effluent S_{bpe} concentration is independent of the influent biodegradable COD concentration (S_{bpi}), a reference K_s (K_{s_ref}) value, relative to a reference S_{bpi} (S_{bpi_ref}) was established from which the actual K_s values were determined relative to the actual S_{bpi} concentrations to keep the % biodegradable COD removed constant at the same sludge age for changing influent COD concentration i.e.:

$$K_{s\_actual} = \left(\frac{K_{s\_ref}}{S_{bpi\_ref}} \right) \cdot S_{bpi\_actual} \qquad (8.2)$$

Where S_{bpi_actual} is the biodegradable particulate organic influent concentration that is specific to a particular AD experiment. The unbiodegradable particulate COD fractions ($f_{SL'up}$) and Monod and saturation hydrolysis kinetic rate constants of the five AD systems fed various sludge types are also listed in Table 8.1.

Table 8.1: Unbiodegradable Particulate Organic (UPO) fractions and hydrolysis kinetic determined by the different methods in the experimental investigation									
Parameter		PS Author	PS[1] Izzett	PS[2] O'Rourke	PS[3] Ristow	WAS MLE 1	WAS MLE 2	WAS NDBEPR	PS -WAS PS + MLE 1
UPO value	Hydrolysis kinetics value	0.31	0.36	0.34	0.34	0.47	0.62	0.54	0.37
	60-day AD value	0.31				0.53	0.66	0.58	0.4
	AS perform-ance value	0.3				0.47	0.62	0.53	0.36
Hydro-lysis kinetic rates	1st Order k_h								
	mk_h	0.013	0.0065	0.398	23205	0.003	0.003	0.033	0.015
	ck_h	-0.077	0.432	1.03	-221130	0.041	0.07	0.004	-0.165
	R^2	0.924	0.78	0.762	0.922	0.842	0.82	0.895	0.981
	Specific 1st order k_H								
	mk_H	0.372	0.007	0.2042	139.79	0.096	0.092	0.216	0.43
	ck_H	-0.303	0.228	-1.5004	-1332.1	0.97	1.147	0.131	-4.331
	R^2	0.852	0.78	0.874	0.922	0.974	0.98	0.872	0.956
	Monod								
	K_m	4.3	3.34	2.004	0.243	2.094	2.482	2.465	5.153
	K_s	1.523	6.76	0.355	640	0.408	0.626	0.607	1.71
	R^2	0.93	0.9	0.429		0.963	0.948	0.826	0.96
	Saturation								
	k_M	1.796	5.27	2.047	11.2	1.603	1.524	1.951	1.919
	K_S	7.962	7.98	0.263	13	5.387	4.838	9.109	7.723
	R^2	0.942	0.9	0.428		0.951	0.951	0.919	0.97

Where:

PS[1] is from Sötemann *et al.* (2005a), determined using data from Izzett *et al.* (1992).

PS[2] is from Sötemann *et al.* (2005a), determined using data from O'Rourke (1968).

PS[3] is from Ristow *et al.* (2004).

3. From Table 8.1, the measured hydrolysis rate kinetic constants selected are unique for each sludge type. However, evaluation of the measured percentage of biodegradable COD removed with sludge age for each of the sludge types show that, while PS hydrolyses faster to yield a higher % COD removal versus sludge age than WAS, there is not a significant difference between the PS and WAS hydrolysis rates. Therefore, it was evident that the AD of WAS together with primary sludge (PS) does not have a significant impact on the hydrolysis rate of WAS compared with anaerobically digesting the WAS by itself.

8.3.2 Determination of Sludge Elemental composition

In both the ASM-3P and ADM-3P models, the composition of the organics (i.e. X, Y, Z, A and B in $C_XH_YO_ZN_AP_B$) are parameterised such that the X, Y, Z, A and B values of the different organic types are required for input to the models. These values for the different organics were measured as follows. Ekama (2009) and Volke *et al.* (2006) show that the organic composition formula can also be written as $Cf_C/12H\ f_H/1O\ f_O/16N\ f_N/14P\ f_P/31$, where the f_C, f_H, f_O, f_N and f_P are the composition mass ratios i.e. gC/gVSS, gH/gVSS, gO/gVSS, gN/gVSS and gP/gVSS. Some of these mass ratios were measured in the experimental investigation at different locations in the plant-wide layout. The five composition ratios require five measurements i.e. VSS, COD, TOC, OrgN and OrgP. In this investigation, the VSS, COD, OrgN and OrgP were measured on the influent and effluent particulate organics (PO) fed to the five ADs. Also, samples were analysed for C and N content by an external laboratory. Unfortunately, these C analysis results lead to unrealistic compositions and so could not be used. Consequently, the C content of the different organics had to be accepted from previous investigations (Wentzel *et al.*, 2006).

The composition of the unbiodegradable organics of the different feed sludges to the 5 ADs (PS, raw wastewater (WW) MLE WAS, settled WW MLE (MLE 1) WAS, settled WW NDBEPR WAS and MLE 1 WAS – PS blend) were measured on the effluent of the 60d

sludge ADs fed these sludges. The composition of the BPO of these sludges was calculated by disaggregating the influent PO (BPO and measured UPO) composition on the effluent.

The results obtained for the different organic types are listed in the Table 8.2 below.

Table 8.2: Composition of the Various Organic Types of Sludge Digested									
Elemental formula	$C_XH_YO_ZN_AP_B$		$C_XH_YO_ZN_AP_B$		$C_XH_YO_ZN_AP_B$		$C_XH_YO_ZN_AP_B$		$q(Mg_cK_dCa_e)$
	Primary Sludge		MLE 1 Activated Sludge		MLE 2 Activated Sludge		NDBEPR Activated Sludge		
Parameter	BPO	UPO	OHO (BPO)	UPO and OHO ER	OHO (BPO)	UPO and OHO ER	OHO and PAO	UPO, OHO ER and PAO ER	Poly-phosphate
f_{cv} (COD/VSS)[a]	1.47	1.51	1.45	1.48	1.41	1.48	1.45	1.45	
f_C (TOC/VSS)[b]	0.46	0.52	0.52	0.52	0.52	0.52	0.52	0.52	
f_N (OrgN/VSS)[a]	0.03	0.06	0.14	0.07	0.13	0.09	0.14	0.04	
f_P (OrgP/VSS)[a]	0.01	0.05	0.04	0.03	0.04	0.03	0.04	0.02	
f_H (H/VSS)[a]	0.08	0.06	0.06	0.06	0.06	0.06	0.25	0.02	
f_O (O/VSS)[a]	0.4	0.31	0.24	0	0.26	0	0.14	0.11	
X	1	1	1	1	1	1	1	1	
Y	2.19	1.32	1.46	1.51	1.35	1.48	1.45	1.42	
Z	0.65	0.44	0.35	0.43	0.37	0.47	0.36	0.54	
A	0.06	0.1	0.23	0.15	0.21	0.11	0.23	0.06	
B	0.01	0.04	0.03	0.02	0.03	0.02	0.03	0.01	
q									0.19
c									0.31
d									0.31
e									0.04

[a] – Obtained from direct measurements on reactor mixed liquor COD (i.e. from unfiltered COD-filtered COD = COD of solids) and VSS (i.e. TSS - ISS).

[b] - The f_c value for OHO, PAO and UPO is given the value (0.515) obtained by Wentzel *et al. (2006)*. The f_c value for S_{bpi}, in PS, is obtained by multiplying the PS AD BPO (mgVSS) to the ratio of TOC removed (from CO_2, CH_4 and H_2CO_3* alkalinity change) to COD removed in the operation of the PS AD at 60 day R_s.

8.3.3 Stoichiometric Section of the Steady State Model

4. Because the BPO of PAOs hydrolyses much slower than its PP content, the stoichiometry, including P, for the AD system of the various municipal sludge types, including WAS from NDBEPR systems, comprises a combination stoichiometry of the AD influent BPO, either in PS or in WAS, with its organically bound N and P and stoichiometry for polyphosphate release. Since the hydrolysis of PP during AD causes release of Mg^{2+} (and K^{+} and Ca^{2+}) and P, which when in high concentrations cause the precipitation of struvite, the steady state AD model includes three phase (solid-liquid-gas) mixed weak acid/base chemistry. This stoichiometry and mixed weak acid/base chemistry was built up from that of Harding (2009) , which extends the two phase (aqueous-gas) steady state stoichiometric model of Sötemann *et al.* (2005a). Added to this stoichiometry for the dynamic AD model is the release of PP by PAOs, with the uptake of acetate (i.e. as would occur in the anaerobic reactor of the NDBEPR system) and multiple (mainly struvite) mineral precipitation.
5. The steady state and dynamic three phase AD model was verified by checking that material (COD, C, H, O N, P, Mg K and Ca) mass balances were obtained between the model input and outputs and was validated (described in Section 8.4 below) by checking how well it fitted the experimentally measured AD data of the 5 AD systems of this investigation.

8.4 THE DEVELOPMENT OF A DYNAMIC PLANT-WIDE THREE PHASE MODEL

6. A plant-wide three phase dynamic model was developed in the simulation program WEST®. This required the selection of a general set of components, which are common to all the biological unit operations of the WWTP (AS, AnAerD and AD). These components were entered into the model in their mass

concentrations (with units of mg/*l*) and additional provisions were made to parameterise the component descriptions (the X, Y, Z, A and B in $C_XH_YO_ZN_AP_B$) in terms of their COD, molar concentrations (molalities) and composition. Thereafter, three separate 3 phase dynamic models were prepared:

i. The aqueous equilibrium Ionic speciation model (Brouckaert *et al.*, 2010), which model includes ion-pairing components.

ii. The three phase Activated Sludge Model 2 (ASM2 – 3P) including the ionic speciation model (Brouckaert *et al.*, 2010) and the Inorganic Settleable Solids (ISS) model of Ekama and Wentzel (2004) with polyphosphate ($Mg_cK_dCa_ePO_3$) formation.

iii. The three phase Anaerobic Digestion Model (ADM-3P), including the hydrolysis of multiple municipal sludge types (PS, ND WAS, NDBEPR WAS and PS-WAS blends), the Ekama and Wentzel (2004) ISS model, the Brouckaert *et al.* (2010) ionic speciation model and multiple mineral precipitation. This ADM-3P model extends the UCTADM1 model developed by Sötemann *et al.* (2005b), by including:

- Additional soluble and particulate biodegradable organic components to represent material that might be combined from different sources in the WWTP and feed to the anaerobic digester.
- Hydrolysis kinetics of the polyphosphate for the digestion of waste activated sludge (WAS) from BEPR systems.
- Precipitation of $MgNH_4PO_4.6H_2O$ (struvite), $MgKPO_4.6H_2O$ (K-struvite) and $Ca_3(PO_4)_2$.
- Modelling separately as algebraic equations, the 'instantaneous' aqueous phase equilibrium and ion-paring reactions to reduce the stiffness of the system of differential equations.

- Parameterised stoichiometry for the bioprocesses so the various organics compositions are entered as X, Y, Z, A and B values.
- Pre-processor and post-processor routines which transform measured influent parameters such as FSA, OP, H_2CO_3 Alk., VFA, pH and TDS to model components and correct equilibrium, Henry's law and solubility products for ionic strength and can form model components back to predicted 'measured' concentrations for comparison with the actual measured concentrations.

The ASM2-3P and ADM-3P models were validated separately and thereafter combined to construct a plant-wide model, which was applied to simulate the whole plant (NDBEPR AS system linked to AD or anoxic-aerobic digestion (AnAerD)).

7. The calibration of the above two models generally involved matching the model results to variables measured from the appropriate systems at selected steady state periods. The ASM2-3P model is calibrated against the NDBEPR UCT and Modified Ludzack Ettinger (MLE) activated sludge systems of the experimental set up of this investigation. The MLE system results of ASM-3P were also compared with simulation results obtained from ASM1 to ensure that the same results are obtained. The ASM2-3P predictions were also compared with the NDBEPR WAS batch aerobic digestion (AerD) tests of Mebrahtu *et al.* (2007) and a NDBEPR UCT AS system linked to an AnAerD system operated and tested by Vogts (2011). The ADM-3P model was calibrated against the ADs fed MLE 1 WAS, MLE 2 WAS and NDBEPR WAS (including batch AD - to ensure that the P release was well matched), primary sludge (PS) and PS-WAS blends of the experimental set up. The ADM-3P predictions were also compared with the predictions of the 2-phase UCTADM1 model of Sötemann *et al.* (2005) and the PS AD results of Izzett *et al.* (1992), whose results were used to validate the UCTADM1 model.

In the calibration procedure, the unbiodegradable particulate COD fraction in the influent WW was kept the same for all ADs and all sludge ages. Also, for all ADs and all sludge ages, the composition of the OHO and PAO biomass and their endogenous residue were kept the same at the composition that was found to be the best over the whole experimental set. It was deemed more important to observe that the model is predicting similar trends to experimentally measured results than to fit the model to each AD sludge age and sludge type (which would yield better correlation) by changing the elemental formulation at each of the different experimental periods and instead provide detailed reasons for the observed differences.

8. The following aspects were noted when modelling the anoxic-aerobic systems (AS, and AerD) with the ASM2-3P model:

i. Since the MLE system with ND does not stimulate BEPR, its effluent P comprises mainly the OP not utilized by the biomass (mainly OHOs) for growth. This growth is limited by the flux of influent biodegradable COD available. With no PAO growth, no PP gets stored. Hence, the WAS produced from this type of system is not likely to cause struvite precipitation during sludge treatment, even with significant thickening before digestion.

ii. The aeration that occurs in the aerobic zone of AS systems strips out most of the CO_2 generated by the bioprocesses. Consequently, this biologically generated CO_2 does not have a significant impact on the pH of the system – pH of the AS system reactors depends mostly on the loss and gain of alkalinity via protein hydrolysis (gain), nitrification (loss), denitrification (gain) and PP storage (loss). The degree of CO_2 super-saturation has little effect on pH.

iii. In MLE systems with little or no nitrification taking place, high quantities of P and acetate in the unaerated ('anoxic') zone will result in the growth PAOs rather than OHO (and ANOs) only as expected in fully aerobic or nitrogen (N) removal

systems. The concentration of acetate available for this PAO growth (and associated excess P removal) depends on the rate of fermentation of biodegradable soluble organics (BSO) that occurs and the concentration of nitrate that gets recycled to the 'anaerobic' reactor in these systems. This also can take place in 3 and 5-stage Bardenpho systems – during the winter months when denitrification is lower than in the summer, the nitrate concentration recycled to the anaerobic reactor can be sufficiently high to suppress BEPR, in which case the WAS is not P-rich and AD of the WAS will not result in mineral precipitation even if thickened to 4 or 5% by flotation. In contrast, in summer the nitrate recycled to the anaerobic reactor is low resulting in BEPR in this system and mineral precipitation in AD and sludge dewatering systems. This happened at the Cape Flats WWTP in Cape Town, where the WAS was thickened to 3 to 4% by dissolved air flotation and anaerobically digested with PS. Seasonal BEPR in the 5-stage Bardenpho system caused mineral precipitation in the AD sludge dewatering centrifuges (van Rensburg *et al.*, 2003). The problem was solved by adding aeration to the post digestion sludge storage tank to raise the digester liquor pH by CO_2 stripping to stimulate mineral precipitation before discharge to the dewatering centrifuges. While not quantitatively validated the plant-wide ASM2-AD-3P does qualitatively predict this behaviour correctly.

iv. In anoxic-aerobic digestion (AnAerD), the absence of VFA and an anaerobic period renders the PAOs unable to compete with the OHOs. Consequently, the PAOs do not grow and undergo endogenous respiration and die, releasing their stored PP as Magnesium, Calcium, potassium and OP. Struvite ($MgNH_4PO_4$) precipitation occurs when the concentration of Mg, ammonia and OP is high enough (i.e. the struvite is supersaturated) in the mixed liquor. If the ammonia is low (< 1mg/N/*l*), due to nitrification, the Mg and P would combine with K to form K-struvite ($MgKPO_4$). The FSA-struvite and K-struvite precipitation is limited by the Mg

concentration, which is usually the lowest of the Mg, K, FSA and P. Once the Mg is limited, no further OP reduction takes place. About one-third of the P released by PP precipitates with the co-released Mg. This was observed in both aerobic and anaerobic digestion.

v. From the application of the ASM2-AerD-3P model to the diluted (4gTSS/*l*) aerobic batch tests of Mebrahtu *et al.* (2007), in which mineral precipitation did not take place, it appears that the PAOs retain their PP until they 'die' at their very slow endogenous respiration rate (0.04/d). This means that after 20d aerobic digestion, a considerable proportion of PAOs, with a high PP content, are still "alive" (> 50%). If the WAS is concentrated (> 2% TSS) FSA-struvite and K-struvite precipitation takes place but will be limited by the co-released Mg. The P release behaviour in aerobic digestion is therefore distinctly different to that in anaerobic digestion, where all the PP is released in less than 5 days (Harding, 2009; Jardin and Pöpel, 1994). The FSA and OP concentrations in dewatering liquor from aerobic digestion of P-rich WAS are therefore much lower than those from AD of P rich WAS.

vi. Application of the model to the AnAerD of the concentrated (~2%TSS) P-rich WAS system of Vogts *et al.* (2010) validated that the effluent FSA and nitrite were very low (< 1mgN/*l*) and that about 1/3rd of released P was precipitated as struvite with co-released Mg. While Vogts *et al.* (2010) also tested the effect of Ca and Mg dosing to the AnAerD on the aqueous OP concentration, this was not simulated but should be done in further work.

9. The following aspects were noted when modelling the AD systems using the steady state and dynamic (ADM-3P) three phase AD models:

vii. In the AD of PS, biodegradable particulate organics (PS BPO) are directly available for hydrolysis but for the AD of WAS, the biomass (OHOs and/or PAOs) die and are converted to BPO rapidly – much faster than their aerobic endogenous respiration rate. The WAS BPO is hydrolyzed at a relatively slow rate (which was

measured in this investigation). This hydrolysis rate of PS BPO and WAS BPO dictates the rate of biomass bound FSA and OP release in AD. The COD removal associated with FSA and OP release increases with increased AD sludge age. This increase is due to the increased time available for the hydrolysis of BPO and associated release of the organically bound N and P, as FSA and OP, into the AD liquor.

viii. Methane is produced via the COD removal. The methane COD depends on the COD of the BPO degraded (minus the very small amount, 2-5% of COD in the AD biomass produced). The C not included in CH_4 (minus the very small amount of C in the biomass) becomes CO_2, either dissolved CO_2 (HCO_3^-) or gaseous CO_2. Being insoluble at close to atmospheric pressure, methane usually all escapes as gas as soon as it is formed by the biological reactions. The mole fraction of the CO_2 in the gas phase [CO_2/ (CO_2 + CH_4)] sets the partial pressure of the gas phase (p_{CO2}), which together with the total alkalinity set the AD pH.

ix. Organically bound N is released with the hydrolysis of BPO in the non-ionic NH_3 form, which are non-reference species for the ammonia weak acid/base system. Therefore, the alkalinity increases by the concentration of NH_3 released. The NH_3, when the ADs are in the 6-8 pH range, reacts with the dissolved CO_2 (H_2CO_3*) forming HCO_3^-, according to $NH_3 + H_2O + CO_2 \rightarrow NH_4^+ + HCO_3^-$. Therefore, the total alkalinity (T.Alk) remains unchanged but is transferred from the FSA system to the inorganic carbon system. This is the main H_2CO_3*alkalinity generation process in an AD treating PS or WAS that is not P-rich. For P-rich systems with PP, H_2CO_3* alkalinity generation also depends on PP and cell bound P release.

x. In the dynamic model but not the steady state model, initially, polyphosphate (PP) release and PHA storage by PAOs takes place with the uptake of acetate, as would happen in the anaerobic part of the parent NDBEPR system. This results in

increased alkalinity because the PP is released as $H_2PO_4^-$. Because the PAOs also require aerobic conditions to supply them with the terminal electron acceptor (oxygen) for their growth, they cannot grow in the AD. Therefore, the PAOs are modelled to "die" in AD at a rate faster than their endogenous respiration rate; releasing their PHA and rest of their stored PP, adding more $H_2PO_4^-$ and alkalinity. Depending on the charge/proton balance requirements, some of the $H_2PO_4^-$ species become HPO_4^{2-} species by reacting with HCO_3^- to form HPO_4^{2-}, H_2O and CO_2. In this exchange, again, the T.Alk remains constant but it causes an additional transfer of alkalinity from the HCO_3^- of the IC system to the HPO_4^{2-} of the OP system and increases the CO_2 that exits the digester as gas and so increases the p_{CO2} of the AD gas. In the steady state model, all the PP is released instantaneously and stoichiometrically to form Mg^{2+}, K^+, Ca^{2+} and OP (which is split between $H_2PO_4^-$ and HPO_4^{2-}). The split between the OP species depends on and has influence towards the IC system, with which it contributes to the establishment of the AD pH.

xi. The organically bound P in the PAO (and OHO) biomass is released as H_3PO_4, at the much slower hydrolysis rate than the rapid PP release rate, which is complete in less than five days (Harding, 2009). Because H_3PO_4 is reference species for the OP weak acid/base system, the T.Alk does not change with this P release. In the AD pH range 7 to 8, the H_3PO_4 reacts with HCO_3^- to become $H_2PO_4^-$ or HPO_4^{2-} species, the HCO_3^- becoming H_2O and CO_2. So while the total alkalinity does not change, the species that represent it do (there is a transfer of alkalinity from the HCO_3^- of the IC system to the $H_2PO_4^-$ and HPO_4^{2-} species of the OP system). The CO_2 that would have been retained in the aqueous phase as HCO_3^- now exits the AD as gas, which increases the p_{CO2} (the CH_4 gas production remains unchanged because it is fixed by the COD of the biodegraded organics).

xii. The rapid release of PP and associated Mg^{2+} and the slow release of biomass N and P generate high concentrations of P, NH_4^+ and Mg^{2+} species in the AD liquor, which promotes struvite precipitation. This struvite precipitation decreases the T.Alk by 3×the struvite concentration precipitated and so results in re-speciation of the IC system, which increases p_{CO2} and decreases AD pH (Loewenthal *et al.*, 1994). If the T.Alk is low due to low N content of the organics and the P-rich WAS concentration high, precipitation of struvite results in decreased alkalinity and pH. However, the digester would not be at risk of failure, since for this precipitation to occur, the AD mixed liquor is required to be at above the required pH for stable AD operation, i.e. > 6.5, but preferably between 7 and 8, as reported by McCarty (1974).

xiii. Because the acetoclastic methanogens utilise only the associated form of VFA (HAc), all dissociated VFA fed to the AD, also cause an increase in alkalinity, i.e. $Ac^- + H_2O + CO_2 \rightarrow HAc + HCO_3^-$.

xiv. Therefore, alkalinity is generated only by the release of N and PP and the utilization of dissociated VFA. These three alkalinity-generating processes (plus the influent alkalinity) establish the T.Alk in the AD. Consequently, the T.Alk generated and p_{CO2} of the gas phase and hence, AD pH are therefore completely defined by the composition of the organics digested and the type of bioprocess, in this case methanogenesis, which itself does not generate alkalinity like sulphate reduction does (Poinapen and Ekama, 2010). The dynamic and steady state models are based on equilibrium conditions between the dissolved CO_2 ($H_2CO_3^*$) and headspace CO_2 concentrations. Therefore, to best match predicted and measured pH in real ADs, this equilibrium condition would need to apply. However, poor mixing of the AD could cause decreased CO_2 expulsion (hence lower p_{CO2}), and decreased pH.

With consideration to the systems complexity of interrelated variables and allowing for the possibilities of error in experimental data (both from AS systems used in characterizing the AD influent and the AD systems, which did not reach 100% mass balances, see Chapter 5) the overall results, when compared to experimental data, showed that the steady state AD and dynamic plant-wide models, assembled with the ASM2-3P and ADM-3P models developed in this investigation, give satisfactory predictions of the wastewater treatment systems performance (i.e. AS and AerD for the ASM2-3P (dynamic model) and AD for the three phase steady state and dynamic (ADM-3P) AD models).

8.5 CLOSURE

The material (COD, C, H, O, N, P, Mg, K and Ca) mass balance based three phase (solid – aqueous – gas) steady state AD and dynamic AD models (ADM-3P) have been developed in three steps, i.e. kinetics of hydrolysis, model stoichiometry and mixed weak acid/base chemistry. The three phase ASM2-3P model (ASM2-3P) was also developed with which to use the ADM-3P model to allow plant-wide simulation.

The 3 phase steady state AD model can be used on its own or linked with a steady state NDBEPR model, such as that developed by Wentzel *et al.* (1990), to construct a steady state plant-wide model, which is useful to make design decisions for the wastewater treatment plant layout and unit operation size (AS, AnAerD and AD sludge age) to achieve a defined effluent quality and sludge stability.

It was necessary to develop the steady state and dynamic models simultaneously because the steady state models were required to determine kinetic rates and sludge compositions from experimental results for dynamic model input and calibration. This was possible because the steady state and dynamic AS and AD models are based on the same basic principles, mass balances stoichiometry, just in simplified form without significant loss of accuracy. Developed in this way and calibrated to the same experimental results make

steady state models a useful complement to dynamic models. They allow the WWTP to be sized and optimized (i.e. for direct calculation of sludge age, reactor volumes and recycle flows) or wastewater characteristics to be determined for existing WWTP before performing simulations and so obviate much of the trial and error use of dynamic models, which require the plant unit operations to be sized and wastewater characteristics to be defined before simulations can be run. Once the WWTP layout is established with steady state models, dynamic models can be applied to its operation to evaluate dynamic behaviour, reduce peak energy consumption and cost while maximizing nutrient recovery and effluent quality.

8.6 RECOMMENDATIONS

The steady state and dynamic three phase AS and AD models have been developed and incorporated into plant-wide settings. However, when developing these models, there are aspects that require further investigation in future research. These include:

1. The effect of assigning different compositions (X, Y, Z, A and B) to the influent unbiodegradable particulate organics (UPO) on the simulation results. A different UPO composition will result in a different BPO composition of the PS and WAS due to the method of calculation of the BPO composition from experimental results – disaggregating the AD influent PO (BPO + UPO) with known (measured) effluent UPO composition. A decrease in N content of UPO would increase the N content of BPO and have an effect on the AD pH. Also, to explore the sensitivity of the plant-wide model to assigning different compositions to the endogenous residue and live biomass – recent research has indicated the compositions of OHOs and their endogenous residue may be different (Randani *et al.*, 2011, currently under review, PAOs not included).
2. Investigate the impact on assigning different OHO and PAO biomass unbiodegradable fractions on the plant-wide model. In this investigation, 0.08 was

assigned to both OHOs (f'_{EH}) and PAOs (f'_{EG}). For OHOs, this fraction is consistent with the endogenous respiration (b_H = 0.24/d; f_{EH} =0.20) and death regeneration (b_H' = 0.62/d, f'_{EH} = 0.08) (Ekama *et al.*, 2006). However, it is not consistent for PAOs (b_G = 0.04/d, f_{EG} = 0.25) because PAOs are not modelled with death regeneration in ASM2 but only endogenous respiration, since it side steps the questions of what happens to the PHA and PP with death regeneration.

3. Investigate the reason behind the different influent WW $f_{S'up}$ fractions calculated for BEPR systems with the steady state BEPR model (with PAOs) and for ND systems treating the same wastewater with the ND AS model (no PAOs). Two possible causes for this higher $f_{S'up}$ values were reviewed (1) Assigning to the PAOs a higher unbiodegradable fraction (f_{EG}) or conversely increasing the PAO biomass concentration (with lower P content) so that more PAO endogenous residue is produced by generating more VFA from hydrolysis of BPO than only the influent readily biodegradable organics (RBCOD) and (2) increase the undegraded BPO organics in the NDBEPR system, which would then appear as UPO in the steady state model, which assumes all biodegradable organics are utilised. This is possible due to the effect of the larger unaerated mass fraction in NDBEPR systems compared with ND systems. This possible reason is not consistent with the observation of this investigation that the higher UPO in the NDBEPR system is reflected in the measured UPO of the AD digesting this WAS. The higher UPO is not due to using membranes in the NDBEPR system (though it contributes) because this higher WW UPO ($f_{S'up}$) has also been observed in NDBEPR systems with settling tanks (Ekama and Wentzel, 1999). For cause (1), the f_{EG} value of 0.25 (measured on enhanced PAO culture activated sludge) can be checked by the determination of f_{EG} experimentally by digesting pure cultures of PAOs at a long AD sludge age (about 60 days or more). The validity of cause (2) can be checked by investigating the biodegradability of WAS from all reactors (aerobic, anoxic and

anaerobic) of the ND and NDBEPR systems when in ADs operated at a long sludge age (about 60 days or more), so confirming whether or not significantly larger unaerated mass fractions and higher mixed liquor concentrations in MBR systems are a cause for higher residual BPO and /or more undegraded influent inert organics enmeshment. From the experience of this investigation, this will require extremely careful and exact experimental work in order to detect small differences in biodegradability of WAS components.

4. It is important to stress that when dealing with systems under non-ideal conditions that are likely to stimulate mineral precipitation, some parameters that are ordinarily not tested require rigorous testing. These include influent (and effluent) pH and alkalinity, ionic conductivity, Mg, K, Ca and for P precipitation, the OP should be tested before and after dissolution of precipitates. Tests that allow distinguishing between the P in PP, organically bound P and P in precipitates should be conducted.
5. The steady state and dynamic plant-wide AD models have been used to predict the output of laboratory scale systems. When applied to simulate full-scale wastewater treatment plants, new challenges may arise, especially regarding the fluid dynamics of reactors (which are assumed to be completely mixed). It should be interesting to explore how well these models predict full-scale systems and to see what type of modifications would be required to achieve this. This work should be of particular interest to the IWA group on Benchmarking of Control Strategies for WWTPs who are planning to include P into an extended BSM model.
6. Over the past years, a number of systematic calibration protocols have been developed for wastewater treatment models, such as the BIOMATH protocol, developed by Vanrolleghem *et al*. (2003) and the Integrated Monte Carlo Methodology (IMCM) of Martin and Ayesa (2010). In order to have a standard procedure for the calibration of a three-phase (aqueous-gas-solid) anaerobic

digestion model (ADM3P) and to promote its widespread utilisation in a reproducible way, a calibration protocol that extends the ones already developed could be prepared. This would include calibration steps fine-tuned for the AD and AerD of P rich sludge such as the observation how well the model makes predictions on the release of phosphorus (i.e. the release of polyphosphate from phosphorus accumulating organisms and polyphosphate hydrolysis) and P precipitation (mainly in the form of struvite).

REFERENCES

1. Allison J.D., Brown D.S. and Novo-Gradac K.J., MINTEQA2, http://www.epa.gov/ceampubl/mmedia/minteq/, accessed 8 Dec 2009.
2. Antoniou P., Hamilton J., Koopman B., Jain R., Holloway B., Lyberatos G. and Svoronos S. A. (1990). Effect of temperature and pH on the effective maximum specific growth rate of nitrifying bacteria. *Water Research,* **24** (1), 97-101.
3. Baader W. (1982). Substratspezifische Stoff-Führung bei anaeroben Verfahren zur Methan-Gewinnung. *Chemie Ingenieur Technik*, **54** (1), 222–228.
4. Batstone D.J., Keller J., Angelidaki I., Kalyuznhyi S.V., Pavlostathis S.G., Rozzi A., Sanders W.T.M., Siegrist H. and Vavilin V.A. (2002). *Anaerobic digestion model No 1 (ADM1)*, Scientific and Technical Report No 9, International Water Association (IWA), London, UK.
5. Batstone D.J. and Keller J. (2003). Industrial applications of the IWA anaerobic digestion model No. 1 (ADM1). *Water Science and Technology*, **47** (12), 199-206.
6. Beeharry A. O., Lee B. J., Cronje G.L, Wentzel M.C. and Ekama G.A. (2002b). Measurement of active heterotrophic organism concentration in nitrification-denitrification activated sludge systems. Paper 025, Procs. 7th WISA Biennial Conf., Durban, South Africa.
7. Beychok M.R. (1971). Performance of surface-aerated basins. *Chemical Engineering Progress Symposium Series*, **67** (107), 322–339.
8. Billing E. and Dold P.L. (1988a). Modelling techniques for biological reaction systems 3: Modelling of the dynamic case. *Water SA,* **14** (4), 207-218.
9. Billing, E. and Dold, P.L. (1988b). Modelling techniques for biological reaction systems 2: Modelling of the steady-state case. *Water SA,* **14** (4), 193-206.

10. Brink I.C., Ekama G.A. and Wentzel M.C. (2007). *A plant-wide stoichiometric steady state WWTP model.* Procs. 10th IWA specialised conference Design, Operation and Economics of large WWTP, Vienna, Australia, 9 – 13 Sept.
11. Brouckaert C.J., Ikumi D.S. and Ekama G.A. (2010a). *Modelling of anaerobic digestion for incorporation into a plant-wide wastewater treatment model*. Procs. WISA Biennial Conference Durban, South Africa, 18-22 April.
12. Brouckaert C.J., Ikumi D.S. and Ekama G.A. (2010b) *A 3-phase anaerobic digestion model.* Procs. 12th IWA Anaerobic Digestion Conference (AD12), Guadalajara, Mexico, 1-4 Nov.
13. Butler J. N. (1964). *Ionic Equilibrium: Solubility and pH calculations*. Wiley –Interscience, New York, USA.
14. Capri M. and Marais G.vR. (1975). pH adjustment in anaerobic digstion. *Water Research*, **9** (3), 307-314.
15. Christensen D. B. and McCarty P. L. (1975). Multi- process biological treatment model. *Journal of water pollution control federation*, **67** (1), 2652.
16. Clayton A.J., Ekama G.A., Wentzel M.C. and Marais G.vR. (1989). *Denitrification kinetics in biological nitrogen and phosphorus removal activated sludge systems*. Research Report W63, Dept. of Civil Eng., Univ. of Cape Town, Rondebosch, 7701, Cape, South Africa.
17. Clayton J.A., Ekama G.A., Wentzel M.C. and Marais G.vR. (1991). Denitrification kinetics in biological nitrogen and phosphorus removal systems treating municipal wastewaters. *Water Science and Technology*, **23** (4/6), 1025–1035.
18. Cole J.A. and Hughes D.E. (1965). The metabolism of polyphosphates in chlorobium thiosulfatophilum. *Journal of General Microbiology*, **38** (1), 65 – 72.
19. Comeau Y., Hall K.J., Hancock R.E.W. and Oldham W.K. (1985). Biochemical model for enhanced biological phosphorus removal. Procs. UBC Conference on New

Directions and Research in Water Treatment and Residuals Management, June, Vancouver, Canada.

20. Davies P.S. (2005). *Biological Basis of Wastewater Treatment*. Strathkelvin Instruments Ltd, Scotland.
21. Daigger T.D., Henry C.L. and Leslie C.P. (1999). *Biological Wastewater Treatment*. 2nd Edn, Marcel Dekker Inc., New York, USA.
22. De-Bashan L.E. and Bashan Y. (2004). Recent advances in removing phosphorus from wastewater and its future use as fertilizer. *Water Research*, **38** (2004), 4222-4246.
23. Dold P.L., Ekama G.A. and Marais G.vR. (1980). A general model for the activated sludge process. *Prog. Wat. Technol*., **12** (Tor) 47-77.
24. Dold P.L., Wentzel M.C., Billing A.E., Ekama G.A. and Marais G.vR. (1991). *Activated sludge simulation programs*. Water Research Commission, Private Bag X03, Gezina, 0031, South Africa.
25. Dold P.L., Wentzel M.C., Billing A.E., Ekama G.A. and Marais G.vR. (1991). *Activated sludge system simulation programs, version 1.0*. Water Research Commission, P O Box 824, Pretoria, 0001, RsA.
26. Downing A.L., Painter H.A. and Knowles G. (1964). Nitrification in the activated sludge process. *Journal and Proceedings. Institute of Sewage Purification.* **64** (2), 130-153.
27. Du Toit G.J.G, Parco V., Ramphao M., Wentzel M.C., Lakay M.T., Mafungwa H. And Ekama G.A. (2010). *The Performance and Kinetics of Biological Nitrogen and Phosphorus Removal with Ultra-Filtration Membranes for Solid-Liquid Separation*. WRC Report No. 1537/1/09. Dept. of Civil Eng., University of Cape Town, Rondebosch, 7701, Cape Town, South Africa.
28. Eastman J.A. and Ferguson J.F. (1981). Solubilization of particulate organic carbon during the acid phase of anaerobic digestion. *Journal of the Water Pollution Control Federation*, **53** (1), 352–366.

29. Ekama G.A. (2009). Using bio-process stoichiometry to build a steady state plant-wide wastewater treatment plant model. *Water Research*, **43**(8), 2101-2120.
30. Ekama G. A. and Marais G. V. R. (1979). Dynamic behaviour of the activated sludge process. *Journal of the Water Pollution Control Federation*, **51** (1), 534-556.
31. Ekama G.A., Siebritz I.P. and Marais G.vR. (1983). Considerations in the process design of nutrient removal activated sludge processes. *Water Science and Technology*, **15** (3/4), 283 – 318.
32. Ekama G.A., Wentzel M.C. and Sötemann S.W. (2006). Mass Balance-Based Plant-Wide Wastewater Treatment Plant Models-Part 1: Biodegradability of Wastewater Organics under Anaerobic Conditions. *Water SA*, **32** (3), 269-275.
33. Ekama G.A., Wentzel M.C. and Sötemann S.W. (2006). Mass Balance-Based Plant-Wide Wastewater Treatment Plant Models-Part 3: Biodegradability of Activated Sludge Organics under Anaerobic Conditions. *Water SA*, **32** (3), 287-296.
34. Ekama G.A. and Marais G.vR. (1978). *The dynamic behaviour of the activated sludge process*. Research Report W27, Department of Civil Engineering, University of Cape Town, Rondebosch, 7701, RSA.
35. Ekama G.A. and Wentzel M.C. (1999). Denitrification kinetics in biological N and P removal activated sludge systems treating municipal wastewaters. *Water Science and Technology*., **39**(6), 69-77.
36. Ekama G.A. and Wentzel M.C. (2004). A predictive model for the reactor inorganic suspended solids concentration in activated sludge systems. *Water Research,* **38**(19), 4093-4106.
37. Ekama G.A., Dold P.L. and Marais G.vR. (1986). Procedures for determining influent COD fractions and the maximum specific growth rate of heterotrophs in activated sludge systems. *Water Science and Technology*., **18**(6), 91-114.
38. Ekama G.A., Mebrahtu M.K., Brink I.C. and Wentzel M.C. (2007). *Mass balances and modelling over wastewater treatment plants*. Final report to the WRC on Project K5/1620,

Report No 1620/1/07, Water Research Commission, Private Bag, 03, Gezina, 0031, Gauteng, RSA.

39. Ferguson J.F. and McCarty P. (1971). Effects of carbonate and magnesium on calcium phosphate precipitation. *Environmental Science and Technoogy*., **5**(6), 534-540.
40. Ghosh S. (1997). *Anaerobic digestion for renewable energy and environmental restoration*, Procs. The 8th International Conference on Anaerobic digestion, Sendai International Center, Sendai, Japan, May 25-29, pp. 9-16.
41. Gossett J.M. and Belser R.L. (1982). Anaerobic digestion of waste activated sludge, *Journal of Environmental Engineering. ASCE*, **108** (1), 1101-1120.
42. Grau P., Vanrolleghem P. and Ayesa E. (2007). BSM2 plant-wide Model construction and comparative analysis with other methodologies for integrated modelling. Procs. The Seventh International IWA Symposium on Systems Analysis and Integrated Assessment in Water Management.Washington, DC, USA, 7–9 May 2007.
43. Gujer W. (1993). *ASIM - Activated Sludge Simulation Program*. EAWAG, Dubendorf, Switzerland.
44. Gujer W. and Zehnder A.J.B (1983). Conversion processes in anaerobic digestion. *Water Science and Technology*, **15** (8/9): 127 – 167.
45. Harding T.H. (2009). *A steady state stoichiometric model describing the anaerobic digestion of BEPR WAS*. MSc. Thesis. Water Research Group, Department of Civil Engineering, University of Cape Town, Rondebosch, 7701, Cape Town, South Africa
46. Harding T.H., Ikumi D.S. and Ekama G.A. (2011a). A steady state stoichiometric model describing the anaerobic digestion of biological excess phosphorus removal waste activated sludge. *Research Report W132*, Dept. of Civil Eng., University of Cape Town, Rondebosch, 7701, Cape Town, South Africa.
47. Harding T.H., Ikumi D.S. and Ekama G.A.(2011b). *Incorporating phosphorus into plant-wide wastewater treatment plant modelling*. Procs.10th IWA Watermatex conference - Anaerobic Digestion, San Sebastian, Spain , 20-22 June.

48. Harding T.H., Ikumi DS and Ekama GA (2011c). A steady state stoichiometric model describing the anaerobic digestion of biological excess phosphorus removal waste activated sludge. Research Report W132 (Harding MSc thesis), Dept. of Civil Eng., Univ of Cape Town, Rondebosch, 7701, Cape, South Africa.
49. Harding T.H., Ikumi D.S., Lakay MT., Mafugwa H., Ekama G.A (2008). *Extending plant-wide WWTP models by including anaerobic digestion of waste activated sludge from biological excess phosphorus removal systems*. Procs. WISA conference (116). Gauteng, South Africa, 18-22 May.
50. Henze M., Grady C.P.L. (Jr.), Gujer W., Marais G.vR. and Matsuo T. (1987). *Activated Sludge Model No. 1(ASM1)*. IAWPRC Scientific and Technical Report No. 1, IAWPRC, London, U.K.
51. Henze M., Gujer W., Mino T., Matsuo T., Wentzel M.C. and Marais G.v.R. (1995). *Activated sludge model No.2 (ASM2)*. IWA Scientific and Technical Report No.3, IWA Publishing, London, U.K.
52. Henze M., Gujer W., Mino T. and van Loosdrecht M.C.M. (2000). *Activated sludge models: ASM1, ASM2, ASM2d and ASM3*. Scientific and Technical Report no. 9. IWA Publishing, London. U.K.
53. Henze M., van Loosdrecht M.C.M., Ekama G.A. and Brdjanovic D. (2008). *Biological wastewater treatment: Principles, modelling and design*. IWA publishing, Alliance house, 12 Caxton Street, London SW1H 0QS, UK.
54. Hill D.T., Young D.T. and Nordstedt R.A. (1980). *Continuously Expanding Anaerobic Digestion— A Technology for the Small Animal Producer*. American Society of Agricultural and Biological Engineers, Michigan, USA.
55. Horton R. and Hawkes D. L. (1979). Anaerobic digester design fundamentals Part II. *Process Biochemistry*, **14** (9), pp. 12-16.

56. Hu Y. and Stuckey D.C. (2006). Treatment of dilute wastewaters using a novel submerged anaerobic membrane bioreactor. *Journal of Environmental Engineering*, **132** (2), 190 -198.
57. Hu Z., Wentzel M.C., Ekama G.A. (2000).External nitrification in biological nutrient removal activated sludge systems. *Water SA,* **26** (2), 225–38.
58. Ikumi D.S., Harding T.H., Brouckaert C.J. and Ekama G.A. (2011). plant-wide *integrated biological, chemical and physical bioprocesses modelling of wastewater treatment plants in 3 phases (aqueous-gas-solid)*. Research Report W136, Dept. of Civil Eng., University of Cape Town, Rondebosch, 7701, Cape, South Africa.
59. Izzett H.B., Wentzel M.C. and Ekama G.A. (1992). *The Effect of Thermophilic Heat Treatment on the Anaerobic Digestibility of Primary Sludge*. MSc Thesis W76, Dept. of Civil Eng., University of Cape Town, Rondebosch, 7701, Cape, South Africa.
60. Jeppsson U., Rosen C., Alex J., Copp J., Gernaey K.V., Pons M.N. and Vanrolleghem, P.A. (2006). Towards a benchmark simulation model for plant-wide control strategy performance evaluation of WWTPs. *Water Science and Technology*, **53** (1), 287–295.
61. Jeyaseelan S. (1997). A simple mathematical model for anaerobic digestion process. *Water Science and Technology*, **35**(8), 185-191.
62. Jones R.M. and Takàcs I. (2004). *Importance of anaerobic digestion modelling on predicting the overall performance of wastewater treatment plants*. Procs. The Anaerobic Digestion Tenth World Congress, Montreal, Canada, 29 Aug.–2 Sept. 2004, pp. 1371–1375.
63. Koutsoukos P., Amjad Z., Tomson M.B. and Nancollas G.H. (1980). Crystallization of calcium phosphates: A constant composition study. *J Am Chem Soc*., **27** (1), 1553-1557.
64. Kotze J.P., Thiel P.G. and Hattingh W.H. J. (1969). Characterization and control of Anaerobic digestion. *Water Research*, **3** (1), 459.
65. Lettinga G. (1995). Anaerobic digestion and wastewater treatment systems. *Antonie Van Leeuwenhoek*, **67** (1), 3–28.

66. Lesjean B., Rosenberger S. and Schrotter J.C. (2004). Membrane-aided biological wastewater treatment – an overview of applied systems. *Membrane Technology*, August 2004.

67. Liu, W.T., Mino T., Matsuo T. and Nakamura K. (1996). Biological phosphorus removal processes – effect of pH on anaerobic substrate metabolism. *Water Science and Technology*., **34** (1), 25–32.

68. Liu T. and Sung S. (2002). Ammonia inhibition on thermophilic aceticlastic methanogens. *Water Science and Technology*, **45** (10), 113-120.

69. Loewenthal R.E., Sötemann S.W., Wentzel M.C. and Ekama G.A. (2004).*Three phase mixed weak acid/base chemistry kinetic modelling of multiple mineral precipitation problems*. Procs. IWA Conference on Struvite: it's Role in Phosphorus Recovery and Re-use, Cranfield University, Bedfordshire, UK, 17-18 June.

70. Loewenthal R.E., Ekama G.A. and Marais G.vR. (1989). Mixed weak acid/base systems: Part I - Mixture characterisation. *Water SA*, **15** (1), 3 - 24.

71. Loewenthal R.E., Wentzel M.C., Ekama G.A. and Marais G.vR. (1991). Mixed weak acid/base systems: Part II - Dosing estimation, aqueous phase. *Water SA*, **17** (2) 107 – 122.

72. Loewenthal R.E., Kornmuller U.R.C. and Van Heerden E.P. (1994). Modelling struvite precipitation in anaerobic treatment systems. *Water Science and Technology*, **30** (12), 107-116.

73. Loveless J.E. and Painter H.A. (1968). The influence of metal ion concentration and pH value in the growth of Nitrosomonas strain isolated from activated sludge. *Journal of General Microbiology*, **52**, 1-14.

74. Luz E., Bashan D.E. and Bashan Y. (2004). Recent advances in removing phosphorus from wastewater and its future use as fertilizer. *Water Research*, **38**, 4222–4246.

75. Marais G.vR. and Ekama G.A. (1976). The activated sludge process: Part I - Steady state behaviour. *Water SA*, **2** (4), 163-200.

76. Martin C. and Ayesa E. (2010). An Integrated Monte Carlo Methodology for the calibration of water quality models. *Ecological modelling*, **221** (22), 2656-2667.
77. McCarty P.L. (1967a). *Anaerobic waste treatment fundamentals. Part One: Chemistry and microbiology*. Public Works 95, September, pp 107-112
78. McCarty P.L. (1967b). *Anaerobic waste treatment fundamentals. Part Two: Environmental requirements and control*. Public Works 95, October, pp 123-126.
79. McCarty P.L. (1974). *Anaerobic processes*. Procs. International Association of Water Pollution Research (IAWPR, now IWA) short course on Design Aspects of Biological Treatment, Birmingham, UK, 18 Sept. 1974.
80. McCarty P.L. (1975). Stoichiometry of biological reactions. *Progress in Water Technology*, **7** (1), 157-172.
81. McCarty P.L. and Mosey F.E. (1991). Modelling of anaerobic digestion processes (a discussion of concepts). *Water Science and Technology*, **24** (1991), 17–33.
82. McKinney R. E. (1962). Complete mixing activated sludge treatment of antibiotic wastes. *Biotechnology and Bioengineering*, **4** (8), 181–195.
83. McInerney M.J. (1988). Anaerobic hydrolysis and fermentation of fats. In: *Zehnder*, (Ed.), Biology of Anaerobic Microorganisms. Wiley, New York, USA, pp. 872.
84. McInerney M.J., Bryant M.P. and Pfenning N. (1979). Anaerobic bacterium that degrades fatty acids in syntrophic association with methanogens. *Arch Microbiology*, 122,129 – 135.
85. Mebrahtu M.K., Wentzel M.C. and Ekama G.A. (2007). *Aerobic digestion of waste activated sludge from biological N ad P removal systems*. Research report No. W126, Dept of Civil Eng., University of Cape Town, Rondebosch, 7701, Cape, RSA.
86. Mebrahtu M.K. (2007). *Aerobic digestion of waste activated sludge from biological nutrient removal activated sludge systems*. MSc. Thesis. Water Research Group, Department of Civil Engineering, University of Cape Town, Rondebosch 7701, Cape Town, RSA., 180 pages.

87. Mebrahtu M.K., Vogts M. and Ekama G.A. (2010). *Anoxic – aerobic digestion of waste activated sludge from biological nitrogen and phosphorus removal systems*. Procs. WISA Biennial Conference Durban, South Africa , 18-22 April.
88. Mellin H.K.O., Lakay M.T., Wentzel M.C. and Ekama G.A. (1997). *The effect of high temperatures (30˚C) on biological nutrient removal performance and AA (low F/M) filament bulking in ND and NDBEPR systems*. Research Report W91, Department of Civil Engineering, University of Cape Town, Rondesbosch 7701, South Africa.
89. Meijer S.C.F., Van Loosdrecht M.C.M. and Heijnen J.J. (2001a). Metabolic modelling of full scale biological nitrogen and phosphorus removing WWTP. *Water Research*, **35**, 2711–2723.
90. Meijer S.C.F., Van der Spoel H., Heijnen J.J. and van Loosdrecht M.C.M. (2001b). Error diagnostics and data reconciliation for Activated sludge modelling purposes using linear conservation relations. *Water Science and Technology*, **45** (6).
91. Mino T., Liu W.T., Kurisu F. and Matsuo T. (1995). Modelling glycogen storage and denitrification capability of microorganisms in enhanced biological phosphate removal processes. *Water Science and Technology.*, **31** (2), 25–34.
92. Mino T., Satoh H. and Matsuo T. (1994). Metabolism of different bacterial populations in enhanced biological phosphate removal processes. *Water Science and Technology*, **29** (7), 67-70.
93. Moen G., Stensel H.D., Lepisto R. and Ferguson J. (2001). *Effect of retention time on the performance of thermophilic and mesophilic digestion*. Procs. 74th Annual Water Environ. Fed. Conf. and Exhib. Atlanta, USA, 13-17 Oct.
94. Monnet F. (2003). *An introduction to anaerobic digestion of organic wastes*. Remade, Scotland.
95. Munz C. and Roberts P.V. (1989). Gas and liquid phase mass transfer resistances of organic compounds during mechanical surface aeration. *Water Research*, **23** (5), 589-601.

96. Moosbrugger R.E., Wentzel M.C., Ekama G.A. and Marais G.vR. (1992). *Simple titration procedures to determine H_2CO_3* alkalinity and short-chain fatty acids in aqueous solutions containing known concentrations of ammonium, phosphate and sulphide weak acid/bases*. Published by Water Research Commission, P/Bag X03, Gezina 0031, South Africa, 1992.

97. Moosbrugger R.E., Wentzel M.C., Ekama G.A. and Marais G.vR. (1993a). Grape wine distillery waste in UASB systems - Feasibility, alkalinity and pH control. *Water SA,* **19** (1), 53-68.

98. Moosbrugger R.E., Wentzel M.C., Ekama G.A., Marais G.vR. (1993b). A five - pH point titration method for determining the carbonate and SCFA weak acid/bases in anaerobic systems. *Water Science and Technology*, **28** (2), 237 – 246.

99. Motlomelo (2011). Treatment of source separated urine in an anoxic-aerobic digester. MSc. Thesis.

100. Musvoto E.V., Casey T.G., Ekama G.A., Wentzel M.C. and Marais G.vR. (1992). *The effect of a large anoxic mass fraction and concentrations of nitrate and nitrite in the primary anoxic zone on low F/M filament bulking in nutrient removalactivated sludge systems*. Research Report W77, Department of Civil Engineering, University of Cape Town, Rondebosch, 7701, Cape Town, South Africa.

101. Musvoto E.V., Wentzel M.C., Loewenthal R.E. and Ekama G.A. (1997). Kinetic based model for weak acid/base systems. Water S.A., **23** (4), 311-322.

102. Musvoto E.V., Wentzel M.C., Loewenthal R.E. and Ekama G.A. (1998). *Mathematical modelling of integrated chemical, physical and biological treatment of wastewaters*. Research Report W97, Dept. Civil Eng., Univ. Cape Town, Rondebosch 7701, Cape Town, South Africa.

103. Musvoto E.V., Wentzel M.C., Loewenthal R.E. and Ekama G.A. (2000). Extension and application of the three phase weak acid/base kinetic model to the aeration treatment of anaerobic digester liquors. *Water S.A.*, **26** (4), 417-437.

104. Musvoto E.V., Wentzel M.C. and Ekama G.A. (2000a). Integrated chemical- physical processes modelling I. Development of a kinetic based model for weak acid/base systems. *Water Research*, **34** (6), 1857-1867.

105. Musvoto E.V., Wentzel M.C. and Ekama G.A. (2000b). Integrated chemical- physical processes modelling II. Simulating aeration treatment of anaerobic digester supernatants. *Water Research*, **34** (6), 1868-1880.

106. Musvoto E.V., Ekama G.A., Wentzel M.C. and Loewenthal R.E. (2000c). Extention and application of the three phase weak acid/base kinetic model to the aeration treatment of anaerobic digester liquors. *Water SA*, **26** (4), 417-438.

107. O'Rourke J.T (1968). *Kinetics of Anaerobic Treatment at Reduced Temperatures*. PhD dissertation, Department of Civil Engineering, Stanford University, USA.

108. Pavlostathis S.G. and Giraldo Gomez E. (1991). Kinetics of anaerobic treatment. *Water Science and Technology*., **24** (8), 35-59.

109. Pijuan M., Saunders A.M.,Guisasola A., Baeza J.A., Casas C. and Blackall L.L. (2004). Enhanced biological phosphorus removal in a sequencing batch reactor using propionate as the sole carbon source. *Biotechnology and Bioengineering*, **85** (1), 56–67.

110. Pilson R.A., Ekama G.A., Wentzel M.C. and Casey T.G. (1995). *The effect of temperature on denitrification kinetics and biological excess phophorus removal in biological nutrient removal systems in temperate climates (12˚C–20˚C).* Research Report W86, Department of Civil Engineerin g, University of Cape Town, Rondesbosch 7701, South Africa.

111. Pohland F. G. (1992). *Managing co-disposal effects on leachate and gas quality. Landfilling of Waste: Leachate*. Christensen, T. H, Cossu, R., and Stegmann, R. Eds., Elsevier Applied Science, London and New York. 139-165.

112. Poinapen J., Ekama G.A., Wentzel M.C. and Loewenthal R.E. (2008). *Development of a steady state model for biological sulphate reduction with primary sewage sludge as substrate*. Procs. WISA Biennial Conference , Gauteng, South Africa, 18-22 May.

113. Ramphao M., Ekama G.A., Lakay M.T., Mafungwa H. and Wentzel M. (2004). The performance and kinetics of biological nitrogen and phosphorus removal with ultra-filtration membranes for solid-liquid separation. Research Report W120, Dept. of Civil Eng., University of Cape Town, Rondebosch, 7701, Cape, South Africa.

114. Ramphao M., Wentzel M.C., Merrit R., Ekama G.A., Young T. and Buckley C.A. (2005). Impact of membrane solid-liquid separation on design of biological nutrient removal activated sludge systems. *Biotechnology and Bioengineering*, **89** (6), 630-646.

115. Reichert, P. (1998). *AQUASIM 2.0 – Tutorial*. Swiss Federal Institute for Environmental Science and Technology (EAWAG), CH-8600 Dübendorf, Switzerland, 213 pages.

116. Ripley L.E., Boyle W.C. and Converse J.C. (1986). Improved alkalimetric monitoring for anaerobic digestion of high strength wastes. *Journal of Water Pollution Control Federation*, **58** (5), 406-411.

117. Ristow N.E., Sötemann S.W., Loewentha R.E., Wentzel M.C. and Ekama G.A. (2004a). *Hydrolysis of Primary Sewage Sludge under Methanogenic, Acidogenic and Sulphate Reducing Conditions*. WRC Report 1216/1/04, Water Research Commission, P/Bag X03, Gezina 0031, South Africa.

118. Ristow N.E., Sötemann S.W., Wentzel M.C., Loewenthal R.E. and Ekama G.A. (2004b). *The effects of hydraulic retention time and feed COD concentration on the rate of hydrolysis of primary sewage sludge*. Procs. 10th World Congress on Anaerobic Digestion, AD2004, Montreal, Canada, 29 Aug. - 2 Sept.

119. Ristow N.E., Sötemann S.W., Wentzel M.C., Loewenthal R.E. and Ekama G.A. (2005). *The effects of hydraulic retention time and feed COD concentration on the hydrolysis rate of primary sewage sludge*. Procs. WISA specialized conference on management of residues emanating from water and wastewater treatment, Johannesburg, RSA, 9-12 Aug.

120. Romansky J., Heider M. and Wiesmann U. (1997). Kinetics of anaerobic ortho-phosphate release and substrate uptake in enhanced biological phosphorus removal from wastewater. *Water Research*, **31**, 3137–3145.

121. Ross W.R., Barnard J.P., Strohwald N.K.H., Grobler C.J. and Sanetra J. (1992). Practical application of the ADUF process to the full-scale treatment of a maize-processing effluent. *Water Science and Technology*, **25** (10), 27-39.

122. Sacks, J. (1997). Anaerobic digestion of high-strength or toxic organic effluents. *A Survey of Anaerobic Digesters in the KwaZulu-Natal Region to Assess their Availability for the Treatment of High-Strength or Toxic Organic Effluents*. MSc. Thesis. Department of Chemical Engineering, University of Natal, Durban, South Africa.

123. Sam-Soon P.A.L.N.S., Wentzel M.C., Dold P.L., Loewenthal R.E. and Marais G.vR. (1991). Mathematical modelling of upflow anaerobic sludge bed (UASB) systems treating carbohydrate waste waters. *Water SA*., **17** (2), 91 - 106.

124. Sawyer C.N., McCarty P.L. and Parkin G.F. (1994). *Chemistry for Environmental Engineering*. McGraw-Hill Inc., New York, USA.

125. Schlegel H.G. (1992). *Allgemeine Mikrobiologie. 7th Ed*., pp 304-307, Stuttgart, New York, USA.

126. Seco A., Ribes J., Serralta J. and Ferrer J. (2004). Biological nutrient removal model no. 1 (BNRM1). *Water Science and Technology*, **50** (6), 69–78.

127. Siegrist H., Vogt D., Garcia-Heras J.L. and Gujer W. (2002). Mathematical Modelling of Meso- and Thermophillic Anaerobic Sewage Sludge. *Environmental Science and Technology*, **36**, 1113-1123.

128. Speece R.E. (1983). Anaerobic biotechnology for industrial wastewater treatment. *Environmental Science and Technology*., **17**, 416 – 427.

129. Smolders G.J.F., van Loosdrecht M.C.M. and Heijnen J.J. (1994). Stoichiometric model of the aerobic metabolism of the biological phosphorus removal process. *Biotechnology and Bioengineering*, **43**, 837–848.

130. Smolders G.J.F., van der Meij J., van Loosdrecht M.C.M. and Heijnen J.J. (1995). A structured metabolic model for the anaerobic and aerobic stoichiometry and kinetics of the biological phosphorus removal process. *Biotechnology and Bioengineering*, **47**, 277–87.

131. Smolders G.J.F. (1995). *A metabolic model of the biological phosphorus removal (stoichiometry, kinetics and dynamic behaviour).* PhD Thesis, Department of Biochemical Engineering, Tech. University Delft, Netherlands.

132. Smolders G.J.F., van Loosdrecht M.C.M. and Heijnen J.J. (1994a). A model of the anaerobic metabolism of the biological phosphorus removal process, stoichiometry and pH influence. *Biotechnology and Bioengineering*, **43**, 461–70.

133. Smolders G.J.F., van Loosdrecht M.C.M. and Heijnen J.J. (1994b). Stoichiometric model of the aerobic metabolism of the biological phosphorus removal process. *Biotechnology and Bioengineering*, **43**, 837–48.

134. Sneyders M.J., Wentzel M.C. and Ekama G.A. (1997). *The effect of unstabilized landfill leachate addition on biological nutrient removal performance in activated sludge systems*. Research Report W95, Department of Civil Engineering, University of Cape Town, Rondebosch, 7701, RSA.

135. Stern L.B. and Marais G.vR. (1974). *Sewage as the electron donor in biological denitrification*. Research Report W7. Dept. of Civil Engineering, University of Cape Town, Rondebosch, 7701, RSA.

136. Sötemann S.W., Musvoto E.V., Wentzel M.C. and Ekama G.A. (2005a). Integrated chemical, physical and biological processes kinetic modelling Part 1 - Anoxic and aerobic processes of carbon and nitrogen removal in the activated sludge system. *Water S.A.*, **31** (4), 529-544.

137. Sötemann S.W., van Rensburg P., Ristow N.E., Wentzel M.C., Loewenthal R.E. and Ekama G.A. (2005b). Integrated chemical, physical and biological processes modelling Part 2 : Anaerobic digestion of sewage sludges. *Water SA.*, **31** (4), 545-568.

138. Sötemann S.W., Ristow N.E., Wentzel M.C. and Ekama G.A. (2005). A steady state model for anaerobic digestion of sewage sludges. *Water SA*., **31** (4), 511 – 528.

139. Sötemann S.W., Wentzel M.C. and Ekama G.A. (2006). Mass balance based plant-wide wastewater treatment plant models – Part 4: Aerobic digestion of primary and waste activated sludges. *Water SA*., **32** (3), 297 – 306.

140. Sötemann S.W. *(2005). Modelling material mass balances over wastewater treatment plants.* PhD.Thesis. Water Research Group, Department of Civil Engineering, University of Cape Town, Rondebosch, 7701, Cape Town, South Africa.

141. Stumm W. and Morgan J. J. (1970). *Aquatic Chemistry: An Introduction Emphasizing Chemical Equilibria in Natural Waters*. New York, London, Sydney, Toronto, Wiley-Interscience , pp 583.

142. Stumm W. and Morgan J.J. (1996). *Aquatic Chemistry: Chemical equilibria and rates in natural waters*. John Wiley & Sons Inc. New York, USA.

143. Takács I. (2008). *Experiments in Activated Sludge Modelling*. PhD Thesis, Ghent University, Belgium, pp 267.

144. Truesdell A.H. and Jones B.F. (1973). *WATEQ, a computer program for calculating chemical equilibria on natural waters*. U.S.Dept. of the Interior, Geological Survey, 73 pages.

145. Ubisi M.F., Wentzel M.C. and Ekama G.A. (1997). *Organic and inorganic components of activated sludge mixed liquor*. Msc. Thesis W94, Dept. Civil Eng., University of Cape Town, Rondebosch 7700, Cape Town, South Africa.

146. Van Haandel A.C., Ekama G.A. and Marais G.vR. (1981).The activated sludge process 3—Single sludge denitrification. *Water Research*, **15** (10), 1135–52.

147. Van Haandel A.C. and Lettinga G. (1994). *Anaerobic Sewage Treatment. A Practical Guide for Regions with a Hot Climate*. John Wiley and Sons, New York, USA.

148. Van Haandel A.C., Catunda P.F.C. and Araujo L. (1998). Biological sludge stabilization Part 1 - Kinetics of aerobic sludge digestion. *Water SA*., **24** (3), 223 - 230.

149. Vanhooren H., Meirlaen J., Amerlinck Y., Claeys F., Vangheluwe H. and Vanrolleghem P.A. (2003). WEST: modelling biological wastewater treatment. *Journal of Hydroinformatics*, **5**, 27- 50.

150. Vanrolleghem P.A., Insel G., Petersen B., Sin G., De Pauw D., Nopens I., Weijers S., Gernaey K.A. (2003). *Comprehensive model calibration procedure for activated sludge models*. Procs. WEFTEC 2003, 76th Annual Technical Exhibition and Conference, Los Angeles, CA, USA, October 11–15.

151. Vanrolleghem P.A., Rosen C., Zaher U., Copp J., Benedetti L., Ayesa E. and Jeppsson U. (2005). Continuity-based interfacing of models for wastewater systems described by Gujer matrices. *Water Science and Technology*, **52** (1 & 2), 493–500.

152. Van Rensburg P., Wentzel M.C. and Ekama G.A. (2001). *Integrated biological, chemical and physical processes kinetic model for the anaerobic digestion of primary sewage sludge*. Research Report W113, University of Cape Town, Department of Civil Engineering, Rondebosch 7701, CapeTown, South Africa.

153. Van Rensburg P., Musvoto E.V., Wentzel M.C. and Ekama G.A. (2003). Modelling multiple mineral precipitation in anaerobic digester liquor. *Water Research*, **37** (13) 3087-3097.

154. Veeken, A., Kalyuzhyi S., Scharff H. and Hamelers B. (2000). Effect of pH and VFA on hydrolysis of organic solid waste. *J Environ Eng*., **126** (12), 1076-1081.

155. Volcke E.I.P, van Loosdrecht M.C.M and Vanrolleghem P. A. (2006). Continuity based model interfacing for plant-wide simulation: A general approach. *Water Research*, **40**, 2817-2828.

156. Vogts M. (2011). *The removal of nitrogen and phosphorus in anoxic-aerobic digestion of nitrification-denitrification biological excess phosphorus removal waste activated sludge*. MSc. Thesis. Water Research Group, Department of Civil Engineering, University of Cape Town, Rondebosch 7701, Cape Town, RSA.

157. Wild H.E., Sawyer C.N. and McMahon T.C. (1971). Factors affecting nitrification kinetics. *Journal of the Water Pollution Control Federation*., September.

158. Warbuton C.A., Lakay M.T., Casey T.G., Ekama G.A., Wentzel M.C. and Marais G.vR. (1991). The effect of sludge age and aerobic mass fraction on low f/m filament bulking intermittent aeration nitrogen removal systems. Department of Civil Engineering, University of Cape Town, Rondebosch 7700, Cape Town, RSA.

159. Water Environment Federation, 1995. *Wastewater Residuals Stabilization*, MOP No. FD-9.: Water Environment Federation, Alexandria, VA.

160. Wentzel M.C., Ekama G.A., Marais G.v.R. (1992). Processes and modelling of nitrification dentirification biological excess phosphorus removal systems—A review. *Water Science and Technology*, **25** (6), 59–82.

161. Wentzel M.C. and Ekama G.A. (1997). Principles in the design of single-sludge activated sludge systems for biological removal of carbon, nitrogen, and phosphorus. *Water Environment Research*, **69** (7), 1222-1231.

162. Wentzel M.C., Ekama G.A., Dold P.L. and Marais G.vR. (1990). Biological excess phosphorus removal-steady state process design. *Water S.A.*, **16** (1), 29-48.

163. Wentzel M.C. (1988). *Biological excess phosphorus removal in activated sludge systems*. PhD Thesis. Water Research Group, Department of Civil Engineering, University of Cape Town, Rondebosch 7701, Cape Town, RSA. 400 pages.

164. Wentzel M.C., Ekama G.A., Loewenthal R.E., Dold P.L. and Marais G.v.R. (1989a). Enhanced polyphosphate organism cultures in activated sludge systems. Part II—Experimental behaviour. *Water SA.*, **15** (2), 71–88.

165. Wentzel M.C., Ekama G.A. and Sötemann S.W. (2006). Mass Balance-Based Plant-Wide Wastewater Treatment Plant Models-Part 2: Tracking the Influent Inorganic Suspended Solids. *Water SA*, **32** (3), 277-285.

166. Wentzel M.C., Dold P.L., Ekama G.A. and Marais G.v.R. (1989b). Enhanced polyphosphate organism cultures in activated sludge systems. Part III—Kinetic model. Water SA., **15** (2), 89–102.

167. Wolfsberger A. and Holubar P. (2006). *WP7 Biokinetic Data*. Modelling and Control Second Year CROPGEN Meeting, Vienna, Austria.

168. WRC (1984). *Theory, design and operation of nutrient removal activated sludge processes*. Water Research Commision, P O Box 824, Pretoria, RSA.

169. Yasui H., Sugimoto M., Komatsu K., Goel R., Li Y.Y. and Noike T. (2006). An approach for substrate mapping between ASM and ADM1 for sludge digestion. *Water Science and Technology*., **54** (4), 83–92.

170. Zaher U., Grau P., Benedetti L., Ayesa E. and Vanrolleghem P.A. (2007). Transformers for interfacing anaerobic digestion models to pre and post-treatment processes. *Environmental Modelling and Software,* **22**, 40–58.

171. Zaher U. E. (2005). *Modelling and monitoring the anaerobic digestion process in view of optimisation and smooth operation of WWTP's*. PhD Thesis in Appl. Biol. Sci.: Environ. Technol., Faculty of Bioscience Engineering, Ghent University, Belgium.

172. Zehnder A.J.B and Wuhrmann K. (1977). Physiology of a Methanobactreian strain. *Archives of Microbiology*., **111**, 199 – 205.

173. Zinder S.H. (1984). Microbiology of anaerobic conversion of organic wastes to methane: recent developments. *ASM news*, **50**, 294 – 298.

APPENDIX

Appendix 1 and 2: General Calculations used in characterisation of waste and material mass balances.

Appendix 3: Experimental Plan Overview.

Appendix 4: Additives used in Feed to Experimental Systems.

Appendix 5: Steady State AD Model Example.

Appendix 6: Three Phase plant-wide Gujer Matrix.

Appendix 7: Raw Results for AS system

Appendix 8: Raw Results for AD system

APPENDIX 1: CALCULATIONS USED FOR DATA EVALUATION

1.1. The Determination of Solids and Hydraulic Retention Times for the AS Systems

Although conceptually the solids retention time is equal to the mass of sludge in the reactor per mass of sludge wasted in a day, the methods for calculating of solids retention time differed between the MLE and NDBEPR AS systems. This is because for the MLE AS systems the solids concentrations were the same in both the anoxic and aerobic reactor, while for the NDBEPR system the solids concentrations differed for each reactor. The flux of total settleable (FX_t) and volatile settleable (FX_v) solids generated and wasted in the MLE system is given as:

$$MX_{v\_Reactor} = X_t \cdot V_{Reactor}$$

$$FX_{t\_wasted} = X_t \cdot Q_w$$

$$FX_{V\_wasted} = X_V \cdot Q_w$$

(A1.1a, A1.1b, A1.1c)

Where:

- V is the total volume of reactors (i.e. sum of anoxic and aerobic volumes) in the MLE system (*l*).
- X_t and X_v are the systems' average total (also given as TSS) and volatile (also given as VSS) settleable solids concentrations respectively (mg/*l*).
- Q_w is the waste sludge flow rate (*l*/d).
- MX_v is the mass of volatile settleable solids in the reactor.

In the NDBEPR system, the solids concentrations in the three reactors (anaerobic, anoxic and aerobic) vary, with the aerobic sludge concentration being the highest. Therefore, the solids concentrations for this system can be given as:

$$MX_v = (V \cdot X_v)_{anaer} + (V \cdot X_v)_{anox} + (V \cdot X_v)_{aer} + (V \cdot X_v)_{re-aer.}$$

(A1.1c)

Where the anaer, anox, aer and re-aer are the subscripts denoting that the preciding-bracketed calculation occurs for the anaerobic, anoxic, aerobic and re-aeration reactors respectively.

$$FX_{V\_wasted} = X_{V\,aer} \cdot Q_w$$

(A1.1d)

In both the MLE and NDBEPR AS systems, the solids are wasted from the aerobic reactor daily to maintain the system sludge age. The sludge age (R_s) is the length of time the sludge stays in the reactor, also known as solids retention time. For the MLE systems, with sludge concentrations being equal in both the anoxic and aerobic reactors, the sludge age is calculated as:

$$R_s = \frac{V}{Q_w}$$

(A1.1e)

For the NDBEPR system, the sludge age ($R_{s\text{-}NDBEPR}$) is calculated as:

$$R_{s-NDBEPR} = \frac{MX_{t-total}}{MX_{t-wasted}} = \left\lfloor \frac{(V \cdot X_t)_{anaer} + (V \cdot X_t)_{anox} + (V \cdot X_t)_{aer} + (V \cdot X_t)_{re-aer.}}{(Q_w \cdot X_{t-aer})} \right\rfloor .$$

(A1.1f)

Also calculated in this system is the hydraulic retention time (R_{hn}), which is the length of time the liquid material remains in the AS system, given by the equation below:

$$R_{hn} = \frac{V}{Q_i} .$$

(A1.1g)

Where Q_i is the influent flow rate (l/d).

1.2. Determination of Nitrogen Generated and De-nitrified in the AS System

In the AS system nitrates are generated in the aerobic zone, through nitrification of ammonia, and de-nitrified (converted to nitrogen (N_2) gas which exits the system) in the anoxic zone. For the MLE systems change in nitrates (ΔNO_3) concentration, relative to influent flow rate, i.e. due to the nitrification and denitrification, is calculated using:

$$\Delta NO_3 = (s \cdot NO_{3underflow} + a \cdot NO_{3recycle}) - ((1 + a + s) \cdot NO_{3anoxic})$$

(A1.2a)

Where:

- $NO_{3\text{-effluent}}$ and $NO_{3\text{-underflow}}$ are the concentrations of nitrates in the effluent and and sludge underflow recycle to the anoxic zone respectively.
- s and a are the recycle flow rates back to the anoxic zone , from the secondary settling and aerobic zone respectively, entered as ratios to the influent flow rate.

The UCT configuration (anaerobic-anoxic-aerobic) allows for biological excess phosphorus removal (BEPR) to be operated independently of the N removal, i.e. zero nitrate recycle to the anaerobic reactor. Provided that the recycles to the anoxic reactor do not get overloaded with nitrate.

In the NDBEPR, UCT process system the ΔNO_3 concentration relative to influent flow rate, i.e. due to the aerobic nitrification and denitrification that occurs in the unaerated zones is:

$$\Delta NO_{3anox.} = \left[(NO_{3anaer} \cdot (1 + r)\right] + (NO_{3aer} \cdot as) - \left[NO_{3anox} \cdot (1 + as + r)\right] + (NO_{3anox} \cdot r) - \left[(NO_{3anaer} \cdot (1 - r)\right]$$

(A1.2b)

The recycles rates (i.e. as, from aerobic to anoxic zone, and r, from anoxic to anaerobic zone) in the above formulas are measured as a ratio to the influent flow rate. Thus, the change in flux of nitrates de-nitrified (FNO_3) equals:

$$\Delta FNO_3 = Q_i \cdot \Delta NO_3$$

(A1.2c)

The nitrification and denitrification processes that take place in the AS systems can be outlined by the following equations:

1. Nitrification:

$$NH_4^+ + 2O_2 \rightarrow NO_3^- + 2H^+ + H_2O$$

(A1.2d)

$$O_2 + 4e^- + 4H^+ \rightarrow 2H_2O$$

(A1.2e)

This equation shows us that every oxygen molecule has four electron equivalents, thus the two oxygen molecules used in nitrification are equivalent to eight electrons.

2. Denitrification:

$$2NO_3^- + 10e^- + 12H^+ \rightarrow N_2 + 6H_2O$$

(A1.2f)

The above equation shows us that each nitrate (NO_3) takes 5 electrons in the denitrification process.

Therefore O_2 (or COD) equivalent of NO_3 is 5/8 of 4.57 (mgO/mgFSA nitrified i.e. 64/14) which equals 2.86. Therefore, the COD in denitrification (MO_D) is given as:

$$MO_D = \Delta MNO_{3\_denit.} \cdot 2.86$$

(A1.2g)

The total change in flux of nitrates generated in the AS system is the sum of nitrates, which were de-nitrified (ΔFNO_{3_denit}), and nitrates not de-nitrified, which are found in the effluent (NO_{3_eff}):.

$$FNO_{3\_gen} = \left(NO_{3\_ef}\ f \cdot Q\right)_i + \Delta FNO_3$$

(A1.2h)

1.3. The Determination of Oxygen Utilized for Nitrification and for Organics Utilization

With knowledge of the mass of nitrates formed, we are able to calculate the flux of oxygen used in the nitrification process (FO_n):

$$FO_n = 4.57 \cdot FNO_{3\_gen}$$

(A1.3a)

Where 4.57 is the mgO/mgFSA nitrified (i.e. 64/14) and FNO_{3_gen} is the mass of nitrates generated aerobically (MgN-NO_3/d).

The measured oxygen utilization rate (OUR_m) includes both the oxygen used in nitrification and that used in formation of active mass and its endogenous respiration. The aerobic section of the membrane NDBEPR system comprises of a fully aerobic, continuously aerated, tank and a reaeration tank, in which the OUR probe was placed. The OUR for the fully aerated tank was obtained by dividing the measured OUR (mgO/*l*/hour) by the mass fraction of the re-aeration tank to the fully aerated tank.

The total mass of oxygen used (FO_M) equals the measured OUR multiplied by the total aerobic volume and hours per day i.e.:

$$FO_M = OUR \cdot V \cdot 24$$

(A1.3b)

We can thus calculate the mass of oxygen used in the conversion of organics ($MOUR_c$) by subtracting the mass of oxygen used in nitrification ($MOUR_n$) from this total mass of oxygen used, with the following Equation A1.3c:

$$FO_c = FO_M - FO_n$$

(A1.3c)

1.4. Calculation of Nutrients Removed from the AS Systems

Below are the calculations of chemical oxygen demand (COD), total Kjeldahl nitrogen (TKN), and total phosphorus (TP) removed from the AS system. The flux of material

removed per total AS reactor volume (V) can be obtained by subtracting its influent flux to the AS from its effluent flux and dividing the difference by the AS systems' volume as shown in Equations A1.4a to c below.

$$COD\ removed = \frac{\left[(Q_i \cdot S_{ti}) - (Q_e \cdot S_{te})\right]}{V} \quad \text{(A1.4a)}$$

Where:

- S_{ti} and S_{te} are the influent and effluent COD concentrations (mgCOD/*l*) respectively.
- Q_e is the effluent flow rate.

$$TKN\ removed = \frac{\left[(Q_i \cdot N_{ti}) - (Q_e \cdot N_{te})\right]}{V} \quad \text{(A1.4b)}$$

Where:

- N_{ti} and N_{te} are the influent and effluent TKN concentrations (mgN/*l*) respectively.

$$P\ removed = \frac{\left((Q_i \cdot P_{ti}) - (Q_e \cdot P_{te})\right)}{V} \quad \text{(A1.4c)}$$

Where:

- P_{ti} and P_{te} are the influent and effluent TP concentrations (mgP/*l*) respectively.

1.5. The Determination of Phosphorus Content in the OHOs and PAOs

The phosphororus (P) content of the sludge (mainly biomass) as would be found in ordinary heterotrophic organisms (OHOs), which excludes the ployphosphates, PP, in the phosphorus accumulating organisms, is given by subtracting the concentration of measured TP and ortho-phosphate (OP) concentrations in the mixed liquor. Thus, the fraction of P in the sludge (mgP/mgVSS) is calculated using the Equation A1.5a below:

$$f_{p\ OHO} = \frac{(TP - OP)_{aer}}{X_{v\ aer}}$$

(A1.5a)

This value is usually about 0.03 mgP/ mgVSS.

If f_{XBGP} is the total mgP/mgVSS for active phosphorus accumulating organism (PAO) mass (including PP), the P removal Equation A1.4c can be broken down further, in the NDBEPR system to the Equation A1.5b below:

$$P\ removed = \left\lfloor \frac{V}{(R_s \cdot Q_i)} \right\rfloor \cdot \left[(X_{BG} \cdot f_{XBGP}) + (f_{p\ OHO} * (X_{BH} + X_{EG} + X_{EH} + X_i)) \right]$$

(A1.5b)

Where:

- X_{BG} and X_{BH} are the concentrations of active and PAO and OHO organisms respectively (in mg/*l*).
- X_{EG} and X_{EH} are the concentrations of endogenous residue (ER, in mg/*l*) from the PAO and OHO organisms respectively.
- X_i is the concentration of influent unbiodegradable particulate organic material (mg/*l*), which is enmeshed with the rest of the sludge in the reactors hence keeps accumulating with sludge age.

$$Then: f_{XBGP} = (P\,removed \cdot R_s \cdot Q_i) - \frac{\left[0.03 \cdot (X_i + X_{BH} + X_{EH} + X_{EG})\right]}{X_{BG}}$$

(A1.5c)

Thus, with 3.286 as the inorganic settleable solids (ISS) content of PP and $f_{p\text{-}OHO}$ is the mgP/ mgVSS, as for normal to OHO's, (i.e. the content of P found in ordinary biomass):

$$f_{iPAO} = f_{iOHO} + 3.286 \cdot \left(f_{XBGP} - f_{p\ OHO} \right)$$

(A1.5d)

Where:

- f_{iPAO} and f_{iOHO} are the fractions of inorganic material taken up (as inorganic dissolved solids, IDS, form) by the PAOs and OHOs respectively, then manifest as ISS in the ISS test.

1.6. AS System Mass Balance Calculations

The mass balance performed over a system considers the conservation of mass of a material characterstic that enters, exits and gained/lost within the boundaries set for the mass balance, as shown in Equation A1.6a,

$$\begin{bmatrix} Mass \\ Change \\ in\ system \end{bmatrix} = \begin{bmatrix} Mass\ flow \\ into\ system \end{bmatrix} - \begin{bmatrix} Mass\ flow \\ out\ of\ system \end{bmatrix} + \begin{bmatrix} Mass\ gain \\ by\ bio-process \end{bmatrix} - \begin{bmatrix} Mass\ loss \\ by\ bio-process \end{bmatrix}.$$

(A1.6a)

The mass balance calculations for COD, TKN and phosphorus are as given below:

i. Chemical Oxygen Demand (COD) Balance:

The COD flux (MS_{ti}) entering the activated sludge system is given by:

$$MS_{ti} = S_{ti} \cdot Q_i$$

(A1.6a)

This influent COD flux is used in the AS system for biomass growth and respiration, hence is lost from the system through the carbonaceous oxygen utilization, the COD used for denitrification and the COD flux that exits the system from the waste or effluent flow. Therefore, the COD flux leaving the activated sludge system (COD_{out}) is given by:

$$COD_{out} = (Q_w \cdot S_{ml}) + MOUR_c + MO_D + Q_e \cdot S_{te}$$

(A1.6b)

Where:

- S_{ml} is the COD of the mixed liquor in the continuously stirred reactor from which the waste sludge is removed (mg COD/*l*).

- MO_D is the COD flux utilized for dentrification.

For the systems' COD to balance, the total COD in should equal the COD out, hence the COD balance (percentage) is calculated by:

$$COD\,balance = \frac{CODout}{M_{sti}} \cdot 100$$

(A1.6c)

ii. Nitrogen Balance:

The total nitrogen flux (MN_{ti}) entering the activated sludge system is given by:

$$MN_{ti} = Q_i \cdot N_{ti}$$

(A1.6d)

The nitrogen flux out of the AS system (MN_{out}) is given by:

$$MN_{out} = (Q_e \cdot N_{te}) + (Q_e \cdot NO_{3effluent}) + (Q_w \cdot NO_{3underflow}) + (Q_w \cdot N_{ml}) + \Delta MNO_{3\_denit.}$$

(A1.6e)

Where:

- $NO_{3\text{-effluent}}$ and $NO_{3\text{-underflow}}$ is the concentration of nitrates in the effluent and sludge underflow recycle to the anoxic zone respectively.
- $\Delta MNO_{3\text{-denit}}$ is the change in mass of nitrates de-nitrified in the AS system, calculated using the above Equation A1.2h.

For the systems' N to balance the total nitrogen in should equal the nitrogen out, hence the N balance (percentage) is calculated by:

$$N\ balance = \frac{MN_{out}}{MN_{ti}} \times 100$$

(A1.6f)

iii. Phosphorus Balance:

The total phosphorus flux (MP_{ti}) entering the activated sludge system in the influent and leaving (MP_{te}) from the effluent is given by:

$$MP_{ti} = Q_i . P_{ti}$$

(A1.6g)

and

$$MP_{te} = (Q_e + Q_w). P_{te} .$$

(A1.6h)

P is removed from the system with its uptake by microorganisms, which get wasted from the system daily to maintain sludge age. This P flux wasted (P_{wasted}) can be measured as the total P concentration of the mixed liquor (P_{ml}) in the reactor from which the sludge is wasted daily.

$$P_{wasted} = P_{ml} . Q_w$$

(A1.6i)

For the systems' P to balance the P removed, as calculated from the difference between the MP_{ti} and MP_{te} should equal the P removed by the mass of sludge wasted from the system (P_{wasted}).

Therefore, the P balance (percentage) is calculated by:

$$P\ balance = \frac{P_{wasted}}{\left((P_{ti} + P_{te}) \cdot Q_i\right)}$$

(A1.6j)

1.7. AD System Mass Balance Calculations

The AD systems that were operated in this project were completely mixed reactors, hence the feed concentration (mg/*l*) was the same in the systems' influent and effluent.

COD Balance

COD in the influent (mgCOD/d) = Q_i x S_{ti}

COD out: COD in the effluent sludge flow = Q_e x S_{te}

COD out: COD content of the CH_4 gas = COD of CH_4

The COD mass balance over the AD system = (Total COD Out / Total COD In) x 100 [%]

Nitrogen Balance

a. N in the influent (mgN/d) = Q_i x N_{ti}

b. N exiting the AD system (mgN/d) = Q_e x N_{te}

c. The N mass balance over the AD system = (Total N Out / Total N In) x 100 [%]

Phosphorus Balance

a. P in the influent (mgP/d) = Q_i x P_{ti}

b. P exiting the AD system (mgP/d) = Q_e x P_{te}

c. The P mass balance over the AD system = (Total P Out / Total P In) x 100 [%]

Carbon Balance

The Carbon Mass Balance performed over the AD system is not a direct measured component on the influent and effluent of the AD system. However, the carbon mass balances were performed at the different sludge ages selected for the AD system based on the assumed fractions allocated to the VSS (PO) and UPO components, at 0.52 and 0.51 respectively, and that calculated for the BPO based on the difference from the PO and UPO component.

a. C in the influent (mgC/d)

(*The carbon mass content of the influent to the AD system was determined from the f_C of the VSS concentration and the H_2CO_3* Alkalinity of the influent WAS)*

i. C content of the influent VSS flow = (PO / MM_{PO}) x $n_{C(in\ PO)}$ x 12

ii. C content of HCO_3^- = (H_2CO_3* Alk)/ 50 x 12 (in *mg as* $CaCO_3$ the MM = 100/2 eq.)

b. C exiting the AD (mgC/d)

{The carbon mass content exiting the AD system was determined as the sum of the C content of (i) UPO C content, (ii) residual BPO C content, (iii) HCO_3^- C content (based on H_2CO_3 Alk), (iv) CH_4 C content , (v) CO_2 C content and (vi) the C content of the Biomass (not included because the Biomass are not measured).}*

i. C content of the UPO flow = (UPO/MM_{UPO}) x $n_{C(in\ UPO)}$ x 12

ii. C content of the Res. BPO flow = (Res. BPO/MM_{BPO}) x $n_{C(in\ BPO)}$ x 12

iii. C content of effluent HCO_3^- = (H_2CO_3*Alk)/50 x 12 (in *mg as* $CaCO_3$ the MM = 100/2 eq.)

iv. C of CH_4 = (nCH_4/Q_e) x 12

v. C of CO_2 = (nCO_2/Q_e) x 12

vi. C in Biomass can be calculated from the predicted results

APPENDIX 2: OHO AND PAO ORGANIC FORMULA DERIVATION

2.1. The Determination of OHO and PAO Biomass Generic Organic Formulae

The generic formula, determined for OHOs and PAOs in the NDBEPR system is $C_XH_YO_ZN_AP_B$ and $C_XH_YO_ZN_AP_B$ $(MePO_3)_q$ respectively. Where, $(MePO_3)_q$ is the inorganic energy storage molecule inside the organic biomass ($C_XH_YO_ZN_AP_B$).

To calculate the molar quantities of each atom in the formula, Y has been chosen to act as the control value with a value of 7 and to be used in the calculation of X, Z, A and B.

Molar fractions of this can be equated to measured mass fractions:

$$fc = \frac{TOC}{VSS} = \frac{12x}{12x + y + 16z + 31b + 14a}$$

$$\therefore x = \frac{fc}{12(1 - fc)} \cdot (y + 16z + 31b + 14a) \quad .$$

(A2.1a)

Similarly,

$$fn = \frac{TKN}{VSS} = \frac{14a}{12x + y + 16z + 31b + 14a} \qquad fp = \frac{TKN}{VSS} = \frac{31b}{12x + y + 16z + 31b + 14a}$$

$$\therefore a = \frac{fn}{14(1 - fn)} \cdot (y + 16z + 31b + 12x) \quad \text{and} \quad \therefore b = \frac{fp}{31(1 - fp)} \cdot (y + 16z + 12x + 14a) \quad .$$

(A2.1b and c)

From the above Equations A2.1a, b and c, let:

$$y + 16x = qk, \quad \frac{fn}{14(1 - fn)} = qa, \quad \frac{fp}{31(1 - fp)} = qb, \quad \frac{fc}{12(1 - fc)} = qc \quad .$$

(A2.1d, e, f and g)

Solving for a from the above Equations, by substituting Equations A2.1a, c, d e and f to Equation A2.1b, gives:

$$a = \frac{x \cdot (12 \cdot qa + 12 \cdot 31 \cdot qa \cdot qb)}{(1 - 31 \cdot qa \cdot qb \cdot 14)} + \frac{(qb \cdot qa + 31 \cdot qa \cdot qb \cdot qk)}{(1 - 31 \cdot qa \cdot qb \cdot 14)} .$$

(A2.1h)

Solving for b, by substituting for a with its expanded expression above, gives:

$$b = x \cdot \left\lfloor \frac{(12 + 14) \cdot qb \cdot (12 \cdot qa + 12 \cdot 31 \cdot qa \cdot qb)}{(1 - 31 \cdot qa \cdot qb \cdot 14)} \right\rfloor + (qk \cdot qb) + 14 \cdot qb \left\lfloor \frac{(qb \cdot qa + 31 \cdot qa \cdot qb \cdot qk)}{(1 - 31 \cdot qa \cdot qb \cdot 14)} \right\rfloor$$

(A2.1i)

Solving for x, by substituting for a and b with their expanded expressions (from Equations A2.1h and i), gives:

$$x = \frac{qk \cdot fc}{12 \cdot (1 - fn - fp - fc)} .$$

(A2.1j)

With y fixed at a value of 7, x can now be calculated with the above Equation A2.1j, using measured variables. Substituting x from its expression in Equation A2.1j into Equation A2.1h above gives us:

$$a = \frac{fn}{14} \cdot \left\lfloor \frac{y + 16z}{(1 - fn - fp - fc)} \right\rfloor ,$$

(A2.1k)

which is equivalent to the fraction of nitrogen (N) in the biomass multiplied by the molar mass of oxygen (O) and hydrogen (H), all divided by the product of the molar mass of N and the fraction of O plus H in the biomass. Solving similarly for b (i.e Equations A2.1i and j solved simultaneously) gives:

$$b = \frac{fp}{31} \cdot \left\lfloor \frac{y + 16z}{(1 - fn - fp - fc)} \right\rfloor$$

(A2.1l)

However, z is still unknown; therefore, the COD to VSS ratio (f_{cv}) is used, where the COD can be equated to the electron donating capacity (Ds) from the equation:

$$C_X H_Y O_Z N_A P_B (MePO_3)_q + aH_2O \rightarrow bCO_2 + CNH_3 + dH_2PO_4 + fMe^{+2} + gH^+ + Ds(H + e^-)$$

(A2.1m)

Thus, with ths equation balanced, Ds is determined as:

$$Ds = 4X + Y - 2Z - 3A + 5B$$

(A2.1n)

With VSS being equated to molar mass, f_{cv} can be given as:

$$fcv = \frac{COD}{VSS} = \frac{4x + y - 2z - 3a + 5b}{12x + y + 16z + 14a + 31b}$$

(A2.1o)

This is because, as explained earlier, for each mole of the organic material COD is equivalent to the electron donating capacity and VSS is equivalent to its molar mass.

After making z the subject of the Equation A2.1o and providing the necessary substitutions for a, b and x (from above Equations A2.1j, k and l) gives:

$$z = \frac{\frac{y}{2} \cdot \left(1 - \frac{fcv}{8} - \frac{17 \cdot fn}{14} - \frac{26 \cdot fp}{31} - \frac{8 \cdot fc}{12}\right)}{\left(\frac{8 \cdot fcv}{8} + 1 - \frac{44 \cdot fc}{12} - \frac{71 \cdot fp}{31} + \frac{10 \cdot fn}{14}\right)}$$

(A2.1p)

2.2. The Determination of Polyphosphate Concentrations in PAOs

Unlike ND or fully aerobic AS systems, where the P content is a small part of the biomass, NDBEPR AS systems contain PAOs which store significant quantities of phosphorus. Apart from the organic P that is a part of all the AS organism biomass (both OHOs and PAOs), the PAOs are able to store P internally, as chains of polyphosphate (PP), a high-

energy storage molecule. The storage of PP occurs at the expense of carbon in the aerobic conditions and carbon at the expense of polyphosphate at the anaerobic zone of the AS system (Daigger *et al.*, 1999). Thus P is removed from the AS system when sludge is wasted from the aerobic zone of the NDBEPR system. This is because it is in the aerobic zone that PAOs take up the phosphorus and store it as PP, in their cell cytoplasm. This PP content has to be included as a characteristic of the WAS as influent to the AD, as it may partake in the stoichiometry and weak acid- base chemistry. The total P removed from the AS system, and hence stored in the waste sludge (for both PAOs and OHOs can thus be given as:

$$P_{removed} = \frac{\left[(Qi * Pti) - (Qe * Pte)\right]}{V} \tag{A2.2a}$$

Our experiment was performed on both ND systems (containing OHOs only) and an NDBEPR system (containing both OHOs and PAOs) operated in parallel. Hence, it was possible to determine fraction of the biomass content of P as would be found in ordinary heterotrophic organisms (which exclude the PP in the phosphorus accumulating organisms) by calculating the organic particulate P content of the VSS:

$$fp_{OHO} = \frac{(TP - OP)_{aer}}{VSS_{aer}} \tag{A2.2b}$$

This value is usually about 0.03 mgP/ mgVSS.

Therefore, if f_{XBGP} is the mgP/mgVSS for active PAO mass, the P removed from the NDBEPR system can be broken down further as:

$$P_{removed} = \left(\frac{1}{(R_s \cdot Q_i)}\right) \cdot \left(\left(MX_{BG} \cdot f_{XBGP}\right) + \left(f_{pOHO} \cdot \left(MX_{BG} + MX_{EG} + MX_{EH} + MX_I\right)\right)\right) \tag{A2.2c}$$

$$Then: f_{XBGP} = \frac{\left(P_{removed} \cdot R_s \cdot Q_i\right) - \left(f_{pOHO} \cdot \left(MX_i + MX_{BH} + MX_{EH} + MX_{EG}\right)\right)}{MX_{BG}}$$

(A2.2d)

With the fraction of total P (fxBGP), the fraction of organic P that is a part of the biomass (fpOHO) and the concentration of active PAO biomass (X_{BG}) known, we can calculate the P concentration in PP concentration in the waste sludge as:

$$PP = \left(f_{XBGP} - f_{p_{OHO}}\right) \cdot X_{BG}$$

(A2.2e)

PP has a molecular formular of $(MePO_3)q$, where Me is the sum of metallic atoms of magnesium (Mg), potassium (K) and Calium (Ca) and q is the factor that links the biomass PAO (CHONP) to PP hence give active PAO the formula of $CHONP(MePO_3)q$. Therefore, the difference in influent and effluent measured Mg, K and Ca is equal to the quantity that is used in the formation of the PP mass.

To know the molar mass of PP, the molar ratio of each metallic component of PP (e.g. Mg) to P is first determined by:

$$\frac{Mg_{mol}}{P_{mol}} = \frac{\left(\frac{Mg_{polyP}}{24}\right)}{\left(\frac{P_{polyP}}{31}\right)},$$

(A2.2f)

Where 24 and 31 are the relative atomic masses of Mg and P respectively. However, PP being a stable molecule, the total Me should have a charge of +1 to balance the charge of P, which is -1. Therefore the molar fraction of each metallic component e.g. Mg:P can be corrected by dividing it by the total metallic charge per mol of P in PP.

i.e: $$Corrected\ \frac{Mg_{mol}}{P_{mol}} = \frac{\left(\frac{Mg_{mol}}{P_{mol}}\right)}{\left[\frac{\left(\frac{2Mg}{24}+\frac{K}{39}+\frac{2Ca}{40}\right)}{\left(\frac{P_{polyP}}{31}\right)}\right]}$$

(A2.2g)

After the above calculations the sum of metallic atoms and oxygen atoms per mol of P in PP are known. Therefore, we can calculate the molar concentration of PP by dividing the concentration of P in PP, which was determined using Equation A2.2e above, by the molar fraction of this P to PP i.e.:

$$MolarMass_{PolyP} = \frac{P_{polyP}}{\left[\frac{31}{31+\left(24\cdot\frac{Mg_{mol}}{P_{mol}}\right)+\left(39\cdot\frac{K_{mol}}{P_{mol}}\right)+\left(40\cdot\frac{Ca_{mol}}{P_{mol}}\right)+(3\cdot16)}\right]}$$

(A2.2h)

Where 39, 40 and 16 are the atomic masses of K, Ca and O respectively and 3 atoms of O are linked to one atom of P in PP.

The corrected Me concentration in PP is then calculated by multiplying the corrected molar fraction of total Me in PP by the molar mass determined, using Equation A2.2h above i.e:

$$Me_{polyP} = MolarMass_{PolyP}\cdot\frac{\left[\left(24\cdot\frac{Mg_{mol}}{P_{mol}}\right)+\left(39\cdot\frac{K_{mol}}{P_{mol}}\right)+\left(40\cdot\frac{Ca_{mol}}{P_{mol}}\right)\right]}{\left[31+\left(24\cdot\frac{Mg_{mol}}{P_{mol}}\right)+\left(39\cdot\frac{K_{mol}}{P_{mol}}\right)+\left(40\cdot\frac{Ca_{mol}}{P_{mol}}\right)+(3\cdot16)\right]}$$

(A2.2i)

Similarly the oxygen in PP is obtained by multiplying its molar fraction in PP by the molar mass of PP, i.e:

$$O_{polyP} = MolarMass_{PolyP} \cdot \frac{[3 \cdot 16]}{\left[31 + \left(24 \cdot \frac{Mg_{mol}}{P_{mol}}\right) + \left(39 \cdot \frac{K_{mol}}{P_{mol}}\right) + \left(40 \cdot \frac{Ca_{mol}}{P_{mol}}\right) + (3 \cdot 16)\right]}$$

(A2.2j)

APPENDIX 3: EXPERIMENTAL SET UP

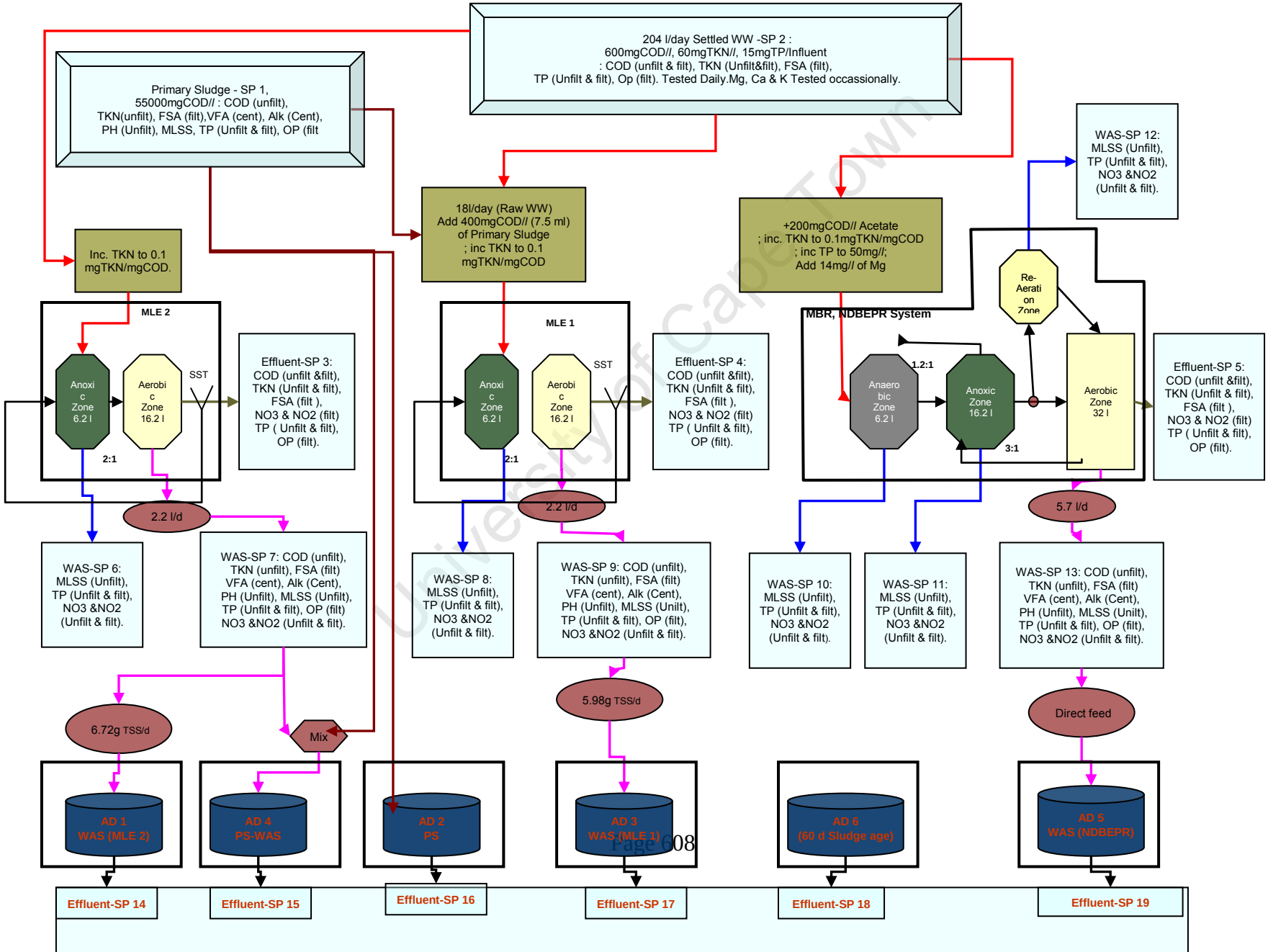

Methane Measurement and COD Removal

The COD concentration removal is directly related to the COD of the CH_4 gas generated in the AD system.

i. The gas volumetric flow rate (ml/d) is measured using the gas flow meter shown in Figure 3.5 described in Section 3.3.8. This unit is connected to a counter that is calibrated in ml per count.

ii. The biogas released from the experimental AD system is captured in gasbags and this gas is then analysed in an external laboratory to determine the CH_4 and CO_2 composition of the biogas. This gas composition is used to determine the volumetric flux f CH_4 (V_{CH4}) and CO_2 (V_{CO2}) released from the AD system as shown below,

$V_{CH4} = Q_{Gas}$ x %Biogas x $\%CH_4$
$V_{CO2} = Q_{Gas}$ x %Biogas x $\%CO_2$

iii. Next, the Ideal Gas Law is applied to determine the molar flux for the CH_4 and CO_2 gases:

$$n_{CH_4} = \frac{[PV_{CH4}]}{RT}$$

and

$$n_{CO_2} = \frac{[PV_{CO2}]}{RT}$$

Where:

P = absolute pressure within the AD system (Pa or atm)
T = AD system temperature (K)
R = universal gas constant = 8.314J/mol K or 0.08206atm. l / mol. K
n_X = moles/d.

The CO_2 gas contains no COD removed from the BPO degraded in the AD system but requires inclusion for carbon balance over the system. Thus,

$$COD_{CH_4} = \frac{n_{CH_4}.MM_{CH_4}.4(gCOD/gCH_4).1000}{Q_i} \qquad \text{(mgCOD/l)}$$

Where:

n_{CH4} = determined in step (a) *(ml/d)*

MM_{CH4} = molar mass of CH_4 = 16 *mg/mol*

Q_i = feed rate *(l/d).*

APPENDIX 4: ADDITIVES USED IN EXPERIMENT

1. Primary sludge added to make Raw WW:

Required is 400mgCOD/*l* (for 40% COD removed),

PS COD is 55000 mg/*l*.

This requires addition of (400 mg/*l* × 1000 ml/*l*)/ 55000mg/*l* = 7.27 ml/*l* of PS, which in 18 l/day equates to 7.27 × 18 = 131 ml of PS.

2. Acetate:

Acetate is taken from from sodium acetate anhydrous (CH_3COONa).

$$CH_3COONa + H_2O \rightarrow CH_3COOH + Na + OH$$
$$CH_3COOH + H_2O \rightarrow 2CO_2 + 8H^+ + 8e^-$$
$$8H^+ + 8e^- + 2O_2 \rightarrow 3H_2O$$

(A4.2)

The COD content = (4× 16)/ 82.03 = 0.7805.

To get 200mgCOD/*l* of this acetate requires 200/ 0.7805 = 256.25 mg/*l*, which in 150 litres = (256.25 × 150) = 38.44 g /day of CH_3COONa.

3. Magnesium:

Required is 0.275 of phosphorus content = 0.275 × 50mg/*l* = 13.8 mg/*l*, i.e. about 14 mg/*l*.

Mg content in $MgCl_2.6H_20$ (Magnesium chloride) = 24.3/ 203.3 = 0.1195.

To get 14 mg/*l* of Mg need, 14/ 0.1195 = 117.13 mg/*l* $MgCl_2.6H_20$.

In 150 l/day, need 117.13mg/*l* × 150l/day = 17.57 g/day.

Prepare stock of 175.7 g/*l* to feed 100ml per day.

4. Phosphorous:

Need 50 mgP/ l.

In Settled WW we already have > 10mgP/*l*.

Need to add 40 mgP/*l*.

P content in K_2HPO_4 (di-Potassium hydrogen ortho-phosphate) = 31/ 174.2 = 0.178

To get 40 mgP/*l*, need 40/ 0.178 = 224.8 mg/*l*.

For 150l/day = 224.8 mg/*l* × 150 l = 33.72 g/day.

Stock = 337.2 g/*l* to feed 100ml/day.

5. Potassium:

Need 0.295 × 50 mgP/*l* = 14.8 mg/*l* of K.

K content in K_2HPO_4 = (39.1× 2)/ 174.2 = 0.449.

To get 14.8 mg/ l need 32.96 mg/*l*, which, in 150 l, gives 4.94 g/day.

In K_2HPO_4 added, we have 33.72g × 0.449 = 15.1 g/day > 4.94.

6. Calcium:

Need 0.05 × 50 mgP/*l* = 2.5mg/*l* of Ca.

Low requirement, assumed to be enough in wastewater.

APPENDIX 5: STEADY STATE AD SPREADSHEET DESIGN EXAMPLE

The most important factor in a successful (most economical and attractive in terms of operability, maintainability and safety) design of an integrated WWTP facility is ensuring that the facility is able to meet the required effluent quality criteria to ensure environmental sustainability. Moreover, it is also important to consider the upstream and downstream effects that each unit process of the plant design has on the performance of the overall WWTP scheme. The plant-wide model can be useful in the design of such a WWTP scheme because it is able to predict, given known influent characteristics, the removals of biodegradable COD, carbon (C), hydrogen (H), oxygen (O), nitrogen (N) and phosphorus (P) and to track the unbiodegradable organic and inorganic material, which cannot be removed but add to the total settleable solids (TSS), hence affect the system volumes, retention times and sludge production.

Presented below is an example of the steady state (assuming constant load and flow conditions) AD model spreadsheet and its use in the design of a wastewater treatment plant (WWTP) for COD, C, H, O, N and P removal. In this example the activated sludge (AS) system volume requirements, oxygen demand and sludge production are calculated, using known influent sewage characteristics and the specified system sludge age. With increased sludge age, it is known that the active fraction of the WAS decreases but the mass of total sludge in the reactor and oxygen consumption increases. Moreover, an AS system treating raw sewage is known to require more oxygen and larger reactor sizes than one treating settled sewage. Other aspects also considered in the plant design include evaluating the impact on design requirements and effluent quality at recycling liquors from the downstream AD unit processes to the upstream AS system.

The WWTP framework for this demonstration are the WWTP layouts of the experimental systems of this investigation i.e. (1) the treatment of raw sewage with

an NDBEPR system (described in Section 2.3.2.2 of Chapter 2) with anaerobic digestion (AD) of its waste activated sludge (WAS); (2) the treatment of settled sewage with the NDBEPR system and the AD of its primary sludge and WAS separately and (3) the treatment of settled wastewater with the same NDBEPR system but with the AD of its primary sludge and WAS blended together are presented. The results obtained from the most favourable design of each of these examples shall thereafter be discussed.

The examples are focused on AD design, purposefully because a major objective of this thesis was to develop and incorporate the three phase AD into the plant-wide steady state model. However, it should be noted that anoxic-aerobic digestion (AerD) is also suitable as a tertiary treatment process for WAS, because it is able to deal with the high N and P sludge concentrations through nitrification-denitrification and promoting P precipitation (Mebrahtu *et al.*, 2010). High N and phosphorus (P) also occurs in AD of P-rich sludge, hence with careful monitoring of the AD and controlled precipitation the AD process can be beneficial in treating secondary sludge. The excess N released from the AD process is commonly treatable later using the SHARON –ANAMMOX process (Volcke 201). Table 2.5 in Section 2.4.4.1 of Chapter 2 shows more about the comparison between AD and AerD treatment processes.

In these simplified design examples, the main design parameters include the sludge age (R_s) and the reasonably selected AS and AD sludge concentrations. Thus for the specified AS sludge age, the AS system volume requirements, oxygen demand, sludge production, sludge active fraction and effluent prediction are determined using the steady state (SS) formulations of an NDBEPR system (developed by Wentzel *et al.*, 1990; see Section 2.3.2.2). Also, for a specified AD sludge age, the AD volume requirements and the quantities of COD, C, H, O, N and P removed are predicted using the SS model (developed in Chapter 6.1 to 6.4). This shows how the SS AD model can be used to aid in predicting system requirements for production of

completely stabilised sludge and effluent that complies with advancing environmental standards.

5.1 Description of Steady State AD Model Spreadsheet

The steady state model developed in Chapter 6 of this thesis (Section 6.1 to 6.4) was programmed into a spreadsheet, with the following model components:

- Biodegradable particulate organics (BPO) of primary sludge (PS) and active biomass of phosphorus accumulating organisms (PAOs) and ordinary heterotrophic organisms (OHOs). These three components get summed up to make the total BPO of the influent AD sludge, which gets hydrolysed to rapidly biodegradable COD as the initial and rate limiting step of the AD process that is modelled by the kinetic section (see Section 6.2).
- Dissociated (Ac^-) and undissociated (HAc) acetic acid and fermentable rapidly biodegradable COD, which make up the influent total rapidly biodegradable COD (RBCOD). The influent RBCOD and that formed from hydrolysis of influent BPO is directly converted during the AD process to methane gas (see Section 6.3).
- Endogenous residue from PAOs and OHOs and unbiodegradable particulate organics (UPO) of PS, which form the total influent UPO. The influent UPO is modelled to accumulate in the AD reactor with sludge age , thus making up a part or all (if the AD sludge age is long enough for complete degradation of biodegradable organics) of the volatile settleable solids (VSS) in the AD effluent. The total VSS in the influent comprises of the total BPO and UPO.
- The influent inorganic settleable solids (ISS) also remain conserved, without being transformed during the AD process. However, the occurrence of precipitation with AD the precipitated minerals add onto the influent ISS causing an increased effluent ISS concentration.

- The total settleable solids (TSS) comprise both the ISS and VSS components and usually dictate the AD volume requirement in the treatment of primary and/or secondary municipal sludge.
- The unbiodegradable soluble COD, which is usually relatively low in the AD of municipal sludge and is conserved in the AD process without undergoing any transformation to form part of the effluent mixed liquor.
- The inorganic soluble material usually comprises of free and saline ammonia (FSA), ortho-phosphates (OP), metallic ions (mainly Magnesium, calcium and potassium) and polyphosphate (PP). Polyphosphate is actually a part of the active PAO mass but has also been included as a separate component in order to unambiguously track its characteristics and stoichiometry. The FSA, OP and PP take part in the AD stoichiometry and weak acid/base chemistry in supplying nutrients or influencing the digester alkalinity hence pH (see Section 6.4).

5.2 Model Spreadsheet Example

Below (Tables A5.1 to A5.8) is an example of the spreadsheet-calculated concentrations for an AD system treating WAS from a nitrification-denitrification biological excess phosphorus removal (NDBEPR) system, at a sludge age of 40 days. This spreadsheet is described in the following sections:

1. The system parameters and kinetic constants (as determined from Section 6.2) are as reported in Table A5.1 below.

Table A5.1: System Parameters in Steady State AD Model Spreadsheet		
Blending factors	PS	**0.00**
	WAS	**1.00**
Thickening factors	Flow into Digester	0.40
	Thickening factor	1.00
Kinetic Constants	K_M	1.92
	K_S	9.15
	Y_{aD}	0.11
	b_{AD}	0.04
	f_{AD}	0.00
Reactor Vol (l)		16.00
AD Sludge age (d)		40.00

2. ***Characterization***: The characteristic fractions (of COD, N and P), which are determined as shown in Chapter 5 are entered into the spreadsheet (highlighted in brown/ dark orange) for the determination the component empirical formulations as shown in Table A5.2 below.

Table A5.2: Characterisation of Feed Sludge in AD Steady State Spreadsheet

Primary Characterisation		Particulate (Residually remaining on .45 micro filter)											Soluble								
Secondary Characterisation				VSS									Organic Soluble				Inorganic Soluble				
Tertiary Characterisation		TSS	ISS	Total VSS	UPO -PS	BPO - PS	PAOs		OHOs		Total BPO	Total UPO	Acetate		F-RBCOD	USCOD	FSA	NO3	OP	metal ions	PP
Characterization	Units						active	endog	active	endog			HAc	Ac-							
Fraction of VSS		1.36	0.00	1.00	0.34	0.00	0.30	0.03	0.22	0.11	0.48	0.52									
Fraction of BPO						0.00	0.58		0.42		1.00										
αCOD				1.45	1.48	1.68	1.43	1.43	1.43	1.43	1.43	1.46	1.07	0.95	1.42	1.42					0.00
αC				0.52	0.52	0.53	0.52	0.52	0.52	0.52	0.52	0.52	0.40	0.41	0.47	0.49					0.00
αN				0.091	0.05	0.01	0.13	0.05	0.13	0.05	0.13	0.06	0.00	0.00	0.00	0.09	0.78	0.23			0.00
αPP											0.00	0.00							0.32		0.28
αPBM				0.03	0.03	0.00	0.036	0.04	0.036	0.04	0.04	0.03	0.00	0.00	0.23	0.30					
fPu				0.02	0.030	0.00	0.003	0.0355	0.003	0.0355	0.00	0.03									
αH				0.050	0.062	0.081	0.061	0.055	0.061	0.055	0.06	0.06	0.067	0.051	0.019	0.002	0.22		0.02		0.00
αO				0.241	0.343	0.381	0.258	0.345	0.258	0.345	0.26	0.34	0.533	0.542	0.281	0.126		0.77	0.66		0.46
αMg																					0.09
αK																					0.20
αCa																					0.02
Carbon	X			13024.55	4099.44	0.00	4254.58	363.90	3053.15	1253.48	6723.11	6301.43	0.00	0.00	0.01	18.81	22.72	31.84			0.00
Hydrogen	Y			63.21	33.78	3.52	91.07	35.03	91.07	35.03	91.07	38.52	0.00	0.00	0.00	62.12					
Oxygen	Z	0.53		0.52	1.00	0.00	0.08	1.00	0.08	1.00	0.08	1.00	0.00	0.00	0.00	1.00					
Nitrogen	A	0.40	0.40	0.40	0.40	0.40	0.40	0.40	0.40	0.40	0.40	0.40	0.40	0.40	0.40	0.40	0.40	0.40	0.40	0.40	0.40
P in Biomass	B						165.26														
linkage factor	q																				
P in polyphosphate				60.52	21.28	0.00	16.92	3.04	12.14	6.88	29.06	31.45	0.00	0.00	0.00	0.00	0.36	0.50	0.53	1.00	18.38
Magnesium (Mg+2)						0.00	6.77		4.86		11.63										
Potasium (K+)				9.81	0.00	0.00	5.71	0.00	4.10	0.00	9.81	0.00	0.00	0.00	0.00						
Calcium (Ca+2)				4.96	4.84	3.80	4.91	5.48	4.91	5.48	4.91	5.00	2.00	2.00	14.46	158.91	0.00	0.00	0.00	0.00	0.00
Metal (K or Mg)	Me +			7.00	7.00	7.00	7.00	7.00	7.00	7.00	7.00	7.00	4.00	3.00	7.00	7.00	4.00	0.00	1.00	0.00	0.00
Charge	e-			2.16	2.42	2.05	1.85	2.75	1.85	2.75	1.85	2.45	2.00	2.00	6.49	30.73	0.00	3.00	4.00	0.00	3.00
Mol Mass biological	g/mol			0.75	0.40	0.04	1.06	0.46	1.06	0.46	1.06	0.47	0.00	0.00	0.00	24.67	1.00	1.00	0.00	0.00	0.00
EDC/mol or Ds	Ds			0.13	0.11	0.00	0.13	0.15	0.13	0.15	0.13	0.12	0.00	0.00	2.74	37.57	0.00	0.00	1.00	0.00	0.00

Table A5.2: Characterisation of Feed Sludge in AD Steady State Spreadsheet

Primary Characterisation		Particulate (Residually remaining on .45 micro filter)											Soluble									
Secondary Characterisation				VSS									Organic Soluble			Inorganic Soluble						
Tertiary Characterisation		TSS	ISS	Total VSS	UPO from PS	BPO from PS	PAOs		OHOs		Total BPO	Total UPO	Acetate		F-RBCOD	USCOD	FSA	NO3 + NO2	Ortho-P	Metals	PP inside PAOs	Mixed Liquor
Substrate Characterization	Units						active	endog (UPO)	active	endog (UPO)			HAc	Ac-								
concentration	mg/l	9494.50	2504.00	6990.50	2399.34	0.00	2104.38	219.74	1510.14	756.90	3325.36	3665.14	0.00	0.00	0.01	10.32	6.39	30.84	51.33		1913.88	9494.50
Biodegradable org or VSS	mgVSS/l	3325.36		3325.36	0.00	0.00	1936.03	0.00	1389.33	0.00	3325.36	0.00	0.00	0.00	0.01	0.00						
Unbio. Organics or VSS	mgVSS/l	3665.14		3665.14	2399.34	0.00	168.35	219.74	120.81	756.90	0.00	3665.14	0.00	0.00	0.00	10.32						
Total COD	mgCOD/l	10104.84		10104.84	3551.02	0.00	3003.97	313.67	2155.70	1080.47	4746.90	5357.94	0.00	0.00	0.01	14.65					0.00	10119.49
Sbi (influent Bio. COD)	mgCOD/l	4746.90		4746.899	0.00	0.00	2763.65	0.00	1983.24	0.00	4746.90	0.00	0.00	0.00	0.01	0.00						
Sui (influent Unbio. COD)	mgCOD/l	5357.94		5357.937	3551.02	0.00	240.32	313.67	172.46	1080.47	0.00	5357.94	0.00	0.00	0.00	14.65						
N	mgN/l	638.69		638.69	119.97	0.00	273.57	10.99	196.32	37.85	432.30	206.39	0.00	0.00	0.00	0.91	4.97	6.96			0.00	644.57
XPGBM	mgP/l	68.80		68.80			68.80				68.80	0.00										
XPGPP (PP)	mgP/l	0.00		0.00							0.00	0.00									583.38	
XPHBM	mgP/l	49.37		49.37					49.37		49.37	0.00										
XBP	mgP/l	118.17		118.17		0.00	68.80		49.37		118.17	0.00							16.41			
XPU	mgP/l	116.96		116.96	71.98		5.98	7.81	4.29	26.90	0.00	116.96										
XTP	mgP/l	235.13		235.13	71.98	0.00	74.78	7.81	53.67	26.90	118.17	116.96	0.00	0.00	0.00	3.07			16.41		583.38	837.98
Mg	mg/l	0.00																		80.60	171.20	251.80
K	mg/l	0.00																		75.40	372.53	447.93
Ca	mg/l	0.00																		21.75	31.11	52.86
Influent VFA																						0.00
Influent Alkalinity	mg/l as $CaCO_3$																					150.00
Influent pH																						8.00

The component characteristics, determined in the Table A5.2 above, are used together with the measured influent component concentrations (highlighted in Table A5.3 below) to determine the various influent component COD, N and P concentrations.

3. ***Predicting the COD removal by hydrolysis and AD stoichiometric products*:** The influent characteristics (Table A5.2) together with the kinetic and stoichiometric constants are used to predict the sludge hydrolysis, COD removal and stoichiometric AD effluent products. These predictions are first done with the assumption of the products being infinitely soluble, i.e. not partaking in mineral precipitation.

Table A5.3: The AD Steady State Model Spreadsheet Calculated Stoichiometric Products for Infinite Solubility

Primary Characterisation		Particulate (Residually remaining on .45 micro filter)											Soluble									
Secondary Characterisation				VSS									Organic Soluble				Inorganic Soluble					
Tertiary Characterisation		TSS	ISS	Total VSS	UPO from PS	BPO from PS	PAOs		OHOs		Total BPO	Total UPO	Acetate		F-RBCOD	USCOD	FSA	NO3 + NO2	Ortho-P	Metals or metal ions	PP inside PAOs	Mixed Liquor
Substrate Characterization	Units						active	endog (UPO)	active	endog (UPO)			HAc	Ac-								
BPO in influent	mmol/d					0.00	6.77		4.86		11.63											
Residual (VSS)	mmol/d			14.39	8.51	0.00	1.05	0.69	0.76	2.37	1.81	12.58	0.00	0.00	0.00	0.00	6.33	0.00	5.17		0.00	
BPO removed	mmole/d			9.81	0.00	0.00	5.71	0.00	4.10	0.00	9.81	0.00	0.00	0.00	0.00							
f value before pptn.				0.63	0.00	0.63	0.63	0.00	0.63	0.00	0.63	0.00	0.00	0.00	0.63	0.00	0.00	0.00	0.63	0.00	0.00	0.63
Water (H_2O)	mmol/*l*			40.89	0.00	0.00	17.13	0.00	17.08	0.00	40.89		0.00	0.00	0.00	0.00		0.00		0.00		40.89
AD Products for infinite solubility of precipitates																						
AD Biomass	mmol/d			0.45		0.00	0.26		0.19		0.45		0.00	0.00	0.00							0.45
Frac Sludge E	E			0.05		0.05	0.05		0.05		0.05				0.05							
CO_2	mmol/d			10.90	0.00	0.00	5.14	0.00	5.75	0.00	10.90	0.00	0.00	0.00	0.00	0.00	0.00	0.00	0.00	0.00	0.00	8.27
Methane (CH_4)	mmol/d			23.89	0.00	0.00	13.91	0.00	9.98	0.00	23.89	0.00	0.00	0.00	0.00	0.00	0.00	0.00	0.00	0.00	0.00	23.89
Ammonia (NH_4^+)	mmol/d			9.99	0.00	0.00	5.82	0.00	4.17	0.00	9.99	0.00	0.00	0.00	0.00	0.00	0.14		0.00	0.00	0.00	10.13
Bicarbonate (HCO_3^-)	mmol/d			10.56	0.00	0.00	7.10	0.00	3.47	0.00	10.56	0.00	0.00	0.00	0.00	0.00	0.00	0.00	0.00	0.00	0.00	11.76
Phosphate ($H_2PO_4^-$)	mmol/d			5.49	0.00	0.00	5.17	0.00	0.32	0.00	5.49	0.00	0.00	0.00	0.00	0.00	0.00	0.00	0.13	0.00		5.63
Phosphate (HPO_4^{2-})	mmol/d			3.27	0.00	0.00	3.07	0.00	0.19	0.00	3.27	0.00	0.00	0.00	0.00	0.00	0.00	0.00	0.08	0.00		3.34
Metallic ions (Me^+)	mmol/d			0.00	0.00	0.00	6.25	0.00	0.00	0.00	6.25	0.00	0.00	0.00	0.00	0.00	0.00	0.00	0.00	2.32		8.57
Magnesium (Mg^{+2})	mmol/d			0.00	0.00	0.00	2.82	0.00	0.00	0.00	2.82	0.00	0.00	0.00	0.00	0.00	0.00	0.00	0.00	1.33	In Active PAO Stoich.	4.14
Potassium (K^+)	mmol/d			0.00	0.00	0.00	3.82	0.00	0.00	0.00	3.82	0.00	0.00	0.00	0.00	0.00	0.00	0.00	0.00	0.77		4.59
Calcium (Ca^{+2})	mmol/d			0.00	0.00	0.00	0.31	0.00	0.00	0.00	0.31	0.00	0.00	0.00	0.00	0.00	0.00	0.00	0.00	0.22		0.53
$H_2CO_3^*$	mmol/d					0.00	1.60		0.78		2.38		0.00	0.00	0.00							2.65

4. ***Calculating precipitation potentials***: The total AD products, assuming their infinite solubility, that form the predicted mixed liquor (shown in the last column of Table A5.3 above) are used to calculate the total concentrations of the species that are likely to participate in mineral precipitation, hence determine the precipitation potential. This is done by weighing the molar products of the species used to form specific precipitate against its solubility product (see Section 6.4). Table A5.4 below shows the precipitation potential output predicted by the spreadsheet, for this example.

Table A5.4: Total Species Concentrations Before Precipitation in Steady State Model Spreadsheet (in mol/*l*)

Total Species Concentrations in Mixed Liquor, Assuming Infinite Solubility (mol/*l*)	CT	0.0360258
	NT	0.0253262
	PT	0.0224275
	Magnesium (Mg^{2+})	0.0103621
	Potassium (K^{+})	0.0114853
	Calcium (Ca^{2+})	0.0013215
Mineral Solubility Products	Struvite (R)	2.51E-13
	ACP (V)	3.47E-26
	Calcite (Q)	3.80E-09
Precipitation potential (mol/*l*)	**Struvite (R)**	**1.04E-02**
	ACP (V)	**0.00**
	Calcite (Q)	**1.32E-03**

5. ***Post- precipitation stoichiometric AD products***: With the precipitation potential determined, as shown above, the AD effluent products can be recalculated, including the precipitates formed and relative reductions in the liquid-phase concentrations of species used to form the precipitates (explained in more detail in Section 6.4). The Table A5.5 below shows the example output for this section of the spreadsheet.

Table A5.5: Post Precipitation AD Stoichiometric Products in AD Steady State Model Spreadsheet

Primary Characterisation		**Particulate (Residually remaining on .45 micro filter)**											**Soluble**									
Secondary Characterisation				**VSS**									**Organic Soluble**				**Inorganic Soluble**					
Tertiary Characterisation		**TSS**	**ISS**	Total VSS	UPO from PS	BPO from PS	PAOs		OHOs		Total BPO	Total UPO	Acetate		F-RBCOD	USCOD	FSA	NO3 + NO2	Ortho-P	Metals or metal ions	PP inside PAOs	Mixed Liquor
Substrate Characterization	**Units**						active	endog (UPO)	active	endog (UPO)			HAc	Ac-								
f value after pptn.	f			0.80	0.00	0.80	0.80	0.00	0.80	0.00	0.80	0.00	0.00	0.00	0.80	0.00	0.00	0.00	0.80	0.00	0.00	0.80
CO_2	mmol/d			16.33	0.00	0.00	7.07	0.00	9.26	0.00	16.33	0.00	0.00	0.00	0.00	0.00	0.00	0.00	0.00	0.00	0.00	13.78
Methane (CH_4)	mmol/d			23.89	0.00	0.00	13.91	0.00	9.98	0.00	23.89	0.00	0.00	0.00	0.00	0.00	0.00	0.00	0.00	0.00	0.00	23.89
Ammonia (NH_4^+)	mmol/d			6.24	0.00	0.00	3.63	0.00	2.61	0.00	6.24	0.00	0.00	0.00	0.00	0.00	0.09	0.00	0.00	0.00	0.00	6.33
Bicarbonate (HCO^{3-})	mmol/d			5.81	0.00	0.00	4.26	0.00	1.54	0.00	5.81	0.00	0.00	0.00	0.00	0.00	0.00	0.00	0.00	0.00	0.00	6.31
Phosphate (H_2PO^{4-})	mmol/d			4.01	0.00	0.00	3.78	0.00	0.24	0.00	4.01	0.00	0.00	0.00	0.00	0.00	0.00	0.00	0.10	0.00	In Active PAO Stoich.	4.11
Phosphate (HPO_4^{2-})	mmol/d			1.03	0.00	0.00	0.97	0.00	0.06	0.00	1.03	0.00	0.00	0.00	0.00	0.00	0.00	0.00	0.03	0.00		1.06
Metallic ions (Me^+)	mmol/d			4.37	0.00	0.00	4.37	0.00	0.00	0.00	4.37	0.00	0.00	0.00	0.00	0.00	0.00	0.00	0.00	1.10		5.47
Magnesium (Mg^{+2})	mmol/d			0.00	0.00	0.00	0.23	0.00	0.00	0.00	0.23	0.00	0.00	0.00	0.00	0.00	0.00	0.00	0.00	0.11		0.34
Potassium (K^+)	mmol/d			0.00	0.00	0.00	3.82	0.00	0.00	0.00	3.82	0.00	0.00	0.00	0.00	0.00	0.00	0.00	0.00	0.77		4.59
Calcium (Ca^{+2})	mmol/d			0.00	0.00	0.00	0.31	0.00	0.00	0.00	0.31	0.00	0.00	0.00	0.00	0.00	0.00	0.00	0.00	0.22		0.53
H_2CO_3*	mmol/d					0.00	2.21		0.80				0.00	0.00	0.00							3.28
Residual (VSS)	mmol/d			14.39	8.51	0.00	1.05	0.69	0.76	2.37	1.81	12.58	0.00	0.00	0.00	0.00	6.33	0.00	5.17		0.00	
Water (H_2O)	mmol/*l*			18.23	0.00	0.00	6.85	0.00	7.62	0.00	18.23		0.00	0.00	0.00	0.00		0.00		0.00		18.23

6. ***Weak acid/base chemistry section for pH prediction*:** To determine the pH requires the determination of the P species (HPO_4^-, H_2PO_4) fractionation (f) value, which is also is required for the stoichiometric section to determine the AD effluent. Therefore the f value has to be calculated iteratively as shown in Section 6.3, using the species weak acid dissociation constants and ensuring that the carbon dioxide liquid and gas phases are in equilibrium, according to Henrys law constant (Table A5.6).

Table A5.6: Weak Acid Dissociation Constants used in Steady State Model

pK_{C1}	6.31
pK_{C2}	10.25
pK_{P2}	7.18
pK_n	8.95
pK_a	38.64
Temp	34.85
Henry's Law constant (pK_H)	1.6

Table A5.7: The Calculated f value (Based on P_T subsystem species) in the Steady State Model Spreadsheet

In the influent	f	0.13
In the AD reactor mixed liquor for Infinite solubility (no precipitation)	f	0.627
	pCO_2 left *	0.29563
	pCO_2 right *	0.25724
Predicted precipitatates to be formed (mmol/day) in AD reactor mixed liquor	Total struvite($MgNH_4PO_3$) precipitation potential	4.1449
	Struvite redissolved due to low pH	0.3449
	R (Net Struvite precipitate)	3.8000
	V (amount of$Ca_3(PO_4)_2$precipitate)	0.000043820
	Q (amount of $CaCO_3$ precipitate)	0
In the AD reactor mixed liquor after precipitation	f new	0.795
	pCO_2 left *	0.3658
	pCO_2 right *	0.3658
Where pCO_2 left represent the pCO_2 calculated from stoichiometrically predicted ratio of CO_2 in the total gases and right is calculated from HCO_3^- using pK values.		

The validation of the steady state model, by comparing the predicted to measured results is done in the following Chapter 7 together with the dynamic model, coded in the WEST® software, when simulated at steady state conditions that replicate the experimental layout of the project. This is possible because all the data accumulated in the experimental investigation was under steady state operation of the systems.

Design Trials for Various Plant-Wide AD Configurations

Below is a design example of how the steady state model can be used in designing plants of various configurations for the treatment of sewage in serving 10000 people at 150 l/person-day =15000m^3/day , with the use of AD in sludge treatment. The Table A5.8 below shows the sewage characteristics.

Table A5.8: Influent Characteristics of Plant for Design Example

Parameters	Raw Sewage	Settled WW	Primary Sludge	Units
Flow	1627.02	1500.00	127.02	m^3/d
Total COD	1467.34	788.77	9480.74	gCOD/m^3
Biodegradable Soluble COD	359.09	260.41	1524.38	gCOD/m^3
VFA	223.72	200.00	503.87	gCOD/m^3
Total Biodegradable COD	1251.41	688.73	7896.31	gCOD/m^3
Biodegradable Particulate COD	892.33	428.32	6371.93	gCOD/m^3
Unbiodegradable Particulate COD	181.80	78.88	1397.21	gCOD/m^3
Unbiodegradable Soluble COD	34.13	21.17	187.22	gCOD/m^3
Total Unbiodegradable COD	215.93	100.05	1584.43	gCOD/m^3
TKN	57.63	46.20	192.62	gN/m^3
FSA	34.05	32.98	46.61	gN/m^3
TP	60.31	30.00	418.26	gP/m^3
OP	30.50	20.00	154.45	gP/m^3
Total settleable solids	534.26	167.00	4871.37	g/m^3
Volatile settleable Solids	433.40	142.80	3865.16	g/m^3
Inorganic settleable Solids	100.86	24.20	1006.21	g/m^3

For the treatment of sewage with the above influent characteristics, the following plant design options are considered:

1. Physical separation of raw wastewater (using a primary settling tank, PST, that produces settled wastewater with an assumed COD removal of 40% from the raw wastewater) to primary sludge and settled wastewater. With this separation, the influent settled sewage is treated with the NDBEPR UCT process AS system and two separate completely mixed, mesophilic anaerobic digesters are used for the treatment of primary sludge (PS, treated in AD1) and WAS (treated in AD2), as shown in the Figure A5.1 below.

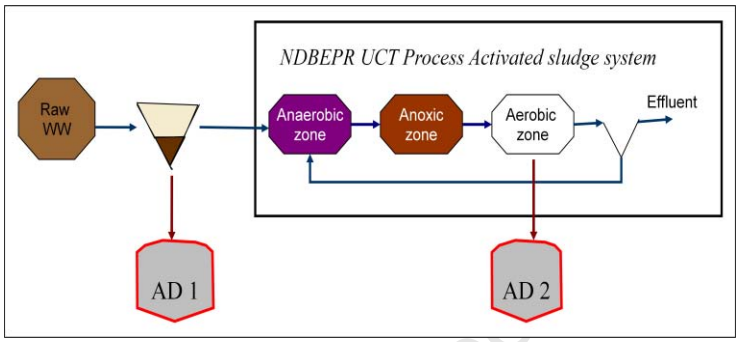

Figure A5.1: *Plant configuration 1*

2. On separation of raw sewage to settled wastewater and PS, the settled wastewater is treated using the NDBEPR UCT process and the PS and WAS are blended into one completely mixed, mesophilic anaerobic digester as shown in the Figure A5.2 below.

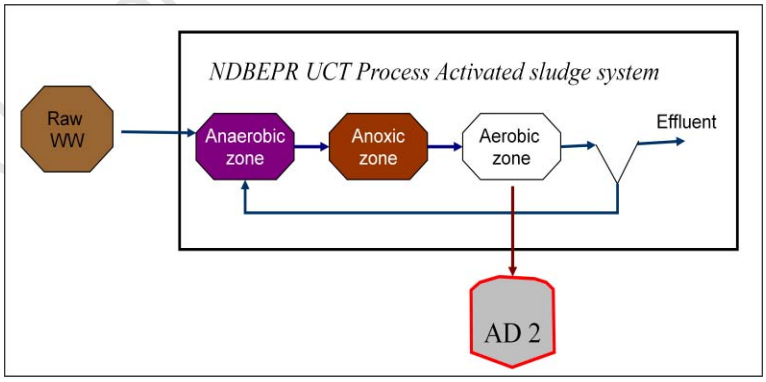

Figure A5.2: *Plant configuration 2*

3. Treatment of influent raw sewage (no primary sludge production) by a NDBEPR UCT process AS system and treatment of the WAS using a completely mixed, mesophilic (operated at 37°C) AD system as shown in the Figure A5.3 below.

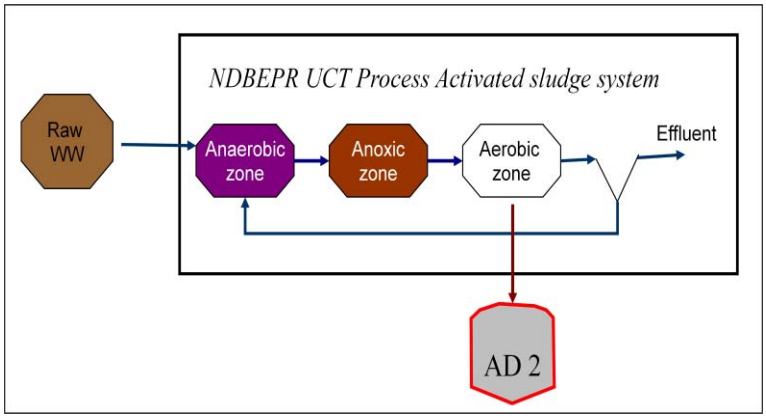

Figure A5.3: *Plant configuration 3*

The Table A5.9 below shows the system requirements for the each of the selected plant–wide configurations.

A crucial step for the design process is to select a suitable total settleable solids (TSS) concentration. Although it is more economical to allocate a higher TSS concentration, other considerations are also made; such as initial and running cost of the sludge recirculation system, limitations of oxygen transfer equipment to supply oxygen at required, increased solids loading on secondary clarifier, which may necessitate a larger surface area, design criteria for the tank and minimum HRT (Henze *et al.*, 2008). In the design of the AD, the first important step made was to determine the correct reactor volume that would ensure sufficient stabilisation of the feed and methane gas production. The calculation of this reactor volume and digester products is based on the selection of the AD sludge retention time (SRT) as the principle design parameter and organic loading rate, which in completely mixed AD systems are directly related. In this case, the AD SRT of 35 days was considered, since it is essentially high enough to ensure that the system does not to fail due to the wash out of methanogens and that the feed sludge is stabilised satisfactorily. The sludge concentration to the AD was selected to be 15000 g/m^3. This concentration was fixed in this way because, as the case with the AS system, despite the cost effectiveness of having higher solids concentration in the AD, over-thickening of the AD feed sludge could interfere with the effective mixing, which helps to keep most of the accumulating scum and grit dispersed through the digesting tank.

Table A5.9a: plant-wide System Requirements for Selected Plant Configurations					
Configuration *		Configuration 1	Configuration 2	Configuration 3	Units
AS System Requirements	Carbonaceous oxygen demand	718473.64	718473.64	1455815.32	gO
	Nitrification oxygen demand	171141.58	171141.58	142286.17	gO
	Oxygen recovery by denitrification	91803.36	91803.36	76324.81	gO
	Net oxygen demand	797811.86	797811.86	1521776.67	gO
	Oxygen utilization rate	24.36	24.36	22.28	mgO/l/d
	Temperature	21.00	21.00	21.00	^{o}C
	Selected sludge age	20.00	20.00	20.00	days
	Selected aerobic TSS	4000.00	4000.00	4000.00	g/m^3
	Required reactor volume	2274.12	2274.12	4743.20	m^3
	Maximum un-aerated mass fraction	0.83	0.83	0.83	
	Minimum primary anoxic sludge mass fraction	0.13	0.13	0.13	
	Chosen un-aerated sludge mass fraction	0.40	0.40	0.40	
	Anaerobic sludge mass fraction	0.15	0.15	0.15	
	anaerobic volume	341.12	341.12	711.48	m^3
	anoxic volume	568.53	568.53	1185.80	m^3
	aerobic volume	1364.47	1364.47	2845.92	m^3
	Optimum a-recycle ratio	10.09	10.09	62.64	
	Selected a-recycle ratio	5.00	5.00	5.00	
	Waste sludge flow rate	113.71	113.71	237.16	m^3/d
AD Systems Requirements	AD 1 sludge total solids concentration	15000.00	0.00	0.00	g/m^3
	AD 1 minimum sludge age	35.00	0.00	0.00	days
	AD 1 volume	2911.90	0.00	0.00	m^3
	PS thickening	3.08	3.08	0.00	
	PS flow to AD	83.20	41.25	0.00	m^3/d
	AD 2 sludge concentration	15000.00	15000.00	15000.00	g/m^3
	AD 2 minimum sludge age	35.00	35.00	35.00	days
	AD 2 volume	1061.25	2505.03	2213.49	m^3
	WAS thickening	3.75	3.75	3.75	
	WAS flow to AD	30.32	30.32	63.24	m^3/d
	AD Temperature	35.00	35.00	35.00	^{o}C
Total Volume requirements		6247.27	4779.14	6956.70	m^3
* The configurations 1, 2 and 3 are described according to the plant design options depicted by Figures A5.1, A5.2 and A5.3 respectively.					

It can be noticed that the total volume requirements for the plant configuration 2, that has an AD treating the blended PS and WAS is the least. Despite this, the

configuration 1 and 2 have the same AS system oxygen requirements, since they are both treating the same loads of settled wastewater and the only difference is that one configuration channels primary and secondary sludge to one large digester instead of two smaller ones. The third configuration requires more volume than the other two configurations and has a higher net oxygen demand. This is because the raw WW in this configuration omits primary treatment, hence higher solids, COD, N and P loads are taken into the AS system. However, this downside could be weighed against the benefits foregone by not including the primary settling tank. The Table A5.9 below shows the predicted effluent quality for the various configurations.

Table A5.9b: AS and AD System Effluent Quality for the Various Selected Plant Configurations

Configuration *			Configuration 1	Configuration 2	Configuration 3	Units
AS System	Effluent	Total COD	21.17	21.17	34.13	gCOD/m^3
		TP	1.19	1.19	17.66	gP/m^3
		OP	0.29	0.29	15.85	gP/m^3
		TKN	1.63	1.63	1.98	gN/m^3
		FSA	0.25	0.25	0.25	gN/m^3
	Waste Sludge	Total settleable solids	454823	454823	948640	g/d
		Volatile settleable solids	294007	294007	594153	g/d
		Inorganic settleable solids	160816	160816	354488	g/d
		Active OHO mass	48906.1	48906.1	110249	g/d
		Active PAO mass	96903.6	96903.6	145247	g/d
		PAO endogenous residue	19942.8	19942.8	29891.8	g/d
		OHO endogenous residue	48311.4	48311.4	108908	g/d
		Total endogenous residue	68254.1	68254.1	138800	g/d
		Inert material from influent	79942.9	79942.9	199857	g/d
		Inert material	148197	148197	338657	g/d
		Polyphosphate	34400.8	34400.8	51562.6	gP/d

Table A5.9b: AS and AD System Effluent Quality for the Various Selected Plant Configurations						
Configuration *			Configuration 1	Configuration 2	Configuration 3	Units
AD System	AD 1 Effluent	CO_2 produced	390740	0	0	g/d
		CH_4 produced	210330	0	0	g/d
		Digester pH	6.8	0	0	
		Digester alkalinity	2108.52	0	0	g/m³ as $CaCO_3$
		Total settleable solids	3740.69	0	0	g/m³
		Volatile settleable solids	2204.45	0	0	g/m³
		Inorganic settleable solids	1536.24	0	0	g/m³
		Total unbiodegradable COD	2133.17	0	0	gCOD/m³
		Total biodegradable COD	1223.44	0	0	gCOD/m³
		TKN	457.74	0	0	gN/m³
		FSA	301.92	0	0	gN/m³
		TP	314.54	0	0	gP/m³
		OP	244.76	0	0	gP/m³
	AD 2 Effluent	CO_2 produced	53905.6	223700	45652.1	gCO_2/d
		CH_4 produced	38901.2	146152	32681.4	gCH_4/d
		Digester pH	6.95	6.96	6.9	
		Digester alkalinity	3233.06	2741.57	2619.83	g/m³ as $CaCO_3$
		Total settleable solids	11595.3	7068.28	12366.4	g/m³
		Volatile settleable solids	6245	3916.23	6495.32	g/m³
		Inorganic settleable solids	5350.27	3152.05	5871.04	g/m³
		Total unbiodegradable COD	7820.81	4542.74	8422.86	gCOD/m³
		Total biodegradable COD	1430.87	1311.32	1202.09	gCOD/m³
		TKN	1926.64	1608.88	2340.7	gN/m³
		FSA	353.06	323.59	309.14	gN/m³
		TP	1429.5	786.83	1161.46	gP/m³
		OP	771.15	467.77	596	gP/m³

Design Options for Plant Expansion

With the increasing growths in populations due to birth rates and rural urban migrations, the WWTP may require expansion after a certain design period. The Table A5.10 below shows the system requirements if the flow to the plant increases from 1500 m^3/d to 2500 m^3/d and ;

a. the same AS system sludge age (20 days) is employed, hence both AS and AD systems are expanded or
b. the AS system sludge age is reduced to 10 days to ensure that it has no further volume requirements but gives out more active biomass and a higher waste flow rate, thereby increasing the volume requirements for the AD system (i.e. the more material loads pushed to the AD systems hence their sole expansion). The AS system R_s was not reduced further, to less than 10 days, to ensure that COD, N and P removal all take place.

Table A5.10: plant-wide System Requirements for Selected Plant Configurations								
Design Options		Expand Both AS and AD systems			Expand AD system			
Configuration *		Config. 1	Config. 2	Config. 3	Config. 1	Config. 2	Config. 3	Units
AS System Requirements	Carbonaceous oxygen demand	1197456.06	1197456.06	2426358.86	1077155.81	1077155.81	2194151.79	gO
	Nitrification oxygen demand	285235.97	285235.97	237143.61	246210.45	246210.45	163516.83	gO
	Oxygen recovery by enitrification	153005.61	153005.61	127208.01	132071.63	132071.63	87713.31	gO
	Net oxygen demand	1329686.43	1329686.43	2536294.46	1191294.63	1191294.63	2269955.31	gO
	Oxygen utilization rate	24.36	24.36	22.28	36.71	36.71	34.35	mgO/l/d
	Temperature	21.00	21.00	21.00	21.00	21.00	21.00	^{o}C
	Selected sludge age (R_s)	20.00	20.00	20.00	10.00	10.00	10.00	days
	Selected aerobic TSS	4000.00	4000.00	4000.00	4000.00	4000.00	4000.00	g/m^3
	Required reactor volume	3790.19	3790.19	7905.34	2253.85	2253.85	4589.16	m^3
	Maximum unaerated mass fraction	0.83	0.83	0.83	0.74	0.74	0.74	
	Minimum primary anoxic sludge mass fraction	0.13	0.13	0.13	0.15	0.15	0.15	
	Chosen unaerated sludge mass fraction	0.40	0.40	0.40	0.40	0.40	0.40	
	Anaerobic sludge mass fraction	0.15	0.15	0.15	0.15	0.15	0.15	
	Anaerobic volume	568.53	568.53	1185.80	338.08	338.08	688.37	m^3
	Anoxic volume	947.55	947.55	1976.33	563.46	563.46	1147.29	m^3
	Aerobic volume	2274.12	2274.12	4743.20	1352.31	1352.31	2753.49	m^3
	Optimum a-recycle ratio	10.09	10.09	62.64	10.78	10.78	63.40	
	Selected a-recycle ratio	5.00	5.00	5.00	5.00	5.00	5.00	
	Waste sludge flow rate	189.51	189.51	395.27	225.38	225.38	458.92	m^3/d
AD Systems Requirements	AD 1 chosen sludge total solids concentration	15000.00	0.00	0.00	15000.00	0.00	0.00	g/m^3
	AD 1 minimum sludge age	35.00	0.00	0.00	35.00	0.00	0.00	days
	AD 1 volume	4853.16	0.00	0.00	4853.16	0.00	0.00	m^3
	PS thickening	3.08	3.08	0.00	3.08	3.08	0.00	
	PS flow to AD	138.66	68.75	0.00	138.66	68.75	0.00	m^3/d
	AD 2 sludge concentration	15000.00	15000.00	15000.00	15000.00	15000.00	15000.00	g/m^3
	AD 2 minimum sludge age	35.00	35.00	35.00	35.00	35.00	35.00	days
	AD 2 volume	1768.76	4175.04	3689.16	2103.59	4509.88	4283.21	m^3
	WAS thickening	3.75	3.75	3.75	3.75	3.75	3.75	
	WAS flow to AD	50.54	50.54	105.40	60.10	60.10	122.38	m^3/d
	AD temperature	35.00	35.00	35.00	35.00	35.00	35.00	^{o}C
Total volume requirements		10412.11	7965.24	11594.49	9210.61	6763.73	8872.37	8872.37

As is notable in Table A5.10, the total volume requirements are generally higher with the expansion of both AS and AD systems. It may be necessary to expand both AS and AD unit operations if the increased influent load would lead to the production of sludge mass that is too high to maintain reasonable reactor concentrations and an adequate system sludge age, without increasing the reactor volumes. The configuration 2 is again found to have the least volume requirements but similar net oxygen demand as configuration 1. However, before selecting it as the best option, other factors also require consideration, such as the energy savings that could be generated by the methane produced and the extra costs from providing required settling tanks.

It is also notable that the capital costs (for the provision of the AS system and sludge handling) may vary according to AS and AD system sludge ages that are selected as acceptable to meet required effluent criteria. Depending on the influent characteristics the sludge age is chosen carefully to cater for COD and nutrient (N and P) removal in the AS system. With increased AS system sludge age:

1. The OUR increases.
2. The sludge mass in reactors (hence volume requirements) increases.
3. The active fraction of sludge decreases hence the connected AD sludge age is lower.
4. The sludge wasted is also less hence, the connected AD volume requirements are decreased.

In the AD system, the selected sludge age would also depend on the sludge type and its hydrolysis (the rate limiting step in AD) rate. The AD system requires its operation to be above the minimum sludge age that would allow all the biodegradable COD to be reduced. The AS and AD system predicted effluent characteristics are presented in the following Table A5.11.

Table A5.11: AS and AD System Effluent Quality for the Various Selected Plant Configurations									
Design Options			Expand Both AS and AD systems			Expand AD system			
Configuration *			Config. 1	Config. 2	Config. 3	Config. 1	Config. 2	Config. 3	Units
AS System	Effluent	Total COD	21.17	21.17	34.13	21.17	21.17	34.13	gCOD/m^3
		TP	1.19	1.19	17.66	0	0	6.88	gP/m^3
		OP	0.29	0.29	15.85	0	0	5.07	gP/m^3
		TKN	1.63	1.63	1.98	1.82	1.82	2.16	gN/m^3
		FSA	0.25	0.25	0.25	0.44	0.44	0.44	gN/m^3
	Waste Sludge	Total settleable solids	758038.64	758038.64	1581067.4	901539.87	901539.87	1835662.1	g/d
		Volatile settleable solids	490011.16	490011.16	990254.28	570699	570699	1146257.5	g/d
		Inorganic settleable solids	268027.48	268027.48	590813.1	330840.86	330840.86	689404.68	g/d
		Active OHO mass	81510.11	81510.11	183747.88	139527.56	139527.56	314536.38	g/d
		Active PAO mass	161506	161506	242077.83	207650.57	207650.57	311242.93	g/d
		PAO endogenous residue	33237.93	33237.93	49819.62	21367.24	21367.24	32026.9	g/d
		OHO endogenous residue	80518.94	80518.94	181513.51	68915.45	68915.45	155355.81	g/d
		Total endogenous residue	113756.88	113756.88	231333.12	90282.7	90282.7	187382.7	g/d
		Inert material from influent	133238.18	133238.18	333095.44	133238.18	133238.18	333095.44	g/d
		Total Inert material	246995.05	246995.05	564428.56	223520.87	223520.87	520478.14	g/d
		Polyphosphate	57334.63	57334.63	85937.63	73715.95	73715.95	110491.24	gP/d

Table A5.11: AS and AD System Effluent Quality for the Various Selected Plant Configurations									
Design Options			Expand Both AS and AD systems			Expand AD system			
Configuration *			Config. 1	Config. 2	Config. 3	Config. 1	Config. 2	Config. 3	Units
AD System	AD 1 Effluent	CO_2 produced	651233.21	0	0	651233.21	0	0	g/d
		CH_4 produced	350549.57	0	0	350549.57	0	0	g/d
		Digester pH	6.8	0	0	6.8	0	0	
		Digester alkalinity	2108.52	0	0	2108.52	0	0	g/m^3 as $CaCO_3$
		Total settleable solids	3740.69	0	0	3740.69	0	0	g/m^3
		Volatile settleable solids	2204.45	0	0	2204.45	0	0	g/m^3
		Inorganic settleable solids	1536.24	0	0	1536.24	0	0	g/m^3
		Total unbiodegradable COD	2133.17	0	0	2133.17	0	0	gCOD/m^3
		Total biodegradable COD	1223.44	0	0	1223.44	0	0	gCOD/m^3
		TKN	457.74	0	0	457.74	0	0	gN/m^3
		FSA	301.92	0	0	301.92	0	0	gN/m^3
		TP	314.54	0	0	314.54	0	0	gP/m^3
		OP	244.76	0	0	244.76	0	0	gP/m^3
		CO_2 produced	89843.43	372834.76	76087.45	129996.54	418716.98	125003.65	gCO_2/d
	AD 2 Effluent	CH_4 produced	64835.27	243587.1	54468.98	92625.05	271376.89	81995.42	gCH_4/d
		Digester pH	6.95	6.96	6.9	7.01	6.97	6.9	
		Digester alkalinity	3233.04	2741.56	2619.82	3935.13	2915.93	2822.91	g/m^3 as $CaCO_3$
		Total settleable solids	11595.27	7068.28	12366.36	10048.75	7050.98	11535.68	g/m^3
		Volatile settleable Solids	6245	3916.23	6495.32	5349.63	3671.49	5696.56	g/m^3
		Inorganic settleable Solids	5350.27	3152.05	5871.04	4699.13	3379.5	5839.12	g/m^3
		Total unbiodegradable COD	7820.81	4542.74	8422.86	6202.24	4031.15	6915.81	gCOD/m^3
		Total biodegradable COD	1430.87	1311.32	1202.09	1718.8	1454.49	1521.55	gCOD/m^3
		TKN	1926.63	1608.88	2340.69	1890.64	1665.13	2339.76	gN/m^3
		FSA	353.05	323.58	309.14	412.76	332.62	346.74	gN/m^3
		TP	1429.5	786.83	1161.46	1514.37	874.12	1207.74	gP/m^3
		OP	771.15	467.77	596	953.03	528.63	638.11	gP/m^3

Closure

The design processes above are simplified conceptual examples that only show how the plant-wide - AD steady state model can be a useful aid in making design choices (i.e. in predicting the effluent quality for given influent flows and material loads and sizing of unit processes. The employment of these models would usually require a more rigorous and detailed process. Usually, other factors, e.g. the continuous fluid mechanics, would be considered since although it is assumed that the reactors are completely mixed, it more than often is not the case and once the variations in concentration are known the model can be employed to the delimited volumes sections of the reactors in the various plant unit processes. Beyond conceptual design, there are many other engineering choices to be made with regard to aspects such as layout and maintenance considerations, constructability, costing, etc.

APPENDIX 6: THE PLANT-WIDE THREE PHASE MODEL GUJER MATRIX

Below is an outline of the three phase AD model Gujer matrix. The following Tables A6.1a to A6.1d provide a more detailed description of the stoichiometric matrix, with references to the stoichiometric coefficients that are presented for each process in the following Sections 6.2 (ASM2) and 6.3 (UCTAD).

Table A6.1a: Outline Formation of the Three phase Plant-Wide Model Gujer Matrix

STOICHIOMETRIC PROCESSES		PROCESS RATES
Soluble Component - Modified ASM2 Section of the Stoichiometric Matrix for the Plant-Wide 3 Phase Model (Table a)	Particulate Component - Modified ASM2 Section of the Stoichiometric Matrix for the Plant-Wide 3 Phase Model (Shown in Table b)	Process Rates for the Modified ASM2 Section in the Stoichiometric Matrix for the Plant-Wide 3 Phase Model
Soluble Component -UCTAD Section of the Stoichiometric Matrix for the Plant-Wide 3 Phase Model (Table c)	Particulate Components - UCTAD Section of the Stoichiometric Matrix for the Plant-Wide 3 Phase Model (Shown in Table d)	Process Rates for the UCTAD Section in the Stoichiometric Matrix for the Plant-Wide 3 Phase Model

Table A6.1b: ASM2-3P Section of the Stoichiometric Matrix for the Plant-Wide 3 Phase Model													
State			**Soluble Components**										
	Expressed as		g/m^3										
	Component		H_2O	H	Na	K	Ca	Mg	NH_4	Cl	Ac	Pr	
AS Processes	1a	Aerobic hydrolysis of BPO_{PS}	A1-1	A1-2					A1-3				
	1b	Anoxic hydrolysis of BPO_{PS}	A1-1	A1-2					A1-3				
	1c	Anaerobic hydrolysis of BPO_{PS}	A1-1	A1-2					A1-3				
	2	Aerobic OHO Growth on FBSO	A2-1	A2-2					A2-3				
	3	Aerobic OHO Growth on Ac	A3-1	A3-2					A3-3		A3-4		
	4	Anoxic OHO Growth on FBSO	A4-1	A4-2					A4-3				
	5	Anoxic OHO Growth on Ac	A5-1	A5-2					A5-3		A5-4		
	6	Fermentation of FBSO	A6-1	A6-2					A6-3		A6-4		
	7	Storage of PHA (by PAOs)	A7-1	A7-2		A7-3	A7-4	A7-5			A7-6		
	8	Aerobic storage of PP	A8-1	A8-2		A8-3	A8-4	A8-5					
	9	Aerobic growth of PAO	A9-1	A9-2					A9-3				
	10	Lysis of PP	A10-1	A10-2		A10-3	A10-4	A10-5					
	11	Lysis of PHA	A11-1	A11-2							A11-3		
	12	Aerobic growth of ANO	A12-1	A12-2					A12-3				
	13a	Lysis of OHO	A13-1	A13-2					A13-3				
	13b	Lysis of PAO	A13-1	A13-2					A13-3				
	13c	Lysis of ANO	A13-1	A13-2					A13-3				
	13d	Aeration											

Table A6.1b: ASM2-3P Section of the Stoichiometric Matrix for the Plant-Wide 3 Phase Model													
State			**Soluble Components**										
	Expressed as		g/m^3										
	Component		CO_3	SO_4	PO_4	H2	USO	FBSO	Glu	O_2	NO_3	S_N2	
AS Processes	1a	Aerobic hydrolysis of BPO_{PS}	A1-4		A1-5			A1-6					
	1b	Anoxic hydrolysis of BPO_{PS}	A1-4		A1-5			A1-6					
	1c	Anaerobic hydrolysis of BPO_{PS}	A1-4		A1-5			A1-6					
	2	Aerobic OHO Growth on FBSO	A2-4		A2-5			A2-6		A2-7			
	3	Aerobic OHO Growth on Ac	A3-5		A3-6					A3-7			
	4	Anoxic OHO Growth on FBSO	A4-4		A4-5			A4-6			A4-7	A4-8	
	5	Anoxic OHO Growth on Ac	A5-5		A5-6						A5-7	A5-8	
	6	Fermentation of FBSO	A6-5		A6-6			A6-7					
	7	Storage of PHA (by PAOs)	A7-7										
	8	Aerobic storage of PP	A8-6		A8-7					A8-8			
	9	Aerobic growth of PAO	A9-4		A9-5					A9-6			
	10	Lysis of PP	A10-6										
	11	Lysis of PHA	A11-4										
	12	Aerobic growth of ANO	A12-4		A12-5					A12-6	A12-7		
	13a	Lysis of OHO	A13-4		A13-5								
	13b	Lysis of PAO	A13-4		A13-5								
	13c	Lysis of ANO	A13-4		A13-5								
	13d	Aeration							1				

Table A6.1c: ASM2-3P Section of the Stoichiometric Matrix for the Plant-Wide 3 Phase Model												
State			**Particulate Components**									
	Expressed as		g/m^3									
	Component		UPO	BPO	PP	PHA	Str	ACP	MgKP	OHO	PAO	
AS Processes	1a	Aerobic hydrolysis of BPO_{PS}										
	1b	Anoxic hydrolysis of BPO_{PS}										
	1c	Anaerobic hydrolysis of BPO_{PS}										
	2	Aerobic OHO Growth on FBSO								A2-8		
	3	Aerobic OHO Growth on Ac								A3-8		
	4	Anoxic OHO Growth on FBSO								A4-9		
	5	Anoxic OHO Growth on Ac								A5-9		
	6	Fermentation of FBSO										
	7	Storage of PHA (by PAOs)			A7-8	A7-9						
	8	Aerobic storage of PP			A8-9	A8-10						
	9	Aerobic growth of PAO				A9-7					A9-8	
	10	Lysis of PP			A10-7							
	11	Lysis of PHA				A11-5						
	12	Aerobic growth of ANO										
	13a	Lysis of OHO								A13-6		
	13b	Lysis of PAO									A13-6	
	13c	Lysis of ANO										
	14	Aeration										

Table A6.1c: SM2-3P Section of the Stoichiometric Matrix for the Plant-Wide 3 Phase Model													
State			Particulate Components										
	Expressed as		g/m^3										
	Component		Z_{AD}	Z_{AC}	Z_{AM}	Z_{HM}	ER	BPO_{PS}	ISS	ANO	CO2	CH4
AS Processes	1a	Aerobic hydrolysis of BPO_{PS}						A1-7				
	1b	Anoxic hydrolysis of BPO_{PS}						A1-7				
	1c	Anaerobic hydrolysis of BPO_{PS}						A1-7				
	2	Aerobic OHO Growth on FBSO										
	3	Aerobic OHO Growth on Ac										
	4	Anoxic OHO Growth on FBSO										
	5	Anoxic OHO Growth on Ac										
	6	Fermentation of FBSO										
	7	Storage of PHA (by PAOs)										
	8	Aerobic storage of PP										
	9	Aerobic growth of PAO										
	10	Lysis of PP										
	11	Lysis of PHA										
	12	Aerobic growth of ANO								A12-8		
	13a	Lysis of OHO					A13-7	A13-8				
	13b	Lysis of PAO					A13-7	A13-8				
	13c	Lysis of ANO					A13-7	A13-8		A13-6		
	14	Aeration										

Table A6.1d: ADM-3P Section of the Stoichiometric Matrix for the Plant-Wide 3 Phase Model												
State			**Soluble Components**									
	Expressed as		g/m^3									
	Component		H_2O	H	Na	K	Ca	Mg	NH_4	Cl	Ac	Pr
s	1	Hydrolysis of FBSO	D1-1	D1-2					D1-3			
	2a	Hydrolysis of OHO $_{BM}$	D2-1	D2-2					D2-3			
	2b	Hydrolysis of PAO $_{BM}$	D2-1	D2-2					D2-3			
	2c	Z_{AD} endogenous decay	D2-1	D2-2					D2-3			
	2d	Z_{AC} endogenous decay	D2-1	D2-2					D2-3			
	2e	Z_{AM} endogenous decay	D2-1	D2-2					D2-3			
	2f	Z_{HM} endogenous decay	D2-1	D2-2					D2-3			
	3	Hydrolysis of BPO_{PSBM}	D3-1	D3-2					D3-3			
	4	Hydrolysis of BPO	D4-1	D4-2					D4-3			
	5	Hydrolysis of PP	D5-1	D5-2		D5-3	D5-4	D5-5				
	6	Lysis of PHA	D6-1	D6-2							D6-3	
	7	Acidogenesis (Low pH)	D7-1	D7-2					D7-3			D7-4
	8	Acidogenesis (high pH)	D8-1	D8-2					D8-3			D8-4
	9	Acetogenesis	D9-1	D9-2					D9-3		D9-4	D9-5
	10	Acetoclastic methanogenesis	D10-1	D10-2					D10-3		D10-4	
	11	Hydrogenotrophic methanogenesis	D11-1	D11-2					D11-3			
	12	Evolution of CO_2 gas	D12-1	D12-2								
	13	Precipitation of $MgNH_4PO_4$	D13-1					D13-2	D13-3			
	14	Precipitation of $Ca_3(PO_4)_2$				D14-1						
	15	Precipitation of $MgKPO_4$	D15-1			D15-2		D15-3				

Table A6.1d: ADM-3P Section of the Stoichiometric Matrix for the Plant-Wide 3 Phase Model												
State			**Soluble Components**									
AD processes	**Expressed as**		g/m^3									
	Component		CO_3	SO_4	PO_4	H2	USO	FBSO	Glu	O_2	NO_3	S_N2
	1	Hydrolysis of FBSO	D1-4		D1-5			D1-6	D1-7			
	2a	Hydrolysis of OHO $_{BM}$	D2-4		D2-5							
	2b	Hydrolysis of PAO $_{BM}$	D2-4		D2-5							
	2c	Z_{AD} endogenous decay	D2-4		D2-5							
	2d	Z_{AC} endogenous decay	D2-4		D2-5							
	2e	Z_{AM} endogenous decay	D2-4		D2-5							
	2f	Z_{HM} endogenous decay	D2-4		D2-5							
	3	Hydrolysis of BPO_{PSBM}	D3-4		D3-5			D3-6	D3-7			
	4	Hydrolysis of BPO	D4-4		D4-5			D4-6	D4-7			
	5	Hydrolysis of PP	D5-6									
	6	Lysis of PHA	D6-4									
	7	Acidogenesis (Low pH)	D7-5		D7-6	D7-7			D7-8			
	8	Acidogenesis (high pH)	D8-5		D8-6	D8-7			D8-8			
	9	Acetogenesis	D9-6		D9-7	D9-8						
	10	Acetoclastic methanogenesis	D10-5		D10-6							
	11	Hydrogenotrophic methanogenesis	D11-4		D11-5	D11-6						
	12	Evolution of CO_2 gas	D12-3									
	13	Precipitation of $MgNH_4PO_4$	D13-4									
	14	Precipitation of $Ca_3(PO_4)_2$			D14-2							
	15	Precipitation of $MgKPO_4$	D15-4									

Table A6.1e: ADM-3P Section of the Stoichiometric Matrix for the Plant-Wide 3 Phase Model											
State			**Particulate Components**								
	Expressed as		g/m^3								
	Component		UPO	BPO	PP	PHA	Str	ACP	MgKP	OHO	PAO
AD processes	2a	Hydrolysis of OHO $_{BM}$								D2-6a	
	2b	Hydrolysis of PAO $_{BM}$									D2-6b
	2c	Z_{AD} endogenous decay									
	2d	Z_{AC} endogenous decay									
	2e	Z_{AM} endogenous decay									
	2f	Z_{HM} endogenous decay									
	3	Hydrolysis of BPO_{PSBM}		D3-8							
	4	Hydrolysis of BPO									
	5	Hydrolysis of PP			D5-7						
	6	Lysis of PHA				D6-5					
	7	Acidogenesis (Low pH)									
	8	Acidogenesis (high pH)									
	9	Acetogenesis									
	10	Acetoclastic methanogenesis									
	11	Hydrogenotrophic methanogenesis									
	12	Evolution of CO_2 gas									
	13	Precipitation of $MgNH_4PO_4$					D13-5				
	14	Precipitation of $Ca_3(PO_4)_2$						D14-3			
	15	Precipitation of $MgKPO_4$							D15-5		

Table A6.1e: ADM-3P Section of the Stoichiometric Matrix for the Plant-Wide 3 Phase Model													
State			**Particulate Components**										
	Expressed as		g/m^3										
	Component		Z_{AD}	Z_{AC}	Z_{AM}	Z_{HM}	ER	BPO_{PS}	ISS	ANO	CO2	CH4
AD processes	2a	Hydrolysis of OHO $_{BM}$										
	2b	Hydrolysis of PAO $_{BM}$										
	2c	Z_{AD} endogenous decay	D2-6c									
	2d	Z_{AC} endogenous decay		D2-6c								
	2e	Z_{AM} endogenous decay			D2-6d							
	2f	Z_{HM} endogenous decay				D2-6e						
	3	Hydrolysis of BPO_{PSBM}										
	4	Hydrolysis of BPO						D4-8				
	5	Hydrolysis of PP										
	6	Lysis of PHA										
	7	Acidogenesis (Low pH)	D7-9									
	8	Acidogenesis (high pH)	D8-9									
	9	Acetogenesis		D9-9								
	10	Acetoclastic methanogenesis			D10-7							D10-8
	11	Hydrogenotrophic methanogenesis				D11-7						D11-8
	12	Evolution of CO_2 gas										
	13	Precipitation of $MgNH_4PO_4$										
	14	Precipitation of $Ca_3(PO_4)_2$										
	15	Precipitation of $MgKPO_4$										

6.1f: Process Rates for the ASM2-3P Section in the Stoichiometric Matrix for the Plant-Wide 3 Phase Model		
No.	Process Description and Rate	
1	Process	AerHydrol:
	Rate	$k\_h \times \{(C[S\_O]) / (K\_O + C[S\_O])\} \times \left\{ \begin{array}{l} (C[BPO\_PS] / C[Xoh]) / (K\_X \div ((8 * gam\_bps) \times Molmass[Xoh]) / (Molmass[BPO\_PS] \times (8 * gam\_bps)) \\ + (C[BPO\_PS] / C[Xoh])) \end{array} \right\} \times C[Xoh]$
2	Process	AnHydrol:
	Rate	$k\_h \times n\_NO\_Hyd \times \{(K\_O) / (K\_O + C[S\_O])) \times (C[S\_NO] / (K\_NO \times 14.007 / 62.004 + C[S\_NO])\} \times \left\{ \begin{array}{l} (C[BPO\_PS] / C[Xoh]) / (K\_X \div ((8 \times gam\_bps) \times Molmass[Xoh]) / (Molmass[BPO\_PS] \times \\ (8 \times gam\_o)) + (C[BPO\_PS] / C[Xoh])) \end{array} \right\} \times C[Xoh]$
3	Process	AnaerHydrol:
	Rate	$k\_h \times n\_fe \times \{(K\_O) / (K\_O + C[S\_O])\} \times \{(K\_NO \times 14.007 / 62.004) / (K\_NO \times 14.007 / 62.004 + C[S\_NO])\} \times \left\{ \begin{array}{l} (C[BPO\_PS] / C[Xoh]) / (K\_X \div ((8 \times gam\_bps) \times Molmass[Xoh]) / (Molmass[BPO\_PS] \times (8 \times gam\_o)) \\ + (C[BPO\_PS] / C[Xoh])) \end{array} \right\} \times C[Xoh]$
4	Process	AerGrowthOnSf:
	Rate	$mu\_H \times \{(C[S\_O]) / (K\_O + C[S\_O])\} \times \left\{ \begin{array}{l} C[FSO] / (K\_F \div (8 \times gam\_f) / Molmass[FSO] + C[FSO])) \\ \times ((C[FSO]) / (C[FSO] + C[Ac\_t])) \times (C[NH4\_t] / (K\_NH \div (14.007 / 18.0386) + C[NH4\_t]) \end{array} \right\} \times$ $\{C[PO4\_t] / (K\_P \div (30.974 / 94.97) + C[PO4\_t])) \times (C[CO3\_t] / (K\_ALK \times 60.008 + C[CO3\_t])\} \times C[Xoh]$
5	Process	AerGrowthOnSa:
	Rate	$mu\_H \times \{(C[S\_O]) / (K\_O + C[S\_O])\} \times \{C[Ac\_t] / (K\_A \div (63.996 / 59.0437) + C[Ac\_t])\} \times$ $\{(C[Ac\_t]) / (C[FSO] + C[Ac\_t])\} \times \{C[NH4\_t] / (K\_NH \div (14.007 / 18.0386) + C[NH4\_t])\} \times$ $\{C[PO4\_t] / (K\_P \div (30.974 / 94.97) + C[PO4\_t])\} \times \{C[CO3\_t] / (K\_ALK \times 60.008 + C[CO3\_t])\} \times C[Xoh]$
6	Process	AnGrowthOnSfDe-nitrif:
	Rate	$mu\_H \times n\_NO\_Het \times \{(K\_O) / (K\_O + C[S\_O])\} \times \{C[FSO] / (K\_F \div ((8 \times gam\_f) / Molmass[FSO]) + C[FSO])\} \times$ $\{(C[FSO]) / (C[FSO] + C[Ac\_t])\} \times \{C[NH4\_t] / (K\_NH \div (14.007 / 18.0386) + C[NH4\_t])\} \times$ $\{C[S\_NO] / (K\_NO \div (14.007 / 62.004) + C[S\_NO])\} \times \{C[PO4\_t] / (K\_P \div (30.974 / 94.97) + C[PO4\_t])\} \times$ $\{C[CO3\_t] / (K\_ALK \times 60.008 + C[CO3\_t])\} \times C[Xoh]$

Process Rates for the ASM2-3P Section in the Stoichiometric Matrix for the Plant-Wide 3 Phase Model		
No.	Process Description and Rate	
7	Process	AnGrowthOnSaDe-nitrif:
	Rate	$mu\_H \times n\_NO\_Het \times \{(K\_O)/(K\_O + C[S\_O])\} \times \{C[Ac\_t]/(K\_A \div (63.996/59.0437) + C[Ac\_t])\} \times \{(C[Ac\_t])/(C[FSO] + C[Ac\_t])\} \times \{C[NH4\_t]/(K\_NH \div (14.007/18.0386) + C[NH4\_t])\} \times \{C[S\_NO]/(K\_NO \times 62.004/14.007 + C[S\_NO])\} \times \{C[PO4\_t]/(K\_P \div (30.974/94.97) + C[PO4\_t])\} \times \{C[CO3\_t]/(K\_ALK \times 60.008 + C[CO3\_t])\} \times C[Xoh$
8	Process	Fermentation:
	Rate	$Q\_fe \times \{(K\_O)/(K\_O + C[S\_O])\} \times \{(K\_NO \div (14.007/62.004))/(K\_NO \div (14.007/62.004) + C[S\_NO])\} \times \{C[FSO]/(K\_fe \div ((8 \times gam\_f)/Molmass[FSO]) + C[FSO])\} \times \{C[CO3\_t]/(K\_ALK \times 60.008 + C[CO3\_t])\} \times C[Xoh]$
9	Process	LysisOfHetero :
	Rate	$b\_H \times C[Xoh]$
10	Process	StorageOfPHA:
	Rate	$Q\_PHA \times \{C[Ac\_t]/(K\_A \div (63.996/59.0437) + C[Ac\_t])\} \times \{C[CO3\_t]/(K\_ALK \times 60.008 + C[CO3\_t])\} \times \{C[PP])/(K\_PP \div ((30.974 \times Molmass[Xpa])/(Molmass[PP] \times (8 \times gam\_o))) + C[PP]/(C[Xpa])\}$
11	Process	StorageOfPP:
	Rate	$Q\_PP \times \{(C[S\_O])/(K\_O + C[S\_O])\} \times \{C[PO4\_t]/(C[PO4\_t] + K\_PS \div (30.974/94.97))\} \times \{C[CO3\_t]/(K\_ALK \times 60.008 + C[CO3\_t])\} \times \{(C[PHA]/C[Xpa])/(K\_PHA \div ((143.991 \times Molmass[Xpa])/(86.0894 \times (8 \times gam\_o))) + C[PHA]/C[Xpa])\} \times \{K\_MAX - C[PP]/C[Xpa])/((K\_IPP \div ((30.974 \times Molmass[Xpa])/(Molmass[PP] \times (8 \times gam\_o)))) + K\_MAX - C[PP]/C[Xpa]) \times C[Xpa]$
12	Process	AerGrowthOnPHA:
	Rate	$mu\_PAO \times \{(C[S\_O])/(K\_O + C[S\_O])\} \times \{C[NH4\_t]/(K\_NH \div (14.007/18.0386) + C[NH4\_t])\} \times \{C[CO3\_t]/(K\_ALK \times 60.008 + C[CO3\_t])\} \times \{C[PO4\_t]/(K\_P \div (30.974/94.97) + C[PO4\_t])\} \times \{(C[PHA]/C[Xpa])/(K\_PHA \div ((143.991 \times Molmass[Xpa])/(86.0894 \times (8 \times gam\_o))) + C[PHA]/C[Xpa])\}$

Process Rates for the ASM2-3P Section in the Stoichiometric Matrix for the Plant-Wide 3 Phase Model		
No.	Process Description and Rate	
13	Process	LysisOfXPAO:
	Rate	$b\_PAO \times C[Xpa] \times \{C[CO3\_t] / (K\_ALK \times 60.008 + C[CO3\_t])\}$
14	Process	LysisOfPP:
	Rate	$b\_PP \times C[PP] \times \{C[CO3\_t] / (K\_ALK \times 60.008 + C[CO3\_t])\}$
15	Process	LysisOfPHA:
	Rate	$b\_PHA \times C[PHA] \times (C[CO3\_t] / (K\_ALK \times 60.008 + C[CO3\_t]))$
16	Process	GrowthOfAuto:
	Rate	$(mu\_AUT \times \{C[S\_O] / (C[S\_O] + K\_O\_AUT)\} \times \{C[NH4\_t] / (C[NH4\_t] + K\_NH\_AUT \div (14.007 / 18.0386))\} \times \{C[PO4\_t] / (K\_P \div (30.974 / 94.97) + C[PO4\_t])\} \times \{C[CO3\_t] / (C[CO3\_t] + K\_ALK\_AUT \times 60.008)\} \times C[X\_AUT])$
17	Process	LysisOfAuto:
	Rate	$b\_AUT \times C[X\_AUT]$
18	Process	ASCO2evol:
	Rate	$KLaCO2 \times (molality[H2CO3] - KA\_CO2) \times 44000$
19	Process	Aeration
	Rate	$Kla\_Actual \times (S\_O\_Sat - C[S\_O])$

6.1g: Process Rates for the ADM-3P Section in the Stoichiometric Matrix for the Plant-Wide 3 Phase Model		
No.	Process Description and Rate	
1	Process	FBSO_Hydrolysis :
	Rate	$(K\_fs \times Tcorr / COD\_per\_mol[FSO]) \times COD[FSO]$
2	Process	BPO_Hydrolysis:
	Rate	$\{K\_bp \times Tcorr / COD\_per\_mol[BPO] \times (COD[BPO] / COD[Xad] / (ks\_bp + COD[BPO] / COD[Xad]))\} \times COD[Xad]$
3	Process	OHO_Lysis:
	Rate	$(K\_oh \times Tcorr / COD\_per\_mol[Xoh]) \times COD[Xoh]$
4	Process	PAO_Lysis:
	Rate	$(K\_pa \times Tcorr / COD\_per\_mol[Xpa]) \times COD[Xpa]$
5	Process	PP_Hydrolysis :
	Rate	$(K\_pp \times Tcorr / Molmass[PP]) \times C[PP]$
6	Process	PP_Release:
	Rate	$(K\_polyp \times Tcorr / Molmass[PP]) \times C[PP]$
7	Process	BPO_{PS}_Hydrolysis:
	Rate	$\{K\_bp \times Tcorr / COD\_per\_mol[BPO] \times (COD[BPO] / COD[Xad] / (ks\_bp + COD[BPO] / COD[Xad]))\} \times COD[Xad]$
8	Process	Acidogenesis_L:
	Rate	$\{mu\_ad / (COD\_per\_mol[Glu] \times Y\_AD) \times Tcorr \times COD[Glu] / (ks\_ad + COD[Glu])\} \times \{1 - COD[H2] / (ki\_H2 + COD[H2])\} \times COD[Xad]$
9	Process	Acidogenesis_H:
	Rate	$\{mu\_ad / (COD\_per\_mol[Glu] \times Y\_AD) \times Tcorr \times COD[Glu] / (ks\_ad + COD[Glu])\} \times \{COD[H2] / (ki\_H2 + COD[H2])\} \times COD[Xad]$

6.1g: Process Rates for the ADM-3P Section in the Stoichiometric Matrix for the Plant-Wide 3 Phase Model		
No.	Process Description and Rate	
10	Process	AD_decay:
	Rate	(K_ad × Tcorr / COD_per_mol[Xad]) × COD[Xad]
11	Process	Acetogenesis
	Rate	{mu_ac / (COD_per_mol[Pr_t] × Y_AC) × Tcorr × COD_HPr / (ks_ac + COD_HPr) × (1 - COD[H2] / (ki_H2 + COD[H2]))} × COD[Xac]
12	Process	AC_decay:
	Rate	(K_ac × Tcorr / COD_per_mol[Xac]) × COD[Xac]
13	Process	Acet_methanogenesis:
	Rate	{mu_am / (COD_per_mol[Ac_t] × Y_AM) × Tcorr × COD_HAc / (ks_am + COD_HAc) × ki_am / (ki_am + molality[H])} × COD[Xam
14	Process	AM_decay:
	Rate	(K_am × Tcorr / COD_per_mol[Xam]) × COD[Xam]
15	Process	Hyd_methanogenesis:
	Rate	{mu_hm × Tcorr / (4.0 × COD_per_mol[H2] × Y_HM) × COD[H2] / (ks_hm + COD[H2]) × ki_hm / (ki_hm + molality[H])} × COD[Xhm]
16	Process	HM_decay:
	Rate	(K_hm × Tcorr / COD_per_mol[Xhm]) × COD[Xhm]
17	Process	CO2_evolution:
	Rate	(K_CO2 × Tcorr / Molmass[CO2]) × {(101300.0 × molality[H2CO3] × gam0 × pow(10,(1.469 + 1028.874 × (1.0 / 298.15 - 1.0 / TK)))) - PCO2_headspace}

6.1g: Process Rates for the ADM-3P Section in the Stoichiometric Matrix for the Plant-Wide 3 Phase Model		
No.	Process Description and Rate	
18	Process	Struvite_diss:
	Rate	Struvite_diss" ProcessRate ="(kdis_stru × Tcorr / Molmass[Str]) × fabs{1.0 - 2.0 / (1.0 + ((Totalmolality[Mg_] × Totalmolality[NH4_] × Totalmolality[PO4_]) × pow(gam1,8) / Ksp_stru))} × Driver_Str
19	Process	ACP_diss:
	Rate	(kdis_cap × Tcorr / Molmass[CaP]) × Driver_cap × fabs{1.0 - 2.0 / (1.0 + (pow(molality[Ca],3) × pow(molality[HPO4],2) / pow(molality[H],2) × pow(gam1,18) / (3.7942 × exp(-12))))}
20	Process	MgKP_diss:
	Rate	(kdis_mgkp × Tcorr / Molmass[MgKP]) × Driver_mgkp × fabs{1.0 - 2.0 / (1.0 + (molality[Mg] × molality[K] × molality[HPO4] / molality[H] × pow(gam1,8) / (8.79508 × exp(-12))))}

APPENDIX 6.2 THREE PHASE ASM2 (ASM2-3P) MODEL STOICHIOMETRY

1. Aerobic hydrolysis of BPO_{PS}				
Component	H_2O	H	NH_4	
Stoichiometric Coefficient	$\left\{\left(\frac{gam_{ps}}{gam_f}\right)\times\left(z_f-3-4b_f\right)-\left(z_{ps}-3-4b_{ps}\right)\right\}\times MolmassH_2O$	$\left\{\left(8b_{ps}-2z_{ps}+6+y_{ps}-4a_{ps}-\right)\left(8b_f-2z_f+6+y_f-4a_f\right)\right\}\times\left(\frac{gam_{ps}}{gam_f}\right)\times MolmassH^+$	$\left\{a_{ps}-\left(\frac{gam_{ps}}{gam_f}\right)\cdot a_f\right\}\times MolmassNH_4^+$	
PM Ref. No.	A1-1	A1-2	A1-3	
Component	CO_3	PO_4	FBSO	BPO_{PS}
Stoichiometric Coefficient	$\left\{1-\left(\frac{gam_{ps}}{gam_f}\right)\right\}\times MolmassCO_3^{2-}$	$\left\{b_{ps}-\left(\frac{gam_{ps}}{gam_f}\right)\cdot b_f\right\}\times MolmassPO_4^{3-}$	$\left(\frac{gam_{ps}}{gam_f}\right)\times MolmassFSO$	$-1\times MolmassBPO\_PS$
PM Ref. No.	A1-4	A1-5	A1-6	A1-7

2. Aerobic OHO Growth on FBSO					
Component	H_2O	H	NH_4		
Stoichiometric Coefficient	$\left\{\left(\frac{\left(z_f-4b_f-3\right)\cdot gam_o}{gam_f\cdot YH}\right)+4b_o-z_o+3+\left(\frac{\left(1-YH\right)\cdot gam_o}{16\cdot YH}\right)\right\}\times MolmassH_2O$	$\left\{\left(\frac{\left(2z_f-8b_f-6-y_f+4a_f\right)\cdot gam_o}{gam_f\cdot YH}\right)+\left(\frac{\left(1-YH\right)\cdot gam_o}{8\cdot YH}\right)-\left(2z_o-8b_o-6-y_o+4a_o\right)\right\}\times -MolmassH^+$	$\left\{a_0-\left(a_f\cdot\frac{gam_o}{gam_f\cdot YH}\right)\right\}\times -MolmassNH_4^+$		
PM Ref. No.	A2-1	A2-2	A2-3		
Component	CO_3	PO_4	FBSO	O_2	OHO
Stoichiometric Coefficient	$\left\{1-\left(\frac{gam_o}{gam_f\cdot YH}\right)\right\}\times -MolmassCO_3^{2-}$	$\left\{b_0-\left(b_f\cdot\frac{gam_o}{gam_f\cdot YH}\right)\right\}\times -MolmassPO_4^{3-}$	$\left(\frac{gam_o}{gam_f\cdot YH}\right)\times -MolmassFSO$	$\left\{\frac{\left(1-YH\right)\cdot}{\frac{gam_o}{YH}\cdot\frac{1}{32}}\right\}\times -MolmassO_2$	$MolmassXoho$
PM Ref. No.	A2-4	A2-5	A2-6	A2-7	A2-8

3. Aerobic OHO Growth on Ac				
Component	H_2O	H	NH_4	Ac
Stoichiometric Coefficient	$\left\{\begin{array}{l}4b_o - z_o + 3 + \\ \left(\frac{gam_o \cdot (2 \cdot (1 - YH) - 2)}{32 \cdot YH}\right)\end{array}\right\}$ $\times \mathrm{MolmassH_2O}$	$\left\{\begin{array}{l}\left(\frac{gam_o \cdot 2 \cdot (1 - YH)}{16 \cdot YH}\right) \\ -\left(\frac{11 \cdot gam_o}{64 \cdot YH}\right) - \\ (2z_o - 8b_o - 6 - y_o + 4a_o)\end{array}\right\}$ $\times -MolmassH^+$	$(a_0)\times$ $-MolmassNH_4^+$	$\left(\frac{gam_o}{64 \cdot YH}\right)$ $\times -MolmassAc$
PM Ref. No.	A3-1	A3-2	A3-3	A3-4

Component	CO_3	PO_4	O_2	OHO
Stoichiometric Coefficient	$\left\{1 - \left(\frac{gam_o}{32 \cdot YH}\right)\right\}$ $\times -MolmassCO_3^{2-}$	$(b_0)\times$ $-MolmassPO_4^{3-}$	$\left\{(1 - YH) \cdot \frac{gam_o}{YH} \cdot \frac{1}{32}\right\}$ $\times -MolmassO_2$	$1\times$ $MolmassXoho$
PM Ref. No.	A3-5	A3-6	A3-7	A3-8

4. Anoxic OHO Growth on FBSO			
Component	H_2O	H	NH_4
Stoichiometric Coefficient	$\left\{\begin{array}{l}\left(\frac{(z_f - 4b_f - 3) \cdot gam_o}{gam_f \cdot YH}\right) \\ + 4b_o - z_o + 3 + \\ \left(\frac{3 \cdot (1 - YH) \cdot gam_o}{2.86 \cdot 14 \cdot YH}\right)\end{array}\right\}$ $\times MolmassH_2O$	$\left\{\begin{array}{l}\left(\frac{(2z_f - 8b_f - 6 - y_f + 4a_f) \cdot gam_o}{gam_f \cdot YH}\right) \\ + \left(\frac{6 \cdot (1 - YH) \cdot gam_o}{2.86 \cdot 14 \cdot YH}\right) \\ - (2z_o - 8b_o - 6 - y_o + 4a_o)\end{array}\right\}$ $\times -MolmassH^+$	$\left\{\begin{array}{l}a_0 - \\ \left(a_f \cdot \frac{gam_o}{gam_f \cdot YH}\right)\end{array}\right\}$ $\times -MolmassNH_4^+$
PM Ref. No.	A4-1	A4-2	A4-3

Component	CO_3	PO_4	FBSO	NO_3	S_N2	OHO
Stoichiometric Coefficient	$\left\{\begin{array}{l}1 - \\ \left(\frac{gam_o}{gam_f \cdot YH}\right)\end{array}\right\}$ $\times -MolmassCO_3^{2-}$	$\left\{\begin{array}{l}b_0 - \\ \left(b_f \cdot \frac{gam_o}{gam_f \cdot YH}\right)\end{array}\right\}$ $\times -MolmassPO_4^{3-}$	$\left(\frac{gam_o}{gam_f \cdot YH}\right)$ $\times -MolmassFSO$	$\left\{\begin{array}{l}(1 - YH) \cdot \frac{gam_o}{YH} \cdot \\ \frac{1}{(2.86 \cdot 14)}\end{array}\right\}$ $\times -MolmassNO_3$	$\left\{\begin{array}{l}(1 - YH) \cdot \frac{gam_o}{YH} \cdot \\ \frac{1}{(2.86)}\end{array}\right\}$ $\times MolmassN_2$	$1\times$ $Molmass$ $Xoho$
PM Ref. No.	A4-4	A4-5	A4-6	A4-7	A4-8	A4-9

	5. Anoxic OHO Growth on Ac			
Component	H_2O	H	NH_4	Ac
Stoichiometric Coefficient	$\left\{\begin{array}{l} 4b_o - z_o + 3 - \\ \left(\frac{2\cdot gam_o}{32\cdot YH}\right) + \\ \left(\frac{3\cdot gam_o\cdot(1-YH)}{2.86\cdot 14\cdot YH}\right) \end{array}\right\} \times MolmassH_2O$	$\left\{\begin{array}{l} \left(\frac{6\cdot gam_o\cdot(1-YH)}{2.86\cdot 14\cdot YH}\right) \\ -\left(\frac{11\cdot gam_o}{64\cdot YH}\right) - \\ (2z_o - 8b_o - 6 - y_o + 4a_o) \end{array}\right\} \times -MolmassH^+$	$(a_0)\times$ $-MolmassNH_4^+$	$\left(\frac{gam_o}{64\cdot YH}\right)$ $\times -MolmassAc$
PM Ref. No.	5-1	5-2	5-3	5-4

Component	CO_3	PO_4	NO_3	S_N2	OHO
Stoichiometric Coefficient	$\left\{1-\left(\frac{gam_o}{32\cdot YH}\right)\right\}$ $\times -MolmassCO_3^{2-}$	$(b_0)\times$ $-MolmassPO_4^{3-}$	$\left\{\begin{array}{l} (1-YH)\cdot\frac{gam_o}{YH}\cdot \\ \frac{1}{(2.86\cdot 14)} \end{array}\right\}$ $\times -MolmassNO_3$	$\left\{\begin{array}{l} (1-YH)\cdot\frac{gam_o}{YH}\cdot \\ \frac{1}{(2.86)} \end{array}\right\}$ $\times MolmassN_2$	$1\times$ $MolmassXoho$
PM Ref. No.	5-5	5-6	5-7	5-8	5-9

6. Fermentation of FBSO			
Component	H_2O	H	NH_4
Stoichiometric Coefficient	$\left\{\begin{array}{l} z_f - 4b_f - 3 + \\ \left(\frac{4\cdot gam_f}{64}\right) \end{array}\right\} \times MolmassH_2O$	$\left\{\begin{array}{l} 8b_f - 2z_f + 6 + y_f - 4a_f - \\ \left(\frac{11\cdot gam_f}{64}\right) \end{array}\right\} \times MolmassH^+$	$(a_0)\times$ $MolmassNH_4^+$
PM Ref. No.	A6-1	A6-2	A6-3

Component	Ac	CO_3	PO_4	FBSO
Stoichiometric Coefficient	$\left(\frac{gam_f}{64\cdot YH}\right)$ $\times MolmassAc$	$\left\{1-\left(\frac{2\cdot gam_f}{64}\right)\right\}$ $\times MolmassCO_3^{2-}$	$(b_0)\times$ $MolmassPO_4^{3-}$	$-1\times$ $MolmassFSO$
PM Ref. No.	A6-4	A6-5	A6-6	A 6-7

7. Storage of PHA (by PAO)					
Component	H_2O	H	K	Ca	Mg
Stoichiometric Coefficient	$\left\{10-\left(4\cdot\frac{144}{64}\right)\right\}$ $\left\{-\left(\frac{144\cdot YPO_4}{31}\right)\right\}$ $\times MolmassH_2O$	$\left\{\left(11\cdot\frac{144}{64}\right)+\right\}$ $\left\{\left(2\cdot\frac{144\cdot YPO_4}{31}\right)-26\right\}$ $\times MolmassH^+$	$\left(\frac{144\cdot YPO_4\cdot 0.32}{31}\right)$ $\times MolmassK^+$	$\left(\frac{144\cdot YPO_4\cdot 0.32}{31}\right)$ $\times MolmassCa^{2+}$	$\left(\frac{144\cdot YPO_4\cdot 0.32}{31}\right)$ $MolmassMg^{2+}$
PM Ref. No.	A7-1	A7-2	A7-3	A7-4	A7-5

Component	Ac	CO_3	PP	PHA
Stoichiometric Coefficient	$\frac{144}{64}$ $\times -MolmassAc$	$\left\{2\cdot\frac{144}{64}-4\right\}$ $MolmassCO_3^{2-}$	$\left(\frac{144\cdot YPO_4}{31}\right)$ $\times -MolmassPP$	$1\times$ $MolmassPHA$
PM Ref. No.	A7-6	A7-7	A7-8	A7-9

8. Aerobic storage of PP					
Component	H_2O	H	K	Ca	Mg
Stoichiometric Coefficient	$\left\{1-\left(10\cdot\frac{YPHA}{144}\right)\right\}$ $\left\{+\left(\frac{YPHA}{16}\right)\right\}$ $\times MolmassH_2O$	$\left\{\left(26\cdot\frac{YPHA}{144}\right)-\right\}$ $\left\{2-\left(\frac{YPHA}{8}\right)\right\}$ $\times MolmassH^+$	K_pp $\times -MolmassK^+$	Ca_pp $\times -MolmassCa^{2+}$	Mg_pp $\times -MolmassMg^{2+}$
PM Ref. No.	A8-1	A8-2	A8-3	A8-4	A8-5

Component	CO_3	PO_4	O_2	PP	PHA
Stoichiometric Coefficient	$\left\{4\cdot\frac{YPHA}{144}\right\}$ $\times MolmassCO_3^{2-}$	$-1\times$ $MolmassPO_4^{3-}$	$\left(\frac{YPHA}{32}\right)$ $\times -MolmassO_2$	$1\times$ $MolmassPP$	$\left(\frac{YPHA}{144}\right)$ $\times -MolmassPHA$
PM Ref. No.	A8-6	A8-7	A8-8	A8-9	A8-10

9. Aerobic growth of PAO					
Component	H_2O		H		NH_4
Stoichiometric Coefficient	$\left\{\left(\frac{(1-YPAO)\cdot gam_o}{16\cdot YPAO}\right) - \left(\frac{10\cdot gam_o}{144\cdot YPAO}\right) + 4b_o - z_o + 3\right\} \times MolmassH_2O$		$\left\{\left(\frac{(1-YPAO)\cdot gam_o}{8\cdot YPAO}\right) - \left(\frac{26\cdot gam_o}{144\cdot YPAO}\right) - (2z_o - 8b_o - 6 - y_o + 4a_o)\right\} \times -MolmassH^+$		$(a_0)\times -MolmassNH_4^+$
PM Ref. No.	A9-1		A9-2		A9-3
Component	CO_3	PO_4	O_2	PHA	PAO
Stoichiometric Coefficient	$\left\{\left(1-\frac{4\cdot gam_o}{144\cdot YPAO}\right)-1\right\} \times -MolmassCO_3^{2-}$	$(b_0)\times -MolmassPO_4^{3-}$	$\left\{(1-YPAO)\cdot\frac{gam_o}{YPAO}\cdot\frac{1}{32}\right\} \times -MolmassO_2$	$\left(\frac{gam_o}{144\cdot YPAO}\right) \times -MolmassPHA$	$1\times MolmassXpao$
PM Ref. No.	A9-4	A9-5	A9-6	A9-7	A9-8

10. Lysis of PP							
Component	H_2O	H	K	Ca	Mg	CO_3	PP
Stoichiometric Coefficient	$1\times MolmassH_2O$	$2\times MolmassH^+$	$K\_pp \times MolmassK^+$	$Ca\_pp \times MolmassCa^{2+}$	$Mg\_pp \times MolmassMg^{2+}$	$1\times MolmassCO_3^{2-}$	$-1\times MolmassPP$
PM Ref. No.	A10-1	A10-2	A10-3	A10-4	A10-5	A10-6	A10-7

11. Lysis of PHA					
Component	H_2O	H	Ac	CO_3	PHA
Stoichiometric Coefficient	$\left\{\frac{4}{64}-\frac{10}{144}\right\} \times MolmassH_2O$	$\left\{\frac{26}{144}-\frac{11}{64}\right\} \times MolmassH^+$	$\frac{1}{64}\times MolmassAc$	$\left\{\frac{4}{144}-\frac{2}{64}\right\} \times MolmassCO_3^{2-}$	$\left(\frac{1}{144}\right)\times -MolmassPHA$
PM Ref. No.	A11-1	A11-2	A11-3	A11-4	A11-5

12. Aerobic growth of ANO			
Component	H_2O	H	NH_4
Stoichiometric Coefficient	$\left\{\left(\frac{4.57-YA}{16\cdot YA}\cdot gam_o\right)-\left(3\cdot\frac{gam_o}{14\cdot YA}+4b_o-z_o+3\right)\right\}\times MolmassH_2O$	$\left\{\left(\frac{4.57-YA}{8\cdot YA}\cdot gam_o\right)-\left(10\cdot\frac{gam_o}{14\cdot YA}\right)-(2z_o-8b_o-6-y_o+4a_o)\right\}\times -MolmassH^+$	$\left(\frac{gam_o}{14\cdot YA}+a_0\right)\times -MolmassNH_4^+$
PM Ref. No.	A12-1	A12-2	A12-3

Component	CO_3	PO_4	O_2	NO_3	ANO
Stoichiometric Coefficient	$-1\times -MolmassCO_3^{2-}$	$(b_0)\times -MolmassPO_4^{3-}$	$\left(\frac{4.57-YA}{32\cdot YA}\cdot gam_o\right)\times -MolmassO_2$	$\left(\frac{gam_o}{14\cdot YA}\right)\times MolmassNO_3$	$1\times MolmassXaut$
PM Ref. No.	A12-4	A12-5	A12-6	A12-7	A12-8

13. Lysis of Biomass			
Component	H_2O	H	NH_4
Stoichiometric Coefficient	$\left\{z_0-\left(f_{ep}\cdot\frac{gam_o}{gam_e}\right)\cdot(z_e-3-4b_e)-\left((1-f_{ep})\cdot\frac{gam_o}{gam_{ps}}\right)\cdot(z_{ps}-3-4b_{ps})-3-4\cdot b_o\right\}\times MolmassH_2O$	$\left\{8b_o-2z_o+6+y_o-4a_o-(8b_e-2z_e+6+y_e-4a_e)\cdot\left(\frac{f_{ep}\cdot gam_o}{gam_e}\right)-(8b_{ps}-2z_{ps}+6+y_{ps}-4a_{ps})\cdot\left(\frac{(1-f_{ep})\cdot gam_o}{gam_{ps}}\right)\right\}\times MolmassH^+$	$\left\{a_0-\left(f_{ep}\cdot\frac{gam_o}{gam_e}\right)\cdot a_e-\left((1-f_{ep})\cdot\frac{gam_o}{gam_{ps}}\right)\cdot a_{ps}\right\}\times MolmassNH_4^+$
PM Ref. No.	A13-1	A13-2	A13-3

Component	CO_3	PO_4	OHO	ER	BPO_{PS}
Stoichiometric Coefficient	$\left\{1-\left(f_{ep}\cdot\frac{gam_o}{gam_e}\right)-\left((1-f_{ep})\cdot\frac{gam_o}{gam_{ps}}\right)\right\}\times MolmassCO_3^{2-}$	$\left\{b_0-\left(f_{ep}\cdot\frac{gam_o}{gam_e}\right)\cdot b_e-\left((1-f_{ep})\cdot\frac{gam_o}{gam_{ps}}\right)\cdot b_{ps}\right\}\times MolmassPO_4^{3-}$	$-1\times Molmass\ Xoho$	$\left(f_{ep}\cdot\frac{gam_o}{gam_e}\right)\times MolmassER$	$\left((1-f_{ep})\cdot\frac{gam_o}{gam_{ps}}\right)\times MolmassBPO\_PS$
PM Ref. No.	A13-4	A13-5	A13-6	A13-7	A13-8

1. AD Hydrolysis of FBSO			
Component	H_2O	H	NH_4
Stoichiometric Coefficient	$\left(z\_f - 3 - 4\cdot b\_f + \frac{gam\_f}{2}\right) \times MolmassH_2O$	$\left(3\cdot b\_f + 2 - a\_f - \frac{gam\_f}{2}\right) \times MolmassH^+$	$(a\_f)\times MolmassNH_4^+$
PM Ref. No.	D1-1	D1-2	D1-3

Component	CO_3	PO_4	FBSO	Glu
Stoichiometric Coefficient	$\left(1-\frac{gam\_f}{4}\right) \times MolmassCO_3^{2-}$	$(b\_f)\times MolmassPO_4^{3-}$	$-1\times MolmassFSO$	$\frac{gam\_f}{24}\times MolmassGLU$
PM Ref. No.	D1-4	D1-5	D1-6	D1-7

2. AD Hydrolysis of PAO and OHO (WAS Biomass)			
Component	H_2O	H	NH_4
Stoichiometric Coefficient	$\left(z\_o - 3 - 4\cdot b\_o + \frac{gam\_o}{2}\right) \times MolmassH_2O$	$\left(3\cdot b\_o + 2 - a\_o - \frac{gam\_o}{2}\right) \times MolmassH^+$	$(a\_o)\times MolmassNH_4^+$
PM Ref. No.	D2-1	D2-2	D2-3

Component	CO_3	PO_4	PAO	Glu
Stoichiometric Coefficient	$\left(1-\frac{gam\_o}{4}\right) \times MolmassCO_3^{2-}$	$(b\_o)\times MolmassPO_4^{3-}$	$-1\times MolmassXpa$	$\frac{gam\_o}{24}\times MolmassGLU$
PM Ref. No.	D2-4	D2-5	D2-6	D2-7

3. Lysis of AD Biomass (Z_{AD}, Z_{AC}, Z_{AM} and Z_{HM})			
Component	H_2O	H	NH_4
Stoichiometric Coefficient	$\left\{\begin{array}{l} z\_o - \\ \left(f_{ep}\cdot\frac{gam\_o}{gam\_e}\right) \\ \cdot(z\_e - 3 - 4b\_e) \\ -\left(\left(1-f_{ep}\right)\cdot\frac{gam\_o}{gam\_bps}\right)\cdot \\ (z\_bps - 3 - 4b\_bps) \\ -3-4\cdot b\_o \end{array}\right\} \times MolmassH_2O$	$\left\{\begin{array}{l} 8b\_o - 2z\_o + 6 + y\_o - 4a\_o - \\ (8b\_e - 2z\_e + 6 + y\_e - 4a\_e)\cdot \\ \left(\frac{f_{ep}\cdot gam\_o}{gam_e}\_e\right) \\ -(8b\_bps - 2z\_bps + 6 + y\_bps - 4a\_bps) \\ \cdot\left(\frac{\left(1-f_{ep}\right)\cdot gam\_o}{gam\_bps}\right) \end{array}\right\} \times MolmassH^+$	$\left\{\begin{array}{l} a\_o - \\ \left(f_{ep}\cdot\frac{gam\_o}{gam\_e}\right)\cdot a\_e \\ -\left(\left(1-f_{ep}\right)\cdot\frac{gam\_o}{gam\_bps}\right)\cdot a\_bps \end{array}\right\} \times MolmassNH_4^+$
PM Ref. No.	A13-1	A13-2	A13-3

Component	CO_3	PO_4	OHO	ER	BPO_{PS}
Stoichiometric Coefficient	$\left\{\begin{array}{l} 1- \\ \left(f_{ep}\cdot\frac{gam\_o}{gam\_e}\right)- \\ \left(\left(1-f_{ep}\right)\cdot\frac{gam\_o}{gam\_bps}\right) \end{array}\right\} \times MolmassCO_3^{2-}$	$\left\{\begin{array}{l} b\_o - \\ \left(f_{ep}\cdot\frac{gam\_o}{gam\_e}\right)\cdot b\_e \\ -\left(\left(1-f_{ep}\right)\cdot\frac{gam\_o}{gam\_bps}\right)\cdot b\_bps \end{array}\right\} \times MolmassPO_4^{3-}$	$-1\times Molmass\ Xad$	$\left(f_{ep}\cdot\frac{gam\_o}{gam\_e}\right) \times MolmassER$	$\left(\left(1-f_{ep}\right)\cdot\frac{gam\_o}{gam\_bps}\right) \times MolmassBPO\_PS$
PM Ref. No.	A13-4	A13-5	A13-6	A13-7	A13-8

4. Hydrolysis of PP							
Component	H_2O	H	K	Ca	Mg	CO_3	PP
Stoichiometric Coefficient	$1\times MolmassH_2O$	$2\times MolmassH^+$	$K\_pp \times MolmassK^+$	$Ca\_pp \times MolmassCa^{2+}$	$Mg\_pp \times MolmassMg^{2+}$	$1\times MolmassCO_3^{2-}$	$-1\times MolmassPP$
PM Ref. No.	D4-1	D4-2	D4-3	D4-4	D4-5	D4-6	D4-7

5. AD hydrolysis of BPO_{PS}			
Component	H_2O	H	NH_4
Stoichiometric Coefficient	$\left(z\_bps - 3 - 4\cdot b\_bps + \frac{gam\_bps}{2}\right) \times MolmassH_2O$	$\left(3\cdot b\_bps + 2 - a\_bps - \frac{gam\_bps}{2}\right) \times MolmassH^+$	$(a\_bps)\times MolmassNH_4^+$
PM Ref. No.	D5-1	D5-2	D5-3

Component	CO_3	PO_4	BPO_{PS}	Glu
Stoichiometric Coefficient	$\left(1-\frac{gam\_bps}{4}\right) \times MolmassCO_3^{2-}$	$(b\_bps)\times MolmassPO_4^{3-}$	$-1\times MolmassBPO\_PS$	$\frac{gam\_bps}{24}\times MolmassGLU$
PM Ref. No.	D5-4	D5-5	D5-6	D5-7

6. Lysis of PHA					
Component	H_2O	H	Glu	CO_3	PHA
Stoichiometric Coefficient	$\left(-\frac{4}{3}\right)\times MolmassH_2O$	$\left(-\frac{4}{3}\right)\times MolmassH^+$	$1\times MolmassAc$	$\left(-\frac{2}{3}\right)\times MolmassCO_3^{2-}$	$\left(-\frac{4}{3}\right)\times MolmassPHA$
PM Ref. No.	D6-1	D6-2	D6-3	D6-4	D6-5

7. Acidogenesis				
Component	H_2O	H	NH_4	Ac
Stoichiometric Coefficient	$\left(\left(\frac{72-24\cdot z\_o+96\cdot b\_o}{gam\_o}-8\right)\cdot Y\_AD - 4\right) \times MolmassH_2O$	$\left(\left(6+\frac{\left(\frac{24\cdot a\_o-}{72\cdot b\_o-48}\right)}{gam\_o}\right)\cdot Y\_AD + 6\right) \times MolmassH^+$	$\left(-\frac{24\cdot Y\_AD}{gam\_o}\cdot a\_o\right) \times MolmassNH_4^+$	$\left(\frac{2-}{2\cdot Y\_AD}\right) \times MolmassAc\_t$
PM Ref. No.	D7-1	D7-2	D7-3	D7-4

Component	CO_3	PO_4	H2	Glu	Z_{AD}
Stoichiometric Coefficient	$\left(4-\left(\frac{24}{gam\_o}\right)\cdot Y\_AD + 2\right) \times MolmassCO_3^{2-}$	$\left(-\frac{24\cdot Y\_AD}{gam\_o}\cdot b\_o\right) \times MolmassPO_4^{3-}$	$(4-4\cdot Y\_AD) \times MolmassH_2$	$-1\times MolmassGLU$	$\left(\frac{24\cdot Y\_AD}{gam\_o}\right) \times MolmassXad$
PM Ref. No.	D7-5	D7-6	D7-7	D7-8	D7-9

8. Acidogenesis				
Component	H_2O	H	NH_4	Pr
Stoichiometric Coefficient	$\left(\left(\frac{72-24\cdot z\_o+96\cdot b\_o}{gam\_o}-14\right)\cdot Y\_AD\right)+2$ $\times MolmassH_2O$	$\left(\left(10+\frac{\left(\frac{24\cdot a\_o-}{72\cdot b\_o-48}\right)}{gam\_o}\right)\cdot Y\_AH+2\right)$ $\times MolmassH^+$	$\left(-\frac{24\cdot Y\_AH}{gam\_o}\cdot a\_o\right)$ $\times MolmassNH4^+$	$\left(\frac{2-}{2\cdot Y\_AH}\right)$ $\times Molmass\,\mathrm{Pr}$
PM Ref. No.	D8-1	D8-2	D8-3	D8-4

Component	CO_3	PO_4	H2	Glu	Z_{AD}
Stoichiometric Coefficient	$\left(\left(6-\frac{24}{gam\_o}\right)\cdot Y\_AH\right)$ $\times MolmassCO_3^{2-}$	$\left(-\frac{24\cdot Y\_AH}{gam\_o}\cdot b\_o\right)$ $\times MolmassPO_4^{3-}$	$\left(-2+2\cdot Y\_AH\right)$ $\times MolmassH_2$	$-1\times$ $Molmass$ GLU	$\left(\frac{24\cdot Y\_AH}{gam\_o}\right)$ $\times MolmassXad$
PM Ref. No.	D8-5	D8-6	D8-7	D8-8	D8-9

9. Acetogenesis				
Component	H_2O	H	NH_4	Ac
Stoichiometric Coefficient	$\left(-3+\left(\frac{42-14z\_o+56b\_o}{gam\_o}-4\right)\cdot Y\_\right.$ $\times MolmassH_2O$	$\left(2+\left(3+\frac{14a\_o-42b\_o-28}{gam\_o}\right)\cdot Y\_AC\right)$ $\times MolmassH^+$	$\left(-\frac{14\cdot Y\_AC}{gam\_o}\cdot a\_o\right)$ $\times MolmassNH_4^+$	$(1-Y\_AC)$ $\times MolmassAc$
PM Ref. No.	D9-1	D9-2	D9-3	D9-4

Component	Pr	CO_3	PO_4	H2	Z_{AC}
Stoichiometric Coefficient	$-1\times$ $Molmass$ Pr	$\left(1+\left(Y\_AC\cdot\left(2-\frac{14}{gam\_o}\right)\right)\right)$ $\times MolmassCO_3^{2-}$	$\left(-\frac{14\cdot Y\_AC}{gam\_o}\cdot b\_o\right)$ $\times MolmassPO_4^{3-}$	$(3-3Y\_AC)$ $\times MolmassH_2$	$\left(\frac{14\cdot Y\_AC}{gam\_o}\right)$ $\times MolmassXad$
PM Ref. No.	D9-5	D9-6	D9-7	D9-8	D9-9

	10. Acetoclastic Methanogenesis		
Component	H_2O	H	NH_4
Stoichiometric Coefficient	$\left(-1+\left(-3+\frac{(24-8\cdot z\_o+32\cdot b\_o)}{gam\_o}\right)\cdot Y\_AM\right)\times MolmassH_2O$	$\left(1+\left(2+\frac{8\cdot a\_o-24\cdot b\_o-16}{gam\_o}\right)\cdot Y\_AM\right)\times MolmassH^+$	$\left(\frac{-8\cdot Y\_AM}{gam\_o}\cdot a\_o\right)\times MolmassNH_4^+$
PM Ref. No.	D10-1	D10-2	D10-3

Component	Ac	CO_3	PO_4	Z_{AM}	CH4
Stoichiometric Coefficient	$-1\times MolmassAc$	$\left(1+\left(1-\frac{8}{gam\_o}\right)\right)\times MolmassCO_3^{2-}$	$\left(-\frac{8\cdot Y\_AM}{gam\_o}\cdot b\_o\right)\times MolmassPO_4^{3-}$	$\left(\frac{8\cdot Y\_AM}{gam\_o}\right)\times MolmassXam$	$(1-Y\_AM)\times MolmassCH_4$
PM Ref. No.	D10-4	D10-5	D10-6	D10-7	D10-8

	11. Hydrogenotrophic Methanogenesis		
Component	H_2O	H	NH_4
Stoichiometric Coefficient	$\left(3+\left(\frac{24-8\cdot z\_o+32\cdot b\_o}{gam\_o}-3\right)\cdot Y\_HM\right)\times MolmassH_2O$	$\left(\left(\frac{8\cdot a\_o-24\cdot b\_o-16}{gam\_o}+2\right)\cdot Y\_HM-2\right)\times MolmassH^+$	$\left(-\frac{8\cdot Y\_HM}{gam\_o}a\_o\right)\times MolmassNH_4^+$
PM Ref. No.	11-1	11-2	11-3

	11. Hydrogenotrophic Methanogenesis		
Component	H_2O	H	NH_4
Stoichiometric Coefficient	$\left(3+\left(\frac{24-8\cdot z\_o+32\cdot b\_o}{gam\_o}-3\right)\cdot Y\_HM\right)\times MolmassH_2O$	$\left(\left(\frac{8\cdot a\_o-24\cdot b\_o-16}{gam\_o}+2\right)\cdot Y\_HM-2\right)\times MolmassH^+$	$\left(-\frac{8\cdot Y\_HM}{gam\_o}a\_o\right)\times MolmassNH_4^+$
PM Ref. No.	11-1	11-2	11-3

Component	CO_3	PO_4	H2	Z_{HM}	CH4
Stoichiometric Coefficient	$\left(1-\left(1-\frac{8}{gam\_o}\right)\cdot Y\_HM\right)\times MolmassCO_3^{2-}$	$\left(-\frac{8\cdot Y\_HM}{gam\_o}b\_o\right)\times MolmassPO_4^{3-}$	$-4\times MolmassH_2$	$\frac{8}{gam\_o}\cdot Y\_HM\times MolmassXhm$	$(1-Y\_HM)\times MolmassCH_4$
PM Ref. No.	11-4	11-5	11-6	11-7	11-8

12. CO_2 Evolution					
Component	**H_2O**	**H**	**CO_3**	**CO2**	
Stoichiometric Coefficient	$1\times MolmassH_2O$	$-2\times MolmassH^+$	$-1\times MolmassCO_3^{2-}$	$1\times MolmassCO_2$	
PM Ref. No.	12-1	12-2	12-3	12-4	

13. Struvite Dissociation					
Component	**H_2O**	**Mg**	**NH_4**	**PO_4**	**Str**
Stoichiometric Coefficient	$-6\times MolmassH_2O$	$-1\times MolmassMg^{2+}$	$-1\times MolmassNH_4^+$	$-1\times MolmassPO_4^-$	$1\times MolmassStr$
PM Ref. No.	13-1	13-2	13-3	13-4	13-5

14. calcium phosphate Dissociation				
Component	**Ca**	**PO_4**	**ACP**	
Stoichiometric Coefficient	$-3\times MolmassCa^{2+}$	$-2\times MolmassPO_4^-$	$1\times MolmassCaP$	
No.	14-1	14-2	14-3	

15. K-Struvite Dissociation					
Component	**H_2O**	**K**	**Mg**	**PO_4**	**MgKP**
Stoichiometric Coefficient	$-6\times MolmassH_2O$	$-1\times MolmassK^+$	$-1\times MolmassMg^{2+}$	$-1\times MolmassPO_4^-$	$1\times MolmassMgKP$
PM Ref. No.	15-1	15-2	15-3	15-4	15-5

APPENDIX 7: RAW DATA FOR AS SYSTEMS

Table A7.1: Raw Measurements for the UCT Process Operated Nitrification-denitrification Biological Excess Phosphorus Removal System, fed settled wastewater and an extra 200mgCOD/*l* of acetate

			Experimental Period 5 (For the AD 10 day R_s)					Experimental Period 1 (For the AD 18 day R_s)				
Samples & Tests		Date	26-Oct-08	27-Oct-08	28-Oct-08	30-Oct-08	1-Nov-08	31-Mar-08	2-Apr-08	4-Apr-08	6-Apr-08	8-Apr-08
Chemical Oxygen Demand (COD)	Reading	Influent	6.9	7.7	6.6	6.6	6.7	3.7	4.0	5.2	4.9	5.5
		Filt. Influent	19.0	17.6	18.8	20.1	17.1	15.4	16.4	15.8	15.9	17.2
		Mixed liquor	14.1	14.2	13.9	14.1	13.5	10.0	11.2	12.0	12.8	12.5
		Effluent	24.2	24.6	24.1	25.2	25.1	21.9	22.9	23.8	23.6	24.3
		Blank	25.0	25.5	25.0	25.2	25.0	22.6	23.5	24.2	24.7	25.1
		FAS Norm.	0.05	0.05	0.05	0.05	0.05	0.05	0.05	0.05	0.05	0.05
	Dill.	Influent	1.0	1.0	1.0	1.0	1.0	1.0	1.0	1.0	1.0	1.0
		Mixed liquor	20.0	20.0	20.0	20.0	20.0	20.0	20.0	20.0	20.0	20.0
	Conc. (mgCOD/*l*)	Influent	757.3	744.8	769.9	778.2	765.7	774.1	798.7	778.2	811.0	790.3
		Filt. Influent	251.0	330.5	259.4	213.4	330.5	294.9	290.8	344.1	360.4	318.5
		Mixed liquor	9121.1	9455.8	9288.5	9288.5	9623.2	10321.9	10051.6	9986.0	9748.5	10201.0
		Effluent	33.5	37.7	37.7			28.7	24.6	16.4	45.1	32.3
Total Kjeldahl Nitrogen (TKN)	Reading	Influent	46.0	46.3	50.2	42.0	44.0	33.5	30.6	32.5	33.1	31.0
		Filt. Influent	40.2	41.7	37.1	35.0	42.0	24.5	23.0	28.0	30.0	30.5
		Mixed liquor	20.5	19.6	18.5	19.8	19.9	21.3	21.6	20.9	21.1	11.0
		Effluent	4.2	3.5	4.2	4.0	4.1	4.5	3.3	3.4	4.5	3.5
	sample size (ml)	Influent	10.0	10.0	10.0	10.0	10.0	1.0	1.0	1.0	1.0	1.0
		Filt. Influent	10.0	10.0	10.0	10.0	10.0	1.0	1.0	1.0	1.0	1.0
		Mixed liquor	10.0	10.0	10.0	10.0	10.0	10.0	10.0	10.0	10.0	5.0
		Effluent	10.0	10.0	10.0	10.0	10.0	1.0	1.0	1.0	1.0	1.0
	Dill.	Mixed liquor	20.0	20.0	20.0	20.0	20.0	20.0	20.0	20.0	20.0	20.0
	Conc. (mgN/*l*)	Influent	64.4	64.8		58.8	61.6	46.9	42.8	45.5	46.3	43.4
		Filt. Influent	56.3	58.4	51.9	49.0	58.8	34.3	32.2	39.2	42.0	42.7
		Mixed liquor	574.0	548.8	518.0	554.4	557.2	596.4	604.8	585.2	590.8	616.0
		Effluent	5.9	4.9	5.9	5.6	5.7	6.3	4.6	4.8	6.3	4.9
Free and Saline Ammonia (FSA)	Read	Influent	36.8	37.5	36.2	33.0	39.1	12.0	22.6	22.0	13.5	27.0
		Effluent	1.2	1.4	1.7	1.2	1.1	4.5	3.0	2.9	2.5	2.5
	sample	Inf & effl.	10.0	10.0	10.0	10.0	10.0	5.0	10.0	10.0	10.0	10.0
	Conc. (mgN/*l*)	Influent	51.5	52.5	50.7	46.2	54.7	33.6	31.6	30.8	37.8	37.8
		Effluent	1.7	2.0	2.4	1.7	1.5	6.3	4.2	4.1	3.5	3.5
MLSS and ISS (mg/*l*)	Anaerobic Tank (Measured)	Weight A	19.28	19.28	19.30	19.32	19.31	48.06	19.40	19.38	19.37	19.38
		Weight B	19.45	19.46	19.47	19.49	19.50	48.25	19.58	19.55	19.56	19.56
		Weight C	19.32	19.33	19.34	19.36	19.37	48.10	19.44	19.41	19.41	19.41
		TSS	3462.0	3572.0	3398.0	3488.0	3822.0	3736.0	3632.0	3426.0	3648.0	3572.0
		VSS	2626.0	2682.0	2590.0	2546.0	2724.0	2942.0	2892.0	2836.0	3012.0	2940.0
		ISS	836.0	890.0	808.0	942.0	1098.0	794.0	740.0	590.0	636.0	632.0
	Anoxic Tank (Measured)	Weight A	39.34	39.34	41.66	41.67	32.17	28.40	32.32	43.60	32.32	32.32
		Weight B	39.65	39.66	41.96	41.96	32.47	28.74	32.64	43.91	32.64	32.65
		Weight C	39.41	39.43	41.74	41.74	32.25	28.50	32.41	43.67	32.39	32.40
		TSS	6238.0	6302.0	6034.0	5744.0	6140.0	6732.0	6444.0	6264.0	6540.0	6642.0
		VSS	4816.0	4570.0	4418.0	4344.0	4574.0	4796.0	4628.0	4832.0	4976.0	5108.0
		ISS	1422.0	1732.0	1616.0	1400.0	1566.0	1936.0	1816.0	1432.0	1564.0	1534.0
	Re-Aeration Tank (Measured)	Weight A	32.09	32.10	32.12	32.15	41.68	53.21	30.39	32.32	43.59	39.41
		Weight B	32.41	32.41	32.43	32.43	41.99	53.54	30.73	32.64	43.92	39.76
		Weight C	32.17	32.19	32.19	32.23	41.77	53.29	30.48	32.41	43.66	39.49
		TSS	6392.0	6096.0	6202.0	5532.0	6186.0	6600.0	6636.0	6334.0	6534.0	6980.0
		VSS	4772.0	4284.0	4782.0	4048.0	4408.0	4908.0	4986.0	4638.0	5112.0	5436.0
		ISS	1620.0	1812.0	1420.0	1484.0	1778.0	1692.0	1650.0	1696.0	1422.0	1544.0
	Aerobic Tank (Measured)	Weight A	41.64	41.65	39.35	39.36	39.37	55.69	43.62	30.40	30.37	30.34
		Weight B	42.06	42.08	39.78	39.78	39.83	56.17	44.09	30.85	30.81	30.80
		Weight C	41.74	41.76	39.46	39.46	39.48	55.81	43.74	30.51	30.47	30.45
		TSS	8334.0	8692.0	8559.4	8314.0	9080.0	9464.0	9336.0	9024.0	8910.0	9144.0
		VSS	6386.0	6410.0	6384.0	6416.0	6816.0	7078.0	7066.0	6708.0	6828.0	6926.0
		ISS	1948.0	2282.0	2175.4	1898.0	2264.0	2386.0	2270.0	2316.0	2082.0	2218.0

Table A7.1

Samples & Tests		Date	Experimental Period 2 (For the AD 25 day R_s)					Experimental Period 4 (For the AD 40 day R_s)				
			2-Jun-08	4-Jun-08	6-Jun-08	8-Jun-08	10-Jun-08	18-Sep-08	20-Sep-08	25-Sep-08	26-Sep-08	28-Sep-08
Chemical Oxygen Demand (COD)	Reading	Influent	6.1	8.5	4.7	4.3	6.5	5.8	5.4	5.3	6.3	4.9
		Filt. Influent	15.7	17.3	16.6	15.8	17.8	18.9	18.8	18.5	18.6	19.5
		Mixed liquor	13.5	12.0	13.0	12.5	10.0	12.5	13.0	12.6	12.7	12.3
		Effluent	23.7	24.0	23.5	23.6	23.1	25.1	24.8	24.7	24.3	24.6
		Blank	24.6	24.4	24.6	24.5	24.4	25.2	25.2	25.0	24.9	25.0
		FAS Norm.	0.05	0.05	0.05	0.05	0.05	0.05	0.05	0.05	0.05	0.05
	Dil.	Influent	1.0	1.0	1.0	1.0	1.0	1.0	1.0	1.0	1.0	1.0
		Mixed liquor	20.0	20.0	20.0	20.0	20.0	20.0	20.0	20.0	20.0	20.0
	Conc. (mgCOD/l)	Influent	757.8	651.3	805.6	817.7	724.6	791.5	807.8	803.8	758.9	810.4
		Filt. Influent	364.5	290.8	323.8	352.2	267.2	257.0	261.1	265.2	257.0	221.8
		Mixed liquor	9093.1	10158.1	9391.4	9715.2		10363.2	9955.2	10118.4	9955.2	10241.3
		Effluent	36.9	16.4	44.5	36.4	52.6	4.1	16.3	12.2	24.5	16.1
Total Kjeldahl Nitrogen (TKN)	Reading	Influent	20.5	18.0	18.0	19.0	18.0	18.0	14.0	18.0	16.0	16.5
		Filt. Influent	14.0	16.0	15.0	15.0	13.0	17.0	11.5	10.5	11.0	13.0
		Mixed liquor	22.0	22.0	21.5	20.0	21.0	21.5	19.5	22.4	18.0	21.5
		Effluent	4.0	3.5	3.5	3.5	3.5	3.5	3.5	4.5	3.5	6.0
	sample size (ml)	Influent	2.0	2.0	2.0	2.0	2.0	2.0	2.0	2.0	2.0	2.0
		Filt. Influent	2.0	2.0	2.0	2.0	2.0	2.0	2.0	2.0	2.0	2.0
		Mixed liquor	10.0	10.0	10.0	10.0	10.0	10.0	10.0	10.0	10.0	10.0
		Effluent	1.0	1.0	1.0	1.0	1.0	1.0	1.0	1.0	1.0	1.0
	Dill.	Mixed liquor	20.0	20.0	20.0	20.0	20.0	20.0	20.0	20.0	20.0	20.0
	Conc. (mgN/l)	Influent	57.4	50.4	50.4	53.2	50.4	50.4	39.2	50.4	44.8	46.2
		Filt. Influent	39.2	44.8	42.0	42.0	36.4	47.6	32.2	29.4	30.8	36.4
		Mixed liquor	616.0	616.0	602.0	560.0	588.0	602.0	546.0	627.2	504.0	602.0
		Effluent	5.6	4.9	4.9	4.9	4.9	4.9	4.9	6.3	4.9	8.4
Free and Saline Ammonia (FSA)	Read	Influent	14.0	15.5	14.5	16.0	14.5	13.5	11.5	13.0	10.5	14.5
		Effluent	3.5	3.0	3.5	4.0	3.5	3.5	6.0	6.5	4.5	3.5
	sample size	Influent	5.0	10.0	10.0	5.0	5.0	5.0	5.0	5.0	5.0	5.0
		Effluent	10.0	10.0	10.0	10.0	10.0	10.0	20.0	20.0	10.0	10.0
	Conc. (mgN/l)	Influent	39.2	21.7	20.3	44.8	40.6	37.8	32.2	36.4	29.4	
		Effluent	4.9	4.2	4.9	5.6	4.9	4.9	4.2	4.6	6.3	4.9
MLSS and ISS (mg/l)	Anaerobic Tank (Measured)	Weight A	55.88	55.88	51.73	12.76		13.55	13.73	13.74	13.75	13.75
		Weight B	56.10	56.07	51.90	12.96		13.93	13.93	13.94	13.93	13.98
		Weight C	55.95	55.93	51.76	12.82		13.77	13.78	13.85	13.80	13.81
		TSS	4470.0	3850.0	3562.0	3892.0		7498.0	4124.0	4040.0	3524.0	4640.0
		VSS	3090.0	2774.0	2892.0	2748.0		3038.0	2960.0	1702.0	2524.0	3488.0
		ISS	1380.0	1076.0	670.0	1144.0		4460.0	1164.0	2338.0	1000.0	1152.0
	Anoxic Tank (Measured)	Weight A	51.69	51.71	48.07	19.39	19.36	39.39	27.35	28.42	27.36	27.36
		Weight B	52.06	52.05	48.41	19.77	19.73	39.74	28.08	28.77	27.71	27.73
		Weight C	51.82	51.82	48.16	19.51	19.50	39.49	27.45	28.54	27.47	27.48
		TSS	7340.0	6834.0	6614.0	7514.0	7276.0	7014.0		7082.0	6988.0	7298.0
		VSS	4640.0	4552.0	4938.0	5154.0	4616.0	4870.0		4700.0	4794.0	5016.0
		ISS	2700.0	2282.0	1676.0	2360.0	2660.0	2144.0		2382.0	2194.0	2282.0
	Re-Aeration Tank (Measured)	Weight A	28.39	41.59	48.46	54.65		39.39	43.59	30.36	30.39	46.47
		Weight B	28.75	41.95	48.82	55.03		39.72	43.95	30.74	30.74	47.10
		Weight C	28.52	41.70	48.56	54.80		39.47	43.70	30.50	30.50	46.00
		TSS	7186.0	7290.0	7086.0	7418.0		6614.0	7274.0	7538.0	7042.0	
		VSS	4520.0	5014.0	5062.0	4568.0		4870.0	5006.0	4772.0	4826.0	
		ISS	2666.0	2276.0	2024.0	2850.0		1744.0	2268.0	2766.0	2216.0	
	Aerobic Tank (Measured)	Weight A	53.24	53.27	50.29	53.83	53.82	43.58	39.41	32.35	30.92	30.93
		Weight B	53.71	53.75	50.76	54.36	54.32	44.04	39.89	32.00	31.39	31.41
		Weight C	53.40	53.44	50.43	54.01	53.98	43.69	39.54	30.51	31.04	31.06
		TSS	9504.0	9676.0	9542.0	10706.0	9982.0	9334.0	9552.0		9468.0	9424.0
		VSS	6312.0	6340.0	6650.0	6950.0	6662.0	7032.0	6992.0		6876.0	6862.0
		ISS	3192.0	3336.0	2892.0	3756.0	3320.0	2302.0	2560.0		2592.0	2562.0

Table A7.1

			Experimental Period 3 (For the AD 60 day R_s)					
Samples & Tests		Date	25-Jun-08	27-Jun-08	29-Jun-08	1-Jul-08	3-Jul-08	4-Jul-08
Chemical Oxygen Demand (COD)	Reading	Influent	3.5	4.1	5.1	3.4	5.0	5.7
		Filt. Influent	16.5	16.3	18.1	17.0	18.1	18.0
		Mixed liquor	12.6	11.8	11.2	11.5	12.1	12.5
		Effluent	24.3	23.7	23.9	23.4	24.3	24.2
		Blank	25.0	24.5	24.2	24.7	24.7	25.1
		FAS Norm.	0.05	0.05	0.05	0.05	0.05	0.05
	Dill.	Influent	1.0	1.0	1.0	1.0	1.0	1.0
		Mixed liquor	20.0	20.0	20.0	20.0	20.0	20.0
	Conc. (mgCOD/l)	Influent	880.6	835.6	782.3	872.4	806.9	782.2
		Filt. Influent	348.2	335.9	249.9	315.4	270.3	286.3
		Mixed liquor	10158.1	10403.8	10649.6	10813.4	10321.9	10160.6
		Effluent	28.7	32.8	12.3	53.2	16.4	36.3
Total Kjeldahl Nitrogen (TKN)	Reading	Influent	32.0	29.6	33.5	33.4	33.4	31.0
		Filt. Influent	18.5	23.0	21.5	24.5	23.9	27.7
		Mixed liquor	24.3	24.6	23.5	23.6	23.6	12.0
		Effluent	4.5	3.0	6.5	5.5	5.5	3.5
	sample size (ml)	Influent	1.0	1.0	1.0	1.0	1.0	1.0
		Mixed liquor	10.0	10.0	10.0	10.0	10.0	5.0
		Effluent	1.0	1.0	1.0	1.0	1.0	1.0
	Dill.	Mixed liquor	20.0	20.0	20.0	20.0	20.0	20.0
	Conc. (mgN/l)	Influent	44.8	41.4	46.9	46.8	46.8	43.4
		Filt. Influent	25.9	32.2	30.1	34.3	33.4	38.7
		Mixed liquor	680.4	688.8	658.0	660.8	660.8	672.0
		Effluent	6.3	4.2	9.1	7.7	7.7	4.9
Free and Saline Ammonia (FSA)	Read	Influent	10.0	18.5	22.0	11.4	9.9	21.5
		Effluent	4.5	3.0	2.9	4.1	4.1	3.2
	sampl e size	Influent	5.0	10.0	10.0	5.0	5.0	10.0
		Effluent	10.0	10.0	10.0	10.0	10.0	10.0
	Conc. (mgN /l)	Influent	28.0	25.9	30.8	31.9	27.7	30.1
		Effluent	6.3	4.2	4.1	5.7	5.7	4.5
MLSS and ISS (mg/l)	Anaerobic Tank (Measured)	Weight A	13.73	19.40	13.74	12.72	12.72	19.38
		Weight B	13.92	19.58	13.94	13.19	12.91	19.56
		Weight C	13.77	19.44	13.78	12.77	12.77	19.41
		TSS	3674.0	3632.0	4122.0	4673.0	3764.0	3572.0
		VSS	2848.0	2892.0	3162.0	4245.0	2864.0	2940.0
		ISS	826.0	740.0	960.0	428.0	900.0	632.0
	Anoxic Tank (Measured)	Weight A	30.38	32.32	28.38	27.94	28.38	32.32
		Weight B	30.74	32.64	28.79	28.31	28.75	32.65
		Weight C	30.47	32.41	28.51	28.03	28.50	32.40
		TSS	7310.0	6444.0	8016.0	7376.0	7374.0	6642.0
		VSS	5472.0	4628.0	5466.0	5594.0	5114.0	5108.0
		ISS	1838.0	1816.0	2550.0	1782.0	2260.0	1534.0
	Re-Aeration Tank (Measured)	Weight A	58.77	30.39	39.39	27.32	51.69	39.41
		Weight B	59.13	30.73	39.81	27.70	52.05	39.76
		Weight C	58.83	30.48	39.54	27.43	51.82	39.49
		TSS	7218.0	6636.0	8498.0	7554.0	7184.0	6980.0
		VSS	5916.0	4986.0	5536.0	5350.0	4558.0	5436.0
		ISS	1302.0	1650.0	2962.0	2204.0	2626.0	1544.0
	Aerobic Tank (Measured)	Weight A	39.40	51.71	30.37	30.82	57.83	30.34
		Weight B	39.89	52.21	30.86	31.32	58.33	30.82
		Weight C	39.54	51.84	30.51	30.96	57.82	30.46
		TSS	9868.0	10084.0	9796.0	10062.0		9544.0
		VSS	6992.0	7380.0	7012.0	7332.0		7126.0
		ISS	2876.0	2704.0	2784.0	2730.0		2418.0

Table A7.1

Samples & Tests			Date (2008)	Experimental Period 5 (For the AD 10 day R_s)					Experimental Period 1 (For the AD 18 day R_s)				
				26-Oct-	27-Oct-	28-Oct-	30-Oct-	1-Nov-	31-Mar-	2-Apr-	4-Apr-	6-Apr-	8-Apr-
OUR (mgO/l)				63.6	61.3	63.2	62.1		55.6		59.2	54.2	53.9
DSVI			ml/gTSS		26.0			26.0		97.0		89.0	
Nitrate (NO_3) and Nitrite (NO_2) Results	Reading (cm)	Nitrate + Nitrite	Anaerobic	0.0	0.0	0.0	0.0	0.0	0.0	0.0	0.0	0.0	0.0
			Anoxic	15.0	15.0	13.5	13.0	11.0	5.0	3.5	5.5	6.5	3.5
			Filt. Effluent	8.5	9.7	9.4	9.3	10.0	5.0	3.5	2.0	1.5	0.0
		Nitrite	Anaerobic	0.0	0.0	0.0	0.0	0.0	0.0	0.0	0.0	0.0	0.0
			Anoxic	18.5	18.0	19.0	16.5	17.0	0.0	0.0	0.0	0.0	0.0
			Filt. Effluent	0.0	0.0	0.0	0.0	0.0	0.0	0.0	0.0	0.0	0.0
	Stds line fn.	NO_2 & NO_3	Slope (m)	0.11	0.11	0.11	0.11	0.11	0.11	0.11	0.09	0.10	0.11
			Intercept (c)	0.22	0.22	0.22	0.22	0.22	0.00	0.00	0.00	0.00	0.00
		NO_2	Slope (m)	0.04	0.04	0.04	0.04	0.04	0.01	0.06	0.07	0.13	0.04
			Intercept (c)	0.01	0.01	0.01	0.01	0.01	0.00	0.00	0.00	0.00	0.00
	Dillution	NO_2 & NO_3	Anaerobic	1.0	1.0	1.0	1.0	1.0	1.0	1.0	1.0	1.0	1.0
			Anoxic	2.0	2.0	2.0	2.0	2.0	2.0	2.0	2.0	2.0	2.0
			Aerobic	10.0	10.0	10.0	10.0	10.0	20.0	20.0	20.0	20.0	20.0
			Filt. Effluent	10.0	10.0	10.0	10.0	10.0	20.0	20.0	20.0	20.0	20.0
	Conc. (mgN/l)	Nitrate	Anaerobic	0.0	0.0	0.0	0.0	0.0	0.0	0.0	0.0	0.0	0.0
			Anoxic	2.8	2.8	2.5	2.4	2.0	1.1	0.7	1.0	1.3	0.8
			Filt. Effluent	7.1	8.4	8.1	8.0	8.7	11.0	7.5	3.6	3.1	0.0
		Nitrite	Anaerobic	0.0	0.0	0.0	0.0	0.0	0.0	0.0	0.0	0.0	0.0
			Anoxic	1.6	1.5	1.6		1.4	0.0	0.0	0.0	0.0	0.0
			Filt. Effluent	0.0	0.0	0.0	0.0	0.0	0.0	0.0	0.0	0.0	0.0
Total Phosphates (TP) and Ortho-Phosphate (OP) Results	Reading	TP	Influent	0.10	0.08	0.08	0.08	0.08	0.10	0.10	0.10	0.09	0.10
			Filt. Influent	0.07	0.07	0.07	0.07	0.08	0.09	0.10	0.09	0.08	0.10
			Anaerobic	0.11	0.11	0.12	0.12	0.14	0.14	0.13	0.13	0.13	0.12
			Anoxic	0.07	0.08	0.07	0.07	0.09	0.10	0.10	0.10	0.08	0.10
			Aerobic	0.06	0.04	0.06	0.09	0.04	0.15	0.07	0.08	0.08	0.08
			Mixed liquor	0.15	0.13	0.11	0.13	0.14	0.15	0.14	0.14	0.15	0.15
			Filt. Effluent	0.06	0.05	0.06	0.09	0.04	0.14	0.07	0.08	0.09	0.07
		OP	Influent	0.11	0.10	0.11	0.11	0.18	0.13	0.13	0.14	0.12	0.13
			Anaerobic	0.21	0.18	0.22	0.17	0.14	0.22	0.15	0.17	0.17	0.19
			Aerobic	0.20	0.16	0.18	0.17	0.13	0.21	0.10	0.17	0.18	0.24
			Filt. Effluent	0.19	0.17	0.18	0.16	0.13	0.20	0.12	0.19	0.20	0.21
	Stds Line fn.	TP	Slope	160.97	160.97	160.97	160.97	160.97	181.40	181.40	178.34	178.34	178.34
			Intercept (-ve)	-0.42	-0.42	-0.42	-0.42	-0.42	3.68	3.68	2.83	2.83	2.83
		OP	Slope	106.25	106.25	106.25	106.25	106.25	108.21	108.21	107.29	107.29	107.29
			Intercept (-ve)	0.03	0.03	0.03	0.03	0.03	1.21	1.21	1.52	1.52	1.52
	Dillution	TP	Influent	4.0	4.0	4.0	4.0	4.0	4.0	4.0	4.0	4.0	4.0
			Filt. Influent	4.0	4.0	4.0	4.0	4.0	4.0	4.0	4.0	4.0	4.0
			Anaerobic	5.0	5.0	5.0	5.0	5.0	5.0	5.0	5.0	5.0	5.0
			Anoxic	4.0	4.0	4.0	4.0	4.0	4.0	4.0	4.0	4.0	4.0
			Aerobic (filt)	2.0	2.0	2.0	2.0	2.0	1.0	2.0	2.0	2.0	2.0
			Mixed liquor	40.0	40.0	40.0	40.0	40.0	40.0	40.0	40.0	40.0	40.0
			Filt. Effluent	2.0	2.0	2.0	2.0	2.0	1.0	2.0	2.0	2.0	2.0
		OP	Influent	4.0	4.0	4.0	4.0	4.0	4.0	4.0	4.0	4.0	4.0
			Anaerobic	1.0	1.0	1.0	1.0	1.0	5.0	5.0	5.0	5.0	4.0
			Filt. Effluent	1.0	1.0	1.0	1.0	1.0	1.0	2.0	1.0	1.0	1.0
	Conc. (mgP/l)	TP	Influent	63.5	51.2	51.9	53.2	55.8	57.8	54.9	58.6	54.3	59.3
			Filt. Influent	46.7	48.7	49.3	46.1	50.0	52.7	54.2	54.3	48.7	56.4
			Anaerobic	87.4	91.4	101.9	94.6	111.5	107.7	97.7	103.5	100.0	96.4
			Anoxic	44.2	50.0	48.7	49.3	58.3	60.7	57.8	60.7	47.9	59.3
			Aerobic (filt)	18.5	13.4	20.1	29.8	13.1	23.5	19.5	22.9	24.3	23.9
			Mixed liquor	995.3	873.0	724.9	853.7	885.9	926.5	875.7	871.1	956.7	942.4
			Filt. Effluent	21.1	16.6	19.5		14.4	21.7	16.6	21.1	24.6	20.0
		OP	Influent	46.6	43.2	45.8	46.2		52.7	49.7	51.8	46.7	49.7
			Aerobic	21.4	16.5	18.9	18.2		21.2	18.8	16.2	18.1	23.7
			Filt. Effluent	20.2	18.0	19.1	17.0	13.8	20.2	22.5	18.4	20.1	20.8

Table A7.1

				Experimental Period 2 (For the AD 25 day R_s)					Experimental Period 4 (For the AD 40 day R_s)				
Samples & Tests			Date	2-Jun-08	4-Jun-08	6-Jun-08	8-Jun-08	10-Jun-08	18-Sep-08	20-Sep-08	25-Sep-08	26-Sep-08	28-Sep-08
OUR (mgO/l)				45.6	51.5	49.2	54.2	53.9	59.0	61.0	60.0	64.2	53.9
DSVI			ml/gTSS			92.6							93.4
Nitrate (NO_3) and Nitrite (NO_2) Results	Reading (cm)	Nitrate + Nitrite	Anaerobic	0.5	0.5	1.5	1.0	2.5	0.0	0.0	2.0	0.0	1.0
			Anoxic	0.5	0.0	1.5	2.5	0.5	3.0	2.5	0.5	0.0	0.0
			Filt. Effluent	5.5	7.5	3.5	6.0	1.5	1.0	1.1	0.9	2.0	3.0
		Nitrite	Anaerobic	0.0	0.0	0.0	0.0	0.5	0.0	0.0	0.0	0.0	1.0
			Anoxic	9.5	0.0	0.0	0.0	0.0	0.0	0.0	0.0	0.0	0.0
			Filt. Effluent	12.5	2.5	3.5	3.5	1.0	0.0	2.5	0.0	0.0	0.0
	Stds line fn.	NO_2 & NO_3	Slope (m)	0.03	0.03	0.06	0.03	0.11	0.13	0.13	0.13	0.12	0.13
			Intercept (c)	-0.05	-0.04	-0.05	-0.05	-0.07	-0.15	-0.19	-0.19	-0.09	-0.13
		NO_2	Slope (m)	0.06	0.11	0.03	0.06	0.07	0.07	0.07	0.07	0.07	0.06
			Intercept (c)	-0.03	-0.20	-0.02	-0.05	0.00	-0.13	-0.10	-0.02	-0.01	-0.04
	Dillution	NO_2 & NO_3	Anaerobic	1.0	1.0	1.0	1.0	1.0	1.0	1.0	1.0	1.0	1.0
			Anoxic	2.0	2.0	2.0	2.0	2.0	2.0	2.0	2.0	2.0	2.0
			Aerobic	20.0	20.0	20.0	20.0	20.0	20.0	20.0	20.0	20.0	20.0
			Filt. Effluent	20.0	20.0	20.0	20.0	20.0	20.0	20.0	20.0	20.0	10.0
	Conc. (mgN/l)	Nitrate	Anaerobic	0.1	0.0	0.1	0.1	0.3	0.2	0.2	0.4	0.1	0.3
			Anoxic	0.1	0.1	0.3	0.3	0.2	1.1	1.0	0.5	0.2	0.3
			Filt. Effluent	4.8	4.6	5.4	5.2	4.7	5.6	6.5	6.0	6.7	5.0
		Nitrite	Anaerobic	0.0	0.2	0.0	0.1	0.0	0.1	0.1	0.0	0.0	0.1
			Anoxic	1.2	0.4	0.0	0.0	0.0	0.3	0.2	0.0	0.0	0.1
			Filt. Effluent	0.0	0.0	0.0	0.0	0.0	0.0	0.0	0.0	0.0	0.0
Total Phosphates (TP) and Ortho-Phosphate (OP) Results	Reading	TP	Influent	0.10	0.13	0.11	0.10	0.12	0.10	0.10	0.10	0.10	0.10
			Filt. Influent	0.08	0.11	0.10	0.09	0.10	0.09	0.09	0.09	0.09	0.09
			Anaerobic	0.14	0.16	0.18	0.20	0.24	0.09	0.12	0.11	0.13	0.13
			Anoxic	0.14	0.14	0.14	0.01	0.03	0.13	0.11	0.12	0.12	0.11
			Aerobic	0.06	0.08	0.20	0.16	0.17	0.08	0.07	0.08	0.07	0.08
			Mixed liquor	0.17	0.14	0.18	0.14	0.18	0.14	0.13	0.15	0.14	0.15
			Filt. Effluent	0.17	0.16	0.19	0.17	0.15	0.08	0.08	0.07	0.08	0.09
		OP	Influent	0.10	0.22	0.14	0.13	0.13	0.13	0.12	0.12	0.13	0.12
			Anaerobic	0.26	0.22	0.26	0.23	0.21	0.14	0.21	0.22	0.22	0.21
			Aerobic	0.30	0.21	0.30	0.28	0.28	0.13	0.20	0.20	0.21	0.20
			Filt. Effluent	0.29	0.25	0.27	0.28	0.28	0.23	0.19	0.20	0.20	0.21
	Stds Line fn.	TP	Slope	177.05	177.05	162.81	162.81	162.81	177.05	177.05	162.81	162.81	162.81
			Intercept (-ve)	3.31	3.31	2.26	2.26	2.26	3.31	3.31	2.26	2.26	2.26
		OP	Slope	93.37	93.37	99.32	99.32	99.32	93.37	93.37	99.32	99.32	99.32
			Intercept (-ve)	0.91	0.91	1.81	1.81	1.81	0.91	0.91	1.81	1.81	1.81
	Dillution	TP	Influent	4.0	4.0	4.0	4.0	4.0	4.0	4.0	4.0	4.0	4.0
			Filt. Influent	4.0	4.0	4.0	4.0	4.0	4.0	4.0	4.0	4.0	4.0
			Anaerobic	5.0	5.0	5.0	5.0	5.0	5.0	5.0	5.0	5.0	5.0
			Anoxic	4.0	4.0	4.0	4.0	4.0	4.0	4.0	4.0	4.0	4.0
			Aerobic (filt)	2.0	2.0	2.0	2.0	2.0	2.0	2.0	2.0	2.0	2.0
			Mixed liquor	40.0	40.0	40.0	40.0	40.0	40.0	40.0	40.0	40.0	40.0
			Filt. Effluent	1.0	1.0	1.0	1.0	1.0	2.0	2.0	2.0	2.0	2.0
		OP	Influent	4.0	4.0	4.0	4.0	4.0	4.0	4.0	4.0	4.0	4.0
			Anaerobic	5.0	5.0	5.0	5.0	4.0	5.0	5.0	5.0	5.0	4.0
			Filt. Effluent	1.0	1.0	1.0	1.0	1.0	1.0	1.0	1.0	1.0	1.0
	Conc. (mgP/l)	TP	Influent	56.9	75.3	63.3	58.7	67.8	54.0	57.6	52.8	56.7	55.4
			Filt. Influent	44.8	65.6	54.8	46.3	55.4	48.4	50.5	46.3	48.3	48.9
			Anaerobic	105.6	126.9	137.7	154.8	184.9	64.9	89.7	78.3	94.5	94.5
			Anoxic	85.9	82.4	82.1	0.1	11.8	76.7	65.4	67.2	65.9	65.2
			Aerobic (filt)	14.6	21.7	61.3	46.0	49.5	21.4	17.5	21.2	18.9	20.6
			Mixed liquor	1071.6	866.3	1075.4	821.4	1108.0	859.2		854.0		886.5
			Filt. Effluent	26.8	25.0	27.9	25.3	22.8	21.7	19.9	18.3	22.2	24.1
		OP	Influent	33.6	78.7	50.1	45.6	43.7	44.2	41.2	41.6	44.0	40.8
			Aerobic	26.6	19.0	27.5	26.0		11.1	17.6	18.3	18.7	18.5
			Filt. Effluent	26.3	22.5	25.1	25.5		20.2	17.0	17.6	18.0	19.0

Table A7.1

				Experimental Period 3 (For the AD 60 day R_s)					
Samples & Tests			Date	25-Jun-08	27-Jun-08	29-Jun-08	1-Jul-08	3-Jul-08	4-Jul-08
OUR (mgO/*l*)				52.0	51.6	52.4	50.0	49.9	50.3
DSVI			ml/gTSS		86.0				
Nitrate (NO_3) and Nitrite (NO_2) Results	Reading (cm)	Nitrate + Nitrite	Anaerobic	10.0	3.5	0.1	3.5	3.5	0.5
			Anoxic	5.0	3.0	0.5	0.5	0.5	3.5
			Filt. Effluent	5.0	1.5	3.9	1.5	1.0	0.0
		Nitrite	Anaerobic	2.0	4.5	0.5	12.0	12.0	2.0
			Anoxic	1.0	11.0	0.5	10.0	10.0	3.5
			Filt. Effluent	6.0	7.5	0.6	10.5	10.5	0.5
	Stds line fn.	NO_2 & NO_3	Slope (m)	0.01	0.09	0.06	0.10	0.10	0.11
			Intercept (c)	-0.12	-0.11	-0.03	-0.15	-0.15	-0.28
		NO_2	Slope (m)	0.01	0.06	0.07	0.13	0.13	0.04
			Intercept (c)	-0.05	-0.03	0.00	-0.08	-0.08	0.01
	Dilution	NO_2 & NO_3	Anaerobic	1.0	1.0	1.0	1.0	1.0	1.0
			Anoxic	2.0	2.0	2.0	2.0	2.0	2.0
			Aerobic	20.0	20.0	20.0	20.0	20.0	20.0
			Filt. Effluent	20.0	20.0	20.0	20.0	20.0	20.0
	Conc. (mgN/*l*)	Nitrate	Anaerobic	0.2	0.4	0.0	0.5	0.5	0.3
			Anoxic	0.3	0.7	0.1	0.4	0.4	1.4
			Filt. Effluent	3.4	4.8	5.3	6.2	5.1	5.5
		Nitrite	Anaerobic	0.1	0.3	0.0	1.7	1.7	0.1
			Anoxic	0.1	1.4	0.1	0.0	0.0	0.3
			Filt. Effluent	0.0	0.0	0.0	0.0	0.0	0.0
Total Phosphates (TP) and Ortho-Phosphate (OP) Results	Reading	TP	Influent	0.10	0.11	0.09	0.10	0.09	0.09
			Filt. Influent	0.08	0.07	0.07	0.07	0.07	0.06
			Anaerobic	0.10	0.12	0.14	0.15	0.15	0.15
			Anoxic	0.11	0.10	0.11	0.13	0.08	0.10
			Aerobic	0.08	0.08	0.08	0.12	0.08	0.08
			Mixed liquor	0.16	0.15	0.13	0.14	0.15	0.15
			Filt. Effluent	0.07	0.08	0.07	0.13	0.07	0.08
		OP	Influent	0.09	0.09	0.11	0.10	0.10	0.09
			Anaerobic	0.23	0.13	0.20	0.23	0.21	0.23
			Aerobic	0.17	0.18	0.20	0.20	0.17	0.19
			Filt. Effluent	0.18	0.19	0.19	0.19	0.16	0.19
	Stds Line fn.	TP	Slope	181.40	181.40	178.34	178.34	178.34	178.34
			Intercept (-ve)	3.68	3.68	2.83	2.83	2.83	2.83
		OP	Slope	108.21	108.21	107.29	107.29	107.29	107.29
			Intercept (-ve)	1.21	1.21	1.52	1.52	1.52	1.52
	Dilution	TP	Influent	4.0	4.0	4.0	4.0	4.0	4.0
			Filt. Influent	4.0	4.0	4.0	4.0	4.0	4.0
			Anaerobic	5.0	5.0	5.0	5.0	5.0	5.0
			Anoxic	4.0	4.0	4.0	4.0	4.0	4.0
			Aerobic (filt)	2.0	2.0	2.0	1.0	2.0	2.0
			Mixed liquor	40.0	40.0	40.0	40.0	40.0	40.0
			Filt. Effluent	2.0	2.0	2.0	1.0	2.0	2.0
		OP	Influent	4.0	4.0	4.0	4.0	4.0	4.0
			Anaerobic	5.0	5.0	5.0	5.0	5.0	4.0
			Filt. Effluent	1.0	1.0	1.0	1.0	1.0	1.0
	Conc. (mgP/*l*)	TP	Influent	57.8	61.5	49.3	57.1	54.3	53.6
			Filt. Influent	39.7	34.6	41.5	35.0	37.9	34.3
			Anaerobic	75.0	90.4	106.2	120.5	118.7	121.4
			Anoxic	63.6	57.8	65.0	81.4	46.4	59.3
			Aerobic (filt)	19.8	20.6	23.2	18.4	21.4	23.2
			Mixed liquor	977.3	962.8	814.0	899.6	956.7	921.0
			Filt. Effluent	19.5	19.8	19.3	20.0	17.5	21.8
		OP	Influent	32.0	34.1	40.7	34.7	35.5	33.8
			Aerobic	17.6	18.6	19.4	19.5		19.3
			Filt. Effluent	18.7	19.3	18.5	18.4		18.9

Table A7.2: Raw Measurements for Modified Ludzack Ettinger System 2 (MLE 2) which carries out nitrification - denitrification process, operated using raw wastewater

			Experimental Period 5 (For the AD 10 day R_s)					Experimental Period 1 (For the AD 18 day R_s)				
Samples & Tests		Date	26-Oct-08	27-Oct-08	28-Oct-08	30-Oct-08	1-Nov-08	31-Mar-08	2-Apr-08	4-Apr-08	6-Apr-08	8-Apr-08
Chemical Oxygen Demand (COD)	Reading	Influent	20.2	19.9	20.8	20.3	20.2	9.2	9.6	11.4	10.2	11.6
		Filt. Influent	22.5	23.0	22.7	23.6	23.1	19.1	18.5	20.4	20.9	21.2
		Mixed liquor	18.2	17.9	17.2	17.5	17.8	7.0	7.5	6.1	7.5	6.3
		Effluent	24.2	24.1	24.1	23.8	24.0	21.7	22.3	23.4	23.8	24.0
		Filtered Eff.	24.2	24.1	24.1	23.8	24.0	21.7	22.3	23.4	23.8	24.0
		Blank	25.0	25.5	25.0	25.2	25.0	22.6	23.5	24.2	24.7	25.1
		FAS Norm.	0.05	0.05	0.05	0.05	0.05	0.05	0.05	0.05	0.05	0.05
	Dill.	Influent	5.0	5.0	5.0	5.0	5.0	2.0	2.0	2.0	2.0	2.0
		Mixed liquor	10.0	10.0	10.0	10.0	10.0	5.0	5.0	5.0	5.0	5.0
	Conc. (mgCOD/l)	Influent	979.2	1142.4	856.8	999.6	979.2	1097.7	1138.7	1048.6	1187.8	1088.6
		Filt. Influent	102.0	102.0	93.8	65.3	77.5	143.4	204.8	155.6	155.6	157.2
		Mixed liquor	2774.4	3100.8	3182.4	3141.6	2937.6	3194.9	3276.8	3706.9	3522.6	3790.1
		Filtered Eff.	32.6		36.7		40.8	36.9	49.2	32.8	36.9	44.4
Total Kjeldahl Nitrogen (TKN)	Reading	Influent	27.5	27.1	24.5	26.5	25.5	20.0	20.5	39.8	39.0	19.0
		Filt. Influent	18.9	21.3	20.0	20.5	15.5	16.5	15.5	31.0	29.0	10.0
		Mixed liquor	13.5	15.5	17.5	15.5	21.0	19.5	18.5	19.0	18.5	18.8
		Effluent	3.5	4.5	3.5	2.5	3.5	3.5	3.5	3.5	4.5	3.5
	sample size	Influent	5.0	5.0	5.0	5.0	5.0	2.0	2.0	1.0	1.0	2.0
		Filt. Influent	10.0	10.0	10.0	10.0	5.0	2.0	2.0	1.0	1.0	2.0
		Mixed liquor	10.0	10.0	10.0	10.0	20.0	10.0	10.0	10.0	10.0	10.0
		Effluent	10.0	10.0	10.0	10.0	10.0	1.0	1.0	1.0	1.0	1.0
	Dill.	Mixed liquor	5.0	10.0	10.0	10.0	10.0	10.0	10.0	10.0	10.0	10.0
	Conc. (mgN/l)	Influent	77.0	75.9	68.6	74.2	71.4	56.0	57.4	55.7	54.6	53.2
		Filt. Influent	26.5	29.8	28.0	28.7	43.4	46.2	43.4	43.4	40.6	28.0
		Mixed liquor	94.5	217.0	245.0	217.0	147.0	273.0	259.0	266.0	259.0	263.2
		Effluent	4.9	6.3	4.9		4.9	4.9	4.9	4.9		4.9
Free and Saline Ammonia (FSA)	Read	Influent	19.5	21.3	17.5	18.0	14.5	10.5	29.0	28.0	28.0	19.9
		Effluent	3.0	4.0	3.5	2.5	2.5	3.5	2.7	3.0	3.5	2.5
	sampl e size	Influent	10.0	10.0	10.0	10.0	10.0	2.5	1.0	1.0	1.0	1.0
		Effluent	10.0	10.0	10.0	10.0	10.0	1.0	1.0	1.0	1.0	1.0
	Conc. (mgN /l)	Influent	27.3	29.8	24.5	25.2	20.3	36.8	40.6	39.2	39.2	27.9
		Effluent	4.2	5.6	4.9	3.5	3.5	4.9	3.8	4.2	4.9	3.5
MLSS and ISS	Anoxic Tank	Weight A	60.13	98.03	49.83	61.09	59.20	53.30	53.30	53.28	53.27	53.27
		Weight B	60.26	98.17	49.96	61.23	59.34	53.44	53.44	53.42	53.41	53.40
		Weight C	60.16	98.06	49.85	61.12	59.24	53.32	53.32	53.31	53.30	53.29
		Sample (ml)	50.0	50.0	50.0	50.0	50.0	50.0	50.0	50.0	50.0	50.0
		TSS	2502.0	2662.0	2450.0	2628.0	2666.0	2896.0	2750.0	2834.0	2806.0	2654.0
		VSS	1920.0	2106.0	2026.0	2120.0	1954.0	2348.0	2254.0	2286.0	2290.0	2260.0
		ISS	582.0	556.0	424.0	508.0	712.0	548.0	496.0	548.0	516.0	394.0
	Aerobic Tank	Weight A	49.16	75.50	50.24	55.67	61.04	58.66	60.81	60.81	60.80	60.80
		Weight B	49.29	75.62	50.36	55.80	61.17	58.80	60.95	60.95	60.94	60.95
		Weight C	49.18	75.52	50.26	55.69	61.06	58.69	60.84	60.84	60.82	60.82
		Sample (ml)	50.0	50.0	50.0	50.0	50.0	50.0	50.0	50.0	50.0	50.0
		TSS	2668.0		2414.0	2714.0	2574.0	2746.0	2782.0	2944.0	2846.0	3070.0
		VSS	2152.0		1926.0	2168.0	2042.0	2250.0	2282.0	2314.0	2350.0	2642.0
		ISS	516.0		488.0	546.0	532.0	496.0	500.0	630.0	496.0	428.0
OUR (mgO/l)			31.6	30.9	29.9	31.9	28.7	30.2	35.5	29.0	34.8	30.6
DSVI (ml/gTSS)			115.1	112.9	110.3	95.1	101.2					

Table A7.2

			Experimental Period 2 (For the AD 25 day R_s)					Experimental Period 4 (For the AD 40 day R_s)				
Samples & Tests		Date	2-Jun-08	4-Jun-08	6-Jun-08	8-Jun-08	10-Jun-08	18-Sep-08	20-Sep-08	25-Sep-08	26-Sep-08	28-Sep-08
Chemical Oxygen Demand (COD)	Reading	Influent	13.8	12.6	10.4	13.0	13.3	13.0	12.0	12.2	11.4	11.5
		Filt. Influent	19.5	20.5	21.0	20.5	19.7	20.7	21.5	22.0	20.9	22.4
		Mixed liquor	8.7	10.0	9.7	9.2	9.2	16.9	9.7	7.5	9.1	8.9
		Effluent	23.6	23.0	23.0	22.8	22.6	24.0	24.4	23.5	23.8	24.0
		Filtered Eff.	23.6	23.0	23.0	22.8	22.6	24.0	24.4	23.5	23.8	24.0
		Blank	24.6	24.4	24.6	24.5	24.4	25.2	25.2	25.0	24.9	25.0
		FAS Norm.	0.05	0.05	0.05	0.05	0.05	0.05	0.05	0.05	0.05	0.05
	Dill.	Influent	2.0	2.0	2.0	2.0	2.0	2.0	2.0	2.0	2.0	2.0
		Mixed liquor	5.0	5.0	5.0	5.0	5.0	10.0	5.0	5.0	5.0	5.0
	Conc. (mgCOD/l)	Influent	884.7	966.7	1149.6	931.0	898.7	995.5	1077.1	1044.5	1101.6	1088.6
		Filt. Influent	208.9	159.7	145.7	161.9	190.3	183.6	151.0	122.4	163.2	104.8
		Mixed liquor	3256.3	2949.1	3015.8	3096.7	3076.5	3386.4	3162.0	3570.0	3223.2	3245.8
		Filtered Eff.	41.0	57.3	64.8	68.8	72.9	49.0	32.6			40.3
Total Kjeldahl Nitrogen (TKN)	Reading	Influent	20.2	19.5	20.5	18.0	20.0	22.0	21.0	39.8	42.5	21.0
		Filt. Influent	15.2	14.5	13.5	14.0	15.0	17.5	15.5	32.0	31.0	13.0
		Mixed liquor	8.5	8.0	7.5	9.0	7.8	19.5	18.5	19.0	18.5	18.8
		Effluent	4.0	4.5	4.2	4.2	3.9	4.5	3.9	3.7	4.0	4.2
	sample size	Influent	2.0	2.0	2.0	2.0	2.0	2.0	2.0	1.0	1.0	2.0
		Filt. Influent	2.0	2.0	2.0	2.0	2.0	2.0	2.0	1.0	1.0	2.0
		Mixed liquor	5.0	5.0	5.0	5.0	5.0	10.0	10.0	10.0	10.0	10.0
		Effluent	1.0	1.0	1.0	1.0	1.0	1.0	1.0	1.0	1.0	1.0
	Dill.	Mixed liquor	10.0	10.0	10.0	10.0	10.0	10.0	10.0	10.0	10.0	10.0
	Conc. (mgN/l)	Influent	56.6	54.6	57.4	50.4	56.0	61.6	58.8	55.7	59.5	58.8
		Filt. Influent	42.6	40.6	37.8	39.2	42.0	49.0	43.4	44.8	43.4	36.4
		Mixed liquor	238.0	224.0	210.0	252.0	218.4	273.0	259.0	266.0	259.0	263.2
		Effluent	5.6	6.3	5.9	5.9	5.5	6.3	5.5	5.2	5.6	5.9
Free and Saline Ammonia (FSA)	Read	Influent	13.0	12.0	12.5	14.0	12.5	16.1	15.5	14.0	13.0	12.5
		Effluent	2.7	2.5	3.0	2.6	3.1	2.8	3.0	3.6	3.5	2.5
	sample size	Influent	2.0	2.0	2.0	2.0	2.0	2.0	2.0	2.0	2.0	2.0
		Effluent	1.0	1.0	1.0	1.0	1.0	1.0	1.0	1.0	1.0	1.0
	Conc. (mgN/l)	Influent	36.4	33.6	35.0	39.2	35.0	45.1	43.4	39.2	36.4	35.0
		Effluent	3.8	3.5	4.2	3.6	4.3	3.9	4.2	5.0	4.9	3.5
MLSS and ISS	Anoxic Tank	Weight A	59.10	59.11	59.12	59.11	59.11	59.35	59.35	59.44	59.39	59.39
		Weight B	59.22	59.23	59.24	59.25	59.26	59.47	59.48	59.57	59.52	59.51
		Weight C	59.12	59.13	59.14	59.14	59.14	59.36	59.36	59.46	59.41	59.40
		Sample (ml)	50.0	50.0	50.0	50.0	50.0	50.0	50.0	50.0	50.0	50.0
		TSS	2560.0	2366.0	2280.0	2832.0	2922.0	2490.0	2688.0	2538.0	2622.0	2422.0
		VSS	2134.0	2014.0	2014.0	2346.0	2352.0	2130.0	2332.0	2256.0	2270.0	2154.0
		ISS	426.0	352.0	266.0	486.0	570.0	360.0	356.0	282.0	352.0	268.0
	Aerobic Tank	Weight A	58.12	58.13	58.15	58.14	58.16	60.80	60.80	60.82	60.80	60.80
		Weight B	58.25	58.24	58.26	58.27	58.30	60.93	60.92	60.95	60.93	60.93
		Weight C	58.14	58.15	58.16	58.16	58.18	60.81	60.81	60.84	60.82	60.82
		Sample (ml)	50.0	50.0	50.0	50.0	50.0	50.0	50.0	50.0	50.0	50.0
		TSS	2550.0	2266.0	2364.0	2726.0	2732.0	2620.0	2566.0	2748.0	2692.0	2598.0
		VSS	2196.0	1784.0	1984.0	2214.0	2210.0	2258.0	2266.0	2296.0	2274.0	2226.0
		ISS	354.0	482.0	380.0	512.0	522.0	362.0	300.0	452.0	418.0	372.0
OUR (mgO/l)			26.2	29.5	28.5	29.5	28.0	32.5	29.6	31.1	28.8	33.2

Table A7.2

Samples & Tests		Date	25-Jun-08	27-Jun-08	29-Jun-08	1-Jul-08	3-Jul-08	4-Jul-08
			Experimental Period 3 (For the AD 60 day R_s)					
Chemical Oxygen Demand (COD)	Reading	Influent	12.3	11.8	12.0	9.0	9.0	12.7
		Filt. Influent	20.9	20.8	20.6	20.6	21.3	19.5
		Mixed liquor	9.0	7.0	16.3	6.7	6.7	6.5
		Effluent	23.4	23.7	23.7	23.3	23.7	24.0
		Filtered Eff.	23.4	23.5	23.0	23.3	23.7	24.0
		Blank	24.5	24.5	24.5	24.5	24.5	24.5
		FAS Norm.	0.05	0.05	0.05	0.05	0.05	0.05
	Dill.	Influent	2.0	2.0	2.0	2.0	2.0	2.0
		Mixed liquor	5.0	5.0	10.0	5.0	5.0	5.0
	Conc. (mgCOD/*l*)	Influent	999.4	1040.4	1024.0	1269.8	1269.8	951.6
		Filt. Influent	147.5	151.6	159.7	159.7	131.1	201.6
		Mixed liquor	3174.4	3584.0	3358.7	3645.4	3645.4	3628.8
		Filtered Eff.	45.1	41.0	61.4	49.2	32.8	20.2
Total Kjeldahl Nitrogen (TKN)	Reading	Influent	19.8	20.1	40.8	43.0	43.0	21.0
		Filt. Influent	16.4	13.4	31.0	29.0	27.0	10.0
		Mixed liquor	20.5	21.5	20.0	18.5	21.0	22.8
		Effluent	3.5	3.5	3.5	4.5	4.7	3.5
	sample size	Influent	2.0	2.0	1.0	1.0	1.0	2.0
		Filt. Influent	2.0	2.0	1.0	1.0	1.0	2.0
		Mixed liquor	10.0	10.0	10.0	10.0	10.0	10.0
		Effluent	1.0	1.0	1.0	1.0	1.0	1.0
	Dill.	Mixed liquor	10.0	10.0	10.0	10.0	10.0	10.0
	Conc. (mgN/*l*)	Influent	55.4	56.3	57.1	60.2	60.2	58.8
		Filt. Influent	45.9	37.5	43.4	40.6	37.8	28.0
		Mixed liquor	287.0	301.0	280.0	259.0	294.0	319.2
		Effluent	4.9	4.9	4.9	6.3	6.6	4.9
Free and Saline Ammonia (FSA)	Read	Influent	10.5	29.0	28.0	26.0	28.0	15.2
		Effluent	3.5	2.9	3.0	3.5	3.8	2.5
	sample size	Influent	2.5	1.0	1.0	1.0	1.0	1.0
		Effluent	1.0	1.0	1.0	1.0	1.0	1.0
	Conc. (mgN/*l*)	Influent	36.8	40.6	39.2	36.4	39.2	21.3
		Effluent	4.9	4.1	4.2	4.9	5.3	3.5
MLSS and ISS	Anoxic Tank	Weight A	53.30	53.30	53.28	53.27	53.27	53.27
		Weight B	53.43	53.44	53.42	53.41	53.42	53.41
		Weight C	53.32	53.32	53.31	53.30	53.30	53.29
		Sample (ml)	50.0	50.0	50.0	50.0	50.0	50.0
		TSS	2696.0	2870.0	2914.0	2686.0	2886.0	2834.0
		VSS	2148.0	2374.0	2366.0	2170.0	2370.0	2440.0
		ISS	548.0	496.0	548.0	516.0	516.0	394.0
	Aerobic Tank	Weight A	58.66	60.81	60.81	60.80	60.80	60.80
		Weight B	58.82	60.95	60.95	60.95	60.94	60.94
		Weight C	58.69	60.84	60.84	60.82	60.82	60.82
		Sample (ml)	50.0	50.0	50.0	50.0	50.0	50.0
		TSS	3086.0	2722.0	2944.0	2926.0	2826.0	2720.0
		VSS	2590.0	2222.0	2314.0	2430.0	2330.0	2342.0
		ISS	496.0	500.0	630.0	496.0	496.0	378.0
OUR (mgO/*l*)			28.0	27.0	26.5	31.8	36.0	36.7

Table A7.2

Samples & Tests			Date	Experimental Period 5 (For the AD 10 day R_s) 26-Oct-08	27-Oct-08	28-Oct-08	30-Oct-08	1-Nov-08	Experimental Period 1 (For the AD 18 day R_s) 31-Mar-08	2-Apr-08	4-Apr-08	6-Apr-08	8-Apr-08
Nitrate (NO_3) and Nitrite (NO_2) Results	Reading (cm)	Nitrate + Nitrite	Anoxic	17.0	20.0	11.5	18.5	19.0	4.0	10.6	9.5	10.5	1.0
			Aerobic	18.0	19.5	12.5	13.0	12.5	1.5	3.9	12.5	12.8	4.5
			Filt. Effluent	22.5	24.5	20.5	10.0	11.5	9.0	7.0	11.0	8.0	4.0
		Nitrite	Anoxic	4.0	3.0	4.5	3.0	3.5	3.5	7.0	12.5	4.0	0.5
			Aerobic	0.0	0.0	0.0	0.0	0.0	1.0	5.5	1.0	2.0	1.5
			Filt. Effluent	0.0	0.0	0.0	0.0	0.0	1.0	1.5	0.5	0.5	0.5
	Stds line fn.	NO_2 + NO_3	Slope (m)	0.11	0.11	0.11	0.11	0.11	0.01	0.09	0.06	0.10	0.11
			Intercept (c)	-0.20	-0.20	-0.20	-0.20	-0.20	-0.12	-0.11	-0.03	-0.15	-0.28
		NO_2	Slope (m)	0.04	0.04	0.04	0.04	0.04	0.01	0.06	0.07	0.10	0.04
			Intercept (c)	0.00	0.00	0.00	0.00	0.00	-0.05	-0.03	0.00	-0.08	0.01
	Dill.	NO_2 + NO_3	Anoxic	5.0	5.0	5.0	5.0	5.0	10.0	10.0	5.0	5.0	10.0
			Aerobic	10.0	10.0	10.0	10.0	10.0	20.0	20.0	10.0	10.0	20.0
			Filt. Effluent	10.0	10.0	10.0	10.0	10.0	20.0	20.0	10.0	10.0	20.0
	Concentration (mgN/l)	Nitrate	Anoxic	10.3	11.9	7.3	11.1	11.4	1.6	10.3	3.0	6.2	3.9
			Aerobic	21.7	23.3	15.7	16.2	15.7	2.7	9.0	7.9	14.7	15.8
			Filt. Effluent	26.6	28.8	24.4	12.9	14.6	4.1	14.4	7.0	9.8	14.7
		Nitrite	Anoxic	0.8	0.6	0.9	0.6	0.7	0.7	4.5	4.2	2.4	0.1
			Aerobic	0.0	0.0	0.0	0.0	0.0	1.0	7.2	0.7	2.8	1.0
			Filt. Effluent	0.0	0.0	0.0	0.0	0.0	1.0	2.4	0.3	1.3	0.2
Total Phosphates (TP) and Ortho-Phosphate (OP) Results	Reading	TP	Influent	0.06	0.04	0.05	0.04	0.04	0.14	0.14	0.14	0.14	0.16
			Filt. Influent	0.08	0.06	0.05	0.04	0.04	0.11	0.12	0.07	0.11	0.11
			Aerobic										
			Filt. Effluent	0.04	0.05	0.04	0.04	0.05	0.12	0.13	0.12	0.12	0.11
		OP	Influent										
			Aerobic	0.04	0.06	0.05	0.06	0.05	0.05	0.09	0.08	0.09	0.08
			Filt. Effluent	0.24	0.13	0.19	0.14	0.19	0.15	0.16	0.15	0.17	0.15
	Stds Line fn.	TP	Slope	0.11	0.12	0.12	0.13	0.11					
			Intercept (-ve)	0.10	0.11	0.11	0.12	0.10	0.11	0.12	0.13	0.12	0.11
		OP	Slope	168.89	168.89	168.89	168.89	168.89	181.40	181.40	178.34	178.34	178.34
			Intercept (-ve)	0.00	0.00	0.00	0.00	0.00	3.68	3.68	2.83	2.83	2.83
	Dillution	TP	Influent	10.0	10.0	10.0	10.0	10.0	10.0	10.0	10.0	10.0	10.0
			Filt. Influent	10.0	10.0	10.0	10.0	10.0	5.0	5.0	5.0	5.0	5.0
			Anoxic	2.0	2.0	2.0	2.0	1.0	2.0	2.0	2.0	2.0	2.0
			Aerobic	1.0	1.0	1.0	1.0	1.0	2.0	1.0	1.0	1.0	1.0
			Aerobic (filt)	1.0	1.0	1.0	1.0	1.0	1.0	1.0	1.0	1.0	1.0
			Effluent	1.0	1.0	1.0	1.0	1.0	1.0	1.0	1.0	1.0	1.0
		OP	Influent	1.0	1.0	1.0	1.0	1.0	1.0	1.0	1.0	1.0	1.0
			Aerobic		18.6	20.3	17.7	18.2	21.5	21.9	22.5	21.2	24.8
			Filt. Effluent	13.2	19.6	15.9	13.8	14.2	16.6	17.9	17.5	16.6	16.4
	Conc. (mgP/l)	TP	Influent	168.9	168.9	168.9	168.9	168.9	181.4	181.4	178.3	178.3	178.3
			Filt Influent	0.0	0.0	0.0	0.0	0.0	3.7	3.7	2.8	2.8	2.8
			Aerobic		79.4	65.9	65.9	77.7	86.8	96.8	91.9	92.8	87.5
			Effluent		9.3	9.1	9.8	8.3	12.2	12.3	11.3	12.5	11.8
		OP	Influent		11.2	15.9	11.7	15.6	15.3	15.9	14.5	16.6	14.7
			Filt. Effluent	8.4	9.0		9.6	7.9	11.0	11.7	11.9	11.7	10.3

Table A7.2

Samples & Tests			Date	Experimental Period 2 (For the AD 25 day R_s)					Experimental Period 4 (For the AD 40 day R_s)				
				2-Jun-08	4-Jun-08	6-Jun-08	8-Jun-08	10-Jun-08	18-Sep-08	20-Sep-08	25-Sep-08	26-Sep-08	28-Sep-08
Nitrate (NO_3) and Nitrite (NO_2) Results	Reading (cm)	Nitrate + Nitrite	Anoxic	7.0	1.0	0.5	0.0	2.0	0.5	2.0	2.0	1.5	3.0
			Aerobic	2.5	0.5	0.5	1.5	0.5	1.5	3.0	3.5	5.0	3.0
			Filt. Effluent	3.0	5.0	7.0	12.7	8.5	2.0	4.0	3.0	4.0	0.5
		Nitrite	Anoxic	7.0	0.0	11.0	7.5	2.0	0.0	2.5	2.5	1.0	0.0
			Aerobic	6.0	6.5	8.5	7.0	2.5	0.0	0.5	1.0	2.0	0.0
			Filt. Effluent	7.5	7.0	0.5	0.0	2.5	0.0	0.0	0.5	1.0	0.0
	Stds line fn.	NO_2+ NO_3	Slope (m)	0.03	0.03	0.06	0.03	0.11	0.13	0.13	0.13	0.12	0.13
			Intercept (c)	-0.05	-0.04	-0.05	-0.05	-0.07	-0.15	-0.19	-0.19	-0.09	-0.13
		NO_2	Slope (m)	0.06	0.11	0.03	0.06	0.07	0.07	0.07	0.07	0.07	0.06
			Intercept (c)	-0.03	-0.20	-0.02	-0.05	0.00	-0.13	-0.10	-0.02	-0.01	-0.04
	Dill.	NO_2 + NO_3	Anoxic	10.0	10.0	5.0	5.0	5.0	10.0	10.0	5.0	5.0	5.0
			Aerobic	20.0	20.0	10.0	10.0	10.0	20.0	20.0	10.0	10.0	10.0
			Filt. Effluent	20.0	20.0	10.0	10.0	10.0	20.0	20.0	10.0	10.0	10.0
	Concentration (mgN/l)	Nitrate	Anoxic	2.9	0.6	0.4	0.2	1.4	2.2	4.4	2.2	1.4	2.5
			Aerobic	2.7	1.0	0.8	1.0	1.2	6.9	11.3	6.3	7.0	5.0
			Filt. Effluent	3.1	3.3	4.9	4.9	10.0	8.2	13.8	5.6	5.8	1.9
		Nitrite	Anoxic	4.7	2.0	2.0	2.6	0.7	1.3	2.7	0.9	0.4	0.2
			Aerobic	8.1	18.0	3.2	4.9	1.9	2.7	2.7	0.8	1.5	0.4
			Filt. Effluent	10.0	19.1	0.4	0.5	1.9	2.7	2.0	0.5	0.8	0.4
Total Phosphates (TP) and Ortho-Phosphate (OP) Results	Reading	TP	Influent	0.07	0.16	0.13	0.14	0.12	0.14	0.18	0.17	0.15	0.16
			Filt. Influent	0.06	0.10	0.10	0.07	0.06	0.07	0.06	0.06	0.07	0.06
			Aerobic										
			Filt. Effluent	0.07	0.23	0.13	0.12	0.19	0.12	0.14	0.13	0.13	0.14
		OP	Influent										
			Aerobic	0.05	0.06	0.08	0.07	0.08	0.05	0.05	0.06	0.05	0.05
			Filt. Effluent	0.15	0.17	0.16	0.16	0.15	0.09	0.11	0.11	0.11	0.09
	Stds Line fn.	TP	Slope										
			Intercept (-ve)	0.09	0.09	0.11	0.11	0.09	0.08	0.09	0.09	0.08	0.10
		OP	Slope	177.05	177.05	162.81	162.81	162.81	164.45	164.45	164.45	164.45	164.45
			Intercept (-ve)	3.31	3.31	2.26	2.26	2.26	-0.10	-0.10	-0.10	-0.10	-0.10
	Dilution	TP	Influent	10.0	10.0	10.0	10.0	10.0	10.0	10.0	10.0	10.0	10.0
			Filt. Influent	10.0	2.0	5.0	5.0	5.0	5.0	5.0	5.0	5.0	5.0
			Anoxic	1.0	1.0	1.0	1.0	1.0	1.0	1.0	1.0	1.0	1.0
			Aerobic	1.0	1.0	1.0	1.0	1.0	2.0	2.0	2.0	2.0	2.0
			Aerobic (filt)	1.0	1.0	1.0	1.0	1.0	2.0	2.0	2.0	2.0	2.0
			Effluent	1.0	1.0	1.0	1.0	1.0	2.0	2.0	2.0	2.0	2.0
		OP	Influent	1.0	1.0	1.0	1.0	1.0	2.0	2.0	2.0	2.0	2.0
			Aerobic	18.2	25.4	18.9	20.5	17.3	23.8	29.5	28.2	23.9	26.4
			Filt. Effluent	12.9	14.4	14.5	17.6	14.7	22.2	20.6	21.3	21.9	19.3
	Conc. (mgP/l)	TP	Influent	177.1	177.1	162.8	162.8	162.8	164.5	164.5	164.5	164.5	164.5
			Filt Influent	3.3	3.3	2.3	2.3	2.3	-0.1	-0.1	-0.1	-0.1	-0.1
			Aerobic	97.9	74.8	94.5	84.0		96.7	112.3	106.6	106.6	
			Effluent	6.3	7.3	10.1	9.0	11.1	18.0	15.0	18.3	16.6	15.3
		OP	Influent	13.2	14.5	13.9	14.0	13.0	15.2	18.7	18.6	17.4	13.5
			Filt. Effluent	7.4	7.5	9.0	8.6	7.4	12.6	15.0	13.3	12.3	15.3
VFA (mg/l)			Aerobic						0.0				
Alk. ($mgCaCO_3/l$)			Aerobic						280.0				
pH			Aerobic						7.5				

Table A7.2

				Experimental Period 3 (For the AD 60 day R_s)					
Samples & Tests			Date	25-Jun-08	27-Jun-08	29-Jun-08	1-Jul-08	3-Jul-08	4-Jul-08
Nitrate (NO_3) and Nitrite (NO_2) Results	Reading (cm)	Nitrate + Nitrite	Anoxic	4.0	11.5	9.5	10.5	10.5	1.0
			Aerobic	1.5	0.0	12.5	12.8	12.8	4.5
			Filt. Effluent	0.5	0.0	9.5	8.0	8.0	4.0
		Nitrite	Anoxic	3.5	7.0	12.5	4.0	4.0	0.5
			Aerobic	1.0	5.5	1.0	2.0	2.0	1.5
			Filt. Effluent	1.0	1.5	0.5	0.5	0.5	0.5
	Stds line fn.	NO_2+ NO_3	Slope (m)	0.01	0.09	0.06	0.10	0.10	0.11
			Intercept (c)	-0.12	-0.11	-0.03	-0.15	-0.15	-0.28
		NO_2	Slope (m)	0.01	0.06	0.07	0.10	0.10	0.04
			Intercept (c)	-0.05	-0.03	0.00	-0.08	-0.08	0.01
	Dill.	NO_2 + NO_3	Anoxic	10.0	10.0	5.0	5.0	5.0	10.0
			Aerobic	20.0	20.0	10.0	10.0	10.0	20.0
			Filt. Effluent	20.0	20.0	10.0	10.0	10.0	20.0
	Concentration (mgN/l)	Nitrate	Anoxic	1.6	11.1	3.0	6.2	6.2	3.9
			Aerobic	2.7	2.2	7.9	14.7	14.7	15.8
			Filt. Effluent	2.5	2.2	6.1	9.8	9.8	14.7
		Nitrite	Anoxic	0.7	4.5	4.2	2.4	2.4	0.1
			Aerobic	1.0	7.2	0.7	2.8	2.8	1.0
			Filt. Effluent	1.0	2.4	0.3	1.3	1.3	0.2
Total Phosphates (TP) and Ortho-Phosphate (OP) Results	Reading	TP	Influent	0.06	0.08	0.08	0.09	0.09	0.08
			Filt. Influent	0.04	0.04	0.03	0.03	0.06	0.06
			Aerobic						
			Filt. Effluent	0.08	0.08	0.08	0.07	0.08	0.07
		OP	Influent						
			Aerobic	0.03	0.03	0.03	0.03	0.05	0.05
			Filt. Effluent	0.16	0.14	0.15	0.15	0.16	0.14
	Stds Line fn.	TP	Slope						
			Intercept (-ve)	0.10	0.10	0.11	0.10	0.11	0.11
		OP	Slope	181.40	181.40	178.34	178.34	178.34	178.34
			Intercept (-ve)	3.68	3.68	2.83	2.83	2.83	2.83
	Dillution	TP	Influent	10.0	10.0	10.0	10.0	10.0	10.0
			Filt. Influent	10.0	10.0	10.0	10.0	10.0	10.0
			Anoxic	2.0	2.0	2.0	2.0	2.0	2.0
			Aerobic	5.0	5.0	5.0	5.0	2.0	2.0
			Aerobic (filt)	1.0	1.0	1.0	1.0	1.0	1.0
			Effluent	1.0	1.0	1.0	1.0	1.0	1.0
		OP	Influent	1.0	1.0	1.0	1.0	1.0	1.0
			Aerobic	14.4	19.8	22.9	25.7	24.6	21.4
			Filt. Effluent	16.5	14.3	16.1	14.4	16.8	14.7
	Conc. (mgP/l)	TP	Influent	181.4	181.4	178.3	178.3	178.3	178.3
			Filt Influent	3.7	3.7	2.8	2.8	2.8	2.8
			Aerobic	106.5	111.9	110.8	96.5	112.5	101.8
			Effluent	10.6	8.8	13.5	9.0	11.5	10.4
		OP	Influent	16.0	13.9	14.7	14.2	15.5	13.5
			Filt. Effluent	10.0	9.1	10.5	9.4	10.7	10.4
VFA (mg/*l*)			Aerobic						
Alk. ($mgCaCO_3$/*l*)			Aerobic						
pH			Aerobic						

Table A7.3: Raw Measurements for Modified Ludzack Ettinger System 1 (MLE 1) which carries out nitrification - denitrification process, operated using settled wastewater

			Experimental Period 5 (For the AD 10 day R_s)					Experimental Period 1 (For the AD 18 day R_s)				
Samples & Tests		Date	26-Oct-08	27-Oct-08	28-Oct-08	30-Oct-08	1-Nov-08	31-Mar-08	2-Apr-08	4-Apr-08	6-Apr-08	8-Apr-08
Chemical Oxygen Demand (COD)	Reading	Influent	17.5	18.4	18.5	18.5	17.1	15.0	8.1	8.0	10.2	10.2
		Filt. Influent	22.9	23.3	23.1	23.5	23.7	19.9	20.6	21.2	21.6	21.9
		Mixed liquor	18.2	18.3	19.5	18.3	16.7	7.2	8.5	10.5	10.3	10.7
		Effluent	24.1	24.8	24.9	24.6	24.1	22.5	22.9	23.4	23.8	24.0
		Filtered Eff.	24.1	24.8	24.9	24.6	24.1	22.5	22.9	23.4	23.8	24.0
		Blank	25.0	25.5	25.0	25.2	25.0	23.0	23.5	24.2	24.7	25.1
		FAS Norm.	0.05	0.05	0.05	0.05	0.05	0.05	0.05	0.05	0.05	0.05
	Dill.	Influent	2.0	2.0	2.0	2.0	2.0	2.0	1.0	1.0	1.0	1.0
		Mixed liquor	10.0	10.0	10.0	10.0	10.0	5.0	5.0	5.0	5.0	5.0
	Conc. (mgCOD/l)	Influent	627.6	594.1	543.9	560.7	661.1	655.4	630.8	663.6	593.9	600.8
		Filt. Influent	87.9		79.5	71.1	54.4	127.0	118.8	122.9	127.0	129.0
		Mixed liquor	2845.1	3012.5		2887.0	3472.7	3235.8	3072.0	2805.8	2949.1	2903.0
		Filtered Eff.	37.7	29.3		25.1	37.7	20.5	24.6	32.8	36.9	44.4
Total Kjeldahl Nitrogen (TKN)	Reading	Influent	22.5	23.5	23.4	23.8	21.4	6.5	13.5	36.5	13.8	29.0
		Filt. Influent	23.1	22.0	21.4	21.2	21.0	5.5	23.0	32.0	28.3	28.5
		Mixed liquor	14.7	14.0	14.1	14.5	14.2	35.6	18.5	18.0	16.0	18.0
		Effluent	6.6	3.6	3.1	3.5	3.1	1.0	3.1	3.0	3.5	3.5
	sample size	Influent	5.0	5.0	5.0	5.0	5.0	5.0	2.0	1.0	2.0	1.0
		Filt. Influent	10.0	10.0	10.0	10.0	10.0	5.0	1.0	1.0	1.0	1.0
		Mixed liquor	10.0	10.0	10.0	10.0	10.0	5.0	10.0	10.0	10.0	10.0
		Effluent	20.0	10.0	10.0	10.0	20.0	1.0	1.0	1.0	1.0	1.0
	Dill..	Mixed liquor	10.0	10.0	10.0	10.0	10.0	10.0	10.0	10.0	10.0	10.0
	Conc. (mgN/l)	Influent	63.0	65.8	65.5	66.6	59.9	45.5	37.8	51.1	38.6	40.6
		Filt. Influent	32.3	30.8	30.0	29.7	29.4	38.5	32.2	44.8	39.6	39.9
		Mixed liquor	205.8	196.0	197.4	203.0	198.8	249.2	259.0	252.0	224.0	252.0
		Effluent	4.6	5.0	4.3	4.9	2.2		4.3	4.2	4.9	4.9
Free and Saline Ammonia (FSA)	Read	Influent	17.6	19.5	17.8	16.8	18.3	10.5	18.0	28.0	25.0	18.0
		Effluent	2.6	2.4	2.7	2.9	2.5	5.0	2.1	3.5	3.0	3.4
	Conc.samp le size (mgN/l)	Influent	10.0	10.0	10.0	10.0	10.0	5.0	2.0	1.0	1.0	1.0
		Effluent	10.0	10.0	10.0	10.0	10.0	10.0	1.0	1.0	1.0	1.0
		Influent	24.6	27.3	24.9	23.5	25.6	29.4	50.4	39.2	35.0	25.2
		Effluent		3.4	3.8	4.1	3.5		2.9	4.9	4.2	4.8
MLSS and ISS	Anoxic Tank	Weight A	62.09	62.09	58.16	58.14	58.14	53.86	13.74	54.03	60.93	30.81
		Weight B	62.21	62.21	58.28	58.25	58.25	53.99	13.86	54.17	61.06	30.93
		Weight C	62.11	62.11	58.18	58.16	58.16	53.88	13.76	54.06	60.95	30.83
		Sample (ml)	50.0	50.0	50.0	50.0	50.0	50.0	50.0	50.0	50.0	50.0
		TSS	2492.0	2286.0	2468.0	2198.0	2274.0	2656.0	2532.0	2664.0	2472.0	2536.0
		VSS	2064.0	1886.0	2012.0	1812.0	1866.0	2280.0	2032.0	2204.0	2016.0	2096.0
		ISS	428.0	400.0	456.0	386.0	408.0	376.0	500.0	460.0	456.0	440.0
	Aerobic Tank	Weight A	55.43	55.42	54.25	54.20	54.16	54.03	12.70	53.84	54.70	32.32
		Weight B	55.56	55.53	54.38	54.32	54.25	54.15	12.83	53.97	54.83	32.44
		Weight C	55.46	55.44	54.28	54.22	0.01	54.05	12.72	53.86	54.72	32.34
		Sample (ml)	50.0	50.0	50.0	50.0	50.0	50.0	50.0	50.0	50.0	50.0
		TSS	2520.0	2326.0	2536.0	2436.0		2440.0	2640.0	2638.0	2518.0	2464.0
		VSS	2080.0	1924.0	2086.0	2052.0		1964.0	2224.0	2252.0	2084.0	1968.0
		ISS	440.0	402.0	450.0	384.0		476.0	416.0	386.0	434.0	496.0
	`settled-ww` Influent settleable solids	Weight A		0.093		0.093	0.092	0.092	0.094	0.092	0.092	0.093
		Weight B		0.116		0.117	0.109	0.113	0.115	0.118	0.114	0.117
		Weight C		0.096		0.096	0.096	0.095	0.097	0.095	0.094	0.096
		Sample (ml)		100.0		100.0	100.0	100.0	100.0	100.0	100.0	100.0
		TSS		229.0			170.0	207.0	212.0	268.0	225.0	245.0
		VSS		199.0			133.0	178.0	183.0	235.0	202.0	208.0
		ISS		30.0			37.0	29.0	29.0	33.0	23.0	37.0

Table A7.3

Samples & Tests		Date	Experimental Period 2 (For the AD 25 day R_s)					Experimental Period 4 (For the AD 40 day R_s)				
			2-Jun-08	4-Jun-08	6-Jun-08	8-Jun-08	10-Jun-08	18-Sep-08	20-Sep-08	25-Sep-08	26-Sep-08	28-Sep-08
Chemical Oxygen Demand (COD)	Reading	Influent	9.7	9.2	10.7	9.1	9.3	10.1	9.6	9.1	8.6	9.5
		Filt. Influent	21.2	21.5	21.8	21.4	21.2	20.7	22.5	22.8	22.6	22.8
		Mixed liquor	10.0	16.5	10.0	9.3	7.9	10.0	10.9	10.5	10.2	9.5
		Effluent	23.2	23.1	23.5	23.2	22.6	24.8	24.6	24.5	24.3	24.3
		Filtered Eff.	23.2	23.1	23.5	23.2	22.6	24.2	24.6	24.5	24.3	24.3
		Blank	24.6	24.4	24.6	24.5	24.4	25.2	25.2	25.0	24.9	25.0
		FAS Norm.	0.05	0.05	0.05	0.05	0.05	0.05	0.05	0.05	0.05	0.05
	Dill.	Influent	1.0	1.0	1.0	1.0	1.0	1.0	1.0	1.0	1.0	1.0
		Mixed liquor	5.0	5.0	5.0	5.0	5.0	5.0	5.0	5.0	5.0	5.0
	Conc. (mgCOD/l)	Influent	610.3	622.6	562.7	623.4	611.2	616.1	636.5	648.7	665.0	625.0
		Filt. Influent	139.3	118.8	113.3	125.5	129.5	183.6	110.2	89.8	93.8	88.7
		Mixed liquor	2990.1		2955.0	3076.5	3339.6	3100.8	2917.2	2958.0	2998.8	3124.8
		Filtered Eff.	57.3	53.2	44.5	52.6	72.9	40.8	24.5	20.4	24.5	28.2
Total Kjeldahl Nitrogen (TKN)	Reading	Influent	15.6	16.0	15.5	16.5	14.9	15.4	16.4	16.7	16.0	16.4
		Filt. Influent	15.2	15.1	14.8	13.5	14.0	15.0	15.5	15.5	15.3	14.1
		Mixed liquor	30.0	32.0	31.5	30.6	32.8	35.0	36.0	34.0	30.0	36.0
		Effluent	4.5	4.0	3.5	3.9	4.0	3.9	3.7	3.4	3.5	3.9
	sample size	Influent	2.0	2.0	2.0	2.0	2.0	2.0	2.0	2.0	2.0	2.0
		Filt. Influent	2.0	2.0	2.0	2.0	2.0	2.0	2.0	2.0	2.0	2.0
		Mixed liquor	5.0	5.0	5.0	5.0	5.0	5.0	5.0	5.0	5.0	5.0
		Effluent	1.0	1.0	1.0	1.0	1.0	1.0	1.0	1.0	1.0	1.0
	Dill.	Mixed liquor	10.0	10.0	10.0	10.0	10.0	10.0	10.0	10.0	10.0	10.0
	Conc. (mgN/l)	Influent	43.7	44.8	43.4	46.2	41.7	43.1	45.9	46.8	44.8	45.9
		Filt. Influent	42.6	42.3	41.4	37.8	39.2	42.0	43.4	43.4	42.8	39.5
		Mixed liquor	210.0	224.0	220.5	214.2	229.6	245.0	252.0	238.0	210.0	252.0
		Effluent	6.3	5.6	4.9	5.5	5.6	5.5	5.2	4.8	4.9	5.5
Free and Saline Ammonia (FSA)	Read	Influent	13.0	13.6	12.7	12.0	14.0	13.4	14.6	13.7	13.5	14.0
		Effluent	3.0	3.0	2.5	2.8	2.5	2.5	3.1	2.2	2.8	3.0
	sample size	Influent	5.0	2.0	2.0	2.0	2.0	2.0	2.0	2.0	2.0	2.0
		Effluent	1.0	1.0	1.0	1.0	1.0	1.0	1.0	1.0	1.0	1.0
	Conc. (mgN/l)	Influent	36.4	38.1	35.6	33.6	39.2	37.5	40.9	38.4	37.8	39.2
		Effluent		4.2	3.5	3.9	3.5	3.5	4.3	3.1	3.9	4.2
MLSS and ISS	Anoxic Tank	Weight A	53.86	13.74	54.03	60.93	30.81	53.86	13.74	54.03	60.93	30.81
		Weight B	53.98	13.86	54.16	61.06	30.93	53.99	13.86	54.16	61.06	30.93
		Weight C	53.88	13.76	54.06	60.96	30.83	53.88	13.76	54.06	60.95	30.83
		Sample (ml)	50.0	50.0	50.0	50.0	50.0	50.0	50.0	50.0	50.0	50.0
		TSS	2456.0	2532.0	2564.0	2472.0	2536.0	2656.0	2532.0	2464.0	2472.0	2536.0
		VSS	2080.0	2032.0	2104.0	1816.0	2096.0	2280.0	2032.0	2004.0	2016.0	2096.0
		ISS	376.0	500.0	460.0	656.0	440.0	376.0	500.0	460.0	456.0	440.0
	Aerobic Tank	Weight A	54.03	12.70	53.84	54.70	32.32	54.03	12.70	53.84	54.70	32.32
		Weight B	54.15	12.83	53.97	54.83	32.44	54.15	12.82	53.96	54.83	32.44
		Weight C	54.05	12.72	53.86	54.72	32.34	54.05	12.72	53.86	54.72	32.34
		Sample (ml)	50.0	50.0	50.0	50.0	50.0	50.0	50.0	50.0	50.0	50.0
		TSS	2440.0	2592.0	2638.0	2518.0	2464.0	2440.0	2480.0	2438.0	2518.0	2464.0
		VSS	1964.0	2176.0	2252.0	2084.0	1968.0	1964.0	2064.0	2052.0	2084.0	1968.0
		ISS	476.0	416.0	386.0	434.0	496.0	476.0	416.0	386.0	434.0	496.0
	`settled-ww' Influent settleable solids	Weight A	0.091	0.099	0.098	0.095	0.095	0.094	0.094	0.090	0.090	0.095
		Weight B	0.146	0.121	0.137	0.131	0.131	0.111	0.111	0.107	0.107	0.111
		Weight C	0.122	0.100	0.115		0.107	0.097	0.096	0.093	0.092	0.097
		Sample (ml)	100.0	100.0	100.0		100.0	100.0	100.0	100.0	100.0	100.0
		TSS	545.0	224.0	396.0		358.0	167.0	174.0	168.0	171.0	155.0
		VSS	240.0	209.0	222.0		234.0	142.0	152.0	141.0	145.0	134.0
		ISS	305.0	15.0	174.0		124.0	25.0	22.0	27.0	26.0	21.0

Table A7.3

Samples & Tests			Experimental Period 3 (For the AD 60 day R_s)					
		Date	25-Jun-08	27-Jun-08	29-Jun-08	1-Jul-08	3-Jul-08	4-Jul-08
Chemical Oxygen Demand (COD)	Reading	Influent	9.8	8.0	9.4	10.2	9.0	9.0
		Filt. Influent	21.3	21.6	21.9	22.1	21.6	20.9
		Mixed liquor	8.0	8.9	17.0	8.2	8.0	8.9
		Effluent	23.6	23.7	23.7	23.5	23.9	23.7
		Filtered Eff.	23.6	23.7	23.7	23.5	23.9	23.7
		Blank	24.5	24.5	24.5	24.5	24.5	24.5
		FAS Norm.	0.05	0.05	0.05	0.05	0.05	0.05
	Dill.	Influent	1.0	1.0	1.0	1.0	1.0	1.0
		Mixed liquor	5.0	5.0	10.0	5.0	5.0	5.0
	Conc. (mgCOD/l)	Influent	602.1	675.8	618.5	585.7	634.9	625.0
		Filt. Influent	131.1	118.8	106.5	98.3	118.8	145.2
		Mixed liquor	3379.2	3194.9	3072.0	3338.2	3379.2	3145.0
		Filtered Eff.	36.9	32.8	32.8	41.0	24.6	32.3
Total Kjeldahl Nitrogen (TKN)	Reading	Influent	6.5	15.5	30.1	16.2	16.8	32.0
		Filt. Influent	5.5	26.0	32.0	25.0	26.1	28.5
		Mixed liquor	35.6	18.5	18.0	16.0	16.0	18.0
		Effluent	3.0	2.5	3.6	4.1	4.5	3.5
	sample size	Influent	5.0	2.0	1.0	2.0	2.0	1.0
		Filt. Influent	5.0	1.0	1.0	1.0	1.0	1.0
		Mixed liquor	5.0	10.0	10.0	10.0	10.0	10.0
		Effluent	1.0	1.0	1.0	1.0	1.0	1.0
	Dill..	Mixed liquor	10.0	10.0	10.0	10.0	10.0	10.0
	Conc. (mgN/l)	Influent	45.5	43.4	42.1	45.4	47.0	44.8
		Filt. Influent	38.5	36.4	44.8	35.0	36.5	39.9
		Mixed liquor	249.2	259.0	252.0	224.0	224.0	252.0
		Effluent	4.2	3.5	5.0	5.7	6.3	4.9
Free and Saline Ammonia (FSA)	Read	Influent	10.5	18.0	28.0	25.0	25.0	18.0
		Effluent	3.0	3.1	3.5	3.0	3.0	3.4
	sample size	Influent	5.0	2.0	1.0	1.0	1.0	1.0
		Effluent	10.0	1.0	1.0	1.0	1.0	1.0
	Conc. (mgN/l)	Influent	29.4	50.4	39.2	35.0	35.0	25.2
		Effluent	4.2	4.3	4.9	4.2	4.2	4.8
MLSS and ISS	Anoxic Tank	Weight A	53.86	13.74	54.03	60.93	60.93	30.81
		Weight B	53.99	13.86	54.17	61.07	61.06	30.93
		Weight C	53.88	13.76	54.06	60.95	60.95	30.83
		Sample (ml)	50.0	50.0	50.0	50.0	50.0	50.0
		TSS	2656.0	2532.0	2664.0	2772.0	2472.0	2536.0
		VSS	2280.0	2032.0	2204.0	2316.0	2016.0	2096.0
		ISS	376.0	500.0	460.0	456.0	456.0	440.0
	Aerobic Tank	Weight A	54.03	12.70	53.84	54.70	54.70	32.32
		Weight B	54.15	12.83	53.97	54.85	54.83	32.45
		Weight C	54.05	12.72	53.86	54.72	54.72	32.34
		Sample (ml)	50.0	50.0	50.0	50.0	50.0	50.0
		TSS	2440.0	2640.0	2638.0	2918.0	2518.0	2664.0
		VSS	1964.0	2224.0	2252.0	2484.0	2084.0	2168.0
		ISS	476.0	416.0	386.0	434.0	434.0	496.0
	`settled-ww` Influent settleable solids	Weight A	0.092	0.094	0.092	0.092	0.092	0.093
		Weight B	0.113	0.115	0.118	0.114	0.114	0.117
		Weight C	0.095	0.097	0.095	0.094	0.094	0.096
		Sample (ml)	100.0	100.0	100.0	100.0	100.0	100.0
		TSS	207.0	212.0	268.0	225.0	225.0	245.0
		VSS	178.0	183.0	235.0	202.0	202.0	208.0
		ISS	29.0	29.0	33.0	23.0	23.0	37.0

Table A7.3

				Experimental Period 5 (For the AD 10 day R_s)					Experimental Period 1 (For the AD 18 day R_s)				
Samples & Tests			Date	26-Oct-08	27-Oct-08	28-Oct-08	30-Oct-08	1-Nov-08	31-Mar-08	2-Apr-08	4-Apr-08	6-Apr-08	8-Apr-08
OUR (mgO/l)			Aerobic	47.3	49.7	50.2	49.5	46.3	47.3	52.7	45.2	39.5	50.5
DSVI (ml/gTSS)			Aerobic	0.2	0.3	0.2		0.2	196.7	189.4	189.5		
Nitrate (NO_3) and Nitrite (NO_2) Results	Reading (cm)	Nitrate + Nitrite	Anoxic	9.6	11.3	12.0	12.5	11.3	7.0	5.0	9.0	10.5	12.6
			Aerobic	5.5	5.8	5.5	5.9	5.8	4.0	5.5	14.5	10.5	12.5
			Filt. Effluent	5.0	5.7	6.3	7.5	4.8	4.0	5.5	14.5	10.5	12.5
		Nitrite	Anoxic	12.0	11.5	11.7	12.1	10.0	10.0	1.0	9.0	8.5	16.0
			Aerobic	0.0	0.0	0.0	0.0	0.0	5.0	0.5	1.0	1.5	9.0
			Filt. Effluent	0.0	0.0	0.0	0.0	0.0	5.0	0.0	0.5	0.5	9.0
	Stds line fn.	NO_2+ NO_3	Slope (m)	0.12	0.12	0.12	0.12	0.12	0.01	0.09	0.06	0.10	0.11
			Intercept (c)	0.02	0.02	0.02	0.02	0.02	-0.12	-0.11	-0.03	-0.15	-0.28
		NO_2	Slope (m)	0.04	0.04	0.04	0.04	0.04	0.01	0.06	0.07	0.10	0.04
			Intercept (c)	0.04	0.04	0.04	0.04	0.04	-0.05	-0.03	0.00	-0.08	0.01
	Dill.	NO_2 + NO_3	Anoxic	10.0	10.0	10.0	10.0	10.0	20.0	20.0	20.0	20.0	20.0
			Aerobic	40.0	40.0	40.0	40.0	40.0	25.0	25.0	25.0	25.0	25.0
			Filt. Effluent	40.0	40.0	40.0	40.0	40.0	25.0	25.0	25.0	25.0	25.0
	Concentration (mgN/l)	Nitrate	Anoxic	11.3	13.4	14.2	14.8	13.4	3.8	10.9	11.5	24.7	34.3
			Aerobic	25.6	27.0	25.6	27.5	27.0	4.0	14.7	22.7	30.9	42.6
			Filt. Effluent	23.2	26.5	29.4	35.2	22.2	4.0	14.7	22.7	30.9	42.6
		Nitrite	Anoxic	4.7	4.5	4.6	4.8	3.9	2.1	1.8	12.0	18.6	13.5
			Aerobic	0.0	0.0	0.0	0.0	0.0	1.9	1.4	1.7	5.8	9.3
			Filt. Effluent	0.0	0.0	0.0	0.0	0.0	1.9	0.7	0.8	3.3	9.3
Total Phosphates (TP) and Ortho-Phosphate (OP) Results	Reading	TP	Influent	0.04	0.05	0.04	0.05	0.04	0.06	0.12	0.11	0.11	0.11
			Filt. Influent	0.04	0.04	0.04	0.04	0.04	0.10	0.12	0.06	0.06	0.10
			Aerobic	0.04	0.04	0.04	0.04	0.04	0.07	0.10	0.07	0.07	0.07
			Filt. Effluent	0.03	0.03	0.03	0.03	0.03	0.09	0.08	0.08	0.08	0.08
		OP	Influent	0.06	0.06	0.06	0.06	0.06	0.14	0.14	0.15	0.15	0.15
			Filt. Effluent	0.10	0.10	0.10	0.10	0.09	0.11	0.11	0.11	0.12	0.12
	Stds Line fn.	TP	Slope	184.81	171.20	180.51	175.95	184.81	181.40	181.40	178.34	178.34	178.34
			Intercept (-ve)	0.00	0.00	0.00	0.00	0.00	3.68	3.68	2.83	2.83	2.83
		OP	Slope	120.08	106.99	108.52	115.37	120.08	108.21	108.21	107.29	107.29	107.29
			Intercept (-ve)	0.00	0.00	0.00	0.00	0.00	1.21	1.21	1.52	1.52	1.52
	Dillution	TP	Influent	2.0	2.0	2.0	2.0	2.0	2.0	1.0	1.0	1.0	1.0
			Filt Influent	2.0	2.0	2.0	2.0	2.0	1.0	1.0	2.0	2.0	1.0
			Anoxic	2.0	2.0	2.0	2.0	2.0	2.0	2.0	2.0	2.0	2.0
			Aerobic	10.0	10.0	10.0	10.0	10.0	10.0	5.0	5.0	5.0	5.0
			Aerobic (filt)	10.0	10.0	10.0	10.0	10.0	10.0	10.0	5.0	10.0	10.0
			Filt. Effluent	2.0	2.0	2.0	2.0	2.0	1.0	1.0	1.0	1.0	1.0
		OP	Influent	2.0	2.0	2.0	2.0	2.0	1.0	1.0	1.0	1.0	1.0
			Aerobic	1.0	1.0	1.0	1.0	1.0	1.0	1.0	1.0	1.0	1.0
			Filt. Effluent	1.0	1.0	1.0	1.0	1.0	1.0	1.0	1.0	1.0	1.0
	Conc. (mgP/l)	TP	Influent	14.4	15.4	15.5		15.2	15.1	18.1	16.2	16.6	15.9
			Filt Influent	14.4	13.7	13.7	14.4	15.5	14.3	17.7	15.4	15.7	14.5
			Aerobic	77.6	66.8	72.2	61.6	73.9	163.8	112.7	80.2	74.8	75.7
			Filt. Effluent	11.8	11.6	11.9	11.6	10.0	11.7	11.4	11.1	11.4	12.0
		OP	Influent		11.8	13.9	12.9	13.2	14.4	13.8	14.5	14.6	14.2
			Filt. Effluent	11.5	11.1	11.2	11.2	10.3	10.9	10.7	10.7	10.8	11.2
VFA (mg/l)			Aerobic	0.0	0.0	0.0		0.0	0.0	61.1	0.0		183.3
Alk. ($mgCaCO_3$/l)			Aerobic	425.0		368.1		554.3	616.0	644.9	855.1		662.8
pH			Aerobic	7.7		7.5		7.9	7.5	8.2	7.9		7.8

Table A7.3

				Experimental Period 2 (For the AD 25 day R_s)					Experimental Period 4 (For the AD 40 day R_s)				
Samples & Tests			Date	2-Jun-08	4-Jun-08	6-Jun-08	8-Jun-08	10-Jun-08	18-Sep-08	20-Sep-08	25-Sep-08	26-Sep-08	28-Sep-08
OUR (mgO/l)			Aerobic	37.3	42.7	40.2	49.5		46.3	46.9	42.0	49.4	47.8
DSVI (ml/gTSS)			Aerobic	196.7	192.9	182.0				193.5	164.7		190.1
Nitrate (NO_3) and Nitrite (NO_2) Results	Reading (cm)	Nitrate + Nitrite	Anoxic	4.5	6.0	4.0	5.5	2.0	8.5	7.5	6.0	8.5	7.5
			Aerobic	8.0	8.0	8.0	8.5	4.5	8.0	6.5	3.5	5.0	7.5
			Filt. Effluent	9.0	8.0	10.5	12.2	6.5	8.0	6.0	3.0	5.5	7.5
		Nitrite	Anoxic	4.5	6.5	3.5	5.5	2.0	3.5	6.5	2.5	7.0	4.0
			Aerobic	1.0	1.0	0.5	0.5	1.5	0.0	0.0	1.0	0.5	0.0
			Filt. Effluent	0.0	0.0	0.5	0.0	0.5	0.0	0.0	0.5	0.5	0.0
	Stds line fn.	NO_2+ NO_3	Slope (m)	0.03	0.03	0.06	0.03	0.11	0.13	0.13	0.13	0.12	0.13
			Intercept (c)	-0.05	-0.04	-0.05	-0.05	-0.07	-0.15	-0.19	-0.19	-0.09	-0.13
		NO_2	Slope (m)	0.06	0.11	0.03	0.06	0.04	0.07	0.07	0.07	0.07	0.06
			Intercept (c)	-0.03	-0.20	-0.02	-0.05	0.00	-0.13	-0.10	-0.02	-0.01	-0.04
	Dill.	NO_2 + NO_3	Anoxic	10.0	10.0	10.0	10.0	10.0	10.0	10.0	10.0	10.0	10.0
			Aerobic	20.0	20.0	20.0	20.0	20.0	20.0	20.0	20.0	20.0	20.0
			Filt. Effluent	20.0	20.0	20.0	20.0	20.0	20.0	20.0	20.0	20.0	20.0
	Concentration (mgN/l)	Nitrate	Anoxic	2.0	1.9	3.0	2.4	2.9	12.6	11.3	9.4	11.3	10.6
			Aerobic	6.5	4.9	11.1	6.9	11.3	23.8	20.0	12.5	14.1	21.3
			Filt. Effluent	7.2	4.9	14.2	9.5	15.6	23.8	18.8	11.3	15.3	21.3
		Nitrite	Anoxic	3.1	9.0	1.4	4.0	0.8	3.8	5.3	1.9	4.9	2.8
			Aerobic	1.9	6.1	0.7	1.7	1.1	2.7	2.0	1.7	0.9	0.9
			Filt. Effluent	0.6	4.0	0.7	1.0	0.4	2.7	2.0	1.0	0.9	0.9
Total Phosphates (TP) and Ortho-Phosphate (OP) Results	Reading	TP	Influent	0.06	0.09	0.10	0.10	0.10	0.12	0.12	0.12	0.11	0.11
			Filt. Influent	0.09	0.07	0.10	0.10	0.08	0.09	0.10	0.11	0.09	0.10
			Aerobic	0.07	0.07	0.09	0.10	0.08	0.12	0.14	0.07	0.13	0.13
			Filt. Effluent	0.07	0.06	0.07	0.07	0.07	0.05	0.05	0.05	0.05	0.05
		OP	Influent	0.14	0.11	0.14	0.14	0.13	0.09	0.09	0.09	0.08	0.09
			Filt. Effluent	0.10	0.08	0.10	0.10	0.10	0.08	0.08	0.08	0.09	0.08
	Stds Line fn.	TP	Slope	177.05	177.05	162.81	162.81	162.81	164.45	164.45	164.45	164.45	164.45
			Intercept (-ve)	3.31	3.31	2.26	2.26	2.26	-0.10	-0.10	-0.10	-0.10	-0.10
		OP	Slope	93.37	93.37	99.32	99.32	99.32	93.37	93.37	99.32	99.32	99.32
			Intercept (-ve)	0.91	0.91	1.81	1.81	1.81	0.91	0.91	1.81	1.81	1.81
	Dillution	TP	Influent	2.0	1.0	1.0	1.0	1.0	1.0	1.0	1.0	1.0	1.0
			Filt Influent	1.0	1.0	1.0	1.0	1.0	1.0	1.0	1.0	1.0	1.0
			Anoxic	2.0	2.0	2.0	2.0	2.0	2.0	2.0	2.0	2.0	2.0
			Aerobic	10.0	10.0	5.0	5.0	5.0	5.0	5.0	10.0	5.0	5.0
			Aerobic (filt)	10.0	10.0	5.0	10.0	10.0	10.0	10.0	5.0	10.0	10.0
			Filt. Effluent	1.0	1.0	1.0	1.0	1.0	2.0	2.0	2.0	2.0	2.0
		OP	Influent	1.0	1.0	1.0	1.0	1.0	2.0	2.0	2.0	2.0	2.0
			Aerobic	1.0	1.0	1.0	1.0	1.0	2.0	2.0	2.0	2.0	2.0
			Filt. Effluent	1.0	1.0	1.0	1.0	1.0	2.0	2.0	2.0	2.0	2.0
	Conc. (mgP/l)	TP	Influent	12.9	11.9	13.5	14.0	13.7	19.3	19.8	19.3	18.8	18.5
			Filt Influent	13.0	9.3	13.2	13.5	11.4	15.2	16.1	17.5	15.4	16.1
			Aerobic	82.0	85.5	86.2	92.7	79.7	98.4	113.2	107.9	107.4	104.9
			Filt. Effluent	8.9	7.5	8.3	9.5	8.7	16.0	16.3	15.7	16.0	16.6
		OP	Influent	11.7	8.9	11.7	12.3	11.4	14.8	14.1	14.7	12.9	14.7
			Filt. Effluent	8.0	6.6	8.3	8.0	8.5	13.9	13.7	12.3	13.5	12.5
VFA (mg/l)			Aerobic	0.0	0.0	0.0		0.0		10.9			183.3
Alk. ($mgCaCO_3/l$)			Aerobic	317.0	654.1	435.8		619.2		408.5			511.4
pH			Aerobic	7.3	8.0	7.4		7.9		7.6			7.7

Table A7.3									
				Experimental Period 3 (For the AD 60 day R_s)					
Samples & Tests			Date	25-Jun-08	27-Jun-08	29-Jun-08	1-Jul-08	3-Jul-08	4-Jul-08
OUR (mgO/*l*)			Aerobic	50.3	49.1	49.1	48.5	49.5	47.6
DSVI (ml/gTSS)			Aerobic		180.3		174.2	163.0	
Nitrate (NO_3) and Nitrite (NO_2) Results	Reading (cm)	Nitrate + Nitrite	Anoxic	7.0	5.0	9.0	10.5	10.5	8.0
			Aerobic	1.0	3.5	12.5	8.5	8.5	12.5
			Filt. Effluent	6.0	0.5	12.5	5.5	5.5	12.5
		Nitrite	Anoxic	10.0	1.0	9.0	8.5	8.5	9.0
			Aerobic	5.0	0.5	1.0	1.5	1.5	2.2
			Filt. Effluent	5.0	0.0	0.5	0.5	0.5	1.0
	Stds line fn.	NO_2 + NO_3	Slope (m)	0.01	0.09	0.06	0.10	0.10	0.11
			Intercept (c)	-0.12	-0.11	-0.03	-0.15	-0.15	-0.28
		NO_2	Slope (m)	0.01	0.06	0.07	0.10	0.10	0.04
			Intercept (c)	-0.05	-0.03	0.00	-0.08	-0.08	0.01
	Dill.	NO_2 + NO_3	Anoxic	10.0	10.0	10.0	10.0	10.0	10.0
			Aerobic	20.0	20.0	20.0	20.0	20.0	20.0
			Filt. Effluent	20.0	20.0	20.0	20.0	20.0	20.0
	Concentration (mgN/*l*)	Nitrate	Anoxic	1.9	5.5	5.7	12.3	12.3	11.9
			Aerobic		8.3	15.7	20.6	20.6	34.1
			Filt. Effluent		3.1	15.7	14.4	14.4	34.1
		Nitrite	Anoxic	1.0	0.9	6.0	9.3	9.3	3.7
			Aerobic	1.5	1.2	1.3	4.6	4.6	1.6
			Filt. Effluent	1.5	0.5	0.7	2.6	2.6	0.6
Total Phosphates (TP) and Ortho-Phosphate (OP) Results	Reading	TP	Influent	0.10	0.10	0.11	0.10	0.11	0.11
			Filt. Influent	0.06	0.06	0.06	0.03	0.06	0.03
			Aerobic	0.13	0.12	0.12	0.05	0.07	0.08
			Filt. Effluent	0.05	0.05	0.03	0.03	0.05	0.04
		OP	Influent	0.14	0.14	0.15	0.15	0.15	0.15
			Filt. Effluent	0.10	0.10	0.11	0.10	0.10	0.11
	Stds Line fn.	TP	Slope	181.40	181.40	178.34	178.34	178.34	178.34
			Intercept (-ve)	3.68	3.68	2.83	2.83	2.83	2.83
		OP	Slope	108.21	108.21	107.29	107.29	107.29	107.29
			Intercept (-ve)	1.21	1.21	1.52	1.52	1.52	1.52
	Dillution	TP	Influent	2.0	1.0	1.0	1.0	1.0	1.0
			Filt Influent	2.0	2.0	2.0	5.0	2.0	5.0
			Anoxic	2.0	2.0	2.0	2.0	2.0	2.0
			Aerobic	10.0	5.0	5.0	5.0	5.0	5.0
			Aerobic (filt)	10.0	10.0	5.0	10.0	10.0	10.0
			Filt. Effluent	2.0	2.0	5.0	5.0	2.0	2.0
		OP	Influent	1.0	1.0	1.0	1.0	1.0	1.0
			Aerobic	1.0	1.0	1.0	1.0	1.0	1.0
			Filt. Effluent	1.0	1.0	1.0	1.0	1.0	1.0
	Conc. (mgP/*l*)	TP	Influent		13.9	16.8	15.7	16.8	16.6
			Filt Influent	14.0	15.5	15.4	15.3	14.7	15.3
			Aerobic	195.4	90.4	121.2	55.2	79.3	86.4
			Filt. Effluent	9.0	10.0	9.9	10.8	10.4	10.0
		OP	Influent	14.0	14.3	14.5	14.6	14.6	14.4
			Filt. Effluent	9.4	10.0	10.0	8.9	9.1	10.1
VFA (mg/*l*)			Aerobic		23.0				
Alk. ($mgCaCO_3$/*l*)			Aerobic		523.0				
pH			Aerobic		7.8				

Table A7.4: Influent for AD 2 (PS) Raw Measurements

Samples & Tests			Experimental Period 5 (For the AD 10 day R_s)					Experimental Period 1 (For the AD 18 day R_s)				
		Date	26-Oct-08	27-Oct-08	28-Oct-08	30-Oct-08	1-Nov-08	31-Mar-08	2-Apr-08	4-Apr-08	6-Apr-08	8-Apr-08
Chemical Oxygen Demand (COD)	Reading	Influent	19.7	17.3	17.1	17.5	18.0	13.2	13.6	14.2	14.1	15.7
		Filt. Influent	16.5	20.0	18.5	19.1	20.0	12.5	14.0	14.6	14.8	14.2
		Blank	24.6	24.4	24.6	24.5	24.4	22.6	23.5	24.2	24.7	25.1
		FAS Norm.	0.1	0.1	0.1	0.1	0.1	0.1	0.1	0.1	0.1	0.1
	Dill.	Influent	20.0	20.0	20.0	20.0	20.0	20.0	20.0	20.0	20.0	20.0
		filt. Influent	2.0	2.0	2.0	2.0	2.0	2.0	2.0	2.0	2.0	2.0
	Conc. (mg/*l*)	Influent		5816.3	6072.0	5667.2	5181.4	7700.5	8110.1	8192.0	8683.5	7580.2
		Filt. Influent	663.6	360.4	493.9	437.2	356.2	827.4	778.2	786.4	811.0	879.0
Total Kjeldahl Nitrogen (TKN)	Read	Influent	21.0	18.0	16.0	17.5	19.0	9.5	10.0	9.5	9.0	7.5
		Filt. Influent	16.0	15.0	11.0	12.0	12.2		2.5	4.5	4.0	8.0
	sample (ml)	Influent	10.0	10.0	10.0	10.0	10.0	10.0	10.0	10.0	10.0	10.0
		filt. influent	10.0	10.0	10.0	10.0	10.0	20.0	20.0	20.0	20.0	20.0
	Dill.	Influent	10.0	10.0	10.0	10.0	10.0	10.0	10.0	10.0	10.0	10.0
		filt. Influent	2.0	2.0	2.0	2.0	2.0	5.0	5.0	5.0	5.0	5.0
	Conc. (mg/*l*)	Influent	294.0	252.0	224.0	245.0	266.0	266.0	280.0	266.0	252.0	210.0
		Filt. Influent	44.8	42.0	30.8	33.6	34.2		17.5	31.5	28.0	56.0
Influent FSA	Reading			2.5	4.1	4.3	4.0		2.7	4.5	4.0	4.5
	Sample Size(ml)	10.0	10.0	10.0	10.0	10.0	10.0	10.0	10.0	10.0	10.0	10.0
	Dillution		5.0	10.0	5.0	5.0	5.0	5.0	5.0	5.0	5.0	5.0
	Conc. (mg/*l*)			35.0	28.7	30.1	28.0		18.9	31.5	28.0	31.5
MLSS (mg/*l*)	Influent	Weight A	30.36	31.34	43.63	43.63		30.82	55.35	48.05	55.68	12.72
		Weight B	30.60	31.57	43.90	43.87		31.11	55.62	48.33	55.95	13.00
		Weight C	30.42	31.38	43.68	43.69		30.87	55.40	48.10	55.74	12.77
	sample size (ml)		50.0	50.0	50.0	50.0		50.0	50.0	50.0	50.0	50.0
	Conc. (mg/*l*)	TSS	4802.0	4696.0	5430.0	4836.0		5796.0	5406.0	5572.0	5352.0	5654.0
		VSS	3620.0	3834.0	4326.0	3580.0		4764.0	4340.0	4518.0	4214.0	4622.0
		ISS	1182.0	862.0	1104.0	1256.0		1032.0	1066.0	1054.0	1138.0	1032.0
Total Phosphates	Readings	Influent	0.05	0.06	0.10	0.12	0.06	0.05	0.07	0.07	0.07	0.07
		Filt. Influent	0.16	0.11	0.11	0.12	0.12	0.06	0.08	0.06	0.06	0.06
	Line fn.	Slope (m)	166.06	166.06	166.06	166.06	166.06	181.40	181.40	178.34	178.34	178.34
		Intercept (c)	-0.19	-0.19	-0.19	-0.19	-0.19	3.68	3.68	2.83	2.83	2.83
	Dill.	Influent	10.0	10.0	10.0	10.0	10.0	40.0	20.0	20.0	20.0	20.0
		Filt. Influent	1.0	1.0	1.0	1.0	1.0	5.0	4.0	4.0	4.0	4.0
	Conc. (mg/*l*)	Influent	81.2	96.1			102.7	186.4	187.5	196.6	203.7	200.1
		Filt. Influent	26.1	18.6	17.4	19.2	18.9	33.3	39.7	34.3	33.6	31.5
Ortho-Phosphates	Readings	Influent	0.22	0.18	0.08	0.08	0.07	0.07	0.09	0.08	0.07	0.17
	Line fn.	Slope	121.90	121.90	121.90	121.90	121.90	108.21	108.21	107.29	107.29	107.29
		Intercept (-ve)	-0.03	-0.03	-0.03	-0.03	-0.03	1.21	1.21	1.52	1.52	1.52
	Dill.	Influent	1.0	1.0	2.0	2.0	2.0	2.0	2.0	2.0	2.0	2.0
	Conc. (mg/*l*)	Influent		22.4	19.2	19.9	16.3	18.2	22.3	20.2	18.1	39.1
VFA (mg/*l*)		Influent		160.0		132.0		55.0	174.7	139.3	207.6	291.5
Alk (mg$CaCO_3$/*l*)		Influent		377.0		419.0		377.4	262.2	308.8	463.5	478.2
pH		Influent		5.8		6.0		5.8	5.9	5.8	6.3	7.0

Table A7.4

Samples & Tests			Experimental Period 2 (For the AD 25 day R_s)					Experimental Period 4 (For the AD 40 day R_s)				
		Date	2-Jun-08	4-Jun-08	6-Jun-08	8-Jun-08	10-Jun-08	18-Sep-08	20-Sep-08	25-Sep-08	26-Sep-08	28-Sep-08
Chemical Oxygen Demand (COD)	Reading	Influent	14.2	14.9	12.9	14.0	13.1	13.7	2.5	2.0	13.5	13.3
		Filt. Influent	9.5	10.0	10.2	8.8	8.4	17.8	17.9	16.1	15.9	16.5
		Blank	24.6	24.4	24.6	24.5	24.4	25.2	25.2	25.0	24.9	25.0
		FAS Norm.	0.1	0.1	0.1	0.1	0.1	0.1	0.1	0.1	0.1	0.1
	Dill.	Influent	20.0	20.0	20.0	20.0	20.0	40.0	20.0	20.0	40.0	40.0
		filt. Influent	2.0	2.0	2.0	2.0	2.0	5.0	5.0	5.0	5.0	5.0
	Conc. (mg/l)	Influent	8519.7		9472.3	8500.8	9148.5	18768.0	18523.2	18768.0	18604.8	18869.8
		Filt. Influent	1237.0		1165.8	1271.1	1295.4	1509.6	1489.2	1815.6	1836.0	1713.6
Total Kjeldahl Nitrogen (TKN)	Read	Influent	18.5	21.5	15.5	16.5	18.0	18.0	16.0	16.0	22.0	18.5
		Filt. Influent	16.0	29.0	20.0	23.5	25.0	8.0	10.0	7.0	10.0	6.0
	sample (ml)	Influent	10.0	10.0	10.0	10.0	10.0	10.0	10.0	10.0	10.0	10.0
		filt. influent	20.0	20.0	20.0	20.0	20.0	20.0	20.0	20.0	20.0	20.0
	Dill.	Influent	10.0	10.0	10.0	10.0	10.0	10.0	10.0	10.0	10.0	10.0
		filt. Influent	5.0	1.0	1.0	1.0	1.0	5.0	5.0	5.0	5.0	5.0
	Conc. (mg/l)	Influent	259.0	301.0	287.0	315.0		504.0	448.0	448.0	616.0	518.0
		Filt. Influent		40.6	28.0	32.9	35.0		70.0	49.0	70.0	42.0
Influent FSA	Reading		2.5	4.1	4.0	3.5	3.4	8.0	8.0	6.0	10.0	6.0
	Sample Size(ml)	10.0	10.0	10.0	10.0	10.0	10.0	10.0	10.0	10.0	10.0	10.0
	Dillution		5.0	5.0	5.0	5.0	5.0	5.0	5.0	5.0	5.0	5.0
	Conc. (mg/l)		17.5	28.7	28.0	24.5	23.8		56.0	42.0	70.0	42.0
MLSS (mg/l)	Influent	Weight A	48.45	48.46	53.29	54.07	53.73	30.49	31.47	43.76	43.76	43.76
		Weight B	48.76	48.83	53.67	54.36	54.10	31.23	32.23	44.46	44.50	44.50
		Weight C	48.51	48.54	53.37	54.13	53.80	30.64	31.62	43.93	43.89	43.89
	sample size (ml)		50.0	50.0	50.0	50.0	50.0	50.0	50.0	50.0	50.0	50.0
	Conc. (mg/l)	TSS	6322.0	7396.0	7658.0	5876.0	7496.0	14802.0	15296.0	14030.0	14810.0	14810.0
		VSS	4988.0	5778.0	6018.0	4622.0	6062.0	11820.0	12234.0	10556.0	12154.0	12154.0
		ISS	1334.0	1618.0	1640.0	1254.0	1434.0	2982.0	3062.0	3474.0	2656.0	2656.0
Total Phosphates	Readings	Influent	0.06	0.06	0.04	0.07	0.06	0.05	0.08	0.08	0.08	0.07
		Filt. Influent	0.05	0.04	0.06	0.05	0.05	0.06	0.08	0.06	0.06	0.06
	Line fn.	Slope (m)	177.05	177.05	162.81	162.81	162.81	177.05	177.05	162.81	162.81	162.81
		Intercept (c)	3.31	3.31	2.26	2.26	2.26	3.31	3.31	2.26	2.26	2.26
	Dill.	Influent	40.0	40.0	40.0	20.0	20.0	40.0	20.0	20.0	20.0	20.0
		Filt. Influent	5.0	10.0	5.0	5.0	5.0	5.0	5.0	5.0	5.0	5.0
	Conc. (mg/l)	Influent	278.5	285.5	170.2	182.8	160.0	214.7	210.1	228.4	225.1	189.3
		Filt. Influent	29.5	32.4	35.1	29.4	27.0	33.9	49.9	40.8	40.0	37.6
Ortho-Phosphates	Readings	Influent	0.07	0.06	0.08	0.08	0.17	0.07	0.06	0.08	0.08	0.07
	Line fn.	Slope	93.37	93.37	93.37	93.37	93.37	99.32	99.32	99.32	99.32	99.32
		Intercept (-ve)	0.91	0.91	0.91	0.91	0.91	1.81	1.81	1.81	1.81	1.81
	Dill.	Influent	5.0	2.0	5.0	2.0	2.0	5.0	4.0	5.0	5.0	2.0
	Conc. (mg/l)	Influent	28.1	9.9	32.3	13.5	29.9	25.7	17.8	30.2	31.7	9.7
VFA (mg/l)		Influent	175.5		185.8	197.4		110.1	262.1	234.0	482.6	370.4
Alk ($mgCaCO_3/l$)		Influent	316.9		342.0	382.6		554.0	807.9	804.9	866.6	812.9
pH		Influent	5.8		5.7	6.3		6.1	6.1	5.7	6.3	6.2

Table A7.4

Samples & Tests			Experimental Period 3 (For the AD 60 day R_s)					
		Date	25-Jun-08	27-Jun-08	29-Jun-08	1-Jul-08	3-Jul-08	5-july-08
Chemical Oxygen Demand (COD)	Reading	Influent	6.3	7.2	6.4	7.3	7.1	7.5
		Filt. Influent	0.1	14.4	11.6	7.8	7.6	8.4
		Blank	24.8	24.7	24.5	24.1	24.8	24.5
		FAS Norm.	0.1	0.1	0.1	0.1	0.1	0.1
	Dill.	Influent	40.0	40.0	40.0	40.0	40.0	40.0
		filt. Influent	4.0	4.0	4.0	4.0	4.0	4.0
	Conc. (mg/*l*)	Influent	29600.0	28000.0	28960.0	27417.6	28886.4	27744.0
		Filt. Influent	3952.0	1648.0	2064.0	2660.2	2807.0	2627.5
Total Kjeldahl Nitrogen (TKN)	Read	Influent	18.5	31.0	18.0	7.0	21.0	27.5
		Filt. Influent	15.5	10.0	10.0	4.5	4.0	5.0
	sample (ml)	Influent	10.0	10.0	10.0	10.0	10.0	10.0
		filt. influent	25.0	20.0	40.0	40.0	25.0	20.0
	Dill.	Influent	10.0	10.0	10.0	10.0	10.0	10.0
		filt. Influent	5.0	5.0	5.0	5.0	5.0	5.0
	Conc. (mg/*l*)	Influent	518.0	560.0	504.0		588.0	770.0
		Filt. Influent		70.0	70.0	31.5		35.0
Influent FSA	Reading		3.0		3.5	4.0	4.0	5.0
	Sample Size(ml)		10	10.0	10.0	10.0	10.0	10.0
	Dillution		10.0	10.0	10.0	10.0	10.0	10.0
	Conc. (mg/*l*)		42.0		49.0		56.0	
MLSS (mg/*l*)	Influent	Weight A	46.75	30.80	28.40	28.39	59.32	32.33
		Weight B	47.71	31.79	29.37	29.45	60.27	33.30
		Weight C	46.90	30.98	28.56	28.58	59.48	32.49
	sample size (ml)		50.0	50.0	50.0	50.0	50.0	50.0
	Conc. (mg/*l*)	TSS	19170.0	19662.0	19438.0	21152.0	18986.0	19390.0
		VSS	16062.0	16168.0	16196.0	17424.0	15664.0	16230.0
		ISS	3108.0	3494.0	3242.0	3728.0	3322.0	3160.0
Total Phosphates	Readings	Influent	0.09	0.10	0.05	0.05	0.08	0.09
		Filt. Influent	0.04	0.06	0.06	0.06	0.03	0.03
	Line fn.	Slope (m)	181.40	181.40	178.34	178.34	178.34	178.34
		Intercept (c)	3.68	3.68	2.83	2.83	2.83	2.83
	Dill.	Influent	40.0	20.0	40.0	40.0	20.0	20.0
		Filt. Influent	5.0	5.0	5.0	5.0	10.0	10.0
	Conc. (mg/*l*)	Influent		303.6	207.6	243.3	228.7	253.6
		Filt. Influent	21.5	38.7	42.0	39.3	23.4	32.3
Ortho-Phosphates	Readings	Influent	0.07	0.22	0.09	0.08	0.08	0.09
	Line fn.	Slope	108.21	108.21	107.29	107.29	107.29	107.29
		Intercept (-ve)	1.21	1.21	1.52	1.52	1.52	1.52
	Dill.	Influent	4.0	1.0	4.0	4.0	4.0	2.0
	Conc. (mg/*l*)	Influent	26.8	22.3	33.4	29.1	27.8	16.1
VFA (mg/*l*)		Influent	363.1		470.0		406.0	
Alk (mg$CaCO_3$/*l*)		Influent	1021.5		1026.9		1082.0	
pH		Influent	5.3		5.3		6.0	

APPENDIX 8: RAW DATA FOR AD SYSTEMS

Table A8.1: Raw Results for Anaerobic Digester 2 (AD 2), fed Primary Sludge (PS), when operated at sludge ages of 10, 18 and 25 days

			10 Day R_s (Experimental Period 5)									
Samples & Tests		Date	26-Oct-08	27-Oct-08	28-Oct-08	29-Oct-08	30-Oct-08	31-Oct-08	2-Nov-08	3-Nov-08	4-Nov-08	5-Nov-08
Chemical Oxygen Demand (COD)	Reading	Effluent	21.0	16.1	20.1	14.9	16.6	14.9	15.7	14.4	16.0	15.5
		Filt. Effluent	22.1	22.3	22.0	21.5	23.0	22.5	22.7	22.1	22.1	22.3
		Blank	25.0	25.5	25.1	25.6	25.0	25.0	25.0	25.0	25.0	25.0
		FAS Norm.	0.05	0.05	0.05	0.05	0.05	0.05	0.05	0.05	0.05	0.05
	Dillution	Effluent	20.0	10.0	20.0	10.0	10.0	10.0	10.0	10.0	10.0	10.0
		Filt. Effluent	1.0	1.0	1.0	1.0	1.0	1.0	1.0	1.0	1.0	1.0
	Conc. (mg/*l*)	Effluent	3289.6	3865.3	4112.0	4399.8	3454.1	4153.1	3824.2	4358.7	3700.8	3906.4
		Filt. Effluent	119.2	131.6	127.5	168.6	82.2	102.8	94.6	119.2	119.2	111.0
Total Kjeldahl Nitrogen (TKN)	Reading	Effluent	19.0	15.0	16.2	16.5	15.5	16.0	17.0	18.0	16.5	17.0
		Filt. Effluent	20.1	14.1	18.2	17.9	16.7	20.6	24.1	19.9	20.4	25.0
	Dillution	Effluent	10.0	10.0	10.0	10.0	10.0	10.0	10.0	10.0	10.0	10.0
		Filt. Effluent	1.0	1.0	1.0	1.0	1.0	1.0	1.0	1.0	1.0	1.0
	Conc. (mg/*l*)	Effluent	266.0		226.8	231.0		224.0	238.0	252.0	231.0	238.0
		Filt. Effluent	56.3	39.5	51.0	50.1	46.8	57.7	67.5	55.7	57.1	70.0
Free and Saline Ammonia (FSA)	Reading	Filt. Effluent	13.4	17.8	18.9	20.5	16.7	16.6	19.2	16.3	15.8	22.0
	Dillution	Filt. Effluent	1.0	1.0	1.0	1.0	1.0	1.0	1.0	1.0	1.0	1.0
	Sample Size	Filt. Effluent	10.0	10.0	10.0	10.0	10.0	10.0	10.0	10.0	10.0	10.0
	Conc. (mg/*l*)	Filt. Effluent		24.92	26.46	28.70	23.38	23.24	26.88	22.82	22.12	30.80
MLSS (mg/*l*)	Reading	Weight A	48.03	19.37	48.04	19.37	27.32	19.39	12.81	27.35		27.34
		Weight B	48.19	19.47	48.18	19.55	27.50	19.57	12.99	27.52		27.51
		Weight C	48.08	19.39	48.09	19.43	27.37	19.44	12.87	27.41		27.39
	Sample Size	Effluent	50.0	50.0	50.0	50.0	50.0	50.0	50.0	50.0		50.0
	Conc. (mg/*l*)	TSS	3302.0			3476.0	3514.0	3700.0	3602.0	3402.0		3376.2
		VSS	2320.0			2292.0	2440.0	2548.0	2534.0	2284.0		2368.2
		ISS	982.0			1184.0	1074.0	1152.0	1068.0	1118.0		1008.0
Total Phosphates (TP) and ortho-phosphates (OP) Results	TP Reading	Effluent	0.05	0.05	0.08	0.07	0.06	0.06	0.05	0.06	0.06	0.07
		Filt. Effluent	0.07	0.09	0.25	0.07	0.07	0.08	0.07	0.07	0.06	0.17
	OP Reading	Filt. Effluent	0.09	0.08	0.10	0.13	0.09	0.09	0.11	0.10	0.09	0.10
	TP Std. line fn.	Slope	166.06	166.06	166.06	166.06	166.06	166.06	166.06	166.06	166.06	166.06
		Intercept	-0.19	-0.19	-0.19	-0.19	-0.19	-0.19	-0.19	-0.19	-0.19	-0.19
	OP) Std. line fn.	Slope	121.90	121.90	121.90	121.90	121.90	121.90	121.90	121.90	121.90	121.90
		Intercept	-0.03	-0.03	-0.03	-0.03	-0.03	-0.03	-0.03	-0.03	-0.03	-0.03
	TP Dillution	Effluent	10.0	10.0	10.0	10.0	10.0	10.0	10.0	10.0	10.0	10.0
		Filt. Effluent	1.0	1.0	1.0	1.0	1.0	1.0	1.0	1.0	1.0	1.0
	OP Dillution	Filt. Effluent	1.0	1.0	1.0	1.0	1.0	1.0	1.0	1.0	1.0	1.0
	TP Conc. (mgP/*l*)	Effluent	84.7	88.0			96.3	91.3	83.0	93.0	99.6	
		Filt. Effluent	11.6			11.8	11.5	13.2	10.8	11.5		
	OP Conc. (mgP/*l*)	Filt. Effluent	11.5	9.8	11.6		11.3	11.1	13.9	11.6		11.8
VFA	Conc. (mgHAc/*l*)	Filt. Effluent	0.0		0.0				0.0		0.0	
Alk	Conc. ($mgCaCO_3/l$)	Filt. Effluent	1077.0		1175.0				1204.0		1086.0	
pH		Effluent	7.03		7.06				7.11		7.04	
Gas Production (l/d)		Effluent	2.90		2.54	2.46		2.60	2.42	2.65	2.63	

Table A8.1

			18 Day R_s (Experimental Period 1)									
Samples & Tests		Date	31-Mar-08	1-Apr-08	2-Apr-08	3-Apr-08	4-Apr-08	5-Apr-08	7-Apr-08	8-Apr-08	9-Apr-08	10-Apr-08
Chemical Oxygen Demand (COD)	Reading	Effluent	17.0	18.3	18.0	17.8	18.8	17.7	18.8	19.3	19.1	19.8
		Filt. Effluent	20.3	19.0	18.6	19.1	19.7	20.3	20.4	20.7	20.7	21.0
		Blank	22.6	23.4	23.5	23.7	24.2	23.8	24.7	25.0	25.1	25.0
		FAS Norm.	0.05	0.05	0.05	0.05	0.05	0.05	0.05	0.05	0.05	0.05
	Dillution	Effluent	20.0	20.0	20.0	20.0	20.0	20.0	20.0	20.0	20.0	20.0
		Filt. Effluent	2.0	1.0	1.0	1.0	1.0	1.0	1.0	1.0	1.0	1.0
	Conc. (mg/*l*)	Effluent	4587.5	4177.9	4505.6	4833.3	4423.7	4997.1	4833.3	4596.5	4838.4	4259.8
		Filt. Effluent	188.4	180.2	200.7	188.4	184.3	143.4	176.1	173.4	177.4	163.8
Total Kjeldahl Nitrogen (TKN)	Reading	Effluent	18.70	17.80	18.50	18.90	18.70	17.90	18.40	19.00	30.50	20.10
		Filt. Effluent	11.20	5.00	10.50	15.80	13.00	14.00	12.40	11.00	10.50	12.50
	Dillution	Effluent	10.00	10.00	10.00	10.00	10.00	10.00	10.00	10.00	5.00	10.00
		Filt. Effluent	5.00	10.00	5.00	5.00	5.00	5.00	5.00	5.00	5.00	5.00
	Conc. (mg/*l*)	Effluent	261.80	249.20	259.00	264.60	261.80	250.60	257.60	266.00		281.40
		Filt. Effluent	78.40	70.00	73.50		91.00	98.00		77.00	73.50	87.50
Free and Saline Ammonia (FSA)	Reading	Filt. Effluent	3.80	23.50	19.20	21.50	19.30	23.70	18.80	21.80	22.40	23.00
	Dillution	Filt. Effluent	1.00	1.00	1.00	1.00	1.00	1.00	1.00	1.00	1.00	1.00
	Sample Size	Filt. Effluent	5.00	5.00	5.00	5.00	5.00	5.00	5.00	5.00	5.00	5.00
	Conc. (mg/*l*)	Filt. Effluent		65.80	53.76	60.20	54.04	66.36	52.64	61.04	62.72	64.40
MLSS (mg/*l*)	Reading	Weight A	30.38	30.82	60.96	30.83	39.40	30.82	27.29	46.81	30.82	30.35
		Weight B	30.59	31.06	61.20	31.05	39.63	31.05	27.51	47.02	31.04	30.57
		Weight C	30.45	30.90	61.05	30.91	39.48	30.90	27.38	46.90	30.91	30.44
	Sample Size	Effluent	50.0	50.0	50.0	50.0	50.0	50.0	50.0	50.0	50.0	50.0
	Conc. (mg/*l*)	TSS	4238.0	4704.0	4806.0	4468.0	4434.0	4466.0	4340.0	4244.0	4356.0	4302.0
		VSS	2800.0	3142.0	2976.0	2748.0	2838.0	2882.0	2572.0	2554.0	2664.0	2566.0
		ISS	1438.0	1562.0	1830.0	1720.0	1596.0	1584.0	1768.0	1690.0	1692.0	1736.0
Total Phosphates (TP) and ortho-phosphates (OP) Results	TP Reading	Effluent	0.03	0.06	0.06	0.05	0.06	0.06	0.02	0.03	0.06	0.06
		Filt. Effluent	0.05	0.05	0.05	0.06	0.05	0.03	0.06	0.04	0.05	0.06
	OP Reading	Filt. Effluent	0.05	0.06	0.05	0.06	0.29	0.06	0.06	0.06	0.07	0.07
	TP Std. line fn.	Slope	181.40	181.40	181.40	181.40	178.34	178.34	178.34	178.34	178.34	178.34
		Intercept	3.68	3.68	3.68	3.68	2.83	2.83	2.83	2.83	2.83	2.83
	OP) Std. line fn.	Slope	108.21	108.21	108.21	108.21	107.29	107.29	107.29	107.29	107.29	107.29
		Intercept	1.21	1.21	1.21	1.21	1.52	1.52	1.52	1.52	1.52	1.52
	TP Dillution	Effluent	40.0	20.0	20.0	20.0	20.0	20.0	40.0	40.0	20.0	20.0
		Filt. Effluent	4.0	4.0	4.0	4.0	4.0	4.0	4.0	4.0	4.0	4.0
	OP Dillution	Filt. Effluent	5.0	5.0	5.0	5.0	1.0	5.0	5.0	5.0	5.0	5.0
	TP Conc. (mgP/*l*)	Effluent	195.9	210.4	199.5	192.3	203.3	199.7	171.2	185.5	203.3	203.3
		Filt. Effluent	33.4	35.6	37.0	39.9	34.2	21.4	39.2	30.7	35.7	42.1
	OP Conc. (mgP/*l*)	Filt. Effluent	29.2	29.8	28.1	31.9	31.1	31.1	31.7	32.7	35.4	34.9
VFA	Conc. (mgHAc/*l*)	Filt. Effluent	133.4		97.7		0.0		30.3		0.0	
Alk	Conc. (mg$CaCO_3$/*l*)	Filt. Effluent	1125.6		1020.5		1065.1		1024.0		1027.9	
pH		Effluent	7.30		7.21		7.25		7.34		7.24	
Gas Production (l/d)		Effluent	1.68	1.83	1.93	1.55	1.37	1.62	1.76			

Table A8.1

			25 Day R_s (Experimental Period 2)									
Samples & Tests		Date	2-Jun-08	3-Jun-08	4-Jun-08	5-Jun-08	6-Jun-08	7-Jun-08	9-Jun-08	10-Jun-08	11-Jun-08	12-Jun-08
Chemical Oxygen Demand (COD)	Reading	Effluent	19.2	19.3	19.4	19.1	19.7	19.2	19.1	19.5	19.0	
		Filt. Effluent	18.8	18.1	19.0	17.2	19.8	15.4	17.0	19.5	19.8	
		Blank	24.5	24.5	24.5	24.5	24.5	24.5	24.5	24.5	24.5	24.5
		FAS Norm.	0.05	0.05	0.05	0.05	0.05	0.05	0.05	0.05	0.05	0.05
	Dillution	Effluent	20.0	20.0	20.0	20.0	20.0	20.0	20.0	20.0	20.0	20.0
		Filt. Effluent	1.0	1.0	1.0	1.0	1.0	1.0	1.0	1.0	1.0	1.0
	Conc. (mg/*l*)	Effluent	4341.8	4259.8	4177.9	4423.7	3932.2	4290.9	4371.8	4048.0	4452.8	
		Filt. Effluent	233.5	262.1	225.3	299.0	192.5	368.4	303.6	202.4	190.3	
Total Kjeldahl Nitrogen (TKN)	Reading	Effluent	14.50	15.00	16.50	16.00	17.50	16.00	17.00	18.00	16.50	18.00
		Filt. Effluent	16.00	16.00	15.00	15.50	15.00	16.00	16.00	13.50	13.50	15.50
	Dillution	Effluent	10.00	10.00	10.00	10.00	10.00	10.00	10.00	10.00	10.00	10.00
		Filt. Effluent	5.00	5.00	5.00	5.00	5.00	5.00	5.00	5.00	5.00	5.00
	Conc. (mg/*l*)	Effluent			231.00	224.00	245.00	224.00	238.00	252.00	231.00	252.00
		Filt. Effluent	112.00	112.00	105.00	108.50	105.00	112.00	112.00	94.50	94.50	108.50
Free and Saline Ammonia (FSA)	Reading	Filt. Effluent	7.00	8.00	7.00	7.50	7.50	6.50	6.00	6.50	7.50	7.00
	Dillution	Filt. Effluent	10.00	10.00	10.00	10.00	10.00	10.00	10.00	10.00	10.00	10.00
	Sample Size	Filt. Effluent	10.00	10.00	10.00	10.00	10.00	10.00	10.00	10.00	10.00	10.00
	Conc. (mg/*l*)	Filt. Effluent	98.00	112.00	98.00	105.00	105.00	91.00	84.00	91.00	105.00	98.00
MLSS (mg/*l*)	Reading	Weight A	48.03	19.37	48.04	19.37	27.32	19.39	12.81	27.35		27.34
		Weight B	48.21	19.49	48.20	19.58	27.54	19.60	13.03	27.54		27.53
		Weight C	48.09	19.40	48.10	19.44	27.39	19.45	12.89	27.42		27.40
	Sample Size	Effluent	50.0	50.0	50.0	50.0	50.0	50.0	50.0	50.0		50.0
	Conc. (mg/*l*)	TSS	3702.0		3220.0	4076.0	4314.0	4300.0	4402.0	3802.0		3776.2
		VSS	2520.0		1984.0	2692.0	2840.0	2948.0	2934.0	2484.0		2568.2
		ISS	1182.0		1236.0	1384.0	1474.0	1352.0	1468.0	1318.0		1208.0
Total Phosphates (TP) and ortho-phosphates (OP) Results	TP Reading	Effluent	0.01	0.04	0.03	0.01	0.03	0.04	0.03	0.04	0.04	0.03
		Filt. Effluent	0.08	0.08	0.07	0.08	0.16	0.08	0.08	0.08	0.16	0.16
	OP Reading	Filt. Effluent	0.12	0.11	0.13	0.22	0.06	0.11	0.15	0.14	1.16	0.24
	TP Std. line fn.	Slope	177.05	177.05	177.05	177.05	177.05	162.81	162.81	162.81	162.81	162.81
		Intercept	3.31	3.31	3.31	3.31	3.31	2.26	2.26	2.26	2.26	2.26
	OP) Std. line fn.	Slope	93.37	93.37	93.37	93.37	93.37	99.32	99.32	99.32	99.32	99.32
		Intercept	0.91	0.91	0.91	0.91	0.91	1.81	1.81	1.81	1.81	1.81
	TP Dillution	Effluent	40.0	40.0	40.0	40.0	40.0	40.0	40.0	40.0	40.0	40.0
		Filt. Effluent	5.0	5.0	5.0	5.0	2.0	5.0	5.0	5.0	2.0	2.0
	OP Dillution	Filt. Effluent	5.0	5.0	5.0	5.0	10.0	5.0	5.0	5.0	1.0	2.0
	TP Conc. (mgP/*l*)	Effluent		247.87	212.46			227.93	162.81	260.50	273.52	221.42
		Filt. Effluent	74.12	70.59	65.30	72.36	56.48	64.92	61.67	64.92	51.93	53.23
	OP Conc. (mgP/*l*)	Filt. Effluent	58.12	52.31	60.61		58.12	55.64	75.95	70.65		46.98
VFA	Conc. (mgHAc/*l*)	Filt. Effluent			0.0		0.0		6.0		0.0	
Alk	Conc. ($mgCaCO_3/l$)	Filt. Effluent			1884.1		1896.2		1838.8		1882.5	
pH		Effluent			7.26		7.27		7.28		7.24	
Gas Production (l/d)		Effluent	1.37	1.07	1.30	1.34		1.37	1.22	1.45		

Table A8.1

Samples & Tests		Date	40 Day R_s (Experimental Period 4)									
			18-Sep-08	19-Sep-08	20-Sep-08	21-Sep-08	22-Sep-08	23-Sep-08	24-Sep-08	25-Sep-08	26-Sep-08	27-Sep-08
Chemical Oxygen Demand (COD)		Effluent	17.6	18.1	17.1	17.0	16.0	17.2	17.6	16.8	17.4	17.0
		Filt. Effluent	19.2	19.8	20.2	18.2	20.4	20.5	20.4	20.0	21.0	21.3
		Blank	25.2	25.1	25.2	25.0	25.0	24.8	24.9	25.0	25.0	25.1
	Reading	FAS Norm.	0.05	0.05	0.05	0.05	0.05	0.05	0.05	0.05	0.05	0.05
		Effluent	20.0	25.0	20.0	20.0	20.0	20.0	25.0	20.0	20.0	20.0
	Dillution	Filt. Effluent	2.0	2.0	2.0	2.0	2.0	2.0	2.0	2.0	2.0	2.0
		Effluent	6201.6	7140.0	6609.6	6528.0	7344.0	6201.6	7446.0	6691.2	6128.6	6531.8
	Conc. (mg/*l*)	Filt. Effluent			408.0		375.4	350.9	367.2	408.0	322.6	
Total Kjeldahl Nitrogen (TKN)	Reading	Effluent	20.0	18.0	18.0	20.0	17.0	18.0	16.5	17.0	18.5	17.5
		Filt. Effluent	17.5	21.5	18.0	21.0	17.0	16.0	17.2	27.0	18.0	18.0
	Dillution	Effluent	20.0	20.0	20.0	20.0	20.0	20.0	20.0	20.0	20.0	20.0
		Filt. Effluent	10.0	10.0	10.0	10.0	10.0	10.0	10.0	10.0	10.0	10.0
	Conc. (mg/*l*)	Effluent	560.0	504.0	504.0	560.0	476.0	504.0	462.0	476.0	518.0	490.0
		Filt. Effluent	245.0	301.0	252.0	294.0	238.0	224.0	240.8	378.0	252.0	252.0
Free and Saline Ammonia (FSA)	Reading	Filt. Effluent	17.5	21.5	17.0	20.0	16.0	16.0	28.5	27.0	18.0	17.5
	Dillution	Filt. Effluent	10.0	10.0	10.0	10.0	10.0	10.0	5.0	10.0	10.0	10.0
	Sample Size	Filt. Effluent	10.0	10.0	10.0	10.0	10.0	10.0	10.0	10.0	10.0	10.0
	Conc. (mg/*l*)	Filt. Effluent	245.0	301.0	238.0	280.0	224.0	224.0	199.5	378.0	252.0	245.0
MLSS (mg/*l*)		Weight A	27.58	32.31	28.42	30.85	27.96	39.38	27.96	32.34	27.92	31.32
		Weight B	27.70	32.66	28.97	31.20	28.27	39.70	28.28	32.70	28.27	32.69
	Reading	Weight C		32.42	28.57	30.96	28.06	39.49	28.07	32.46	28.04	32.44
	Sample Size	Effluent	50.0	50.0	50.0	50.0	50.0	50.0	50.0	50.0	50.0	50.0
		TSS		6862.0		6992.0	6258.0	6384.0	6274.0	7308.0	6890.0	
		VSS		4720.0		4826.0	4172.0	4178.0	4244.0	4778.0	4430.0	
	Conc. (mg/*l*)	ISS		2142.0		2166.0	2086.0	2206.0	2030.0	2530.0	2460.0	
Total Phosphates (TP) and ortho-phosphates (OP) Results	TP Reading	Effluent	0.03	0.03	0.03	0.04	0.03	0.03	0.04	0.03	0.03	0.03
		Filt. Effluent	0.03	0.04	0.03	0.04	0.04	0.04	0.03	0.03	0.03	0.03
	OP Reading	Filt. Effluent	0.09	0.08	0.14	0.25	0.10	0.08	0.08	0.08	0.65	0.08
	TP Std. line fn.	Slope	177.05	177.05	177.05	177.05	177.05	162.81	162.81	162.81	162.81	162.81
		Intercept	3.31	3.31	3.31	3.31	3.31	2.26	2.26	2.26	2.26	2.26
	OP) Std. line fn.	Slope	93.37	93.37	93.37	93.37	93.37	99.32	99.32	99.32	99.32	99.32
		Intercept	0.91	0.91	0.91	0.91	0.91	1.81	1.81	1.81	1.81	1.81
	TP Dillution	Effluent	40.0	40.0	40.0	40.0	40.0	40.0	40.0	40.0	40.0	40.0
		Filt. Effluent	10.0	10.0	10.0	10.0	10.0	10.0	10.0	10.0	10.0	10.0
	OP Dillution	Filt. Effluent	5.0	5.0	5.0	5.0	5.0	5.0	5.0	5.0	5.0	5.0
		Effluent	212.5	198.3	226.6	290.4	240.8	201.9	227.9	208.4	169.3	221.4
	TP Conc. (mgP/*l*)	Filt. Effluent		64.7	55.6	66.0	68.6	58.3	54.7	50.0	52.3	53.5
	OP Conc. (mgP/*l*)	Filt. Effluent	40.2	37.3	65.4	118.6	47.6	39.2	39.2	40.2		37.7
VFA	Conc. (mgHAc/*l*)	Filt. Effluent	9.1		41.6		0.0		66.2		45.7	
Alk	Conc. (mg$CaCO_3$/*l*)	Filt. Effluent	1893.3		1886.5		1796.2		1833.8		1812.5	
pH		Effluent	7.25		7.27		7.18		7.28		7.26	
Gas Production (l/d)		Effluent	1.13	1.16	1.01	0.92		0.99	1.24	1.03	0.78	

Table A8.1

Samples & Tests		Date	60 Day Rs (Experimental Period 3)									
			25-Jun-08	26-Jun-08	27-Jun-08	28-Jun-08	29-Jun-08	30-Jun-08	2-Jul-08	3-Jul-08	4-Jul-08	5-Jul-08
Chemical Oxygen Demand (COD)	Reading	Effluent	11.5	11.3	11.4	5.4	12.3	12.1	11.6	11.5	6.8	6.0
		Filt. Effluent	17.2	20.1	20.9	19.5	20.9	20.5	19.8	20.6	21.0	21.5
		Blank	24.8	24.5	24.7	24.6	24.5	24.3	24.0	24.2	24.8	24.5
		FAS Norm.	0.05	0.05	0.05	0.05	0.05	0.05	0.05	0.05	0.05	0.05
	Dillution	Effluent	20.0	20.0	20.0	20.0	20.0	20.0	20.0	20.0	20.0	20.0
		Filt. Effluent	2.0	2.0	2.0	2.0	2.0	2.0	2.0	2.0	2.0	2.0
	Conc. (mg/*l*)	Effluent	10640.0	10560.0	10640.0		9760.0	9955.2	10118.4	10363.2		
		Filt. Effluent		352.0	304.0	408.0	288.0	310.1	342.7	293.8	310.1	
Total Kjeldahl Nitrogen (TKN)	Reading	Effluent	21.50	22.80	20.50	21.90	21.70	17.90	21.40	21.00	39.50	22.10
		Filt. Effluent	9.36	15.85	13.98	22.34	20.23	21.06	21.53	19.06	20.98	21.57
	Dillution	Effluent	20.00	20.00	20.00	20.00	20.00	20.00	20.00	20.00	10.00	20.00
		Filt. Effluent	20.00	10.00	10.00	10.00	10.00	10.00	10.00	10.00	10.00	10.00
	Conc. (mg/*l*)	Effluent	602.00	638.40	574.00	613.20	607.60		599.20	588.00	553.00	618.80
		Filt. Effluent	262.07	221.90	195.78	312.69	283.21	294.83	301.38	266.83	293.78	301.97
Free and Saline Ammonia (FSA)	Reading	Filt. Effluent	7.37	19.47	20.21	20.52	18.21	18.21	18.73	18.94	20.42	21.05
	Dillution	Filt. Effluent	10.00	10.00	10.00	10.00	10.00	10.00	10.00	10.00	10.00	10.00
	Sample Size	Filt. Effluent	10.00	10.00	10.00	10.00	10.00	10.00	10.00	10.00	10.00	10.00
	Conc. (mg/*l*)	Filt. Effluent		272.57	282.88	287.30	254.89	254.89	262.25	265.20	285.83	294.67
MLSS (mg/*l*)	Reading	Weight A	28.39	27.32	27.31	27.31	27.95	32.43			39.39	30.11
		Weight B	28.85	27.75	27.83	27.72	28.35	32.83			39.86	30.57
		Weight C	28.55	27.45	27.48	27.44	28.06	32.54			39.51	30.26
	Sample Size	Effluent	45.0	45.0	50.0	40.0	35.0	45.0	40.0	50.0	50.0	50.0
	Conc. (mg/*l*)	TSS	10338.8	9839.3	10416.0	10305.0	10025.0	9962.3			9408.0	10239.8
		VSS	6747.8	6777.0	7020.0	7130.0	7172.5	7142.3			7034.0	6936.7
		ISS	3591.0	3062.2	3396.0	3175.0	2852.5	2820.0			2374.0	3303.0
Total Phosphates (TP) and ortho-phosphates (OP) Results	TP Reading	Effluent	0.11	0.08	0.11	0.10	0.06	0.06	0.06	0.06	0.12	0.11
		Filt. Effluent	0.10	0.10	0.12	0.10	0.09	0.09	0.12	0.09	0.09	0.09
	OP Reading	Filt. Effluent	0.17	0.13	0.14	0.13	0.15	0.16	0.12	0.12	0.15	0.11
	TP Std. line fn.	Slope	181.40	181.40	181.40	181.40	178.34	178.34	178.34	178.34	178.34	178.34
		Intercept	3.68	3.68	3.68	3.68	2.83	2.83	2.83	2.83	2.83	2.83
	OP) Std. line fn.	Slope	108.21	108.21	108.21	108.21	107.29	107.29	107.29	107.29	107.29	107.29
		Intercept	1.21	1.21	1.21	1.21	1.52	1.52	1.52	1.52	1.52	1.52
	TP Dillution	Effluent	10.0	20.0	10.0	20.0	20.0	20.0	20.0	20.0	10.0	20.0
		Filt. Effluent	5.0	5.0	5.0	5.0	5.0	5.0	5.0	5.0	5.0	5.0
	OP Dillution	Filt. Effluent	5.0	5.0	5.0	5.0	5.0	5.0	5.0	5.0	5.0	5.0
	TP Conc. (mgP/*l*)	Effluent	199.54	300.61	191.77		203.82		203.82	219.10	216.56	
		Filt. Effluent	87.84	94.02	110.14	94.02	81.87	83.19	103.00	84.51	76.59	79.23
	OP Conc. (mgP/*l*)	Filt. Effluent	89.35	71.38	74.46	71.42	80.79	84.87	66.70	63.14	82.83	56.52
VFA	Conc. (mgHAc/*l*)	Filt. Effluent	41.50		59.50		31.90		0.10		51.00	
Alk	Conc. (mgCaCO$_3$/*l*)	Filt. Effluent	2036.00		2049.50		2058.20		1984.90		2026.70	
pH		Effluent	7.08		7.14		7.15		7.18		7.11	
Gas Production (l/d)		Effluent										

Table A8.2: Raw Results for Anaerobic Digester 4 (AD 4), fed primary sludge blended with waste activated sludge (WAS) from MLE 1, when operated at sludge ages of 10, 18 and 25 days

			10 Day R_s (Experimental Period 5)									
Samples & Tests		Date	26-Oct-08	27-Oct-08	28-Oct-08	29-Oct-08	30-Oct-08	31-Oct-08	2-Nov-08	3-Nov-08	4-Nov-08	5-Nov-08
Chemical Oxygen Demand (COD)		Effluent	16.7	11.9	10.6	10.4	10.1	10.6	13.2	12.1	9.8	9.5
		Filt. Effluent	21.8	22.0	19.4	21.0	20.9	19.4	20.5	21.1	19.9	22.0
		Blank	25.0	25.5	25.1	25.6	25.0	25.0	25.0	25.0	25.0	25.0
	Reading	FAS Norm.	0.05	0.05	0.05	0.05	0.05	0.05	0.05	0.05	0.05	0.05
		Effluent	20.0	10.0	10.0	10.0	10.0	10.0	10.0	10.0	10.0	10.0
	Dillution	Filt. Effluent	1.0	1.0	1.0	1.0	1.0	1.0	1.0	1.0	1.0	1.0
		Effluent		5592.3	5962.4	6250.2	6126.9	5921.3		5304.5	6250.2	6373.6
	Conc. (mg/*l*)	Filt. Effluent	131.6	143.9	234.4	189.2	168.6	230.3	185.0	160.4	209.7	123.4
Total Kjeldahl Nitrogen (TKN)	Reading	Effluent	14.80	17.80	20.30	18.80	12.80	15.30	13.30	15.30	13.80	17.30
		Filt. Effluent	28.40	30.48	31.87	0.00	27.02	27.71	27.71	33.94	31.17	28.40
		Effluent	20.00	20.00	20.00	20.00	20.00	20.00	20.00	20.00	20.00	20.00
	Dillution	Filt. Effluent	1.00	1.00	1.00	1.00	1.00	1.00	1.00	1.00	1.00	1.00
		Effluent	414.40	498.40			358.40	428.40	372.40	428.40	386.40	484.40
	Conc. (mg/*l*)	Filt. Effluent	39.76	42.67	44.61		37.82	38.79	38.79	47.52	43.64	39.76
Free and Saline Ammonia (FSA)	Reading	Filt. Effluent	29.35	30.03	31.40	26.62	27.30	27.30	29.35	25.94	0.00	23.89
	Dillution	Filt. Effluent	1.00	1.00	1.00	1.00	1.00	1.00	1.00	1.00	1.00	1.00
	Sample Size	Filt. Effluent	10.00	10.00	10.00	10.00	10.00	10.00	10.00	10.00	10.00	10.00
	Conc. (mg/*l*)	Filt. Effluent	41.09	42.05	43.96	37.27	38.22	38.22	41.09	36.31		33.45
MLSS (mg/*l*)		Weight A	27.30	12.73	27.30	12.74	28.40	12.75	28.41		43.45	
		Weight B	27.60	12.95	27.61	13.03	28.68	12.96	28.69		43.71	
	Reading	Weight C	27.37	12.80	27.40	12.82	28.49	12.83	28.50		43.53	
	Sample Size	Effluent	50.0	50.0	50.0	50.0	50.0	50.0	50.0	50.0	50.0	50.0
		TSS	6170.0		6136.0	5702.0	5510.0		5434.0		5394.0	
		VSS	4674.0		4252.0	4144.0	3762.0		3702.0		3670.0	
	Conc. (mg/*l*)	ISS	1496.0		1884.0	1558.0	1748.0		1732.0		1724.0	
Total Phosphates (TP) and ortho-phosphates (OP) Results	TP Reading	Effluent	0.05	0.06	0.05	0.06	0.06	0.06	0.06	0.05	0.10	0.12
		Filt. Effluent	0.12	0.13	0.14	0.12	0.13	0.12	0.12	0.12	0.12	0.12
	OP Reading	Filt. Effluent	0.16	0.15	0.17	0.16	0.15	0.16	0.16	0.16	0.16	0.16
	TP Std. line fn.	Slope	166.06	166.06	166.06	166.06	166.06	166.06	166.06	166.06	166.06	166.06
		Intercept	-0.19	-0.19	-0.19	-0.19	-0.19	-0.19	-0.19	-0.19	-0.19	-0.19
	OP) Std. line fn.	Slope	121.90	121.90	121.90	121.90	121.90	121.90	121.90	121.90	121.90	121.90
		Intercept	-0.03	-0.03	-0.03	-0.03	-0.03	-0.03	-0.03	-0.03	-0.03	-0.03
	TP Dillution	Effluent	10.0	10.0	10.0	10.0	10.0	10.0	5.0	10.0	5.0	5.0
		Filt. Effluent	1.0	1.0	1.0	1.0	1.0	1.0	1.0	1.0	1.0	1.0
	OP Dillution	Filt. Effluent	1.0	1.0	1.0	1.0	1.0	1.0	1.0	1.0	1.0	1.0
	TP Conc. (mgP/*l*)	Effluent	153.20		176.44	186.41			104.83	163.16	161.29	
		Filt. Effluent	20.78	21.44	23.10	19.95	20.94	20.11	19.78	19.62	20.45	19.95
	OP Conc. (mgP/*l*)	Filt. Effluent	19.29	18.68	20.51	19.41	18.56	19.53	18.92	19.17	20.02	19.78
VFA	Conc. (mgHAc/*l*)	Filt. Effluent	0.00		0.00				0.00			
H2CO3 Alk	Conc. (mg$CaCO_3$/*l*)	Filt. Effluent	1435.00		1276.00				1304.00			
pH		Effluent	7.11		7.15				7.20			
Gas Production (l/d)			3.96	3.65	3.55	3.77	3.48			4.13		3.89

Table A8.2

Samples & Tests		Date	18 Day R_s (Experimental Period 1)									
			31-Mar-08	1-Apr-08	2-Apr-08	3-Apr-08	4-Apr-08	5-Apr-08	7-Apr-08	8-Apr-08	9-Apr-08	10-Apr-08
Chemical Oxygen Demand (COD)		Effluent	13.8	15.3	13.8	16.1	15.8	15.4	16.8	14.7	16.9	16.1
		Filt. Effluent	18.7	18.0	17.9	18.9	19.4	19.2	20.2	19.5	20.5	20.7
		Blank	22.6	23.4	23.5	23.7	24.2	23.8	24.7	25.0	25.1	25.0
	Reading	FAS Norm.	0.05	0.05	0.05	0.05	0.05	0.05	0.05	0.05	0.05	0.05
		Effluent	20.0	20.0	20.0	20.0	20.0	20.0	20.0	20.0	20.0	20.0
	Dillution	Filt. Effluent	1.0	1.0	1.0	1.0	1.0	1.0	1.0	1.0	1.0	1.0
		Effluent	7209.0	6635.5	7946.2	6225.9	6881.3	6881.3	6471.7		6612.5	7290.9
	Conc. (mg/l)	Filt. Effluent	159.7	221.2	229.4	196.6	196.6	188.4	184.3	221.8	185.5	176.1
Total Kjeldahl Nitrogen (TKN)	Reading	Effluent	19.80	15.20	21.00	29.00	16.00	17.00	19.00	15.50	16.50	14.90
		Filt. Effluent	15.70		24.00	32.00	34.00	32.00	32.00	30.00	15.50	30.50
		Effluent	20.00	20.00	20.00	10.00	20.00	20.00	20.00	20.00	20.00	20.00
	Dillution	Filt. Effluent	5.00	5.00	2.00	2.00	2.00	2.00	2.00	2.00	2.00	2.00
		Effluent	554.40	425.60		406.00	448.00	476.00	532.00	434.00	462.00	
	Conc. (mg/l)	Filt. Effluent	109.90			89.60	95.20	89.60	89.60	84.00		85.40
Free and Saline Ammonia (FSA)	Reading	Filt. Effluent	16.70		24.00	31.00	29.00	31.50	32.00	29.00	30.00	29.80
	Dillution	Filt. Effluent	5.00	5.00	2.00	2.00	2.00	2.00	2.00	2.00	2.00	2.00
	Sample Size	Filt. Effluent	10.00	10.00	10.00	10.00	10.00	10.00	10.00	10.00	10.00	10.00
	Conc. (mg/l)	Filt. Effluent	116.90		67.20	86.80	81.20	88.20	89.60	81.20	84.00	83.44
MLSS (mg/l)		Weight A	32.31	39.40	54.71	39.41	30.83	39.41	28.41	48.05	43.58	32.33
		Weight B	32.73	39.79	55.13	39.79	31.22	39.82	28.80	48.42	43.94	32.71
	Reading	Weight C	32.40	39.48	54.82	39.49	30.50	39.50	28.50	48.13	43.65	32.41
	Sample Size	Effluent	50.0	50.0	50.0	50.0	50.0	50.0	50.0	50.0	50.0	50.0
		TSS	8520.0	7808.0	8318.0	7670.0		8174.0	7744.0	7400.0	7046.0	7708.0
		VSS	6670.0	6216.0	6224.0	5982.0		6296.0	5996.0	5872.0	5694.0	6058.0
	Conc. (mg/l)	ISS	1850.0	1592.0	2094.0	1688.0		1878.0	1748.0	1528.0	1352.0	1650.0
Total Phosphates (TP) and ortho-phosphates (OP) Results	TP Reading	Effluent	0.09	0.10	0.10	0.11	0.09	0.10	0.09	0.09	0.09	0.10
		Filt. Effluent	0.04	0.07	0.06	0.04	0.06	0.06	0.06	0.04	0.04	0.06
	OP Reading	Filt. Effluent	0.04	0.07	0.07	0.07	0.29	0.09	0.10	0.18	0.07	0.10
	TP Std. line fn.	Slope	181.40	181.40	181.40	181.40	178.34	178.34	178.34	178.34	178.34	178.34
		Intercept	3.68	3.68	3.68	3.68	2.83	2.83	2.83	2.83	2.83	2.83
	OP) Std. line fn.	Slope	108.21	108.21	108.21	108.21	107.29	107.29	107.29	107.29	107.29	107.29
		Intercept	1.21	1.21	1.21	1.21	1.52	1.52	1.52	1.52	1.52	1.52
	TP Dillution	Effluent	10.0	10.0	10.0	10.0	10.0	10.0	10.0	10.0	10.0	10.0
		Filt. Effluent	10.0	5.0	5.0	10.0	5.0	5.0	5.0	10.0	10.0	5.0
	OP Dillution	Filt. Effluent	5.0	5.0	5.0	5.0	2.0	5.0	5.0	5.0	5.0	5.0
		Effluent	263.72	300.00	281.86	318.14	260.76	285.72	257.19	275.02	264.32	296.43
	TP Conc. (mgP/l)	Filt. Effluent	33.91	40.54	34.19	35.72	42.01	37.55	36.65	41.21	35.86	37.55
	OP Conc. (mgP/l)	Filt. Effluent		32.91	33.99	30.20		41.74	46.57		28.33	
VFA	Conc. (mgHAc/l)	Filt. Effluent	26.00		91.50		0.00		37.30		0.00	
H2CO3 Alk	Conc. (mgCaCO$_3$/l)	Filt. Effluent	1456.40		1347.40		1524.70		1488.60		1442.20	
pH		Effluent	7.37		7.29		7.27		7.28		7.24	
Gas Production (l/d)			2.16	1.80	2.11	1.78	1.34			1.87	1.61	2.28

Table A8.2

Samples & Tests		Date	25 Day R_s (Experimental Period 2)									
			2-Jun-08	3-Jun-08	4-Jun-08	5-Jun-08	6-Jun-08	7-Jun-08	9-Jun-08	10-Jun-08	11-Jun-08	12-Jun-08
Chemical Oxygen Demand (COD)		Effluent	15.6	16.3	16.2	15.8	16.6	15.9	15.5	16.5	16.2	
		Filt. Effluent	19.7	18.7	19.8	19.4	19.6	19.4	19.0	19.1	19.9	
		Blank	24.5	24.5	24.5	24.5	24.5	24.5	24.5	24.5	24.5	24.5
	Reading	FAS Norm.	0.05	0.05	0.05	0.05	0.05	0.05	0.05	0.05	0.05	0.05
		Effluent	20.0	20.0	20.0	20.0	20.0	20.0	20.0	20.0	20.0	20.0
	Dillution	Filt. Effluent	1.0	1.0	1.0	1.0	1.0	1.0	1.0	1.0	1.0	1.0
		Effluent	7290.9	6717.4	6799.4	7127.0	6471.7	6962.6	7286.4	6476.8	6719.7	
	Conc. (mg/*l*)	Filt. Effluent	196.6	237.6	192.5	208.9	200.7	206.4	222.6	218.6	186.2	
Total Kjeldahl Nitrogen (TKN)	Reading	Effluent	17.50	20.00	21.50	20.50	16.00	17.50	16.00	18.00	16.50	19.50
		Filt. Effluent	28.50	30.50	32.00	0.00	27.00	27.50	27.71	34.00	31.00	28.40
		Effluent	20.00	20.00	20.00	20.00	20.00	20.00	20.00	20.00	20.00	20.00
	Dillution	Filt. Effluent	5.00	5.00	5.00	5.00	5.00	5.00	5.00	5.00	5.00	5.00
		Effluent	490.00	560.00	602.00	574.00	448.00	490.00	448.00	504.00	462.00	546.00
	Conc. (mg/*l*)	Filt. Effluent	199.50	213.50	224.00		189.00	192.50	193.96	238.00	217.00	198.81
Free and Saline Ammonia (FSA)	Reading	Filt. Effluent	29.50	30.00	31.50	27.00	27.00	27.00	29.50	26.00	0.00	24.00
	Dillution	Filt. Effluent	2.00	2.00	2.00	2.00	2.00	2.00	2.00	2.00	2.00	2.00
	Sample Size	Filt. Effluent	5.00	5.00	5.00	5.00	5.00	5.00	5.00	5.00	5.00	5.00
	Conc. (mg/*l*)	Filt. Effluent	165.20	168.00	176.40	151.20	151.20	151.20	165.20	145.60		134.40
MLSS (mg/*l*)		Weight A	27.30	12.73	27.30	12.74	28.40	12.75	28.41		43.45	
		Weight B	27.69	13.08	27.69	13.16	28.81	13.09	28.82		43.84	
	Reading	Weight C	27.39	12.82	27.42	12.84	28.51	12.85	28.52		43.55	
	Sample Size	Effluent	50.0	50.0	50.0	50.0	50.0	50.0	50.0	50.0	50.0	50.0
		TSS	7970.0	6914.0	7736.0	8302.0	8110.0	6762.0	8034.0		7994.0	
		VSS	6074.0	5100.0	5452.0	6344.0	5962.0	4874.0	5902.0		5870.0	
	Conc. (mg/*l*)	ISS	1896.0	1814.0	2284.0	1958.0	2148.0	1888.0	2132.0		2124.0	
Total Phosphates (TP) and ortho-phosphates (OP) Results	TP Reading	Effluent	0.07	0.09	0.08	0.09	0.07	0.07	0.07	0.07	0.09	0.08
		Filt. Effluent	0.09	0.09	0.10	0.10	0.08	0.09	0.08	0.07	0.08	0.08
	OP Reading	Filt. Effluent	0.17	0.13	0.14	0.08	0.15	0.17	0.11	0.11	0.12	0.13
	TP Std. line fn.	Slope	177.05	177.05	177.05	177.05	177.05	162.81	162.81	162.81	162.81	162.81
		Intercept	3.31	3.31	3.31	3.31	3.31	2.26	2.26	2.26	2.26	2.26
	OP) Std. line fn.	Slope	93.37	93.37	93.37	93.37	93.37	99.32	99.32	99.32	99.32	99.32
		Intercept	0.91	0.91	0.91	0.91	0.91	1.81	1.81	1.81	1.81	1.81
	TP Dillution	Effluent	20.0	20.0	20.0	20.0	20.0	20.0	20.0	20.0	20.0	20.0
		Filt. Effluent	5.0	5.0	5.0	5.0	5.0	5.0	5.0	5.0	5.0	5.0
	OP Dillution	Filt. Effluent	5.0	5.0	5.0	5.0	5.0	5.0	5.0	5.0	5.0	5.0
		Effluent	363.44	252.54		245.46	349.28	372.05	365.54	346.00		
	TP Conc. (mgP/*l*)	Filt. Effluent	58.71	64.02	67.56	69.33	53.40	62.79	49.76	45.69	56.28	53.83
	OP Conc. (mgP/*l*)	Filt. Effluent		55.20	62.21	33.73	64.54	75.40	47.09	47.59	52.06	56.03
VFA	Conc. (mgHAc/*l*)	Filt. Effluent	0.00		0.00		2.30		0.00		0.00	
H2CO3 Alk	Conc. (mgCaCO$_3$/*l*)	Filt. Effluent	2025.70		2076.70		2024.80		2102.00		2032.10	
pH		Effluent	7.25		7.29		7.25		7.30		7.26	
Gas Production (l/d)			1.08	1.25	1.32	0.91		0.98	1.10		0.96	1.25

Table A8.2

Samples & Tests			Date	40 Day Rs (Experimental Period 4)									
				18-Sep-08	19-Sep-08	20-Sep-08	21-Sep-08	22-Sep-08	23-Sep-08	24-Sep-08	25-Sep-08	26-Sep-08	27-Sep-08
Chemical Oxygen Demand (COD)	Reading	Effluent		10.9	9.1	9.7	10.4	8.9	9.6	8.8	9.7	10.3	10.4
		Filt. Effluent		20.0	21.8	20.9	20.6	20.9	20.9	22.8	20.5	22.3	22.8
		Blank		25.2	25.1	25.2	25.0	25.0	24.8	24.9	25.0	25.0	25.1
		FAS Norm.		0.05	0.05	0.05	0.05	0.05	0.05	0.05	0.05	0.05	0.05
	Dillution	Effluent		20.0	20.0	20.0	20.0	20.0	20.0	20.0	20.0	20.0	20.0
		Filt. Effluent		2.0	1.0	1.0	1.0	1.0	1.0	1.0	1.0	1.0	1.0
	Conc. (mg/*l*)	Effluent		11668.8	13056.0	12648.0	11913.6	13137.6	12403.2	13137.6	12484.8	11854.1	11854.1
		Filt. Effluent			134.6	175.4	179.5	167.3	159.1		183.6	108.9	92.7
Total Kjeldahl Nitrogen (TKN)	Reading	Effluent		30.00	33.00	33.00	15.50	14.00	13.50	34.00	35.00	31.00	33.00
		Filt. Effluent		29.50	29.00	28.00	16.50	30.00	29.50	28.00	6.50	29.00	29.00
	Dillution	Effluent		20.00	20.00	20.00	40.00	40.00	40.00	20.00	20.00	20.00	20.00
		Filt. Effluent		10.00	10.00	10.00	20.00	10.00	10.00	10.00	10.00	10.00	10.00
	Conc. (mg/*l*)	Effluent			924.00	924.00	868.00			952.00	980.00	868.00	924.00
		Filt. Effluent		413.00	406.00	392.00	462.00	420.00	413.00	392.00		406.00	406.00
Free and Saline Ammonia (FSA)	Reading	Filt. Effluent		30.00	19.50	28.00	24.00	30.00	28.00	28.00	29.50	27.00	29.00
	Dillution	Filt. Effluent		10.00	10.00	10.00	10.00	10.00	10.00	10.00	10.00	10.00	10.00
	Sample Size	Filt. Effluent		10.00	10.00	10.00	10.00	10.00	10.00	10.00	10.00	10.00	10.00
	Conc. (mg/*l*)	Filt. Effluent		420.00		392.00	336.00	420.00	392.00	392.00	413.00	378.00	406.00
MLSS (mg/*l*)	Reading	Weight A		27.35	30.84	27.93	32.35	43.61	28.35	39.41	39.33	28.41	28.43
		Weight B		27.80	31.38	28.24	32.89	44.13	28.90	39.95	39.87	28.94	28.93
		Weight C		27.49	31.00	28.05	32.51	43.78	28.53	39.58	39.51	28.58	28.59
	Sample Size	Effluent		50.0	50.0	50.0	50.0	50.0	50.0	50.0	50.0	50.0	50.0
	Conc. (mg/*l*)	TSS			10840.0		10770.0	10406.0	11052.0	10884.0	10852.0	10626.0	
		VSS			7534.0		7600.0	7040.0	7526.0	7502.0	7344.0	7196.0	
		ISS			3306.0		3170.0	3366.0	3526.0	3382.0	3508.0	3430.0	
Total Phosphates (TP) and ortho-phosphates (OP) Results	TP Reading	Effluent		0.07	0.09	0.08	0.09	0.07	0.07	0.07	0.07	0.09	0.08
		Filt. Effluent		0.09	0.09	0.10	0.10	0.08	0.09	0.08	0.07	0.08	0.08
	OP Reading	Filt. Effluent		0.17	0.13	0.14	0.08	0.15	0.17	0.11	0.11	0.12	0.13
	TP Std. line fn.	Slope		177.05	177.05	177.05	177.05	177.05	162.81	162.81	162.81	162.81	162.81
		Intercept		3.31	3.31	3.31	3.31	3.31	2.26	2.26	2.26	2.26	2.26
	OP) Std. line fn.	Slope		93.37	93.37	93.37	93.37	93.37	99.32	99.32	99.32	99.32	99.32
		Intercept		0.91	0.91	0.91	0.91	0.91	1.81	1.81	1.81	1.81	1.81
	TP Dillution	Effluent		40.0	40.0	40.0	40.0	40.0	40.0	40.0	40.0	40.0	40.0
		Filt. Effluent		10.0	10.0	10.0	10.0	10.0	10.0	10.0	10.0	10.0	10.0
	OP Dillution	Filt. Effluent		10.0	10.0	10.0	10.0	10.0	10.0	10.0	10.0	10.0	10.0
	TP Conc. (mgP/*l*)	Effluent		363.44		420.10		349.28	372.05	365.54	346.00		
		Filt. Effluent		117.42	128.04	135.12	138.66	106.80	125.58	99.53	91.39	112.55	107.67
	OP Conc. (mgP/*l*)	Filt. Effluent		149.63	110.41	124.42	67.46	129.08	150.79	94.18	95.17	104.11	112.06
VFA	Conc. (mgHAc/*l*)	Filt. Effluent		47.90		58.50		9.30		20.60		0.00	
H_2CO_3 Alk	Conc. (mg$CaCO_3$/*l*)	Filt. Effluent		2514.60		2446.60		2414.80		2509.00		2433.70	
pH		Effluent		7.37		7.39		7.25		7.40		7.30	
Gas Production (l/d)				0.77	0.91	0.98	1.06	0.72					

Table A8.2

Samples & Tests		Date	60 Day R_s (Experimental Period 3)									
			25-Jun-08	26-Jun-08	27-Jun-08	28-Jun-08	29-Jun-08	30-Jun-08	2-Jul-08	3-Jul-08	4-Jul-08	5-Jul-08
Chemical Oxygen Demand (COD)	Reading	Effluent	14.4	13.7	12.8	13.3	13.7	14.0	12.3	14.4	14.6	14.2
		Filt. Effluent	19.6	19.4	17.7	19.7	19.2	19.0	20.0	19.2	20.0	20.3
		Blank	24.8	24.5	24.7	24.6	24.5	24.3	24.0	24.2	24.8	24.5
		FAS Norm.	0.05	0.05	0.05	0.05	0.05	0.05	0.05	0.05	0.05	0.05
	Dillution	Effluent	40.0	40.0	40.0	40.0	40.0	40.0	40.0	40.0	40.0	40.0
		Filt. Effluent	1.0	1.0	1.0	1.0	1.0	1.0	1.0	1.0	1.0	1.0
	Conc. (mg/*l*)	Effluent	16640.0	17280.0		18080.0	17280.0	16809.6		15993.6	16646.4	16809.6
		Filt. Effluent	208.0	204.0		196.0	212.0	216.2	163.2	204.0	195.8	171.4
Total Kjeldahl Nitrogen (TKN)	Reading	Effluent	39.00	35.00	38.00	36.00	32.00			34.00	42.50	38.50
		Filt. Effluent	48.50	38.00		41.00	39.50	72.00	35.00	36.00	42.00	36.50
	Dillution	Effluent	20.00	20.00	20.00	20.00	20.00	20.00	20.00	20.00	20.00	20.00
		Filt. Effluent	10.00	10.00	10.00	10.00	10.00	5.00	10.00	10.00	10.00	10.00
	Conc. (mg/*l*)	Effluent	1092.00	980.00	1064.00	1008.00	896.00			952.00	1190.00	1078.00
		Filt. Effluent	679.00	532.00		574.00	553.00	504.00	490.00	504.00	588.00	511.00
Free and Saline Ammonia (FSA)	Reading	Filt. Effluent	48.50	35.00	34.50	39.00	39.50	38.50	27.50	41.00		36.00
	Dillution	Filt. Effluent	10.00	10.00	10.00	10.00	10.00	10.00	10.00	10.00	10.00	10.00
	Sample Size	Filt. Effluent	10.00	10.00	10.00	10.00	10.00	10.00	10.00	10.00	10.00	10.00
	Conc. (mg/*l*)	Filt. Effluent	679.00	490.00	483.00	546.00	553.00	539.00	385.00	574.00		504.00
MLSS (mg/*l*)	Reading	Weight A	32.31	39.40	54.71	39.41	30.83	39.41	28.41	48.05	43.58	32.33
		Weight B	32.93	40.14	55.47	40.13	31.66	40.12	29.17	48.27	44.38	32.56
		Weight C	32.53	39.62	54.94	39.59	31.06	39.61	28.62	48.27	43.79	32.54
	Sample Size	Effluent	50.0	50.0	50.0	50.0	50.0	50.0	50.0	50.0	50.0	50.0
	Conc. (mg/*l*)	TSS	12420.0	14708.0	15218.0	14570.0	16696.0	14274.0	15044.0		15946.0	
		VSS	7970.0	10316.0	10724.0	10882.0	12006.0	10196.0	10896.0		11794.0	
		ISS	4450.0	4392.0	4494.0	3688.0	4690.0	4078.0	4148.0		4152.0	
Total Phosphates (TP) and ortho-phosphates (OP) Results	TP Reading	Effluent	0.09	0.08	0.07	0.09	0.04	0.04	0.04	0.09	0.09	0.10
		Filt. Effluent	0.12	0.12	0.13	0.12	0.06	0.07	0.08	0.11	0.12	0.11
	OP Reading	Filt. Effluent	0.17	0.16	0.23	0.17	0.20	0.22	0.12	0.11	0.16	0.16
	TP Std. line fn.	Slope	181.40	181.40	181.40	181.40	178.34	178.34	178.34	178.34	178.34	178.34
		Intercept	3.68	3.68	3.68	3.68	2.83	2.83	2.83	2.83	2.83	2.83
	OP) Std. line fn.	Slope	108.21	108.21	108.21	108.21	107.29	107.29	107.29	107.29	107.29	107.29
		Intercept	1.21	1.21	1.21	1.21	1.52	1.52	1.52	1.52	1.52	1.52
	TP Dillution	Effluent	40.0	40.0	40.0	40.0	40.0	40.0	40.0	40.0	40.0	40.0
		Filt. Effluent	10.0	10.0	10.0	10.0	20.0	20.0	20.0	10.0	10.0	10.0
	OP Dillution	Filt. Effluent	10.0	10.0	10.0	10.0	10.0	10.0	10.0	10.0	10.0	10.0
	TP Conc. (mgP/*l*)	Effluent	505.68	462.14		476.66				507.25	528.65	564.32
		Filt. Effluent	189.46	174.37	193.59	174.37	166.86	191.58	233.25	162.00	194.14	169.42
	OP Conc. (mgP/*l*)	Filt. Effluent	167.24	160.60	233.67	167.24	195.52		117.81	105.95	156.01	158.64
VFA	Conc. (mgHAc/*l*)	Filt. Effluent	84.50		76.30		50.20		67.30		65.00	
H_2CO_3 Alk	Conc. (mg$CaCO_3$/*l*)	Filt. Effluent	2525.20		2542.60		2562.00		2518.60		2541.20	
pH		Effluent	7.27		7.26		7.25		7.28		7.24	
Gas Production (l/d)												

Table A8.3: Raw Results for Anaerobic Digester 1 (AD 1), fed waste activated sludge (WAS) from the NDBEPR UCT Process System, when operated at sludge ages of 10, 18 and 25 days

Samples & Tests				10 Day R_s (Experimental Period 5)									
			Date	26-Oct-08	27-Oct-08	28-Oct-08	29-Oct-08	30-Oct-08	31-Oct-08	2-Nov-08	3-Nov-08	4-Nov-08	5-Nov-08
Chemical Oxygen Demand (COD)			Effluent	15.8	6.6	6.5	7.4	7.2	6.8	8.5	6.7	7.1	
			Filt. Effluent	23.3	22.0	23.0	22.4	22.5	23.0	22.8	23.1	22.9	
			Blank	25.0	25.5	25.1	25.6	25.0	25.0	25.0	25.0	25.0	
		Reading	FAS Norm.	0.05	0.05	0.05	0.05	0.05	0.05	0.05	0.05	0.05	0.05
			Effluent	20.0	10.0	10.0	10.0	10.0	10.0	10.0	10.0	10.0	10.0
		Dillution	Filt. Effluent	1,0	1,0	1.0	1.0	1.0	1.0	1 .0	1.0	1.0	
			Effluent	7566.1	7771.7	7648.3	7483.8	7319.4	7483.8		7525.0	7360.5	
		Conc. (mg/l)	Filt. Effluent	69.9	143.9	86.4	131.6	102.8	82.2	90.5	78.1	86.4	
Total Kjeldahl Nitrogen (TKN)			Effluent	19.5	23.0	20.0	23.0	24.0	20.5	20.0	19.5	21.5	22.0
		Reading	Filt. Effluent	11.4	12.3	12.3	13.3	16.6	11.4	13.8	12.8	14.2	13.8
			Effluent	20.0	20.0	20.0	20.0	20.0	20.0	20.0	20.0	20.0	20.0
		Dillution	Filt. Effluent	5.0	5.0	5.0	5.0	5.0	5.0	5.0	5.0	5.0	5.0
			Effluent	546.0	644.0	560.0	644.0	672.0	574.0	560.0	546.0	602.0	616.0
		Conc. (mg/l)	Filt. Effluent	79.7	86.3	86.3	93.0	116.2	79.7	96.3	89.6	99.6	96.3
Free and Saline Ammonia (FSA)		Reading	Filt. Effluent	11.8	12.3	12.8	13.2	16.7	11.8	12.8	12.8	13.7	13.2
		Dillution	Filt. Effluent	5.0	5.0	5.0	5.0	5.0	5.0	5.0	5.0	5.0	5.0
		Sample Size	Filt. Effluent	10.0	10.0	10.0	10.0	10.0	10.0	10.0	10.0	10.0	10.0
		Conc. (mg/l)	Filt. Effluent	82.4	85.8	89.3	92.7		82.4	89.3	89.3	96.1	92.7
MLSS (mg/l)			Weight A	54.74	54.72	58.12	58.11	58.12	58.16	58.12	58.13	59.56	
			Weight B	55.10	55.07	58.48	58.48	58.47	58.51	58.52	58.49	59.89	0.05
		Reading	Weight C	54.83	54.82	58.22	58.22	58.25	58.21	58.26	58.24	59.64	0.06
		Sample Size	Effluent	50.0	50.0	50.0	50.0	50.0	50.0	50.0	50.0	50.0	50.0
			TSS	7240.0	6960.0	7246.0	7292.0	7008.0		8099.0	7166.0	6668.0	
			VSS	5426.0	4948.0	5202.0	5160.0	4422.0		5243.0	4980.0	4960.0	
		Conc. (mg/l)	ISS	1814.0	2012.0	2044.0	2132.0	2586.0		2856.0	2186.0	1708.0	
Total Phosphates (TP) and ortho-phosphates (OP) Results		TP Reading	Effluent	0.14	0.17	0.14	0.16	0.13	0.13	0.15	0.14	0.14	0.13
			Filt. Effluent	0.07	0.06	0.08	0.08	0.09	0.07	0.08	0.07	0.11	0.08
		OP Reading	Filt. Effluent	0.09	0.08	0.11	0.10	0.12	0.11	0.10	0.10	0.17	0.09
			Slope	166.06	166.06	166.06	166.06	166.06	166.06	166.06	166.06	166.06	166.06
		TP Std. line fn.	Intercept	-0.19	-0.19	-0.19	-0.19	-0.19	-0.19	-0.19	-0.19	-0.19	-0.19
			Slope	121.90	121.90	121.90	121.90	121.90	121.90	121.90	121.90	121.90	121.90
		OP) Std. line fn.	Intercept	-0.03	-0.03	-0.03	-0.03	-0.03	-0.03	-0.03	-0.03	-0.03	-0.03
			Effluent	40.0	40.0	40.0	40.0	40.0	40.0	40.0	40.0	40.0	40.0
		TP Dillution	Filt. Effluent	40.0	40.0	40.0	40.0	40.0	40.0	40.0	40.0	40.0	40.0
		OP Dillution	Filt. Effluent	40.0	40.0	40.0	40.0	40.0	40.0	40.0	40.0	40.0	40.0
			Effluent	957.3		930.8		871.0	884.3		917.5	950.7	877.6
		TP Conc. (mgP/l)	Filt. Effluent	492.4	379.5	532.2	552.2	592.0	499.0	505.7	485.7		545.5
		OP Conc. (mgP/l)	Filt. Effluent	454.7	410.8	537.6	498.6	581.5	522.9	498.6	464.4		459.6
VFA		Conc. (mgHAc/l)	Filt. Effluent	32.0	30.0	1.0	10.0	40.0	48.0	28.0	58.0	0.0	0.0
H_2CO_3Alk		Conc. (mg$CaCO_3$/l)	Filt. Effluent	178.0	286.9	146.0	310.0	130.0	226.0	270.0	433.0	250.0	243.0
Total Alk.		Conc. (mg$CaCO_3$/l)	Filt. Effluent										
pH				6.81		6.66		6.76		6.71			
Gas Production (l/d)				3.71	4.21	4.41	4.26	4.11	4.36	4.26	4.36	4.21	4.01

Table A8.3

Samples & Tests			Date	31-Mar-08	1-Apr-08	2-Apr-08	3-Apr-08	4-Apr-08	5-Apr-08	7-Apr-08	8-Apr-08	9-Apr-08	10-Apr-08
				18 Day R_s (Experimental Period 1)									
Chemical Oxygen mand (COD)	Reading	Effluent		13.7	14.1	14.4	14.9	15.6	15.1	15.6	15.9	16.2	15.7
		Filt. Effluent		19.5	20.7	20.4	19.9	21.4	20.9	21.7	21.8	22.1	22.6
		Blank		22.6	23.4	23.5	23.7	24.2	23.8	24.7	25.0	25.1	25.0
		FAS Norm.		0.05	0.05	0.05	0.05	0.05	0.05	0.05	0.05	0.05	0.05
	Dillution	Effluent		20.0	20.0	20.0	20.0	20.0	20.0	20.0	20.0	20.0	20.0
		Filt. Effluent		1,0	1,0	1.0	1.0	1.0	1.0	1 .0	1.0	1.0	1,0
	Conc. (mg/*l*)	Effluent		7290.9			7209.0	7045.1	7127.0	7454.7	7338.2	7177.0	
		Filt. Effluent		127.0	110.6	127.0	155.6	114.7	118.8	122.9	129.0	121.0	98.3
Total Kjeldahl rogen (TKN)	Reading	Effluent		22.6	23.5	19.5	20.1	19.9	19.6	20.2	21.5	21.5	22.0
		Filt. Effluent		10.0	23.0	24.5	24.0	19.5	21.5	18.5	18.0	19.0	22.0
	Dillution	Effluent		20.0	20.0	20.0	20.0	20.0	20.0	20.0	20.0	20.0	20.0
		Filt. Effluent		10.0	5.0	5.0	5.0	5.0	5.0	5.0	5.0	5.0	5.0
	Conc. (mg/*l*)	Effluent		632.8	658.0	546.0	562.8	557.2	548.8	565.6	602.0	602.0	616.0
		Filt. Effluent		140.0	161.0	171.5	168.0	136.5	150.5	129.5	126.0	133.0	154.0
Free and Saline monia (FSA)	Reading	Filt. Effluent		9.8	22.0	23.0	21.5	19.5	21.5	18.0	18.0	19.0	20.0
	Dillution	Filt. Effluent		10.0	5.0	5.0	5.0	5.0	5.0	5.0	5.0	5.0	5.0
	Sample Size	Filt. Effluent		10.0	10.0	10.0	10.0	10.0	10.0	10.0	10.0	10.0	10.0
	Conc. (mg/*l*)	Filt. Effluent		137.2	154.0	161.0	150.5	136.5	150.5	126.0	126.0	133.0	140.0
MLSS (mg/*l*)	Reading	Weight A		54.74	54.72	58.12	58.11	58.12	58.16	58.12	58.13	59.56	
		Weight B		55.11	55.08	58.49	58.49	58.49	58.49	58.54	58.51	59.91	
		Weight C		54.86	54.84	58.24	58.24	58.27	58.23	58.28	58.26	59.66	
	Sample Size	Effluent		50.0	50.0	50.0	50.0	50.0	50.0	50.0	50.0	50.0	50.0
	Conc. (mg/*l*)	TSS		7400.0	7260.0	7546.0	7592.0	7308.0	6616.0	8399.0	7466.0	6968.0	
		VSS		4986.0	4848.0	5102.0	5060.0	4322.0	5196.0	5143.0	4880.0	4860.0	
		ISS		2414.0	2412.0	2444.0	2532.0	2986.0	1420.0	3256.0	2586.0	2108.0	
Total Phosphates (TP) and ortho-phosphates (OP) ults	TP Reading	Effluent		0.17	0.15	0.14	0.15	0.14	0.09	0.09	0.10	0.11	0.14
		Filt. Effluent		0.09	0.08	0.10	0.07	0.10	0.13	0.07	0.07	0.07	0.08
	OP Reading	Filt. Effluent		0.12	0.09	0.13	0.06	0.16		0.09	0.09	0.17	
	TP Std. line fn.	Slope		181.40	181.40	181.40	181.40	178.34	178.34	178.34	178.34	178.34	178.34
		Intercept		3.68	3.68	3.68	3.68	2.83	2.83	2.83	2.83	2.83	2.83
	OP) Std. line fn.	Slope		108.21	108.21	108.21	108.21	107.29	107.29	107.29	107.29	107.29	107.29
		Intercept		1.21	1.21	1.21	1.21	1.52	1.52	1.52	1.52	1.52	1.52
	TP Dillution	Effluent		40.0	40.0	40.0	40.0	40.0	50.0	50.0	50.0	50.0	50.0
		Filt. Effluent		40.0	40.0	40.0	40.0	40.0	40.0	40.0	40.0	40.0	40.0
	OP Dillution	Filt. Effluent		40.0	40.0	40.0	40.0	40.0	40.0	40.0	40.0	40.0	40.0
	TP Conc. (mgP/*l*)	Effluent		1086.2	933.8	832.2	904.8	885.3	802.5	802.5	882.8	954.1	1062.1
		Filt. Effluent		481.3	411.0	557.7		572.2		413.1	350.5	386.8	433.4
	OP Conc. (mgP/*l*)	Filt. Effluent		471.0	319.5	505.6		621.5		303.9	333.9	655.8	
VFA	Conc. (mgHAc/*l*)	Filt. Effluent		0.0	0.0	0.0	0.0	0.0	0.0	0.0	0.0	0.0	0.0
H_2CO_3Alk	Conc. (mg$CaCO_3$/*l*)	Filt. Effluent		378.0	286.9	346.0	310.0	330.0	226.0	270.0	433.0	350.0	243.0
Total Alk.	Conc. (mg$CaCO_3$/*l*)	Filt. Effluent		819.0		799.0	901.0	851.0	822.0	857.0	851.0	899.0	892.0
pH				6.89	6.85	6.92	6.81	6.98	6.86	6.89	7.09	7.00	7.04
Gas Production (l/d)				1.91	2.01	2.04	1.94	1.91	1.84	1.91	1.97	1.94	1.97

Table A8.3

Samples & Tests			25 Day R_s (Experimental Period 2)									
		Date	2-Jun-08	3-Jun-08	4-Jun-08	5-Jun-08	6-Jun-08	7-Jun-08	9-Jun-08	10-Jun-08	11-Jun-08	12-Jun-08
Chemical Oxygen Demand (COD)		Effluent	16.0	16.3	15.9	16.0	15.8	15.7	16.1	16.1	15.8	
		Filt. Effluent	21.8	21.9	22.2	21.7	22.1	19.8	21.6	22.0	22.4	
		Blank	24.5	24.5	24.5	24.5	24.5	24.5	24.5	24.5	24.5	24.5
	Reading	FAS Norm.	0.05	0.05	0.05	0.05	0.05	0.05	0.05	0.05	0.05	0.05
		Effluent	20.0	20.0	20.0	20.0	20.0	20.0	20.0	20.0	20.0	20.0
	Dillution	Filt. Effluent	1,0	1.0	1.0	1.0	1.0	1 .0	1.0	1.0	1,0	
		Effluent	6963.2	6717.4	7045.1	6963.2	7127.0	7124.5	6800.6	6800.6	7043.5	
	Conc. (mg/*l*)	Filt. Effluent	110.6	106.5	94.2	114.7	98.3	190.3	117.4	101.2	85.0	
Total Kjeldahl Nitrogen (TKN)	Reading	Effluent	19.5	23.0	20.0	23.0	24.0	20.5	20.0	19.5	21.5	22.0
		Filt. Effluent	11.4	12.3	12.3	13.3	16.6	11.4	13.8	12.8	14.2	13.8
		Effluent	20.0	20.0	20.0	20.0	20.0	20.0	20.0	20.0	20.0	20.0
	Dillution	Filt. Effluent	10.0	10.0	10.0	10.0	10.0	10.0	10.0	10.0	10.0	10.0
		Effluent	546.0	644.0	560.0	644.0	672.0	574.0	560.0	546.0	602.0	616.0
	Conc. (mg/*l*)	Filt. Effluent	159.4	172.6	172.6	185.9	232.4	159.4	192.6	179.3	199.2	192.6
Free and Saline Ammonia (FSA)	Reading	Filt. Effluent	11.8	12.3	12.8	13.2	16.7	11.8	12.8	12.8	13.7	13.2
	Dillution	Filt. Effluent	10.0	10.0	10.0	10.0	10.0	10.0	10.0	10.0	10.0	10.0
	Sample Size	Filt. Effluent	10.0	10.0	10.0	10.0	10.0	10.0	10.0	10.0	10.0	10.0
	Conc. (mg/*l*)	Filt. Effluent	164.8	171.7	178.5	185.4		164.8	178.5	178.5	192.3	185.4
MLSS (mg/*l*)		Weight A	54.74	54.72	58.12	58.11	58.12	58.16	58.12	58.13	59.56	
		Weight B	55.10	55.07	58.48	58.48	58.47	58.51	58.52	58.49	59.89	
	Reading	Weight C	54.85	54.84	58.24	58.24	58.27	58.23	58.28	58.26	59.66	
	Sample Size	Effluent	50.0	50.0	50.0	50.0	50.0	50.0	50.0	50.0	50.0	50.0
		TSS	7240.0	6960.0	7246.0	7292.0	7008.0	7116.0	8099.0	7166.0	6668.0	
		VSS	5026.0	4548.0	4802.0	4760.0	4022.0	5696.0	4843.0	4580.0	4560.0	
	Conc. (mg/*l*)	ISS	2214.0	2412.0	2444.0	2532.0	2986.0	1420.0	3256.0	2586.0	2108.0	
Total Phosphates (TP) and ortho-phosphates (OP) Results	TP Reading	Effluent	0.15	0.15	0.14	0.13	0.14	0.14	0.15	0.15	0.15	0.13
		Filt. Effluent	0.06	0.09	0.09	0.07	0.08	0.11	0.09	0.09	0.11	0.07
	OP Reading	Filt. Effluent	0.10	0.13	0.14	0.10	0.13	0.12	0.15	0.14	0.17	0.11
		Slope	177.05	177.05	177.05	177.05	177.05	162.81	162.81	162.81	162.81	162.81
	TP Std. line fn.	Intercept	3.31	3.31	3.31	3.31	3.31	2.26	2.26	2.26	2.26	2.26
		Slope	93.37	93.37	93.37	93.37	93.37	99.32	99.32	99.32	99.32	99.32
	OP) Std. line fn.	Intercept	0.91	0.91	0.91	0.91	0.91	1.81	1.81	1.81	1.81	1.81
		Effluent	40.0	40.0	40.0	40.0	40.0	40.0	40.0	40.0	40.0	40.0
	TP Dillution	Filt. Effluent	60.0	40.0	40.0	40.0	40.0	40.0	40.0	40.0	40.0	40.0
	OP Dillution	Filt. Effluent	60.0	40.0	40.0	40.0	40.0	40.0	40.0	40.0	40.0	40.0
		Effluent	930.0	915.8	887.5	753.0	880.4	821.4	886.5	867.0	854.0	756.3
	TP Conc. (mgP/*l*)	Filt. Effluent	407.1	483.8	512.2	328.0	413.0	613.0	463.2	482.8	593.5	372.1
	OP Conc. (mgP/*l*)	Filt. Effluent	505.6	449.1	490.2	337.1	445.4	416.4	531.7	464.1	583.3	380.7
VFA	Conc. (mgHAc/*l*)	Filt. Effluent	37.3		0.0		3.0		2.3		20.7	
H_2CO_3Alk	Conc. (mgCaCO$_3$/*l*)	Filt. Effluent	612.0	606.0	744.0	625.0	612.0	599.0	508.0	724.0	721.0	
Total Alk.	Conc. (mgCaCO$_3$/*l*)	Filt. Effluent	901.0	926.0	913.0	927.0	844.0	901.0	978.0	965.0	985.0	
pH			6.80	6.75	6.80	6.82	6.80	6.83	6.79	6.79	6.85	6.82
Gas Production (l/d)			1.02	0.99	0.96	0.99	0.94	0.91	0.99	0.96	0.96	0.94

Table A8.3

Samples & Tests		Date	40 Day R_s (Experimental Period 4)									
			18-Sep-08	19-Sep-08	20-Sep-08	21-Sep-08	22-Sep-08	23-Sep-08	24-Sep-08	25-Sep-08	26-Sep-08	27-Sep-08
Chemical Oxygen Demand (COD)	Reading	Effluent	17.0	17.5	17.6	16.8	16.5	16.8	17.6	17.4	16.9	16.6
		Filt. Effluent	23.2	23.1	22.5	22.6	22.2	23.1	22.4	22.8	22.8	23.1
		Blank	25.2	25.1	25.2	25.0	25.0	24.8	24.9	25.0	25.0	25.1
		FAS Norm.	0.05	0.05	0.05	0.05	0.05	0.05	0.05	0.05	0.05	0.05
	Dillution	Effluent	20.0	20.0	20.0	20.0	20.0	20.0	20.0	20.0	20.0	20.0
		Filt. Effluent	1.00	1.00	1.00	1.00	1.00	1.00	1.00	1.00	1.00	1.00
	Conc. (mg/*l*)	Effluent	6691.2	6201.6	6201.6	6691.2		6528.0	5956.8	6201.6	6531.8	
		Filt. Effluent	81.6	81.6	110.2	97.9	114.2	69.4	102.0	89.8	88.7	80.6
Total Kjeldahl Nitrogen (TKN)	Reading	Effluent	22.0	21.0	23.0	21.0	19.0	22.0	18.5	23.0	21.0	24.5
		Filt. Effluent	14.0	14.0	17.5	15.0	14.5	18.0	17.5	16.5	16.5	13.0
	Dillution	Effluent	20.0	20.0	20.0	20.0	20.0	20.0	20.0	20.0	20.0	20.0
		Filt. Effluent	10.0	10.0	10.0	10.0	10.0	10.0	10.0	10.0	10.0	10.0
	Conc. (mg/*l*)	Effluent	616.0	588.0	644.0	588.0	532.0	616.0	518.0	644.0	588.0	686.0
		Filt. Effluent	196.0	196.0	245.0	210.0	203.0	252.0	245.0	231.0	231.0	182.0
Free and Saline Ammonia (FSA)	Reading	Filt. Effluent	13.0	13.0	17.5	14.0	14.0	17.5	17.0	16.5	15.0	13.0
	Dillution	Filt. Effluent	10.0	10.0	10.0	10.0	10.0	10.0	10.0	10.0	10.0	10.0
	Sample Size	Filt. Effluent	10.0	10.0	10.0	10.0	10.0	10.0	10.0	10.0	10.0	10.0
	Conc. (mg/*l*)	Filt. Effluent	182.0	182.0	245.0	196.0	196.0	245.0	238.0	231.0	210.0	182.0
MLSS (mg/*l*)	Reading	Weight A	52.75	52.72	52.75	52.78	52.80	52.79	52.77	52.77	59.37	52.77
		Weight B	53.10	53.06	53.09	53.10	53.06	53.05	53.11	53.12	59.70	53.09
		Weight C	52.88	52.85	52.88	52.90	52.85	52.85	52.88	52.90	59.48	52.89
	Sample Size	Effluent	50.0	50.0	50.0	50.0	50.0	50.0	50.0	50.0	50.0	50.0
	Conc. (mg/*l*)	TSS	6918.0	6820.0	6870.0	6366.0			6816.0	6992.0	6644.0	6390.0
		VSS	4276.0	4378.0	4238.0	4002.0			4668.0	4554.0	4356.0	4086.0
		ISS	2642.0	2442.0	2632.0	2364.0			2148.0	2438.0	2288.0	2304.0
Total Phosphates (TP) and ortho-phosphates (OP) Results	TP Reading	Effluent	0.15	0.15	0.14	0.15	0.14	0.15	0.15	0.15	0.16	0.15
		Filt. Effluent		0.10	0.10	0.10	0.10	0.11	0.10	0.11	0.09	0.10
	OP Reading	Filt. Effluent	0.15	0.14	0.15	0.15	0.15	0.17	0.15	0.17	0.15	0.15
	TP Std. line fn.	Slope	177.05	177.05	177.05	177.05	177.05	162.81	162.81	162.81	162.81	162.81
		Intercept	3.31	3.31	3.31	3.31	3.31	2.26	2.26	2.26	2.26	2.26
	OP) Std. line fn.	Slope	93.37	93.37	93.37	93.37	93.37	99.32	99.32	99.32	99.32	99.32
		Intercept	0.91	0.91	0.91	0.91	0.91	1.81	1.81	1.81	1.81	1.81
	TP Dillution	Effluent	40.0	40.0	40.0	40.0	40.0	40.0	40.0	40.0	40.0	40.0
		Filt. Effluent	40.0	40.0	40.0	40.0	40.0	40.0	40.0	40.0	40.0	40.0
	OP Dillution	Filt. Effluent	40.0	40.0	40.0	40.0	40.0	40.0	40.0	40.0	40.0	40.0
	TP Conc. (mgP/*l*)	Effluent	901.7	894.6	823.8	922.9	873.3	860.5	886.5	873.5	938.6	886.5
		Filt. Effluent		583.0	590.1	575.9	604.2	593.5	560.9		521.8	534.9
	OP Conc. (mgP/*l*)	Filt. Effluent	508.9	501.4	535.0	516.3	523.8		527.7		503.8	523.7
VFA	Conc. (mgHAc/*l*)	Filt. Effluent	32.0	30.0	1.0	10.0	40.0	48.0	28.0	58.0	0.0	0.0
H_2CO_3 Alk.	Conc. (mg$CaCO_3$/*l*)	Filt. Effluent	696.0	713.0	888.6	676.0	680.0	862.0	731.0	752.0	736.0	760.0
Total Alk.	Conc. (mg$CaCO_3$/*l*)	Filt. Effluent	926.0	942.0	1002.0	734.0	885.0	1029.0	999.7	913.0	917.0	975.0
pH		Effluent	6.97	6.98	6.95	6.97	6.95	6.99	6.95	6.95	7.01	6.97
Gas Production (l/d)			0.41	0.50	0.41	0.47	0.47	0.50	0.47	0.52	0.52	0.50

Table A8.3

Samples & Tests			60 Day R_s (Experimental Period 3)									
		Date	25-Jun-08	26-Jun-08	27-Jun-08	28-Jun-08	29-Jun-08	30-Jun-08	2-Jul-08	3-Jul-08	4-Jul-08	5-Jul-08
Chemical Oxygen Demand (COD)		Effluent	17.0	17.4	17.0	17.0	16.7	17.0	16.1	16.9	17.3	17.9
		Filt. Effluent	19.6	21.5	20.8	20.0	20.4	20.8	21.1	20.7	22.9	21.3
		Blank	24.8	24.5	24.7	24.6	24.5	24.3	24.0	24.2	24.8	24.5
	Reading	FAS Norm.	0.05	0.05	0.05	0.05	0.05	0.05	0.05	0.05	0.05	0.05
		Effluent	20.0	20.0	20.0	20.0	20.0	20.0	20.0	20.0	20.0	20.0
	Dillution	Filt. Effluent	1.00	1.00	1.00	1.00	1.00	1.00	1.00	1.00	1.00	1.00
		Effluent	6240.0	5680.0	6160.0	6080.0		5956.8	6446.4	5956.8	6120.0	
	Conc. (mg/*l*)	Filt. Effluent	208.0	120.0	156.0	184.0	164.0	142.8	118.3	142.8	77.5	130.6
Total Kjeldahl Nitrogen (TKN)	Reading	Effluent	22.6	23.5	19.5	20.1	19.9	19.6	20.2	21.5	21.5	22.0
		Filt. Effluent	10.0	23.0	24.5	24.0	19.5	21.5	18.5	18.0	19.0	22.0
		Effluent	20.0	20.0	20.0	20.0	20.0	20.0	20.0	20.0	20.0	20.0
	Dillution	Filt. Effluent	20.0	10.0	10.0	10.0	10.0	10.0	10.0	10.0	10.0	10.0
		Effluent	632.8	658.0	546.0	562.8	557.2	548.8	565.6	602.0	602.0	616.0
	Conc. (mg/*l*)	Filt. Effluent	280.0	322.0	343.0	336.0	273.0	301.0	259.0	252.0	266.0	308.0
Free and Saline Ammonia (FSA)	Reading	Filt. Effluent	9.8	22.0	23.0	21.5	19.5	21.5	18.0	18.0	19.0	20.0
	Dillution	Filt. Effluent	20.0	10.0	10.0	10.0	10.0	10.0	10.0	10.0	10.0	10.0
	Sample Size	Filt. Effluent	10.0	10.0	10.0	10.0	10.0	10.0	10.0	10.0	10.0	10.0
	Conc. (mg/*l*)	Filt. Effluent	274.4	308.0	322.0	301.0	273.0	301.0	252.0	252.0	266.0	280.0
MLSS (mg/*l*)		Weight A	54.74	54.72	58.12	58.11	58.12	58.16	58.12	58.13	59.56	
		Weight B	55.08	55.05	58.45	58.45	58.46	58.45	58.48	58.47	59.85	
	Reading	Weight C	54.88	54.85	58.23	58.22	58.26	58.28	58.26	58.21	59.61	
	Sample Size	Effluent	50.0	50.0	50.0	50.0	50.0	50.0	50.0	50.0	50.0	50.0
		TSS	6740.0	6660.0	6746.0	6792.0	6708.0	5816.0	7199.0	6666.0	5768.0	
		VSS	4026.0	3948.0	4402.0	4760.0	3822.0	3496.0	4243.0		4760.0	
	Conc. (mg/*l*)	ISS	2714.0	2712.0	2344.0	2032.0	2886.0	2320.0	2956.0	1486.0	1008.0	
Total Phosphates (TP) and ortho-phosphates (OP) Results	TP Reading	Effluent	0.12	0.11	0.12	0.12	0.12	0.12	0.13	0.11	0.12	0.12
		Filt. Effluent	0.06	0.06	0.08	0.07	0.07	0.07	0.06	0.08	0.06	0.07
	OP Reading	Filt. Effluent	0.09	0.09	0.10	0.10	0.10	0.10	0.10	0.11	0.09	0.10
		Slope	181.40	181.40	181.40	181.40	178.34	178.34	178.34	178.34	178.34	178.34
	TP Std. line fn.	Intercept	3.68	3.68	3.68	3.68	2.83	2.83	2.83	2.83	2.83	2.83
		Slope	108.21	108.21	108.21	108.21	107.29	107.29	107.29	107.29	107.29	107.29
	OP) Std. line fn.	Intercept	1.21	1.21	1.21	1.21	1.52	1.52	1.52	1.52	1.52	1.52
		Effluent	40.0	40.0	40.0	40.0	40.0	40.0	40.0	40.0	40.0	40.0
	TP Dillution	Filt. Effluent	40.0	40.0	40.0	40.0	40.0	40.0	40.0	40.0	40.0	40.0
	OP Dillution	Filt. Effluent	40.0	40.0	40.0	40.0	40.0	40.0	40.0	40.0	40.0	40.0
		Effluent	870.7	827.2	841.7	863.5	877.4	834.6	927.4	799.0	848.9	841.8
	TP Conc. (mgP/*l*)	Filt. Effluent	464.4	413.6	544.2	471.6	463.7	492.2	428.0	542.2	420.9	463.7
	OP Conc. (mgP/*l*)	Filt. Effluent	389.6	393.9	445.8	424.2	442.0	429.2	429.2	467.8	373.4	433.5
VFA	Conc. (mgHAc/*l*)	Filt. Effluent	22.0			20.0		22.0			18.0	
H_2CO_3 Alk.	Conc. (mg$CaCO_3$/*l*)	Filt. Effluent	1025.0	785.0	876.0		1024.0	1017.0	940.0	792.0	916.0	972.0
Total Alk.	Conc. (mg$CaCO_3$/*l*)	Filt. Effluent	1238.0	1130.0	1285.0		1399.0	1424.0	1284.0	1228.0	1238.0	1304.0
pH		Effluent	6.97	6.99	7.05		7.08	7.08	7.10	7.07	7.13	7.08
Gas Production (l/d)			0.36	0.28	0.32	0.30	0.34	0.34	0.34	0.34	0.36	0.36

Table A8.4: Raw Results for Anaerobic Digester 3 (AD 3), fed waste activated sludge (WAS) from MLE 1 system, when operated at sludge ages of 10, 18 and 25 days

Samples & Tests		Date	10 Day R_s (Experimental Period 5)									
			26-Oct-08	27-Oct-08	28-Oct-08	29-Oct-08	30-Oct-08	31-Oct-08	2-Nov-08	3-Nov-08	4-Nov-08	5-Nov-08
Chemical Oxygen Demand (COD)		Effluent	17.6	14.4	13.5	13.8	13.1	13.5	13.8	14.9	13.7	13.8
		Filt. Effluent	23.8	23.9	23.4	23.0	23.2	23.5	23.0	23.1	22.8	23.3
		Blank	25.0	25.5	25.1	25.6	25.0	25.0	25.0	25.0	25.0	25.0
	Reading	FAS Norm.	0.05	0.05	0.05	0.05	0.05	0.05	0.05	0.05	0.05	0.05
		Effluent	10.0	5.0	5.0	5.0	5.0	5.0	5.0	5.0	5.0	5.0
	Dillution	Filt. Effluent	1.00	1.00	1.00	1.00	1.00	1.00	1.00	1.00	1.00	1.00
		Effluent		2282.2	2385.0			2364.4	2302.7	2076.6	2323.3	2302.7
	Conc. (mg/*l*)	Filt. Effluent	49.3	65.8	69.9	106.9	74.0	61.7	82.2	78.1	90.5	69.9
Total Kjeldahl Nitrogen (TKN)	Reading	Effluent	31.5	30.0	27.0	29.5	26.5	25.5	23.5	28.5	25.0	21.0
		Filt. Effluent	10.7	11.3	13.5	11.3	10.1	8.4	12.9	14.6	15.8	10.7
	Dillution	Effluent	5.0	5.0	5.0	5.0	5.0	5.0	5.0	5.0	5.0	5.0
		Filt. Effluent	2.5	2.5	2.5	2.5	2.5	2.5	2.5	2.5	2.5	2.5
		Effluent			189.0		185.5	178.5	164.5	199.5	175.0	147.0
	Conc. (mg/*l*)	Filt. Effluent	37.4	39.4	47.3	39.4	35.5		45.3	51.2	55.2	37.4
Free and Saline Ammonia (FSA)	Reading	Filt. Effluent	9.0	9.5	12.0	9.5	11.0	9.7	11.0	12.0	12.5	9.5
	Dillution	Filt. Effluent	2.5	2.5	2.5	2.5	2.5	2.5	2.5	2.5	2.5	2.5
	Sample Size	Filt. Effluent	10.0	10.0	10.0	10.0	10.0	10.0	10.0	10.0	10.0	10.0
	Conc. (mg/*l*)	Filt. Effluent	31.5	33.3	42.0	33.3	38.5	34.0	38.5	42.0	43.8	33.3
MLSS (mg/*l*)		Weight A	55.38	55.38	58.66	58.65	58.64	58.62	58.61	58.60	59.30	
		Weight B	55.48	55.47	58.76	58.74	58.72	58.71	58.73	58.70	59.40	
	Reading	Weight C	55.40	55.40	58.68	58.67	58.65	58.63	58.63	58.63	59.32	
	Sample Size	Effluent	50.0	50.0	50.0	50.0	50.0	50.0	50.0	50.0	50.0	50.0
		TSS	1924.0	1948.0	2014.0	1880.0		1750.0		1978.0	1958.0	
		VSS	1582.0	1504.0	1628.0	1474.0		1488.0		1538.0	1564.0	
	Conc. (mg/*l*)	ISS	342.0	444.0	386.0	406.0		262.0		440.0	394.0	
Total Phosphates (TP) and ortho-phosphates (OP) Results	TP Reading	Effluent	0.07	0.07	0.05	0.06	0.07	0.07	0.09	0.08	0.08	0.09
		Filt. Effluent	0.24	0.26	0.17	0.20	0.16	0.15	0.20	0.17	0.10	0.09
	OP Reading	Filt. Effluent	0.20	0.19	0.13	0.15	0.07	0.15	0.15	0.16	0.15	0.13
	TP Std. line fn.	Slope	166.06	166.06	166.06	166.06	166.06	166.06	166.06	166.06	166.06	166.06
		Intercept	-0.19	-0.19	-0.19	-0.19	-0.19	-0.19	-0.19	-0.19	-0.19	-0.19
	OP) Std. line fn.	Slope	121.90	121.90	121.90	121.90	121.90	121.90	121.90	121.90	121.90	121.90
		Intercept	-0.03	-0.03	-0.03	-0.03	-0.03	-0.03	-0.03	-0.03	-0.03	-0.03
	TP Dillution	Effluent	5.0	5.0	5.0	5.0	5.0	5.0	5.0	5.0	5.0	5.0
		Filt. Effluent	1.0	1.0	1.0	1.0	1.0	1.0	1.0	1.0	1.0	1.0
	OP Dillution	Filt. Effluent	1.0	1.0	1.0	1.0	1.0	1.0	1.0	1.0	1.0	1.0
		Effluent	62.4	59.9	42.5	46.6	56.6	54.9	71.5	65.7	66.5	75.7
	TP Conc. (mgP/*l*)	Filt. Effluent			28.7			24.6		27.9	16.8	15.1
	OP Conc. (mgP/*l*)	Filt. Effluent			15.4	18.8	8.2	18.7	18.3	19.7	17.7	15.9
VFA	Conc. (mgHAc/*l*)	Filt. Effluent	0.0		135.2		11.4		0.0		13.3	
H_2CO_3 Alk	Conc. (mg$CaCO_3$/*l*)	Filt. Effluent	485.2		320.6		420.5		435.0		415.0	
pH		Effluent	7.23		6.92		7.01		6.86		7.10	
Gas Production (l/d)		Effluent	0.30	0.19								

Table A8.4

Samples & Tests		Date	18 Day R_s (Experimental Period 1)									
			31-Mar-08	1-Apr-08	2-Apr-08	3-Apr-08	4-Apr-08	5-Apr-08	7-Apr-08	8-Apr-08	9-Apr-08	10-Apr-08
Chemical Oxygen Demand (COD)	Reading	Effluent	16.8	17.5	17.1	17.7	18.0	18.6	18.4	19.2	18.3	18.9
		Filt. Effluent	21.0	21.9	21.7	22.4	22.0	22.4	22.8	23.5	23.1	23.4
		Blank	22.6	23.4	23.5	23.7	24.2	23.8	24.7	25.0	25.1	25.0
		FAS Norm.	0.05	0.05	0.05	0.05	0.05	0.05	0.05	0.05	0.05	0.05
	Dillution	Effluent	10.0	10.0	10.0	10.0	10.0	10.0	10.0	10.0	10.0	10.0
		Filt. Effluent	1.00	1.00	1.00	1.00	1.00	1.00	1.00	1.00	1.00	1.00
	Conc. (mg/*l*)	Effluent	2375.7	2416.6	2621.4	2457.6	2539.5		2580.5	2338.6	2741.8	2498.6
		Filt. Effluent	65.5	61.4	73.7	53.2	90.1	57.3	77.8	60.5	80.6	65.5
Total Kjeldahl Nitrogen (TKN)	Reading	Effluent	19.5	17.4	20.1	18.7	17.6	19.9	21.1	20.7	18.5	19.8
		Filt. Effluent	7.8	15.8	15.8	14.5	14.5	15.8	13.5	12.5	17.0	16.5
	Dillution	Effluent	10.0	10.0	10.0	10.0	10.0	10.0	10.0	10.0	10.0	10.0
		Filt. Effluent	10.0	5.0	5.0	5.0	5.0	5.0	5.0	5.0	5.0	5.0
	Conc. (mg/*l*)	Effluent	273.0	243.6	281.4	261.8	246.4	278.6	295.4	289.8	259.0	277.2
		Filt. Effluent	109.2	110.6	110.6	101.5	101.5	110.6			119.0	115.5
Free and Saline Ammonia (FSA)	Reading	Filt. Effluent	7.7	15.5	15.5	14.0	14.5	15.0	13.0	11.8	16.0	15.5
	Dillution	Filt. Effluent	10.0	5.0	5.0	5.0	5.0	5.0	5.0	5.0	5.0	5.0
	Sample Size	Filt. Effluent	10.0	10.0	10.0	10.0	10.0	10.0	10.0	10.0	10.0	10.0
	Conc. (mg/*l*)	Filt. Effluent	107.8	108.5	108.5	98.0	101.5	105.0	91.0	82.6	112.0	108.5
MLSS (mg/*l*)	Reading	Weight A	55.38	55.38	58.66	58.65	58.64	58.62	58.61	58.60	59.30	
		Weight B	55.49	55.47	58.76	58.75	58.73	58.72	58.74	58.70	59.38	
		Weight C	55.41	55.40	58.69	58.68	58.66	58.64	58.66	58.63	59.31	
	Sample Size	Effluent	50.0	50.0	50.0	50.0	50.0	50.0	50.0	50.0	50.0	50.0
	Conc. (mg/*l*)	TSS	2104.0	1928.0	1994.0	2060.0	1800.0	2050.0		1958.0		
		VSS	1662.0	1384.0	1508.0	1554.0	1352.0	1568.0		1418.0		
		ISS	442.0	544.0	486.0	506.0	448.0	482.0		540.0		
Total Phosphates (TP) and ortho-phosphates (OP) Results	TP Reading	Effluent	0.08	0.08	0.07	0.07	0.06	0.07	0.07	0.08	0.07	0.07
		Filt. Effluent	0.07	0.18	0.18	0.27	0.15	0.15	0.09	0.14	0.13	0.14
	OP Reading	Filt. Effluent	0.12	0.26	0.26	0.25	0.20	0.17	0.08	0.22	0.20	0.21
	TP Std. line fn.	Slope	181.40	181.40	181.40	181.40	178.34	178.34	178.34	178.34	178.34	178.34
		Intercept	3.68	3.68	3.68	3.68	2.83	2.83	2.83	2.83	2.83	2.83
	OP) Std. line fn.	Slope	108.21	108.21	108.21	108.21	107.29	107.29	107.29	107.29	107.29	107.29
		Intercept	1.21	1.21	1.21	1.21	1.52	1.52	1.52	1.52	1.52	1.52
	TP Dillution	Effluent	10.0	10.0	10.0	10.0	10.0	10.0	10.0	10.0	10.0	10.0
		Filt. Effluent	5.0	2.0	2.0	1.0	2.0	2.0	2.0	2.0	2.0	2.0
	OP Dillution	Filt. Effluent	5.0	2.0	2.0	2.0	2.0	2.0	4.0	2.0	2.0	2.0
	TP Conc. (mgP/*l*)	Effluent	108.3	99.2	84.7	88.3	82.2	100.1	96.5	109.0	87.6	92.9
		Filt. Effluent	46.9			45.7	46.0	48.9		45.7	41.4	43.6
	OP Conc. (mgP/*l*)	Filt. Effluent		53.6	54.3	52.1	39.7	34.3		43.9	39.7	42.9
VFA	Conc. (mgHAc/*l*)	Filt. Effluent	77.0	0.0	0.0	0.0	22.0	23.0	0.0	0.0	0.0	0.0
H_2CO_3 Alk	Conc. (mg$CaCO_3$/*l*)	Filt. Effluent	650.0	700.0	723.0	748.0	767.0	743.0	760.0	735.0	806.0	790.0
pH		Effluent	7.20	7.21	7.19	7.23	7.12	7.10	7.05	7.15	7.12	7.28
Gas Production (l/d)		Effluent	0.30	0.47	0.23	0.38	0.41					

Table A8.4

Samples & Tests		Date	25 Day R_s (Experimental Period 2)									
			2-Jun-08	3-Jun-08	4-Jun-08	5-Jun-08	6-Jun-08	7-Jun-08	9-Jun-08	10-Jun-08	11-Jun-08	12-Jun-08
Chemical Oxygen Demand (COD)		Effluent	13.8	14.9	15.7	13.1	21.1	18.0	18.5	17.8	17.2	
		Filt. Effluent	21.3	22.9	23.7	22.2	22.8	21.5	22.2	22.0	22.8	
	Reading	Blank	24.5	24.5	24.5	24.5	24.5	24.5	24.5	24.5	24.5	24.5
		FAS Norm.	0.05	0.05	0.05	0.05	0.05	0.05	0.05	0.05	0.05	0.05
	Dillution	Effluent	10.0	10.0	10.0	10.0	20.0	10.0	10.0	10.0	10.0	10.0
		Filt. Effluent	1.00	1.00	1.00	1.00	1.00	1.00	1.00	1.00	1.00	1.00
	Conc. (mg/*l*)	Effluent		3932.2	3604.5		2785.3	2631.2	2428.8	2712.2	2955.0	
		Filt. Effluent	131.1	65.5	32.8	94.2	69.6	121.4	93.1	101.2	68.8	
Total Kjeldahl Nitrogen (TKN)	Reading	Effluent	31.5	30.0	27.0	29.5	26.5	25.5	23.5	28.5	25.0	21.0
		Filt. Effluent	10.7	11.3	13.5	11.3	10.1	8.4	12.9	14.6	15.8	10.7
	Dillution	Effluent	10.0	10.0	10.0	10.0	10.0	10.0	10.0	10.0	10.0	10.0
		Filt. Effluent	10.0	10.0	10.0	10.0	10.0	10.0	10.0	10.0	10.0	10.0
	Conc. (mg/*l*)	Effluent	441.0	420.0	378.0	413.0	371.0	357.0	329.0	399.0	350.0	294.0
		Filt. Effluent	149.7	157.6	189.1	157.6	141.8		181.2	204.9	220.6	149.7
Free and Saline Ammonia (FSA)	Reading	Filt. Effluent	9.0	9.5	12.0	9.5	11.0	9.7	11.0	12.0	12.5	9.5
	Dillution	Filt. Effluent	10.0	10.0	10.0	10.0	10.0	10.0	10.0	10.0	10.0	10.0
	Sample Size	Filt. Effluent	10.0	10.0	10.0	10.0	10.0	10.0	10.0	10.0	10.0	10.0
	Conc. (mg/*l*)	Filt. Effluent	126.0	133.0	168.0	133.0	154.0	135.8	154.0	168.0	175.0	133.0
MLSS (mg/*l*)	Reading	Weight A	55.38	55.38	58.66	58.65	58.64	58.62	58.61	58.60	59.30	
		Weight B	55.51	55.49	58.78	58.77	58.75	58.74	58.76	58.72	59.41	
		Weight C	55.41	55.41	58.70	58.68	58.67	58.65	58.64	58.64	59.32	
	Sample Size	Effluent	50.0	50.0	50.0	50.0	50.0	50.0	50.0	50.0	50.0	50.0
	Conc. (mg/*l*)	TSS	2524.0	2348.0	2414.0	2480.0	2220.0	2350.0	2996.0	2378.0	2158.0	
		VSS	1942.0	1664.0	1788.0	1834.0	1632.0	1848.0	2396.0	1698.0	1724.0	
		ISS	582.0	684.0	626.0	646.0	588.0	502.0	600.0	680.0	434.0	
Total Phosphates (TP) and ortho-phosphates (OP) Results	TP Reading	Effluent	0.07	0.14	0.10	0.05	0.08	0.07	0.13	0.11	0.12	0.12
		Filt. Effluent	0.12	0.24	0.10	0.03	0.06	0.10	0.10	0.07	0.10	0.09
	OP Reading	Filt. Effluent	0.20	0.19	0.13	0.15	0.07	0.15	0.15	0.16	0.15	0.13
	TP Std. line fn.	Slope	177.05	177.05	177.05	177.05	177.05	162.81	162.81	162.81	162.81	162.81
		Intercept	3.31	3.31	3.31	3.31	3.31	2.26	2.26	2.26	2.26	2.26
	OP) Std. line fn.	Slope	93.37	93.37	93.37	93.37	93.37	99.32	99.32	99.32	99.32	99.32
		Intercept	0.91	0.91	0.91	0.91	0.91	1.81	1.81	1.81	1.81	1.81
	TP Dillution	Effluent	10.0	10.0	10.0	10.0	10.0	10.0	10.0	10.0	10.0	10.0
		Filt. Effluent	5.0	5.0	5.0	5.0	10.0	5.0	5.0	10.0	5.0	5.0
	OP Dillution	Filt. Effluent	5.0	5.0	5.0	5.0	5.0	5.0	5.0	5.0	5.0	5.0
	TP Conc. (mgP/*l*)	Effluent	90.9	221.9	135.1	48.4	108.6	83.2	180.9	153.3	171.2	172.8
		Filt. Effluent	85.3		71.1		76.7	68.5	71.7	86.5	70.1	62.0
	OP Conc. (mgP/*l*)	Filt. Effluent	88.8	85.6	54.3	67.3		67.0	65.5	70.9	63.0	55.5
VFA	Conc. (mgHAc/*l*)	Filt. Effluent	0.0	0.0	95.9	0.0		46.0		75.6		
H_2CO_3 Alk	Conc. (mg$CaCO_3$/*l*)	Filt. Effluent	766.0		841.0	821.7		794.0		723.9		
pH		Effluent	7.14		7.05	7.06		7.05		7.15		
Gas Production (l/d)		Effluent	0.32	0.34	0.34	0.32	0.28	0.30	0.30	0.32	0.34	0.41

Table A8.4

Samples & Tests		Date	40 Day R_s (Experimental Period 4)									
			18-Sep-08	19-Sep-08	20-Sep-08	21-Sep-08	22-Sep-08	23-Sep-08	24-Sep-08	25-Sep-08	26-Sep-08	27-Sep-08
Chemical Oxygen Demand (COD)		Effluent	18.6	19.1	18.8	19.8	19.1	19.2	20.1	19.6	19.8	19.4
		Filt. Effluent	23.5	23.4	23.7	21.8	22.5	23.1	22.0	23.2	22.8	23.1
		Blank	25.2	25.1	25.2	25.0	25.0	24.8	24.9	25.0	25.0	25.1
	Reading	FAS Norm.	0.05	0.05	0.05	0.05	0.05	0.05	0.05	0.05	0.05	0.05
		Effluent	20.00	20.00	20.00	20.00	20.00	20.00	20.00	20.00	20.00	20.00
	Dillution	Filt. Effluent	1.00	1.00	1.00	1.00	1.00	1.00	1.00	1.00	1.00	1.00
		Effluent		4896.0		4243.2	4814.4	4569.6	3916.8	4406.4	4193.3	4596.5
	Conc. (mg/*l*)	Filt. Effluent	69.4	69.4	61.2	130.6	102.0	69.4	118.3	73.4	88.7	80.6
Total Kjeldahl Nitrogen (TKN)	Reading	Effluent	19.5	20.5	20.0	18.0	19.5	12.5	21.0	19.0	17.0	17.5
		Filt. Effluent	12.8	14.3	12.3	23.7	10.4	10.4	15.8	10.9	12.8	10.9
		Effluent	20.0	20.0	20.0	20.0	20.0	20.0	20.0	20.0	20.0	20.0
	Dillution	Filt. Effluent	20.0	20.0	20.0	10.0	20.0	20.0	20.0	20.0	20.0	20.0
		Effluent	546.0	574.0	560.0	504.0	546.0		588.0	532.0	476.0	490.0
	Conc. (mg/*l*)	Filt. Effluent	359.1	400.6	345.3	331.5	290.1	290.1	442.0	303.9	359.1	303.9
Free and Saline Ammonia (FSA)	Reading	Filt. Effluent	20.5	23.4	17.5	29.2	17.5	18.3	24.9	21.2	21.2	19.0
	Dillution	Filt. Effluent	10.0	10.0	10.0	10.0	10.0	10.0	10.0	10.0	10.0	10.0
	Sample Size	Filt. Effluent	10.0	10.0	10.0	10.0	10.0	10.0	10.0	10.0	10.0	10.0
	Conc. (mg/*l*)	Filt. Effluent	286.6	327.6	245.7	409.5	245.7	255.9	348.0	296.9	296.9	266.1
MLSS (mg/*l*)		Weight A	58.10	58.08	58.09	58.11	58.12	58.10	58.09	58.09	58.09	58.09
		Weight B	58.30	58.28	58.29	58.31	58.33	58.29	58.34	58.27	58.26	58.28
	Reading	Weight C	58.13	58.14	58.16	58.17	58.18	58.15	58.16	58.14	58.14	58.14
	Sample Size	Effluent	50.0	50.0	50.0	50.0	50.0	50.0	50.0	50.0	50.0	50.0
		TSS		4030.0	4026.0	4060.0	4190.0	3804.0	4982.0	3702.0	3396.0	
		VSS		2878.0	2548.0	2770.0	2970.0	2784.0	3586.0	2696.0	2316.0	
	Conc. (mg/*l*)	ISS		1152.0	1478.0	1290.0	1220.0	1020.0	1396.0	1006.0	1080.0	
Total Phosphates (TP) and ortho-phosphates (OP) Results	TP Reading	Effluent	0.05	0.10	0.05	0.05	0.05	0.05	0.05	0.05	0.05	0.06
		Filt. Effluent	0.09	0.10	0.07	0.09	0.09	0.06	0.12	0.08	0.11	0.07
	OP Reading	Filt. Effluent	0.14	0.15	0.10	0.14	0.13	0.09	0.19	0.13	0.16	0.11
		Slope	177.05	177.05	177.05	177.05	177.05	162.81	162.81	162.81	162.81	162.81
	TP Std. line fn.	Intercept	3.31	3.31	3.31	3.31	3.31	2.26	2.26	2.26	2.26	2.26
		Slope	93.37	93.37	93.37	93.37	93.37	99.32	99.32	99.32	99.32	99.32
	OP) Std. line fn.	Intercept	0.91	0.91	0.91	0.91	0.91	1.81	1.81	1.81	1.81	1.81
		Effluent	40.0	40.0	40.0	40.0	40.0	40.0	40.0	40.0	40.0	40.0
	TP Dillution	Filt. Effluent	10.0	10.0	10.0	10.0	10.0	10.0	10.0	10.0	10.0	10.0
	OP Dillution	Filt. Effluent	10.0	10.0	10.0	10.0	10.0	10.0	10.0	10.0	10.0	10.0
		Effluent	228.9		221.8	243.1	214.7	235.3	215.8	241.8	254.8	267.9
	TP Conc. (mgP/*l*)	Filt. Effluent	122.0	141.3		123.6	123.6		179.4	115.5	160.1	
	OP Conc. (mgP/*l*)	Filt. Effluent	120.0	129.1		120.0	113.4		166.9	112.3	144.0	
VFA	Conc. (mgHAc/*l*)	Filt. Effluent	0.0	62.0		0.0		0.0		0.0		0.0
H_2CO_3 Alk	Conc. (mg$CaCO_3$/*l*)	Filt. Effluent	1254.0	1227.0		1247.0		1299.0		1188.0		1247.0
pH		Effluent	7.09	7.28		7.44		7.25		7.38		7.39
Gas Production (l/d)		Effluent	0.24	0.28	0.15	0.19	0.23	0.30				

Table A8.4

Samples & Tests		Date	60 Day R_s (Experimental Period 3)									
			25-Jun-08	26-Jun-08	27-Jun-08	28-Jun-08	29-Jun-08	30-Jun-08	2-Jul-08	3-Jul-08	4-Jul-08	5-Jul-08
Chemical Oxygen Demand (COD)		Effluent	17.2	16.7	16.8	16.9	16.6	16.4	16.2	17.1	12.4	13.8
		Filt. Effluent	19.8	22.5	19.2	21.3	20.0	20.7	20.9	20.6	20.0	20.3
		Blank	24.8	24.5	24.7	24.6	24.5	24.3	24.0	24.2	24.8	24.5
	Reading	FAS Norm.	0.05	0.05	0.05	0.05	0.05	0.05	0.05	0.05	0.05	0.05
		Effluent	20.00	20.00	20.00	20.00	20.00	20.00	20.00	20.00	20.00	20.00
	Dillution	Filt. Effluent	1.00	1.00	1.00	1.00	1.00	1.00	1.00	1.00	1.00	1.00
		Effluent	6080.0	6240.0	6320.0	6160.0	6320.0	6446.4	6364.8	5793.6		
	Conc. (mg/*l*)	Filt. Effluent	200.0	80.0	220.0	132.0	180.0	146.9	126.5	146.9	195.8	171.4
Total Kjeldahl Nitrogen (TKN)	Reading	Effluent	17.5	17.4	16.1	18.7	17.6	15.9	18.1	14.7	18.5	19.8
		Filt. Effluent	9.3	18.8	18.8	17.2	17.2	18.8	16.1	14.9	20.2	19.6
	Dillution	Effluent	50.0	50.0	50.0	50.0	50.0	50.0	50.0	50.0	50.0	50.0
		Filt. Effluent	20.0	20.0	20.0	20.0	20.0	20.0	20.0	20.0	20.0	20.0
		Effluent	612.5	609.0	563.5	654.5	616.0	556.5	633.5	514.5	1295.0	1386.0
	Conc. (mg/*l*)	Filt. Effluent	259.8	526.2	526.2	482.9	482.9	526.2	449.6	416.3	566.1	549.5
Free and Saline Ammonia (FSA)	Reading	Filt. Effluent	8.8	17.6	17.6	15.9	16.5	17.1	14.8	13.4	18.2	17.6
	Dillution	Filt. Effluent	40.0	20.0	20.0	20.0	20.0	20.0	20.0	20.0	20.0	20.0
	Sample Size	Filt. Effluent	10.0	10.0	10.0	10.0	10.0	10.0	10.0	10.0	10.0	10.0
	Conc. (mg/*l*)	Filt. Effluent	490.5	493.7	493.7	445.9	461.8	477.8	414.1	375.8	509.6	493.7
MLSS (mg/*l*)		Weight A	55.38	55.38	58.66	58.65	58.64	58.62	58.61	58.60	59.30	
		Weight B	55.65	55.66	58.92	58.91	58.91	58.88	58.90	58.86	59.57	
	Reading	Weight C	55.46	55.44	58.73	58.74	58.70	58.70	58.68	58.68	59.37	
	Sample Size	Effluent	50.0	50.0	50.0	50.0	50.0	50.0	50.0	50.0	50.0	50.0
		TSS	5304.0	5728.0	5194.0	5260.0	5400.0	5130.0	5776.0	5158.0	5538.0	
		VSS	3862.0	4384.0	3908.0	3554.0	4152.0	3568.0	4426.0	3618.0	4080.0	
	Conc. (mg/*l*)	ISS	1442.0	1344.0	1286.0	1706.0	1248.0	1562.0	1350.0	1540.0	1458.0	
Total Phosphates (TP) and ortho-phosphates (OP) Results	TP Reading	Effluent	0.06	0.07	0.06	0.07	0.07	0.10	0.09	0.04	0.07	0.09
		Filt. Effluent	0.15	0.19	0.15	0.16	0.14	0.10	0.13	0.11	0.13	0.10
	OP Reading	Filt. Effluent	0.26	0.26	0.22	0.22	0.21	0.14	0.18	0.14	0.18	0.15
		Slope	181.40	181.40	181.40	181.40	178.34	178.34	178.34	178.34	178.34	178.34
	TP Std. line fn.	Intercept	3.68	3.68	3.68	3.68	2.83	2.83	2.83	2.83	2.83	2.83
		Slope	108.21	108.21	108.21	108.21	107.29	107.29	107.29	107.29	107.29	107.29
	OP) Std. line fn.	Intercept	1.21	1.21	1.21	1.21	1.52	1.52	1.52	1.52	1.52	1.52
		Effluent	40.0	40.0	40.0	40.0	40.0	20.0	40.0	40.0	40.0	20.0
	TP Dillution	Filt. Effluent	10.0	10.0	10.0	10.0	10.0	10.0	10.0	10.0	10.0	10.0
	OP Dillution	Filt. Effluent	10.0	10.0	10.0	10.0	10.0	10.0	10.0	10.0	10.0	10.0
		Effluent	317.0	324.3	288.0	360.6	357.4	296.4			350.3	
	TP Conc. (mgP/*l*)	Filt. Effluent	229.2	300.9	234.9	259.4	224.0	147.9	205.4	166.4	207.3	147.9
	OP Conc. (mgP/*l*)	Filt. Effluent	264.6	269.6	229.4	229.4	205.2	137.4	174.3	139.4	181.3	141.4
VFA	Conc. (mgHAc/*l*)	Filt. Effluent	36.0	0.0	0.0	0.0		0.0		100.0		39.0
H_2CO_3 Alk	Conc. (mg$CaCO_3$/*l*)	Filt. Effluent	1370.0	1374.0	1511.0	1806.0		1456.0		1515.0		1496.0
pH		Effluent	7.35	7.48	7.46	7.49		7.26		7.29		7.30
Gas Production (l/d)		Effluent										

Table A8.5: Raw Results for Anaerobic Digester 5 (AD 5), fed waste activated sludge (WAS) from MLE 2 System, when operated at sludge ages of 10, 18 and 25 days

			10 Day R_s (Experimental Period 5)									
Samples & Tests		Date	26-Oct-08	27-Oct-08	28-Oct-08	29-Oct-08	30-Oct-08	31-Oct-08	2-Nov-08	3-Nov-08	4-Nov-08	5-Nov-08
Chemical Oxygen Demand (COD)		Effluent	21.5	19.4	18.9	19.0	19.2	18.0	18.8	18.8	19.0	19.1
		Filt. Effluent	21.5	22.6	22.7	22.7	22.3	22.5	23.0	21.9	22.4	22.0
		Blank	25.0	25.5	25.1	25.6	25.0	25.0	25.0	25.0	25.0	25.0
	Reading	FAS Norm.	0.05	0.05	0.05	0.05	0.05	0.05	0.05	0.05	0.05	0.05
		Effluent	20.0	10.0	10.0	10.0	10.0	10.0	10.0	10.0	10.0	10.0
	Dillution	Filt. Effluent	1.00	1.00	1.00	1.00	1.00	1.00	1.00	1.00	1.00	1.00
		Effluent	2878.4	2508.3	2549.4	2713.9	2385.0	2878.4	2549.4	2549.4	2467.2	2426.1
	Conc. (mg/*l*)	Filt. Effluent	143.9	119.2	98.7	119.2	111.0	102.8	82.2	127.5	106.9	123.4
Total Kjeldahl Nitrogen (TKN)	Reading	Effluent	35.0	32.0	33.0	36.0	30.5	34.0	29.5	33.0	36.0	33.0
		Filt. Effluent	14.5	18.0	14.5	12.0	20.0	12.0	12.5	15.0	11.0	12.5
		Effluent	2.0	2.0	2.0	2.0	2.0	2.0	2.0	2.0	2.0	2.0
	Dillution	Filt. Effluent	2.0	2.0	2.0	2.0	2.0	2.0	2.0	2.0	2.0	2.0
		Effluent	196.0	179.2	184.8	201.6	170.8	190.4	165.2	184.8	100.8	184.8
	Conc. (mg/*l*)	Filt. Effluent	40.6	50.4	40.6	33.6	56.0	33.6	35.0	42.0	30.8	35.0
Free and Saline Ammonia (FSA)	Reading	Filt. Effluent	15.0	19.0	16.5	11.5	19.0	14.0	13.5		13.0	12.5
	Dillution	Filt. Effluent	2.0	2.0	2.0	2.0	2.0	2.0	2.0	2.0	2.0	2.0
	Sample Size	Filt. Effluent	10.0	10.0	10.0	10.0	10.0	10.0	10.0	10.0	10.0	10.0
	Conc. (mg/*l*)	Filt. Effluent	42.0		46.2	32.2		39.2	37.8		36.4	35.0
MLSS (mg/*l*)		Weight A	60.96	60.95	53.21	53.20	53.20	53.19	53.20	53.20	52.72	
		Weight B	61.07	61.06	53.33	53.31	53.30	53.31	53.32	53.31	52.82	
	Reading	Weight C	60.98	60.98	53.23	53.23	53.22	53.22	53.23	53.23	52.74	
	Sample Size	Effluent	50.0	50.0	50.0	50.0	50.0	50.0	50.0	50.0	50.0	50.0
		TSS	2180.0	2210.0	2390.0	2252.0	2132.0	2352.0			2172.0	
		VSS	1690.0	1586.0	1900.0	1628.0	1642.0	1764.0			1694.0	
	Conc. (mg/*l*)	ISS	490.0	624.0	490.0	624.0	490.0	588.0			478.0	
Total Phosphates (TP) and ortho-phosphates (OP) Results	TP Reading	Effluent	0.04	0.05	0.05	0.05	0.06	0.05	0.05	0.05	0.05	0.04
		Filt. Effluent	0.10	0.08	0.10	0.07	0.08	0.09	0.07	0.09	0.10	0.09
	OP Reading	Filt. Effluent	0.15	0.13	0.13	0.13	0.12	0.11	0.10	0.11	0.12	0.12
		Slope	166.06	166.06	166.06	166.06	166.06	166.06	166.06	166.06	166.06	166.06
	TP Std. line fn.	Intercept	-0.19	-0.19	-0.19	-0.19	-0.19	-0.19	-0.19	-0.19	-0.19	-0.19
		Slope	121.90	121.90	121.90	121.90	121.90	121.90	121.90	121.90	121.90	121.90
	OP) Std. line fn.	Intercept	-0.03	-0.03	-0.03	-0.03	-0.03	-0.03	-0.03	-0.03	-0.03	-0.03
		Effluent	10.0	10.0	10.0	10.0	10.0	10.0	10.0	10.0	10.0	10.0
	TP Dillution	Filt. Effluent	1.0	1.0	1.0	1.0	1.0	1.0	1.0	1.0	1.0	1.0
	OP Dillution	Filt. Effluent	1.0	1.0	1.0	1.0	1.0	1.0	1.0	1.0	1.0	1.0
		Effluent	69.7	83.0	74.7	81.4		79.7	76.4		88.0	73.1
	TP Conc. (mgP/*l*)	Filt. Effluent	16.3	13.9	16.6			14.9	11.8	14.3	16.6	14.9
	OP Conc. (mgP/*l*)	Filt. Effluent		16.3	16.1	16.2	14.9	13.4	12.4	13.5	14.6	15.1
VFA	Conc. (mgHAc/*l*)	Filt. Effluent	15.4		66.7		12.1		24.3			
Alk.	Conc. ($mgCaCO_3$/*l*)	Filt. Effluent	975.7		910.6		982.6		916.0			
pH		Effluent	7.20		7.39		7.41		7.18			
Gas Production (l/d)		Effluent	0.88	0.68	0.95	0.88	1.00	1.00	0.80	0.58	0.70	0.75

Table A8.5

Samples & Tests		Date	40 Day R_s (Experimental Period 4)									
			18-Sep-08	19-Sep-08	20-Sep-08	21-Sep-08	22-Sep-08	23-Sep-08	24-Sep-08	25-Sep-08	26-Sep-08	27-Sep-08
Chemical Oxygen Demand (COD)		Effluent	14.4	13.1	12.9	15.4	13.5	13.2	13.1	12.8	12.7	13.0
		Filt. Effluent	22.7	22.6	22.5	23.3	21.5	21.7	21.8	22.9	22.0	22.1
		Blank	25.2	25.1	25.2	25.0	25.0	24.8	24.9	25.0	25.0	25.1
	Reading	FAS Norm.	0.05	0.05	0.05	0.05	0.05	0.05	0.05	0.05	0.05	0.05
		Effluent	25.0	25.0	25.0	25.0	25.0	25.0	25.0	25.0	25.0	25.0
	Dillution	Filt. Effluent	1.00	1.00	1.00	1.00	1.00	1.00	1.00	1.00	1.00	1.00
		Effluent	11016.0	12240.0	12546.0		11730.0	11832.0	12036.0	12444.0	12398.4	12196.8
	Conc. (mg/*l*)	Filt. Effluent	102.0	102.0	110.2	69.4	142.8	126.5	126.5	85.7	121.0	121.0
Total Kjeldahl Nitrogen (TKN)	Reading	Effluent	18.5	20.0	22.0	24.0	14.0	22.0	21.5	21.5	18.0	25.0
		Filt. Effluent	19.4	19.4	20.5	14.8	15.4	16.0	18.8	20.5	17.7	21.1
		Effluent	20.0	20.0	20.0	20.0	20.0	20.0	20.0	20.0	20.0	20.0
	Dillution	Filt. Effluent	20.0	20.0	20.0	20.0	20.0	20.0	20.0	20.0	20.0	20.0
		Effluent	1036.0		1232.0	1344.0		1232.0	1204.0	1204.0		1400.0
	Conc. (mg/*l*)	Filt. Effluent	543.0		575.0	415.3	431.2	447.2	527.1	575.0	495.1	591.0
Free and Saline Ammonia (FSA)	Reading	Filt. Effluent	20.8	18.6	18.1	16.4	14.8	17.0	19.1	18.1	19.1	19.1
	Dillution	Filt. Effluent	20.0	20.0	20.0	20.0	20.0	20.0	20.0	20.0	20.0	20.0
	Sample Size	Filt. Effluent	10.0	10.0	10.0	10.0	10.0	10.0	10.0	10.0	10.0	10.0
	Conc. (mg/*l*)	Filt. Effluent	582.1	520.8	505.5	459.5	413.6	474.8	536.1	505.5	536.1	536.1
MLSS (mg/*l*)		Weight A	53.21	53.19	53.20	53.22	53.24	53.22	53.21	53.22	53.21	53.22
		Weight B	53.66	53.66	53.66	53.66	53.75	53.72	53.72	53.72	53.72	53.73
	Reading	Weight C	53.30	53.29	53.30	53.30	53.33	53.32	53.30	53.31	53.31	53.32
	Sample Size	Effluent	50.0	50.0	50.0	50.0	50.0	50.0	50.0	50.0	50.0	50.0
		TSS	9066.0	9410.0	9262.0	8964.0	10230.0	10174.0	10126.0	10090.0	10034.0	10238.0
		VSS	7242.0	7462.0	7236.0	7190.0	8372.0	8188.0	8422.0	8162.0	8036.0	8160.0
	Conc. (mg/*l*)	ISS	1824.0	1948.0	2026.0	1774.0	1858.0	1986.0	1704.0	1928.0	1998.0	2078.0
Total Phosphates (TP) and ortho-phosphates (OP) Results	TP Reading	Effluent	0.04	0.07	0.07	0.08	0.06	0.06	0.06	0.04	0.07	0.09
		Filt. Effluent	0.11	0.11	0.11	0.10	0.12	0.11	0.12	0.10	0.12	0.16
	OP Reading	Filt. Effluent		0.16	0.20	0.15	0.17	0.16	0.19	0.18	0.18	0.26
		Slope	177.05	177.05	177.05	177.05	177.05	162.81	162.81	162.81	162.81	162.81
	TP Std. line fn.	Intercept	3.31	3.31	3.31	3.31	3.31	2.26	2.26	2.26	2.26	2.26
		Slope	93.37	93.37	93.37	93.37	93.37	99.32	99.32	99.32	99.32	99.32
	OP) Std. line fn.	Intercept	0.91	0.91	0.91	0.91	0.91	1.81	1.81	1.81	1.81	1.81
		Effluent	40.0	40.0	40.0	40.0	40.0	40.0	40.0	40.0	40.0	40.0
	TP Dillution	Filt. Effluent	10.0	10.0	10.0	10.0	10.0	10.0	10.0	10.0	10.0	10.0
	OP Dillution	Filt. Effluent	10.0	10.0	10.0	10.0	10.0	10.0	10.0	10.0	10.0	10.0
		Effluent		474.5	481.6	531.2	417.8	377.7	390.7		436.3	566.6
	TP Conc. (mgP/*l*)	Filt. Effluent	196.7	191.9	199.0	180.1	206.2	172.1	196.1	170.0	196.1	254.9
	OP Conc. (mgP/*l*)	Filt. Effluent		150.2	182.6	137.0	158.6	157.2	184.0	178.9	173.8	254.3
VFA	Conc. (mgHAc/*l*)	Filt. Effluent	0.0		4.1		0.0		0.0		0.0	
Alk.	Conc. (mg$CaCO_3$/*l*)	Filt. Effluent	1030.0		947.0		780.0		1092.0		972.1	
pH		Effluent	7.05		7.00		7.07		7.04		7.18	
Gas Production (l/d)		Effluent	0.450	0.425	0.450	0.450	0.425	0.375	0.350	0.450	0.400	0.425

Table A8.5

Samples & Tests		Date	60 Day R. (Experimental Period 3)									
			25-Jun-08	26-Jun-08	27-Jun-08	28-Jun-08	29-Jun-08	30-Jun-08	2-Jul-08	3-Jul-08	4-Jul-08	5-Jul-08
Chemical Oxygen Demand (COD)		Effluent	8.6	8.4	7.5	8.4	8.5	7.7	7.9	7.7	8.4	7.6
		Filt. Effluent	22.0	21.3	17.8	17.9	20.1	16.7	19.6	16.3	21.7	21.0
		Blank	24.8	24.5	24.7	24.6	24.5	24.3	24.0	24.2	24.8	24.5
	Reading	FAS Norm.	0.05	0.05	0.05	0.05	0.05	0.05	0.05	0.05	0.05	0.05
		Effluent	25.0	25.0	25.0	25.0	25.0	25.0	25.0	25.0	25.0	25.0
	Dillution	Filt. Effluent	1.00	1.00	1.00	1.00	1.00	1.00	1.00	1.00	1.00	1.00
		Effluent	16200.0	16100.0		16200.0	16000.0	16932.0	16422.0	16830.0	16728.0	
	Conc. (mg/l)	Filt. Effluent	112.0	128.0	276.0	268.0	176.0	310.1	179.5	322.3	126.5	142.8
Total Kjeldahl Nitrogen (TKN)	Reading	Effluent	15.1		14.7	13.4	14.0	13.5	12.0	12.5	24.5	15.0
		Filt. Effluent	12.8	0.0	28.0	28.0	28.0	26.8	26.8	27.4	16.4	29.8
		Effluent	50.0	50.0	50.0	50.0	50.0	50.0	50.0	50.0	50.0	50.0
	Dillution	Filt. Effluent	40.0	20.0	20.0	20.0	20.0	20.0	20.0	20.0	40.0	20.0
		Effluent	2114.0		2058.0	1876.0	1960.0	1890.0	1680.0	1750.0	1715.0	2100.0
	Conc. (mg/l)	Filt. Effluent	716.2		784.4	784.4	784.4	750.3	750.3	767.3		835.5
Free and Saline Ammonia (FSA)	Reading	Filt. Effluent	12.5	28.1	26.9	28.8	29.4	27.5	28.1	28.1	28.1	30.1
	Dillution	Filt. Effluent	40.0	20.0	20.0	20.0	20.0	20.0	20.0	20.0	20.0	20.0
	Sample Size	Filt. Effluent	10.0	10.0	10.0	10.0	10.0	10.0	10.0	10.0	10.0	10.0
	Conc. (mg/l)	Filt. Effluent	702.4	788.0	752.2	805.9	823.8	770.1	788.0	788.0	788.0	841.7
MLSS (mg/l)		Weight A	60.96	60.95	53.21	53.20	53.20	53.19	53.20	53.20	52.72	
		Weight B	61.61	61.59	53.85	53.85	53.83	53.85	53.86	53.85	53.40	0.12
	Reading	Weight C	61.10	61.10	53.35	53.35	53.34	53.34	53.35	53.35	52.86	
	Sample Size	Effluent	50.0	50.0	50.0	50.0	50.0	50.0	50.0	50.0	50.0	50.0
		TSS	12980.0	12810.0	12790.0	13052.0	12732.0	13152.0	13292.0	13088.0	13772.0	
		VSS	10090.0	9786.0	9900.0	10028.0	9842.0	10164.0	10120.0	10020.0	10894.0	
	Conc. (mg/l)	ISS	2890.0	3024.0	2890.0	3024.0	2890.0	2988.0	3172.0	3068.0	2878.0	
Total Phosphates (TP) and ortho-phosphates (OP) Results	TP Reading	Effluent	0.06	0.09	0.09	0.01	0.09	0.09	0.09	0.05	0.09	0.08
		Filt. Effluent	0.09	0.11	0.08	0.09	0.08	0.09	0.09	0.09	0.09	0.08
	OP Reading	Filt. Effluent	0.17	0.15	0.13	0.14	0.11	0.14	0.13	0.06	0.11	0.11
		Slope	181.40	181.40	181.40	181.40	178.34	178.34	178.34	178.34	178.34	178.34
	TP Std. line fn.	Intercept	3.68	3.68	3.68	3.68	2.83	2.83	2.83	2.83	2.83	2.83
		Slope	108.21	108.21	108.21	108.21	107.29	107.29	107.29	107.29	107.29	107.29
	OP) Std. line fn.	Intercept	1.21	1.21	1.21	1.21	1.52	1.52	1.52	1.52	1.52	1.52
		Effluent	40.0	40.0	40.0	40.0	40.0	40.0	40.0	40.0	40.0	20.0
	TP Dillution	Filt. Effluent	20.0	20.0	20.0	20.0	20.0	20.0	20.0	20.0	20.0	20.0
	OP Dillution	Filt. Effluent	20.0	20.0	20.0	20.0	20.0	20.0	20.0	20.0	20.0	20.0
		Effluent		624.0	667.6		620.6	642.0	613.5		642.0	
	TP Conc. (mgP/l)	Filt. Effluent	316.1	409.4	305.8	344.6	295.5	305.7	305.7	310.8	305.7	272.6
	OP Conc. (mgP/l)	Filt. Effluent	374.5	333.0	280.9	306.3	238.7	306.3	271.9		238.7	228.1
VFA	Conc. (mgHAc/l)	Filt. Effluent	19.0	10.0		0.0	0.0		80.0		0.0	0.0
Alk.	Conc. ($mgCaCO_3/l$)	Filt. Effluent	1828.0	1839.0		1918.0	1668.0		1804.0		1842.0	1789.0
pH		Effluent	7.25	7.36		7.36	7.30		7.25		7.32	7.23
Gas Production (l/d)		Effluent										